GEOMORPHOLOGY OF DESERT ENVIRONMENTS

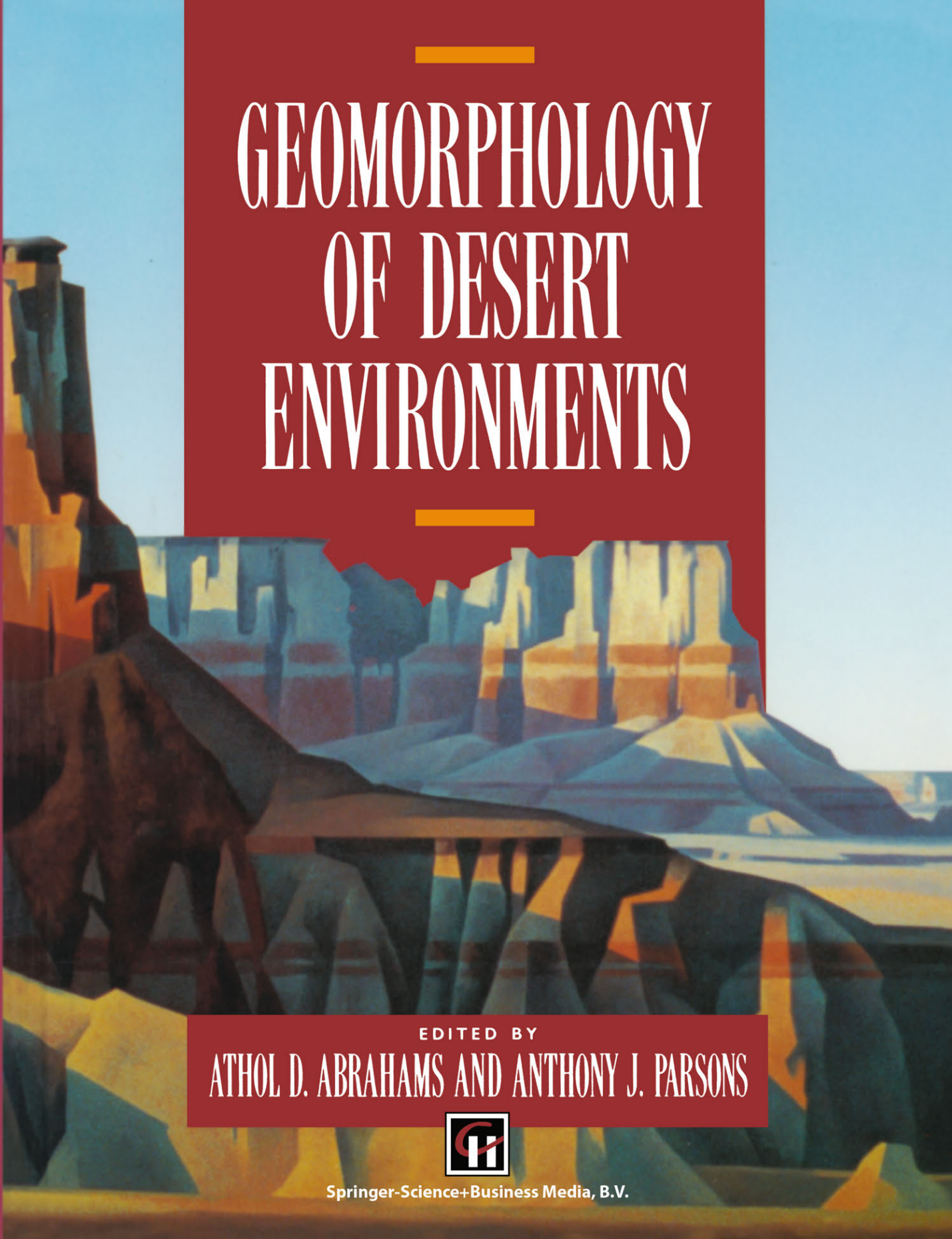

EDITED BY
ATHOL D. ABRAHAMS AND ANTHONY J. PARSONS

Springer-Science+Business Media, B.V.

GEOMORPHOLOGY OF DESERT ENVIRONMENTS

GEOMORPHOLOGY OF DESERT ENVIRONMENTS

Edited by

Athol D. Abrahams

and

Anthony J. Parsons

Springer-Science+Business Media, B.V.

First edition 1994

ISBN 978-94-015-8256-8 ISBN 978-94-015-8254-4 (eBook)
DOI 10.1007/978-94-015-8254-4

Originally published by Chapman & Hall in 1994.

Typeset in 9/11pt Palatino by Keyset Composition, Colchester, Essex

A catalogue record for this book is available from the British Library

Library of Congress Cataloging-in-Publication data

Geomorphology of desert environments/edited by Athol D. Abrahams and Anthony J. Parsons. — 1st ed.
p. cm.
Includes index.

1. Deserts. 2. Geomorphology. I. Abrahams, A. D. (Athol D.), 1946– . II. Parsons, A. J.
GB611.G465 1993
551.4'15—dc20 93-33947
CIP

CONTENTS

CONTRIBUTORS

ATHOL D. ABRAHAMS
Department of Geography, State University of New York at Buffalo, Buffalo, NY 14261, USA

TERENCE C. BLAIR
Blair & Associates, 1949 Hardscrabble Place, Boulder, CO 80303, USA

DONALD R. CURREY
Department of Geography, University of Utah, Salt Lake City, UT 84112, USA

JOHN C. DIXON
Department of Geography, University of Arkansas, Fayetteville, AR 72701, USA

JOHN C. DOHRENWEND
U.S. Geological Survey, MS 901, 345 Middlefield Road, Menlo Park, CA 94025, USA

RONALD I. DORN
Department of Geography, Arizona State University, Tempe, AZ 85287, USA

CAROLYN F. FRANCIS
Sir William Halcrow & Partners, Burderop Park, Swindon, Wiltshire SN4 0QD, UK

ALAN D. HOWARD
Department of Environmental Sciences, University of Virginia, Charlottesville, VA 22903, USA

JULIE E. LAITY
Department of Geography, California State University, Northridge, CA 91330, USA

NICHOLAS LANCASTER
Desert Research Institute, University of Nevada, P.O. Box 60220, Reno, NV 89506, USA

JOHN G. McPHERSON
Mobil Research and Development Corporation, Mobil Exploration and Producing Technical Center, P.O. Box 650232, Dallas, TX 75265, USA

WILLIAM G. NICKLING
Department of Geography, University of Guelph, Guelph, Ontario N1G 2W1, Canada

THEODORE M. OBERLANDER
Department of Geography, University of California, Berkeley, CA 94720, USA

ANTHONY J. PARSONS
Department of Geography, University of Keele, Keele, Staffordshire ST5 5BG, UK

IAN REID
Department of Geography, Loughborough University of Technology, Loughborough, LE11 3TU, UK

DOROTHY SACK
Department of Geography, University of Wisconsin, Madison, WI 53706, USA

KARL-HEINZ SCHMIDT
Geomorphologisches Laboratorium, Freie Universitat Berlin, Altensteinstrasse 19, D-1000 Berlin 33, Germany

MICHAEL J. SELBY
Department of Earth Sciences, University of Waikato, Private Bag 3105, Hamilton, New Zealand

B.J. SMITH
Department of Geosciences, Queen's University of Belfast, Belfast BT7 1NN, UK

VATCHE P. TCHAKERIAN
Department of Geography, Texas A & M University, College Station, TX 77843, USA

JOHN B. THORNES
Department of Geography, King's College London, Strand, London WC2R 2LS, UK

M.A.J. WILLIAMS
Mawson Graduate Centre for Environmental Studies, University of Adelaide, GPO Box 498, Adelaide, SA 5001, Australia

PREFACE

About one-third of the Earth's land surface experiences a hyperarid, arid, or semi-arid climate, and this area supports approximately 15% of the planet's population. This percentage continues to grow and with this growth comes the need to learn more about the desert environment. Geomorphology is only one aspect of this environment, but an important one, as geomorphic phenomena such as salt weathering, debris flows, flash flooding, and dune encroachment pose major problems to desert settlement and transportation.

The geomorphology of deserts has been the subject of scientific enquiry for more than a century, but desert geomorphology did not emerge as an identifiable subdiscipline in geomorphology until the 1970s when the first textbooks on the subject appeared, namely *Geomorphology in deserts* in 1973 and *Desert landforms* in 1977. Also, in 1977 the Eighth Annual (Binghamton) Geomorphology Symposium was devoted to the theme 'Geomorphology in Arid Lands' and the proceedings of the symposium were published in the same year. The 1980s have seen the appearance of titles dealing with particular topics within desert geomorphology, the most notable of these being *Urban geomorphology in drylands* and *Dryland rivers*. As we enter the 1990s, a new generation of textbooks on desert geomorphology has reached the bookstores. *Arid zone geomorphology* and *Desert geomorphology* incorporate the advances in knowledge that have occurred during the past 20 years but are primarily written for the college student. By contrast, the present volume assumes that the reader already has some knowledge of desert geomorphology. It is pitched at a level somewhat higher than the standard text and is intended to serve mainly as a reference work.

To achieve this goal we sought out authors who were active researchers and authorities in their fields. We asked each to write an up-to-date review of an assigned topic related to their speciality. These reviews are assembled in this book and together represent a comprehensive treatment of the state of knowledge in desert geomorphology. The treatment, perhaps inevitably, contains a geographical bias, in that 14 of the 22 authors are based in North America. Although most of them have experience in deserts on other continents, their discussions and the examples they draw upon are lop-sidedly American. The bias was perhaps inevitable (despite our best efforts to avoid it) because modern research in desert geomorphology published in English is dominated by investigations conducted in the deserts of the American South-west. Faced with this geographical bias, we specifically requested authors to include research conducted outside North America. Different authors have succeeded in this regard in varying degrees. Thus in spite of the bias, we believe this book will have appeal and relevance beyond North America and will be useful to geomorphologists working in deserts around the globe.

The idea for this volume emerged during an informal field trip of desert geomorphologists through the Mojave Desert and Death Valley prior to the Annual Meeting of the Association of American Geographers in Phoenix in April 1988. One author submitted his chapter in September, even before we had found a publisher! As we write this Preface, almost four years later, the final chapter has just arrived. Assembling within a limited time frame 26 chapters from 22 authors, all of whom have busy schedules and other commitments and obligations, is a daunting task. Those who submitted their chapters early or on time have waited patiently for those less prompt, while those running late have had to sustain regular badgering by the editors. Finally, however, the book is complete. As is generally the case with edited volumes, the quality of the product depends very heavily on the quality of the individual chapters, and the quality of the chapters depends on the authors. Recognizing this, we would like to thank the authors for their efforts in writing this book. We are pleased with the final product, and we hope they are too.

Athol D. Abrahams
Buffalo, USA

Anthony J. Parsons
Keele, UK

ACKNOWLEDGEMENTS

We would like to thank the following publishers, organizations, and individuals for permission to reproduce the following figures.

Figure 1.5	Belhaven Press and D.S.G. Thomas
Figure 7.9	Selby, M.J. 1987. Rock slopes. In *Slope stability: geotechnical engineering and geomorphology*, M.G. Anderson and K.S. Richards (eds), 475–504. Reprinted by permission of John Wiley & Sons, Ltd.
Figure 7.22	Donald O. Doehring
Figure 7.29	Van Nostrand Reinhold
Figure 7.33	Zeitschrift fur Geomorphologie
Figure 7.34	Arthur L. Lange
Figure 8.2a	Elsevier Science Publishers
Figure 8.3	Academic Press
Figure 8.5	Elsevier Science Publishers
Figure 8.7	Elsevier Science Publishers
Figure 8.8	Elsevier Science Publishers
Figure 8.17	Kirkby, M.J. 1969. Erosion by water on hillslopes. In *Water, earth and man*, R.J. Chorley (ed.), 229–38. Reproduced by permission of Methuen & Co.
Figure 8.18	Catena Verlag
Figure 8.21	American Society of Agricultural Engineers
Figure 8.22	Catena Verlag
Figure 8.23	Catena Verlag
Figure 9.4	Elsevier Science Publishers
Figure 9.5	Catena Verlag
Figure 22.1	M. Servant
Figure 22.2	M.R. Talbot
Figure 22.3	Frostick, L.E. and I. Reid 1989. Is structure the main control of river drainage and sedimentation in rifts? *Journal of African Earth Sciences* **8**, 165–82. Reprinted with permission of Pergamon Press PLC.
Figure 22.5	D.A. Adamson
Figure 22.8	Maizels, J.K. 1987. Plio-Pleistocene raised channel systems of the western Sharqiya (Wahiba), Oman. In *Desert sediments: ancient and modern*, L.E. Frostick and I. Reid (eds), 35–50. Reproduced by permission of the Geological Society and J.K. Maizels.
Figure 22.10	Baker, V.R. 1978. Adjustment of fluvial systems to climate and source terrain in tropical and subtropical environments. In *Fluvial sedimentology*, A.D. Miall (ed.), 211–30. Reproduced with permission of the Canadian Society of Petroleum Geologists.
Figure 22.12a, b	W.L. Graf
Figure 22.12c	Graf, W.L. 1979. The development of montane arroyos and gullies. *Earth Surface Processes* **4**, 1–14. Copyright 1979 John Wiley & Sons, Ltd. Reprinted by permission of John Wiley & Sons, Ltd.
Figure 22.13	Schumm, S.A. and R.F. Hadley 1957. Arroyos and the semiarid cycle of erosion. *American Journal of Science* **255**, 161–74. Reprinted by permission of American Journal of Science and S.A. Schumm.
Figure 22.14	M.R. Talbot
Figure 22.16	Grossman, S. and R. Gerson 1987. Fluviatile deposits and morphology of alluvial

surfaces as indicators of Quaternary environmental changes in the southern Negev, Israel. In *Desert sediments: ancient and modern*, L.E. Frostick and I. Reid (eds), 17–29. Reproduced by permission of the Geological Society and S. Grossman.

Figure 22.17 Maizels, J.K. 1987. Plio-Pleistocene raised channel systems of the western Sharqiya (Wahiba), Oman. In *Desert sediments: ancient and modern*, L.E. Frostick & I. Reid (eds), 31–50. Reproduced by permission of the Geological Society and J.K. Maizels.

Figure 22.18 D. Adamson

Figure 24.4 Elsevier Science Publishers and D.R. Currey

Figure 26.2 Williams, M.A.J., P.I. Abell and B.W. Sparks 1987. Quaternary landforms, sediments, and depositional environments and gastropod isotope ratios at Adrar Bous, Tenere Desert of Niger, south-central Sahara. In *Desert sediments: ancient and modern*, L.E. Frostick and I. Reid (eds), 105–25. Reproduced by permission of the Geological Society and I. Reid.

Figures 26.5, 6 and 7 Williams, M.A.J. 1984. Quaternary environments. In *Phanerozoic earth history of Australia*, J.J. Veevers (ed.), 42–7. Reproduced by permission of Oxford University Press.

PART ONE

INTRODUCTION

GEOMORPHOLOGY OF DESERT ENVIRONMENTS

1

Anthony J. Parsons and Athol D. Abrahams

DESERT AREAS OF THE WORLD

In popular concept, a desert should be hot, barren, and, preferably, sandy. In reality, many deserts are few, or none of these things. Most deserts are, however, areas of aridity, and it is upon this property that the scientific definition of deserts has generally hinged. Even so, providing an acceptable measure of aridity upon which to base a definition of desert areas has not been straightforward, and several attempts based upon a variety of geomorphic, climatic, and/or vegetational indices of aridity have been made to identify the world distribution of deserts.

Probably the first attempt that achieved widespread acceptance was the map of the distribution of arid and semi-arid homoclimates produced by Meigs (1953) on behalf of UNESCO, and based upon Thornthwaite's (1948) index of moisture availability. Since that time, new climatic data from a denser meteorological network together with more information on soils, biology, and vegetation of arid zones have become available. In addition, a better understanding of the relationships among climate, soils, and vegetation has been achieved. In response to these data and to the growing interests in problems of aridity and desertification, a new map (a simplified version of which is presented in Fig. 1.1) has been produced (UNESCO 1977). For this map, arid regions were delimited partly on the basis of aridity indices and partly from consideration of all available data on soil, relief, and vegetation. The degree of bioclimatic aridity was defined by the ratio of the mean annual precipitation P to the mean annual potential evapotranspiration Etp. Values of this ratio at 1600 meteorological stations were mapped and the limits of bioclimatic regions were interpolated taking into account, for the regions where there were few climatic data, the information given on the FAO/UNESCO *Soil Map of the World* and maps of vegetation. The map defines four main classes of aridity: the hyperarid zone ($P/Etp < 0.03$), the arid zone ($0.03 < P/Etp < 0.20$), the semi-arid zone ($0.20 < P/Etp < 0.50$) and the subhumid zone ($0.50 < P/Etp < 0.75$).

Taking this map as a definition, deserts encompass a much larger tract of land than would be included in any popular delimitation. None the less, in some regards the popular image of deserts dominates. More than 40% of the world's deserts can be classified as hot and the remainder have hot summers but can be differentiated on the basis of the coolness of their winters (UNESCO 1977). In other respects, however, the popular image is erroneous. Only about 20% of deserts are covered by aeolian sand deposits, and truly barren areas occupy only 13% of deserts. Mountains are the commonest landforms, and if any surface cover is typical, it is sparse grasses and shrubs, which cover 59% of deserts.

As Figure 1.1 shows, the largest expanses of deserts are in zones approximately centred on the tropics. Here, stable descending air of the tropical high pressure systems maintains aridity throughout most of the year. Three other factors may contribute to aridity in these zones, or maintain it elsewhere. The first of these is the presence of a large land mass. Large land areas disrupt the zonal pattern of global pressure systems and impose their own strongly seasonal one. In winter, the land mass, cooler than its surrounding ocean, becomes the location of a high pressure system. In summer, despite being the centre of a low pressure system, distance from the ocean prevents the ingress of substantial quantities of rain-bearing air. The large desert area of northern Africa and Arabia is due to a combination of this factor with the location of the

Geomorphology of Desert Environments. Edited by Athol D. Abrahams and Anthony J. Parsons. Published in 1994 by Chapman & Hall, London. ISBN 978-94-015-8256-8

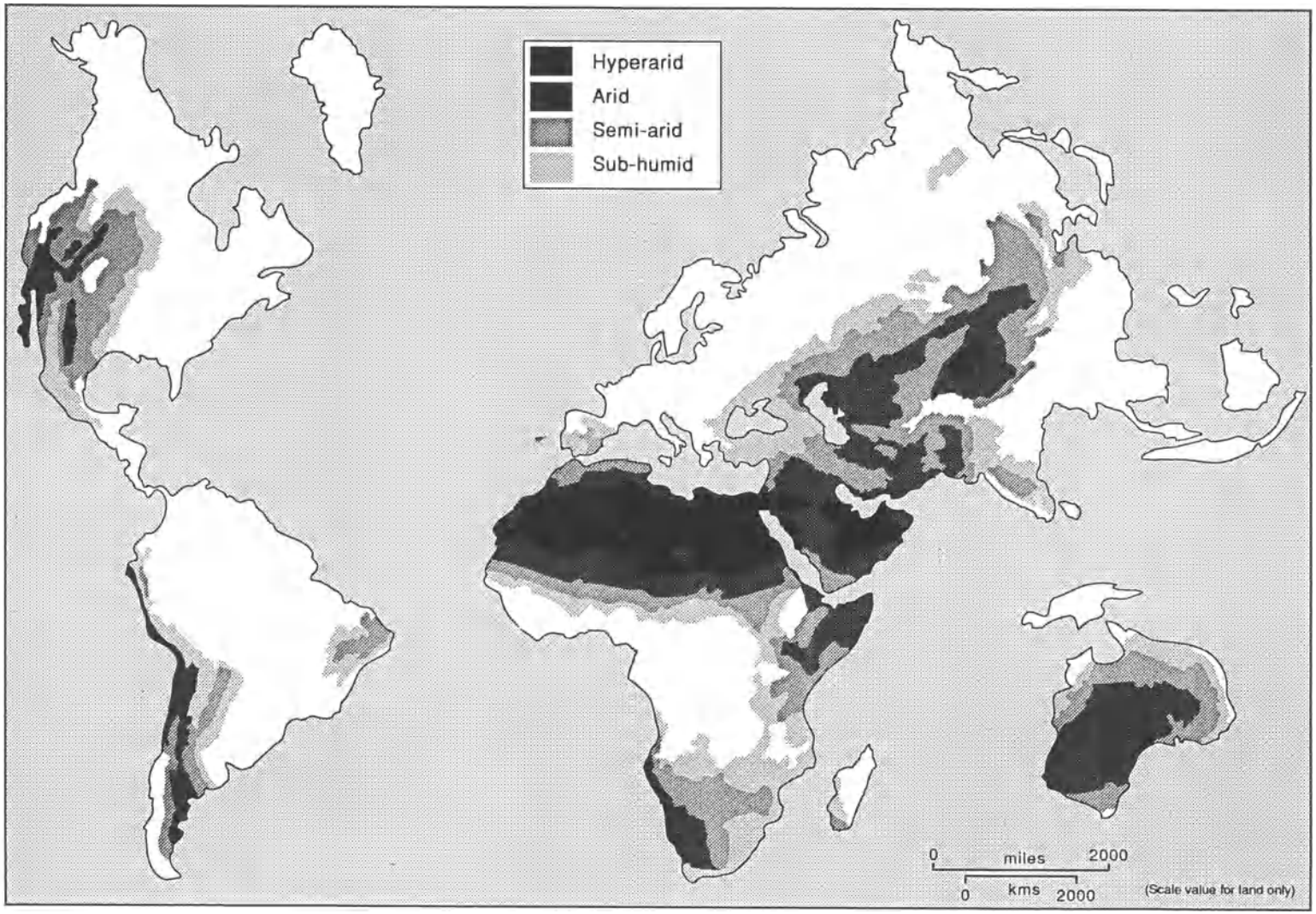

Figure 1.1 World distribution of deserts (after UNESCO 1977).

Tropic of Cancer. This desert area extends northward into central Asia as a result of the size of this land mass. Mountain barriers are the second additional cause of aridity. Areas in the lee of mountain ranges are both shielded from rain-bearing winds and are subject to descending winds. The extratropical deserts of North and South America owe their presence to this effect. Finally, there is the influence of cold currents on the eastern margins of oceans. This factor accounts for the extension of hyperarid conditions in the Atacama desert to near-equatorial latitudes.

DESERT CLIMATES

Whether due to their presence beneath the tropical high pressure systems, in the far interior of continents, or in the lee of mountain ranges, in most deserts a lack of rainfall is accompanied by a high diurnal range of temperature, low average humidity, and predominantly cloud-free skies (Figs 1.2a, b and c). It is also a characteristic of deserts that they experience great climatic variability at all scales. At the daily scale it is fluctuation in temperature which is most marked, typically very similar to the annual range in mean daily temperature. The effect of this is to raise pre-dawn relative humidity substantially so that for some part of the year dew is present for brief periods of the day in many desert areas. On a longer timescale it is variability in precipitation which is most marked. Of all parts of the Earth's surface, arid areas have the highest average deviation in annual rainfall (Morales 1977) and, generally, this deviation increases as the mean annual precipitation decreases. Although for many purposes it is the probability that the mean annual rainfall will not occur which is significant, for geomorphology the more important element of this variability is the rare occurrence of extremely large rainfall events. Baker (1984) documented the effects of between 170 and 267 mm of rain (between 64 and 100% the mean annual rainfall) falling during five days in the Tucson area in 1983. Flood peaks in the Santa Cruz and Rillito Rivers resulted in immense channel changes and pronounced bank erosion in the incised reaches of these rivers (Fig. 1.3). Baker (1984, p. 217) drew attention to differences between observed and predicted channel responses. 'So much channel enlargement occurred during the 1983 flooding that even the 1470 m^3/sec (52 000 cfs) flood peak failed to achieve the extent of overbank flooding predicted . . . for a much smaller flow. On the other hand, local channel migration moved the active floodway into zones predicted to have only the risk of overbank floods rarer than the 500-year event.'

Precipitation in deserts is subject not only to temporal variability but also to extreme spatial variability. Figure 1.4 shows isohyets for Walnut Gulch experimental watershed for summer rainfall in 1967 and 1969. In the former year there is a more than twofold variation in summer rainfall across the watershed and in the latter a near threefold variation. Furthermore, the two years show no similarity in the spatial distribution of the rainfall.

The exceptions to this general pattern of desert climates are the coastal deserts adjacent to cold ocean currents (Fig. 1.2d). These deserts are characterized by smaller annual and daily temperature ranges, cloudiness, high humidity but, typically, hyperaridity. Like all other deserts, however, variability in precipitation is characteristic. At Arica, for example, the 10 mm of rain that fell in one day in January 1918 accounted for about a third of the total rainfall received during half a century (Miller 1976).

THE CONCEPT OF DESERT GEOMORPHOLOGY

The notion that the desert areas of the world possess a distinct geomorphology has a long history and, in many ways, is informed by the popular concept of deserts. Not surprisingly, early explorers in deserts, particularly Europeans travelling in the Sahara from the late 18th century onwards, were impressed by, and reported on, the unusual features of these areas. Rock pedestals, sand dunes, and bare-rock hills rising almost vertically from near-horizontal, gravel-covered plains all contributed to the impression of a unique landscape. This spirit of exploration in a totally alien landscape continued into the 20th century, so that as late as 1935 R.A. Bagnold wrote of his travels in North Africa during the preceding decade under the title *Libyan sands: travels in a dead world* (Bagnold 1935). Emphasis on the unusual and remarkable landforms of desert areas and a coincident emphasis on the hot tropical deserts had a profound impact on attempts to explain the geomorphology of deserts.

Of particular influence in shaping a view of the uniqueness of desert landscapes, due in large measure to his influence in shaping geomorphology overall, was W.M. Davis who was sufficiently persuaded of the distinctiveness of desert landscapes that in 1905 he published his cycle of erosion in arid climates. Davis held the opinion that, notwithstanding the infrequency of rainfall in desert areas, the landforms resulted primarily from fluvial processes. Only towards the end of his cycle of erosion did aeolian processes come to play a dominant role.

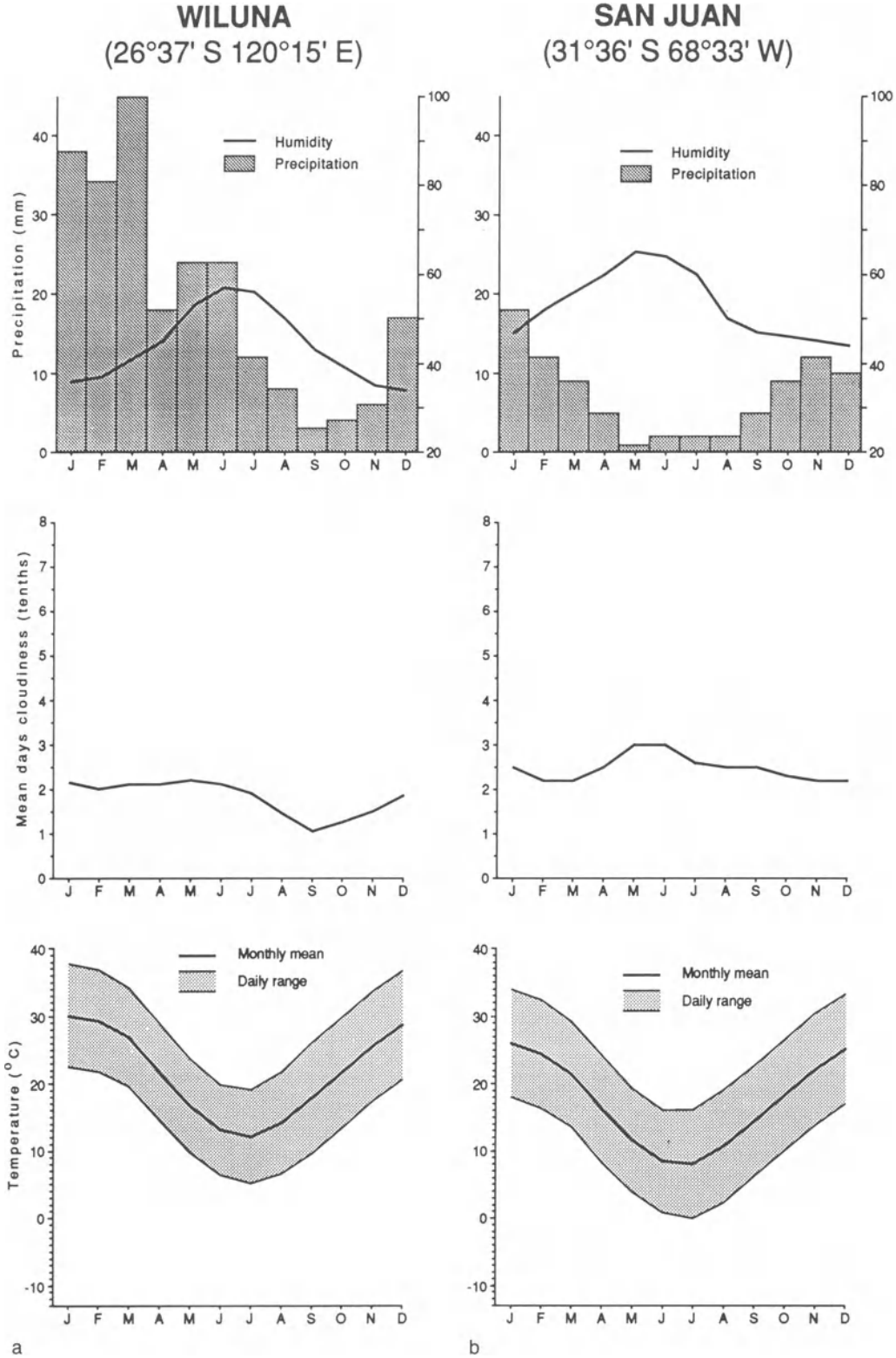

Figure 1.2 Climatic characteristics of (a) Wiluna, Australia; (b) San Juan, Argentina; (c) Khorog, Tadzhikstan; and (d) Swakopmund, Namibia (source: Landsberg 1972).

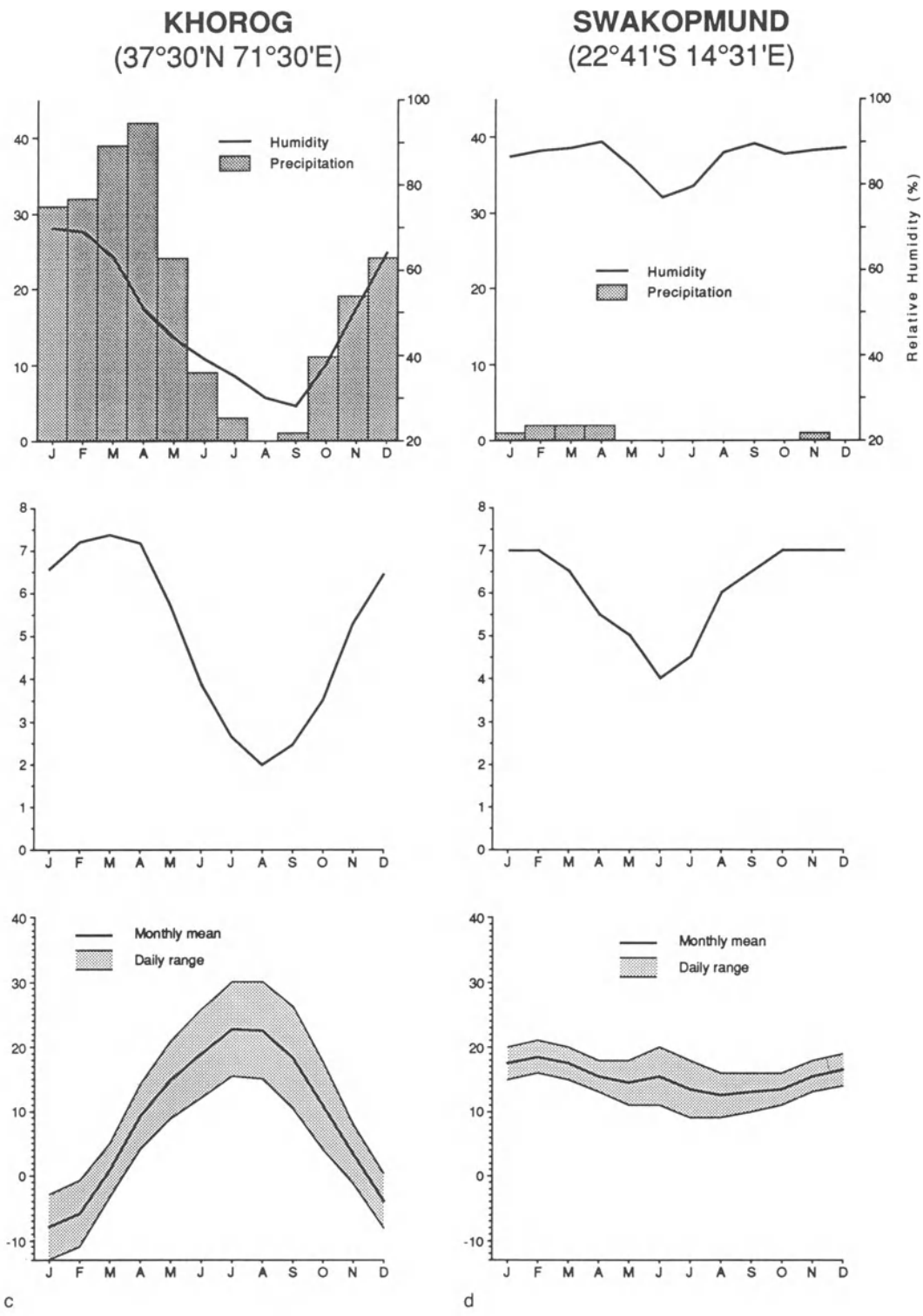
KHOROG
(37°30'N 71°30'E)
SWAKOPMUND
(22°41'S 14°31'E)
Humidity
Precipitation
Relative Humidity (%)
Monthly mean
Daily range
J F M A M J J A S O N D
c
d

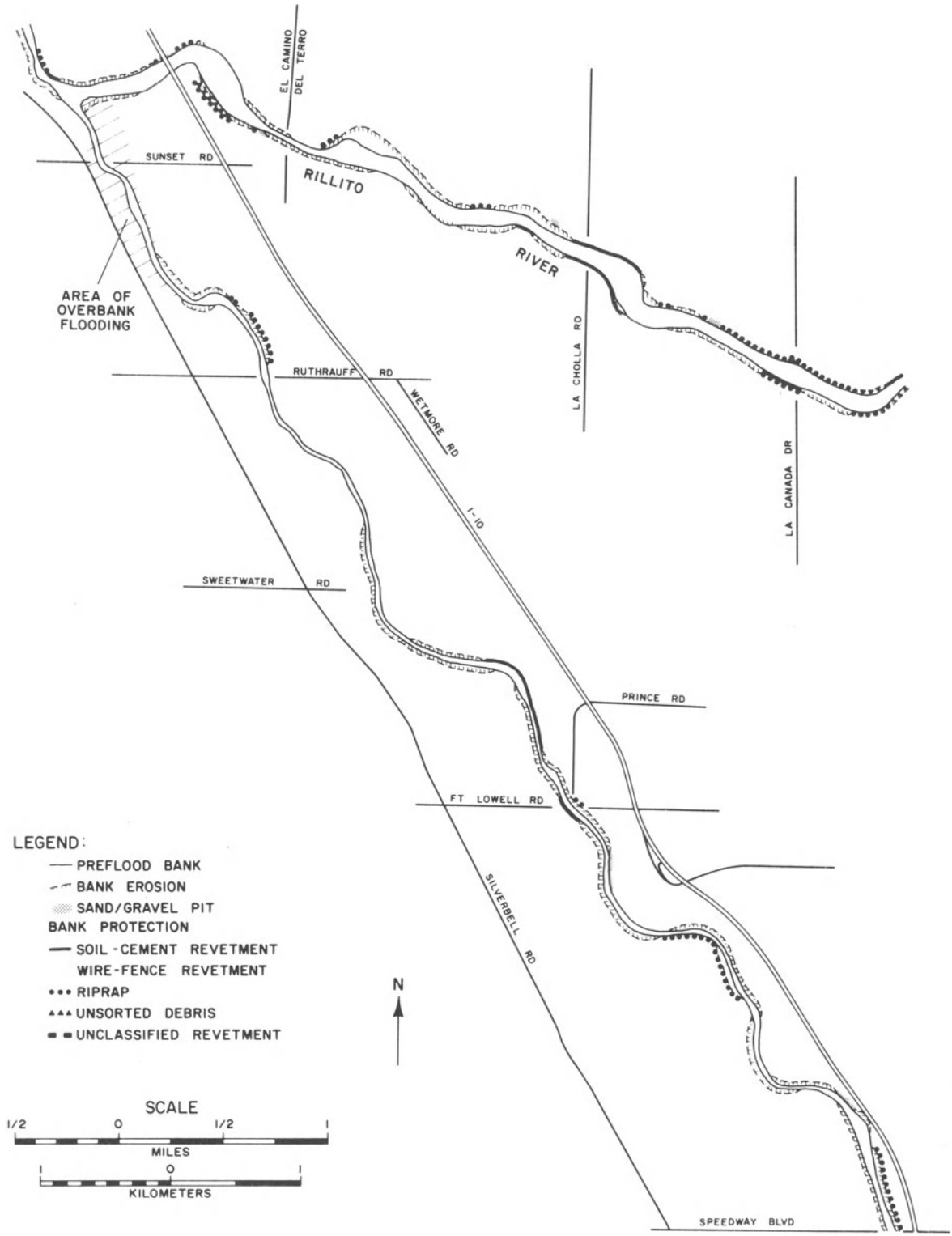

Figure 1.3 Channel changes along the Santa Cruz and Rillito Rivers, Tucson, Arizona, following an extreme rainfall event (after Baker 1984).

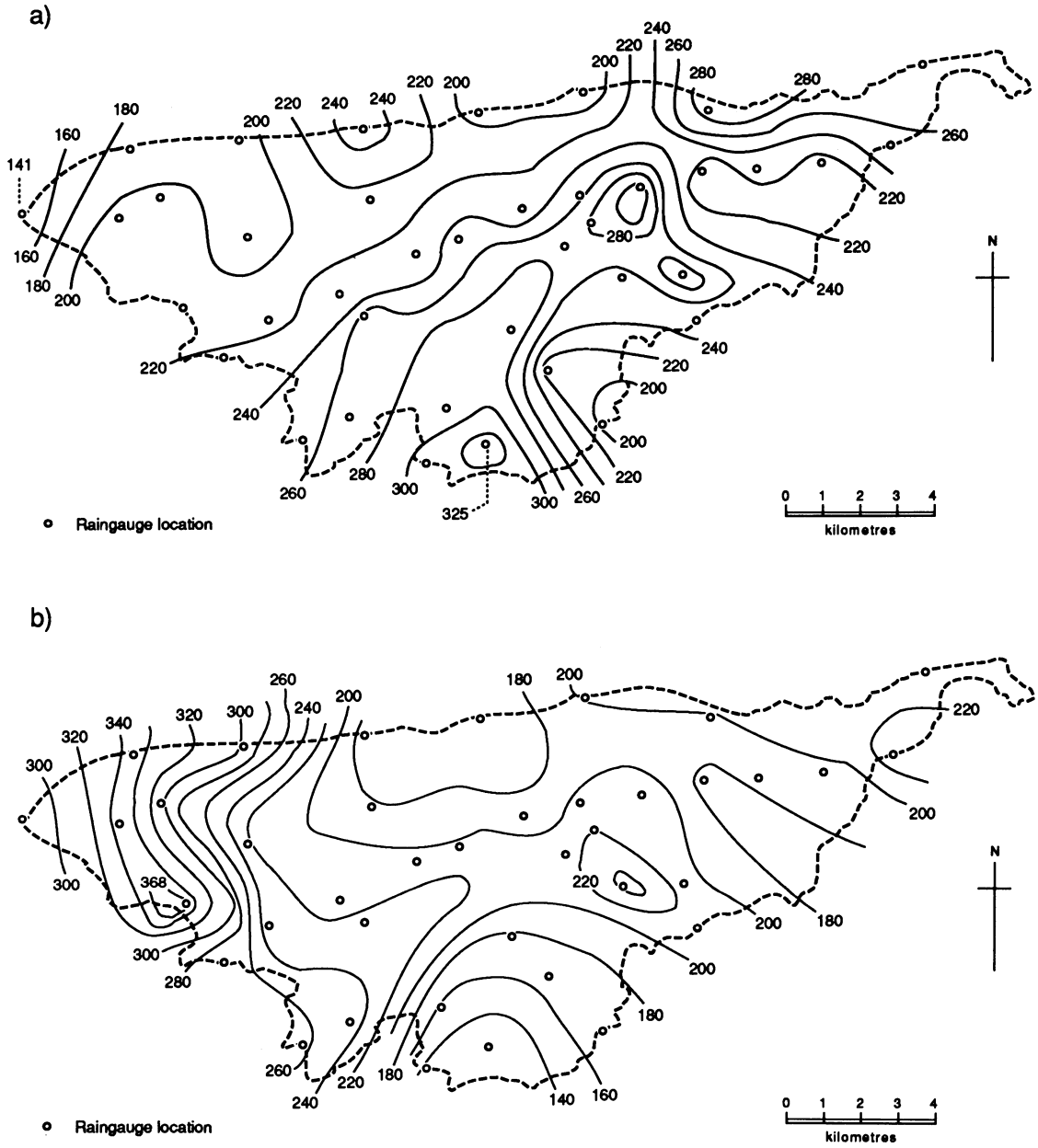

Figure 1.4 Isohyets for summer rainfall in (a) 1967 and (b) 1969 at Walnut Gulch experimental watershed, Arizona (after Osborne 1983).

Subsequently, there has been substantial debate on the relative importance of fluvial and aeolian processes in desert landform evolution. However, the essence of Davis's viewpoint, namely that arid areas are subject to a unique cycle of erosion, was maintained for much of the 20th century in the work of, for example, Cotton (1947) and, in a wider context, in the many writings that stem from the concept of climatic geomorphology (e.g. Birot 1960, Tricart and Cailleux 1969, Budel 1963).

Central to this concept of desert landforms and landform evolution is the assumption that similar-

ities of climate throughout desert areas outweigh differences that may arise from other influences. Three such influences are worth mentioning here.

First, there is the effect of geologic differences. Whereas some deserts, for example the Kalahari and the deserts of central Australia, are located within areas of tectonic stability, others, such as those in western North and South America and in the Jordan valley, are on active plate boundaries. Furthermore, deserts are underlain by a variety of substrates. In northern Sudan, for example, the area to the west of the Nile is dominantly underlain by Nubian sandstone, whereas to the east it is mainly underlain by schists, gneisses, and granites of the Basement Complex. There is no reason to expect all these areas to exhibit any greater landform similarity than the landscapes of Amazonia and Papua New Guinea which, likewise, share a similar climate but differ in their geologic setting.

Second, there is the influence of climatic change. It has long been recognized that desert areas have had different climates in the past and that some of their landform features may owe more to former, more humid, climates than to the present arid one. But, as Thomas (1989) has shown, just as different climates have been experienced by all desert areas in the past, so different desert areas have different climatic histories (Fig. 1.5). To the extent that aridity may preserve landforms created under more humid conditions (Peel 1960) different histories of the world's deserts may explain some of their landform differences. But, conversely, similar landforms may be accounted for by similar histories.

Finally, there is the effect of man on the vegetation cover of deserts. One of the most obvious differences between the deserts of the Middle East and North Africa, on the one hand, and those of the New World, on the other, is the comparative sparseness of vegetation of the former. In part, such differences may be due to differences of aridity, but even comparing two areas of very similar rainfall a difference is apparent. At a more local level, there are striking differences in vegetation cover either side of the boundaries of Indian reservations in the American South-west that reflect differences of grazing intensities by stock animals. In so far as vegetation cover is a control of geomorphic processes (e.g. Parsons *et al.* 1992), the study of desert landforms must take account of the history of human occupancy.

In more recent times, the emphasis of geomorphology has shifted away from morphogenesis within specific areas towards the study of processes *per se*. This shift, coupled with recognition that deserts extend to areas beyond the tropical high pressure belts, in large measure undermines the distinctiveness of desert geomorphology. Thus, for example, Schumann (1989) in his study of anabranching of Red Creek in arid Wyoming (mean annual precipitation of 165 mm) drew a parallel between the flashy regime of this river and that of the Yallahs River studied by Gupta (1975) in Jamaica, where the mean annual rainfall exceeds 2000 mm. Likewise, Abrahams and Parsons (1991) compared their findings of the relationship between resistance to overland flow and gravel concentration on piedmont hillslopes in southern Arizona (mean annual precipitation of 288 mm) to similar work undertaken by Roels (1984) in the Ardeche basin, France (mean annual rainfall of 1036 mm). An emphasis on process studies, together with the recognition that similar processes may operate in diverse environments, therefore raises the question whether it is now meaningful to use the term desert geomorphology and, if so, what should it denote?

Notwithstanding all the problems that may be encountered in defining a set of unique and characteristic landforms for the world's arid lands, the fact remains that in travelling over the Earth's surface, for example equatorward from the temperate areas or poleward from the wet tropical areas, there are progressive climatic and vegetational changes. Along some directions rainfall becomes less, more infrequent, and sporadic, vegetation becomes smaller and patchy, and bare ground becomes more common. Desert geomorphology can effectively be defined as the geomorphic consequences of these climatic and vegetational changes. Under this definition, as in Figure 1.1, the term desert is used in this volume broadly to include all hot, warm, and temperate, arid and semi-arid areas of the world.

ORGANIZATION OF THE BOOK

This book focuses on geomorphic processes and their effects in desert areas. The effects of most processes are spatially limited so that it is possible to identify within any landscape a set of process domains within which particular processes are preeminent. The book is organized around these process domains. Different domains dominate different deserts so that a first consideration needs to be the distribution of these domains across the deserts of the world. In the second chapter of the introductory section, therefore, the world's deserts are compared from the point of view of these process domains.

Some processes, particularly weathering and soil formation, are less constrained into specific process

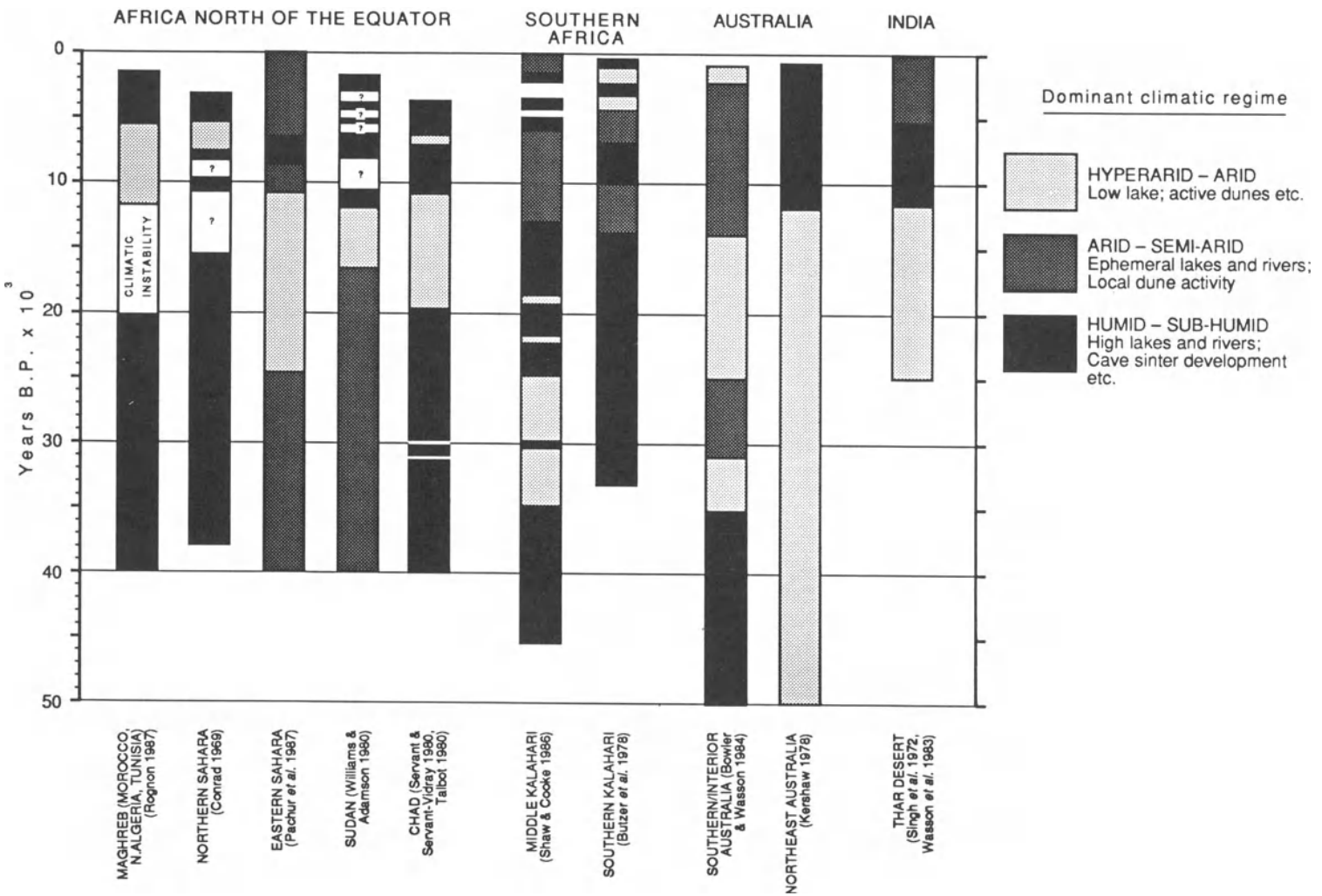

Figure 1.5 Late Quaternary climatic changes in the world's desert areas (after Thomas 1989).

domains than others. Because of their widespread effects across all desert terrain types, these processes are considered in the second section of the book. The next five sections examine the processes of the five main process domains of deserts: hillslopes, rivers, piedmonts, lake basins, and aeolian surfaces. In the final section of the book, we step outside the present spatial pattern of processes and process domains, which are no more than a short-term expression of the contemporary climate, to examine how the processes and process domains of deserts respond to and are able to provide information about climatic change.

REFERENCES

Abrahams, A.D. and A.J. Parsons 1991. Resistance to overland flow on desert pavement and its implications for sediment transport modeling. *Water Resources Research* **27**, 1827–36.

Bagnold, R.A. 1935. *Libyan sands: travels in a dead world.* London: The Travel Book Club.

Baker, V.R. 1984. Questions raised by the Tucson flood of 1983. *Hydrology and Water Resources in Arizona and the Southwest* **14**, 211–9.

Birot, P. 1960. *Le cycle d'erosion sous les differents climats.* Rio de Janeiro: University of Brazil. English translation by C.I. Jackson and K.M. Clayton, London: Batsford, 1968.

Bowler, J.M. and R.J. Wasson 1984. Glacial age environments of inland Australia. In *Late Cainozoic palaeoclimates of the southern hemisphere*, J.C. Vogel (ed.), 183–208. Rotterdam: Balkema.

Budel, J. 1963. Klima-genetische Geomorphologie. *Geographische Rundschau* **15**, 269–85.

Butzer, K.W., R. Stuckenrath, A.J. Bruzewicz and D.M. Helgren 1978. Late Cenozoic palaeoclimates of the Gaap Escarpment, Kalahari margin, South Africa. *Quaternary Research* **10**, 310–39.

Conrad, G. 1969. *L'évolution continental post-hercynienne du Sahara algerien.* CNRS: Paris.

Cotton, C.A. 1947. *Climatic accidents in landscape-making.* Christchurch: Whitcombe & Tombs.

Davis, W.M. 1905. The Geographical Cycle in an arid climate. *Journal of Geology* **13**, 381–407.

Gupta, A. 1975. Stream characteristics in eastern Jamaica, an environment of seasonal flow and large floods. *American Journal of Science* **275**, 825–47.

Kershaw, A.P. 1978. Record of the last interglacial–glacial cycle from northeastern Queensland. *Nature* **272**, 159–61.

Landsberg, H.E. (ed.) 1972. *World survey of climatology.* Amsterdam: Elsevier.

Meigs, P. 1953. World distribution of arid and semi-arid homoclimates. *Arid zone hydrology. UNESCO Arid Zone Research Series* 1, 203–9.

Miller, A. 1976. The climate of Chile. In *Climates of Central and South America*, W. Schwerdfeger (ed.), 113–45. Amsterdam: Elsevier.

Morales, C. 1977. Rainfall variability – a natural phenomenon. *Ambio* **6**, 30–3.

Osborne, H.B. 1983. *Precipitation characteristics affecting hydrologic response of southwestern rangelands.* U.S. Department of Agriculture Reviews and Manuals, Western Series 3. Oakland, CA.

Pachur, H.J., H.P Roper, S. Kropelin and M. Groschin 1987. Late Quaternary hydrography of the Eastern Sahara. *Berliner Geowissenschaften Abhandlungen* (A) **75**, 331–84.

Parsons, A.J., A.D. Abrahams & J.R. Simanton. 1992. Microtopography and soil-surface materials on a semi-arid piedmont hillslope, southern Arizona. *Journal of Arid Environments* **22**, 107–15.

Peel, R.F. 1960. Some aspects of desert geomorphology. *Geography* **45**, 241–62.

Roels, J.M. 1984. Flow resistance in concentrated overland flow on rough slope surfaces. *Earth Surface Processes and Landforms* **9**, 541–51.

Rognon, P. 1987. Late Quaternary climatic reconstruction for the Maghreb (north Africa). *Palaeogeography, Palaeoclimatology, Palaeoecology* **58**, 11–34.

Schumann, R.R. 1989. Morphology of Red Creek, Wyoming, an arid-region anastomosing channel system. *Earth Surface Processes and Landforms* **14**, 277–88.

Servant, M. and S. Servant-Vidary 1980. L'environment quaternaire du basin du Tchad. In *The Sahara and the Nile*, M.A.J. Williams & H. Faure (eds), 133–62. Rotterdam: Balkema.

Shaw, P.A. and H.J. Cooke 1986. Geomorphic evidence for the Late Quaternary palaeoclimate of the Middle Kalahari of Northern Botswana. *Catena* **13**, 349–59.

Singh, G., R.D. Joshi and A.B. Singh 1972. Stratigraphic and radiocarbon evidence for the age and development of the three salt lake deposits in Rajasthan, India. *Quaternary Research* **2**, 496–505.

Talbot, M.R. 1980. Environmental responses to climatic change in the West African Sahel over the past 20,000 years. In *The Sahara and the Nile*, M.A.J. Williams and H. Faure (eds), 37–62. Rotterdam: Balkema.

Thomas, D.S.G. 1989. Reconstructing ancient arid environments. In *Arid zone geomorphology*, D.S.G. Thomas (ed.), 311–34. London: Belhaven.

Thornthwaite, C.W. 1948. An approach towards a rational classification of climate. *Geographical Review* **38**, 55–94.

Tricart, J. and A. Cailleux 1969. *Traite de geomorphology IV: le modele des regions seches.* Paris: Societe d'edition d'enseignement superieur.

UNESCO 1977. *World distribution of arid regions.* Paris: Laboratoire de Cartographie thématique du CERCG, CNRS.

Wasson, R.J., S.N. Rajaguru, N.N. Misra, D.P. Agrawal *et al.* 1983. Geomorphology, Late Quaternary stratigraphy and palaeoclimatology of the Thar Desert. *Zeitschrift für Geomorphologie Supplement Band* **45**, 117–52.

Williams, M.A.J. and D.A. Adamson 1980. Late Quaternary depositional history of the Blue and White Nile rivers in central Sudan. In *The Sahara and the Nile*, M.A.J. Williams and H. Faure (eds), 281–304. Rotterdam: Balkema.

GLOBAL DESERTS: A GEOMORPHIC COMPARISON

2

Theodore M. Oberlander

INTRODUCTION

Among the most fascinating aspects of deserts is their diversity. The North American deserts (or 'semi-deserts' in the terminology of Old World observers) exemplify the range in climates, landforms, and biota possible in a relatively small area of year-around moisture deficiency. Clearly, Utah's Canyonlands, California's Death Valley, and Arizona's Saguaro National Monument present altogether different landform associations, each of which can be understood only by independent analysis. However, even such diverse landscapes as these hardly prepare one for the unique phenomena encountered in portions of the hyperarid 'true deserts', such as the Chilean Atacama and the eastern Sahara of Libya and Egypt, each of which is itself morphologically distinctive.

Differences in the landform associations of the various desert regions of the Earth are inevitable in view of the contrasting geologic and climatic histories of those portions of the continents that escape the influence of precipitation-generating atmospheric mechanisms. While ensuing chapters will make clear the complexity of specific desert geomorphic phenomena, this chapter will attempt to establish that the desert regions of the Earth are distinctive individually, each presenting certain unique landforms and analytical problems. As space limitations preclude scrutiny of every major desert region, four instructive examples are compared: the North American deserts, including both platform and mountain and basin (basin and range) types of deserts according to Mabbutt's morpho-structural classification (Mabbutt 1977); the Saharo-Arabian realm, including platform, shield, and sand deserts; the Australian deserts, comprised of platform, shield, sand, and clay deserts; and the Atacama Desert of Chile, which includes basin and range topography and ignimbrite blankets. Additional treatments of the Thar, Namib-Kalahari, Irano-Afghan and Inner Asian deserts, and Patagonia would introduce a host of additional unique geomorphic phenomena. In the following, there is no attempt to present complete or even balanced descriptions of regional geology and physiography. The objective throughout is to highlight the unique phenomena of major deserts, not to inventory their geographies in a systematic manner. Because of space constraints, the characteristics of the North American deserts are sketched in a cursory manner, without detailed references, as a point of departure for consideration of less-familiar regions.

THE NORTH AMERICAN DESERTS

The disparate scenery visible in a relatively small area makes the North American deserts the most geomorphologically diverse of all desert regions. The extreme contrast between the fluvially dissected platform setting of the Colorado Plateau, dominated by cuestas and canyons, the tectonically dominated extensional terranes of the Great Basin region to the west, and the older erosional relics of the Basin and Range area farther to the south has no equivalent elsewhere.

The North American dry realm (Fig. 2.1) is rather moderate in the climatic sense, with xerophytic vegetation, including arborescent species, visible almost everywhere. Only Death Valley, California, and the Lower Colorado River region qualify as hyperarid, with a ratio of precipitation to estimated potential evapotranspiration (P/Etp) less than 0.03. Rainfall is recorded annually at all stations, with

Geomorphology of Desert Environments. Edited by Athol D. Abrahams and Anthony J. Parsons. Published in 1994 by Chapman & Hall, London. ISBN 978-94-015-8256-8

Figure 2.1 North American deserts. Stipple shows arid areas in which P/Etp is less than 0.20. Solid lines within stipple indicate hyperarid regions in which P/Etp is less than 0.03. Only Death Valley and the Lower Colorado River region are hyperarid by this definition (adapted from UNESCO 1977).

seasonality shifting from winter in California to summer in Arizona and New Mexico. In addition to the pluvial/interpluvial oscillations of the Quaternary, a more humid past is evident in the Tertiary flora of the region which indicate a gradual drying trend beginning in Miocene time, when the southwestern United States and adjacent Mexico supported vegetation ranging from temperate and tropical forest and woodland to semi-arid woodland and chaparral (Axelrod 1983).

THE COLORADO PLATEAU

Were it not for the incised Colorado River, the platform desert of the Colorado Plateau, centred on the common corners of Utah, Arizona, Colorado, and New Mexico, would be an erg-spattered low-relief cuestaform desert, like the Saharo-Arabian example. This was indeed the case intermittently for 100 m.y. prior to the disintegration of the Pangaean supercontinent. The platform sediments overlying the craton here are more thoroughly arenaceous than those of the Sahara, being dominated by lithified dune sands and shales from Permian through Jurassic time. However, the mid-Tertiary uplift of the region, the collapse of the Great Basin to the west, and the linkage of separate fluvial elements to form an incised through-flowing Colorado River system by 4 Ma has evacuated the sandy sediments that would otherwise be trapped in a regional aeolian system of the Saharo-Arabian type, likewise evident in relict form in the Kalahari and Australian deserts.

Current understanding of the tectonic and hydrologic evolution of the region has been summarized by Patton and Morrison (1991) and the geomorphology is treated systematically by Graf *et al.* (1987). The plateau landscape is a textbook illustrating the

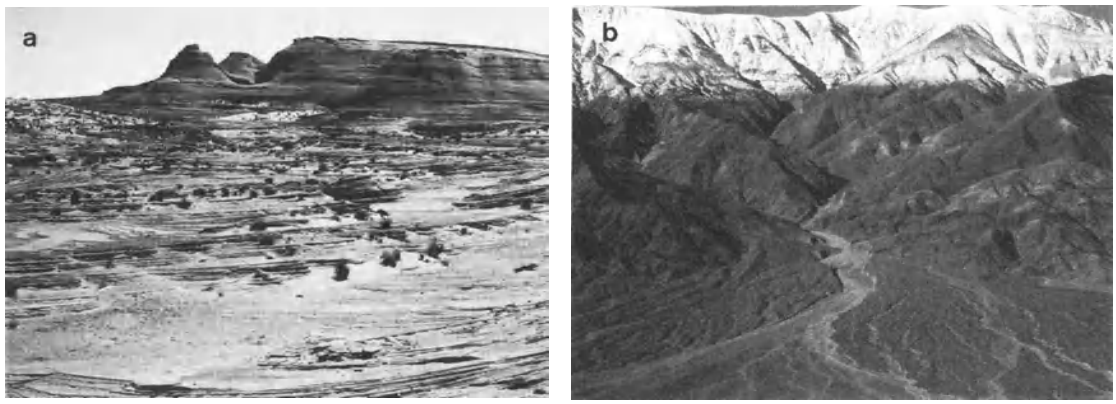

Figure 2.2 (a) Aerodynamically streamlined slickrock form in aeolian sandstone on the Colorado Plateau: possibly a rock yardang. (b) Alluvial fan in Death Valley, California, with aggradational surfaces of at least six different ages evident.

effects of differential erosion in lightly deformed sedimentary strata of varying strength. Canyons, cuesta scarps, and plains stripped to bedrock dominate, with details including major discordances between stream courses and geologic structures; the presence of both ingrown and entrenched stream meanders; canyon sinuosity variations related to jointing and stratigraphic dips; evidence that groundwater sapping has influenced the growth of tributary canyons; rock arches, natural bridges, and exfoliation effects in massive sandstones; relict large-scale slope detachments; small areas of active sand dunes; and recently recognized aerodynamic forms (yardangs) resulting from aeolian erosion of consolidated rock (Fig. 2.2). Evidence of cycles of arroyo cutting and filling is common to all arid regions.

Rates of retreat of composite cliffs on the Colorado Plateau have been estimated by a variety of methods, including recession from datable lava drapes, positions of datable packrat middens in caves, canyon geometry, and inferred ancient scarp positions based on strike valleys. Results vary from 0.16 to 6.7 m per 1000 years. A range of results is inevitable given varying jointing, caprock loads, and strengths of substrates. Young (1987) has stressed that the majority of scarp retreat on the Colorado Plateau occurred prior to canyon incision, perhaps as long ago as Laramide time. Consequently, most cuesta scarp retreat in Dutton's famed 'Great Denudation' occurred under climatic and base level conditions quite unlike the present.

THE BASIN AND RANGE REGION

The basin and range region of western North America contains several subdivisions based on geology and tectonics, but the most significant geomorphic contrast is between the area of ongoing relief generation by tensional faulting, extending from the east face of California's Sierra Nevada to the front of the Wasatch Range in central Utah, and the area extending southward from southern California, Arizona, and New Mexico into Sonora and Chihuahua, Mexico, in which lateral movements and broad warping disturb a dominantly erosional landscape. The geomorphology of the region has been discussed comprehensively by Dohrenwend (1987).

The area of active crustal extension centred in Nevada is a remarkable display of linear subparallel mountains, mostly either rotated listric slabs or horsts, bounded on one or both sides by faults rooting at depth in a horizontal ductile zone of regional extent. Increasing numbers of smoothly descending range 'noses' composed of Precambrian to Mesozoic complexes of metamorphic rocks are being identified as tectonically stripped detachment surfaces – essentially the tectonically unloaded, exposed, and arched soles of listric faults. Wernicke *et al.* (1988) computed east–west extension of the basin and range region at the latitude of Las Vegas at nearly 250 km. In the region of ongoing extension, range front morphologies reflect the recency of vertical movements on range-bounding faults. Straight or rhombic range fronts with faceted spur ends indicate active vertical displacements, whereas erosionally frayed base lines bespeak lengthy tectonic stagnation. Scarps breaking late Pleistocene glacial moraines and Holocene alluvium clearly indicate continuing seismic activity throughout the region.

The transition from eroding mountain block to adjacent subsiding basin takes the form of an apron

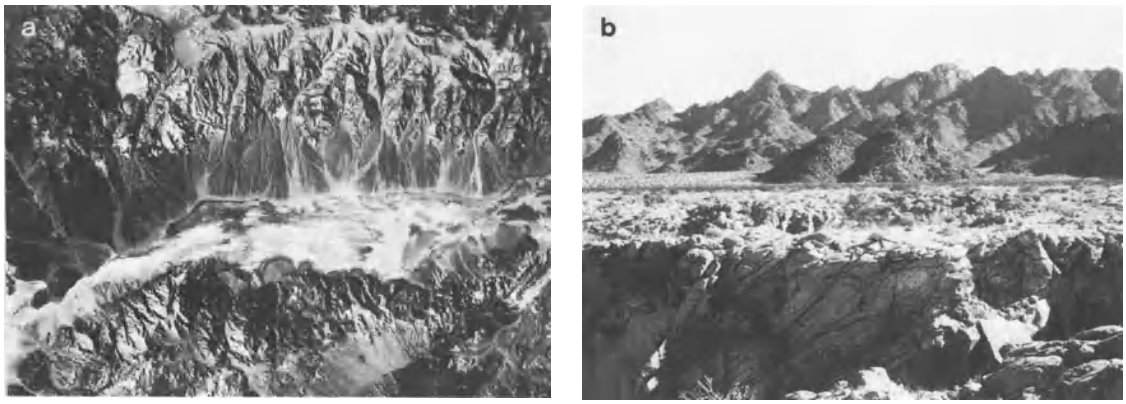

Figure 2.3 (a) SPOT (Satellite Probatoire pour l'Observation de la Terre) image of Death Valley displaying typical basin and range form asymmetries. Higher Panamint Range (top) nourishes large alluvial fans having multiple surfaces evident in tonal variations reflecting degrees of rock varnish development. Abrupt scarp of lower Black Mountains (bottom) displays recent fault displacement and small, steep, faulted alluvial fans. North is to the right. (b) Bedrock pediment of Coxcomb Range, Mojave Desert, California, with a younger alluvial fan superimposed in the distance.

of coalescing alluvial fans. These usually exhibit multiple surfaces of contrasting age and geomorphic character, indicating periodicity in fan aggradation and/or frequent shifts in the loci of deposition (Fig. 2.3). Fan surfaces vary with respect to preservation of depositional bedforms, development of desert pavement and desert varnish, clast size, degree of dissection, and presence of age-diagnostic pedogenic features. Multiple fan surfaces in the basin and range region have been attributed to tectonic warping, climatic oscillations, and steady-state development involving repeated diversions of the aggrading fan-building wash by gullies heading on the fan surface. Episodes of fan aggradation have been attributed to humid phases when destructive debris flows are minimized, arid phases when constructive debris flows dominate, and the humid-to-arid transition when loss of vegetative protection causes colluvial mantles developed during pluvial episodes to be stripped and translocated to fan surfaces (Wells *et al.* 1987) (Chapter 23).

Tectonic depressions in the basin and range region contain clay and evaporite pans and relict channel systems that indicate past overflows from one pluvial lake to another. Late Pleistocene deep lake conditions (not necessarily synchronous) in the endoreic basin and range region have been imprinted on hillslopes and piedmonts as conspicuous relict shorelines composed of cliffed bedrock and depositional spits, deltas, and shoreline tufa particularly in the Lahontan and Bonneville basins in western Nevada and western Utah, respectively.

Dunes are present in many of the basins and are usually dominated by transverse barchanoid forms or stellate dunes with multiple arms converging on central peaks as much as 200 m high. The latter appear to reflect seasonal changes in sand-moving winds. Great Basin dune fields are small, with occasional draa-scale forms, and most are proximal to Pleistocene lake shorelines, with little or no progressive displacement of dune forms under modern conditions.

South of a line from California's Tehachapi Mountains to Phoenix, Arizona, active listric normal faulting ceases and endoreic basin and range landscapes have been dominated since Miocene time by erosion of a former extensional terrane of complex origin that has been reduced to isolated ranges surrounded by extensive ramp-like bedrock pediments. In the deserts of southern California, Arizona, and northern Mexico, granite is a dominant lithology, which is reflected in abrupt piedmont angles at the junctions of boulder-clad hillslopes and grus- or sand-covered pediments with slopes of 2° to 7°. These ramps expose bedrock to distances of kilometres from boulder-clad hillslopes (Fig. 2.3). Shallow Quaternary alluvial fans are commonly superimposed over, and may completely obscure, the antecedent bedrock pediments of the larger ranges.

In California's Mojave Desert metres-deep, strongly oxidized granitic weathering profiles preserved under early to mid-Pliocene basalts and alluvial fills indicate that pedimentation by parallel rectilinear slope retreat occurred in a prior soil-covered semi-

arid landscape pre-dating the onset of full desert conditions in this portion of North America. Although cycles of colluvial generation and stripping have occurred on jointed rock during the Pleistocene (Wells *et al.* 1987), the distribution of dated volcanic remnants indicates that the major slope retreat producing the broad pediments occurred in pre-Quaternary time.

The basin and range area of western North America includes several large volcanic fields, each with age control by K/Ar dating. The time spans represented, from late Pliocene to Holocene, have been useful in establishing rates of a number of geomorphic processes, including chemical leaching trends in rock varnish, the accretion of aeolian dust that lifts desert pavements, drainage formation and subsequent cone dissection, and surface lowering by erosion below datum levels.

SAHARO-ARABIAN DESERT

The Red Sea Rift interrupts the world's greatest continuous desert expanse (Fig. 2.4), which dwarfs the North American arid zone, reaching 7500 km across North Africa and Arabia, from the Atlantic Ocean to the Persian Gulf, comprising some 12×10^6 km^2 of shield and platform desert – about 9% of the Earth's ice-free land area. The vastness of the Saharo-Arabian desert realm can be appreciated by the fact that all of France could be swallowed in Arabia's Rub Al Khali sand sea, which itself constitutes less than one-twentieth of the desert region. The vast majority of this expanse is free of perennial vegetation and is classified as hyperarid ($P/Etp < 0.03$), with extremely hot summers and mild winters. The eastern and western margins average less than 100 mm of rainfall annually, declining to less than 10 mm in the Nile Valley and Libyan Desert region. Annual Etp values are between 1100 and 1700 mm. Computed water deficits for the single month of least moisture stress can exceed the total annual precipitation by 10 to 20 times (Oberlander 1979).

GEOLOGIC STRUCTURE

The Afro-Arabian (Nubian) craton has been exposed by erosional stripping of platform sediments during the rise of the Red Sea arch that began to rupture in the late Eocene. The Arabian peninsula is the eastern half of the ruptured swell, with a series of well-defined cuestas composed of Precambrian to late Tertiary platform sediments backing toward the Persian Gulf, exposing a progressively expanding area of ancient crystalline rock to the west. Eocene–Oligocene flood basalts veneer the high edge of the Arabian shield and episodic basaltic volcanism has continued into the Holocene.

Crystalline rocks of the craton also form the surface west of the Red Sea in Egypt and the Sudan, disappearing under a Paleozoic to Eocene sedimentary succession along the margins of the Nile Valley. The immense accumulation of flood basalts at the junction of the East African, Red Sea, and Gulf of Aden rifts lifts Ethiopia out of the desert climatic zone. Across North Africa, the geologic structure consists of a series of basement uplifts that expose ancient crystalline rocks, separated by expanses of platform sediments and cuestaform landscapes. Over large areas the sedimentary series is obscured by sand seas (ergs). Surmounting the basement uplifts, and rising to 3000 m in the Ahaggar and 3400 m in the Tibesti of the central Sahara are younger volcanic forms, both constructional and denudational, including sizeable volcanic calderas and clusters of volcanic necks.

North Africa and Arabia entered the Tertiary as a realm of tropical forests, which gave way to savannas during the Oligocene. True aridity is first evident in the Oligocene in the form of aeolian sand deposited in the Atlantic (Sarntheim 1978). From Pliocene time onward, Saharo-Arabian climates have oscillated between subhumid and arid, with moist intervals recorded by soil development, fluvial activity, tufa deposition, and the appearance of lakes and marshes, while aridity is evidenced by fragmentation of fluvial systems, lake desiccation, and increased aeolian activity. Detailed reviews of the evidence for late Quaternary climatic changes affecting the Sahara and adjacent regions are given by Rognon (1976) and Alimen (1982). While the southern and central Sahara were gripped by aridity during the height of the late Pleistocene glacial phase, the northern Sahara and Arabia experienced a climate more humid than the present, with wadis carrying water from the High Atlas ranges far into the desert.

Except for unusual intervals from *c.* 12 000 to 11 000 years BP, when aridity seems to have expanded to both the north and the south and a generally humid phase from *c.* 9000 to 8000 years BP, the different precipitation-generating mechanisms of the middle and low latitudes have kept the climates of the northern and southern Sahara in opposition. The late Pleistocene desiccation of the southern margins (the Sahel) coincided with pluvial climates in the northern Sahara and Arabia, whereas at present the northern and central Sahara are desic-

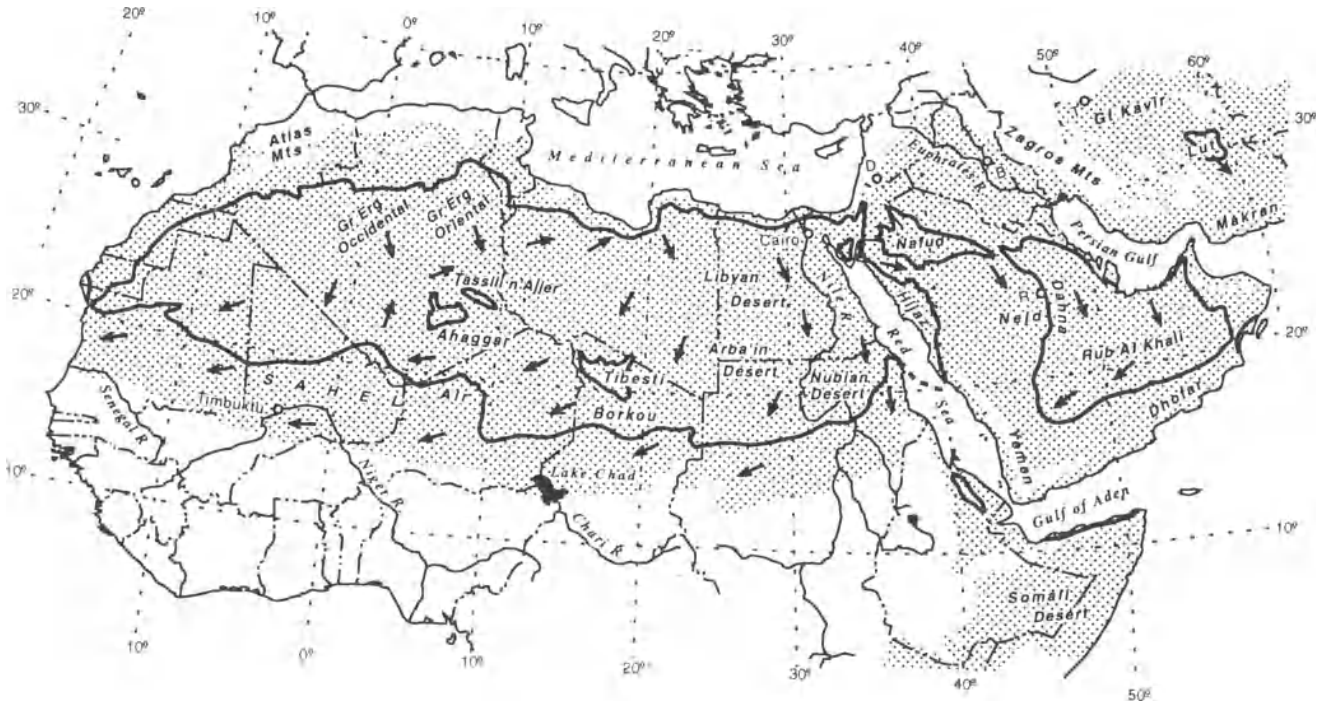

Figure 2.4 Saharo-Arabian desert region. Symbols as in Figure 2.1, emphasizing the vastness of the desert's hyperarid core. Arrows indicate dominant winds based upon aeolian erosional and depositional landforms (adapted from UNESCO 1977 and Mainguet 1983).

cated and the Sahelian dunes overlook marshes and permanent streams.

AEOLIAN LANDSCAPES

An exceptional aspect of the Saharo-Arabian deserts, other than their vast extent, is the fact that large areas within them truly are dominated by the factor popularly (but usually incorrectly) identified as the prime creator of desert scenery – the action of wind! Although some 80% of Saharo-Arabian platform and shield landscapes consist of gravel regs and rocky hamadas, themselves bearing evidence of aeolian scour, the most arresting phenomenon of these deserts is their spectacular sand seas, or ergs. Orbital photography and Landsat images stimulated interest in ergs and resulted in the first general theories of erg formation and evolution (Wilson 1971, 1973, McKee *et al.* 1977, Mainguet 1978, Fryberger and Ahlbrandt 1979). Soon afterward, McCauley *et al.* (1977) began to revolutionize thinking about aerodynamically streamlined forms in consolidated rock in desert regions, vastly expanding our appreciation of the importance of aeolian erosion.

In the Saharo-Arabian region sand accumulation has occurred at some 20 important depocentres separated by gravel regs or rock hamadas. The sand accumulations in the Saharo-Arabian ergs are enormous relative to ergs in most other locations, with spread-out (mean) sand thicknesses of 20 to 43 m, and mean local thicknesses exceeding 100 m (Wilson 1973). By comparison, the mean sand thickness in Australia's Simpson Desert is estimated by Wilson at about 1 m.

Most Saharan ergs do not appear to be downwind from alluvial sediment sources as in the North American deserts: rather, the sands appear to be cycled from one erg to the next by sand flows across intervening surfaces. While Saharan sands seem to have their provenance in the continental platform series (continental intercalaire), itself derived from the craton, the specific sources and histories of the erg sands have yet to be elucidated.

Aeolian scour producing bedrock yardangs in dune-free hamada regions has greatly assisted in the verification of regional sand flows between linked aeolian depocentres. This is especially clear west of the Nile in Egypt and in the Tibesti region of Libya and Chad. In the Saharo-Arabian region the flow of sand tends to be clockwise in a general sense. Along the northern fringe of the Sahara, the drift of sand and dust is toward the east-north-east along the Mediterranean coast and south-east farther inland. Sand streaks and dune forms reveal that this flow curves strongly to the south-east from Libya to central Arabia and to the south and south-west in the Rub Al Khali of southern Arabia, where it corresponds to the directional trend all across the southern Sahara – aligned with the infamous harmattan 'trade' winds of the Sahel region, but driven by less frequent winds of greater force.

Complications appear in the interior of the Sahara, where wind roses, yardangs, and dune forms reveal subsidiary circulations induced by the pattern of highlands, particularly the Ahaggar and Tibesti massifs. Large ergs are absent from the central Saharan region (southern Algeria) despite nearby sand sources in the large wadis (episodic or fossil at present) that issue from the Saharan highlands (see Fragmented fluvial systems below).

The Saharo-Arabian ergs include every type of desert dune, with many instances of abrupt transition from one type to another. Anomalous relationships between adjacent dune forms in the large Saharo-Arabian ergs, as seen on morphological maps and satellite images, indicate controls and histories that are far from clear at present.

The aeolian forms visible on standard satellite images are actually all very large draas, or megadunes up to 300 m in height and spaced at intervals of 1 to 2.5 km, which support smaller subsidiary dunes. Some individual ergs, like the Grand Erg Occidental of Algeria, contain an astonishing variety of draa morphologies, as seen on the maps in Breed *et al.* (1979). In the most general sense, a tripartite categorization of forms seems apparent, including unlinked pyramidal draas, both linked and unlinked crescentic transverse draas, and linear draas. Numerous transitional and variant forms are present, such as grid dunes with perpendicular transverse elements, linear chains of pyramid dunes, and feathered linear dunes. The western extremities of both the Sahara and Arabian deserts are dominated by parallel, evenly spaced, south-west-trending linear draa, the western Rub Al Khali being conspicuous for its perfect 'raked' appearance and the longitudinal persistence of its seif dunes.

According to Mainguet (1983), transverse and pyramid dunes indicate net sand gains, and parallel longitudinal dunes signify net sand loss or erosion. Mainguet and Chemin (1983) claim that the ergs of the north-west are the only areas of net gain in the Sahara at present. The eastern, central, and southern Sahara are seen as areas of sand loss to the Sahel region, which is an area of major gain currently. Maps of dune morphology in Breed *et al.* (1979) more or less support this; however, wind roses in

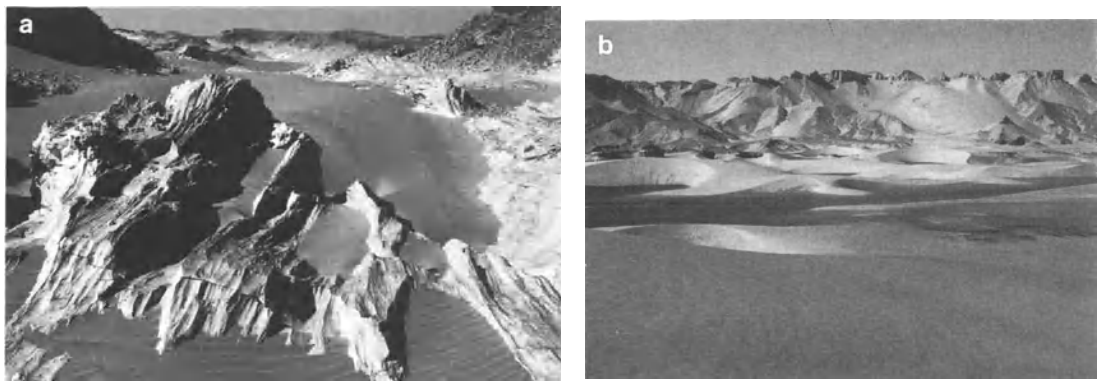

Figure 2.5 Aeolian landforms of the eastern Sahara. (a) Ventifacted limestone in the Libyan Desert between the Nile Valley and Kharga Depression, Egypt. Limestone possibly karstified under pre-desert climate. (b) Moribund cuesta scarp forming north rim of Kharga Depression. Active sand blankets the scarp and remobilizes into dunes moving southward through the Kharga region.

Mainguet and Canon (1976) and Breed *et al.* (1979) suggest that the relationship claimed by Mainguet is far from simple.

In their present forms, the great ergs of the Saharo-Arabian deserts, composed of red-coloured aeolian sands, are geologically recent constructs. According to Conrad (1969), the major phase of accumulation of Algeria's Grand Erg Occidental, on the northern portion of the Saharo-Arabian gyre, was between 10 000 and 11 000 years BP. To the south and east, on the southern half of the Saharo-Arabian gyre, McClure (1978) and Clark (1989) found that the linear seif dunes of the western Rub Al Khali were built as recently as 7000 years BP. Beneath the active dune crests of the western Rub Al Khali, McClure found an earlier mass of aeolian sand that was active in the late Pleistocene (17 000 to 10 000 years BP) in the form of ancestral seif dunes. According to McClure, no red aeolian sands in the Rub Al Khali are older than 17 000 years BP, suggesting that the present hyperaridity of southern Arabia did not occur before that date.

AEOLIAN SCOUR OF HAMADAS

Images of the eastern Sahara have shown comprehensive remodelling of the land surface by both corrasion and deflation in areas of unidirectional winds. Among the most spectacular forms are the linear rock yardangs of the Borkou area (Chad), south of the Tibesti, described by Hagedorn (1968) and Mainguet (1968). These are visible on satellite images as linear striations covering areas of thousands of square kilometres being inscribed in both sandstone and granitic rock. Climatic oscillations are evident in younger yardangs eroded into freshwater lacustrine deposits interfingered with older bedrock yardangs (Busche 1979). Equally impressive is the complete erasure of all fluvial features in the wind-sculptured limestone plateau between the Nile Valley and the Kharga Depression (Fig. 2.5). In the latter area, scattered anomalous pits and clefts in the marble-like silicified limestone suggest the former presence of a karst landscape, removed to its roots by true sandblasting (Breed *et al.* 1989).

FRAGMENTED FLUVIAL SYSTEMS

Both the Sahara Desert and the Arabian peninsula display unequivocal evidence of major climatic change in the form of fossilized large-scale fluvial systems that appear to have been moribund for much of the Holocene. In their upper portions these hydrographic systems include sizeable canyons, their floors now clogged by dunes and talus, their thalwegs disrupted by autogenous and tributary alluvial cones. The distal portions of these fluvial systems are extensive inactive sand and gravel fans or sand seas. Ergs now submerge the middle portions of some of the largest of the fluvial systems in both Arabia and North Africa.

Every highland in the Saharo-Arabian desert realm is a source of conspicuous relict drainage systems: the Atlas Mountains in the north-west, the individual massifs of the Central Sahara (Air, Adrar des Iforas, Ahaggar, Tibesti), the Red Sea (Nubian) Hills of Egypt and the Sudan, and the western rim of the Arabian peninsula (the Hijaz and Asir). Some

of the ancient through-flowing streams of the Sahara and Arabia were equal in length to the greatest streams of Europe (Wadi Igharghar, Wadi Soura, Wadis Tamanrasset and Tafassasset in the Sahara, and Wadi Ar Rimah, Wadi Birk and Wadi Dawasir on the Arabian peninsula).

Currently, aggradation prevails even in the upper portions of the fossil wadis of Arabia and the Sahara, disrupted wadi profiles being evident in frequent appearances of salt or gypsum crusts or salty clays ('wadi sabkha sediments' of Hötzl *et al.* 1978a) on dune-blocked valley floors. Episodic flow occurs within portions of the fossil wadis, resulting from runoff on local pediments and cuesta backslopes, but this is so restricted that the wadis disrupt their thalwegs with their own alluvial fans, which form at successive points of debouchure from canyons and narrows.

The surprising outcome of a radar-imaging experiment in the sandy Arba'in Desert of southern Egypt, west of the Nile Valley, was the revelation of an otherwise invisible sand-entombed system of bedrock channels, individually 10 to 30 km wide – equal in breadth to the present Nile River floodplain (McCauley *et al.* 1982). McCauley *et al.* hypothesized that this hydrographic system, which underlies the most arid portion of the entire Sahara, carried runoff westward into the basin of Lake Chad, and perhaps through to the Atlantic Ocean (McCauley *et al.* 1986). What could have produced a hydrographic system of such magnitude other than the escape of drainage from the Red Sea Hills and also from tropical Africa – in other words, the palaeo-Nile itself?

McCauley *et al.* proposed that tectonic uplift, along with associated volcanism, formed a topographic barrier some 15 m.y. ago, disrupting a westward-draining hydrographic system that had functioned for some 10 to 20 m.y. They suggest that desiccation of the Mediterranean some 6 m.y. ago produced a phenomenal fall in base level, stimulating headward erosion by the ancestor of the Egyptian Nile, which eventually captured the upper Nile and diverted it from the Chad Basin to the Mediterranean. The buried channels nevertheless seem to have remained functional until about 4000 years BP. Burke and Wells (1989) have dissented from this interpretation and offer several lines of evidence indicating that the so-called 'radar river valleys' were merely east-draining components of the ancient Nile, which they believe has drained to the Mediterranean since Eocene time.

McCauley's hypothesis is not contrary to earlier findings indicating that the connection of the Egyptian Nile to its present source in Ethiopia did not occur until perhaps 500 000 years ago, when Ethiopian sediments and tropical pollen make their first appearance in Egypt (Malay 1969, Hassan 1976). Butzer (1980) argued for an essentially modern Nile by about 200 000 years BP.

The crescent-shaped Qattara Depression in northern Egypt, an expanse of sabkha, sand, and reg, 19 000 km^2 of which lie below sea level, has also been attributed to ancient fluvial action. The depression, Africa's largest and deepest (−134 m), was long regarded as a classic example of large-scale aeolian deflation following dissolution of a limestone caprock. However, recent investigators have attributed the feature to fluvial erosion following the strike of north-dipping strata, followed by either aeolian deflation (Said 1981) or subsurface karstification and collapse (Stringfield *et al.* 1974) – the one implying climatic desiccation, the other demanding a humid climate. Albritton *et al.* (1990) utilize the Miocene desiccation of the Mediterranean as a means of activating ground water in seaward-dipping aquifers, resulting in subsurface solution and collapse of the floor of a former Qattara fluvial valley tributary to the Mediterranean.

KARST DEVELOPMENT IN CARBONATE AND SILICATE ROCKS

Relict karst forms in carbonate rocks are widespread in the Saharo-Arabian region and include collapse features, subterranean passages, and large pits similar to the cenotes of the Mayan realm in Mexico. The modern spring outflows on the floor of the Persian Gulf and in the Qatif and Hasa oasis districts of eastern Arabia are well known (Job 1978) and appear to be overflows from separate Miocene and Plio-Pleistocene phases of karstification (Hötzl *et al.* 1978b).

In eastern Arabia, some near-surface cavern systems older than the range of radiocarbon dating were completely filled with aeolian sand that was subsequently indurated by calcium carbonate in the form of a duricrust including stalactites and stalagmites (Felber *et al.* 1978). The duricrust carbonate has a date of 30 000 to 32 000 years BP. This unusual complex attesting to major climatic change has been modified by a second phase of solution that has produced a modern generation of caverns.

Stranger still are solution forms in sandstones in many parts of the Sahara. The phenomenon was first noted by Peel (1941) in the Libyan Desert of Egypt. Busche and Erbe (1987) have described solution effects in bleached quartz sandstones under silcrete and laterite duricrusts in southern Libya and

northern Niger, west of the Tibesti. Crusted sandstone plateaux here display multitudes of vertical-walled collapse dolines, sinuous uvala-like channels, subsurface corkscrew tubes, and intersecting cylindrical passages that outlet on cuesta scarps – all apparently formed by ground water circulating slowly along joints in sandstone weathered to friability in a tropical wet environment. Busche and Erbe regard the period of formation as pre-late Miocene. Similar sandstone karst in Algeria was described earlier by Renault (1953) and Mainguet (1972). All of these researchers seem to concur that the subterranean drainage systems antedated much of the dissection of the plateaux and the separation of erosional outliers that are conspicuously perforated. This phenomenon, which seems ubiquitous in the sandstone terranes of the Sahara (Mainguet 1972), seems to be one of piping on a massive scale. Busche and Erbe suggest that the absence of fluvial features on many of the Saharan plateaux reflects widespread silicate karst development in the Tertiary rather than aridity in the Quaternary.

Very similar phenomena have been described in sandstones in the Hasa oasis region of Saudi Arabia, very close to the area of active limestone springs, but are associated with Plio-Pleistocene marine terraces and have been attributed to marine erosion (Hötzl *et al.* 1978b). Maps and photographs of these 'sea caves', which form rectangular, joint-guided labyrinths, including numbers of interior rooms with areas greater than 100 m^2, seem to leave little doubt that the phenomena are not marine in origin, but are another example of silicate karst inherited from the pre-desert epoch of Arabian history.

SCARP-FOOT FORMS

Associated with subterranean silicate karst forms throughout the Sahara are conspicuous scarp-foot depressions, or moats, 40 to 60 m deep, first noted in the Libyan Desert by Peel (1941). These fringe sandstone cuestas and encircle inselbergs, isolating them from adjacent erosional surfaces. Several Saharan oases occur in such moats. Busche and Erbe (1987) attributed the depressions to a continuation of aggressive weathering in the zone of surface runoff and subsurface water outflow at the base of scarps in the late Pliocene, as aridity began to dry out the rest of the landscape. They propose that the major depressions of Egypt's Western Desert, Kharga and Dakhla, one aligned with the wind, the other transverse to it, are similar forms.

Both Peel (1941) and Büdel (1982) noted an absence of ramp-like pediments of the North American type around inselbergs in the Libyan Desert and in the central Sahara. According to Büdel, all surfaces peripheral to scarps in the Central Sahara are flat remnants of tropical etchplains, with deeply oxidized Tertiary soils preserved locally under later volcanics. A final aspect of the Saharo-Arabian scenery is the presence, as on the Colorado Plateau, of ancient landslides and rotational slumps along many cuesta scarps. As these are attributed to past periods of humidity and cover erosional surfaces, the latter are shown to be older still, and probably Tertiary in age (Busche and Hagedorn 1980, Grunert and Busche 1980). In the arid core of the Sahara, scarps of all types appear to be essentially fossilized at present.

THE AUSTRALIAN DESERTS

Geologically, the closest analogue to the Saharo-Arabian platform and shield desert is that of central Australia (Fig. 2.6), the second largest continental area lying in the subtropical zone. Like the Saharo-Arabian region, Australia as a whole has been free of tectonic activity other than vertical flexing through most of Phanerozoic time. As in the Sahara, exposed rock surfaces in the Australian arid region reveal an ancient episode of continental glaciation, in this case of Permian age, during which Australia was situated just west of the South Pole. Finally, the landscape of the Australian interior, like that of the Saharo-Arabian region, preserves an array of relict forms overlain by younger aeolian features. But similarities between the largest deserts of the Northern and Southern Hemispheres extend little further than these generalizations.

Whereas the Saharo-Arabian desert is hyperarid, the Australian desert is in the arid category, with P/Etp ratios between 0.20 and 0.03, equivalent to the marginal regions of the Saharo-Arabian desert. Nowhere is the average precipitation less than 100 mm, and more generally it ranges from 200 to 400 mm. The majority of the Australian arid zone receives summer rainfall, which extends well across the Tropic of Capricorn and far south of the desert centre. The southern third of the desert lies in a zone of unreliable rainfall seasonality, with a winter rainfall zone barely touching the southern desert fringe. While Saharan aridity indices (Ia = 100[(P/Etp) − 1]) generally exceed 95 (the hyperarid threshold) and frequently surpass 99, no Australian station has recorded an Ia value higher than 88.6 (Charlotte Waters, Northern Territory). At the most xeric station in water balance terms (Tennant Creek, Northern Territory) the moisture deficit in the least

Figure 2.6 Australian deserts. Symbols as in Figure 2.1. No hyperarid climates (P/Etp < 0.03) are present as summer rainfall amounts are relatively high, though offset by evapotranspiration.

xeric month is 7.7% of the annual precipitation. These statistics are reflected in the biota, with xerophytic shrubs and grasses supporting large foraging animals throughout the arid interior.

The Australian desert landscape is conspicuously flat, between 150 and 300 m in elevation, with two central highland areas in the parallel east–west-trending Macdonnel and Musgrave ranges, each cresting at elevations close to 1500 m. In the west the land rises somewhat above 1000 m in the Hammersley Range, which generates more radial drainage than the somewhat higher interior ranges. The central uplands are a region of denuded folds in Cambrian and older sediments; to the east is a platform, known as The Channel Country, veneered by Jurassic and later sandstones of the Great Artesian Basin; to the west is a shield exposing ancient igneous and metamorphic rocks etched into variable relief and spattered with dry lake beds that appear to represent ancient fossilized drainage lines. France and a unified Germany would together be swallowed by the arid expanses to either the east or the west of the central uplands.

The Australian arid zone displays many peculiar geomorphic phenomena and poses numbers of yet unresolved questions of landscape genesis. Among these are very extensive aeolian landscapes, problematical hydrographic features, vast areas of relict duricrusts of varying type, unusual soil phenomena, and distinctive relief features in granites of the craton as well as in various rocks of the platform areas.

THE AUSTRALIAN ERGS

Aeolian deposits cover close to 50% of the Australian arid region, the highest proportion of all of the Earth's deserts. However, the aeolian landscape is conspicuously dominated by longitudinal sand ridges (King 1960, Mabbutt 1968, Mabbutt and Sullivan 1968), suggesting overall negative sand budgets according to Mainguet's criterion. Transverse dunes are present, but are developed on a much smaller scale in terms of both area and size. Pyramid and dome-shaped forms seem absent from the Australian ergs. The ubiquitous longitudinal

dunes are normally less than 30 m high, averaging only 13 m in the Simpson Desert, but can be unusually persistent, in a few instances, continuing for as much as 300 km. For the most part, the Australian longitudinal dunes are morphologically simple sand ridges, with single crests that often merge downwind, unlike the far higher and more complex seif and uruk draa of the Saharo-Arabian ergs. While dune crests may remain active, dune flanks in most areas support sparse grasses or shrubs, and in many areas seem immobilized. A vegetation cover is clearly evident in Landsat images, in which striated landscapes are often spattered with irregular fire scars. Nevertheless, extensive areas of active dunes, both longitudinal and transverse, do exist, as in the Simpson and Great Sandy deserts.

The striations created by the linear dunes veer around Australia in a Southern Hemisphere anticyclonic (anticlockwise) manner, producing a mirror image of the Saharo-Arabian aeolian pattern. As in the latter, the eastern (high-to-low-latitude) portion of the gyre is strongly developed, but there is no corresponding low-to-high-latitude closure in the west, where all dunes have a westerly trend. The desert centre is an upland in which large longitudinal dunes are replaced by scattered areas of transverse dunes. Dune-free areas break the otherwise continuous ellipse only north-east of Alice Springs and in the Flinders Range and Lake Torrens area of the south-east.

Most Australian sand ridges, like much of the Australian Desert, are reddish in colour. Generally, red coloration in dune sands has been attributed to time, with reddening increasing in the downwind direction (Gardner and Pye 1981). Wasson (1983) found that in the Strzelcki-Simpson mobile dunefield the reddest dunes (2.5 YR 5/8) were derived from older 'pre-reddened' sediments of local provenance, with lighter colorations (10 YR 7/4) in low topographic situations associated with the intrusion into the erg of large modern streams (Cooper Creek, Diamantina River). Wasson admitted downwind reddening in the Simpson Desert, but maintained the importance of different sediment sources to account for it.

AGE OF THE DUNES

Like the dunes of the African Sahel, the Australian sand ridges extend well beyond the desert area into regions of marshes and seasonal streams. Clearly, such dunes are relict, as are large expanses of dunes in the drier interior. Wasson (1983) established that his mobile 'pale dunes' in the Simson-Strzelski Desert (at the eastern end of the Australian gyre) developed between 23 000 and 13 000 years BP and have been active only in their crestal areas in the late Holocene. Apparently large dunes were not generated during the Holocene, as the dune chains of the Great Sandy Desert in the north-western portion of the gyre continue across the coastline to at least 15 m below sea level, where they are overlain by Holocene marine deposits (Jennings 1975). There is as yet no conclusive evidence constraining the maximum ages of the existing Australian dunes.

LUNETTES

Australia is the classic locality for lunettes (Bowler 1973, 1976), which are crescent-shaped clay dunes at the downwind end of ephemeral lakes. They consist of clays deflated from desiccated lake beds in the form of pellets produced by the flocculating effect of salines. Frequently the clays are blown into areas of sand dunes that form the lunette core. The sands represent lake high stands and beach activity, while the clays indicate desiccation of the lake shore during falling stages. Lunette stratigraphy, which often includes charcoal and datable carbonates, records a long period of desiccation in southern Australia prior to 45 000 years BP, a humid period from 45 000 to 26 000 years BP, low-level saline lakes from 26 000 to about 18 000 years BP, and sustained aridity from about 17 000 years BP to the present (Bettenay 1962, Dury 1973, Bowler 1976).

FOSSIL DRAINAGE SYSTEMS

Like the Saharo-Arabian Desert, Australia is a museum of fossilized stream systems. Certain summer-active stream systems of the Channel Country east of the Centre, with braided reaches as much as 40 km wide (Eyre Creek, Queensland) amid impeding dunefields (Francis and Jones 1984) bear a stunning resemblance to the major defunct drainage systems of Arabia and the Sahara, suggesting that truly humid climates may not be required for the development of such phenomena. The breadth of some of the region's channels may be a result of the ease of planation in deeply weathered silcrete substrates.

Both the Channel Country of the north-east and the Riverine Plains draining to the Murray and Darling Rivers in the south-east display what appears to be three stages of drainage development from the late Pleistocene through the Holocene. However, these differ quite distinctly.

In the Channel Country of western Queensland, north-east of the Centre, is a ubiquitous surface cover of transported clays, some 5 m thick, overlying sands deposited by older braided stream systems (Veevers and Rundle 1979). Modern streams are underfit and braided within the larger clay-coated braided channels. Thus climatic oscillations from semi-arid to humid to arid seem evident. Baker (1986) has suggested that the change from clay deposition to the modern pattern may have occurred with a transition from more humid conditions to present aridity *c.* 7000 to 5000 years BP.

Considerably more attention has been given to the Riverine Plains of semi-arid New South Wales, south-east of the Centre, where the current drainage to the Murray and Darling Rivers is overprinted on two earlier hydrologic systems having unmistakably different morphologies (Butler 1950, Langford-Smith 1960, Pels 1964, Schumm 1968). The modern underfit channels meander through floodplains developed by older 'ancestral rivers' that have meander geometries and wavelengths an order of magnitude greater than those of the present streams. The interfluves between the ancestral rivers display a system of infilled palaeochannels known as 'prior streams'. These have very low sinuosities, are almost always fringed by aeolian sand accumulations, and clearly are very ancient bedload channels.

Pels (1969) attributed the ancestral rivers to the Pleistocene, with a change to the modern regime *c.* 15 000 to 13 000 years BP. This is hard to reconcile with the oxbow lakes and well-preserved bar and swale topography persisting in the ancestral system, which Schumm logically regarded as 'very recent'. All observers place the prior channels well back in the Pleistocene – beyond the limit of radiocarbon dating, according to Pels – and Schumm's analysis appears to establish that they signify a time of accentuated aridity in south-eastern Australia.

In the ancient, deeply weathered and stripped shield area of Western Australia many sinuous lines of dry lake beds suggest a former comprehensive hydrographic network similar to the fossil wadi systems of the Sahara and Arabia. According to Ollier (1977) and Van de Graaf *et al.* (1977), these broad infilled valleys are far more ancient than the Saharo-Arabian fossil wadis, having been beheaded about 75 Ma by the rifting that initiated separation of Australia from Antarctica.

In the centre of the desert region, the highly denuded folds of the Macdonnell, Kirchauff, and James ranges, produced by Palaeozoic compression, are cleft by the Finke River and its tributaries, in courses of uncertain origin that presumably evolved under non-desert conditions (Mabbutt 1966). Büdel (1982) made this area a cornerstone for his theory of tropical etchplain development, citing the drainage pattern as evidence of evolution on a deeply weathered surface of insignificant relief.

DURICRUSTS

An obtrusive characteristic of the Australian arid zone is the importance of ancient weathering phenomena in the form of laterite and silcrete duricrusts. Angular silcrete fragments known as gibbers or billy, litter vast expanses; *in situ* silcrete is the source of precious opal; and laterite or silcrete-capped mesas are often the only features breaking a dead-level horizon. Laterite and silcrete remnants are found in many of the world's deserts, reflecting quite different climates in the early Tertiary (Goudie 1973), but nowhere outside of Australia are relict duricrusts a dominant geomorphic element over large areas. While the exact genesis of laterite in any setting provokes continuing argument, the formation of silcrete poses even more difficult questions (Goudie 1973, Langford-Smith 1978). In the Australian interior two generations of pre-Miocene mesa-capping silcretes with underlying pallid zones form tablelands above Miocene aluminous laterite crusts, with some ferruginization atop the silcrete mesas as well.

According to Wopfner (1974) and Langford-Smith and Watts (1978), the conspicuous deep pallid zone underlying the mesa duricrusts is a product of pre-Miocene silcrete formation rather than of the Miocene ferralitization process. Late Miocene to early Pliocene desiccation then terminated the development of laterite duricrusts and initiated stripping of the inherited deeply weathered land surface (Mabbutt 1965).

Rather than being a product of aridity, as often proposed (Langford-Smith and Dury 1965, Goudie 1973, Mabbutt 1977), silcrete is now seen by Langford-Smith (1982) and others as a product of a warm and wet climate, which is in accord with palaeobotanical evidence for the period of silcrete formation (Wopfner 1978). Langford-Smith (1982) suggested that the change to ferralitization may have resulted from increased rainfall seasonality. This seems to accord with the interposition of laterization (ending about 13.5 Ma) between the earlier hyperhumid and later arid climatic regimes in central and eastern Australia. Ferruginous laterite is dominant in western Australia, with few traces of silcrete present, suggesting a persistent seasonal rainfall regime in a tropical setting throughout the Tertiary.

ETCHPLAINS

The laterite and silcrete duricrusts discussed in the preceding section are but the superficial aspect of tropical humid etchplain development that dominated Australia until the late Tertiary. Silcrete and laterite caprocks protect weaker substrates including the deeply decomposed bedrock of a continent flattened by tens of millions of years of erosion under warm and seasonally wet conditions. The etchplain concept involves double planation (Büdel 1982), in which a slowly eroding land surface is well separated from an irregular, structurally controlled basal surface of chemical weathering at a depth of tens to hundreds of metres. If the sinking land surface is lowered to a protuberance on the basal surface of chemical etching, solid rock is exposed locally at the surface, where it endures essentially unchanged as the surrounding area continues to rot and be pared down, always maintaining a planar surface. Relief generation by stream incision in bedrock is paralysed as the thoroughness of rock decay deprives streams of abrasive tools.

In arid Australia this development has been terminated by the onset of aridity, which accelerated surface erosion and ended deep weathering, so that former basal surfaces of chemical etching have been widely exposed. The ancient deep weathering profiles are preserved as remnants, including the ubiquitous mesas capped by laterite and/or silcrete duricrusts atop conspicuous white pallid zones. Finkl and Churchward (1973) made clear the variety of landscape types that can result from varying degrees of etching, stripping, and duricrust preservation in south-western Australia.

INSELBERGS

The erosional flattening of Australia is so thorough that any sharp protuberance constitutes a major landmark. Among the latter are Ayers Rock and the Olgas near the Centre, and low granitic domes in many locations north, west, and south of the Centre. All of these features rise abruptly above vast expanses of level plains and appear to be extremely ancient landforms.

The Australian inselbergs are smooth, boulder-free domes of the type often known as bornhardts and are composed of both sedimentary and granitic rock. Ayers Rock is an isolated rhombic slab, some 9 km in circumference and 340 to 350 m high, composed of steeply dipping, coarse-grained, Cambrian arkose. It had been wholly or partially exhumed from a Cenozoic cover by late Mesozoic or early Tertiary erosion (Twidale 1978) with three sides fringed by flat pediments that expose the arkose as much as 800 m from the base of the inselberg. The Olgas, some 30 km west of Ayers Rock, are a cluster of about 30 joint-defined rock domes composed of massive, gently dipping cobble- to boulder-conglomerate of Upper Palaeozoic age (Ollier and Tuddenham 1961). Granitic inselbergs are widely distributed, taking the form of low domes with steepened or 'flared' margins (discussed below).

Estimates of the great age of the Australian bornhardts are based upon the facts that those in Western Australia project from plains laterized in Oligocene or earlier time, those in central Australia stand above early to middle Tertiary silcretes, and the Olgas and Ayers Rock overlook early Tertiary sediments (Twidale 1982).

Whereas Ollier and Tuddenham accepted major erosional backwearing of inselberg slopes, Twidale has insisted that backwearing is minimal, with the inselbergs being a product of greater resistance (less joint density) than surrounding rocks (Twidale and Bourne 1978, Twidale 1982).

In common with granitic bornhardts, Ayers Rock displays 'flared slopes', being girdled by a smooth basal concavity with an overhanging brow as much as 10 m above the land surface. Twidale (1962, 1982) has attributed flares to subsurface scarp-foot weathering, with a former ground surface present at the brow above the concavity. Perched flares, or niche lines, are present well above the land surface on inselbergs composed of both clastics and granites in Australia. Twidale and Bourne (1975) thus referred to the 'episodic exposure' of inselbergs by multiple phases of land surface downwearing and surface stabilization and slope foot weathering, with terraced dome flanks preserving this history. Similar features, including perched niche lines, are present in many desert areas, but nowhere else appear to be developed on the scale or with the elegance seen in Australia.

As part of his emphasis on the age of the Australian bornhardt domes, and on their explanation in terms of rock resistance, Twidale regarded the backwearing of rock slopes between successive phases of ground surface lowering as relatively insignificant – no more than 60 m in granite (Twidale and Bourne 1978). In the arkose of Ayers Rock, Twidale (1978) admitted rock slope recession of 30 to 90 m while surrounding plains composed of weaker materials were lowered some 60 m. This is far from the kilometres of slope backwearing invoked by others to explain North American desert pediments. The long history of tropical weathering of an un-

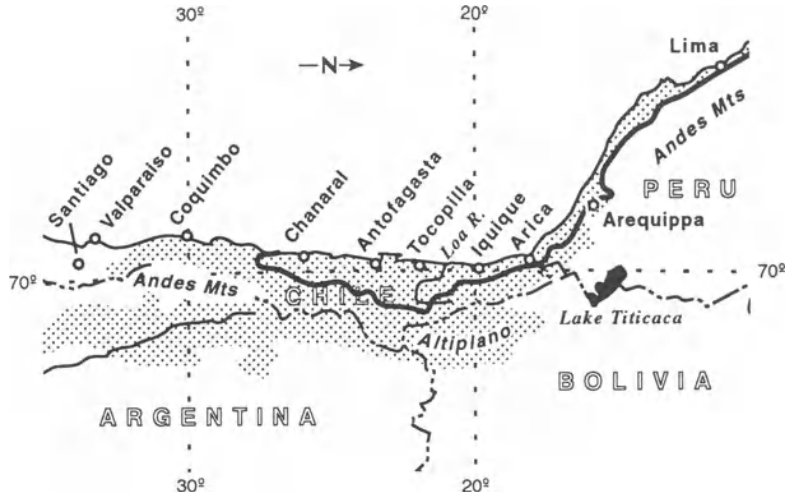

Figure 2.7 Atacama Desert, Chile. Symbols as in Figure 2.1.

usually stable landscape seems to have produced a distinctive geomorphic phenomenon in the flared slopes of Australian inselbergs.

THE ATACAMA DESERT

The coastal desert of Peru, Chile, and Ecuador is the world's driest region, and the only desert that reaches across the Equator from the subtropics (Fig. 2.7). Drought here results from atmospheric subsidence and offshore cold water upwelling reinforced by a coastal trend parallel to the eastern limb of the South Pacific anticyclonic gyre. The region of most accentuated drought – the Atacama Desert of northern Chile – extends high into the Andean cordillera from a narrow plain (or terrace) fringing a coastal escarpment up to 2000 m high. In the Atacama, measurable rainfall occurs at intervals of many years, usually when El Niño conditions prevail. Annual rainfall averages are in fractions of a millimetre. As a consequence, the landscape below about 3000 m is completely barren over vast areas. Trewartha (1981) noted that rainfall becomes more frequent beyond the Peru–Chile frontier where the coast swings west, producing onshore flow of the anticyclonic gyre. It may be equally significant that the high coastal escarpment of northern Chile, which extends nearly 1000 km from Chanaral to Arica, disappears at the same point. While this desert is almost rainless (P/Etp < 0.03), its coastal location and influence by advection fog places it in the warm-summer rather than very-warm-summer category (UNESCO 1977). Coastal fog advects inland from the sea almost daily through passes lower than about 1000 m and condenses on rock surfaces in the desert interior. The long-sustained extreme aridity of the coast and interior has created several peculiar geomorphic phenomena, particularly saline deposits that are unusual in type, origin, distribution, and influences on the land surface.

Although the accumulations of highly soluble materials in the Atacama Desert, including surface nitrate deposits, have convinced their investigators that aridity may have been sustained over a period of millions of years (Ericksen 1981, 1983), Ochsenius (1977, 1982) has claimed that the region was merely semi-arid and populated by a rich megafauna until the Holocene, when salines began to accumulate. This seems contradicted by the distinctive paucity of sediments in the Peru–Chile ocean trench, indicating sustained aridity in the late Tertiary. Alpers and Brimhall (1988) concluded that copper enrichment by aggressive leaching conditions in the Atacama occurred from 18 to *c.* 15 Ma, based on K/Ar dating of supergene minerals, declining thereafter due to increasing aridity, with hyperarid conditions established by the middle Miocene. In the absence of some mechanism for extraordinary rapid Holocene concentration of salines, the geomorphic phenomena seen in the Atacama accord much better with the latter view than with Ochsenius' interpretation. Nevertheless, relict Pleistocene shorelines surrounding at least 35 basins in Chile and Bolivia (Stoertz and Ericksen 1974) indicate either periodic moist intervals or intrusions of Andean runoff that have produced long-lasting lakes in the desert environment.

PHYSIOGRAPHY

The gross configuration of the Atacama Desert of Chile consists of a central trough at an elevation of about 1000 m, hemmed in on the east by a gradual rise to the 4000- to 5500-m volcanic axis of the Andes, and to the west by a variably expressed coastal range that locally rises about 3000 m and contains many closed basins. In the north a deep blanket of andesitic and rhyodacitic ashflows, lahars, and interbedded sediments slopes from the Andes to the crest of the coastal escarpment. South of Antofagasta the Andes and the coast are again linked by integrated channel systems crossing a dissected pediplain. Desert basin and range topography occurs both east and west of the central depression, and granitic hamadas dominate the coastal areas in the southern portion of the desert. Narrow marine terraces at the foot of the coastal escarpment attest to the recent tectonic rise of the littoral of northern Chile.

The Atacama has its own highly distinctive landforms but lacks some of the staples of desert scenery elsewhere, such as well-developed desert varnish, true desert pavements, and large areas of sand dunes. As in the Namib, classic mosaic-like desert pavement does not appear to be present, although staged alluvial surfaces and segmented alluvial fans are present. In all settings, bare ground is exposed between surface clasts. Pavement formation in the Atacama seems to be inhibited by soil disturbance related to salt crystallization and solution under the influence of fog and dew, along with clast fragmentation by salt cracking.

Desert varnish of the conspicuous black, manganese-rich type (see Chapter 6) is a product of Mn-oxidizing bacteria that do not thrive in alkaline environments. The Atacama geochemical setting appears to resemble the alkaline undersides of desert pavement cobbles, which in other deserts bear an Mn-deficient and Fe-rich orange-red patina. It is hardly surprising that the Atacama is over large areas a reddish desert, in which surface clasts and underlying fines are the same colour. Instead of reddish ventral coatings, the undersides of Atacama clasts are commonly encrusted with white halite or gypsum. Even at elevations above 2000 m, staged alluvial surfaces that in the western United States would bear a systematic age sequence of rock varnish colours from grey to black show only the most subtle variations of buff tones in the Atacama. The darkest rock varnish found in the Atacama by this observer occurs in the most humid microenvironments, such as fog gaps and on terraces above the riparian marshes of the Loa River. Over pure white flint substrates this varnish is Fe-rich and orange in close view, with black Mn-rich speckles and pit fillings.

The interior Atacama displays areas of ventifacted bedrock and cobbles, but is conspicuously free of large dune fields. Individual dunes, some quite large, occur in scattered locations along the coast, but the interior Atacama contains no true ergs. The change in coastal trend and loss of the high escarpment at the Peruvian border are reflected in the greater development of sand dunes along the Peruvian coast. As in the Namib (Lancaster 1989), onshore movement of sand appears to be favoured where coastlines cut across the major atmospheric flows. The Atacama coastline is cliffed, virtually straight, and parallel to the eastern edge of the South Pacific anticyclone.

DRAINAGE EVOLUTION

Mortimer (1980) has analysed the profiles of the major Atacama quebradas, concluding that, in the northern Atacama, Andean drainage has been incised 300 to 900 m from consequent courses on the volcanic blanket, whereas farther south Andean streams terminated in the central depression until the latter was aggraded to the point of sediment overspill or stream capture by steep-gradient gorges working headward through the coastal range. The course of the exotic Loa River, in particular, suggests a linkage of segments of differing origin, either by headward extension of a coastal range canyon, or by overspill to the coast of a large interior lake. The relict shorelines of an ancient lake some 200 m deep (Lago Soledad) remain conspicuous in the landscape at the potential spillway elevation, more than 1000 m above the Loa River's passage through the coastal range. The preserved shorelines are completely encased by halite and anhydrite crusts at least 10 m thick. Stoertz and Ericksen (1974) and Paskoff (1977), apparently borrowing from Bruggen (1950), vastly understated the depth of this hydrologically significant pre-late Pleistocene palaeolake.

In the southern portion of the Atacama the central depression disappears, and an erosional pediplain-like surface is dissected by stream systems issuing from the Andes (Galli-Olivier 1967). Longitudinal profiles of the trunk channels crossing the southern Atacama become convex-upward near the coast. This reflects either valley shortening due to rapid cliff recession by marine erosion where the coast is subsiding (Mortimer 1980) or tectonic uplift where the coast is fronted by marine terraces capped by

shelly coquinas. Whatever the cause of the profile convexity, regrading of channels to compensate for base level change or valley shortening is ineffective in the current hyperarid climate.

THE COASTAL ESCARPMENT

One of the most remarkable features of the Atacama region is the 300- to 1000-m-high coastal wall of northern Chile, which locally rises above 2000 m. North and south of the Loa River (the single Andean stream that persists through the desert to the sea) the coastal scarp truncates a basin and range landscape, so that basin fills including Miocene tephras are exposed in cross-section. Nearby, the land surface interrupted by the scarp can be seen to be a pediment truncating inclined sediments and volcanics. At its northernmost point the coastal scarp cuts the volcanic blanket; to the south it exposes granitic and metamorphic rocks.

The high coastal escarpment was initially thought to have been produced directly by en échelon faulting (Bruggen 1950). This interpretation has subsequently been rejected (Mortimer and Sarič 1975). The trench of the Loa River through a coastal terrace fails to expose a fault at the cliff base. Mortimer (1972) attributed the cliff entirely to wave attack along a subsiding shoreline, while Paskoff (1976, 1980) preferred 1 to 2 km of cliff retreat by marine erosion following scarp formation by extensional faulting. In some locations the escarpment has the rhombic geometry of basin and range faults, causing the present author to believe that faulting initiated the scarp a short distance seaward of the current shoreline. Paskoff (1980) established that Pliocene marine deposits are present up to the foot of the scarp, which seems to have existed in its present position since the late Tertiary.

Where the cliff descends to the sea it is gouged by ravines, with geological structures etched in relief. But where a narrow coastal plain or terrace is present, ravines are almost entirely absent, and the wall is a smooth equiplanation surface, often veneered from top to bottom by colluvium of variable thickness. In such areas the coastal escarpment resembles the smooth quebrada walls of the north, which are cut and fill surfaces that have a truly lunar appearance. The upward expansion of colluvial mantles is apparent in many locations where small areas of rough rock are still preserved above immense talus aprons. Where mantles are complete, their materials seem to have undergone a fining process, possibly resulting from salt-cracking of clasts. The contrast between the smoothed colluviated slopes of the coastal escarpment and the rough rock walls of the Loa River canyon at the coast indicates that the lower Loa River canyon is significantly younger than the coastal scarp, reinforcing the impression of canyon initiation at a relatively late date by overspill of an interior deep lake.

SLOPE EQUIPLANATION

In the driest portion of the Atacama, north of the 24th parallel, the completely barren landscape has a smoothed lunar appearance. Many long slopes are devoid of any features indicative of surface water erosion and instead display peculiar mass wasting phenomena in the form of fish-scale patterns or inclined terracettes (Fig. 2.8). Where soils are saturated with halite and anhydrite, patterned gilgae-like surfaces often run smoothly from valley floors over hillcrests. Roadcuts on quebrada walls in ignimbrite areas reveal that long smooth slopes consist of both cut and fill surfaces, resulting in near-perfect slope equiplanation. Differential weathering and erosion, ravining, rilling, and badland dissection of the type dominating most mountainous deserts is so highly localized in the northern Atacama as to demand a photograph when it is seen!

Abele (1983) asserted that the smoothed slopes of the Atacama were restricted to the zone of coastal fog below about 1100 m, with normal dissection prevailing above this elevation. Abele attributed this phenomenon to the intensification of salt weathering by daily wetting and drying in the fog zone. However, the roughness of the coastal scarp at Arica and Tocopilla contradict this generalization, as do smooth slopes well above and to the east of the fog zone.

Three rather unusual factors appear to influence the Atacama's distinctive scenery. The most obvious is the insignificance of rainfall, which rarely appears sufficient to generate overland flow. Second is the unique abundance of salines in the environment, including encrustation of slopes by halite, anhydrite, and sodium nitrate (see below). Initial crystallization, and later expansion and contraction of salines due to daily thermal and humidity fluctuations may be crucial in rock disintegration and slope equiplanation, trimming projections and maintaining a colluvial mantle over slopes in and beyond the fog zone.

The third unusual influence that may be pervasive in the Atacama is seismic activity. Colluvial terracettes and fish-scale mass wasting can easily be visualized as material shunted downslope during major earthquakes, which are a distinctive aspect of this desert's location above one of the Earth's most

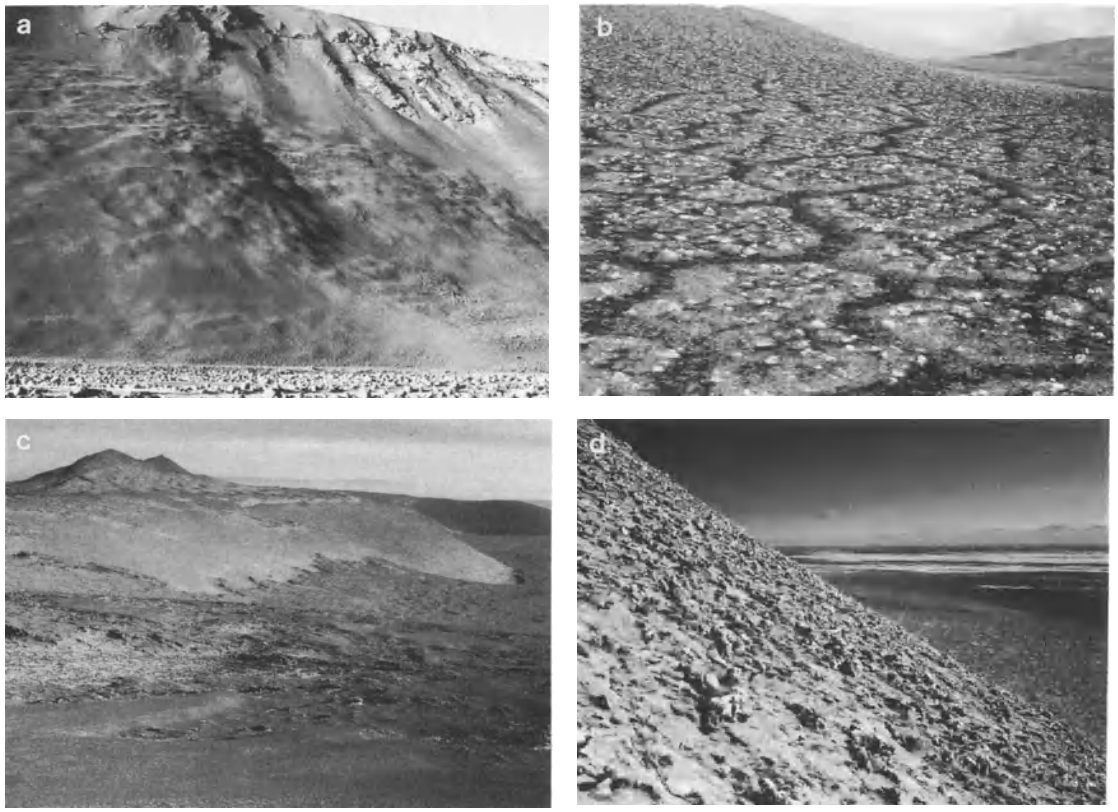

Figure 2.8 Unusual landforms of the Atacama Desert, Chile. (a) Quebrada wall, some 500 m high, showing colluvial mantle and terracettes possibly generated by repeated major seismic events. (b) Gypsum-rich gilgae soils mantling smooth terrain north of the Loa River's outlet to the sea. (c) Halite and anhydrite blankets completely encasing terrain north of the Loa River. Relief is about 300 m. The anhydrite cap, 1 to 2 m thick, has been partially stripped from the subjacent halite and is darker in the photograph. (d) Morphology of the halite crust on a 200-m-long slope in the vicinity of (c). This crust is at least 10 m thick.

active subduction zones. The total absence of stabilizing vegetation and root systems would abet seismically induced regolith creep, and, although not verified, seismically induced creep of incoherent surficial materials may be accentuated by the presence of coherent saline crusts underlying slopes and acting as shaking tables.

SALINE CRUSTS

The conspicuous saline deposits of the Atacama Desert present difficult interpretive problems. The origin of the highly unusual nitrate beds has remained a matter of conjecture for more than a century, with ten different explanatory hypotheses summarized by Ericksen (1983). Nitrate deposits in the form of cements, veins, and dykes occur on all types of topography, in association with bedrock, alluvium, and colluvium of diverse lithologies. The deposits contain substances not known from any other location: perchlorate, and unique iodate, nitrate, chromate, and diachromate minerals. Some of the nitrate minerals are those normally associated with the decay of bat guano and are rare in saline complexes (Ericksen 1983). Based on the high ammonium content of sea spray and the iodine content of nitrate deposits, Bloch and Luecke (1972) supported a long history of importation and deposition of aerosol nitrogen released by photochemical oxidation of atmospheric ammonium derived from sea spray. However, Ericksen (1983) found very little nitrate in soil samples from the coastal region.

Nitrate crusts are best developed on the interior side of the coastal ranges, near the base of long slopes, suggesting a period of secondary enrichment by hillslope throughflow. Ericksen proposed that the nitrates were produced by bacteria and blue-green algae in interior saline playas and were blown against the coastal ranges from the east, subsequently experiencing a lengthy history of leaching and redeposition.

Other salines are equally problematical, for they are not confined to ancient lake beds, but blanket the topography. North of the westward bend of the Loa River a surface halite blanket capped by anhydrite and loess has a relief of more than 200 m, and a thickness of at least 10 m on slopes, as revealed in an isolated doline containing NaCl speleothems. Here the salt crust, complete with typical salt polygons, is inclined at an angle of 33° over a 200 m rise (Fig. 2.8). In this same region are salt-encased spits on a relict shoreline and salt pan hummocks 4 m high that appear to be salt-encased sand dunes.

The superposition of the less soluble anhydrite atop massive halite on steep slopes is the reverse of the evaporite sequence produced by lake desiccation or capillary rise of ground water and suggests aerosol input and downward leaching, with chlorides more mobile than sulphates. Local removal of the loess and anhydrite veneer and solutional lowering of underlying halite by 2 m or more could be interpreted as evidence of humid phases within the overall hyperarid climate. However, the present surface morphology of the lowered salt crusts on slopes is accretionary; forms indicative of recent corrosion of the salt are not present.

In the hills north of the Loa River canyon, loess directly overlies salt on slopes and is being stripped to expose the brilliant white salt in swales. Possibly the chlorides were a component of the loess and were subsequently leached downward from it. North of the Loa River canyon, coulee-like ridges of massive salt capped by loess protrude from bordering hillslopes into the vast salt pan of Salar Grande. This suggests a general solutional lowering of the salt pan surface at some time in the past, producing local instances of relief inversion. At present solution is not occurring here; as on the slopes described above, only growth forms are visible.

SALT EJECTION OF REGOLITH CLASTS

Some granitic hillslopes west of the Loa River bristle with tabular blocks. Examination of these crests and the slopes leading to them indicates extrusion of granitic masses, from 2-m blocks to finger-size prisms. The surface soil is a sandy, saline mud that has been dragged outward as a cuff around the smaller extruded fragments. This salt heave mimics the frost push (and pull) phenomena of cold-winter areas. Shallow swales draining the summits are choked with granitic blocks apparently extruded and toppled farther upslope.

Although typical boulder tors and forms of cavernous salt weathering in granite appear in the coastal area, hillslopes consisting of rounded granitic boulders and exfoliating domes, typical of most deserts – including the Atacama's closest climatic parallel, the Namib – do not appear to be a component of granitic scenery in the interior of the Atacama, which to an elevation of some 2300 m is a virtually lunar landscape.

CONCLUSION

Although desert landscapes are visually similar in the broad sense, the preceding pages should demonstrate how varied individual deserts are in the particulars that constitute modern research challenges. Each of the major deserts examined contains certain unique landform associations and peculiar geomorphic problems, many of which remain unresolved, and, in some cases, uninvestigated. Effective process systems vary significantly even in arid settings, and, except in the Atacama, have been applied for relatively brief timespans to quite diverse antecedent landscapes. The North American deserts have presented a cornucopia of research problems and findings as a result of unusually diverse geologic and tectonic conditions, though even here the precise effects of climatic oscillations during the Quaternary and the influence of the remote past on present landscapes remain elusive. Nevertheless, the scenery of the North American arid realm is clearly dominated by the erosional and depositional effects of surface water. Not so in the eastern Sahara, where aeolian processes are paramount, nor in the Atacama, where inexplicably high saline inputs and seismically abetted mass wasting generate landforms of unique character. Our knowledge of the arid regions extending from Iran through Inner Asia is merely at the reconnaissance level, and fuller investigation there will surely reveal hitherto undescribed geomorphic phenomena. A suggestion of this has already appeared in the work of Jackson *et al.* (1991) on the salt diapirs of the evaporite-dominated heart of Iran.

The point of this contribution is that deserts are far from uniform geomorphically even when they fall into the same structural category. Basin and

range (or 'mountainous') deserts, with similar structural features, such as those of Nevada, Chile, and Iran, exhibit dissimilar geomorphic phenomena related to the degree and duration of aridity. Cuesta-form (or platform) deserts of the Colorado Plateau and Saharo-Arabian region display unlike scenery as a result of both climate and tectonics. Australian shield and platform landforms differ significantly from those of the Saharo-Arabian region, probably as a consequence of antecedent climates. Dune-dominated deserts are of strikingly different types. The Saharo-Arabian realm, the Namib erg of south-west Africa, and the Taklamakan erg of Chinese Xinjiang are active on a large scale, while the sands of the Sahel, Australia, Kalahari, and Thar (India–Pakistan) are largely fixed and inactive, as the presently active ergs have been several times in the last 100 000 years. Wider coverage would reveal the Thar to be a well-populated and over-utilized sand desert as a consequence of subsurface water and agriculturally useful mollic geosols within the sands. The Kalahari would be seen to display countless pans of controversial origin and unique (possibly solution-influenced) valley forms, called mekgachas, cutting massive intertonguing calcrete, silcrete, and ferricrete duricrusts. The Namib displays a sea wall of sand attaining volumes encountered nowhere else in a coastal zone, marine terraces completely entombed in these sands, and also sprawling erosion surfaces epitomizing (according to the observer) either long-distance scarp recession *à la* L.C. King or *in situ* scarp generation at a tectonic flexure in a tropical savanna as envisaged by J. Büdel. In the heart of Iran are vast expanses of deformed and eroded evaporites intruded by complexes of salt diapirs, and farther south a desert dominated by wind-scoured yardangs of unique persistence and perfection of form. Finally, in the cold deserts of Mongolia, western China, and the central Asian republics of the former Soviet Union are sand seas, erosional plains, and depositional cones of magnitudes that utterly dwarf any New World parallels, but which have received little outside recognition and analysis, and which would remain largely unknown in the absence of satellite imaging.

Rather than developing a unifying perspective, the preceding account emphasizes diversity, with the single unifying theme being the instability of climates in the desert realm, the recency of non-desert conditions in most of the currently arid zone, the resulting superposition of humid and arid landforms, and the role of pre-Quaternary non-desert conditions in the differentiation of existing desert landscapes.

REFERENCES

Abele, G. 1983. Flachenhafte Hanggestaltung und Hangzerschneidung im chilenisch – peruanischen Trockengebiet. *Zeitschrift für Geomorphologie Supplement Band* **48**, 197–201.

Albritton, C.C., J.W. Brooks, B. Issawi and A. Swedan 1990. Origin of the Qattara Depression, Egypt. *Bulletin of the Geological Society of America* **102**, 952–60.

Alimen, Marie-Henriette 1982. Le Sahara: Grande Zone Désertique Nord-Africaine. *Striae* **17**, 35–51.

Alpers, C.N. and G.H. Brimhall 1988. Middle Miocene climatic change in the Atacama Desert, northern Chile: Evidence from supergene mineralization at La Escondida. *Bulletin of the Geological Society of America* **100**, 1640–56.

Axelrod, D.I. 1983. Paleobotanical history of the Western Deserts. In *Origin and evolution of deserts*, S.G. Wells and D.R. Haragan (eds), 113–29. Albuquerque NM: University of New Mexico Press.

Baker, V.R. 1986. Fluvial landforms. In *Geomorphology from space*, N.M. Short and R.W. Blair Jr. (eds), 255–315, Washington, DC: National Aeronautics and Space Administration.

Bettenay, E. 1962. The salt lake systems and their associated aeolian features in the semi-arid regions of Western Australia. *Journal of Soil Science* **13**, 10–17.

Bloch, M.R. and W. Luecke 1972. Geochemistry of ocean water bubble spray. *Journal of Geophysical Research* **77**, 5100–5.

Bowler, J.M. 1973. Clay dunes: their occurrence and environmental significance. *Earth Science Reviews* **9**, 315–38.

Bowler, J.M. 1976. Aridity in Australia: age, origin, and expression in eolian landforms and sediments. *Earth Science Reviews* **12**, 279–310.

Breed, C.S., S.C. Fryberger, S. Andrews, C. McCauley *et al.* 1979. Regional studies of sand seas using Landsat (ERTS) imagery. In a study of global sand seas. E.D. McKee (ed.), *U.S. Geological Survey Professional Paper* 1052, 305–97.

Breed, C.S., J.F. McCauley and M.I. Whitney, 1989. Wind erosion forms. In *Arid zone geomorphology*, D.S.G. Thomas (ed.), 284–307. New York: Halsted.

Bruggen, J. 1950. *Fundamentos de la Geologia de Chile*. Santiago: Instituto Geografico Militaire.

Büdel, J. 1982. *Climatic geomorphology*, translated by L. Fisher and D. Busche. Princeton, NJ: Princeton University Press.

Burke, K. and G.L. Wells 1989. Trans-African drainage system of the Sahara: Was it the Nile? *Geology* **17**, 743–7.

Busche, D. 1979. Planation surfaces and the problem of scarp retreat on the western margin of the Murzuk basin, central Sahara. *Palaeoecology of Africa* **10**, 50–5.

Busche, D. and W. Erbe, 1987. Silicate karst landforms of the Southern Sahara. *Zeitschrift für Geomorphologie Supplement Band* **64**, 55–72.

Busche, D. and H. Hagedorn 1980. Landform development in warm deserts – the central Saharan example. *Zeitschrift für Geomorphologie Supplement Band* **36**, 123–39.

Butler, B.E. 1950. A theory of prior streams as a causal factor of soil occurrence in the Riverine Plain of Southeastern Australia. *Australian Journal of Agricultural Research* **1**, 231–52.

Butzer, K.W. 1980. Pleistocene history of the Nile Valley in Egypt and Lower Nubia. In *The Sahara and the Nile*, M.A.J. Williams and H. Faure (eds), 253–80. Rotterdam: Balkema.

Clark, A. 1989. Lakes of the Rub'al Khali. *Aramco World* **40**(3), 28–33.

Conrad, 1969. Le'Evolution continentale Post-Hercynienne au Sahara algeriénne (Saoura, Erg, Chech, Tanezrouft, Ahnet-Mouydir). *Publication Centre de Recherches sur les Zones arids*, C.N.R.S., Serie geologie 10, 24.

Dohrenwend, J.C. 1987. Basin and range. In *Geomorphic systems of North America*, W.L. Graf (ed.), 303–42. Boulder, CO: Geological Society of America.

Dury, G.H. 1973. Paleohydrologic implications of some pluvial lakes in northwestern New South Wales, Australia. *Bulletin of the Geological Society of America* **84**, 3663–76.

Ericksen, G.E. 1981. Geology and origin of the Chilean nitrate deposits. *U.S. Geological Survey Professional Paper* 1188.

Ericksen, G.E. 1983. The Chilean nitrate deposits. *American Scientist* **71**, 366–74.

Felber, H., H. Hötzl, H. Moser, W. Ravert *et al.* 1978. Karstification and geomorphology of As Sulb Plateau. In *Quaternary Period in Saudi Arabia*, Vol. 1., S.S. Al-Sayari and J.G. Zötl (eds), 166–72. New York: Springer.

Finkl, C.S. Jr and H.M. Churchward 1973. The etched landsurfaces of southwestern Australia. *Journal of the Geological Society of Australia* **20**, 295–307.

Francis, P. and P. Jones 1984. *Images of Earth*. Englewood Cliffs, NJ: Prentice Hall.

Fryberger, S.G. and T.S. Ahlbrandt 1979. Mechanisms for the formation of aeolian sand seas. *Zeitschrift für Geomorphologie* **23**, 440–60.

Galli-Olivier, C. 1967. Pediplain in northern Chile and the Andean uplift. *Science* **158**, 653–5.

Gardner, R. and K. Pye 1981. Nature, origin, and paleoenvironmental significance of red coastal and desert dune sands. *Progress in Physical Geography* **5**, 514–34.

Goudie, A.S. 1973. *Duricrusts in tropical and subtropical landscapes*. Oxford: Clarendon Press.

Graf, W.L., R. Heresford, J. Laity and R.A. Young 1987. Colorado Plateau. *Geomorphic systems of North America*, W.L. Graf (ed.), 259–302. Boulder, CO: Geological Society of America.

Grunert, J. and D. Busche 1980. Large-scale fossil landslides of the Msak Malat and Plateau du Maughini escarpment. *Proceedings of the 2nd Symposium on the Geology of Libya*. New York: Academic Press.

Hagedorn, H. 1968. Über äolische Abtragung und Formung in der Südost-Sahara. Ein Beitrag zur Gliederung der Oberflachenformen in der Wüste. *Erdkunde* **22**, 257–69.

Hassan, F.A. 1976. Heavy minerals and the evolution of the modern Nile. *Quaternary Research* **6**, 425–44.

Hötzl, H., F. Kramer, and V. Maurin 1978a. Quaternary sediments. In *Quaternary period in Saudi Arabia*, Vol. 1, S.S. Al-Sayari and J.G. Zötl (eds), 264–301. New York: Springer.

Hötzl, H., V. Maurin and J.G. Zötl 1978b. Geologic history of the al Hasa area since the Pliocene. In *Quaternary period in Saudi Arabia* Vol. 1, S.S. Al-Sayari and J.G. Zötl (eds), 58–77. New York: Springer.

Jackson, M.P.A., R.R. Cornelius, C.H. Craig, A. Gansser *et al.* 1991. Salt diapirs of the Great Kavir, Central Iran. *Geological Society of America Memoir* 177.

Jennings, J.N. 1975. Desert dunes and estuarine fill in the Fitzroy estuary (north-western Australia). *Catena* **2**, 215–62.

Job, C. 1978. Hydrochemical investigations in the area of al Qatif, al Hasa. In *Quaternary period in Saudi Arabia*, Vol. 1, S.S. Al-Sayari and J.G. Zötl (eds), 93–105. New York: Springer.

King, D. 1960. The sand ridge deserts of South Australia and related aeolian landforms of the Quaternary arid cycles. *Transactions of the Royal Society of South Australia* **83**, 99–109.

Lancaster, N. 1989. *The Namib sand sea: dune forms, processes, and sediments*. Rotterdam: Balkema.

Langford-Smith, T. 1960. The dead river systems of the Murrumbidgee. *Geographical Review* **50**, 368–89.

Langford-Smith, T. 1978. *Silcrete in Australia*. Armidale, NSW: Department of Geography, University of New England.

Langford-Smith, T. 1982. The Geomorphic history of the Australian deserts. *Striae* **17**, 4–19.

Langford-Smith, T. and G.H. Dury 1965. Distribution, character and attitude of the duricrust in the northwest of New South Wales and adjacent areas of Queensland. *American Journal of Science* **263**, 179–90.

Langford-Smith, T. and S.H. Watts 1978. The significance of coexisting siliceous and ferruginous weathering products at select Australian localities. In *Silcrete in Australia*, T. Langford-Smith (ed.), 143–65. Armidale, NSW: Department of Geography, University of New England.

Mabbutt, J.A. 1965. The weathered land surface in Central Australia. *Zeitschrift für Geomorphologie* **9**, 82–114.

Mabbutt, J.A. 1966. Landforms of the Western Macdonnell Ranges. In *Essays in geomorphology*, G.H. Dury (ed.), 83–119. London: Elsevier.

Mabbutt, J.A. 1968. Aeolian landforms in Central Australia. *Australian Geographical Studies* **6**, 139–50.

Mabbutt, J.A. 1977. *Desert Landforms*. Cambridge, MA: MIT Press.

Mabbutt, J.A. and M.E. Sullivan 1968. The formation of longitudinal dunes: evidence from the Simpson Desert. *Australian Geographer* **10**, 483–7.

Mainguet, M. 1968. LeBorkou, Aspects d'une modelé eolien. *Annales Geographie* **77**, 296–322.

Mainguet, M. 1972. *Le Modelé des grés*. Paris: Institut Geographique National.

Mainguet, M. 1978. The influence of trade winds, local air-masses and typographic obstacles on the aeolian movement of sand particles and the origin and distribution of dunes and ergs in the Sahara and Australia. *Geoforum* **9**, 17–28.

Mainguet, M. 1983. Tentative mega-morphological study of the Sahara. In *Mega-geomorphology*, R. Gardner and H. Scoging (eds), 111–33. Oxford: Clarendon Press.

Mainguet, M. and L. Canon, 1976. Vents et Paléovents du Sahara, Tentative d'Appreche Paléoclimatique. *Revue de Géographie Physique et de Géologie Dynamique*, **18**, 241–50.

Mainguet, M. and M.C. Chemin 1983. Sand seas of the Sahara and Sahel: an explanation of their thickness and sand dune type by the sand budget principle. In *Eolian*

sediments and processes, M.E. Brookfield and T.S. Ahlbrandt (eds), 353–63. Amsterdam: Elsevier.

Malay, Jean 1969. Le Nil: données nouvelles et essai de synthèse de son histoire géologique. *Bulletin Association Senegal et Quaternaire Ouest Afrique* **21**, 40–8.

McCauley, J.F., M.J. Grolier and C.S. Breed 1977. Yardangs. In *Geomorphology in arid regions*, D.O. Doehring (ed.), 233–69. Binghamton: Publications in Geomorphology.

McCauley, J., G.G. Schaber, C.S. Breed, M.J. Grolier *et al.* 1982. Subsurface valleys and geoarcheology of the eastern Sahara revealed by Shuttle radar. *Science* **218**, 1004–19.

McCauley, J., C.S. Breed, G.G. Schaber, W.P. McHugh *et al.* 1986. Paleodrainages of the eastern Sahara – the radar rivers revisited. *Institute of Electrical and Electronics Engineers, Transactions on Geoscience and Remote Sensing*, **GE-24**, 624–48.

McClure, H.A. 1978. Ar Rub 'Al Khali. In *Quaternary period in Saudi Arabia*. Vol. 1, S.S. Al-Sayari and J.G. Zötl (eds), 252–64. New York: Springer.

McKee, E.D. 1983. Eolian sand bodies of the world. In *Eolian sediments and processes*, M.E. Brookfield and T.S. Ahlbrandt (eds), 1–25. Amsterdam: Elsevier.

McKee, E.D., C.D. Breed and S.G. Fryberger 1977. Desert sand seas. In *Skylab explores the Earth*, 5–47, Washington, DC: National Aeronautics and Space Administration.

Mortimer, C. 1972. The evolution of the continental margin of northern Chile. *XXIV International Geological Congress, Montreal, Canada*, Section 8, 48–52.

Mortimer, C. 1980. Drainage evolution in the Atacama Desert of northernmost Chile. *Revista Geologica de Chile* **11**, 3–28.

Mortimer, C. and N. Sarič 1975. Cenozoic studies in northernmost Chile. *Geologische Rundschau* **2**, 395–420.

Oberlander, T.M. 1979. Characterization of arid climates according to combined water balance parameters. *Journal of Arid Environments* **2**, 219–41.

Ochsenius, C. 1977. El Pleistoceno en del Desierto de Atacama. Tropico de Capricornio. Doctoral Thesis, University of Sao Paulo.

Ochsenius, C. 1982. The Hologenesis of the Pacific coastal desert in the context of the South American Quaternary. *Striae* **17**, 112–31.

Ollier, C.D. 1977. Early landform evolution. In *Australia: a geography*. D.N. Jeans (ed.). London: St Martin's Press.

Ollier, C.D. and W.G. Tuddenham 1961. Inselbergs of Central Australia. *Zeitschrift für Geomorphologie* **5**, 257–76.

Paskoff, R.P. 1976. Sur l'origine du grand escarpement cotier du desert chilien. *XXIIII International Geographical Congress, Moscow, USSR, Abstracts* 1, 207–11.

Paskoff, R.P. 1977. Quaternary of Chile: the state of the research. *Quaternary Research* **8**, 2–31.

Paskoff, R.P. 1980. Late Cenozoic crustal movements and sea level variations in the coastal area of northern Chile. In *Earth rheology, isostacy, and eustacy*, N. Moerner (ed.), 487–95. New York: Wiley.

Patton, P.C. and R.B. Morrison 1991. Introduction to the Quaternary geology of the Colorado Plateau. In *Quaternary nonglacial geology: conterminous U.S.* R.B. Morrison (ed.), 373–8. Boulder, CO: Geological Society of America.

Peel, R.G. 1941. Denudational landforms of the central Libyan Desert. *Journal of Geomorphology* **4**, 3–23.

Pels, S. 1964. The present and ancestral Murray River system. *Australian Geographical Studies* **2**, 111–9.

Pels, S. 1969. Radio-carbon datings of ancestral river sediments on the Riverine Plain of south-eastern Australia and their interpretation. *Journal and Proceedings of the Royal Society of New South Wales* **102**, 189–95.

Renault, P. 1953. Caracteres généraux des grottes gréseuses du Sahara méridional. *Premier Congress Internationale de Spéléologie, Paris* **2**, 275–89.

Rognon, P. 1976. Essai d'interpretation des variation climatiques au Sahara depuis 40,000 ans. *Revue de Geographie Physique et de Geologie Dynamique* **18**, 251–82.

Said, Rushdi 1981. *The geological evolution of the River Nile*. New York: Springer.

Sarntheim, M. 1978. Sand deserts during glacial maximum and climatic optimum. *Nature* **272**, 43–6.

Schumm, S.A. 1968. River adjustment to altered hydrologic regimen – Murrumbidgee River and Paleochannels. *U.S. Geological Survey Professional Paper* 598.

Stoertz, G.E. and G.E. Ericksen 1974. Geology of salars in Northern Chile. *U.S. Geological Survey Professional Paper* 811.

Stringfield, V.T., P.E. LaMoreaux and H.E. LaGrand 1974. Karst and paleohydrology of carbonate rock terranes in semiarid regions, with a comparison to the humid karst of Alabama. *Geological Survey of Alabama Bulletin* 105.

Trewartha, G.T. 1981. *The Earth's problem climates*, 2nd edn. Madison, WI: University of Wisconsin Press.

Twidale, C.R. 1962. Steepened margins of inselbergs from north-western Eyre Peninsula, South Australia. *Zeitschrift für Geomorphologie* **6**, 51–69.

Twidale, C.R. 1978. On the origin of Ayers Rock, Central Australia. *Zeitschrift für Geomorphologie Supplement Band* **31**, 177–206.

Twidale, C.R. 1982. The evolution of bornhardts. *American Scientist* **70**, 268–76.

Twidale, C.R. and J.A. Bourne 1975. Episodic exposure of inselbergs. *Bulletin of the Geological Society of America* **86**, 1473–81.

Twidale, C.R. and J.A. Bourne 1978. Bornhardts. *Zeitschrift für Geomorphologie, Supplement Band* **31**, 111–37.

UNESCO 1977. *World distribution of arid regions*. Map 1:25 000 000. New York: United Nations.

Van de Graaff, W.J.E., R.W.A. Browe, J.A. Buntin and N.J. Mackson 1977. Relict early Cainozoic drainages in arid western Australia. *Zeitschrift für Geomorphologie* **21**, 379–400.

Veevers, J.J. and A.S. Rundle 1979. Channel country fluvial sands and associated facies of central-eastern Australia: modern analogues of Mesozoic desert sands of South America. *Palaeogeography, Palaeoclimatology, Palaeoecology* **26**, 1–16.

Wasson, R.J. 1983. Dune sediment type, sand colour, sediment provenance and hydrology in the Strzelecki-Simpson dunefield, Australia. In *Aeolian sediments and processes*, M.E. Brookfield and T.S. Ahlbrandt (eds), 165–95. Amsterdam: Elsevier.

Wells, S.G., L.D. McFadden and J.C. Dohrenwend 1987. Influence of late Quaternary climatic changes on geomorphic and pedogenic processes on a desert piedmont, eastern Mojave Desert, California. *Quaternary Research* **27**, 130–46.

Wernicke, B., G.J. Axen and J.K. Snow 1988. Basin and

range extensional tectonics at the latitude of Las Vegas, Nevada. *Bulletin of the Geological Society of America* **100**, 1738–57.

Wilson, I.G. 1971. Desert sandflow basins and a model for the development of ergs. *Geographical Journal* **137**, 180–99.

Wilson, I.G. 1973. Ergs. *Sedimentary Geology* **10**, 77–106.

Wopfner, H. 1974. Post-Eocene history and stratigraphy of northeastern Australia. *Transactions of the Royal Society of South Australia* **98**, 1–12.

Wopfner, H. 1978. Silcretes of northern South Australia and adjacent regions. In *Silcrete in Australia*, T. Langford-Smith (ed.), 93–141. Armidale, NSW: Department of Geography, University of New England.

Young, R.A. 1987. The Colorado Plateau: landscape development during the Tertiary. In *Geomorphic systems of North America*, W.L. Graf (ed.) 265–76. Boulder, CO: Geological Society of America.

PART TWO

WEATHERING

WEATHERING PROCESSES AND FORMS 3

B. J. Smith

INTRODUCTION

Recent studies of weathering in deserts (e.g. Goudie 1989, Cooke *et al.* 1993) have given detailed reviews of the mechanisms considered to operate and the landforms with which they are generally associated. Invariably such reviews – especially if orientated towards students – deal primarily with the perceived certainties of our knowledge. In reality, however, weathering studies are more characterized by uncertainties and gaps in knowledge. Weathering research is thus not a question of what we know about desert weathering, but what we do not know; those points we secretly hope will not be raised in lectures or paper presentations. This chapter will therefore concentrate upon some of the less certain issues in weathering studies. The aim is not to be exhaustive or comprehensive, but hopefully to question some traditionally held views and stimulate future research.

BACKGROUND TO WEATHERING STUDIES IN DESERTS

Because of difficulties of access and the harshness of desert environments, desert geomorphology has remained something of an infant science when compared with landscape studies in many other regions. Much work is still at the exploratory stage; the nature of desert environments is incompletely understood, and many features have yet to be described. Because of a comparative paucity of rigorous fieldwork, many geomorphological studies have relied upon the uncorroborated reports of explorers and upon data collected for other purposes. This has particularly applied to weathering studies where, for example, views on temperature and moisture regimes have been influenced by accounts of 'freezing nights' and 'splitting rocks'. Such reports understandably stress the environmental extremes encountered by travellers, but unfortunately extremes of temperature variability and absence of moisture have become widely accepted as the norm for all desert regions. This has in turn influenced our perception of how processes operate and encouraged a concentration upon the role of extreme events, be they the highest ever rock temperature or the longest period between rainfall. Because many desert weathering concepts were initially borrowed from other disciplines and because of the short history of enquiry, weathering studies have been riven by numerous arguments, revisions, and reinterpretations. Paramount amongst these controversies is the debate over the efficacy or even existence of insolation weathering, but it has also encompassed the weathering roles of both moisture and wind.

The recent emergence of desert weathering studies in any great number has coincided – at least in the English-speaking world – with a tendency in geomorphology to concentrate upon studies of process. Within weathering research there has also been a reductionist element whereby weathering mechanisms are reduced to the basic physical and chemical processes that control their operation. This is an inevitable consequence of a desire to understand geomorphic processes, but brings with it problems, some of which are particularly appropriate to weathering in deserts. First, the majority of *in situ* observations of weathering mechanisms tend to be short term and of restricted spatial extent. This creates problems as to their long-term significance in regions where few areas have been mapped in detail, and where little is known about medium- and long-term climatic variability. Second, process studies focus attention upon features that exhibit measurable change within the one or two years over which the fieldwork for most research projects is

Geomorphology of Desert Environments. Edited by Athol D. Abrahams and Anthony J. Parsons. Published in 1994 by Chapman & Hall, London. ISBN 978-94-015-8256-8

carried out. As a consequence, there are numerous studies of features such as cavernous hollows (tafoni) but few of, for example, the intervening cliff faces or the debris slopes below them. Third, the reductionist tendency has fostered a segregationist approach, wherein specific mechanisms such as insolation weathering, salt crystallization, or freeze–thaw are examined in isolation. This approach is prevalent in desert weathering investigations where there has been a reliance upon laboratory-based simulation studies. It is the aim, and the virtue, of these studies that they can examine a particular mechanism under controlled conditions. In doing this, however, environmental conditions may be unrealistically simplified and possible synergisms between weathering mechanisms and other geomorphic processes discounted. Finally, in common with other areas of geomorphology, we have yet to use our new-found understanding of weathering mechanisms successfully to explain either the present configuration of most desert landscapes or their long-term evolution. Process studies are only a limited end in themselves. If we are to justify our preoccupation with them we must ultimately breach the spatial and temporal boundaries that separate individual, short-term studies at the microscale from their cumulative impact on the landscape. If we fail to do this we betray the existence of geomorphology as a distinctive discipline.

Despite the above observation our understanding of weathering processes and environments and the landforms they produce has steadily progressed. Many of the early misconceptions concerning weathering have been dismissed or modified and we are beginning to understand some fundamental controls upon rock breakdown. For example, Cooke *et al.* (1992) have listed six observations that they consider should guide our understanding of weathering in deserts.

(a) Weathering processes (and presumably forms) are likely to be distinctive because of distinctive diurnal and seasonal temperature and relative humidity regimes.
(b) Contrary to popular belief, moisture for weathering is widely available, from rainfall, dew, and fogs.
(c) Relative humidity is often high at night.
(d) Physical processes are probably significantly more important than elsewhere, but the role of chemical processes should not be ignored.
(e) Some of the debris and weathering features seen today may well be inherited from different climatic conditions.
(f) Despite a common emphasis upon weathering landforms, the most important role of weathering is to provide debris for fluvial and aeolian systems.

Laudable as these observations are, they are, like all generalizations, open to question and qualification. It is these qualifications that will identify directions for future research.

THE ROLE OF TEMPERATURE

Discussions concerning the role of temperature in desert weathering have concentrated upon the extremes of diurnal variability, normally under summer conditions. Associated with this has been a preoccupation with the search for maximum ground surface temperatures (Goudie 1989; McGreevy and Smith 1982). These observations have in turn played an essential role in the design of laboratory simulation experiments of, for example, insolation and salt weathering. However, the use of extreme diurnal temperature regimes raises a number of questions. These concern their representativeness of weathering environments and the realism of using one temperature regime to characterize a complex climatic zone (Jenkins and Smith 1990). There is also the possibility that unrealistically high rock temperatures trigger weathering mechanisms for which there is no field evidence or which are additional to those aimed for in a particular simulation.

With regard to the first of these points, it has long been known, and frequently reiterated, that desert weathering concentrates in so-called 'shadow areas' (e.g. Evans 1970) to produce features such as cavernous hollows (tafoni), honeycombs, and pedestal rocks. Rock surface temperatures and diurnal ranges associated with these features are reduced compared with those on surrounding exposed surfaces (Dragovich 1967, 1981, Rögner 1987). Within these features moisture availability appears to be the critical control upon rock breakdown rather than extreme temperatures. Rapid, early morning temperature rises on exposed surfaces should inhibit absorption of any moisture deposited overnight and hence restrict the operation of processes such as hydration, solution, and hydrolysis. High rock temperatures may therefore not only be unnecessary but undesirable for many desert weathering processes.

There is also debate concerning the representativeness of many of the very high rock surface temperatures recorded, even for exposed surfaces. This has been reviewed in detail by McGreevy and Smith (1982, 1983), where it was noted that many early

Table 3.1 Selected rock surface temperature (°C) measurements from desert environments

Surface temperature °C	*Material*	*Location (altitude)*	*Time of year*	*Source*
74.4	Black bulb	Egypt	August	Williams (1923)
62	Limestone	Egypt	August	Sutton (1945)
49	Quartz Monzanite	California	August	Roth (1965)
72.5	Rock	Sudan	September	Cloudsley-Thompson and Chadwick (1969)
78.5	Basalt	Tibesti	August	Peel (1974)
79.3	Dark Sandstone	Tibesti	August	Peel (1974)
78.8	Light Sandstone	Tibesti	August	Peel (1974)
57	Basalt	Tibesti	March	Jäkel and Dronia (1976)
46	Granite	Tibesti	March	Jäkel and Dronia (1976)
48	Sandstone	Tibesti	March	Jäkel and Dronia (1976)
48.1	Limestone	Morocco	August	Smith (1977)
21.1	Limestone	Morocco	January	Smith (1977)
62	Asphalt	Abu Dhabi	Summer	Potocki (1978)
73	Asphalt	Abu Dhabi	Summer	Potocki (1978)
41.0	Basalt	Karakoram Mountains	July/August	Whalley *et al.* (1984)
33.5	Basalt	Karakoram Mountains	July/August	Whalley *et al.* (1984)
46.3	Desert Varnish	Karakoram Mountains	July/August	Whalley *et al.* (1984)
54.0	Sandstone	Karakoram Mountains	July/August	Whalley *et al.* (1984)
50.8	Limestone	Negev	August	Rögner (1987)
56	Rock	Algeria	June	George (1986)
52.2	Sandstone	Tenerife (2070 m)	June	Jenkins and Smith (1990)
42.5	Sandstone	Tenerife (2070 m)	January	Jenkins and Smith (1990)
35.0	Sandstone	Tenerife (950 m)	June	Jenkins and Smith (1990)
29.0	Sandstone	Tenerife (950 m)	January	Jenkins and Smith (1990)
50.0	Sandstone	Tenerife (50 m)	June	Jenkins and Smith (1990)
41.0	Sandstone	Tenerife (50 m)	January	Jenkins and Smith (1990)

measurements, often in excess of 70°C, were made when equipment was less sophisticated than that now used. Peel (1974), for example, used thermocouples without a 0°C datum, and Williams (1923) used a black bulb thermometer. With the advent of reliable thermistors and, more recently, infrared thermometers, many of the maxima recorded from a wide range of desert conditions are below 60°C (Table 3.1). Where 60°C is exceeded there may also be exceptional circumstance, such as the bitumen-coated road surfaces measured by Potocki (1978). The significance of these observations is that very high absolute temperatures and temperature ranges have invariably been used in, for example, salt weathering simulation studies. Data from similar tests used for assessing building stone durability have shown that rates of breakdown are closely related to the maximum temperatures to which samples are heated. Minty (1965) showed that when samples of dolerite were cycled in sea water between 105 and 110°C the rate of disaggregation was approximately 40 times greater than when similar samples were cycled between 48.9 and 65.6°C. Other workers have also noted that the type of damage caused during salt crystallization durability tests varies with different heating cycles. Marschner (1978) found that damage was restricted to surface layers in samples heated to 60°C but that deeper cracking occurred in samples heated to 105°C. The critical nature of the 60 to 70°C range was also demonstrated by Yong and Wang (1980), who found that microcracking could be initiated in granite only after samples were heated above 60 to 70°C. Thus, as pointed out by McGreevy and Smith (1983), the use of very high rock temperatures in simulation experiments of salt crystallization under 'desert conditions' may enhance breakdown by increasing crystallization pressures, ensuring complete crystallization from solution and perhaps better crystal development, and by instigating purely thermal effects such as thermal expansion of salts and/or thermal fracturing of the rock itself. Thus, by subjecting rocks to unnaturally high temperatures, especially for salt weathering environments, it may not be possible to limit or identify the mechanisms responsible for any breakdown. There may also 'be the danger of introducing thermal effects which

would not be encountered in nature' (McGreevy and Smith 1983, p. 300). Laboratory studies which use extreme temperature cycles to produce insolation weathering (e.g. Rodriguez-Rey and Montoto 1978) must therefore be approached with considerable caution.

The use of diurnally based thermal cycles in laboratory-based weathering simulations also presupposes that this is the primary variable in influencing physical breakdown. Yet, as noted by Cooke *et al.* (1993), there can also be significant seasonal variations in temperature. Under winter conditions freezing temperatures may be frequently experienced at rock surfaces and freeze–thaw activity becomes a possibility. Both seasonal and diurnal variability are clearly systematic, but superimposed upon these are other degrees of spatial and temporal variability which, although far less predictable, may be of considerable significance. Air and rock temperature reductions within caverns have already been noted, but to these must be added other aspect-related differences. This applies not only to obvious variations between north- and south-facing slopes, but also between east- and west-facing slopes. On these slopes any overnight moisture should be retained for longer in low latitudes on those facing west. This moisture is then rapidly driven off as the slopes come out of shadow and experience rapid rock temperature rises and accentuated internal temperature gradients when heated by a sun already high above the horizon (Smith 1977).

Added to these effects must be the amelioration of rock temperature regimes resulting from maritime influences in coastal deserts, and a variety of effects associated with increasing altitude. Unfortunately, there have been relatively few studies of rock temperature variations in high altitude desert areas, but those that have been made have recorded surface maxima similar to those observed in low altitude environments (e.g. Whalley *et al.* 1984). These high surface temperatures frequently occur in conjunction with low air temperatures, and any interruption of incident radiation can result in rapid falls in surface temperatures. This phenomenon was recently illustrated by Jenkins and Smith (1990) in a study of altitudinal and seasonal variability in daytime temperatures on the island of Tenerife. By continuous measurement of surface temperatures on a standard sandstone block moved between three sites at different altitude, they showed that at an altitude of 2070 m there were numerous short-term fluctuations of 3 to 15 minutes duration related to shading by a light cloud cover and wind speed variations. During these fluctuations surface temperatures could drop up to 15°C with temperature gradients sometimes in excess of 2°C per minute. At mid-altitude (950 m) and coastal (50 m) sites, where cloud cover was greater, additional fluctuations of 1 to 2 hours duration were noted which effectively destroyed the daytime element of any generalized diurnal temperature curve. The frequency and intensity of these short-term variations suggests that they could play an important role in disruptive processes such as granular disintegration and the formation of thin surface flakes. Generally these short-term fluctuations have either failed to register when desert temperatures were recorded at set intervals (every 15, 30 minutes, etc.) or have been disregarded in insolation and salt weathering simulations based upon diurnal cycles of heating and cooling or wetting and drying. It is interesting to note, however, that in one of the few sets of experiments to register detectable alteration (using reflectance and microhardness changes) resulting from thermal fatigue (insolation weathering), the heating and cooling cycle was of only 15 minutes duration (Aires-Barros *et al.* 1975, Aires-Barros 1977, 1978).

Patterns of thermal stress experienced by desert rock surfaces are thus exceedingly complex. In addition to seasonal and diurnal cycles there are various short-term fluctuations related to local weather conditions (wind, cloud cover, air temperature, and cooling by rainfall). Superimposed upon these are a range of 'shadow effects' related not only to generalized aspect but to shading within hollows at a variety of scales by local topographic irregularities (boulders, etc.) and vegetation. Any laboratory assessment of the effectiveness of thermally related weathering mechanisms in deserts (insolation, salt, and frost weathering specifically) should take this variability into account. Recognition of the range of stresses to which rocks are subjected suggests that rarely, if ever, is rock breakdown a function of a single mechanism acting in isolation. Invariably it is a product of two or more mechanisms acting together or in alternation (Jenkins and Smith 1990). The most obvious example of this is insolation weathering itself. It is difficult to envisage any situation in which desert rocks are subjected to temperature fluctuations in isolation. It has already been noted that moisture is universally available in some form within hot deserts (see also next section). Additionally, all rocks exposed at desert surfaces will have experienced a unique stress history which will have left them weakened to a greater or lesser extent, and more or less susceptible to either mechanical breakdown or chemical decay. Possible excep-

tions may be some chemical precipitates such as certain silcretes, but even these rarely form at the desert surface.

Sources of pre-stressing in desert rocks are numerous. They include chemical alteration, either under present conditions of limited, but assured, moisture availability or inherited from former periods of moister climate; dilatation acting at a range of scales; and previous subjection to mechanical weathering processes such a salt and frost weathering. Frost weathering is particularly relevant when one considers that mountains consistently constitute the dominant terrain type in the world's major desert areas. A study by Fookes (1976) identified, for example, 43% of the Sahara desert, 39% of the Libyan Desert, 47% of Arabia, and 38.1% of the deserts in the south-western United States as mountainous. Other studies of desert terrain (e.g. Cooke *et al.* 1982) also identified a range of mountain–plain models as the most representative of the world's desert landscapes. Within these models most debris mantling alluvial fans and plains is derived initially from adjacent mountain catchments, where moisture may be more readily available and temperatures can frequently fall below 0°C. Debris produced under these conditions is likely to carry with it inbuilt stresses that can be exploited by other weathering processes more characteristic of hot desert environments *per se*.

Potentially exploitable weaknesses in the form of microfractures can also be created within the rock mass prior to exposure. These will then be carried over into any debris derived from these rocks. The range of microfractures found within near-surface rocks has been discussed by Nur and Simmons (1970) and Simmons and Richter (1970), and was summarized by Whalley *et al.* (1982a) as consisting of (a) cracks at grain boundaries produced during ascent to the Earth's surface; (b) stress-induced cracks produced by the principle of non-hydrostatic stress; (c) radial and concentric cracks about grains enclosed by material with different volumetric properties; (d) tube cracks produced by magmatic fluid solution, dislocation, etching, etc.; (e) cracks induced by thermal shocks and gradients; and (f) cleavage cracks. To these crack-opening processes should be added potential weathering lines comprised of, for example, certain mineralogical concentrations.

Understandably, microfractures and lines of potential weathering are normally associated with igneous and metamorphic rocks. Stress relief does, however, also occur within sedimentary rocks, where unequal release of confining pressures by erosion of once deeply buried rocks can lead to exfoliation and splitting (e.g. Bradley 1963). Similarly, sedimentary and metamorphic rocks can contain a wide range of different lineations associated with stylolites, cleavage, and bedding plains and alignments of grain boundaries and/or voids even in apparently unbedded sandstones (e.g. Smith and McGreevy 1988).

Weathering susceptibility is also influenced by alteration skins, rock varnish (see Chapter 6) and case-hardened layers (e.g. Conca and Rossman 1982) which frequently cover desert rock surfaces. Indeed it is not unknown for the presence of rock varnish, and consequently reduced albedo, to be used as a justification for the high rock surface temperatures recorded in deserts (e.g. Peel 1974). Should it not, therefore, be reasonable to explore the possibility of insolation weathering occurring in the presence of such crusts? Work on other materials such as concrete has shown that durability problems frequently occur because of expansion in materials with different surface layers. This can lead to patterns of rupture redolent of those found on desert rocks (Fig. 3.1).

Within rocks exposed to insolation, a wide range of potential weaknesses thus exists that can be exploited during thermally induced surface expansion and contraction. Folk and Begle-Paton (1982) and Rice (1976) have pointed out that the early experiments of Blackwelder (1925, 1933) and Griggs (1936) may have been more successful in producing fatigue failure if they had used larger blocks that were in some way confined. Similarly, such experiments may have produced a more realistic assessment of fatigue weathering in deserts if they had used samples characteristic of those exposed by erosion and transport at desert surfaces; rather than freshly quarried blocks selected for their purity, freedom from imperfections and absence of recognizable weathering.

Studies of other weathering processes have also identified the significance of physical and chemical variability in rocks as catalysts to breakdown. Experiments using 'coupled' samples of two rock types exposed to simulated salt weathering conditions have, for example, shown how moisture can be retained for longer at boundaries between different stone types. This can lead ultimately to a concentration of crystallized salt, if available, and enhanced disaggregation (Haneef *et al.* 1990a, b). Other salt weathering simulations (McGreevy and Smith 1984) have shown how the presence of swelling clays in sandstone samples, coupled with increases in microporosity, can enhance breakdown through flaking.

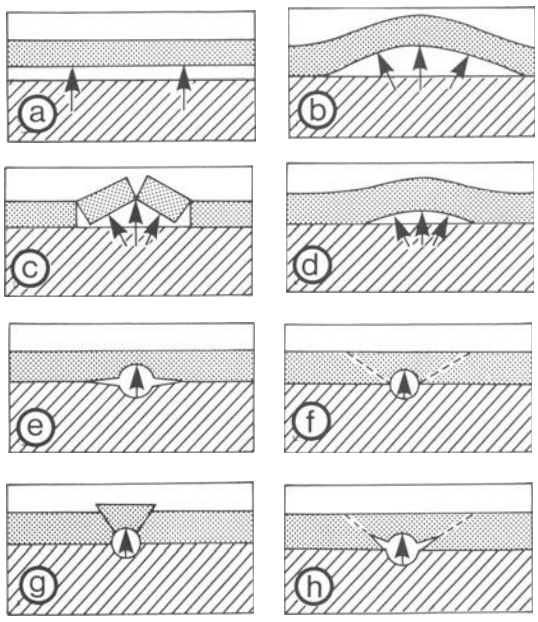

Figure 3.1 Typical failure patterns in an elastic outer layer on a rigid base due to forces concentrated at the interface. a–d illustrate force concentrated along the interface, e–f illustrate force exerted through expansion at a point. a, parallel separation of rigid plate; b, peeling from base; c, bending – plastic failure; d, bending – elastic sudden failure; e, cleavage – sudden failure; f–h, punching or pop-out failure – pattern of failure depends upon brittleness of outer layer. At high brittleness numbers failure occurs suddenly (f). At low brittleness material behaves in a ductile fashion (g). At intermediate brittleness failure occurs through stable crack growth (h) (adapted from Bache 1985).

Exploitation of potential cracks comprising aligned grain boundaries and pores in sandstones may be a factor in salt-induced contour scaling of sandstones (Smith and McGreevy 1988). Breakdown following the cyclical wetting and drying of basalts has similarly been attributed to the swelling of hydrothermally derived smectite clays (McGreevy 1982a). More systematic studies of the physical rock properties that influence mechanical breakdown have identified water absorption capacity, porosity and microporosity, saturation coefficient, and tensile strength as amongst the most important properties (Cooke 1979). Compressive strength, specific gravity, compactness, hardness texture, shape, anisotropy, microfractures, and cleavage as characteristics that influence rock durability can also be added (Fookes *et al.* 1988). Additional factors which are of specific relevance to insolation weathering are variations in thermal properties such as albedo, specific heat capacity, and thermal conductivity. These not only influence rock surface temperatures and internal temperature gradients (Kerr *et al.* 1984, McGreevy 1985), but also the establishment of other internal stresses as rock constituents with varying thermal properties, including additions such as clays and salts, expand and contract differentially. Natural differences in all these rock properties, and variability induced by earlier physical and chemical weathering, must contribute greatly to the variable breakdown of rocks exposed to hot desert conditions. The presence of physical variability, pre-stressing, and chemical alteration within rocks is one possible explanation of why insolation weathering continues to find support from field studies (Ollier 1963, 1984). The fact that laboratory simulations using unconfined, freshly cut and polished blocks have historically discounted thermal fatigue may find an explanation in that they did not continue for long enough, or that the weathering that did take place was not detected (Goudie 1989). This last point will be discussed further towards the end of the chapter.

THE ROLE OF MOISTURE

The role of moisture in shaping desert environments has for many years appeared anomalous. On the one hand, deserts are perceived as areas of little if any moisture, while on the other we are faced with landscapes in which many elements are of patently fluvial origin. For many years explorers denied these origins by invoking other processes including: 'sculpture due to solar heat shattering the rocks and wind removing the pulverised residue' (Peel 1975, p. 110). But as understanding of fluvial processes progressed through the early part of this century, alternative explanations became necessary. Many fluvial features were thus interpreted either as legacies from some former climate of more assured rainfall, or as products of infrequent but intense rainfall operating over long timespans. It is only relatively recently that alternative viewpoints have been explored in which moisture is seen as being more readily available in many hot deserts than previously surmised (e.g. Peel 1975, Goudie 1989). In his paper on water action in deserts, for example, Peel referenced Slatyer and Mabbutt (1964) who found that intense, 'catastrophic' rainfall of the kind traditionally associated with deserts is much more common around the margins of deserts. In a survey of various deserts, they found that 50% of the rain that falls usually occurs in gentle showers of moderate intensity. Similarly, Peel drew on observations

by Dubief (1965) who showed that mean rainfall intensities over the whole of the Sahara are little higher than those in France. Rainfall of lower intensities is less likely to generate overland flow, more likely to be absorbed by rocks and soil, and will most probably play a more important role in promoting a range of weathering processes. In his review of desert weathering, Goudie (1989) tabulated data from a range of world deserts which demonstrate that even in 'quite dry locations there may be an appreciable number of days in which measurable quantities of rain are received' (p. 15). Frequent wetting enhances the efficacy of both mechanical and chemical weathering processes.

Rainfall can also concentrate locally within the environment and thus might lead to enhanced scope for weathering in certain situations. Apart from obvious orographic controls, it seems that there may be a spatial organization to desert storms (e.g. Sharon 1981) related to phenomena such as Rayleigh cells within the atmosphere, although there is no significant long-term tendency for storms to occur at preferred locations. However, local rainfall is not randomly scattered and there is evidence that it can concentrate in valley areas which also receive rainfall deflected away from exposed interfluves by higher winds (Sharon 1970). Windward slopes will likewise receive substantially more rainfall than adjacent leeward slopes. Yair *et al.* (1978) suggested that windward slopes of 20° with incident rainfall of 40° would receive almost twice as much rainfall as opposing valley sides. Similar observations were made in Sinai by Schattner (1961) who noted that granular disintegration of granites was more rapid and penetrated more deeply on rocks that were not exposed to the 'strongest and largest insolation' (p. 254). Instead, disintegration is most intensive on surfaces facing north and west into the dominant rain-bearing winds. South-facing slopes, he found, rarely exhibited intensive disintegration.

The degree to which water is concentrated into certain areas is also dependent upon surface controls, such as the extent of soil and rock cover. Where bare rock dominates, surface runoff is more frequent and extensive, and infiltration concentrates in certain parts of catchments, such as slope foot zones of colluvial accumulation (Yair and Berkowicz 1989). Because of between-catchment differences in hydrological response, Yair and Berkowicz (1989) suggested that climatic parameters such as temperature and rainfall alone provide insufficient indication of ground surface aridity.

Both Peel (1975) and Goudie (1989) drew attention to the importance of moisture from fogs. Goudie tabulated the relative contributions of rainfall and fog as moisture sources at Gobabeb in Namibia over the period 1963–84. He found that rainfall averaged 24.5 mm and fog 31.7 mm per annum. More universally appreciated is the contribution that direct precipitation in the form of dew can make to the moisture budget of desert areas (Verheye 1976). Little is known in any detail of dewfall from many of the world's deserts, and most opinions concerning its significance have been based upon pioneering work by Duvdevani (e.g. 1947, 1953) and Evenari *et al.* (1971) in Israel, especially at the ancient city of Avdat in the Negev Desert. On occasions they reported that dewfall can exceed annual rainfall (28.4 mm as opposed to 25.6 mm in 1962–63), but over the four-year period 1963–66 mean dewfall at the ground surface was 33 mm from an average of 195 dew nights and, at a height of 100 cm, 28 mm from 172 dew nights. This compares with an average annual rainfall at Avdat of 83 mm for the period 1960–67 (Evenari *et al.* 1971, p. 30). Clearly these figures suggest that although dewfall is frequent, the amounts per night are small and are a product of low ground surface temperatures and low moisture contents of the contact zone rather than high levels of air moisture (Verheye 1976). None the less, Verheye pointed out that such moisture is important as one of the main promoters of biological life in deserts. Similarly, it has not prevented the invocation of direct precipitation as a major moisture source and key component in the accentuated weathering associated with features such as tafoni and other cavernous hollows (e.g. Smith 1978, Rögner 1988a) and in low-lying areas (e.g. Schattner 1961). The weathering significance of dew is further enhanced by its chemical composition. This is largely a function of the aerosols and dissolved salts that it can scavenge from the atmosphere as well as any dry fallout previously deposited on to rock surfaces and mobilized during condensation of dew. The greatest potential for this mobilization is normally associated with polluted urban environments (e.g. Wisniewski 1982, Ashton and Sereda 1982). What observations there are from arid to semi-arid areas have, however, also shown markedly enhanced concentrations of calcium, bicarbonate, and sulphate ions in dewfall compared with rainfall (Yaalon and Ganor 1968). The most likely source for these ions is sea salts, but chemical analysis of airborne dusts blowing from desert areas suggests that they can contain elevated concentrations of numerous minerals. These include a range of clay minerals and soil nutrients (e.g. Wilke *et al.* 1984) as well as salts (Pye 1987, table 6.3, p. 130).

Before ascribing too much importance to dewfall for rock weathering, certain other factors must be considered. First, the information we do have is drawn from meteorological observations which are not necessarily relevant to conditions experienced at rock surfaces under a wide variety of local topographic conditions. Second, we have little knowledge of the controls that humidity conditions exert upon weathering (McGreevy and Smith 1982). Is, for example, all moisture that condenses at a rock surface absorbed and, if so, what role does it play in mobilizing salts?

Meteorological observations are normally collected to reflect standard conditions, with figures invariably averaged over a given time period. The figures for dewfall at Avdat (only 80 km from the Mediterranean) are, for example, given in Evenari *et al.* (1971) as annual averages showing higher deposition at ground level than at 100 cm. Duvdevani (1953) showed, however, that under dry summer conditions dew deposition at various sites in Israel increases from ground level upwards – his so-called 'arid gradient'. It is only during moist winter months, when moisture can be drawn up from below, that dew deposition is greatest nearer the ground.

The mechanism of moisture deposition can itself be complicated. Under clear sky conditions with rapid radiative heat loss at night, surface temperatures can fall below ambient air temperature. As they do so, condensation will occur at relative humidities progressively below 100%, especially if hygroscopic salts are present (Arnold 1982). Moisture flux from atmosphere to rock surface may, however, take place first in the vapour phase within pores before dew point is reached and before spontaneous condensation of liquid water. In his review of condensation–evaporation cycles in capillary systems, Camuffo (1984) suggested that condensation begins with an adsorbed film of molecular moisture. This can form at relative humidities below 100% because 'the binding forces between the water molecules and the solid surface are larger than the binding forces between the first adsorbed layer and newly arriving vapour' (p. 152). As relative humidity in the environment increases, further molecular layers can accumulate which may eventually collapse under gravity into larger pores and take on 'bulk-liquid structure'. Such patterns of deposition have been observed within buildings (e.g. Camuffo 1983) under conditions which are otherwise effectively arid. Advantages of this mechanism are that it can promote deep moisture penetration, carrying with it gases scavenged from the atmosphere, and that moisture absorption occurs very frequently (Camuffo 1983). Such relatively small quantities of moisture may also be important in fractured rocks where, if it can form near crack tips, it may generate stresses through the formation of an electrical double layer (Ravina and Zaslavsky 1974).

As rock surface temperatures fall overnight and the relative humidity of air in contact increases, eventually a point is reached where surface condensation occurs. Whether such moisture is absorbed by the rock will depend on pore size and geometry. In the case of a small, hemispheric cavity facing the external environment (Fig. 3.2a) it will remain empty except for the monolayer of moisture until the radius of the meniscus of condensed moisture r_m equals the pore radius r_p, after which the cavity will progressively fill with moisture. This process works in reverse when relative humidity falls and the cavity progressively empties. In the case of large 'spheric pores' which open to the atmosphere via a small opening (Fig. 3.2b), the cavity remains empty until relative humidity reaches a critical level where r_m equals r_p. Thereafter the cavity will completely fill with no increase in relative humidity. If relative humidity subsequently falls, however, the pore will remain filled until a critical relative humidity is

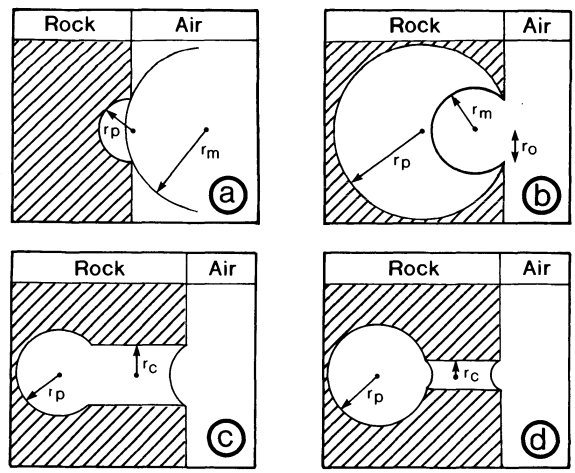

Figure 3.2 Influences of pore and capillary characteristics upon moisture deposition and condensation at a rock–air interface. r_p = pore radius, r_m = radius of meniscus of liquid water (which increases with relative humidity such that $r_m = \infty$ at RH = 100%), r_c = capillary radius. (a) Hemispherical cavity facing large pore or external environment; (b) spheric cavity open to the environment through a small hole; (c) pore connected to environment by wide capillary ($r_c > r_p/2$); (d) pore connected to environment by narrow capillary ($r_c < r_p/2$) (adapted from Camuffo 1984).

reached where r_m equals r_o, the radius of the opening, which then triggers evaporation of moisture. Where pores are connected to the atmosphere via capillaries, the pattern of filling and emptying depends upon the ratio of the pore radius r_p to that of the capillary r_c. Where $r_c > r_p/2$ (Fig. 3.2c) condensation occurs first in the pore and then in the capillary. On the other hand, where $r_c < r_p/2$ (Fig. 3.2d), condensation will occur within the capillary, trapping air within the pore. This trapped air can act as an effective block against further moisture ingress even though relative humidity may rise above 100%. Camuffo (1983) pointed out in fact that in rocks with pores showing this 'ink-bottle effect' the only way to fill inner cavities with moisture would be to submerge them in liquid water, although some moisture may be 'sucked in' if temperature falls and trapped air contracts. Conversely, if temperature were to rise, trapped air could expand and expel water without evaporation.

Drying does, however, normally involve evaporation. This occurs in two stages (Hall *et al.* 1984). In the first stage, drying is strongly influenced by both temperature and wind speed. A 10°C rise in temperature will approximately double the drying rate, as will a quadrupling of wind speed. The drying rate in the first stage is also directly proportional to relative humidity. A second phase will eventually be reached when the drying rate declines substantially. During this phase drying is not significantly affected by humidity. Towards the later stages of drying in a porous body 'liquid phase capillary continuity is lost and vapour phase diffusion no doubt becomes the only transport mechanism within the pores' (Hall *et al.* 1984, p. 18). A similar situation can be reached earlier under conditions of either very rapid surface moisture loss or where the rate of evaporation is greater than the rate of replenishment of capillary moisture from within the rock (Amoroso and Fassina 1983, Lewin 1981). Under these conditions work on building stones has shown that the liquid-to-vapour transition will occur at some depth below the rock surface. This can have very significant implications if the moisture contains dissolved salts, which will begin to crystallize out of solution at this depth as a subflorescence (Fig. 3.3a). Growth of crystals at this wet–dry interface has been found experimentally by Lewin and Charola (1979) to cause the outer surface of stonework to separate or crumble (also reported in Amoroso and Fassina 1983, pp. 33–34). If the rate of drying is less than that of moisture replenishment from within the stone (Fig. 3.3b), then evaporation will take place from the surface and an efflorescence of crystallized salt will develop. Under these conditions observations on the behaviour of building materials suggest that disruption will be reduced compared with subsurface crystallization (Amoroso and Fassina 1983, p. 29).

Under desert conditions, salt-rich moisture migrating from within a rock is most likely to derive from rising ground water. Indeed, ground water is now recognized by many as a major source of moisture and salts in numerous low-lying and/or coastal desert areas. It has, for example, been identified as a major cause of building decay in these areas as well as being instrumental in the formation of many natural salt weathering phenomena such as tafoni and honeycombs (see Cooke *et al.* 1982, Chapter 5 for a review). In urban areas from other environments, rising damp is seen to produce characteristic weathering zones above ground level (e.g. Arnold 1982), with maximum deterioration in a periodically dried zone some distance above the ground. Experimental work has also demonstrated the rapid effectiveness of salts derived from rising capillary moisture in causing rock breakdown in tests lasting just two weeks and drying conditions of only 20°C and 60% relative humidity (Lewin 1981). Salts deposited from ground water are often complex mixtures and occur in high concentrations (e.g. Goudie and Cooke 1984). As a consequence, these salts can exploit a wide range of environmental conditions to exert stresses within rocks through repeated expansion and contraction. Complete pore-filling by salts enhances the efficacy of differential thermal expansion, whereas mixtures of salts acting singly or synergistically hydrate and dehydrate or dissolve and crystallize across a wide range of temperature and humidity conditions.

Most desert environments are not, however, characterized either by an abundance of salts or of moisture. Instead, as already argued, moisture is frequently derived in small amounts from direct precipitation overnight at or near an exposed surface from where it is lost during the following day. Under these conditions large quantities of salt might even inhibit certain disruptive forces by acting in effect as a 'passive pore-filler' which prevents ingress of small quantities of moisture (Smith and McAlister 1986). Under conditions of limited moisture availability it might be expected that differing internal salt distributions might occur. Experimental work by Smith and McGreevy (1988) has shown that where sandstone blocks receive limited, daily applications of weak salt solutions to one face, salts preferentially concentrated in response to diurnal heating and cooling between approximately 20°C and 52°C. The precise disposition of crystallized salts

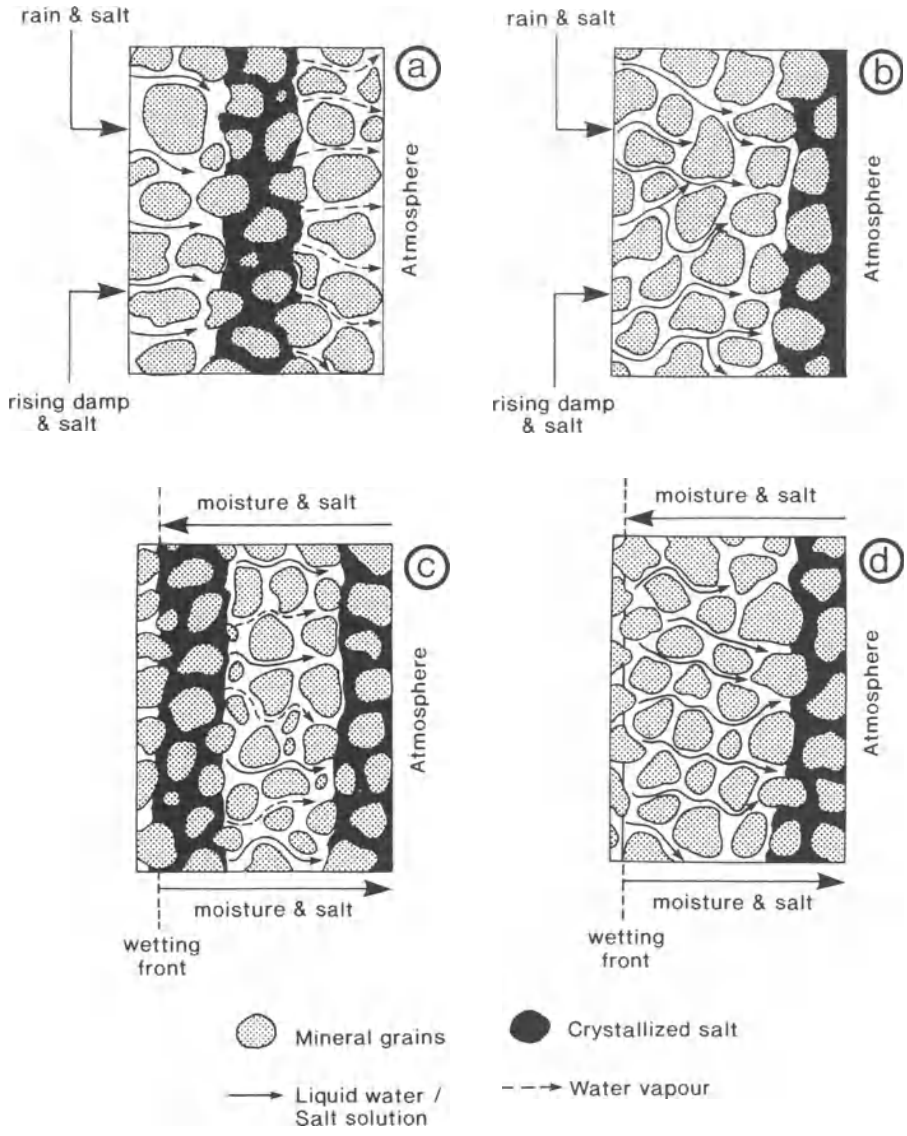

Figure 3.3 Patterns of salt crystallization within a porous rock: (a) subsurface deposition where there is a high rate of surface evaporation and salt solution drawn from within the rock; (b) surface deposition where the rate of evaporation is less than the potential rate of outward salt solution migration; (c) surface and subsurface salt deposition after evaporation of surface-wetted rock (sodium sulphate, magnesium sulphate); (d) surface salt deposition after evaporation of surface-wetted rock (sodium chloride).

appears to depend upon salt type. In blocks treated with 10% solutions of sodium sulphate and magnesium sulphate, accumulations occurred at or near the approximate diurnal wetting depth and just below the surface (Fig. 3.3c). This segregation is thought to result from the outward migration of some salt in solution during the early stages of drying, followed by a transition to vapour transfer before all of the salt is brought to the surface. Loss of moisture during this transition appears to concentrate the salt solution to the point where salts crystallize. During the next wetting phase the salt retained at depth is mobilized again and migrates down towards the wetting front. In this manner salt progressively accumulates at depth, while at least some always reaches the surface to crystallize as an

efflorescence. In a block treated with the more soluble sodium chloride, however, salt was only seen to accumulate in a narrow zone at and beneath the stone surface (Fig. 3.3d). This surface accumulation in all blocks was associated with varying degrees of granular disintegration of the sandstone and production of a rock meal. Where salts accumulated at depth they eventually resulted in contour scaling, with scales 1 to 2 cm thick lifting away from the block surface.

Similar suggestions of scaling being associated with wetting depths were made by Dragovich (1969) working on granites in Australia. This explanation would not seem to account, however, for the thinner, multiple flakes of 1 to 2 mm thickness which are often seen breaking away from, for example, the walls of cavernous hollows. No satisfactory explanation of these 'booklets' of flakes has yet been forthcoming. If they are associated with variable wetting depths it could imply that salt-induced rupture can occur over relatively few wetting and drying cycles especially if, perhaps, the subsurface layer has already been weakened during the formation of a thicker contour scale.

Clearly, the effectiveness of any salts precipitated out of solution in causing rock breakdown is not solely a matter of where they crystallize. It must also depend on the manner of their crystallization and the stresses that they can exert from within pores and capillaries on surrounding mineral grains. The process of crystal growth out of solution itself is considered by many to be the most important mechanism by which stresses are exerted and rock fabric disrupted (Cooke *et al.* 1993). A situation is normally envisaged where crystals bridge across a pore and continue to grow against confining pressures provided there is a film of solution at the salt–rock interface (Correns 1949). Observations of crystallized salts within pores from a range of environments suggest that pore-filling begins with a layer of salts crystallizing around the boundary of the pore. Bernardi *et al.* (1985), for example, identify authigenic calcite and gypsum growing around ooliths in limestones from the Ducal Palace in Urbino. These salts come into contact first either in capillaries or the narrow necks connecting pores. By concentrating stresses here they could cause disruption without the necessity either for pore-bridging or pore-filling. Indeed, although there are now numerous descriptions of salt efflorescences from many environments and of subfluorescences exposed when blisters are removed, there are few, if any, examples of pore-bridging within sound rock. Long, acicular gypsum crystals have been frequently described growing out of carbonaceous nucleii (e.g. Del Monte and Sabbioni 1984, Del Monte *et al.* 1984, Del Monte and Vittori 1985). But these are observed growing on the surface of polluted stonework or subsequently under moist laboratory conditions from sources such as fly-ash.

As an alternative to partial pore-filling by crystalline salts, relatively rapid evaporation under laboratory conditions can fill pores with microcrystalline salts (e.g. Smith and McGreevy 1988). Complete pore-filling of this kind may cause breakdown by crystallization if salts continue to migrate towards the pore, but will also result in stresses due to differential thermal expansion and/or hydration if environmental conditions and salt types permit it (Stambolov 1976, Sperling and Cooke 1980a, b).

The areal distribution of salt accumulation and ultimately salt-induced decay is very dependent upon the wetting and drying characteristics of stone surfaces. Varying pore size and shape characteristics will, as already discussed, lead to differing patterns of moisture condensation, absorption, and loss as well as affecting susceptibility to various salt weathering mechanisms. Variability of this kind has often been used, but with little evidence, to explain the location of so-called sidewall tafoni on cliff faces (e.g. Bryan 1925, Mustoe 1983). In contrast, basal tafoni are normally ascribed to greater moisture availability in cliff foot zones from either groundwater seepage or enhanced direct precipitation near ground level (Dragovich 1967, Smith 1978). Once created, any hollows protected from rainfall become sites of preferential salt accumulation and, it has been proposed, sites of accelerated weathering related to higher average levels of relative humidity and protection from direct insolation (see previous section). This proposition, however, has always required that at some stage moisture is evaporated from within the rock. This may be achieved through insolation reaching the interior of the hollow later in the day or through a general rise in air temperatures and fall in relative humidity. The former is special pleading, while the latter would be unlikely to produce the rapid evaporation required for salt crystallization beneath the rock surface. Work on building stone decay has suggested that rapid drying might be achieved in honeycomb features through air turbulence related to strong winds (Torraca 1981). Differential drying on more uniform surfaces may also be related to consistent local patterns of air turbulence and is reflected on many buildings in polluted areas by the uneven distribution of black gypsum crusts. Unfortunately, little systematic work has been carried out on wind-

related drying patterns, salt accumulation, and rock breakdown in urban or desert environments.

It would seem, therefore, that moisture is available for weathering in deserts from a variety of sources. Often this moisture is spatially concentrated, but although it may occur frequently (e.g. as dewfall), it is normally available in limited quantities. The concentration of weathering in shadow zones where moisture is retained the longest rather than in areas experiencing the highest rock surface temperatures suggests that moisture availability is the critical control upon processes such as salt weathering in deserts.

CHEMICAL WEATHERING AND CLIMATIC INHERITANCE

It is appropriate to consider these two aspects of desert weathering together. Most debate about chemical weathering in deserts concerns the question of how much can be attributed to present-day climatic conditions and how much is inherited from past conditions of greater moisture availability. Conversely, the presence of chemical decay in desert areas is often used to support the existence of former pluvial conditions. The best-documented use of this reasoning is the work of climatic geomorphologists such as Büdel, who proposed a climatogenetic interpretation of desert landscapes which combined them with tropical savanna and rainforest areas as a zone of Tropical Planation (e.g. Büdel 1982, pp. 120–85). Of paramount importance in this planation process is prior deep weathering, which he envisaged as having occurred at some stage across the whole zone. According to Büdel, most of the deeply weathered material has been removed from present-day desert areas under a geomorphic regime in which long-term fluvial erosion and aeolian deflation exceeds debris supply through weathering. Because of this, much of the evidence of former deep weathering consists not of weathered profiles but of the gross similarity between, for example, the inselberg and plain landscape of tropical West Africa and that of the Sahara to the north. Morphological evidence of this kind must be approached with caution, especially in light of the great antiquity of the land surfaces in these areas and the likelihood of morphological convergence towards landforms and landscapes conditioned by geological controls. In addition, there are few studies and a relatively poor understanding of what constitutes chemical weathering under hot desert conditions and the extent to which chemical processes are currently active in desert environments.

The clearest evidence that chemical weathering occurs in hot deserts is the already stated argument that moisture is readily available. This is supported by the widely held belief that salt weathering constitutes the principal mode of rock breakdown (e.g. Cooke and Smalley 1968, Evans 1970, Goudie 1985) which presupposes a major role for moisture absorption by rocks. Indeed, it is arguable whether certain salt weathering mechanisms are not themselves partly chemical in nature. Thus Winkler (1987a), writing about the distinction between chemical and physical weathering, made the point that

'On both natural outcrops and urban buildings the process (weathering), turns out to be more complex, and not readily separable into chemical and physical components. Where can we draw the line between crystallization and hydration pressure, as these are physiochemical processes? There is also evidence of chemical reaction between salts in the masonry and the masonry substance (Arnold 1981) leading to new compounds. Today we still do not understand the physical behaviour and chemical effect of water trapped in capillaries under pressure in most types of stone' (p. 85).

Despite the presumption that desert environments are not conducive to chemical weathering, we can no longer assume that where deeply weathered rock is found it is inherited from moister conditions. In a study of saprolites on igneous rocks in the Negev, Singer (1984) has shown that the climate during their formation has never been moister than semi-arid. None the less, clay contents of 45%, 53%, 11.3%, and 37% were found on andesitic basalt, Na–basanite, microgranite, and microdiorite. Moreover, a wide range of alteration products were identified (Table 3.2), which runs counter to traditional associations of arid conditions with limited alteration of silicate rocks only to smectite clays except under exceptional local circumstances (Barshad 1966, Tardy *et al.* 1973, Singer 1980). Crystallized iron oxides

Table 3.2 Alteration products of deep weathering in the Negev Desert (Singer 1984)

Parent material	*Alteration product*
Na–basanite	Dioctahedral smectite
Andesite basalt	Hydroxy: interlayered, high charge smectite
Microgranite	Principally smectite and chlorite with moderate amounts of kaolinite
Microdiorite	Mica: after sericitization of feldspars and osmectite

were also found in the clay mineral fraction of saprolites from basic rocks and argillation seemed to affect mafic minerals preferentially. Significantly, the alteration that Singer observed was not associated with, and thus not dependent upon, significant leaching of the weathered profiles.

The formation of iron oxides and their movement through rocks by capillary action has also been reported from other deserts. Selby (1977) described red stainings, principally of limonite, but also possibly of goethite, from granites in Namibia associated with scaling features. The staining could sometimes be seen emanating from biotite crystals and a few feldspar crystals showed evidence of moderate kaolinization and sericitization. This, together with some possible chloride formation, was taken to indicate slight chemical weathering. Selby also noted some strong leaching and decomposition of biotites in granites experiencing granular disintegration in the central Sahara. Conca and Rossman (1985) similarly noted haematite coatings on tonalite boulders in California derived from the leaching of biotite, while Osborn and Duford (1981) described streaks of iron oxide running down the sides of sandstone inselbergs in south-western Jordan. They also noted iron-rich weathering rinds up to 1 cm thick on many boulders. The rinds were found to reduce the degree of disintegration when boulders were dropped from cliffs and to offer a degree of protection to the underlying sandstone. Similar protection has been assumed by those who see tafoni and other cavernous features as forming through the breaching of weathering rinds. Breaching is followed by excavation of rock behind the rind that was preferentially weakened during rind formation by weathering and outward migration of certain constituents (e.g. Wilhemy 1964, Winkler 1979). Apart from iron, case-hardening is also produced by the outward migration in solution and precipitation of calcium carbonate, which may be derived from within the rock or in non-calcareous rocks from lime-rich ground water (e.g. Bryan 1926). Calcite deposition can alternatively weaken rock structure when, for example, it crystallizes within the pores of a quartz sandstone (Laity 1983). The constituents of case-hardened coatings can also originate as external additions of wind-blown dusts which are subsequently mobilized by surface moisture. Conca and Rossman (1982) have described thin case-hardened layers on quartz sandstone in Nevada which contain calcite, hydrated calcium barite, and raised levels of kaolinite of possibly aeolian origin.

Behind these crusts the interior of boulders may be weakened by a process termed core softening by Conca and Rossman (1985). They describe how tonalite boulders in Baja California have undergone preferential decay beneath iron-rich surface layers. This decay consists of kaolinization of feldspars (normally along cleavage planes and grain boundaries), a loss of iron from biotite, and the formation of authigenic silica and traces of calcite and gypsum. They proposed that the weathering is accomplished by migrating capillary moisture. This may have an elevated chemical reactivity due to increased dissolved CO_2 and organic acids if it had previously flowed through the upper soil horizons within which the boulders are partly buried. Weakening of rock structure may similarly be accomplished in quartz sandstone by selective silica dissolution under saline conditions, revealed as solutional etching on grain surfaces (e.g. Young 1987). In light of these observations, Young proposed that this dissolution can lead to the development of cavernous hollows. Mustoe (1983) also made the point that such cavities can be produced by chemical weathering in addition to the normally assumed salt weathering. This weathering is possible given that the cycles of hydration and dehydration required for most salt weathering will also encourage a range of chemical reactions leading, for example, to the decay of feldspars. Silica solubility is also enhanced under saline conditions, and Winkler (1987b) described silica coatings on tuffs in Texas, which he attributed to the 'high solubility of silica in a dry and hot west Texas . . . enhanced by probably alkalic waters' (p. 975).

The increase in solubility of both quartz and amorphous silica with increasing pH is well established (Goudie 1989) and is reflected in the formation of extensive silicate deposits within the evaporite sequences of alkaline lakes (e.g. Eugster 1967, 1969, Eugster and Jones 1968). The corollary of this is that quartz and silicate rocks will be corroded if they come into contact with alkaline lake water. This is illustrated by Butler and Mount (1986) who described corroded cobbles along former lacustrine strandlines in Death Valley. This corrosion manifests itself in the form of pits and honeycombs, and it derives principally from the dissolution of quartz, feldspars, and phyllosilicates in a variety of rock types. Corrosion occurs preferentially along grain boundaries, laminations, cross beds, and foliations and can enlarge vesicles in extrusive igneous rocks. This can lead to development of a secondary porosity, which increases moisture penetration and encourages further corrosion but can also increase susceptibility to salt weathering if the water is high in total dissolved solids.

In their study of alkaline corrosion, Butler and Mount (1986) observed little corrosion of limestone or dolomite. Again, it would seem that environmental factors, such as high temperatures and paucity of soil and vegetation giving low dissolved CO_2 contents in desert moisture, generally combine to produce little karstic weathering in deserts. Thus the traditional view is that espoused by Jennings (1983) who concluded that carbonate karst decreases with precipitation. This does not mean that karstic phenomena are absent; simply that they are invariably explained away as relics of former climates (Table 3.3). As such they are described as being destroyed by arid processes including aeolian abrasion (Krason 1961), mechanical weathering (Smith 1978), and fluvial incision (Marker 1972). Some features do, however, manage to retain a degree of development under arid conditions. Thus, Hunt *et al.* (1985) reported active karst on gypsum and anhydrite deposits of the Tripolitanian pre-desert in Libya, and Castellani and Dragoni (1987) described active erosion of solution pipes in south-eastern Morocco. The moisture for the latter erosion condenses as dew and is blown along the limestone surface. The ability of rivulets of coalesced dew to effect solution is further evidenced by studies of building stone, where they can cause serious damage (e.g. Camuffo *et al.* 1986). It is not likely that dew could initiate features such as extensive solution piping. Instead, they probably formed under conditions of more assured rainfall, but continue to develop slowly at the present time.

Dewfall does, however, appear to play significant direct and indirect roles in the formation of microkarstic features found in deserts (Smith 1988). Wind-driven dew can form microrills or rillensteine (Laudermilk and Woodford 1932) and plays an important part in the solution facetting of limestone pebbles (Bryan 1929) and micropitting of pebbles buried within the vesicular layer beneath stone pavements (Smith 1988). Other active karst described from arid areas have included rillenkarren (Sweeting and Lancaster 1982) and solution pans (Smith 1987).

In addition to highlighting the role of direct precipitation, karst studies have stressed the predominance of features such as pans and pits which trap moisture and, in recent years, the role of organisms in promoting solution (Smith 1988). The general role of organisms in erosion of limestone has been recently reviewed by Viles (1988) and their role in desert weathering by Cooke *et al.* (1993). In deserts emphasis has been placed on endolithic cyanobacteria and blue-green algae in, for example, the formation of weathering pits (Danin *et al.* 1982, Danin and Garty 1983); on endolithic algae in the 'solubilizing' of minerals, including silicates (Friedman 1971); and on lichen in exfoliation (e.g. Friedman 1982). The widespread occurrence of these organisms in deserts such as the Negev is generally attributed to the high frequency and regularity of dewfalls (Kappen *et al.* 1979) as a source of essential moisture. Because of the crucial role of dew, the distributions of these organisms show a marked variability with aspect. Lichen, for example, were found by Kappen *et al.* (1980) to be much more productive on shaded north-facing slopes in the Negev than on drier east-facing slopes exposed to strong insolation from the rising sun. Danin and Garty (1983) similarly found that north-facing slopes were characterized by epilithic lichens, whereas south-facing slopes were inhabited by endolithic cyanobacteria which are more capable of surviving drought conditions (see also Viles 1988). Care must be taken in attributing all microsolutional phenomena to present-day biotic weathering. Danin *et al.* (1982) found, for example, that although lichen and blue-green algae can produce characteristic jigsaw-like patterns of microgrooves at the boundaries between lichen colonies in Israel, they are only active in Mediterranean areas. Where these grooves

Table 3.3 Karstic features described from desert environments

Principal features	*Location*	*Source*
Dayas (dolines)	Algeria, Morocco	Conrad (1959, 1969), Clark *et al.* (1974), Castellani and Dragoni (1977)
Caves	Algeria	Conrad *et al.* (1967)
Solution hollows	Algeria	Quinif (1983)
Caves/hollows/ karren	Morocco	Smith (1987)
Cone karst	Egypt	El Aref *et al.* (1986, 1987)
Caves	Australia	Grodzicki (1985)
Caves	Morocco	Castellani and Dragoni (1987)

occur in arid areas they are interpreted as indicating more humid conditions in the past.

From this very brief overview of chemical weathering, it would seem that there are very few chemical processes that cease completely or are totally excluded under desert conditions. Their rates of action, mode of operation, and frequency of occurrence do change significantly. Limestone solution, for example, does not cease, but it no longer produces clearly defined macro- and mesoscale karstic phenomena. Instead it is responsible for a complex variety of microscale features and, it would seem, an indifferentiated slow loss of limestone in solution (Smith 1988).

WEATHERING OF DEBRIS IN DESERTS

As noted in Cooke *et al.* (1993), weathering of debris in deserts has tended to be neglected in favour of investigations into rock masses or, at best, boulders of a size that can support features such as cavernous hollows. Yet weathering does not cease with the production of coarse debris but continues as long as the debris remains at or near the desert surface (Smith 1988). Indeed, weathering of debris exercises an important control upon the overall rate of erosion of many landscapes mantled and protected by stone pavements. Even when such debris is fractured or disaggregates, further comminution may be required before it can be removed by either low energy fluvial erosion or aeolian deflation. A crucial stage in this process is the reduction of sand-sized or coarser debris into silt-sized fragments that are the principal constituents of many wind-borne dusts that blow out of the world's deserts.

Clearly, exceptions to this generalization exist and many of the experimental studies into salt weathering have used 'debris-sized' blocks of stone (e.g. Goudie *et al.* 1970, Goudie 1974, Fahey 1986, Cooke 1979). Unfortunately, these studies have rarely been used to explain debris behaviour *per se*. Instead, results have invariably been applied to generalized questions such as relative stone durability, the effectiveness of various salts and salt combinations in causing weight loss, or the nature of weathering mechanisms. Little attention has been paid to patterns of decay or, with some exceptions (e.g. Smith and McGreevy 1983, 1988), to the reproduction of weathering features similar to those observed under field conditions. The effectiveness of salt weathering in causing debris breakdown has been further demonstrated through studies of natural debris (e.g. Goudie and Day 1980) and cut blocks of stone (e.g. Goudie and Watson 1984) in salt-rich desert environments. Progress has been made despite the problems envisaged earlier in causing mechanical breakdown in small, unconstrained blocks which can themselves expand and contract in response to temperature variations.

Salt weathering is not, however, the only weathering process to operate in deserts, and rock debris should be subject to the full range of weathering processes active in these environments. Such debris may originate in a high mountain environment where it is released from the rock mass by frost-related processes exploiting intrinsic microfractures. It may then experience abrasion and high energy collisions during subsequent fluvial transport and finally be exposed to extreme temperature variations and partial or complete burial in a salt-rich environment such as an alluvial fan. As a result, the debris found mantling many desert surfaces exhibits a wide range of different stress histories, which in turn may explain the variety of weathering patterns observed and the comparative ease with which some debris is seen to breakdown in response, for example, to temperature cycling. The stress history described represents a form of climatic change brought about by spatial relocation. While there has been some work on the combined effects of different weathering regimes on rock breakdown (e.g. frost and salt weathering, Williams and Robinson 1981, McGreevy 1982b, Robinson and Jerwood 1987, Jerwood *et al.* 1990), there has been little work on sequential exposure of rocks to different weathering mechanisms. This situation obtains despite the recognition that many weathering mechanisms, such as salt crystallization weathering and wedging by expanding lattice clays, are exploitative in character and only operate in many originally non-porous rocks once fractures or microcracks have been initiated by other mechanisms (e.g. Smith and Magee 1990).

A wide range of weathering patterns has been observed on desert debris (see Table 3.4), but it is possible to identify a number of underlying characteristics. First, enhanced moisture and salt availability (via upward migration in low-lying alluvial and lacustrine environments) can produce rapid and thorough disintegration. Second, processes such as insolation and salt weathering are enhanced where debris is partially buried within finer material. Partial burial can produce accentuated internal temperature gradients around the exposure and burial boundary, constraint upon the expansion of the buried portion, and possibly enhanced chemical weathering within the subsurface environment. Third, many recent studies have stressed the role of biological agencies in facilitating the solution of

Table 3.4 Weathering features associated with debris on stone pavements

Weathering phenomena	*Sources*
Parallel stone cracking	Yaalon (1970), Cooke (1970)
Desert varnish	Verheye (1986), Bowman (1982), Dorn (1983)
Solution pitting	Amit and Gerson (1986), Rögner (1988a)
Vesicular weathering	Smith (1988)
Solution facetting	Bryan (1929)
Solution pinnacles	Joly (1962)
Microrills	Laudermilk and Woodford (1932)
Case hardening	Smith (1988)
Shattered rocks	Ollier (1963), Rögner (1988b)
Polygonal cracking	Soleilhavoup (1977), Bertouille *et al.* (1979)
Dirt cracking	Ollier (1965)
Granular disintegration	Cooke (1970), Goudie and Day (1980)
Honeycombing	Butler and Mount (1986)
Split/cleaved boulders	Whitaker (1974), Ollier (1984)
Weathering rinds	Osborn and Duford (1981)

limestone and the fixation of iron and manganese in desert varnishes. Finally, contrary to normal expectations, weathering need not be dominated by physical breakdown. On limestone debris, for example, it was noted in the previous section that a range of microsolutional features can be observed which are the most likely representatives of a truly arid karst.

Comminution of boulder and cobble-sized debris produces a variety of material ranging from rock fragments to individual mineral grains and, less frequently, fragmented grains. This material is in turn subject to further weathering and/or attrition which can, under suitable conditions, reduce material to fine sands or silts. Silt-sized particles make up the loess (e.g. Yaalon and Dan 1974, Caudé-Gaussen *et al.* 1982, Caudé-Gaussen 1984) and loess-like deposits of desert marginal areas (e.g. Smith and Whalley 1981, McTainsh 1984). It is generally considered that the transformation of quartz sands into silts requires either the precise application of disruptive stresses or the general application of very large stresses. Thus glacial grinding has been invoked to explain the loess deposits of high latitudes. Indeed, the apparent pre-eminence of glacial theories for loess-silt formation has meant that, even where silts are blown out of deserts such as the Gobi, it has been proposed that they must have originated initially from surrounding mountains (e.g. Smalley and Krinsley 1978).

There is, however, increasing evidence that a number of weathering and other processes which operate in deserts are capable of producing quartz silt of loess size (20 to 60 μm). These processes are reviewed in Table 3.5 and also by Pye (1987), McTainsh (1987) and Smith and Whalley (1993).

Table 3.5 Possible origins of loess-sized quartz silt in desert environments

Process	*Source*
Salt weathering of loose granular material	Goudie *et al.* (1979), Pye and Sperling (1983), Peterson (1980)
Salt weathering of sandstone	Goudie (1986), Smith *et al.* (1987)
Frost weathering	Moss *et al.* (1981), Lautridou and Ozouf (1982)
Biotite weathering in granitic profiles	Pye (1985)
Inherited tropical deep weathering	Boulet (1973), Leprun (1979), Nahon and Trompette (1982)
Inherited silica dissolution of dune sands	Little *et al.* (1978), Pye (1983)
Inherited weathering from temperate soils	Pye (1987)
Silica dissolution in saline environments	Young (1987), Magee *et al.* (1988)
Inherited glacial grinding	Smalley and Vita-Finzi (1968), Boulton (1978)
Aeolian abrasion	Whalley *et al.* (1982b, 1988)
Fluviatile abrasion	Moss (1972), Moss *et al.* (1973)
Fracturing and/or dissolution in duricrusts	Nahon and Trompette (1982)
Microdilation in granitic profiles	Nur and Simmons (1970), Moss and Green (1975), White (1976), Power *et al.* (1990)

Some of the proposed processes, including salt weathering and aeolian and fluviatile abrasion, clearly act under hot desert conditions. Others, such as frost shattering, are most likely to be effective in either desert marginal areas or 'climatic islands' within deserts induced by altitude. A further and important group comprises processes which operate under moist tropical or temperate conditions, the effects of which may represent climatic inheritance when encountered in present-day deserts. It is a characteristic of many of the mechanisms listed in Table 3.5 that they operate through exploiting flaws in sand-sized and larger grains. These flaws could be inherited microfractures (Moss and Green 1975), cleavage planes (Wilson 1979), or dislocations formed by tectonic deformation (White 1976). Such flaws are not always necessary and within sandstones fractures could be initiated by compressive loading of sand grains when salts expand within adjacent pores (Smith *et al.* 1987). It is difficult to envisage, however, how other processes such as salt weathering of loose grains could be effective in the absence of pre-existing flaws or microfractures.

In keeping with larger debris, therefore, sand-sized material exposed at desert surfaces is invariably the product of a complex stress history. This history may represent sequential exposure to different stress mechanisms through climatic fluctuations, long-distance transport, and/or release from parent rock. Grains may additionally be subject to processes such as frost and salt weathering acting alternatively or in conjunction. The end products of exposure to these stresses are either comparatively flawless core grains of the type found in many dune sands or silt-sized fragments of a calibre prone to deflation and removal from the desert environment.

FUTURE DIRECTIONS

There are many aspects of desert weathering that require further investigation and refinement. In particular, it is clear that the weathering environments of hot deserts are numerous and varied. We need much more information on the range of environmental conditions experienced before rock responses can be fully understood. Moreover, the distinction must be made between conditions as measured for meteorological purposes and the temperature and moisture regimes experienced at the rock–atmosphere interface. The overall significance of weathering achieved within these environments cannot be appreciated until (a) we improve the precision with which weathering damage is recognized and assessed, and (b) we begin to investigate the overall contribution of weathering not only in the development of individual landforms but also in the long-term evolution of desert landscapes as a whole.

DAMAGE RECOGNITION AND ASSESSMENT

A criticism levelled at many early rock weathering simulation studies is that they dismissed weathering mechanisms such as insolation-related fatigue failure, simply because they employed techniques of damage assessment insufficiently sensitive to register changes that might have been expected over the duration of the experiment (see Rice 1976). Similarly, many weathering changes are threshold phenomena, in that specimens may exhibit little surface change while experiencing internal changes that can lead to sudden and catastrophic damage as strength thresholds are breached and, for example, large contour scales break away. As a result, damage assessment by weight loss alone can lead to misleading estimates of relative durability if simulation experiments are of limited duration. Alternatively, there is a temptation to increase the aggressivity of such tests to the point that while measurable damage is achieved, conditions no longer relate to those encountered in nature. There is a need, therefore, for more precise and consistent methods of assessing surface and internal changes in rock properties consequent upon weathering. Ideally such methods should be applicable under both field and laboratory conditions to permit work to be integrated between the two situations.

Considerable progress has been made in recent years in terms of damage assessment by civil engineers in general, and by those concerned in building stone decay in particular. Some of the techniques used which might be appropriate for desert weathering studies are given in Table 3.6 together with examples of their adoption and use by geomorphologists. The studies listed concentrate upon four particular aspects: (a) the non-destructive testing of rock for internal damage principally using ultrasonic techniques; (b) improved assessments of small-scale surface changes using, for example, surface profilometers, microerosion meters, survey by scanning electron microscopy and optical reflectance; (c) methods such as the Schmidt Hammer which assess rock hardness; and (d) the need for a rigorous terminology when defining weathering damage. Table 3.6 does not extend to the more standard engineering tests for rock strength which tend to be destructive of samples. Reviews of these

Table 3.6 Tests and procedures of possible relevance to the study of weathering in deserts

Rock characteristics	*Method*	*Source*
Degree of weathering	Weathering grades based on range of criteria from field and laboratory tests. For review see Fookes *et al.* (1988)	Irfan and Dearman (1978a, b, c), Fookes *et al.* (1971), Dearman *et al.* (1978), Dibb *et al.* (1983a, b), Baynes and Dearman (1978), Lewin and Charola (1981)
Rock strength (dynamic Young's Modulus)	Ultrasonic pulse velocity	Allison (1988, 1990)
Rock hardness (coefficient of restitution)	Schmidt Hammer	Day and Goudie (1977), Williams and Robinson (1983)
Rock hardness	Abrasion resistance	Conca and Cubba (1986)
Rock hardness/abrasion resistance	Sandblast index	Verhoef (1987)
Crack detection	Fluorescent dye	Coffey (1988)
Crack location and measurement	Ultrasonic probe	Coffey (1988), Hall (1976, 1977), Hall and Farley (1978)
Crack growth	Acoustic emission/ultrasonic velocity measurement	Tassios and Economou (1976), Delgado-Rodrigues (1978, 1982), Honeybourne (1982)
Crack visualization	Impregnation with metal alloy	Anonymous (1987)
Crack patterns	Optical microscopy	Nolen-Hoeksèma and Gordon (1987)
Surface roughness change	Reflectance	Aires-Barros (1977)
Surface roughness	Microroughness meter/surface roughness scanner	McCarroll (1990), Lam and Johnston (1985)
Surface loss	Microerosion meter	Trudgill *et al.* (1989), High and Hanna (1970), Viles and Trudgill (1984)
Crack expansion	Strain gauges	Douglas *et al.* (1987)
Rock block expansion	Displacement transducer	Manning (1987), Cassaro *et al.* (1982), Pissart and Lautridou (1984)
Time of wetness/condensation	Relative humidity probes, circuit grids, limestone-block resistors	See *et al.* (1987, 1988), Yamasaki *et al.* (1983)

and other tests can be found in, for example, Fookes *et al.* (1988) and Price (1975a, b).

AN INTEGRATED APPROACH TO DESERT WEATHERING

There has been a long-term tendency in studies of desert weathering to isolate individual weathering mechanisms and to seek an understanding of weathering phenomena through segregation rather than integration. This tendency has, as indicated in the introduction, reflected a general trend in geomorphological investigations which have become increasingly process orientated and reductionist in character. Like these studies, understanding of desert weathering mechanisms is not an end in itself; ultimately such mechanisms must be set within wide temporal and spatial contexts to understand the landscapes within which weathering occurs (Smith 1987). In doing this, it must be recognized that weathering mechanisms do not operate in isolation from one another and that integration must take place at a variety of levels. Specifically, integration must occur:

(a) *Between different mechanisms acting simultaneously and in sequence.* These mechanisms should include pressure release, limited but varied chemical alteration, and temperature variations – alone and in the presence of moisture and salts – which combine frost weathering with other mechanisms and diurnal cycles with shorter-term fluctuations. Attempts should be made to identify similarities in the underlying controls on mechanical disruption. These similarities are suggested by the observation that most breakdown occurs in conjunction with thermally induced expansion and contraction. If underlying similarities can be identified, these may point the way towards a unified approach to the study of mechanical weathering, within which a knowledge of one mechanism will facilitate the understanding of others.

(b) *Between observations of how mechanisms operate and the landforms they produce.* Links between the two are frequently made, though usually at the level of circular argument. Features such as tafoni are used to infer the operation of salt weathering, although it is known that such forms are equifin-

al and the reasons why salt weathering should produce such distinctive features are incompletely understood.

(c) *Between weathering landforms and landscape.* Individual landscapes frequently experience a range of weathering processes and contain numerous weathering features. Few attempts have been made in desert environments to examine the overall contribution of weathering to landscape evolution. In particular, the control exerted by weathering upon rates of debris supply, debris character, and, ultimately, the rate of landscape development has received little attention.

(d) *Between field and laboratory studies.* In addition to the obvious requirement that laboratory simulations should, as far as possible, reflect field environments, efforts should be made to combine field and laboratory experimentation. This could involve, for example, field exposure trials using pre-treated blocks linked to exposure of similar blocks to simulated weathering environments under controlled laboratory conditions. In terms of field exposure trials, geomorphologists have much to learn from work on stone decay in polluted environments (e.g. Building Effects Review Group 1989) where a wide range of sophisticated exposure programmes has been initiated in recent years.

REFERENCES

Aires-Barros, L. 1977. Experiments on thermal fatigue of non-igneous rocks. *Engineering Geology* **11**, 227–38.

Aires-Barros, L. 1978. Comparative study between rates of experimental laboratory weathering of rocks and their natural environmental weathering decay. *Bulletin of the International Association of Engineering Geology* **18**, 169–74.

Aires-Barros, L., R.C. Graça and A. Velez 1975. Dry and wet laboratory tests and thermal fatigue of rocks. *Engineering Geology* **9**, 249–65.

Allison, R.J. 1988. A non-destructive method of determining rock strength. *Earth Surface Processes and Landforms* **13**, 729–36.

Allison, R.J. 1990. Developments in a non-destructive method of determining rock strength. *Earth Surface Processes and Landforms* **15**, 571–7.

Amit, R. and R. Gerson 1986. The evolution of Holocene reg (gravelly) soils in deserts – an example from the Dead Sea region. *Catena* **13**, 59–79.

Amoroso, G.G. and V. Fassina 1983. *Stone decay and conservation.* Amsterdam: Elsevier.

Anonymous 1987. First cast of limestone microcracks. *New Scientist*, **17 December**, 13.

Arnold, A. 1981. Nature and reactions of saline minerals in walls. In *The conservation of stone II*, 13–23. Bologna: Centro Cesare Gnudi.

Arnold, A. 1982. Rising damp and saline minerals. In *Proceedings of the 4th International Congress on Deterioration and Preservation of Stone Objects*, K.L. Gauri and J.A. Gwinn (eds) 11–28. Louisville, KY: University of Louisville.

Ashton, H.E. and P.J. Sereda 1982. Environment, microenvironment and durability of building materials. *Durability of Building Materials* **1**, 49–65.

Bache, H.H. 1985. Durability of concrete fracture mechanical aspects. *Nordic Concrete Research Publication* **4**, 7–25.

Barshad, I. 1966. The effects of variation of precipitation on the nature of clay minerals formed in soils from acid and basic igneous rocks. *Proceedings of International Clay Conference, Jerusalem* **1**, 167–73.

Baynes, F.J. and W.R. Dearman 1978. Scanning electron microscope studies of weathered rocks: a review of nomenclature and methods. *Bulletin of the International Association of Engineering Geology* **18**, 199–204.

Bernardi, A., D. Camuffo and C. Sabbioni 1985. Microclimate and weathering of a historical building: the Ducal Palace in Urbino. *The Science of the Total Environment* **46**, 243–60.

Bertouille, H., J.P. Coutard, F. Soleilhavoup and J. Pellerin 1979. Les galets fissures: étude de la fissuration des galets Sahariens et comparaison avec issus de diverses zones climatiques. *Révue de Géomorphologie* **28**, 33–48.

Blackwelder, E. 1925. Exfoliations as a phase of rock weathering. *Journal of Geology* **33**, 793–806.

Blackwelder, E. 1933. The insolation hypothesis of rock weathering. *American Journal of Science* **266**, 97–113.

Boulet, R. 1973. Toposéquence de sols tropicaux en Haute Volta. Equilibre et deséquilibre pédobioclimatique. *Memoires ORSTOM* **85**, 1–272.

Boulton, G.S. 1978. Boulder shapes and grain size distribution of debris as indicators of transport paths through a glacier and till genesis. *Sedimentology* **25**, 773–99.

Bowman, D. 1982. Iron coating in recent terrace sequences under extremely arid conditions. *Catena* **9**, 353–9.

Bradley, W.C. 1963. Large-scale exfoliation in massive sandstones of the Colorado Plateau. *Bulletin of the Geological Society of America* **74**, 519–28.

Bryan, K. 1925. The Papago Country, Arizona. *U.S. Geological Survey Water-Supply Paper* 499.

Bryan, K. 1926. Niches and other cavities in sandstone at Chaco Canyon, New Mexico. *Zeitschrift für Geomorphologie* **3**, 125–40.

Bryan, K. 1929. Solution facetted limestone pebbles. *American Journal of Science* **18**, 193–208.

Büdel, J. 1982. *Climatic geomorphology*, Princeton, NJ: Princeton University Press.

Building Effects Review Group 1989. *The effects of acid deposition on buildings and building materials in the United Kingdom.* London: HMSO.

Butler, P.R. and J.F. Mount 1986. Corroded cobbles in southern Death Valley: their relationship to honeycomb weathering and lake shorelines. *Earth Surface Processes and Landforms* **11**, 377–87.

Camuffo, D. 1983. Indoor dynamic climatology: investigations on the interactions between walls and indoor environment. *Atmospheric Environment* **17**, 1803–9.

Camuffo, D. 1984. Condensation–evaporation cycles in pore and capillary systems according to the Kelvin model. *Water, Air and Soil Pollution* **21**, 151–9.

Camuffo, D., A. Bernardi and A. Ongaro 1986. The challenges of the microclimate and the conservation of works of art. *2emes Rencontres Internationals pour la Protection du Patrimoine Cultural, Avignon, Nov. 1986*, 215–28.

Cassaro, M.A., K.L. Gauri, M. Sharifinassab and A. Sharifian 1982. On the strength and deformation properties of Indiana limestone and concrete in the presence of salts. In *Proceedings of the 4th International Congress on Deterioration and Preservation of Stone Objects*, K.L. Gauri and J.A. Gwinn (eds) 57–76. Louisville, KY: University of Louisville.

Castellani, V. and W. Dragoni 1977. Surface Karst landforms in the Moroccan Hamada of Guir. *Proceedings of the 7th Congress of Speleology*, 98–101.

Castellani, V. and W. Dragoni 1987. Some considerations regarding Karstic evolution of desert limestone plateaus. In *International geomorphology*, V. Gardiner (ed.), 1199–206. Chichester: Wiley.

Caudé-Gaussen, G. 1984. Le cycle des poussieres éoliennes désertiques actuelles et la sédimentation des péridésertiques Quaternaires. *Bulletin des Centres de Récherches Exploration-Production Elf Aquitaine* **8**, 167–82.

Caudé-Gaussen, G., C. Mosser, P. Rognon and J. Torenq 1982. Une accumulation de loess Pleistocene superient dans le sud-Tunisien: la coupe de Techine. *Bulletin de la Société Géologique de France* **24**, 283–92.

Clark, D.M., C.W. Mitchell and J.A. Varley 1974. Geomorphic evolution of sediment-filled solution hollows in some arid regions. *Zeitschrift für Geomorphologie Supplement Band* **20**, 193–208.

Cloudsley-Thompson, J.L. and M.J. Chadwick 1969. *Life in deserts*. London: Foulis.

Coffey, J.M. 1988. Non-destructive testing – the technology of measuring defects. *CEGB Research* **21**, 36–47.

Conca, J.L. and R. Cubba 1986. Abrasion resistance hardness testing of rock materials. *International Journal of Rock Mechanics Mineral Science and Geomechanics Abstracts* **23**, 141–9.

Conca, J.L. and G.R. Rossman 1982. Case hardening of sandstone. *Geology* **10**, 520–3.

Conca, J.L. and G.R. Rossman 1985. Core softening of cavernously weathered tonalite. *Journal of Geology* **93**, 59–73.

Conrad, G. 1959. Observations preliminaires sur la sedimentation dans les daias de la Hamada du Guir. *Compte Rendu Société Géologique Français* **7**, 156–62.

Conrad, G. 1969. *L'évolution continentale post-Hercynienne du Sahara Algerien*. Paris: Centre National du Récherche Scientifique.

Conrad, G., B. Geze and Y. Paloc 1967. Phénomenes Karstiques et pseudokarstiques du Sahara. *Révue de Géographie Physique et Géologie Dynamique* **9**, 357–69.

Cooke, R.U. 1970. Stone pavements in deserts. *Annals of the Association of American Geographers* **4**, 560–77.

Cooke, R.U. 1979. Laboratory simulation of salt weathering processes in arid environments. *Earth Surface Processes and Landforms* **4**, 347–59.

Cooke, R.U. and I.J. Smalley 1968. Salt weathering in deserts. *Nature* **220**, 1226–7.

Cooke, R.U., D. Brunsden, J.C. Doornkamp and D.K.C. Jones 1982. *Urban geomorphology in drylands*. Oxford: Oxford University Press.

Cooke, R.U., A. Warren and A.S. Goudie 1993. *Desert geomorphology*. London: UCL Press.

Correns, C.W. 1949. Growth and dissolution of crystals under linear pressure. *Discussions of the Faraday Society* **5**, 267–71.

Danin, A. and J. Garty 1983. Distribution of cyanobacteria and lichens on hillsides of the Negev highlands and their impact on biogenic weathering. *Zeitschrift für Geomorphologie* **27**, 423–44.

Danin, A., R. Gerson, K. Marton and J. Garty 1982. Patterns of limestone and dolomite weathering by lichens and blue-green algae and their palaeoclimatic significance. *Palaeogeography, Palaeoclimatology, Palaeoecology* **37**, 221–33.

Day, M.J. and A.S. Goudie 1977. Field assessment of rock hardness using the Schmidt Test Hammer. *British Geomorphological Research Group Technical Bulletin* **18**, 19–29.

Dearman, W.R., F.J. Baynes and T.Y. Irfan 1978. Engineering grading of weathered granite. *Engineering Geology* **12**, 345–74.

Delgado-Rodrigues, J. 1978. Some problems raised by the study of the weathering of igneous rocks. In *Deterioration and protection of stone monuments*. UNESCO/RILEM Conference, Paris, Section 2.4.

Delgado-Rodrigues, J. 1982. Laboratory study of thermally-fissured rocks. In *Proceedings of the 4th International Congress on the Deterioration and Preservation of Stone Objects*, K.L. Gauri and J.A. Gwinn (eds) 281–94. Louisville, KY: University of Louisville.

Del Monte, M. and C. Sabbioni 1984. Gypsum crusts and fly ash particles on carbonate outcrops. *Archives for Meteorology, Geophysics and Bioclimatology Series B* **35**, 105–11.

Del Monte, M. and O. Vittori 1985. Air pollution and stone decay: the case of Venice. *Endeavour, New Series* **9**, 117–22.

Del Monte, M., C. Sabbioni, A. Ventura and G. Zappia 1984. Crystal growth from carbonaceous particles. *The Science of the Total Environment* **36**, 247–54.

Dibb, T.E., D.W. Hughes and A.B. Poole 1983a. The identification of critical factors affecting rock durability in marine environments. *Quarterly Journal of Engineering Geology* **16**, 149–61.

Dibb, T.E., D.W. Hughes and A.B. Poole 1983b. Controls of size and shape of natural armourstone. *Quarterly Journal of Engineering Geology* **16**, 31–42.

Dorn, R.I. 1983. Cation ratio dating: a new rock varnish age-determination technique. *Quaternary Research* **20**, 49–73.

Douglas, G.R., J.P. McGreevy and W.B. Whalley 1987. The use of strain gauges for experimental frost weathering studies. In *International geomorphology*, V. Gardiner (ed.), 605–21. Chichester: Wiley.

Dragovich, D. 1967. Flaking, a weathering process operating on cavernous rock surfaces. *Bulletin of the Geological Society of America* **78**, 801–4.

Dragovich, D. 1969. The origin of cavernous surfaces (tafoni) in granitic rocks of Southern Australia. *Zeitschrift für Geomorphologie* **13**, 163–81.

Dragovich, D. 1981. Cavern microclimates in relation to preservation of rock art. *Studies in Conservation* **26**, 143–9.

Dubief, J. 1965. Le probleme de l'eau superficielle au Sahara. *La Météorologie* **77**, 3–32.

Duvdevani, S. 1947. Dew in Palestine. *Nature* **159**, 4041.

Duvdevani, S. 1953. Dew gradients in relation to climate, soil and topography. *Desert Research Symposium, Jerusalem*, 136–52.

El Aref, M.M., F. Awadalah and S. Ahmed 1986. Karst landform development and related sediments in the Miocene rocks of the Red Sea coastal zone. *Geologie Rundschau* **76**, 781–90.

El Aref, M.M., A.M. Abou Khadrah and Z.H. Lofty 1987. Karst topography and karstification processes in the Eocene limestone plateau of El Bhahariya Oasis, Western Desert, Egypt. *Zeitschrift für Geomorphologie* **31**, 45–64.

Eugster, H.P. 1967. Hydrous sodium silicates from Lake Magadi, Kenya: precursors of bedded chert. *Science* **157**, 1177–80.

Eugster, H.P. 1969. Inorganic bedded cherts from the Magadi area, Kenya. *Contributions to Mineralogy and Petrology*, **22**, 1–31.

Eugster, H.P. and B.F. Jones 1968. Gels composed of sodium aluminium silicate, Lake Magadi, Kenya. *Science* **162**, 160–4.

Evans, I.S. 1970. Salt crystallization and rock weathering. *Revue de Géomorphologie Dynamique* **19**, 153–77.

Evenari, M., L. Shanan and N. Tadmor 1971. *The Negev*. Cambridge, MA: Harvard University Press.

Fahey, B.D. 1986. A comparative laboratory study of salt crystallisation and salt hydration as potential weathering agents in deserts. *Geografiska Annaler* **68A**, 107–11.

Folk, R.L. and E. Begle-Patton 1982. Buttressed expansion of granite and development of grus in Central Texas. *Zeitschrift für Geomorphologie* **26**, 17–32.

Fookes, P.G. 1976. Middle East – inherent ground problems. In *Geological Society, Conference on Engineering Problems, November 1976*, 7–23.

Fookes, P.G., W.R. Dearman and J.A. Franklin, 1971. Some engineering aspects of rock weathering with field examples from Dartmoor and elsewhere. *Quarterly Journal of Engineering Geology* **4**, 139–85.

Fookes, P.G., C.S. Gourlay and C. Ohikere 1988. Rock weathering in engineering time. *Quarterly Journal of Engineering Geology* **21**, 33–57.

Friedman, E.I. 1971. Light and scanning electron microscopy of endolithic desert algal habitat. *Phycologia* **10**, 411–28.

Friedman, E.I. 1982. Endolithic micro-organisms in the Antarctic cold desert. *Science* **215**, 1045–53.

George, V. 1986. The thermal niche: desert sand and desert rock. *Journal of Arid Environments* **10**, 213–24.

Goudie, A.S. 1974. Further experimental investigation of rock weathering by salt and other mechanical processes. *Zeitschrift für Geomorphologie Supplement Band* **21**, 1–12.

Goudie, A.S. 1985. Salt weathering. *Oxford School of Geography Research Paper* **8**.

Goudie, A.S. 1986. Laboratory simulation of the 'wick effect' in salt weathering of rock. *Earth Surface Processes and Landforms* **11**, 275–85.

Goudie, A.S. 1989. Weathering Processes. In *Arid zone geomorphology*, D.S.G. Thomas (ed.), 11–24. London: Belhaven Press.

Goudie, A.S. and R.U. Cooke 1984. Salt efflorescences and saline lakes; a distributional analysis. *Geoforum* **15**, 563–82.

Goudie, A.S. and M.J. Day 1980. Disintegration of fan sediments in Death Valley, California by salt weathering. *Physical Geography* **1**, 126–37.

Goudie, A.S. and A. Watson 1984. Rock block monitoring of rapid salt weathering in southern Tunisia. *Earth Surface Processes and Landforms* **9**, 95–8.

Goudie, A.S., R.U. Cooke and I. Evans 1970. Experimental investigation of rock weathering by salts *Area* **4**, 42–8.

Goudie, A.S., R.U. Cooke and J.C. Doornkamp 1979. The formation of silt from quartz dune sand by salt processes in deserts. *Journal of Arid Environments* **2**, 105–12.

Griggs, D.T. 1936. The factor of fatigue in rock exfoliation. *Journal of Geology* **74**, 733–96.

Grodzicki, J. 1985. Genesis of Nullarbor caves in southern Australia. *Zeitschrift für Geomorphologie* **29**, 37–49.

Hall, C., W.D. Hoff and M.R. Nixon 1984. Water movement in porous building materials VI. Evaporation and drying in brick and block materials. *Building and Environment* **19**, 13–20.

Hall, K.G. 1976. Crack depth measurement in rail steel by Rayleigh waves aided by photoelastic visualization. *British Journal of Non-Destructive Testing*, June 1976, 121–6.

Hall, K.G. 1977. Ultrasonic wave visualization as a teaching aid in non-destructive testing. *Ultrasonics*, March 1977, 57–69.

Hall, K.G. and P.G. Farley 1978. An evaluation of ultrasonic probes by the photoelastic visualization method. *British Journal of Non-Destructive Testing*, July 1978, 171–84.

Haneef, S.J., C. Dickinson, J.B. Johnson, G.E. Thompson *et al.* 1990a. Degradation of coupled stones by artificial acid rain solution. In *Science technology and the european cultural heritage*, N.S. Baer, C. Sabbioni and A.I. Sors (eds), 469–73, Oxford: Butterworth-Heinemann.

Haneef, S.J., C. Dickinson, J.B. Johnson, G.E. Thompson *et al.* 1990b. Laboratory-based testing and simulation of dry and wet deposition of pollutants and their interaction with building stone. *European Cultural Heritage Newsletter* **4**, 9–16.

High, C.J. and F.K. Hanna 1970. A method for the direct measurement of erosion of rock surfaces. *British Geomorphological Research Group Technical Bulletin* **5**, 3–17.

Honeybourne, D.B. 1982. *The building limestones of France*. London: HMSO.

Hunt, C.O., S.J. Gale and D.D. Gilbertson 1985. The UNESCO Libyan valleys survey IX: anhydrite and limestone karst in the Tripolitanian pre-desert. *Libyan Studies* **16**, 1–13.

Irfan, T.Y. and W.R. Dearman 1978a. Characterization of weathering grades in granite using standard tests on aggregates. *Annales de la Société Géologique de Belgique* **101**, 67–9.

Irfan, T.Y. and W.R. Dearman 1978b. Micropetrographic and engineering characterization of a weathered granite. *Annales de la Société Géologique de Belgique* **101**, 71–7.

Irfan, T.Y. and W.R. Dearman 1978c. The engineering petrography of a weathered granite in Cornwall, England. *Quarterly Journal of Engineering Geology* **11**, 233–44.

Jäkel, D. and H. Dronia 1976. Ergebrisse von boden- und

Gesteintemperatur-messungen in der Sahara. *Berliner Geographische Abhandlungen* **24**, 55–64.

Jenkins, K.A. and B.J. Smith 1990. Daytime rock surface temperature variability and its implications for mechanical rock weathering: Tenerife, Canary Islands. *Catena* **17**, 449–59.

Jennings, J.N. 1983. The disregarded Karst of the arid and semi-arid domain. *Karstologia* **1**, 61–73.

Jerwood, L.C., D.A. Robinson and R.B.G. Williams 1990. Experimental frost and salt weathering of Chalk – 1. *Earth Surface Processes and Landforms* **15**, 611–24.

Joly, F. 1962. Etude sur le relief du sud-est Morocain. *Institute Scientifique Chérifien, Travaux* 10.

Kappen, L. O.L. Lange, E.-D. Schulze, M. Evenari *et al.* 1979. Ecophysiological investigations on lichens of the Negev Desert. VI. Annual course of the photosynthetic production. *Flora* **168**, 85–108.

Kappen, L., O.L. Lange, E.-D. Schulze, U. Buschbom *et al.* 1980. Ecophysiological investigations on lichens of the Negev Desert VII. The influence of the habitat exposure on dew inhibition and photosynthetic productivity. *Flora* **169**, 216–29.

Kerr, A., B.J. Smith, W.B. Whalley and J.P. McGreevy 1984. Rock temperature measurements from southeast Morocco and their significance for experimental rock weather studies. *Geology* **12**, 306–9.

Krason, J. 1961. The caves in Maestrichtian limestone in the Arabic Desert. *Hohle* **12**, 57.

Laity, J.E. 1983. Diagenetic controls on groundwater sapping and valley formation, Colorado Plateau, revealed by optical and electron microscopy. *Physical Geography* **4**, 103–25.

Lam, S.K. and I.W. Johnston 1985. A scanning device to quantify joint surface roughness. *Geotechnical Testing Journal* **8**, 117–24.

Laudermilk, J.D. and A.O. Woodford 1932. Concerning rillensteine. *American Journal of Science* **23**, 135–54.

Lautridou, J.P. and J.C. Ozouf 1982. Experimental frost shattering: fifteen years of research at the Centre de Geomorphologie du CNRS. *Progress in Physical Geography* **6**, 215–32.

Leprun, J.C. 1979. *Les cuirasses ferrugineuses des pays cristallins de l'Afrique Occidentale séche: genese, transformations, degradation.* Unpublished Doctorate thesis. Université de Strasbourg.

Lewin, S.Z. 1981. The mechanism of masonry decay through crystallization. In *Conservation of historic stone buildings and monuments*, S.M. Barkin (ed.), 1–31. Washington, D.C.: National Academy of Sciences.

Lewin, S.Z. and A.E. Charola 1979. The physical chemistry of deteriorated brick and its impregnation techniques. In *Atti del Convegno Internazionale il Mattone di Venezia, Venice October 22–23*, 189–214 (cited by Amoroso and Fassina 1983).

Lewin, S.Z. and A.E. Charola 1981. An HF-SEM technique for characterization of the weathering properties of building stone. I. Granite. *Scanning Electron Microscopy*, 555–61.

Little, I.P., T.M. Armitage and R.J. Gilkes 1978. Weathering of quartz in dune sands under subtropical conditions in Eastern Australia. *Geoderma* **20**, 225–37.

Magee, A.W., P.A. Bull and A.S. Goudie 1988. Chemical textures on quartz grains. An experimental approach using salts. *Earth Surface Processes and Landforms* **13**, 665–76.

Manning, M.I. 1987. Acid rain: effects on structural materials. *CEGB Research* **20**, 53–61.

Marker, M.E. 1972. Karst landform analysis as evidence for climatic change in the Transvaal, South Africa. *South African Geographical Journal* **54**, 152–62.

Marschner, H. 1978. Application of salt crystallization test to impregnated stones. In *Deterioration and Protection of Stone Monuments*. UNESCO/RILEM Conference, Paris, Section 3.4.

McCarroll, D. 1990. Differential weathering of feldspar and pyroxene in an Arctic-Alpine environment. *Earth Surface Processes and Landforms* **15**, 641–51.

McGreevy, J.P. 1982a. Hydrothermal alteration and earth surface rock weathering: a basalt example. *Earth Surface Processes and Landforms* **7**, 189–95.

McGreevy, J.P. 1982b. Frost and salt weathering: Further experimental results. *Earth Surface Processes and Landforms* **7**, 475–88.

McGreevy, J.P. 1985. Thermal rock properties as controls on rock surface temperature maxima, and possible implications for rock weathering. *Earth Surface Processes and Landforms* **10**, 125–36.

McGreevy, J.P. and B.J. Smith 1982. Salt weathering in hot deserts: observations on the design of simulation experiments. *Geografiska Annaler* **64A**, 161–70.

McGreevy, J.P. and B.J. Smith 1983. Salt weathering in hot deserts: observations on the design of simulation experiments. A reply. *Geografiska Annaler* **65A**, 298–302.

McGreevy, J.P. and B.J. Smith 1984. The possible role of clay minerals in salt weathering. *Catena* **11**, 169–75.

McTainsh, G. 1984. The nature and origin of aeolian mantles in northern Nigeria. *Geoderma* **33**, 13–37.

McTainsh, G. 1987. Desert loess in northern Nigeria. *Zeitschrift für Geomorphologie* **31**, 145–65.

Minty, E.J. 1965. Preliminary reports on an investigation into the influence of several factors on the sodium sulphate test for aggregate. *Australian Road Research* **22**, 49–52.

Moss, A.J. 1972. Initial fluviatile fragmentation of granitic quartz. *Journal of Sedimentary Petrology* **42**, 905–16.

Moss, A.J. and P. Green 1975. Sand and silt grains: predetermination of their formation and properties by microfractures in quartz. *Journal of the Geological Society of Australia* **22**, 485–95.

Moss, A.J., P.H. Walker and J. Hutka 1973. Fragmentation of granitic quartz in water. *Sedimentology* **20**, 1489–511.

Moss, A.J., P. Green and J. Hutka 1981. Static breakage of granitic detritus by ice and water in comparison with breakage by flowing water. *Sedimentology* **28**, 261–72.

Mustoe, G.E. 1983. Cavernous weathering in the Capitol Reef Desert, Utah. *Earth Surface Processes and Landforms* **8**, 517–26.

Nahon, D. and R. Trompette 1982. Origin of siltstones: glacial grinding versus weathering. *Sedimentology* **29**, 25–35.

Nolen-Hoeksèma, R.C. and R.B. Gordon 1987. Optical detection of crack patterns in the opening-mode fracture of marble. *International Journal of Rock Mechanics, Mineral Science and Geomechanics Abstracts* **24**, 135–44.

Nur, A. and G. Simmons 1970. The origin of small cracks in igneous rocks. *International Journal of Rock Mechanics and Mineral Science* **7**, 307–14.

Ollier, C.D. 1963. Insolation weathering: examples from central Australia. *American Journal of Science* **261**, 376–87.

Ollier, C.D. 1965. Dirt cracking – a type of insolation weathering. *Journal of Geology* **73**, 454–68.

Ollier, C.D. 1984. *Weathering*, 2nd edn. London: Longman.

Osborn, G. and J.M. Duford 1981. Geomorphological processes in the inselberg region of south-west Jordan. *Palestine Exploration Quarterly* January–June, 1–17.

Peel, R.F. 1974. Insolation weathering: some measurements of diurnal temperature changes in exposed rocks in the Tibesti region, central Sahara. *Zeitschrift für Geomorphologie Supplement Band* **21**, 19–28.

Peel, R.F. 1975. Water action in deserts. In *Processes in physical and human geography*, R.F. Peel, M. Chisholm and P. Haggett (eds), 110–29. London: Heinemann.

Peterson, G.L. 1980. Sediment size reduction by salt weathering in arid environments. *Geological Society of America Abstracts with Programs* **12**, 301.

Pissart, A. and J.P. Lautridou 1984. Variations de longueur de cylindres de pierre de Caen (calcaire bathonien) sous l'effet de séchage et d'humidification. *Zeitschrift für Geomorphologie Supplement Band* **49**, 111–16.

Potocki, F.P. 1978. Road temperatures and climatological observations in the Emirate of Abu Dhabi. *U.K. Transport and Road Research Laboratory, Supplementary Report* 412.

Power, E.T., B.J. Smith and W.B. Whalley 1990. Fracture patterns and grain release in physically weathered granitic rocks. In *Soil micromorphology: a basic and applied science*, L.A. Douglas (ed.), 545–50. Amsterdam: Elsevier.

Price, C. 1975a. Testing porous building stone. *The Architects Journal*, August 13, 337–9.

Price, C. 1975b. Thermal transmittance. *The Architects Journal*, August 13, 345–7.

Pye, K. 1983. Formation of quartz silt during humid tropical weathering of dune sands. *Sedimentary Geology* **34**, 267–82.

Pye, K. 1985. Granular disintegration of gneiss and migmatites. *Catena* 12, 191–9.

Pye, K. 1987. *Aeolian dust and dust deposits*. London: Academic Press.

Pye, K. and H.B. Sperling 1983. Experimental investigation of silt formation by static breakage processes: the effect of temperature, moisture and salt on quartz dune sand and granitic regolith. *Sedimentology* **30**, 49–62.

Quinif, Y. 1983. La reculée et le réseau karstique de Bou Akous (Hammamet, Algérie de l'Est) Geomorphologie et aspects évolutifs. *Révue Belge de Geographie* **107**, 89–111.

Ravina, I. and D. Zaslavsky 1974. The electrical double layer as a possible factor in desert weathering. *Zeitschrift für Geomorphologie Supplement Band* **21**, 13–18.

Rice, A. 1976. Insolation warmed over. *Geology* **4**, 61–2.

Robinson, D.A. and L.C. Jerwood 1987. Frost and salt weathering of chalk shore platforms near Brighton, Sussex, U.K. *Transactions of the Institute of British Geographers* **12**, 217–26.

Rodriguez-Rey, A. and M. Montoto 1978. Insolation weathering phenomena in crystalline rocks. In *Deterioration and Protection of Stone Monuments*. UNESCO/RILEM Conference, Paris, Section 2.7.

Rögner, K. 1987. Temperature measurements of rock surfaces in hot deserts (Negev Israel). In *International geomorphology*, V. Gardiner (ed.), 1271–87. Chichester: Wiley.

Rögner, K. 1988a. Measurements of cavernous weathering at Machtesh Hagadol (Negev Israel). A semi-quantitative study. *Catena Supplement* **12**, 67–76.

Rögner, K. 1988b. Der Verwitterungsgrad von Geröllen auf Terrassenoberflächen. *Die Erde* **119**, 31–45.

Roth, E.S. 1965. Temperature and water content as factors in desert weathering. *Journal of Geology* **73**, 454–68.

Schattner, I. 1961. Weathering phenomena in the crystalline of the Sinai in the light of current notions. *The Bulletin of the Research Council of Israel* **10G**, 247–66.

See, R.B., M.M. Reddy and R.G. Martin 1987. Description and testing of three moisture sensors for measuring surface wetness on carbonate building stones. *U.S. Geological Survey, Water Resources Investigations Report* 87-4177.

See, R.B., M.M. Reddy and R.G. Martin 1988. Description and testing of three moisture sensors for measuring surface wetness of carbonate building stones. *Review of Scientific Instrumentation* **59**, 2279–84.

Selby, M.J. 1977. On the origin of sheeting and laminae in granitic rocks: evidence from Antarctica, the Namib Desert and the Central Sahara. *Madoqua* **10**, 171–9.

Sharon, D. 1970. Topography-conditioned variations in rainfall related to the runoff-contributing areas in a small watershed. *Israel Journal of Earth Sciences* **19**, 85–9.

Sharon, D. 1981. The distribution in space of local rainfall in the Namib Desert. *Journal of Climatology* **1**, 69–75.

Simmons, G. and D. Richter 1976. Microcracks in rocks. In *The physics and chemistry of minerals and rocks*, R.G.J. Strens (ed.) 105–37. Chichester: Wiley.

Singer, A. 1980. The palaeoclimatic interpretation of clay minerals in sediments – a review. *Earth-Science Reviews* **21**, 251–93.

Singer, A. 1984. Clay formation in saprolites of igneous rocks under semiarid to arid conditions, Negev, southern Israel. *Soil Science* **137**, 332–40.

Slatyer, R.O. and J.A. Mabbutt 1964. Hydrology of arid and semi-arid regions. In *Handbook of applied hydrology*, V.T. Chow (ed.), New York: McGraw Hill.

Smalley, I.J. and D.H. Krinsley 1978. Loess deposits associated with deserts. *Catena* **5**, 53–66.

Smalley, I.J. and C. Vita-Finzi 1968. The formation of fine particles in sandy deserts and the nature of desert loess. *Journal of Sedimentary Petrology* **38**, 766–74.

Smith, B.J. 1977. Rock temperature measurements from the northwest Sahara and their implications for rock weathering. *Catena* **41**, 41–63.

Smith, B.J. 1978. The origin and geomorphic implications of cliff foot recesses and tafoni on limestone hamadas in the northwest Sahara. *Zeitschrift für Geomorphologie* **22**, 21–43.

Smith, B.J. 1987. An integrated approach to the weathering of limestone in an arid area and its role in landscape evolution: a case study from southeast Morocco. In *International geomorphology*, V. Gardiner (ed.), 637–57. Chichester: Wiley.

Smith, B.J. 1988. Weathering of superficial limestone debris in a hot desert environment. *Geomorphology* **1**, 355–67.

Smith, B.J. and R.W. Magee 1990. Weathering of granite in

an urban environment: a case study from Rio de Janeiro. *Journal of Tropical Geography*, **11**, 143–53.

Smith, B.J. and J.J. McAlister 1986. Observations on the occurrence and origins of salt weathering phenomena near Lake Magadi, southern Kenya. *Zeitschrift für Geomorphologie* **30**, 445–60.

Smith, B.J. and J.P. McGreevy 1983. A simulation study of salt weathering in hot deserts. *Geografiska Annaler* **64a**, 127–33.

Smith, B.J. and J.P. McGreevy 1988. Contour scaling of a sandstone by salt weathering under simulated hot desert conditions. *Earth Surface Processes and Landforms* **13**, 697–706.

Smith, B.J. and W.B. Whalley 1981. Late Quaternary drift deposits of north-central Nigeria examined by scanning electron microscopy. *Catena* **8**, 345–68.

Smith, B.J. and W.B. Whalley 1993. Non-glacial, loess-sized quartz silt: implications for the origins of 'desert loess'. Review and further data. In *Loess and China, essays for Lin Tung-shen*, E. Derbyshire and I.J. Smalley (eds). Leicester: Leicester University Press, in press.

Smith, B.J., J.P. McGreevy and W.B. Whalley 1987. The production of silt-size quartz by experimental salt weathering of a sandstone. *Journal of Arid Environments* **12**, 199–214.

Soleilhavoup, F. 1977. Les cailleux fissurés des regs Sahariens: étude descriptive et typologie. *Géologie Mediterraneé* **4**, 335–64.

Sperling, C.H.B. and R.U. Cooke 1980a. Salt weathering in arid environments. I Theoretical considerations. *Bedford College London Papers in Geography* 8.

Sperling, C.H.B. and R.U. Cooke 1980b. Salt weathering in arid environments. II Laboratory studies. *Bedford College London Papers in Geography* 9.

Stambolov, T. 1976. The corrosive action of salts. *Lithoclastia* **I**, 5–8.

Sutton, L.J. 1945. Meteorological conditions in caves and ancient tombs in Egypt. *Ministry of Public Works, Egypt, Physical Department Paper* 52.

Sweeting, M.M. and N. Lancaster 1982. Solutional and wind erosion forms on limestone in the central Namib Desert. *Zeitschrift für Geomorphologie* **26**, 197–207.

Tardy, Y., C. Bocquir, H. Paquet and G. Millet 1973. Formation of clay from granite and its distribution in relation to climate and topography. *Geoderma* **10**, 271–84.

Tassios, T.P. and C. Economou 1976. Non-destructive evaluation of marble quality on the west part of the Parthenon. In *2nd International Symposium on the Deterioration of Building Stones, Athens*, 299–308.

Torraca, G. 1981. *Porous Materials – Materials Science for Architectural Conservation*. Rome: ICCROM.

Trudgill, S.T., H.A. Viles, R.J. Inkpen and R.U. Cooke 1989. Remeasurement of weathering rates of St. Paul's Cathedral, London. *Earth Surface Processes and Landforms* **14**, 175–96.

Verheye, W. 1976. Nature and impact of temperature and moisture in arid weathering and soil forming processes. *Pédologie* **26**, 205–24.

Verheye, W. 1986. Observations on desert pavements and desert patinas. *Pedologie* **36**, 303–13.

Verhoef, P.N.W. 1987. Sandblast testing of rock. *International Journal of Rock Mechanics Mineral Science and Geomechanics Abstracts* **24**, 185–92.

Viles, H. 1988. Organisms and karst geomorphology. In *Biogeomorphology*, H.A. Viles (ed.) 319–50. Oxford: Basil Blackwell.

Viles, H. and S.T. Trudgill 1984. Long-term remeasurements of micro-erosion meter rates, Aldabra Atoll, Indian Ocean. *Earth Surface Processes and Landforms* **9**, 89–94.

Whalley, W.B., G.R. Douglas and J.P. McGreevy 1982a. Crack propagation and associated weathering in igneous rocks. *Zeitschrift für Geomorphologie* **26**, 33–54.

Whalley, W.B., J.R. Marshall and B.J. Smith 1982b. Origin of desert loess from some experimental observations. *Nature* **300**, 433–5.

Whalley, W.B., J.P. McGreevy and R.I. Ferguson 1984. Rock temperature observations and chemical weathering in the Hunza region, Karakorum: preliminary data. In *Proceedings of the International Karakorum Project*, K.J. Miller (ed.), 616–33. Cambridge: Cambridge University Press.

Whalley, W.B., B.J. Smith, J.J. McAlister and A.J. Edwards 1988. Aeolian abrasion of quartz particles and the production of silt-size fragments. Preliminary results and some possible implications for loess and silcrete formation. In *Desert sediments: ancient and modern*, L. Frostick and I. Reid (eds), 129–38. Oxford: Blackwell Scientific, Geological Society of London Special Publication 135.

Whitaker, C.R. 1974. Split boulder. *Australian Geographer* **12**, 562–3.

White, S. 1976. The role of dislocation processes during tectonic deformation, with particular reference to quartz. In *The physics and chemistry of minerals and rocks*, R.G.J. Strens (ed.), 75–91. Chichester: Wiley.

Wilhelmy, H. 1964. Cavernous rock surfaces (tafoni) in semi-arid and arid climates. *Pakistan Geographical Review* **19**, 9–13.

Wilke, B.M., B.J. Duke and W.L.O. Jimoh 1984. Mineralogy and chemistry of harmattan dust in northern Nigeria. *Catena* **11**, 91–6.

Williams, C.B. 1923. A short bio-climatic study in the Egyptian Desert. *Ministry of Agriculture, Egypt Technical and Scientific Service Bulletin* 29.

Williams, R.B.G. and D.A. Robinson 1981. Weathering of a sandstone by the combined action of frost and salt. *Earth Surface Processes and Landforms* **6**, 1–9.

Williams, R.B.G. and D.A. Robinson 1983. The effect of surface texture on the determination of the surface hardness of rock using the Schmidt Hammer. *Earth Surface Processes and Landforms* **8**, 289–92.

Wilson, P. 1979. Experimental investigation of etch pit formation on quartz sand grains. *Geological Magazine* **116**, 447–82.

Winkler, E.M. 1979. The role of salts in development of granitic tafoni, South Australia. A discussion. *Journal of Geology* **87**, 119–20.

Winkler, E.M. 1987a. Weathering and weathering rates of natural stone. *Environmental Geology and Water Science* **9**, 85–92.

Winkler, E.M. 1987b. Comment on 'Capillary moisture flow and the origin of cavernous weathering in dolerites of Bull Pass, Antarctica.' *Geology* **15**, 975.

Wisniewski, J. 1982. The potential acidity associated with dews, frosts and fogs. *Water Air and Soil Pollution* **17**, 361–77.

Yaalon, D.H. 1970. Parallel stone cracking, a weathering

process on desert surfaces. *Geological Institute Technical Economic Bulletin (Bucharest)* **18**, 107–10.

Yaalon, D.H. and J. Dan 1974. Accumulation and distribution of loess-derived deposits in the semi-arid desert fringe areas of Israel. *Zeitschrift für Geomorphologie Supplement Band* **20**, 27–32.

Yaalon, D.H. and E. Ganor 1968. Chemical composition of dew and dry fallout in Jerusalem, Israel. *Nature* **217**, 1139–40.

Yair, A. and S.M. Berkowicz 1989. Climatic and non-climatic controls of aridity: the case of the northern Negev of Israel. *Catena Supplement* **14**, 145–58.

Yair, A., D. Sharon and H. Lavee 1978. An instrumental watershed for the study of partial area contribution of runoff in the arid zone. *Zeitschrift für Geomorphologie Supplement Band* **29**, 71–82.

Yamasaki, R.S., H.F. Slade and P.J. Sereda 1983. Determination of time-of-wetness due to condensed moisture. *Durability of Building Materials* **I**, 353–61.

Yong, C. and C.Y. Wang 1980. Thermally induced acoustic emission in Westerly granite. *Geophysical Research Letters* **7**, 1089–92.

Young, A.R.M. 1987. Salt as an agent in the development of cavernous weathering. *Geology* **15**, 962–6.

ARIDIC SOILS, PATTERNED GROUND, AND DESERT PAVEMENTS

4

John C. Dixon

INTRODUCTION

Pedogenic and geomorphic processes operating in deserts are inextricably linked. These linkages are particularly well expressed in the development of patterned ground and desert pavement. In addition, the nature and efficacy of hydraulic, gravitational, and aeolian processes on desert surfaces are strongly influenced by the physical and chemical characteristics of the underlying soils. As a result, the evolution of a diversity of desert landforms is either directly or indirectly linked to pedogenic processes.

The significant role played by pedogenic processes in desert landscape evolution is also strongly reflected in the development of duricrusts – indurated accumulations of calcium carbonate, gypsum, and silica. These essentially pedogenic materials impart considerable relief in the form of tablelands, mesas, and buttes to otherwise low-relief landscapes. Erosion of these topographic eminences in turn provides the coarse debris for the formation of patterned ground and desert pavement.

In this chapter the nature and genesis of soils in arid and semi-arid environments are examined. This discussion is followed by an examination of the major types of patterned ground and the processes responsible for its formation. Finally, the nature and origin of desert pavements are examined. The characteristics and origin of duricrusts are discussed in Chapter 5.

ARIDIC SOILS

CHARACTERISTICS

Aridic soils display a variety of distinctive morphological features. Among these are the presence of gravel surfaces, the development of surficial crusts, and the widespread occurrence of vesicular A horizons. Such soils commonly possess ochric and mollic epipedons and are characterized by the formation of a variety of diagnostic subsurface horizons including cambic, argillic, calcic, petrocalcic, gypsic, petrogypsic, natric, salic, and duripan horizons.

Vesicular Horizons

Immediately beneath the gravel surface layer of many aridic soils a vesicular A horizon (Fig. 4.1) commonly occurs and is often associated with a surface crust. Formation of the vesicular horizon has been widely attributed to the saturation of the fine grained soil surface horizon (Miller 1971). Nettleton and Peterson (1983) argued that in the saturated state the soil plasma of this upper horizon is free to move and in so doing traps air. With repeated episodes of saturation and air entrapment, the vesicles in the surface horizon increase in size. Repeated destruction of the vesicular horizon is thought to be caused by wetting and drying cycles (Springer 1958, Miller 1971). Nettleton and Peterson (1983) alternatively suggested that vesicular horizon destruction is primarily the result of soil trampling by animals. Upon destruction, the formation of the vesicular horizon begins anew as soil saturation episodes begin and air entrapment resumes.

More recently, a substantially different explanation for the origin of the vesicular horizon has been proposed by Wells *et al.* (1985) and McFadden *et al.* (1986, 1987). These workers attributed the origin of the fine grained surface horizon and accompanying vesicular structure to aeolian addition of fine grained materials and associated soluble salts, carbonates, and iron oxides. The development of vesicles was attributed to entrapment of air by aeolian infall with subsequent expansion due to heating following sum-

Geomorphology of Desert Environments. Edited by Athol D. Abrahams and Anthony J. Parsons. Published in 1994 by Chapman & Hall, London. ISBN 978-94-015-8256-8

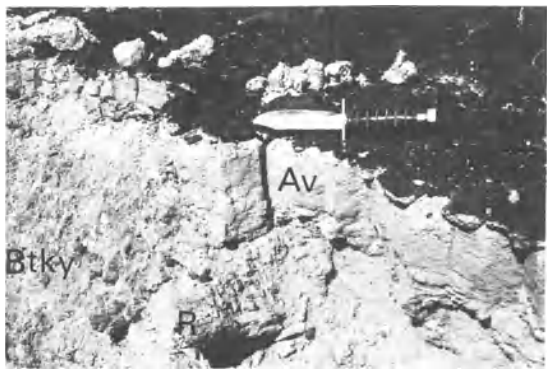

Figure 4.1 Soil developed beneath desert pavement showing vesicular A horizon (Av) and carbonate and gypsum enriched B horizon (Btky). Bedrock rubble is designated (R) (photo courtesy of L.D. McFadden).

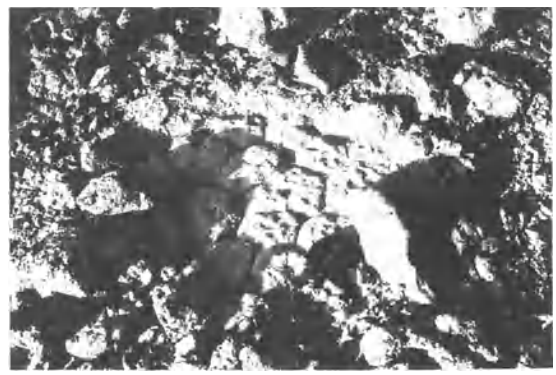

Figure 4.2 Columnar structure of vesicular A horizon resulting from high shrink–swell capacity (photo courtesy of L. D. McFadden).

mer rainfall events. This model follows that of Evenari *et al.* (1974) for vesicular horizons developed in soils in Israel. While aeolian infall was envisaged as the primary source of the fine grained surface layer, McFadden *et al.* (1987) also suggested that some of the sand and silt fraction may be the result of mechanical weathering of the surface gravels. The presence, and successive accumulation, of clay in the aeolian mantle leads to the development of a distinctive columnar structure in the Av horizon due to enhanced shrink–swell capacity (McFadden *et al.* 1986) (Fig. 4.2). Recently, Sullivan and Koppi (1991), working on desert loams in Australia, have also proposed that the fine grained materials in the vesicular horizon are externally derived. They suggested a combination of aeolian, colluvial, and overland flow sources.

Cambic Horizons

Intimately associated with the vesicular, ochric epipedons are cambic horizons. These horizons are found below ochric epipedons and are typically reddish or brownish in colour. There is evidence of alteration in the horizon in the form of obliteration of original structures due to mixing, development of new structure, accumulation of clay, and carbonate translocation through and into the horizon (Nettleton and Peterson 1983). The source of the fine material and the carbonates in this horizon is widely attributed to aeolian infall (Gile 1970, 1975, Gerson *et al.* 1985, McFadden *et al.* 1986, Gerson and Amit 1987, Reheis 1987a, Wells *et al.* 1987, Birkeland 1990). McFadden *et al.* (1986) suggested that as the vesicular horizon thickens due to continued aeolian addition, plasma migration near the base of the horizon results in destruction of vesicles and a slowing of the migration of infiltrating waters. This slowing of infiltration results in ferrous iron alteration as well as the accumulation of authigenic ferric iron oxyhydroxides. Soil reddening results, and a cambic horizon slowly develops. Clay and carbonate added by aeolian infall also migrate to the cambic horizon.

Argillic Horizons

Many aridic soils are characterized by the occurrence of strongly developed argillic (clay-rich) horizons. This horizon differs markedly from the aforedescribed cambic horizon in that it is substantially more abundant in clay and commonly has a non-calcareous matrix. Research on the origin of the argillic horizon has focused on two contrasting sources of clay. Smith and Buol (1968) and Nettleton *et al.* (1975) have shown that the degree of mineral weathering in A horizons of some argids in the south-western United States is comparable to, or greater than, that in underlying Bt horizons. This finding therefore suggests that chemical weathering in A horizons is a possible source of illuvial clay. Further, these authors have pointed to the occurrence of clay skins on mineral grains and pebbles in the argillic horizon as evidence for clay illuviation. The frequent lack of clay skins on ped faces is attributed by Nettleton and Peterson (1983) to destruction by swell–shrink mechanisms, bioturbation, and calcium carbonate crystal growth. Nettleton *et al.* (1975) also argued for clay illuviation on the basis of patterns of distribution of fine and coarse clay and total iron and aluminium down the profile. Finally,

Nettleton and Peterson (1983) reasoned that the occurrence of clay skins on the walls of deep pipes or as downward extensions of the argillic horizon support an illuvial origin for the clay. Chartres (1982), on the other hand, has stressed the importance of the aeolian addition of fine debris in the formation of argillic horizons, citing a relative lack of weathered soil particles in the A horizon as evidence against an in-profile source of clay.

Carbonates are commonly associated with the argillic horizon. In some cases they may dominate the soil matrix (Gile 1967), but more commonly they occur as nodules which have displaced the previously deposited clays (Gile and Grossman 1968, McFadden *et al.* 1986). Accumulation of carbonates in argillic horizons is widely interpreted to be indicative of significant climate change from humid to arid climatic regimes with an accompanying reduction in depth of leaching (Nettleton and Peterson 1983, McFadden and Tinsley 1985, McFadden *et al.* 1986, Reheis 1987b, Wells *et al.* 1987). Thick argillic horizons in Aridisols are therefore widely regarded as being largely relics of the Pleistocene.

Natric and Salic Horizons

The accumulation of soluble salts is a further characteristic of aridic soils. Accumulation results in the formation of either natric (sodic) or salic (saline) horizons. Natric horizons are characterized by high ($\geq$15%) exchangeable sodium and by the development of prismatic or columnar soil structure (Soil Survey Staff 1975). In Holocene age soils these horizons are typically thin, while in Pleistocene soils they thicken considerably (Nettleton and Peterson 1983). These horizons typically occur above or in a zone of calcium carbonate accumulation (Nettleton and Peterson 1983). Although there is sodium accumulation, there is insufficient for these horizons to be classified as salic. Salic horizons are characterized by accumulation of salts in such abundance that the product of horizon thickness in centimetres and percentage salt content is not less than 60.

Soluble salt-rich horizons appear to be the result of three principal processes. Airborne addition of salts has been suggested for these horizons in aridic soils in the United States by Alexander and Nettleton (1977), Peterson (1980), Nettleton and Peterson (1983), and McFadden *et al.* (1991). An airborne source of salts has also been suggested for saline soils in Israel (Yaalon 1964, Yaalon and Ganor 1973, Dan *et al.* 1982, Amit and Gerson 1986). The source of salts in sodic soils in Australia has also been widely attributed to airborne sources, particularly for those soils within about 200 km of the coastal environment (Hutton and Leslie 1958, Wetselaar and Hutton 1963, Chartres 1983, Isbell *et al.* 1983).

A second source of the sodium is from the incursion of very shallow ground waters. Nettleton and Peterson (1983) suggested such an origin for some of the natric horizons in soils in the United States. These workers also proposed that this process is particularly important in the formation of salic horizons. This process appears to be especially significant for soils occurring in the Riverine Plain of south-eastern Australia (Northcote and Skene 1972, Isbell *et al.* 1983). Detailed discussion of salinization of soils in Western Australia by saline ground waters is provided by Conacher (1975). Secondary salinization as a result of groundwater pumping for irrigation is a growing problem in some arid Australian soils.

The third explanation for the formation of natric or salic horizons is the inheritance of salts from parent materials. Three parent material sources have been suggested by workers from Australia. Chartres (1983) suggested that sodic horizons developed well below the depth of contemporary infiltration may well have originated in older sodic soils which have subsequently been eroded. A number of studies of sodic soils from western Queensland strongly suggest that many have derived their sodium from the underlying bedrock (Gunn and Richardson 1979, Isbell *et al.* 1983). In a related fashion, some sodic soils derive their salts from underlying deeply weathered parent materials which have in turn been derived from salt-rich bedrock. Sodic soils developed on laterite in Western Australia have been reported by Bettenay *et al.* (1964) and Dimmock *et al.* (1974). The significance of the deep sodic horizons as sources of secondary salinization have been investigated by Peck and Hurle (1973) and Peck (1978). Sodic soils developed in deeply weathered materials have also been reported from Queensland by Hubble and Isbell (1958) and Isbell (1962). More recently, Gunn (1967) has suggested that deep weathering profiles are also the source of salts in solodic and solodized–solonetz soils in central Queensland.

Calcic and Gypsic Horizons

Aridic soils are frequently dominated by calcium carbonate and/or gypsum. With progressive concentration of carbonate or gypsum and accompanying induration, petrocalcic and petrogypsic horizons develop. These horizons are collectively referred to as duricrusts, which are discussed fully in Chapter 5. Calcic and gypsic soils are characterized by the

occurrence of non-indurated accumulations of calcite and/or dolomite in the former and gypsum in the latter. These materials occur in a variety of forms including powdery fillings, nodules, pendents, or crusts beneath pebbles and cobbles. Crusts in calcic and gypsic soils slake in water. In the United States, calcic soil horizons must be 15 cm or more thick, contain the equivalent of ≥15% $CaCO_3$, and have a carbonate content ≥5% greater than the C horizon. Gypsic soil horizons must also be 15 cm or more thick, contain at least 5% more gypsum than the underlying horizon, and have a product of horizon thickness in centimetres and percentage gypsum content not less than 150 (Soil Survey Staff 1975).

Descriptions of calcic and gypsic soils are common in the desert soils literature. It is important to point out that many aridic soils contain intergrades of calcic–gypsic horizons. Calcic soils in the United States have been extensively investigated by Bachman and Machette (1977), Shlemon (1978), Gile *et al.* (1981), Nettleton and Peterson (1983), Machette (1985), Weide (1985), Reheis *et al.* (1989), Harden *et al.* (1991), McFadden *et al.* (1991), Monger *et al.* (1991), Rabenhorst *et al.* (1991), and Nettleton *et al.* (1991). Studies of gypsic soils in the United States are notably fewer but include those of Nelson *et al.* (1978), Nettleton *et al.* (1982), and Harden *et al.* (1991). Detailed descriptions of gypsic soils in Wyoming have been provided by Reheis (1987a) Figs 4.3, 4.4 and 4.5). Studies of calcic soils from Australia have been summarized by Stace *et al.* (1968) and Northcote and Skene (1972), and more recently by Hutton and Dixon (1981), Milnes and Hutton (1983), Isbell *et al.* (1983), and Akpokodje (1984). Early descriptions of gypsic soils in Australia were provided by Jessop (1960) and Bettenay (1962). Calcic and gypsic soils have been reported from many other arid and semi-arid environments, some of which were summarized by Eswaran and Zi-Tong (1991). These authors reported the extensive occurrence of gypsic soils in China, India, Pakistan, the Middle East, and Africa. More limited occurrences of gypsic soils were recorded in southern Europe. Dan (1983) and Dan *et al.* (1982) described gypsic soils from Israel.

The source of the gypsum and carbonate in aridic soils is widely believed to be from atmospheric addition as either dust or carbonate dissolved in rainwater (Bull 1991, Dohrenwend *et al.* 1991, Gustavson *et al.* 1991). However, some studies such as those by Akpokodje (1984) suggest an *in situ* origin of the carbonate and gypsum. Recently, Boettinger and Southard (1991) have provided compelling evidence from Aridisols developed on pediments in the

Figure 4.3 Stage I gypsum (arrows) in soil developed on alluvial fan, Bighorn Basin, Wyoming (photo courtesy of M. Reheis (U.S. Geological Survey Bulletin 1590-C)).

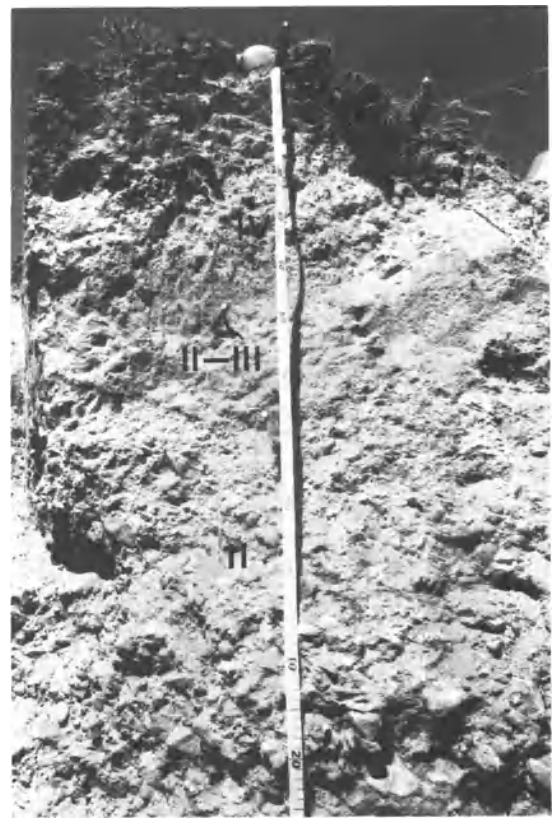

Figure 4.4 Complex gypsic soil developed on alluvial fan, Bighorn Basin, Wyoming. Stage IV gypsum 20–50 cm, Stage II/III gypsum 50–75 cm, Stage II gypsum 75+ cm (photo courtesy of M. Reheis (U.S. Geological Survey Bulletin 1590-C)).

Figure 4.5 Stage IV gypsum (g) in soil developed on alluvial fan, Bighorn Basin, Wyoming (photo courtesy of M. Reheis (U.S. Geological Survey Bulletin 1590-C)).

Mojave Desert of California that the source of carbonate deep within calcareous Haplargids is derived from the weathering of the granite and accompanying release of calcium from plagioclase.

Duripans

Many arid soils possess a duripan. These pans are subsurface indurations of predominantly silica, but may grade to petrocalcic (calcrete) horizons (Soil Survey Staff 1975, Nettleton and Peterson 1983). In gross morphology, chemistry, and mineralogy they are analogous to silcretes described in detail in Chapter 5. Duripans are generally platy in structure with individual plates ranging in thickness from 1 to 15 cm. Pores and surfaces of the plates are commonly coated with opal, chalcedony, and/or microcrystalline silica. For a soil horizon to be classified as a duripan, at least one of three criteria must be met. The soil must display (a) some vertical coatings of opal, (b) siliceous nodule development, or (c) the development of silica pendents on the undersides of coarse fragments. In addition, opal or other forms of silica must partly fill interstices and form bridges between sand grains (Soil Survey Staff 1975).

Duripans in the United States appear to be most strongly developed in soils formed on volcanic ash or other pyroclastic parent materials containing abundant silica (Flach *et al.* 1969, 1973, Brasher *et al.* 1976, Nettleton and Peterson 1983). Duripans have recently been examined by Boettinger and Southard (1991) from a Durorthid pedon developed in grus on a pediment in the Mojave Desert. These workers suggested that the source of the silica is not volcanic glass, which is essentially absent from the profile, but the weathering of feldspars. In Australia, Stace *et al.* (1968) reported hardpan soils commonly occurring on strongly weathered alluvial and colluvial deposits as well as on eroded laterites. Duripans are most strongly developed on older landscape surfaces where there has been sufficient time for prolonged silica dissolution, translocation, and deposition. They form at the average depth of wetting, which progressively diminishes with increasing aridity. Duripans commonly form below or in the lower part of argillic or natric horizons and have also been observed to be interlayered with illuvial clay (Nettleton and Peterson 1983). In Australia, hardpan soils have been reported from Western Australia by Litchfield and Mabbutt (1962), Stace *et al.* (1968), and Brewer *et al.* (1972), from South Australia by Stace *et al.* (1968), Wright (1983), and Milnes *et al.* (1991), and from New South Wales by Chartres (1985).

ARIDIC SOILS AND LANDSCAPE DEVELOPMENT

Research on aridic soils in the United States in recent years has focused heavily on the relationship between soil development and landscape evolution. These studies have been concerned with the age of landscapes, correlation of Quaternary deposits, and climate change. The use of aridic soils as relative age indicators is well illustrated in studies from the western and south-western United States (Christianson and Purcell 1985, Harden *et al.* 1985, Machette 1985, Ponti 1985, Dohrenwend *et al.* 1991).

Detailed studies of soil development as an indicator of environmental change have been undertaken by many workers in the south-western United States. Major differences in aeolian dust addition to soils between the Holocene and Pleistocene are reported by Machette (1985), McFadden *et al.* (1984, 1986, 1987), Wells *et al.* (1987), Chadwick and Davis (1990), Reheis (1987a, b, 1990), and Bull (1991). Studies of carbonate accumulation amounts and rates, and depth of infiltration have been undertaken by Machette (1985), McFadden and Tinsley (1985), Reheis (1987a, b), and Bull (1991). These studies all point to maximum carbonate accumulation during the Holocene and accompanying reduction in the depth of carbonate infiltration. The polygenetic nature of many aridic soils is also highlighted in studies by Reheis (1987a, b) Nettleton *et al.* (1989), and Bull (1991). Variability in rates of soil formation depending on geomorphic setting and climate is stressed by Reheis *et al.* (1989) and Bull (1991).

Soils in arid environments in the western United States have also been widely used as stratigraphic markers and as indicators of periods of stability

within Quaternary depositional systems. Such studies are well exemplified by the work of Gustavson and Winkler (1988), Gustavson *et al.* (1991), and Holliday (1985a, b, c, 1988, 1989, 1990) from the southern High Plains of Texas and New Mexico. A similar study in an aeolian environment in the southern Colorado Plateau by Wells *et al.* (1990) further demonstrates the importance of soils in studies of landscape evolution in desert environments.

CLASSIFICATION

In the United States, the soil order dominating the warm desert regions of the country is Aridisol. Two principal suborders, Argids and Orthids, are recognized. Argids are Aridisols that are characterized by the development of argillic or natric horizons. Orthids are Aridisols which lack an argillic or natric horizon.

Each of these suborders can be further divided into a number of great groups. The principal great groups of Argids are Durargids, Haplargids, Natrargids, Nadurargids, and Paleargids (Guthrie 1982). Durargids possess a duripan that underlies an argillic horizon and lack natric horizons. The top of the duripan is within a metre of the ground surface. Haplargids lack a natric horizon and do not have a duripan or petrocalcic horizon within a metre of the surface. They have weakly developed argillic horizons with less than 35% clay accumulation. Natrargids are characterized by the occurrence of a natric horizon but lack a duripan or petrocalcic horizon within a metre of the ground surface. Nadurargids are Argids that possess a natric horizon above a duripan, and the surface of the duripan is within a metre of the ground surface. Paleargids are Argids that develop on old land surfaces. They are characterized by either a petrocalcic horizon below an argillic horizon or an argillic horizon with greater than 35% clay and an abrupt upper boundary (Soil Survey Staff 1975).

Orthids are aridic soils with one or more pedogenic horizons. However, they lack a natric or argillic horizon. They commonly have an accumulic horizon of soluble salts and calcium carbonate. Some orthids possess salic, calcic, gypsic, petrocalcic, petrogypsic, cambic, and duripan horizons (Soil Survey Staff 1975). Orthids are divided into six great groups: Calciorthids, Camborthids, Durorthids, Gypsiorthids, Paleorthids, and Salorthids. Calciorthids contain abundant amounts of lime derived from either the parent material or added from aeolian dust. Camborthids are characterized by the development of a cambic horizon that results in a brownish to reddish brown soil of uniform texture. Durorthids possess a duripan within a metre of the surface and are commonly calcareous throughout. Gypsiorthids contain a gypsic or petrogypsic horizon with an upper boundary within a metre of the soil surface. Paleorthids contain a petrocalcic horizon within a metre of the ground surface. They commonly display evidence of calcium carbonate engulfing a pre-existing argillic horizon. Salorthids are very salty soils commonly associated with the accumulation of salts from capilliary rise of salty waters. They are characterized by a salic horizon (Soil Survey Staff 1975).

Aridisols, however, are not the only soil order found in warm desert environments. In one of the most comprehensive studies of arid lands soils in the United States, the Desert Project (Gile *et al.* 1981) recognized that large parts of the study sites in New Mexico are occupied by Entisols, Mollisols, and some Vertisols. Recent studies of the desert region in the south-western United States have recorded the widespread development of Entisols on Holocene age surficial deposits (McFadden 1988, Bull 1991).

The classification of soils in the arid environments of Australia is based on the Great Soil Groups originally proposed by Prescott (1931), modified by Stephens (1962), and more recently modified again by Stace *et al.* (1968). The Australian arid zone possesses a complex mozaic of Great Soil Groups, including Solonchaks, Lithosols, Siliceous Sands, Desert Loams, Grey Brown and Red Clays, Red and Brown Hardpan Soils, Solonized Brown Soil and Red Earths.

PATTERNED GROUND

GILGAI

Patterned ground associated with both stony deserts and playa surfaces is a widespread phenomenon in warm deserts (Cooke and Warren 1973, pp. 129–49, Mabbutt 1977, pp. 130–4). Perhaps the most common and widespread type of patterned ground is gilgai. Gilgai is an Australian aboriginal word meaning small water hole, and while originally applied to small depressions that held water, it is now used to refer to a wide variety of soil patterned ground phenomena. Although the distribution and diversity of gilgai forms is perhaps greatest on the Australian continent, gilgai has also been reported from the Middle East by Harris (1958, 1959) and White and Law (1969), from South Dakota by White and Bones-

tall (1960), and from Death Valley, California, by Denny (1965, 1967) and Hunt and Washburn (1960). In addition to gilgai being frequently associated with soils of high swelling potential such as Vertisols, it is also a common feature in arid and semi-arid environments where strong textural contrasts exist within soils and where the climate is characterized by pronounced seasonality of precipitation. Gilgai morphology occurs in soils with annual rainfalls ranging from less than 150 mm to more than 1500 mm.

Gilgai Types

In early work on gilgai (Hallsworth and Robertson 1951, Hallsworth *et al.* 1955, Stace *et al.* 1968, pp. 417 and 420, Hubble *et al.* 1983), six principal types of morphology were recognized (Fig. 4.6). (a) Normal gilgai is the most common form and is characterized by the development of randomly oriented mounds and shelves. The magnitude of these features ranges from imperceptible to as much as 3 m vertically with a wavelength of 15 m. If mounds are subcircular, they are referred to as puffy gilgai. (b) Melon-hole gilgai consists of large mounds separated by shelves of complex morphology. The shelves are commonly depressions with one or more sinkholes at the bottom; they are typically 1 to 3 m wide and 15 to 20 cm deep. (c) Stony gilgai, which most closely resembles the patterned ground found at high latitudes and high altitudes, has stone-covered mounds which are wide and flat in form. (d) Lattice gilgai is complex in morphology. It includes mounds that are discontinuous and oriented parallel to the direction of the slope as well as semi-continuous mounds that form networks of diverse orientation. (e) Linear or wavy gilgai develops on hillslopes ranging in gradient from 15″ to 3°. Mounds and shelves are continuous and are arranged at right angles to the contour. These forms are 5 to 10 cm in height, and in the dry season they are very puffy in appearance. (f) Tank gilgai is large-scale gilgai that is usually rectangular in shape. Vertical dimensions range from 60 cm to 1.5 m, while depressions are 10 to 20 m long and 15 to 20 m wide.

The most widely developed type of gilgai in the Australian desert is stony gilgai. Ollier (1966) and Mabbutt (1977, p. 131, 1979) recognized two principal types: circular and stepped (Fig. 4.6c i and ii). Circular gilgai is characterized by the development of a relatively fine grained inner depression surrounded by a slightly raised stony rim. The depressions are commonly about 3 m in diameter, while the outer rims have diameters of approximately 8 m. This type of stony gilgai commonly forms on surfaces of low slope. The soil beneath the stony mound is generally clay-rich and has a silt crust with embedded pebbles. In contrast, the soil beneath the depression is typically sandier in the upper 30 to 50 cm but at depth resembles the mound soil and has abundant coarse fragments. Circular gilgai may occur either in random patterns or in networks. Stepped gilgai – or, as Mabbutt (1977, 1979) calls them, lattice systems – occur on steeper slopes with gradients of 0.5° to 6°. These forms are essentially distorted gilgai that become aligned across the slope. They are characterized by the development of stony risers upslope and downslope of practically stone-free treads. As with the circular gilgai forms, the risers are underlain by fine grained soils, while sandier soils underlie the treads. Treads commonly display sink holes at the base of the upslope riser (Ollier 1966, Cooke and Warren 1973, Mabbutt 1979).

Mabbutt (1979) recognized a third type of stony gilgai in the desert pavement-covered areas of the Northern Territory. He referred to this type as sorted stone polygons (Fig. 4.6c iii). These polygons are between 40 and 80 cm in diameter and are outlined by a rim of silcrete boulders sitting on a pavement of smaller pebbles. The silcrete boulders are absent from the interior depression, though the smaller pebbles are still present. Top soil thicknesses are generally greater in the interior of the polygon (Mabbutt 1977).

Although gilgai in the arid areas of Australia is primarily associated with Desert Loams (Stace *et al.* 1968), it is also associated with a variety of other soils with strong textural contrasts in seasonally wet–dry environments. In particular, gilgai is strongly developed on grey cracking clays in west-central Queensland and in north-central and south-central New South Wales (Stace *et al.* 1968).

Detailed analyses of gilgai morphology have been undertaken by Paton (1974) and Knight (1980). Knight analysed gilgai in south-eastern Australia using structural geological techniques. He recognized five recurring patterns based on the spatial arrangement of mounds, depressions, and shelves.

Gilgai Formation

A large literature exists on the origin of gilgai. Knight (1980) identified four types of gilgai-forming mechanisms: (a) heave between cracks, (b) heave over cracks, (c) contraction over cracks, and (d) heave due to loading (Fig. 4.7). Within the first type of mechanism he distinguished three subtypes (Fig. 4.7a). The first subtype involves soil compres-

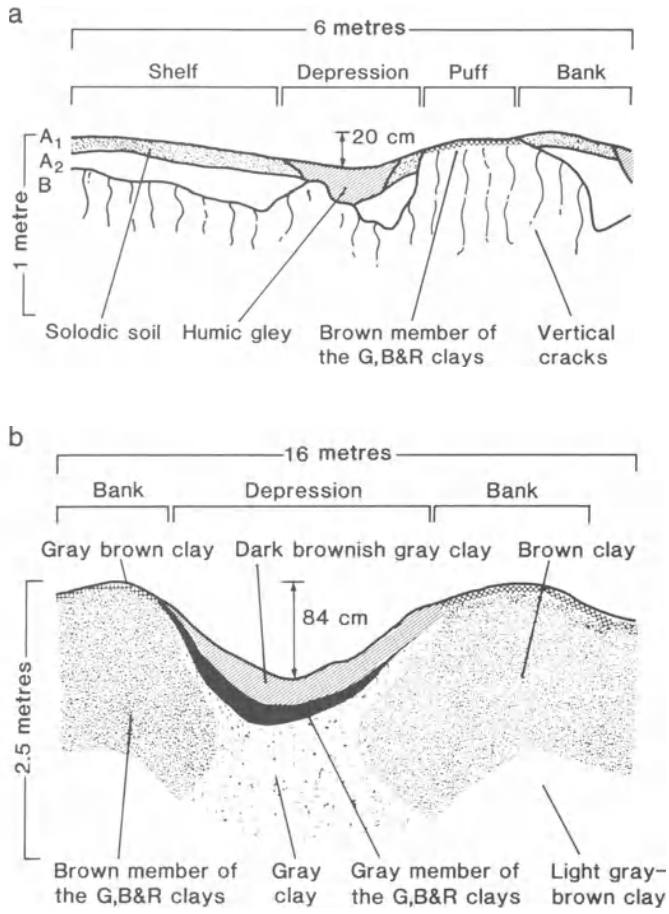

Figure 4.6 Cross-sections of principal types of gilgai: (a) normal; (b) melon-hole; (c) stony: (i) circular, (ii) stepped, (iii) polygonal; (d) lattice; (e) linear; (f) tank. (After Ollier 1966, Mabbutt 1977, Hubble *et al.* 1983.)

sion, extrusion, and associated plastic flow, with resulting upward movement of the mound. This mechanism was originally proposed by Leeper *et al.* (1936). The second subtype is perhaps one of the most widely accepted mechanisms of gilgai development and involves compression and block fracture (Hallsworth *et al.* 1955). This mechanism envisages the falling or washing of surface materials into cracks with subsequent exertion of force on subsurface clays resulting in vertical upthrusting. The third subtype calls for compression and oblique slip. This mechanism was originally proposed by White and Bonestall (1960). However, these three subtypes are all regarded by Knight (1980) as being mechanically unsound.

Two subtypes of the heave-over-cracks mechanism were recognized by Knight (1980) (Fig. 4.7b). The first he classified as being due to cumulative internal vertical movements due to small oblique slips. The second subtype is that of vertical block movement due to heave and was proposed by Howard (1939). It is also the mechanism proposed by Ollier (1966) for stony gilgai.

The contraction-over-cracks mechanism is a hypothetical one proposed by McGarity (1953) (Fig. 4.7c). It envisages the formation of depressions in the vicinity of adjacent cracks and mounds between cracks. The depressions are the result of downward movement of soil due to drying.

The heave-due-to-loading mechanism can be divided into two subtypes (Fig. 4.7d). The first involves the upward flow of soil due to density contrasts between layers (Beckman 1966, Paton 1974), whereas the second involves the flow of fluidized soil up a crack through a solid layer (Hallsworth and Beckman 1969).

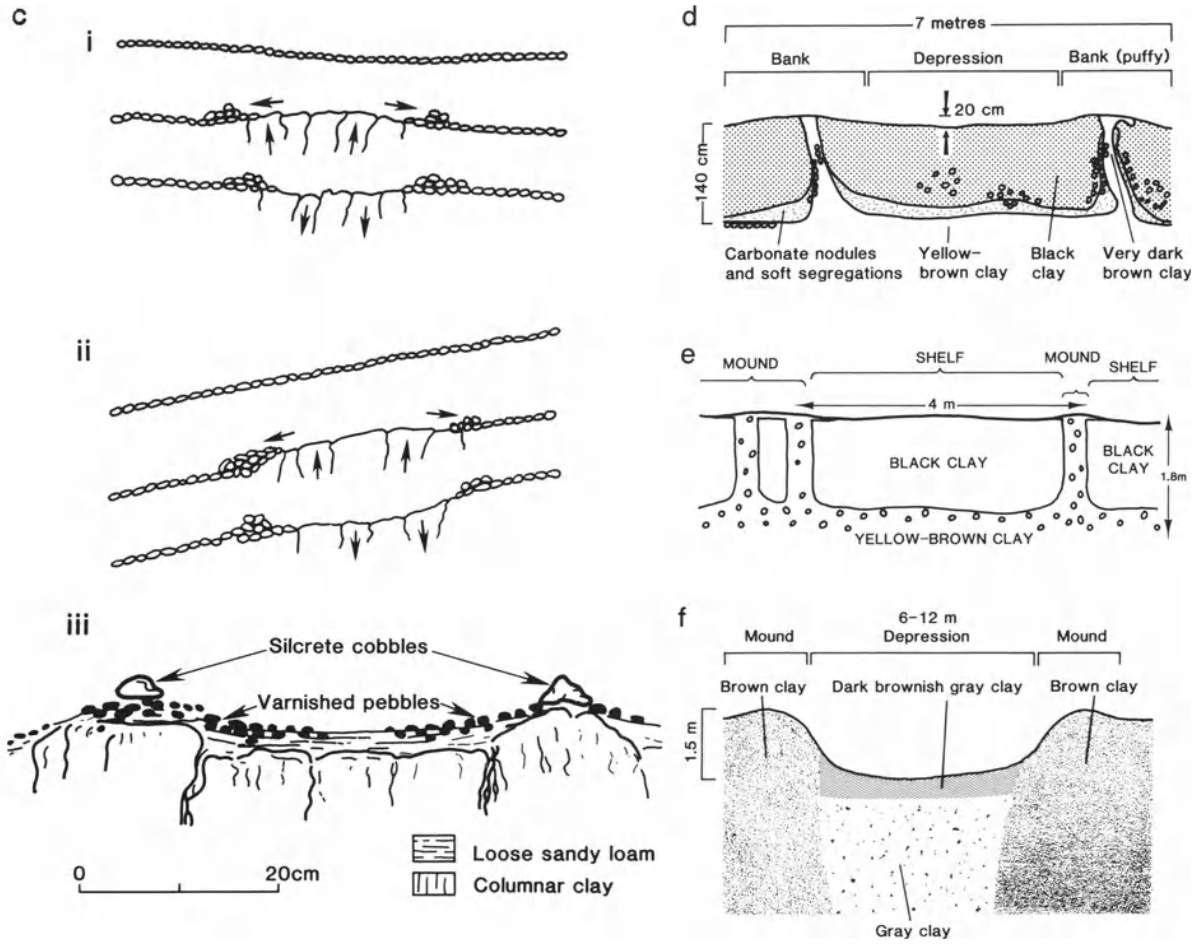

SURFACE CRACKING

The second major type of patterned ground in warm deserts is related to surface cracking. This cracking is interpreted to be largely a desiccation feature caused by drying of the surface crust (Cooke and Warren 1973, pp. 139–40). Considerable literature exists on the nature and origin of cracks in sediments. However, there has been relatively little discussion of the origin of small-scale surface cracks in deserts. An exception is the work by Tucker (1978) in northern Iraq on the origin of patterned ground associated with gypsum crusts. Tucker examined non-orthogonal crack types (Lachenbruch 1962) which range in diameter from 50 cm to 2 m, with the cracks themselves being no wider than 5 cm. The cracks are commonly infilled with gypsum and stand as ridges above the general level of the surface crust. Polygons commonly are upturned at their edges. Tucker suggested that the development of cracks and resulting polygons is the result of changes in volume of the gypsum crust. These volume changes he attributed to diurnal and seasonal changes in temperature.

Another prominent type of patterned ground in deserts is found on playa lake surfaces and is characterized by large-scale desiccation fissures (Fig. 4.8). Such fissures have received considerable attention in the literature. In the United States extensive work on the nature and origin of these features has been undertaken in California by Neal (1965, 1968a, b, 1969), Neal and Motts (1967) and by Neal *et al.* (1968). These features are primarily the result of desiccation and subsequent cracking of crusts rich in swelling clays.

A great variety of patterned ground forms has

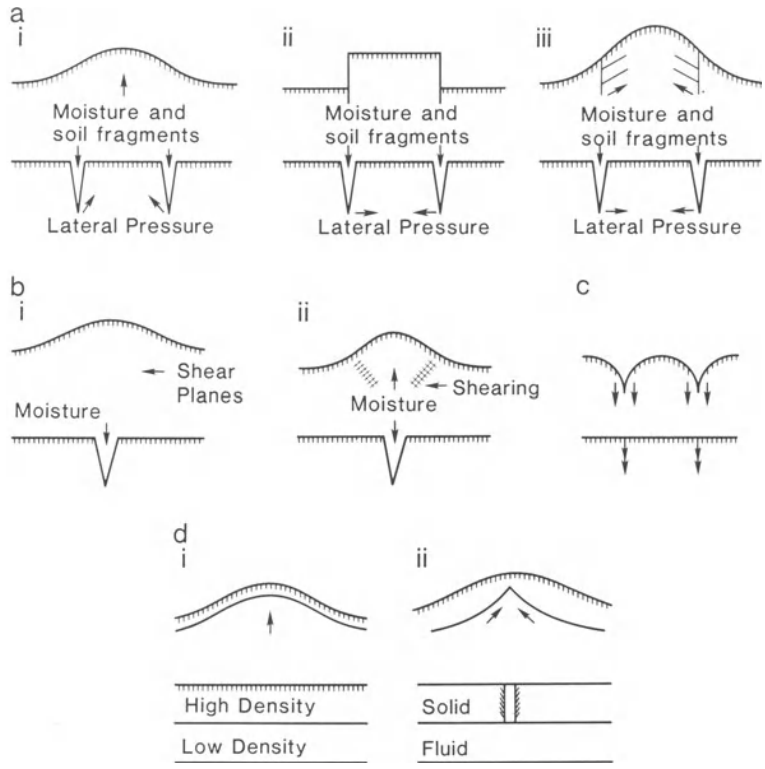

Figure 4.7 Principal mechanisms of gilgai formation. (a) Heave between cracks: (i) by compression, extrusion and plastic flow, (ii) by compression and block fracture, (iii) by compression and oblique slip; (b) heave over cracks: (i) by cumulative internal oblique slip, (ii) by vertical block movement; (c) contraction over cracks due to downward movement associated with desiccation; (d) heave due to loading: (i) by upward flow due to density differences between layers, (ii) by upward flow of fluid soil through cracks in solid layer. (After Knight 1980.)

been described from playa lakes in the western United States by Hunt and Washburn (1960, 1966). These forms are associated with different types of salt crusts. Smooth silt-rich surfaces with desiccation cracks and solution pits occur in the chloride zone beyond the limits of playa flooding. In the areas of gypsum crust, nets and polygons develop. In the carbonate zone near the edge of the salinas, sorted and non-sorted nets develop. The sorted nets form as a result of the washing of debris into the cracks. Sorted polygons develop where rock salt occurs beneath the surface. Coarse debris accumulates in depressions within silt overlying the salts. In addition, Hunt and Washburn (1966) have described a variety of patterned ground features developed on alluvial fan surfaces, including sorted steps, sorted polygons, and stone stripes.

The various patterned ground phenomena described from playa lake basins are all essentially the result of the action of salt crystallization. In addition to the desiccation of salt-rich sediment crusts on and adjacent to playas, the expansion and contraction of salts as a result of heating and cooling as well as wetting and drying play an important role in the development of patterned ground features.

Patterned ground phenomena have been described from the Great Kavi of Iran. Krinsley (1968, 1970) reported a variety of morphologies including salt polygons, thrust polygons, desiccation cracks, and mud pinnacles. He attributed these features largely to the influx and episodic evaporation and subsequent desiccation of salt-rich ground waters. Patterned ground has also been described from the bed of Lake Eyre in central Australia, where its origin has been ascribed to the growth of salt crystals in unconsolidated muds and accompanying ground heave along desiccation cracks (Summerfield 1991, p. 147).

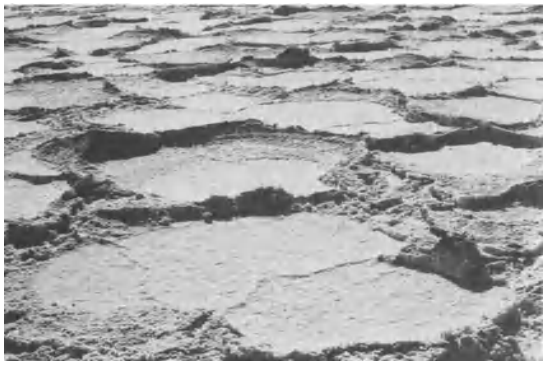

Figure 4.8 Salt polygons, Death Valley Salt Pan, California.

Figure 4.9 Desert pavement, Cima volcanic field, California. Pavement underlain by a thick layer of aeolian-derived fine sediment (photo courtesy of L.D. McFadden).

MICROTOPOGRAPHIC PATTERNED GROUND

Microtopographic patterned ground forms are also common in desert environments. These forms are often not apparent to the casual observer but are highlighted by patterns of vegetation growth, such as vegetation arcs and water lanes recognized by MacFadyen (1950) and Hemming (1965) in Somalia. Water lanes have also been described from the Somaliland Plateau by Boaler and Hodge (1962). Similar patterns have been observed in Western Australia by Mabbutt (1963). He attributed the sorting of sediment to the combined action of wind and sheet flow. Large arcuate ripples have been described in Utah by Ives (1946).

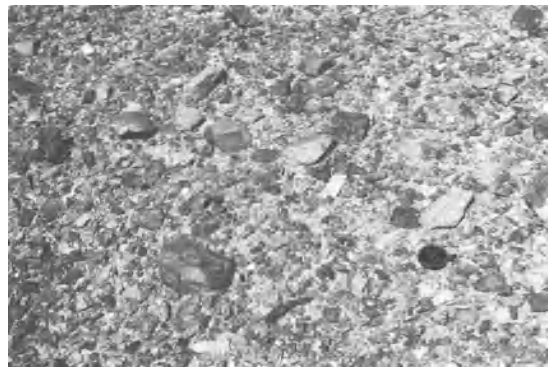

Figure 4.10 Desert pavement, Afton Canyon, California. Pavement underlain by a thick layer of aeolian-derived fine sediment.

DESERT PAVEMENT

MORPHOLOGY

Desert pavement is a stony surface generally composed of a layer of angular or subrounded gravels one or two stones thick sitting on a mantle of finer stone-free material (Mabbutt 1965, 1977, p. 119, Cooke and Warren 1973, p. 120) (Figs 4.9 and 4.10). Desert pavement occurs widely in the warm deserts of the world (Cooke and Warren 1973, p. 121, Mabbutt 1977, p. 119). This surficial phenomenon is known by a variety of names depending on the particular character of the pavement and the region of the world in which it occurs. Where the pavement is dominated by rock outcrops and boulders are relatively few, the landscape is referred to as hamada, an Arabic word meaning 'unfruitful'. Boulder hamada consists of extensive surfaces of large angular rock fragments and occurs extensively in deserts such as the Libyan Sahara (Mabbutt 1977, p. 121). Pavement dominated by smaller size gravel is referred to as reg in the old world and derives its name from the Arabic word meaning 'becoming smaller' (Dan *et al.* 1982, Amit and Gerson 1986). In the central Sahara, reg surfaces are referred to as serir (Mabbutt 1977). In Australia stone pavements are called gibber.

GENESIS

Deflation

The development of desert pavement is generally attributed to one of five stone-concentrating processes. Perhaps the most commonly invoked process is that of deflation. The concentration of the coarse debris is believed to be the result of the removal of

fine-grained material from the desert surface by wind, leaving the coarser debris behind as a lag deposit (e.g. Cooke 1970, Dan *et al.* 1981, 1982). Many workers, however, have questioned the ability of wind to transport fine-grained materials from desert surfaces. These materials are often incorporated into crusts which effectively preclude subsequent transportation (Cooke 1970). Several workers have also shown that as a gravel surface develops, the areas between the coarse fragments in fact become sheltered from the wind and fine-grained materials in these locations become progressively less likely to be transported (Pandastico and Ashaye 1956, Symmons and Hemming 1968). Finally, the fact that many desert pavements are underlain by a relatively thick layer of fine debris suggests the relative inefficiency of aeolian transport of fines from the desert surface. Some desert pavements, however, may in fact be the result of deflation, such as those observed in the Peruvian desert by Crolier *et al.* (1979). These workers noted that the cobbles forming the pavement are not supported by silts and clays but rather rest on sands and gravels (Fig. 4.11).

Figure 4.11 Deflation pavement on marine terrace near Punta Carballes, southern Peru. Pavement supported by sand and cobbles (photo courtesy of R. Dorn).

Wash

A second mechanism for gravel concentration that has been widely proposed is the winnowing of fines by surface wash (Lowdermilk and Sudling 1950, Sharon 1962, Denny 1965, Cooke 1970, Dan *et al.* 1981, 1982). Several of these workers have shown quantitatively that erosion of disturbed pavements yields considerable amounts of fine wash debris (Sharon 1962, Cooke 1970). McHargue (1981), working in the vicinity of the Aguila Mountains in Arizona, demonstrated that surface wash is a necessary component of pavement formation. He argued that incipient pavements form after the erosion of 1 to 3 cm of fine sediment and that stable pavements form after the removal of 3 to 15 cm of sediment. McHargue envisaged long-term stability of the pavement being related to subsequent addition of fine-grained aeolian materials to the landscape. However, the widespread development of surface crusts probably precludes extensive pavement development by wash processes.

Upward Migration of Stones

The third and perhaps most widely accepted explanation for the origin of desert pavements is the progressive upward migration of coarse particles through the underlying finer material. The mechanism most commonly invoked for this upward movement is alternate wetting and drying and associated swelling and shrinking of the fine-grained subpavement materials (Springer 1958, Jessop 1960, Cooke 1970, Dan *et al.* 1982). As the fine debris swells, coarse material is forced upward. When shrinkage occurs the coarse material fails to return to its former position which is occupied by fines. Repetition of this sequence of events causes the coarse material slowly to make its way to the ground surface. This process is clearly most pronounced in subpavement soils which are characterized by strong textural contrasts between the A and B horizons. The presence of gypsic horizons beneath pavements may also impede the vertical migration of cobbles from the subsurface (Fig. 4.12). Cooke and Warren (1973, p. 128) have suggested that freeze–thaw processes

Figure 4.12 Desert pavement with geoglyphs (arrows) near Nazca, Peru. Pavement has partially reformed after geoglyph construction. Underlying substrate is gypcrete (photo courtesy of R. Dorn).

may also account for the formation of stone pavements in high altitude deserts such as those in South America and central Asia. The appeal of this mechanism is the fact that it offers an explanation for the fine-grained material found beneath the pavement. One of the limitations of this explanation is the fact that seldom are stones observed to be 'in transit' from below the fine-grained mantle to the ground surface (Mabbutt 1979). Further, adequate wetting depths for coarse fragment migration in deserts are difficult to invoke.

Cumulic Pedogenesis

Mabbutt (1977, 1979) proposed that perhaps some of the desert pavements in central Australia are the result of upward sorting above a fine textured mantle that is largely aeolian in origin. He suggested that aeolian dust is trapped by the rough surface of the pavement and that there is a consequent upward displacement of the pavement as dust accumulation proceeds. Sorting, if any, is limited to the uppermost part of the fine-grained aeolian mantle. More recently, a similar mechanism of pavement formation has been suggested by McFadden *et al.* (1987), who argued that the formation of desert pavement in the Cima volcanic field, California, is the result of the *in situ* mechanical weathering and accompanying downslope transport of basalt at the ground surface and the subsequent raising of the pavement as aeolian silts and clays accumulate below the gravels. In essence, the pavement is born at the earth's surface and, once formed, changes little through time. Soil development proceeds in the aeolian mantle beneath the pavement. Recent support for this model has been provided by Wells *et al.* (1991) through cosmogenic dating of gravel clasts. These workers found that, using ^{3}He and ^{21}Ne, lava flow samples and clast samples have ages that are statistically inseparable from each other.

Subsurface Weathering

Mabbutt (1977) suggested a fifth process to account for the formation of desert pavement, namely differential weathering. He argued that moisture conditions are more favourable for rock weathering in the subsoil environment than at the desiccated surface, leading to the more rapid breakdown of coarse debris. The result of this enhanced weathering at depth is a layer of relatively fine materials with a lack of coarse debris. Mabbutt reasoned that this process may be particularly important in the generation of pavements in granitic terranes and that salt weathering may also be effective in the breakdown of coarse debris below the surface.

Desert pavements clearly result from a variety of processes. Some processes act independently, while others act in combination. The processes responsible for the formation of pavements vary from location to location depending on the climate, geomorphic setting, the nature of the clastic materials available, and the nature of the local soils (Bull 1991, p. 66).

GRAVEL SOURCE

Central to an understanding of the origin of desert pavements is the source of the gravels. Two principal sources are generally recognized. Some pavements are composed of gravels that are fluvial in origin (Denny 1965, Cooke 1970, Mabbutt 1977, p. 122, Dan *et al.* 1982, Bull 1991, p. 65). These gravels are commonly rounded and occur in landscape settings in close proximity to stream channels. Some rounding of gravels can be accomplished by surface weathering processes, and so grain shape alone is not necessarily indicative of a fluvial origin. The second source is mechanical weathering of the local bedrock. This source has frequently been associated with the origin of hamadas (Cooke 1970, Mabbutt 1977, p. 121) but is now widely ascribed to finer grained pavement surfaces as well (Wells *et al.* 1985, McFadden *et al.* 1987).

Various processes have been postulated for the disintegration of bedrock and production of pavement gravels. Cooke (1970) suggested that pavement gravels in California and Chile might result from the combined influences of diurnal changes in insolation, the growth of frost needles and salt crystals, and a variety of chemical weathering processes. Peel (1974) proposed that gravels on pavements in the central Sahara are the result of insolation weathering, a view reiterated by Dan *et al.* (1982) for pavements in southern Israel and the Sinai. However, Dan *et al.* stress that cracking associated with salt crystal growth is a more important mechanism. In their detailed study of pavements in the Cima volcanic field, McFadden *et al.* (1987) suggested that much of the disintegration of the basalt flows is the result of mechanical disintegration processes. They proposed that salt- and clay-rich aeolian material deposited in fractures in the lava-flow surfaces experiences volumetric increase due to crystal growth and wetting and drying. These processes result in the vertical and lateral displacement of basalt clasts from the parent flows as well as subsequent breakdown of dislodged fragments.

McFadden *et al.* suggested that some of the sand and silt in the fine-grained mantle may be derived from the mechanical breakdown of surface clasts. Some chemical alteration of the clasts has also occurred but appears to be limited to alteration of volcanic glass and iron oxides as well as olivine in the groundmass. Some authigenic clay formation is also suggested. However, much of the clay alteration seems to be related to chemical weathering of aeolian fines. A detailed discussion of weathering processes in arid environments is provided in Chapter 3.

CONCLUSIONS

Desert soils display a distinctive assemblage of physical chemical and biological characteristics. They are typically thin, gravelly, salt-dominated, and organic-poor. Their surfaces are characterized by the development of crusts and gravel lag deposits. The processes responsible for the development of these distinctive soils also result in the development of an assemblage of distinctive landform features.

The addition of considerable amounts of airborne clay to landscape surfaces in desert environments results in the development of soils with considerable swell–shrink capacity. Repeated swelling and shrinking of soils leads to the development of a variety of patterned ground forms.

Aeolian processes not only contribute significantly to soil formation and patterned ground development but they represent an important component of desert pavement formation. Silts and clays added to the desert landscape act to buoy the coarse gravel lag on the landscape surface. In addition, these fine particles as well as airborne salts serve as important agents of weathering, producing coarse debris that dominates some desert landscapes.

From the preceding discussion it is clear that a complete understanding of the geomorphic processes operating in desert environments cannot be obtained without a careful assessment of the nature of desert pedogenic processes.

REFERENCES

Akpokodje, E.G. 1984. The influence of rock weathering on the genesis of gypsum and carbonates in some Australian arid zone soils. *Australian Journal of Soil Research* **22**, 243–51.

Alexander, E.B. and W.D. Nettleton 1977. Post-Mazama Natrargids in Dixie Valley, Nevada. *Soil Science Society of America Journal* **41**, 1210–12.

Amit, R. and R. Gerson 1986. The evolution of Holocene reg (gravelly) soils in deserts: an example from the Dead Sea region. *Catena* **13**, 59–79.

Bachman, G.O. and M.N. Machette 1977. Calcic soils and calcretes in the southwestern United States. *U.S. Geological Survey Open File Report* 77-796.

Beckman, G.G. 1966. Gilgai phenomena as geologic structures: a theoretical discussion. *Proceedings of the Australian Conference of Soil Science* **3**, 1–2.

Bettenay, E. 1962. The salt lake systems and their associated aeolian features in the semi-arid region of Western Australia. *Journal of Soil Science* **13**, 10–17.

Bettenay, E., A.V. Blackmore and F.J. Hingston 1964. Aspects of the hydrological cycle and related salinity in the Belka Valley, Western Australia. *Australian Journal of Soil Research* **2**, 187–210.

Birkeland, P.W. 1990 Soil-geomorphic research – a selected overview. *Geomorphology* **3**, 207–24.

Boaler, S.B. and C.A.H. Hodge 1962. Vegetation stripes in Somaliland. *Journal of Ecology* **50**, 465–76.

Boettinger, J.L. and R.J. Southard 1991. Silica and carbonate sources for aridisols on a granitic pediment, western Mojave Desert. *Soil Science Society of America Journal* **55**, 1057–67.

Brasher, B.R., G. Borst and W.D. Nettleton 1976. Weak duripans in weathered rock in a Mediterranean climate. *Annual Meeting, American Society of Agronomy, Abstracts* 158.

Brewer, R., E. Bettenay and H.M. Churchward 1972. Some aspects of the origin and development of the red and brown hardpan soils of Bulloo Downs, W.A. *CSIRO (Australia) Division of Soils Technical Paper* 1B.

Bull, W.B. 1991. *Geomorphic responses to climate change*. New York: Oxford University Press.

Chadwick, O.A. and J.O. Davis 1990. Soil forming intervals caused by eolian sediment pulses in the Lahonton Basin, northwestern Nevada. *Geology* **18**, 243–6.

Chartres, C.J. 1982. The pedogenesis of desert loams in the Barrier Range, Western New South Wales, I. Soil parent materials. *Australian Journal of Soil Research* **20**, 269–81.

Chartres, C.J. 1983. The pedogenesis of desert loam soils in the Barrier Range, Western New South Wales. II. Weathering and soil formation. *Australian Journal of Soil Research* **21**, 1–13.

Chartres, C.J. 1985. A preliminary investigation of hardpan horizons in north-west New South Wales. *Australian Journal of Soil Research* **23**, 325–37.

Christianson, G.E. and C. Purcell 1985. Correlation and age of Quaternary alluvial fan sequences, Basin and Range province, southwestern United States. In *Soils and Quaternary geology of the southwestern United States*, D.L. Weide (ed.), 115–22. Geological Society of America Special Paper 203.

Conacher, A.J. 1975. Throughflow as a mechanism responsible for excessive soil salinization in non-irrigated, previously arable lands in the Western Australia wheat belt: a field study. *Catena* **2**, 31–67.

Cooke, R.U. 1970. Stone pavements in deserts. *Annals of the Association of American Geographers* **60**, 560–77.

Cooke, R.U. and A. Warren 1973. *Geomorphology in deserts*. Berkeley: University of California Press.

Crolier, M.J., G.E. Ericksen, J.F. McCauley and P.C. Morris 1979. The desert landforms of Peru; a preliminary photographic atlas. *U.S. Geological Survey Interagency Report: Astrogeology* 57.

Dan, J. 1983. Soil chronosequences in Israel. *Catena* **10**, 287–399.

Dan, J., R. Gerson, H. Kogumdjisky and D.H. Yaalon 1981. *Arid Soils of Israel*. Agricultural Research Organization, Special Publication 190.

Dan, J., D.H. Yaalon, R. Moshe and S. Nissim 1982. Evolution of reg soils in southern Israel and Sinai. *Geoderma* **28**, 173–202.

Denny, C.S. 1965. Alluvial fans in the Death Valley region, California and Nevada. *U.S. Geological Survey, Professional Paper* 466.

Denny, C.S. 1967. Fans and pediments. *American Journal of Science* **265**, 81–105.

Dimmock, G.M., E. Bettenay and M.J. Mulcahy 1974. Salt content of laterite profiles in the Darling Range, Western Australia. *Australian Journal of Soil Research* **12**, 63–9.

Dohrenwend, J.C., W.B. Bull, L.D. McFadden, G.I. Smith *et al.* 1991. Quaternary geology of the Basin and Range Province in California. In *Quaternary non-glacial geology: conterminous United States*, R.B. Morrison (ed.), 321–52. Geology of North America, Vol. K-2. Boulder, CO: Geological Society of America.

Eswaran, H. and G. Zi-Tong 1991. Properties, genesis, classification and distribution of soils with gypsum. In *Occurrence, characteristics, and genesis of carbonate, gypsum and silica accumulations in soils*, W.D. Nettleton (ed.), 89–119. Soil Science Society of America Special Publication 26.

Evenari, J., D.H. Yaalon and Y. Gutterman 1974. Note on soils with vesicular structures in deserts. *Zeitschrift für Geomorphologie* **18**, 162–72.

Flach, K.W., W.D. Nettleton, L.H. Gile and J.G. Cady 1969. Pedocementation: induration by silica, carbonates, and sesquioxides in the Quaternary. *Soil Science* **107**, 442–53.

Flach, K.W., W.D. Nettleton and R.E. Nelson 1973. The micro-morphology of silica cemented soil horizons in western North America. In *Soil microscopy*, G.K. Rutherford (ed.) 714–29. Kingston: Queens University.

Gerson, R. and R. Amit 1987. Rates and modes of dust accretion and deposition in an arid region: the Negev, Israel. In *Desert sediments: ancient and modern*, L. Fostick and I. Reid (eds), 157–69. Geological Society Special Publication 35.

Gerson, R., R. Amit and S. Grossman 1985. *Dust availability in desert terrains, a study in the deserts of Israel, and the Sinai*. Jerusalem: Institute of Earth Sciences, the Hebrew University of Jerusalem.

Gile, L.H. 1967. Soils of an ancient basin floor near Las Cruces, New Mexico. *Soil Science* **103**, 265–76.

Gile, L.H. 1970. Soil of the Rio Grande Valley border in southern New Mexico. *Soil Science Society of America Journal* **34**, 465–72.

Gile, L.H. 1975. Holocene soils and soil geomorphic relations in an arid region of southern New Mexico. *Quaternary Research* **5**, 321–60.

Gile, L.H. and R.B. Grossman 1968. Morphology of the argillic horizon in desert soils of southern New Mexico. *Soil Science* **106**, 6–15.

Gile, L.H., J.W. Hawley and R.B. Grossman 1981. Soils and geomorphology in the Basin and Range area of Southern New Mexico: guidebook to the Desert Project, *New Mexico Bureau of Mines and Mineral Resources Memoir* 39.

Gunn, R.H. 1967. A soil catena on denuded laterite profiles in Queensland. *Australian Journal of Soil Research* **5**, 117–32.

Gunn, R.H. and D.P. Richardson 1979. The nature and possible origins of soluble salts in deeply weathered landscapes of eastern Australia. *Australian Journal of Soil Research* **17**, 197–215.

Gustavson, T.C., R.W. Baumgardner Jr, S.C. Caran, V.T. Holliday *et al.* 1991. Quaternary geology of the Southern Great Plains and an adjacent segment of the Rolling Plains. In *Quaternary non-glacial geology: conterminous United States*, R.B. Morrison (ed.), 477–501. Geology of North America, Vol. K-2. Boulder, CO: Geological Society of America.

Gustavson, T.C. and D.A. Winkler 1988. Depositional facies of the Miocene–Pliocene Ogallola Formation, northwestern Texas and eastern New Mexico. *Geology* **16**, 203–6.

Guthrie, P.L. 1982. Distribution of great groups of aridisols in the United States. *Catena Supplement* **1**, 29–36.

Hallsworth, E.G. and G.G. Beckman 1969. Gilgai in the Quaternary. *Soil Science* **10**, 409–20.

Hallsworth, E.G. and G.K. Robertson 1951. The nature of gilgai and melonhole soils. *Australian Journal of Science* **13**, 181.

Hallsworth, E.G., G.K. Robertson and F.R. Gibbons 1955. Studies in pedogenesis in New South Wales. VII. The gilgai soils. *Journal of Soil Science* **6**, 1–31.

Harden, D.R., N.E. Biggar and M.L. Gillam 1985. Quaternary deposits and soils in and around Spanish Valley, Utah. In *Soils and Quaternary geology of the southwestern United States*, D.L. Weide (ed.), 43–64. Geological Society of America Special Paper 203.

Harden, J.W., E.M. Taylor, L.D. McFadden and M.C. Reheis 1991. Calcic, gypsic, and siliceous soil chronosequences in arid and semiarid environments. In *Occurrence, characteristics, and genesis of carbonate, gypsum and silica accumulations in soils*, W.D. Nettleton (ed.), 1–16. Soil Science Society of America. Special Publication 26.

Harris, S.A. 1958. Gilgaied and land structured soils of central Iraq. *Journal of Soil Science* **9**, 169–85.

Harris, S.A. 1959. The classification of gilgaied soils: some evidence from northern Iraq. *Journal of Soil Science* **10**, 27–33.

Hemming, C.F. 1965. Vegetation arcs in Somaliland. *Journal of Ecology* **53**, 57–67.

Holliday, V.T. 1985a. Holocene soil geomorphological relations in a semi-arid environment: the Southern High Plains of Texas. In *Soils and Quaternary landscape evolution*, J. Boardman (ed.), 325–57. New York: Wiley.

Holliday, V.T. 1985b. Morphology of late Holocene soils at the Lubbock Lake archeological site, Texas. *Soil Science Society of America Journal* **49**, 938–46.

Holliday, V.T. 1985c. Early and middle Holocene soils at the Lubbock Lake archeological site, Texas. *Catena* **12**, 61–78.

Holliday, V.T. 1988. Genesis of late Holocene soils at the Lubbock Lake archaeological site, Texas. *Annals of the Association of American Geographers* **78**, 594–610.

Holliday, V.T. 1989. The Blackwater Draw Formation (Quaternary). A 1.4 + m.y. record of eolian sedimentation and soil formation on the Southern High Plains. *Bulletin of the Geological Society of America* **101**, 1598–607.

Holliday, V.T. 1990. Soils and landscape evolution of eolian plains: the Southern High Plains of Texas and New Mexico. *Geomorphology* **3**, 489–515.

Howard, A. 1939. Crab-hole gilgai and self-mulching soils of the Murrumbidgee Irrigation Area. *Pedology* **8**, 14–8.

Hubble, G.D. and R.F. Isbell 1958. The occurrence of strongly acid clays beneath alkaline soils in Queensland. *Australian Journal of Science* **20**, 186–7.

Hubble, G.D., R.F. Isbell and K.H. Northcote 1983. Features of Australian soils. In *Soils: an Australian viewpoint*, 17–47. Melbourne: CSIRO/London: Academic Press.

Hunt, C.B. and A.L. Washburn 1960. Salt features that simulate ground patterns formed in cold climates. *U.S. Geological Survey Professional Paper* 400-B.

Hunt, C.B. and A.L. Washburn 1966. Patterned ground. *U.S. Geological Survey Professional Paper* 494-B, 104–33.

Hutton, J.T. and J.C. Dixon 1981. The chemistry and mineralogy of some South Australian calcretes and associated soft carbonates and their dolmitization. *Journal of the Geological Society of Australia* **28**, 71–9.

Hutton, J.T. and T.I. Leslie 1958. Accession of non-nitrogenous ions dissolved in rainwater to soils in Victoria. *Australian Journal of Agricultural Research* **14**, 319–29.

Isbell, R.F. 1962. Soils and vegetation of the brigalow lands, eastern Australia. *CSIRO (Australia) Division of Soils, Soils and Landuse Series* 43.

Isbell, R.F., R. Reeve and J.T. Hutton 1983. Salt and sodicity. In *Soils: an Australian viewpoint*, 107–17, Melbourne: CSIRO/London: Academic Press.

Ives, R.L. 1946. Desert ripples. *American Journal of Science* **244**, 492–501.

Jessop, R.W. 1960. The lateritic soils of the southeastern portion of the Australian Arid Zone. *Journal of Soil Science* **11**, 106–13.

Knight, M.J. 1980. Structural analysis and mechanical origins of gilgai at Boorook, Victoria, Australia. *Geoderma* **23**, 245–83.

Krinsley, D.B. 1968. Geomorphology of three kavirs in northern Iran. *Air Force Cambridge Research Laboratories Environmental Research Papers* 283.

Krinsley, D.B. 1970. A geomorphological and paleoclimatological study of the playas of Iran. *U.S. Geological Survey. Final Scientific Report Contract PROCP-70-800.*

Lachenbruch, A.H. 1962. Mechanics of thermal contraction cracks and ice-wedge polygons in permafrost. *Geological Society of America Special Paper* 70.

Leeper, G.W., A. Nicholls and S.M. Wadham 1936. Soil and pasture studies in the Mount Gellibrand area, Western District of Victoria. *Proceedings of the Royal Society of Victoria* **49**, 77–138.

Litchfield, W.H. and J.A. Mabbutt 1962. Hardpan soils of semi-arid Western Australia. *Journal of Soil Science* **13**, 148–60.

Lowdermilk, W.C. and H.L. Sundling 1950. Erosion pavement, its formation and significance. *Transactions of the American Geophysical Union* **31**, 96–100.

Mabbutt, J.A. 1963. Wanderrie banks: micro-relief patterns in semiarid Western Australia. *Bulletin of the Geological Society of America* **74**, 529–40.

Mabbutt, J.A. 1965. Stone distribution in a stony tableland soil. *Australian Journal of Soil Research* **3**, 131–42.

Mabbutt, J.A. 1977. *Desert landforms*, Cambridge, Mass. MIT Press.

Mabbutt, J.A. 1979. Pavements and patterned ground in the Australian stony deserts. *Stuttgarter Geographische Studen* **93**, 107–23.

Machette, M.N. 1985. Calcic soils of the Southwestern United States. In *Soils and Quaternary geology of the southwestern United States*, D.L. Wide (ed.) 1–21. Geological Society of America Special Paper 203.

McFadden, L.D. 1988. Climatic influences on rates and processes of soil development in Quaternary deposits of southern California. In *Paleosols and weathering through geologic time: principles and applications*, J. Reinhardt and W.R. Sigleo (eds), 153–77, Geological Society of America Special Paper 206.

McFadden, L.D. and J.C. Tinsley 1985. Rate and depth of pedogenic-carbonate accumulation in soils: formulation and testing of a comparintment model. In *Soils and Quaternary geology of the southwestern United States*, D.L. Weide (ed.), 23–41. Geological Society of America Special Paper 203.

McFadden, L.D., S.G. Wells, J.C. Dohrenwend and B.D. Turrin 1984. Cumulic soils formed in eolian parent materials on flows of the late Cenozoic Cima volcanic field, California. In *Surficial geology of the eastern Mojave Desert, California*, J.C. Dohrenwend (ed.), 134–49. Field Trip Guide, 97th Annual Meeting of the Geological Society of America.

McFadden, L.D., S.G. Wells, and J.C. Dohrenwend 1986. Influences of Quaternary climate changes on processes of soil development on desert loess deposits of the Cima volcanic field; California. *Catena* **13**, 361–89.

McFadden, L.D., S.G. Wells and M.J. Jercinovich 1987. Influences of eolian and pedogenic processes on the origin and evolution of desert pavements. *Geology* **15**, 504–8.

McFadden, L.D., R.G. Amundson and O.A. Chadwick 1991. Numerical modeling, chemical, and isotopic studies of carbonate accumulation in soils of arid regions. In *Occurrence, characteristics, and genesis of carbonate, gypsum and silica accumulation in soils*, W.D. Nettleton (ed.), 17–35. Soil Science Society of America. Special Publication 26.

MacFadyen, W.A. 1950. Vegetation patterns in the semi-desert plains of British Somalia. *Geographical Journal* **116**, 199–211.

McGarity, J.W. 1953. Melon hole formation in the Richmond River District of New South Wales. *Proceedings of the Australian Conference on Soil Science* **2**, 1–7.

McHargue, L.E. 1981. Late Quaternary deposition and pedogenesis on the Aquila Mountains piedmont, southeastern Arizona. M.S. thesis, University of Arizona, Tucson.

Miller, D.E. 1971. Formation of vesicular structure in soil. *Soil Science Society of America Journal* **35**, 635–7.

Milnes, A.R. and J.T. Hutton 1983. Calcretes in Australia. In *Soils: an Australian viewpoint*, 119–62, Melbourne: CSIRO/London: Academic Press.

Milnes, A.R., M.J. Wright and M. Thiry 1991. Silica accumulations in saprolites and soils in South Australia. In *Occurrence, characteristics, and genesis of carbonate, gypsum and silica accumulations in soils*, W.D. Nettleton (ed.) 121–49. Soil Science Society of America Special Publication 26.

Monger, H.C., L.A. Daugherty and L.H. Gile 1991. A microscopic examination of pedogenic calcite in an aridisol of southern New Mexico. In *Occurrence, characteristics, and genesis of carbonate, gypsum and silica accumulations in soils*, W.D. Nettleton (ed.), 37–60. Soil Science Society of America. Special Publication 26.

Neal, J.T. 1965. Giant desiccation polygons of Great Basin playas. *Air Force Cambridge Research Laboratories Environmental Research Papers* 123, 1–30.

Neal, J.T. 1968a. Playa surface changes at Harper Lake California: 1962–1967. *Air Force Cambridge Research Laboratories Environmental Research Papers* 283.

Neal, J.T. (ed.) 1968b. Playa surface morphology: miscellaneous investigations. *Air Force Cambridge Research Laboratories Environmental Research Papers* 283.

Neal, J.T. 1969. Playa variations. In *Arid lands in perspective*, W.G. McGimies and B.J. Goldman (eds), 13–44. Tucson: University of Arizona Press.

Neal, J.T. and W.S. Motts 1967. Recent geomorphic changes in playas of the western United States. *Journal of Geology* **75**, 511–25.

Neal, J.T., A.M. Langer and P.F. Kerr 1968. Giant desiccation polygons of Great Basin playas. *Bulletin of the Geological Society of America* **79**, 69–90.

Nelson, R.E., L.C. Klameth and W.D. Nettleton 1978. Determining soil gypsum content and expressing properties of gypsiferous soils. *Soil Science Society of America Journal* **42**, 659–61.

Nettleton, W.D. and F.F. Peterson 1983. Aridisols. In *Pedogenesis and soil taxonomy II. The soil orders. Developments in Soil Science IIB*, L.P. Wilding, N.E. Smeck and G.F. Hall (eds), 165–215. Amsterdam: Elsevier.

Nettleton, W.D., J.G. Witty, R.E. Nelson and J.W. Hanley 1975. Genesis of argillic horizons in soils of desert areas of the southwestern U.S. *Soil Science Society of America Journal* **39**, 919–26.

Nettleton, W.D., R.E. Nelson, B.R. Brasher and P.S. Deer 1982. Gypsiferous soils in the western United States. In *Acid sulfate weathering*, J.A. Kittrick, D.S. Fanning and L.R. Hossner (eds), 147–68. Soil Science Society of America. Special Publication 10.

Nettleton, W.D., E.E. Gamble, B.L. Allen, G. Borst *et al.* 1989. Relief soils of subtropical regions of the United States. *Catena Supplement* **16**, 59–93.

Nettleton, W.D., B.R. Brasher and S.L. Baird 1991. Carbonate clay characterization by statistical methods. In *Occurrence, characteristics, and genesis of carbonate, gypsum and silica accumulations in soils* W.D. Nettleton (ed.), 75–88. Soil Science Society of America. Special Publication 25.

Northcote, K.H. and J.K.M. Skene 1972. Australian soils with saline and sodic properties. *CSIRO (Australia) Soil Publication* 27.

Ollier, C.D. 1966. Desert gilgai. *Nature* **212**, 581–3.

Pandastico, E.B. and T.I. Ashaye 1956. Demonstration of the effect of stone layers on soil transport and accretion. In *Experimental pedology*, E.G. Hallsworth and D.V. Crawford (eds), 384–90. London: Butterworth.

Paton, T.A. 1974. Origin and terminology for gilgai in Australia. *Geoderma* **11**, 221–42.

Peck, A.J. 1978. Salinization of non-irrigated soils and associated streams: a review. *Australian Journal of Soil Research* **16**, 157–68.

Peck, A.J. and D.H. Hurle 1973. Chloride balance of some farmed and forested catchments in southwestern Australia. *Water Resource Research* **9**, 648–57.

Peel, R.F. 1974. Insolation weathering: some measurements of diurnal temperature change in exposed rocks in the Tibest region, central Sahara. *Zeitschrift für Geomorphologie Supplement Band* **21**, 19–28.

Peterson, F.F. 1980. Holocene desert soil formation under sodium salt influence in a playa-margin environment. *Quaternary Research* **13**, 172–86.

Ponti, D.J. 1985. The Quaternary alluvial sequence of the Antelope Valley, California. In *Soils and Quaternary geology of the southwestern United States*, D.L. Weide (ed.), 79–96. Geological Society of America Special Paper 203.

Prescott, J.A. 1931. The soils of Australia in relation to vegetation and climate. *CSIRO (Australia) Bulletin* 52.

Rabenhorst, M.C., L.T. West and L.P. Wilding 1991. Genesis of calcic and petrocalcic horizons in soils over carbonate rocks. In *Occurrence, characteristics, and genesis of carbonate, gypsum and silica accumulations in soils*, W.D. Nettleton (ed.), 61–74, Soil Science Society of America. Special Publication 26.

Reheis, M.C. 1987a. Gypsic soils on the Kane alluvial fans, Big Horn Country, Wyoming. *U.S. Geological Survey Bulletin* 159-C.

Reheis, M.C. 1987b. Climate implications of alternating clay and carbonate formation in semi arid soils of south-central Montana. *Quaternary Research* **29**, 270–82.

Reheis, M.C. 1990. Influence of climate and eolian dust on major-element chemistry and clay mineralogy of soils in the northern Bighorn Basin, U.S.A. *Catena* **17**, 219–48.

Reheis, M.C., J.W. Harden, L.D. McFadden and R.R. Shroba 1989. Development rates of late Quaternary soils: Silver Lake Playa, California. *Soil Science Society of America Journal* **53**, 1127–40.

Sharon, D. 1962. On the nature of hamadas in Israel. *Zeitschrift für Geomorphologie* **6**, 129–47.

Shlemon, R.J. 1978. Quaternary soil–geomorphic relationships, southeastern Mojave Desert, California and Arizona. In *Quaternary soils*, W.C. Mahany (ed.), 187–207, Norwich: Geo Books.

Smith, B.R. and S.W. Buol 1968. Genesis and relative weathering intensity studies in three semirarid soils. *Soil Science Society of America Journal* **32**, 261–5.

Soil Survey Staff 1975. Soil taxonomy: a basic system of soil classification for making and interpreting soil survey. *U.S. Department of Agriculture Agriculture Handbook* 436.

Springer, M.E. 1958. Desert pavement and vesicular layer in some soils of the Lahontan Basin, Nevada. *Soil Science Society of America Journal* **22**, 63–6.

Stace, H.C.T., G.D. Hubble, R. Brewer, K.H. Northcote *et al.* 1968. *A handbook of Australian soils*, Glenside, South Australia: Rellim Technical Publications.

Stephens, C.G. 1962. *Manual of Australian soils*. 3rd edn. Melbourne: CSIRO.

Sullivan, L.A. and A.J. Koppi 1991. Morphology and genesis of silt and clay coatings in the vesicular layer of a desert loam soil. *Australian Journal of Soil Research* **29**, 579–86.

Summerfield, M.A. 1991. *Global geomorphology*, New York: Wiley.

Symmons, P.M. and C.F. Hemming 1968. A note on wind-stable stone-mantles in the southern Sahara. *Geographical Journal* **134**, 60–4.

Tucker, M.E. 1978. Gypsum crusts (gypcrete) and patterned ground from northern Iraq. *Zeitschrift für Geomorphologie* **22**, 89–100.

Weide, D.L. (ed.) 1985. Soils and Quaternary geology of the southwestern United States. *Geological Society of America Special Paper* 203.

Wells, S.G., J.C. Dohrenwend, L.D. McFadden, B.D. Turrin *et al.* 1985. Late Cenozoic landscape evolution on lava flow surfaces of the Cima volcanic field, Mojave Desert, California *Bulletin of the Geological Society of America* **96**, 1518–29.

Wells, S.G., L.D. McFadden and J.C. Dohrenwend 1987. Influence of late Quaternary climatic changes on geomorphic and pedogenic processes on a desert piedmont eastern Mojave Desert, California. *Quaternary Research* **27**, 130–46.

Wells, S.G., L.D. McFadden and J.D. Schultz 1990. Eolian landscape evolution and soil formation in the Chaco dune field, southern Colorado Plateau, New Mexico. *Geomorphology* **3**, 517–46.

Wells, S.G., L.D. McFadden and C.T. Olinger 1991. Use of cosmogenic 3Ne and 21Ne to understand desert pavement formation. *Geological Society of America Abstracts with Programs* **23** (5), 206.

Wetselaar, R. and J.T. Hutton 1963. The ionic composition of rainwater of Katherine, N.T. and its part in the cycling of plant nutrients. *Australian Journal of Agricultural Research* **14**, 319–29.

White, E.M. and R.G. Bonestall 1960. Some gilgaied soils of South Dakota. *Soil Science Society of America Journal* **24**, 305–9.

White, L.P. and R. Law 1969. Channeling of alluvial depression soils in Iraq and Sudan. *Journal of Soil Science* **20**, 84–90.

Wright, M.J. 1983. Red-brown hardpans and associated soils in Australia. *Transactions of the Royal Society of South Australia* **107**, 252–4.

Yaalon, D.H. 1964. Airborne salt as an active agent in pedogenic processes. *Transactions of the 8th Congress of the International Soil Science Society* **5**, 994–1000.

Yaalon, D.H. and E. Ganor 1973. The influence of dust on soils during the Quaternary. *Soil Science* **116**, 146–55.

DURICRUSTS 5

John C. Dixon

INTRODUCTION

Warm desert environments are characterized by the occurrence of a variety of surface and near-surface, chemically precipitated crusts, including calcrete, silcrete, and gypcrete. Collectively, these are referred to as duricrusts (Woolnough 1930). This chapter focuses on the morphology, chemistry, mineralogy, and origin of the major types of crusts. Particular attention is given to recent research from Australia, the United States, and Africa.

CALCRETE

TERMINOLOGY

Calcrete was defined by Netterberg (1969, p. 88) as almost any terrestrial material which has been cemented and/or replaced by dominantly calcium carbonate. The mechanism of calcification is not restricted and may be of pedogenic or non-pedogenic origin or both. Goudie (1983, p. 94–5) offered a more comprehensive definition. He defined calcrete as terrestrial materials composed dominantly, but not exclusively, of calcium carbonate, which occurs in states ranging from powdery to highly indurated. These materials involve the cementation of, accumulation in, and/or replacement of greater or lesser quantities of soil, rock, or weathered material primarily in the vadose zone. Goudie recognized some limitations of this definition, pointing out that not all calcretes are indurated nor are they necessarily all formed in the vadose zone.

The term calcrete was introduced into the geomorphological literature by Lamplugh (1902) in reference to lime cemented gravels from Dublin, Ireland. Five years later Lamplugh (1907) introduced the related term valley calcretes to refer to calcareous deposits in the valley of the Zambezi River. In the same year that Lamplugh introduced the term calcrete, Blake (1902) used the term caliche in the United States to refer to carbonate accumulations at or near the Earth's surface in Arizona and New Mexico. While these two terms are the most commonly used in the English-speaking literature, they are by no means the only ones. A detailed summary of the various terms used to refer to terrestrial carbonates is provided by Goudie (1973). Some of the more commonly used terms include nari in Israel (Dan 1977), kankar in India and croute calcaire in the French literature (Durand 1963).

Preference is growing for the use of the term calcrete because of inconsistencies in the use of terms such as caliche and travertine (Hay and Reeder 1978, Netterberg and Caiger 1983). In the United States the term caliche is becoming less commonly used and is being replaced by the terms calcrete when referring to indurated terrestrial deposits (Machette 1985) and calcified soils in the case of non-indurated calcic accumulations (Machette 1985). Disfavour with the term caliche has grown as a result of its misapplication to a variety of surficial crusts. In addition to being applied to carbonate deposits, the term has been applied to many varieties of duricrust (Price 1933). In South America the term caliche has been applied to accumulations of sodium nitrate. Hunt and Mabey (1966) used the term to refer to calcium sulphate cemented gravels in Death Valley, California. Attempts to re-define caliche in order to avoid these confusions were made by Bretz and Horberg (1949) and Brown (1956), who both stressed restricting the term caliche to calcareous deposits that had accumulated in place in the weathering zone.

In Australia, early geologists referred to the widespread surficial accumulations of carbonate as travertine (Woolnough 1930, Crocker 1946). In the

Geomorphology of Desert Environments. Edited by Athol D. Abrahams and Anthony J. Parsons. Published in 1994 by Chapman & Hall, London. ISBN 978-94-015-8256-8

1960s the term travertine was largely replaced by the term kunkar which is derived from the hindi term kankar meaning gravel (Goudie 1973, p. 9). The term kunkar was widely applied to indurated calcareous masses present within soil profiles (Johns 1963). Firman (1963, 1964) used the term to refer to limey B horizons present in many soils of South Australia. Crawford (1965) used the term for complex calcrete profiles on Yorke Peninsula in southern South Australia. In the mid-1960s Firman (1966) proposed that the term calcrete be adopted.

Throughout the past two decades the term calcrete has been widely used in the Australian literature on terrestrial carbonates (Dixon 1978, Hutton and Dixon 1981, Milnes and Hutton 1983, Phillips and Self 1987, Phillips *et al.* 1987).

Figure 5.1 Nodular and glaebular calcrete, Yorke Peninsula, South Australia.

DISTRIBUTION

Calcrete covers approximately 13% of the Earth's land surface (Yaalon 1981) and occurs in areas where the annual precipitation is between 400 and 600 mm (Goudie 1983). Calcrete is widely distributed throughout Africa, Israel, southern Europe (Goudie 1973, pp. 73–9, 1983), and the semi-arid parts of India (Patil 1991). In the United States it occurs widely in the south-western states of New Mexico, Nevada, Arizona, Texas, and California (Reeves 1976, Machette 1985). It is also found in southern and central South Australia (Milnes and Hutton 1983), central Western Australia (Mann and Horwitz 1979), and the Northern Territory (Jacobson *et al.* 1988).

MORPHOLOGY

Macromorphology

Calcrete morphology has been described from many locations. However, only a few systematic, non-genetic, systems of calcrete classification have been developed. Durand (1949) recognized eight different types of calcrete crust: croute zonaire, encroutement, racine petrifiee, calcaire pulverulent, efflorescences, nodules, vernis desertique, and tufa or travertine. Today, however, desert varnish and tufa are not regarded as calcrete types.

In the late 1960s, a non-genetic, evolutionary, morphological sequence of calcrete types was developed by Netterberg (1969) for South Africa. Netterberg distinguished six fundamental calcrete types. The least strongly developed calcrete is a calcified soil which is cemented by carbonate to a firm or stiff consistency. With progressive calcification the calcified soil becomes a powder calcrete which is composed of loose carbonate silt or sand particles with few or no host soil particles or nodules present. Nodular or glaebular calcrete consists of silt- to gravel-sized particles of soil material cemented by carbonate (Fig. 5.1). Included within the nodular calcrete type are calcified pedotubules and crotovinas. As calcrete nodules increase in size due to the progressive accumulation of carbonate, they begin to coalesce to form honeycomb calcrete. In this type of calcrete the coalesced nodules are separated by host soil material. When the voids of the honeycomb calcrete become infilled and cemented with carbonate, hardpan calcrete develops. Hardpan calcretes are firm to very hard sheet-like masses of calcrete and represent the most advanced stage of calcrete development (Fig. 5.2). They commonly overlie less strongly indurated materials (Fig. 5.3). Hardpan calcretes are commonly capped with a thin layer of laminar calcrete (Fig. 5.4). As hardpan calcretes are weathered and eroded, they break down into rounded, subrounded, subangular, and blocky masses which are referred to as boulder calcrete (Fig. 5.5). Netterberg's classification system has been adopted in modified form by several workers in Australia (e.g. Hutton and Dixon 1981, Milnes and Hutton 1983, Phillips and Milnes 1988).

In the United States, the most widely used system of morphological description of pedogenic calcretes is that of Gile *et al.* (1965). These authors introduced the concept of the K horizon to refer to layers of accumulated carbonate. To qualify as a K horizon a carbonate layer must consist of more than 90% K fabric. Such fabric consists of continuous authigenic carbonate that has engulfed and cemented pebble-, sand-, and silt-sized grains. Gile *et al.* (1966) iden-

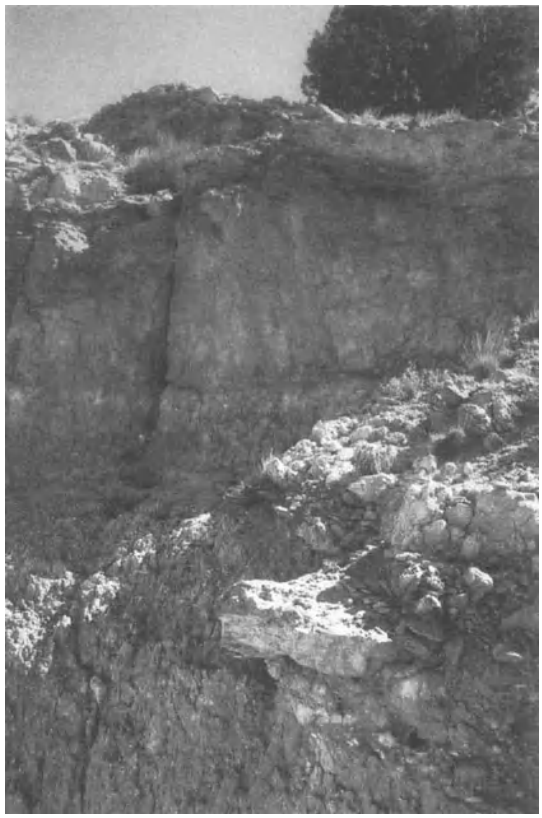

Figure 5.2 Hardpan calcrete caprock, High Plains, eastern New Mexico.

Figure 5.3 Calcrete profile, Murray River valley, South Australia, showing powder calcrete horizon in lower half of photo, massive hardpan calcrete with incorporated nodules in upper half.

tified a morphological sequence of carbonate accumulation in calcic soils based on the degree of calcification. They proposed a four-stage sequence based in part on the nature of the texture of the parent material (Table 5.1).

Recently, the morphological scheme of Gile *et al.* (1966) has been modified by the inclusion of two additional stages of carbonate development which more completely describe later phases of carbonate induration (Bachman and Machette 1977, Machette 1985) (Table 5.2).

Multiple calcrete profiles displaying a variety of stages of development may be exposed in a single geological unit (Fig. 5.6). Gustavson and Winkler (1988) reported the occurrence of multiple calcretes in the Pleistocene age Ogallala Formation of west Texas and eastern New Mexico. Holliday (1989) recorded similar occurrences of multiple calcretes in the Holocene age Blackwater Draw Formation of west Texas.

Reeves (1976, pp. 42–65) recognized a diversity of calcrete morphologies largely related to the degree of induration of the carbonate mass. At the two extremes of induration he distinguished hard massive and soft powdery calcrete. Other macromorphological forms include breccia, conglomerate, concretions, glaebules (Brewer and Sleeman 1964), honeycomb calcrete, irregular masses of poorly indurated carbonate including cylindrical masses, laminar calcrete, nodules, pisolites, plates, and septaria. In Australia there is no widely agreed upon descriptive scheme of calcrete morphology. Early workers including Crocker (1946), Ward (1965, 1966), and Firman (1966) described field occurrences of calcrete as sheets, pans, or nodules. One of the earliest detailed descriptions of calcrete morphology was that of Crawford (1965) who recognized an upper unit of nodular calcrete overlying a unit of massive calcrete which was in turn underlain by a unit of calcrete nodules embedded in a matrix of marl.

Figure 5.4 Calcrete profile from Murray River valley, South Australia, showing progressive decrease in the degree of carbonate induration with depth and development of thin laminar layer at top of profile.

Figure 5.5 Boulder calcrete horizon overlying weakly indurated nodular calcrete horizon, Yorke Peninsula, South Australia.

Similar terminologies had been used by Crocker (1946) in his brief descriptions of calcretes from southern South Australia.

Systematic detailed descriptions of the macromorphology of calcrete from Australia are relatively recent. Wetherby and Oades (1975) developed a scheme for calcrete descriptions based on texture, the amount and nature of the carbonate, and the nature of the horizon boundaries. Dixon (1978) and Hutton and Dixon (1981) adapted Netterberg's (1969) morphological scheme from South Africa to calcretes in the Murray River valley and on Yorke Peninsula, South Australia. Recently, detailed macromorphological description of calcretes from the St Vincents Basin of southern South Australia has been undertaken (Phillips and Milnes 1988). These workers identified a wide variety of the calcrete morphologies, and to some they applied terms previously used by Netterberg, including carbonate silt, nodules, hardpan calcrete, and laminar zones. They recognized a variety of additional morphologies, including biscuits, pisoliths, coated clasts, wedges, stringers, and blotches.

Micromorphology

Micromorphological analysis of calcretes has largely developed within the last decade in an attempt to come to a more detailed and precise understanding of calcrete genesis. One of the earliest studies of calcrete micromorphology was undertaken in India by Sehgal and Stoops (1972). These workers identified seven distinct types of carbonate micromorphology: (a) microcrystalline interflorescences which consist of equant grains 2 to 3 μm in size; (b) neocalcitons which refer to calcite in the soil matrix surrounding pores; (c) spongy calcitic nodules comprised of irregular, diffuse nodules 100 to 200 μm in diameter; (d) compact calcitic soil nodules which are large dense nodules 250 to 500 μm in diameter; (e)

Table 5.1 Stages of the morphogenetic sequence of carbonate deposition in calcic soils[a]

Stage	*Diagnostic carbonate morphology*	
	Gravelly soils	*Non-gravelly soils*
I	Thin, discontinuous pebble coatings	Few filaments or faint coatings
II	Continuous pebble coatings, some interpebble fillings	Few to common nodules
III	Many interpebble fillings	Many nodules and internodular fillings
IV	Laminar horizon overlying plugged horizon. Thickened laminar and plugged horizons	Increasing carbonate impregnation. Laminar horizon overlying plugged horizon

[a]Modified from Gile *et al.* (1966, p. 348, table 1).

crystal chambers filled with coarse calcite crystals; (f) needle-shaped calcite efflorescences consisting of calcite needles less than 50 μm in length; and (g) rounded calcite grains. Working in the West Indies at the same time, James (1972) recognized three distinct forms of calcite in calcretes: flower spar, needles, and micrite.

Wieder and Yaalon (1974) identified three distinct types of nodules within calcic soils in Israel: orthic, disorthic, and allothic nodules. This subdivision was based on the apparent origin of the grains. Orthic nodules have formed in place and are similar in appearance to the surrounding matrix; disorthic nodules show evidence of displacement; and allothic nodules are relict nodules related to some other soil.

Detailed studies of the micromorphology of calcretes were undertaken in Africa in the late 1970s. Hay and Reeder (1978) described calcretes from Olduvai gorge in Tanzania, providing detailed micromorphological descriptions of laminar calcrete as well as of pisoliths above the laminar zone. N.A. Watts (1978, 1980) working in the Kalahari desert provided detailed micromorphological descriptions of calcrete and associated diagenetic structures. Bachman and Machette (1977) described a diversity of micromorphological features from calcretes of the

Table 5.2 Stages in the morphogenetic sequence of carbonate deposition used in this report[a]

Stage	*Diagnostic carbonate morphology*
I	Filaments or faint coatings. Thin, discontinuous coatings on lower surface of pebbles
II	Firm carbonate nodules few to common but isolated from one another. Matrix may include friable interstitial accumulations of carbonate. Pebble coatings continuous
III	Coalesced nodules in disseminated carbonate matrix
IV	Platy, massive indurated matrix. Relict nodules may be visible in places. Plugged. May have weak incipient laminae in upper surface. Case hardening common on vertical exposures
V	Platy to tabular, dense and firmly cemented. Well-developed laminar layer on upper surface. May have scattered incipient pisoliths in laminar zone. Case hardening common
VI	Massive, multilaminar and brecciated, with pisoliths common. Case hardening common

[a]From Bachman and Machette (1977, p. 40, tables 2 and 3).

Figure 5.6 Multiple, buried calcrete profiles developed in the Ogalalla Formation, High Plains, west Texas.

south-western United States, including micrite, microsparite, ooids, and pisoliths.

In the early 1980s attention shifted to detailed examination of the micromorphology of the various concentric forms of calcrete. Hay and Wiggins (1980), working on calcretes from a number of locations in the south-western United States, recognized three fundamental concentric forms of calcrete: pellets, ooids, and pisoliths. They distinguished among these forms on the basis of their internal structure and size. Similarly, Shafetz and Butler (1980) described the micromorphology of calcrete nodules and pisoliths from central Texas. A variety of other micromorphological forms have been recognized from the calcretes of central Texas, including calcans, neocalcans, needle efflorescences, concretions, crystal chambers, and intercalary crystals (Rabenhorst *et al.* 1984, Drees and Wilding 1987, West *et al.* 1988).

Several workers have identified micromorphological features which have been interpreted to be the result of biological activity. Early work by James (1972) identified tubular structures in calcretes which he attributed to algal activity. Kahle (1977) suggested that calcretes might be formed by the combined influences of algae and fungi, while Knox (1977) suggested that bacteria also play an important role in calcrete formation. In a series of papers, Klappa (1978, 1979a, b) recognized a wide variety of micromorphological structures which he ascribed to biological activity. Klappa (1979a) recognized microborings, algal filaments, fungal hyphae, calcite spherules, spherical structures, and deci-micron calcite grains arranged in thin parallel layers in laminar calcrete from coastal Mediterranean sites and suggested that they were indicative of lichen stromatolites. Klappa (1979b), in a detailed discussion of calcified filamentous structures, including root hairs, algal filaments, Actinomycete, and fungal hyphae in calcretes from the Mediterranean, suggested that these features were indicative of organic templates for subsequent calcrete formation.

Recent detailed studies of the micromorphological characteristics of calcretes from South Australia reveal the widespread occurrence of needle fibre calcite and calcified filaments in voids within powder, nodular, platy, and hardpan calcrete (Phillips and Self 1987, Phillips *et al.* 1987). These workers have interpreted the needle fibre calcite as having two distinct biological origins, depending on the size of the needles. Micro-rods frequently associated with organic matter are interpreted as being calcified rod-shaped bacteria. The larger needles are interpreted as forming within mycelial strands from which they are later released. The calcified filaments are interpreted to be the remains of fungal hyphae.

CHEMISTRY

Based on some 300 chemical analyses of calcrete from around the world, Goudie (1972) found the average composition of calcretes to consist of 79.28% $CaCO_3$, 12.30% SiO_2, 2.12% Al_2O_3, 2.03% Fe_2O_3, 3.05% MgO, and 42.62% CaO. There is, however, considerable variability in the chemistry of calcretes from one location to another. For example, Goudie (1973) pointed out that calcretes from India are on average less calcareous than the global average and that Australian calcretes are considerably more calcareous. Calcretes particularly abundant in magnesium have been reported from South Africa, Namibia, and Australia (Goudie 1973).

Aristarain (1970), working in the United States, cited numerous chemical analyses of calcretes from Oklahoma and New Mexico. These analyses reveal North American calcretes to be chemically different from the global average. Compilation of Aristarain's data, based on 22 analyses, reveals on average 34.93% CaO, 30.68% SiO_2, 1.81% MgO, 1.88 Al_2O_3, and 1.00% Fe_2O_3. He observed that calcium, carbon, oxygen, and hydrogen were added to the upper parts of the calcrete profile and decreased in abundance downward.

Magnesium, sulphur, and ferric iron were added in decreasing amounts from top to bottom of the profiles. Silicon and titanium increase slightly in the upper part of the profiles but appreciably in the middle. Potassium and phosphorus remain constant down the profiles. There are no clear profile trends in sodium and ferrous iron.

Chemical characteristics of calcretes from Nevada were reported by Gardner (1972). Unfortunately, these data were presented in parts per million concentrations and so are not comparable with other available data. More recently, a comprehensive survey of the major and minor element geochemistry of calcretes from the south-western United States has been presented by Bachman and Machette (1977).

Detailed chemical analyses of calcretes have been undertaken in Australia by numerous workers. Results of these investigations are summarized in a comprehensive discussion of Australian calcretes by Milnes and Hutton (1983). Recent investigations of the chemistry of calcretes in Australia have been undertaken by Dixon in the St Vincents Basin of South Australia which add to earlier work from the Murray Basin and Yorke Peninsula, South Australia (Dixon 1978, Hutton and Dixon 1981). Typical

Table 5.3 Major element bulk chemistry of calcretes from the Murray Basin, South Australia

Location	*Description*	*CaO*	*SiO_2*	*MgO*	*Al_2O_3*	*Fe_2O_3*	*TiO_2*	*K_2O*	*P_2O_5*	*Loss on ignition*	*Total*
Taleim Bend	Massive	40.4	9.4	6.8	1.2	0.6	0.08	0.22	0.04	41.3	100.04
	Massive	35.8	18.7	7.0	2.1	0.9	0.17	0.40	0.04	36.4	101.51
	Massive	29.0	32.2	5.0	2.7	1.0	0.21	0.84	0.05	29.3	100.59
	Massive	40.9	15.7	3.8	2.0	0.9	0.20	0.67	0.07	37.3	101.62
	Massive	28.8	17.7	13.2	2.1	0.8	0.16	0.58	0.04	37.5	101.01
	Nodular	31.9	20.3	9.1	2.0	0.8	0.20	0.56	0.04	35.5	100.49
	Nodular	33.2	13.4	12.4	1.5	0.8	0.15	0.40	0.05	39.7	101.75
	Nodular	36.1	23.6	3.6	2.2	0.7	0.17	0.50	0.05	33.8	101.15
	Powder	22.8	30.5	8.5	2.7	1.3	0.20	0.31	0.04	32.8	99.15
Monteith (A)	Massive	33.9	26.4	3.4	1.9	0.7	0.14	0.46	0.05	33.0	99.96
	Massive	36.5	20.7	4.2	1.9	0.7	0.13	0.46	0.07	35.4	100.10
	Massive	36.3	27.3	2.5	1.6	1.3	0.20	0.54	0.08	31.1	101.03
	Massive	37.9	14.8	9.3	1.4	0.7	0.13	0.28	0.04	38.7	103.34
	Nodular	33.5	24.0	5.8	2.1	0.9	0.18	0.56	0.05	33.5	100.70
	Nodular	31.2	24.3	8.0	2.4	0.9	0.19	0.54	0.04	33.4	101.10
	Powder	12.6	38.0	20.4	4.1	1.5	0.31	0.61	0.02	23.4	101.00
Monteith (B)	Massive	39.4	17.8	4.6	1.3	1.2	0.12	0.54	0.08	36.2	101.45
	Massive	35.7	24.3	4.3	1.8	0.8	0.15	0.49	0.04	33.7	101.44
	Nodular	34.2	10.8	13.3	1.3	0.6	0.12	0.41	0.04	41.1	102.00
Murray Bridge	Massive	38.1	10.4	9.6	1.4	0.6	0.93	0.35	0.04	40.5	101.20
	Nodular	40.0	12.3	7.0	1.7	0.8	0.14	0.41	0.05	39.2	101.44
Black Hill	Massive	37.6	17.0	4.1	2.7	1.3	0.22	0.35	0.08	36.7	99.60
	Massive	37.3	16.8	4.1	2.7	1.3	0.22	0.26	0.07	36.4	99.70

Table 5.4 Major element bulk chemistry of calcretes from Yorke Peninsula, South Australia

Location	*Description*	*CaO*	*SiO_2*	*MgO*	*Al_2O_3*	*Fe_2O_3*	*TiO_2*	*K_2O*	*P_2O_5*	*Loss on ignition*	*Total*
Yorktown	Massive	40.4	15.1	3.0	2.7	1.1	0.14	0.83	0.06	36.8	100.1
	Nodular	40.3	16.0	3.1	3.1	1.1	0.16	0.75	0.08	36.8	101.5
Melton	Massive	51.1	4.4	1.1	1.0	0.4	0.06	0.51	0.12	43.2	101.9
	Massive	53.0	2.5	1.1	0.7	0.3	0.04	0.19	0.07	43.3	101.2
	Powder	22.8	30.5	8.5	2.7	1.3	0.20	0.31	0.04	32.8	99.2
Port Vincent	Massive	31.5	32.3	2.4	1.7	0.8	0.09	0.42	0.11	32.8	99.1
	Nodular	31.4	33.2	2.5	2.2	0.9	0.11	0.35	0.13	29.8	100.6
Moonta Bay	Massive	39.3	20.9	2.1	2.3	0.8	0.13	0.44	0.08	35.0	101.1
	Nodular	27.3	36.0	5.0	1.2	0.5	0.06	0.40	0.07	29.2	99.7
Port Julia	Massive	42.8	11.5	3.6	1.5	0.5	0.07	0.35	0.05	40.1	100.5
	Nodular	43.5	12.8	2.0	2.0	0.7	0.10	0.47	0.10	39.3	101.0
Wool Bay	Massive	42.0	14.8	3.5	2.4	0.9	0.12	0.32	0.08	38.4	102.5
	Nodular	44.9	8.8	4.8	1.9	0.7	0.07	0.34	0.07	41.5	103.1

chemical analyses of calcretes from numerous sites in southern South Australia are presented in Tables 5.3 and 5.4.

Considerable variability in chemistry occurs in South Australian calcretes. Dixon (1978) and Hutton and Dixon (1981) found that this variability is related to both calcrete morphology and to profile position. Dixon (1978) showed that as the degree of induration of calcretes increases, so does their chemical purity, with hardpan calcretes being the most calcareous and powder calcretes the least (Tables 5.3 and 5.4). Hutton and Dixon (1981) found that there is a systematic decrease in CaO and an accompanying increase in MgO in calcretes with increasing depth.

This trend was explained in terms of depth of leaching and associated degree of replacement of host materials by carbonate.

Dixon has examined the role of topography in accounting for spatial variations in calcrete chemistry. He examined six calcrete profiles down a toposequence in the St Vincents Basin and found that there was a systematic decrease in calcium from top to bottom of the toposequence and an accompanying increase in magnesium, as well as systematic decreases in calcium with depth (Table 5.5).

At a larger spatial scale, Milnes and Hutton (1983) recognized two distinct geochemical provinces of calcrete formation. The first province is associated with Pleistocene beach complexes and aeolianites and was given the name Bridgewater Formation province. The second province is a largely non-calcareous continental province in which calcretes are associated with a diversity of bedrock types. It was named the Continental province. In the Bridgewater Formation province the chemistry of the calcretes is very similar to that of the calcareous parent materials. The chemistry of calcretes from the Continental province, on the other hand, is highly variable. Hutton *et al.* (1977) suggested that calcrete developed on norite (hypersthene gabbro) in the Murray Basin at Black Hill was in part derived from the weathering of this rock. Dixon (1978) also showed that calcrete chemistry varied markedly depending on the underlying lithology. Hutton and Dixon (1981) established that the chemistry of the insoluble residue strongly reflected the chemistry of the underlying bedrock. Detailed discussion of the calcrete chemistry from each of the two provinces is provided by Milnes and Hutton (1983).

Recently, attention has been given to the uranium content of calcretes. Groundwater calcretes in particular have been the source of economic abundances of uranium minerals. Uranium-rich calcretes have been reported from Western Australia by Butt *et al.* (1977) and Carlisle (1983). Goudie (1983) also recorded uranium in calcretes from the Namib, Angola, Mauritania, and Somalia.

Chemical studies of calcrete in recent years have been focused on the isotopic compositions of these materials. These studies have been ultimately interested in determining the source of the carbon and thereby ascertaining the origin of the calcretes. Attention has been given to the stable isotopes of both carbon and oxygen. Salomons *et al.* (1978) conducted extensive isotopic analyses of calcretes from Europe, Africa, and India. These workers found that despite a considerable spread in isotopic values for both carbon and oxygen, there was, in general, good agreement between values in calcrete and prevailing precipitation. From this observation they concluded that evaporation was not a significant factor in calcrete formation. Nor did they find any systematic difference in isotopic content with depth. Isotopic studies of calcretes in Africa have also been undertaken by Cerling and Hay (1986), who found that calcretes in Olduvai Gorge display progressive increases in ^{18}O and ^{13}C isotopes with time. From these data the researchers concluded that there had been a progressive drying of the climate and an accompanying increase in C_4 grasses.

Isotopic studies of calcretes in the United States are relatively limited. However, Gardner (1972) conducted an extensive analysis of the isotopic chemistry of calcretes from Nevada and New Mexico. More recently Amundson *et al.* (1988) examined the isotopic chemistry of calcic soils from the Mojave Desert. Following on from that study, Amundson *et al.* (1989) report on oxygen and carbon isotopes in calcretes from Kyle Canyon in the Mojave Desert. Amundson *et al.* concluded that the isotopic composition of the calcretes is consistent with the prevailing climatic regime. These workers also determined the ages of calcrete lamelli using ^{14}C composition, but were unsure of the reliability of their dates due to possibility of contamination.

Early isotopic work on calcretes from Australia focused on ^{14}C concentrations in an attempt to determine the age of the calcretes (Williams and Polach 1969, 1971, Bowler and Polach 1971). These same workers also examined $^{12}C/^{13}C$ ratios in an attempt to come to some understanding of the origin of the carbonate in the calcrete. More recently Milnes and Hutton (1983) have examined the ^{13}C content of calcretes from a variety of locations in southern South Australia. The significance of these data with respect to calcrete genesis is still poorly understood.

MINERALOGY

The carbonate mineralogy of calcretes is dominated by calcite and dolomite, while the non-carbonate mineral fraction consists of quartz, opal, feldspars, and clay minerals (e.g. Goudie 1973, pp. 25–6, Reeves 1976, pp. 25–41, Milnes and Hutton 1983). The calcite is generally low-Mg calcite, though Watts (1980) reported high-Mg calcite from calcretes in southern Africa. Aragonite is also occasionally found in calcretes (Watts 1980, Milnes and Hutton 1983). Minor non-carbonate minerals in calcretes include iron sulphide and glauconite (Goudie 1972, 1973). Gypsum has also been reported widely in

Table 5.5 Major element bulk chemistry of calcretes from St Vincents Basin, South Australia (normalized to 100%)

Location	*Description*	*Depth (cm)*	*CaO*	*SiO_2*	*MgO*	*Al_2O_3*	*Fe_2O_3*	*TiO_2*	*K_2O*	*P_2O_5*	*Loss on ignition*
Onkaparinga R.	Massive	10	36.50	17.50	1.58	4.50	2.03	0.18	1.05	0.05	36.61
	Massive	30	37.76	17.30	1.92	4.06	1.87	0.19	0.94	0.05	35.91
	Powder	35	30.97	26.71	1.96	4.78	2.34	0.27	1.17	0.04	31.76
	Powder	55	30.13	26.68	2.45	4.49	2.36	0.26	1.14	0.03	32.46
	Powder	95	25.87	27.15	6.10	4.12	2.12	0.24	1.07	0.03	33.30
	Powder	125	28.03	23.65	7.30	3.40	1.84	0.19	0.84	0.02	34.73
	Powder	160	26.20	21.73	9.20	3.17	1.71	0.18	0.79	0.02	37.00
	Powder	185	24.86	22.86	10.20	3.63	1.87	0.20	0.90	0.01	35.67
	Powder	215	22.98	22.29	11.40	4.43	2.10	0.21	0.91	0.01	35.67
Onkaparinga	Massive	10	36.50	20.76	1.29	2.94	1.62	0.15	0.67	0.04	36.03
Trig	Massive	30	30.72	27.75	1.58	3.72	1.98	0.20	0.90	0.02	33.13
A	Powder	35	28.61	32.57	1.76	4.06	2.13	0.23	0.98	0.03	29.63
	Powder	60	26.02	35.34	3.66	4.29	2.33	0.24	1.08	0.21	26.83
	Powder	85	23.17	32.68	6.40	3.62	1.92	0.20	0.86	0.02	31.13
	Powder	125	23.42	35.49	6.10	3.79	1.95	0.20	0.94	0.03	28.08
	Powder	150	20.57	32.50	9.80	3.43	1.92	0.19	0.85	0.01	30.73
	Powder	180	20.51	33.01	9.50	3.34	1.94	0.19	0.83	0.01	30.67
	Powder	210	18.09	38.11	8.30	4.15	2.25	0.23	0.98	0.02	27.87
Onkaparinga	Massive	30	35.71	22.89	1.88	3.13	1.63	0.17	0.71	0.03	53.85
Trig	Powder	40	29.13	31.28	2.72	3.57	1.87	0.20	0.84	0.02	30.37
B	Powder	85	22.86	30.45	8.50	3.40	1.72	0.19	0.84	0.01	32.03
	Powder	110	20.88	30.52	10.90	3.34	1.85	0.19	0.84	0.01	31.47
	Wedge	150	25.77	14.50	16.50	1.64	1.03	0.07	0.39	0.01	40.15
Onkaparinga	Massive	30	35.22	25.09	2.04	3.25	1.80	0.18	0.79	0.03	31.60
Trig	Powder	35	30.07	29.68	3.78	3.64	1.86	0.20	0.93	0.02	29.82
C	Powder	60	28.74	31.45	6.39	4.13	2.07	0.23	1.03	0.02	28.94
	Powder	100	23.71	30.64	8.22	3.79	2.03	0.21	0.97	0.02	30.41
	Powder	130	21.78	31.80	9.16	4.02	2.05	0.23	1.00	0.01	29.94
	Wedge	170	27.67	14.54	14.20	2.19	1.17	0.13	0.50	0.01	29.59
	Wedge	170	25.56	18.28	14.00	2.54	1.29	0.15	0.60	0.01	37.57
	Powder	175	23.51	25.39	11.10	3.48	1.82	0.19	0.86	0.01	33.64
	Wedge	220	27.68	12.91	14.60	2.35	1.23	0.13	0.46	0.01	40.63
	Powder	220	19.23	34.98	7.80	5.46	2.68	0.28	1.11	0.01	28.45
Lonsdale A	Weak Massive	10	20.25	43.49	6.29	2.52	1.71	0.15	0.51	0.01	25.07
	Massive	30	19.36	44.27	6.41	2.72	1.86	0.14	0.54	0.01	24.69
	Massive	30	13.58	51.81	6.96	3.38	2.27	0.19	0.66	0.01	21.14
	Massive	70	16.09	49.65	6.45	2.96	2.14	0.18	0.59	0.02	21.92
	Massive	80	16.75	49.65	6.45	3.00	1.88	0.14	0.52	0.01	21.60
	Massive	90	13.22	51.16	8.08	3.12	2.06	0.16	0.62	0.01	21.57
	Massive	100	10.13	57.14	6.90	3.37	2.34	0.23	0.66	0.01	19.22
	Massive	110	9.68	63.12	4.68	3.51	2.50	0.19	0.70	0.01	15.61
	Wedge	–	21.83	33.84	10.30	1.47	1.37	0.07	0.30	0.01	30.81
	Wedge	–	16.00	44.30	10.26	1.95	1.65	0.11	0.41	0.01	25.31
Lonsdale B	Massive	30	25.74	41.98	1.40	3.16	2.07	0.19	0.61	0.04	24.81
	Powder	50	27.42	39.38	1.55	3.02	1.83	0.20	0.57	0.04	25.99
	Weak Massive	70	25.62	39.64	2.91	3.12	1.90	0.18	0.54	0.03	26.06
	Weak Massive	90	18.12	50.36	2.93	4.31	2.48	0.25	0.73	0.02	20.80
	Massive	110	16.56	53.48	3.05	3.94	2.49	0.23	0.70	0.02	19.53
	Massive	130	13.13	57.66	3.95	3.90	2.47	0.22	0.71	0.02	17.94
	Massive	150	11.76	59.77	4.84	3.72	2.47	0.22	0.68	0.01	16.53
Lonsdale C	Coated Clast		27.03	42.52	0.94	2.15	1.79	0.20	0.40	0.03	24.94
	Massive	30	20.71	51.28	1.08	2.43	1.83	0.23	0.43	0.03	21.98
	Massive	50	24.81	43.63	1.74	2.16	1.86	0.17	0.31	0.03	25.24
	Massive	70	26.31	37.60	3.05	2.33	1.77	0.16	0.40	0.02	28.36
	Massive	90	25.86	36.59	4.00	2.45	1.74	0.16	0.41	0.11	28.78

Table 5.5—contd.

Location	*Description*	*Depth (cm)*	*CaO*	*SiO_2*	*MgO*	*Al_2O_3*	*Fe_2O_3*	*TiO_2*	*K_2O*	*P_2O_5*	*Loss on ignition*
Lonsdale D	Nodule	10	25.81	44.03	0.94	2.79	2.05	0.22	0.50	0.03	23.63
	Strong Massive	30	26.39	43.78	0.97	2.51	1.80	0.18	0.45	0.02	23.90
	Massive	50	21.27	50.75	0.99	3.46	2.29	0.23	0.58	0.03	20.40
	Massive	70	23.84	43.87	1.45	3.60	2.24	0.24	0.55	0.02	24.19
	Massive	90	20.73	52.76	1.10	2.39	1.85	0.24	0.41	0.02	20.50
	Weak Massive	110	17.23	59.54	0.93	2.62	2.23	0.24	0.54	0.02	16.60
	Massive	130	10.88	68.10	1.19	3.94	2.71	0.30	0.71	0.02	12.15
	Massive	140	14.82	61.43	0.92	3.59	2.62	0.28	0.64	0.01	15.69
Lonsdale E	Nodule	10	27.33	41.48	1.01	2.72	1.93	0.20	0.50	0.03	24.80
	Weakly Massive	30	17.72	58.70	0.88	2.95	2.10	0.25	0.57	0.03	16.80
	Massive	50	20.66	52.06	1.46	3.11	2.12	0.22	0.55	0.02	19.80
	Massive	70	21.34	50.44	1.64	3.02	2.13	0.25	0.51	0.02	20.65
	Massive	90	28.22	34.01	2.66	3.03	1.86	0.14	0.46	0.01	29.61
	Massive	110	19.89	55.00	2.69	3.04	1.89	0.15	0.46	0.01	16.87
	Massive	130	15.18	62.92	1.80	2.18	1.86	0.21	0.41	0.01	15.43
	Massive	150	13.90	63.02	2.25	2.48	2.04	0.24	0.48	0.01	15.43
	Massive	170	22.29	50.67	1.40	2.06	1.66	0.19	0.39	0.02	21.32
	Massive	180	10.37	69.59	2.43	2.75	2.23	0.26	0.55	0.01	11.78

calcretes (Reeves and Suggs 1964, Aristarain 1971, Goudie 1973). Haematite, grossularite, magnetite, muscovite, rutile, tourmaline, and zircon have all been reported from calcretes in New Mexico by Aristarain (1971).

Mineralogical studies have focused primarily on the clay mineral fraction and have been largely concerned with the origin of the clays and the light they may throw on calcrete genesis. Clay mineral assemblages in calcretes appear to be characterized by a relatively small number of mineral species. In the United States, the dominant clay minerals appear to be palygorskite and sepiolite, and there are smaller abundances of illite, kaolinite, montmorillonite, interlayered illite–montmorillonite, and chlorite (Van den Heuvel 1966, Gile 1967, Aristarain 1970, 1971, Gardner 1972, Frye *et al.* 1974, Reeves 1976, pp. 37–9, Bachman and Machette 1977, Hay and Wiggins 1980). Many authors have ascribed the origin of the palygorskite and sepiolite to the alteration of montmorillonite and interlayered montmorillonite–illite. Hay and Wiggins (1980) believed that the sepiolite in calcretes from various locations in the south-western United States is neo-formational in origin. However, they argued for the formation of palygorskite from montmorillonite.

In Australia, the dominant clay minerals in calcretes are illite, kaolinite, and interstratified minerals (Milnes and Hutton 1983, Phillips and Milnes 1988). However, Dixon (1978) and Hutton and Dixon (1981) found that palygorskite and sepiolite are the dominant clay minerals in calcretes in selected areas of the Murray Basin of southern South Australia. These authors ascribed the origin of these minerals to neo-formation in an environment abundant in Mg, specifically a favourable underlying lithology that provides the necessary cations upon weathering. Clay mineralogy of calcretes appears to be strongly related to the provenance of the calcrete. Calcretes in the Bridgewater Formation province appear to be dominated by illite, kaolinite, and interlayered clays. In the Continental province the clay mineralogy is more diverse and includes sepiolite and palygorskite.

Recent clay mineralogical investigations of calcretes from Africa (Watts 1980) reveal mineral assemblages similar to those from the United States and Australia. Watts (1980) found that the calcretes from the Kalahari Desert were dominated by palygorskite and sepiolite. These clay minerals were interpreted to be primarily neo-formational in origin. However, Watts suggested that some of the palygorskite may be derived from the alteration of montmorillonite. The remainder of the clay mineral assemblage consists of illite, montmorillonite, mixed layer illite–montmorillonite, kaolinite, chlorite, and glauconite. Watts (1980) interpreted the minor clay mineral species present in the calcretes to be pre-

dominantly detrital. The mixed layer clays, however, appear to be weathering products derived from illite.

Detailed studies of dolomite in calcretes have recently been undertaken in both Australia and Africa (Dixon 1978, Watts 1980, Hutton and Dixon 1981, Phillips and Milnes 1988). Dixon (1978) and Hutton and Dixon (1981) identified abundant amounts of dolomite in calcretes from the southern Murray Basin and Yorke Peninsula, South Australia. Dolomite abundances were greatest in the fine carbonate silt at the base of the calcrete profile and decreased progressively upward in the profiles as the degree of induration increased. Similar dolomite trends have been reported from calcrete profiles in the St Vincents Basin of southern South Australia (Phillips and Milnes 1988). These authors pointed out that dolomite abundances are greatest in wedges and blotches developed in the calcretes. In southern Africa, Watts (1980) reported generally similar trends with respect to the distribution of dolomite within the profiles. Dolomite is intimately associated with palygorskite and sepiolite in calcretes from both of these continents. Dolomite appears to be closely associated with the less indurated varieties of calcrete.

Dixon has examined in detail the distribution of dolomite and calcite in calcrete profiles from the St Vincents Basin in South Australia. He conducted a study down a single hillslope developed on weakly indurated calcrete and found that there was a systematic decrease in calcite and an accompanying increase in dolomite. The calcrete profile at the top of the catena is characterized by a complete lack of dolomite through its entire thickness. The profile at the base of the catena contains only dolomite with a complete absence of calcite. The greater solubility of $MgCO_3$ compared with $CaCO_3$ accompanied by lateral transportation of Mg-rich waters may be responsible for this trend.

Quartz is often the dominant non-carbonate mineral in both bulk samples and clay size fractions of the calcretes (Reeves 1976, p. 30, Milnes and Hutton 1983, Phillips and Milnes 1988). Silica also occurs in various other forms, including opal and chalcedony. Opal has been widely reported from calcretes in west Texas (Reeves 1976, p. 28) as well as from the south-western United States (Hay and Wiggins 1980). Watts reports the occurrence of opal in calcretes from southern Africa along with both length-slow and length-fast chalcedony. Much of the silica in calcretes occurs as cement. However, in some cases quartz is a replacement mineral of calcite.

ORIGIN

Calcretes may be pedogenic or non-pedogenic in origin. However, most areally extensive calcretes appear to form in the soil environment. The specific processes responsible for calcrete formation in the soil environment are variable. Goudie (1973, pp. 141–4, 1983) suggested several models for the formation of pedogenic calcretes. These include the concentration of carbonate by downward translocation in percolating soil waters, the concentration of carbonate by capillary rise waters, *in situ* case hardening by carbonate, and cementation of calcrete detritus. Of these models, the accumulation of carbonate in soils as a result of vertical translocation is the most widely accepted. Precipitation of the carbonate results from a variety of processes. Schlesinger (1985), working in the Mojave Desert, suggests that carbonate precipitation results from evaporation, increases in pH, and decreases in CO_2 partial pressure. Other mechanisms of carbonate precipitation include increases in temperature and accompanying loss of CO_2 (Barnes 1965), the common ion effect (Wigley 1973), and evaporation (Watts 1980, Watson 1989). Biological processes have also been shown to be important in calcite precipitation. Several authors have clearly established the significance of micro-organisms in calcrete formation (e.g. Klappa 1978, 1979a, b, Phillips and Self 1987, Phillips *et al.* 1987). In addition, the formation of calcrete around plant roots has been widely documented (Gill 1975, Klappa 1979a, b, Semeniuk and Meagher 1981, Warren 1983, Semeniuk and Searle 1985).

Central to the question of the origin of calcretes has been the origin of the calcium carbonate contained within them. In the United States there has been a long history of appealing to atmospheric sources for the carbonate. As early as 1956, Brown (1956) suggested that all of the carbonate necessary for the formation of calcretes could be derived from atmospheric dust and calcium dissolved in rainwater. Similar arguments have been presented by subsequent workers including Gile (1967), Ruhe (1967), Reeves (1970), Bachman and Machette (1977), Machette (1985), and McFadden and Tinsley (1985). Gardner (1972) provided quantitative support to the notion of an aeolian origin for the carbonate by showing that extreme thicknesses of overlying sediments would have to be weathered and leached in order to account for the thick calcrete caprocks in Nevada. Similar conclusions had earlier been reached by several authors who had shown that there was little evidence for significant depletion of

calcium from sediments overlying calcrete horizons (Gile *et al.* 1966, Van den Heuvel 1966, Aristarain 1970, McFadden 1982).

In southern Australia, the carbonate mantle is also widely interpreted to be aeolian in origin. Early workers (Crocker 1946) interpreted the mantle to have been derived from the winnowing of the finer size fraction from coastal dune deposits. Recent studies by Milnes and Hutton (1983), Milnes *et al* (1987) and Phillips and Milnes (1988) essentially concur but point out that the original sediments have been considerably modified since deposition and may also contain some inclusions of sediments from non-aeolian sources. Hutton and Dixon (1981) suggested that some of the carbonate, especially that in continental settings, was lacustrine in origin and had been modified in place by pedogenic processes. *In situ* formation of calcretes has occurred within calcareous coastal dunes and sand sheets on Yorke Peninsula (Dixon 1978, Hutton and Dixon 1981) as well as in similar deposits in Western Australia (Arakel 1985). In both locations cementation of host materials by percolating vadose waters is responsible for calcrete development.

Non-pedogenic calcretes have also long been recognized. As mentioned earlier, at approximately the same time that Lamplugh introduced the term calcrete he specifically recognized the existence of calcretes in association with river valleys. Considerable research in central and Western Australia has focused on the association of calcrete with present and palaeo-drainage ways. Much of this research has been undertaken in association with uranium exploration (e.g. Mann and Horwitz 1979, Arakel and McConchie 1982, Arakel 1986, Jacobson *et al.* 1988). In these calcretes the calcium carbonate is derived from groundwater sources and is subsequently precipitated in drainage channels as a result of low-precipitation and high-evaporation climatic regimes.

SILCRETE

TERMINOLOGY

The term silcrete was introduced into the geomorphological literature at the same time as calcrete. Lamplugh (1902) originally used the term to refer to silicified sandstones and conglomerates and later (Lamplugh 1907) to indurated sandstones and quartzites cemented by chalcedony occurring in the Zambesi River basin. Today, silcrete is widely defined as a surface or near-surface deposit of saprolite, sediment, or soil that has been cemented by secondary silica (Milnes and Twidale 1983). Silicification has occurred at low temperatures and is not a product of volcanism, plutonism, metamorphism, or deep diagenesis (Summerfield 1983a).

Figure 5.7 Breakaway capped with silcrete and associated weathered pallid zone, northern New South Wales, Australia (photo courtesy of S.H. Watts).

Early work on silcretes linked them genetically to the deep weathering profile which frequently occurs beneath many massive silcrete caprocks (Woolnough 1930, Wopfner 1978) (Fig. 5.7). Silcrete in Australia and Africa has also commonly been related to surfaces of low relief (Woolnough 1927, Langford-Smith and Dury 1965, Wopfner and Twidale 1967, Twidale *et al.* 1970).

DISTRIBUTION

Silcretes are most widely distributed in Australia and southern Africa but have also been reported from a variety of other locations. In Africa they have been reported from such diverse areas as the Sahara and its margins, the Congo Basin, Zambesi Basin, Botswana, Namibia, South Africa, and some areas of east Africa (Summerfield 1982, Watson 1989).

In Australia, silcretes have been reported from the states of Queensland (e.g. Gunn and Galloway 1978, Senior 1978, van Dijk and Beckman 1978), New South Wales (Dury 1966, S.H. Watts 1978b, Taylor 1978), and South Australia (Hutton *et al.* 1972, 1978, Wopfner 1978, 1983, Milnes and Twidale 1983, Milnes *et al.* 1991), and Western Australia (Butt 1983, 1985).

Silcrete has not been widely reported from the United States. However, silicification of calcrete has been recognized in Texas (Price 1933, Reeves 1970, 1976, pp. 26–32). Where silicification of calcrete has been virtually complete, these deposits might be appropriately referred to as silcretes.

MORPHOLOGY

Macromorphology

Macroscopically, silcrete displays a diversity of forms. In a detailed study of the silcretes of western New South Wales, S.H. Watts (1978b) described a wide variety of silcrete morphologies both at the landform scale as well as at the outcrop scale. Watts recorded the common occurrence of massive, columnar jointed silcretes capping upland surfaces (Fig. 5.8). Individual columns often extend the complete thickness of the silcrete outcrop. Individual columns may be up to 5 m thick with widths of 2 m. In outcrop, silcrete surfaces frequently display concentric ring patterns, ropy surfaces, and nodular to concretionary weathering forms. Watts also described piping silcrete and accompanying rounded, lobe-like ridges and rings.

In a study of silcrete in northern South Australia (Wopfner 1978) observed a similar diverse assemblage of macroscopic forms. He recognized polygonal prismatic or columnar silcrete as the most common morphological type. The columns or prisms are commonly 50 to 120 cm high with diameters of 25 to 80 cm. The columns are frequently draped with a thin skin of silica. Often associated with columnar silcrete is platy silcrete which occurs as large slabs from 8 to 15 cm thick. In detail, platy silcretes are either massive or pseudopebbly. Wopfner identified two other principal macromorphological types. Botryoidal silcrete is characteristically rough and jagged and occurs in thick profiles, whereas pillowy silcrete resembles the surface of lava. Like S.H. Watts (1978b), Wopfner described pipe silcrete as commonly occurring within outcroppings of botryoidal silcrete. On the basis of Wopfner's (1978) observations of silcrete macromorphology, Watts developed a comprehensive classification of silcretes. In addition to macroscopic characteristics, the classification includes microscopic parameters. The classification is based on the characteristics of the silcrete matrix mineralogy, macroscopic texture, host rock texture, and profile thickness and type.

A recent comprehensive summary of the macroscopic characteristics of silcretes in central Australia was provided by Milnes and Twidale (1983). These workers recognized a variety of silcrete types occurring on mesa surfaces, including columnar, massive, bedded, and conglomeratic or nodular silcrete. Silcrete outcrop surfaces commonly display ropy, whorled, and custard-like forms as well as liesegang ring-like structures. Pipe-like structures are widespread, as are silcrete skins on bedrock outcrops (Twidale *et al.* 1970, Hutton *et al.* 1972).

Micromorphology

Microscopically, silcretes reflect characteristics of both the host material and the silicification process (S.H. Watts 1978a, Summerfield 1983b, Milnes *et al.* 1991). Primary characteristics of silcretes usually relate to such features as grain size, grain shape, mineralogy, and grain fabric. Secondary characteristics include cryptocrystalline and microcrystalline silcrete matrices, extensive embayment of quartz grains (Fig. 5.9), grain pitting and replacement by secondary silica, and textural modification of sediments from a grain-supported to a floating matrix texture (Watts 1978a). Summerfield (1982, 1983a) discussed a variety of secondary micromorphological

Figure 5.8 Silcrete outcrop, showing typical columnar structure, Mount Stuart Station, New South Wales, Australia (photo courtesy of S.H. Watts).

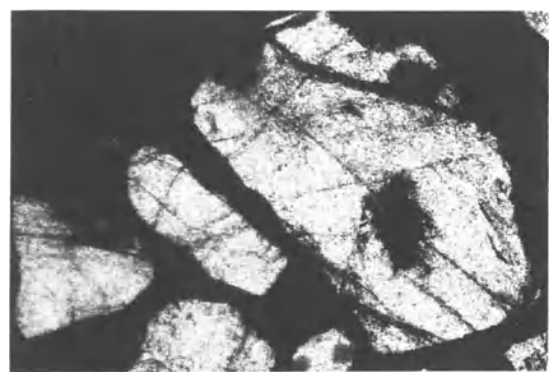

Figure 5.9 Photomicrograph of silcrete, showing solutional embayments of original detrital quartz (photo courtesy of S.H. Watts). Field of view is 1.8 mm.

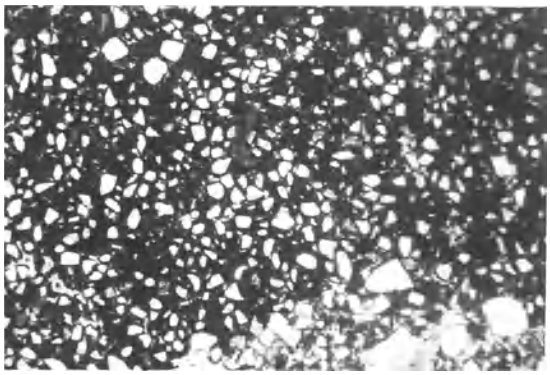

Figure 5.10 Photomicrograph of silcrete from west Texas, showing floating (F) fabric with quartz grains separated by finer matrix materials. Field of view is 1.1 mm.

Figure 5.11 Photomicrograph of silcrete from west Texas, showing conglomeratic (C) fabric. Field of view is 1.1 mm.

features developed in silcretes from southern Africa. Detailed studies of the micromorphology of silcretes in Australia have been undertaken by Hutton *et al.* (1972), Milnes and Hutton (1974), Hutton *et al.* (1978), and Milnes and Twidale (1983).

A number of classification schemes based on micromorphological features have been developed, including those of Smale (1973), S.H. Watts (1978a), and Wopfner (1978, 1983). Perhaps the most comprehensive of these is that developed by Summerfield (1982, 1983a). He recognized four major fabric types with associated subtypes. The principal fabric types are GS (grain-supported) fabric, F (floating) fabric, M (matrix) fabric, and C (conglomeratic) fabric. Grain-supported fabrics are those in which skeletal grains of the silcrete are self-supporting. Skeletal grains may display overgrowths of chalcedony or microquartz. The matrix of grain-supported silcrete fabrics is commonly characterized by microquartz and cryptocrystalline and opaline silica. Floating fabrics are those in which the skeletal grains float in a matrix of microcrystalline, cryptocrystalline, and opaline silica. The skeletal grain content of these fabrics is greater than 5%. Floating fabrics may be massive or glaebular (Fig. 5.10). Matrix fabrics are similar to F fabrics with the difference being they possess a skeletal grain content of less than 5%. As with F fabrics, M fabrics occur as massive and glaebular subtypes. Conglomeratic fabrics possess a discernible detrital fabric. The fabric is determined primarily on the basis of the size of the detrital grains which exceed 4 mm in diameter (Fig. 5.11).

CHEMISTRY

The chemistry of silcretes is overwhelmingly dominated by silica, which may be as much as 99% by weight, with negligible amounts of other chemical constituents. Silcretes are characteristically poor in alkalis and alkali earths, though often they display enhanced concentrations of iron, titanium, zirconium, and aluminium. The enhanced titanium concentrations are associated with the presence of anatase and rutile (Hutton *et al.* 1972, Milnes and Twidale 1983). Aluminium concentrations are associated with clay minerals.

Chemical analyses of silcretes have been published by Goudie (1973, pp. 18–21) for Africa and by Summerfield (1982, 1983b, c) for Botswana and South Africa. The analyses of Summerfield were concerned with the chemical variability vertically down through the weathering profile. An examination of some 50 silcrete profiles reveals a mean silica abundance of 94.7%. The second most abundant constituent is titanium at 1.82%. Iron and aluminium are present in small and variable abundances. Silcrete profiles show enrichment in silica and often titanium but display depletion of aluminium, alkalis, and alkali earths. In some profiles there is also enrichment of iron where silcrete is associated with ferricrete and where late-stage surface weathering has occurred. On the basis of silcrete chemistry, distinction is made between weathering and non-weathering silcretes. Weathering silcretes are characterized by the enrichment of titanium as a result of the leaching of more soluble materials, while non-weathering silcretes are deficient in titanium (Summerfield 1983c).

Detailed chemical analyses of Australian silcretes are available from a number of studies. Hutton *et al.* (1972) examined the chemistry of silcretes and silcrete skins in South Australia. This study was significant in heightening awareness of concentrations of titanium and zirconium in silcretes. A

comprehensive collection of papers edited by Langford-Smith (1978) provided a wide sampling of silcrete chemistries from a variety of areas in arid and semi-arid Australia (Gunn and Galloway 1978, Hutton *et al.* 1978, Langford-Smith and Watts 1978, Senior 1978, Wopfner 1978). Watts (1977) presented a detailed discussion of the chemistry of silcretes from western New South Wales. A summary of silcrete chemical analyses from a variety of sites in central and southern Australia has been presented by Milnes and Twidale (1983). Consistent with previous studies of silcrete chemistry these authors found the silcretes to be dominated by silica, enriched in titanium and zirconium, low in calcium and alkalis, and characterized by accumulations of iron oxides and aluminium. Recent work on pedogenic and groundwater silcretes from the opal fields of South Australia by Milnes *et al.* (1991) and Thiry and Milnes (1991) provided detailed chemical analyses of these diverse materials. These studies again revealed the trends in silcrete chemistry outlined above. An interesting finding of these studies was that as shale is transformed to opalite, there is a loss of aluminium, titanium, iron and water, and an accompanying accumulation of silica.

Silicification of calcrete in the south-western United States is widespread and has been widely reported in the literature (Price 1933, Sidwell 1943, Brown 1956, Swineford and Franks 1959, Aristarain 1970, Reeves 1976). However, published chemical analyses are few. Field observations (Fig. 5.12) of massive calcretes in the Ogallala Formation showed that many of them are extensively replaced by silica and, therefore, are more accurately referred to as silici-calcretes (Table 5.6). Considerable scope exists for the systematic study of silcretes in the south-western United States where these materials are undoubtedly more widespread than previously recognized (B.L. Allen, personal communication, 1991).

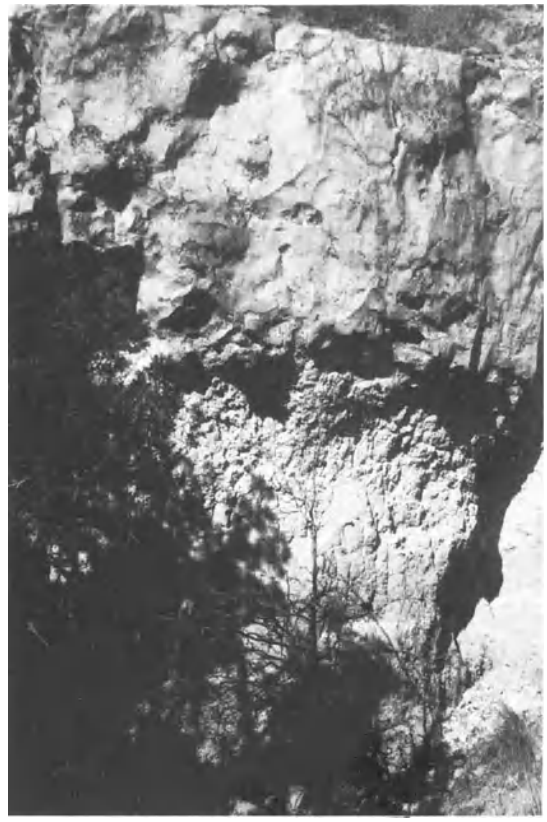

Figure 5.12 Silcreted caprock calcrete, Ogalalla Formation, Palo Duro Canyon, west Texas.

MINERALOGY

Like its chemistry, the mineralogy of silcrete is relatively simple. However, the mineralogy is a reflection of both host materials as well as secondary alteration. Typically, silcretes are dominated by quartz, with minor amounts of opaline silica, feldspars, and heavy minerals and clay minerals (Summerfield 1983a, c).

Detailed mineralogical studies of silcretes from southern Africa (Summerfield 1982) revealed a mineralogy dominated by quartz with the presence of opal CT (cristobalite and tridymite) in the ground mass. Chalcedony was recognized in voids and

Table 5.6 Major element bulk chemistry of silicified calcretes. High Plains, west Texas

Sample	SiO_2	Al_2O_3	Fe_2O_3	MgO	CaO	Na_2O	K_2O	TiO_2	*Loss on ignition*	*Total*
S1A	65.7	2.2	0.83	1.4	14.4	0.28	0.45	0.13	15.1	100.5
S1B	65.5	2.2	0.79	1.3	14.5	0.29	0.46	0.12	15.1	100.3
S2A	71.1	2.7	0.97	1.4	10.8	0.35	0.66	0.14	11.8	99.9
S2B	70.8	2.7	0.95	1.4	10.8	0.35	0.67	0.14	11.8	99.9

vughs. The clay mineral fraction was dominated by glauconite–illite.

Similar mineralogies were reported from central and southern Australian silcretes by Milnes and Twidale (1983). These authors observed framework grains dominated by quartz with variable size lithic clasts. The micro- and cryptocrystalline matrix is a mixture of opal-C, opal-CT, and quartz. Overgrowths on framework grains consist of chalcedony and quartz. In some skin silcretes, in particular, the groundmass contains an abundance of anatase (Hutton *et al.* 1972, 1978). Other accessory minerals in Australian silcretes commonly include zircon and rutile. Mineralogical characteristics of silcretes from various locations in the Australian arid zone are reported by Gunn and Galloway 1978, Wopfner 1978, S.H. Watts 1978a).

A variety of clay minerals have been identified in the matrix of the silcretes. Van Dijk and Beckman (1978) found the clay size fraction of silcretes from south-eastern Queensland to be dominated by quartz and kaolinite, with smaller amounts of interstratified clay minerals, illite, and montmorillonite. Detailed mineralogical analyses of silcretes in the opal fields of South Australia (Milnes *et al.* 1991) revealed a diverse mineralogy dominated by kaolinite and smectite.

ORIGIN

Silcrete formation involves the interaction of three elements: a silica source, silica transfer, and silica precipitation. Numerous sources of silica are possible for the formation of silcrete. Silica may be derived *in situ* from the dissolution of the host materials followed by reprecipitation. Evidence for this is seen in the frequent occurrence of embayed quartz and other aluminosilicate mineral grains within silcrete (Hutton *et al.* 1978, S.H. Watts 1978a).

Silcretes with accompanying weathering profiles or in close proximity to weathered sediments may derive the silica for their formation from the weathering of aluminosilicate minerals and/or dissolution of quartz (Senior 1978, Wopfner 1978, Summerfield 1982, 1983c, Milnes and Twidale 1983).

A long history exists in Australia of attempts to genetically link silcrete formation to the presence of basalt because of a common spatial association between the two. Many workers have suggested that silica released as a result of weathering is redeposited beneath the basalt as silcrete (Gunn and Galloway 1978, Ollier 1978). Taylor and Smith (1975), however, had previously argued against any genetic link between basalt and silcrete, suggesting that their frequent spatial association was merely fortuitous.

Silica sources for the formation of silcrete in southern Africa have been attributed to aeolian influx. Summerfield (1982, 1983a) has suggested that aeolian-transported quartz and aluminosilicate sediments are especially susceptible to dissolution because of the abrasion and associated disordering of their surfaces experienced during transport. In addition, grain size reduction during transport results in a greatly enhanced surface area to volume relationship, which increases their solubility.

Concentration of silica is common amongst some grasses and represents another source of silica (Summerfield 1982, 1983a). In lacustrine and fluvial environments, diatoms may also represent an important silica source (Summerfield 1982).

Silica solution and transport takes place in normal aqueous systems as either silicic acid or as an aqueous sol (Milnes and Twidale 1983). Such solution and transport appears to occur at normal temperatures and under neutral to low pH conditions. However, it is widely known that the solubility and concentration of silica in solution in the soil environment is greatly increased in environments where pH is above 9 (Wilding *et al.* 1977).

Summerfield (1982, 1983a), based on his studies of silcrete genesis in southern Africa, distinguished between lateral transfer models and vertical transfer models of silcrete formation. Lateral transfer models, which include the formation of silcrete in lacustrine and fluvial models environments, have long been applied to the origin of silcretes in Australia and Africa. In some of the earliest work on the genesis of silcretes in Australia, Stephens (1964, 1971) suggested that the silcretes in central Australia were the result of the accumulation of silica leached and transported from the Eastern Highlands during the formation of lateritic iron crusts. Short-distance lateral transport models have been proposed by Milnes and Twidale (1983), Wopfner (1978), and Hutton *et al.* (1972, 1978). Summerfield (1982, 1983b), working in southern Africa, described silcretes from a variety of landscape settings whose origin can be best ascribed to the lateral transfer model. He reported the occurrence of silcretes in pan (lacustrine) settings in Botswana and the Northern Cape Province, South Africa, as well as on the floors of river valleys and in association with river terraces. Ambrose and Flint (1981) described silcretes associated with strandlines of a receding Miocene lake in northern South Australia.

Perhaps more widely applicable than the lateral transfer models are the vertical transfer models. The

latter models include the *per ascendum, per descendum,* and groundwater models of Goudie (1973). Silcretes resulting from the vertical rise of soil waters (the *per ascendum* model) and subsequent deposition of silica as a result of evaporation and/or pH change were described in early investigations of silcrete genesis in Australia (Woolnough 1927) and Africa (Frankel and Kent 1938). Severe limitations with this model with respect to the distance of capillary rise through sands (Summerfield 1982) as well as the efficiency of evaporative precipitation at depth (Summerfield 1983b) have cast serious doubts on its widespread applicability to silcrete genesis.

Of broader applicability is the *per descendum* model in which silica-charged waters percolate to depth under the influence of gravity, eventually resulting in the deposition of silica. These models were championed early in the history of silcrete research by workers such as Whitehouse (1940) and more recently by Gunn and Galloway (1978) and S.H. Watts (1978a, b). Thiry and Milnes (1991) described pedogenic silcretes from the opal fields of South Australia in which they envisaged the accumulation of silica to be the result of the downward percolation of silica-rich waters derived from the weathering of overlying quartzite.

Transport of silica in ground water (the groundwater model) and subsequent deposition with associated silcrete formation has received considerable attention in the literature. Groundwater silcretes have been described from arid central Australia by Ambrose and Flint (1981). Thiry and Milnes (1991), working in the opal fields of South Australia, proposed a model of silcrete formation in association with silica-laden ground waters. This model led them to conclude that multiple silcrete layers could be attributed to silicification associated with progressive water table lowering as a landscape denudation proceeds.

GYPSUM CRUSTS

OCCURRENCE

Gypsic crusts occur in warm desert environments receiving less than 200 to 250 mm of rainfall per annum (Watson 1983). Gypcretes have been reported from virtually every continent of the world (Watson 1983). In Australia, gypcretes have been described by Wopfner and Twidale (1967), Arakel and McConchie (1982), Warren (1982), Jacobson *et al.* (1988), and Milnes *et al.* (1991). In Africa, extensive areas of gypsum crusts have been recorded in Tunisia (Watson 1979, 1985, 1988), Algeria (Horta 1980), and the Namib Desert of southern Africa (Martin 1963, Scholz 1972, Watson 1983, 1985, 1988). Gypsic crusts have also been reported from the Middle East, specifically from Israel (Dan *et al.* 1982, Amit and Gerson 1986), Egypt (Ali and West 1983), and Iraq (Tucker 1978). In North America there have been limited reports of gypcretes from the south-western United States (Nettleton *et al.* 1982) and the semi-arid Rocky Mountain states (Reider *et al.* 1974, Reheis 1987).

MORPHOLOGY

Watson (1979, 1983) recognized three principal types of gypsum crust in Africa. (a) Evaporitic crust characteristically consists of packed microcrystalline gypsum strata. (b) True gypsum or *croute de nappe* occurs in two forms: either as lightly cemented gypsum crystals up to 1 mm in length commonly developed beneath non-gypsic sediment or as desert rose crust consisting of interlocking lenticular gypsum crystals ranging in size from a few millimetres to 20 cm. (c) Surface crust also occurs in two principal forms: gypsum powder which is composed of loose accumulations of small gypsum crystals, and indurated crust which is characteristically polygonal or columnar in appearance and consists of an outer zone of densely packed microcrystalline gypsum and a core of soft or puggy coarsely crystalline gypsum.

In a recent study of gypsic soils in the Rocky Mountain states, Reheis (1987) described gypsum accumulations in soils in terms of the morphologic sequence developed by Gile *et al.* (1966) for calcretes from the south-western United States. Reheis (1987) identified four stages of gypcrete development. Stage I gypcrete is characterized by thin, discontinuous gypsum coatings on the undersides of stones. Stage II gypcrete has abundant gypsum pendents under stones and gypsum crystals scattered through the matrix or forming small, soft powdery nodules. Stage III gypcrete is distinguished by the presence of continuous gypsum through the soil matrix and large gypsum pendents beneath stones. Stage IV gypcrete consists of a continuous gypsum-plugged matrix, with stones and smaller debris floating in the gypsum matrix.

Detailed descriptions of gypcrete from Australia are limited. Wopfner and Twidale (1967) recognized two main forms of gypsum. The first is an upper crystalline unit which these authors specifically referred to as gypcrete. This unit consists of coarsely crystalline double-twinned gypsum, together with fine to coarse clastic gypsum. The second lies below

Table 5.7 Typical bulk chemical analyses of gypcretes from Wyoming (from Reheis 1987)

			Percentage of size fraction <2 mm									
Location	*Depth (cm)*	*Stage*	SiO_2	Al_2O_3	Fe_2O_3	MgO	CaO	Na_2O	K_2O	TiO_2	Mn	ZrO_2
Kane Fan 4	28–75	II	13.0	1.74	0.80	6.17	33.3	0.24	0.36	0.08	0.02	0.01
Site B-16	75–135	II	19.0	2.44	1.04	6.72	27.6	0.40	0.48	0.12	0.02	0.01
	135–237+	I+	45.0	5.44	2.23	3.35	14.0	0.59	0.96	0.30	0.01	0.03
Kane Fan 5	19–40	IV	9.0	1.19	0.46	2.31	29.5	0.19	0.24	0.05	0.01	0.00
Site B-17	40–89	II+	16.0	2.04	1.09	9.67	27.4	0.23	0.48	0.12	0.02	0.01
	89–179	II	23.0	3.35	1.43	7.96	23.9	0.38	0.72	0.18	0.03	0.01
	179–249	I+	24.0	3.25	1.32	7.89	25.6	0.38	0.72	0.17	0.03	0.02
Kane Fan 6	22–51	IV	24.0	2.89	1.27	3.25	23.5	0.38	0.60	0.17	0.03	0.02
Site B-16	51–75	II+	25.0	4.20	1.63	7.55	23.1	0.49	0.84	0.18	0.03	0.01
	75–130	II	32.0	3.72	3.08	6.57	22.5	0.53	0.84	0.20	0.19	0.02
	130–255+	I	41.0	4.88	2.58	5.24	20.3	0.65	1.20	0.27	0.09	0.03
Kane Fan 7	14–25	II	47.0	4.10	1.63	2.32	18.0	0.36	0.84	0.22	0.05	0.03
Site B19	25–40	IV	20.0	2.63	1.19	4.15	24.2	0.26	0.48	0.13	0.07	0.01
	40–85	III	33.0	4.39	2.05	4.38	19.2	0.35	0.84	0.23	0.08	0.02
	85–137	II	42.0	5.14	2.56	5.01	16.2	0.49	1.08	0.27	0.11	0.02
	137–262	I	44.0	5.63	3.33	3.57	18.0	0.54	1.33	0.32	0.17	0.03

the crystalline unit and is a gypsum-rich sedimentary unit. These two units together constitute what is referred to as a gypsite profile. The underlying unit consists of finely crystalline gypsum dispersed throughout the clastic sediments. Gypsum prisms also occur within the matrix of the unit.

Gypcretes and gypsites have been described from Western Australia by Arakel and McConchie (1982) and the Northern Territory by Jacobson *et al.* (1988). The gypsites are morphologically diverse depending on whether they originate in the vadose or phreatic zones. Phreatic gypsite bodies are typically wedge or lensoid in shape. They consist of acicular and/or discoidal gypsum crystals with massive, tabular, or clotted micromorphologies. Vadose gypsites are typically massive in appearance and consist of loosely to tightly packed gypsum crystals, crystallites, or gypsic fragments. Grain sizes are variable and display a variety of micromorphological fabrics. Surface gypcretes are commonly thick and massive. They possess a variety of grain sizes and occasionally exhibit graded bedding. The gypcretes form benches adjacent to lake basins and occur as lenses in lake-bordering dunes. The gypcretes consist of weathered gypsum crystals that have undergone repeated solution and recrystallization (Jacobson *et al.* 1988).

CHEMISTRY

A comprehensive summary of the characteristics of the chemistry of gypcretes from Tunisia and the Namib Desert was provided by Watson (1983, 1985). These analyses reflect the considerable diversity of gypcrete chemistries which vary with the degree of induration. Typically, the African gypcretes contain small abundances of calcium carbonate but are enriched in sodium, potassium, and magnesium. Iron and aluminium occur in smaller abundances than the soluble salts and probably reflect the mineralogy of the insoluble residue.

Comprehensive chemical analyses of gypcretes from North America are presented by Reheis (1987). Typical analyses are presented in Table 5.7. The gypcretes are dominated by calcium which usually occurs in abundances of approximately 30%. Silicon is co-dominant in abundance with calcium and is indicative of the mineralogy of the insoluble residue. Magnesium is present in abundances of less than 10% and may be indicative of the presence of carbonates. As with the African gypcretes, iron and aluminium occur in substantially smaller abundances than the aforementioned elements. Like the silicon, these two elements are representative of the clay mineral fraction of the insoluble residue. Minor abundances of the other elements are present in the gypcretes. Sodium has been widely regarded as an important chemical constituent in gypcretes from Africa and linked to the role of ground water in its formation (Watson 1983). Chemical analyses of gypcretes from Wyoming, however, contain less than half a percent of sodium which may indicate minimal ground water effects.

Relatively little work has been undertaken on the

Table 5.8 Mineralogies of gypcrete from Wyoming (from Reheis 1987)

			Clay mineral percentage				
Location	*Depth (cm)*	*Stage*	*Gypsum*	*Kaolinite*	*Mica*	*Smectite*	*Palygorskite*
Kane Fan 4	28–75	II	31.4	21	23	42	7
Site B-16	75–135	II	43.8	35	20	33	6
	135–237	I+	29.6	34	17	37	6
Kane Fan 5	19–40	IV	70.3	9	25	13	9
Site B-17	40–89	II+	28.0	28	26	28	9
	89–179	II	37.2	21	30	30	10
	179–249	I+	27.2	10	37	27	10
Kane Fan 6	22–51	IV	58.8	24	22	39	15
Site B-18	51–75	II+	32.6	14	8	44	4
	75–130	II	14.1	23	23	33	8
	130–255	I	8.5	24	22	37	7
Kane Fan 7	14–25	II	20.2	19	16	50	11
Site B-19	25–40	IV	56.0	18	18	41	6
	40–85	III	41.3	17	13	28	5
	85–137	II	31.3	28	16	39	5
	137–262	I	18.1	24	19	42	6

mineralogy of gypcretes. Gypsum is the dominant mineral species. Analysis of about 150 samples from Tunisia and the Namib by Watson (1983) shows the mean abundance of this mineral to range from 61% in powdery gypcrete to greater than 77% in indurated surface crusts. Quartz is also an important constituent in the insoluble residue. Gypcretes from Wyoming (Reheis 1987) contain gypsum abundances of less than 10% in some stage I gypcretes to as much as 70% in stage IV materials (Table 5.8).

A variety of clay minerals is present in the insoluble residue, the most abundant one being the fibrous mineral palygorskite (Reheis 1987, Watson 1989). Other clay mineral species have been reported by Reheis (1987) from the insoluble residue of gypcretes from Wyoming, including kaolinite, smectite, and mica.

ORIGIN

A diversity of models has been presented in the literature for the origin of different forms of gypcrete. These models fall basically into either pedogenic or non-pedogenic categories. It has been proposed that pedogenic gypcretes may result from the vertical rise and subsequent evaporation of gypsum-laden soil waters. This model, however, has been extensively criticized by Keen (1936) and more recently by Watson (1979, 1983, 1985). Keen argued that the structure of most desert soils precluded the capillary rise of waters, and Watson stressed the problem of the great quantities of water necessary to precipitate even thin gypsum crusts.

Pedogenic gypcretes resulting from the downward movement of gypsum have been more widely embraced (Watson 1979, 1983, 1985), the source of gypsum being generally regarded as aeolian (Page 1972, Watson 1979). Recent studies of gypsic soils in the Middle East have stressed the importance of wind-derived gypsum (Dan *et al.* 1982, Amit and Gerson 1986). This gypsum is then translocated to shallow depths and deposited by evaporation. Where gypsum occurs deeper in the soil profile, wetter climatic regimes are implied. Reheis (1987) also ascribed the gypcretes in Wyoming to vertical translocation of aerosolically derived gypsum, the gypsum having been derived from nearby dunes and surrounding bedrock sources. Watson (1985) likewise recognized the significance of aeolian-derived gypsum as a source for surface and subsurface crusts in Tunisia and the Namib Desert. In Tunisia he considered the source to be deflation of seasonally flooded basins, while in the Namib he emphasized the importance of fog in carrying dissolved salts.

Non-pedogenic models of gypcrete formation are related to deposition of gypsum in ground water or lacustrine environments. Extensive gypsite and gypcretes have recently been discovered in a series of playa lakes in central Australia (Jacobson *et al.* 1988). The gypsite and gypcretes result from the complex interaction of phreatic and vadose ground waters

and infiltrating meteoric waters. Lacustrine gypcretes have also been found by Watson (1985) in the warm desert environments of Tunisia and the Nabib. Watson described bedded gypsum crusts, which he attributed to evaporation of shallow lakes, and subsurface desert rose gypsum crusts, which he ascribed to the evaporation of shallow ground water.

CONCLUSIONS

From the foregoing discussion a number of general conclusions can be reached.

(a) Calcretes, silcretes, and gypcretes are widely distributed throughout the warm desert environments of Australia, Africa, North America, and the Middle East.

(b) Each of the principal types of duricrust displays considerable variability with respect to morphology, micromorphology, chemistry, and mineralogy. This variability reflects the diversity of environments of duricrust formation.

(c) The formation of duricrusts is the result of diverse processes which may be fundamentally divided into pedogenic and non-pedogenic categories. Complex interactions between formative processes also commonly occur.

(d) While the nature and origin of duricrusts have received considerable attention in the literature, considerable gaps exist geographically.

(e) There is a need for more work on the nature and origin of duricrusts in general in the American south-west. In Australia considerable opportunity exists for future research on the nature and origin of gypcretes.

(f) In all warm desert environments there is great scope for the assessment of the genetic relationship between different duricrust types.

REFERENCES

Ali, Y.A. and I. West 1983. Relationships of modern gypsum nodules in sabkhas of loess to composition of brines and sediments in northern Egypt. *Journal of Sedimentary Petrology* **53**, 1151–68.

Ambrose, G.J. and R. Flint 1981. A regressive Miocene lake system and silicified strand lines in northern South Australia: implications for regional stratigraphy and silcrete genesis. *Journal of the Geological Society of Australia* **28**, 81–94.

Amit, R. and R. Gerson 1986. The evolution of Holocene reg (gravelly) soils in deserts – an example from the Dead Sea region. *Catena* **13**, 59–79.

Amundson, R.G., O. Chadwick, J. Sowers and H. Donner 1988. The relationship between modern climate and vegetation and the stable isotope chemistry of Mojave Desert soils. *Quaternary Research* **29**, 245–54.

Amundson, R.G., O. Chadwick, J. Sowers and H. Donner 1989. The stable isotope chemistry of pedogenic carbonate at Kyle Canyon, Nevada. *Soil Science Society of America Journal* **53**, 201–10.

Arakel, A.V. 1985. Vadose diagenesis and multiple calcrete soil profile development in Hutt Lagoon area, Western Australia. *Revue de Geologie Dynamique et de Geographie Physique* **26**, 243–54.

Arakel, A.V. 1986. Evolution of calcrete in palaeodranages of the Lake Napperby Area, central Australia. *Palaeogeography, Palaeoclimatology, Palaeoecology* **54**, 283–303.

Arakel, A.V. and D. McConchie 1982. Classification and genesis of calcrete and gypsite lithofacies in paleodrainage systems of inland Australia and their relationship to carnotite mineralization. *Journal of Sedimentary Petrology* **52**, 1149–70.

Aristarain, L.F. 1970. Chemical analysis of caliche profiles from High Plains, New Mexico. *Journal of Geology* **78**, 201–12.

Aristarain, L.F. 1971. On the definition of caliche deposits. *Zeitschrift für Geomorphologie* **15**, 274–89.

Bachman, G.O. and M.N. Machette 1977 Calcic soils and calcretes in the southwestern United States. *U.S. Geological Survey Open-File Report* 77-794.

Barnes, I. 1965. Geochemistry of Birch Creek, Inyo County, California, a travertine depositing creek in an arid environment. *Geochimica et Cosmochimica Acta* **29**, 85–112.

Blake, W.P. 1902. The caliche of southern Arizona: an example of deposition by vadose circulation. *Transactions of the American Institute of Mining and Metalurgical Engineers* **31**, 220–6.

Bowler, J.M. and H.A. Polak 1971. Radiocarbon analysis of soil carbonates: an evaluation from paleosols in southeastern Australia. In *Paleopedology – origin, nature, and dating of paleosols*, D. Yaalon (ed.), 97–108. Jerusalem: Israel University Press.

Bretz, J.H. and L. Horberg 1949. Caliche in southeastern New Mexico. *Journal of Geology* **57**, 491–511.

Brewer, R. and J.R. Sleeman 1964. Glaebules: their definition, classification and interpretation. *Journal of Soil Science* **15**, 66–78.

Brown, C.N. 1956. The origin of caliche in the northeastern Llano Estacado, Texas. *Journal of Geology* **64**, 1–15.

Butt, C.R.M. 1983. Aluminosilicate cementation of saprolites, grits and silcretes in Western Australia. *Journal of the Geological Society of Australia* **30**, 179–86.

Butt, C.R.M. 1985. Granite weathering and silcrete formation on the Yilgarn Block, Western Australia. *Australian Journal of Earth Sciences* **32**, 415–32.

Butt, C.R.M., R.C. Horwitz and A.W. Mann 1977. Uranium occurrences in calcretes and associated sediments in Western Australia. *CSIRO Mineral Research Laboratories Division of Mineralogy. Report* FP 16.

Carlisle, D. 1983. Concentration of uranium and vanadium in calcretes and gypcretes. In *Residual deposits: surface related weathering processes and materials*, R.C.L. Wilson (ed.) 185–95. Geological Society of London Special Publication 11.

Cerling, T.E. and R.L. Hay 1986. An isotopic study of paleosol carbonates from Olduvai Gorge. *Quaternary Research* **25**, 63–78.

Crawford, A.R. 1965. The geology of Yorke Peninsula. *Geological Survey of South Australia Bulletin* 39.

Crocker, R.L. 1946. Post-Miocene climatic and geologic history and its significance in relation to the genesis of the major soil types of South Australia. *CSIRO Bulletin* 193.

Dan, J. 1977. The distribution and origin of nari and other lime crusts in Israel. *Israel Journal of Earth Sciences* **26**, 68–83.

Dan, J., D.H. Yaalon, R. Moshe and S. Nissim 1982. Evolution of reg soils in southern Israel and Sinai. *Geoderma* **28**, 173–202.

Dixon, J.C. 1978. Morphology and genesis of calcrete in South Australia with special reference to the southern Murray Basin and Yorke Peninsula. M.A. thesis. University of Adelaide, South Australia.

Drees, L.R. and L.P. Wilding 1987. Micromorphic record and interpretation of carbonate forms in the Rolling Plains of Texas. *Geoderma* **40**, 157–76.

Durand, G.H. 1949. Essai de nomenclature des croutes. *Bulletin Societe des Sciences Nautrelles de Tunisie* **3/4**, 141–2.

Durand, J.H. 1963. Les croutes calcaires et gypseuses en Algerie: formation et age. *Bulletin Societe Geologique de France, Series 7* **6**, 959–68.

Dury, G.H. 1966. Duricrusted residuals on the Barrier and Cobar pediplains of New South Wales. *Journal of the Geological Society of Australia* **13**, 299–307.

Firman, J.B. 1963. Quaternary geological events near Swan Reach in the Murray Basin, South Australia. *Quarterly Notes of the Geological Survey of South Australia* **5**, 2–4.

Firman, J.B. 1966. Stratigraphy of the Chowilla area in the Murray Basin. *Quarterly Notes of the Geological Survey of South Australia* **20**, 3–7.

Frankel, J.J. and L.E. Kent 1938. Grahamstown surface quartzites (silcretes). *Transactions of the Geological Society of South Africa* **15**, 1–42.

Frye, J.C., H.D. Glass, A.B. Leonard and D. Coleman 1974. Caliche and clay mineral zonation of the Ogallala Formation, central-eastern New Mexico. *New Mexico Bureau of Mines and Mineral Resources Circular* 144.

Gardner, L.R. 1972. Origin of the Mormon Mesa caliche, Clark County, Nevada. *Bulletin of the Geological Society of America* **83**, 143–56.

Gile, L.H. 1967. Soils of an ancient basin floor near Las Cruces. *Soil Science* **103**, 264–76.

Gile, L.H., F.F. Peterson and R.B. Grossman 1965. The K horizon – a master soil horizon of carbonate accumulation. *Soil Science* **99**, 74–82.

Gile, L.H., F.F. Peterson and R.B. Grossman 1966. Morphological and genetic sequences of carbonate accumulation in desert soils. *Soil Science* **101**, 347–60.

Gill, E.D. 1975. Calcrete hardpans and rhizomorphs in western Victoria, Australia. *Pacific Geology* **9**, 1–16.

Goudie, A. 1972. The chemistry of world calcretes. *Journal of Geology* **80**, 449–63.

Goudie, A. 1973. *Duricrusts in tropical and subtropical landscapes*. Oxford: Clarendon Press.

Goudie, A. 1983. Calcrete. In *Chemical sediments and geomorphology: precipitates and residua in the near surface environment*, A.S. Goudie and K. Pye (eds) 93–131. New York: Academic Press.

Gunn, R.H. and R.W. Galloway 1978. Silcretes in south-central Queensland. In *Silcrete in Australia*, T. Langford-Smith (ed.), 51–71. Armidale: Department of Geography, University of New England.

Gustavson, T.C. and D.A. Winkler 1988. Depositional facies of the Miocene–Pliocene Ogallala Formation, northwestern Texas and eastern New Mexico. *Geology* **16**, 203–6.

Hay, R.L. and R.J. Reeder 1978. Calcretes of Olduvai Gorge and the Ndolanya Beds of northern Tanzania. *Sedimentology* **25**, 649–73.

Hay, R.L. and B. Wiggins 1980. Pellets, ooids, sepiolite and silica in three calcretes of the southwest United States. *Sedimentology* **27**, 559–76.

Holliday, V.T. 1989. The Blackwater Draw Formation (Quaternary): a 1.4-plus-m.y. record of eolian sedimentation and soil formation on the southern High Plains. *Bulletin of the Geological Society of America* **101**, 1598–607.

Horta, O.S. 1980. Calcrete, gypcrete, and soil classification in Algeria. *Engineering Geology* **15**, 15–52.

Hunt, C.B. and D.R. Mabey 1966. Stratigraphy and structure, Death Valley, California. *U.S. Geological Survey Professional Paper* 494A.

Hutton, J.T. and J.C. Dixon, 1981. The chemistry and mineralogy of some South Australian calcretes and associated soft carbonates and their dolomitization. *Journal of the Geological Society of Australia* **28**, 71–9.

Hutton, J.T., C.R. Twidale, A.R. Milnes and H. Rosser 1972. Composition and genesis of silcretes and silcrete skins from the Beda Valley, southern Arcoona Plateau, South Australia. *Journal of the Geological Society of Australia* **19**, 31–9.

Hutton, J.T., D.S. Lindsay and C.R. Twidale. 1977. The weathering of norite at Black Hill. *Journal of the Geological Society of Australia* **24**, 37–50.

Hutton, J.T., C.R. Twidale and A.R. Milnes 1978. Characteristics and origins of some Australian silcretes. In *Silcrete in Australia*, T. Langford-Smith (ed.), 19–40. Armidale: Department of Geography, University of New England.

Jacobson, G., A.V. Arakel and C. Yijian 1988. The central Australian groundwater discharge zone: evolution of associated calcrete and gypcrete deposits. *Australian Journal of Earth Sciences* **35**, 549–65.

James, N.P. 1972. Holocene and Pleistocene calcareous crust (caliche) profiles: criteria for subaerial exposure. *Journal of Sedimentary Petrology* **42**, 817–36.

Johns, R.K. 1963. Limestone, dolomite, and magnesite resources of South Australia. *Geological Survey of South Australia Bulletin* 38.

Keen, B.A. 1936. The circulation of water in the soil between the surface and the level of underground water. *Bulletin of the International Association of Scientific Hydrology* **22**, 328–31.

Klappa, C.F. 1978. Biolithogenesis of microcodium. *Sedimentology* **25**, 489–522.

Klappa, C.F. 1979a. Lichen stromatolites: criterion for subaerial exposure and a mechanism for the formation of laminar calcretes (caliche). *Journal of Sedimentary Petrology* **49**, 387–400.

Klappa, C.F. 1979b. Calcified filaments in Quaternary calcretes: organo-mineral interactions in the subaerial

vadose environment. *Journal of Sedimentary Petrology* **49**, 955–68.

Knox, G.J. 1977. Caliche profile formation, Saldanha Bay (South Africa). *Sedimentology* **24**, 657–74.

Lamplugh, G.H. 1907. The geology of the Zambezi Basin around the Batoka Gorge (Rhodesia). *Quarterly Journal of the Geological Society of London* **63**, 162–216.

Lamplugh, G.W. 1902. 'Calcrete'. *Geological Magazine* **9**, 575.

Langford-Smith, T. 1978. *Silcrete in Australia*. Armidale: Department of Geography, University of New England.

Langford-Smith, T. and G.H. Dury 1965. Distribution, character and attitude of the duricrust in the northwest of New South Wales and adjacent areas of Queensland. *American Journal of Science* **263**, 170–90.

Langford-Smith, T. and S.H. Watts 1978. The significance of co-existing siliceous and ferruginous weathering products at selected Australian localities. In *Silcrete in Australia*, T. Langford-Smith (ed.), 143–65. Armidale: Department of Geography, University of New England.

Machette, M.N. 1985. Calcic soils of the southwestern United States. In *Soils and Quaternary geology of the southwestern United States*, D. Weide (ed.) 1–21. Geological Society of America Special Paper 203.

Mann, A.W. and R.C. Horwitz 1979. Groundwater calcretes in Australia: some observations from Western Australia. *Journal of the Geological Society of Australia* **26**, 293–303.

Martin, H. 1963. A suggested theory for the origin and a brief description of some gypsum deposits of South West Africa. *Transactions of the Geological Society of South Africa* **55**, 345–50.

McFadden, L.D. 1982. The impacts of temporal and spatial climatic changes on alluvial soil genesis in southern California. Ph.D. thesis. University of Arizona, Tucson.

McFadden, L.D. and J.C. Tinsley 1983. Rate and depth of pedogenic–carbonate accumulation in soils: formulation and testing of a compartment model. In *Soils and Quaternary geology of the southwestern United States*, D. Weide (ed.), 23–41. Geological Society of America Special Paper 203.

Milnes, A.R. and J.T. Hutton 1974. The nature of microcryptocrystalline titania in 'silcrete' skins from the Beda Hill area of South Australia. *Search* **5**, 153–4.

Milnes, A.R. and J.T. Hutton 1983. Calcretes in Australia. In *Soils: an Australian viewpoint*, 119–62. Melbourne: CSIRO/London: Academic Press.

Milnes, A.R. and C.R. Twidale 1983. An overview of silicification in Cainozoic landscapes of arid central and southern Australia. *Australian Journal of Soil Research* **21**, 387–410.

Milnes, A.R., R.W. Kimber and S.E. Phillips 1987. Studies in eolian calcareous landscapes of southern Australia. In *Aspects of loess research*, L. Tungsheng (ed.), 130–9. Beijing: China Ocean Press.

Milnes, A.R., M. Thiry and M.J. Wright 1991. Silica accumulations in saprolite and soils in South Australia. In *Occurrence, characteristics, and genesis of carbonate, gypsum and silica accumulation in soils*, W.D. Nettleton (ed.), 121–49. Soil Science Society of America, Special Publication 26.

Netterberg, F. 1969. Ages of calcretes in southern Africa. *South African Archeological Bulletin* **24**, 117–22.

Netterberg, F. and J.H. Caiger 1983. A geotechnical classification of calcretes and other pedocretes. In *Residual deposits: surface and related weathering processes and materials*, R.C.L. Wilson (ed.), 235–43, Geological Society of London Special Publication 11.

Nettleton, W.D., R.E. Nelson, B.R. Brasher and P.S. Derr. 1982. Gypsiferous soils of the western United States. In *Acid sulphate weathering*, J.A. Kittrick, D.S. Fanning and L.R. Hossner (eds), 147–68. Soil Science Society of America Special Publication 10.

Ollier, C.D. 1978. Silcrete and weathering. In *Silcrete in Australia*, T. Langford-Smith (ed.), 13–17. Armidale: Department of Geography, University of New England.

Page, W.D. 1972. The geological setting of the archeological site at Oued al Akarit and the paleoenvironmental significance of gypsum soils, southern Tunisia. Ph.D. thesis. University of Colorado, Boulder.

Patil, D.N. 1991. Basalt weathering and related chemical sediments and residuals from the Deccan volcanic province, Maharashtra, India. *Tropical Geomorphology Newsletter* **11**, 1–3.

Phillips, S.E. and A.R. Milnes 1988. The Pleistocene terrestrial carbonate mantle on the southeastern margin of the St Vincent Basin, South Australia. *Australian Journal of Earth Sciences* **35**, 463–81.

Phillips, S.E. and P.G. Self 1987. Morphology, crystallography and origin of needle-fibre calcite in Quaternary pedogenic calcretes of South Australia. *Australian Journal of Soil Research* **25**, 429–44.

Phillips, S.E., A.R. Milnes and R.C. Foster 1987. Calcified filaments: an example of biological influences in the formation of calcrete in South Australia. *Australian Journal of Soil Research* **25**, 405–28.

Price, W.A. 1933. The Reynosa problem of south Texas and the origin of caliche. *Bulletin of the Association of Petroleum Geologists* **17**, 488–522.

Rabenhorst, M.C., L.P. Wilding and C.L. Girdner 1984. Airborn dust in the Edwards Plateau region of Texas. *Soil Science Society of America Journal* **48**, 621–7.

Reeves, C.C. 1970. Origin, classification, and geological history of caliche on the southern High Plains, Texas and eastern New Mexico. *Journal of Geology* **78**, 352–62.

Reeves, C.C. 1976. *Caliche: origin, classification, morphology and uses*. Lubbock: Estacado Books.

Reeves, C.C. and J.D. Suggs 1964. Caliche of central, and southern Llano Estacado, Texas. *Journal of Sedimentary Petrology* **34**, 669–72.

Reheis, M.C. 1987. Gypsic soils on the Kane alluvial fans, Big Horn County, Wyoming. *U.S. Geological Survey Bulletin* 1590C.

Reider, R.G., N.J. Kuniansky, D.M. Stiller and P.J. Uhl 1974. Preliminary investigation of comparative soil development on Pleistocene and Holocene geomorphic surfaces of the Laramie Basin, Wyoming. In *Applied Geology and Archeology: The Holocene History of Wyoming*, M. Wilson (ed.), 27–33. Geological Survey of Wyoming Report of Investigations 10.

Ruhe, R.V. 1967. Geomorphic surfaces and surficial deposits in southern New Mexico. *New Mexico Bureau of Mines and Mineral Resources Memoir* 18.

Salomons, W., A. Goudie and W.G. Mook 1978. Isotopic

composition of calcrete deposits from Europe, Africa, and India. *Earth Surface Processes* **3**, 43–57.

Schlesinger, W.H. 1985. The formation of caliche in soils of the Mojave Desert, California. *Geochimica et Cosmochimica Acta* **49**, 57–66.

Scholz, H. 1972. The soils of the central Namib Desert with special consideration of the soils in the vicinity of Gobabeb. *Madoqua* **2**, 33–51.

Sehgal, J.L. and G. Stoops 1972. Pedogenic calcite accumulations in arid and semi-arid regions of the Indo-Gangetic alluvial plain of erstwhile Punjab. *Geoderma* **8**, 59–72.

Semeniuk, V. and T.D. Meagher 1981. Calcrete in Quaternary coastal dunes in southwestern Australia: a capillary-rise phenomenon associated with plants. *Journal of Sedimentary Petrology* **51**, 47–68.

Semeniuk, V. and D.J. Searle 1985. Distribution of calcrete in Holocene coastal sands in relationship to climate, southwestern Australia. *Journal of Sedimentary Petrology* **55**, 86–95.

Senior, B.R. 1978. Silcrete and chemically weathered sediments in southwest Queensland. In *Silcrete in Australia*, T. Langford-Smith (ed.), 41–50. Armidale: Department of Geography, University of New England.

Shafetz, H.S. and J.C. Butler 1980. Petrology of recent caliche pisolites, spherules and speleothems deposits from central Texas. *Sedimentology* **27**, 497–518.

Sidwell, R. 1943. Caliche deposits of the southern High Plains, Texas. *American Journal of Science* **241**, 257–61.

Smale, D. 1973. Silcretes and associated silica diagenesis in southern Africa and Australia. *Journal of Sedimentary Petrology* **43**, 1077–89.

Stephens, C.G. 1964. Silcretes of central Australia. *Nature* **203**, 1407.

Stephens, C.G. 1971. Laterite and silcrete in Australia: a study of the genetic relationships of laterite and silcrete and their companion materials, and their collective significance in the weathered mantle, soils, relief, and drainage of the Australian continent. *Geoderma* **5**, 5–52.

Summerfield, M.A. 1982. Distribution, nature and probable genesis of silcrete in arid and semi-arid southern Africa. *Catena Supplement* **1**, 37–65

Summerfield, M.A. 1983a. Silcrete. In *Chemical sediments and geomorphology: precipitates and residua in the near surface environment*, A.S. Goudie and K. Pye (eds), 59–91. New York: Academic Press.

Summerfield, M.A. 1983b. Petrology and diagenesis of silcrete from the Kalahari Basin and Cape coastal zone, southern Africa. *Journal of Sedimentary Petrology* **53**, 895–909.

Summerfield, M.A. 1983c. Geochemistry of weathering profile silcretes, southern Cape Province, South Africa. In *Residual deposits: surface and related weathering processes and materials*, R.C.L. Wilson (ed.), 167–78. Geological Society of London Special Publication 11.

Swineford, A. and P.C. Franks 1959. Opal in the Ogalalla Formation in Kansas. *Society of Economic Paleontologists and Mineralogists Special Publication 7*.

Taylor, G. 1978. Silcretes in the Walgett-Cumborah Region of New South Wales. In *Silcrete in Australia*, T. Langford-Smith (ed.), 187–93. Armidale: Department of Geography, University of New England.

Taylor, G. and I.E. Smith 1975. The genesis of sub-basaltic silcretes from the Monaro, New South Wales. *Journal of the Geological Society of Australia* **22**, 377–85.

Thiry, M. and A.R. Milnes 1991. Pedogenic and groundwater silcretes at Sturt Creek opal field, South Australia. *Journal of Sedimentary Petrology* **61**, 111–27.

Tucker, M.E. 1978. Gypsum crusts (gypcrete) and patterned ground from northern Iraq. *Zeitschrift für Geomorphologie* **22**, 89–100.

Twidale, C.R., J.A. Shepard and R.M. Thompson 1970. Geomorphology of the southern part of the Arcoona Plateau and the Tent Hill Region, west and north of Port Augusta, South Australia. *Transactions of the Royal Society of South Australia* **94**, 55–69.

Van den Heuvel, R.C. 1966. The occurrence of sepiolite and attapulgite in the calcareous zone of a soil near Las Cruces, New Mexico. *Clays and Clay Minerals* **25**, 193–207.

van Dijk, D.C. and G.G. Beckman 1978. The Yuleba hardpan and its relationship to soil geomorphic history in the Yuleba-Tora region, southeast Queensland. In *Silcrete in Australia*, T. Langford-Smith (ed.), 73–92. Armidale: Department of Geography, University of New England.

Ward, W.T. 1965. Eustatic and climatic history of the Adelaide area, South Australia. *Journal of Geology* **73**, 592–602.

Ward, W.T. 1966. Geology, geomorphology and soils of the southwestern part of County Adelaide. *CSIRO Soil Publication* 23.

Warren, J.K. 1982. The hydrological setting, occurrence, and significance of gypsum in late Qaternary salt lakes in South Australia. *Sedimentology* **29**, 609–37.

Warren, J.K. 1983. Pedogenic calcrete as it occurs in Quaternary calcareous dunes in coastal South Australia. *Journal of Sedimentary Petrology* **53**, 787–96.

Watson, A. 1979. Gypsum crusts in deserts. *Journal of Arid Environments* **2**, 3–20.

Watson, A. 1983. Gypsum crusts. In *Chemical sediments and geomorphology: precipitates and residua in the near surface environment*. A.S. Goudie and K. Pye (eds), 133–6. New York: Academic Press.

Watson, A. 1985. Structure, chemistry and origins of gypsum crusts in southern Tunisia and the central Namib Desert. *Sedimentology* **32**, 855–75.

Watson, A. 1988. Desert gypsum crusts as palaeoenvironmental indicators: a micropetrographic study of crusts from southern Tunisia and the central Namib desert. *Journal of Arid Environments* **15**, 19–42.

Watson, A. 1989. Desert crusts and varnishes. In *Arid zone geomorphology*, D.S.G. Thomas (ed.), 25–55. New York: Hallstead Press.

Watts, N.L. 1978. Displacive calcite: evidence from recent and ancient calcretes. *Geology* **6**, 699–703.

Watts, N.L. 1980. Quaternary pedogenic calcretes from the Kalahari (southern Africa): mineralogy, genesis and diagenesis. *Sedimentology* 27, 661–86.

Watts, S.H. 1977. Major element geochemistry of silcrete from a portion of inland Australia. *Geochimica et Cosmochimica Acta* **41**, 1164–7.

Watts, S.H. 1978a. A petrographic study of silcrete from inland Australia. *Journal of Sedimentary Petrology* **48**, 987–94.

Watts, S.H. 1978b. The nature and occurrence of silcrete in the Tibooburra area of northwestern New South Wales. In *Silcrete in Australia*, T. Langford-Smith (ed.), 167–85. Armidale: Department of Geography, University of New England.

Weatherby, K.G. and J.M. Oades 1975. Classification of carbonate layers in highland soils of the northern Murray Valley, South Australia and their use in stratigraphic and land-use studies. *Australian Journal of Soil Research* **13**, 119–32.

West, L.T., L.R. Drees, L.P. Wilding and M.C. Rabenhorst 1988. Differentiation of pedogenic and lithogenic carbonate forms in Texas. *Geoderma* **43**, 271–87.

Whitehouse, F.W. 1940. *Studies in the late geological history of Queensland*. University of Queensland Papers in Geology 1.

Wieder, M. and D. Yaalon 1974. Effects of matrix composition on carbonate nodule crystallization. *Geoderma* **11**, 95–121.

Wigley, T.M.L. 1973. Chemical evolution of the system calcite–gypsum–water. *Canadian Journal of Earth Sciences* **10**, 306–15.

Wilding, L.P., N.E. Smeck and L.R. Drees 1977. Silica in soils: quartz, cristobalite, tridymite, and opal. In *Minerals in soil environments*, J.B. Dixon and S.B. Weed (eds), 471–522. Madison: Soil Science Society of America.

Williams, G.E. and H.A. Polach 1969. The evaluation of C-14 ages for soil carbonate from the arid zone. *Earth and Planetary Science Letters* **7**, 240–2.

Williams, G.E. and H.A. Polach 1971. Radiocarbon dating of arid zone calcareous paleosols. *Bulletin of the Geological Society of America* **82**, 3069–86.

Woolnough, W.G. 1927. The duricrust of Australia. *Journal and Proceedings of the Royal Society of New South Wales* **61**, 24–53.

Woolnough, W.G. 1930. Influence of climate and topography in the formation and distribution of products of weathering. *Geological Magazine* **67**, 123–32.

Wopfner, H. 1978. Silcretes of northern South Australia and adjacent regions. In *Silcrete in Australia*, T. Langford-Smith (ed.), 93–141. Armidale: Department of Geography, University of New England.

Wopfner, H. 1983. Environment of silcrete formation: A comparison of examples from Australia and the Cologne Embayment, West Germany. In *Residual deposits: surface and related weathering processes and materials*, R.C.L. Wilson (ed.), 151–8. Geological Society of London Special Publication 11.

Wopfner, H. and C.R. Twidale 1967. Geomorphological history of the Lake Eyre Basin. In *Landform studies from Australia and New Guinea*, J.N. Jennings and J.A. Mabbutt (eds), 118–43. Canberra: A.N.U. Press.

Yaalon, D.H. 1981. Pedogenic carbonate in aridic soils: magnitude of the pool and annual fluxes. *Abstract, International Conference on Aridic Soils, Jerusalem.*

ROCK VARNISH IN DESERTS

6

Theodore M. Oberlander

INTRODUCTION

Dark surficial coatings on rocks in diverse environments have been an object of scientific curiosity since their first description by Alexander von Humboldt (1819). These surface films are most conspicuous in arid regions (e.g. Laudermilk 1931), where exposed rock outcrops and rubble deposits are ubiquitous and frequently are covered by glossy, brown to black, iron- and/or manganese-rich patinas, giving rise to the term desert varnish. Beyond the arid realm, non-riverine chemical films on rocks are dull and black in colour and attracted little attention, being presumed to be vaguely 'organic'. In seasonally flooded tropical riverine environments, vitreous silica-rich films of brown to purple-black colour are sometimes present on exposed bedrock potholes (Tricart 1972) and point bar cobbles, which may be cemented together to form a resistant carapace. Although the origin of non-riverine chemical films remained an enigma for a century and a half following Humboldt's description, relative degrees of rock surface darkening, or patination, have long been utilized as an age indicator in the fields of archaeology and geomorphology (e.g. Goodwin 1960, Hunt and Mabey 1966, and Fig. 6.1).

The long period of pure conjecture regarding the exact nature and origin of chemical coatings on rock surfaces came to an end with the application of modern analytical tools such as the scanning electron microscope and the electron microprobe, both of which permit precise chemical characterization of natural varnish films from point to point on the micrometre scale. The pioneering work was done by Engle and Sharp (1958), who used spectrographic analysis of varnish scrapings to reveal the vast enhancement in varnish films of Mn and other elements relative to local rock, soil, or airborne dust. Hooke *et al.* (1969) produced the first varnish chemical transects by electron microprobe analyses; Baumann (1976) pointed out the chemical similarities between desert varnish and marine ferromanganese nodules; Potter and Rossman (1977) demonstrated the high clay content of varnish films, and, along with Allen (1978), established that varnish constituents are derived from sources external to the subjacent rock. Perry and Adams (1978) revealed that varnish films contain sequences of Mn-rich and Mn-poor laminations. Dorn and Oberlander (1981b, 1982) analysed dark coatings from a variety of arid and humid settings and concluded that Mn-rich films in highly dissimilar environments were closely related in chemical composition and mineralogy and originated similarly as microbial products. Thus they suggested the general term rock varnish and viewed desert varnish as the most familiar type of rock varnish. Although the following discussion is concerned with desert varnish, for simplicity the more general term rock varnish will be used throughout the remainder of the chapter.

With several specialists now focusing their attention on rock varnish research, new findings and new hypotheses are appearing at such a pace that any current synopsis can only be a snapshot of a rapidly changing scene. The following presents the state of rock varnish research as we move into the last decade of the 20th century.

VARNISH CHARACTERISTICS

Rock varnish varies widely in chemical and physical characteristics; indeed many generalizations put forward in the pioneering studies cited above were based on limited sampling and have been disproved by later work. It is not difficult to find rock surface phenomena that resemble thick black, brown, or red rock varnish but are concentrations of substrate substances under a surficial varnish of the same colour. This should be suspected whenever macroscopic inspection seems to reveal an exceptionally thick varnish – that is, >0.4 mm (400 μm). Most rock

Geomorphology of Desert Environments. Edited by Athol D. Abrahams and Anthony J. Parsons. Published in 1994 by Chapman & Hall, London ISBN 978-94-015-8256-8

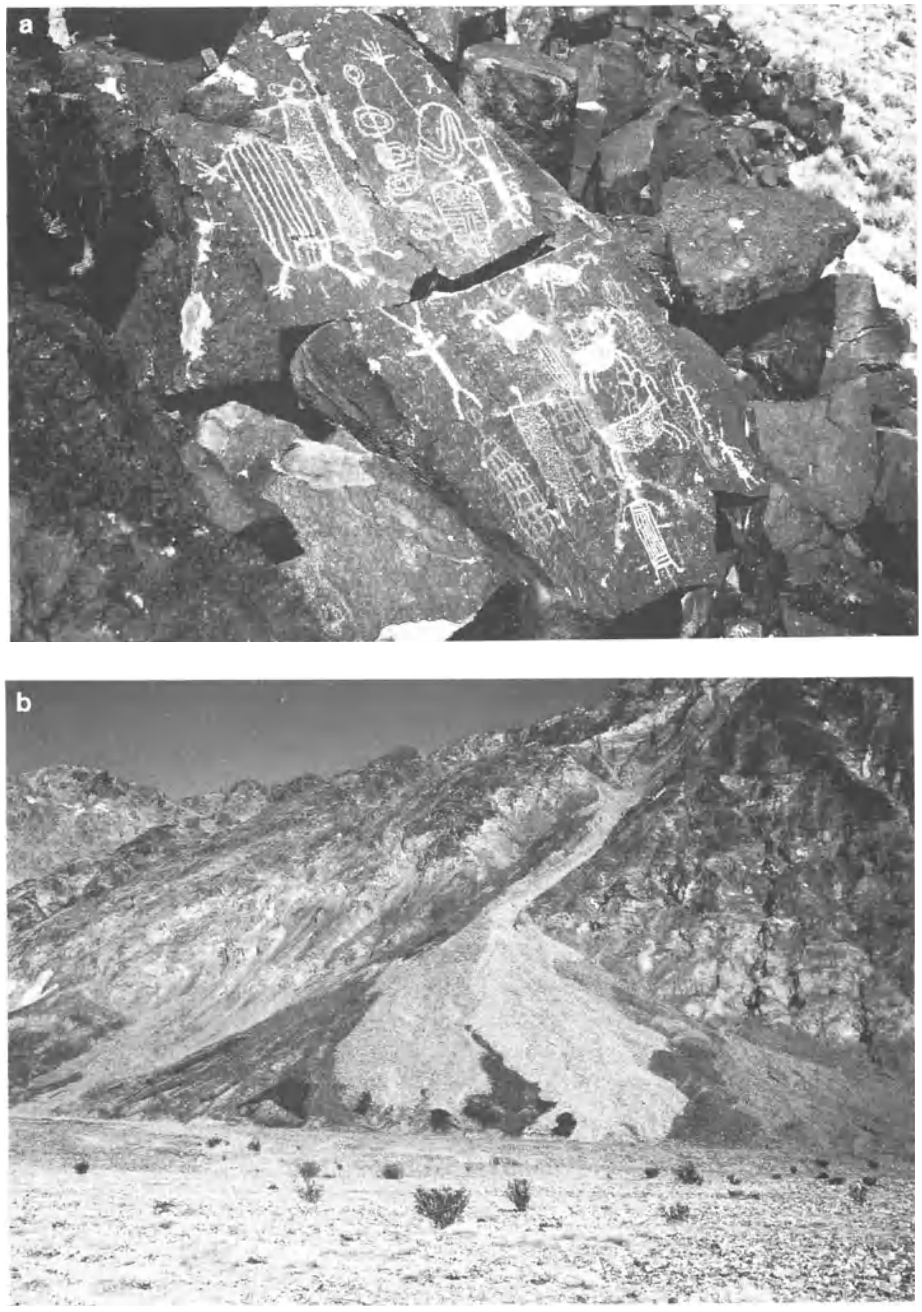

Figure 6.1 (a) Petroglyphs inscribed in desert varnish in the Coso area, eastern California. Revarnishing of older petroglyphs suggests that this rock art spans thousands of years. (b) Debris cone in Death Valley, California, with individual debris slides distinguished by degree of coloration by desert varnish.

varnish films are less than 300 μm in depth. Whereas rock varnish having a high Si content can barely be scratched with a tungsten–carbide needle, some similar appearing clay- and Fe-rich varnish can be skimmed off rock surfaces like butter, and on very smooth surfaces may even be removed by the friction of a fingertip. Rarity of well-developed rock varnish on Holocene surfaces and artifacts suggests that in most desert environments the formation of continuous black varnish coatings requires at least 10 000 years. Varnish forms much more rapidly in humid regions and in arid locales where channelled flows of water periodically stream over rock surfaces. A frequently cited report of rock varnish formation in some 25 years (Engle and Sharp 1958) is demonstrably erroneous (Dorn and Oberlander 1982, Elvidge 1982).

Rock varnish has been observed on every lithology, including limestone and marble in humid environments, but is best developed on durable silicate rocks. Many recent investigators have demonstrated that varnish films contain elements not present in the varnish substrate and clearly have not been derived from weathering of substrate material. This is especially obvious in the case of Mn- and Fe-rich varnish films on natural clasts and lithic artifacts composed of pure silica. Either the varnish-forming process, varnish clay minerals, or the major elements incorporated in varnish scavenge a host of elements present in the environment, which are transported to rock surfaces as dust or in solution in water. The major elements detectable in most rock varnish, in addition to Si, Al, Mn, and Fe, are Ca, K, Na, Ba, Ti, Sr, and Cu. Minor elements, locally assuming major significance, include Pb, V, P, Sr, Co, Ni, Cd, Zn, La, Y, B, and Zr. A host of additional elements also appears in trace amounts, suggesting that rock varnish could be useful as a geochemical prospecting tool (Lakin *et al.* 1963, Potter 1979).

The major determinants of rock varnish physical characteristics are the relative contents of clay minerals (commonly 60 to 80%) and hydrous non-crystalline oxides of Mn, Fe, and Si, each of which can attain values of 50% or more. Potter (1979) found that clays and oxides are intimately mixed, with the clays adsorbing oxides and the oxides cementing the clay minerals together. Clays are principally mixed layer illite–montmorillonite, but Potter also found some varnish specimens to be dominated by kaolinite. Varnish colour indicates the balance between the oxides of Mn (purple-black: possibly birnessite) and Fe (orange: haematite), with many varnish specimens containing equivalent amounts of the two, imparting a dusky-brown hue. Clasts composing desert pavements generally have a dusky-brown to black, Mn- and Fe-rich dorsal surface, and an orange, Fe-rich ventral surface in contact with a vesicular silty substrate. The Fe-rich bottom coat also seems to develop on the undersides of clast-supported rubble deposits that presently lack any fine matrix. Mineralogically, the bottom coat is distinctive only by the absence of Mn. Where clasts are partially embedded in fines, an Mn-rich, 'ground-band', 1 to 4 cm wide, that is darker and glossier than dorsal varnish, separates the dorsal and ventral varnishes (Fig. 6.2). Bauman (1976) noted that marine ferromanganese nodules have a similar ground-band. Resurfacing of orange, Fe-rich ventral varnish by dark, Mn-dominated dorsal varnish is often visible where surface clasts have been overturned by some agency.

Figure 6.2 Clast on alluvial fan in Death Valley, overturned to expose the darker Mn-rich band that forms at the ground-line, with orange Fe-rich ventral varnish below and dark grey Mn- and Fe-rich varnish above. Pen to the left for scale.

Black, Mn-rich rock varnish expands by growing outward from initial scattered points that are usually microdepressions favouring moisture retention after rainfall or dew formation. Thus Mn-rich varnish appears to expand from points of colonization in the manner of lichens, suggesting a biotic origin (Blackwelder 1954), and appears to be associated with water concentration. Fe-rich ventral varnish, on the other hand, appears to accrete and darken uniformly regardless of rock surface microtopography, suggesting a non-biotic physico-chemical origin.

The dorsal and ventral sides of pavement clasts have quite different chemical environments. The dorsal side, darkened by Mn-rich varnish, is flushed periodically by rainfall and dew drainage, while the ventral side, coloured orange by haematite, is usual-

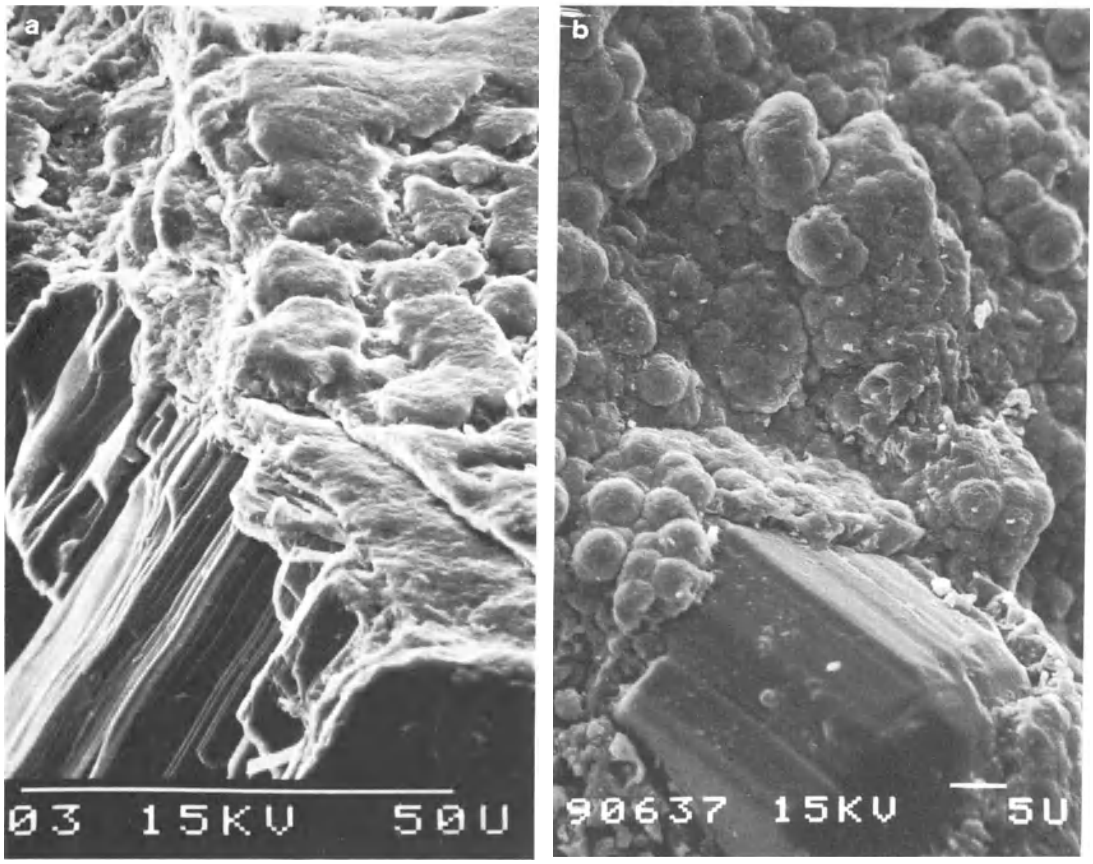

Figure 6.3 (a) Scanning electron microscopy image of shiny brown Mn- and Fe-rich lamellate varnish typical of hyperarid locations, superimposed over mineral crystal, from Death Valley debris cone in Figure 6.1b (50-μm scale bar shown). (b) Scanning electron microscopy image of Mn-rich dull black botryoidal varnish typical of semi-arid to subhumid locations, from west Texas (5-μm scale bar). Images by R. I. Dorn.

ly in contact with alkaline soil. Rock varnish in non-desert settings resembles the black dorsal patinas in most deserts, with a low content of clay and aeolian detritus and a high content of Mn. Varnish formed in regions that are hyperarid – essentially rainless on a timescale of years – resembles that of clast ventral surfaces in the more mesic deserts, being Fe-rich and reddish in colour, with high clay and detrital components of aeolian origin (Oberlander 1982, Jones 1991).

Varnish sheen reflects the micromorphology of varnish surfaces on the micrometre scale together with the content of Mn and Si (Fig. 6.3). Shiny black varnishes – the classic type that has long attracted attention – are Mn-rich, with a platy or a smoothly lamellate morphology as viewed under high magnification (>500×). Dull black varnish has a low content of clay and Fe, is Mn-rich, and has a surface morphology composed of spherical botryoids having diameters of 2 to 10 μm. Such varnish is seen in non-desert settings where rocks are periodically wetted and dried, as in alpine vernal pools, river point bars, and saltwater intertidal environments, including the Giant's Causeway in Ulster, Ireland (Fig. 6.4), and Scottish lochs, in which ferromanganese nodules are also present (Calvert and Price 1970).

Some Fe-rich rock varnish contains high amounts of Si or is encased by a glassy Si glaze. This varnish variant seems to have been overlooked by archaeologists, and it is possible that certain examples of the 'sickle-sheen' or 'phytolith polish' on microlithic artifacts, regarded as a product of human harvesting of phytolith-rich grass, are actually a natural Si glaze. On the eastern pediment of the Cargo Muchacho Mountains of southern California, hard Si glazes cover countless spherical pebbles that clearly are not artifacts. Scanning electron micros-

Figure 6.4 Black, Mn-rich rock varnish on columnar basalt in saltwater spray zone, Giant's Causeway, Ulster, Ireland. Black varnish also forms where column tops are concave and hold intermittent pools of rainwater.

Figure 6.5 Rock varnish degrading and accreting simultaneously on weathered and fresh sandstone faces, near Moab, Utah. The role of water in conveying Mn is evident in varnish streaking on the new rock face exposed by collapse.

copy views of some examples of 'use-polished' surfaces (Kamminga 1979) resemble lamellate-over-botryoidal accretionary varnish morphologies rather than abraded surfaces.

Within most deserts there is a vast range in varnish morphologies and chemical compositions. As varnish constituents arrive on rock surfaces either in dissolved form or as airborne dust, surface orientation is a partial control of varnish type. High-Mn varnish forms on steep rock faces where dust is not trapped, but where streaming water is present on occasion. Fe-rich varnishes, usually having high contents of clay and silt to fine sand detritus, form in dust-trapping microenvironments such as small pits, vesicles, and rock fissures in areas having large dust fluxes including alkaline substances such as salt and gypsum. Depressions ranging in size from large lava vesicles to microscopic roughness elements collect both water and dust, but generally are points of higher than average Mn concentration. This seems true even in hyperarid alkaline environments where varnish films are conspicuously Fe-dominated. Clearly, periodic wetting or moisture retention favours Mn accumulation on rock surfaces, even where alkaline dust also accumulates.

ELEMENT-CONCENTRATING MECHANISM

Throughout the long preliminary phase of varnish investigation, the popular view, still cited in recent years, was that varnish elements were 'sweated out' of rocks being weathered in dry, high-temperature environments. The earliest SEM and microprobe analyses disproved this by demonstrating a lack of continuity or interpenetration between weathered rock surfaces and varnish films (Potter and Rossman 1977). Both chemically and morphologically, basal varnish layers are conspicuously separate from and superimposed upon unweathered crystals of rock substrates along sharp interfaces (Fig. 6.3). Clearly, varnish elements are transported to rock surfaces from exterior sources either as particulate matter or in solution, as is apparent in Figure 6.5.

However, the 40 to 60 times enhancement of Mn in rock varnish as compared with average ambient levels of this element (Engle and Sharp 1958) suggests a preferential concentrating factor for Mn. Many researchers have attempted to explain the striking increase in Mn relative to Fe and other varnish elements on the basis of purely physicochemical processes involving fractionation and precipitation from solution of more soluble Mn relative to less soluble Fe under the high Eh–pH conditions of arid environments (Engle and Sharp 1958, Hooke *et al.* 1969, Elvidge and Moore 1979). While it is difficult to disprove a purely physicochemical explanation for Mn enhancement in arid environments, such explanations disregard the presence of Mn-rich varnish in humid macro- and microenvironments where Eh–pH conditions are quite unlike those of arid regions. While Mn should be dissolved from source materials much more rapidly than Fe, producing Mn-enhanced solutions as varnish sources, the far greater abundance of Fe in the environment and the disposition of Fe in solution prior to the deposition of the more soluble Mn present problems. Moreover, the literature on Mn deposits in a wide variety of surface, subsurface, and aquatic settings makes a strong case for a biotic concentrating mechanism for Mn films, with several specific bacterial taxa implicated (Bauman 1976,

Ehrlich 1978, Crerar *et al.* 1980, Dorn and Oberlander 1982, Palmer *et al.* 1985).

Scanning electron microscopy X-ray analysis of varnish specimens from surface and subsurface settings in the south-western United States convinced Dorn and Oberlander (1981a) that bacteria visible on varnish surfaces concentrated Mn that had been oxidized as a microbial energy source in environments lacking organic nutrients (Ehrlich 1978). Our experiments indicated that mixotrophic Mn-concentrating microbes could be cultured in neutral pH conditions, but were inhibited by both alkaline and acidic environments. This concurs with previous work on one of the most ubiquitous and distinctive of the Mn-concentrating bacteria identified by us, *Metallogenium personatum*, which is the oldest known living organism, occurring in its present form in 2.0×10^9-year-old Precambrian rocks (Crerar *et al.* 1980). Fungi, proposed by others (Krumbein and Jens 1981) as the source of Mn enhancement in rock varnish, support visible bacterial populations, and we found that the latter were the specific sources of the Mn concentrations present. In fact, the organic acids generated by flourishing communities of microcolonial fungi or lichens appear to erode Mn-rich rock varnish. Thus the viable environment for organisms producing Mn-rich rock varnish appears to be neutral-pH surfaces that are intermediate between the alkaline setting of dust-filled rock cracks and pebble ventral surfaces and moister situations in which life forms higher than mixotrophic bacteria begin to thrive and generate inimical and corrosive organic acids.

Potter (1979) and Raymond *et al.* (1992) discovered biogenic stromatolite-like accretionary structures in varnish films, and the latter concluded that Mn-oxidizing bacteria not only produce varnish structures but also account for the amorphous (non-crystalline) nature of the Mn in rock varnish. Microscopic stromatolite-like accretionary structures appear to be common in Mn-rich varnish films and have been recognized in unequivocal form in this author's specimens. Dorn (pers. comm. 1991) has attributed the columnar morphology to biogenic erosion by microcolonial fungi; however, varnish laminae parallel to column faces seem contrary to this interpretation.

The wide occurrence of Mn-rich varnish coatings on fracture surfaces far below ground level (Weaver 1978), often with a gloss equivalent to the best surface varnish, suggests that the controls of Mn deposition are complex. Glossy subsurface varnishes on semi-consolidated lacustrine silts collected by this author near Barstow, California, are densely populated by bacteria that appear to be filamentous–trichospheric *Metallogenium personatum* in stage 4 of this microbe's life cycle in the presence of dissolved manganese (Crerar *et al.* 1980). Although the microbial origin of Mn-rich rock varnish has been supported by subsequent research (Jones 1991, Raymond *et al.* 1992), some researchers continue to advocate a role for fungi, based on their own SEM analyses (e.g. Krumbein and Jens 1981). In addition, advocates of a pure or partial physicochemical Mn-concentrating mechanism continue to debate the issue of rock varnish origin (Elvidge and Iverson 1983, Smith and Whalley 1988).

The mechanism producing Fe-rich varnishes with high clay contents in alkaline settings has received little attention, but both biotic and physicochemical processes appear to be implicated (Jones 1991). Scanning electron microscopy X-ray analysis of desert varnish bacteria reveals minor enhancement in Fe along with the dominant Mn spike, and many different Fe-concentrating bacteria have been recognized in non-desert settings. Fe-rich films on rocks in streams and at springs in acidic environments in humid regions are common and are ordinarily attributed to chemolithotrophic bacteria and Eh and pH changes. However, orange Fe films in aquatic settings are free of clays and occupy an entirely different chemical environment from that of Fe-rich rock varnish.

MICROCHEMICAL LAMINATIONS

The first electron microprobe investigations of rock varnish by Hooke *et al.* (1969) revealed variations in chemistry through the depth of varnish films. Hooke *et al.* believed that these were systematic, permitting certain generalizations to be made about chemical trends in rock varnish transects. These generalizations have not been sustained by subsequent work, which indicates far more variability in varnish chemistry. Perry and Adams (1978) discovered that rock varnish films contained sequences of Mn-rich and Mn-poor laminations, which they regarded as primary depositional features. Dorn and Oberlander (1982) found the same laminations in their specimens and likened the Mn-poor laminae to the Mn-deficient (Fe-rich) varnishes on the undersides of desert pavement clasts, stressing the negative influence of alkalinity on microbial oxidation of Mn. We proposed that microchemical laminations resulted from oscillations between moderately mesic and hyperarid climates, as in pluvial and interpluvial intervals in arid regions. Hyperarid phases were equated with higher dust fluxes, more alkaline

environments, reduced microbial activity, and a falloff in Mn fixation by mixotrophic bacteria while non-biogenic Fe accretion continues. Thus it was proposed that rock varnish microchemical laminations provided an on-land proxy palaeoclimatic record analogous to the oceanic oxygen isotope record (Dorn and Oberlander 1982, Dorn 1984, 1990a). Dragovich (1988) has commented upon the care required in the interpretation of rock varnish microchemical laminations.

VARNISH CHEMISTRY AS AN ENVIRONMENTAL INDICATOR

Alternating Fe-rich and Mn-rich laminae are evident in varnish transects from areas known to have oscillated between arid and semi-arid (or subhumid) climates in Holocene and Pleistocene time (e.g. the Mojave and Sahara deserts) (Fig. 6.6). The Fe trend in varnish films is usually paralleled by Si and Al (varnish clays), while Mn trends tend to be echoed by Ca and Ba. Dorn (1990a) found that at 18 meteorological stations where rock varnish was present, Mn/Fe was inversely correlated with two different indices of climatic aridity as well as with $\delta^{13}C$ indications of plant xericity. In Death Valley, California, varnish on alluvial fans on the upwind and downwind sides of the central evaporite pan, a major alkaline dust source, varies significantly. West-side (upwind) alluvial fans issuing from the Panamint Mountains bear black, Mn-rich varnish, while east-side (downwind) fans rimming the Black Mountains are stained by orange to brown Fe-rich varnish. The basal varnish of older portions of Black Mountain fans (downwind) is Mn-rich, possibly reflecting a lacustrine phase that reduced the local dust flux. In both relative and absolute terms, Mn declines outward while Fe increases, so that the youngest portions of varnish films are consistently Fe-dominated. Varnish on younger fan segments is Fe-dominated throughout, seeming to reflect the contemporary post-lacustrine hyperarid condition.

In the alkaline, hyperarid Atacama Desert of Chile, which records rainfall at intervals of about a decade, conspicuous rock varnish is rare, but, where present, is Fe-rich, with Mn sparse through the full depth of all varnish films examined. In this area many hillslopes, dune fields, and relict shorelines are encrusted by salines including halite, gypsum, and highly soluble nitrates. Here there is no clear record of late Pleistocene moisture increases. Although relict shorelines are visible, they are undated, and the most prominent are encased by salt derived from aerosols over an immense span of time (see Chapter 2). These ancient shorelines could not be reoccupied, as they lack topographic closure owing to large-scale post-lacustral erosion of bedrock. In the Atacama Desert every rare occurrence of rock varnish having a significant Mn content can be accounted for in terms of a microclimatic setting that increases humidity: either proximity to the exotic Loa River or a sag in the coastal escarpment that permits occasional ingress of the persistent coastal fog. In the fog-shrouded but barren coastal zone,

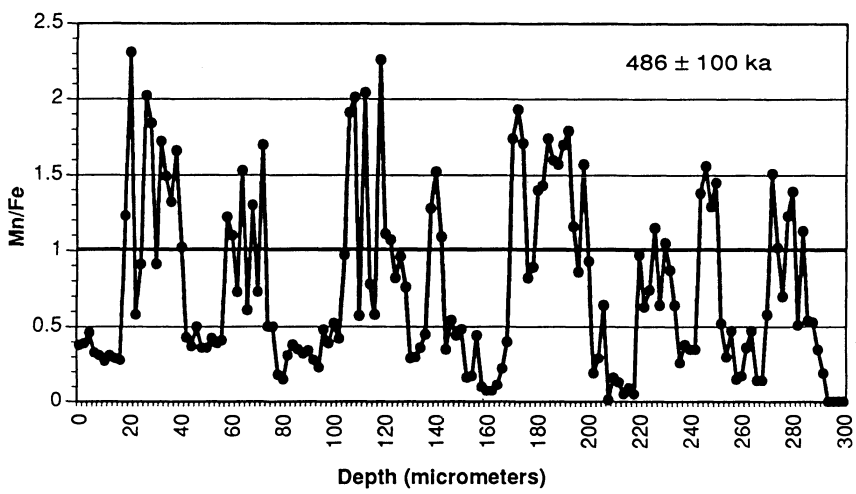

Figure 6.6 Ratios of Mn to Fe through depth of varnish film on volcanic surface with K/Ar date of 486 ± 100 ka, Coso area, California. Periods of minimum Mn accretion (troughs) interpreted as arid (alkaline) intervals in a record of pluvial–interpluvial climatic oscillations.

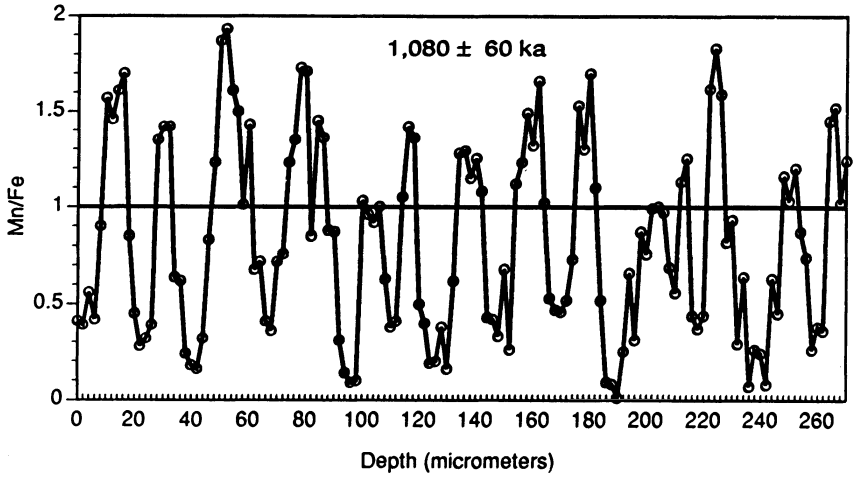

Figure 6.7 Ratios of Mn to Fe through rock varnish on volcanics with K/Ar date of 1080 ± 60 ka, Coso area, California. Peaks and troughs are supported by multiple data points, but record appears too variable to be convincing as an index of climatic oscillations.

rock varnish is not present and clasts are encrusted by lichens.

The Mn/Fe relationship to present climate along with consistency of the trends noted in Death Valley and the Atacama Desert lends credence to the palaeoclimatic significance of Mn/Fe ratios in varnish cross-sections. However, complications in a simple climatic interpretation of Mn/Fe ratios were noted by Jones (1991). Raymond *et al.* (1992) suggested that Mn is associated with the stromatolite-like structures noted above, with Fe being abundant in interstices that collect aeolian detritus. However, not all Mn-rich varnish exhibits visible stromatolitic structures, and vertical stratigraphic superposition of Mn- and Fe-rich laminae is often clearly visible in SEM views. Harrington *et al.* (1990) found that in areas of Pleistocene and Holocene volcanism, the Fe content of varnish films and the number of Fe-rich varnish laminae correlate with proximity to eruptive vents rather than with climatic oscillations. This becomes a further problem in varnish age determinations based on Ti content (see below), as titanomagnetite grains are likely to be indicators of tephra horizons in varnish. Isolated Fe spikes appear in many transects through Mn-rich varnish and usually correlate with high-Ti anomalies.

Despite broad consistencies in the relationship between alkalinity and the Mn/Fe balance in rock varnish, microchemical laminations in varnish cross-sections from southern California (Mojave Desert, Imperial Valley, southern Owens Valley) display considerable local variability. Whereas some varnish cross-sections seem indicative of true climatic oscillations, with plateaux and troughs in Mn/Fe ratios defined by multiple points, other cross-sections from the same surfaces are a hash of unconvincing single-point peaks and valleys (Fig. 6.7). Obtrusive variations in the micromorphology of varnish presumably accreting simultaneously at sites only millimetres apart suggest complexity in varnish-forming processes. Observations of dew distribution on desert pavement rocks indicate that moisture condensation and retention on rock surfaces varies markedly with substrate mineralogy, possibly creating complexes of humid and arid climates on the micrometre to millimetre scale. Raymond *et al.* (1992) found that substrate elements influenced varnish elements adsorbed to the rock surface even though the varnish elements were derived from exterior sources.

Further testing of the Mn/Fe ratio as a palaeoclimatic index is essential, including analysis of the effects of substrate mineralogy, the field orientation of varnished surfaces, and specimen height above soil surfaces, and future varnish collection should control all of these influences. Core sampling from faces (not tops) of outcrops and large clasts would probably decrease varnish detrital content as well as the water pooling and chemical fractionation effects noted by Jones (1991) and would increase sample comparability.

VARNISH AGE DETERMINATION

The degree of rock varnish development or patination has long been used in geomorphology as an

indicator of the relative ages of eroding rock surfaces and rubble deposits such as alluvial fan and talus components. Surface lithic artifacts likewise are assigned relative ages on the basis of degrees of patination, as are petroglyphs that have undergone various degrees of repatination. What has been utilized is the increase in value (in the hue/value/chroma system of colour classification) or relative darkness of a particular hue. However, the element composition of the varnish disturbs any straightforward interpretation, as Mn-rich varnish appears older (darker) than Fe-dominated varnish. Varnish thickness is an unreliable age index, being thinner on smoother substrates and thicker over irregular dust- and moisture-trapping substrates. Varnishes that are obviously young are often surprisingly thick, suggesting a rapid rate of accretion until surfaces are smoothed, after which accumulation seems to proceed much more slowly. Certain lithologies likewise appear to influence varnish thickness, or perhaps the onset of varnish deposition: for example, basalt appears to rapidly develop thick, easily removed varnish, while cryptocrystalline quartz (flint, chalcedony) varnishes slowly and may have a thin, Si-rich, abrasion-resistant veneer. Finally, on many rock surfaces varnish accretion is periodically interrupted by surface scaling, aeolian abrasion, or corrosion by organic acids associated with fungi or lichens. Varnished ventifacts are not uncommon in most deserts, suggesting that ventifacted varnish should also be expected.

Attempts have been made to determine the absolute age of rock varnish using neutron activation analysis (Bard *et al.* 1978) and U-series dating (Knauss and Ku 1980). Reasonable ages were obtained, but the absence of corroborating evidence and the specialized laboratory apparates required seem to have stifled further attempts along these lines. Potter (1979) determined that there is too little organic matter in rock varnish to date by conventional radiocarbon analysis. Accelerator mass spectrometer radiocarbon dating of rock varnish is discussed below. Potter also tested palaeomagnetic dating, but found that the magnetic signal of both dorsal and ventral varnishes was too weak to be of use. However, Clayton *et al.* (1990) were able to detect a palaeomagnetic signal in rock varnish on quartzite, suggesting that varnish ages older than *c.* 700 000 years could indeed be distinguished.

VARNISH CATION RATIO DATING

Dorn and Oberlander (1981b) suggested that the relative ages of rock varnish films could be estimated semi-quantitatively by comparison of the proportions of relatively mobile and immobile elements incorporated in varnish films. By analogy with soil chronosequences, we assumed that in older varnish immobile substances would accumulate relative to more abundant mobile cations that would be incorporated and later leached to varying degrees. The most stable substance incorporated in all rock varnishes in significant amounts is TiO_2. Of the mobile cations Na, Mg, Ca and K, only the latter two are heavy enough to be reliably counted by various microanalytical techniques. This suggested the ratio (Ca + K)/Ti as a leaching index, later termed the varnish cation ratio or VCR (Dorn 1983, 1990a). When applied to test sites with landforms of varying age, cation ratios of bulk samples of varnish scraped from rock surfaces gave both consistent and logical results. Harrington and Whitney (1987) found that cation ratios could be obtained by non-destructive SEM energy dispersive X-ray (EDAX) analysis of intact varnish specimens, permitting point-specific resampling where anomalies are detected. In this procedure, depth penetration of an electron beam normal to the varnish surface is achieved by progressive acceleration of beam voltage (Reneau *et al.* 1991a). Dorn (1989) and Dorn *et al.* (1990) have criticized this approach, which requires removal of a portion of the varnish substrate.

Cation ratios of varnish bulk samples scraped from K/Ar-dated volcanic rocks and analysed chemically by the proton-induced X-ray emission (PIXE) method have been used to generate rock varnish absolute age determination curves for archaeological and geomorphic use in nearby areas (Dorn 1989). These age determination curves (Fig. 6.8) assume that the (Ca + K)/Ti ratio of dust incorporated into varnish at a site remains constant through time. As indicated below, this critical assumption may be erroneous. Bierman and Gillespie (1991b) warn that natural fires in semi-arid regions cause boulder spalling, particularly in granite, causing loss of older varnish. As climatic oscillations have induced earlier vegetation enrichment in presently desertified areas, fire-related spalling may have affected sites in which such a phenomenon now seems inconceivable. Nevertheless, VCR age determinations based on curves calibrated by varnish chemistry on dated volcanic rocks and by AMS ^{14}C age determinations (see below) are now routinely used by both geomorphologists and archaeologists (Wells and McFadden 1987, Dorn *et al.* 1988, Pineda *et al.* 1988, Whitney *et al.* 1988, Dorn 1990b, Loendorf 1991).

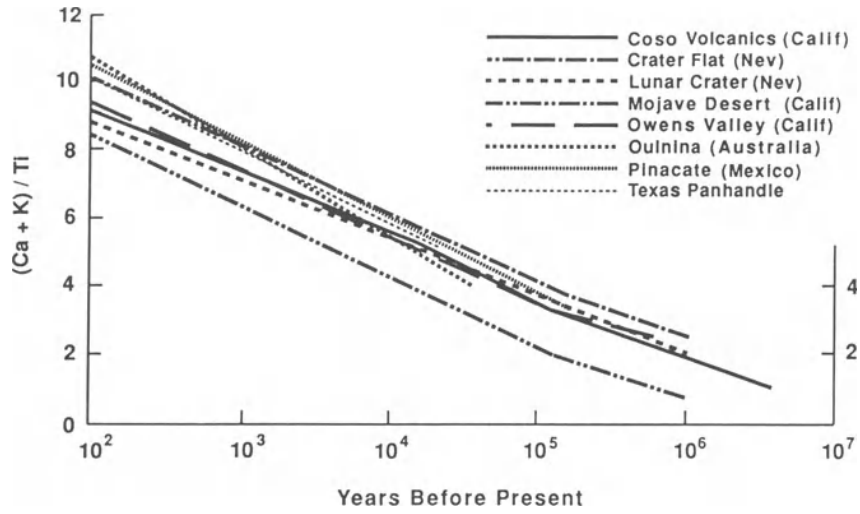

Figure 6.8 Rock varnish leaching curves, showing cation ratios (Ca + K)/Ti plotted against K/Ar ages of volcanic rocks. Recent end of scale based on modern dust compositions (adapted from Dorn 1989).

PROBLEMATICAL ASPECTS OF VCR AGE DETERMINATIONS

Questions have been raised concerning the precision of the chemical analyses underlying rock varnish age determination curves. Bierman and Gillespie (1991a), Bierman *et al.* (1991), and Harrington *et al.* (1991) pointed out that many VCR age determinations are unreliable because, in the absence of a special deconvolution, standard PIXE analysis of varnish scrapings does not separate Ba from the Ti used to compute cation ratios. This, in turn, invalidates the varnish leaching curves that are the basis of varnish age determinations. Barium is associated with Mn in virtually all rock varnish, occasionally attaining values equal to Mn and often exceeding Ti, but may not be recorded in standard energy-dispersive spectroscopy used in SEMs, electron microprobes, and proton beam (PIXE) analysis because L_α and L_β peaks for Ba coincide with K_α and K_β peaks for Ti. Thus Ba and Ti are cumulated as Ti, resulting in erroneously large Ti amounts and erroneously low VCR values. Harrington *et al.* (1991) pointed out that Ba concentrations seem to be inversely related to varnish age, so that the Ba/Ti problem is greatest with younger varnish films.

The standard pitfalls of VCR dating are discussed by Dorn (1989) and Krinsley *et al.* (1990). However, the very premise of VCR dating – the leaching of varnish cations – has been questioned by Reneau and Raymond (1991), Raymond *et al.* (1992), and Reneau *et al.* (1992), who recognized that there is no evidence of element translocation in varnish chemical transects – that is, basal rock varnish is no more leached than recently accreted surficial layers. This seems true of all varnish cross-sections produced by the present author using both electron microprobe and SEM-EDAX analyses (e.g. Fig. 6.9) and has been acknowledged by Dorn (1989). In response, Dorn and Krinsley (1991) offered visual (SEM) evidence of porous textures thought to be created by varnish leaching and also performed leaching experiments with both scrapings and *in situ* varnish. However, the visible textures are not easily distinguished from primary depositional features, particularly detritus-filled gaps between Mn-rich laminae or adjacent microstromatolites. Raymond *et al.* (1992) believe that VCR results are considerably disturbed by the distribution of detritus within rock varnish, with Ca, K, and Ti all being major detrital components. Unfortunately, Dorn and Krinsley's SEM images are reproduced at too small a size to be conclusive, and chemical profiles of indicated transects are not offered.

Bearing on the question of varnish leaching, the present researcher's analyses of varnish from lithic artifacts in the hyperarid (and hyperalkaline) central Atacama Desert reveal an *increase* of cation ratios over time, with VCRs *lower* (less cation-rich) on younger flaked surfaces than on older cortex areas. This suggests that in areas experiencing intervals of hyperalkaline conditions, particularly near playas, VCRs may be ratcheted backward by each extended desiccation event.

Perhaps a more important complication is the

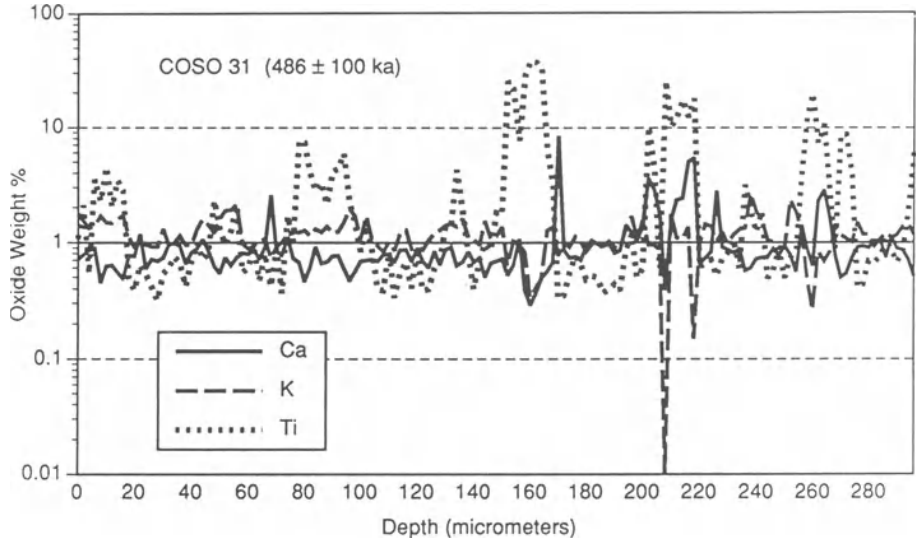

Figure 6.9 Oxide weight percentages of Ca, K, and Ti (logarithmic scale) through depth of the varnish film in Figure 6.6. Contrary to the leaching hypothesis there is no relative loss of Ca and K in the older (deeper) varnish. Ti appears as discrete spikes that may reflect volcanic tephra inputs rather than leaching residues.

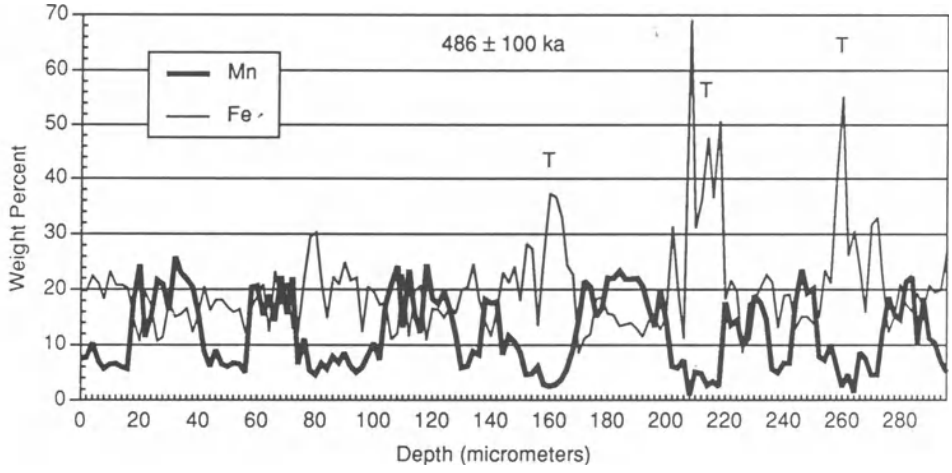

Figure 6.10 Manganese and iron oxide weight percentages through the varnish film analysed in Figures 6.6 and 6.9. Highest Fe peaks are also Ti spikes in Figure 6.9, suggesting that the most striking Fe-rich and Mn-poor laminae may be volcanic tephra intercalations.

possibility, first raised by Harrington *et al.* (1990) and Krier *et al.* (1990), that Ti-rich horizons in rock varnish are tephra layers rather than biogenic growth forms or the residuum of leaching. In fact, while K and Ca percentages do not decline through the depth of varnish films, neither does the percentage of Ti increase with varnish depth and age as the leaching hypothesis would predict. Titanium percentages in varnish cross-sections maintain rather constant levels except for isolated spikes, as seen in Figure 6.9. Older varnishes differ from younger varnishes merely by including a larger number of discrete Ti spikes (often coinciding with Fe spikes) that probably represent tephra falls (Fig. 6.10). Harrington *et al.* (1990) and Krier *et al.* (1990) noted that Ti content decreases and varnish cation ratios

increase with distance from eruptive vents. The present writer has observed that the number and prominence of Ti spikes are much greater in rock varnish collected in volcanic fields than they are in rock varnish collected in nearby non-volcanic areas. Accordingly, it would be perilous to extrapolate VCR curves derived from sites of repeated volcanism (e.g. the first five curves in Fig. 6.8) to nearby non-volcanic settings. In non-volcanic settings, Ti-dominated horizons are less abundant and less prominent in rock varnish, causing varnish ages to be grossly underestimated by VCR extrapolation from volcanic areas. This becomes a significant problem in areas lacking other means of chronological control and may invalidate VCR dates on surfaces beyond the limit of ^{14}C age determinations.

Although published VCR age determinations seem to correspond well with age determinations by other means, the above criticisms are cogent. Until there is a better understanding of varnish diagenesis through time, it would seem wise to treat VCR age determinations with caution.

AMS RADIOCARBON DATING OF ROCK VARNISH

Multiple VCR age determinations clearly evince greater scatter on short timescales, possibly because of the Ba effect, the influence of volcanic Ti, and unsystematic variations in the colonization of substrates by varnish-generating organisms. To resolve the problem of late Pleistocene and Holocene age determinations, and as a check on VCR dating, Dorn *et al.* (1989) introduced the use of accelerator mass spectrometry (AMS) to obtain radiocarbon dates on organic matter beneath or within basal varnish layers, thus constraining the ages of rock substrates. The organic matter consists of varnish organisms, pollen, and plant debris embedded in the accreting clays and oxides composing varnish films. To obtain adequate organic matter for AMS analysis, the basal varnish covering a surface area of 0.5 m^2 or more must be collected. This entails removing the outer (younger) varnish overburden down to a consistent depth above the substrate, then detaching the remaining basal layer for AMS analysis. According to Dorn *et al.*, the outer 90% of the varnish is removed by hand under magnification, using a tungsten–carbide needle (later 'dental tools'), to a uniform depth on the micrometre scale over a surface area of 0.5 m^2. Lithologies that would promote time-transgressive varnish (beginning in roughness elements and delayed on smooth crystal faces) are avoided. It should be noted that the varnishes utilized for this analysis are often quite thin, having been formed in 1 000 to 50 000 years (in the case of petroglyphs, 1 000 to 10 000 years), exacerbating the problem of overburden removal to a consistent stratigraphic horizon.

Dorn *et al.* (1989) achieved excellent agreement between rock varnish AMS ^{14}C dates and dates measured or inferred by other means at a large number of test sites, with varnish dates being about 10% younger than controls as a consequence of the expected lag in colonization by varnish-generating organisms. The procedure has been extended to the dating of petroglyphs (Dorn *et al.* 1992a), moraines (Dorn *et al.* 1987, Dorn *et al.* 1991), alluvial fan segments (Dorn 1988), and lava flows (Dorn *et al.* 1992b). In all instances the published AMS ^{14}C dates correspond strikingly with age estimates by other methods. This seems remarkable considering the difficulty of stripping varnish from large surfaces to a specified depth with a sharp-pointed hand-held tool, the limitations of the human hand, operating on the micrometre scale, being far more critical than the specific scraping tool used. Questions concerning AMS ^{14}C age determinations on rock varnish have been raised by Reneau *et al.* (1991b). These have to do with the time-transgressive nature of basal varnish, the precision of the mechanical procedure that isolates basal varnish of a consistent age, and the possibility of incorporation of older organic debris in basal varnish. Dorn *et al.* (1992a) have recently asserted that the organic material in basal varnish samples actually is subvarnish organic debris located at the rock–varnish interface, so that consistency in sampling depth is not truly critical for AMS age determinations.

CONCLUSION

Research on rock varnish has advanced enormously in the past two decades, taking the phenomenon from the category of a complete enigma to a possible tool for both absolute age determination and palaeoenvironmental analysis. However, details of the formative mechanisms, the nature of diagenetic changes in varnish films, and the most appropriate methods for varnish chemical analysis have become subjects of ongoing debates. The basic premises underlying the use of rock varnish for both age determination and palaeoenvironmental research have come into question and will remain in doubt pending future substantive findings concerning varnish-forming processes. Nevertheless, the consistency of cation ratio results and of some systems of microchemical laminations have convinced a number of researchers that rock varnish contains usable

environmental records that may be applied in studies of fault activity, rates of cliff retreat, and the ages of Quaternary geological deposits as well as lithic artifacts. Systematic analyses of rock varnish characteristics and processes are being undertaken by an increasing number of individuals along with very well-equipped research teams. It would be surprising if the attention presently focused on rock varnish does not eventually yield unequivocal answers to the questions raised by detailed analyses of varnish in recent years. However, as rock varnish chemical and physical characteristics are highly site-specific, researchers should be warned against generalizing too confidently from studies of single localities.

REFERENCES

Allen, C.C. 1978. Desert varnish of the Sonoran Desert: optical and electron probe microanalysis. *Journal of Geology* **86**, 743–52.

Bard, J.C., F. Asaro and R.F. Heizer 1978. Perspectives on the dating of prehistoric Great Basin petroglyphs by neutron activation analysis. *Archaeometry* **20**, 85–8.

Bauman, A.J. 1976. Desert varnish and marine ferromanganese oxide nodules: cogeneric phenomena. *Nature* **259**, 387–8.

Bierman, P.R. and A.R. Gillespie 1991a. Accuracy of rock-varnish chemical analyses: implications for cation-ratio dating. *Geology* **19**, 196–9.

Bierman, P.R. and A.R. Gillespie 1991b. Range fires: a significant factor in exposure-age determination and geomorphic surface evolution. *Geology* **19**, 641–4.

Bierman, P.R., A.R. Gillespie and S. Kuehner, 1991. Precision of rock varnish chemical analysis and cation ratio ages. *Geology* **19**, 135–8.

Blackwelder, E. 1954. Geomorphic processes in the desert. *California Division of Mines Bulletin* **170**, V11–V20.

Calvert, S.E. and N.B. Price 1970. Composition of manganese nodules and manganese carbonate from Loch Fyne, Scotland. *Contributions to Mineralogy and Petrology* **29**, 215–33.

Clayton, J.A., K.L. Verosub and C.D. Harrington 1990. Magnetic techniques applied to the study of rock varnish. *Geophysical Research Letters* **17**, 787–90.

Crerar, D.A., A.G. Fischer and C.L. Plaza 1980. Metallogenium and biogenic deposition of manganese from Precambrian to recent time. In *Geology and geochemistry of manganese, Volume III: Manganese on the bottom of recent basins*. I.M. Varentsov and G. Grasselly (eds), 285–303. Stuttgart: E. Schweizerbart'sche Verlagsbuchhandlung.

Dorn, R.I. 1983. Cation-ratio dating: a new rock varnish age-determination technique. *Quaternary Research* **20**, 49–73.

Dorn, R.I. 1984. Cause and implications of rock varnish microchemical laminations. *Nature* **310**, 767–70.

Dorn, R.I. 1988. A rock varnish interpretation of alluvial fan development in Death Valley, California. *National Geographic Research* **4**, 56–73.

Dorn, R.I. 1989. Cation-ratio dating of rock varnish: a geographic assessment. *Progress in Physical Geography* **13**, 559–96.

Dorn, R.I. 1990a Quaternary alkalinity fluctuations recorded in rock varnish microlaminations on western U.S.A. volcanics. *Palaeogeography, Palaeoclimatology, Palaeoecology* **76**, 291–310.

Dorn, R.I. 1990b. Rock varnish dating of rock art: state of the art perspective. *La Pintura* **17**(2), 1–2, 9–10.

Dorn, R.I. and D.H. Krinsley 1991. Cation-leaching sites in rock varnish. *Geology* **19**, 1077–80.

Dorn, R.I. and T.M. Oberlander 1981a. Microbial origin of desert varnish. *Science* **213**, 1245–7.

Dorn, R.I. and T.M. Oberlander 1981b. Rock varnish origin, characteristics, and usage. *Zeitschrift für Geomorphologie* **25**, 420–36.

Dorn, R.I. and T.M. Oberlander 1982. Rock varnish. *Progress in Physical Geography* **6**, 317–67.

Dorn, R.I., B.D. Turrin, A.J.T. Jull, T.W. Linick *et al.* 1987. Radiocarbon and cation ratio ages for rock varnish on Tioga and Tahoe morainal boulders of Pine Creek, eastern Sierra Nevada, California, and their paleoclimatic implications. *Quaternary Research* **28**, 38–49.

Dorn, R.I., M. Nobbs and T.A. Cahill 1988. Cation-ratio-dating of rock engravings from the Olary Province of arid South Australia. *Antiquity* **62**, 681–9.

Dorn, R.I., A.J.T. Jull, D.J. Donahue, T.W. Linick *et al.* 1989. Accelerator mass spectrometry radiocarbon dating of rock varnish. *Bulletin of the Geological Society of America* **101**, 1363–72.

Dorn, R.I., T.A. Cahill, R.A. Eldred, T.E. Gill *et al.* 1990. Dating rock varnishes by the cation ratio method with PIXE, ICP, and the electron microprobe. *International Journal of PIXE* **1**, 157–95.

Dorn, R.I., F.M. Phillips, M.G. Zreda, E.W. Wolfe *et al.* 1991. Glacial chronology of Mauna Kea, Hawaii, as constrained by surface-exposure dating. *National Geographic Research and Exploration* **7**, 456–71.

Dorn, R.I., P.B. Clarkson, M.F. Nobbs, L.L. Leondorf *et al.* 1992a. New approach to the radiocarbon dating of rock varnish, with examples from drylands. *Annals of the Association of American Geographers* **82**, 136–51.

Dorn, R.I., A.J.T. Jull, D.J. Donahue, T.W. Linick *et al.* 1992b. Rock varnish on Hualalai and Mauna Kea volcanoes, Hawaii. *Pacific Science* **46**, 11–34.

Dragovich, D. 1988. A preliminary electron microprobe study of microchemical laminations in desert varnish in western New South Wales. *Earth Surface Processes and Landforms* **13**, 259–70.

Ehrlich, H.L. 1978. Inorganic energy sources for chemolithotrophic and mixotrophic bacteria. *Geomicrobiology Journal* **1**, 65–83.

Elvidge, C.D. 1982. Reexamination of the rate of desert varnish formation reported south of Barstow, California. *Earth Surface Processes and Landforms* **7**, 345–8.

Elvidge, C.D. and R.M. Iverson 1983. Regeneration of desert pavement and varnish. In *Environmental effects of off-road vehicles*. R.H. Webb and H.G. Wilshire (eds), 225–43. New York: Springer.

Elvidge, C.D. and C.B. Moore 1979. A model for desert varnish formation. *Geological Society of America Abstracts with Programs* **11**, 271.

Engle, C.G. and R.S. Sharp 1958. Chemical data on desert varnish. *Bulletin of the Geological Society of America* **69**, 487–518.

Goodwin, A.J.H. 1960. Chemical alteration (patination) of stone. *Viking Fund Publications in Anthropology* **28**, 300–24.

Harrington, C.D. and J.W. Whitney 1987. A scanning-electron microscope method for rock varnish dating. *Geology* **15**, 967–970.

Harrington, C.D., S.L. Reneau and D.J. Krier 1990. Incorporation of volcanic ash into rock varnish, and implications for geochronologic and paleoenvironmental research. *American Geophysical Union Program Abstracts*, December 1990, 1341.

Harrington, C.D., D.J. Krier, R. Raymond, Jr. and S.L. Reneau 1991. Barium concentration in rock varnish: implications for calibrated rock varnish dating curves. *Scanning Microscopy* **5**, 55–62.

Hooke, R. LeB., H. Yang and P.W. Weiblin, 1969. Desert varnish: an electron microprobe study. *Journal of Geology* **77**, 275–88.

von Humboldt, A. 1819. *Voyage aux régions équinoxiales du nouveau continent* v. 2. Paris: N. Maze.

Hunt, C.B. and D.R. Mabey 1966. Stratigraphy and structure, Death Valley, California. *U.S. Geological Survey Professional Paper* 494-A.

Jones, C.E. 1991. Characteristics and origin of rock varnish from the hyperarid coastal deserts of northern Peru. *Quaternary Research* **35**, 116–29.

Kamminga, J. 1979. The nature of use-polish and abrasive smoothing on stone tools. In *Lithic Use-Wear Analysis*, B. Hayden (ed.), 143–57. New York: Academic Press.

Knauss, K.G. and T.L. Ku, 1980. Desert varnish: potential for age-dating via uranium series isotopes. *Journal of Geology* **88**, 95–100.

Krier, D.J., C.D. Harrington, R. Raymond Jr and S.L. Reneau 1990. Pitfalls in the construction of rock varnish cation-ratio dating curves for young volcanic fields: examples from the Cima volcanic field, California. *American Geophysical Union Program Abstracts*, December 1990, 1341–2.

Krinsley, D.H., R.I. Dorn and S. Anderson 1990. Factors that may interfere with the dating of rock varnish. *Physical Geography* **11**, 97–119.

Krumbein, W.E. and K. Jens 1981. Biogenic rock varnishes of the Negev Desert (Israel): an ecological study of iron and manganese transformation by cyanobacteria and fungi. *Oecologia* **50**, 25–38.

Lakin, H.W., C.B. Hunt, D.F. Davidson and U. Odea 1963. Variation in minor element content of desert varnish. *U.S. Geological Survey Professional Paper* 475-B, B28–B31.

Laudermilk, J.C. 1931. On the origin of desert varnish. *American Journal of Science* **21**, 51–66.

Loendorf, L.L. 1991. Cation-ratio varnish dating and petroglyph chronology in southeastern Colorado. *Antiquity* **65**, 246–55.

Oberlander, T.M. 1982. Interpretation of rock varnish from the Atacama Desert, Chile. *Program Abstracts, Association of American Geographers*, San Antonio, 311.

Palmer, F.E., J.T. Staley, R.G.E. Murray, T. Counsell *et al.* 1985. Identification of manganese-oxidizing bacteria from desert varnish. *Geomicrobiology Journal* **4**, 343–60.

Perry, R.S. and J. Adams 1978. Desert varnish: evidence for cyclic deposition of manganese. *Nature* **276**, 489–91.

Pineda, C.A., M. Peisach and L. Jacobson 1988. Ion beam anaysis for the determination of cation ratios as a means of dating South African rock art. *Nuclear Instruments and Methods in Physics Research* **B35**, 463–6.

Potter, R.M. 1979. The tetravalent manganese oxides: clarification of their structural variations and relationships and characterization of their occurrence in the terrestrial weathering environment as desert varnish and other manganese oxide concentrations. PhD dissertation, California Institute of Technology.

Potter, R.M. and G.R. Rossman 1977. Desert varnish: the importance of clay minerals. *Science* **196**, 1446–8.

Raymond, R. Jr, G.D. Guthrie, Jr, D.L. Bish, S.L. Reneau *et al.* 1992. Biomineralization of manganese within rock varnish. *Catena Supplement*, **21**, 321–35.

Reneau, S.L. and R. Raymond, Jr 1991. Cation-ratio dating of rock varnish: why does it work? *Geology* **19**, 937–40.

Reneau, S.L., R.C. Hagan, C.D. Harrington and R. Raymond, Jr 1991a. Scanning electron microscope analysis of rock varnish for cation-ratio dating: an examination of electron beam penetration depths. *Scanning Microscopy* **5**, 47–54.

Reneau, S.L., T.M. Oberlander and C.D. Harrington 1991b. Accelerator mass spectrometry dating of rock varnish: discussion. *Bulletin of the Geological Society of America* **103**, 310–11.

Reneau S.L., R. Raymond, Jr and C.D. Harrington 1992. Elemental relationships in rock varnish stratigraphic layers, Cima volcanic field, California: implications for varnish development and the interpretation of varnish chemistry. *American Journal of Science* **292**, 684–723.

Smith, B.J. and W.B. Whalley 1988. A note on the characteristics and possible origins of desert varnishes from southeast Morocco. *Earth Surface Processes and Landforms* **13**, 251–8.

Tricart, J. 1972. *The landforms of the humid tropics, forests and savannas*, translated by C.J.K. de Jonge, New York: St Martin's Press.

Weaver, C.E. 1978. Mn–Fe coatings on saprolite fracture surfaces. *Journal of Sedimentary Petrology* **48**, 595–610.

Wells, S.G. and L.D. McFadden 1987. Comment on 'Isotopic evidence for climatic influence on alluvial fan development in Death Valley, California'. *Geology* **15**, 1178.

Whitney, J.W., C.D. Harrington and P.A. Glancy 1988. Deciphering Quaternary alluvial history in Las Vegas Wash, Nevada, by radiocarbon and rock varnish dating. *Geological Society of America Abstracts with Programs* **20**, 243.

PART THREE

HILLSLOPES

ROCK SLOPES 7

Alan D. Howard and Michael J. Selby

INTRODUCTION

The very slow chemical and physical weathering rates in desert areas coupled with a relatively high efficiency of wash processes, due to the general sparseness of vegetation, results in more widespread occurrence of slopes with little or no regolith than in areas with humid climates. This chapter outlines the processes and landforms occurring on desert slopes that are either massive bedrock or are scarps and cuestas in layered rocks dominated by outcropping resistant rock layers.

SLOPES IN MASSIVE ROCKS

by Michael J. Selby

Hillslopes formed on bodies of massive rock – that is, with few joints and high intact strength – are found in most of the world's deserts. These deserts vary in age, past climatic regimes, structure, and geological history. It seems inherently improbable, therefore, that all hillslopes will have one set of controls on their form, or even that the same controls have prevailed throughout the evolution of the hillslope. In this section the following influences on hillslope form will be considered: rock mass strength and slope forms; structural influences; sheeting; bornhardts; karst in siliceous rocks; etch processes and inherited forms.

ROCK MASS STRENGTH AND SLOPE FORMS

There has been a general recognition by geomorphologists that rock resistance to processes of erosion has played a part in controlling the form of hillslopes, particularly in arid regions, but attempts to study such relationships in detail were dependent upon the development of rock mechanics as a discipline. The work of tunnelling and mining engineers has been important in the establishment of methods of investigation (see, for example, Terzaghi 1962, Brown 1981, Hoek and Bray 1981, Brady and Brown 1985, Bieniawski 1989). The application of rock mechanics approaches to the understanding of hillslopes has been particularly fruitful in arid and semi-arid areas where excellent exposure of rock outcrops is available (Selby 1980, 1982a, b, c, d, Moon and Selby 1983, Moon 1984a, 1986, Allison and Goudie 1990a, b).

The underpinning of the geomorphological studies listed above was the formulation of a semi-quantitative method of evaluating the strength of rock masses (Selby 1980). The method involves a five-level ordinal rating of seven characteristics of exposed rock related to mass strength. These are intact rock strength (typically measured by Schmidt hammer), degree of weathering, spacing of joints, orientation of joints relative to the slope surface, joint width, joint continuity, and degree of groundwater outflow. The individual ratings of these characteristics are incorporated into a weighted sum characterizing rock mass strength. Details of this method have been referred to in accessible sources, such as Selby (1982d) and Gardiner and Dackombe (1983). The original method is fundamentally unchanged but Moon (1984b) has suggested some refinements to measurements and Abrahams and Parsons (1987) have improved the definition of the envelope defining strength equilibrium slopes.

The contention that strength equilibrium slopes are widespread is confirmed by independent and recent work and has a number of implications. (a) Rock slopes in strength equilibrium retreat to angles which preserve that equilibrium: if the process of retreat brings to the slope surface rocks of lower mass strength the slope angle will become lower; if higher strength rock masses are exposed, slope angles will steepen; only if rock mass strength is

Geomorphology of Desert Environments. Edited by Athol D. Abrahams and Anthony J. Parsons. Published in 1994 by Chapman & Hall, London. ISBN 978-94-015-8256-8

constant will slopes retreat parallel to themselves. (b) Only if controls other than those of mass strength supervene will the above generalization be invalid. (c) Rock slopes evolve to equilibrium angles relatively quickly. If this were not so, slope angles too high or too low for equilibrium would be more common than they are. (d) Gentle rock slopes remain essentially uneroded until either weakened by weathering or steepened by undercutting to the strength equilibrium gradient. Application of the technique is useful for distinguishing the effects of controls other than rock mass strength on slope inclination.

The assessment of strength equilibrium for hillslopes forming escarpments and inselbergs in South Africa, the Namib Desert, and Australia and on a great variety of lithologies has demonstrated that there is no simplistic model for slope evolution of the kind implied in such terms as parallel retreat or downwearing. If such ideas have any validity, it can only be in application to a particular variation in mass strength into a rock mass as the slopes on it evolve.

In all of the early work on the form of rock slopes the units for assessment were chosen as having a uniform slope and angle or an obvious uniformity of rock properties. Such a selection process has certain advantages, but it limits the application of statistical assessment of parameters. Allison and Goudie (1990a) have introduced the use of a 'kennedy parameter' for measuring slope shape and a fixed distance of 5 m over which slope angle changes are recorded. This method permits assessment of slope curvature. The kennedy parameter has a value of 0.5 for straight slopes, increasingly concave slopes have values tending towards 0.0 and increasingly convex slopes towards 1.0. Symmetrical concavo-convex or convexo-concave slopes also have a value of 0.5. Profile records must therefore include profile plots if errors are to be avoided. The same workers also advocate the use of the sine of the slope angle if frequency distributions and statistical analyses are to be applied to slope profile data.

STRUCTURAL INFLUENCES

The rock mass strength rating system is insensitive to the condition in which critical joints or weak bedding planes dip steeply out of a slope – that is, where the stability of the overall slope is controlled by deep-seated structural influences rather than processes and resistance operating at the scale of individual joint blocks. If joints are infilled with weak materials, such as clays, the critical angle for stability could be as low as 10° (see Selby 1982d, pp. 72 and 158). A careful assessment of the shear strength along critical joints is then required. Basic methods are described by Brown (1981) and their application to geomorphic studies by Selby (1987).

Moon (1984a) has studied steep slopes in the Cape Mountains and recognized both unbuttressed and buttressed slopes with units which are as steep as 90°. Buttressed slopes are supported by rock units lower on the hillslope whenever the dominant joints fail to outcrop. This happens most obviously where bedding joints plunge at the same angle as the hillslope angle. Buttressed slopes have slope angles less than their apparent strength based upon the rock mass strength parameters due to lack of exposed dominant jointing. Such slopes demonstrate the importance of a lack of weathering along the joints and the lack of dilation which would otherwise allow sliding to take place. The effective friction angle along critical joints is assumed to exceed 55° in some cases, as there are few signs of mass failure of scarp faces. The elimination of buttressing by weathering, buckling, or other processes is an essential prerequisite to the development of strength equilibrium.

Rock slopes out of equilibrium with the rock mass strength rating can also result from rapid undercutting (by stream erosion of mass wasting lower on the slope), form dominance by non-mass-wasting processes (such as solution of limestones), rocks with a regolith cover, exhumation (for example, structural plains on resistant caprocks exposed by erosion of overlying weak rocks, former Richter slopes denuded of their debris cover, and some bornhardts), and slopes dominated by sheeting fracturing.

SHEETING

The formation of planar or gently curved joints conformable with the face of a cliff or valley floor is called sheeting. To merit this name there usually is evidence that the joints form more than one layer of separating rock. Such evidence is obtained from exposures which reveal parallel shells of rock separating from the parent rock mass, which is massive. Sheeting joints have been described from several rock types which can form massive bodies; granite and hard, dense sandstones (Bradley 1963) are the most common. In deserts domed inselbergs, called bornhardts, and high cliffs are the most common features which develop sheet structures (Figs 7.1 and 7.2).

At least four major hypotheses have been proposed to account for sheeting: (a) sheeting results

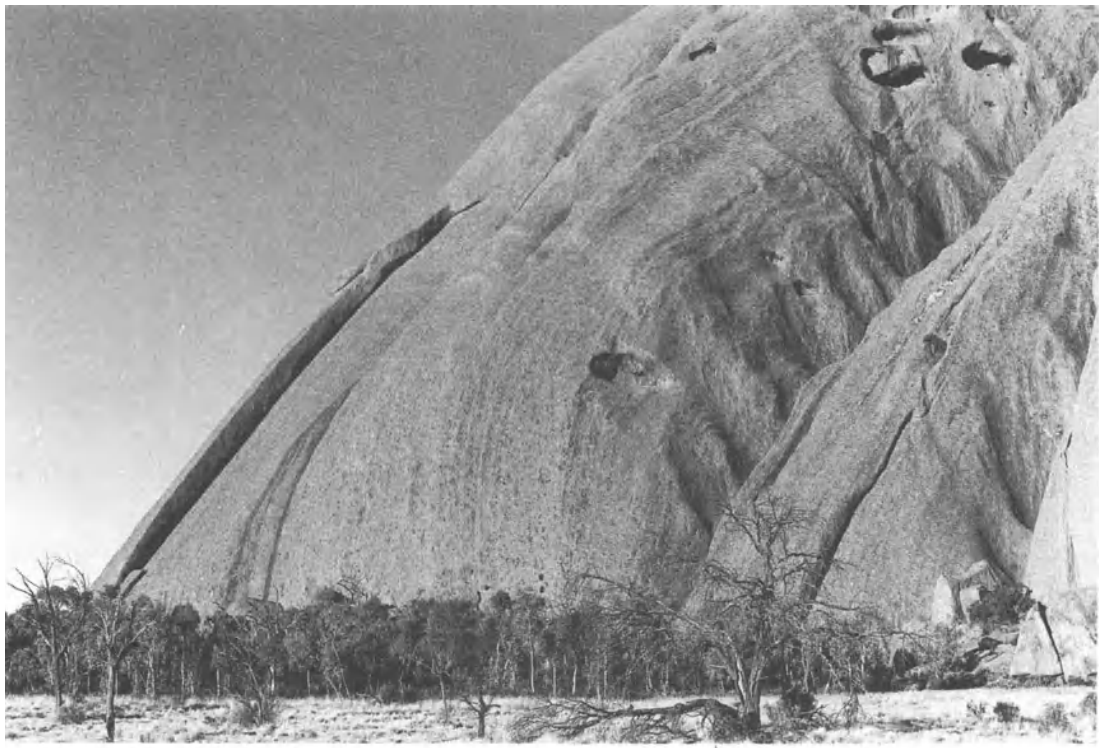

Figure 7.1 A sheet of arkosic sandstone has separated from the dome of Ayers Rock, central Australia. The bedding of the rock lies in a vertical plane and has no influence on the sheeting. Note the tafoni on the dome face, which have been interpreted as having an origin within a weathering mantle (photo M.J. Selby).

from stress release; (b) sheet structures are developed in granitic rocks by the formation of stretching planes during intrusion into the crust; (c) sheeting is the result of faulting with the development of secondary shears; and (d) lateral compression within the crust creates dome-like forms with concentric jointing being developed during the compression. The expansion of rock during weathering produces thin slabs of rock which, if confined laterally, may arch and create small-scale features which are similar to the larger-scale forms created by crustal stresses.

The unloading or stress release hypothesis was expressed in its most persuasive form by Gilbert (1904). He, like many geologists, was impressed by the evidence of rock bursts in mines and deep tunnels, of the springing up of rock slabs after retreat of glaciers and by the common occurrence of sheeting on the walls of deglaciated valleys and in quarries. Work in quarries (Dale 1923, Jahns 1943) showed clearly that the thickness of sheets increases with depth into the rock mass. Sheet thicknesses range from less than one metre to more than ten metres and transect rock structures, or even dykes in rock bodies, which have few or no other joint sets. Sheet structures terminate laterally where they meet other joints or weak rock units.

Stresses in the upper crust are usually described as being derived from four major sources: gravitational, tectonic, residual, and thermal (see Selby *et al.* 1988 for a review).

Gravitational stresses at a point within a rock body are induced by the weight of the column of rock above that point. Rocks under load tend to expand transversely to the direction of the applied load, with the resulting transverse stress having a magnitude which is approximately one-third that of the vertical stress. Even if the overburden is removed the tendency for transverse expansion to occur is locked into the rock mass as a residual stress (Haxby and Turcotte 1976).

Tectonic stresses result from convergence, and their presence is indicated by thrust faulting and conjugate joint sets. Stress fields in areas of convergence may yield horizontal stresses which exceed the local vertical stresses (McGarr and Gay, 1978).

Thermal stresses result from the prevention of

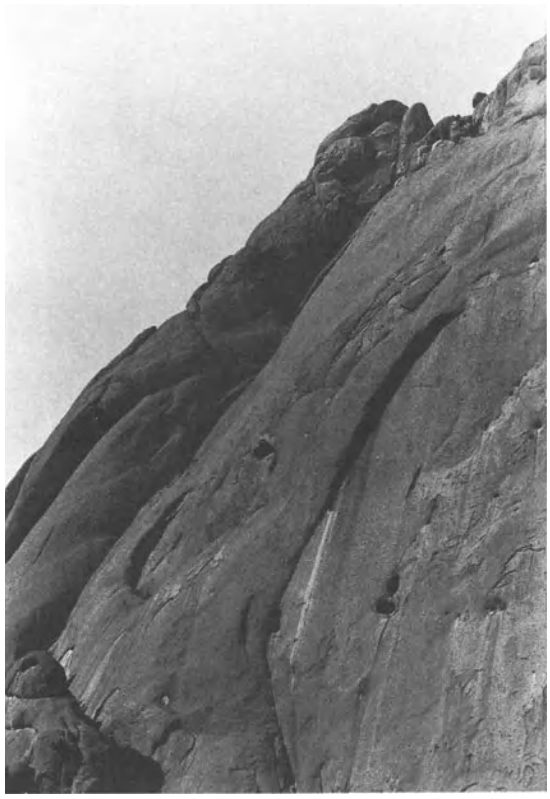

Figure 7.2 Sheeting on the surface of a granite dome, showing various degrees of separation. Gross Spitzkoppe, Namibia (photo M.J. Selby).

expansion or contraction of a solid during heating or cooling. The magnitude of the stresses in a confined rock body which cools through 100°C may exceed the tensile strength of the rock (Voight and St Pierre 1974).

The stresses from gravitational, tectonic, and thermal effects may all be locked in the rock body as residual stresses if they cannot be relieved by expansion of the rock, internal deformation, or the development of joints.

In weak rocks and soils, continuous joint systems do not develop freely because the high void space and the presence of many microcracks and plastic clays within their structure prevent fracture propagation. In dense, strong rocks, by contrast, joints can propagate with few impediments (for a discussion of fracture mechanics and crack propagation see Einstein and Dershowitz 1990).

The tendency of rock bodies to expand as a result of gravitational loading and thermal stress from cooling has been analysed in some detail by finite-element analyses. Such analyses have now been applied to a number of geomorphic phenomena at scales ranging from small cliffs and individual slopes to mountain peaks and mountain massifs (see, for example, Yu and Coates 1970, Sturgul *et al.* 1976, Lee 1978, Augustinus and Selby 1990). It is evident from such analyses that all of the four forms of stress described above can create a tendency for rock masses to expand laterally and for stresses to be concentrated at particular sites along cliff faces, usually at the bases of cliffs (Yu and Coates 1970). Furthermore, the magnitude of the stresses commonly exceeds the tensile strength of the rock. As fractures are propagated in directions which are normal to the direction of the principal stress (Einstein and Dershowitz 1990), it is evident that stress relief can be a major cause of sheeting which can operate when the confining pressure of surrounding rock masses is removed by erosion.

Yatsu (1988) has offered a dissenting view of the role of residual or 'locked-in' stresses on development of sheeting and rock bursts, maintaining that steady-state creep can erase such stresses over the long timescales required for exposure of formerly deeply buried rock. Yatsu emphasized the role of neotectonic stress fields and gravitational stress related to present-day topography.

The evidence for steady-state creep is likely to be found in thin sections taken from rock at shallow depth. Such sections may be expected to show alignment of minerals such as micas and development of shears in crystals and silica overgrowths in orientations which are unrelated to original rock microstructure and are aligned downslope. No such evidence has been reported.

Neotectonic stress fields would be expected to create preferred alignments of sheeting joints, but sheeting occurs parallel to valley walls and dome surfaces with many orientations in a small area. Furthermore, many areas of sheeting occur in cratons far from areas of Cenozoic tectonism.

Gravitational stress is caused by existing overburdens and is relevant to flanks of steep-sided peaks and ridges and to walls of deep valleys. It is not relevant to areas of low relative relief where many examples of stress relief are found. It should be noted also that, although a few studies of stresses in individual boulders have been carried out, residual stresses have been measured in joint-bounded columns of basaltic lava (Bock 1979). Much further work is needed, but Bock's work has the implication that residual stresses, of thermal or gravitational origin, may be locked into small rock units.

The alternative mechanisms listed in the second paragraph of this section are not necessarily ex-

cluded from being contributing factors to sheeting but are, in essence, special cases which can apply to only a few cases in specific environments.

MASS WASTING INFLUENCES

Many steep bedrock slopes in desert environments exhibit chutes – linear depressions oriented downslope. Although most of these are developed along zones of structural weakness, their deepening and downslope integration may be enhanced by the motion of rockfalls and avalanches through the chutes. Such features are most elegantly developed as 'spur and gully' terrain in arctic and alpine environments where competition from runoff processes is negligible (Matthes 1938, Blackwelder 1942, Rapp 1960a, b, Luckman 1977, 1978, Akerman 1984, Rudberg 1986) and on the sides of steep scarps on Mars (Sharp and Malin 1975, Blasius *et al.* 1977, Lucchitta 1978). In arctic and alpine terrain dry rockfalls, debris avalanches, and snow avalanches appear to be capable of rock erosion (Matthes 1938, Blackwelder 1942, Rapp 1960a, b, Peev 1966, Gardiner 1970, 1983, Hewett 1972, Luckman 1977, 1978, Corner 1980, O'Loughlin and Pearce 1982, Ackroyd 1987). Lucchitta (1978) and Patton (1981) cited examples from desert areas, but competition from fluvial erosion makes the evidence for rockfall and avalanche erosion equivocal.

Howard (1990) has modelled gully erosion by avalanching using an avalanche rheology similar to equation 8.13 and an approach similar to that used from modelling of snow avalanches (Perla *et al.* 1980, Dent and Lang 1980, 1983, Martinelli *et al.* 1980) and some debris avalanches (Cannon and Savage 1988, McEwen and Malin 1990). These models generally assume that the avalanche moves as a unit with the net downslope surface shear τ being expressed by a relationship

$$\tau = \rho_b g h(\cos\theta \tan\phi - \sin\theta) - \rho_b C_f V^n \quad (7.1)$$

where h is the avalanche thickness (often assumed to be constant during the avalanche motion), g is the gravitational acceleration, θ is the slope angle, ϕ is a friction angle, V is the avalanche velocity, ρ_b is the flow bulk density, n is an exponent, and C_f is a friction coefficient. A theoretical basis for C_f is not firmly established and may represent air drag, internal frictional dissipation, and 'ploughing' of surface material (Perla *et al.* 1980). Some models utilize a 'turbulent' friction with $n = 2$, and others assume 'laminar' friction with $n = 1$ (Buser and Frutiger 1980, Dent and Lang 1980, 1983, Lang and Dent 1982, Perla *et al.* 1980, Martinelli *et al.* 1980, McClung and Schaerer 1983, Schiewiller and Hunter 1983, McEwen and Malin 1990, Cannon and Savage 1988). Rather than finding analytical solutions for travel distance, in these models avalanche motion is generally routed downslope over the existing terrain, with deposition where V drops to zero. These models also often account for lack of flow contact in overhangs and momentum loss at sudden decreases of slope angle. Howard (1990) showed that chutes can be created either through the action of debris motion triggering failure of partially weathered bedrock or regolith under conditions where they would otherwise be stable or through direct scour of the substrate.

BORNHARDTS

Bornhardts are steep-sided, domical hills with substantial surfaces of exposed rock (Willis 1936; Fig. 7.3). In detail they vary considerably in form from being nearly perfect hemispheres, through cylinders with domed tops, to elongated ovoids. These different forms have been given a variety of local and general descriptive names (see Twidale 1981, 1982a, b).

The name bornhardt honours the German geologist Wilhelm Bornhardt who gave evocative accounts of the landscapes of East Africa where granite domes stand above extensive plains (Bornhardt 1900, Willis 1936). The association of granite with isolated domical hills standing above plains is clearly implicit in the original designation, but hills with similar forms occur on other rock types of which Ayres Rock and the Olgas of central Australia are among the best known. Ayres Rock is formed of a coarse-grained arkose – that is, a sandstone rich in feldspars. The Olgas, on the other hand, consist of a massive conglomerate, the matrix of which is as resistant as the boulder- and gravel-sized clasts (Twidale, 1978) (Figs 7.3 and 7.4).

The outstanding feature of bornhardts is their massive form with few major or continuous joints passing through the body of rock, but the margins of bornhardts can often be seen to be determined by bounding joints. Large rock masses may be partitioned by widely spaced joints which then separate the mass into a series of domes. Such partitioning can be seen in the Pondok Mountains of the Namib Desert (Selby 1982a) and in the Olgas (Fig. 7.4). Sheeting, with separation of curved plates of rock conformable with the dome surface, is a feature of many bornhardts. It is easily recognized that such jointing will permit survival of the dome form even after successive sheets are broken by cross joints,

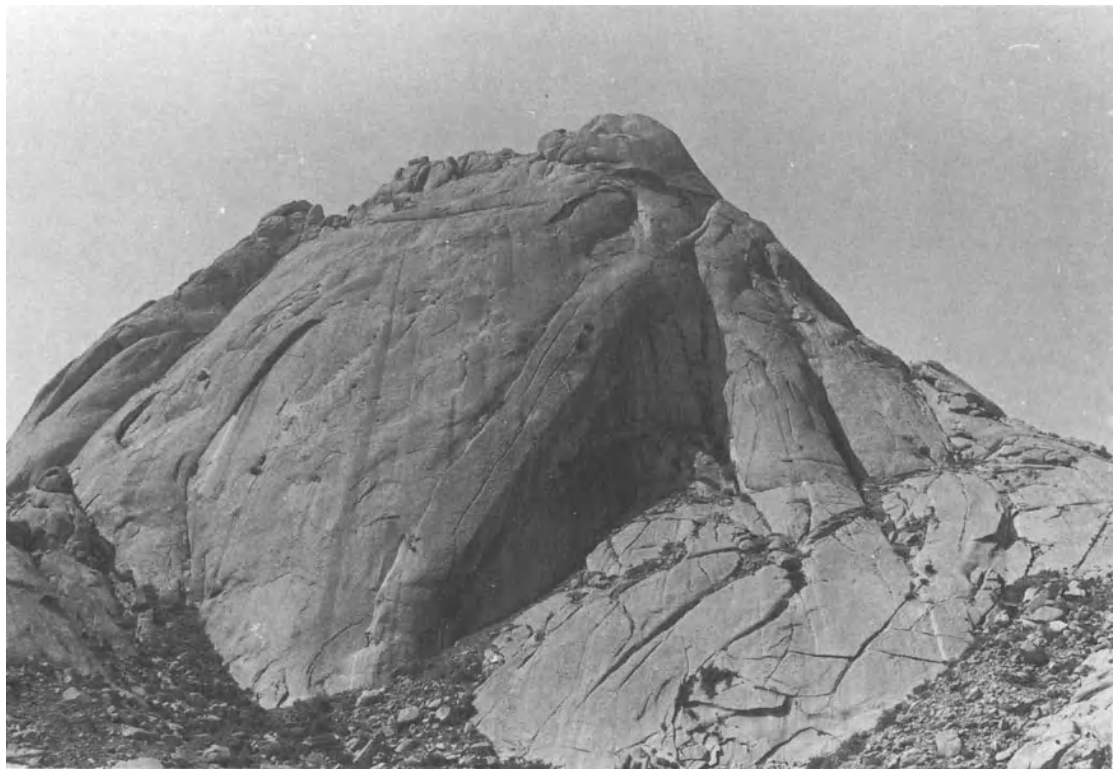

Figure 7.3 Gross Spitzkoppe, Namibia, is a granite bornhardt which rises 600 m above the surrounding desert plain. Sheeting is occurring on the main face and at depth in the central section which is in deep shadow. On the right, sheets are being subdivided by cross-joints (photo M.J. Selby).

and weathering has caused disintegration of the resulting slabs. Sheet jointing, however, is not always concentric with the dome surface, and where it has a curvature with a shorter radius or longer radius than that of the dome, the result will be a steepening or flattening of the ultimate dome form.

Bornhardts have been reported from virtually all climatic zones, but they are especially abundant in the humid, subhumid, and arid landscapes of the Gondwana cratons where large exposed intrusions of granitic rocks are common. In areas of younger granitic and gneissic intrusions, granitic domes form the cores of mountain massifs and may be revealed by valley erosion along their flanks, as in the Yosemite Valley, California, or as growing intrusions in areas of active uplift, as in Papua New Guinea (Ollier and Pain 1981). In other continental settings diapiric intrusions form domed hills, as at Mount Duval, Australia (Korsch 1982). Such features, and the recognition that granite domes are created as part of the intrusion process and revealed as cover beds are removed, as in the inland Namib escarpment (Selby 1977), indicate clearly that some dome forms are entirely structural in origin and have forms maintained by sheeting processes (Fig. 7.5).

There is no evidence, or process known, for a structural origin for domes of sedimentary rock; for them, and possibly for some domes of igneous rock, other mechanisms have to be considered. It is widely recognized that rounded core stones develop from cuboid joint blocks within weathering profiles. On much larger scales, it is often assumed that similar rounding of corners will form domical rock masses within weathering profiles. Such processes may be aided, or even made possible, by stress release joints opening along the edges of large blocks and thus promoting the formation of rounded forms.

Construction of railways, roads, and mine tunnels (Boyé and Fritsch 1973) has revealed that many domes occur as compartments of solid relatively unjointed rock within a deeply weathered regolith. The widely accepted hypothesis that many bornhardts are resistant bodies of rock which have

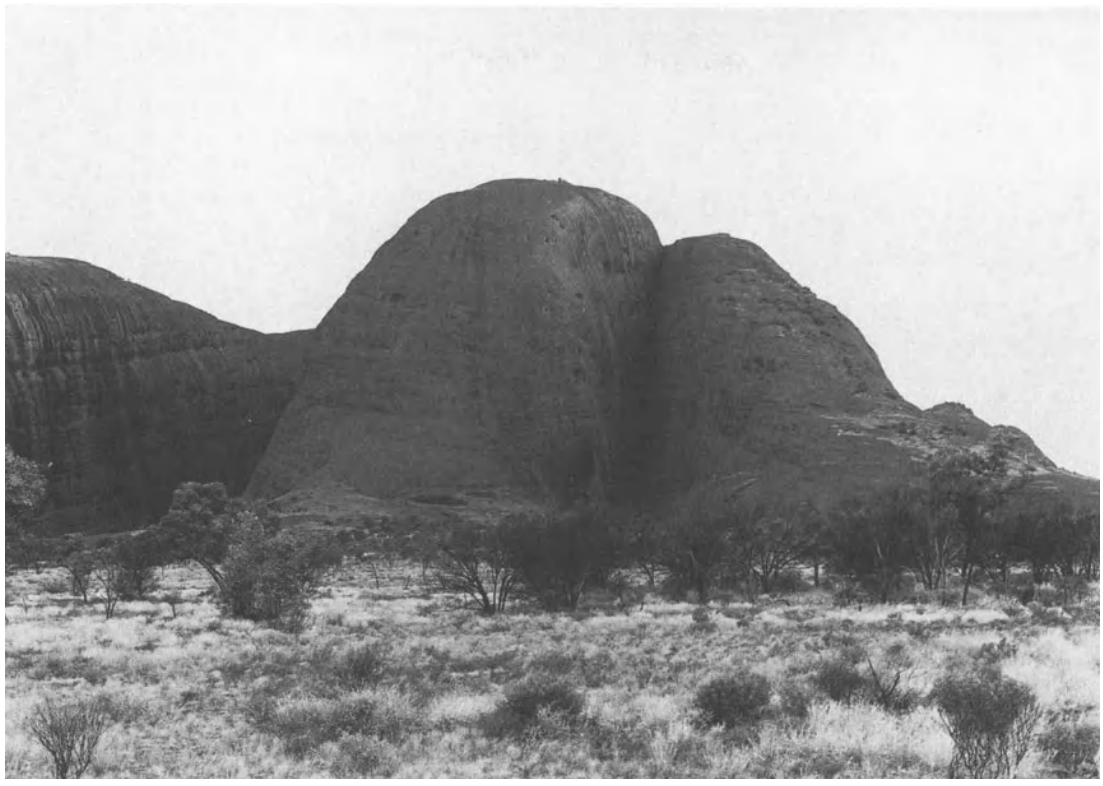

Figure 7.4 Domes of the Olgas, central Australia, showing the effect of major joints in subdividing the massif into elongated domes (photo M.J. Selby).

survived attack by subsurface weathering and then been revealed by erosional stripping of the regolith (Falconer 1911) is clearly demonstrable where domes stand above erosion surfaces below which deep regoliths survive. For example, in central Australia the exposure of Ayres Rock and the Olgas can be put at the end of the Mesozoic, yet these inselbergs stand above plains that have silcretes of early to middle Tertiary age at the surface (Twidale 1978).

Much of the controversy about bornhardts has been concerned with why bodies of rock should be relatively free of major joints while the rock around them is more closely jointed and therefore subject to penetration by water and chemical alteration. The focus of the debate has been on the lack of joints which has commonly been ascribed to the massive bodies being in a state of compression due to horizontal stresses in the crust (e.g. Twidale 1981, 1982a, b). The arguments, however, will be convincing only when stress levels in the rock are measured. Standard methods exist (Brady and Brown 1985) and have been used by mining engineers for some time. The difficulty is that the material around the bornhardt usually has either been removed by erosion or been deeply weathered, so comparable data cannot be obtained from the dome and its surroundings. In the Namib Desert, however, emerging domes and their surrounds are available for study.

It is evident from the above discussion that domed hills are not unique to any climatic environment. They are found in many of the world's deserts, but primarily because these lie on the surfaces of cratons which have been deeply weathered and stripped. The distinct feature of domes in deserts is their excellent exposure, with limited weathering of their surfaces by modern processes because the domes shed to their margins such rain as falls on them. Even the tafoni, pits, and other superficial features are usually attributed to weathering within the regolith. The process of stripping, whether it be by downwearing or backwearing of the surrounding material is irrelevant to understanding the origins of the domes. Similarly, the mineralogy and petrology

Figure 7.5 Domes of granite being stripped of their cover rocks which are unweathered schists. This exposure is one of the best pieces of evidence for the creation of domes by intrusive emplacement and the inheritance of that form in the landscape as cover rocks are removed by erosion (photo M.J. Selby).

of the rock is relevant only in so far as any bornhardt that survives has had to resist the processes acting on it.

KARST IN SILICEOUS ROCKS

Karst forms, possibly inherited from past more humid environments, may be important parts of some present desert environments. Such an area is the Bungle Bungle of the south-eastern Kimberley region of north-western Australia (Young 1986, 1987, 1988) and similar areas have been reported from the Sahara (Mainguet 1972). In both of these areas the rocks are quartzose sandstones and quartzites.

The siliceous rocks of the south-eastern Kimberley region are nearly horizontally bedded and of Devonian age. Their karstic features include complex fields of towers and sharp ridges, cliff-lined gullies, steep escarpments with cave and tube systems and conical hills standing above flat-floored valleys which debouch on to pediments which may have near right-angle junctions with the scarps. The local relief between the pediment surface and the ridge crests is seldom greater than 300 m (Fig. 7.6). The present climate is semi-arid with a dry season lasting from April to November and a wetter season occurring between December and March. The best estimate for the annual rainfall is 600 mm. On pediment surfaces, to the south, are widely spaced sand dunes now fixed by stable vegetation but indicating a formerly dry climate; the last arid phase ended 10 000 to 15 000 years BP (Wyrwoll 1979).

Studies by Young (1988) have indicated the processes which have contributed to, or perhaps controlled, the development of the present landscape. The primary evidence comes from scanning electron microscope analyses of the rocks. The sandstones have quartz grains cemented by quartz overgrowths which did not eliminate all primary porosity. As a result water could circulate through the rock and etch the grains and dissolve much of the overgrowth silica. The sandstones have, in some formations, been left as granular interlocking grains with few cementing bonds.

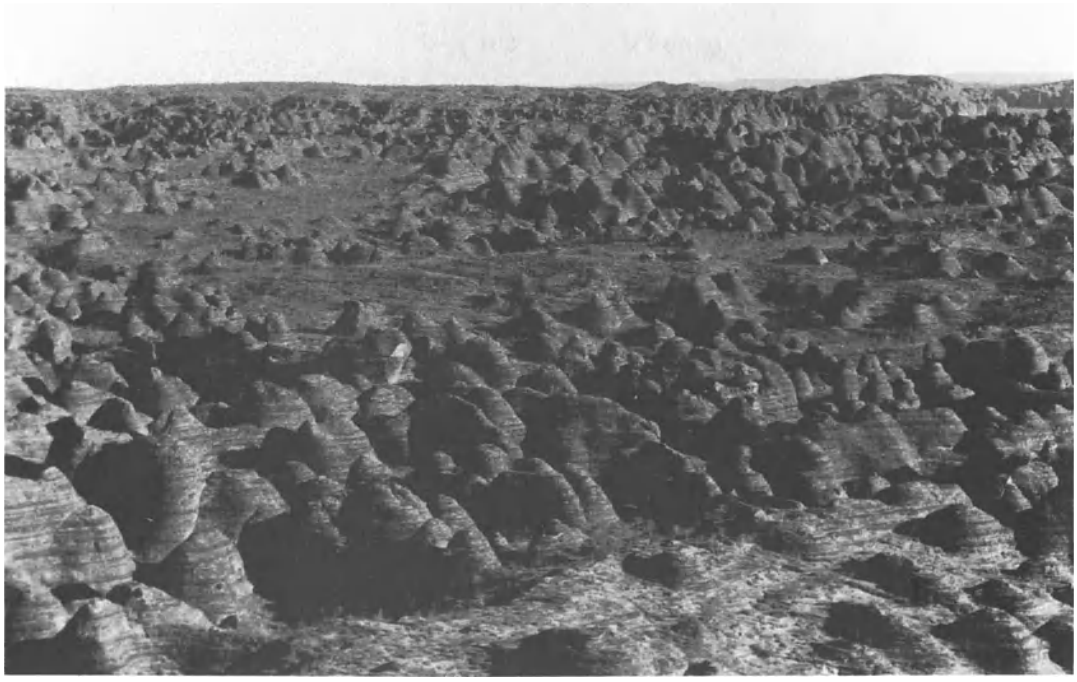

Figure 7.6 Conical hills and sinuous ridges of the Bungle Bungle, northern Australia, rising above a pediment (photo M.J. Selby).

The rock bodies now have relatively high compressive strength (35 to 55 MPa), as applied loads are transmitted by point-to-point contacts between grains, but very low tensile or shear strengths because of weak cementation. The sandstones are now friable and are readily broken down into small blocks or single grains by sediment-laden water. On cliff faces, bedding forms stand out clearly where small-scale fretting and granular exfoliation has undercut more coherent rock units (Fig. 7.7). Stream channels have obviously followed major joints and, in many canyons, streams have undercut valley walls. Below cliffs and escarpments the boundary between the cliff and the pediment is extremely sharp and has angles as high as 90°. Sheet flows crossing the pediments can readily transport the dominantly sand-size grains carried by wet-season flows.

Stream flow and sheet wash are clearly active and the presence of streams in the month of May suggests substantial storage of water in the rocks and the possibility of sapping as a significant factor in slope development. Case hardening is common on most of the slopes to depths of 1 to 10 mm, but whether the deposition of silica and clays to form the casing is still active or is a relic from former dry periods is unclear. There are a few sites in the Bungle Bungle, and in Hidden Valley near Kununurra to the north (see R.W. Young 1987), where thin slab exfoliation has occurred in the relatively recent past and left bare unfretted faces which do not show evidence of case hardening; this may indicate either inactivity of case hardening or just very slow hardening.

The evidence for solution and weakening of the rocks is very clear, but the period over which this has occurred is much more difficult to establish. Caves and dolines in sandstone have usually been attributed to removal of silica in acidic solutions under tropical humid conditions (Pouyllau and Seurin 1985) where there is an abundance of organic molecules. Palaeoclimatic data from Australia indicate that much of the continent had a rainforest cover under which deep weathering profiles and lateritized surfaces developed until at least the middle Miocene when grasslands became common (Kemp 1981). However, laboratory studies of the solubility of silica show that this is greatest when pH is high and that it is enhanced by high chloride concentrations (A.R.M. Young 1987). Potassium chloride crystals have been found in close association with etched quartz grains in the Kimberley

Figure 7.7 Kings Canyon, central Australia, with bedding forms of the sandstone exposed (photo M.J. Selby).

sandstones. Whether much, or all, of the solution took place in humid or in arid conditions is not clear, but it seems probable that it may have occurred in both of these extreme tropical environments.

Some of the landforms described in this section have very similar forms to those found closer to the heart of the Australian arid zone near Alice Springs, where annual rainfall is in the range of 200 to 300 mm (Slatyer 1962). The horizontally bedded sandstones of Kings Canyon area (Fig. 7.7), for example, exemplify a joint-controlled incised landscape in which the canyon walls have a generally convex form and stand above flat-floored valleys and pediments.

Local controls by hard bands in the rock create a waterfall and plunge pool long profile to channel beds. Local rock falls are of greater significance here than they are in the Bungle Bungle. Whether or not solution of the silicate rocks has played any part in the evolution of these landforms is unknown.

The case for calling landforms developed under dominant solution processes 'karstic' has been made by Jennings (1983). These are relatively common in the tropical zone of the Gondwana continents and are of significance in several desert areas. The extent to which they are wholly or only partly inherited from humid environments is unclear.

ETCH PROCESSES AND INHERITED FORMS

Discussions of the development of hillslopes in terms of rock resistance to modern processes and of the effect of modern processes are inevitably limited in their relevance to slopes which may have a history of 100 m.y. or more. The idea of very long periods for landscape development in the core zones of the continents is not new and has a history which can be traced back at least to Suess (German edition, 1885–1909; English edition, 1904–1924) who introduced the word 'shield' for describing the exposed nuclear core of each major land mass. The addition of the word 'craton', by Stille (1924) to distinguish the long-stabilized foundations of Precambrian age of every continent, added to the recognition of great geological age for extensive parts of all continents. Only the platforms of relatively undeformed sedimentary rocks deposited predominantly during marine transgressions, the marginal mobile belts, and the hotspot generated zones of volcanism and rifting disturb the pattern of continental stability. The relevance of these comments to desert hillslopes is that many of the world's most extensive deserts are on cratons and may therefore have had upland masses with a long evolutionary history for their hillslopes.

Remote sensing has given a clear indication of both the extent of bedrock exposures and of features veneered by thin cover beds on desert cratonic surfaces (for example, Brown *et al.* 1989; Burke and Wells 1989). Broad swells and undulations of cratonic surfaces and continental rifting with elevation of rift margins may be attributable to mantle convection. It has been suggested by Fairbridge (1988) that tectono-eustasy related to seafloor spreading has given rise to a thalossostatic condition linked to a biostatic regime (Erhart 1956) marked by a world-wide moist and warm climate with low relief, continuous vegetation cover, abundant non-seasonal rainfall, and strong biochemical weathering. This thalossostatic condition alternated with a disturbed or rhexistatic state in which high-standing continental surfaces (epeirostatic conditions) with low base levels, rejuvenation of fluvial systems, land erosion, seasonal rainfalls, zonally contrasting climates, formation of deserts, and monsoonal weather patterns were major features. Cratonic regions, according to this concept, tend to be characterized throughout geological history by alternation of chemical leaching, weathering, and duricrust formation with periods of erosion, desiccation, and offshore deposition.

Whether or not this grand but simple scheme is valid, it does add a possible explanation for the clear evidence of periodic stripping of weathering mantles from cratonic surfaces with the consequence that many hillforms, and especially those of inselbergs and related forms, have features that have been attributed to weathering beneath deep regoliths, followed by erosional stripping of the mantles and exposure of bedrock.

The idea of nearly world-wide cratonic weathering mantles was most vigorously expressed by Budel (1957) and has subsequently been vigorously espoused as the basis of many geomorphological explanations by Ollier (1988), Thomas (1989a, b), and Twidale (1990). The essence of the theory is that deep weathering mantles are developed through the action of meteoric waters penetrating along joints and fissures and progressively forming a mantle of saprolite which may extend to depths of tens or even hundreds of metres. The processes of alteration are fundamentally chemical, with the production of a residual soil which is leached of soluble material and which is depleted of the colloids removed by drainage waters. That the saprolite is formed without loss of volume is indicated by the survival in it of relict joints, veins of quartz and other structural forms derived from the original bedrock. The loss of mobile elements leaves a low-density residuum.

Weathering mantles commonly develop two major zones: an upper unsaturated zone which has a red coloration and is oxidized and a lower saturated zone which has white to pale green coloration and a reducing environment. The boundary between the two zones is the water table which fluctuates in level seasonally or as a result of storms and droughts. At depth a zone is reached where joints are closed, water cannot penetrate, and therefore weathering cannot operate; this is the basal weathering front. All that is required for deep weathering is deep penetration of ground water in the liquid state (i.e. not frozen) and time. There is no necessary relationship between climate at the ground surface and chemical weathering at depth. At depths ranging from about one to ten metres, depending upon climatic zones and penetration of fresh water, soil temperatures are constant at the mean annual surface temperature. At greater depths the geothermal heat flow controls soil temperatures. The availability of ground water depends mostly on fresh inputs from percolation but is commonly available as 'old' water in arid and semi-arid zones.

It has been pointed out by Habermehl (1980) and Ollier (1988) that the Great Artesian Basin of Australia has ground water extending to depths of 3000 m, so weathering by hydrolysis can also extend to this depth. Stable isotope studies show that the water is of meteoric origin (not connate) and flow rates indicate that it takes two million years for the ground water to flow from recharge areas to discharge zones in artesian springs. The present land surface is a desert, but weathering of the basal rock is occurring under the control of geothermal heat and Pliocene, or early Pleistocene, meteoric water. The Great Artesian Basin is, no doubt, an extreme example but it illustrates the general principle.

Deep weathering profiles have often been associated with current humid tropical climates, perhaps because the surfaces of cratons which are now within the tropics have many land surfaces formed upon deeply weathered mantles. There is increasing evidence that some weathering profiles are of great age; in Australia, for example, Mesozoic and early Cenozoic ages are recognized (Idnurm and Senior 1978). More widely it has been recognized that relics of deep weathering profiles occur in areas which are far from the tropics. Hack (1980) noted saprolite in the Piedmont and Blue Ridge areas of the Appalachians with an average depth of 18 m and a maximum depth which may exceed 90 m; Hall (1986) identified preglacial saprolites in Buchan, Scotland, up to 50 m deep, and in the Gaick area of the Grampian Mountains up to 17 m (Hall 1988);

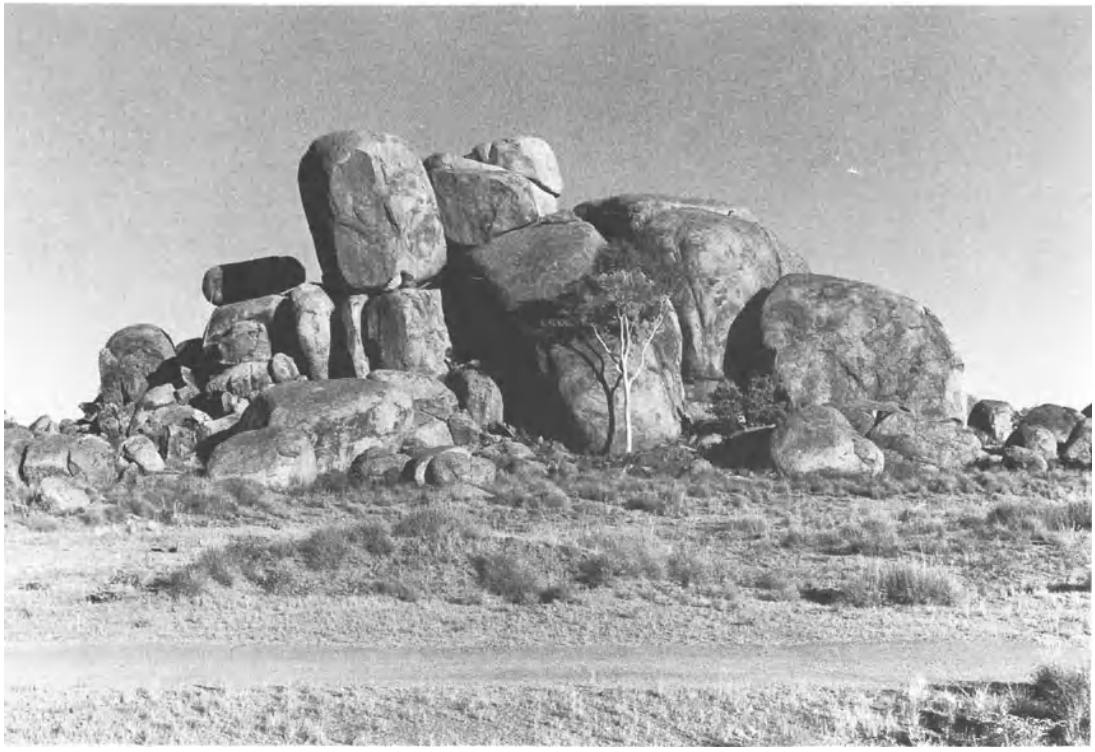

Figure 7.8 Devils Marbles, central Australia, which have been interpreted as residual etchforms developed within a weathering mantle which has now been stripped (photo M.J. Selby).

Bouchard (1985) has found saprolites up to 15 m thick at protected sites covered by Quaternary ice sheets in Canada.

The relevance of all of these observations for an understanding of hillslope development in the modern desert zones is that many features now visible may have developed at the basal weathering front and later been exposed at the ground surface as regolith was stripped in periods of rhexistasy.

ETCH FORMS OF DESERTS

The recognition that boulders, and other minor and major forms, have developed within weathering mantles and at the weathering front has a long history which goes back to the beginning of modern geology (Twidale 1990). These forms when exposed by mantle stripping are collectively known as etch forms (Wayland 1933). Weathering fronts are particularly sharp in granitic and other crystalline rocks of low permeability. The front is more diffuse, and essentially a zone, in the weaker sedimentary rocks. Crystalline rocks commonly form the bedrock of cratons, and the various associations of boulders recognized as boulder-strewn platforms (Oberlander 1972), tors or koppies (Fig. 7.8) are readily identified as remnants of corestones because corestones are common in exposures through weathering mantles. Perhaps more significant was the proposal by Falconer (1911) that the inselberg landscapes of northern Nigeria were shaped not by epigene processes but by chemical action of waters acting at the weathering front. Furthermore, he recognized that the variations in depth of penetration of the front were controlled by the spacing of joints in the bedrock. The result of mantle stripping was therefore an irregular land surface with inselbergs standing above plains with residual mantles of varying depth. Such ideas were elaborated into a system of geomorphological evolution of the cratonic surfaces by Budel (1957, 1982).

The evidence in favour of the concept of etchforms developing on cratonic surfaces is now very strong. It indicates the development of currently exposed land surfaces over periods of 100 m.y. or more. This timespan far exceeds the period of existence of the world's major deserts which are mid to late Tertiary in origin (see Selby 1985 for a review). The obvious

conclusion is that many of the major hill mass and plain landforms had an origin beneath deep weathering mantles of ancient origin. Subsequent mantle stripping has exposed them to subaerial processes of weathering and erosion. In the time since exposure, denudation of bare rock has been sufficient for many hillslopes to achieve slope angles which are in equilibrium with the mass strength of their rocks, but on hillslopes formed of massive rocks with little pre-existing jointing the possible controls on form include survival of etch forms; survival of the original form through stress release joints developing nearly parallel to the original rock surface; the development of cross fractures which permit an incomplete adjustment to the slope angle controlled by rock mass strength; survival of structural influences and controls; dominance by solution processes; control by talus covers and formation of Richter-denudation slope units; undercutting of upper slope units by sapping, stream action, or recession of an underlying weak rock unit.

SLOPES IN LAYERED ROCKS
by Alan D. Howard

Many desert areas are underlain by generally flat-lying sedimentary rocks of varied composition, sometimes intermingled with tabular intrusive or extrusive volcanic rocks. Examples include the Colorado Plateau in the south-western United States, North Africa, the Arabian peninsula, and portions of the other major deserts. The erosion of such sedimentary sequences creates a landscape of scarps or cuestas capped by the more resistant rock units. By contrast, a few desert areas, such as the Zagros Mountains region of Iran, have complex patterns of cuestas, hogbacks, strike valleys, etc. developed in strongly folded or faulted layered sedimentary rocks. The discussion here will focus on the simple cuesta landforms of flat or inclined beds, although the general principles are applicable in areas of more complicated structure.

The classification of rock slope types introduced by Selby (1980, 1987) and Moon (1984b) can also be applied to cuesta landforms. Figure 7.9 shows a classification of slope elements on an eroded anticline in layered rocks. Strength equilibrium slopes (shown by =) occur primarily on cliff faces eroded by small rockfalls, but where such cliffs are actively eroded by stream undercutting (+U+) they may be steeper than strength equilibrium. Scarp faces dominantly eroded by landslides may be less steep than strength equilibrium and those dominantly wasted by rockfalls involving the entire cliff face may be steeper than strength equilibrium. Structurally controlled slopes (−S−) occur where erosion of weaker layers exposes the top surface of resistant rocks. Normal slopes in weak rock (typically badlands with shallow regolith) are shown by −E−. Rampart slopes in weak rocks below cliffs of resistant rock will generally be talus (−D−) or Richter slopes (not shown).

In a general sense cuestas are an automatic adjustment of the landscape to permit rocks of varied erosional resistance to be eroded at roughly equivalent rates (Hack 1966). When a resistant rock layer is first exposed the erosion rate diminishes on the exposed top of the resistant layer as the overlying weaker rocks are removed, often creating lithologically controlled near-planar upland surfaces called stripped plains. As the resistant layer becomes more elevated relative to surrounding areas of weaker rocks, the caprock is eventually breached, exposing underlying weaker rock units, whose rapid erosion creates a steep scarp and accelerated caprock erosion by virtue of the steep gradients relative to the superjacent stripped plain. This discussion of such scarps is organized into two general headings: evolution of scarps in profile and evolution of scarp planforms. Examples are taken primarily from the Colorado Plateau, south-western United States. Additional illustrations of the features described here and a road log of sapping and geologic features are given in Howard and Kochel (1988).

EVOLUTION OF SCARPS IN PROFILE

Resistant sandstones, limestones, and volcanic flows and sills in desert areas are generally exposed as bare rock slopes except where mantled with aeolian sands or alluvium. However, areas of very low relief, such as stripped plains, may be mantled with sandy, cobbly, poorly horizonated soils and scrubby vegetation. Two morphological end members characterize the resistant rock exposures, low to high relief slopes in massive rock (in particular, the rounded sandstone exposures termed 'slickrock') and cliff or scarp slopes developed where the caprocks are being undermined. Emphasis in this section is placed on scarp-front processes and morphology. An intermediate landform type, termed segmented cliffs by Oberlander (1977), will also be discussed.

The more readily weathered and eroded rock units, generally shales or poorly cemented sandstones or alluvium, are commonly eroded into badlands where they are thick (Chapter 9). But in areas with thick interbedded caprock-forming units the

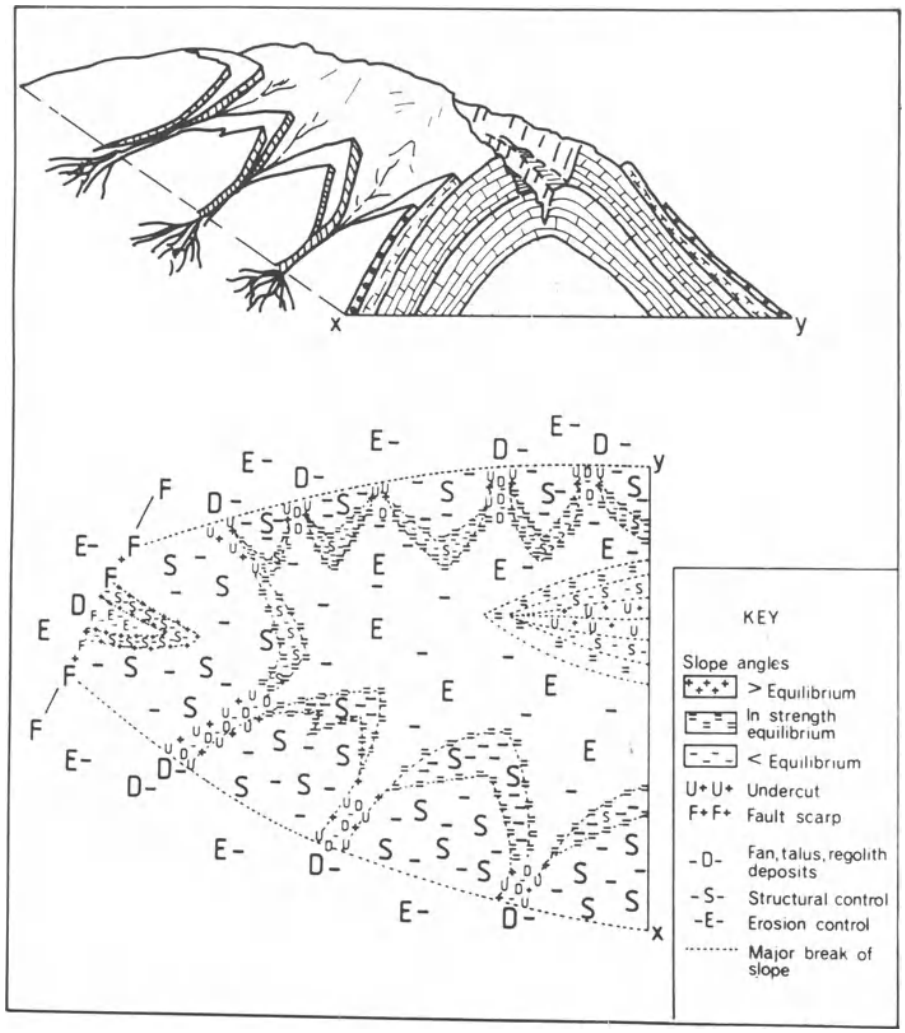

Figure 7.9 Identification of landform elements on cuestas in folded rocks (from Selby 1987, fig. 15.13).

easily eroded strata are usually exposed primarily on the subcaprock slopes or ramparts. Terms used here to describe the characteristic parts of an escarpment are shown in Figure 7.10. Several alternative terms have been used to denote the rampart, including subtalus slope (Koons 1955), debris-covered slope (Cooke and Warren 1973), footslope (Ahnert 1960, Oberlander 1977), lower slope (Schmidt 1987), and substrate ramp (Oberlander 1989).

The exposure of weaker strata (generally shales or poorly cemented and/or highly fractured sandstones) beneath massive sandstones causes undermining of the sandstone, leading to cliff development and rapid scarp backwasting. A far greater volume of rock is initially broken up by scarp retreat than by erosion on backslopes when considering average rates over large areas. Because of the rapid retreat of scarp slopes, the cliffs generally eat back into pre-existing backslopes. Figure 7.11 shows an example where updip exposure of shale near the stream level (right side of picture) has caused development of cliffs and their backwasting into sandstone slickrock slopes; such undermining was discussed by Ahnert (1960) and Oberlander (1977). The relief developed on scarp backslopes depends upon the erodibility of the caprock unit compared with overlying units, the thickness of the caprock, the types of weathering and erosional processes acting on the exposed rock, and rates of basel level lowering.

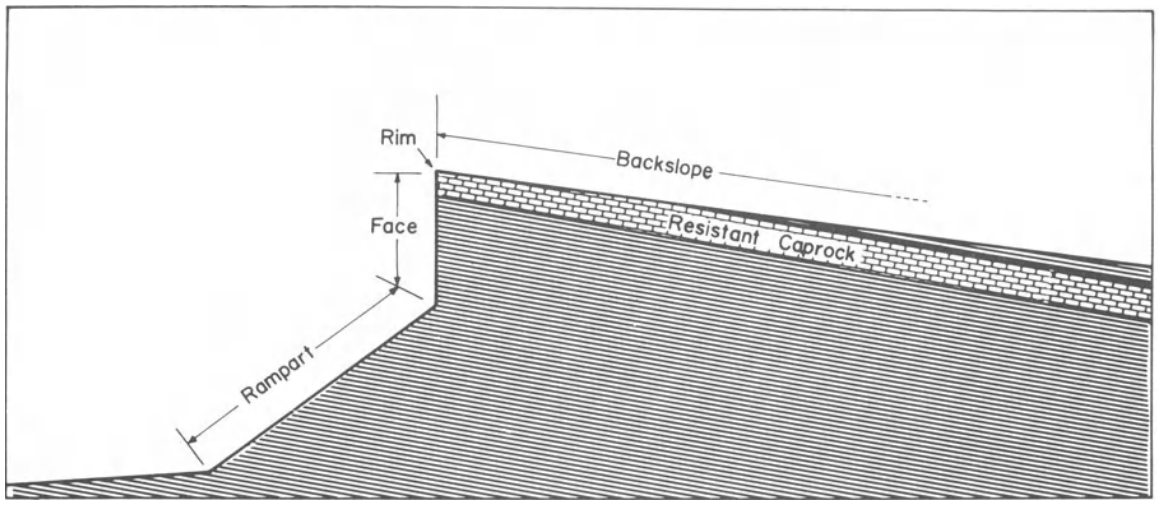

Figure 7.10 Escarpment components. The face is the vertical to near-vertical cliff developed at the top of the escarpment mostly in the caprock but occasionally extending into the non-resistant layer beneath. The rampart is a slope of lesser inclination extending from the bottom of the face to the base of the escarpment which is commonly partly mantled with debris from backwasting of the face (from Howard 1970, fig. 55).

Figure 7.11 Landforms of De Chelly Sandstone north of Kayenta, Arizona along US Highway 163. Slickrock slopes to left give way to vertical scarps at right where undermining is active due to exposure of shaly Organ Rock Tongue at the base of the scarps (photo A. Howard).

Processes of Scarp Erosion

Wasting of caprocks occurs primarily by rockfall, block-by-block undermining, and slumping. Some sandstone caprocks (e.g. the Morrison Formation of the American South-west) are undermined block-by-block by weathering and erosion of the underlying shale without rapid fall of the undermined blocks (Fig. 7.12). The blocks may be repeatedly lowered with little downslope sliding or rolling, but typically the blocks slide and occasionally roll a short distance upon being undermined. Block-by-block undermining requires a relatively thin caprock, well-developed jointing, and shale that weathers easily by addition of water (e.g. the smectitic Morrison Shale). Slumping is prevalent on relatively few escarpments, where it may dominate as the mechanism of scarp retreat (Fig. 7.13). The Toreva block slumps are a classic example (Reiche 1937), and other examples have been discussed by Strahler (1940) and Watson and Wright (1963). Conditions leading to slumping failure have not been firmly established, but a low shear strength of the unweathered subcaprock unit is probably the major factor. Low shear strength can

Figure 7.12 Block-by-block undermining of channel sandstones in shales of Morrison Formation, near Hanksville, Utah (a and b) (photo A. Howard).

Figure 7.13 Slump failure of Morrison–Summerville escarpment near Hanksville, Utah (photo A. Howard).

result from low bulk strength or a high degree of fracturing and/or abundant bedding plane partings. Other factors may be deep weathering of the subcaprock unit by groundwater flow and high pore water pressures. Landslide and rockfall processes were summarized in Anderson and Richards (1987) and Brunsden and Prior (1984).

Rockfall is the most common form of scarp retreat (Fig. 7.14), involving events ranging from calving of individual blocks to the failure and fall of a wide segment of the face, resulting in a rock avalanche on the scarp rampart. Debris produced by rockfalls with high potential energy may result in powdering of a large percentage of the original rock (Schumm and Chorley 1966), but on most scarps the coarse debris produced by the rockfalls must be weathered and eroded before further scarp retreat can occur (Fig. 7.15). Weathering processes acting on the debris are similar to those occurring on slickrock slopes, including splitting or shattering, granular disintegration, and solution of cement (or the rock *en masse* in the case of limestones). The necessity for weathering of scarp-front debris before further erosion of the subcaprock unit leads to a natural episodic nature of rockfalls and scarp morphology, as outlined by Koons (1955), Schipull (1980), and Schmidt (1987) (Fig. 7.14). Where caprocks are eroded primarily by large rockfalls continued erosion of the subcaprock unit at the margins or base of the rockfall eventually raise the debris blanket into relief, sometimes forming subsidiary small escarpments where the debris blanket is subject to further mass wasting. Thus old rockfalls stand well above surrounding slopes of both exposed subcaprock unit and younger rockfalls. When these old rockfalls are contiguous with the scarp face, they prevent the development of high relief at the cliff face, and thereby inhibit further rockfalls until the talus is weathered and eroded. In some cases the talus at the foot of the rampart becomes isolated from the scarp face as erosion of the subcaprock unit continues, forming a talus flatiron (Koons 1955, Schipull 1980, Gerson 1982, Schmidt 1987). Talus flatirons thus formed have been termed non-cyclic flatirons as contrasted with similar features resulting from climatic fluctuations (Schmidt 1989a) (Chapter 21). Schmidt (1987, 1989a) suggested that flatirons are best developed in scarps with heterogeneous subcaprock strata, including beds of variable resistance and slope inclination. However, flatirons are also well developed on the scarps of the Colorado Plateau composed of massive sandstones over homogeneous marine shales. Gerson and Grossman (1987) noted that flatirons are absent on desert scarps lacking a strong caprock over a weaker subcaprock unit.

Most prominent scarps on the Colorado Plateau are formed of massive sandstone underlain by shale or other easily weathered rock, so that backwasting

Figure 7.14 Portion of escarpment of Emery Sandstone over Mancos Shale on North Caineville Mesa near Hanksville, Utah, along Utah Highway 24. Note extensive deposits of rockfall debris that are dissected by continuing erosion of shale on rampart. Cliff in alcove extends far into the underlying Mancos Shale. Seepage line is present at base of the Emery Sandstone in the alcove. High debris blankets to right and left of alcove that extend upward to the base of the sandstone are strongly dissected at their base. Presence of the debris blanket inhibits further scarp backwasting until the debris is weathered and eroded. These high debris blankets are probably a Bull Lake equivalent (Illinoisan?) pluvial deposit. The badlands in the foreground resulted from dissection of a Bull Lake pediment extending from the escarpment to Bull Lake gravels (now terraces) along the Fremont River behind the photographer (photo A. Howard).

is caused by a combination of weathering of exposed caprocks (e.g. off-loading fracturing, freeze–thaw, and groundwater sapping) and loss of bulk strength of the underlying layer accompanied by erosion of the scarp rampart. However, some of the incompetent layers producing scarps are strong in bulk but are eroded primarily because of denser fracturing relative to more massive (but not necessarily stronger) overlying sandstones (Oberlander 1977, Nicholas and Dixon 1986). Creep of subcaprock shales has been implicated in breakup of caprocks (block gliding) in humid environments (e.g. Zaruba and Mencl 1982) but has not been noted on desert scarps. It is possible that slight creep or off-loading expansion in shales may locally be a factor in development of off-loading fractures in overlying sandstone caprocks. Gravity-induced creep of evaporite beds has been suggested as the mechanism responsible for creating the miniature horst and graben structure of the Needles District in Canyonlands National Park, Utah (McGill and Stromquist 1975).

Although rockfall and slumping are the major transport processes in scarp backwasting, weathering and erosion by groundwater commonly can be as, or more, important in weakening the scarp face than is undermining by erosion of the rampart. The role of groundwater sapping is discussed separately below.

The amount of caprock talus exposed on scarp ramparts depends in part on the planform curvature of scarps, being greater in re-entrants where caprock debris converges on the lower rampart and lesser in front of headlands or projections (or around small buttes) where debris is spread radially. The amount of debris is also controlled by spatial variations in rates of scarp retreat (generally higher at the head of re-entrants) and by the volume of caprock eroded per unit amount of backwasting, which is higher in re-entrants and lower at headlands.

Scarp ramparts are eroded by a variety of processes, including normal slope and rill erosion where the subcaprock unit is exposed and weathering and erosional processes act on caprock detritus. Weathering processes on talus include frost and/or hydration splitting or shattering, spalling due to salt crystallization (primarily on unexposed surfaces), granular disintegration, and solution. The relative mix of these weathering processes depends upon

Figure 7.15 Recent rockfall in Navajo Sandstone in the Inscription House area of the Navajo indian reservation showing abundant rockfall debris (photo A. Howard). Cliff above rockfall is approximately 30 m tall.

the size and composition of the talus. Calcareous-cemented sandstones, common on the Colorado Plateau, are primarily shattered in large blocks, but succumb to granular disintegration in small blocks, yielding easily eroded sand-sized detritus. On the other hand, siliceous-cemented sandstones do not weather by granular disintegration, and large blocks of caprock commonly remain behind as the scarp retreats (Fig. 7.12b).

Where caprock debris is copious or very resistant, the talus material may be reworked several times before its final removal due to continuing erosion of the subcaprock unit, forming elevated blankets eroded at its margins as subsidiary scarps (e.g. the flatirons discussed above), development of individual rocks on subcaprock unit pedestals (damoiselles), or less dramatic undermining and rolling of individual boulders. Slopewash and gullying are important in removing sand- to gravel-sized weathering products, and some talus blankets are extensively modified by, or even emplaced by, wet debris flows (Gerson and Grossman 1987).

Absolute and Relative Rates of Scarp Erosion

A variety of methods has been used to date regional rates of scarp retreat in desert areas, including archaeological dating (Sancho *et al.* 1988), beheading of consequent valleys (Schmidt 1980, 1989b), stratigraphic relationships with dated volcanic or sedimentary deposits (Lucchitta 1975), and age of faulting initiating scarp retreat (Yair and Gerson 1974). Inferred retreat rates vary over two decades from about 0.1 to 10 m $1000\,y^{-1}$ (Schmidt 1988, 1989b, Oberlander 1989). The primary long-term controls over erosion rates are rate of base level lowering and rock dip, as discussed below. However, short-term erosion rates are strongly influenced by climate variations and climate-related changes in local base level.

The relative rates of erosion on different parts of cuestas can be illustrated by considering, as a first approximation, that the form elements maintain a constant gradient and a constant position relative to the stratigraphic layers through time. These assump-

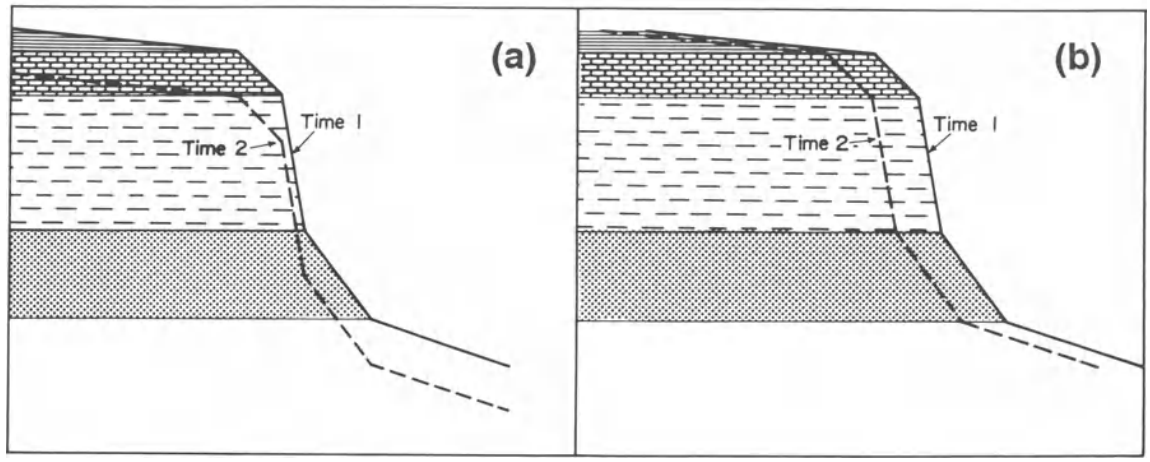

Figure 7.16 Erosion of a compound hillslope under the assumptions of (a), uniform rate of downwasting on all slope elements, and (b), maintenance of correlations between slope elements and stratigraphic units. Both assume that gradients of the respective elements remain constant through time. Under the first assumption (a) the volume of material removed increases with decrease of gradient, whereas the volume decreases in (b) (from Howard 1970, fig. 56).

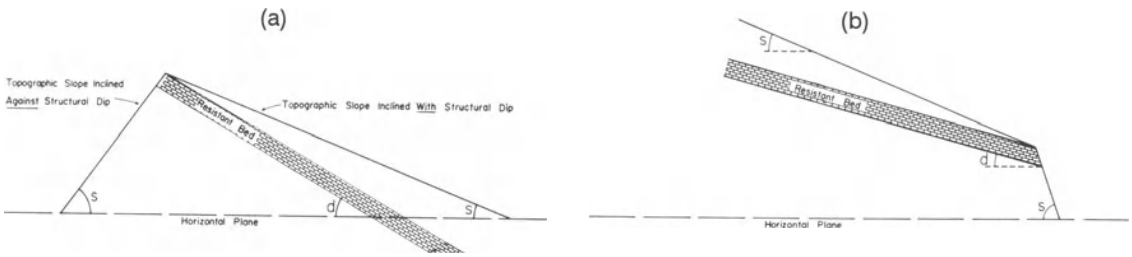

Figure 7.17 Definition of angles and slope elements on escarpments in dipping strata (from Howard 1970, fig. 58).

tions require a constancy of both stream erosion and slope processes through time, which probably approximates the long-term average behaviour of scarp erosion but not the short-term changes due to climatic fluctuations. The assumption of a constant position of slope elements relative to the stratigraphy (Fig. 7.16b) is clearly a closer approximation to scarp evolution than the assumption that slope elements retain a constant position through time (i.e. a constant rate of vertical erosion on all elements of the scarp (Fig. 7.16a)).

In horizontal stratified rock these assumptions predict a rate of vertical erosion proportional to the slope tangent, whereas the horizontal rate of erosion (lateral backwasting) is identical on all slope elements (Fig. 7.16b). This implies an infinite rate of downwasting for a vertical cliff, which is an artifact of considering cliff retreat as continuous erosion rather than as discrete events such as rockfalls. Therefore, as mentioned above, on a typical escarpment the downwasting of the slickrock slope on top of the caprock is very slow compared with both cliff retreat and vertical erosion below the rim.

The relative rates of erosion on various slope elements are also affected by the structural dip. If all form elements erode at an equal rate parallel to the structure (that is, in a downdip direction) with constant gradient, then the instantaneous rate of vertical downwasting V_t is given by the structural dip d, the slope angle s, and the rate of downdip backwasting of the escarpment D_t. Where the slope is inclined with the dip (Fig. 7.17a),

$$V_t = D_t(\sin d - \cos d \tan s), \text{ for } 90° > d > s > 0° \tag{7.2}$$

and (Fig. 7.17b),

$$V_t = D_t(\tan s \cos d - \sin d), \text{ for } 90° > s > d > 0° \tag{7.3}$$

Where the slope opposes the structural dip (Fig. 7.17a):

$$V_t = D_t(\sin d + \cos d \tan s), \text{ for } 90° > s > 0°. \tag{7.4}$$

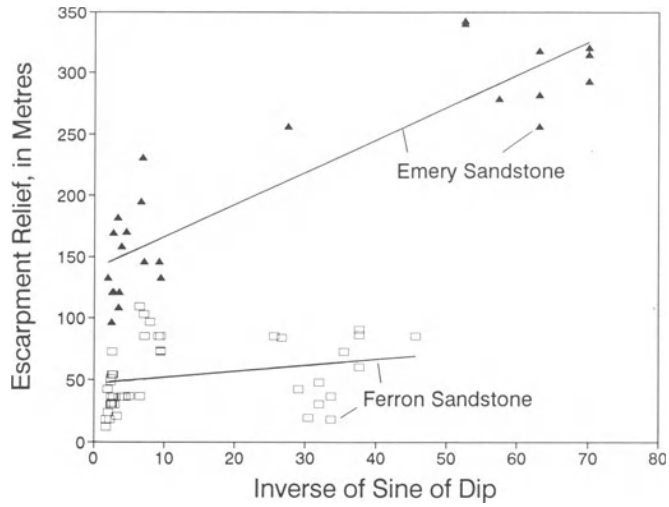

Figure 7.18 Relief of escarpments in dipping strata as a function of the angle of dip for two sandstones sandwiched between over- and underlying shales. Relief is measured from crest of escarpment to base of scarp rampart (see Fig. 7.10). Each data point is a measurement from a separate location along the western edge of the Henry Mountains, Utah. A least-squares regression line has been fitted to observations from each sandstone scarp (based on Howard 1970, fig. 59).

During continued downcutting by streams draining the escarpment, the relief should adjust until downdip exposure of new caprock and updip removal by backwasting are roughly balanced. Therefore the rate of vertical reduction of the rim should be independent of the dip (maintaining a constant relief through time), whereas horizontal retreat of the escarpment would be inversely proportional to the tangent of the dip, and the volume of caprock eroded per unit time would be inversely proportional to the sine of the dip. The very rapid rate of horizontal retreat predicted for low dips does not occur because the escarpment becomes segmented by erosion along drainage lines into isolated mesas and buttes whose local relief, distance from the main escarpment, and rate of backwasting increase through time. Nevertheless, these considerations imply that, in general, a greater volume of rock must be eroded per unit time from gently dipping scarps than from steeper ones. The gradients and total relief on a given scarp should increase where the structural dip decreases to maintain relatively constant rates of vertical reduction of the rim. Figure 7.18 compares relief of escarpments on two sandstones in the Henry Mountains area, Utah, as a function of the reciprocal of the sine of the dip, showing that there is a relationship of the type predicted for the Emery Sandstone. The relationship is poor for the low escarpment of Ferron Sandstone. Areal variations in fluvial incision at the scarp base since the Bull Lake glacial maximum (varying from about 60 m along Fremont River to a few metres in remote locations) may be responsible for the large scatter for this low scarp.

The overall height and steepness of a given scarp should be controlled by one of three factors: (a) development of sufficient relief to trigger caprock mass wasting (which will be related to caprock resistance); (b) the rate of weathering and erosion of caprock debris on scarp ramparts; and (c) the rate of erosion of the subcaprock unit.

Caprock resistance has been suggested as a controlling factor by Schumm and Chorley (1966), Nicholas and Dixon (1986) (who related scarp backwasting rates to degree of fracturing of the lower caprock unit), and Schmidt (1989b) (who found a strong relationship between regional backwasting rates and the product of caprock thickness and a measure of caprock resistance). To the degree that scarps adjust over long time intervals to balance rate of caprock removal with long-term rates of base level lowering (i.e. V_t in Equations 7.2–7.4 is areally uniform), relationships between backwasting *rate* and caprock resistance of the type found by Nicholas and Dixon (1986) and Schmidt (1989b) cannot be universally valid (although *local* variations in backwasting rates on a given scarp may be related to caprock resistance as found by Nicholas and Dixon (1986) due to exposure of zones of caprock of differing resistance to erosion). Rather, the backwasting rate D_t will adjust to be a function only of rock dip and regional erosion rate V_t. As suggested

above, overall scarp height and steepness adjust to equalize erosion rates, and these should be related to caprock resistance and thickness (the scarps in the thin Ferron Sandstone are lower than those of the massive, thick Emery Sandstone (Fig. 7.18)). It seems reasonable that a threshold scarp steepness and/or height would be required to trigger the more energetic types of mass wasting processes, such as rock avalanche and landsliding. Block-by-block undermining small rockfalls and caprock weakening by groundwater sapping are less clearly related to overall scarp relief.

Koons (1955) emphasized that accumulated caprock talus protects the caprock from further large rockfalls until it is removed. Koons (1955) and Howard (1970) suggested that the length of the rampart self-adjusts over the long run to provide a surface area sufficient to weather talus at the rate that it is supplied. Schumm and Chorley (1966) introduced the talus weathering ratio, which they defined as the ratio of the rate of talus production from the cliff to the rate of talus destruction on the rampart. They noted that a ratio greater than unity leads to a moribund scarp choked in its own detritus, similar to the models of Lehmann (1933) and others (summary in Scheidegger 1991, pp. 130–4). Schumm and Chorley (1966) suggested that ratios less than unity characterize certain nearly debris-free scarps encountered on the Colorado Plateau. However, over the long run, continuing scarp retreat implies the talus weathering ratio equals unity, since only as much talus can be weathered as is produced (Gerson and Grossman 1987, Howard and Kochel 1988). This concept can be illustrated by letting P equal the volumetric rate of supply of caprock talus per unit time per unit width of scarp, K equal the potential volumetric erosion rate (either weathering- or erosion-limited) of talus per unit area of scarp rampart, and L the required rampart length. Then for balance of addition and removal

$$L = P/K \tag{7.5}$$

However, as discussed below, this ratio may vary considerably as a result of climatic fluctuations as well as local short-term imbalances of P and K, as discussed by Koons (1955). Since talus on ramparts is composed of caprock debris, scarp relief controlled by talus weathering will be indirectly controlled by caprock resistance.

The rate of erosion of the subcaprock bedrock (commonly shales) has been cited as the controlling factor for scarp erosion rates by Gerson and Grossman (1987) and Schipull (1980). Strictly speaking, if the rate of subcaprock bedrock erosion were the dominant factor in scarp retreat, scarps should not be higher or different in form than other slopes in the subcaprock unit where no caprock is present. None the less, it is true that base level control is transmitted to the scarp via the channels and slopes developed in the subcaprock unit.

It is likely that these three factors vary in relative importance in controlling scarp form from scarp to scarp, from place to place on the same scarp, and through time as climate and/or base level control varies. Scarps that backwaste largely by rockfall are most likely to have planforms controlled over the long run by requirements for weathering of caprock debris, leading to the observation that 50 to 80% of the scarp front is covered by talus at equilibrium (Gerson and Grossman 1987). As will be discussed further below, many scarps on the Colorado Plateau are quite stable under the present climatic regime, so that the ramparts are nearly bare of talus, and tall cliffs have developed in both the caprock and in the subcaprock shales. Thus both base level control and talus weathering at present have little influence on scarp form, and the backwasting that does occur is largely due to caprock weathering and small rockfalls. On the other hand, for escarpments characterized by block-by-block undermining (Fig. 7.12) caprock resistance is less important than erosion of the subcaprock shales. In fact, where the caprocks consist of hard-to-weather silica-cemented sandstones, caprock boulders may be gradually let down by undermining and rolling while the escarpment continues to retreat, leaving piles of large caprock fragments (Fig. 7.12b).

Schmidt (1989b) noted that very resistant caprocks often include less resistant beds in the subcaprock strata that, in the absence of the more resistant overlying bed, would independently form scarps. In sections of scarp that are linear or indented, debris shed from the overlying caprock largely prevents development of subsidiary lower scarps, but in front of headlands, where rapid retreat of the main caprock and radial dispersal of its detritus leave the subcaprock units largely free of talus, the lower resistant units commonly form low scarps.

Backslopes on Caprock

In the classic case of a scarp composed of a thin resistant layer sandwiched between thick, easily eroded strata (Fig. 7.10) the caprock is exposed as a low-relief stripped plain on the scarp backslope, and caprock erosion occurs primarily at the scarp face. However, when the caprock is thick, erosional

Figure 7.19 Polygonal superficial fracturing of Navajo Sandstone along Utah Highway 12 west of Boulder, Utah. Individual 'elephant-hide' polygons are about 1 to 2 m in size (photo A. Howard).

sculpting of the backslope may be as or more important than the lateral attack at scarp faces. Landform development on thick, homogeneous rocks is discussed in the Slopes in Massive Rocks section, but processes and landforms on slickrock slopes are outlined here because of their importance in development of segmented scarps.

The striking and unusual slickrock slopes occur on desert sandstone exposures as low, generally rolling relief on bare rock slopes (Figs 7.11 and 7.19). Hill forms are generally convex to convexo-concave and rather irregular due to the prevalence of small-scale structural and lithologic controls exerted by the exposed rock upon weathering and erosional processes. Slickrock slopes occur most commonly on the backslopes of cuestas, but high relief forms occur in thick, massive sandstones such as the Navajo Sandstone. Where strong structural control by jointing or faulting occurs, the fractures tend to be eroded into furrows or valleys, and the sandstone landscape takes on a reticulated or maze-like appearance as at Arches National Park, Utah. Doelling (1985) noted that sandy colluvium collecting along depressions developed on joints accelerates weathering of the sandstone by providing a moist environment; thus the influence of fractures on the topography is enhanced by a positive feedback on weathering rates. Small-scale horst-and-graben development associated with extension caused by flow of underlying evaporites has created the 'needles' section of Canyonlands National Park, Utah (McGill and Stromquist 1975).

Slickrock slopes are weathering-limited (Carson and Kirkby 1972, pp. 104–6) in that transport processes are potentially more rapid than weathering processes. That is, loose debris is removed from the slopes as fast as it is produced by weathering so that little or no loose residuum covers the bedrock. On slickrock slopes the bedding is emphasized by the grain-by-grain loosening or disintegration of thin surface crusts or whole layers of the sandstone exposed on these weathering-limited slopes, particularly on exposures of the massively cross-bedded Navajo Sandstone (Fig. 7.20). Coarser sand layers with fewer grain-to-grain contacts weather and loosen most readily, aiding differential surface expression of minor lithologic variations (Hamilton 1984). Despite these microscale lithologic controls, the slickrock slopes generally show only minor form control by bedding and the fairly planar to rounded slopes cut across bedding planes (Figs 7.11, 7.19).

The major reason for development of smooth, generally convex slopes is the development of exfoliation or sheeting fractures in massive, poorly

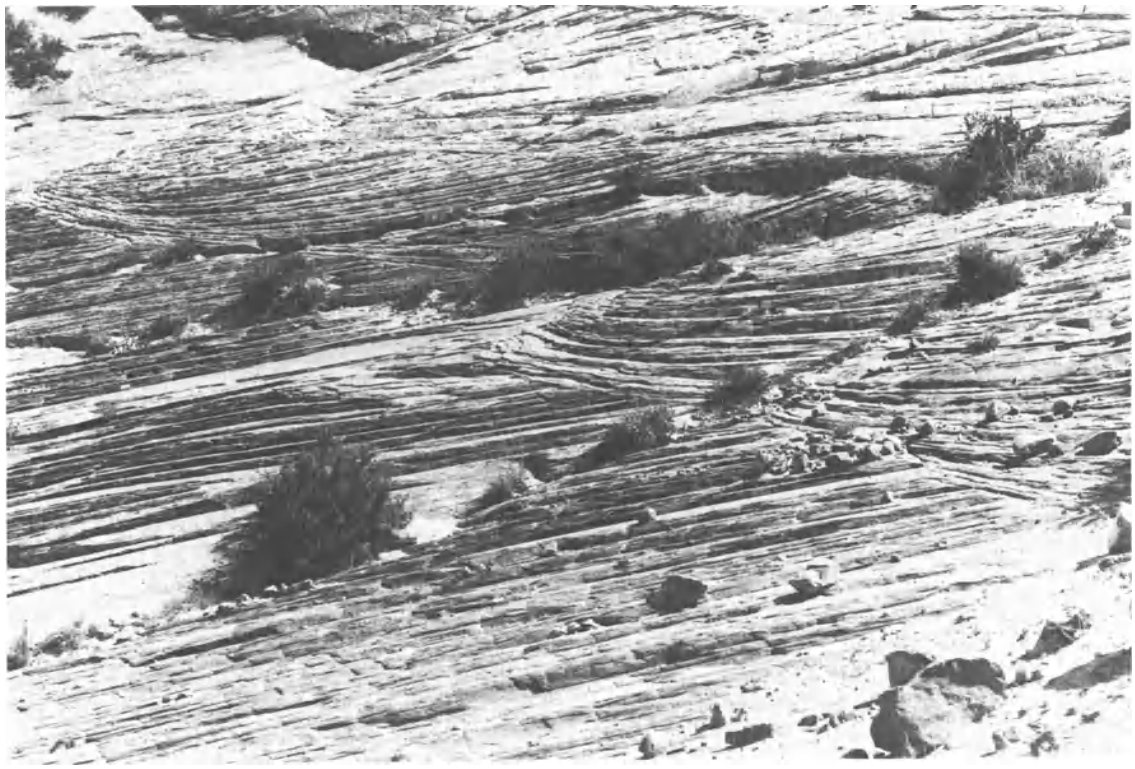

Figure 7.20 Expression of bedding in slickrock slopes in Navajo Sandstone near Utah Highway 12 west of Boulder, Utah (photo A. Howard).

jointed (referring here to pre-existing regional or systematic jointing) sandstones such as the Navajo Sandstone (Bradley 1963). The fracturing may be due to stress relief (Bradley 1963), expansive stresses due to weathering of near-surface beds (Hamilton 1984), and possibly freeze–thaw. These mechanisms produce lenticular sheets of thickness ranging from a few centimetres to a metre or so, with more widely spaced fractures below these, fading out within 10 to 20 m from the surface. Thus the exfoliation joints form 'a crude, somewhat subdued replica of the surface form' (Bradley 1963, p. 521). Although grain-by-grain removal of sand grains loosened by solution of the calcite cement or peeling of thin (<1 cm) weathered rinds seems to be the dominant erosional process, deeper weathering is indicated locally by the presence of shallow jointing perpendicular to the sandstone surface. In massive sandstones these cracks create a network pattern with a scale of 1 to 5 m that clearly wrap around existing topography, creating an 'elephant hide' pattern (Fig. 7.19). Where strong layering is exposed in cross-section, the cracks follow bedding planes and also create fractures cutting across the bedding, forming a 'checkerboard' or 'waffle' pattern as at Checkerboard Mesa, Zion National Park, Utah. The effective depth of these fractures is probably about 1/5 to 1/2 their lateral spacing. Hamilton (1984, pp. 32–4) suggested the fractures result from cyclic near-surface volume changes resulting from thermal cycling, wetting and drying, or freeze–thaw.

In addition to exfoliation, any weathering process that acts through some depth from the surface will tend to erode away projecting masses due to the greater surface area relative to volume and lead to a 'grading' of surface slopes, with a characteristic scale of action of the same order of magnitude as the depth of weathering (presumably a few centimetres to a few metres). Such processes may include solution of cement, weathering of feldspars and clays, disruption of the rock along microfractures and between grains due to differential volume changes produced by temperature changes, freeze–thaw, or shrink–swell of clays.

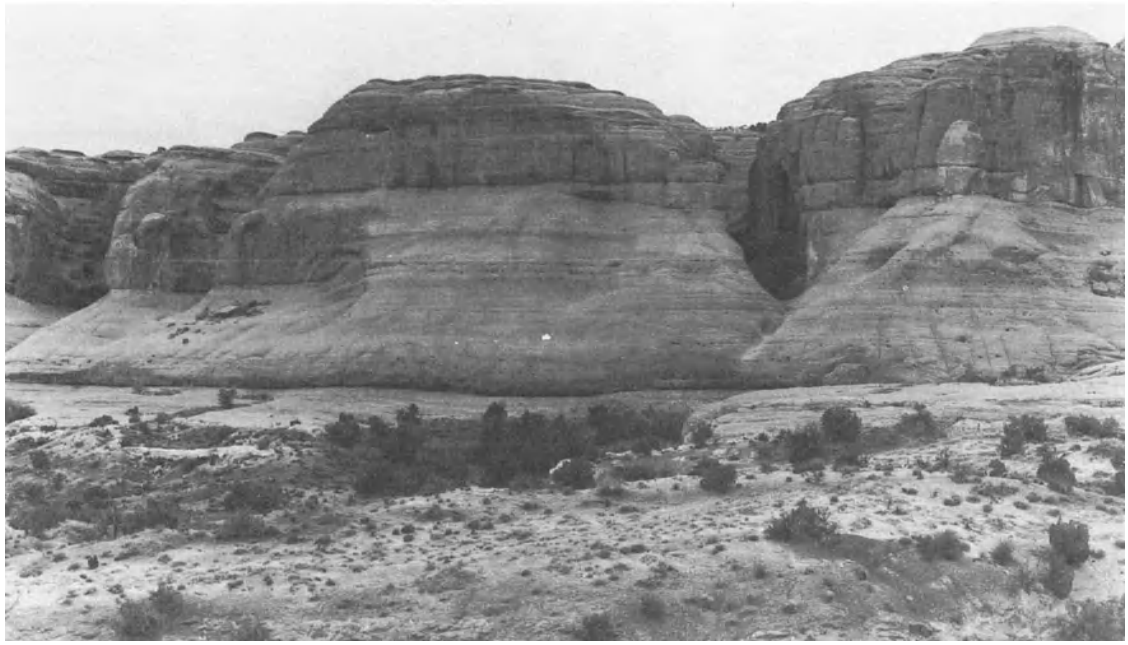

Figure 7.21 Segmented scarp in Entrada Sandstone at Arches National Park, Utah, showing slickrock slopes, slab walls, and effective partings at base of slab walls. Note that the prominent slab wall in the middle of the scarp at left dies out before the centre of the photo due to pinching out of the effective parting (photo A. Howard).

Segmented Scarps

Many areas of moderate relief on sandstones on the Colorado Plateau exhibit a complex topography embodying both elements of slickrock morphology and of scarps. Such landscapes developed in the Slick Rock member of the Entrada Sandstone at Arches National Park, Utah, were the object of a comprehensive study by Oberlander (1977). In this area slickrock slopes are interrupted by nearly vertical cliffs which Oberlander termed slab walls due to their erosion by failure along sheeting (off-loading) fractures parallel to the scarp face. The slab walls terminate at their base at indentations developed in thin weak zones (partings) whose weathering and erosion cause the slab wall backwasting (Fig. 7.21). Partings that readily weather (effective partings) are either closely spaced bedding planes with highly fractured sandstone sandwiched in between, or are one or more thin (2 to 5 cm) layers of fissile ferriferous shale. The partings commonly are of limited horizontal extent, so that slab walls die out laterally (Fig. 7.21). Some slopes may have more than one slab wall where partings occur at two or more levels.

Oberlander presented convincing evidence that slope erosion occurs both by erosion of slickrock slopes and slab wall backwasting. This, coupled with intersection of new partings and lateral dying out of other partings during slope retreat, leads to progressive changes in slope profile form (Fig. 7.22). In Oberlander's model the gradient of slickrock slopes below effective partings largely depends upon the relative rates of scarp backwasting by parting erosion and the rate of weathering and erosion on the slickrock slopes, with gentler slickrock slopes associated with rapid parting erosion. Sometimes backwasting at a parting may cease, either due to playing out of the parting or local conditions less conducive to parting erosion. In such cases continued erosion of the slickrock slope below the parting leads to development of a near-vertical slope below the parting; such slopes were called secondary walls by Oberlander. Such inactive slab walls also commonly develop alveolar weathering, discussed further below. An important conclusion of Oberlander's study is that thin partings in otherwise massive bedrock cause a complicated slope form (in particular the slab wall), so that slope breaks are not necessarily an indication of lithologic contrast above and below the break, but may imply only a thin discontinuity.

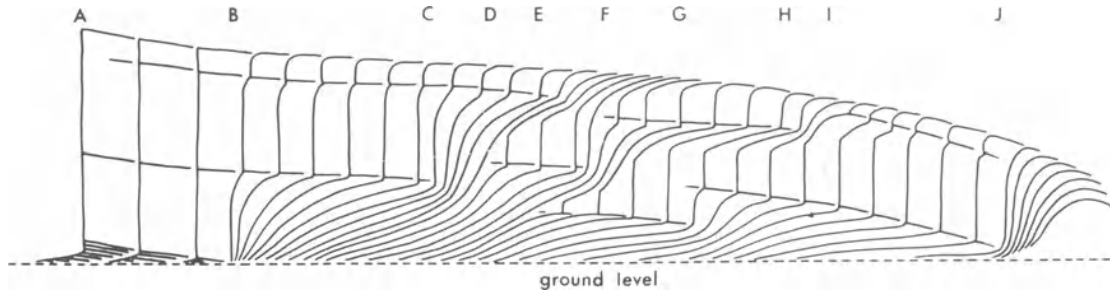

Figure 7.22 Development of scarp forms in massive sandstone through time and space. For simplicity a constant ground level (dashed line) is assumed during scarp retreat, along with equal thicknesses of removal from major slab walls in each unit of time. At A a through-going cliff is present due to sapping above a thin-bedded substrate. At B the thin-bedded substrate passes below ground level, scarp retreat slows, and effective intraformational partings assume control of scarp form. Effective partings close at C, E, F, G, H, and J, leading to local slab wall stagnation and rounding into slickrock. Partings that open at D, E, F, G, and I, initiate growth of new slab walls. Note that the effect of former partings in rocks that have been removed continues to be expressed in the form of slickrock ramps and concave slope breaks. Lowering of ground level during backwearing would cause cliff extension upward from major contact (caption and illustration from Oberlander 1977, fig. 8).

Similar slope forms occur in other sandstone units on the Colorado Plateau, especially the Navajo Sandstone and the Cedar Mesa Sandstone at Natural Bridges National Monument, Utah. In these formations the slab wall is commonly strongly overhung into a thin two-dimensional arch or alcove presumably backwasted along sheeting fractures. One puzzling aspect of these prominent indentations is a general paucity of mass wasting debris on the lower floor. Schumm and Chorley (1966) cited the ready breakup of the wasted debris as an explanation, but slab wall failures from relatively short cliffs yield abundant debris (Fig. 7.15), and the alcoves are a relatively protected environment. Another possible explanation is present-day inactivity of parting erosion and resulting slab failure due to aridity. The effects of climatic change on scarp morphology are discussed further below.

Hoodoos and Demoiselles

A few scarps are sculpted into highly intricate forms, such as occur at Bryce Canyon, Utah, and smaller forests of boulders on shale pedestals called hoodoos (Fig. 7.23). These forms occur where the caprock unit is discontinuous but massive and the underlying shales are readily eroded where exposed to rain but easily protected from weathering by slight overhangs. Many scarps in the south-western United States are composed of cliffs that extend well below the caprock unit into the underlying shales (Fig. 7.24). These cliffs are remarkably stable, having persisted and grown vertically (downward) throughout the Holocene (and late Pleistocene?), showing the efficacy of overhangs as small as a few tens of centimetres in restricting surface weathering of shales in a desert environment. Typically the caprock units are concretions or discontinuous interbeds of cemented sandstones or limestones. They are embedded in shales or shaly, poorly cemented sandstones that typically erode into badlands where relief is sufficient and caprocks are absent. Exposure of the concretion or resistant interbed greatly reduces erosion rates while the surrounding shale

Figure 7.23 Hoodoos in Entrada Sandstone near Hanksville, Utah. Hoodoos are capped by resistant concretions, whereas nearby poorly cemented sandy shales exhibit regolith-mantled badland slopes. Hoodoos are often supported by thin pedestals of shale (photo A. Howard).

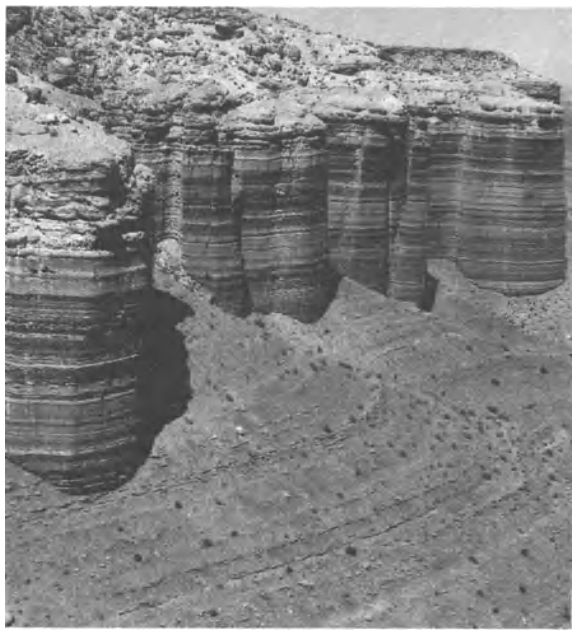

Figure 7.24 Typical view of Morrison–Summerville escarpment at Sandslide Point off Utah Highway 95 near Hanksville, Utah, showing the cliff face extending into the weakly resistant Summerville Formation, the badland rampart in the same formation abutting the escarpment face, and the absence of debris on the rampart. Note that the rampart is shallowly underlain by bedrock and is not a colluvial apron (photo A. Howard).

badlands continue to erode, producing a dichotomy in the shales between the vertical slopes protected by the caprock and the subjacent badlands. Development of stucco-like coatings of clay and lime by vertical drainage on the shale cliffs may be a contributing factor in protecting the shale from erosion (Lindquist 1979). Rates of vertical erosion in the shale badlands may be 40 times the rate of lateral retreat of the vertical shale cliffs (Lindquist 1979).

Role of Sapping Processes in Scarp Erosion and Morphology

Various geomorphologists have suggested that rock weathering and erosion at zones of groundwater discharge have contributed to the backwasting of scarps and valleys in sandstones exposed on the Colorado Plateau (Gregory 1917, Bryan 1928, Ahnert 1960, Campbell 1973, Laity and Malin 1985). General discussions of groundwater sapping and its landforms have been provided in Higgins (1984), Howard *et al.* (1988), Baker *et al.* (1990), and Higgins and Osterkamp (1990). Laity and Malin (1985, p. 203) defined sapping as 'the process leading to the undermining and collapse of valley head and side walls by weakening or removal of basal support as a result of enhanced weathering and erosion by concentrated fluid flow at a site of seepage'. Higgins (1984) distinguished between 'spring sapping' caused by concentrated water discharge and 'seepage erosion' resulting from diffuse discharge at lithologic contacts or other lithologic boundaries. This discussion addresses both the role of seepage groundwater in scarp erosion and the development of deeply incised valleys in sandstone by spring sapping.

Such definitions of sapping and seepage erosion are complicated by marginal and transitional situations. Scarp erosion processes that are clearly not sapping erosion include plunge-pool undermining and rock weathering by moisture delivered to the scarp face by precipitation, condensation, or absorption of water vapour. However, other circumstances are not as clear-cut. For example, water penetrating into tensional and exfoliation joints close to cliff faces may cause rockfalls as a result of freezing or water pressure but would probably not be classified as sapping by most geomorphologists. Similarly, corrasional erosion of shale beneath sandstone by water penetrating along wide fractures (termed subterranean wash by Ahnert 1960) is similar to piping, but probably should not be included as a process of groundwater sapping. On the other hand, rockfall caused by weathering of shales beneath a sandstone scarp in which water is delivered by flow along joints within the sandstone is more likely to be considered to be sapping, even in the absence of obvious water discharge along the scarp face. Weathering processes resulting from intergranular flow within sandstone would generally be considered sapping.

Groundwater flow plays an uncertain role in weathering of the shales and weakly cemented layers whose erosion causes scarp retreat in overlying sandstones. Oberlander (1977, 1989) mentioned spring sapping of shale partings as a possible process of scarp retreat in segmented scarps. Schumm and Chorley (1966), while providing experiments and observations on surface weathering of caprock units, essentially avoided the issue of processes of caprock undermining. Koons (1955) was similarly vague. Ahnert (1960) clearly felt that sapping processes are of general importance in scarp retreat in sandstone–shale scarps of the South-west, but he provided little evidence. Laity and Malin (1985) suggested that disruption of surface expo-

sures by salt crystal growth where seepage emerges and sloughing of thin sheets of the bedrock are the major processes of sapping erosion in massive sandstones, and that sapping is usually concentrated in thin zones above less permeable boundaries within or below the sandstone. This backwasting and undermining of the overlying sandstone then occasions development of slab failure and, locally, alcove development associated with development of exfoliation jointing as outlined by Bradley (1963). Laity and Malin primarily discussed spring sapping processes occurring at canyon headwalls, and it is uncertain the degree to which they felt sapping or seepage erosion occurs more generally on sandstone scarps. Observations reported below suggest an important role of shallow groundwater circulation in scarp retreat in sandstone–shale sequences of the South-west under present climates.

Many scarps are indented by V-shaped re-entrants or canyons excavated by erosion along streams passing over the escarpment. Such erosion is generally considered to result from corrasion of the bed (e.g. Howard and Kerby 1983) or from plunge-pool action. However, examination of canyon heads in sandstone suggests that sapping processes may play a role in channel erosion, at least for washes with drainage areas less than several square kilometres. Washes passing over scarps in sandstone commonly occupy only a fraction of the total scarp width. In addition, the scarps are commonly overhung when developed in massive sandstone and plunge pools are rare and small below the waterfalls. Even steep streams on thin sandstone beds sandwiched between shale layers exhibit overhangs considerably wider than the stream bed and show little development of plunge pools. Much of the erosion of the sandstone beds in such cases may occur due to sapping, with a very localized water source from the overlying stream. Additionally, small washes developed on slickrock slopes above scarps are commonly interrupted by solution pits and the washes exhibit flutes and furrows that suggest that solutional removal of calcite cement is more important than mechanical corrasion in bed erosion.

Weathering and erosion of sandstone by the effects of crystal growth occur at a variety of scales in sheltered locations. Steep slopes and scarps in sandstone are frequently interrupted by rounded depressions, often overlapping, which intersect sharply with the general slope (Fig. 7.25). Such alveolar weathering, or tafoni, occurs not only in sandstone, but also in granites, tuff, and other massive rocks (Mustoe 1982, 1983). Both accelerated erosion in the hollows and case hardening of the exposed portions of the slope (Conca and Rossman 1982) may contribute to development of tafoni. Salt

Figure 7.25 Alveolar weathering, or tafoni, developed in Navajo Sandstone at Capital Reef National Monument, along Utah Highway 24. Note highway reflector for scale and uneroded ribs where surface wash occurs (photo A. Howard).

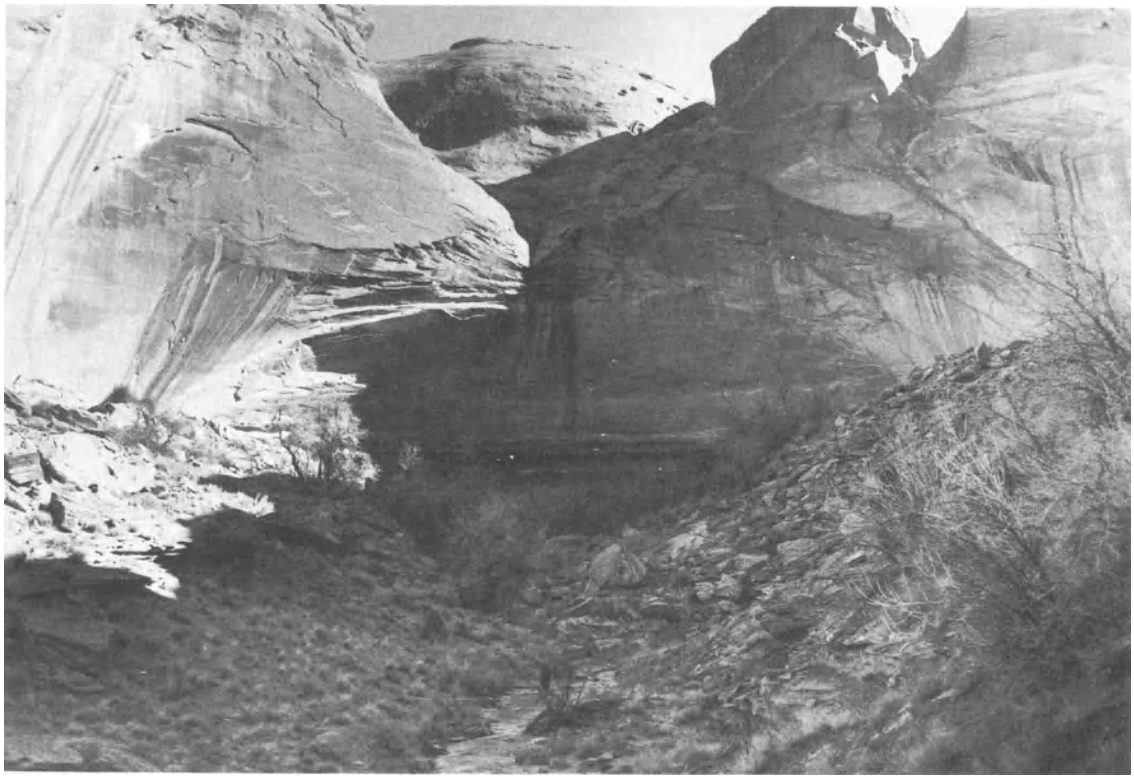

Figure 7.26 Theatre-headed valley in Navajo Sandstone near Utah Highway 95 along North Wash (southern Henry Mountains area). Note cottonwood trees and dark figure in wash at bottom centre of photo for scale. The active seep is the dark band at the base of the alcove. Note the evidence of offloading fracturing. The stream passing over the top of the alcove is clearly inadequate in size to have created the alcove as a plunge pool. Water draining down the face of the alcove from the lip of the falls has created the dark streaks. However, delivery of water along the alcove walls occurs only locally, and is insufficient to account for the backwasting of the alcove (photo A. Howard).

accumulations are often quite apparent in the cavernous hollows, and the backwasting results in spalling of sheets of weathered rock up to a few centimetres in thickness. Mustoe (1983) noted high soluble cation contents in the spall detritus in tafoni and the presence of the mineral gypsum. Laity (1983) and Laity and Malin (1985) found calcite deposition on spalling walls. The mechanisms by which such mineral deposition may contribute to the spalling include pressures exerted by crystal growth, thermal expansion and contraction of the crystal-filled rock, and expansion and contraction due to hydration of deposited minerals (Cooke and Smalley 1968). Freeze–thaw disruption on the moist seepage faces may also contribute, and spalling may be aided by the weight of accumulated winter ice (Laity and Malin 1985).

A surface protected from surface runoff is a necessary condition for tafoni and alcove development. On steep sandstone scarps surface runoff commonly flows as sheets down the scarp, held by surface tension on slightly overhung slopes. Such runoff paths are commonly accentuated by rock varnish. Where such runoff paths cross zones of tafoni development, backwasting is inhibited, and the tafoni are separated by columns that often resemble flowstone columns in caves (Fig. 7.25). Surface runoff might inhibit salt fretting simply by solution and removal of salts brought to the surface by evaporating groundwater or more actively by case hardening of the exposed surface by deposition of clays or calcite (Conca and Rossman 1982).

Two intergrading types of sapping landforms develop on massive sandstones. The more exotic form is the development of tafoni on steep scarps and on large talus blocks. Such tafoni may literally riddle certain steep slopes (Fig. 7.25), with the tafoni concentrated along certain beds that are either more

Figure 7.27 Seepage face at a theatre head alcove. Zone of seepage is 1 to 2 m thick. Floor of alcove is highly weathered sandstone debris supporting a vegetative cover. The seepage face is incrusted with ferns, mosses, algae, and other phreatophytes. Salt efflorescences occur above moist zone (photo A. Howard).

susceptible to the salt fretting or receive greater groundwater discharge. Talus blocks generally develop tafoni on their lower, overhung portions. The concentration of tafoni development at the base of such blocks may be due both to the protection from surface wash as well as upward wicking of salts from underlying soils or shales, a process that contributes to weathering of the bases of tombstones (Mustoe 1983, Hamilton 1984). Oberlander (1977) pointed out that tafoni develop most strongly on scarps initially steepened by basal undermining but presently no longer backwasting because alluviation or aeolian deposition covers and protects the basal backwasting face. Thus generalized tafoni development on a scarp indicates relative inactivity of backwasting by surface attack or basal undercutting.

On the other hand, large alcoves are common in massive sandstones and are often actively retreating as a result of sapping erosion (Fig. 7.26). However, direct sapping usually is localized to zones less than 2 m thick along permeability discontinuities where the discharge of groundwater is concentrated (Fig. 7.27), although at major valley heads the seepage zone may be 20 to 25 m thick. These sapping zones generally backwaste by processes similar to those of tafoni, and locally tafoni are superimposed upon the sapping face. In addition to salt fretting, backwasting by groundwater discharge can also occur by cement dissolution and by weathering of shale beneath or interbedded in the sandstone. The retreat of the active zone of sapping undermines the sandstone above, with the result that occasional rockfalls occur (Fig. 7.15). In massive sandstone the undermining occasions the development of exfoliation sheeting fractures, resulting in large arches or alcoves, with the deepest parts of the alcoves presumably corresponding to the most rapid sapping attack (Fig. 7.27). In well-jointed sandstones, such as the Wingate Sandstone, arches and overhanging cliffs are less common, and the role of scarp retreat by sapping processes is not as obvious but may be just as important.

The major aquiclude for the Navajo Sandstone is the underlying Kayenta Formation, and the major seeps develop at this discontinuity (Figs 7.26 and 7.27). However, thin shales and limestone interbeds (interdunal deposits) create minor aquicludes within the Navajo (Laity 1988, Kochel and Riley 1988),

leading to frequent development of multiple levels of seeps and associated alcoves at valley headwalls.

A distinction may be made between wet sapping with a damp rock face and an effluent discharge and dry sapping, where the rock face is generally incrusted with mineral salts (Laity and Malin 1985). In general, tafoni are associated with dry sapping because of their localized development, whereas large alcoves are generally associated with a more regional groundwater flow and exhibit faces that are at least seasonally wet.

Neither active seepage nor deposition of mineral crusts on protected sandstone walls are necessarily correlated with rapid weathering and backcutting of the sandstone walls. For example, the Weeping Wall at Zion National Park, Utah, is an impressive seep emerging from the Navajo Sandstone, but the associated alcove and canyon are small. Many other examples of fairly high discharge rates but only minor, or non-existent, alcoves can be found throughout the Colorado Plateau. Too rapid a seepage may in fact discourage deposition of salts. Although rapid seepage can also cause backwasting by dissolution of calcite or gypsum cement, this would only occur if the groundwater were undersaturated. Similarly, many examples of thick mineral incrustations at seeps lacking evidence of backwasting can be found on sandstones throughout the South-west. Several factors control whether minerals deposited by evaporating seepage are deposited intergranularly within the rock (encouraging exfoliation and granular disintegration) or at the rock surface (with little resulting sapping), including the type and concentration of salts, the average and variance of water discharge to the surface, the distribution of pore sizes and their interconnectivity, the presence and size of fractures, the temperature regime at the rock face, local humidity and winds, and the frequency of occurrence of wetting of the rock face by rain or submergence (if along a stream or river). The interaction of these factors is poorly understood. Discrepancies between size of alcove or sapping valley and the magnitude of the seep can also result from differences in the length of time that sapping has been active. Despite these cautions, it is reasonable to expect within a specific physiographic, structural, and stratigraphic setting that the degree of alcove development and degree of headward erosion of sapping valleys would correlate with the discharge of the seeps involved (Laity and Malin 1985).

In summary, most evidence suggests that sapping processes are common in sandstones of the Colorado Plateau and the processes result in the widespread development of tafoni and alcoves. The major caution is the evidence cited by Oberlander suggesting that groundwater sapping is unimportant in erosion of effective partings at thin shale layers in the Entrada and other sandstones. One of several possibilities may account for this difference in interpretation. The effective shale partings may, in fact, be so readily weathered by atmospheric moisture due to high salt content or other factors that seepage is not required for such partings as it is for cavernous weathering and alcove development elsewhere. The Entrada Sandstone exhibits considerable variation in lithology and cementation both vertically and areally, so that in the Arches National Park the Slick Rock Member may be relatively impermeable. However, well-developed arches and tafoni with evidence of active salt fretting are found a few tens of kilometres south in this same member. Another possibility is that backwasting along effective partings is not very active under present climatic conditions, but was more active during the late Pleistocene. The evidence for relatively inactive scarp retreat (and, by extension, seepage erosion) under present climatic conditions is discussed below.

Climatic Change and Scarp Morphology

Most recent discussions of scarp morphology and associated weathering and erosional processes have implied that the morphological elements can be explained by presently active processes (e.g. Koons 1955, Schumm and Chorley 1966, Oberlander 1977). However, other authors have maintained that escarpments in the Colorado Plateau region are undergoing considerably less caprock erosion under the present climate than during the late Pleistocene (Reiche 1937, Ahnert 1960, Howard 1970).

Given our poor understanding of present scarp processes and little historical control, it is not surprising that different conclusions have been drawn about present activity and the presence or the lack of a direct relationship between present processes and present scarp form. For example, Schumm and Chorley (1964, 1966) cited numerous examples of historical rockfalls as evidence for present activity of scarps. However, a simple analysis suggests just the opposite. Inferred long-term rates of scarp retreat on the Colorado Plateau average about 3 m per 1000 years (Schmidt 1989b). If rockfalls occur randomly through time and characteristically involve a block of caprock 1 m thick and 10 m in horizontal dimension, then one should expect about three rockfalls per year on 10 km of scarp front. If the characteristic

rockfall is larger, say 3 m thick and 100 m long, then there should be a rockfall every ten years. Since there are tens to hundreds of thousands of kilometres of scarp front on the Colorado Plateau, occurrences of large rockfalls should be much more frequent than appears to be the case, possibly by as much as an order of magnitude.

The escarpment of Emery Sandstone near Caineville, Utah, is a case in point. Extensive old rockfall deposits on North and South Caineville Mesas, dissected to a depth of as much as 50 m at their lower and lateral margins, were interpreted by Howard (1970) to be Bull Lake equivalent in age (Illinoian?) because some of the debris blankets interfinger with pediment deposits of Bull Lake age, whereas the remainder extend no further downslope than the level of the former pediment surface (Fig. 7.28). The old debris blankets have been dissected by a similar amount and project concordantly laterally along the escarpment. Much of the scarp rampart is now devoid of extensive debris, so that extensive badlands have developed on the underlying Mancos Shale. In places the cliff capped by the Emery Sandstone extends downward by as much as 70 m into the underlying shale (Fig. 7.14). Koons (1955) demonstrated that development of cliff faces in the non-resistant subcaprock unit is a normal occurrence in the cycle of rockfall, debris blanket erosion, and erosion of the subcaprock unit which triggers the next rockfall. However, for reasons outlined above, extensive cliff development in the subcaprock unit may also indicate stagnation of caprock mass wasting while erosion of the subcaprock unit continues on the scarp rampart.

Schmidt (1988, 1989a) and Gerson and Grossman (1987) noted similar remnant debris blankets related to climatic change and, in particular, talus flatirons and associated pediment flatirons (Fig. 7.29). Schmidt (1988, 1989a) termed climatically controlled flatiron development cyclical flatirons as contrasted with the non-cyclic flatirons discussed previously, and also cited the presence of associated dissected pediments (pediment flatirons) as a distinguishing characteristic of cyclic flatirons.

An outstanding example of a presently stagnant scarp morphology is the escarpment capped by the lower units of the Morrison Formation overlying the thin bedded sand and shale beds of the Summerville Formation near Hanksville, Utah. Much of the escarpment is capped by a thin gypsum layer which is stable enough to support vertical cliffs up to 30 m high in the Summerville Formation (Fig. 7.24). The gypsum cap has been eroded into small crenellations mimicked in the underlying Summerville, indicating

Figure 7.28 Pleistocene-age (Illinoisan?) rockfall on escarpment of Emery Sandstone over Mancos Shale on South Caineville Mesa near Hanksville, Utah. Note heavy dissection of lower end of rockfall blanket. Note remnant of pediment of same age in front of escarpment on left side of photo (photo A. Howard).

that the caprock protects the vertical face from weathering and erosional processes. The rampart generally consists of debris-free badlands likewise carved in the Summerville Formation, which meet the vertical face at an abrupt angle. The rampart is bordered downslope by dissected pluvial (Bull Lake?) pediments paved with agate derived from the caprock, giving evidence that abundant debris was transported from the escarpment during that time. Where a caprock of gypsum is present, even a thick sequence of overlying sandstone sheds little debris on to the rampart. But where the gypsum unit is discontinuous or missing (Fig. 7.30), the overlying sandstone wastes by undermining and rockfall. However, during the Bull Lake pluvial climate the gypsum caprock evidently succumbed more readily to rockfall and occasional slumping (Fig. 7.31). The scarps illustrated in photos 3 and 22 of Schumm and Chorley (1966) are probably further examples of such presently inactive scarps.

In canyon areas, a cliff in a massive sandstone often is underlain by a nearly bare rock slope with a gradient of about 30° to 40°. No obvious lithologic break separates these slope elements. In some cases, such as at Canyon de Chelly, Arizona, examples can be found where such bare rock slopes yield laterally to rock slopes of similar gradient but mantled with rockfall debris (Fig. 7.32). One explanation for such features is that they are Richter slopes, forming at the characteristic friction angle of rockfall debris under conditions where removal of rockfall debris (by weathering or erosion at the scarp base) just balances production at the superjacent cliff face (Richter 1901, Bakker and Le Heux 1952, Cotton and Wilson 1971, Selby 1982d, pp. 204–8, Scheidegger

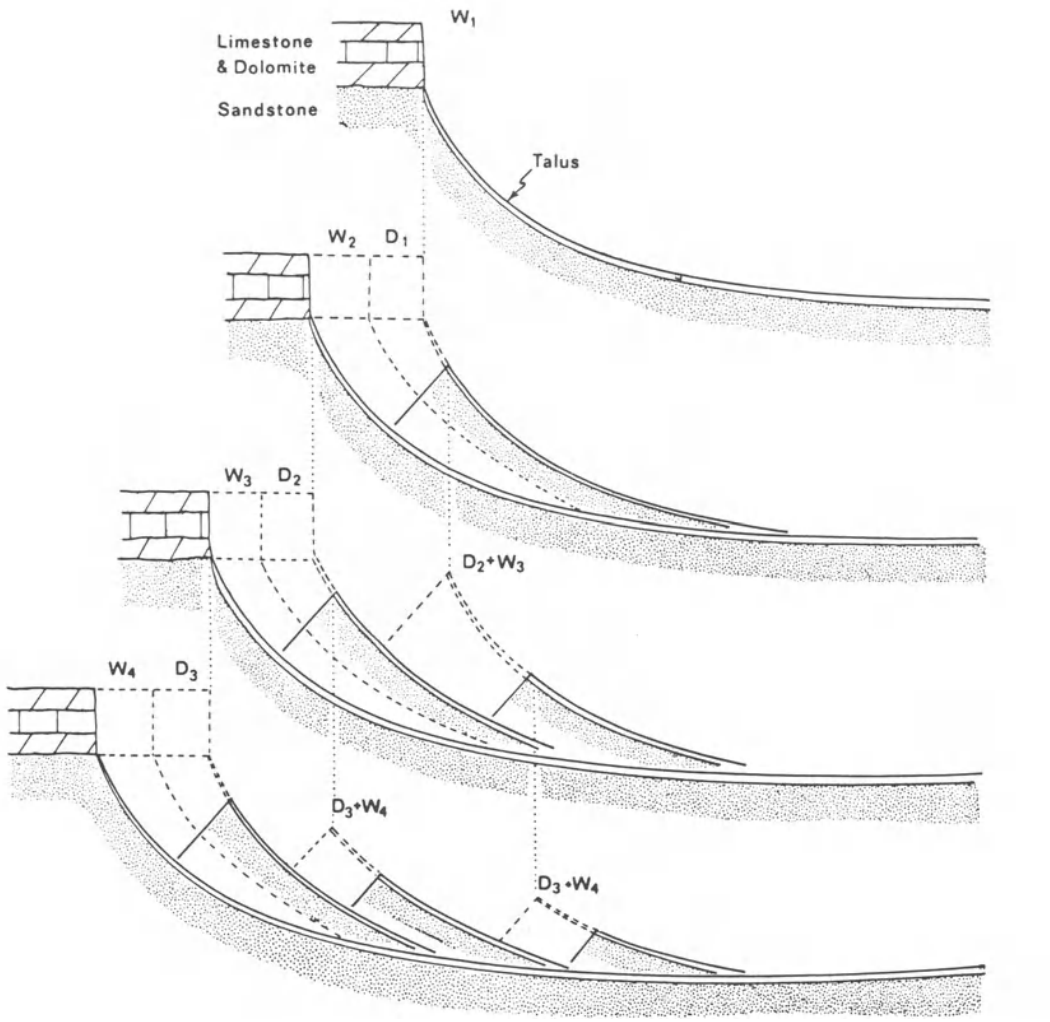

Figure 7.29 Talus flatirons developed by alternating wet (W) and dry (D) climates. Talus aprons and associated pediments develop during enhanced weathering and transport of wet periods and are dissected during dry epochs (from Gerson and Grossman, 1987, fig. 17-8).

1991, p. 132; also equivalent to the case of Schumm and Chorley's (1966) unity weathering ratio). However, at least in the Colorado Plateau examples, it is difficult to imagine how such a scattered debris cover protects the underlying rock from weathering and erosion. One possible explanation is that the moving talus has erosive capability which planes the rock down to the friction angle of the moving talus. Erosion by rock and ice avalanches has been used to explain spur-and-gully development on steep arctic and alpine mountain slopes (Rapp 1960a, b, Howard 1989, 1990). However, in this case erosion tends to become localized in chutes.

A more direct explanation is that the bare rock slopes were formerly mantled with rock debris produced by cliff retreat and that the debris mantle protected the underlying rock from weathering and erosion, forming threshold slopes (Carson 1971, Carson and Petley 1970). The cover of debris on such slopes is now obviously inadequate to protect the rock from weathering and erosion with the implication that scarp backwasting is presently largely inactive, permitting the weathering and stripping of the former debris mantle. Somewhat similar forms can be found in the areas of segmented scarps in Entrada Sandstone at Arches National Monument

Figure 7.30 View of northwest face of Goatwater Point, along Utah Highway 95 near Hanksville, Utah, showing rapid backwasting of the sandstones capping the Morrison–Summerville escarpment in the absence of the gypsum caprock. Vertical cliffs in the Summerville Formation occur only where the gypsum unit is present, such as on the left edge and centre of the picture (photo A. Howard).

(the area studied by Oberlander 1977) (Fig. 7.21). Oberlander interpreted the low-gradient slickrock slopes to be a normal feature of erosion of segmented scarps (Fig. 7.22), but it is possible that some of the slickrock slopes below vertical cliffs may have formerly been mantled by a debris blanket under a different climate (a scattering of debris can be seen on many of these segmented slopes).

Ahnert's (1960) historical interpretation of scarp morphology contrasts sharply with the 'dynamic equilibrium' interpretations of Schumm and Chorley (1966) and Oberlander (1977). Ahnert suggested that scarp retreat occurs by erosion of shales and other weakly resistant layers by sapping-related processes that have only been active during pluvial episodes characterized by abundant, gentle precipitation. By contrast, he felt that slickrock slopes are eroded largely by sheetwash, which has been active during the sparse but intense rainfall of interpluvials. Ahnert felt that the generally sharp breaks between slickrock slopes and subjacent scarps were evidence of the non-contemporaneous origin of the two features, whereas Oberlander (1977) and Howard and Kochel (1988) felt that such sharp breaks can result from contemporaneous slickrock erosion and scarp retreat. Ahnert's assertion that slickrock slopes are eroded primarily by sheetwash misses the importance of the initial weathering that must occur on these weathering-limited slopes. This weathering, which makes debris capable of slopewash transport, is probably not optimal under present climatic conditions of brief, intense rainstorms, but is favoured by winter precipitation and freeze–thaw.

Despite these objections to Ahnert's interpretations, the examples presented previously suggest that there have been changes throughout the Pleistocene and Holocene in the relative rates of the major processes producing cuesta landforms: scarp undermining by sapping, undermining, or surface-directed weathering; weathering and erosion of rockfall debris; weathering and erosion of slickrock slopes; erosion of interbedded shale layers; and, locally, slumping and landsliding. Changes in the relative importance of these processes have produced landforms that in many cases can only be understood by knowledge of the temporal process changes (i.e. relict landforms). These examples of remnant effects of past climates add a complicating element in unravelling the geomorphic history of cuesta landforms and interpretation of scarp morphologies which would greatly benefit from application of modern techniques of geomorphic surface dating.

The greater rainfall during the Bull Lake pluvial maximum would suggest greater sapping activity then relative to now, but that same moisture supply would also contribute to surface-directed weathering, particularly freeze–thaw weathering. Also, more abundant groundwater does not necessarily produce more sapping in sandstones because if seepage is sufficient and humidity high enough to permit runoff of the seepage, little salt accumulation will occur. However, other groundwater-related weathering processes would be enhanced by greater available moisture, such as hydration and leaching of shale interbeds. Thus during the pluvial epochs we

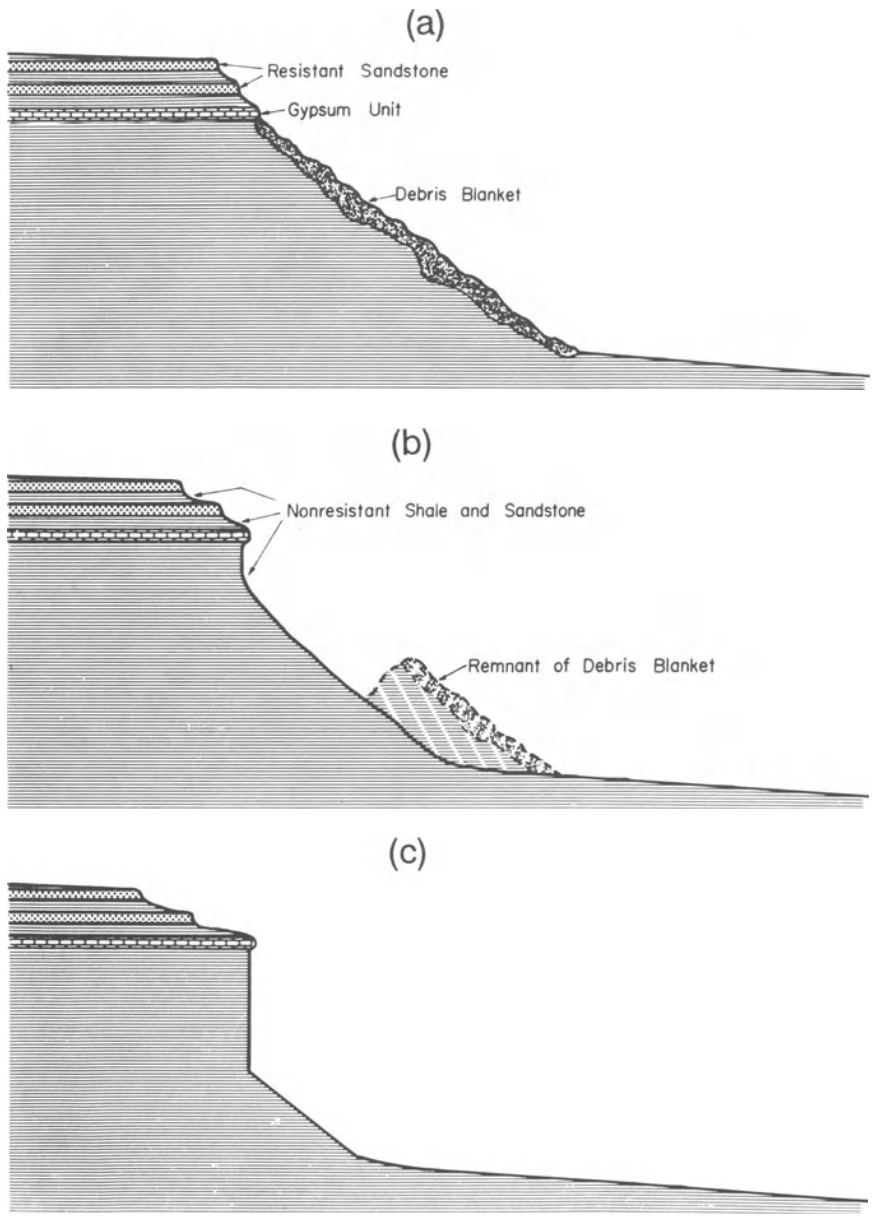

Figure 7.31 Cross-sections through the Morrison–Summerville escarpment showing presumed Pleistocene conditions compared with the present-day profile. During the Pleistocene pluvials, backwasting of the caprock units by rockfall and block-by-block undermining was probably rapid, and the debris-covered rampart extended up to the caprock without tall vertical cliffs in the underlying Summerville Formation (cross-section a). Between rockfalls, weathering and erosion eventually removed the sandstone and gypsum debris, and a cliff would begin to form in the Summerville Formation (b). Because of the greater supply of water and lower temperatures, vertical cliffs higher than those in profile (b) were probably unstable, for another rockfall would return the escarpment to the conditions at (a). However, under the drier and warmer Holocene conditions, the gypsum caprock has become very resistant, and backwasting of the escarpment has essentially halted, with the result that the escarpment rampart is rapidly eroding away, leaving behind high cliffs in the Summerville Formation (c) (from Howard 1970, fig. 81).

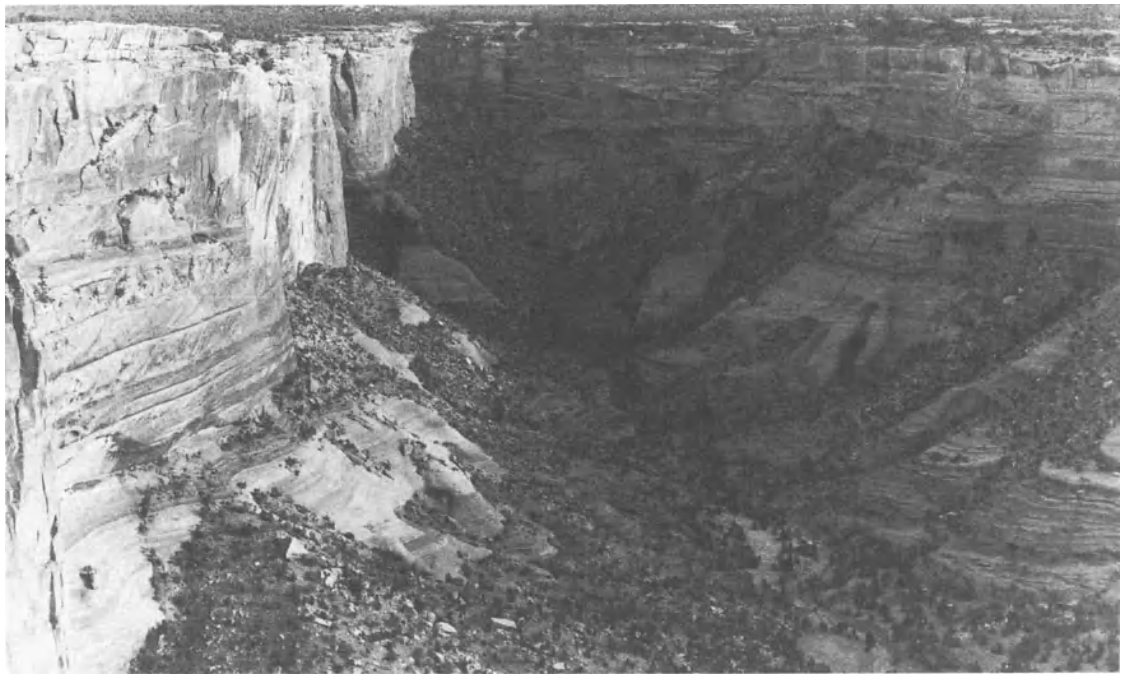

Figure 7.32 View of a small tributary re-entrant to Canyon De Chelly, Arizona, showing prominent vertical cliffs in upper parts of the De Chelly Sandstone with slickrock slopes of 30 to 40° inclination below the cliffs and also developed in the De Chelly Sandstone. Note partial mantling of lower slopes with talus and the suggestion that the other slickrock slopes were formerly mantled (photo A. Howard).

might expect more debris production by freeze–thaw, less alveolar weathering, but greater backwasting at the contact between sandstones and underlying shales and along shale interbeds. The present paucity of rockfall debris, rather than indicating nearly complete breakup and rapid weathering of the debris, as suggested by Schumm and Chorley (1966), may simply indicate relative inactivity of many scarps in present climates.

Another prominent feature of the theatre headwalls at seeps is the paucity of rockfall debris. This commonly contrasts with abundant rockfall debris along the sides of the valley downstream from the seep (Fig. 7.26). Laity (1988) suggested that both initial pulverization of rockfall debris and rapid weathering in the moist environment of the headwall account for the paucity of debris. However, recent rockfalls in alcoves generate abundant debris, and the rockfall debris along valley walls also suggests that the backwasting of scarp walls produces a considerable volume of coarse debris that must be further weathered before it is transported from the rampart and backwasting can continue. The paucity of rockfall debris at headwater scarps is therefore interpreted as further evidence of greater sapping activity during past pluvial periods and relative inactivity during the present climatic regime.

In the western desert of Egypt, particularly the Gilf Kebir, scarp retreat via groundwater sapping during wet episodes of the Pleistocene and present erosional inactivity has been inferred by Peel (1941), Maxwell (1982), and Higgins and Osterkamp (1990).

Quantitative Models of Scarp Profile Evolution

A variety of quantitative models of scarp profiles has been developed over the years. Most notable are the models of scarp backwasting and talus accumulation that predict the evolutionary slope history and the subtalus bedrock profile (Lehmann 1933, Bakker and Le Heux 1952, Gerber and Scheidegger 1973, and others: see summary in Scheidegger 1991, pp. 130–4). These have been developed for the case of a horizontal, fixed base level with no provision for weathering and removal of talus except through a constant ratio of rock eroded to talus produced.

Other slope evolution models permit resistant

layers, but some express resistance solely in terms of resistance to weathering and do not allow for the effects of mass movement and surface wash (e.g. Scheidegger 1991, pp. 144–7; Aronsson and Linde 1982), or they include creep-like mass movement but not the effects of surface wash, rockfall, and talus weathering (Ahnert 1976, Pollack 1969).

Developing of realistic scarp profile models will prove challenging owing to the range of processes and materials that must be considered. The first component must be the accounting of weathering and failure of the caprock, addressing rates of weathering, effects of slope steepness and profile, and predicting size and frequency of rockfall, undermining, or slumps, possibly including the role of groundwater sapping. A second component should follow the distribution, comminution during emplacement, weathering, and erosion of caprock debris, as well as the protective influence of the debris on underlying bedrock. The third component should address erosion of the subcaprock unit where exposed. Finally, initial and boundary conditions must be addressed, including stratigraphy, dip, base level changes, and possible process variations through time. A final problem with profile evolution on ramparts with rockfall talus is that production and erosion of the talus is inherently three-dimensional (e.g. the development of flatirons).

EVOLUTION OF SCARP PLANFORM

The planimetric form of canyons and escarpments is the most obvious signature of the erosional processes involved in scarp retreat in layered rocks. The processes of scarp erosion create characteristic shapes of planform features such as re-entrants, projections, and inset canyons. For example, some scarps have rounded projections, or headlands, whereas others are sharply terminated. Similarly, some scarps are inset with deep, narrow canyons, while others have shallow, broadly rounded re-entrants. The scarp form is determined by the spatial distribution of the processes discussed earlier as well as the lithologic and structural influences such as rock thickness and dip. Several generalities about scarp planform have been noted for many years.

(a) In areas of strong structural dip (more than a few degrees) scarps tend to be oriented updip with a linear to gently curving planform that closely follows the structural strike, locally interrupted by through-flowing streams. At least two factors contribute to the linearity of scarps with steep dip. Drainage divides tend to be at or very close to the scarp crest, so that little fluvial or sapping erosion occurs. In addition, escarpment height is a strong function of crest location, so that portions of the scarp that lag in erosion rapidly become higher than surrounding locations, tending to enhance average rates of retreat. Thus the remarkable linearity of scarps in steeply dipping rocks is *prima facie* evidence for the sensitive dependency of scarp backwasting rates on scarp relief.

(b) Where the structural dip is slight, scarp planforms are highly textured, with deep embayments and canyons as well as headlands and detached mesas. Scarps may face either updip or downdip, with downdip portions being more deeply embayed because drainage areas on top of such scarps are generally larger.

(c) Resistant rock units generally become first breached by stream erosion, forming scarps, where structural elevations are high (e.g. at the top of anticlines) and/or where gradients are steepest (e.g. on dip-slope stripped plains on the resistant unit). Both factors are combined in the common scenario of breaching of caprocks just below the crest of monoclines.

Since caprock erosion occurs dominantly by scarp retreat, the scarp planform reflects areal variations in rate of scarp retreat. One factor controlling scarp retreat rates is the erosional resistance of the caprock and/or subcaprock units. Nicholas and Dixon (1986) examined the role of variations in inherent caprock resistance (e.g. compressive strength, slake durability, cementation) and caprock fabric (fracture orientation and spacing) in controlling relative rates of caprock erosion. They found that embayments in the Organ Rock Formation escarpment, Utah, have a higher density of fractures at the base of the caprock than occurs beneath headlands. However, caprock resistance is nearly equal on headlands and escarpments. Accordingly, they suggest that areal variations in caprock fabric are a dominant control on scarp planform (Fig. 7.33).

The other factor controlling scarp form is areal variations in process rates. Erosion of the scarp face by rockfall, slumping, and undermining of the caprock, weathering of the caprock debris, and erosion of subcaprock units will be termed scarp backwasting. Deep re-entrant canyons are clearly created by rapid erosion along a linear zone, generally by fluvial erosion or groundwater sapping. Structure often plays an indirect role by channelling surface or subsurface water along fractures. The role of areal variations in intensity of these three classes

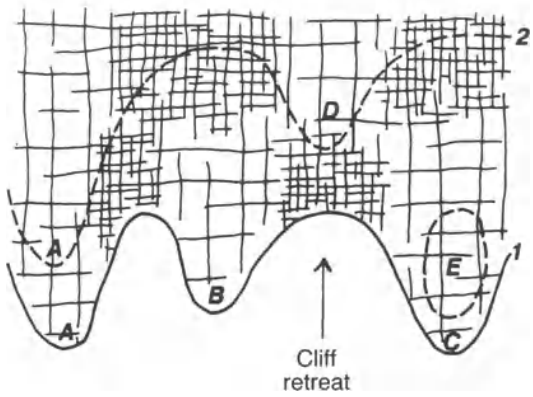

Figure 7.33 Plan view of scarp retreat, showing variable rates of backwasting governed by differences in fracture density. Particularly unfractured masses may persist as isolated buttes, as at A, B, D and E (from Nicholas and Dixon 1986, fig. 8).

of processes and in rock resistance in creating scarp planforms is discussed below based upon both field evidence and theoretical modelling. The discussion will concentrate on the development of Schumm and Chorley's (1964) compound scarps consisting of one scarp-forming unit sandwiched between easily eroded rocks.

Scarp Backwasting

Natural scarps commonly exhibit a planform characterized by sharply pointed or cuspate projections (headlands, spurs) and broadly concave re-entrants (embayments). The role of essentially uniform rates of scarp retreat in creating pointed headlands and broad embayments was first discussed by Dutton (1882, pp. 258–9) and Davis (1901, pp. 178–80), who noted the nearly uniform spacing between successively lower scarps on the walls of the Grand Canyon. Attack of an escarpment by areally uniform backwasting gradually makes embayments more shallow and the planform of the scarp face close to linear (Fig. 7.34). Similar observations were made by Howard (1970) and Schipull (1980). Lange (1959) systematically studied the consequences of uniform erosional attack (uniform decrescence) on two- and three-dimensional surfaces, showing that uniform erosion acting on any arbitrary, rough surface produces rounded re-entrants and cuspate spurs. He also showed that scarp retreat in the Grand Canyon is uniform to a first approximation, with some tendency towards more rapid erosion of embayments (Fig. 7.34). Furthermore, uniform decrescence and uniform addition of material (accrescence) are not reversible (Lange 1959), so that the position of an escarpment rim during the past cannot be uniquely inferred from its present configuration, even if subject to uniform retreat in the past, especially in the case of former spurs that first eroded into outliers and then wasted away.

A simple numerical model of scarp backwasting (Howard 1988, in preparation) lumps local variations in process rates and rock resistance into a single 'erodibility', which is assumed to vary randomly from location to location. The erodibility is assumed to be a self-similar fractal with variations at both large and small scales. The spatial variability of erodibility is characterized by three parameters, an average value, a variance, and a rate of change of variance with scale. The rate of lateral backwasting is assumed to be linearly dependent upon the erodibility. Figure 7.35 shows a plan view of successive scarp positions starting from a square 'mesa'. All simulations discussed here assume a scarp such as is shown in Figure 7.10, with a single caprock over shale and a superjacent stripped plain. As expected, scarps produced by this type of backwasting are characterized by sharply terminating projections and broad re-entrants (as in the Grand Canyon, Fig. 7.34), with re-entrants produced by erosion through more erodible rocks.

The projections of some natural scarps are rounded rather than sharply pointed. This suggests that the lateral erosion rates on the projections are enhanced relative to straight or concave portions of the scarp. Several mechanisms may account for this. The rate of erosion of many scarps is limited by the rate that debris shed from the cliff face can be weathered and removed from the underlying rampart on the less resistant rocks. Debris from convex portions of scarps (projections) is spread over a larger area of rampart, so that weathering rates may be enhanced. Additionally, headlands commonly stand in higher relief than re-entrants, leading to longer and/or steeper ramparts and enhanced erosion rates. Finally, some scarp caprock may be eroded by undermining due to outward creep or weathering of the rocks beneath the caprock. Both processes are enhanced at convex scarp projections. Figure 7.36 shows a model scarp in which backwasting rates are enhanced by scarp convexity and restricted by concavity, and Figure 7.37 shows a similar natural scarp.

By contrast, some natural scarps exhibit narrow, talon-like headlands that are unlikely to have resulted from pure uniform retreat (Figs 7.34 and 7.38). Occasional thin headlands may result from narrow-

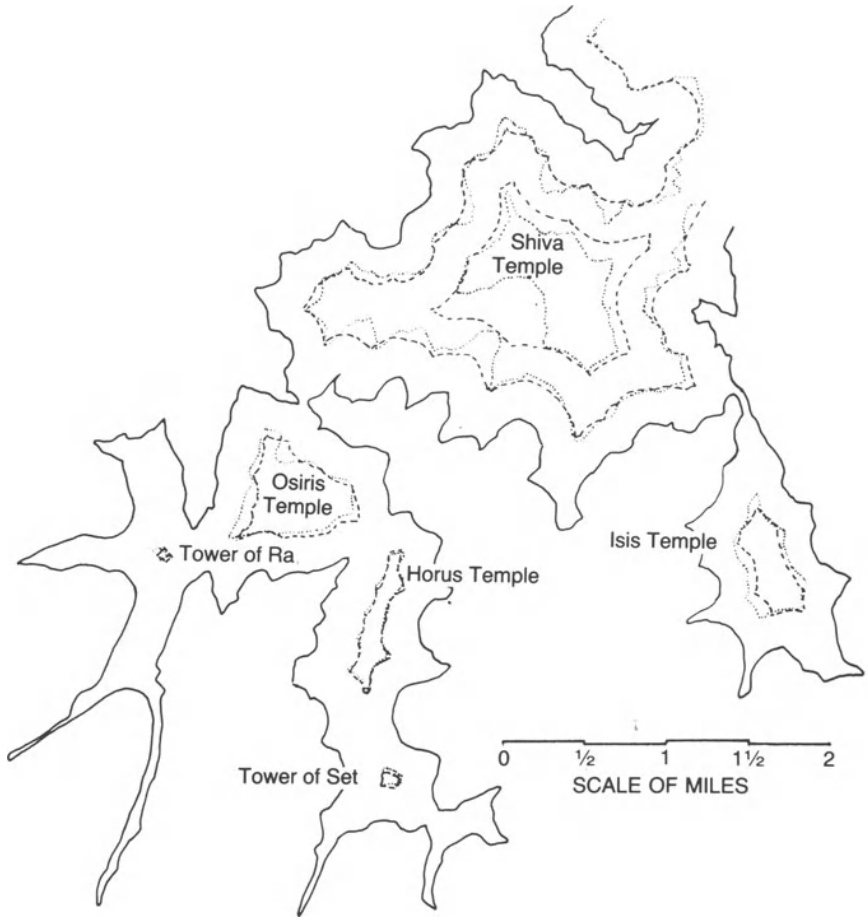

Figure 7.34 Process of uniform erosional attack illustrated on the Redwall, Coconino, and Kaibab escarpments within the Grand Canyon. The rim outline of both the Coconino and Kaibab escarpments (dotted lines) may be approximately duplicated by uniform erosional attack of the Redwall escarpment rim (dashed lines). In a few cases the hollows, or re-entrants, are deeper than would be produced by uniform backwasting of the next lower escarpment; sapping backwasting may be involved (from Lange 1959, fig. 7.17).

ing of divides between canyons by uniform backwasting, but where such sharp cusps are frequent it is likely that they result from slowed erosion of narrow projections. Impeding of erosion on such headlands may be due to a lack of uplands contributing surface or subsurface drainage to the scarp face, thus inhibiting chemical and physical weathering of the cliff face or its undermining. Scarps that have been broken up into numerous small buttes, such as occurs at Monument Valley, Arizona, may be further examples of inhibition of scarp retreat where upland areas are small. An alternative explanation may be that these occur in locations with minimal caprock jointing, in the manner suggested by Nicholas and Dixon (1986).

Almost all escarpments in gently dipping rocks exhibit deep re-entrants and, as erosion progresses, break up into isolated mesas and buttes. This indicates erosion concentrated along generally linear zones of either structural weakness, fluvial erosion, or sapping (often acting in combination). One indicator of the role of either or both fluvial erosion and groundwater sapping is the asymmetry of scarps in gently tilted rocks. The planform of segments where the scarp faces updip is generally similar to that expected by uniform decrescence,

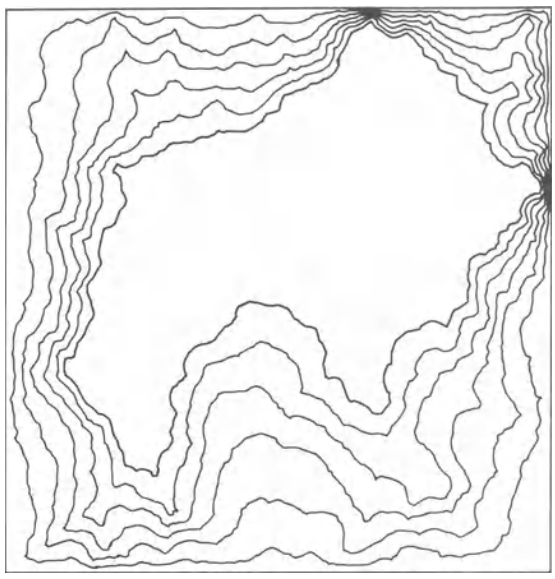

Figure 7.35 Stages of simulated scarp retreat by uniform erosional attack of caprock with spatially variable resistance. The simulation starts from an assumed square mesa and the lines show successive stages of retreat of the edge of the scarp. Note that the lines are not contours.

Figure 7.37 Plan view of a natural scarp with rounded headlands in sandstone underlain by shale in north-eastern New Mexico (1:100 000 Capulin Mountain quadrangle). Note that fluvial incision has created numerous sharply terminated embayments. The uneroded portion of the scarp is patterned. Length of bar is 5 km, and arrow points north.

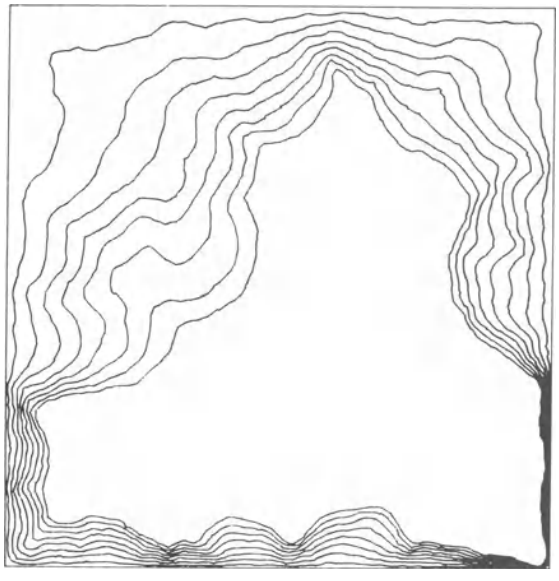

Figure 7.36 Plan view of simulated scarp evolution by uniform erosional attack with an assumed dependency of retreat rate on planform convexity. Note rounding of scarp headlands.

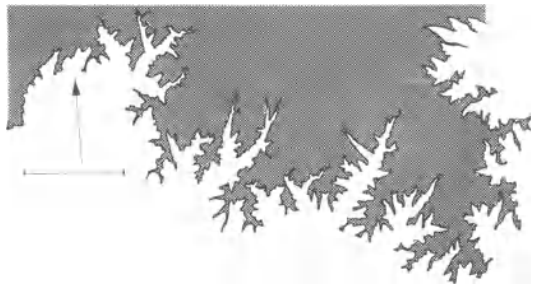

Figure 7.38 Natural scarp with sharply pointed projections and sharply pointed, gradually narrowing box canyon embayments due to stream incision (scarp of the Redwall limestone in Grand Canyon National Park: Grand Canyon 1:100 000 quadrangle). The uneroded portion of the scarp is patterned. Length of bar is 10 km, and arrow points north.

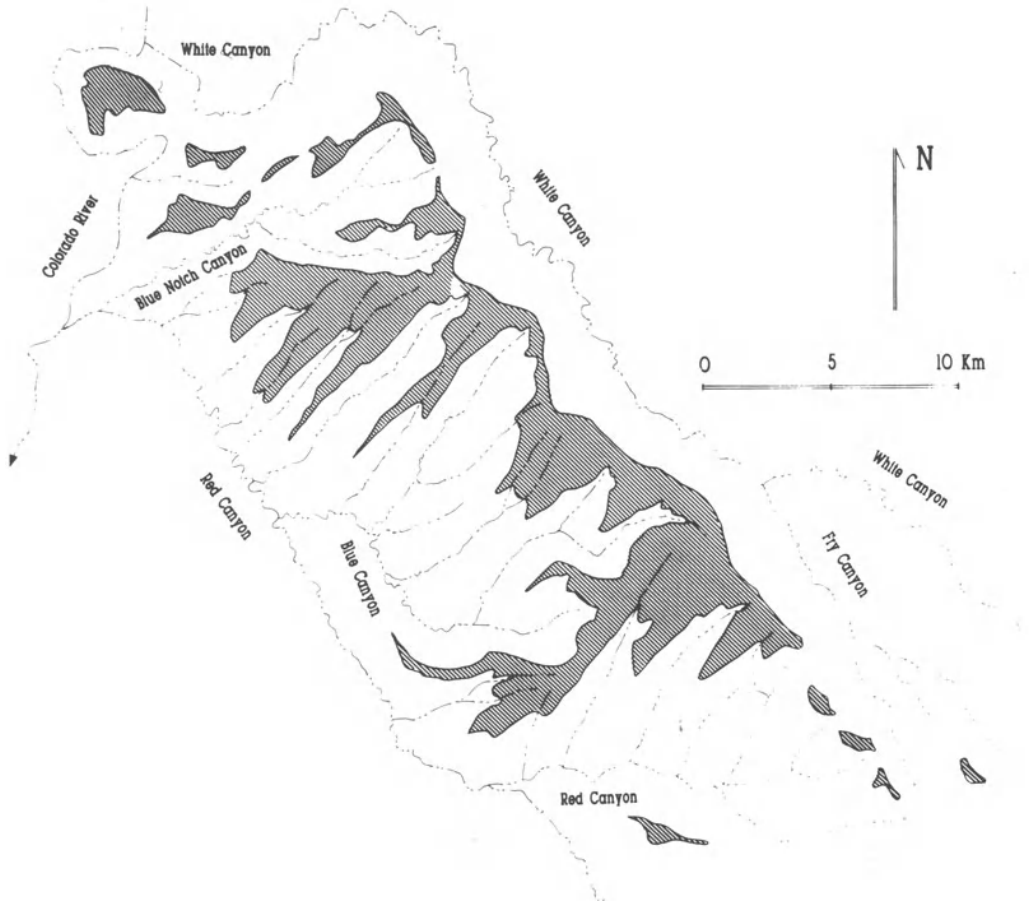

Figure 7.39 Plan view of an escarpment of gently dipping Wingate Sandstone showing smooth, nearly straight planform on updip side and deeply embayed downdip side. Strata dip about 1.5° due west. Mesa is located to south-west of Utah Highway 95 between the Colorado River and Natural Bridges National Monument.

since little drainage passes over the scarp, but segments facing downdip ('back scarps' of Ahnert 1960) are deeply indented as a result of fluvial or sapping erosion (Fig. 7.39) (Ahnert 1960, Laity and Malin 1985).

Nicholas and Dixon (1986) emphasized the role of variable density of fracturing of incompetent and caprock layers in controlling the rate of scarp retreat and the development of re-entrants, projections, and isolated buttes. Their evidence suggests that variable density of fracturing is important on certain scarps, but it probably controls primarily the small-scale planform features. Variable density of fracturing cannot account for the remarkable asymmetry of gently dipping scarps (Fig. 7.39) and the general association of embayments with the drainage basins on the overlying stripped surface of the caprock.

Fluvial Downcutting

One process creating deep re-entrants is downcutting by streams which originate on the top of the escarpment and pass over its front. Such caprock erosion is localized to the width of the stream, which is generally very small compared with overall scarp dimensions, so that the heads of fluvially eroded canyons are quite narrow, but increase gradually in width downstream by scarp backwasting, as noted by Ahnert (1960) and Laity and Malin (1985). Examples of such gradually narrowing, deep re-entrants

are common on the Colorado Plateau (Figs 7.37 and 7.38).

Scarp erosion by combined fluvial erosion and scarp backwasting can be numerically modelled by superimposing a stream system on to a simulated scarp and allowing it to downcut through time. If a resistant layer is present, the stream develops a profile characterized by a low gradient section on top of the resistant layer and a very steep section (rapids or falls in natural streams) which rapidly cuts headward. In the model shown here, erosion is assumed to be proportional to the product of the bed erodibility and the average channel bed shear stress (Howard and Kerby 1983). Between streams, scarps are assumed to erode by the backwasting process described above. Figure 7.40 shows a simulated scarp eroded by both fluvial downcutting and scarp backwasting, and Figure 7.41 is similar but with convexity-enhanced scarp backwasting. Figures 7.37 and 7.38 are natural scarps similar to Figures 7.41 and 7.40, respectively. Scarp morphology is similar to that produced by scarp backwasting, with the addition of several deep re-entrants characterized by a gradually narrowing width and projections that are sharply pointed in the linear case and rounded in the convexity-enhanced case.

All of the fluvial models combine scarp backwasting with downcutting and scarp retreat due to fluvial erosion, with valleys gradually enlarging downstream due to longer duration since fluvial backwasting passed through that location. The angle subtended by the valley walls ψ is related to the ratio of the scarp backwasting rate R_b to the stream headcutting rate R_s by the expression

$$R_b/R_s = \sin \psi/2. \qquad (7.6)$$

The rate of downstream increase of valley width has been used by Schmidt (1980, 1989b) to estimate scarp recession rates.

Groundwater Sapping

Groundwater sapping is an important process in scarp retreat throughout the Colorado Plateau (Ahnert 1960) and probably contributes to the scarp backwasting process discussed above. However, the deep, narrow, bluntly terminated canyon networks of the type discussed by Laity and Malin (1985) and Howard and Kochel (1988) are the scarp form most clearly dominated by sapping processes.

Ahnert (1960) and Laity and Malin (1985) suggested that while fluvial erosion produces V-shaped canyon heads that widen consistently downstream,

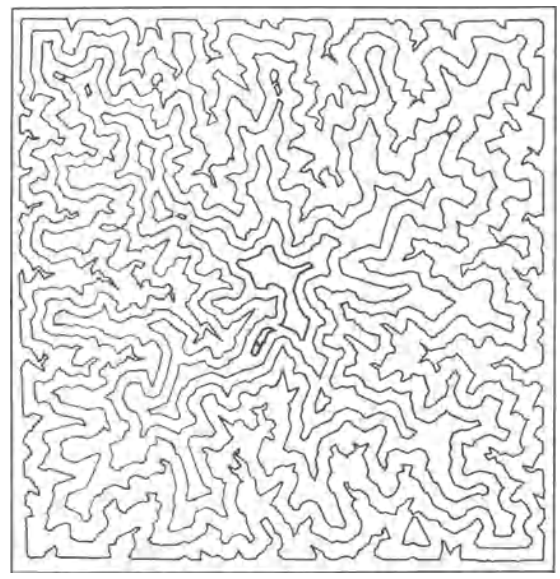

Figure 7.40 Plan view of successive stages of simulated erosion of an initially square mesa by combined action of fluvial downcutting and uniform scarp retreat.

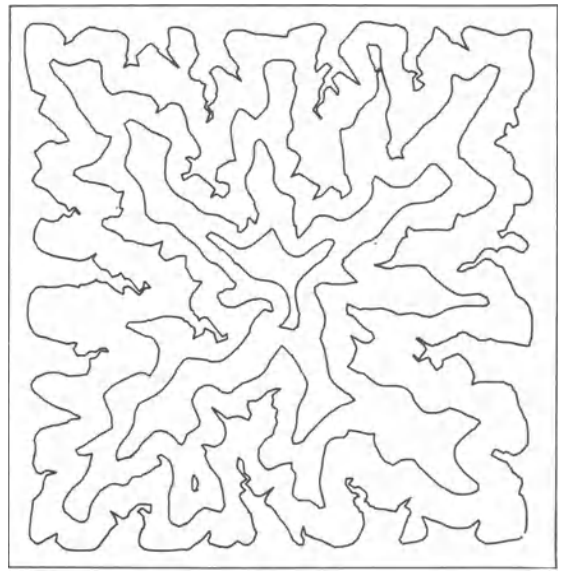

Figure 7.41 Plan view of successive stages of simulated erosion of an initially square mesa by combined action of fluvial downcutting and uniform erosion with a curvature rate dependence.

sapping produces U-shaped, theatre-headed canyons of relatively constant width downstream (the terms U- and V-shaped refer here to valley planform, not valley cross-section). Other planform features diagnostic of sapping-dominated canyon extension and widening include theatre-shaped heads of first-order tributaries with active seeps (Figs 7.26 and 7.42), relatively constant valley width from source to outlet (Figs 7.42 and 7.43), high and steep valley sidewalls, pervasive structure control, and frequent hanging valleys. The most direct evidence of sapping processes are the numerous alcoves, both in valley heads and along sidewalls, and the many springs on the valley walls and bottoms. Although many valley headwalls occur as deeply undercut alcoves, some terminate in V or half-U shapes with obvious extension along major fractures (Fig. 7.43). Although sapping action is fairly evident where alcoves occur at valley heads, sapping may also occur in fracture-controlled headwalls. Evidence for erosion by streams passing over the valley headwalls is slight, and plunge pools are not obvious. The valley extension along fracture traces suggests control by groundwater flowing along the fractures, and a preponderance of the major valley heads are oriented updip, which is consistent with sapping by a regional downdip groundwater flow. One striking feature of these canyon networks is frequent discrepancy between the extent of headward canyon growth and the relative upland area contributing drainage to the canyon head, including situations where the upland drainage enters the side rather than the end of the canyon (Fig. 7.42). Such circumstances suggest that goundwater flow rather than surface runoff controls headward extension of the canyons. Another indication of sapping control is the extension of canyons right up to major topographic divides (Fig. 7.42), sometimes causing the divides to be displaced. In contrast to surface runoff, groundwater flow can locally cross topographic divides. Divide migration can also occur in surface runoff drainage basins (see discussion of badlands), but is associated with the presence of slopes that are well graded from stream to divide. In the case of headward migration of canyons, streams above the scarp are perched on the upper slickrock slopes, so that base level control is very indirect.

The pattern of valley development and the relative contribution of sapping processes versus fluvial erosion is influenced by many structural, stratigraphic, and physiographic features. Infiltration may be restricted where overlying aquicludes were not stripped from the sandstone (Laity and Malin 1985, Laity 1988). The permeability of the sandstone is influenced not only by primary minerals but by diagenetic cements and overgrowths. These secondary minerals vary considerably from layer to layer and location to location (Laity 1983, 1988). Kochel and Riley (1988) and Laity (1988) discussed the important role that thin aquicludes (generally interdune deposits) and bedding strikes and dips have in controlling groundwater flow through the sandstone. Primary and off-loading (sheeting) fractures are important avenues of groundwater migration (Laity and Malin 1985, Laity 1988, Kochel and Riley 1988). On the other hand, dense primary fracturing, such as occurs in the Wingate Sandstone, restricts development of alcoves and probably diminishes weathering by cement solution and salt fretting (Laity 1988), although sapping processes may still be important but lack the spectacular alcoves commonly developed in the Navajo Sandstone. Relatively flat uplands on sandstones should encourage infiltration, whereas steep slickrock slopes probably lose much precipitation to runoff. Weathering pits and thin covers of windblown sand may also encourage infiltration.

A simulation model of scarp backwasting by groundwater sapping assumes a planar caprock aquifer (that may be tilted) with uniform areal recharge and a self-similar areal variation in permeability. The rate of sapping backwasting E is assumed to depend upon the amount by which the linear discharge rate at the scarp face q exceeds a critical discharge q_c: $E = k(q - q_c)^a$, where k and a are coefficients. Scarp erosion is simulated by solving for the groundwater flow, eroding the scarp by a small amount, with repeated iterations. Figure 7.44 shows a simulated scarp with $q_c = 0$ and $a = 1$. Figure 7.45 shows a case with $q_c = 0$ and $a = 2$. Figure 7.46 shows a case with $q_c = 0$ and $a = 2$ and superimposed scarp backwasting. Figure 7.43 is a natural scarp in Navajo Sandstone formed largely by sapping. Valleys developed by groundwater sapping tend to be linear or crudely dendritic, with nearly constant width and rounded rather than sharp terminations, in accord with the predictions of Ahnert (1960) and Laity and Malin (1985).

Deep re-entrants that are essentially constant in width with rounded ends imply either that almost all valley enlargement occurs at the headward end of the valley (see, for example, the simulations in Figs 7.44 and 7.45) or that a period of rapid headward canyon growth (either by sapping or fluvial incision) is succeeded by a period of uniform scarp retreat. This latter case is exemplified by the simulations in Figure 7.46 combining groundwater sapping and uniform backwasting in which rapid valley erosion

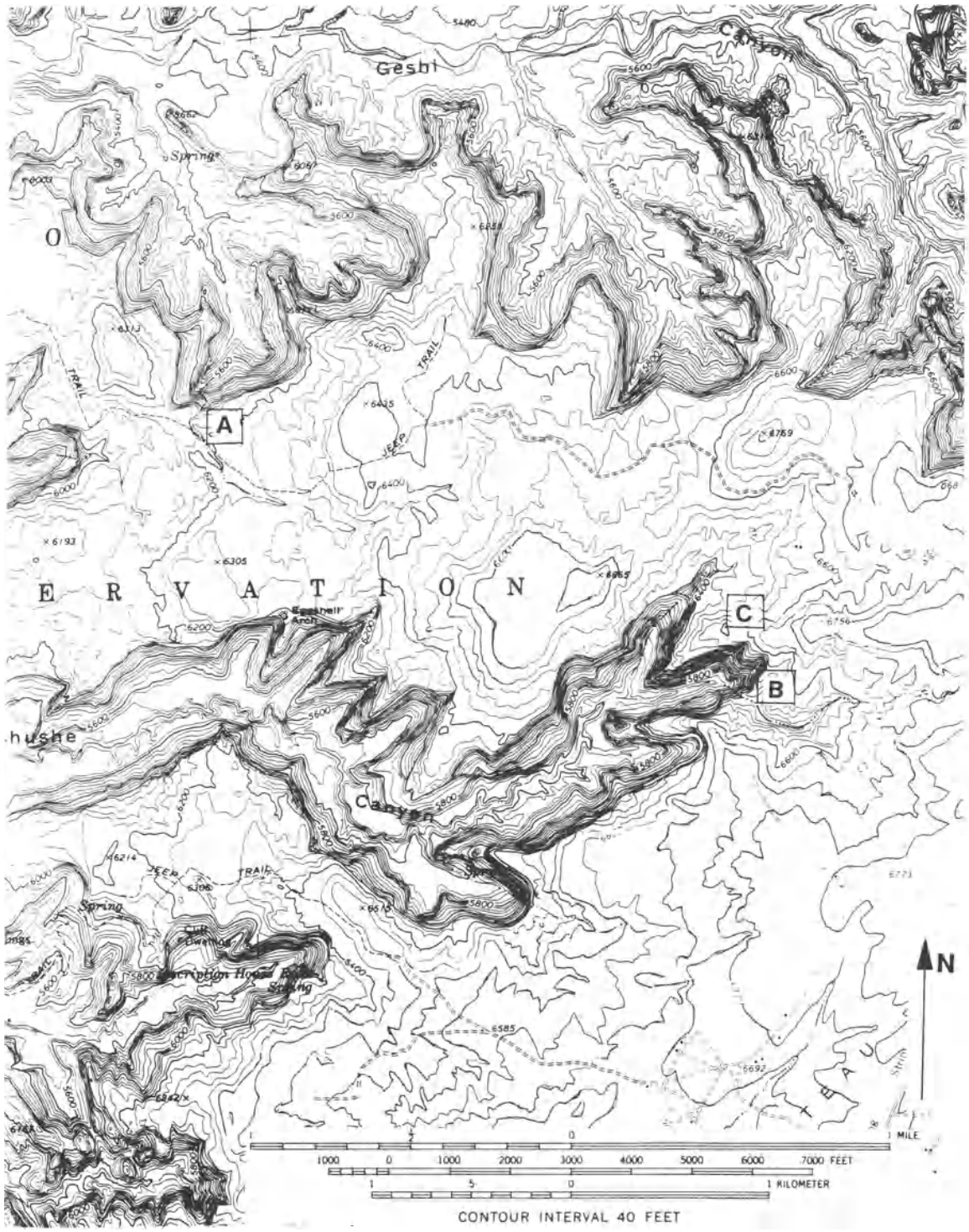

Figure 7.42 Topographic map of box canyons eroded into Navajo Sandstone in the Inscription House area of the Navajo indian reservation, Arizona (part of the Inscription House Ruin 1:24 000 quadrangle). Note that the backslope drainage at B does not enter the canyon at its head and that the canyon headwalls at C extend nearly to the backslope divide with little contributing drainage area. The extensive upslope drainage enters the large alcove at A at a minor niche. Also note the rounded, theatre-like canyon headwalls, most of which have active seeps.

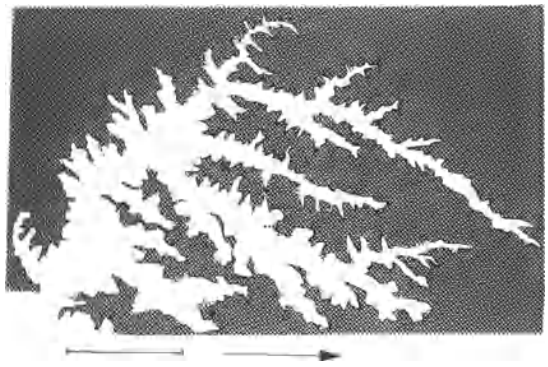

Figure 7.43 Planform of cuesta in Navajo Sandstone at Betatakin National Monument, Arizona, showing rounded canyon headwalls, weak branching, and nearly uniform canyon width. Re-entrants locally show strong control of orientation by fractures (Kayenta 1:100 000 quadrangle). The uneroded portion of the scarp is patterned.

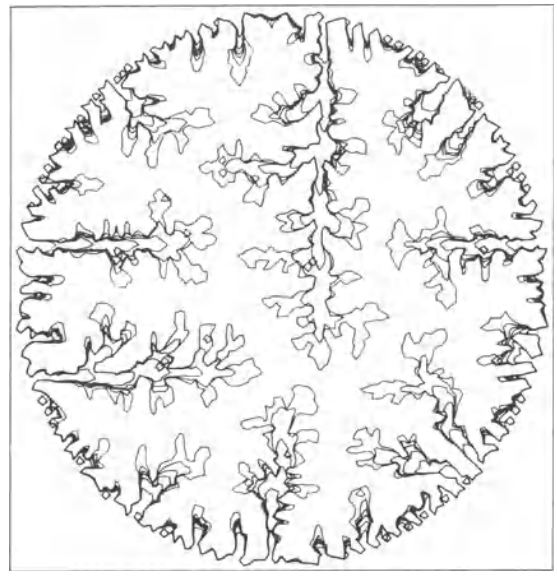

Figure 7.45 Simulated sapping erosion of an initially round mesa as in Figure 7.42, but with erosion rate proportional to the square of seepage discharge rate.

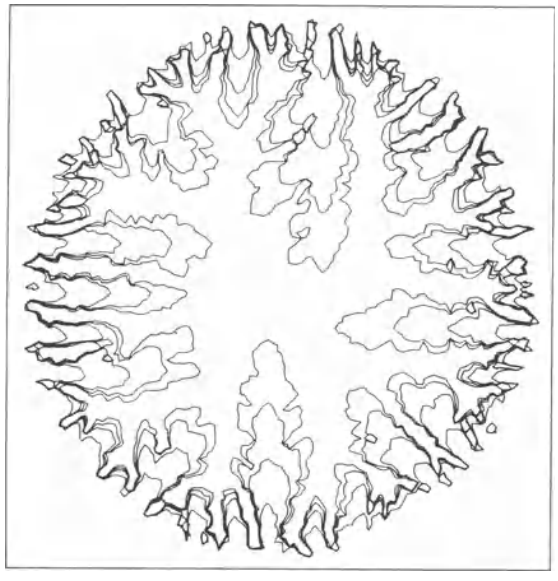

Figure 7.44 Plan view of successive stages of simulated erosion of an initially round mesa by groundwater sapping. Caprock aquifer is assumed to undergo uniform recharge from above and water flows along the base of the caprock at the contact with underlying shale until it emerges at the edges of the mesa. Erosion rate is proportional to seepage discharge rate per unit width of scarp face.

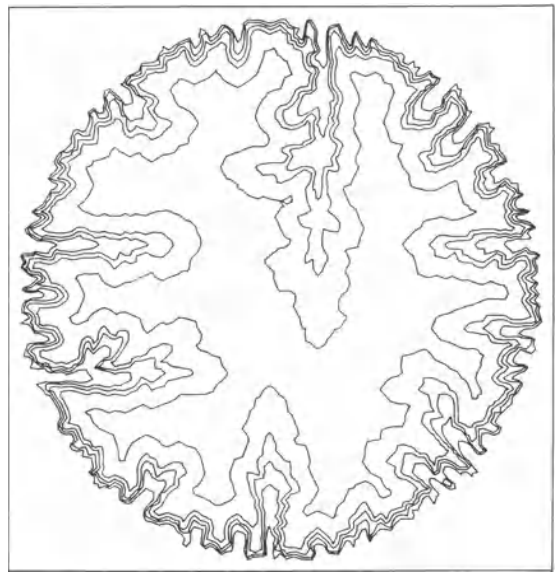

Figure 7.46 Simulated sapping erosion of an initially round mesa as in Figure 7.43, but with superimposed uniform scarp retreat.

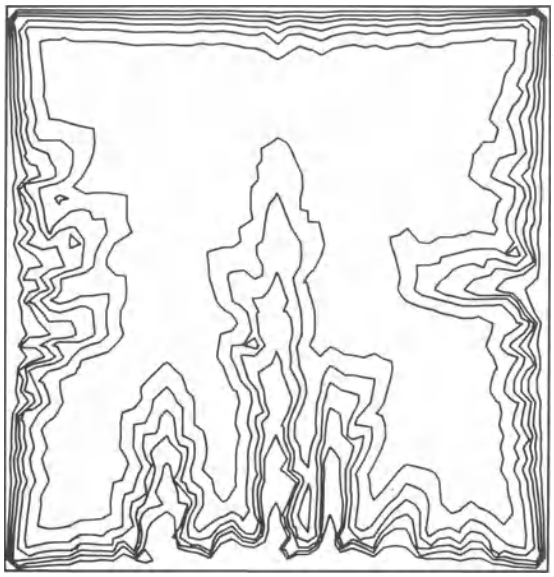

Figure 7.47 Simulated sapping erosion of a slightly tilted square mesa by groundwater sapping. The caprock tilts to the bottom. Note the strongly asymmetrical development of re-entrant canyons.

by sapping early in the simulation is succeeded by a dominance of uniform backwasting in later stages of erosion as upland areas contributing to groundwater sapping diminish in size.

Summary of Scarp Modelling

These simulations illustrate a common evolutionary sequence in scarp erosion. Early stages are characterized by a planform determined largely by the agency first exposing the scarp, generally fluvial downcutting. Thus scarp walls parallel the stream course with small re-entrants along tributaries draining over the scarp. Continuing tributary erosion by fluvial or sapping processes with modest rates of scarp backwasting between streams eventually creates a maximally crenulate scarp planform. As erosion continues and upland areas diminish, rates of stream or sapping backcutting diminish relative to more uniform scarp backwasting (which may accelerate as relief increases) so that the scarp planform becomes characterized by broad re-entrants, sharp cusps, and often isolated small buttes during the last stages before complete caprock removal. This is illustrated in Figures 7.40 and 7.46. This sequence can occur sequentially on a single large mesa, as takes place in the simulations, but it is also illustrated by spatial sequences during long-continued erosion of a given caprock from newly exposed scarps in structurally low areas to the last caprock remnants in structurally high areas.

Even slight structural dips create a strong asymmetry of rates of fluvial and sapping headcutting on down- and updip facing portions of the scarp, since drainage divides tend to be located close to the updip crest. General scarp backwasting is less affected by dip, so that updip scarp segments are nearly linear, whereas downdip sections are highly crenulate. This is illustrated in the natural scarp in Figure 7.39 and the simulated sapping erosion of a tilted scarp in Figure 7.47.

The planform of escarpments gradually develops through scarp retreat of hundreds to thousands of metres. Thus it is unlikely that planforms reflect to any great extent Quaternary climatic oscillations. Longer-term climatic changes may have influenced scarp planforms, but such influences would probably be hard to detect.

CONCLUSIONS

Weathering and erosional processes on exposed bedrock are generally either very slow-acting or occur as large and often rapid mass wasting events. As a result, process studies of the sort that have been conducted on badland and rock-mantled slopes are rare. Furthermore, the slow development of bedrock landforms often implies a strong influence of climate changes on slope form. Among the issues that need further study are (a) the relative roles of stress-release fracturing and contemporary gravitational, neotectonic, or weathering-induced stresses in generating broadly rounded bedrock exposures, (b) weathering processes involved in groundwater sapping, (c) controls on rates of scarp backwasting and scarp height and steepness, and (d) processes of talus weathering and removal on scarp ramparts. We anticipate that the study of landform development on bedrock will benefit greatly from application of modern techniques for dating of geomorphic surfaces, including use of rock varnish (Chapters 6 and 20) and thermoluminescence, fission-track, and radiogenic or cosmogenic isotopes.

REFERENCES

Abrahams, A.D. and A.J. Parsons 1987. Identification of strength equilibrium rock slopes: further statistical considerations. *Earth Surface Processes and Landforms* **12**, 631–5.

Ackroyd, P. 1987. Erosion by snow avalanche and implications for geomorphic stability, Torlesse Range, New Zealand. *Arctic and Alpine Research* **19**, 65–80.

Ahnert, F. 1960. The influence of Pleistocene climates upon the morphology of cuesta scarps on the Colorado Plateau. *Annals of the American Association of Geographers* **50**, 139–56.

Ahnert, F. 1976. Darstellung des Structureinflusses auf de Oberflachenformen in theoretischen Modell. *Zeitschrift für Geomorphologie Supplement Band* **24**, 11–22.

Akerman, H.J. 1984. Notes on talus morphology and processes in Spitsbergen. *Geografiska Annaler* **66A**, 267–84.

Allison, R.J. and A.S. Goudie 1990a. The form of rock slopes in tropical limestone and their associations with rock mass strength. *Zeitschrift für Geomorphologie* **34**, 129–48.

Allison, R.J. and A.S. Goudie 1990b. Rock control and slope profiles in a tropical limestone environment: the Napier Range of Western Australia. *Geographical Journal* **156**, 200–11.

Anderson, M.G. and K.S. Richards (eds) 1987. *Slope stability – geotechnical engineering and geology*. Chichester: Wiley.

Aronsson, G.K. and K. Linde 1982. Grand Canyon – a quantitative approach to the erosion and weathering of a stratified bedrock. *Earth Surface Processes and Landforms* **7**, 589–99.

Augustinus, P.C. and M.J. Selby 1990. Rock slope development in McMurdo Oasis, Antarctica, and implications for interpretation of glacial history. *Geografiska Annaler* **72A**, 55–62.

Baker, V.R., R.C. Kochel, J.E. Laity and A.D. Howard 1990. Spring sapping and valley network development. In *Groundwater geomorphology*, C.G. Higgins and D.R. Coates (eds), 235–65. Geological Society of America Special Paper **252**.

Bakker, J.P. and J.W.N. Le Heux 1952. A remarkable new geomorphological law. *Koninklijke Nederlandsche Academie van Wetenschappen* **B55**, 399–410, 554–71.

Bieniawski, Z.T. 1989. *Engineering rock mass classifications*. New York: Wiley.

Blackwelder, E. 1942. The process of mountain sculpture by rolling debris. *Journal of Geomorphology* **4**, 324–8.

Blasius, K.R., J.A. Cutts, J.E. Guest and H. Masursky 1977, Geology of the Valles Marineris: first analysis of imaging from Viking 1 orbiter primary mission. *Journal of Geophysical Research* **82**, 4067–91.

Bock, H. 1979. Experimental determination of the residual stress field in a basaltic column. *Proceedings of the International Congress on Rock Mechanics Montreux* **1**, 45–9; **3**, 136–7.

Bornhardt, W. 1900. *Zur Oberflachengestaltung und Geologie Deutsch-Ostafrikas*. Berlin: Reimer.

Bouchard, M. 1985. Weathering and weathering residuals on the Canadian Shield. *Fennia* **163**, 327–32.

Boyé, M. and P. Fritsch 1973. Degagement artificiel d'un dome cristallin au Sud Cameroun. In *Cinq etudes de geomorphologie et de palynologie travaux et documents de geographie tropicale*. CEGET-CNRS **8**, 31–63.

Bradley, W.C. 1963. Large-scale exfoliation in massive sandstones of the Colorado Plateau. *Bulletin of the Geological Society of America* **74**, 519–28.

Brady, B.H.G. and E.T. Brown 1985. *Rock mechanics for underground mining*. London: George Allen & Unwin.

Brown, E.T. 1981. *Rock characterization testing and monitoring: ISRM suggested methods*. Oxford: Pergamon.

Brown, G.F., D.L. Schmidt and A.C. Huffman 1989. Geology of the Arabian Peninsula: shield area of western Saudi Arabia. *U.S. Geological Survey Professional Paper* 560-A.

Brunsden, D. and D.B. Prior (eds) 1984. *Slope instability*. Chichester: Wiley.

Bryan, K. 1928. Niches and other cavities in sandstones at Chaco Canyon, N. Mexico. *Zeitschrift für Geomorphologie* **3**, 125–40.

Budel, J. 1957. Die 'doppelten Einebnungsflachen' in den feuchten Tropen. *Zeitschrift für Geomorphologie* **1**, 201–88.

Budel, J. 1982. *Climatic geomorphologie* (translated by L. Fischer and D. Busche). Princeton: Princeton University Press.

Burke, K. and G.L. Wells 1989. Trans-African drainage system of the Sahara: was it the Nile? *Geology* **17**, 743–7.

Buser, O. and H. Frutiger 1980. Observed maximum run-out distance of snow avalanches and the determination of the friction coefficients mu and epsilon. *Journal of Glaciology* **94**, 121–30.

Campbell, I.A. 1973. Controls of canyon and meander forms by jointing. *Area* **5**, 291–6.

Cannon, S.H. and W.Z. Savage 1988. A mass-change model for the estimation of debris-flow runout. *Journal of Geology* **96**, 221–7.

Carson, M.A. 1971. An application of the concept of threshold slopes to the Laramie Mountains, Wyoming. *Institute of British Geographers Special Publication* 3, 31–47.

Carson, M.A. and M.J. Kirkby 1972. *Hillslope form and process*. Cambridge: Cambridge University Press.

Carson, M.A. and D.J. Petley 1970. The existence of threshold slopes in the denudation of the landscape. *Transactions of the Institute of British Geographers* **49**, 71–95.

Conca, J.L. and G.R. Rossman 1982. Case hardening of sandstone. *Geology* **10**, 520–33.

Cooke, R.U. and I.J. Smalley 1968. Salt weathering in deserts. *Nature* **220**, 1226–7.

Cooke, R.U. and A. Warren 1973. *Geomorphology in deserts*. Berkeley: University of California Press.

Corner, C.D. 1980. Avalanche impact landforms in Troms, north Norway. *Geografiska Annaler* **62A**, 1–10.

Cotton, C.A. and A.T. Wilson 1971. Ramp forms that result from weathering and retreat of precipitous slopes. *Zeitschrift für Geomorphologie* **15**, 199–211.

Dale, T.N. 1923. The commercial granites of New England. *U.S. Geological Survey Bulletin* **738**.

Davis, W.M. 1901. An excursion into the Grand Canyon of the Colorado. *Harvard Museum of Comparative Zoology and Geology* **5**, 105–201.

Dent, J.D. and T.E. Lang 1980. Modeling of snow flow. *Journal of Glaciology* **26**, 131–40.

Dent, J.D. and T.E. Lang 1983. A biviscous modified Bingham model of snow avalanche motion. *Annals of Glaciology* **4**, 42–6.

Doelling, H.H. 1985. *Geology of Arches National Park*. Utah Geological and Mineral Survey, Map 74.

Dutton, C.E. 1882. Tertiary history of the Grand Canyon district. *U.S. Geological Survey Monograph* 2.

Einstein, H.H. and W.S. Dershowitz 1990. Tensile and

shear fracturing in predominantly compressive stress fields – a review. *Engineering Geology* **29**, 149–72.

Erhart, H. 1956. *La genese des sols. Esquise d'une theorie geologique*. Paris: Masson.

Fairbridge, R.W. 1988. Cyclical patterns of exposure, weathering and burial of cratonic surfaces, with some examples from North America and Australia. *Geografiska Annaler* **70A**, 277–83.

Falconer, J.D. 1911. *The geology and geography of northern Nigeria*. London: Macmillan.

Gardiner, J. 1970. Geomorphic significance of avalanches in the Lake Louise area, Alberta, Canada. *Arctic and Alpine Research* **2**, 135–44.

Gardiner, J. 1983. Observations on erosion by wet snow avalanches, Mount Rae area, Alberta, Canada. *Arctic and Alpine Research* **15**, 271–4.

Gardiner, V. and R. Dackombe 1983. *Geomorphological field manual*. London: George Allen and Unwin.

Gerber, E.K. and A.E. Scheidegger 1973. Erosional and stress-induced features on steep slopes. *Zeitschrift für Geomorphologie Supplement Band* **18**, 38–49.

Gerson, R. 1982. Talus relics in deserts: a key to major climatic fluctuations. *Israel Journal of Earth Sciences* **31**, 123–32.

Gerson, R. and S. Grossman 1987. Geomorphic activity on escarpments and associated fluvial systems in hot deserts. In *Climate history, periodicity, predictability*, M.R. Rampino, J.S. Sanders, R.E. Newman and L.K. Konigsson (eds), 300–22. New York: Van Nostrand Reinhold.

Gilbert, G.K. 1904. Domes and dome structures of the High Sierra. *Bulletin of the Geological Society of America* **15**, 29–36.

Gregory, H.E. 1917. Geology of the Navajo country. *U.S. Geological Survey Professional Paper* 93.

Habermehl, M.A. 1980. The Great Artesian Basin, Australia. *BMR Journal of Geology and Geophysics* **5**, 9–38.

Hack, J.T. 1966. Interpretation of Cumberland escarpment and Highland rim, South-central Tennessee and northeast Alabama. *U.S. Geological Survey Professional Paper* 524-C.

Hack, J.T. 1980. Rock control and tectonism; their importance in shaping the Appalachian Highlands. *U.S. Geological Survey Professional Paper* 1126-A–J, pp. B1–B17.

Hall, A.M. 1986. Deep weathering patterns in north-east Scotland and their geomorphological significance. *Zeitschrift für Geomorphologie* **30**, 407–22.

Hall, A.M. 1988. The characteristics and significance of deep weathering in the Gaick area, Grampian Highlands, Scotland. *Geografiska Annaler* **70A**, 309–14.

Hamilton, W.L. 1984. *The sculpturing of Zion*. Zion National Park: Zion Natural History Association.

Haxby, W.F. and D.L. Turcotte 1976. Stresses induced by the addition or removal of overburden and associated thermal effects. *Geology* **4**, 181–4.

Hewett, K. 1972. The mountain environment and geomorphic processes. In *Mountain geomorphology*, H.O. Slaymaker and H.J. McPherson (eds), 17–34. Vancouver: Tantalus Press.

Higgins, C.G. 1984. Piping and sapping: development of landforms by groundwater flow. In *Groundwater as a geomorphic agent*, R.G. LaFleur (ed.), 18–58. Boston: Allen & Unwin.

Higgins, C.G. and W.R. Osterkamp 1990. Seepage-induced cliff recession and regional denudation. In *Groundwater geomorphology*, C.G. Higgins and D.R. Coates (eds), 291–317, Geological Society of America Special Paper 252.

Hoek, E. and J.W. Bray 1981. *Rock slope engineering*. London: Institution of Mining and Metallurgy.

Howard, A.D. 1970. A study of process and history in desert landforms near the Henry Mountains, Utah. Unpublished Ph.D. dissertation. Baltimore: Johns Hopkins University.

Howard, A.D. 1988. Groundwater sapping experiments and modeling. In *Sapping features of the Colorado Plateau*, A.D. Howard, R.C. Kochel and H.E. Holt (eds), 71–83, Washington: National Aeronautics and Space Administration SP-491.

Howard, A.D. 1989. Miniature analog of spur-and-gully landforms in Valles Marineris scarps. *Reports of the planetary geology and geophysics program – 1988*. Washington: National Aeronautics and Space Administration TM 4130, 355–7.

Howard, A.D. 1990. Preliminary model of processes forming spur-and-gully terrain. *Reports of the planetary geology and geophysics program – 1989*. Washington: National Aeronautical and Space Administration TM 4210, 345–7.

Howard, A.D. and G.R. Kerby 1983. Channel changes in badlands. *Bulletin of the Geological Society of America* **94**, 739–52.

Howard, A.D. and R.C. Kochel 1988. Introduction to cuesta landforms and sapping processes on the Colorado Plateau. In *Sapping features of the Colorado Plateau*. A.D. Howard, R.C. Kochel and H.E. Holt (eds), 6–56. Washington: National Aeronautics and Space Administration SP-491.

Howard, A.D., R.C. Kochel and H.E. Holt (eds) 1988. *Sapping features of the Colorado Plateau*. Washington: National Aeronautics and Space Administration SP-491.

Idnurm, M. and B.R. Senior 1978. Palaeomagnetic ages of Late Cretaceous and Tertiary weathered profiles in the Eromanga Basin, Queensland. *Palaeogeography, Palaeoclimatology, Palaeoecology* **24**, 263–77.

Jahns, R.H. 1943. Sheet structure in granites, its origin and use as a measure of glacial erosion in New England. *Journal of Geology* **51**, 71–98.

Jennings, J.N. 1983. Sandstone pseudokarst or karst. In *Aspects of Australian sandstone landscapes*, Australian and New Zealand Geomorphology Group, Special Publication 1, 21–30.

Kemp, E.M. 1981. Tertiary palaeogeography and the evolution of Australian climate. In *Ecological biogeography of Australia*, A. Keast (ed.), 33–49. The Hague: W. Junk.

Kochel, R.C. and G.W. Riley 1988. Sedimentologic and stratigraphic variations in sandstones of the Colorado Plateau and their implications for groundwater sapping. In *Sapping features of the Colorado Plateau*, A.D. Howard, R.C. Kochel and H.E. Holt (eds), 57–62. Washington: National Aeronautics and Space Administration SP-491.

Koons, D. 1955. Cliff retreat in the southwestern United States. *American Journal of Science* **253**, 44–52.

Korsch, R.J. 1982. Mount Duval: geomorphology of a near-surface granite diapir. *Zeitschrift für Geomorphologie* **26**, 151–62.

Laity, J.E. 1983. Diagenetic controls on groundwater sapping and the valley formation, Colorado Plateau, as

revealed by optical and electron microscopy. *Physical Geography* **4**, 103–25.

Laity, J. 1988. The role of groundwater sapping in valley evolution on the Colorado Plateau. In *Sapping features of the Colorado Plateau*. A.D. Howard, R.C. Kochel and H.E. Holt (eds), 63–70. Washington: National Aeronautics and Space Administration SP-491.

Laity, J.E. and M.C. Malin 1985. Sapping processes and the development of theater-headed valley networks in the Colorado Plateau. *Bulletin of the Geological Society of America* **96**, 203–17.

Lang, T.E. and J.D. Dent 1982. Review of surface friction, surface resistance, and flow of snow. *Reviews of Geophysics and Space Physics* **20**, 21–37.

Lange, A.L. 1959. Introductory notes on the changing geometry of cave structures. *Cave Studies* **11**.

Lee, C.F. 1978. Stress relief and cliff stability at a power station near Niagara Falls. *Engineering Geology* **12**, 193–204.

Lehmann, O. 1933. Morphologishe Theorie der Vervitterung von Steinschlag Wandern. *Vierteljahrschrift der Naturforschende Gesellschaft in Zürich* **87**, 83–126.

Lindquist, R.C. 1979. Genesis of the erosional forms of Bryce Canyon National Park. *Proceedings of the 1st conference on scientific research in the National Parks* **2**, 827–34. Washington, DC: National Park Service.

Lucchitta, B.K. 1978. Morphology of chasma walls, Mars. *Journal of Research, U.S. Geological Survey* **6**, 651–62.

Lucchitta, I. 1975. Application of ERTS images and image processing to regional geologic problems and geologic mapping in northern Arizona – Part IV B, the Shivwits Plateau. *National Aeronautics and Space Administration Technical Report* 32-1597, 41–72.

Luckman, B.H. 1977. The geomorphic activity of snow avalanches. *Geografiska Annaler* **59A**, 31–48.

Luckman, B.H. 1978. Geomorphic work of snow avalanches in the Canadian Rocky Mountains. *Arctic and Alpine Research* **10**, 261–76.

Mainguet, M. 1972. *Le modelegdes gres*. Paris: Institut Geographique National.

Martinelli, M. Jr, T.E. Lang and A.I. Mears 1980. Calculations of avalanche friction coefficients from field data. *Journal of Glaciology* **26**, 109–19.

Matthes, F.E. 1938. Avalanche sculpture in the Sierra Nevada of California. *International Association of Scientific Hydrology Bulletin* **23**, 631–7.

Maxwell, T.A. 1982. Erosional patterns of the Gilf Kebir Plateau and implications of the origin of Martian canyonlands. In *Desert landforms of southwest Egypt: a basis for comparison with Mars*, F. El-Baz and T.A. Maxwell (eds), 207–39. Washington: National Aeronautics and Space Administration CR-3611.

McClung, D.M. and P.A. Schaerer 1983. Determination of avalanche dynamics friction coefficients from measured speeds. *Annals of Glaciology* **4**, 170–3.

McEwen, A.S. and M.C. Malin 1990. Dynamics of Mount St. Helens' 1980 pyroclastic flows, rockslide-avalanche, lahars, and blast. *Journal of Volcanology and Geothermal Research* **37**, 205–31.

McGarr, A. and N.C. Gay 1978. State of stress in the earth's crust. *Annual Review of Earth and Planetary Sciences* **6**, 405–36.

McGill, G.E. and A.W. Stromquist 1975. Origin of graben in the Needles District, Canyonlands National Park, Utah. *Four Corners Geological Society Guidebook, 8th Field Conference*, 235–43.

Moon, B.P. 1984a. The form of rock slopes in the Cape Fold Mountains. *The South African Geographical Journal* **66**, 16–31.

Moon, B.P. 1984b. Refinement of a technique for measuring rock mass strength for geomorphological purposes. *Earth Surface Processes and Landforms* **9**, 189–93.

Moon, B.P. 1986. Controls on the form and development of rock slopes in fold terrane. In *Hillslope processes*, A.D. Abrahams (ed.), 225–43. Boston: Allen & Unwin.

Moon, B.P. and M.J. Selby 1983. Rock mass strength and scarp forms in southern Africa. *Geografiska Annaler* **65A**, 135–45.

Mustoe, G.E. 1982. Origin of honeycomb weathering. *Bulletin of the Geological Society of America* **93**, 108–15.

Mustoe, G.E. 1983. Cavernous weathering in the Capitol Reef Desert, Utah. *Earth Surface Processes and Landforms* **8**, 517–26.

Nicholas, R.M. and J.C. Dixon 1986. Sandstone scarp form and retreat in the Land of Standing Rocks, Canyonlands National Park, Utah. *Zeitschrift für Geomorphologie* **30**, 167–87.

Oberlander, T.M. 1972. Morphogenesis of granitic boulder slopes in the Mojave Desert California. *Journal of Geology* **80**, 1–20.

Oberlander, T.M. 1977. Origin of segmented cliffs in massive sandstones of southeastern Utah. In *Geomorphology in arid regions*, D.O. Doehring (ed.), 79–114. Binghamton, NY: Publications in Geomorphology.

Oberlander, T.M. 1989. Slope and pediment systems. In *Arid zone geomorphology*, D.S.G. Thomas (ed.), 56–84. New York: Halsted Press.

Ollier, C.D. 1988. Deep weathering, groundwater and climate. *Geografiska Annaler* **70A**, 285–90.

Ollier, C.D. and C.F. Pain 1981. Active gneiss domes in Papua New Guinea, new tectonic landforms. *Zeitschrift für Geomorphologie* **25**, 133–45.

O'Loughlin, C.L. and A.J. Pearce 1982. Erosional processes in the mountains. In *Landforms of New Zealand*, J.M. Soons and M.J. Selby (eds), 67–79. Auckland: Longman Paul.

Patton, P.C. 1981. Evolution of the spur and gully topography on the Valles Marineris wall scarps. *Reports of the planetary geology program 1981*. National Aeronautics and Space Administration Technical Memorandum 84211, 324–5.

Peel, R.F. 1941. Denudational landforms of the central Libyan Desert. *Journal of Geomorphology* **4**, 3–23.

Peev, C.D. 1966. Geomorphic activity of snow avalanches. *International Association of Scientific Hydrology Publication* 69, 357–68.

Perla, R., T.T. Cheng and D.M. McClung 1980. A two-parameter model of snow-avalanche motion. *Journal of Glaciology* **26**, 197–207.

Pollack, H.N. 1969. A numerical model of Grand Canyon. *Four Corners Geological Society, Geology and Natural History of the Grand Canyon Region*, 61–2.

Pouyllau, M. and M. Seurin 1985. Pseudo-karst dans des roches greso-quartzitiques de la formation Roraima. *Kar-*

stologia **5**, 45–52.
Rapp, A. 1960a. Recent development of mountain slopes in Karkevagge and surroundings, northern Scandinavia. *Geografiska Annaler* **42**, 73–200.
Rapp, A. 1960b. Talus slopes and mountain walls at Templefjorden, Spitzbergen. *Norsk Polarinstitutt Scrifter* **119**, 96 pp.
Reiche, P. 1937. The Toreva Block, a distinctive landform type. *Journal of Geology* **45**, 538–48.
Richter, E. 1901. Geomorphologische Untersuchungen in den Hochalpen. *Dr. A. Petermann's Mitteilungen aus Justus Perthes' geographischer Ansalt, Ergänzungsheft* 132.
Rudberg, S. 1986. Present-day geomorphological processes in Prins Oscars Land, Svalvard. *Geografiska Annaler* **68A**, 41–63.
Sancho, C., M. Gutierrez, J.L. Pena and F. Burillo 1988. A quantitative approach to scarp retreat starting from triangular slope facets, central Ebro Basin, Spain. *Catena Supplement* **13**, 139–46.
Scheidegger, A.E. 1991. *Theoretical geomorphology* (3rd edn). Berlin: Springer.
Schiewiller, T. and K. Hunter 1983. Avalanche dynamics. Review of experiments and theoretical models of flow and powder-snow avalanches. *Journal of Glaciology* **29**, 283–5.
Schipull, K. 1980. Die Cedar Mesa – Schichtstufe aud dem Colorado Plateau – ein Beispiel für die Morphodynamik arider Schichtstufen. *Zeitschrift für Geomorphologie* **24**, 318–31.
Schmidt, K.-H. 1980. Eine neue Metode zur Ermittlung von Stufenruckwanderungsraten, dargestellt am Beispiel der Black Mesa Schichtstufen, Colorado Plateau, USA. *Zeitschrift für Geomorphologie* **24**, 180–91.
Schmidt, K.-H. 1987. Factors influencing structural landform dynamics on the Colorado Plateau – about the necessity of calibrating theoretical models by empirical data. *Catena Supplement* **10**, 51–66.
Schmidt, K.-H. 1988. Rates of scarp retreat: a means of dating neotectonic activity. In *The Atlas system of Morocco – studies on its geodynamic evolution*, V.H. Jacobshagen (ed.), 445–62. Berlin: Lecture Notes in Earth Science **15**.
Schmidt, K.-H. 1989a. Talus and pediment flatirons – erosional and depositional features of dryland cuesta scarps. *Catena Supplement* **14**, 107–18.
Schmidt, K.-H. 1989b. The significance of scarp retreat for Cenozoic landform evolution on the Colorado Plateau, USA. *Earth Surface Processes and Landforms* **14**, 93–105.
Schumm, S.A. and R.J. Chorley 1964. The fall of threatening rock. *American Journal of Science* **262**, 1041–54.
Schumm, S.A. and R.J. Chorley 1966. Talus weathering and scarp recession in the Colorado Plateau. *Zeitschrift für Geomorphologie* **10**, 11–36.
Selby, M.J. 1977. Bornhardts of the Namib Desert. *Zeitschrift für Geomorphologie* **21**, 1–13.
Selby, M.J. 1980. A rock mass strength classification for geomorphic purposes: with tests from Antarctica and New Zealand. *Zeitschrift für Geomorphologie* **24**, 31–51.
Selby, M.J. 1982a. Form and origin of some bornhardts of the Namib Desert. *Zeitschrift für Geomorphologie* **26**, 1–15.
Selby, M.J. 1982b. Rock mass strength and the form of some inselbergs in the Central Namib Desert. *Earth Surface Processes and Landforms* **7**, 489–97.
Selby, M.J. 1982c. Controls on the stability and inclinations of hillslopes formed on hard rock. *Earth Surface Processes and Landforms* **7**, 449–67.
Selby, M.J. 1982d. *Hillslope materials and processes*. Oxford: Oxford University Press.
Selby, M.J. 1985. *Earth's changing surface*. Oxford: Clarendon Press.
Selby, M.J. 1987. Rock slopes. In *Slope stability: geotechnical engineering and geomorphology*, M.G. Anderson and K.S. Richards (eds), 475–504. Chichester: Wiley.
Selby, M.J., P. Augustinus, V.G. Moon and R.J. Stevenson 1988. Slopes on strong rock masses: modelling and influences of stress distributions and geomechanical properties. In *Modelling geomorphological systems*, M.G. Anderson (ed.), 341–74. Chichester: Wiley.
Sharp, R.P. and M.C. Malin 1975. Channels on Mars. *Bulletin of the Geological Society of America* **86**, 593–609.
Slatyer, R.O. 1962. Climate of the Alice Springs area. *Land Research Series* **6**, CSIRO, Melbourne, 109–28.
Stille, H. 1924. *Grundfragen der vergleichenden Tektonic*. Berlin: Gebruder Borntraeger.
Strahler, A.N. 1940. Landslides of the Vermillion and Echo Cliffs, northern Arizona. *Journal of Geomorphology* **3**, 285–300.
Sturgul, J.R., A.E. Scheidegger and Z. Grinshpan 1976. Finite-element model of a mountain massif. *Geology* **4**, 439–42.
Suess, E. 1904–24. *The face of the Earth* (translated H.B.C. Sollas), 5 vols. Oxford: Clarendon Press. (German edition 1885–1909, Vienna: Tempsky.)
Terzaghi, K. 1962. Stability of steep slopes in hard unweathered rock. *Geotechnique* **12**, 251–70.
Thomas, M.F. 1989a. The role of etch processes in landform development: I. etching concepts and their applications. *Zeitschrift für Geomorphologie* **33**, 129–42.
Thomas, M.F. 1989b. The role of etch processes in landform development: II. etching and the formation of relief. *Zeitschrift für Geomorphologie* **33**, 257–74.
Twidale, C.R. 1978. On the origin of Ayres Rock, central Australia. *Zeitschrift für Geomorphologie Supplement Band* **31**, 177–206.
Twidale, C.R. 1981. Granite Inselbergs. *Geographical Journal* **147**, 54–71.
Twidale, C.R. 1982a. The evolution of bornhardts. *American Scientist* **70**, 268–76.
Twidale, C.R. 1982b. *Granite landforms*. Amsterdam: Elsevier.
Twidale, C.R. 1990. The origin and implications of some erosional landforms. *Journal of Geology* **98**, 343–64.
Voight, B. and B.H.P. St Pierre 1974. Stress history and rock stress. *Proceedings of the Third Congress of the International Society for Rock Mechanics, Denver* **2**, 580–2.
Watson, R.A. and H.E. Wright, Jr, 1963. Landslides on the east flank of the Chuska Mountains, northwestern New Mexico. *American Journal of Science* **261**, 525–48.
Wayland, E.J. 1933. Peneplains and some other erosional platforms. *Annual Report and Bulletin of the Protectorate of Uganda Geological Survey and Department of Mines, Note* 1, 77–9.
Willis, B. 1936. *East African plateaus and rift valleys. Studies in comparative seismology*. Washington, DC: Carnegie Institution.

Wyrwoll, K.H. 1979. Late Quaternary climates of Western Australia: evidence and mechanisms. *Journal of the Royal Society of Western Australia* **62**, 129–42.

Yair, A. and R. Gerson 1974. Mode and rate of escarpment retreat in an extremely arid environment (Sharm el Sheikh, southern Sinai Peninsula). *Zeitschrift für Geomorphologie* **21**, 106–21.

Yatsu, E. 1988. *The nature of weathering: an introduction*. Tokyo: Sozosha.

Young, A.R.M. 1987. Salt as an agent in cavernous weathering. *Geology* **15**, 962–6.

Young, R.W. 1986. Tower karst in sandstone Bungle Bungle massif, northwestern Australia. *Zeitschrift für Geomorphologie* **30**, 189–202.

Young, R.W. 1987. Sandstone landforms of the tropical East Kimberley region, northwestern Australia. *Journal of Geology* **95**, 205–18.

Young, R.W. 1988. Quartz etching and sandstone karst: examples from the East Kimberleys, northwestern Australia. *Zeitschrift für Geomorphologie* **32**, 409–23.

Yu, Y.S. and D.F. Coates 1970. Analysis of rock slopes using the finite element method. *Department of Energy, Mines and Resources, Mines Branch, Mining Research Centre, Research Report* R229, Ottawa.

Zaruba, Q. and V. Mencl 1988. *Landslides and their control* (2nd edn). Amsterdam: Elsevier.

ROCK-MANTLED SLOPES 8

Athol D. Abrahams, Alan D. Howard, and Anthony J. Parsons

INTRODUCTION

This chapter will consider hillslopes with gradients less than 40° that are neither active, undissected piedmonts (i.e. pediments and alluvial fans, which are dealt with in Chapters 13 and 14) nor are developed in highly erodible, fine-grained sedimentary rocks (i.e. badlands slopes, which are treated in Chapter 9). Such hillslopes in desert (arid and semi-arid) climates are usually mantled with a thin layer of coarse debris that has either weathered out of the underlying substrate or fallen from a superincumbent cliff. The former hillslopes are herein referred to as debris slopes and the latter as talus slopes. In this chapter we shall first consider the processes acting on these rock-mantled slopes and then consider the forms they produce. These processes are not only important in terms of understanding hillslope form but because they give rise to a variety of hydrologic and geomorphic phenomena such as flash flooding, extreme soil erosion, and hazardous debris flows. More generally, they exert a major control over the flux of water and sediment that passes through desert river systems, across active piedmonts, and into closed lake basins. Thus an understanding of many, if not most, desert geomorphic systems must begin with a comprehension of the processes operating on desert hillslopes.

HYDRAULIC PROCESSES

INFILTRATION AND RUNOFF

Model

Virtually all runoff from desert hillslopes occurs in the form of overland flow that is generated when the rainfall intensity exceeds the surface infiltration rate. Such rainfall-excess overland flow is widely termed Horton overland flow (Horton 1933). The infiltration process may be modelled by the Richards (1931) equation:

$$\frac{\partial \Theta}{\partial t} = \frac{\partial}{\partial z}\left[K_s k_r(\Psi) \frac{\partial \Psi}{\partial z} \right] - \frac{\partial}{\partial z}\left[K_s k_r(\Psi) \right] \quad (8.1)$$

where Θ is the volumetric water content, Ψ is the pressure head, z is the distance (positive) below the surface, t is time, K_s is the saturated hydraulic conductivity, and $k_r(\Psi)$ is the relative hydraulic conductivity as a function of Ψ (Smith and Woolhiser 1971). Smith (1972) and Mein and Larson (1973) developed solutions to this equation which enable infiltration curves to be predicted for particular soils for different rainfall rates and initial soil-water contents (Fig. 8.1). The Richards equation is especially useful where the rainfall intensity initially does not exceed the surface infiltration rate.

Although the Richards equation is a powerful analytical tool, its application to desert hillslopes is complicated by the widespread occurrence of surface sealing (Moore 1981, Romkens *et al.* 1990). Surface sealing may be caused by swelling of soil aggregates or soil structure breakdown due to physico-chemical processes, clogging of soil pores as a result of the deposition of fine particles in ponded water, or aggregate breakdown and compaction by raindrops (Romkens *et al.* 1990). The last mechanism is particularly important on desert hillslopes where the effectiveness of raindrops in sealing the surface appears to be contingent on the extent to which the surface is covered with stones and vegetation. Simanton and Renard (1982) conducted rainfall simulation experiments on three different soils on semi-arid hillslopes at Walnut Gulch, Arizona, and compared runoff rates in the spring and autumn. In the spring the soil surface was loosened by frost action and wetting and drying during the preceding winter, whereas in the autumn the surface was compacted by the

Geomorphology of Desert Environments. Edited by Athol D. Abrahams and Anthony J. Parsons. Published in 1994 by Chapman & Hall, London. ISBN 978-94-015-8256-8

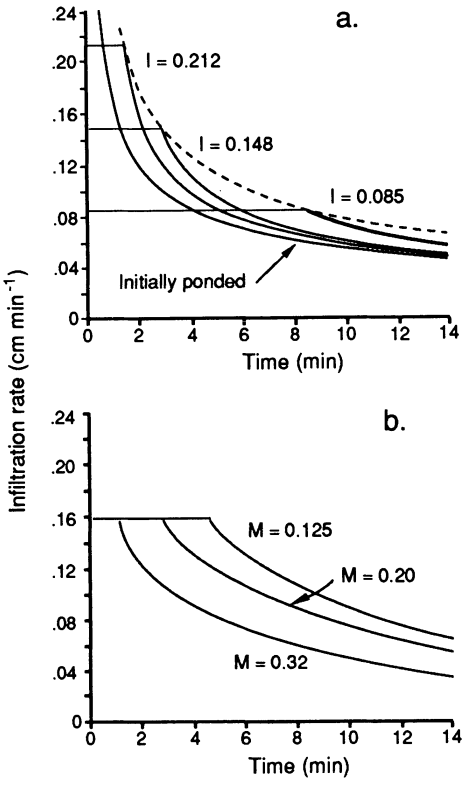

Figure 8.1 Graphs of infiltration rate against time since the start of rainfall obtained by solving the Richards equation. These graphs show how the infiltration curve varies with (a) rainfall rate I and (b) initial moisture content M (volume per unit volume).

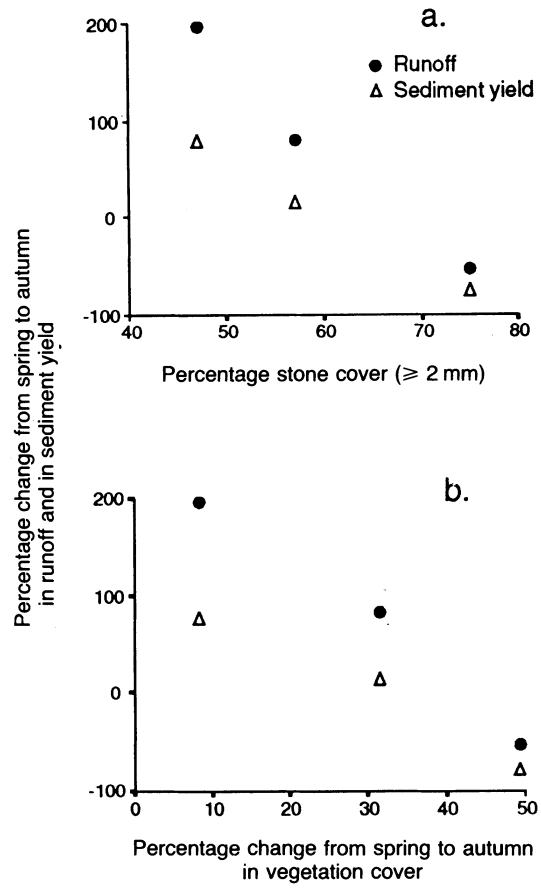

Figure 8.2 Graphs of percentage change from spring to autumn in runoff and sediment yield against (a) percentage stone cover and (b) percentage change from spring to autumn in vegetation cover for three soils at Walnut Gulch, Arizona.

previous summer's thunderstorm rainfall. Figure 8.2 shows that the change in runoff from spring to autumn is inversely related to the proportion of the surface covered with stones (≥2 mm) and the percentage change in vegetation from spring to autumn. This is because higher stone and vegetation covers afford the soil surface greater protection from raindrop impact and, hence, inhibit surface sealing by summer rainfall.

Controlling Factors

Infiltration rates on desert hillslopes vary greatly over short distances (e.g. Blackburn 1975, Sharma *et al.* 1980, Yair and Lavee 1985, Berndtsson and Larson 1987, Johnson and Gordon 1988). This variation may reflect variation in surface or subsurface properties. However, much less is known about the role of the latter than the former. Among the surface properties controlling infiltration and runoff are the ratio of bedrock to soil, surface and subsurface stone size, stone cover, and vegetation.

Given the widespread occurrence of bedrock outcrops on many desert hillslopes, an important control of infiltration and runoff is the ratio of bedrock to soil. Figure 8.3 shows the infiltration curves for rocky and soil-covered surfaces at Sede Boquer and the Hovav Plateau in the northern Negev, Israel (Yair 1987). The infiltration capacities are lower for the bedrock than for the soil-covered surfaces at both sites. The difference is especially pronounced for the Sede Boquer site because the rock is a smooth, massive crystalline limestone, whereas at the Hovav Plateau it is densely jointed and chalky. Data from natural rainfall events at Sede Boquer

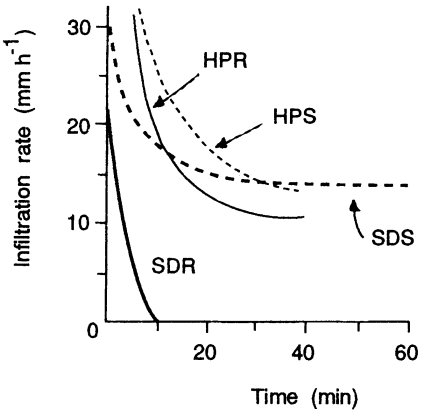

Figure 8.3 Infiltration curves for rocky and soil-covered surfaces in the northern Negev, Israel: Sede Boquer (rainfall intensity 36 mm h^{-1}) massive limestone (SDR), Sede Boquer stony colluvium soil (SDS), Hovav Plateau (rain intensity 33 mm h^{-1}) densely jointed and chalky limestone (HPR), and Hovav Plateau stoneless colluvial soil (HPS) (after Yair 1987).

(Yair 1983) indicate that the threshold level of daily rainfall necessary to generate runoff in the rocky areas is 1 to 3 mm, whereas it is 3 to 5 mm for the colluvial soils. As rain showers of less than 3 mm represent 60% of the rain events, the frequency and magnitude of runoff events are both much greater on the rocky than on the soil-covered areas.

The effect of surface stones on runoff is quite complex and has been the subject of numerous field and laboratory studies (e.g. Jung 1960, Seginer *et al.* 1962, Epstein *et al.* 1966, Yair and Klein 1973, Yair and Lavee 1976, Box 1981, Poesen *et al.* 1990, Abrahams and Parsons 1991b, Lavee and Poesen 1991, Poesen and Lavee 1991). Figure 8.4, which is based on laboratory experiments by Poesen and Lavee (1991, fig. 3), is an attempt to summarize the present state of knowledge for surfaces devoid of vegetation. Basically, surface stones affect runoff by two groups of mechanisms. First, increasing stone size and stone cover increasingly protect the soil surface from raindrop impact and thereby inhibit surface sealing and reduce runoff. Increasing stone size and stone cover also increase depression storage which promotes infiltration. Second, increasing stone size and stone cover result in greater quantities of water being shed by the stones (stone flow) and concentrated in the interstone areas, where the water overwhelms the ability of the underlying soil to absorb it and runs off in increasing amounts. Both groups of mechanisms operate simultaneously. In general, it appears that as stone size increases the

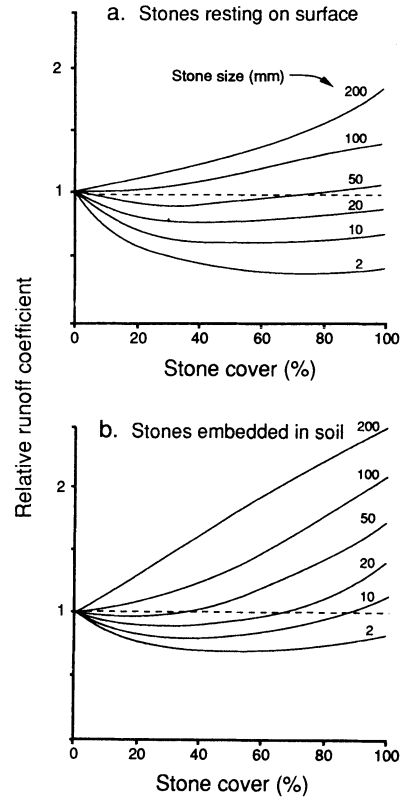

Figure 8.4 Graphs showing relations between runoff coefficient and stone cover for different stone sizes: (a) stones resting on the soil surface and (b) stones partially embedded in the soil. The graphs are generalizations of the experimental results of Poesen and Lavee (1991).

second group dominates. As a result, runoff increases with stone size irrespective of stone cover. The relation between runoff and stone cover is less straightforward. Where stone sizes and stone covers are small, the first group of mechanisms dominates, and runoff is negatively related to stone cover. However, for other combinations of stone size and stone cover the second group dominates, and runoff is positively related to stone cover. Stone position also affects runoff. A comparison of Figures 8.4a and 8.4b reveals that where stones are embedded in the soil runoff rates are higher than where they are resting on the surface. Interestingly, for intermediate (mean) stone sizes (i.e. 20 to 50 mm), the sign of the relation between runoff and stone cover may actually change from negative for stones resting on the surface to positive for stones embedded in the soil. (Poesen 1990, Poesen *et al.* 1990).

Figure 8.4 applies to areas devoid of vegetation.

Where there is a significant vegetation cover, particularly of shrubs, the controls of infiltration and runoff are quite different. This is reflected in the correlation between infiltration and stone cover. Abrahams and Parsons (1991a) noted that both positive and negative correlations between infiltration and stone cover have been reported for semi-arid hillslopes in the American South-west. They observed that positive correlations (Tromble 1976, Abrahams and Parsons 1991b) have been obtained when infiltration measurements were confined to (bare) stone-covered areas between shrubs (lower curves in Fig. 8.4), and they attributed these correlations to increasing stone cover progressively impeding surface sealing. In contrast, negative correlations have been found when infiltration was measured in shrub as well as intershrub areas (e.g. Tromble *et al.* 1974, Simanton and Renard 1982, Wilcox *et al.* 1988, Abrahams and Parsons 1991a). Abrahams and Parsons ascribed these correlations to infiltration rates under shrubs being greater than those between shrubs (Lyford and Qashu 1969), and percentage stone cover being negatively correlated to percentage shrub canopy (Wilcox *et al.* 1988). The mechanisms giving rise to higher infiltration rates under shrubs than between them are summarized in Figure 8.5. As might be expected, positive correlations have been recorded between infiltration rate and percentage plant canopy (Kincaid *et al.* 1964, Simanton *et al.* 1973, Tromble *et al.* 1974).

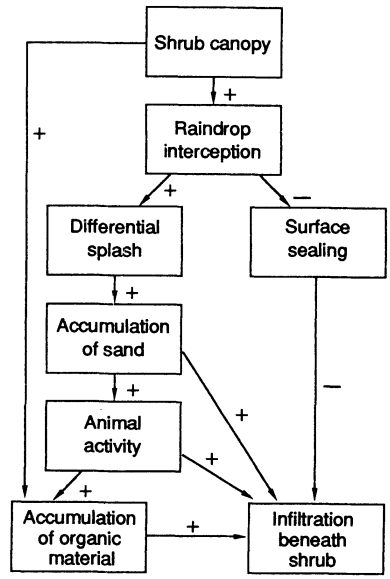

Figure 8.5 Causal diagram showing the mechanisms whereby a shrub's canopy promotes infiltration under the shrub at Walnut Gulch, Arizona (after Abrahams and Parsons 1991a).

Finally, an oft-neglected factor influencing infiltration and runoff on desert hillslopes is the presence of cryptogamic crusts. Such crusts may be composed of algae, lichen, or moss. They are surprisingly common on desert surfaces and help to stabilize such surfaces. They also have a water-repellent property that results in their generating runoff during relatively light showers of short duration. For example, in the Nizzana sand field, southern Israel, Yair (1990a) found that less than 1 mm of rainfall was sufficient to initiate runoff at a relatively low rainfall intensity of 18.4 mm h^{-1}. He concluded that some runoff could be expected over the crusted surface during any rainstorm exceeding 2 to 3 mm.

Partial Areas

The spatial variability in the factors controlling point infiltration rates means that overland flow is not generated uniformly over a desert hillslope but preferentially from those parts of the hillslope, termed partial areas, where the infiltration rates are lowest. Overland flow generated by partial areas then travels downslope where it may encounter other areas whose infiltration capacity remains higher than the rainfall intensity. Some or all of the flow may infiltrate into these areas (Smith and Hebbert 1979, Hawkins and Cundy 1987). As a result of this runon infiltration, runoff per unit area may decrease downslope. This phenomenon is illustrated in Figure 8.6 for a small piedmont watershed at Walnut Gulch, Arizona (Kincaid *et al.* 1966).

Another example of runon infiltration has been documented at the Sede Boquer experimental site studied by Yair and his colleagues in the northern Negev, Israel. The upper part of the hillslope consists largely of exposed bedrock, whereas the lower part is covered by stony colluvium. A series of sprinkling experiments showed that runoff generated on the upper part of the hillslope usually infiltrates into the colluvium. Only when both the antecedent moisture and rainfall intensity are exceptionally high, does overland flow cross the colluvial footslope and reach the stream channel (Fig. 8.7). Runoff data for natural rainfall events collected over a ten-year period revealed that continuous flow down the 60-m hillslope occurs in only about 5% of the rainstorms, thus representing rather extreme conditions (Yair and Lavee 1985).

Yair and Shachak (1987) suggested that desert hillslopes are often divided into a rocky upper slope and a soil-covered lower slope. Certainly, in the

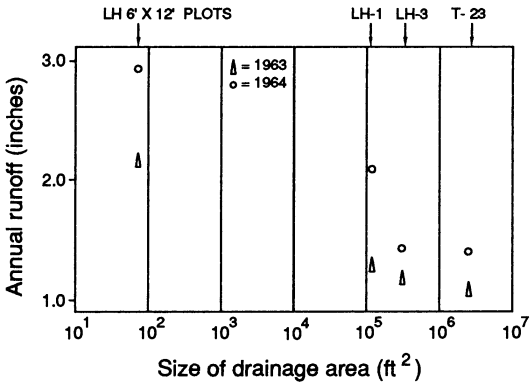

Figure 8.6 Graph of annual runoff against size of drainage area for runoff plots and very small watersheds (>10^5 ft^2) at Walnut Gulch, Arizona (after Kincaid *et al.* 1966).

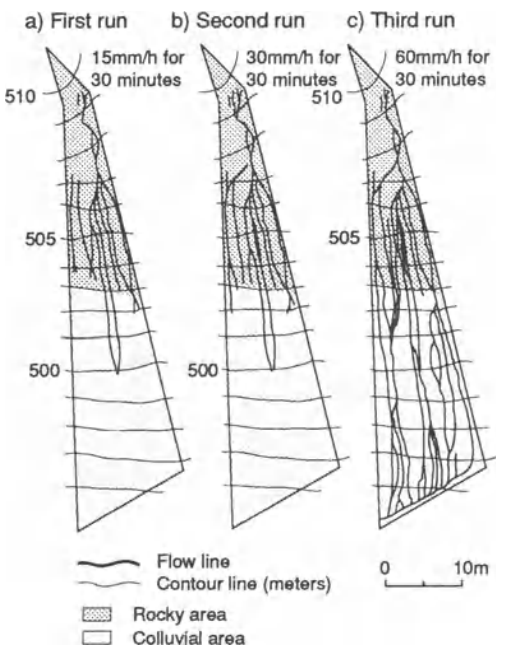

Figure 8.7 Flowlines during three consecutive rainfall simulation experiments on a runoff plot at Sede Boquer, northern Negev, Israel (after Yair 1990b).

Mojave Desert, California, there is a tendency for bedrock to crop out more widely on the upper part of hillslopes (i.e. the upper convexity and rectilinear elements) than on the lower part (i.e. the lower concavity) (Parsons and Abrahams 1987). Inasmuch as this pattern of a rocky upper slope and colluvial lower slope appears to be common and runoff coefficients for bedrock are generally higher than those for colluvium, runon infiltration is likely to be an important phenomenon on desert hillslopes and must be taken into account in modelling and predicting hillslope hydrographs.

OVERLAND FLOW HYDRAULICS

On desert hillslopes virtually all runoff occurs in the form of overland flow. Although there is pedogenic evidence of throughflow on some hillslopes (Wieder *et al.* 1985, Lavee *et al.* 1989), this process appears to contribute little water to stream channels and to play a minor role in hillslope erosion. Consequently, the process of throughflow will not be discussed further.

Interrill Areas

Interrill overland flow on desert hillslopes generally appears as a sheet of water with threads of deeper, faster flow diverging and converging around surface protuberances, rocks, and vegetation. As a result of these diverging and converging threads, flow depth and velocity may vary markedly over short distances, giving rise to changes in the state of flow. Thus over a small area the flow may be wholly laminar, wholly turbulent, wholly transitional, or consist of patches of any of these three flow states. Resistance to overland flow may be quantified by the dimensionless Darcy–Weisbach friction factor

$$f = 8ghS/V^2 \qquad (8.2)$$

where g is the acceleration of gravity, h the mean depth of flow, S the energy slope, and V the mean flow velocity. Flow resistance f consists of grain resistance, form resistance, and rain resistance. Grain resistance f_g is imparted by soil particles and microaggregates that protrude into the flow less than about ten times the thickness of the viscous sublayer (Yen 1965). Form resistance f_f is exerted by microtopographic protuberances, stones, and vegetation that protrude further into the flow and control the shape of the flow cross-sections (Sadeghian and Mitchell 1990). Finally, rain resistance f_r is due to velocity retardation as flow momentum is transferred to accelerate the raindrop mass from zero velocity to the velocity of the flow (Yoon and Wenzel 1971). For laminar flow on gentle slopes f_r may attain 20% of f (Savat 1977). However, generally it is a much smaller proportion, and the proportion becomes still smaller as the state of flow changes from transitional to turbulent (Yoon and Wenzel 1971, Shen and Li 1973). Because f_r is typically several orders of magnitude less than f on

desert hillslopes (Dunne and Dietrich 1980), the following discussion will focus on f_g and f_f.

Resistance to flow generally varies with the intensity of flow, which is represented by the dimensionless Reynolds Number

$$R_e = 4Vh/\nu \tag{8.3}$$

where ν is the kinematic fluid viscosity. Laboratory experiments and theoretical analyses since the 1930s have established that where f is due entirely to grain resistance the power relation between f and R_e for shallow flow over a plane bed is a function of the state of flow. The relation has a slope of -1.0 where the flow is laminar and a slope close to -0.25 where it is turbulent. Virtually all models of hillslope runoff have employed this relation between f and R_e (or surrogates thereof) for plane beds. However, the surfaces of desert hillslopes are rarely, if ever, planar, and the anastomosing pattern of overland flow around microtopographic protuberances, rocks, and vegetation attests to the importance of form resistance. If form resistance is important, its influence might be expected to be reflected in the shape of the f–R_e relation.

This was first recognized in a set of field experiments conducted by Abrahams *et al.* (1986) on small runoff plots located in intershrub areas on piedmont hillslopes at Walnut Gulch, southern Arizona. Although the plot surfaces were mantled with gravel, clipped plant stems occupied as much as 10% of their area, and the steeper plots had quite irregular surfaces. Analyses of 14 cross-sections yielded f–R_e relations that were positively sloping, negatively sloping, and convex-upward (Fig. 8.8). These shapes were attributed to the progressive inundation of the roughness elements (i.e. gravel, plant stems, and microtopographic protuberances) that impart form resistance. So long as these elements are emergent from the flow, f increases with R_e as the upstream wetted projected area of the elements increases. However, once the elements become submerged, f decreases as R_e increases and the ability of the elements to retard the flow progressively decreases.

In a second set of field experiments on small plots sited in gravel-covered intershrub areas at Walnut Gulch, Abrahams and Parsons (1991c) obtained the regression equation

$$\log f = -5.960 - 0.306 \log R_e + 3.481 \log \%G + 0.998 \log D_g \tag{8.4}$$

where %G is the percentage of the surface covered with gravel, D_g is the mean size of the gravel (mm), and $R^2 = 0.61$. Of the independent variables in Equation 8.4, %G was by far the single best predictor of f, explaining 50.1% of the variance. The dominance of %G implies that $f_f >> f_g$ on these gravel-covered hillslopes. This was confirmed using a procedure developed by Govers and Rauws (1986) for calculating the relative magnitudes of f_g and f_f in overland flow. For the 73 experiments performed on the small plots the modal and median values of $\%f_g$, which denotes grain resistance expressed as a percentage of total resistance, were 4.55% and 4.53% (Fig. 8.9). Thus on these gravel-covered hillslopes, f_g is typically about one-twentieth of f_f. This conclusion has important implications for sediment transport which will be explored below.

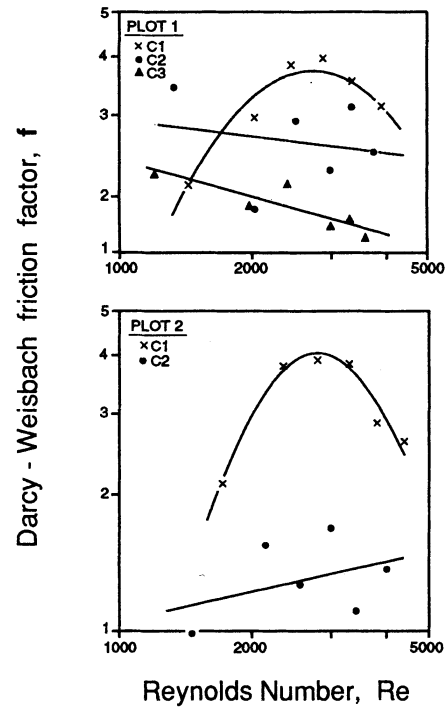

Figure 8.8 Graphs of Darcy–Weisbach friction factor against Reynolds Number for five cross-sections on two runoff plots at Walnut Gulch, Arizona. The cross-sections are denoted by C1, C2, etc. (after Abrahams *et al.* 1986).

The findings of Abrahams *et al.* (1986) and Abrahams and Parsons (1991c) are supported by some recent laboratory experiments by Gilley *et al.* (1992) in which varying rates of flow were introduced into a flume covered with different concentrations and sizes of gravel. Gilley *et al.* also recorded positively sloping, negatively sloping, and convex-upward f–R_e relations which they attributed to the progressive

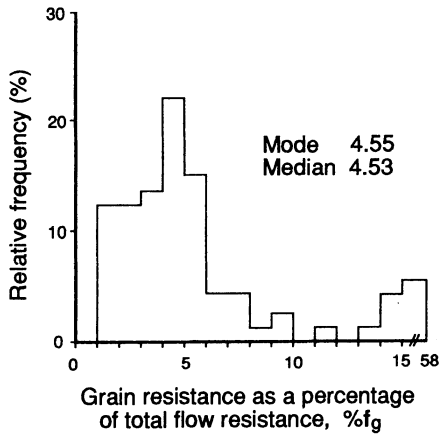

Figure 8.9 Relative frequency distribution of grain resistance expressed as a percentage of total flow resistance for 73 experiments on 8 runoff plots at Walnut Gulch, Arizona.

inundation of the gravel. In addition, they obtained regression equations of the form

$$\log f = \log a_1 - a_2 \log R_e + a_3 \log \%G \qquad (8.5)$$

for each gravel size class. The R^2 value for each regression exceeded 0.94. These flume experiments confirm the important role of gravel cover in controlling resistance to overland flow through its influence on form resistance.

The hydraulics of overland flow over an entire interrill area were investigated by Parsons *et al.* (1990) using simulated rainfall on a plot 18 m wide and 35 m long also located on a shrub-covered piedmont hillslope at Walnut Gulch. These shrubs sit atop low mounds formed largely by differential splash (see Rainsplash below). Between the shrubs are gravel-covered surfaces where overland flow is generated and travels downslope. The h, V, and R_e values were computed for two measured sections situated 12.5 and 21 m from the top of the plot. At-a-section h–R_e and V-R_e relations show that increases in R_e are accommodated largely by increases in h. These hydraulic relations are principally the result of f increasing with R_e as overland flow spreads laterally into new areas. Downslope hydraulic relations differ strikingly from at-a-section relations. Under equilibrium (steady state) runoff conditions, f decreases rapidly as R_e increases, permitting increases in R_e to be accommodated entirely by increases in V. The decrease in f is due to the progressive downslope concentration of flow into fewer, larger threads. Under non-equilibrium conditions, downslope hydraulic relations are different from those at equilibrium, but f always decreases downslope. This is the result of low flows following pathways formed by higher flows that concentrate downslope.

Rills

The tendency for threads of overland flow to increase in depth and velocity downslope coupled with the convergence (and divergence) of these threads around obstructions may lead to the formation of small channels or rills. Such features are very common on desert hillslopes, particularly where the underlying material is easily eroded. However, to our knowledge, there have been no quantitative studies of either the form or hydraulics of rills on such hillslopes. All the data available on rills come from agricultural fields in more humid environments. The following discussion, therefore, is based on these data on the assumption that the mechanics of rill formation are similar in desert and humid settings and that, consequently, the findings for agricultural fields can with appropriate caution be generalized to desert hillslopes.

Studies of rill morphology suggest that rill width is a function of soil erodibility, whereas rill spacing is related to hillslope gradient (Parsons 1987) (Fig. 8.10). Rill depth usually reflects the degree of rill development or the depth to a resistant layer in the soil. Small rills may exist for only short intervals before being obliterated by other slope processes, such as frost action, soil creep, or hydraulic deposition. Large rills, on the other hand, may persist for decades. Rills grade into gullies. The boundary is necessarily arbitrary, but one that has been widely adopted specifies that gullies are wider than 0.33 m and deeper than 0.67 m (Brice 1966). Gully processes and forms are discussed in Chapter 12.

Because rills are irregular in profile and cross-section, rill flow varies markedly in depth and velocity over short distances. The flow may be laminar, transitional, or turbulent (Roels 1984c, Gilley *et al.* 1990, Sadeghian and Mitchell 1990), but it is more often turbulent than is interrill flow. Field and laboratory studies of rill flow reveal that f–R_e relations are consistently inverse with slopes ranging from 0 to −1.85 and averaging about −1.0 (Roels 1984c, Foster *et al.* 1984a, Gilley *et al.* 1990, Sadeghian and Mitchell 1990). These slopes reflect the dominant influence of rill form on f. Specifically, as R_e increases f decreases because any roughness elements on the bed are covered by progressively greater depths of water and because the flow better follows the waviness of the bed (Foster *et al.* 1984a, Abrahams *et al.* 1986). In a study of flow through a

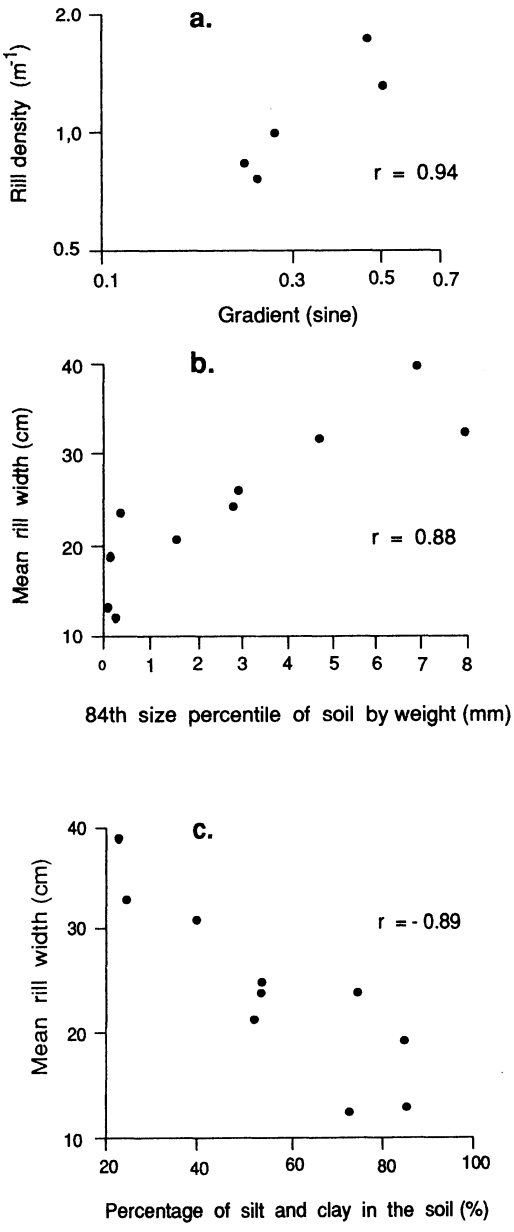

Figure 8.10 Graphs of (a) rill density against hillslope gradient, (b) mean rill width against the 84th size percentile of the soil, and (c) mean rill width against percentage of silt and clay in the soil.

fibreglass replica of a rill, Foster *et al.* (1984b) found that $\%f_g$ increased from 8.6 to 38.5% as R_e increased from 16 000 to 80 000. As in interrill flow, form resistance dominates, but it becomes less dominant as R_e increases.

Using hot-film anemometry, Foster *et al.* (1984a) also investigated velocity profiles in their rill replica. They found that the profiles were well described by the Prandtl–von Karman velocity distribution law:

$$v = (v_*/\kappa) \ln(z/z_0) \qquad (8.6)$$

where v is point velocity, κ is von Karman's constand, v_* is shear velocity, z is height above the bed, and z_0 is roughness length. However, κ, which is normally assumed to equal 0.4, took values between 0.2 and 1.3. In general, κ varied with position along the rill and increased with discharge. Because rill flows are deeper and more turbulent than interrill flows, rainfall has less effect on flow velocity. Foster *et al.* (1984a) showed that mean flow velocities were 2 to 10% less with a rainfall intensity of 127 mm h^{-1} than with no rain.

To our knowledge, the hydraulic geometry of rills on desert hillslopes has never been investigated. Studies have been made by agricultural engineers of the hydraulic geometry of rills on croplands, but with one exception these studies have examined rills developed on preformed (furrowed) surfaces. Consequently, their hydraulic geometry may not be representative of natural rills. The exception is a recent study by Gilley *et al.* (1990), who analysed the at-a-section relation between rill width and discharge for ten soils scattered across the eastern and mid-western United States. The exponent of the power relation ranged from 0.144 to 0.467 and averaged 0.303. This average exponent is comparable to that for river channels (Ferguson 1986), suggesting that rills and river channels are hydraulically similar (Moore and Foster 1990). However, whereas the hydraulic geometry of individual rivers fluctuates about some equilibrium, that of individual rills is in a state of constant evolution. Moreover, although average exponents may be similar, there is considerable variation about these averages especially in response to differences in bank strength (Ferguson 1986). Thus, caution is recommended in drawing conclusions from the above similarity.

EROSION BY HYDRAULIC PROCESSES

Rates

There are very few data on rates of erosion by hydraulic processes on desert hillslopes. A survey by Saunders and Young (1983) indicated that rates exceed 1 mm y^{-1} on normal rocks in semi-arid climates but are less than 0.01 mm y^{-1} in arid climates. These rates of erosion for semi-arid climates are amongst the highest in the world. Although

debris flows may be an important agent of erosion on slopes steeper than 30°, Young and Saunders (1986) concluded that hydraulic action is the predominant denudational process in semi-arid climates, and probably in arid ones as well. Within a given climate, however, there is considerable variability in rates of hydraulic erosion, even over a single hillslope. This variability is largely the result of differences in surface properties affecting runoff generation and sediment supply. Among these properties are stone size, stone cover, vegetation cover, and biotic activity.

Controlling Factors

Abrahams and Parsons (1991b) investigated the relation between hydraulic erosion and gradient at Walnut Gulch by conducting three sets of field experiments on small runoff plots under simulated rainfall on two different substrates. Each set of experiments yielded a convex-upward sediment-yield–gradient relation with a vertex at about 12° (Fig. 8.11). The key to understanding this relation is the relation between runoff and gradient. On slopes less than 12° runoff increases very slowly with gradient, so sediment yield increases with gradient mainly in response to the increase in the downslope component of gravity. On slopes steeper than 12° runoff decreases rapidly as gradient increases. This decrease in runoff outweighs the increase in the downslope component of gravity and causes sediment yield to decrease.

Although sediment yield is curvilinearly related to gradient, it is actually controlled in a complex way by a combination of stone size, surface roughness, and gradient. The nature of this control is outlined in Figure 8.12 (Abrahams *et al.* 1988). Where gradients exceed 12° sediment yield is positively correlated with runoff which, in turn, is negatively correlated with gradient, stone size, and surface roughness (Yair and Klein 1973). Where gradients are less than 12° runoff is almost constant, and sediment yield is positively correlated with these variables. Thus the controls of sediment yield depend on the range of gradient being considered. Where gradients exceed 12° stone size and surface roughness have a strong influence on runoff and, through runoff, affect sediment yield. On the other hand, where gradients are less than 12°, stone size and surface roughness have little effect on runoff. However, they are correlated with gradient, and gradient determines sediment yield. The interesting question raised by these results for slopes steeper than 12° is if stoniness increases with gradient causing runoff and erosion to decrease, how does one explain the increase of stoniness with gradient? The most likely explanation is that the small plot experiments that produced the above results do not take into account overland flow from upslope which would presumably be highly effective in eroding the steeper portions of desert hillslopes.

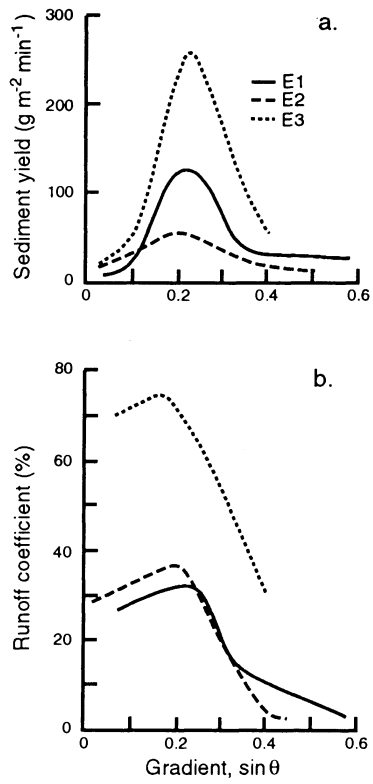

Figure 8.11 Curves fitted to graphs of (a) sediment yield and (b) runoff coefficient against gradient for three sets of experiments denoted by E1, E2, and E3 at Walnut Gulch, Arizona. Experiments E1 and E2 were conducted on plots underlain by Quaternary alluvium, with the ground vegetation being clipped for E1 but not for E2. Experiment E3 was performed on plots underlain by the Bisbee Formation.

The relation between stone cover and sediment yield on semi-arid hillslopes has been investigated by Iverson (1980) and Simanton *et al.* (1984) using simulated rainfall. For 21 plots in the Mojave Desert, California, Iverson obtained a correlation of −0.56 between sediment yield and percentage stones (>2 mm) in the surface soil. However, these plots ranged in gradient from 4° to 25°, which contributed greatly to the scatter. In a better controlled study in which all the plots had similar gradients (5.1° to

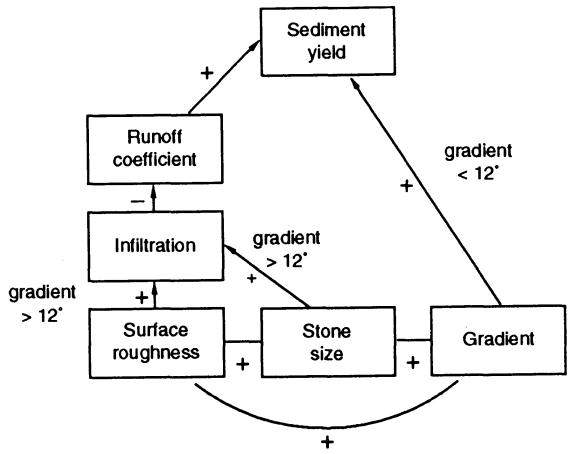

Figure 8.12 Causal diagram showing the factors controlling the runoff coefficient and sediment yield on desert hillslopes.

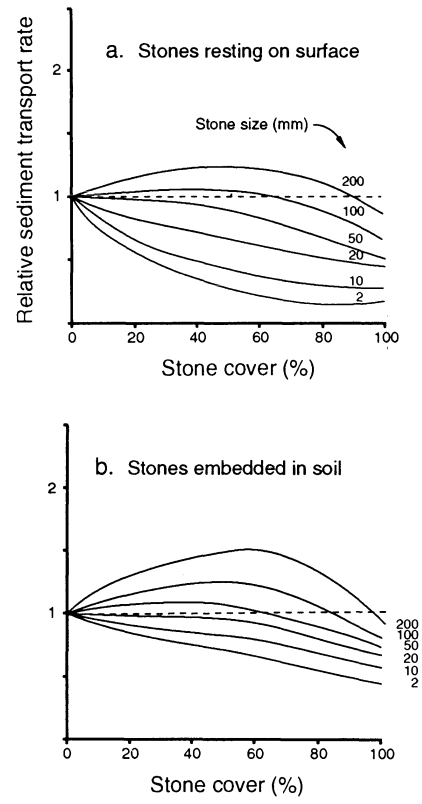

Figure 8.13 Graphs showing relations between sediment transport rate and stone cover for different stone sizes: (a) stones resting on the soil surface, and (b) stones partially embedded in the soil. The graphs are generalizations of the experimental results of Poesen and Lavee (1991).

6.8°), Simanton *et al.* obtained a correlation of −0.98 between sediment yield and percentage stone cover (>5 mm) for eight plots at Walnut Gulch, Arizona. These negative correlations can be attributed to several factors: the stones protect the soil structure against aggregate breakdown and surface sealing by raindrop impact; enhance infiltration and diminish runoff; increase surface roughness which decreases overland flow velocities; and reduce soil detachment and, hence, interrill erosion rates (Poesen 1990).

Laboratory experiments by Poesen and Lavee (1991), however, suggest that the correlation between sediment yield and stone cover is not always negative. Figure 8.13, which is a generalization of Poesen and Lavee's results, indicates that the correlation becomes positive where the stones are embedded in the soil and are larger than 50 mm. In these circumstances, the increasing stone-flow effect outweighs the increasing protection-from-raindrop-impact and flow-retardation effects as stone cover increases, and the increasing concentration of water between the stones results in greater flow detachment and transport of soil particles. However, once stone cover increases above about 70%, sediment yield begins to decline toward a minimum at 100%, when the stone cover affords complete protection of the soil beneath. Poesen and Lavee's experiments also show that for a given stone cover, sediment yield consistently increases with stone size due to increasing stone flow.

Simanton and Renard (1982) used simulated rainfall to examine seasonal variations in the erosion of three soils at Walnut Gulch. In the spring the soil surface is loose due mainly to freeze–thaw during the preceding winter, whereas in the autumn it is compacted as a result of summer thunderstorms. Nevertheless, sediment yields in the spring are not always greater than those in the autumn. Figure 8.2a shows that the change in sediment yield is closely related to the change in runoff, which is inversely related to the percentage of the surface covered with stones (>2 mm). This relation can be attributed at least in part to an increase in stone cover inhibiting surface sealing. However, between spring and fall there is also an increase in vegetation cover in response to the summer rains. This increase is negatively correlated with the change in runoff and sediment yield (Fig. 8.2b), suggesting that the change in sediment yield is also a function of differences in summer vegetation growth.

The bulk of desert flora consists of ephemerals and annuals that germinate in response to rainfall

events (Thomas 1988). This is very significant geomorphologically, as ephemerals typically appear 2 to 3 days after a rainfall event and annuals a few days later. Thus major rainfalls that trigger growth at the end of dry periods are erosionally very effective. Conversely, erosion rates at the end of wet periods, during which the plant canopy has thickened, are generally much lower than at other times. The plant canopy impedes soil erosion in a variety of ways, including protecting the ground surface from raindrop impact, which promotes infiltration and reduces soil detachment, and slowing overland flow. However, given that interrill erosion is governed by soil detachment rates (even if it is not detachment-limited) and that detachment on most desert hillslopes is accomplished mainly by raindrop impact, the principal mechanism whereby the plant canopy reduces erosion is probably through its influence on soil detachment.

Semi-arid ecosystems are dominated by either shrubs or grasses. Although semi-arid grasses are often clumped, they are more effective than shrubs as interceptors of rainfall (Thomas 1988). As a consequence, erosion rates at Walnut Gulch are two to three times greater for watersheds with predominantly shrub cover than for those with predominantly grass cover, even though runoff rates are similar (Kincaid *et al.* 1966). In general, erosion rates in semi-arid environments are inversely related to plant canopy or biomass. Kincaid *et al.* (1966) provide an example of such a relation for grass-covered watersheds at Walnut Gulch, whereas Johnson and Blackburn (1989) offer one for sagebrush-dominated sites in Idaho.

On some desert hillslopes, biological activity, in the way of digging and burrowing by animals or insects, plays a significant part in determining spatial and temporal variations in erosion rates. In a study conducted at the Sede Boquer experimental site, northern Negev, Israel, Yair and Lavee (1981) recorded intense digging and burrowing by porcupines and isopods (woodlice). Porcupines seeking bulbs for food break the soil crust which otherwise, due to its mechanical properties and cover of soil lichens and algae, inhibits soil erosion. Thus fine soil particles and loose aggregates are made available for transport by overland flow. Similarly, burrowing isopods produce small faeces which disintegrate easily under the impact of raindrops. Measurements of sediment produced by this biological activity on different plots revealed amounts that were of the same order of magnitude as eroded from the plots during a single rainy season (Fig. 8.14). Erosion rates were greater on the Shivta than on the Drorim and

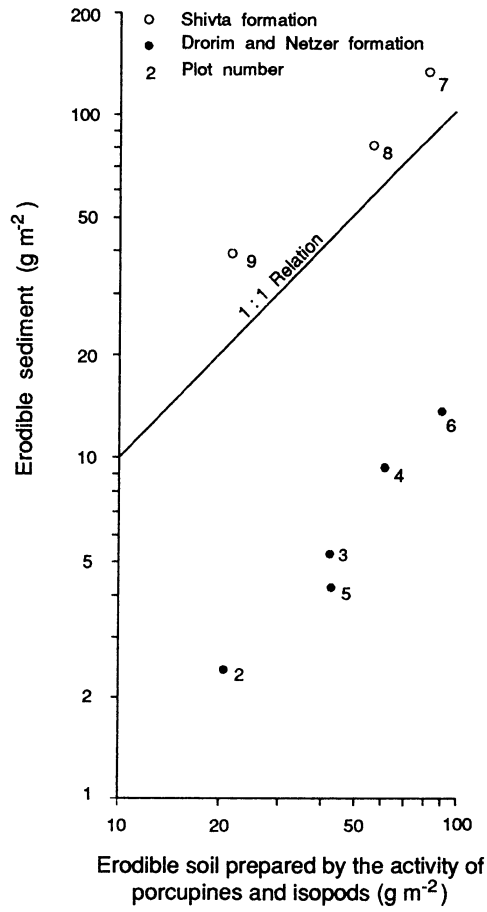

Figure 8.14 Graph of eroded sediment against erodible soil prepared by porcupines and isopods for the Sede Boquer experimental site, northern Negev, Israel. Data from Yair and Shachak (1987, table 10.4).

Netzer Formations (a) because of the proximity of biotic sediment to the measuring stations at the slope base, and (b) because of the higher magnitude and frequency of overland flow on the massive Shivta Formation. Yair and Rutin (1981) investigated the availability of biotic sediment across the northern Negev and found that it increased from 3 to 70 g m^{-1} as mean annual precipitation increased from 65 to 310 mm. These authors also noted that biotic sediment may be produced in desert environments by a variety of animals and insects other than porcupines and isopods, including moles, prairie dogs, and ants (Table 8.1).

RAINDROP EROSION

On desert hillslopes where the vegetation cover is generally sparse (Thomas 1988), the impact of rain-

Table 8.1 Biological activity and sediment production in northern Negev, Israel (data from Yair and Rutin 1981)

Plot name	*Annual rainfall (mm)*	*Sediment production ($g\ m^{-2}$)*			
		Isopods	*Porcupines*	*Moles*	*Total*
Yattir	310	41.3	30.2	100	171.6
Dimona	110	4.5	3.5	0	8.0
Shivta	100	5.3	3.3	0	8.6
Sede Boquer	93	11.9	8.7	0	20.6
Mount Nafha	85	2.1	6.6	0	8.7
Tamar-Zafit	65	0	2.9	0	2.9

drops is an important mechanism in the erosion process. Raindrop impact gives rise to rainsplash and rain dislodgement. Each of these processes will be discussed in turn.

Rainsplash

Rainsplash occurs when raindrops strike the ground surface or a thin layer of water covering the ground and rebound carrying small particles of soil in the splash droplets. On a horizontal surface the mass of material splashed decreases exponentially with distance from the point of impact (Savat and Poesen 1981, Torri *et al.* 1987). The presence of a thin film of water appears to promote splash. Although Palmer (1963) reported that maximum splash occurs when the ratio of water depth to drop diameter is approximately 1, other workers have found that the maximum occurs at much smaller ratios (Ellison 1944, Mutchler and Larson 1971). Mass of soil splashed then decreases as the ratio increases (Poesen and Savat 1981, Park *et al.* 1982, Torri *et al.* 1987).

The most complete model currently available for predicting the net downslope splash transport rate for vertical rainfall has been proposed by Poesen (1985):

$$Q_{rs} = \frac{E \cos\theta}{R\gamma_b}[0.301 \sin\theta + 0.019 D_{50}^{-0.220} (1 - \exp^{-2.42 \sin\theta})] \quad (8.7)$$

where Q_{rs} is net downslope splash transport rate ($m^3\ m^{-1}\ y^{-1}$), E is kinetic rainfall energy ($J\ m^{-2}\ y^{-1}$), R is resistance of the soil to splash ($J\ kg^{-1}$), γ_b is bulk density of the soil ($kg\ m^{-3}$), θ is slope gradient (degrees of arc), and D_{50} is median grain size (mm).

This model indicates that Q_{rs} is positively related to rainfall kinetic energy corrected for surface gradient and negatively related to the bulk density of the soil and its resistance to splash. Resistance is, in turn, a function of D_{50} with a minimum at about 100 μm (Fig. 8.15). Coarser particles are more difficult to splash by virtue of their greater mass, while finer particles are more susceptible to compaction, are more cohesive, and promote the formation of a water layer that impedes splash (Poesen and Savat 1981). The first two terms inside the brackets respectively represent the effects of gradient and particle size on the mean splash distance, whereas the expression inside the parentheses reflects the influence of gradient on the difference between the volumes of soil splashed upslope and downslope. The model is based on laboratory experiments. However, Poesen (1986) assembled field data from a number of sources suggesting that it produces order-of-magnitude estimates of splash transport on bare slopes.

There have been few field studies of rainsplash in desert environments. Kirkby and Kirkby (1974) monitored painted stone lines near Tucson, Arizona, over a two-month period during the summer thunderstorm season. They found that mean travel distance due to rainsplash and unconcentrated overland flow increases with gradient and decreases with particle size (Fig. 8.16). By multiplying the travel distances in Figure 8.16 by the grain diameters, they obtained the mass transport for each grain size per unit area. Then combining these data with data on storm frequency and assuming that rainsplash is completely suppressed under vegetation, Kirkby (1969) produced Figure 8.17, which shows that erosion by rainsplash and unconcentrated overland flow reaches a maximum at annual precipitations of 300 to 400 mm. In other parts of the world, the maximum may occur at somewhat different precipitations, reflecting differences in the distribution of intense storms, seasonality of rainfall, and vegetation characteristics.

Kotarba (1980) monitored splash transport on two plots with gradients of 12° and 15° on the Mongolian

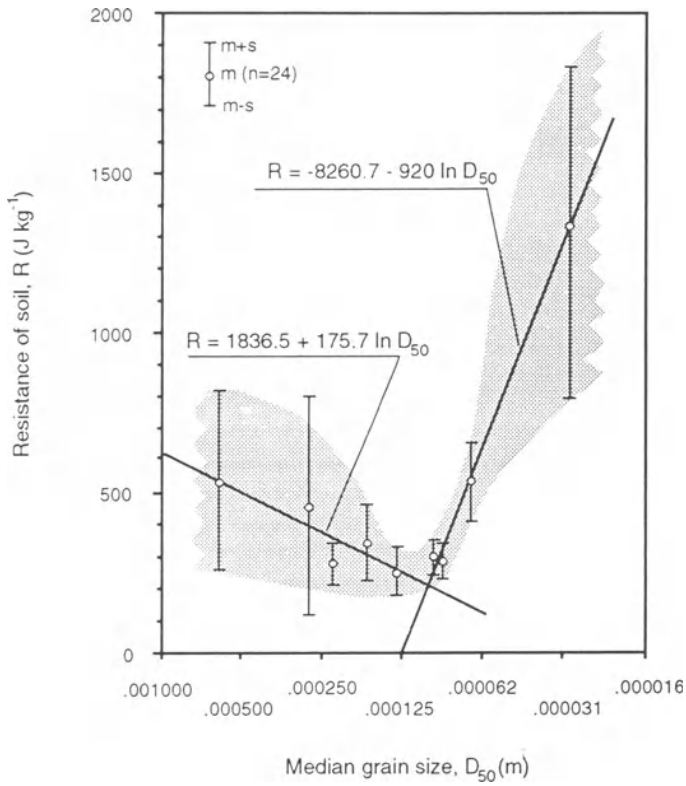

Figure 8.15 Relation between the mean resistance of loose sediments to rainsplash and their median grain size. The standard deviation (s) of experimental values is shown with each mean (m).

steppe. During a single summer he found that length of transportation was closely related to rainfall intensity and grain diameter for particles coarser than 2.5 mm but weakly related to these variables for particles 2.0 to 2.5 mm in size. He attributed these weak correlations to the finer particles being transported by wind as well as splash. Kotarba pointed out that although the region has an annual precipitation of about 250 mm, 80% of which occurs as rainfall during June, July, and August, overland flow is confined to very limited areas, and rainsplash is the dominant erosional agent. Stones as large as 12 mm were moved by this process. The average displacement of stones during a single summer was 2 to 4 cm, with some stones travelling as far as 50 cm.

Martinez *et al.* (1979) measured rainsplash under simulated rainfall at six sites in southern Arizona. They found that mass of splashed material decreases as the proportion and size of stones in the surface pavement increase. Moreover, the presence of an undisturbed stone pavement seems to damp the effect of increasing rainfall intensity, causing mass of splashed material to increase with rainfall intensity to the 0.48 power, whereas for bare agricultural fields the exponent is usually in the range of 1.5 to 2.5 (Meyer 1981, Watson and Laflen 1986). Finally, these authors noted that rainsplash is greatest for particles with diameters between 100 and 300 μm (i.e. fine sand), consistent with the laboratory findings of Poesen and Savat (1981).

Parsons *et al.* (1991b) pointed out that on many semi-arid hillslopes, shrubs are located atop small mounds of fine material, whereas the intervening intershrub areas are swales with a desert pavement surface. Applying simulated rainfall to seven shrubs at Walnut Gulch, Arizona, they showed that these mounds were formed largely by differential rainsplash – that is, to more sediment being splashed into the areas beneath shrubs than is splashed outward. Parsons *et al.* also demonstrated that both the splashed sediment and the sediment forming the mounds were richer in sand than the matrix soil in the intershrub areas, reflecting the tendency of rainsplash to preferentially transport sand-sized particles.

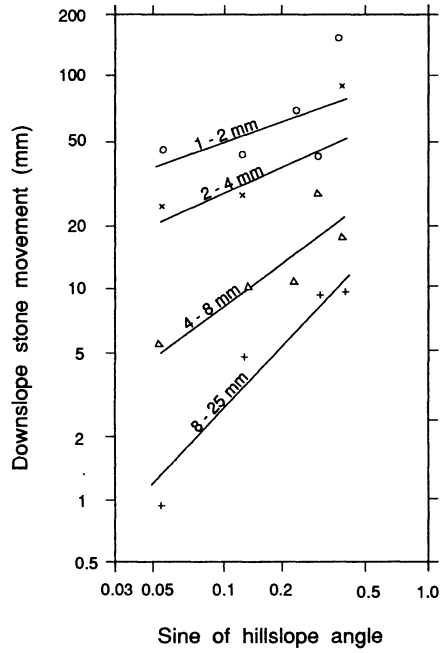

Figure 8.16 Graph of downslope stone movement by rainsplash and unconcentrated overland flow against hillslope gradient for different stone sizes. Data were collected by Kirkby and Kirkby (1974) from painted stone lines on hillslopes near Tucson, Arizona.

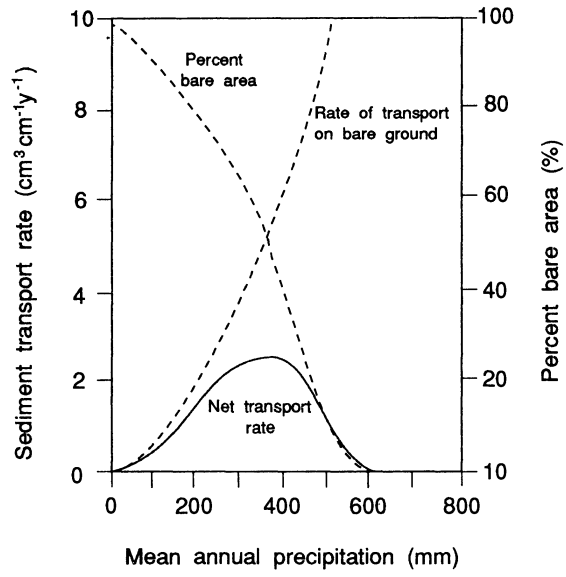

Figure 8.17 Generalized relations of sediment transport rate, percentage bare area, and net transport rate (calculated as the product of the former two variables) to mean annual precipitation for the southern United States (after Kirkby 1969).

Rain Dislodgement

Rain dislodgement refers to the movement of soil particles by raindrops where the particles are not transported in splash droplets. Ghadiri and Payne (1988) showed that a large proportion of the splash corona (and hence detached sediment) fails to separate into droplets and falls back into the impact area. This proportion increases as the layer of water covering the surface becomes deeper. Moeyersons (1975) coined the term splash creep for the lateral movement of gravel by raindrop impact. He observed that stones as large as 20 mm could be moved in this manner, and using simulated rainfall he demonstrated that splash creep rate increases with gradient and rainfall intensity (Fig. 8.18).

Raindrop-detached sediment includes that which is dislodged by raindrops as well as that carried in splash droplets. In laboratory experiments, Schultz *et al.* (1985) found that the total weight of detached sediment was 14 to 20 times greater than that transported by splash. This finding underscores the fact that the most important role of raindrop impact is not in directly transporting sediment but in detaching soil particles from the surface prior to their removal by overland flow.

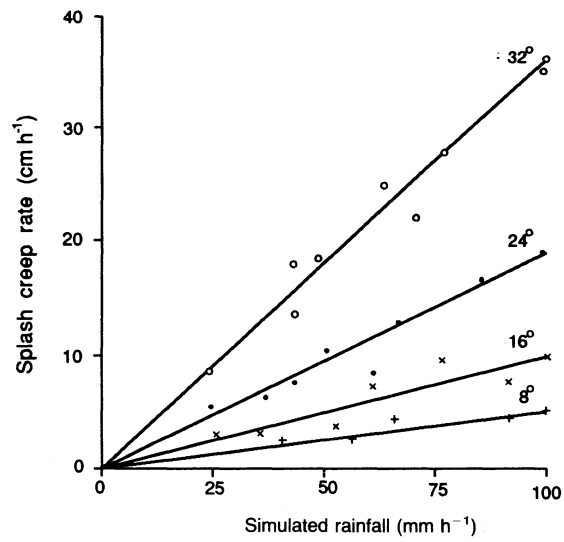

Figure 8.18 Graph of splash creep rate measured in the laboratory against rainfall intensity for different slope gradients (after Moeyersons 1975).

INTERRILL EROSION

Soil Detachment

Detachment of soil particles from the soil mass may be due to raindrop impact or flowing water. Numerous studies have established that on agricultural lands detachment occurs chiefly by raindrop impact (Borst and Woodburn 1942, Ellison 1945, Woodruff 1947, Young and Wiersma 1973, Lattanzi *et al.* 1974, Quansah 1985). To ascertain whether the same is true on undisturbed semi-arid hillslopes, five paired runoff plots, one covered with an insect screen to absorb the kinetic energy of the falling raindrops and the other uncovered, were established at Walnut Gulch, Arizona. Assuming that there is no raindrop detachment on the covered plots, the proportion of the sediment load detached by flowing water may be estimated by dividing the sediment load from the covered plot by that from the uncovered plot. As can be seen in Table 8.2, the proportions for all the plots are less than or equal to 0.25. These results support the proposition that raindrop impact is the dominant mode of detachment.

Although soil detachment in interrill areas on desert hillslopes appears to occur mainly by raindrop impact, as flow paths become longer and threads of flow deeper, flow detachment may come to dominate in these threads both because critical flow shear stresses are exceeded and because the deeper water protects the soil surface from raindrop impact. This line of reasoning is supported by Roels' (1984a, b) findings on a rangeland hillslope in the Ardeche drainage basin, France. Roels observed that natural irregularities in the ground surface cause runoff to concentrate into interrill flow paths, which range in length up to 20 m, and he termed the longest of these flow paths prerills. He derived separate regression models for soil loss from the prerill and non-prerill interrill areas. In prerill sites 87% of the variation in soil loss was accounted for by a runoff erosivity factor $REF = Q \times Q_p^{0.33}/A$, where Q is the runoff volume, Q_p the peak discharge, and A the drainage area. In contrast, in non-prerill interrill areas, 85% of the variation in soil loss was explained by a rainfall erosivity factor $EA \times IM$, where EA is the excess rainfall amount and IM is the maximum 5-minute rainfall intensity. These results imply that flow detachment dominates in the prerill portions of these areas, whereas raindrop detachment dominates elsewhere. Unless the prerills migrate laterally or are periodically infilled by other processes, flow detachment will inevitably cause them to evolve into rills.

Most process-based soil erosion models include an equation for the interrill erosion rate D_i that attempts to incorporate the factors that have the greatest influence on this process. For example, the equation in the WEPP (Water Erosion Prediction Project) model has the form (Nearing *et al.* 1989)

$$D_i = K_i I_e^2 C_e G_e (R_s/w) \qquad (8.8)$$

In this equation K_i denotes the base line erodibility which is a function of soil properties; I_e is the effective rainfall intensity during the interval when rainfall intensity exceeds the infiltration rate (i.e. during runoff); C_e represents the effect of the plant canopy in reducing raindrop detachment by intercepting and absorbing its kinetic energy; G_e captures the effect of ground cover on both raindrop and flow detachment – ground cover impedes raindrop detachment by intercepting rainfall and hinders flow

Table 8.2 Sediment yields for covered and uncovered runoff plots, Walnut Gulch, Arizona

Plot number	*Status*	*Gradient (degrees)*	*Percentage vegetation*	*Percentage stones*	*Sediment yield, G* ($g\ m^{-2}\ min^{-1}$)	*G for covered plot / G for uncovered plot*
1	Covered	7.7	38.1	43.8	6.0	0.19
1	Uncovered	7.5	44.8	33.3	31.9	
2	Covered	11.7	15.2	41.9	6.4	0.10
2	Uncovered	11.5	19.1	44.8	61.0	
3	Covered	16.0	27.6	48.6	1.2	0.086
3	Uncovered	17.5	18.1	55.2	13.4	
4	Covered	14.0	25.7	54.3	2.3	0.087
4	Uncovered	14.0	35.2	38.1	26.2	
5	Covered	17.0	18.1	48.6	8.9	0.25
5	Uncovered	17.7	34.3	44.8	36.3	

detachment by reducing flow velocities; R_s denotes rill spacing; and w rill width. That D_i increases with R_s is presumably due to flow detachment increasing with R_s. The efficacy of equation 8.8 in predicting interrill erosion on desert hillslopes has yet to be evaluated. Work by Simanton *et al.* (1984) suggests that the definition of ground cover may need to be extended to include stones. Furthermore, the fact that desert hillslopes generally have wider interrill zones than the croplands for which the equation was designed may present problems (see below).

It is interesting to note that equation 8.8 does not include a gradient term, though revised versions of the WEPP model are expected to correct this oversight (Liebenow *et al.* 1990). The omission of a gradient term from equation 8.8 is due to the fact that in the WEPP model interrill detachment is assumed to occur wholly by raindrop impact, and detachment by this mechanism increases slowly with gradient (Meyer *et al.* 1975, Quansah 1985). However, desert hillslopes may be steeper and their interrill flow paths longer than those for which the WEPP model was designed. Consequently, gradient is likely to have a significant influence on interrill detachment on such hillslopes and should be included in models for estimating this quantity. Inasmuch as the interrill erosion rate is largely governed by the detachment rate, interrill erosion varies with gradient, but the relation is less steep than that for rill erosion, where detachment is caused almost entirely by flowing water (Meyer *et al.* 1975).

Sediment Transport

Sediment transport in interrill areas may be accomplished by rainsplash and overland flow. Field and laboratory experiments have indicated that sediment transport by rainsplash on bare surfaces is only about one-twentieth of that by overland flow (Young and Wiersma 1973, Lattanzi *et al.* 1974, Morgan 1978). The proportion for natural desert hillslopes is probably fairly similar.

Sediment transport by interrill overland flow is generally represented by either bedload or total load formulae originally developed for rivers (e.g. Komura 1976, Moore and Burch 1986) or simple empirical formulae in which transport capacity is related to a measure of flow intensity (e.g. Foster 1982, Gilley *et al.* 1985a, b, Hartley 1987, Everaert 1991). Although a variety of hydraulic variables is used in these formulae to predict sediment transport capacity, for illustrative purposes, the following discussion will focus on formulae employing total shear stress $\tau = \rho_f g h S$, where ρ_f is the density of the fluid. The use of such formulae overlooks two major considerations.

The first is that the measure of flow intensity controlling sediment transport capacity is not τ but grain shear stress τ_g (Govers and Rauws 1986, Nearing *et al.* 1989), and that grain shear stress expressed as a percentage of total shear stress $\%\tau_g$ is equal to $\%f_g$. Abrahams and Parsons (1991c) found that on gravel-covered hillslopes at Walnut Gulch, $\%f_g$ is typically about 5% (Fig. 8.9), which signifies that $\%\tau_g$ too is about 5%. Therefore, τ must be replaced by τ_g when the above formulae are applied to overland flow otherwise sediment transport capacity will be grossly overestimated. Figure 8.19 illustrates the rapid decrease in transport capacity as form resistance increases in shallow overland flow in a laboratory flume. Inasmuch as form resistance is likely to be large and, hence, $\%\tau_g$ small on all desert hillslopes, it is vital that sediment transport modelling be based on τ_g rather than τ.

The second consideration that the use of formulae that relate sediment transport capacity to flow properties disregards is the influence of raindrop impact on transport capacity. Guy *et al.* (1987) found that raindrop impact was responsible for 85% of the sediment transport capacity in flow depths 0.15 to 0.39 times the mean raindrop diameter. These are very shallow flows (maximum depth 1.5 mm), and the influence of raindrop impact might be expected

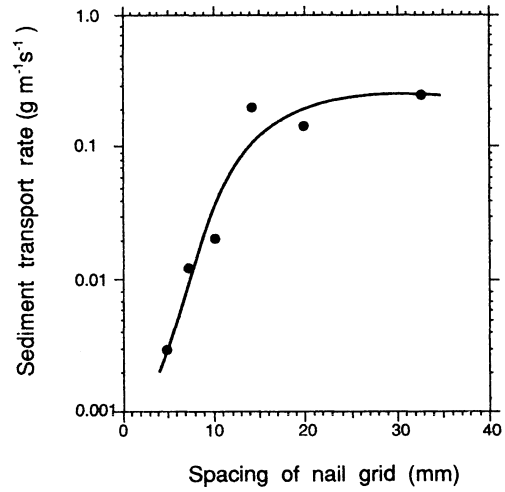

Figure 8.19 Graph of sediment transport rate against nail spacing for a series of flume experiments on beds of well-sorted sands. The nails were arranged in a grid and imparted form resistance to the flow. Thus form resistance increases as nail spacing decreases (after Moss 1980).

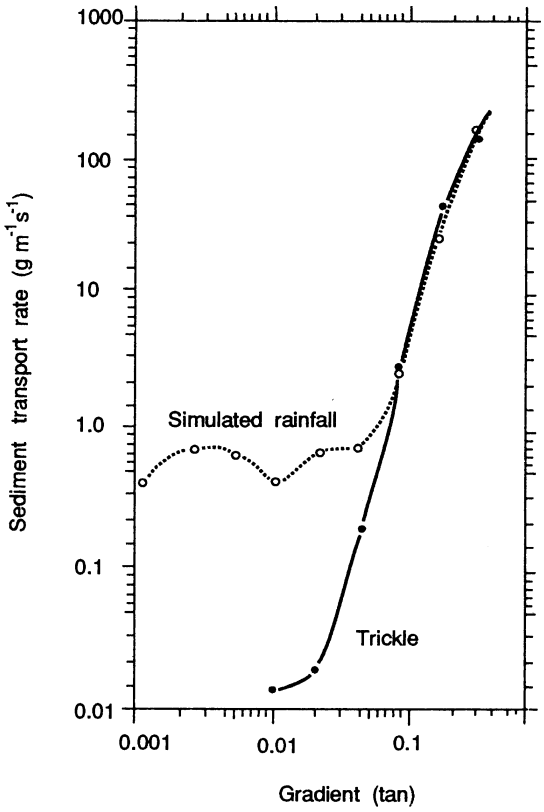

Figure 8.20 Graph of sediment transport rate against gradient for overland flow generated by simulated rainfall and trickle on a bed of poorly sorted sands (after Moss 1980).

to decrease as flow depth increases. Moreover, the laboratory experiments by Moss (1980) suggest that the effect of raindrop impact diminishes as gradient increases and becomes insignificant on hillslopes steeper than 5° (Fig. 8.20). Nevertheless, these findings demonstrate that raindrop impact enhances sediment transport capacity independently of its effect on soil detachment and that in shallow flows on gentle slopes rainfall properties are far more important than flow properties in controlling transport capacity.

In a recent series of laboratory experiments, Kinnell (1991) examined the controls of sediment transport rate in shallow flows where the transport rate was not at capacity and soil particles were detached by raindrop impact. Figure 8.21 shows that the sediment transport rate peaks when the flow depth is about 1.5 times the drop diameter. It decreases as flow depth increases and becomes negligible at depths equal to about 3 times the drop diameter. This negative relation reflects the fact that soil

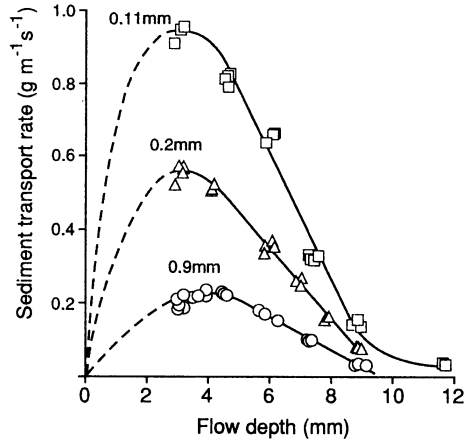

Figure 8.21 Graph of sediment transport rate against flow depth for three sizes of particle (after Kinnell 1991).

detachment decreases as greater depths of flow increasingly cushion the bed from raindrop impact. For flow depths smaller than 1.5 drop diameters, the sediment transport rate in the flow decreases as flow depth decreases because increasing amounts of sediment are transported by splash. Kinnell found that sediment transport rate also varied linearly with rainfall intensity and flow velocity: greater rainfall intensities eject more particles from the bed into the flow, and greater flow velocities transport these particles farther downstream before they settle back to the bed. However, because flow velocity increases with rainfall intensity in natural rainstorms, these two factors augment one another to cause soil detachment capacity to appear to vary with rainfall intensity squared (equation 8.8).

RILL EROSION

Two conditions must be met in order for rills to form: (a) overland flow must exert sufficient shear stress on the ground surface to detach soil particles, and (b) the transport capacity of the flow must not be satisfied by sediment supplies by raindrop detachment or flow from upslope (Meyer 1986). Many studies have emphasized the first condition (e.g. Moeyersons 1975, Savat and de Ploey 1982, Rauws 1987). However, as Dunne and Aubrey (1986) have shown, rills will not develop, even where the flow is competent to scour its bed, if the flow is fully loaded with raindrop-detached sediment.

Rills develop as a result of significant flow detachment and, once formed, continue to erode chiefly by this mechanism. Field experiments suggest that flow detachment in rills is linearly related to effective shear stress (Van Liew and Saxton 1983). In the

WEPP model the relation has the form (Nearing *et al.* 1989)

$$D_c = K_r(\tau_g - \tau_c) \quad (8.9)$$

where D_c is the detachment capacity of the flow (kg s^{-1} m^{-2}), K_r is a rill soil erodibility parameter (s m^{-1}), τ_g is grain shear stress (Pa), and τ_c is the critical shear stress of the soil (Pa). Note that τ_g is used in place of τ in equation 8.9. As in interrill flow, form resistance dominates grain resistance, and τ_g is a relatively small proportion of τ. Foster *et al.*'s (1984b) analysis of flows through a fibreglass replica of a rill yielded values for $\%\tau_g$ ranging from 8.6 to 38.5%.

In interrill areas detachment is accomplished principally by raindrops and is independent of the sediment load. In contrast, in rills detachment is mainly the result of flow shear stresses and is dependent on the sediment load in the flow. This concept was expressed mathematically by Foster and Meyer (1972) in the equation

$$D_f = D_c[1 - (G/T_c)] \quad (8.10)$$

where D_f is the rill erosion rate (kg s^{-1} m^{-2}), G is the sediment load (kg s^{-1} m^{-1}), and T_c is the sediment transport capacity in the rill (kg s^{-1} m^{-1}). The basic idea here is that as the sediment load approaches the transport capacity, the rill erosion rate becomes a progressively smaller proportion of the detachment capacity of the flow. Equation 8.10 applies where $T_c \geq G$ and D_f is positive. Where $T_c < G$ and D_f is negative, deposition occurs at a rate estimated in the WEPP model by (Nearing *et al.* 1989)

$$D_f = [v_f/(h\ V)](T_c - G) \quad (8.11)$$

where v_f is the fall velocity of the sediment (m s^{-1}).

Perhaps the best equations available for estimating T_c for rill flows are those developed by Govers (1990) from a series of flume experiments using sediment ranging in size from silt to coarse sand. Different empirical equations were developed using shear stress, Bagnold's (1980) effective stream power, and Yang's (1972) unit stream power as the predictive hydraulic variable, and nomograms were produced indicating how the coefficients in these equations vary with sediment size. As in the case of interrill flow, sediment transport capacity of rill flow is affected by raindrop impact and the expenditure of energy in overcoming form resistance. Because rill flows are usually deeper than a few millimetres, the effect of raindrops can for practical purposes be neglected. Form resistance, however, dominates in rill flow as it does in interrill flow (Foster *et al.* 1984b), and this must be taken into account when using Govers' equations to estimate T_c.

MODELLING OVERLAND FLOW EROSION

The concepts employed in process-based erosion models have evolved gradually since Meyer and Wischmeier (1969) suggested mathematical expressions for detachment and transport by rainfall and runoff as conceptualized by Ellison (1944). Important subsequent developments were the proposal of equation 8.10 by Foster and Meyer (1972) and the distinction between rill and interrill sources of sediment by Meyer *et al.* (1975). A variety of process-based erosion models has been formulated during the past 15 years (e.g. Foster *et al.* 1977, 1981, Beasley *et al.* 1980, Gilley *et al.* 1985a, b, Woolhiser *et al.* 1990). One such model has been the WEPP model (Nearing *et al.* 1989). It is extremely tempting to apply soil erosion models such as the WEPP model to desert hillslopes, as the technology is both advanced and accessible and there is no alternative model available in the geomorphic literature. However, existing process-based soil erosion models in general and the WEPP model in particular have a number of deficiencies with respect to desert hillslopes.

First, the WEPP model assumes that the interrill erosion rate can be estimated by equation 8.8. Although this equation allows for soil detachment and sediment transport by interrill overland flow, it was developed for cropland where most detachment and transport is accomplished by raindrops and interrill zones are narrow (typically 0.5 m: Gilley *et al.* 1990). On desert hillslopes interrill zones are much wider (in extreme cases up to 500 to 600 m: Dunne and Aubrey 1986), and soil detachment and especially sediment transport by overland flow become more important.

Not all process-based soil erosion models minimize the role of interrill overland flow. The interrill erosion model of Gilley *et al.* (1985a, b) assumes that detachment of soil particles occurs wholly by raindrop impact and that the transport of these particles downslope is accomplished wholly by overland flow. An example of the output of this model is given in Figure 8.22. Gilley *et al.*'s model suggests that over the greater part of most interrill areas the erosion rate is equal to the detachment capacity – that is, it is detachment-limited. Only on very gentle slopes (e.g. near divides) and in areas of deposition (e.g. concave footslopes) is it equal to the transport capacity – that is, transport-limited. Indeed, because the portion of the interrill zone where erosion is

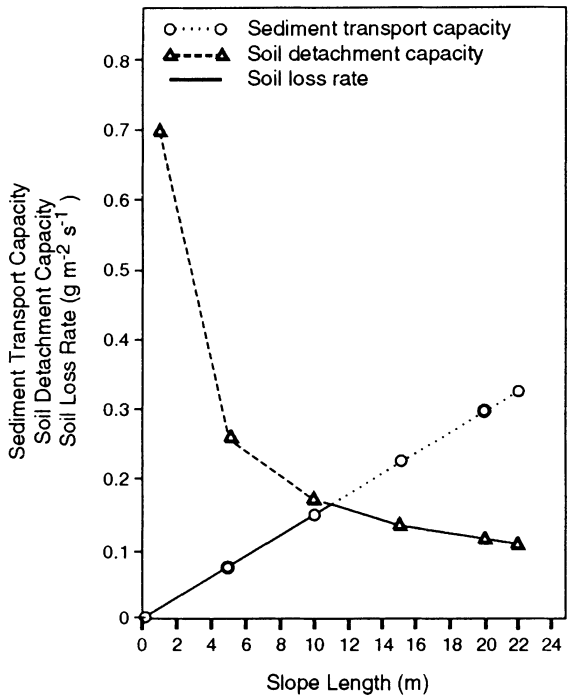

Figure 8.22 An example of the output of the interrill erosion model of Gilley *et al.* (1985a, b). The gradient of the interrill area is 6% (3.4°).

transport-limited is small, some models (e.g. Dillaha and Beasley 1983) have simply assumed that erosion over the entire interrill area is detachment-limited.

Recent work by Parsons and Abrahams (1992), however, has indicated that on a semi-arid hillslope at Walnut Gulch, the interrill erosion rate is less than the detachment capacity. Two types of evidence support this contention. First, particle size analyses reveal that splashed sediment is coarser than sediment being transported by overland flow, signifying that the coarser detached particles are not eroded from the hillslope (Parsons *et al.* 1991a). Second, although raindrop detachment occurs over the entire hillslope except where overland flow is too deep, the detached sediment is transported downslope only where it is splashed into or dislodged within overland flow competent to transport it. Using a simulation model and detailed measurements of the cross-slope variation in overland flow depth and velocity, Abrahams *et al.* (1991) showed that there are significant proportions of the hillslope where soil is detached but there is no flow competent to transport it downslope. Inasmuch as overland flow on all desert hillslopes displays across-slope variations in depth and velocity, soil detachment rates probably always exceed actual sediment transport rates. Thus the notion that interrill erosion is detachment-limited appears to be an oversimplification. In reality the erosion rate will always be smaller than the detachment capacity. However, the magnitude of the disparity is difficult to estimate and is probably highly variable over both time and space.

A second weakness of available process-based models is that they assume that soil detachment takes place only while runoff is occurring. Such models overlook the accumulation of loose sediment on the ground surface at the start of runoff. This accumulated sediment, which may be considerable on desert hillslopes owing to the typically long intervals between runoff events, has three origins: (a) it is detached by rainfall or flowing water during preceding storms but not removed by overland flow (David and Beer 1975); (b) it is detached by rainfall during the current storm prior to the start of runoff (Yair and Lavee 1977); and (c) it is detached by weathering processes between storms (Ellison 1945, Emmett 1970). The accumulated loose sediment exerts a strong influence on interrill erosion. This influence is commonly manifested in (a) a decline in sediment concentration after the start of runoff reflecting the progressive depletion of detachment storage (Ellison 1945, Yair and Lavee 1977, Abrahams *et al.* 1988) (Fig. 8.23) and (b) a positive correlation between storm soil loss and either the amount of biological activity or intensity of weathering prior to the storm (Yair and Lavee 1981, Roels 1984a) (Fig. 8.14). As a result, erosion rates do not always correlate well with rainfall or surface variables such as appear in equation 8.8.

A third weakness of current process-based erosion models that limits their utility on desert hillslopes is that they were not designed for use on steep hillslopes (>10°) covered with coarse debris, as many desert hillslopes are. Some models may perform quite well on gentle hillslopes where the surface debris is relatively fine. However, on steep hillslopes with nearly complete covers of coarse debris, the hydrology, hydraulics, and erosion mechanics are very different, and these models are unlikely to give good results.

GRAVITATIONAL PROCESSES

The movement of weathered detritus under the influence of gravity encompasses a very wide range of phenomena differing in depth and mass of material being mobilized, rates of motion, transport mechanisms, and relative volumes of debris, water,

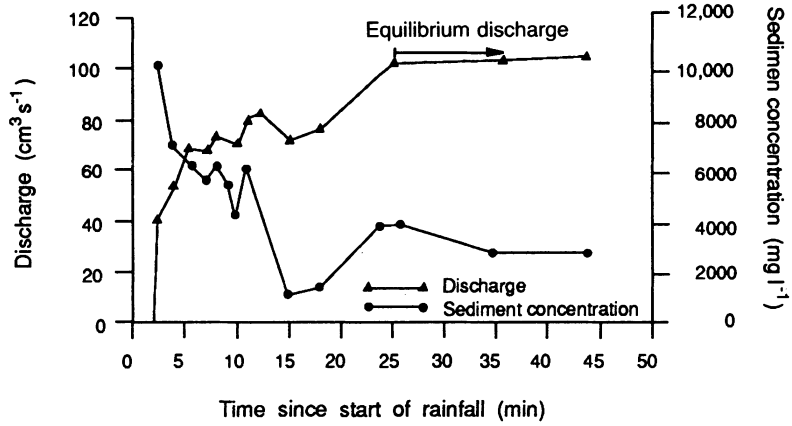

Figure 8.23 Graphs of overland flow discharge and sediment concentration against time since the start of rainfall for a runoff plot at Walnut Gulch, Arizona (after Abrahams *et al.* 1988).

ice, and air. A thorough review is not possible here; the emphasis will be on processes most common in arid environments. Weathering and mass wasting in arid climates generally conform to the following patterns: (a) classic creep processes are relatively unimportant due to the dry regolith and the paucity of fines; (b) deep-seated failures and landsliding are uncommon; and (c) mass movement is dominated by mobilization of surficial layers and their rapid transport ranging from motion of individual particles (talus falls) to debris flows.

CREEP PROCESSES

Slow, relatively continuous movement of thick regolith by matrix deformation is uncommon in arid regions because of the general dryness of the regolith and the paucity of plastic fines. Exceptions may include cold deserts with winter freeze–thaw and clay-rich badland regolith (see Chapter 9). Therefore most coarse-grained desert regolith beneath slopes less than about 25° are generally eroded primarily by wash processes unless mobilized into debris flows due to shallow regolith failure. Where creep is important, a rate of movement proportional to the gravitational stress ($\rho_b g h \sin\theta$) is probably sufficient, where ρ_b is the bulk soil density and h is the effective depth of creep (see Carson and Kirkby (1972) for further discussion of creep mechanics and Chapter 9 for use of creep processes in simulation modelling of slope evolution).

MOVEMENT OF DRY DEBRIS ON SCREE SLOPES

Steep, unstable slopes (talus slopes) of accumulated loose scree arriving from superjacent steep, bedrock slopes are common in desert environments, occurring most noticeably below cliffs (such as the cuesta scarps discussed in Chapter 7) but also as more localized patches on the flanks of many bedrock hills and mountains. Debris may be shed from the bedrock source slopes in a spectrum of events ranging from fall of individual rocks to large debris avalanches. The motion and deposition of individual rocks has been investigated in experiments and theoretical studies (Kirkby and Statham 1976, Statham and Francis 1986). It is generally hypothesized that a rock particle of mass M_p falls to the head of a scree slope from a freefall through a distance z, so that its initial velocity v_0 is

$$v_0 = \sqrt{2gz} \tag{8.12}$$

After the initial impact at the head of the scree slope of inclination θ only the downslope momentum is preserved, so that its initial velocity u_0 parallel to the slope is $v_0 \sin\theta$. As the particle progresses down the slope it bounces, rolls, and slides over particles already on the scree. The net downslope force F acting on the particle of mass M_p is the difference between the downslope component of gravity $M_p g \sin\theta$, and a frictional force $M_p g \cos\theta \tan\phi_d$, where ϕ_d is the dynamic angle of friction. The model assumes that ϕ_d is a constant when averaged over a large number of collisions and a large number of particles, and it ignores non-elastic effects such as particle shattering and exchange of momentum between the falling rock and scree surface rocks through cratering effects. The model thus assumes that the average movement can be treated as a sliding friction over a rough surface. Assuming that the actual slope is less than the dynamic angle of

friction, the particle will come to rest in a mean distance $\bar{x}$ given by

$$\bar{x} = \frac{M_p u_0^2}{2F} = \frac{z \sin^2 \theta}{\cos \theta \tan \phi_d - \sin \theta} \quad (8.13)$$

Experiments involving dropping stones on to inclined boards (Kirkby and Statham 1976) have shown that the actual travel distance down the slope varies considerably, but can be represented by an exponential distribution

$$P(x) = e^{-x/\bar{x}} \quad (8.14)$$

where $P(x)$ is the probability of the rock travelling at least the distance x downslope. The exponential distribution implies that the probability of stopping in a given distance interval remains constant downslope (so long as θ and ϕ_d remain constant).

Large rocks move more readily over smaller scree than over a scree equal or larger in size to the mobile particle. Kirkby and Statham's experiments have shown that the friction angle ϕ_d varies with the grain size D^* of the particle and of the particles forming the scree surface D

$$\tan \phi_d = \tan \phi_0 + kD/D^* \quad (8.15)$$

The parameter k depends upon the shapes of the impacting and scree particles and ϕ_0 is the friction value for mobile rocks very much coarser than the scree. Kirkby and Statham (1976) indicated that equation 8.15 is not valid for mobile rocks much smaller in size than the scree.

This model ignores a number of processes and conditions which may be important under some conditions, including air friction on both the freefalling and moving rock, rocks arriving at the scree surface after moving over a sloping bedrock surface (rather than freefall), momentum loss due to cratering (particularly at the first impact at the head of the scree), and interaction between moving particles. None the less, the model provides an excellent fit to experimental data and explains both the concave planform and downslope sorting found on many talus slopes (see below).

On some steep, tall scarps failure may involve a considerable volume of rock and the motion may be by avalanche rather than by motion of individual particles. Gerber and Scheidegger (1974) assume that motion of an avalanche can be described by equations analogous to 8.12 and 8.13. The most common approach to modelling avalanche utilizes the same equations of motion for debris flows that are discussed below.

DEBRIS FLOWS

The movement of mixtures of particulates, water, and air exhibits different flow behaviour depending upon relative amounts of these components and on the grain size distribution of the particulates (Pierson and Costa 1987, Costa 1988). Water flows with cohesionless sediment loads less than about 20% by volume transport sediment via turbulent suspension or by traction at the bed. In these 'water flood' flows (considered under Hydraulic Processes, above and in Chapter 12) the suspended sediment has little effect on flow viscosity and standard fluid flow and sediment transport equations for overwash and channel flows are appropriate. When sediment concentration ranges from 20% to about 47% by volume the flow is 'hyperconcentrated' in that sediment increases flow viscosity and decreases turbulent intensity. A slight shear strength may also be imparted to the flow. Flow density attains values (bulk specific gravity of 1.3 to 1.8) such that buoyant suspension becomes important, and grain-to-grain contacts introduce dispersive stresses (Costa 1984, 1988). The transition to hyperconcentrated flow may occur at sediment concentrations less than 10% by volume for clays (Hampton 1972, 1975). Sediment in hyperconcentrated flows still behaves largely as individual grains, such that larger grains are deposited first as flow velocity diminishes and the resulting sedimentary deposits resemble those of water floods (Costa 1988).

When sediment concentrations exceed about 47% by volume (20% or even less for clay–water mixtures) particle interactions become strong enough that the flow has a well-defined shear strength and a viscosity much greater than water; these are generally called 'debris flows' (Costa 1988). In these flows cohesion, buoyancy, grain-to-grain support, and dispersive stresses resulting from grain collisions (Bagnold 1954) become the dominant mechanisms of sediment suspension and transport, whereas turbulent suspension is greatly diminished relative to water floods. The rheology or resistance to flow in debris flows is a complicated function of sediment concentration, sediment size range, and rate of shearing.

At the highest concentrations of debris relative to matrix the grains are essentially completely supported by grain-to-grain contacts and collisions. Such flows are called granular flows by Pierson and Costa (1987) and include such phenomena as debris and rock avalanches, earthflows, and shallow slides on talus slopes and dune slip faces.

Debris flows generally exhibit a consistent range

of behaviour (Blackwelder 1928, Johnson 1970, Fisher 1971, Costa 1984, Johnson and Rodine 1984). The flows occur as a series of blunt-nosed pulses with the first pulse commonly being the largest. The maximum depth of each pulse occurs near the nose, with a long tailing flow that is commonly more fluid than the nose, often changing to hyperconcentrated or water flood flows during the waning stages. Debris flows are noted for the wide range of grain sizes transported and the tendency for large boulders to be concentrated near the flow surface and at the leading edge of the flow. Deposits from debris flows often show inverse grading. Characteristics of debris flow deposits are considered in Chapter 14.

A wide variety of constitutive laws relating resisting shearing stress τ_r to flow and sediment properties have been proposed (see, for example, the reviews in Iverson 1985, Chen 1987, Iverson and Denlinger 1987, Major and Pierson 1992). A fairly general one-dimensional relationship can be expressed as

$$\tau_r = c + \sigma \tan \phi + m' \left(\frac{dv}{dz} \right)^{n'}, \qquad (8.16)$$

where c is shear strength, σ is normal stress (acting on a surface parallel to the bed), ϕ is a dynamic friction angle (not necessarily the same as in equation 8.13), m' and n' are coefficients, and v is downstream velocity at a height z above the bed. A more general three-dimensional formulation of a similar relationship can be found in Iverson (1985, 1986), where it is also applied to slow earthflow landslides. Flows for which $0 < n' < 1$ are called pseudo-plastic (shear-thinning) as contrasted with dilatent (shear-thickening) for $n' > 1$ (Major and Pierson 1992). Two commonly assumed special cases are Bingham plastics for which $n' = 1$, $\phi = 0$, and $m' = \eta_p$ (the plastic viscosity), and Coulomb–Bingham plastics with $n' = 1$, $m' = \eta_p$, but $\phi > 0$.

Flows that are well characterized by the Coulomb–Bingham and Bingham models exhibit a characteristic flow pattern in which the boundaries of the flow are in a laminar shear with a parabolic velocity profile, whereas the centre and top of the flow, where shear stresses are low, is a rigid plug. A rigid central plug has been observed or inferred for many debris flows (Johnson 1965, 1970, Costa 1984, Johnson and Rodine 1984, Pierson 1986). For a two-dimensional flow that is steady and uniform, such that $\sigma = \rho_b g h \cos \theta$ and the gravitational shearing stress is $\tau = \rho_b g h \sin \theta$, the thickness h_c of the plug in Coulomb–Bingham flow occurs for $dv/dz = 0$ and $\tau_r = \tau$:

$$h_c = \frac{c}{\rho_b g (\sin \theta - \cos \theta \tan \phi)} \qquad (8.17)$$

Johnson (1970) and Johnson and Rodine (1984) presented solutions for the plug thickness and velocity distribution for both two-dimensional flows and flows in circular channels. Coulomb–Bingham flows will cease flowing if the flow thickness becomes less than or equal to h_c through thinning of the flow, downstream decrease in θ, or increase in c or ϕ through loss of water or incorporation of more debris.

In a series of experiments with various mixture ratios and total concentrations of sand, silt, and clay Major and Pierson (1992) found estimated values of n' ranging from 0.3 to 3.3. Greatest variability in rheological properties occurs for shear rates (dv/dz) less than 5 s^{-1}, particularly when the volume concentration of sand exceeds 20% and frictional interactions between sand grains dominate shearing resistance. Major and Pierson (1992) found that the Bingham model is a reasonable description of flow behaviour for shear rates greater than 5 s^{-1}. However, both c and η_p increase exponentially with volumetric sediment concentration C_v:

$$c = k_1 e^{b_1 C_v} \text{ and } \eta_p = k_2 e^{b_2 C_v} \qquad (8.18)$$

where k_i and b_i are experimentally determined coefficients (Major and Pierson 1992). Increase of sediment concentration of a few percent can produce order-of-magnitude increases in c and η_p. Very strong dependencies of shear strength of debris flows on sediment concentration have also been noted by Rodine and Johnson (1976), Johnson and Rodine (1984), Costa (1984), Pierson (1986), O'Brien and Julien (1988), and Phillips and Davies (1991).

Clasts may be supported by a variety of mechanisms, including buoyancy (up to 75% to 90% of their weight) (Johnson 1970, Hampton 1975, 1979, Middleton and Hampton 1976, Rodine and Johnson 1976, Costa 1984, 1988), dispersive stresses due to collisions between particles (Bagnold 1954), cohesion (Johnson 1970, Hampton 1975, Rodine and Johnson 1976), structural support from grain to grain contacts which can support up to one-third the weight of coarse particles in flows with solid volumetric concentrations greater than 35% (Pierson 1981), and turbulence in dilute flows. The mechanisms that concentrate coarse grains at the surface may include dispersive stresses introduced by the greater number of collisions with smaller grains on the bottom

relative to the top of clasts in shear flow (Iverson and Denlinger 1987), kinetic sieving in which fines settle through voids between coarse clasts during particle vibrations (Middleton 1970, Bridgewater 1980), and angular momentum applied to large particles in shear flows (with clast tops rotating downstream) such that large clasts can roll over smaller ones (Iverson and Denlinger 1987).

A comprehensive theoretical foundation for constitutive relationships (e.g. equation 8.16) for debris flows based upon the mechanics of the matrix and solid interactions (including grain-to-grain collisions) is lacking. Iverson and Denlinger (1987) pointed out the complexity of the processes involved in debris flows, including collisions, rubbing, rotations, vibrations and possibly fracturing of the solid phase and flow, compression, vibration and cavitation of the matrix. The Bingham and Coulomb–Bingham models (Johnson 1965, 1970, Yano and Daido 1965) do not include dynamic particle interactions but can explain flow over diverse slopes, formation of a rigid plug, support of large clasts, and the blunt nose of debris flows (Iverson and Denlinger 1987).

Takahashi (1978, 1980, 1981) and McTigue (1979) have proposed theoretical models based upon Bagnold's (1954) observations that mutual particle collisions in granular flows produce dispersive stresses that can help support such flows. These theories assume a uniform grain size and uniform particle concentration, and result in constitutive equations with no cohesive term and shear stresses proportional to the square of the shear rate ($n' = 2$ in equation 8.16). These theories can explain some observed velocity profiles in debris flows, inverse grading, and segregation of coarse particles in the snout of debris flows. However, the limitation of uniform grain size and particle concentration, as well as neglect of particle–matrix interactions, is a major shortcoming (Iverson and Denlinger 1987). More general experiments and theoretical formulations of particle collisions in dry grain flows (e.g. Lowe 1976, Middleton and Hampton 1976, Savage 1979, 1984, 1989, Lun *et al.* 1984, Campbell and Brennen 1985, Drake and Shreve 1986, Haff 1986, Hui and Haff 1986, Melosh 1987, Drake 1990) may ultimately provide better debris flow models that incorporate inelastic collisions and variable particle sizes and concentrations. However, Iverson and Denlinger (1987) pointed out that solid–fluid interactions are important in debris flows, particularly the cushioning effect on collisions afforded by the matrix (Biot 1956, Davis *et al.* 1986, Iverson and LaHusen, 1989).

Source area characteristics and mechanisms for initiation of debris flows are not well understood. The role of steep relief and high rainfall intensity/duration is cited by nearly every study (e.g. Rice *et al.* 1969, Scott 1971, Campbell 1975, Nilsen *et al.* 1976, Cooley *et al.* 1977, Scott and Williams 1978, Weiczorek 1987, Florsheim *et al.* 1991). However, Hooke (1987, p. 512) pointed out that overland flow and water floods cannot be converted to mudflows simply by entrainment of sediment from flow boundaries due to the lack of turbulent mixing in debris flows. A variety of mechanisms have been identified (see general discussions in Johnson and Rahn 1970, pp. 310–33, Costa 1984, Johnson and Rodine 1984, Hooke 1987). The most common mechanism is probably the conversion of slumps and small landslides into debris flows either through dilation through incorporation of additional water in hollows and channels or through liquefaction if the original deposit has high intergranular porosity or extensive macropores (see reviews of the extensive literature in Costa 1984, Johnson and Rodine 1984; also see Ellen and Fleming 1987, McDonnell 1990, Guzzetti 1991). Johnson and Rodine (1984, pp. 313–7, 329–31) described the transformation of slumps into debris flows within a few seconds and after travel of only a metre or less. Slumps of slope or channel banks into rill and gully flows is another mechanism (Johnson and Rodine 1984, pp. 321–4). Such slumping may occur during flow events or between flows; in the latter case the debris forms small dams that create debris flows when they fail, incorporating the ponded water into the debris. The flow of water draining from bedrock slopes and chutes on to loose talus may be one of the most important mechanisms of debris flow generation on arid slopes (Johnson and Rodine 1984, pp. 329–31); such flows occur as high velocity jets that sluice the upper portions of talus slopes, and additional debris will be incorporated from the unstable talus slopes as the flow progresses downslope.

Debris flows from slopes in semi-arid and strongly seasonal climates commonly occur shortly after fire has destroyed the natural vegetation cover (Sidle *et al.* 1985, Wohl and Pearthree 1991). Fire may contribute to failure by reducing evapotranspiration while creating a hydrophobic fire-sealed soil layer that promotes surface soil saturation and runoff (Wells 1981, 1987, Laird and Harvey 1986, Campbell *et al.* 1987, Wells *et al.* 1987). However, Florsheim *et al.* (1991) noted that wildfire often is not followed by large debris flows even though sediment yield is increased, and they suggest that rainfall intensity and duration is much more important in triggering debris flow than is wildfire.

The role of water floods in creating rills and gullies on desert slopes is reasonably well understood (discussion above and in Chapters 9 and 12). However, the role of rockfalls, avalanches, and debris flows in slope sculpture is poorly characterized. Debris flows generally are confined to established channels, at least until they debouch on to pediments or fans, but there is disagreement as to the efficacy of such flows in creating or deepening channels. Lustig (1965), Pierson (1980), Janda *et al.* (1981), Johnson and Rodine (1984, p. 273) and Costa (1984, p. 274) cited evidence for erosion by debris flows, but Hooke (1987) disagreed, citing the lack of turbulence in such flows and the possibility that most observed channel erosion occurs from the waning-stage water floods occurring after the passage of the debris flow; similar views were advanced by Blackwelder (1928) and Morton and Campbell (1973). None the less, the momentum of debris flows is sufficient to shear trees and demolish structures, so that it is certainly capable of incorporating additional large boulders along the channel margins. Furthermore, debris flows exert shear stresses along their margins that may cause failure of partially weathered bedrock or loose regolith.

SLOPE STABILITY

Deep rotational landslides and slow-moving earthflows (Iverson 1986, Keefer and Johnson 1983) are rare in arid regions because of the shallowness and general aridity of the regolith. Slope failures generally involve stripping of thin surficial regolith layers, so that a stability analysis involving finite slopes with a potential failure surface parallel to the surface and flow likewise parallel to the surface (equations 9.1 to 9.5) is often sufficient. However, failures are often initiated at zones of groundwater seepage; such seepage will produce instability on gentler slopes than indicated by equations 9.1 to 9.5 (Iverson and Major 1986). Surficial regolith may be acted upon by a combination of gravity, seepage, and overland flow. A simplified torque-balance approach has been formulated by Kochel *et al.* (1985), Howard and McLane (1988), and Dunne (1990) for the critical stability of a surficial particle (Fig. 8.24).

$$F_g D \sin(\alpha - \theta) + F_c D - F_w D \cos \alpha - F_s D \cos(\theta + \psi - \alpha) = 0 \quad (8.19)$$

where the forces due to gravity F_g, seepage F_s, cohesion F_c, and surface water flow F_w are assumed to be related to the particle size D by

$$F_g = C_1(\rho_s - \rho_f)gD^3 \quad (8.20)$$

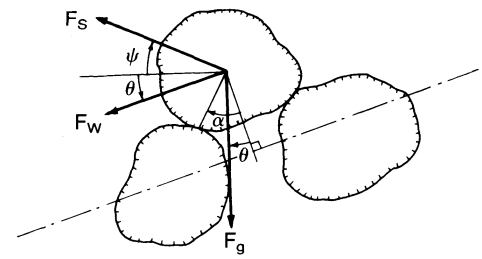

Figure 8.24 Definition of angles and forces on a surficial particle acted upon by seepage and runoff.

$$F_s = C_2 \rho_f g i D^3 \quad (8.21)$$

$$F_c = C_3 c D^2 \quad (8.22)$$

$$F_w = C_4 \tau_s D^2 \quad (8.23)$$

where the C_i are coefficients determined by particle geometry, ρ_s is particle density, i is the hydraulic gradient, and τ_s is the shear stress exerted by the surface flow. Kochel *et al.* (1985) and Howard and McLane (1988) showed that the hydraulic gradient is uniquely related to the slope and seepage exit angles by the expression

$$i = \sin \theta / \cos(\psi + \theta) \quad (8.24)$$

Howard and McLane (1988) investigated the mechanisms of combined seepage and runoff erosion for cohesionless sediments ($c = 0$).

Iverson and Reid (1992) and Reid and Iverson (1992) combined two-dimensional elastic solutions of regolith stress–strain behaviour, Darcian groundwater flow, and a Coulomb failure criterion to investigate slope stability with groundwater flow for saturated conditions. They concluded that stability of slopes with deep, saturated regolith is underestimated by infinite slope analysis such as conducted by Iverson and Major (1986). Slope conditions conducive to failure are high steepness and convexity of slope profiles and outcrop of low-conductivity materials that direct seepage vectors outward.

TRANSPORT OF COARSE DEBRIS

As the name implies, rock-mantled slopes are covered with a layer of coarse debris. Field observations have established that at least some of this debris moves downslope (as opposed to weathering *in situ*). However, the identity and relative importance of the processes causing this movement have been the subject of considerable debate. These processes will be discussed in this section.

The investigation of these processes has been dominated by studies in the American South-west. Lawson (1915) recognized that rock-mantled slopes (termed 'rock slopes' by him) have gradients less than 35° and are inclined at angles less than the angle of repose of the loose material on their surface. He maintained (p. 29) that 'sheets of water . . . wash down the detritus in times of cloud-burst', but 'rain wash co-operates with gravity and transportation is far more efficient' (p. 26). Bryan (1922, 1940), on the other hand, placed greater emphasis on the role of gravitational processes, such as falling, rolling, sliding, and creep, in transporting coarse surface debris. However, he conceded that smaller surface debris can also be undermined and carried away by rain wash, and that the development of gullies during 'cloud bursts' can strip surface debris from whole sections of hillslope. Melton (1965) appears to have held similar views to Bryan. He claimed that particles up to 64 mm in diameter could be transported downslope by hydraulic processes, whereas larger cobbles and boulders moved only by rolling and sliding on slopes steeper than about 28°, which he equated with the angle of sliding friction.

Two studies have recorded the actual movement of stones in the American South-west. Kirkby and Kirkby (1974) painted lines across 12 hillslopes with gradient up to 20° in the Sonoran Desert of southern Arizona. During a two-month period they measured after each rainstorm the movement of all particles with diameters $\geq$1 mm. Field observations confirmed that the processes moving these particles were rainsplash and unconcentrated overland flow, and statistical analyses indicated that the distance moved was directly related to hillslope gradient and inversely related to grain size.

Abrahams *et al.* (1984) analysed 16 years of stone movement on two hillslopes with gradients up to 24° in the Mojave Desert, California. They found that the distance each particle moved was directly related to both length of overland flow (a surrogate for overland flow discharge) and hillslope gradient and inversely related to particle size. These results were interpreted as indicating that the stones, which ranged in size up to 65 mm, were moved mainly by hydraulic action. Citing Kirkby and Kirkby's findings as well as their own, Abrahams *et al.* (1984, p. 369) concluded 'that hydraulic action is probably the dominant process transporting coarse debris down hillslopes with gradients up to at least 24° over most of the Mojave and Sonoran Deserts'.

Although Melton (1965) emphasized gravitational processes while Kirkby and Kirkby (1974) and Abrahams *et al.* (1984) stressed hydraulic ones, their findings are not incompatible, as they examined different ranges of gradient. Indeed, a hypothesis consistent with all the findings is that coarse debris moves mainly by sliding and rolling on slopes steeper than 28° and by hydraulic activity on gentler slopes. Abrahams *et al.* (1990) investigated this hypothesis by analysing the fabric of coarse particles mantling a debris slope on Bell Mountain in the Mojave Desert. The slope is typical of debris slopes in the Mojave Desert underlain by closely jointed or mechanically weak rocks. Samples of rod- and disc-shaped particles from five sites ranging in gradient from 11.7° to 33.17° were found to display essentially the same fabric: particles tend to be aligned downslope and to lie flat on the ground surface. There is no evidence of imbrication signifying sliding or creep nor of transverse modes indicating rolling. Abrahams *et al.* concluded that the fabric is probably produced by hydraulic action, and that this process is mainly responsible for moving coarse particles on gradients up to 33° on these debris slopes.

Cumulative size distributions of the particles sampled at the two sites with gradients greater than 28° reveal that about 25% of the particles are larger than 64 mm and that the largest particle in each sample has a diameter in excess of 300 mm. It is difficult to imagine particles of this size being entrained by overland flow a few millimetres deep and transported as bed load. Abrahams *et al.* (1990) suggested that such particles may be moved downslope by a process termed runoff creep. De Ploey and Moeyersons (1975) observed this process on steep hillslopes in Nigeria and then replicated it in a laboratory flume. Their flume experiments disclosed that under the influence of overland flow (a) blocks shifted and tilted downslope when smaller gravel particles on which they were resting became wet and collapsed; (b) pebbles moved forward and tilted downslope during liquefaction of the underlying soil layer; (c) erosion of underlying finer material caused pebbles to settle downslope; and (d) scour on the upslope side of pebbles resulted in them being drawn into the holes and tilted upslope.

That hydraulic processes, including runoff creep, appear to be the main mechanism whereby coarse debris is moved downslope on Bell Mountain does not necessarily mean that all the coarse debris is transported by this mechanism. Nor does it mean that hydraulic processes necessarily dominate on other desert hillslopes either in the American South-west or elsewhere. In the semi-arid mountains of southern California, coarse debris is moved down hillslopes close to their angle of repose (Melton's angle of static friction) by a combination of gravita-

tional and hydraulic processes. Gravitational processes are locally referred to as dry erosion and hydraulic processes as wet erosion. Dry erosion includes surface creep, particle sliding, and particle flow and may be triggered by wetting and drying, earthquakes, wind, or animals. This process involves a wide range of debris sizes and is sensitive to vegetation cover, with rates of movement being greater under shrubs than under grass (Wohlgemuth 1986). Field measurements have established that dry erosion is more rapid than wet erosion, which includes rainsplash, unconcentrated overland flow, and rilling (Rice 1982, Wohlgemuth 1986).

A combination of gravitational and hydraulic processes also seems to be at work on hillslopes in semi-arid northern Kenya. Over a two-year period Frostick and Reid (1982, Reid and Frostick 1986) monitored the movements of three lines of painted stones $\geq$10 mm in diameter on a 30° hillslope. On the planar portion of the hillslope they found that the distance moved was positively correlated with size of particle (cf. Kirkby and Kirkby 1974, Abrahams *et al.* 1984), which led them to infer that these movements were due to unspecified gravitational processes. In contrast, in the chutes and rills, the particles moved much farther, but the distance moved was uncorrelated with particle size. The movement of particles in the chutes and rills was attributed to concentrated overland flow eroding interstitial fines, thereby undermining the coarse particles and facilitating their downslope movement (i.e. runoff creep).

Finally, there is ample evidence that on still other desert hillslopes, debris flows are largely responsible for the downslope transport of coarse debris. Such hillslopes are generally steep – that is, they are at or near the angle of repose of their surface material. Moreover, the relative importance of debris flows appears to vary with the character of the substrate. Substrates that produce an abundance of fine debris upon weathering are more likely to generate debris flows than those that do not. Similarly, substrates that favour the formation of a relatively impermeable caliche layer close to the surface, thereby aiding saturation of the surface materials, are more susceptible to debris flows than those that do not. Hillslopes where debris flows are the dominant process transporting coarse debris have been described by Mabbutt (1977, pp. 45–6), Gerson (1982), and Gerson and Grossman (1987).

To conclude, desert hillslopes appear to lie along a continuum with respect to the manner in which coarse debris is moved downslope (Carson and Kirkby 1972, p. 345). At one end of the continuum are slopes inclined at the angle of repose of their mantling debris. On these slopes gravitational processes, both dry and wet, dominate. On slightly less steep slopes, gravitational processes remain important, but quite coarse debris can also be moved directly by overland flow; in addition, much debris is probably moved indirectly by runoff creep. At the other end of the continuum are gentler slopes where hydraulic processes are largely responsible for the downslope movement of coarse debris by both direct and indirect means and gravitational processes such as creep are of little significance.

DEBRIS SLOPES

SLOPE FORM AND ADJUSTMENT

Debris slopes are usually thought of as relatively steep – that is, with gradients in excess of 10° – but in this chapter they include all rock-covered slopes, regardless of gradient, whose surface accumulation of coarse debris has weathered from the underlying rock. Typically the profiles of such slopes are convex–rectilinear–concave, though either the rectilinear or concave elements may be missing. Generally the upper convexity is narrow, and the profile is dominated by either the rectilinear or concave element. The rectilinear element tends to dominate on slopes affected by stream undercutting (Strahler 1950), and the concave element on slopes unaffected by this process. However, even in the latter circumstances, a rectilinear element may be present and occupy a significant proportion of the profile, especially where the slope is long or steep.

The coarse debris mantling debris slopes is often embedded within and/or resting upon a matrix of fines, particularly toward the base of slopes or where gradients are gentle. These fines are produced by the chemical and physical breakdown of the coarse debris. As the weathering particles become finer, they are preferentially transported downslope by hydraulic processes, so that usually the proportion of fines increases and the proportion of coarse debris decreases in this direction. Inasmuch as gradient also tends to decrease downslope, positive correlations between gradient and various measures of particle size often obtain, particularly on weak to moderately resistant rocks (e.g., Cooke and Reeves 1972, Kirkby and Kirkby 1974, Akagi 1980, Abrahams *et al.* 1985, Simanton *et al.* 1993) (Fig. 8.25).

A more detailed picture of the variation in mean particle (fines plus debris) size with gradient down a debris slope profile is presented in Figure 8.26. This

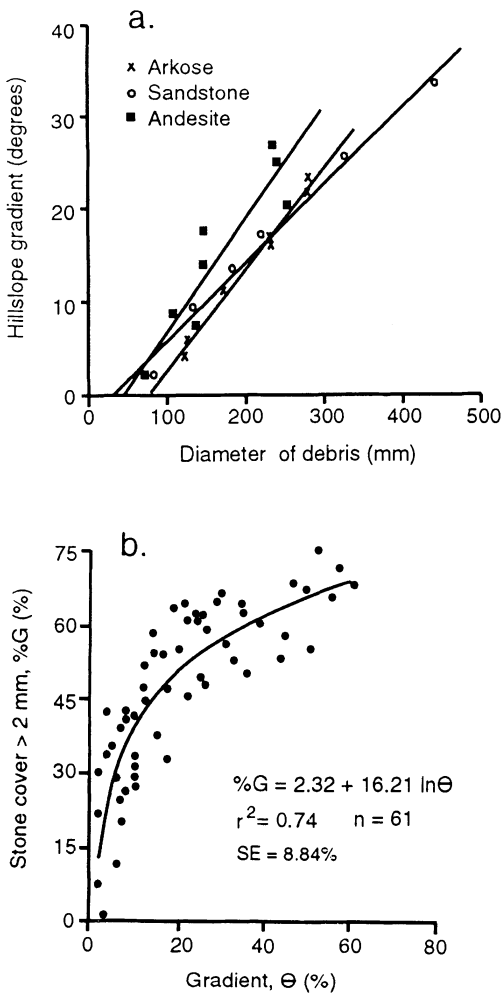

Figure 8.25 Graphs of hillslope gradient against various measures of particle size. (a) Graph of hillslope gradient against the mean size of the ten largest debris particles for three debris slopes on three rock types in southern Arizona (after Akagi 1980). (b) Graph of stone cover against hillslope gradient for 12 debris slopes in Walnut Gulch Experimental Watershed, Arizona.

profile is located in the Mojave Desert, California, and is underlain by closely jointed latitic porphyry (Fig. 8.27). Beginning at the divide, mean particle size increases with gradient down the upper convexity. Note, however, that the particles are much larger than at comparable gradients on the basal concavity. This is because the weathering mantle is thinner and bedrock outcrops are more common on the convexity. Downslope from the convexity is a substantial rectilinear element. Mean particle size is at a maximum at the top of this element and decreases down the element. The decrease continues down the long concave element. This downslope pattern of change in particle size is representative of many, if not most, debris slopes without basal streams, including those that are both much steeper and much gentler than this example, and appears to be primarily due to the selective transport of fine sediment by hydraulic processes.

That hydraulic processes play a dominant role in removing sediment from and fashioning many debris slopes is suggested by a recent study of the relation between gradient S and mean particle size $\bar{D}$ for debris slopes underlain by weak to moderately resistant rocks in the Mojave Desert, California. In this study, Abrahams *et al.* (1985) found that plan-planar slopes on different rocks have S–$\bar{D}$ relations with similar slope coefficients but different intercepts (Fig. 8.28). However, on a given rock the slope coefficient varies with debris slope planform, being greater for plan-concave slopes than for plan-convex ones (Fig. 8.29).

To explain their findings Abrahams *et al.* assumed that sediment transport by hydraulic processes can be characterized by an equation of the form

$$G \propto X^m S^n / \bar{D}^p \tag{8.26}$$

where G is sediment transport rate, X is horizontal distance from the divide, and m, n, and p are positive coefficients. Now if debris slopes are formed by and adjusted to hydraulic processes, equation 8.26 may be manipulated to ascertain how the S–$\bar{D}$ relation varies with debris slope planform. Because $\bar{D} \propto X^q$, where $q < 0$,

$$G \propto \bar{D}^{[(m/n)-p]} S^n \tag{8.27}$$

Rearranging equation 8.27, one obtains

$$S \propto G^{1/n} / \bar{D}^{[(m/q)-p]/n} \tag{8.28}$$

From equation 8.26 it can be seen that m is larger for plan-concave slopes, where overland flow converges, than for plan-convex slopes, where overland flow diverges. The larger the value of m, the larger is the exponent (i.e. slope coefficient) of $\bar{D}$ in equation 8.28, and the steeper is the S–$\bar{D}$ relation. Thus the analysis predicts that plan-concave debris slopes have steeper S–$\bar{D}$ relations than plan-convex ones. The agreement between the analysis and observed variation in the S–$\bar{D}$ relation with planform implies that the debris slopes are formed by and adjusted to hydraulic processes.

In the above sediment transport equation (equation 8.26), the arithmetic mean particle size $\bar{D}$ was used as the measure of particle size because, of the several measures of particle size tested, it correlated

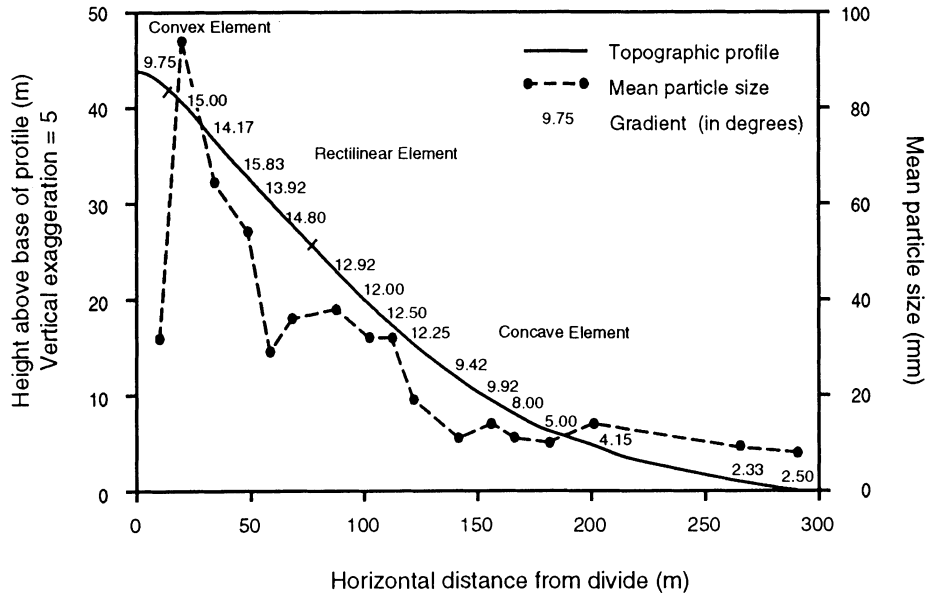

Figure 8.26 Debris slope profile showing the downslope variation in mean particle size (sample size 100) and gradient (measured length 5 m). The debris slope is depicted in Figure 8.27.

most highly with gradient. Variable $\bar{D}$ worked best in this instance possibly because it represented resistance to flow, and the contribution by each piece of debris to flow resistance was additive rather than multiplicative. However, there are other measures of particle size, and in different circumstances they may be better predictors of G than is $\bar{D}$. For example, $\bar{D}$ is very insensitive to size of fines. Therefore where this property has a significant effect on G, a more sensitive sediment size variable should be used.

Figure 8.27 Photograph of well-adjusted debris slope underlain by latitic porphyry in Turtle Valley, Mojave Desert, California.

Laboratory experiments by Poesen and Lavee (1991) showed that the proportion of the surface covered with coarse debris (i.e. percentage stone cover) and the size of debris (stones) have an important influence on G (Fig. 8.13). Usually G decreases as stone cover increases due to increased resistance to flow and increased protection of the underlying fines. However, where stones are larger than about 50 mm and cover less than 70% of the surface, the opposite is true because the stones tend to concentrate the flow. Most interesting is the fact that for a given stone cover, G consistently increases with stone size, again because the stones tend to concentrate the flow. These findings by Poesen and Lavee suggest that although equation 8.26 may be a useful start to the modelling of debris slope form, the situation on actual debris slopes is probably far more complex, and that a great deal more work is required to elucidate the effect of debris size and cover on sediment transport rate.

A discussion of debris slopes would be incomplete if it did not consider the effects of climatic change. Major climatic fluctuations have probably occurred in every desert during the Cenozoic (Chapter 26) and have strongly influenced the form of many debris slopes (Chapter 21). The imprint of these former climates appears to be most pronounced where rock resistance is greatest. This is well illustrated by Oberlander's (1972) classic study of boul-

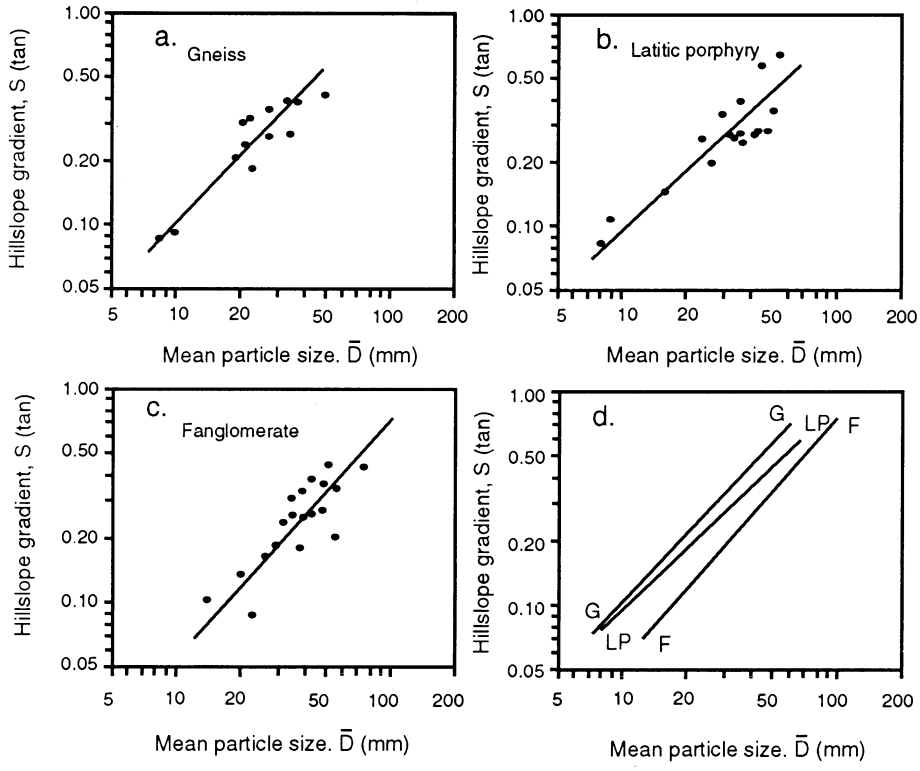

Figure 8.28 Graphs of hillslope gradient against mean particle size for plan-planar debris slopes underlain by (a) gneiss, (b) latitic porphyry, and (c) fanglomerate. The fitted lines in (a), (b), and (c) are reproduced in (d) for comparative purposes (after Abrahams *et al.* 1985).

der-covered slopes on resistant quartz monzonite in the Mojave Desert, California. These slopes consist of a 'jumble of subangular to spheroidal boulders of a variety of shapes and sizes clearly derived from plane-faced blocks bounded by intersecting joints' (Oberlander 1972, p. 4) (Fig. 8.30). Oberlander argued that the boulders formed as corestones within a deep weathering profile under a wetter climate, and that these corestones became stranded on bedrock slopes as the supporting matrices of fines were removed under the more arid climate of the late Tertiary and the Quaternary. Not surprisingly, Oberlander could find no correlation between hillslope gradient and boulder size. Other investigators too have reported an absence of any relation between gradient and debris size on slopes underlain by resistant rocks (e.g. Melton 1965, Cooke and Reeves 1972, Kesel 1977), suggesting that these slopes also owe much of their form and sedimentology to climatic change.

Legacies from past climates are probably more prevalent on debris slopes than is generally realized. Certainly, Oberlander's description of boulder-clad slopes in the Mojave Desert applies to debris slopes in most granitic terranes. Erosion on such slopes is often characterized as weathering-limited (e.g. Young 1972, p. 206, Mabbut 1977, p. 41). However, if this were truly the case, such slopes would be more or less devoid of fine material because, by definition, such material should be removed as rapidly as it is produced. Instead, what we often find are boulders or bedrock outcrops protruding from a matrix of fines that becomes progressively more extensive downslope. Parsons and Abrahams (1987) investigated this phenomenon in the Mojave Desert and concluded that the presence of the fines indicates adjustment by the hillslope to extant hydraulic processes, and that the degree of adjustment is inversely related to slope gradient and rock resistance (Fig. 8.31). It is interesting to note that inasmuch as particle size decreases as degree of adjustment increases, the hillslopes studied by Parsons and Abrahams display strong correlations between gradient and particle size, even though they

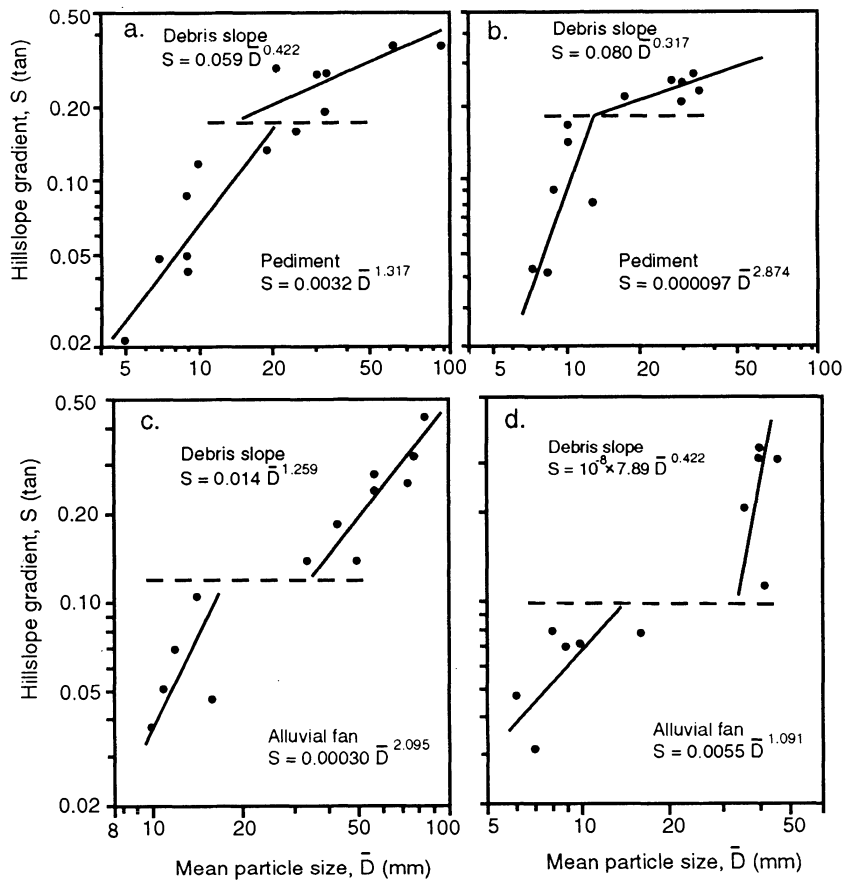

Figure 8.29 Graphs of hillslope gradient against mean particle size for two (a, b) plan-convex debris slopes and their basal pediments and two (c, d) plan-concave slopes and their basal alluvial fans (after Abrahams 1987). Note that the S–D̄ relations are much steeper for the plan-concave slopes than for the plan-convex ones.

are far from being adjusted to contemporary hydraulic processes, especially in their steeper parts.

PIEDMONT JUNCTIONS

In desert landscapes, hills and mountains generally arise abruptly from their surrounding plains or piedmont. The transition zone between the piedmont and these upland areas has been variously referred to as the transition slope (Fair 1948), the nickpoint (Rahn 1966), the break in slope (Kirkby and Kirkby 1974), the piedmont angle (Twidale 1967, Young 1972, pp. 204–8, Cooke and Warren 1973, p. 199), and the piedmont junction (Mabbutt 1977, p. 82, Parsons and Abrahams 1984). In this chapter we use the term piedmont junction. At many locations the piedmont junction marks the boundary between the operation of different processes: for example, where an alluvial fan abuts against a hillslope. At other locations, the morphology of the piedmont junction is manifestly influenced by geological structure (e.g. Twidale 1967) or subsurface weathering (e.g. Twidale 1962, Mabbutt 1966). We are concerned with none of these situations here. Rather we focus on piedmont junctions that are simply concavities in debris slope profiles. These piedmont junctions occur at the transition between a pediment and its backing hillslope and extend from 15° on the lower part of the backing hillslope to 5° on the upper part of the pediment (Kirkby and Kirkby 1974).

Piedmont junctions vary greatly in concavity. At one extreme are features that are so concave that they take the form of a true break in slope and can be identified only as a point on the hillslope profile (Fig. 8.32a). At the other extreme are features whose concavity is so slight that they can reach lengths of 750 m (Fig. 8.32b) (Kirkby and Kirkby 1974). Numer-

Figure 8.30 Photograph of a steep, poorly adjusted debris slope developed on widely jointed quartz monzonite in the Mojave Desert, California.

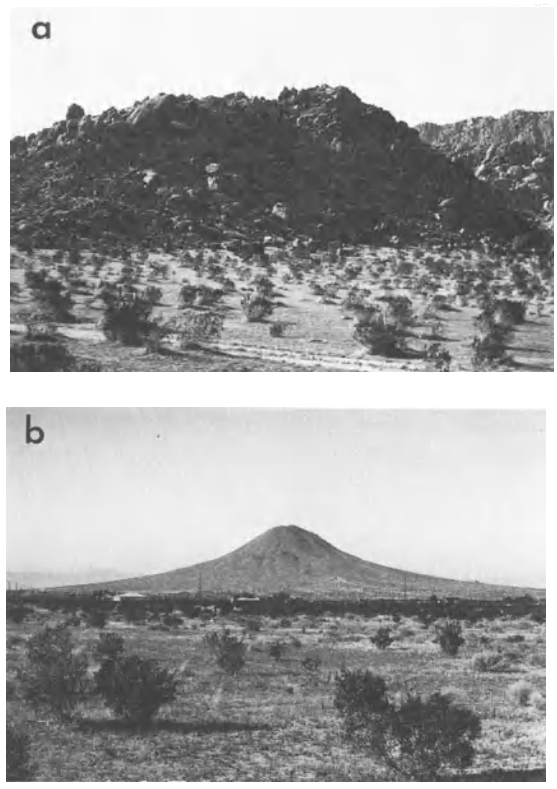

Figure 8.32 Photographs of piedmont junctions, showing (a) a narrow, highly concave one formed on widely jointed quartz monzonite, Mojave Desert, California, and (b) a broad, gently concave one developed on quartz monzonite with a latitic porphyry debris mantle derived from the caprock of the residual.

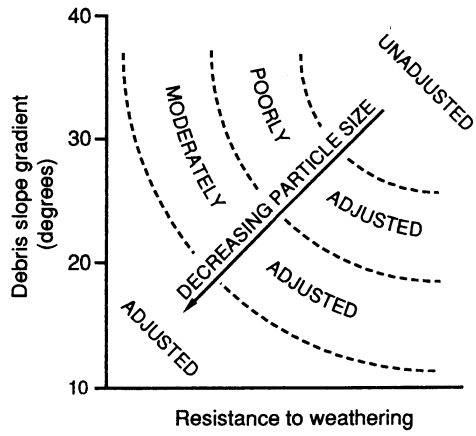

Figure 8.31 Graph of debris slope gradient against resistance to weathering, showing how the degree of debris slope adjustment varies with these variables (after Parsons and Abrahams 1987).

ous workers have noted that piedmont junctions in many locations conform to two general tendencies. First, under a given climate they tend to vary in concavity from one rock type to another (e.g. Kirkby and Kirkby 1974, Mabbutt 1977, pp. 85–7). Second, on a given rock type they tend to decrease in concavity as precipitation increases (e.g. Bryan 1940, Fair 1947, 1948, Young 1972, p. 208, Mabbutt 1977, p. 85). The latter tendency is of course implicit in the fact that piedmont junctions (i.e. pronounced concavities) are generally associated with desert landscapes and not humid ones.

Both these tendencies derive from the fact that on debris slopes adjusted to present-day processes of sediment transport, gradient varies directly with particle size, which in turn varies inversely with distance downslope at different rates on different rock types and in different climates. Early workers

claimed that gradient was related to particle size (e.g. Lawson 1915, Bryan 1922, Gilluly 1937), and in the past two decades this relation has been verified quantitatively (e.g. Kirkby and Kirkby 1974, Abrahams *et al.* 1985). M.J. Kirkby (Carson and Kirkby 1972, pp. 346–7, Kirkby and Kirkby 1974) was perhaps the first to point out that different rock types have different comminution sequences and that, because hydraulic processes selectively transport finer particles further downslope than coarser ones, the comminution sequence is reflected in the downslope rate of change in particle size and, hence, gradient. At one extreme are rocks, such as basalts and schists, that have fairly continuous comminution sequences from boulder- to silt-sized particles. The debris slopes that form in these rocks exhibit a progressive decrease in particle size accompanied by a steady decline in gradient downslope, forming a broad and gently curving piedmont junction. At the other extreme are rocks, such as widely jointed granites, that are characterized by markedly discontinuous comminution sequences in which boulders disintegrate directly into granules and sands. On these rocks, steep backing slopes mantled with boulders give way abruptly downslope to gentle pediments covered with granules and sands, and an extremely narrow, almost angular piedmont junction is produced. It is therefore evident that given the relationship between hillslope gradient and particle size, the concavity of piedmont junctions in a desert climate depends on the comminution sequence of the underlying rock.

The same line of reasoning may be applied to explaining the variation in piedmont junction concavity with climate. In desert climates, particle size decreases across piedmont junctions in accordance with the comminution sequence of the underlying rock, as explained above. In humid climates, on the other hand, soils with fine-grained A horizons are developed on both the backing hillslopes and the footslopes, and the size of surface particles decreases very little, if at all, downslope (e.g. Furley 1968, Birkeland 1974, p. 186). Because the decrease in particle size across the piedmont junction is more pronounced in desert climates than in humid ones, the piedmont junctions are typically narrower and more concave.

The foregoing discussion applies to debris slopes that are adjusted to present-day processes, at least in the vicinity of the piedmont junction. However, not all debris slopes are so adjusted. Where they are not, particle size may be unrelated to gradient, and the preceding analysis is irrelevant. The situation most commonly encountered is where a pediment covered with fines and presumably adjusted to contemporary processes is backed by a weathering-limited slope that is clearly not adjusted to current transport processes (Fig. 8.30). The form of the backing slope might be controlled by rock mass strength (Selby 1980, 1982a, b, pp. 199–203) or rock structure (Oberlander 1972) or inherited from a previous climate. Thus the concavity of the piedmont junction cannot be understood in terms of contemporary hydraulic processes. About all that can be said about piedmont junctions of this type is that they tend to be more concave than most. The reason for this is that in a given (desert) climate, steep backing slopes are more likely to become weathering-limited than are gentle ones, and piedmont junctions with steep backing slopes are likely to be more concave than those with gentle backing slopes.

TALUS SLOPES

Talus or scree slopes are a ubiquitous accompaniment to steep bedrock slopes. Most occur as small fillets in breaks-of-slope in bedrock slopes, but more extensive talus occurs below resistant caprocks in layered rock (Chapter 7). Most studies of scree slope development and sedimentology have been undertaken in arctic and alpine environments (see references in Kirkby and Statham 1976, Statham and Francis 1986). Delivery of debris to talus slopes may occur as falls ranging from individual rocks to debris avalanches. A model of debris motion and deposition has been presented above (equations 8.12 to 8.15). Two characteristics of talus slopes are explained by this model (Kirkby and Statham 1976). Talus is commonly sorted downslope, with coarser blocks at the foot of the slope. The differential movement of rocks over a scree of a different size (equation 8.15) explains this sorting, since the largest rocks have enhanced mobility. Furthermore, talus slopes are generally concave due to the exponential travel distance decay function (equation 8.14); the concave tail is created by rocks composing the higher-mobility tail of the distribution. The concavity is best developed on short talus slopes and on talus extending out on to a horizontal rather than downward sloping basal surfaces (Kirkby and Statham 1976).

Because the dynamic friction angle of moving debris, which controls deposition, is 5° or more greater than the static friction angle, scree slopes are at least marginally stable when deposited (Statham and Francis 1986). Weathering of scree may increase mechanical stability of the slope due to generation and movement of fine debris leading to a well-

graded and dense packing. However, weathering also decreases infiltration capacity and can lead to enhanced runoff erosion and regolith saturation during precipitation events, which can decrease slope stability (e.g. equations 9.1 to 9.5) (Statham and Francis 1986). Concentrated runoff from bedrock slopes above the scree means that instability will occur most commonly at the head of the talus slope (Statham and Francis 1986), including mobilization of debris flows as discussed above.

Classic models of scree slope development assume an initially high cliff bordering a basal slope of low inclination, with the cliff backwasting, forming talus that gradually swamps the cliff face, leading ultimately to the entire slope becoming talus and a characteristic convex profile of the talus–bedrock contact (Fisher 1866, Lehmann 1933, Bakker and Le Heux 1946, 1947, 1950, 1952). This idealized pattern of evolution seldom occurs in nature (Statham and Francis 1986). Many small scree slopes in depressions on bedrock slopes are essentially surfaces of transportation, delivering as much material to the bedrock slope at the foot of the scree as arrives from upslope. Such scree may wax or wane in size depending upon the pattern of weathering and erosion of the super- and subjacent bedrock slopes. A similar pattern occurs on many basal screes debouching directly into fluvial washes or chutes, where input from above is balanced by erosion from below. In fact, the ideal model presented above is probably the exception, occurring primarily where a scarp is created fairly suddenly from faulting, landsliding, or fluvial undercutting. Even more complex relationships between talus emplacement and erosional removal occur on cuesta scarps due to the difference in erosional resistance between the caprock talus and the weak subcaprock unit. In these circumstances the talus may be eroded laterally and undergo several episodes of remobilization prior to removal (Chapter 7). Over the long run talus slopes exhibit a balance between addition of debris from above and its removal through weathering, runoff erosion, mass wasting, and basal erosion, although individual talus slopes may wax or wane in size due to changes in geo-topographic setting or climatic changes.

DISCUSSION

As with most of the landforms and processes in deserts, our knowledge of rock-mantled slopes is deficient and there are many opportunities for further field observations and experimentation, laboratory investigations, and theoretical modelling. Our understanding of weathering processes of regolith generation is poor, and the relative roles of present and past climates is uncertain. Mechanisms of debris mobilization, deposition, and further weathering are reasonably well understood both in a quantitative and qualitative sense, but the long-term interaction of processes and materials to create specific types of desert slopes is poorly characterized.

ACKNOWLEDGEMENTS

The experiments reported in Table 8.2 were funded by NSF grant SES-8812587.

REFERENCES

Abrahams, A.D. 1987. Hydraulic processes in the formation of debris slopes in the Mojave Desert, California. In *Processes and measurement of erosion*, A. Godard (ed.), 187–97. Paris: Centre National de la Recherche Scientifique.

Abrahams, A.D. and A.J. Parsons 1991a. Relation between infiltration and stone cover on a semiarid hillslope, southern Arizona. *Journal of Hydrology* **122**, 49–59.

Abrahams, A.D. and A.J. Parsons 1991b. Relation between sediment yield and gradient on debris-covered hillslopes, Walnut Gulch, Arizona. *Bulletin of the Geological Society of America* **103**, 1109–13.

Abrahams, A.D. and A.J. Parsons 1991c. Resistance to overland flow on desert pavement and its implications for sediment transport modeling. *Water Resources Research* **27**, 1827–36.

Abrahams, A.D., A.J. Parsons, R.U. Cooke and R.W. Reeves 1984. Stone movement on hillslopes in the Mojave Desert, California: a 16-year record. *Earth Surface Processes and Landforms* **9**, 365–70.

Abrahams, A.D., A.J. Parsons and P.J. Hirsch 1985. Hillslope gradient-particle size relations: evidence for the formation of debris slopes by hydraulic processes in the Mojave Desert. *Journal of Geology* **93**, 347–57.

Abrahams, A.D., A.J. Parsons and S.-H. Luk 1986. Resistance to overland flow on desert hillslopes. *Journal of Hydrology* **88**, 343–63.

Abrahams, A.D., A.J. Parsons and S.-H. Luk 1988. Hydrologic and sediment responses to simulated rainfall on desert hillslopes in southern Arizona. *Catena* **15**, 103–17.

Abrahams, A.D., A.J. Parsons and S.-H. Luk 1991. The effect of spatial variability in overland flow on the downslope pattern of soil loss on a semiarid hillslope, southern Arizona. *Catena* **18**, 255–70.

Abrahams, A.D., N. Soltyka, A.J. Parsons and P.J. Hirsch 1990. Fabric analysis of a desert debris slope: Bell Mountain, California. *Journal of Geology* **98**, 264–72.

Akagi, Y. 1980. Relations between rock type and the slope form in the Sonoran Desert, Arizona. *Zeitschrift für Geomorphologie* **24**, 129–40.

Bagnold, R.A. 1954. Experiments on a gravity-free dispersion of large solid spheres in a Newtonian fluid under shear. *Proceedings of the Royal Society of London, Series A*, **225**, 49–63.

Bagnold, R.A. 1980. An empirical correlation of the bedload transport rates in flumes and natural rivers. *Proceedings of the Royal Society of London, Series A*, **372**, 453–73.

Bakker, J.P. and J.W.N. Le Heux 1946. Projective geometry treatment of G. Lehmann's theory of the transformation of mountain slopes. *Koninklijke Nederlandshe Akademie van Wetenschapen, Amsterdam*, **49**, 532–47.

Bakker, J.P. and J.W.N. Le Heux 1947. Theory on central rectilinear recession of slopes *Koninklijke Nederlandshe Akademie van Wetenschapen, Amsterdam*, **50**, 959–66, 1154–62.

Bakker, J.P. and J.W.N. Le Heux 1950. Theory on central rectilinear recession of slopes. *Koninklijke Nederlandshe Akademie van Wetenschapen, Amsterdam*, **53**, 1072–84, 1364–74.

Bakker, J.P. and J.W.N. Le Heux 1952. A remarkable new geomorphological law. *Koninklijke Nederlandshe Akademie van Wetenschapen, Amsterdam*, **55**, 399–410, 554–71.

Beasley, D.B., L.F. Huggins and E.J. Monke 1980. ANSWERS: a model for watershed planning. *Transactions of the American Society of Agricultural Engineers* **23**, 938–44.

Berndtsson, R. and M. Larson 1987. Spatial variability of infiltration in a semi-arid environment. *Journal of Hydrology* **90**, 117–33.

Biot, M.A. 1956. Theory of propagation of elastic waves in a fluid-saturated porous solid. I. Low-frequency range. *Journal of the Acoustical Society of America* **28**, 168–78.

Birkeland, P.W. 1974. *Pedology, weathering, and geomorphological research*. Oxford: Oxford University Press.

Blackburn, W.H. 1975. Factors influencing infiltration and sediment production of semiarid rangelands in Nevada. *Water Resources Research* **11**, 929–37.

Blackwelder, E. 1928. Mudflow as a geologic agent in semi-arid regions. *Bulletin of the Geological Society of America* **39**, 465–84.

Borst, H.L. and R. Woodburn 1942. The effect of mulching and methods of cultivation on run-off and erosion from Muskingum silt loam. *Agricultural Engineering* **23**, 19–22.

Box, J.E. 1981. The effects of surface slaty fragments on soil erosion by water. *Soil Science Society of America Journal* **45**, 111–16.

Brice, J.C. 1966. Erosion and deposition in the loess-mantled Great Plains, Medicine Creek drainage basin, Nebraska. *U.S. Geological Survey Professional Paper* 352-H.

Bridgewater, J. 1980. On the width of failure zones. *Geotechnique* **30**, 533–6.

Bryan, K. 1922. Erosion and sedimentation in the Papago Country, Arizona. *U.S. Geological Survey Bulletin* 730-B, 19–90.

Bryan, K. 1940. The retreat of slopes. *Annals of the Association of American Geographers* **30**, 254–68.

Campbell, A.G., P.M. Wohlgemuth and W.W. Wells 1987, Post-fire response of a boulder bed channel. *International Association of Scientific Hydrology Publication* 165, 277–8.

Campbell, C.S. and C.E. Brennen 1985. Chute flows of granular material: some computer simulations. *Journal of Applied Mechanics* **52**, 172–8.

Campbell, R.H. 1975. Soil slips, debris flows, and rainstroms in the Santa Monica Mountains and vicinity, southern California. *U.S. Geological Survey Professional Paper* 851.

Carson, M.A. and M.J. Kirkby 1972. *Hillslope form and process*. Cambridge: Cambridge University Press.

Chen, C.-I. 1987. Comprehensive review of debris flow modeling concepts in Japan. In *Debris flows/avalanches: processes, recognition and mitigation*, J.E. Costa and G.F. Weiczorek (eds), 13–29. Reviews in Engineering Geology 7. Boulder: Geological Society of America.

Cooke, R.U. and R.W. Reeves 1972. Relations between debris size and the slope of mountain fronts and pediments in the Mojave Desert, California. *Zeitschrift für Geomorphologie* **16**, 76–82.

Cooke, R.U. and A. Warren 1973. *Geomorphology in deserts*. Berkeley: University of California Press.

Cooley, M.E., B.N. Aldridge and R.C. Euler 1977. Effects of the catastrophic flood of December 1966, north rim area, eastern Grand Canyon, Arizona. *U.S. Geological Survey Professional Paper* 980.

Costa, J.E. 1984. Physical geomorphology of debris flows. In *Developments and applications of geomorphology*, J.E. Costa and P.J. Fleisher (eds), 268–317. Berlin: Springer.

Costa, J.E. 1988. Rheologic, geomorphic, and sedimentologic differentiation of water floods, hyperconcentrated flows, and debris flows. In *Flood geomorphology*, V.R. Baker, R.C. Kochel and P.C. Patten (eds), 113–22. New York: Wiley.

David, W.P. and C.E. Beer 1975. Simulation of soil erosion – Part I. Development of a mathematical erosion model. *Transactions of the American Society of Agricultural Engineers* **18**, 126–9, 133.

Davis, R.H., J.-M. Serayssol and E.J. Hinch 1986. The elastohydrodynamic collision of two spheres. *Journal of Fluid Mechanics* **163**, 479–97.

De Ploey, J. and J. Moeyersons 1975. Runoff creep of coarse debris: experimental data and some field observations. *Catena* **2**, 275–88.

Dillaha, T.A., III and D.B. Beasley 1983. Distributed parameter modeling of sediment movement and particle size distributions. *Transactions of the American Society of Agricultural Engineers* **26**, 1766–72, 1777.

Drake, T.G. 1990. Structural features in granular flow. *Journal of Geophysical Research* **95**, 8681–96.

Drake, T.G. and R.L. Shreve 1986. High-speed motion pictures of nearly steady, uniform, two-dimensional, inertial flows of granular material. *Journal of Rheology* **30**, 981–93.

Dunne, T. 1990. Hydrology, mechanics, and geomorphic implications of erosion by subsurface flow. In *Groundwater geomorphology*, C.G. Higgins and D.R. Coates (eds), 1–28. Geological Society of America Special Paper 252.

Dunne, T. and B.F. Aubry 1986. Evaluation of Horton's theory of sheetwash and rill erosion on the basis of field experiments. In *Hillslope processes*, A.D. Abrahams (ed.), 31–53. Boston: Allen & Unwin.

Dunne, T. and W.E. Dietrich 1980. Experimental study of Horton overland flow on tropical hillslopes. 2. Hydraulic characteristics and hillslope hydrographs. *Zeitschrift für Geomorphologie Supplement Band* **35**, 60–80.

Ellen, S.D. and R.W. Fleming 1987. Mobilization of debris flows from soil slips, San Francisco Bay region, California. In *Debris flows/avalanches: processes, recognition and mitigation*, J.E. Costa and G.F. Weiczorek (eds), 31–40. Reviews in Engineering Geology 7. Boulder: Geological Society of America.

Ellison, W.D. 1944. Studies of raindrop erosion. *Agricultural Engineering* **25**, 131–6, 181–2.

Ellison, W.D. 1945. Some effects of raindrops and surface flow on soil erosion and infiltration. *Transactions of the American Geophysical Union* **26**, 415–29.

Emmett, W.W. 1970. The hydraulics of overland flow on hillslopes. *U.S. Geological Survey Professional Paper* 662-A.

Epstein, E., W.J. Grant and R.A. Struchtemeyer 1966. Effects of stone on runoff, erosion, and soil moisture. *Soil Science Society of America Proceedings* **30**, 638–40.

Everaert, W. 1991. Empirical relations for the sediment transport capacity of interrill flow. *Earth Surface Processes and Landforms* **16**, 513–32.

Fair, T.J.D. 1947. Slope form and development in the interior of Natal, South Africa. *Transactions of the Geological Society of South Africa* **50**, 105–19.

Fair, T.J.D. 1948. Hill-slopes and pediments of the semi-arid Karoo. *South African Geography Journal* **30**, 71–9.

Ferguson, R.I. 1986. Hydraulics and hydraulic geometry. *Progress in Physical Geography* **10**, 1–31.

Fisher, O. 1866. On the disintegration of a chalk cliff. *Geological Magazine* **3**, 354–6.

Fisher, R.V. 1971. Features of coarse-grained, high-concentration fluids and their deposits. *Journal of Sedimentary Petrology* **41**, 916–27.

Florsheim, J.L., E.A. Keller and D.W. Best 1991. Fluvial sediment transport in response to moderate storm flows following chaparral wildfire, Ventura County, Southern California. *Bulletin of the Geological Society of America* **103**, 504–11.

Foster, G.R. 1982. Modeling the erosion process. In *Hydrologic modeling of small watersheds*, C.T. Haan, H.P. Johnson and D.L. Brakensiek (eds), 296–380. St Joseph, MI: American Society of Agricultural Engineers.

Foster, G.R. and L.D. Meyer 1972. A closed-form soil erosion equation for upland areas. In *Sedimentation: Symposium to Honor Professor H.A. Einstein*, H.W. Shen (ed.), 12.1–12.19. Fort Collins, CO: H.W. Shen.

Foster, G.R. and L.D. Meyer 1975. Mathematical simulation of upland erosion using fundamental erosion mechanics. In *Present and prospective technology for predicting sediment yields and sources*, U.S. Agricultural Research Service Report ARS-S-40, 190–207. Oxford, MS: U.S. Department of Agriculture.

Foster, G.R., L.D. Meyer and C.A. Onstad 1977. An erosion equation derived from basic erosion principles. *Transactions of the American Society of Agricultural Engineers* **20**, 678–82.

Foster, G.R., L.J. Lane, J.D. Nowlin, J.M. Laflen *et al.* 1981. Estimating erosion and sediment yield on field-sized areas. *Transactions of the American Society of Agricultural Engineers* **24**, 1253–62.

Foster, G.R., L.F. Huggins and L.D. Meyer 1984a. A laboratory study of rill hydraulics: I. Velocity relationships. *Transactions of the American Society of Agricultural Engineers* **27**, 790–6.

Foster, G.R., L.F. Huggins and L.D. Meyer 1984b. A laboratory study of rill hydraulics: II. Shear stress relationships. *Transactions of the American Society of Agricultural Engineers* **27**, 797–804.

Frostick, L.E. and I. Reid 1982. Talluvial processes, mass wasting and slope evolution in arid environments. *Zeitschrift für Geomorphologie Supplement Band* **44**, 53–67.

Furley, P.A. 1968. Soil formation and slope development 2. The relationship between soil formation and gradient angle in the Oxford area. *Zeitschrift für Geomorphologie* **12**, 25–42.

Gerber, E. and A.E. Scheidegger 1974. On the dynamics of scree slopes. *Rock Mechanics* **6**, 25–38.

Gerson, R. 1982. Talus relicts in deserts: a key to major climatic fluctuations. *Israel Journal of Earth Sciences* **31**, 123–32.

Gerson, R. and S. Grossman 1987. Geomorphic activity on escarpments and associated fluvial systems in hot deserts as an indicator of environmental regimes and cyclic climatic changes. In *Climate: history, periodicity, predictability*, M.R. Rampino, J.E. Sanders and W.S. Newman (eds), 300–22. Stroudsburg, PA: Van Nostrand Reinhold.

Ghadiri, H. and D. Payne 1988. The formation and characteristics of splash following raindrop impact on soil. *Journal of Soil Science* **39**, 563–75.

Gilley, J.E., D.A. Woolhiser and D.B. McWhorter 1985a. Interrill soil erosion – Part I: development of model equations. *Transactions of the American Society of Agricultural Engineers* **28**, 147–53, 159.

Gilley, J.E., D.A. Woolhiser and D.B. McWhorter 1985b. Interrill soil erosion – Part II; testing and use of model equations. *Transactions of the American Society of Agricultural Engineers* **28**, 154–9.

Gilley, J.E., E.R. Kottwitz and J.R. Simanton 1990. Hydraulic characteristics of rills. *Transactions of the American Society of Agricultural Engineers* **33**, 1900–6.

Gilley, J.E., E.R. Kottwitz and G.A. Weiman 1992. Darcy-Weisbach roughness coefficients for gravel and cobble surfaces. *Journal of Irrigation and Drainage Engineering* **118**, 104–12.

Gilluly, J. 1937. Physiography of the Ajo region, Arizona. *Bulletin of the Geological Society of America* **48**, 323–48.

Govers, G. 1990. Empirical relationships for the transport capacity of overland flow. *International Association of Hydrological Sciences Publication* **189**, 45–63.

Govers, G. and G. Rauws 1986. Transporting capacity of overland flow on plane and on irregular beds. *Earth Surface Processes and Landforms* **11**, 515–24.

Guy, B.T., W.T. Dickinson and R.P. Rudra 1987. The roles of rainfall and runoff in the sediment transport capacity of interrill flow. *Transactions of the American Society of Agricultural Engineers* **30**, 1378–86.

Guzetti, F. 1991. Debris-flow phenomena in the central Apennines of Italy. *Terra Nova* **3**, 619–27.

Haff, P.K. 1986. A physical picture of kinetic granular fluids. *Journal of Rheology* **30**, 931–48.

Hampton, M.A. 1972. The role of subaqueous debris flow in generating turbidity currents. *Journal of Sedimentary Petrology* **42**, 775–93.

Hampton, M.A. 1975. Competence of fine-grained debris flows. *Journal of Sedimentary Petrology* **45**, 834–44.

Hampton, M.A. 1979. Buoyancy in debris flows. *Journal of Sedimentary Petrology* **49**, 753–8.

Hartley, D.M. 1987. Simplified process model for water sediment yield from single storms. Part I – Model formulation. *Transactions of the American Society of Agricultural Engineers* **30**, 710–17.

Hawkins, R.H. and T.W. Cundy 1987. Steady-state analysis of infiltration and overland flow for spatially-varied hillslopes. *Water Resources Bulletin* **23**, 215–16.

Hooke, R. Le B. 1987. Mass movement in semi-arid environments and the morphology of alluvial fans. In

Slope stability, M.G. Anderson and K.S. Richards (eds), 505–29. New York: Wiley.

Horton, R.E. 1933. The role of infiltration in the hydrologic cycle. *Transactions of the American Geophysical Union* **14**, 446–60.

Howard, A.D. and C.F. McLane 1988. Erosion of cohesionless sediment by groundwater seepage. *Water Resources Research* **24**, 1659–74.

Hui, K. and P.K. Haff 1986. Kinetic grain flow in a vertical channel. *International Journal of Multiphase Flow* **12**, 289–98.

Iverson, R.M. 1980. Processes of accelerated pluvial erosion on desert hillslopes modified by vehicular traffic. *Earth Surface Processes* **5**, 369–88.

Iverson, R.M. 1985. A constitutive equation for mass-movement behavior. *Journal of Geology* **93**, 143–60.

Iverson, R.M. 1986. Dynamics of slow landslides: a theory for time-dependent behavior. In *Hillslope processes*, A.D. Abrahams (ed.), 297–317. Boston: Allen & Unwin.

Iverson, R.M. and R.P. Denlinger 1987. The physics of debris flows – a conceptual assessment. *International Association of Scientific Hydrology Publication* 165, 155–65.

Iverson, R.M. and LaHusen, R.G. 1989. Dynamic pore-pressure fluctuations in rapidly shearing granular materials. *Science* **246**, 796–9.

Iverson, R.M. and J.J. Major 1986. Groundwater seepage vectors and the potential for hillslope failure and debris flow mobilization. *Water Resources Research* **22**, 1543–8.

Iverson, R.M. and M.E. Reid 1992. Gravity-driven groundwater flow and slope failure potential 1. Elastic effective-stress model. *Water Resources Research* **28**, 925–38.

Janda, R.J., K.M. Scott, K.M. Nolan and H.A. Martinson 1981. Lahar movement, effects and deposits. In *The 1980 eruptions of Mount St. Helens, Washington*, P.W. Lipmann and D.R. Mullineaux (eds), 461–78. U.S. Geological Survey Professional Paper 1250.

Johnson, A.M. 1965. A model for debris flow. Unpublished Ph.D. dissertation. State College, Pennsylvania: Pennsylvania State University.

Johnson, A.M. 1970. *Physical processes in geology*. San Francisco: Freeman & Cooper.

Johnson, A.M. and P.H. Rahn 1970. Mobilization of debris flows. *Zeitschrift für Geomorphologie* **9**, 168–86.

Johnson, A.M. and J.R. Rodine 1984. Debris flow. In *Slope instability*, D. Brunsden and D.B. Prior (eds), 257–361. New York: Wiley.

Johnson, C.W. and W.H. Blackburn 1989. Factors contributing to sagebrush rangeland soil loss. *Transactions of the American Society of Agricultural Engineers* **32**, 155–60.

Johnson, C.W. and N.D. Gordon 1988. Runoff and erosion from rainfall simulator plots on sagebrush rangeland. *Transactions of the American Society of Agricultural Engineers* **31**, 421–7.

Jung, L. 1960. The influence of the stone cover on runoff and erosion on slate soils. *International Association of Scientific Hydrology Publication* 53, 143–53.

Keefer, D.K. and A.M. Johnson 1983. Earthflows: morphology, mobilization and movement. *U.S. Geological Survey Professional Paper* 1264.

Kesel, R.H. 1977. Some aspects of the geomorphology of inselbergs in central Arizona, USA. *Zeitschrift für Geomorphologie* **21**, 120–46.

Kincaid, D.R., J.L. Gardner and H.A. Schreiber 1964. Soil and vegetation parameters affecting infiltration under semiarid conditions. *International Association of Scientific Hydrology Publication* 65, 440–53.

Kincaid, D.R., H.B. Osborn and J.L. Gardner 1966. Use of unit-source watersheds for hydrologic investigations in the semiarid Southwest. *Water Resources Research* **2**, 381–92.

Kinnell, P.I.A. 1991. The effect of flow depth on sediment transport induced by raindrops impacting shallow flows. *Transactions of the American Society of Agricultural Engineers* **34**, 161–8.

Kirkby, A. and M.J. Kirkby 1974. Surface wash at the semi-arid break in slope. *Zeitschrift für Geomorphologie Supplement Band* **21**, 151–76.

Kirkby, M.J. 1969. Erosion by water on hillslopes. In *Water, earth and man*, R.J. Chorley (ed.) 229–38. London: Methuen.

Kirkby, M.J. and I. Statham 1976. Surface stone movement and scree formation. *Journal of Geology* **83**, 349–62.

Kochel, R.C., A.D. Howard and C. McLane 1985. Channel networks developed by groundwater sapping in fine-grained sediments: analogs to some Martian valleys. In *Models in geomorphology*, M.J. Woldenberg (ed.), 313–41. Boston: Allen & Unwin.

Komura, S. 1976. Hydraulics of slope erosion by overland flow. *Journal of the Hydraulics Division, Proceedings of the American Society of Civil Engineers* **102**, 1573–86.

Kotarba, A. 1980. Splash transport in the steppe zone of Mongolia. *Zeitschrift für Geomorphologie Supplement Band* **35**, 92–102.

Laird, J.R. and M.D. Harvey 1986. Complex-response of a chaparral drainage basin to fire. *International Association of Scientific Hydrology Publication* 159, 165–83.

Lattanzi, A.R., L.D. Meyer and M.F. Baumgardner 1974. Influences of mulch rate and slope steepness on interrill erosion. *Soil Science Society of America Proceedings* **38**, 946–50.

Lavee, H. and J. Poesen 1991. Overland flow generation and continuity on stone-covered soil surfaces. *Hydrological Processes* **5**, 345–60.

Lavee, H., M. Wieder and S. Pariente 1989. Pedogenic indicators of subsurface flow on Judean desert hillslopes. *Earth Surface Processes and Landforms* **14**, 545–55.

Lawson, A.C. 1915. The epigene profiles of the desert. *University of California Publications, Bulletin of the Department of Geology* **9**(3), 23–48.

Lehmann, O. 1933. Morphologishe Theorie der Viervitterung von Steinschlagwande. *Viertel Jahrschaft der Naturforschenden Gesellschaft im Zürich*, **78**, 83–126.

Liebenow, A.M., W.J. Elliott, J.M. Laflen and K.D. Kohl 1990. Interrill erodibility: collection and analysis of data from cropland soils. *Transactions of the American Society of Agricultural Engineers* **33**, 1882–8.

Lowe, D.R. 1976. Grain flow and grain flow deposits. *Journal of Sedimentary Petrology* **46**, 188–99.

Lun, C.K.K., S.B. Savage, D.J. Jeffrey and N. Chipurniy 1984. Kinetic theories of granular flow: inelastic particles in a Couette flow and slightly inelastic particles in a general flow-field. *Journal of Fluid Mechanics* **140**, 223–56.

Lustig, L.K. 1965. Clastic sedimentation in Deep Springs Valley, California. *U.S. Geological Survey Professional Paper* 352-F, 131–92.

Lyford, F.P. and H.K. Qashu 1969. Infiltration rates as

affected by desert vegetation. *Water Resources Research* **5**, 1373–6.

Mabbutt, J.A. 1966. Mantle-controlled planation of pediments. *American Journal of Science* **264**, 78–91.

Mabbutt, J.A. 1977. *Desert landforms*. Canberra: Australian National University Press.

Major, J.J. and T.C. Pierson 1992. Debris flow rheology: experimental analysis of fine-grained slurries. *Water Resources Research* **28**, 841–57.

Martinez, M., L.J. Lane and M.M. Fogel 1979. Experimental investigation of soil detachment by raindrop impacts. *Proceedings of the Rainfall Simulation Workshop, Tucson, Arizona, March 7–9, 1979*. USDA Agricultural Reviews and Manuals ARM-W-10, 153–5. Oakland, CA: U.S. Department of Agriculture.

McDonnell, J.J. 1990. The influence of macropores on debris flow initiation. *Quarterly Journal of Engineering Geology* **23**, 325–31.

McTigue, D.F. 1979. A nonlinear continuum model for flowing granular materials. Unpublished Ph.D. dissertation, 165 pp. Stanford: Stanford University.

Mein, R.G. and C.L. Larson 1973. Modeling infiltration during steady rain. *Water Resources Research* **9**, 384–94.

Melosh, H.J. 1987. The mechanics of large rock avalanches. In *Debris flows/avalanches: processes, recognition and mitigation*, J.E. Costa and G.F. Weiczorek (eds), 41–9. Reviews in Engineering Geology 7. Boulder: Geological Society of America.

Melton, M.A. 1965. Debris-covered hillslopes of the southern Arizona desert – consideration of their stability and sediment contribution. *Journal of Geology* **73**, 715–29.

Meyer, L.D. 1981. How rainfall intensity affects interrill erosion. *Transactions of the American Society of Agricultural Engineers* **24**, 1472–5.

Meyer, L.D. 1986. Erosion processes and sediment properties for agricultural cropland. In *Hillslope processes*, A.D. Abrahams (ed.), 55–76. Boston: Allen & Unwin.

Meyer, L.D. and W.H. Wischmeier 1969. Mathematical simulation of the process of soil erosion by water. *Transactions of the American Society of Agricultural Engineers* **12**, 754–8, 762.

Meyer, L.D., G.R. Foster and M.J.M. Romkens 1975. Source of soil eroded by water from upland slopes. In *Present and prospective technology for predicting sediment yields and sources*, U.S. Agricultural Research Service Report ARS-S-40, 177–89, Oxford, MS: U.S. Department of Agriculture.

Middleton, G.V. 1970. Experimental studies related to the problems of flysch sedimentation. *Geological Society of Canada Special Paper* 7, 253–72.

Middleton, G.V. and M.A. Hampton 1976. Subaqueous sediment transport and deposition by sediment gravity flows. In *Marine sediment transport and environmental management*, D.D. Stanly and J.P. Swift (eds), 197–218. New York: Wiley.

Moeyersons, J. 1975. An experimental study of pluvial processes on granite gruss. *Catena* **2**, 289–308.

Moore, I.D. 1981. Effect of surface sealing on infiltration. *Transactions of the American Society of Agricultural Engineers* **24**, 1546–52, 1561.

Moore, I.D. and G.J. Burch 1986. Sediment transport capacity of sheet and rill flow: application of unit stream power theory. *Water Resources Research* **22**, 1350–60.

Moore, I.D. and G.R. Foster 1990. Hydraulics and overland flow. In *Process studies in hillslope hydrology*, M.G. Anderson and T.P. Burt (eds), 215–54. Chichester: Wiley.

Morgan, R.P.C. 1978. Field studies of rainsplash erosion. *Earth Surface Processes and Landforms* **3**, 295–9.

Morton, D.M. and R.H. Campbell 1973. Mudflows at Wrightwood, southern California, spring 1969. *Quarterly Journal of Engineering Geology* **7**, 377–84.

Moss, A.J. 1980. Thin-flow transportation of solids in arid and non-arid areas: a comparison of processes. The hydrology of areas of low precipitation. *International Association of Hydrological Sciences Publication* 128, 435–45.

Mutchler, C.K. and C.L. Larson 1971. Splash amounts from waterdrop impact on a smooth surface. *Water Resources Research* **7**, 195–200.

Nearing, M.A., G.R. Foster, L.J. Lane and S.C. Finkner 1989. A process based soil erosion model for USDA-Water Erosion Prediction Project technology. *Transactions of the American Society of Agricultural Engineers* **32**, 1587–93.

Nilsen, T.H., F.A. Taylor and R.M. Dean 1976. Natural conditions that control landsliding in the San Francisco Bay Region – an analysis based on data from the 1968–69 and 1972–73 rainy seasons. *U.S. Geological Survey Bulletin* 1424.

Oberlander, T.M. 1972. Morphogenesis of granite boulder slopes in the Mojave Desert, California. *Journal of Geology* **80**, 1–20.

Oberlander, T.M. 1989. Slope and pediment systems. In *Arid zone geomorphology*, D.S.G. Thomas (ed.), 56–84. London: Belhaven Press.

O'Brien J.S. and P.Y. Julien 1988. Laboratory analysis of mudflow properties. *Journal of Hydraulic Engineering* **114**, 877–87.

Palmer, R.S. 1963. The influence of a thin water layer on waterdrop impact forces. *International Association of Scientific Hydrology Publication* 64, 141–8.

Park, S.W., J.K. Mitchell and G.D. Bubenzer 1982. Splash erosion modeling: physical analyses. *Transactions of the American Society of Agricultural Engineers* **25**, 357–61.

Parsons, A.J. 1987. The role of slope and sediment characteristics in the initiation and development of rills. In *Processes and measurement of erosion*, A. Godard (ed.), 211–20. Paris: Centre National de la Recherche Scientifique.

Parsons, A.J. and A.D. Abrahams 1984. Mountain mass denudation and piedmont formation in the Mojave and Sonoran Deserts. *American Journal of Science* **284**, 255–71.

Parsons, A.J. and A.D. Abrahams 1987. Gradient–particle size relations on quartz monzonite debris slopes in the Mojave Desert. *Journal of Geology* **95**, 423–32.

Parsons, A.J. and A.D. Abrahams 1992. Controls on sediment removal by interrill overland flow on semi-arid hillslopes. *Israel Journal of Earth Sciences*, **41**, 177–88.

Parsons, A.J., A.D. Abrahams and S.-H. Luk 1990. Hydraulics of interrill overland flow on a semi-arid hillslope, southern Arizona. *Journal of Hydrology* **117**, 255–73.

Parsons, A.J., A.D. Abrahams and S.-H. Luk 1991a. Size characteristics of sediment in interrill overland flow on a semiarid hillslope, southern Arizona. *Earth Surface Processes and Landforms* **16**, 143–52.

Parsons, A.J., A.D. Abrahams and J.R. Simanton 1991b. Microtopography and soil-surface materials on semi-arid

piedmont hillslopes, southern Arizona, *Journal of Arid Environments* **22**, 107–15.

Phillips, C.J. and T.R.H. Davies 1991. Determining rheological parameters of debris flow material. *Geomorphology* **4**, 101–10.

Pierson, T.C. 1980. Erosion and deposition by debris flows at Mount Thomas, North Canterbury, New Zealand. *Earth Surface Processes* **5**, 227–47.

Pierson, T.C. 1981. Dominant particle support mechanisms in debris flow at Mount Thomas, New Zealand, and implications for flow mobility. *Sedimentology* **28**, 49–60.

Pierson, T.C. 1986. Flow behavior of channelized debris flows, Mount St. Helens, Washington. In *Hillslope processes*, A.D. Abrahams (ed.), 269–96. Boston: Allen & Unwin.

Pierson, T.C. and J.E. Costa 1987. A rheologic classification of subaerial sediment-water flows. In *Debris flows/avalanches: processes, recognition and mitigation*, J.E. Costa and G.F. Weiczorek (eds), 1–12. Reviews in Engineering Geology 7. Boulder: Geological Society of America.

Poesen, J. 1985. An improved splash transport model. *Zeitschrift für Geomorphologie* **29**, 193–211.

Poesen, J. 1986. Field measurements of splash erosion to validate a splash transport model. *Zeitschrift für Geomorphologie Supplement Band* **58**, 81–91.

Poesen, J. 1990. Erosion process research in relation to soil erodibility and some implications for improving soil quality. In *Soil degradation and rehabilitation in Mediterranean environmental conditions*, J. Albaladejo, M.A. Stocking and E. Diaz (eds), 159–70. Madrid: Consejo Superior de Investigaciones Cientificas.

Poesen, J. and H. Lavee 1991. Effects of size and incorporation of synthetic mulch on runoff and sediment yield from interrills in a laboratory study with simulated rainfall. *Soil and Tillage Research* **21**, 209–23.

Poesen, J. and J. Savat 1981. Detachment and transportation of loose sediments by raindrop splash. Part II. Detachability and transportability measurements. *Catena* **8**, 19–41.

Poesen, J., F. Ingelmo-Sanchez and H. Mucher 1990. The hydrological response of soil surfaces to rainfall as affected by cover and position of rock fragments in the top layer. *Earth Surface Processes and Landforms* **15**, 653–71.

Quansah, C. 1985. Rate of soil detachment by overland flow, with and without rain, and its relationship with discharge, slope steepness, and soil type. In *Soil erosion and conservation*, S.A. El-Swaify, W.C. Moldenhauer and A. Lo (eds), 406–23. Ankeny, IA: Soil Conservation Society of America.

Rahn, P.H. 1966. Inselbergs and nickpoints in southwestern Arizona. *Zeitschrift für Geomorphologie* **10**, 215–24.

Rauws, G. 1987. The initiation of rills on plane beds of non-cohesive sediments. *Catena Supplement* **8**, 107–18.

Reid, I. and L.E. Frostick 1986. Slope processes, sediment derivation and landform evolution in a rift valley basin, northern Kenya. In *Sedimentation in the African rifts*, L.E. Frostick *et al.* (eds), 99–111, Geological Society Special Publication 25.

Reid, M.E. and R.M. Iverson 1992. Gravity-driven groundwater flow and slope failure potential 2. Effects of slope morphology, material properties and hydraulic heterogeneity. *Water Resources Research* **28**, 939–50.

Rice, R.M. 1982. Sedimentation in the chaparral: how do you handle unusual events? In *Sediment budgets and routing in forested drainage basins*, F.J. Swanson, R.J. Janda, T. Dunne and D.N. Swanson (eds), 39–49. General Technical Report PNW-141, Portland, OR: USDA Forest Service.

Rice, R.M., E.S. Corbett and R.G. Bailey 1969. Soil slips related to vegetation, topography, and soil in southern California. *Water Resources Research* **5**, 647–59.

Richards, L.A. 1931. Capillary conduction of liquids through porous mediums. *Physics* **1**, 318–33.

Rodine, J.D. and A.M. Johnson 1976. The ability of debris, heavily weighted with coarse clastic material, to flow on gentle slopes. *Sedimentology* **23**, 213–34.

Roels, J.M. 1984a. Surface runoff and sediment yield in the Ardeche rangelands. *Earth Surface Processes and Landforms* **9**, 371–81.

Roels, J.M. 1984b. Modelling soil losses from the Ardeche rangelands. *Catena* **11**, 377–89.

Roels, J.M. 1984c. Flow resistance in concentrated overland flow on rough slope surfaces. *Earth Surface Processes and Landforms* **9**, 541–51.

Romkens, M.J.M., S.N. Prasad and F.D. Whisler 1990. Surface sealing and infiltration. In *Process studies in hillslope hydrology*, M.G. Anderson and T.P. Burt (eds), 127–72. Chichester: Wiley.

Sadeghian, M.R. and J.K. Mitchell 1990. Hydraulics of micro-braided channels: resistance to flow on tilled soils. *Transactions of the American Society of Agricultural Engineers* **33**, 458–68.

Saunders, I. and A. Young 1983. Rate of surface processes on slopes, slope retreat and denudation. *Earth Surface Processes and Landforms* **8**, 473–501.

Savage, S.B. 1979. Gravity flow of cohesionless granular materials in chutes and channels. *Journal of Fluid Mechanics* **92**, 53–96.

Savage, S.B. 1984. The mechanics of rapid granular flows. *Advances in Applied Mechanics* **24**, 289–366.

Savage, S.B. 1989. Flow of granular materials. In *Theoretical and applied mechanics*, P. Germain, M. Piau and D. Caillerie (eds), 241–66. Amsterdam: Elsevier.

Savat, J. 1977. The hydraulics of sheet flow on a smooth surface and the effect of simulated rainfall. *Earth Surface Processes* **2**, 125–40.

Savat, J. and J. De Ploey 1982. Sheetwash and rill development by surface flow. In *Badland geomorphology and piping*, R. Bryan and A. Yair (eds), 113–26. Norwich: Geo Books.

Savat, J. and J. Poesen 1981. Detachment and transportation of loose sediments by raindrop splash. Part I. The calculation of absolute data on detachability and transportability. *Catena* **8**, 1–17.

Schultz, J.P., A.R. Jarrett and J.R. Hoover 1985. Detachment and splash of a cohesive soil by rainfall. *Transactions of the American Society of Agricultural Engineers* **28**, 1878–84.

Scott, K.M. 1971. Origin and sedimentology of 1969 debris flows near Glendora, California. *U.S. Geological Survey Professional Paper* 422-M.

Scott, K.M. and R.P. Williams 1978. Erosion and sediment yields in the Transverse Ranges, southern California. *U.S. Geological Survey Professional Paper* 1030.

Seginer, I., J. Morin and A. Shachori 1962. Runoff and erosion studies in a mountaneous Terra Rosa region in

Israel. *Bulletin of the International Association of Scientific Hydrology* **7**(4), 79–92.

Selby, M.J. 1980. A rock mass strength classification for geomorphic purposes: with tests from Antarctica and New Zealand. *Zeitschrift für Geomorphologie* **24**, 31–51.

Selby, M.J. 1982a. Controls on the stability and inclinations of hillslopes formed on hard rock. *Earth Surface Processes and Landforms* **7**, 449–67.

Selby, M.J. 1982b. *Hillslope materials and processes*. Oxford: Oxford University Press.

Sharma, M.L., G.A. Gander and C.G. Hunt 1980. Spatial variability of infiltration in a watershed. *Journal of Hydrology* **45**, 101–22.

Shen, H.W. and R.-M. Li 1973. Rainfall effect on sheet flow over smooth surface. *Journal of the Hydraulics Division, Proceedings of the American Society of Civil Engineers* **99**, 771–92.

Sidle, R.C., A.J. Pearce and C. O'Loughlin 1985. *Hillslope stability and land use*. American Geophysical Union Water Resources Monograph 11.

Simanton, J.R. and K.G. Renard 1982. Seasonal change in infiltration and erosion from USLE plots in southeastern Arizona. *Hydrology and Water Resources in Arizona and the Southwest* **12**, 37–46.

Simanton, J.R., K.G. Renard and N.G. Sutter 1973. *Procedure for identifying parameters affecting storm runoff volumes in a semiarid environment*. U.S. Agricultural Research Service Report ARS-W-1.

Simanton, J.R., E. Rawitz and E. Shirley 1984. Effects of rock fragments on erosion of semiarid rangeland soils. *Soil Science Society of America Special Publication* 13, 65–72.

Simanton, J.R., K.G. Renard, L.J. Lane and C.E. Christiansen 1993. Spatial distribution of surface rock fragments along catenas in a semiarid area. *Catena Supplement* **24**, in press.

Smith, R.E. 1972. The infiltration envelope: results from a theoretical infiltrometer. *Journal of Hydrology* **17**, 1–21.

Smith, R.E. and R.H.B. Hebbert 1979. A Monte Carlo analysis of the hydrologic effects of spatial variability of infiltration. *Water Resources Research* **15**, 419–29.

Smith, R.E. and D.A. Woolhiser 1971. *Mathematical simulation of infiltrating watersheds*. Hydrology Paper 47, Colorado State University, Ft Collins.

Statham, I. and S.C. Francis 1986. Influence of scree accumulation and weathering on the development of steep mountain slopes. In *Hillslope processes*, A.D. Abrahams (ed.), 245–67. Boston: Allen & Unwin.

Strahler, A.N. 1950. Equilibrium theory of erosional slopes, approached by frequency distribution analysis. *American Journal of Science* **248**, 673–96, 800–14.

Takahashi, T. 1978. Mechanical characteristics of debris flows. *Journal of the Hydraulics Division, Proceedings of the American Society of Civil Engineers* **104**, 1153–69.

Takahashi, T. 1980. Debris flows on prismatic channel. *Journal of the Hydraulics Division, Proceedings of the American Society of Civil Engineers* **106**, 381–96.

Takahashi, T. 1981. Debris flows. *Annual Reviews of Fluid Mechanics* **13**, 57–77.

Thomas, D.S.G. 1988. The biogeomorphology of arid and semi-arid environments. In *Biogeomorphology*, H.A. Viles (ed.), 193–221. Oxford: Blackwell.

Torri, D., M. Sfalanga and M. Del Sette 1987. Splash detachment: runoff depth and soil cohesion. *Catena* **14**, 149–55.

Tromble, J.M. 1976. Semiarid rangeland treatment and surface runoff. *Journal of Range Management* **29**, 215–5.

Tromble, J.M., K.G. Renard and A.P. Thatcher 1974. Infiltration for three rangeland soil-vegetation complexes. *Journal of Range Management* **27**, 318–21.

Twidale, C.R. 1962. Steepened margins of inselbergs from northwestern Eyre Peninsula, South Australia. *Zeitschrift für Geomorphologie* **6**, 51–9.

Twidale, C.R. 1967. Origin of the piedmont angle as evidenced in South Australia. *Journal of Geology* **75**, 393–411.

Van Liew, M.W. and K.E. Saxton 1983. Slope steepness and incorporated residue effects on rill erosion. *Transactions of the American Society of Agricultural Engineers* **26**, 1738–43.

Watson, D.A. and J.M. Laflen 1986. Soil strength, slope, and rainfall intensity effects on interrill erosion. *Transactions of the American Society of Agricultural Engineers* **29**, 98–102.

Weiczorek, G.F. 1987. Effect of rainfall intensity and duration on debris flow in central Santa Cruz Mountains, California. In *Debris flows/avalanches: processes, recognition and mitigation*, J.E. Costa and G.F. Weiczorek (eds), 93–104. Reviews in Engineering Geology 7. Boulder: Geological Society of America.

Wells, W.G. 1981. Some effects of brush fires on erosion processes in southern California. *International Association of Scientific Hydrology Publication* 165, 305–42.

Wells, W.G. 1987. The effects of fire on the generation of debris flows in southern California. In *Debris flows/avalanches: processes, recognition and mitigation*, J.E. Costa and G.F. Weiczorek (eds), 105–14. Reviews in Engineering Geology 7. Boulder: Geological Society of America.

Wells, W.G., P.M. Wohlgemuth and A.G. Campbell 1987. Post-fire sediment movement by debris flows in the Santa Ynez Mountains, California. *International Association of Scientific Hydrology Publication* 165, 275–6.

Wieder, M., A. Yair and A. Arzi 1985. Caternary soil relationships on arid hillslopes. *Catena Supplement* **6**, 41–57.

Wilcox, B.P., M.K. Wood and J.M. Tromble 1988. Factors influencing infiltrability of semiarid mountain slopes. *Journal of Range Management* **41**, 197–206.

Wohl, E.E. and P.P. Pearthree 1991. Debris flow as geomorphic agents in the Huachuca Mountains of southeastern Arizona. *Geomorphology* **4**, 273–92.

Wohlgemuth, P.M. 1986. Spatial and temporal distribution of surface sediment transport in southern California steeplands. In *Proceedings of the chaparral ecosystems research conference, Santa Barbara, California, May 16–17, 1985*, J.J. DeVries (ed.), 29–32. Report No. 62, Davis, CA: Water Resources Center, University of California.

Woodruff, C.M. 1947. Erosion in relation to rainfall, crop cover, and slope on a greenhouse plot. *Soil Science Society of America Proceedings* **12**, 475–8.

Woolhiser, D.A., R.E. Smith and D.C. Goodrich 1990. *KINEROS, a kinematic runoff and erosion model: documentation and user manual*. U.S. Department of Agriculture, Agriculture Research Service, ARS-77.

Yair, A. 1983. Hillslope hydrology water harvesting and areal distribution of some ancient agricultural systems in

the northern Negev Desert. *Journal of Arid Environments* **6**, 283–301.

Yair, A. 1987. Environmental effects of loess penetration into the northern Negev Desert. *Journal of Arid Environments* **13**, 9–24.

Yair, A. 1990a. Runoff generation in a sandy area – the Nizzana Sands, western Negev, Israel. *Earth Surface Processes and Landforms* **15**, 597–609.

Yair, A. 1990b. The role of topography and surface cover upon soil formation along hillslopes in arid climates. *Geomorphology* **3**, 287–99.

Yair, A. and M. Klein 1973. The influence of surface properties on flow and erosion processes on debris covered slopes in an arid area. *Catena* **1**, 1–18.

Yair, A. and H. Lavee 1976. Runoff generative process and runoff yield from arid talus mantled slopes. *Earth Surface Processes* **1**, 235–47.

Yair, A. and H. Lavee 1977. Trends of sediment removal from arid scree slopes under simulated rainstorm experiments. *Hydrological Sciences Bulletin* **22**, 379–91.

Yair, A. and H. Lavee 1981. An investigation of source areas of sediment and sediment transport by overland flow along arid hillslopes. *International Association of Hydrological Sciences Publication* 133, 433–46.

Yair, A. and H. Lavee 1985. Runoff generation in arid and semiarid zones. In *Hydrological forecasting*, M.G. Anderson and T.P. Burt (eds), 183–220. New York: Wiley.

Yair, A. and J. Rutin 1981. Some aspects of the regional variation in the amount of available sediment produced by isopods and porcupines, northern Negev, Israel. *Earth Surface Processes and Landforms* **6**, 221–34.

Yair, A. and M. Shachak 1987. Studies in watershed ecology of an arid area. In *Progress in desert research*, L. Berkofsky and M.G. Wurtele (eds), 145–93. Totowa, NJ: Rowman and Littlefield.

Yang, C.T. 1972. Unit stream power and sediment transport. *Journal of the Hydraulics Division, Proceedings of the American Society of Civil Engineers* **98**, 1805–25.

Yano, K. and A. Daido 1965. Fundamental study on mud flow. *Bulletin of the Disaster Prevention Research Institute, Kyoto* **14**, 69–83.

Yen, B.-C. 1965. Discussion of 'Large-scale roughness in open channel flow'. *Journal of the Hydraulics Division, Proceedings of the American Society of Civil Engineers* **91**(5), 257–62.

Yoon, Y.N. and H.G. Wenzel 1971. Mechanics of sheet flow under simulated rainfall. *Journal of the Hydraulics Division, Proceedings of the American Society of Civil Engineers* **97**, 1367–86.

Young, A. 1972. *Slopes*. London: Longman.

Young, A. and I. Saunders 1986. Rates of surface processes and denudation. In *Hillslope processes*, A.D. Abrahams (ed.), 3–27. Boston: Allen & Unwin.

Young, R.A. and J.L. Wiersma 1973. The role of rainfall impact in soil detachment and transport. *Water Resources Research* **9**, 1629–36.

BADLANDS

9

Alan D. Howard

BADLAND REGOLITH AND PROCESSES

Badlands have fascinated geomorphologists for the same reasons that they inhibit agricultural use: lack of vegetation, steep slopes, high drainage density, shallow to non-existent regolith, and rapid erosion rates. Badlands appear to offer in a miniature spatial scale and a shortened temporal scale many of the processes and landforms exhibited by more normal fluvial landscapes, including a variety of slope forms, bedrock or alluvium-floored rills and washes, and flat alluvial expanses similar to large-scale pediments. The often (but not universally) rapid landform evolution provides the prospect of direct observational coupling of process and landform evolution in both natural and man-induced badlands. However, Campbell (1989) and Campbell and Honsaker (1982) caution about problems of scaling between processes on badland slopes and channels to larger landforms. Furthermore, although badland slopes are commonly quite regular in appearance (Fig. 9.1), recent studies have demonstrated that weathering, mass wasting, and water erosional processes on badland slopes exhibit complex spatial and temporal variability, and that the weathering and erosional processes are largely hidden from direct observation in cracks and micropipes (Bryan *et al.* 1978, Yair *et al.* 1980).

This chapter will emphasize the relationship between process and form in badland landscapes and the long-term evolution of badland landscapes through both descriptive and quantitative modelling. More general reviews of badlands and badland processes are provided by Campbell (1989) and Bryan and Yair (1982a), including discussion of the climatic, geologic, and geographic setting of badlands, sediment yields, host rock and regolith variations among badlands, field measurements of processes, and badland gullies and piping.

AN EXAMPLE: BADLANDS IN THE HENRY MOUNTAINS AREA, UTAH

Shales of Jurassic and Cretaceous age exposed in the vicinity of the Henry Mountains, Utah, have in places been sculpted into dramatic badlands. The climate in the desert areas at about 1500 m above mean sea level is arid, with about 125 mm of annual precipitation, most of which occurs as summer thunderstorms. These badlands provide premier examples of the erosional conditions favouring badlands, badland slope form and process, relationship between fluvial and slope processes, and variations of badland form with rock type. In particular, the great thickness and uniform lithology of the Upper Cretaceous Mancos Shale (Hunt 1953) results in an unusual regularity of slope form and process (Fig. 9.1), first described by Gilbert (1880). Badlands developed in this area on the Mancos Shale, the Morrison Formation, and the Summerville Formation will be used here as examples. These badlands are discussed more fully by Howard (1970).

BADLAND REGOLITH

Badlands generally have very thin regoliths in arid regions, ranging from about 30 cm to essentially unweathered bedrock. Many badland areas share a similar regolith profile. The top 1 to 5 cm is a surface layer exhibiting desiccation cracks when dry. This surface layer is compact with narrow polygonal cracking in the case of shales with modest shrink–swell (<25%) behaviour, such as the Mancos Shale badlands in Utah (Fig. 9.1), the Brule Formation badlands in South Dakota (Schumm 1956a, b), and portions of the Dinosaur Badlands, Canada (Bryan *et al.* 1978, 1984, Hodges and Bryan 1982). With higher shrink–swell behaviour the surface layer is broken into irregular, loose 'popcorn' fragments with large intervening voids, as exemplified in badlands on the

Geomorphology of Desert Environments. Edited by Athol D. Abrahams and Anthony J. Parsons. Published in 1994 by Chapman & Hall, London. ISBN 978-94-015-8256-8

Figure 9.1 Badlands in Mancos Shale, near the Henry Mountains, Utah. Note linearity of slope profile and narrowness of divides.

Chadron Formation in South Dakota, the Morrison (Fig. 9.2) and Chinle Formations in Utah, and portions of the Dinosaur Badlands, Canada. The surface layer may be thicker (≥10 cm) in such cases. Although the surface layer may contain a few partially weathered fragments of shale, vein fillings, nodules, etc., it is primarily composed of disaggregated and remoulded shale, silt, and sand weathered from the shale which is leached of highly soluble components (particularly when derived from marine shales such as the Mancos Shale: Laronne 1982).

Beneath the surface layer is a sublayer (crust) averaging about 5 to 10 cm in thickness which may range from a dense, amorphous crust (Hodges and Bryan 1982, Gerits *et al.* 1987) to a loose, granular layer (Howard 1970, Schumm and Lusby 1963). Part of the apparent variability of surface layer and crust may be due to differences among researchers in locating the division between these units. Below the crust there occurs a transitional 'shard layer' ranging from 10 to 40 cm in thickness consisting of partially disaggregated and weathered shale chips grading to firm, unweathered shale.

However, there is considerable variability in badland regoliths. Well-cemented sandstone layers outcrop as bare rock, often creating ledges or caprocks. Slightly cemented sand layers (often with $CaCO_3$ cement) generally form steep slopes with regolith 1 to 5 mm thick or less (Hodges and Bryan 1982, Bowyer-Bower and Bryan 1986, Gerits *et al.* 1987). Carman (1958) described a regolith in fluted badlands in a clay matrix-supported conglomerate com-

Figure 9.2 Rounded badland slopes in Morrison Formation.

posed of a hard veneer of sandy clay 1 to 15 cm thick over a softer interior layer and a hard core. Badlands on shaly sandstones in the Summerville Formation have a non-cohesive surface layer of sand grains and shale chips which grades fairly uniformly to unweathered bedrock within 10 to 20 cm. Some badland surfaces are cemented with a biological crust of algae or lichens (Yair *et al.* 1980, Finlayson *et al.* 1987). Badlands in marine shales, such as the Mancos Shale, may have salt recrystallization in the sublayers and local areas of salt surface crusts (Laronne 1982). Due to the frequent occurrence of rapid mass wasting on steep badland slopes, recently denuded areas have atypically thin regoliths with poor development of the surface layer.

Systematic variations in regolith properties may be associated with slope aspect. Churchill (1981), in a comparison of north- and south-facing slopes in Brule Formation Badlands (South Dakota), found the north-facing slopes to be more gently sloping, more densely rilled, with deeper regoliths, and characterized by infrequent mass-wasting involving much of the regolith (20 to 30 cm). By contrast, south-facing slopes have frequent shallow (3 to 10 cm thick) sloughing failures. Churchill suggested that slower evaporation promotes deeper infiltration on north-facing slopes. Yair *et al.* (1980) found north-facing slopes in the Zin badlands of the Negev Desert to have a rough, lichen-covered surface, a deeper regolith, few rills, and relatively high runoff and erosion. South-facing slopes are smoother, with greater runoff, frequent mudflows, and pipe development, but they experience less runoff erosion overall.

Weathering processes of badland regolith development involve relatively modest changes in mineralogy, since the source rocks are poorly lithified sedimentary rocks. Simple wetting may be sufficient to disaggregate the shale and disperse the clay minerals. For example, unweathered blocks of Morrison Formation smectitic shales will completely disaggregate and disperse within a few minutes to a few hours in just enough water to completely saturate the sample (this may be a considerable relative volume of water because of the pronounced swelling). Rapid slaking accompanies this disaggregation. The shallow regolith on these slopes testifies to the absorptive capacity and impermeability of the surface layers. On the other hand, samples of unweathered Mancos Shale, a marine shale with *illite* dominant, decompose more slowly, with less swelling and incomplete dispersion. A yellowish liquor of dissolved salts (mostly sodium and calcium sulphates: Laronne 1981, 1982) is produced, whose accumulation apparently inhibits further disintegration. Leaching of these solutes is apparently required for complete weathering, and salt concentrations decrease upwards within the regolith (Laronne 1982). Some clayey sandstones may have a calcite cementing which requires dissolution before erosion, and the regolith is only a few millimetres thick (Bowyer-Bower and Bryan 1986). On the other hand, marls composed of more than 50% calcite and gypsum may be essentially free from cementation. Consequently clay mineral dispersion is all that is required to form a disaggregated regolith (Imeson and Verstraten 1985, Finlayson *et al.* 1987). Some unconsolidated sediments require no weathering prior to entrainment by rainsplash and runoff, so that regoliths are absent or only seasonally present due to frost heaving (for example, the artificial Perth Amboy badlands studied by Schumm 1956a).

The physical and chemical properties of clay minerals, grain size distribution, density, and cementation affect the weathering by wetting and leaching, runoff characteristics, sediment and solute yields, and badland form. The properties of shales relevant to their erosional behaviour can be measured by a number of simple physico-chemical tests of cation-exchange capacity, solute extracts (concentration and chemistry), Atterberg (consistency) limits, vane shear strength, dispersion index, aggregate stability, and shrink–swell behaviour (Imeson *et al.* 1982, Hodges and Bryan 1982, Bryan *et al.* 1984, Gerits *et al.* 1987, Imeson and Verstraten 1988).

EROSIONAL PROCESSES ON BADLAND SLOPES

Discussion of slope erosional processes is conventionally divided into wash processes (runoff and rainsplash erosion) and mass-wasting (creep, sliding, and flowage). This discussion follows that division, although these processes are so interrelated and intergraded that such divisions are primarily for convenience.

Mass Wasting

The rounded slopes of the Morrison (Fig. 9.2), Chinle, and Chadron Formations have been attributed to the dominance of creep as a slope-forming process (Davis 1892, Schumm 1956b, Howard 1970). These formations contain clays with high dispersive and shrink–swell potential. The volume changes occurring during wetting together with the loss of bulk strength encourage downslope sag and creep of surface layers. Schumm (1963) found surface creep rates to be proportional to the sine of the slope

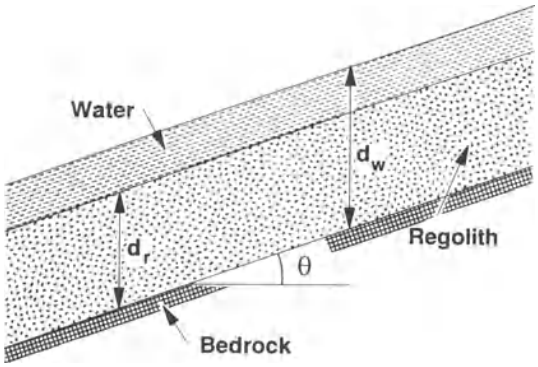

Figure 9.3 Definition of terms for infinite slope failure with water flowing parallel to the slope.

gradient for slope gradients less than 40° on Mancos Shale, and such a relationship is likely to be a good approximation to mass wasting rates for low slope gradients.

Many badland sideslopes are close to their maximum angle of stability, as long, narrow, shallow slips are common occurrences. Because these slopes are generally at angles of 40° or more, and failures occur during rainstorms, slope stability can be analysed by the well-known infinite slope model for saturated regolith and flow parallel to the slope (e.g. Lambe and Whitman 1969, pp. 352–6, Carson 1969, p. 87, Carson and Kirkby 1972, pp. 152–9). Figure 9.3 shows the definitions for an analysis similar to Lambe and Whitman's except that uniform surface flow is also allowed. Conditions for failure at a depth d_r below the surface are assumed to be approximated by a linear relationship

$$\tau_f = c + \sigma_e \tan\phi, \tag{9.1}$$

where τ_f is the shear stress on the failure plane, σ_e is the effective normal stress on the failure plane, c is the saturated cohesion, and ϕ is the saturated friction angle for the regolith material.

Based upon Figure 9.3 for the case when $d_w \geq d_r$ the shear and effective normal stresses on the potential failure plane are

$$\sigma_e = \rho_b d_r g \cos^2\theta \tag{9.2}$$

and

$$\tau = [\rho_t d_r + \rho_w(d_w - d_r)]g \sin\theta\cos\theta \tag{9.3}$$

where ρ_b and ρ_t are the buoyant and total densities of the regolith, respectively, ρ_w is the water density, g is the gravitational constant, θ is the slope angle, and d_w is the depth of water flow above the regolith surface. For the case when $d_w < d_r$

$$\sigma_e = [\rho_u(d_r - d_w) + \rho_b d_w]g\cos^2\theta \tag{9.4}$$

and

$$\tau = [\rho_u(d_r - d_w) + \rho_t d_w]g \sin\theta\cos\theta, \tag{9.5}$$

where ρ_u is the unsaturated unit weight of the regolith (which is likely to be very close to ρ_t).

Failure occurs when $\tau \geq \tau_f$. For the shallow badland regoliths only slight cohesion is necessary to permit slopes greater than 40° if water flow depths are small.

Wash Processes

Wash processes on badlands occur only during and immediately after rainstorms. If a rainstorm starts with a dry regolith (the usual case) much of the initial rainfall is absorbed by the regolith and initially penetrates deeply along cracks and between popcorn aggregates, where present. Runoff from badland slopes is delayed for several minutes after rainfall initiates; for example, Bryan *et al.* (1984) noted a delay of 10 to 15 minutes after initiation of sprinkling at a rate of 10 to 20 mm h^{-1}. The depth of wetting is limited either by absorption along crack and fissure edges or by ponding on top of the dense crust layer, where present (Hodges and Bryan 1982). Swelling of the regolith clays rapidly begins to close the cracks and gaps, so that flow is increasingly restricted to lateral flow in larger cracks and, in many cases, to micropipes developed near the crust–shard layer boundary (Hodges and Bryan 1982) (Fig. 9.4). The flow in the larger cracks, especially where appreciable flow is received from upslope, may be able to erode crack walls and keep pace with regolith swelling (Engelen 1973). Most of these cracks will form ephemeral rills, which are partly or wholly eradicated by continued swelling and subsequent drying and cracking of the surface layer. Sediment is added to the flow both by shear and dispersion of clay minerals, and the sediment load may range up to mudflow concentrations. Flow in the cracks and micropipes eventually feeds into rills or on to alluvial surfaces. Badland interflow has been compared to intergranular flow to drains (the rills) (Gerits *et al.* 1987, Imeson and Verstraten 1988) (Fig. 9.5). Through liquefaction of saturated, dispersed crust above the shard layer with accompanying runout, surface rills may initiate pipe formation and surface collapse in the zones of greatest depth of saturation between surface rills (Fig. 9.5).

Hodges and Bryan (1982) pointed out that in Dinosaur Badlands, Canada, runoff occurs more

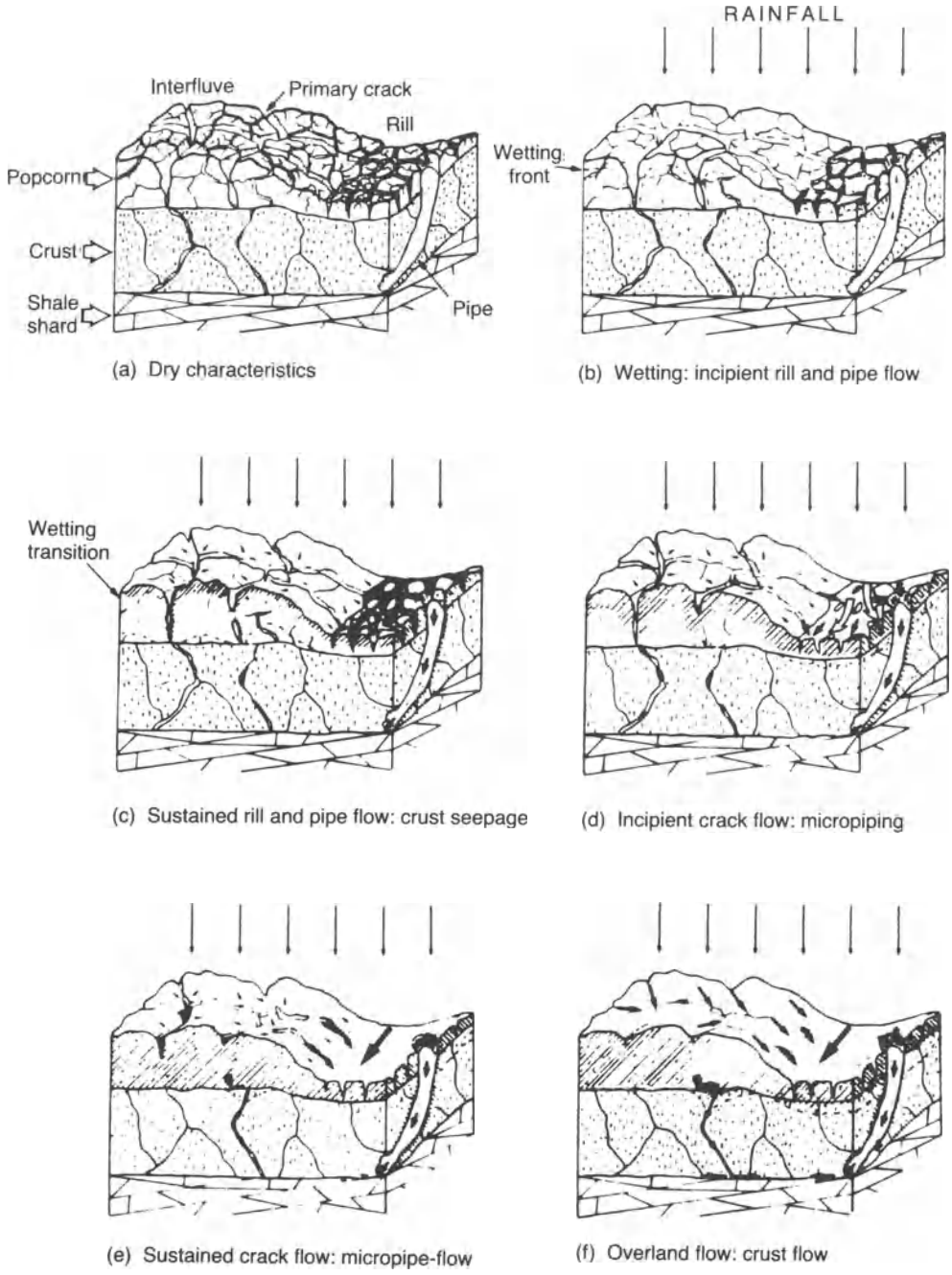

Figure 9.4 Regolith structure and runoff behaviour on shale badland slopes. Diagrams (a) through to (f) portray successive stages in wetting and runoff development (after Hodges and Bryan 1982).

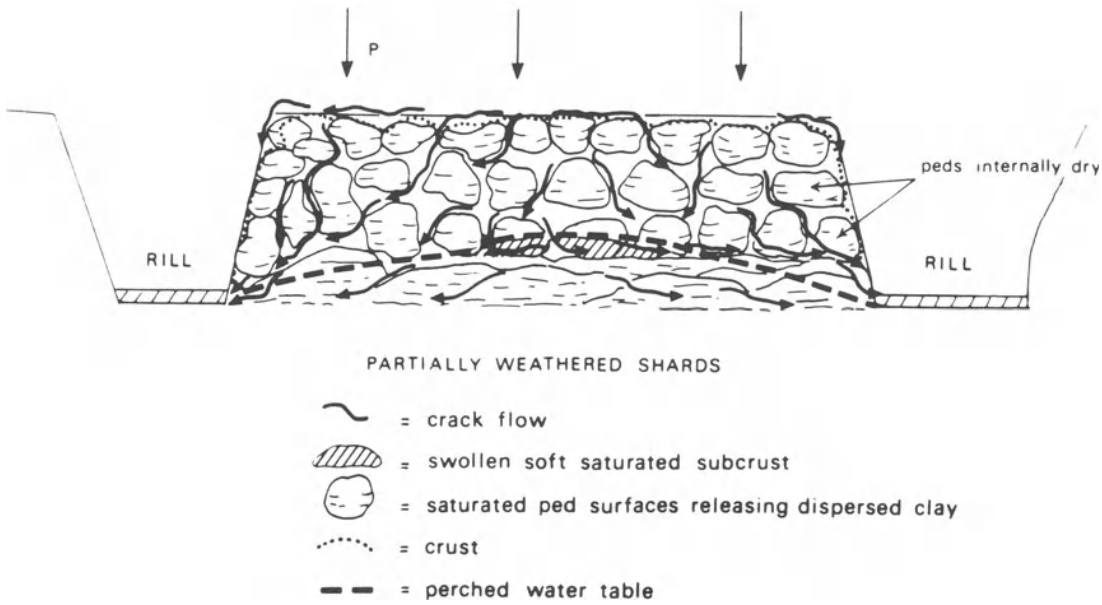

Figure 9.5 Development of a perched water table on top of shard layer in badland regolith and lateral drainage to rills. Note development of a saturated, soft layer between the rills which may fail, forming a pipe and eventually a new rill (after Imeson and Verstraten 1988).

rapidly and more completely on silty surfaces which locally encrust badland rills than on the cracked surface layers of badland slopes. Such silty layers in rills are uncommon on badlands in the Henry Mountains region, but alluvial surfaces are generally covered by such sediment and have rapid runoff response. A very few gentle badland slopes in Morrison Shale exhibit a banding alternating between typical popcorn-textured badland slopes and short alluvial surfaces (Fig. 9.6). The absence of shrink–swell cracking of the alluvial surfaces suggests that the silt layers are very effective at preventing infiltration. The banding may be an expression of layering in the shale or it may indicate a natural bifurcation at low slope gradient between normal badland slopes with swelling enhanced by water shed from upslope alluvial patches and alluvial surfaces graded downstream to the swollen shale bands.

In some badlands much of the slope drainage is routed through deep, corrasional pipe networks (see reviews by Harvey 1982, Campbell 1989, Jones 1990, Parker *et al.* 1990 and several papers in the volume edited by Bryan and Yair 1982b). Piping in susceptible lithologies is encouraged by prominent jointing and steeper hydraulic gradients via underground rather than surface paths caused by layering in the bedrock or through dissection of an originally flat upland (Campbell 1989). Piping is rare in the Henry Mountains badlands discussed here.

Rainsplash

Rainsplash erosion is important on badlands both as a direct agent of detachment and splash transport and indirectly as detachment contributes to runoff erosion and affects the flow hydraulics of shallow flows. A considerable experimental literature exists on rainsplash erosion mechanics (Chapter 8); the major controlling variables are raindrop size and velocity, rain intensity, and regolith characteristics. Few direct measurements exist of the contribution of rainsplash to badland slope erosion. Howard (1970) and Moseley (1973) attributed narrow, rounded divides on some badlands to the action of rainsplash rather than to creep (see below). Carson and Kirkby (1972, p. 221) also suggested that divide convexity may be caused by rainsplash on some arid slopes. The influence of rainsplash may be limited at the beginning of rainstorms by the cohesiveness of the dry clay, and biotic crusts, where present, protect shale regolith from rainsplash entrainment (Yair *et al.* 1980, Finlayson *et al.* 1987). In contrast to agricultural slopes, rainsplash has modest direct influence on overland flow hydraulics due to the concentration of flow into cracks and micropipes.

Figure 9.6 Low, terraced hillslope on shale in Morrison Formation. White bands are small segments of alluvial surface.

Runoff Erosion

Runoff on badlands seldom exemplifies the classic characteristics of overland flow on agricultural land because of the concentration of flow into cracks, micropipes, and ephemeral rills. The rate of erosion in such channelled overland flow and interflow, as well as in larger rills and washes, functionally depends upon flow conditions and resistance of the bedrock or regolith to weathering or detachment. The processes of erosion are poorly understood but may involve direct detachment from the bedrock, scour by sediment, and weathering processes such as leaching and wetting with dispersion.

Several approaches have been used to quantify runoff erosion in both rills and interrill areas. The most common approach on agricultural slopes is to estimate sediment transport rates using bedload or total load transport formulae assuming that the flow is loaded to capacity in the sand size ranges (transport-limited conditions). These are often empirically corrected for rainsplash effects based upon results of plot experiments in non-cohesive sediments or weakly cohesive soils (e.g. Meyer and Monke 1965, Komura 1976, Gilley *et al.* 1985, Julien and Simons 1985, Kinnell 1990, 1991, Everaert 1991). Detachment by rainsplash is assumed to assure capacity transport even where soils are moderately cohesive. Theoretical and empirical runoff erosion models commonly assume capacity transport (e.g. Kirkby 1971, Carson and Kirkby 1972, pp. 207–19, Smith and Bretherton 1972, Hirano 1975), but such assumptions often overestimate actual transport rates severalfold (Dunne and Aubrey 1986). Due to the cohesion and the small sand-sized component of badland regoliths, coupled with the steep slope gradients, runoff and interflow are likely to carry bed sediment loads well below capacity.

A few researchers have recognized that flow on steep slopes is commonly detachment-limited and suggest that the detachment (or deposition) by the flow D_f is related to an intrinsic detachment capacity D_c (for zero sediment load), the actual sediment load G and the flow transport capacity T_c (Foster and Meyer 1972, Meyer 1986, Lane *et al.* 1988, Foster 1990)

$$D_f = D_c(1 - G/T_c). \tag{9.6}$$

This relationship implies an interaction between

deposition and entrainment on the bed. However, rills and badland slopes seldom show evidence of sediment redeposition or partial surface mantling until flow reaches alluvial washes or alluvial surfaces (miniature pediments). The downstream transition from bare regolith to sand- and silt-mantled alluvial surfaces is generally abrupt (Schumm 1956a, b, Smith 1958, Howard 1970). The high roughness and possibly the greater grain rebound on badland regolith may make transport capacity greater than for an alluvial surface at the same gradient (Howard 1980). This suggests that on steep badland slopes and rills actual detachment D_f can reasonably be assumed to equal the intrinsic detachment D_c. This approach is used in the following models.

Howard and Kerby (1983) successfully related areal variations in observed rates of erosion of bedrock channels on shales to the pattern that would be expected if erosion rates were determined by dominant shear stress in the channel. Following Howard (1970), they suggested that erosion rate $\partial y/\partial t$ (detachment rate) is determined by shear stress τ:

$$\partial y/\partial t = K_c(\tau - \tau_c)^{\beta}, \tag{9.7}$$

where τ_c is a critical shear stress, β is an exponent, and the constant of proportionality K_c depends upon both flow durations and bedrock erodibility. Foster (1982) and Foster and Lane (1983) assume a similar relationship (with $\beta = 1$) for rill detachment capacity. Numerous experiments on fluvial erosion of cohesive deposits indicate scour rates that correlate with the applied shear stress (Parthenaides 1965, Parthenaides and Paaswell 1970, Akky and Shen 1973, Parchure and Mehta 1985, Ariathurai and Arulandan 1986, Kuijper *et al.* 1989). Assuming certain hydraulic geometry and resistance equations, and further assuming that the dominant values of shear stress greatly exceed the critical value, then equation 9.7 can be re-expressed as a function of local gradient S and contributing drainage area A_d:

$$\partial y/\partial t = K_e A_d{}^{\gamma} S^{\delta} \tag{9.8}$$

where the constant of proportionality K_e likewise depends upon flow durations and bedrock erodibility as well as constants in the hydraulic geometry equations. Theoretical values for γ and δ for the assumed hydraulic geometry relationships are 0.4 and 0.8, respectively, with observed values being 0.45 and 0.7. Seidl and Dietrich (1991) suggest stream power per unit channel length rather than shear stress may be the controlling factor for bedrock erosion. If so, $\delta = 1$ and γ is the exponent of proportionality between effective discharge and drainage area.

In some badland washes and in much of the throughflow in badland regolith the limiting factor may be the rate of decrease of shear strength of surface rinds either due to weathering of the bedrock or to wetting and dispersion of regolith crusts and shards. Even though the weathering rate is a limiting factor, flow conditions can still affect erosion rates, as illustrated in the following simple model.

Assume that the flow characteristically removes rinds or flocs of thickness δd and that the weathering at that depth decreases the shearing resistance c at a decreasing exponential rate from the initial shale cohesion c_i to a minimum value c_f:

$$c = c_f + (c_i - c_f)e^{-\lambda \delta t}, \tag{9.9}$$

where δt is the elapsed time since weathering has begun and λ is a characteristic weathering rate that depends upon wetting duration, bedrock or regolith permeability, and shale properties. Dislodgement of the weathered layer occurs when $\tau \geq c$, giving the time to dislodgement as

$$\delta t = \frac{1}{\lambda} \frac{(c_i - c_f)}{(\tau - c_f)} \tag{9.10}$$

Assuming that weathering begins anew when a layer is stripped by the flow and that τ_e is the effective shear stress, then the average erosion rate would be given by

$$\frac{\partial y}{\partial t} = \frac{\delta d}{\delta t} = \delta d\, \lambda / \ln \left[\frac{(c_i - c_f)}{(\tau_e - c_f)} \right] \tag{9.11}$$

Although this is a simplistic model, it does illustrate that if $\tau_e < c_f$ no erosion occurs; if $\tau_e > c_f$ there is a minimum erosion rate given by the weathering rate $\partial d \lambda$, and if $\tau_e > c_i$ the erosion rate is infinite. For the more interesting case of $c_i > \tau_e > c_f$ the erosion rate increases with τ_e, and where $c_i \gg \tau_e > c_f$ the rate of increase is nearly linear.

Both of these models suggest an erosion rate that increases with some measure of the strength of the effective flow. However, data on erosion rates in badland channels is limited, and that on the accompanying flow is essentially non-existent.

In some cases flows in bedrock rills may become so sediment laden that they exhibit Bingham flow properties (discussed in Chapter 8) with development of levees on rills and depositional mudflow fans. The common occurrence of localized slumps and draping flows on badland slopes might be

appropriately characterized by Bingham flow as well.

Requisite conditions for rill development and the overall control of drainage density in badlands has been a continuing theme in badlands geomorphology, starting with Schumm's (1956a) introduction of the 'constant of channel maintenance', a characteristic length from the divide to the head of rills. Rills have been discussed in two contexts. The first is the critical hydraulic conditions required for the transition from dispersed overland flow to channelized rill flow (see general discussions in Bryan 1987, Gerits *et al.* 1987, Torri *et al.* 1987, Rauws and Govers 1988). Several criteria have been proposed, including critical slope gradients (Savat and de Ploey 1982), a critical Froude number (Savat 1976, 1980, Karcz and Kersey 1980, Hodges 1982, Savat and de Ploey 1982), and a critical shear stress or shear velocity (Moss and Walker 1978, Moss *et al.* 1979, 1982, Savat 1982, Chisci *et al.* 1985, Govers 1985, Govers and Rauws 1985, Rauws 1987). On the steep badland slopes with strongly channelized flow in cracks, microrills, and pipes much of the flow exceeds critical conditions for rill initiation by any of these criteria. Rill initiation on badland slopes has also been related to unroofing of tunnels and micropipes (Hodges and Bryan 1982) which may be related as much to saturation, swelling, and softening of badland regolith as to the hydraulic factors mentioned above (see Fig. 9.5, Gerits *et al.* 1987, Imeson and Verstraten 1988).

Runoff thus seems to be capable of rill initiation over most badland slope surfaces, with the possible exception of sandstone layers with thin regoliths. The development and maintenance of semi-permanent rills require a balance between the tendency of runoff to incise and other processes that tend to destroy small rills (Schumm 1956a, Kirkby 1980). Such processes include shrink–swell of the surface layers, which destroys microrills (Engelen 1973), needle-ice growth (Howard and Kerby 1983), mass wasting by creep and shallow slides (Schumm 1956a, b, Howard and Kerby 1983), and rainsplash (Howard 1970, Moseley 1973, Dunne and Aubrey 1986). On badlands in humid climates a well-defined seasonal cycle of rill creation and obliteration occurs (Schumm 1956a, Howard and Kerby 1983). In arid regions advance and retreat of rill systems on slopes may occur over much longer timescales, but may also be dramatically altered by a single heavy summer rainfall or a winter mass wasting event. In the discussion below the emphasis is on 'permanent' rills and gullies that have persisted long enough to have created well-defined valleys. In the simulation modelling discussed at the end of the chapter, the location of permanent rills is determined by the balance between runoff erosion using equation 9.7 (with or without a critical shear stress) and diffusive processes (rainsplash or mass wasting).

BADLAND ARCHITECTURE AND EVOLUTION

The remainder of this chapter emphasizes the spatial process variations that determine the overall architecture of both slope and channel features of badlands. Furthermore, the temporal evolution of badlands will be examined both through reference to the specific case of the Henry Mountains area and through the use of simulation models.

EVOLUTION AND AREAL DISTRIBUTION OF BADLANDS

The rapid erosion of badland slopes means that they occur only where high relief has been created in shaly rocks. In the Henry Mountains area this has occurred through erosional removal of a protective caprock or through rapid master stream downcutting. The ramparts of sandstone cuestas feature local badlands in subcaprock shales, and more extensive badland areas occur where buttes have been recently denuded of their caprock. However, the badlands on cuesta ramparts are well developed only during relatively arid epochs (such as the present) when mass wasting of caprocks is relatively quiescent (see discussion in Chapter 7).

The master stream is the Dirty Devil–Fremont River system, which during the Quaternary has had a history of alternating stability or slight aggradation during pluvial epochs with rapid downcutting, followed by stability at the close of non-pluvial epochs (Howard 1970, 1986). During the pluvial epochs the stable base level coupled with physical weathering and mass wasting of the sandstone cuestas resulted in development of extensive talus slopes on the ramparts of the escarpments coupled with gravel-veneered alluvial surfaces (pediments) mantling the shales. Thus badlands were rare during pluvial epochs, probably occurring only locally on scarp ramparts or caprock-stripped buttes. The post-pluvial (Bull Lake) dissection of river terraces and alluvial surfaces underlain by Mancos Shale has created the spectacular badland landscape near Caineville, Utah (Fig. 9.1). The river apparently downcut about 65 m shortly after the close of the Bull Lake pluvial, followed by stability at about its present level (Howard 1970). As a result, a wave of dissection has moved headwards towards the sand-

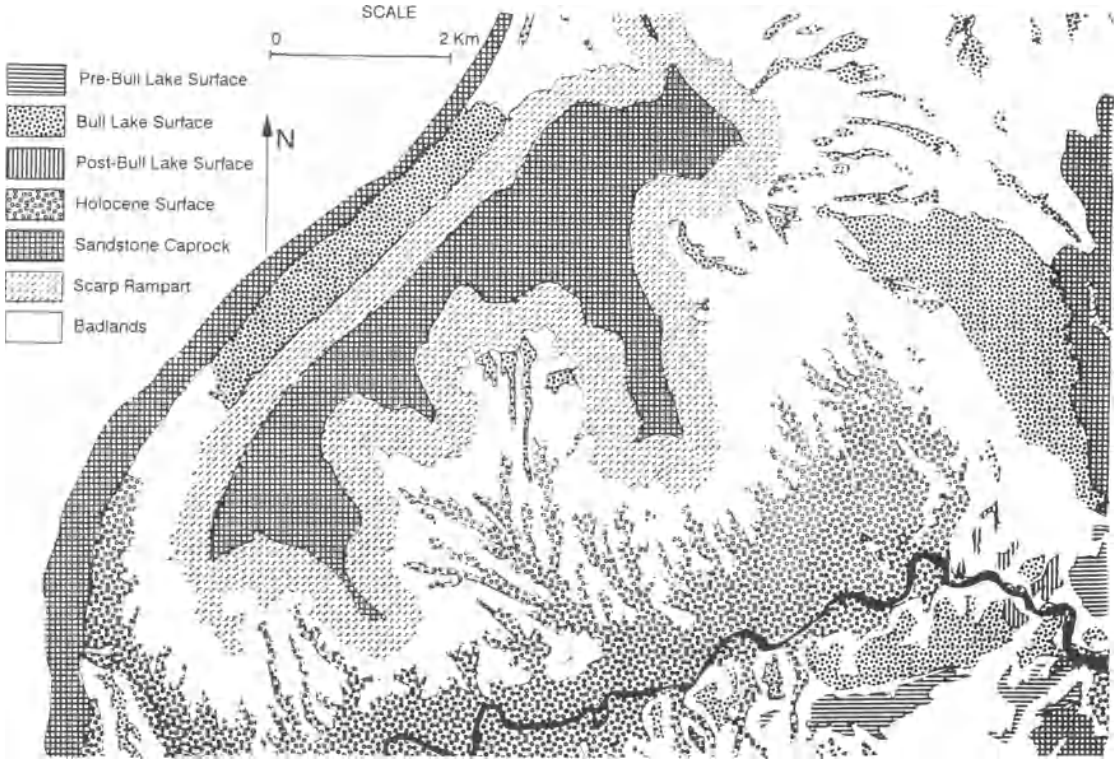

Figure 9.7 Geomorphic map of part of the Caineville Area, near the Henry Mountains, Utah. Bull Lake terrace may be early Wisconsin or Illinoian in age.

stone cuestas to which the alluvial surfaces were graded, producing a sequence of landforms from scattered Bull Lake alluvial surface remnants near the scarps (remaining primarily where the capping gravels were thickest) through a zone of high-relief (50 to 60 m) badlands to modern alluvial surfaces near the master drainage where the badlands have been completely eroded (Fig. 9.7). Shale areas that are either remote from the master drainage or have been protected from stream downcutting by downstream sandstone exposures are either undissected Pleistocene alluvial surfaces or very low-relief badlands.

Similar post-glacial downcutting has been implicated in forming the shale badland landscapes of the Great Plains of the United States and Canada (Slaymaker 1982, Wells and Guiterrez 1982, Bryan *et al.* 1987, Campbell 1989), with a similar progression from undissected uplands (often capped by a protective grassland cover) through high-relief badlands to modern alluvial surfaces. In semi-arid and humid regions, badlands occur primarily where a former vegetation has been removed from shales or easily eroded regolith. Thus such occurrences are similar to relief generation through a protective caprock and its subsequent removal.

FORM AND PROCESSES ON BADLAND SLOPES

Badlands exhibit a surprisingly wide range of slope form. A contrast between steep, straight-sloped badlands with very narrow divides and a convex form with generally gentler slopes was noted quite early in the literature on badlands and is exemplified in the classic South Dakota badlands by slopes in the Brule and Chadron Formations, respectively (Schumm 1956b). In the Henry Mountains area a similar contrast occurs between badlands on the Mancos Shale and those in the Morrison Formation (compare Figs 9.1 and 9.2). Badlands in the Summerville Formation are similar to the Mancos Shale badlands in having straight slopes and narrow divides, but they have significantly lower maximum slope gradients (Table 9.1). Many badlands have quite complicated slope forms due to contrasting lithology and interbedded resistant layers (e.g. the

Table 9.1 Comparison of slope angles (in degrees) on badlands in Mancos Shale, the Summerville Formation, and the Morrison Formation

Formation	*Angle-of-repose slopes*[a]	*Unstable slopes*[b]	*Average slope angle*[c]
Summerville	31.5	31.7	27
Mancos	32	34.8	40
Morrison	–	34.8	–

[a]Slopes constructed of unweathered shale shards.
[b]Constructional talus slopes of mass-wasted regolith below vertical cliffs in shale.
[c]Average gradient of long natural slopes in areas of moderate to high relief.

Dinosaur Badlands of Canada). Occasionally, pinnacle forms of badlands are found that are characterized by extremely high drainage density, knife-edge divides, and generally concave slope form (Fig. 9.8). The following discussion of badland erosional processes links these differences in slope form to variations in lithology and climate.

The broadly rounded upper slopes of the Morrison, Chinle, and Chadron Formations are probably due to creep processes (see above). The popcorn texture of surface aggregates allows relatively large relative movements of the aggregates as their edges become wet and slippery. However, lower sideslopes sometimes exceed 40°, locally resulting in rapid flowage of the popcorn surface layer off the slope. This results in long, narrow tracks of exposed subsoil on the lower slopes which rapidly develop a new surface layer of popcorn aggregates. Convex slopes develop through creep in any circumstance where the creep rate increases monotonically with slope gradient and where creep is the dominant erosional process; this was first elaborated by Davis (1892) and Gilbert (1909).

Even on these rounded slopes runoff erosion becomes increasingly important downslope, becoming dominant in rills and locally within shallow pipes and cracks in the thin regolith.

The Mancos badlands have a nearly linear profile with narrow, rounded divides, which range in width from less than 0.5 m in high-relief badlands to 1 to 2 m in low-relief areas (Fig. 9.1). Because of the very thin regolith on these narrow divides and a tendency for development of a shale-chip surface armouring, Howard (1970) and Moseley (1973) attributed

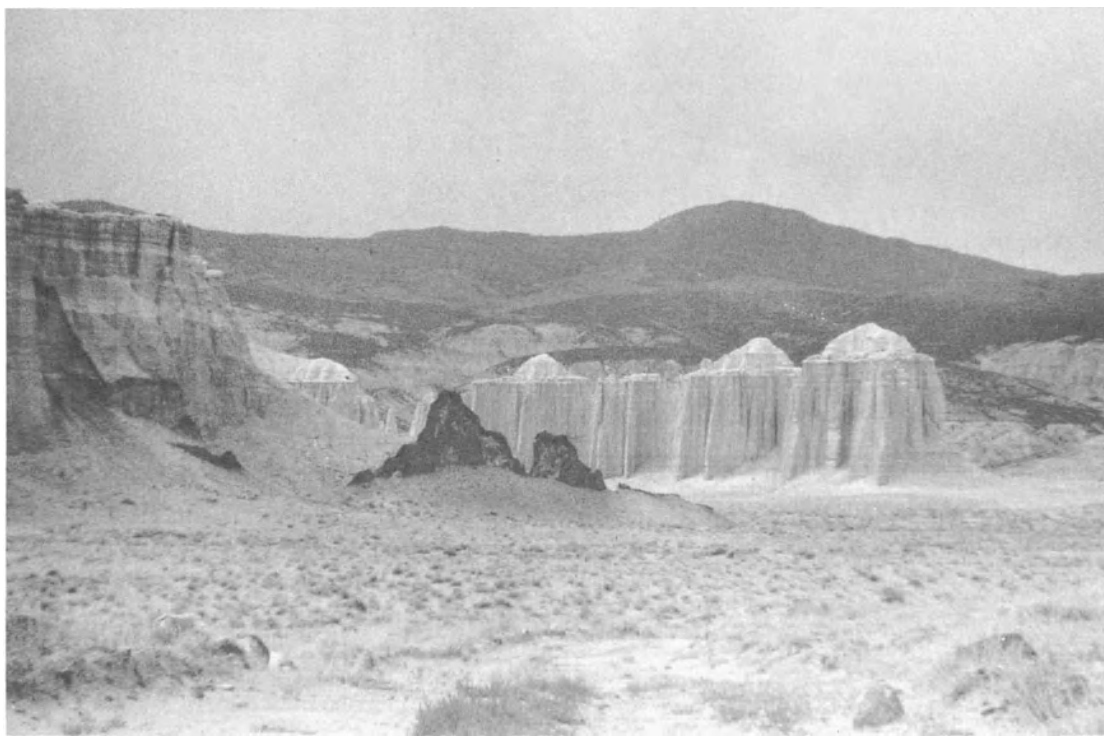

Figure 9.8 Pinnacle badland slopes in Cathedral Valley, near Caineville, Utah. The steep slopes were formerly protected by a caprock. Note the low-gradient slopes in the same formation (Entrada Sandstone).

Figure 9.9 Meandering bedrock wash in Mancos Shale, showing undercutting of slopes and tendency for shallow slumping of undercut slopes.

the divide rounding to rainsplash. This process is effective on narrow divides even at low gradient because the maximum splash distance is greater than the divide width.

Virtually all high-relief badland slopes in the Henry Mountains region have nearly constant gradient on their lower portions, even on the broadly convex slopes in the Morrison Formation. These maximum gradients are usually within a few degrees of the angle of repose of dry detritus weathered from the formations. Maximum gradients on the Summerville Formation, with its loose weathered layer, are 3° to 5° less than the angle of repose, probably due to seepage flow decreasing the maximum stable slope angle (implied in equations 9.1 to 9.5; see Lambe and Whitman, 1969, p. 354). However, in the Morrison and Mancos badlands the slopes are 3° to 10° higher than the repose angle for loose weathered shale due to cohesion. Consequently, many lower slopes are on the verge of failing by flowage and slipping. Many such slopes do occasionally fail, involving only the thin surface layer (5 to 10 cm) and leaving long, narrow tracks of exposed subsoil on the lower slopes. Such flows are numerous on steep slopes on the Morrison and Summerville Formations but are rare on the Mancos badlands. However, on the Mancos badlands, whole sections of hillside appear to slip or slump short distances downhill during rainstorms, producing tension cracks arranged in waves suggesting differential movement and, rarely, extensive shallow slumping (Fig. 9.9). Tension cracks are the more numerous and wider the steeper the gradient, particularly on slopes undercut by meandering washes (Fig. 9.9).

On low-gradient portions of slopes, creep-like movement of the surface layer predominates. However, for the gradients approaching the limiting slope angle (which in actuality is temporally and spatially variable), mass wasting rates can be func-

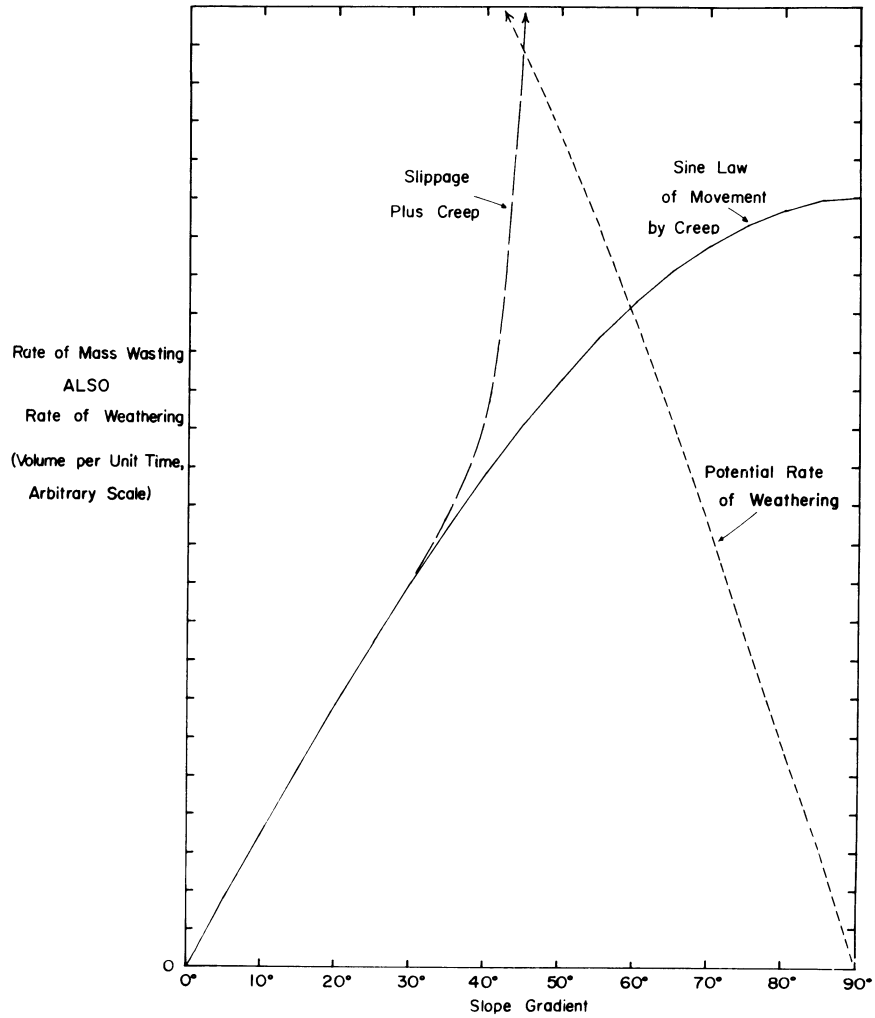

Figure 9.10 Conceptual plots of rate of mass wasting on badlands and potential rate of weathering as a function of slope gradient.

tionally represented by a rapid rate increase (Fig. 9.10). A similar approach was used by Kirkby (1984, 1985b).

Nearly linear lower slopes on regolith mantled, high-relief badlands would be expected if mass wasting determines slope form. Close to the divide, where creep rates are low (due to modest amounts of regolith supplied from upslope) and corresponding gradients are low, mass wasting rate follows the sine relationship. Consequently, gradients increase rapidly downslope. Rainsplash erosion is also a diffusive process, producing divide convexity. As a total volume of mass wasting debris increases downslope, equivalent rates of erosion may require gradients approaching the limiting slope angle where slippage or flowage becomes important. In these lower slope regions the incremental addition of weathered material along the slope can be accommodated by a very slight increase in gradient, thereby creating a nearly straight profile. Such lower slopes are essentially equivalent to the threshold slopes of Carson (1971) and Carson and Petley (1970), except that they are probably best modelled by a rapid but continuous increase in mass wasting rate as the limiting angle is approached rather than by an abrupt threshold.

Indirect evidence for threshold slopes in steep badlands comes from areal variations in badland

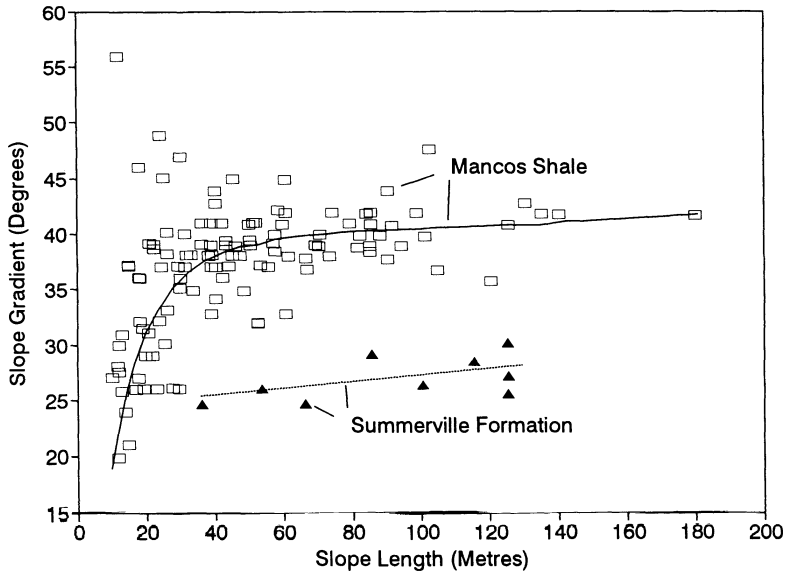

Figure 9.11 Plot of hillslope gradient versus slope length in badlands in the Summerville Formation and Mancos Shale.

form. Average hillslope gradients in badlands of the Summerville and Mancos Formations show little variation with slope length except for very short slopes (Fig. 9.11). However, the drainage density exhibits a complicated relationship to relief ratio, generally increasing with relief ratio up to a value of about 0.5, but decreasing in very high-relief badlands (Fig. 9.12). The relatively low drainage density of areas with very high relief ratio may be explained by the onset of sliding and slumping on steep slopes. In areas of high relief, large increases of the rate of erosion of a slope at its base should be accompanied by only a slight change in slope gradient (Fig. 9.10). But the small increase in slope angle increases the efficiency of erosion on the slope relative to the channel, so that the critical drainage area necessary to support a channel increases, with a resulting decrease in drainage density. Average slope length L and drainage density D are related to the average slope angle θ by (Schumm 1956a, p. 99)

$$L\cos\theta = 2/D. \qquad (9.12)$$

Because slope angles vary little with relief ratio in steep badlands, the decrease in drainage density accompanying increase in relief ratio is accompanied by a proportional increase in slope length. By contrast, in areas of low overall gradient, increase in relief ratio is accompanied by increases in drainage density. Therefore, slope length decreases nearly in proportion, since the cosine term is near unity.

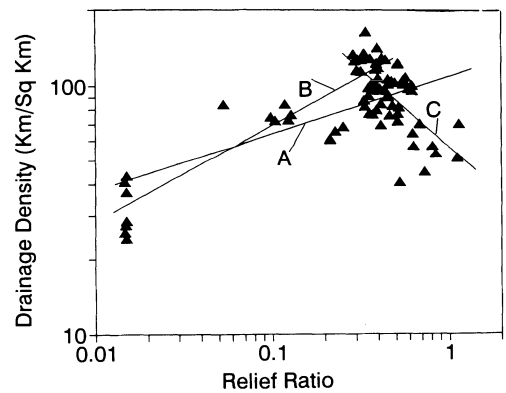

Figure 9.12 Drainage density versus relief ratio for badland areas in the Mancos Shale. Least-squares regression lines (A) for the data as a whole, (B) for values of relief ratio less than 0.35, and (C) for values greater than 0.2. Drainage density and relief ratio measured from aerial photographs with scale of 1:12 000. Each point represents measurement of a circular quadrat with radius of 150 m centred on a major badland divide. The relief ratio is defined from the quadrat centre to the lowest point on the quadrat circumference.

At least four types of surfaces occur on badlands: (a) slopes with exposed bedrock; (b) regolith-mantled slopes; (c) rills and washes with exposed bedrock; and (d) alluvium-mantled surfaces. These surfaces generally sharply abut against each other, with

Figure 9.13 Near-vertical slopes in shales of the Morrison Formation formed by past undercutting by the Fremont River. Differences in bedding are strongly expressed in vertical slopes in contrast to the smoother, gentler slopes mantled by 20+ cm of regolith.

the transitions corresponding to thresholds in the relative importance of processes. Most badland slopes are regolith-mantled, albeit shallowly. However, on steep slopes or where bedrock is resistant to weathering, regolith is absent and the surface is irregular, expressing variations in weathering characteristics of the rock, jointing, and stratigraphy (Fig. 9.13). In contrast, minor differences in lithology of the rocks underlying regolith-mantled badlands (non-undercut areas in Fig. 9.13) do not affect slope form, for the geometry is determined by processes of downslope transport of the weathered debris. The threshold between bare and regolith-mantled slopes is commonly equated with weathering- versus transport-limited conditions, respectively (Culling 1963, Carson and Kirkby 1972, pp. 104–6). However, there are four factors that may limit overall slope erosion rate, the potential weathering rate PW, the potential mass wasting rate PM, the potential detachment rate by runoff (combined splash and runoff detachment) PD, and the potential fluvial transport rate PT. On regolith-mantled slopes $PW > (PM + PD)$ and $PD < PT$. Either mass wasting or runoff detachment may be quantitatively dominant on such slopes; measurements by Schumm (1963) suggest runoff dominance. The use of the term transport-limiting for these mantled slopes is inaccurate, because the runoff component of erosion is detachment- rather than transport-limited. Bare bedrock slopes have $PW < (PM + PD)$ and $PD < PT$, so that the term weathering-limiting is appropriate. Alluvial surfaces have $PD > PT$, and generally $PM \approx 0$ because of the low gradients. Bedrock-floored rills and washes have similar conditions to bare rock slopes except that $PM \approx 0$. The rock-mantled slopes considered in Chapter 8 would appear to be similar to badland regolith-mantled slopes. However, the surface layer is often a lag pavement that greatly restricts runoff erosion, so that the overall rate of erosion is often determined either by (a) the rate of breakdown of the pavement by weathering or (b) the rate of upward migration of fines due to freeze–thaw or bioturbation, or (c) mass wasting rates.

The supply of moisture is the primary factor determining the weathering rate of the soft rocks forming badlands. For vertically falling precipitation the interception per unit surface area of slope diminishes with the cosine of the slope angle (in actuality some water attacks vertical or overhanging slopes, for escarpment caprocks often project beyond underlying shales). This suggests that overall slope erosion rates on badlands follow the relationships shown in Figure 9.10, where a critical gradient separates mantled slopes on which rates of mass wasting increase with slope gradient from steeper bedrock slopes which erode less rapidly as gradients increase (at least until slope relief is great enough to cause bulk failure in the shale bedrock).

Badlands with steep slopes and exposed bedrock commonly develop pinnacle forms (alternatively termed needle-like, serrate, or fluted) (Fig. 9.8). Examples include the Brice Canyon pinnacles, the badlands described by Carman (1958), the spires of Cathedral Valley, Utah, and portions of the badlands of South Dakota. Pinnacle badlands commonly are initiated as a result of near-vertical slopes developing in non-resistant shales lying beneath a resistant caprock which erodes very slowly as compared with downwearing in the surrounding badlands. Eventually the caprock is weathered away or fails, and the underlying shales rapidly erode, developing the fluted form due to rapid rill incision because of the steep relief. Drainage densities are exceedingly high on these slopes and, owing to the absence of a mantling regolith and mass wasting processes, divides are knife-edged. Slope profiles are generally concave, indicating the dominant role of runoff (both unconcentrated and in rills) in erosion. Although the steepness of the fluted slopes is partially due to the high initial relief, the slopes at divides generally steepen during development of fluted badlands because rill erosion rapidly erodes slope bases and weathering and erosion rates on sideslopes *decrease* with increasing slope gradient (Fig. 9.10). As the fluted slopes downwaste, they are generally replaced by mantled badland slopes with lower drainage density at a very sharp transition (Fig. 9.8).

FLUVIAL PROCESSES AND LANDFORMS OF BADLAND LANDSCAPES

Howard (1980) distinguished three types of fluvial channels: bedrock, fine-bed alluvial, and coarse-bed alluvial. In most cases these types of channel are separated by clear thresholds in form and process. In badlands coarse-bed alluvial channels usually occur only where gravel interbeds are present.

Alluvial Surfaces

Few contrasts in landscape are as distinct as that between badland and alluvial surfaces on shaly rocks. Low-relief, alluvium-mantled surfaces in badland areas have been referred to by a variety of names, including miniature pediment (Bradley 1940, Schumm 1956b, 1962, Smith 1958), pseudo- and peri-pediment (Hodges 1982), and alluvial surface (Howard 1970, Howard and Kerby 1983). The last term is used here because of its neutral connotation regarding the numerous and conflicting definitions of pediment.

Flow on alluvial surfaces is either unconfined or concentrated in wide, braided washes inset very slightly below the general level of the alluvial surface (Fig. 9.14). Alluvial surfaces may be of any width compared with that of the surrounding badlands, contrasting with the confinement of flow in bedrock rills and washes. The alluvium underlying most alluvial surfaces is bedload carried during runoff events and redeposited as the flow wanes, but adjacent to major washes overbank flood deposits may predominate. Although the surface of alluvial surfaces and washes is very smooth when dry, during runoff events flow is characterized by ephemeral roll waves and shallow chute rilling which heals during recessional flows (Hodges 1982).

An alluvial surface and badlands commonly meet at a sharp, angular discordance (Fig. 9.15). At such junctures slopes, rills and small washes with inclinations up to 45° abut alluvial surfaces with gradients of a few degrees. In most instances the alluvial surfaces receive their drainage from badlands upstream and are lower in gradient than the slopes or washes. The layer of active alluvium beneath an alluvial surface may be as thin as 2 mm, but increases to 10 cm or more below larger braided washes. Below the active alluvium there occurs either a thin weathered layer grading to bedrock or, in cases where the alluvial surface has been aggrading, more alluvium.

Generally alluvial surfaces and their alluvial washes obey the same pattern of smaller gradients

Figure 9.14 Runoff on alluvial surfaces on Morrison Formation Shales. Photo was taken during waning flow stages.

Figure 9.15 Sharp junction between steep badland slopes and alluvial surface (a and b).

Figure 9.16 Badlands and dissected alluvial surface in Mancos Shale. The former boundary between badland slopes and the alluvial surface occurred at the light–dark transition.

for larger contributing areas. Howard (1970, 1980) and Howard and Kerby (1983) showed that the gradient of alluvial surfaces is systematically related to the contributing drainage area per unit width (or equivalent length) A_L in badlands both in arid and humid climates:

$$S = CA_L^z \tag{9.13}$$

where the exponent z may range from -0.25 to -0.3. The equivalent length for washes on alluvial surfaces is simply the drainage area divided by the channel width, but for unconfined flow on smaller alluvial surfaces it is the drainage area contributing to an arbitrary unit width perpendicular to the gradient. The proportionality constant C can be functionally related to areal variations in sediment yield, runoff, and alluvium grain size. Howard (1980) and Howard and Kerby (1983) showed that the value of the exponent z is consistent with the assumption that alluvial surface gradients are adjusted to transport sand-sized bedload at high transport rates.

Badland alluvial surfaces are therefore comparable to sand-bedded alluvial river systems in general in that gradients decrease with increasing contributing area (downstream). The major contrast is the presence of unchannelled areas in the headward portion of alluvial surfaces. Their presence is probably related to the absence of vegetation and flashy flow, which discourages formation of banks and floodplains. The alluvial surfaces contrast with alluvial fans in that the former are through-flowing systems with only minor losses of water downstream and contribution of water and sediment from the entire drainage area. Furthermore, the alluvial surfaces are generally slowly lowering. If they are aggrading, they do so at a very slow rate. Thus the downstream spreading of discharge characteristic of alluvial fans (and deltas) generally does not occur on alluvial surfaces.

Alluvial surfaces are surfaces of transportation, with a gradient determined by the long-term balance between supplied load and discharge (Smith 1958). Thus they are graded surfaces in the sense of Mackin (1948). Howard (1982) and Howard and Kerby (1983) discussed the applicability of this concept in the context of seasonal and long-term changes in the balance of sediment load and discharge, and the limits to the concept of grade. Interestingly, most badland alluvial surfaces slowly lower through time, as indicated both by direct measurements (Schumm 1962, Howard and Kerby 1983) and by the presence of rocks on pedestals of shale surrounded by an alluvial surface that has lowered around it. Thus the alluvial surfaces are not destroyed by slow lowering of base level, but they become readily dissected by bedrock washes if base level drops too rapidly (Fig. 9.16). Howard (1970) and Howard and Kerby (1983) presented evidence that larger alluvial channels are capable of more rapid erosion than smaller ones without being converted to bedrock channels. Howard and Kerby (1983) suggested that the maximum erosion rate is proportional to about the 0.2 power of drainage area. It is uncertain whether the erosion (or aggradation) rate on alluvial surfaces systematically influences their gradients.

Bedrock Channels

Badland washes and rills are usually floored by slightly weathered bedrock. Beneath the smallest

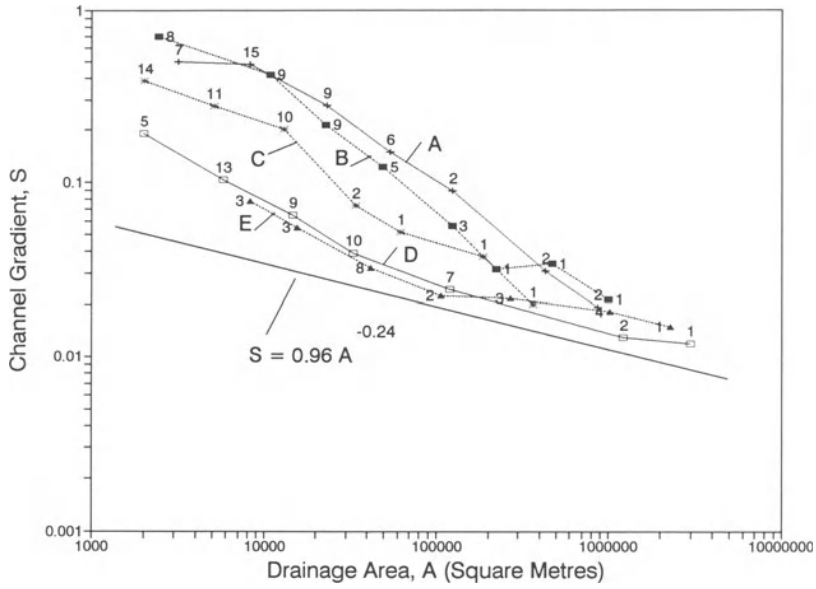

Figure 9.17 Relationship between size of drainage area and stream gradient for selected basins in the Mancos Shale near Caineville, Utah. Figures beside points show number of sample points that are averaged for clearer presentation. For comparison, the relationship between gradient and drainage area for alluvial surfaces on the Morrison Formation is shown.

rills the weathered zone is about as thick as that on adjacent unrilled slopes, although this thickness varies with the seasonal rill cycle (Schumm 1956a, 1964, Schumm and Lusby 1963). In larger badland washes, weathering products are rapidly removed, exposing bedrock. Deposits of alluvium occur only locally in scour depressions.

Larger bedrock washes often display marked meandering (Fig. 9.1) with the wavelength increasing systematically with the 0.4 power of drainage area (Howard 1970), which is consistent with meander wavelength in alluvial streams.

In contrast to the alluvial surfaces, the gradient of bedrock washes is not uniquely related to the size of contributing drainage area and their gradient is steeper than alluvial washes of equivalent area (Howard 1970, Howard and Kerby 1983). Figure 9.17 shows this relationship for bedrock badland drainage basins in the Mancos Shale near Caineville, Utah. Steep-gradient wash systems (A and B in Fig. 9.17) are either locations of complete dissection of the Pleistocene alluvial surface or locations recently denuded of a protective caprock. Low-gradient bedrock wash systems (D and E in Fig. 9.17) occur where dissection of the Pleistocene alluvial surface has been inhibited by a high local base level in the form of a resistant rock unit. The gradients for all of the basins converge for high drainage areas, because the downstream ends of these wash systems are generally alluvial surfaces.

Slope–Channel Interactions in Badlands

Erosion in large bedrock streams may be nearly independent of the sediment load supplied by slope erosion (e.g. equations 9.7 and 9.11), so that the nature of the surrounding slopes has minor influence on stream erosion rates. Thus, in general, evolution of hillslopes follows rather than leads that of the stream network.

However, the low-order tributaries, including rills, interact with adjacent slopes and their gradients are largely determined by hillslope gradients. The smallest rills are ephemeral (Schumm 1956a, Schumm and Lusby 1963, Howard and Kerby 1983) and have gradients essentially equal to hillslope gradients.

The nature of hillslope–channel interactions is poorly understood. Permanent channels occur only where runoff is sufficient such that streams erode as rapidly as the surrounding slopes and with a lesser gradient. Diffusive processes (creep and rainsplash) are more efficient than channel erosion for small contributing areas. This is suggested by models of bedrock channel erosion (e.g. equation 9.8) where,

for a given erosion rate, gradients would have to approach infinity as contributing area approaches zero. In contrast, mass wasting slope processes and rainsplash function even at divides. Ephemeral rills are generally not inset into the slope because seasonal (or year-to-year) mass wasting by needle ice or shallow slips and direct frost heaving episodically destroys them. Permanent rills and washes are distinguished by (and can be defined by) being inset within a definable drainage basin, so that they have a lower gradient than surrounding slopes. Even so, such permanent rills may occasionally be partially infilled by mass wasting debris.

The sharpness of the junction between badland slopes and adjacent alluvial surface (e.g. Fig. 9.15) as well as its spatio-temporal persistence has fascinated generations of geomorphologists, and a variety of hypotheses have been offered for its origin and maintenance. Badlands rising from alluvial surfaces have gradients nearly equal to nearby slopes terminating at bedrock channels (Fig. 9.18), implying nearly equal rates of erosion, even though the alluvial surfaces may be stable or very slowly degrading. Moreover the slope form (straight-sided or broadly convex) remains the same. In Figure 9.18 successive profiles across the valley in a downstream direction may be similar to changes in profiles through time at one location, assuming that the alluvial surface remains at a stable level. The alluvial surfaces expand at the expense of the adjacent slope, as measured by Schumm (1962).

Schumm (1962), Smith (1958), Emmett (1970), and Hodges (1982) suggested that the abrupt contact is created and maintained by erosion concentrated at the foot of the slope, due perhaps to spreading of discharge from the rills at the base of the slope (a type of lateral planation), re-emergence of interflow, and changes of flow regime (subcritical to supercritical) at the slope–alluvial-surface junction. Engelen (1973) suggested that spreading of water emerging on to alluvial surfaces from ephemeral microrills may be as important as spreading flow from more permanent rills. Hodges (1982) provided experimental information and observations on flow on badland slopes, rills, and alluvial surfaces. These data indicate the complicated nature of flow on these surfaces, including ephemeral rilling of the alluvial surface.

Howard (1970) suggested that the abrupt change of gradient at the head of an alluvial surface can be maintained without recourse to special processes acting at this location. Simulation modelling of coupled bedrock and alluvial channel evolution (using an equation similar to equation 9.8 for bedrock erosion) indicated that bedrock channels maintained a nearly uniform gradient as they downcut until they were abruptly replaced by alluvial surface when elevations dropped to the level that the gradients were just sufficient to transport supplied alluvium (Figs 9.23 and 9.24, discussed below). Although these simulations were targeted to the bedrock channel system on badlands, a similar situation may pertain to unrilled badland slopes. Water erosion is the dominant erosional process at the base of badland slopes (Schumm and Lusby 1963) and may be governed by similar rate laws as permanent rills and washes. As noted above, most seemingly unrilled badland slopes are primarily drained by concentrated flow either through an ephemeral surface network of crack flows (which are obliterated during the swelling and reshrinking of the surface layer) or as interflow in deeper cracks and micropipes.

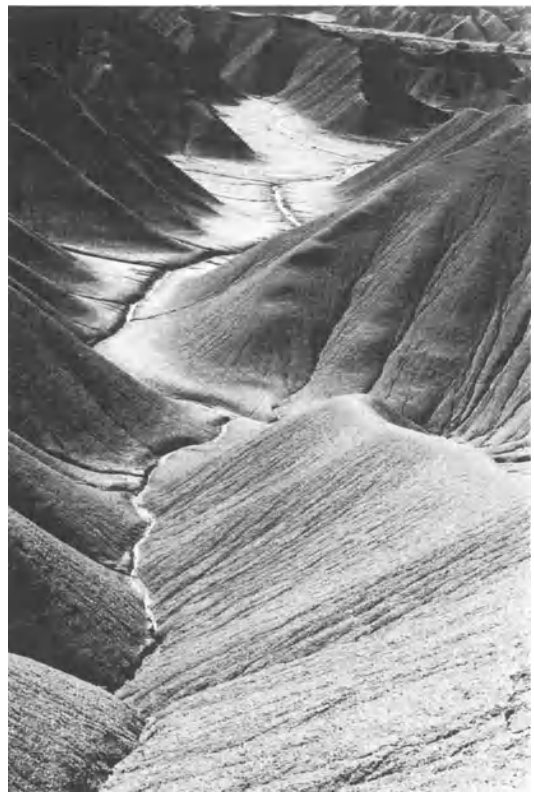

Figure 9.18 Downstream transition between bedrock wash and alluvial surface. Slope gradients are about the same whether grading to bedrock wash or alluvial surface.

Theoretical Models of Badland Evolution

There has been a rich history of quantitative modelling of slope and channel processes. These models

have not primarily been directed towards specific issues related to badland slopes, but they have a general formulation that could be adapted to specific processes and materials in badlands. Early models were primarily applied to evolution of slopes in profile only, either for ease of analytical solutions or for numerical solutions with modest computational demands. A variety of approaches have been used, but two end members can be identified. Some investigators, as exemplified by the approaches of Kirkby (Kirkby 1971, 1976a, b, 1985a, b, Carson and Kirkby 1972), have attempted to quantify almost all of the processes thought to be acting on slopes and their distribution both on the surface and throughout the regolith. This approach offers the promise of detailed understanding of the spatio-temporal evolution of regolith and soils as well as the potential for addressing site-specific issues of erosion processes, slope hydrology, surface water geochemistry, and soil and water pollution. Some attempts have been made to apply such models to cover areal as well as profile characteristics of slopes, including issues of initiation of drainage (Kirkby 1986, 1990). However, the generality of such models restricts their use over large spatial or temporal domains due to present limitations of computer resources and the large number of parameters that must be specified.

Another approach has been to deliberately simplify models in order to address issues of drainage basin morphology and landscape evolution. Ahnert (1976, 1977) has been a pioneer in developing three-dimensional models of landscape evolution, although most of his efforts have been directed to cross-sectional evolution of slope profiles (Ahnert 1987a, b, 1988). Recent advances in computer capabilities have permitted more general modelling of drainage basin evolution. The model of Willgoose *et al.* (1991a, b, c) was formulated to examine long-term evolution of drainage basin morphology through combined slope and channel process. Modelling with deliberately simplified process assumptions, they assume a combination of diffusional processes (such as creep or rainsplash erosion) on regolith-mantled slopes and sediment transport through a fine-bed alluvial stream network. Diffusion is modelled by a linear function of local slope gradient, and fluvial sediment transport rate is parameterized as a function of drainage area and channel gradient by assuming appropriate equations of hydraulic geometry and sediment transport rates.

A similar approach has been taken by Howard (in preparation) to examine variations in slope and drainage network geometry as a function of model parameters. This model is based upon the observation that drainage basins result from simultaneous action of diffusional and concentrative processes. For example, creep, rainsplash, and possibly some forms of overland flow (Dunne and Aubrey 1986) are diffusional, whereas most fluvial processes (excepting those on fans and deltas) are concentrative. The simulation model reported here includes creep (diffusional) and runoff (concentrative) erosion. The model was not specifically constructed to represent badland slopes. In particular, the model assumes gradients of only a few degrees such that $\sin\theta \simeq \tan\theta = S$ and $\cos\theta \simeq 1$. Weathering is assumed not to be a limiting factor and is not explicitly modelled. Creep is assumed to be limited to surface soil layers and thus is independent of total soil depth. The creep flux $\mathbf{q}$ is a function of the slope gradient $\mathbf{S}$:

$$\mathbf{q} = K_s \mathbf{S}^{\alpha} + K_t/(1 - C_t S^{\varepsilon}), \tag{9.14}$$

where K_s and K_t are rate constants, α and ε are constant exponents, and a constant $C_t > 0$ allows for threshold-limiting slopes (bold type indicates vector quantities). The rate of erosion due to creep E_s equals the divergence of creep:

$$E_s = \nabla \cdot \mathbf{q}. \tag{9.15}$$

Channels and rills are assumed to be bedrock-floored, with channel erosion rate E_c depending upon overland flow shear stress τ as given by equation 9.7, which is parameterized as a function of drainage area and local gradient (equation 9.8). The assumption of bedrock-floored channels means that explicit sediment routing in channels is not required. It also means that the development of alluvial washes and alluvial surfaces cannot be simulated with the present version of the model.

The total erosion at any location E_t is given by:

$$E_t = \begin{cases} E_s & \text{if } E_c = 0 \\ E_s/\eta + E_c & \text{if } E_c < 0 \end{cases} \tag{9.16}$$

where $\eta > 1$ models the easier erosion of soil debris than bedrock.

Simulations have been conducted with this model on a 100×100 matrix. The simulations generally assume that the bottom boundary is a horizontal outflow which is lowered at a constant rate E_b so that a steady state topography gradually develops. The top boundary is a drainage divide, and the side boundaries are periodic (elevations on the left boundary are continuous with those on the right, and soil or water leaving the left boundary enters at the same relative position at the right boundary).

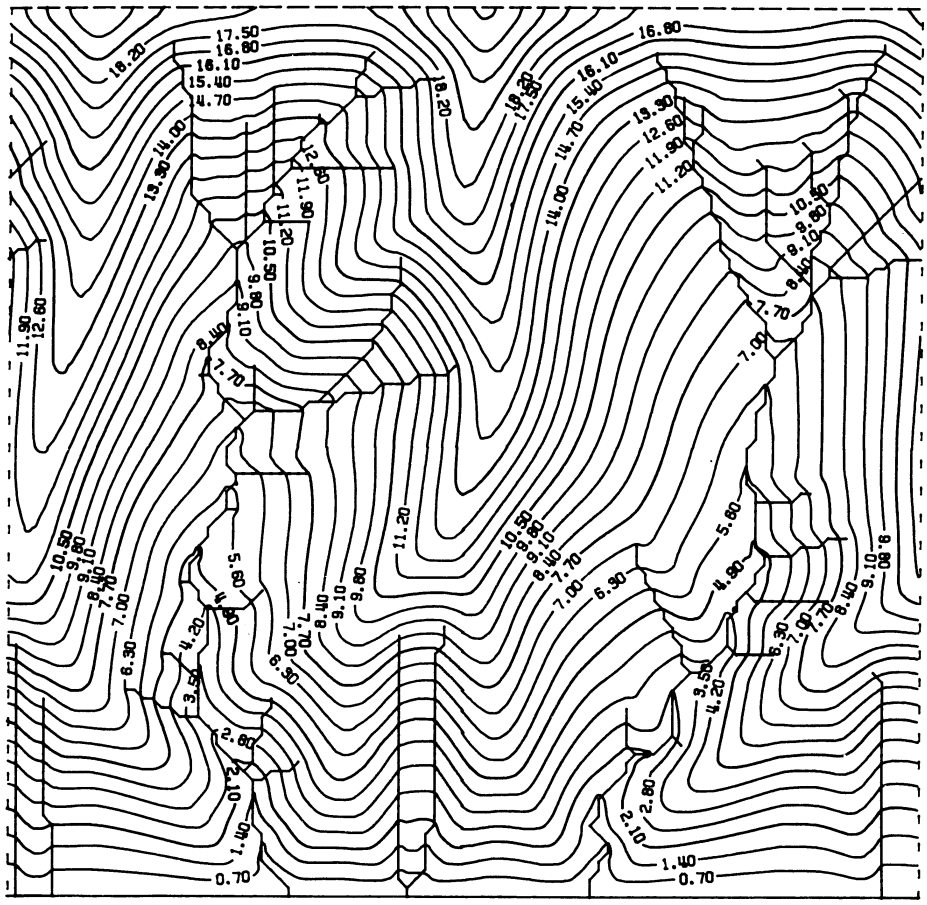

Figure 9.19 Topographic map of simulated drainage basins. Simulations are conducted on a 100×100 matrix. The lower boundary is assumed to be a horizontal base level which is being lowered at a constant rate. The upper boundary is a drainage divide (no water or sediment may cross that boundary), and the lateral boundary is periodic, in that water or mass leaving one boundary comes in at the other. See text for further explanation.

Initial conditions are usually a very low relief, nearly level surface with a random initial topography (including undrained depressions). The simulation is run to a nearly steady state topography ($\approx$15 000 iterations). The simplest model assumes $\alpha = 1$, $\tau_c = 0$, $K_t = 0$, $\eta = 1$ and $\beta = 1$. This results in a superposition of regolith creep proportional to slope angle and water erosion proportional to the shear stress. For an assumed grid spacing of unity the following values give a reasonable drainage density: $K_c = K_e = 1$, $K_s = 2$, $\gamma = 0.35$, $\delta = 0.7$ with an erosion rate $E_t = 1$. This produces a dominantly concave topography with narrow rounded divides that is unlike most natural drainage basins (Fig. 9.19). In these simulations no attempt has been made to match the vertical scale or absolute gradients to a particular landscape; in other words, the vertical scale is arbitrary. We are concerned here primarily with areal variations in relative gradients and forms.

A more badlands-like topography is formed if a critical shear stress for water erosion is introduced. The topography shown in Figure 9.20 has parameter values as above except that $\tau_c = 2.5$. The divides are narrow but rounded, and the slope profiles are slightly concave. This topography is similar to that in the Mancos Shale badlands except for the concave lower slopes. A topography similar to that in the very rounded Morrison Shale badlands results if the critical shear stress is made higher and weathered shale is considered to be more easily eroded than bedrock (Fig. 9.21, with $\eta = 6$ and $\tau_c = 5.0$).

The lower slopes of high-relief badlands in all three formations (Morrison, Summerville, and Mancos) were inferred above to have gradients close

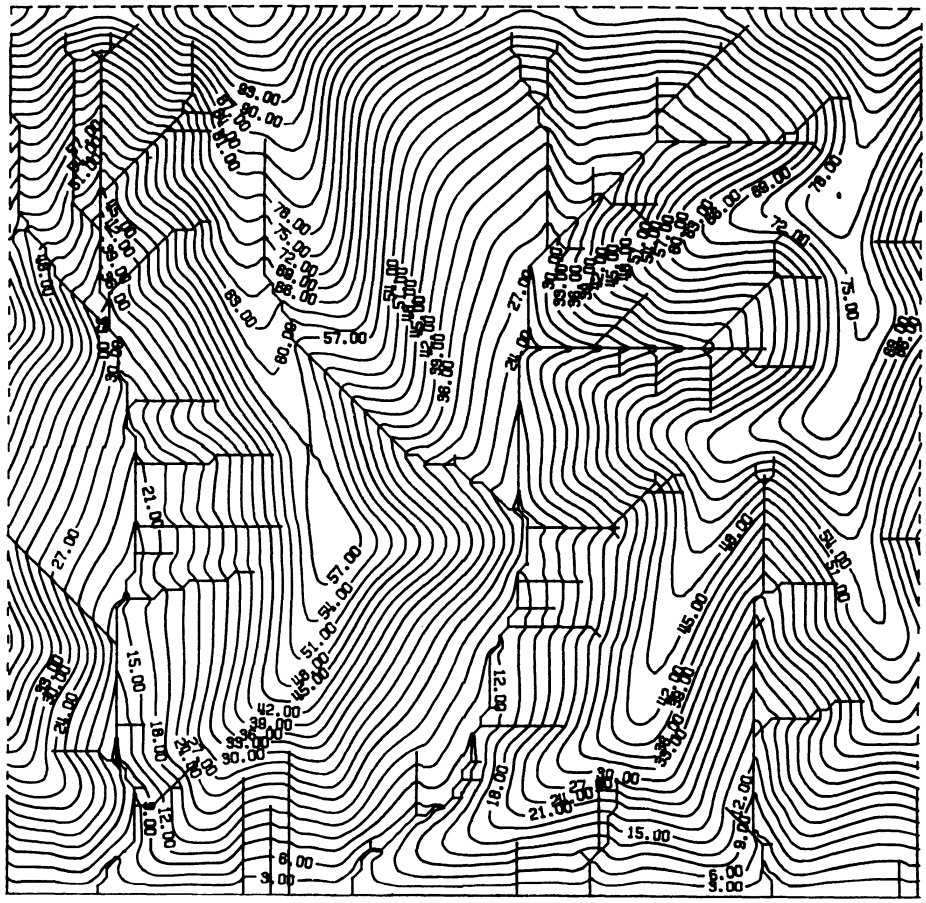

Figure 9.20 Topographic map of simulated drainage basins. Conditions are as for Figure 9.19 except that a critical threshold for fluvial erosion is assumed.

enough to the bulk stability of the weathered mantle that average mass wasting rates are enhanced relative to normal creep processes. This can be simulated in the model by giving non-zero values to K_t and ε. Figure 9.22 shows a simulation with parameters similar to Figure 9.21 except that $E_s = 0.5$, $K_t = 2.5$, and $\varepsilon = 3$. Slopes in this simulation have nearly linear profiles except for a narrow, rounded crest. This simulation has slope forms most similar to the Summerville Formation badlands of any of the simulations shown here, and is also similar to those on the Mancos Shale except for the less rounded divides on Mancos Shale.

The simulations shown here have assumed a constant rate of base level lowering, so that steady state topography eventually develops from any initial conditions. Under these conditions all parts of the landscape erode vertically at a constant rate, and the volume of regolith eroded per unit surface area per unit time V_{at} decreases with the slope angle θ:

$$V_{at} = h_t \cos\theta \tag{9.17}$$

The simulation model at present assumes low slope gradients so that the cosine term can be approximated by unity. However, for explicit modelling of badland slopes this correction should be made. Equation 9.17 also explains the common lack of correlation between slope steepness and badland erosion rates (Schumm 1956a, Schumm and Lusby 1963, Campbell 1970, 1974, 1982); little correlation would be expected for steady state badland slopes.

The model does not directly specify the drainage density or the source locations of streams. Rather, the simulation parameters determine the transition from convex slopes to linear channels. A critical value of the convergence of slope gradient $-\nabla \cdot \mathbf{S}/\hat{S}$,

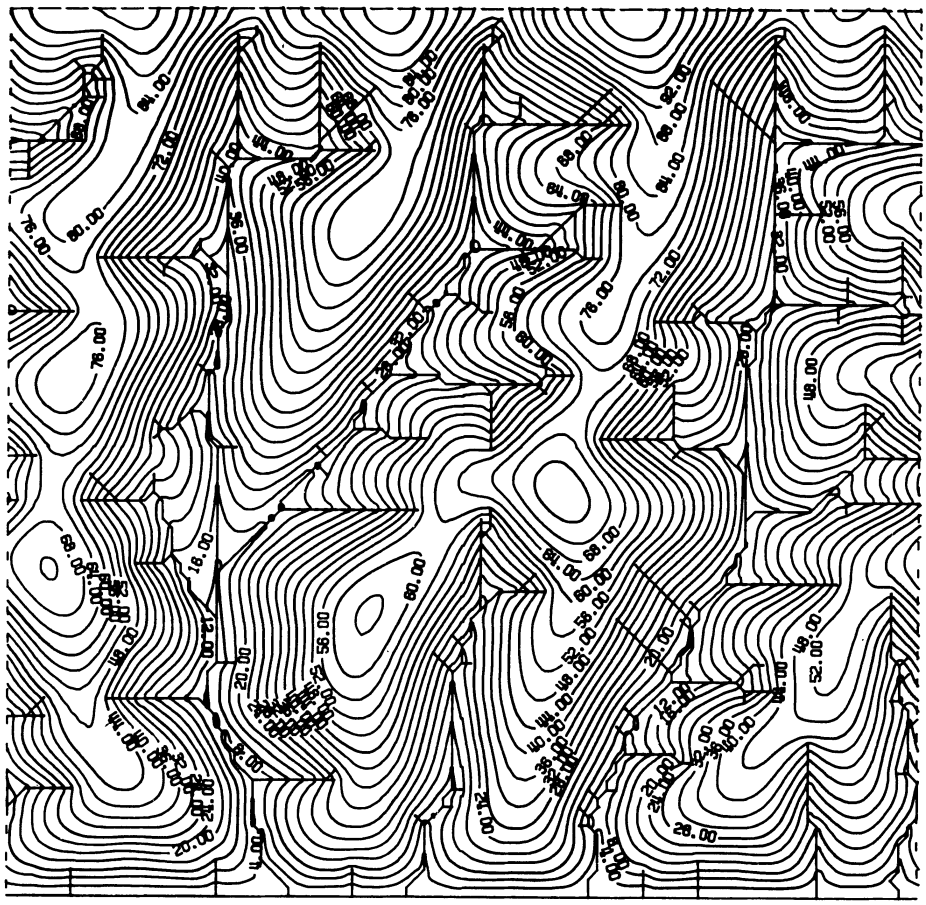

Figure 9.21 Topographic map of simulated drainage basins. Conditions are as in Figure 9.20 except that the threshold for channel erosion is higher and mass wasted regolith is assumed to be easier to fluvially erode than is bedrock.

where $\hat{S}$ is the average basin gradient, provides a reasonable definition of channel locations, giving a generally connected drainage network that corresponds closely with the usual contour crenelation method. This criterion has been used to define the drainage pattern in the illustrated basins.

Several generalities can be made about the landform development and spatial organization of process and topography in these steady state models.

(a) The model is deterministic, with randomness involved only in the development of the initial low-relief topography. The simulations show that even a small random component, either as initial or boundary conditions, is sufficient to provide the rich variation in landform texture that characterizes natural landscapes.

(b) For a constant rate of base level lowering a steady state topography is eventually developed for any arbitrary initial topography. The steady state topographies produced from different initial conditions are all different in detail but similar in general form (e.g. distributions of hillslope and channel gradients, drainage density, and slope profile characteristics).

(c) Very simple additive models of erosional processes produce landforms with spatial properties similar to natural drainage basins. This suggests that, despite the temporal and spatial complexity of processes acting in badlands, long-term erosion of badlands can be approximated through the use of reasonably simple models.

(d) Validation of simulation models of drainage basin development is hampered by very limited

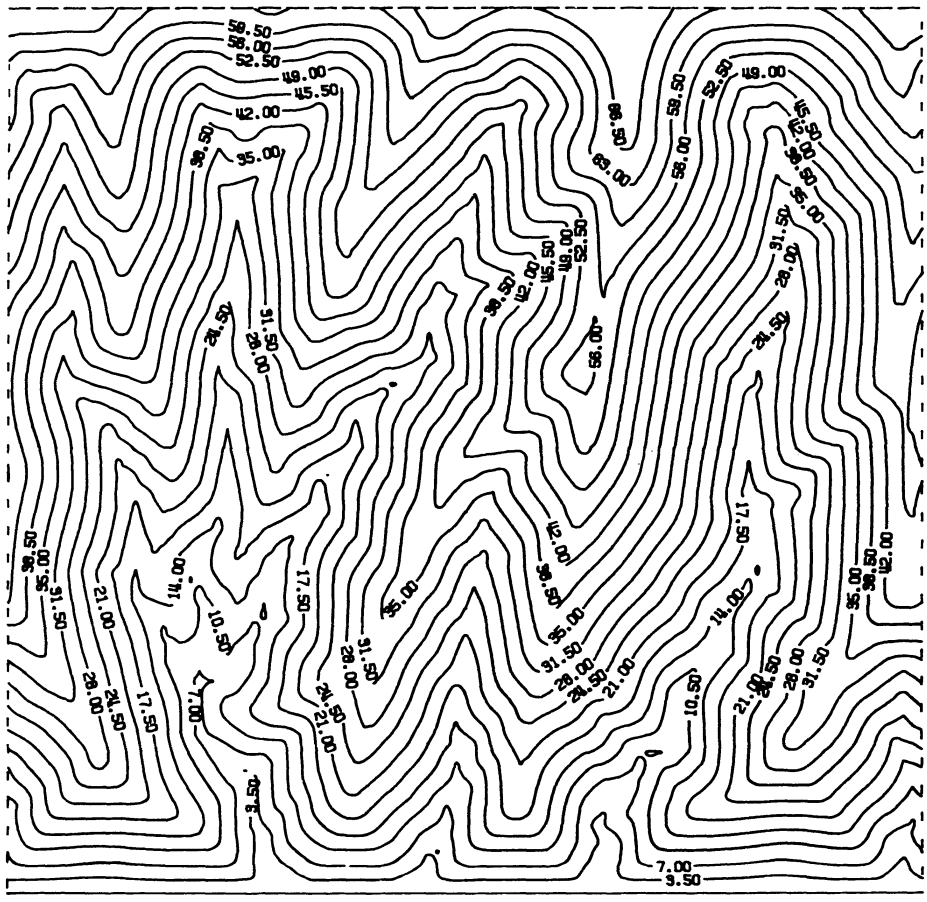

Figure 9.22 Topographic map of simulated drainage basins with a critical gradient for slope failure.

opportunity to compare predicted with observed landform evolution. Therefore, morphometric comparison of simulated and natural drainage basins is a useful technique but will require development of new means of characterizing landform scale, length, orientation, and relief properties. Possible approaches include statistical measures of hypsometry, gradients, junction angles, slope profiles, fractal properties, topology, and frequency-domain analysis.

(e) As has been noted in field measurements of badland erosion, the relative importance of water erosion increases from the divide through the lower slopes to the streams. Even where there is a critical threshold for water erosion ($\tau_c > 0$, as in Figs 9.20 and 9.21) the lower, unchannelled portions of the slopes are commonly partly eroded by water runoff.

(f) The drainage pattern exhibits strong pattern optimization in the sense used by Howard (1990), in that drainage paths from source to outlet are reasonably direct and the drainage density is nearly uniform.

The overall spatial variation in badland morphology may be an indicator of the erosional history of the area. As an obvious example, dissection of a terrace progresses inward from the terrace edge, progressing fastest along streams with the greatest drainage (Schumm 1956a). Because the model at present does not encompass alluvial washes and alluvial surfaces, it cannot be used to simulate erosional history of the Mancos Shale badlands in the Caineville area, where such surfaces are presently expanding into the badlands. However, Howard (1970) utilized a model that investigated the evolution of both bedrock

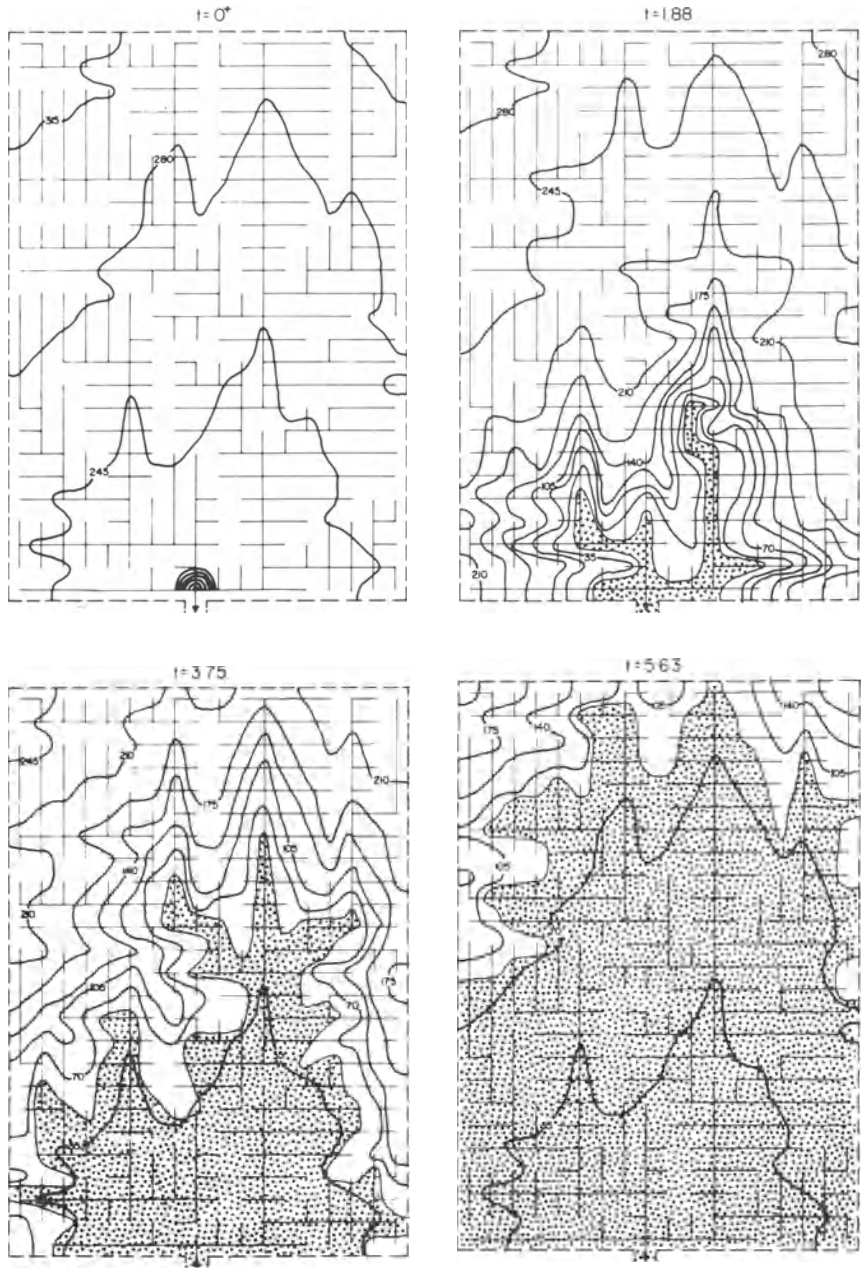

Figure 9.23 Successive stages in the dissection of an alluvial surface after an instantaneous lowering of the downstream end of the basin, followed by stability. Where erosion proceeds to the point that stream gradients reach the assumed minimum value necessary to transport sediment supplied from upstream (equation 9.13), no further erosion is permitted and an alluvial surface is formed (shaded pattern). The relative time since the beginning of the dissection is given by t.

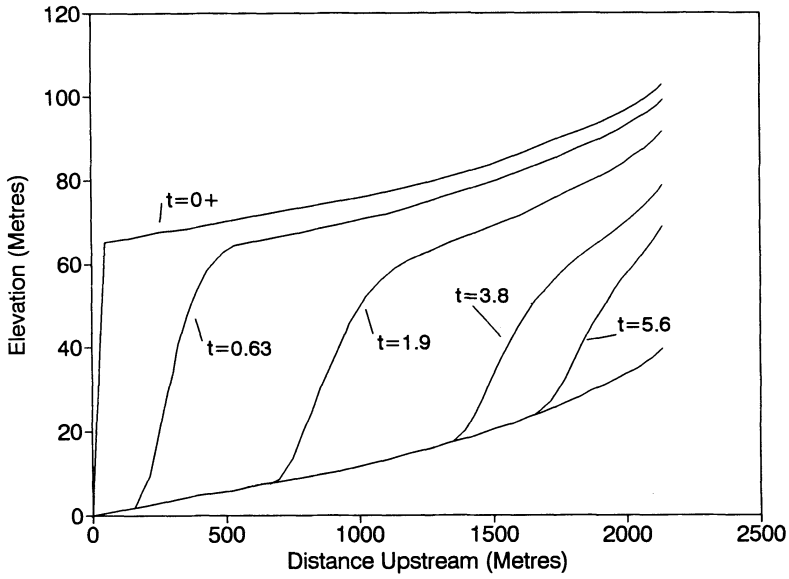

Figure 9.24 Stream profiles developed at successive stages in the dissection of the alluvial surface shown in Figure 9.23. The profile is taken along the stream heading in the upper left-hand corner of Figure 9.23.

washes (using the same approach as indicated in equations 9.7 and 9.8) and alluvial surfaces in this area. But this model does not simulate slope development and assumes a uniform drainage density. Two scenarios were investigated. In both the initial conditions are a flat, undissected alluvial surface assumed to represent the Bull Lake surface. In the first scenario it is assumed that the downstream end of the alluvial surface is instantaneously lowered but then remains stable at the lower level. This scenario represents a sudden downcutting of the Fremont River followed by stability at its present level. Figure 9.23 shows successive stages of dissection of the surface with contours on the badland washes and the extent of development of new alluvial surface graded to the lower river level; Figure 9.24 shows successive stream profles along the main stream. In the second scenario there is a uniform rate of base level lowering (Fig. 9.25), and the extent of alluvial surface depends upon the rate of lowering. In this simulation the extent of alluvial surface does not vary with time and occupies all areas greater than a critical drainage area whose value decreases with increasing downcutting rate. Howard (1970) concluded that the sudden downcutting followed by stability provides a better representation of the actual distribution of alluvial surface (Fig. 9.7), which is greater near the Fremont River and is not a simple function of contributing area.

In conclusion, the use of simulation models for addressing landform evolution in badlands (and drainage basins in general) has a bright future. The most important challenges in using such models are (a) developing appropriate process rate laws; (b) determining the boundary conditions (temporal and spatial) for the given situation; and (c) validation of the model through comparison of process rates or landform morphology between the model and the target natural landscape. Each of these issues is complicated. For example, because of the sensitivity of exact landform morphology to initial and boundary conditions, long-term simulations of landform development cannot be expected to exactly duplicate a specific natural landscape. Comparisons between simulated and natural landscape will need to be statistical; this involves judgments on what variables are most important in making such comparisons and what level of agreement is satisfactory. Similarly, it may be uncertain to what degree the process assumptions in the model are validated by successful statistical comparisons with a natural landscape; rather different mathematical models may be capable of producing similar landforms. Even if the mathematical structure of the model is validated by strong statistical correspondences, it may still be uncertain what actual processes correspond to the mathematical model (e.g. diffusive transport can be produced by regolith creep, rain-splash, or some types of runoff: Dunne and Aubrey 1986).

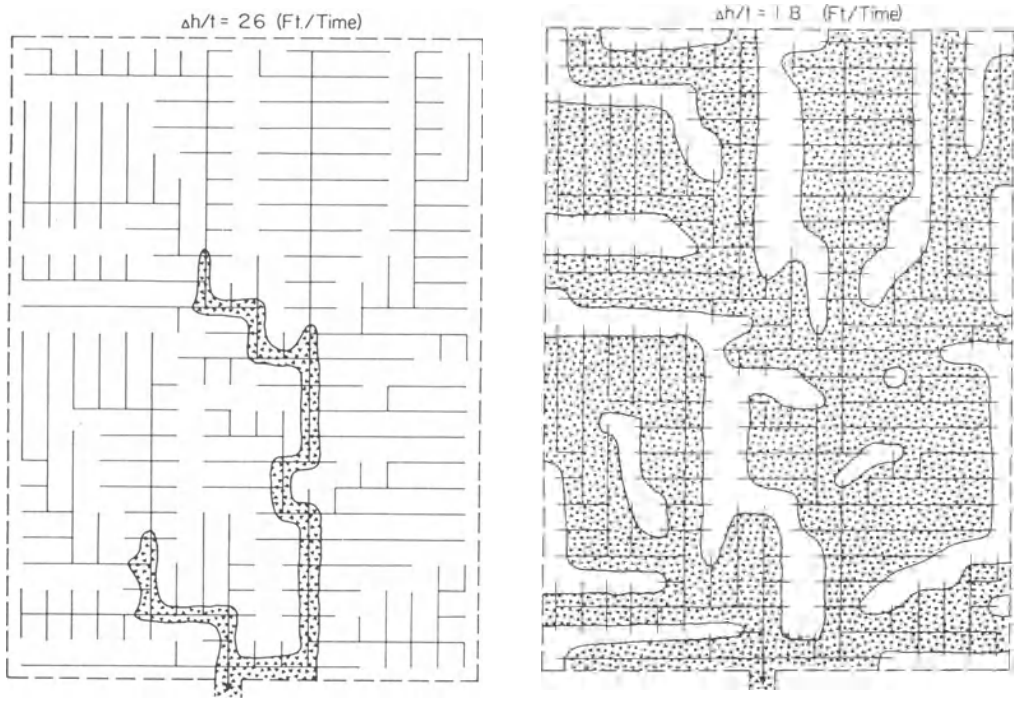

Figure 9.25 Distribution of alluvial surface (shaded) and bedrock channels (unshaded) during dissection of an alluvial surface by a constant rate of lowering of the downstream end of the basin. The vertical downcutting rate per unit time (arbitrary units) is given by $\Delta h/t$. For a value of $\Delta h/t$ less than about 13 the entire area remains as alluvial surface, while for values greater than 53 no alluvial surface remains.

CONCLUSIONS

Despite a long history of badland studies, many uncertainties remain concerning badland processes and landform development. Further understanding of badlands will require studies conducted at a range of temporal and spatial scales. There is a need for observational and experimental studies of hydraulic processes, regolith weathering, and erosion at the scale of small plots to small drainage basins at the timescale of individual precipitation events to extend the pioneering work of Bryan *et al.* (1978, 1984), Hodges (1982), and Yair *et al.* (1980) to the full range of bedrock types, relief, and climates supporting badlands. At an intermediate spatio-temporal scale there is a paucity of coordinated measurement of total, rainsplash, runoff, and mass wasting erosion and regolith development on the scale of small drainage basins and over a period of several years. The relative roles of these processes and their spatial distribution within badland drainage basins is still largely unconstrained. At the largest scale is the opportunity to decipher regional landform evolution in badlands and to relate variations in badland form to erosional history. Finally, comparative study of badlands of different rock type, climate, or erosional histories can be productive at any of these scales.

Badlands offer a unique opportunity for development and testing of quantitative landform models because we not only have the landform morphology to compare with theoretical models but processes are rapid enough that rates of landform change can be measured with reasonable accuracy over periods of just a few years.

REFERENCES

Ahnert, F. 1976. Brief description of a comprehensive three-dimensional process-response model of landform development. *Zeitschrift für Geomorphologie Supplement Band* **25**, 29–49.

Ahnert, F. 1977. Some comments on the quantitative formulation of geomorphological processes in a theoretical model. *Earth Surface Processes* **2**, 191–202.

Ahnert, F. 1987a. Approaches to dynamic equilibrium in theoretical simulations of slope development. *Earth Surface Processes and Landforms* **12**, 3–15.

Ahnert, F. 1987b. Process-response models of denudation at different spatial scales. *Catena Supplement* **10**, 31–50.

Ahnert, F. 1988. Modelling landform change. In *Modelling Geomorphological Processes*, M.G. Anderson (ed.), 375–400. Chichester: Wiley.

Akky, M.R. and C.K. Shen 1973. Erodibility of a cement-stabilized sandy soil. In *Soil erosion: causes and mechanisms*. U.S. Highway Research Board Special Report 135, 30–41.

Ariathurai, R. and K. Arulandan 1986. Erosion rates of cohesive soils. *Journal of the Hydraulics Division, Proceedings of the American Society of Civil Engineers* **104**, 279–98.

Bowyer-Bower, T.A.S. & R.B. Bryan 1986. Rill initiation: concepts and evaluation on badland slopes. *Zeitschrift für Geomorphologie Supplement Band* **59**, 161–75.

Bradley, W.H. 1940. Pediments and pedestals in miniature. *Journal of Geomorphology* **3**, 244–54.

Bryan, R.B. 1987. Processes and significance of rill development. *Catena Supplement* **8**, 1–15

Bryan, R.B., I.A. Campbell and A. Yair 1987. Postglacial geomorphic development of the Dinosaur Provincial Park badlands, Alberta. *Canadian Journal of Earth Sciences* **24**, 135–46.

Bryan, R.B., A.C. Imeson and I.A. Campbell 1984. Solute release and sediment entrainment on microcatchments in the Dinosaur Park badlands, Alberta, Canada. *Journal of Hydrology* **71**, 79–106.

Bryan, R. and A. Yair, 1982a. Perspectives on studies of badland geomorphology. In *Badland geomorphology and piping*. R. Bryan and A. Yair (eds), 1–13. Norwich: Geo Books.

Bryan, R. and A. Yair (eds) 1982b. *Badland geomorphology and piping*. Norwich: Geo Books.

Bryan, R.B., A. Yair and W.K. Hodges 1978. Factors controlling the initiation of runoff and piping in Dinosaur Provincial Park badlands, Alberta, Canada. *Zeitschrift für Geomorphologie Supplement Band* **34**, 48–62.

Campbell, I.A. 1970. Erosion rates in the Steveville badlands, Alberta. *The Canadian Geographer* **14**, 202–16.

Campbell, I.A. 1974. Measurements of erosion on badlands surfaces. *Zeitschrift für Geomorphologie Supplement Band* **21**, 122–37.

Campbell, I.A. 1982. Surface morphology and rates of change during a ten-year period in the Alberta badlands. In *Badland geomorphology and piping*, R. Bryan and A. Yair (eds), 221–36. Norwich: Geo Books.

Campbell, I.A. 1989. Badlands and badland gullies. In *Arid zone geomorphology*, D.S.G. Thomas (ed.), 159–93. New York: Halstead Press.

Campbell, I.A. and J.L. Honsaker 1982. Variability in badlands erosion; problems of scale and threshold identification. In *Space and time in geomorphology*, C.E. Thorn, (ed.), 59–79. London: George Allen & Unwin.

Carman, M.F., Jr 1958. Formation of badland topography. *Bulletin of the Geological Society of America* **69**, 789–90.

Carson, M.A. 1969. Models of hillslope development under mass failure. *Geographical Analysis* **1**, 76–100.

Carson, M.A. 1971. An application of the concept of threshold slopes to the Laramie Mountains, Wyoming. *Institute of British Geographers Special Publication* 3, 31–47.

Carson, M.A. and M.J. Kirkby 1972. *Hillslope form and process*. Cambridge: Cambridge University Press.

Carson, M.A. and D.J. Petley 1970. The existence of threshold slopes in the denudation of the landscape. *Transactions of the Institute of British Geographers* **49**, 71–95.

Chisci, G., M. Sfalanga and D. Torri 1985. An experimental model for evaluating soil erosion on a single-rainstorm basis. In *Soil erosion and conservation*, S.A. Swaify, W.C. Moldenhauer and A. Lo (eds), 558–65. Ankeny, IA: Soil Conservation Society of America.

Churchill, R.R. 1981. Aspect-related differences in badlands slope morphology. *Annals of the Association of American Geographers* **71**, 374–88.

Culling, W.E.H. 1963. Soil creep and the development of hillside slopes. *Journal of Geology* **71**, 127–61.

Davis, W.M. 1892. The convex profile of bad-land divides. *Science* **20**, 245.

Dunne, T. and B.F. Aubrey 1986. Evaluation of Horton's theory of sheetwash and rill erosion on the basis of field experiments. In *Hillslope processes*, A.D. Abrahams (ed.), 31–53. Boston: Allen & Unwin.

Emmett, W.W. 1970. The hydraulics of overland flow on hillslopes. *U.S. Geological Survey Professional Paper* 662-A.

Engelen, G.B. 1973. Runoff processes and slope development in Badlands National Monument, South Dakota. *Journal of Hydrology* **18**, 55–79.

Everaert, W. 1991. Empirical relations for the sediment transport capacity of interrill flow. *Earth Surface Processes and Landforms* **16**, 513–32.

Finlayson, B.L., J. Gerits and B. van Wesemael 1987. Crusted microtopography on badland slopes in southeast Spain. *Catena* **14**, 131–44.

Foster, G.R. 1982. Modeling the erosion process. In *Hydrologic modeling of small watersheds*, C.T. Hahn, H.P. Johnson and D.L. Brakensiek (eds), 297–382. St Joseph, MI: American Society of Agricultural Engineers.

Foster, G.R. 1990. Process-based modelling of soil erosion by water on agricultural land. In *Soil erosion on agricultural land*, J. Boardman, I.D.L. Foster and J.A. Dearing (eds), 429–45. Chichester: Wiley.

Foster, G.R. and L.J. Lane 1983. Erosion by concentrated flow in farm fields. In *Proceedings of the D.B. Simons symposium on erosion and sedimentation, 9.65–9.82*. Fort Collins, CO: Colorado State University.

Foster, G.R. and L.D. Meyer 1972. A closed-form soil erosion equation for upland areas. In *Sedimentation (Einstein)*, H.W. Shen (ed.), 12.1–12.19. Fort Collins, CO: Colorado State University.

Gerits, J., A.C. Imeson, J.M. Verstraten and R.B. Bryan 1987. Rill development and badland regolith properties. *Catena Supplement* **8**, 141–60.

Gilbert, G.K. 1880. *Report on the geology of the Henry Mountains*. Washington: U.S. Geographical and Geological Survey of the Rocky Mountain Region.

Gilbert, G.K. 1909. The convexity of hilltops. *Journal of Geology* **17**, 344–51.

Gilley, J.E., D.A. Woolhiser and D.B. McWhorter 1985. Interrill soil erosion – part I: development of model equations. *Transactions of the American Society of Agricultural Engineers* **28**, 147–53, 159.

Govers, G. 1985. Selectivity and transport capacity of thin flows in relation to rill erosion. *Catena* **12**, 35–49.

Govers, G. and G. Rauws 1986. Transporting capacity of overland flow on plane and on irregular beds. *Earth Surface Processes and Landforms* **11**, 515–24.

Harvey, A. 1982. The role of piping in the development of badlands and gully systems in south-east Spain. In

Badland geomorphology and piping, R. Bryan and A. Yair (eds), 317–35. Norwich: Geo Books.

Hirano, M. 1975. Simulation of developmental process of interfluvial slopes with reference to graded form. *Journal of Geology* **83**, 113–23.

Hodges, W.K. 1982. Hydraulic characteristics of a badland pseudo-pediment slope system during simulated rainstorm experiments. In *Badland geomorphology and piping*, R. Bryan and A. Yair (eds), 127–51. Norwich: Geo Books.

Hodges, W.K. and R.B. Bryan 1982. The influence of material behavior on runoff initiation in the Dinosaur Badlands, Canada. In *Badland geomorphology and piping*, R. Bryan and A. Yair (eds), 13–46. Norwich: Geo Books.

Howard, A.D. 1970. A study of process and history in desert landforms near the Henry Mountains, Utah. Unpublished Ph.D. dissertation. Baltimore: Johns Hopkins University.

Howard, A.D. 1980. Thresholds in river regime. In *Thresholds in geomorphology*, D.R. Coates and J.D. Vitek (eds), 227–58. London: George Allen & Unwin.

Howard, A.D.. 1982. Equilibrium and time scales in geomorphology: application to sand-bed alluvial channels. *Earth Surface Processes and Landforms* **7**, 303–25.

Howard, A.D. 1986. Quaternary landform evolution of the Dirty Devil River system, Utah. *Geological Society of America Abstracts with Program*, 641.

Howard, A.D. 1990. Theoretical model of optimal drainage networks. *Water Resources Research* **26**, 2107–17.

Howard, A.D. 1992. Issues in drainage basin modelling: drainage density, drainage pattern, randomness, and validation. *In preparation*.

Howard, A.D. and G. Kerby 1983. Channel changes in badlands. *Bulletin of the Geological Society of America* **94**, 739–52.

Hunt, C.B. 1953. Geology and geography of the Henry Mountains region. *U.S. Geological Survey Professional Paper* 228.

Imeson, A.C. and J.M. Verstraten 1985. The erodibility of highly calcareous soil material from southern Spain. *Catena* **12**, 291–306.

Imeson, A.C. and J.M. Verstraten 1988. Rills on badland slopes: a physico-chemically controlled phenomenon. *Catena Supplement* **12**, 139–50.

Imeson, A.C., F.J.P.M. Kwaad and J.M. Verstraten 1982. The relationship of soil physical and chemical properties to the development of badlands in Morocco. In *Badland geomorphology and piping*, R. Bryan and A. Yair (eds), 47–69. Norwich: Geo Books.

Jones, J.A.A. 1990. Piping effects in drylands. *Geological Society of America Special Paper* 252, 111–38.

Julian, P.Y. and D.B. Simons 1985. Sediment transport capacity of overland flow. *Transactions of the American Society of Agricultural Engineers* **28**, 755–62.

Karcz, I. and D. Kersey, 1980. Experimental study of free-surface flow instability and bedforms in shallow flows. *Sedimentary Geology* **27**, 263–300.

Kinnell, P.I.A. 1990 Modelling erosion by rain-impacted flow. *Catena Supplement* **17**, 55–66.

Kinnell, P.I.A. 1991. The effect of flow depth on sediment transport induced by raindrops impacting shallow flows. *Transactions of the American Society of Agricultural Engineers* **34**, 161–8.

Kirkby, M.J. 1971. Hillslope process-response models based on the continuity equation. *Institute of British Geographers Special Publication* 3, 15–30.

Kirkby, M.J. 1976a. Soil development models as a component of slope models. *Earth Surface Processes* **2**, 203–30.

Kirkby, M.J. 1976b. Deterministic continuous slope models. *Zeitschrift für Geomorphology Supplement Band* **25**, 1–19.

Kirkby, M.J. 1980. Modelling water erosion processes. In *Soil erosion*, M.J. Kirkby and R.P.C. Morgan (eds), 183–216. Chichester: Wiley.

Kirkby, M.J. 1984. Modelling cliff development in south Wales. Savigear re-viewed. *Zeitschrift für Geomorphologie* **28**, 405–26.

Kirkby, M.J. 1985a. The basis for soil profile modelling in a geomorphic context. *Journal of Soil Science* **36**, 97–122.

Kirkby, M.J. 1985b. A model for the evolution of regolith-mantled slopes. In *Models in geomorphology*, M.J. Woldenberg (ed.), 213–37. Boston: Allen & Unwin.

Kirkby, M.J. 1986. A two-dimensional simulation model for slope and stream evolution. In *Hillslope processes*, A.D. Abrahams (ed.), 203–22. Boston: Allen & Unwin.

Kirkby, M.J. 1990. A one-dimensional model for rill inter-rill interactions. *Catena Supplement* **17**, 133–46.

Komura, S. 1976. Hydraulics of slope erosion by overland flow. *Journal of the Hydraulics Division, Proceedings of the American Society of Civil Engineers* **102**, 1573–86.

Kuijper, C., J.M. Cornelisse and J.C. Winterwerp 1989. Research on erosive properties of cohesive sediments. *Journal of Geophysical Research* **94**, 14341–50.

Lambe, T.W. and R.V. Whitman 1969. *Soil mechanics*. New York: Wiley.

Lane, L.J., E.D. Shirley and V.P. Singh 1988. Modelling erosion on hillslopes. In *Modelling geomorphological systems*, M.G. Anderson (ed.), 287–308. Chichester: Wiley.

Laronne, J.B. 1981. Dissolution kinetics of Mancos Shale – associated alluvium. *Earth Surface Processes and Landforms* **6**, 541–52.

Laronne, J.B. 1982. Sediment and solute yield from Mancos Shale hillslopes, Colorado and Utah. In *Badland geomorphology and piping*, R. Bryan and A. Yair (eds), 181–92. Norwich: Geo Books.

Mackin, J.H. 1948. Concept of the graded river. *Bulletin of the Geological Society of America* **59**, 463–512.

Meyer, L.D. 1986. Erosion processes and sediment properties for agricultural cropland. In *Hillslope processes*, A.D. Abrahams (ed.), 55–76. Boston: Allen & Unwin.

Meyer, L.D. and E.J. Monke 1965. Mechanics of soil erosion by rainfall and overland flow. *Transactions of the American Society of Agricultural Engineers* **8**, 572–7, 580.

Moseley, M.P. 1973. Rainsplash and the convexity of badland divides. *Zeitschrift für Geomorphologie Supplement Band* **18**, 10–25.

Moss, A.J. and P.H. Walker 1978. Particle transport by continental water flow in relation to erosion, deposition, soils and human activities. *Sedimentary Geology* **20**, 81–139.

Moss, A.J., P.H. Walker and J. Hutka 1979. Raindrop-stimulated transportation in shallow water flows: an experimental study. *Sedimentary Geology* **22**, 165–84.

Moss, A.J., P. Green and J. Hutka 1982. Small channels: their experimental formation, nature and significance. *Earth Surface Processes and Landforms* **7**, 401–16.

Parchure, T.M. and A.J. Mehta 1985. Erosion of soft cohesive sediment deposits. *Journal of the Hydaulics Divi-*

sion, Proceedings of the American Society of Civil Engineers **111**, 1308–26.

Parker, G.G., Sr, C.G. Higgins and W.W. Wood 1990. Piping and pseudokarst in drylands. *Geological Society of America Special Paper* **252**, 77–110.

Parthenaides, E. 1965. Erosion and deposition of cohesive soils. *Journal of the Hydraulics Division, Proceedings of the American Society of Civil Engineers* **91**, 105–39.

Parthenaides, E. and R.R. Paaswell 1970. Erodibility of channels with cohesive banks. *Journal of the Hydraulics Division, Proceedings of the American Society of Civil Engineers* **96**, 755–71.

Rauws, G. 1987. The initiation of rills on plane beds of non-cohesive sediments. *Catena Supplement* **8**, 107–18.

Rauws, G. and G. Govers 1988. Hydraulic and soil mechanical aspects of rill generation on agricultural soils. *Journal of Soil Science* **39**, 111–24.

Savat, J. 1976. Discharge velocities and total erosion of a calcareous loess: a comparison between pluvial and terminal runoff. *Revue Geomorphologie Dynamique* **24**, 113–22.

Savat, J. 1980. Resistance to flow in rough supercritical sheetflow. *Earth Surface Processes* **5**, 103–22.

Savat, J. 1982. Common and uncommon selectivity in the process of fluid transportation: field observations and laboratory experiments on bare surfaces. *Catena Supplement* **1**, 139–60.

Savat, J. and J. De Ploey 1982. Sheetwash and rill development by surface flow. In *Badland geomorphology and piping*, R. Bryan and A. Yair (eds), 113–25. Norwich: Geo Books.

Schumm, S.A. 1956a. Evolution of drainage systems and slopes in badlands at Perth Amboy, New Jersey. *Bulletin of the Geological Society of America* **67**, 597–646.

Schumm, S.A. 1956b. The role of creep and rainwash on the retreat of badland slopes. *American Journal of Science* **254**, 693–706.

Schumm, S.A. 1962. Erosion on miniature pediments in Badlands National Monument, South Dakota. *Bulletin of the Geological Society of America* **73**, 719–24.

Schumm, S.A. 1963. Rates of surficial rock creep on hillslopes in western Colorado. *Science* **155**, 560–1.

Schumm, S.A. 1964. Seasonal variations of erosion rates and processes on hillslopes in western Colorado. *Zeitschrift für Geomorphologie Supplement Band* **5**, 215–38.

Schumm, S.A. and G.C. Lusby 1963. Seasonal variation of infiltration capacity and runoff on hillslopes in western Colorado. *Journal of Geophysical Research* **68**, 3655–66.

Seidl, M.A. and W.E. Dietrich 1991. Bedrock channel incision: an examination of Playfair's Law. *Geological Society of America Abstracts with Program*, A240.

Slaymaker, O. 1982. The occurrence of piping and gullying in the Penticton glacio-lacustrine silts, Okanagan Valley, B.C. In *Badland geomorphology and piping*, R. Bryan and A. Yair (eds), 305–16. Norwich: Geo Books.

Smith, K.G. 1958. Erosional processes and landforms in Badlands National Monument, South Dakota. *Bulletin of the Geological Society of America* **69**, 975–1008.

Smith, T.R. and F.P. Bretherton 1972. Stability and the conservation of mass in drainage basin evolution. *Water Resources Research* **8**, 1506–29.

Torri, D., M. Sfalanga and G. Chisci 1987. Threshold conditions for incipient rilling. *Catena Supplement* **8**, 97–115.

Wells, S.G. and A.A. Gutierrez 1982. Quaternary evolution of badlands in the southeastern Colorado Plateau, U.S.A. In *Badland geomorphology and piping*, R. Bryan and A. Yair (eds), 239–57. Norwich: Geo Books.

Willgoose, G., R.L. Bras and I. Rodriguez-Iturbe 1991a. A coupled channel network growth and hillslope evolution model, 1. theory. *Water Resources Research* **27**, 1671–84.

Willgoose, G., R.L. Bras and I. Rodriguez-Iturbe 1991b. A coupled channel network growth and hillslope evolution model, 2, nondimensionalization and applications. *Water Resources Research* **27**, 1685–96.

Willgoose, G., R.L. Bras and I. Rodriguez-Iturbe 1991c. Results from a new model of river basin evolution. *Earth Surface Processes and Landforms* **16**, 237–54.

Yair, A., H. Lavee, R.B. Bryan and E. Adar 1980. Runoff and erosion processes and rates in the Zion Valley badlands, northern Negev, Israel. *Earth Surface Processes* **5**, 205–25.

PLANTS ON DESERT HILLSLOPES 10

Carolyn F. Francis

INTRODUCTION

Texts on desert geomorphology have tended to pay little attention to the presence of vegetation. The main landforming processes in desert environments are fluvial and aeolian, which operate on a surface with a very reduced vegetation cover. Indeed vegetation is absent in many areas. Even in more favourable locations plant cover may not reach 50%, giving an impression of the predominance of bare ground. Biogenic processes affecting landform evolution have threrefore been overlooked or associated with minor, localized impacts.

During the last two decades, there has been a considerable increase in research on desert ecosystems, due largely to the activities of the International Biological Programme, resulting in the publication of several major texts such as Goodall and Perry (1979, 1981) and Evenari *et al.* (1985, 1986) on arid lands, and Miller (1981), Di Castri *et al.* (1981), and Kruger *et al.* (1983) on semi-arid and Mediterranean-type ecosystems. These studies have covered such topics as plant associations and ecosystem structure and functioning in the main semi-arid and arid zones.

Desert ecosystems are terrestrial systems occurring where rainfall is less than 300 to 500 mm y^{-1}. This upper boundary describes the conditions below which arboreal growth is restricted, where there is no deep percolation of soil moisture to groundwater storage, and where plant communities are increasingly characterized by xerophytic flora (Shmida 1985, Orshan 1986). The main limit to tree growth is the lack of water, which in turn varies with factors such as climate, geology, soil type, aspect, and groundwater conditions – hence the wide band defining the upper boundary to the desert zone. Within the desert zone there is a distinction between the spatially diffuse, steppic shrublands and grasslands of the semi-arid environments and the contracted vegetation patterns of the arid environments. Similar differences may be found between vegetation communities that benefit from runon or other sources of water to supplement annual rainfall and those that do not. The boundary between the semi-arid and arid zones has frequently been described as the 200- to 250-mm isohyet in many deserts and as the 100- to 150-mm isohyet in the North African and Middle Eastern deserts (Adams *et al.* 1978).

In the semi-arid zone, where annual rainfall may vary between 100 and 500 mm, a wide range of vegetation communities occurs, including woodland, shrubland, and grassland (Le Houérou 1981, 1986, Evenari *et al.* 1985, 1986, Shmida 1985, Shmida *et al.* 1986). The woodland, which may represent the original climax vegetation, has often been degraded by man and supports trees over 2 m high with canopy covers ranging between 20 and 80%. The shrubland may be evergreen or deciduous, with bushes between 0.5 and 2 m high, covering 30 to 50% of the ground in favourable conditions. Under more xeric conditions or where shrublands have been degraded by overgrazing, chamaephytic vegetation is found, dominated by dwarf shrubs with ground cover falling to 10 to 30%. Grasslands tend to be dominated by perennial species.

In the arid zone, precipitation falls below about 100 mm, vegetation cover contracts to the drainage lines, leaving the interfluves and pediments bare. The vegetation is characterized by chamaephytes, with ground cover falling below 10%, although this may increase significantly to over 50% after sufficient rainfall due to the growth of opportunistic plants such as annuals. Diffuse shrublands or grasslands may persist on deeper or stony soils, north-facing slopes, and sand dunes.

In hyperarid areas where annual precipitation may be less than 25 mm, perennial vegetation is concen-

Geomorphology of Desert Environments. Edited by Athol D. Abrahams and Anthony J. Parsons. Published in 1994 by Chapman & Hall, London. ISBN 978-94-015-8256-8

trated in the main wadis and depressions which have high water tables or receive substantial amounts of runon from surrounding areas or from sources outside the desert region. Perennial vegetation also occurs in areas with high mist and fog inputs. Opportunistic plants may still germinate and grow following rainfall.

The lack of available water is the most important limit to vegetation growth in deserts and is evident at different spatial and temporal scales. On a transect from humid environments to deserts there is a general, positive correlation between vegetation parameters (be they cover, plant size, biomass, or productivity) and average annual precipitation (Whittaker and Niering 1975, Noy-Meir 1985, Shmida *et al.* 1986). Annual rainfall is highly variable, and this variability increases with aridity, so that in semi-arid areas with 300 to 400 mm y^{-1} rainfall variability may be 30 to 40%, while in arid areas with about 100 mm y^{-1} variability rises to 60 to 80% and exceeds 100% in hyperarid regions. Given the strong correlation between vegetation and rainfall, this will lead to significant inter-annual variations in productivity, particularly in areas where the vegetation is rainfed or is dominated by annuals and short-lived perennials. As the environment becomes more arid, the lack of water increasingly dominates over other limits to growth.

Other climatic factors cause stress in plants, limiting their growth in deserts. The interception of solar irradiance, compounded by the reflection of solar radiation from light-coloured soils with a high albedo, creates high heat loads on leaves during the day. These loads affect plant temperature, transpiration, and photosynthesis (Miller 1983). Extreme diurnal temperature ranges and air dryness also cause plant stress.

Physical characteristics of the environment affect vegetation in various ways. Rock domes, pavements, pediments, and duricrusts are inhospitable locations for plants given the lack of soil and moisture. Mobile sand dunes are generally devoid of vegetation due to both the inability of plants to germinate and grow in an unstable substrate and the blasting action of wind-driven sand grains. Events such as extensive flooding and accelerated soil erosion may destroy existing vegetation and permanently alter the plant associations on revegetating slopes by irreversibly changing soil parameters.

The topography, geology, and soil type all affect the redistribution of rainfall through their influence on rates of soil infiltration, soil moisture storage, and runoff patterns (Noy-Meir 1981, Olsvig-Whittaker *et al.* 1983). Areas shedding water, such as interfluves, steep slopes, rock outcrops, and soils with low infiltration rates, have proportionately less available water for plant growth for a given rainstorm than receiving areas such as small depressions, runnels, channels, alluvial fans, and plains. The storage capacities of soils and lithology vary, thus influencing vegetation quantity. For example sandy and gravelly soils usually have higher soil moisture values than adjacent silty and clayey soils due to higher infiltration rates. The microtopography of slopes provides many niches for water storage such as microdepressions, crevices, and pockets under stones.

The lack of nutrients in the soil, especially nitrogen and to a lesser extent phosphorus, has been observed to limit growth, as evidenced by lower productivity during the second year of two consecutive wet seasons with above average rainfall (Lee 1981). The excess of certain chemicals in the soil, notably soluble salts (which induce physiological aridity), and also boron and selenium, restrict growth of non-tolerant species (West 1981).

In addition, interactions between plants may limit plant growth through their influence on spatial patterns and species composition. There has been considerable debate on the effect on competition for resources, particularly water but also nutrients, on spatial patterns of plants. Allelopathic substances in litter from some arid species inhibit the germination and growth of plants nearby.

It is perhaps not surprising that vegetation patterns are highly correlated with geomorphological features. The spatial distributions of plant associations in the main deserts of the world often respond to topographical units, geology, or soil type (e.g. Ayyad 1981, Evenari *et al.* 1985, 1986). Changes in vegetation composition have also been explained in terms of environmental gradients from the continental scale to the mesoscale (e.g. along bajadas and across playas: Bowers and Lowe 1986, Wondzell *et al.* 1990) to the microscale (e.g. across dunes: Yeaton 1988).

As a result of the limits to plant growth in deserts, the amount of vegetation is low compared with other more humid environments. It is also highly variable both spatially and temporally, and it shows a strong response in amount, pattern, and species composition to the constraints of the physical environment. In its presence and functioning, the vegetation is also interacting with the surrounding environment, for example by protecting the ground from erosional processes, redistributing water and nutrients, and influencing soil formation. This interaction, if significant, can result in plants changing

the physical environment, and having a proactive role in landform development. In order to assess the role of plants in desert geomorphology, it is necessary to address four questions.

(a) Do plants significantly affect geomorphological processes in deserts?
(b) Does the presence of vegetation cause the development of specific landforms which would otherwise not occur in deserts?
(c) Do changes in vegetation cause significant changes in landform development?
(d) Which desert environments are most sensitive to changes in vegetation?

Before trying to answer these questions, it is necessary first to review the ways in which vegetation has evolved in response to the environment.

PLANT ADAPTATIONS TO ARIDITY

Plants have developed a range of strategies, which may be classified as physiological, morphological, and behavioural, to cope with the environmental constraints in deserts (Evenari *et al.* 1971). Physiological adaptations refer to the mechanisms by which plants function – for example, transpiration and photosynthesis – and these are often coupled with changes in the morphology of the plant – for example, leaf structure – and behavioural patterns. These developments have occurred over a long timespan and are continuing. The result is that plants evolve to improve their chances of survival in a given environment and with time colonize more extreme environments, thereby extending their influence. As the environment becomes more severe, the adaptations to aridity become more pronounced.

Plant adaptations to arid conditions are covered extensively in the ecological literature (Evenari *et al.* 1971, Adams *et al.* 1978, Harris and Campbell 1981, MacMahon and Schimpf 1981, Heathcote 1983, Evenari 1985), and only a brief outline is considered here. This outline pays particular attention to those adaptions which have a bearing on geomorphic processes principally through their effect on spatial and temporal variations in plant cover, resource use, and nutrient cycling.

There are three basic types of plants, hydrophytes, mesophytes, and xerophytes which are adapted to live in, respectively, waterlogged soils or water, moist conditions, and deserts. Both mesophytes and xerophytes live in arid environments, but xerophytes become more common with increasing aridity. Xerophytes can be divided into three broad groups according to the strategy adopted for coping with drought: (a) plants which withstand desiccation, (b) plants which are active during the dry season, and (c) plants which are inactive during the dry season. Within each group, typical physiological, morphological, and behavioural strategies are discussed.

Some algae and lichen are capable of withstanding prolonged desiccation and rehydration over many cycles. In a dehydrated state they are metabolically inactive and are resistant to temperature extremes. Following rain, algae and lichen switch rapidly to a metabolic state and can take up water from dew, mist, and water vapour (if the relative humidity exceeds 70%) as well as rain. Additionally, many lichens can photosynthesize at low temperatures, and hypolithic algae can photosynthesize at low light intensities. Lichen and algae in deserts have low growth rates but may play a significant role in weathering and hydrological processes.

Plants which remain active during the dry season include trees, shrubs, dwarf shrubs, and biseasonal annuals which form the permanent framework of vegetation in deserts. Drought-avoiding species rely on adaptations to reduce transpiration losses, store water within tissue matter, or metabolize more efficiently. The leaves and stems of these plants may have thick, dense cuticles and sunken stomata to reduce transpiration and hairy leaves to trap a thin layer of saturated air around the plant which reduces transpiration further. Under extreme conditions plants may shed parts such as leaves, cortex and branches to reduce the transpiring area, although photosynthesis may continue through the green stems of some species. During a growing season, the replacement of large winter leaves with small, more drought-resistant leaves, results in increased efficiency in transpiration, particularly as the summer leaves may not only be smaller but also anatomically distinct. High water losses during the day through transpiration can be replenished during the night as the root systems continue to absorb soil moisture while transpiration losses are negligible. Succulents absorb and store water in order to continue to function during the dry period.

In areas with a high water table, such as oases, salt marshes, and main wadis, plants have access to moisture throughout the dry season and may be characterized by features indicative of high rates of water loss such as a high ratio of conducting to non-conducting tissue or high root to shoot ratios.

Plants which are inactive during the dry season include those with bulbs or rhizomes (geophytes), small perennial herbs (nanochamaephytes and hemicryptophytes), and ephemerals (therophytes).

The bulbs and rhizomes lie dormant, possibly for several years, until sufficient rain encourages root growth. The dwarf herbaceous plants avoid drought conditions by shedding leaves and stems and by becoming inactive during the dry season. Ephemerals may account for 50 to 60% of all desert plants and avoid drought by completing their life cycle from germination to reproduction within a few weeks or months following rainfall. Ephemerals have often developed special seed dispersion and germination mechanisms to improve reproductive success rates and are often characterized by an inability to vary their transpiration rate, have shallow root systems, and regulate their size according to the available moisture.

Studies of some desert plants have shown that they follow photosynthetic pathways distinct from species living in mesic environments. Plants which absorb CO_2 during the day via open stomata for immediate photosynthesis are referred to as C_3 plants. However, some plants follow the C_4 pathway whereby the stomata are open at night, and CO_2 is absorbed and stored temporarily in organic acids in the plant. Photosynthesis still occurs during the day, but the stomata are closed to minimize transpiration losses, making the C_4 pathway more efficient during high stress conditions. Some plants can select either pathway, depending upon the prevailing conditions, and the choice is closely related to water shortage, high temperatures, or high salinity. This ability to select the most appropriate pathway is described as crassulacean acid metabolism (CAM), and plant families exhibiting this strategy include Agavaceae and Cactaceae.

It has been suggested that the development from C_3 to C_4 and CAM plants represents an evolutionary sequence responding to drought conditions. It has been observed that C_3 plants occur in more mesic areas, and as rainfall decreases and becomes more variable, these are replaced by C_4 and finally CAM plants.

The adaptations to environmental constraints described so far relate largely to stress imposed by climatic factors. However, some plants have also developed ways of adapting to their physical environment, most notably plants growing in areas of sandy dunes. Plants which succeed in mobile sand have to be able to survive lack of water particularly during germination, rapid burial or exposure of seedlings and the stems and roots of mature plants, and lesions caused by sand blasting. Special adaptations include rapid elongation of seedling roots and the reproduction of adventitious roots and new stems near the new ground level (Bendali *et al.* 1990, Danin 1991).

The phenology (e.g. germination, plant growth, flowering, litterfall, and dormancy) of desert plants is closely related to plant type and climatic factors, particularly rainfall but also temperature and light. There are numerous studies of the phenology of semi-arid ecosystems (Lieth 1974, Di Castri *et al.* 1981, Kummerow *et al.* 1981) but relatively few of arid environments (Ackerman and Bamberg 1974, Ludwig and Whitford 1981, Bertiller *et al.* 1991).

In areas with markedly seasonal climates, there is generally a corresponding seasonal variation in plant phenology. This variation may be triggered by changes in soil moisture, temperature, or length of day, although the timing and magnitude of this variation vary between species, regions, and years. A common pattern of variation in plant phenology is for a period of vegetation growth during the rainy season to be followed by litterfall and plant death during the dry season.

With respect to geomorphic processes, the onset of the rainy season may be associated with a period of reduced vegetation cover, particularly in communities dominated by plants which are inactive during the dry season, leaving relatively more soil exposed to erosive forces. During the dry season plants which remain active, standing dead, and litterfall afford some protection to the soil surface, the effect being greater in more humid areas. For example, Table 10.1 presents rates of annual litterfall from arid and semi-arid environments. The lower plant densities in arid areas result in low overall litterfall inputs to the soil, although litterfall rates from individual plants may be similar between arid and semi-arid environments. However, in some arid areas rainfall is so sporadic and unpredictable that it is not possible to talk about a rainy season nor of seasonal variations in plant phenology. Instead, in these areas variations in plant phenology are better viewed as a series of pulsed responses to rainfall.

THE IMPACT OF PLANTS ON GEOMORPHIC PROCESSES IN DESERTS

The structure and functioning of plants affect erosional forces and the redistribution of resources in desert environments. Here, structure refers to static attributes such as the three-dimensional shape of plants, both above and below ground, spatial distribution of plants, and species composition of communities. The above-ground structure of plants changes the micro-climate under and around plants and modifies the characteristics of rainfall and wind. These in turn have implications for the magnitude of erosional processes. The functioning of plants refers to dynamic attributes of the growth of individual

Table 10.1 Annual litterfall rates ($g\ m^{-2}\ y^{-1}$) from arid and semi-arid environments

Vegetation type	*Dominant plant*	*Region*	*Litterfall*	*Source*
Desert ecosystems – shrubland	*Ambrosia dumosa* and *Larrea tridentata*	Mojave Desert	19.4–53.0	Strojan *et al.* (1979)
Semi-arid ecosystems – matorral	Mixed shrubland *Anthyllis cytisoides* *Pinus halepensis*	Murcia, Spain	121.9 47.9 93.7	Francis and Thornes (unpublished)
Fynbos	*Leucospermum parile*	South Africa	71.5–84.0	Mitchell *et al.* (1986)
Coastal sage scrub	*Salvia leucophylla* and *Artemisia californica*	Southern California	194	Gray and Schlesinger (1981)
Garrigue	*Quercus coccifera*	Southern France	228–261	Rapp and Lossaint (1981)
Sclerophyll scrub	Mixed	Sydney, Australia	490	Maggs and Pearson (1977)

plants and communities which cause the redistribution of resources, such as the soil moisture and nutrients, and changes in soil structure. The combined effect of both structure and function is to interact significantly with geomorphic processes associated with weathering and soil formation and hydrologic and aeolian processes acting on hillslopes.

WEATHERING AND SOIL FORMATION

Flora in desert environments cause both chemical and mechanical weathering of bedrock and rock fragments. A wide range of microflora (epilithic, chasmolithic, and endolithic lichens, free-living cyanobacteria, fungi, and bacteria) and the root systems of some plants (rhizophagolithophytes) weather rocks. The microflora attack the face of soft rocks producing a microbial weathering front (Krumbein and Jens 1981). This weathering causes patterns of microperforations on the rock surface, exfoliation of rock flakes, and etches out pebbles and boulders. Biogenic rock varnishes (Chapter 6) develop when the microbial weathering fronts attack harder rocks or harder layers within soft rock, such that secretions of iron and manganese are formed at rates greater than the rate of penetration of the weathering front. The result is a varnish consisting of iron and manganese hydroxides, organic matter, clay minerals, and other matter which, once formed, protects the microflora trapped between the varnish and the rock from the climatic extremes of the desert environment.

Desert soils (Chapter 4) vary considerably in their texture and mineral content. Mature soils tend to occur on sites which have been vegetated over a long time. However, typically desert soils are characterized by low levels of organic matter and nutrients and accumulations of soluble salts (such as sodium and chloride), carbonates, and gypsum. Furthermore, organic matter and nutrients tend to be concentrated in the upper soil horizons (10 cm) and decrease rapidly with depth. The presence of plants changes the physical and chemical characteristics of soils and exacerbates the spatial heterogeneity.

Comparative studies of soil properties from locations under bushes and in interbush areas have identified strong spatial variations. Fireman and Hayward (1952) found a correlation between crown size and increases in pH, total soluble salts, and exchangeable sodium. Increases in exchangeable sodium under *Sarcobatus vermiculatus* had a marked effect on soil tilth, as indicated by permeability and moisture retention. Romney *et al.* (1977) and Rostagno *et al.* (1991) found significantly higher values of exchangeable cations (sodium and potassium), organic carbon, and nitrogen under plants compared with interplant locations.

Litterfall is the main contributor of organic matter and nutrients to the soil. This may be trapped around the plant itself or be redistributed by wind until it is deposited in depressions or around obstacles, including other plants (West 1979, Binet 1981). As a result, the distribution of litter is low and uneven, with concentrations tending to occur around plants.

Litter may decompose (a) by abiotic processes such as the leaching of solubles, photochemical degradation and disintegration due to wind, trampling, or raindrops, or (b) by biotic processes such as the action of microflora, termites, and other fauna. Biotic processes are restricted by lack of moisture, particularly on the soil surface, but can be significant in soils (Moorhead and Reynolds 1989). Decomposition is favoured around plants compared with open ground because of locally higher soil moisture levels, shading, nutrients, and denser root networks which promote soil microbial activity (Binet 1981).

Litterfall may also increase soil salinity around

plants, as some species concentrate salts in leaves which are then shed. This salinization process may be complemented by soil moisture movements around the root system and the build-up of a saline horizon. Alkalization and calcification may also develop locally around root systems (West 1981).

The root systems of arid plants have not been well studied, although they are thought to improve soil permeability, redistribute soil moisture and soluble chemicals, and add to soil organic matter through root death. Kummerow (1981) found that within a given community different species have distinct root structures in order to take advantage of different soil moisture stores. Some species have shallow but horizontally extensive root networks to maximize use of infiltrating rainwater. Alternatively Adams *et al.* (1978) recorded examples of mesquite roots reaching 20 m and tamarisk roots 50 m. Soil depth has a significant impact on root structures, such that deep-rooting species adopt shallower rooting patterns where soil depth is limited. However, the roots of chasmophytes will penetrate rock fissures in search of water, particularly where the lithology is limestone or dolomite.

HYDROLOGIC PROCESSES

Comparative studies of vegetated and unvegetated slopes in desert environments have shown that vegetation significantly affects the distribution of water on hillslopes. During storms, vegetation can alter the amount and spatial variability of rainfall reaching the ground by intercepting the raindrops which may then either evaporate, drip on to the soil surface, or be channelled as stemflow to the base of the plant. For example, Návar and Bryan (1990) studied interception losses and rainfall redistribution in individual shrubs of *Diospyrus texana*, *Acacia farnesiana*, and *Prosopis laevigata* for a semi-arid vegetation community in north-east Mexico. They found that of the 230 mm of rainfall occurring during 17 storms, interception losses accounted for 27%, throughfall for 70%, and about 3% of the gross rainfall became stemflow. Furthermore they found significant variations in stemflow between and within species, with stemflow averaging 321 ml min^{-1} for *D. texana*, and 115 ml min^{-1} for both *A. farnesiana* and *P. laevigata*, showing that the structure of some plants favours soil moisture accumulation around the stem.

The vegetation canopy also alters the kinetic energy of the rainfall by changing the distribution of drop sizes and velocities. Under low growing, dense shrubs and grassland, the kinetic energy is reduced as the raindrops impact the soil at less than terminal velocity, leading to lower rates of soil particle detachment. However, under high growing trees, such as found in oases, riverine galleries, or in the semi-arid woodlands, the kinetic energy of rainfall may be increased compared with areas of open ground due to the coalescence of droplets in the canopy which fall and reach terminal velocity before impacting on the soil.

Soil evaporation is usually more rapid from the bare ground between plants than from the shaded area under plants, and this differential further contributes to the spatial variation in soil moisture. Shading under plants also reduces the light intensity and air temperature, often providing a more favourable microclimate for many smaller plants. However, it is difficult to determine which factors encourage the understorey, for example, the increased soil moisture or nutrients, or lower temperatures. Walker (1974) found that artificial shading resulted in increased herbaceous production and that the plants remained greener for longer. Smith *et al.* (1987) reported that responses to artificial shading varied between species: species composition of annuals became more diverse but biomass fell, evergreen plants *Larrea tridentata* exhibited higher growth rates in sunny locations, while the deciduous *Ambrosia deltoidea* had higher growth rates in shaded microsites.

Infiltration rates are known to be spatially variable due to factors governing soil surface characteristics, soil structure, permeability, and vegetation. Infiltration tends to be higher under plants due to the ameliorating influence they have on soil structure. In matorral shrublands in south-east Spain, López *et al.* (1984) recorded infiltration rates after one hour ranging between 0.23 and 1.49 cm min^{-1} under a variety of vegetation species, compared with 0.1 to 0.29 cm min^{-1} on weathered, bare marl soils, and 0.04 to 0.12 cm min^{-1} on unweathered, bare marl soils. Stark (1973) found that infiltration rates were eight to ten times greater under shrubs than in the open on desert soils with a high clay fraction. Rostagno *et al.* (1991) found that mean infiltration rates after 35 minutes of simulated rainfall applied at a rate of 70 mm h^{-1} were significantly higher beneath shrub clumps (3.3 cm h^{-1}) than in the intervening unvegetated areas (0.5 cm h^{-1}).

The presence of a litter layer and soils with high organic matter tend to promote infiltration through higher permeability. Walker (1974) noted that infiltration rates correlated with the percentage of litter cover and basal cover of caespitose, perennial grasses, and were nine times faster on a litter-covered

sandy loam than on bare soil sites in a semi-arid ecosystem in south-central Africa. The bare soil surface was characterized by impermeable, hydrophobic, algal crusts, which in laboratory experiments required two hours to soften and allow absorption. As storms in the study area are usually of less duration, infiltration rates are inhibited on bare soils. In comparison, the caespitose grass tufts on the vegetated soils funnel water rapidly to their own roots. With vegetation affecting spatial patterns of infiltration and runoff, it will also potentially affect spatial patterns in soil erosion (Romero-Díaz *et al.* 1988).

AEOLIAN PROCESSES

Plants also affect rates and patterns of wind erosion. The above-ground biomass acts as an obstacle to air flow, increasing near-ground turbulence, reducing velocities in and leewards of the plant, and promoting eddy circulation. Lichens and algal crusts protect the soil surface from entrainment, and near-surface root systems may help to stabilize the soil. On a flat surface, wind velocities may increase up to 120% on the flank side of the bush and decrease to between 20 and 50% of the upwind velocity in the lee of the bush (Ash and Wasson 1983). Both the change in velocity and the physical obstruction of branches and stems cause the deposition of airborne particles within the plant, including dust, sand, microflora and fauna, litter, seeds, and nutrients attached to dust nucleii. The accumulation of such material around plants increases soil fertility and may create phytogenic mounds.

Ash and Wasson (1983) observed that on a transect from semi-arid to arid zones in Australia, there was an increase in mobility on dune crests and upper flanks associated with a decrease in vegetation. On the basis of these field observations, a simple model suggested that sand mobility would occur for vegetation covers up to 35%.

As plants colonize sand dunes they improve the soil stability by trapping silt-sized particles and organics which make the soil more cohesive and nutrient-rich and help to improve soil structure, moisture retention, and fertility. These factors, in turn, promote higher levels of plant productivity. Vegetation is clearly an important means of stabilizing dunes, and a decrease in vegetation may lead to increased erosion, loss of nutrients, further reductions in vegetation, and the reactivation of sand fields (Tsoar and Møller 1986, Bendali *et al.* 1990).

Active dunes tend to occur in areas with annual precipitation less than 150 mm, and where vegetation is sparse or absent. However, vegetated dunes do occur in areas with 100 mm of rainfall, and perennial vegetation has been found on dunes in north-west Sinai where annual precipitation is about 50 mm y^{-1} (Tsoar and Møller 1986). Relict desert dunes also occur in areas where annual rainfall currently exceeds 800 mm, indicating previous changes in climate.

DO PLANTS GIVE RISE TO CHARACTERISTIC LANDFORMS?

Landforms which owe their origin to plants consist of hillocks or hummocky ground where plants have acted as a focus for deposition or differential soil erosion rates. Both rehboub and nebka are mounds caused by the deposition of windborne particles around plants. Rehboub are generally small, reaching 0.1 to 1.0 m high and 0.5 to 5.0 m long, with the main axis oriented parallel with the prevailing wind direction. They tend to be strongly asymmetrical, with a steep face on the windward side and shallow tail in the lee of the obstacle. These hillocks can be very mobile and tend to occur on sandy plains where the annual rainfall lies between 50 and 200 mm and vegetation cover is less than 20% (Le Houérou 1986). Nebka develop where plants grow sufficiently rapidly to remain on top of the mound as detritus is deposited around the plant. The mounds may eventually reach 1 to 5 m in height and 2 to 10 m in diameter and are often ovoid or ellipsoid in form. If periods of accumulation are episodic, layers of dust and sand may alternate with layers of plant litter. With time the mounds also tend to become relatively rich in organic matter, nutrients, microorganisms, flora, and fauna.

The distribution of loess in semi-arid and arid areas may be due to vegetation as well as topographical controls. Yaalon and Dan (1974) found that in the most arid parts of the south and east Negev, wind-deposited loess accumulated in areas of dense vegetation (e.g. by springs), but elsewhere the loess was reworked by wind and wash erosion. In less arid areas of the central Negev highlands, the diffuse vegetation was still not sufficient to prevent erosion, but loess was trapped in hollows and pockets on hillslopes, and accumulated in the valleys where it was colonized by vegetation. In the semi-arid areas, loess covers large areas, including the steeper slopes, partly as a result of the effectiveness of the denser vegetation cover in trapping and stabilizing the sediments.

Differential rates in soil erosion due to splash and runoff result in the development of hummocky

terrain. Rostagno and del Valle (1988) examined such terrain in north-eastern Patagonia. Here discrete shrub clumps between 0.8 and 2.0 m high grow on mounds averaging 0.4 m high and up to 3.55 m long with a density of 450 mounds per hectare. In this area wind is thought to play a minor role as the soil surface particles are too coarse to be entrained. A comparison of permeabilities does favour a theory of differential soil erosion rates due to preferential overland flow production between mounds.

Parsons *et al.* (1992) suggested a combined mechanism of rainsplash (causing the accumulation of sediment under bushes) and wash erosion (causing a lowering of the interbush areas) leading to the creation of the mounded topography. They found that rainsplash during simulated storms resulted in net accretion on the mounds under shrubs and that the particle size of the rain-splashed material was similar to that forming the upper part of the mounds. The coarser, armour deposit in the intermound areas was consistent with the loss of fines by rain splash and sheet erosion.

The presence of vegetation has also contributed to the development of patterned ground described as *steppe tigrée* landscape in Algeria and eastern Morocco, *brousse tigrée* of Niger and Mali, vegetation arcs in Somalia and Jordan (Le Houérou 1981), and the grove and intergrove patterns of eastern Australia (Mabbutt and Fanning 1987, Tongway and Ludwig 1990). This patterned ground consists of alternating vegetated (plant cover 30 to 60%) and unvegetated (plant cover 5 to 10%) bands lying along the contour (also see Chapter 4). Species composition also varies between the bands, with more xeric species occurring in the bare runoff areas. This type of pattern ground occurs typically on shallow slopes (3 to 7%), on silty soils in open low woodlands, with the bands reaching over 1 km in length. The vegetated bands are usually 10 to 20 m wide and the bare strips 50 to 100 m wide (Tongway and Ludwig 1990). Runoff occurs on the bare strips causing soil erosion, which in turn leads to the development of armoured or crusted soils or the exposure of more compact soil. The runoff infiltrates into the more permeable soils in the vegetated bands, and sediment is deposited, leading to further improvements in soil conditions. The bands appear to move downslope with time, although rates have not been estimated. Both Mabbutt and Fanning (1987) and Tongway and Ludwig (1990) associated the grove and intergrove patterns with microtopography. Also Mabbutt and Fanning (1987) found that in areas characterized by narrow banding patterns, the vegetation bands tended to coincide with greater depths to the hard pan. They also found that variations in soil texture between the grove and intergrove locations only occurred in the upper few centimetres, indicating preferential patterns of sediment transport and deposition.

DO CHANGES IN VEGETATION CAUSE SIGNIFICANT CHANGES IN LANDFORM DEVELOPMENT?

It has been shown that the presence of plants affects the environment through a variety of ways, such as by redistributing soil moisture and nutrients and by altering erosional processes. It has also been shown that vegetation parameters are highly variable both spatially and temporally. If there are conditions under which vegetation has a significant impact on the environment, then it follows that changes in vegetation may be expected to cause changes in the environment. The evidence for such an interrelationship between vegetation and environment can be found in the historical record, from observations in the recent past, and by modelling, and such evidence relates mainly to the process of desertification.

Le Houérou (1981) reconstructed changes in vegetation in the northern Sahara over the last 2500 years. These changes, he argued, have led to the creation and extension of desert landforms in areas with annual average rainfall between 50 and 250 mm. During this period there is no evidence of climatic change, but historical records, and archaeological, sedimentological, and vegetation studies, point to changes in vegetation resulting from agriculture. Between 2500 and 2200 years BP the arid zone of North Africa receiving more than 100 mm of precipitation annually was thought to be covered by forest. From 2300 to 1330 years BP, this region was cultivated extensively, resulting in intense soil erosion and vegetation degradation. These processes may have contributed to the decline of agriculture by exhausting soil fertility. The agricultural society collapsed and was succeeded by a low density, pastoral society between 1330 and 100 years BP. During the past 100 years, an exponential population increase has led to a second phase of desertification.

Similar patterns of widespread degradation attributed to agricultural development have been observed in other deserts over the past 100 years. This degradation is usually due to the introduction of grazing and settlement in the desert margins. Williams and Calaby (1985) noted that whilst soil erosion is low in the arid areas of Australia, it is widespread in the semi-arid areas associated with

population centres and agriculture and has resulted in, among other things, the exposure of salt scalds.

Walker *et al.* (1981) described the changes in vegetation which typically occur in semi-arid savanna lands with the introduction of ranging and associated changes in soil parameters and erosion processes. The original vegetation community consists of open grassland with occasional shrubs and trees. The cattle graze preferentially on the grasses reducing their biomass, and they compact the soil by trampling. The composition of grass species changes first as a response to grazing. There follows a decline in perennial grasses and an increase in woody vegetation. Both the depletion of the herbaceous layer and trampling reduce infiltration rates and hence water inputs to the soil, and this desiccation of the soil favours the growth of deeper rooting shrubs and trees compared with the herbaceous layer. Once the nature of the surface soil has changes may have little effect on landform but soil may require a long time to recuperate. Such changes may have little affect on landform but significantly affect the productivity of ecosystems.

In north-eastern Sinai, widespread denudation of the vegetation on the dune systems is thought to account for a change in the morphology of dunes from smoothly rounded, straight, linear dunes, to sinuous, sharp-crested seif dunes (Tsoar and Møller 1986). This change has come about since 1948 due to an increase in the concentration of the bedouin population and pressure on the vegetation from overgrazing and collecting wood for fuel and shelter.

WHICH DESERT ENVIRONMENTS ARE MOST SENSITIVE TO CHANGES IN VEGETATION?

In order to assess which desert environments are susceptible to changes in vegetation, it is necessary to consider both the stability of landforms and desert ecosystems, as well as feedback mechanisms between the biotic and abiotic components of the environment. The stability of a system refers to its ability to remain the same or at least to return rapidly to the same conditions following some perturbation. If the system is stable, positive feedback mechanisms will ensure the return of the system to its characteristic state, but if it is unstable, negative feedback mechanisms may lead to the creation of a new stable state.

Certain types of landforms are more sensitive to erosion due to the erodibility of the substrate, the nature of the erosional forces, and relief. Areas of bedrock outcrops and heavily armoured surfaces are relatively unsusceptible to erosion and would be little affected by the presence or absence of vegetation. Such areas include hammadas, inselbergs, rock domes and other bedrock outcrops, and soil or rock surfaces capped by duricrusts or coarse fragments such as regs. Where the main erosive agent is running water, areas with relief such as alluvial fans and valley-side slopes provide more scope for erosion than flat alluvial floodplains and broad valley floors. For example, the subdued relief of much of Australia (Williams and Calaby 1985) dampens the potential for erosion. Finally, the erosive forces need to occur with sufficient force and frequency to erode the soil. Although some 20% of the area of Australia is covered by sand dunefields (much with an average of 10% vegetation cover rising to 30% in the south), Ash and Wasson (1983) suggested that the present-day wind system is not strong enough to erode the soil, even if all the vegetation were removed, and that an increase in windiness by 20 to 30% is required to cause widespread erosion.

Desert ecosystems appear to be unstable in the short term as plant populations, productivity, biomass, and species composition fluctuate widely within and between years depending on rainfall patterns. In the longer term they appear to be stable in the sense that vegetation responds similarly to a given set of conditions. In a humid year, vegetation cover, productivity, and species composition will tend to be similar to other favourable years and not necessarily to the previous poor season. Thus desert ecosystems tend to have low persistence, which reflects their dependence on rainfall, and high resilience, which refers to their ability to recover under favourable conditions (Noy-Meir 1974).

Because vegetation responds to available resources, resource richness and reliability are important attributes in determining the spatial and temporal characteristics of vegetation (Shmida *et al.* 1986). Where resources are reliable and rich, vegetation cover would be expected to be high and stable. Such conditions are rare in deserts (for example oases) where resources are more likely to be rich but unreliable (for example, on well-drained soils in areas with periodic rainfall), poor but reliable (for example, where moisture is permanently available but of low quantity or quality such as dew or saline groundwaters), or poor and unreliable (for example, in hyperarid regions with low nutrient soils and sporadic rainfall). From the hyperarid to semi-arid zones the resources become increasingly reliable and richer, allowing greater abundance of vegetation.

Vegetation variability now has to be linked with the sensitivity of the environment to change. Field studies have shown that soil erosion increases, often

non-linearly, as vegetation cover falls. In particular, the rate of increase in soil erosion is most rapid when vegetation cover falls between 40 and 10%. At lower values, the amount of cover has little protective effect on erosion rates, so areas with consistently low quantities of vegetation are little affected by variability in plant cover. Similarly where cover normally exceeds 50%, erosional processes are dampened. Consequently, it is the areas where vegetation cover varies between 40 and 10% on erodible substrate which potentially are affected by erosional processes and, hence, landform change.

Soil erosion is a destabilizing factor in desert ecosystems because of the concentration of nutrients and the seedbank in the upper few centimetres of the soil horizon. Erosion of this layer rapidly reduces soil fertility, infiltration, and the moisture retention capacity of soils, which in turn affect the viability of the remaining vegetation. This can result in a negative feedback leading to the predominance of bare, eroded slopes (Thornes 1985). This process may be irreversible leading to changes in species composition, ecosystem productivity, the development of eroded landscapes or unstable dune systems.

Other feedback systems may also be operating. For example, Charney (1975) suggested that a decrease in vegetation cover over a region may significantly increase albedo levels for light coloured desert soils which would lead to local heat losses and changes in air circulation. In the Sahel this could result in lower rainfall which would reinforce further reductions in vegetation cover. Ettahir (1989) suggested that high levels of evapotranspiration are an important source of moisture for summer rainfall in neighbouring deserts and a reduction in evapotranspiration, resulting from changes in albedo, could also lead to the persistence of droughts in deserts.

CONCLUSIONS

While it is evident that vegetation variability occurs due to natural processes, reports of widespread desertification invariably involve the activities of humans. This impact arises through the development of unsuitable agricultural practices around the desert margins and in semi-arid areas. The resulting decrease in vegetation may result in an increase in the effectiveness of erosion processes, causing the reactivation of vegetated dune systems or the development of badland topography. To prevent such consequences, it is necessary to manage these rangelands successfully and improve our understanding of the interactions between biotic and abiotic components of the environment.

REFERENCES

Ackerman, T.L. and S.A. Bamberg 1974. Phenological studies in the Mojave Desert at Rock Valley (Nevada Test Site). In *Phenology and seasonality modeling*, H. Lieth (ed.), Ecological Studies, Volume 8, 215–26. New York: Springer.

Adams, R., M. Adams, A. Willens and A. Willens 1978. *Dry lands: man and plants*. London: The Architectural Press.

Ash, J.E. and R.J. Wasson 1983. Vegetation and sand mobility in the Australian desert dunefield. *Zeitschrift für Geomorphologie Supplement Band* **45**, 7–25.

Ayyad, M.A. 1981. Soil-vegetation-atmosphere interactions. In *Arid land ecosystems: structure, functioning and management, Volume 2*, D.W. Goodall and R.A. Perry (eds), 9–31. Cambridge: Cambridge University Press.

Bendali, F., C. Floret, E. le Floc'h and R. Pontanier 1990. The dynamics of vegetation and sand mobility in arid regions of Tunisia. *Journal of Arid Environments* **18**, 21–32.

Bertiller, M.B., A.M. Beeskow and F. Coronato 1991. Seasonal environmental variation and plant phenology in arid Patagonia (Argentina). *Journal of Arid Environments* **21**, 1–11.

Binet, P. 1981. Short-term dynamics of minerals in arid ecosystems. In *Arid land ecosystems: structure, functioning and management, Volume 2*, D.W. Goodall and R.A. Perry (eds), 325–56. Cambridge: Cambridge University Press.

Bowers, M.A. and C.H. Lowe 1986. Plant form gradients on Sonoran desert bajadas. *Oikos* **46**, 284–91.

Charney, J.G. 1975. A biogeophysical feedback mechanism in arid lands. In *Arid zone development: potentialities and problems*, Y. Mundlak and S.F. Singer (eds), 181–8. Cambridge, MA: Ballinger.

Danin, A. 1991. Plant adaptations in desert dunes. *Journal of Arid Environments* **21**, 193–212.

Di Castri, F., D.W. Goodall and R.L. Specht (eds) 1981. *Ecosystems of the World, Volume 11: Mediterranean-type shrublands*. Amsterdam: Elsevier.

Ettahir, E.A.B. 1989. A feedback mechanism in annual rainfall, Central Sudan. *Journal of Hydrology*, **110**, 323–34.

Evenari, M. 1985. Adaptations of plants and animals to the desert environment. In *Ecosystems of the World, Volume 12A: hot deserts and arid shrublands*, M. Evenari, I. Noy-Meir and D.W. Goodall (eds), 79–92. Amsterdam: Elsevier.

Evenari, M., I. Noy-Meir and D.W. Goodall (eds) 1985. *Ecosystems of the World, Volume 12A: hot deserts and arid shrublands*. Amsterdam: Elsevier.

Evenari, M., I. Noy-Meir and D.W. Goodall (eds) 1986. *Ecosystems of the World, Volume 12B: hot deserts and arid shrublands*. Amsterdam: Elsevier.

Evenari, M., L. Shanan and N.H. Tadmor 1971. *The Negev: the challenge of a desert*. Cambridge, MA: Harvard University Press.

Fireman, M. and H.E. Hayward 1952. Indicator significance of some shrubs in the Escalante Desert, UT: *Botanical Gazette* **114**, 143–55.

Goodall, D.W. and R.A. Perry (eds) 1979. *Arid-land ecosystems: structure, functioning and management, Volume 1*. Cambridge: Cambridge University Press.

Goodall, D.W. and R.A. Perry (eds) 1981. *Arid-land eco-*

systems: structure, functioning and management, Volume 2. Cambridge: Cambridge University Press.

Gray, J.T. and W.H. Schlesinger 1981. Biomass, production and litterfall in the coastal sage scrub of southern California. *American Journal of Botany* **68**, 24–33.

Harris, G.A. and G.S. Campbell 1981. Morphological and physiological characteristics of desert plants. In *Water in Desert Ecosystems*, D.D. Evans and J.L. Thames (eds), 59–74. Stroudsburg, PA: Dowden, Hutchinson and Ross.

Heathcote, R.L. 1983. *The arid lands: their use and abuse*. London: Longman.

Kruger, F.J., D.T. Mitchell and J.U.M. Jarvis 1983. *Mediterranean-type ecosystems: the role of nutrients*, Ecological Studies, Volume 43. Berlin: Springer.

Krumbein, W.E. and K. Jens 1981. Biogenic rock varnishes of the Negev Desert (Israel) – an ecological study of iron and manganese transformation by cyanobacteria and fungi. *Oecologia* **50**, 25–38.

Kummerow, J. 1981. Structure of roots and root systems. In *Ecosystems of the World, Volume 11: Mediterranean-type shrublands*, F. Di Castri, D.W. Goodall and R.L. Specht (eds), 269–88. Amsterdam: Elsevier.

Kummerow, J., G. Montenegro and D. Krause 1981. Biomass, phenology, and growth. In *Resource use by chaparral and matorral*, P.C. Miller (ed.), Ecological Studies, Volume 39, 69–96. New York: Springer.

Lee, K.E. 1981. Effects of biotic components on abiotic components. In *Arid land ecosystems: structure, functioning and management, Volume 2*, D.W. Goodall and R.A. Perry (eds), 105–23. Cambridge: Cambridge University Press.

Le Houérou, H.N. 1981. Long-term dynamics in arid-land vegetation and ecosystems in North Africa. In *Arid land ecosystems: structure, functioning and management, Volume 2*, D.W. Goodall and R.A. Perry (eds), 357–84. Cambridge: Cambridge University Press.

Le Houérou, H.N. 1986. The desert and arid zones of northern Africa. In *Ecosystems of the World, Volume 12B: hot deserts and arid shrublands*, M. Evenari, I. Noy-Meir and D.W. Goodall (eds), 101–47. Amsterdam: Elsevier.

Lieth, H. (ed.), 1974. *Phenology and seasonality modeling*, Ecological Studies, Volume 8. New York: Springer.

López, F., M.A. Romero, A. Ruíz, G.C. Fisher *et al.* 1984. Eroséon y ecología en la España semiarida. *Cuadernos de Investigacion geografica* X, Vol. 1, 113–26.

Ludwig, J.A. and W.G. Whitford 1981. Short-term water and energy flow in arid ecosystems. In *Arid land ecosystems: structure, functioning and management Volume 2*, D.W. Goodall and R.A. Perry (eds), 271–99. Cambridge: Cambridge University Press.

Mabbutt, J.A. and P.C. Fanning 1987. Vegetation banding in arid Western Australia. *Journal of Arid Environments* **12**, 41–59.

MacMahon, J.A. and D.J. Schimpf 1981. Water as a factor in the biology of North American desert plants. In *Water in desert ecosystems*, D.D. Evans and J.L. Thames (eds), 114–71. Stroudsburg, PA: Dowden, Hutchinson & Ross.

Maggs, J. and C.J. Pearson 1977. Litter fall and litter decay in coastal scrub at Sydney, Australia. *Oecologia* **31**, 239–50.

Miller, P.C. (ed.) 1981. *Resource use by chaparral and matorral*, Ecological Studies, Volume 39. New York: Springer.

Miller, P.C. 1983. Canopy structure of Mediterranean-type shrubs in relation to heat and moisture. In *Mediterranean-type ecosystems: the role of nutrients*, F.J. Kruger, D.T. Mitchell and J.U.M. Jarvis (eds), Ecological Studies, Volume 43, 133–66. Berlin: Springer.

Mitchell, D.T., P.G.F. Coley, S. Webb and N. Allsopp, 1986. Litterfall and decomposition processes in the coastal fynbos vegetation, south-western cape, South Africa. *Journal of Ecology* **74**, 977–93.

Moorhead, D.L. and J.F. Reynolds 1989. Mechanisms of surface litter mass loss in the northern Chihuahuan desert: a reinterpretation. *Journal of Arid Environments* **16**, 157–63.

Návar, J. and R. Bryan 1990. Interception loss and rainfall redistribution by three semi-arid growing shrubs in northeastern Mexico. *Journal of Hydrology* **115**, 51–63.

Noy-Meir, I. 1974. Stability in arid ecosystems and the effects of man on it. In *Structure, function and management of ecosystems*, A.J. Cavé (ed.), 220–5. Wageningen: Centre for Agricultural Publications.

Noy-Meir, I. 1981. Spatial effects in modelling of arid ecosystems. In *Arid land ecosystems: structure, functioning and management, Volume 2*, D.W. Goodall and R.A. Perry (eds), 411–32. Cambridge: Cambridge University Press.

Noy-Meir, I. 1985. Desert ecosystem structure and function. In *Ecosystems of the World, Volume 12A: hot deserts and arid shrublands*, M. Evenari, I. Noy-Meir and D.W. Goodall (eds), 93–103. Amsterdam: Elsevier.

Olsvig-Whittaker, L., M. Shachak and A. Yair 1983. Vegetation patterns related to environmental factors in a Negev Desert watershed. *Vegetatio* **54**, 153–65.

Orshan, G. 1986. The deserts of the Middle East. In *Ecosystems of the World, Volume 12B: hot deserts and arid shrublands*, M. Evenari, I. Noy-Meir and D.W. Goodall (eds), 1–28. Amsterdam: Elsevier.

Parsons, A.J., A.D. Abrahams and J.R. Simanton (1992). Microtopography and soil-surface materials on semi-arid piedmont hillslopes, southern Arizona. *Journal of Arid Environments* **22**, 107–15.

Rapp, M. and P. Lossaint 1981. Some aspects of mineral cycling in the garrigue of southern France. In *Ecosystems of the World, Volume 11: Mediterranean-type shrublands*, F. Di Castri, D.W. Goodall and R.L. Specht (eds), 289–301. Amsterdam: Elsevier.

Romero-Díaz, M.A., F. López-Bermúdez, J.B. Thornes, C.F. Francis *et al.* 1988. Variability of overland flow erosion rates in a semi-arid Mediterranean environment under matorral cover, Murcia, Spain. *Catena Supplement* **13**, 1–11.

Romney, E.M., A. Wallace, H. Kaaz, V.Q. Hale *et al.* 1977. Effect of shrubs on redistribution of mineral nutrients in zones near roots in the Mojave Desert. In *The belowground ecosystem: a synthesis of plant-associated processes*. J.K. Marshall (ed.), Science Series No. 26, 303–10. Fort Collins, CO: Colorado State University.

Rostagno, C.M. and H.F. del Valle 1988. Mounds associated with shrubs in aridic soils of northeastern Patagonia: characteristics and probable genesis. *Catena* **15**, 347–59.

Rostagno, C.M., H.F. del Valle and L. Videla 1991. The influence of shrubs on some chemical and physical properties of an aridic soil in north-eastern Patagonia, Argentina. *Journal of Arid Environments* **20**, 179–88.

Shmida, A. 1985. Biogeography of the desert flora. In *Ecosystems of the World, Volume 12A: hot deserts and arid shrublands*, M. Evenari, I. Noy-Meir and D.W. Goodall (eds), 23–77. Amsterdam: Elsevier.

Shmida, A., M. Evenari and I. Noy-Meir 1986. Hot desert ecosystems: an integrated view. In *Ecosystems of the World, Volume 12B: hot deserts and arid shrublands*, M. Evenari, I. Noy-Meir and D.W. Goodall (eds), 379–87. Amsterdam: Elsevier.

Smith, S.D., D.T. Patten and R.K. Monson 1987. Effects of artificially imposed shade on a Sonoran Desert ecosystem: microclimate and vegetation. *Journal of Arid Environments* **13**, 65–82.

Stark, N. 1973. Nutrient cycling in a desert ecosystem. *Bulletin of the Ecological Society of America* **54**, 21–30.

Strojan, C.L., F.B. Turner and R. Castetter 1979. Litter fall from shrubs in the northern Mojave Desert. *Ecology* **60**, 891–900.

Thornes, J.B. 1985. The ecology of erosion. *Geography* **70**, 222–36.

Tongway, D.J. and J.A. Ludwig 1990. Vegetation and soil patterning in semi arid mulga lands of Eastern Australia. *Australian Journal of Ecology* **15**, 23–34.

Tsoar, H. and J.T. Møller 1986. The role of vegetation in the formation of linear sand dunes. In *Aeolian geomorphology*, W.G. Nickling (ed.), 75–95. Boston: Allen & Unwin.

Walker, B.H. 1974. Ecological considerations in the management of semi-arid ecosystems in south-central Africa. In *Structure, function and management of ecosystems*, A.J. Cavé (ed.), 124–9. Wageningen: Centre for Agricultural Publications.

Walker, B.H., D. Ludwig, C.S. Holling and R.M. Peterman 1981. Stability of semi-arid savanna grazing systems. *Journal of Ecology* **69**, 473–98.

West, N.E. 1979. Formation, distribution and function of plant litter in desert ecosystems. In *Arid land ecosystems: structure, functioning and management, Volume 1*, D.W. Goodall and R.A. Perry (eds), 647–59. Cambridge: Cambridge University Press.

West, N.E. 1981. Nutrient cycling in desert ecosystems. In *Arid land ecosystems: structure, functioning and management, Volume 2*, D.W. Goodall and R.A. Perry (eds), 301–24. Cambridge: Cambridge University Press.

Whittaker, R.H. and W.A. Niering 1975. Vegetation of the Santa Catalina Mountains, Arizona. V. Biomass, production, and diversity along the elevation gradient. *Ecology* **56**, 771–90.

Williams, O.B. and J.H. Calaby 1985. The hot deserts of Australia. In *Ecosystems of the World, Volume 12A: hot deserts and arid shrublands*, M. Evenari, I. Noy-Meir and D.W. Goodall (eds), 269–312. Amsterdam: Elsevier.

Wondzell, S.M., J.M. Cornelius and G. Cunningham 1990. Vegetation patterns, microtopography and soils on a Chihuahuan desert playa. *Journal of Vegetation Science* **1**, 403–10.

Yaalon, D.H. and J. Dan 1974. Accumulation and distribution of loess-derived deposits in the semi-desert and desert fringe areas of Israel. *Zeitschrift für Geomorphologie Supplement Band* **20**, 91–105.

Yeaton, R.I. 1988. Structure and function of the Namib dune grasslands: characteristics of the environmental gradients and species distributions. *Journal of Ecology* **76**, 744–58.

PART FOUR

RIVERS

CATCHMENT AND CHANNEL HYDROLOGY

11

John B. Thornes

INTRODUCTION

Solar radiation, wind, and water are the driving agents of desert landscapes. Water has four major roles to play. First, in sustaining any life forms that exist; secondly, as a chemical substance which interacts with other chemical substances, notably salts; third, as a medium of transport of mass; and, fourth, as a direct source of energy. The last role, though small by comparison with the roles of solar and wind energy, may none the less be critical in determining the threshold of operation of runoff, through its impact on infiltration. Since infiltration is one of the major thresholds in dryland morphological development, the factors which control it have a role out of all proportion to the energy involved.

We have come to take for granted the well-known hydrological cycle of arid lands (as illustrated in Fig. 11.1). The hydrological cycle of desert environments has the same inputs and outputs, and there is the same requirement for the conservation of mass and energy.

It is the relative importance of the different components which is critical. In temperate environments percolation, throughflow, saturated flow, and groundwater play a most significant role. In dry environments infiltration normally only occurs to shallow depths, soil moisture is consistently low or very low, and overland flow is important, with deep percolation and groundwater being relatively unimportant except in suballuvial or externally recharged aquifers. This relative importance also varies spatially and through time more than in temperate environments. For example, under even sparse vegetation infiltration becomes relatively much more important than between vegetation. Under seasonal control, infiltration may be much more important in the wetter than in the drier season, and so on. As this balance changes so does the relative role of different geomorphic processes. The differences between desert and temperate hydrology from a geomorphological point of view are therefore more complex than simply a shift in the magnitude and frequency of events.

The major differences, which are illustrated and developed in the remainder of this chapter, can be summarized as follows.

(a) Rainfall occurs at high intensities, with low overall amounts, at irregular intervals, often with a strong seasonal bias and usually with a very large interannual variability.
(b) The rain falls on ground with a sparse or non-existent vegetation cover, which is irregular in its distribution and especially adapted to collect rainfall. Interception rates are low and highly variable and rapid direct evaporation of excess surface water is characteristic.
(c) Infiltration is largely controlled by the bare surface characteristics which range from sands to organic crusts and from stones to chemical precipitates.
(d) Losses due to evapotranspiration are dominated by soil-water availability and controlled by profile characteristics as well as by atmospheric stress; subsurface water movement may be significantly affected by regolith chemistry.
(e) Overland flow is relatively more likely when storms occur and the terrain over which it occurs may be exceptionally rough.
(f) Channel flow is ephemeral and, hence, significantly influenced by boundary conditions, especially transmission losses to alluvium.
(g) Groundwater obeys the same rules as in

Geomorphology of Desert Environments. Edited by Athol D. Abrahams and Anthony J. Parsons. Published in 1994 by Chapman & Hall, London. ISBN 978-94-015-8256-8

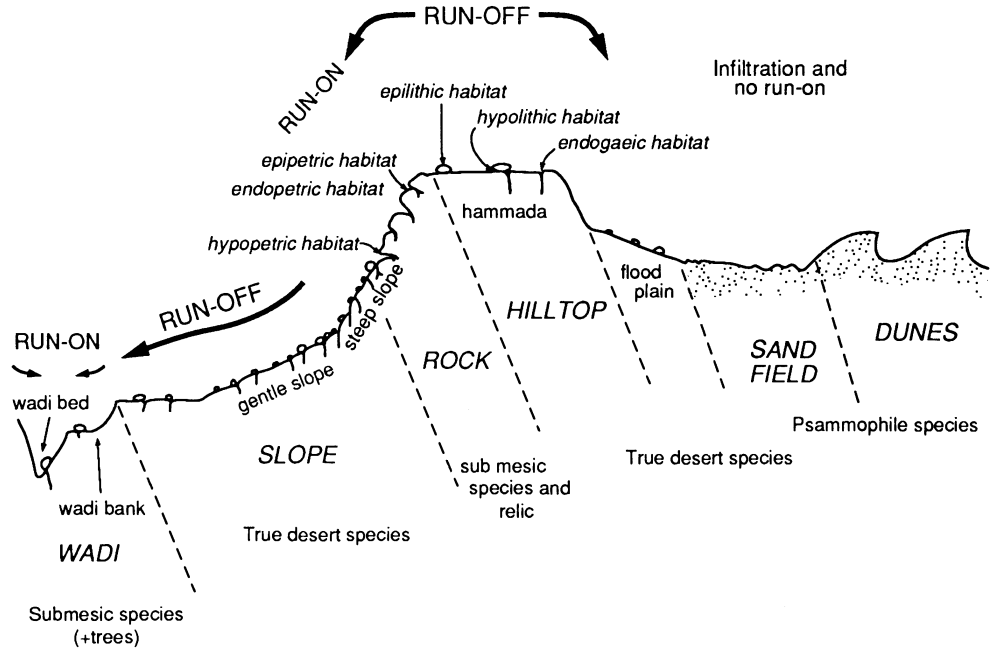

Figure 11.1 Elements of the hydrological cycle in arid lands (after Shmida *et al.* 1986).

temperate environments, but suballuvial aquifers assume a more significant hydrological role with ephemeral channel flow.

PRECIPITATION

MAGNITUDES AT DIFFERENT TIMESCALES

From a geomorphological point of view, annual rainfalls tend to determine the overall character of the environment through the vegetation condition because, to a first approximation, the gross vegetation biomass and productivity are determined by rainfall for areas with less than about 600 mm (Walter 1971, Leith and Whittaker 1975). Above this figure nutrients become more significant in limiting plant growth. Below it the physiological response of plants in biomass terms to gross precipitation may actually be quite variable because ultimately it is the available moisture for plant growth that is the controlling factor. This availability reflects evapotranspiration amounts and the water use efficiency of particular species (Woodward 1987). Shrubs and dwarf shrubs are the most conspicuous life forms in desert regions. At the wetter margin shrubs such as *Artemisia, Atriplex, Cassia, Ephedra, Larrea,* and *Retama* prevail, whereas in extreme deserts dwarf shrub communities are present, such as the Chenopodiacae, Zygophillaceae, and the Asteraceae (such as *Artemisia*). Typically the semi-deserts have 150 to 350 mm of rain, whereas the extreme deserts have less than 70 mm, according to Shmida (1985).

Generally here we follow Le Houerou (1979) in restricting deserts to environments with less than 400 mm y^{-1}, which in North Africa and in southern Europe corresponds to the northern limit of steppe vegetation, such as *Stipa tenacissima* and *Artemisia herba-alba*. Le Houerou differentiates extreme desert lands as those with less than 100 mm, corresponding to the northern border of typical desert plants, such as *Calligonium comosum* and *Cornulaca monacantha*.

Annual rainfall magnitudes are also reflected in altitudinal variations in plant cover. Whittaker and Niering (1964), for example, show the clear gradation from desert to forest developed in the Santa Catalina mountains of Arizona.

There have been several models which relate geomorphic processes or responses to annual rainfall amounts and temperature (Peltier 1950, Langbein and Schumm 1958, Carson and Kirkby 1972), and these consistently show low total magnitudes of rainfall having low rates of geomorphic activity but with sharply increasing rates up to a maximum at about 300 mm.

There is an enormous interannual variability in total amounts in dry areas. Figure 11.2 shows

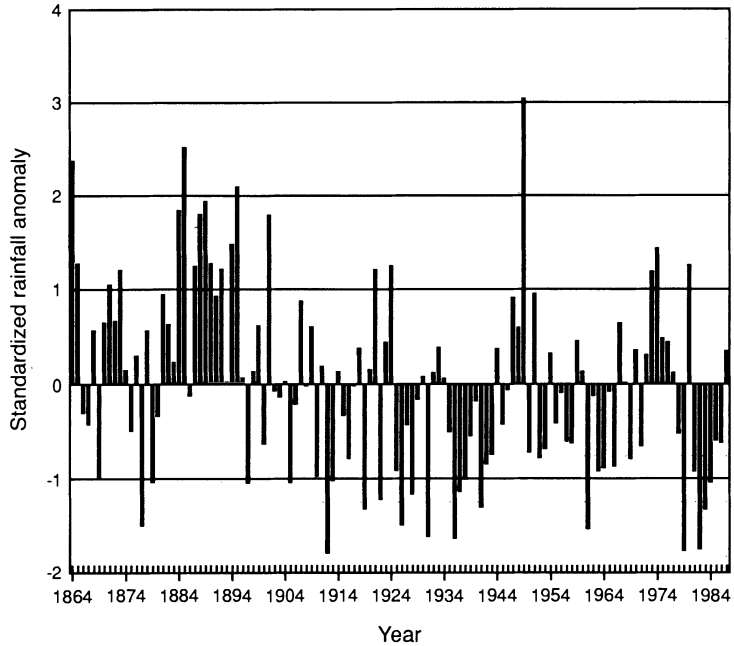

Figure 11.2 Annual rainfall anomalies for Murcia, south-east Spain (after Thornes 1991).

interannual variations of rainfall totals for Murcia, south-east Spain, for the last 30 years, expressed as rainfall anomalies (mean annual rainfall/standard deviation). Here the mean annual rainfall is 300 mm, and the interannual coefficient of variation 35%, a figure typical of semi-arid environments. Bell (1979) has shown that, in general, annual precipitation variability is highest in zones of extreme aridity and that the lowest variations are at the poleward margins of the deserts, where frontal rainfall forms a greater proportion of the total annual rainfall. As a general rule the standardized rainfall anomaly decreases as the mean annual rainfall increases.

The geomorphic significance of seasonal rainfall distribution varies with evapotranspiration because these together determine soil moisture conditions and infiltration rates, decomposition rates for organic matter, soil erodibility, evaporation rates, solute movement, and chemical precipitates.

Figure 11.3 shows the annual pattern of soil moisture for the Murcia site shown in Figure 11.2. The relative importance of seasonal rainfall totals depends on how much the plant cover varies. Typically in arid and semi-arid conditions the seasonal impact is principally on annual herbs. In semi-arid environments these may account for as little as 5% of the total cover, the amount increasing as the conditions become drier. The seasonality of rainfall is generally expressed in some ratio of monthly to annual rainfall. For example the Fournier index (Fournier 1960) expressed seasonality by the index p^2/P, where p is the rainfall of the wettest month and P the annual rainfall. By regression analysis he showed that this index is related to total sediment yield. The yield increases with seasonality and relief, and the rate of increase is greater in desert areas. More recently Kirkby and Neale (1987) indicated that it is seasonality, expressed as the degree of rainfall concentration, which leads to the characteristic Langbein and Schumm (1958) curve.

In areas of extreme aridity the rainfall is not strongly seasonal in amount except in the Gobi–Tarim basin, where cyclonic storms are blocked by the persistent Siberian High in winter. Towards the desert margins rainfall seasonality increases and most significant is the distribution of rainfall in relation to temperature. Around the central Australian desert, for example, long periods without rain are usual in the northern winter and the southern summer. In the Mojave Desert rain occurs in winter, in the Chihuahuan Desert in the summer, and the Sonoran Desert has both winter and summer rainfalls.

Event rainfall magnitudes are important in deter-

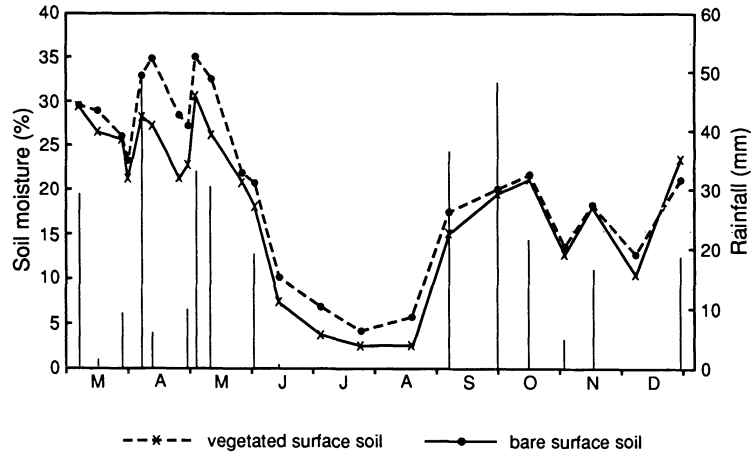

Figure 11.3 Seasonal fluctuations in soil moisture for the El Ardal site, Murcia, 1989–1990 under different ground conditions based on data for the MEDALUS project.

mining soil moisture characteristics, but generally in desert areas it is the high intensity that is geomorphologically important, as discussed below.

The idea of coupling magnitude and frequency was first developed comprehensively in geomorphology by Wolman and Miller (1960). Put simply it draws attention to the fact that it is not only the magnitude of the force applied by a process but also how frequently the force is applied which determines the work done by the process. In temperate environments their results suggest that it is the medium scale events of medium frequency that perform most geomorphic work. Ahnert (1987) has used the same concept to express the magnitude and frequency of climatic events. Plotting the event magnitude on the vertical axis and the log (base 10) of the recurrence interval of the event on the horizontal axis provides an alternative representation of the relationship. By fitting a regression model to the data he obtained the relationship

$$P_{24} = Y + A \log_{10}(\mathrm{RI}) \qquad (11.1)$$

where P_{24} is the daily precipitation of an event with recurrence interval of RI (in years), and the recurrence interval is obtained from RI = $(N+1)$/rank by magnitude in a list of n daily rainfall totals. Ahnert showed that Y and A are characteristics of the rainfall, and he used them as indices of magnitude and frequency. The map of California (Fig. 11.4a) indicates that both A and Y are generally low in the Mojave Desert. The indices can be obtained for other time intervals, for partial series (such as *P*-threshold), and for other variables such as frost frequency. Moreover, it is possible to derive the magnitude and frequency product and plot this against return period. For example, Ahnert calculated the curve for $(P - T_r)F$, where P is the daily rainfall, T_r a threshold value, and F the frequency of the event of magnitude $(P - T_r)$, and plotted this against recurrence interval. The family of curves (Fig. 11.4b) shows that in desert areas the overall product is low and that the maximum of the product occurs in tens of years rather than several times a year. This implies that most work is done by rather less frequent events, but not by very rare events. Recently De Ploey *et al.* (1991) have developed this idea further to provide an index of cumulative erosion potential.

In temperate environments there are a large number of small events and a much smaller number of large events, so the distribution tends to negative exponential and gives a straight line on the semi-log plot. Ahnert (1987) used this relationship to explore the characteristics of storm events, and this provides a useful comparison of the models for desert and temperate environments (Fig. 11.4). This pattern of magnitude and frequency can also be expressed for individual seasons.

RAINFALL INTENSITY

The intensity of rainfalls is especially important in determining the canopy storage and gross interception losses as well as the production of overland flow. Intensity also determines the compaction of soils and thus indirectly affects the infiltration capacity (Roo and Riezebos 1992). One of the simplest measures of intensity is the mean rainfall per rain

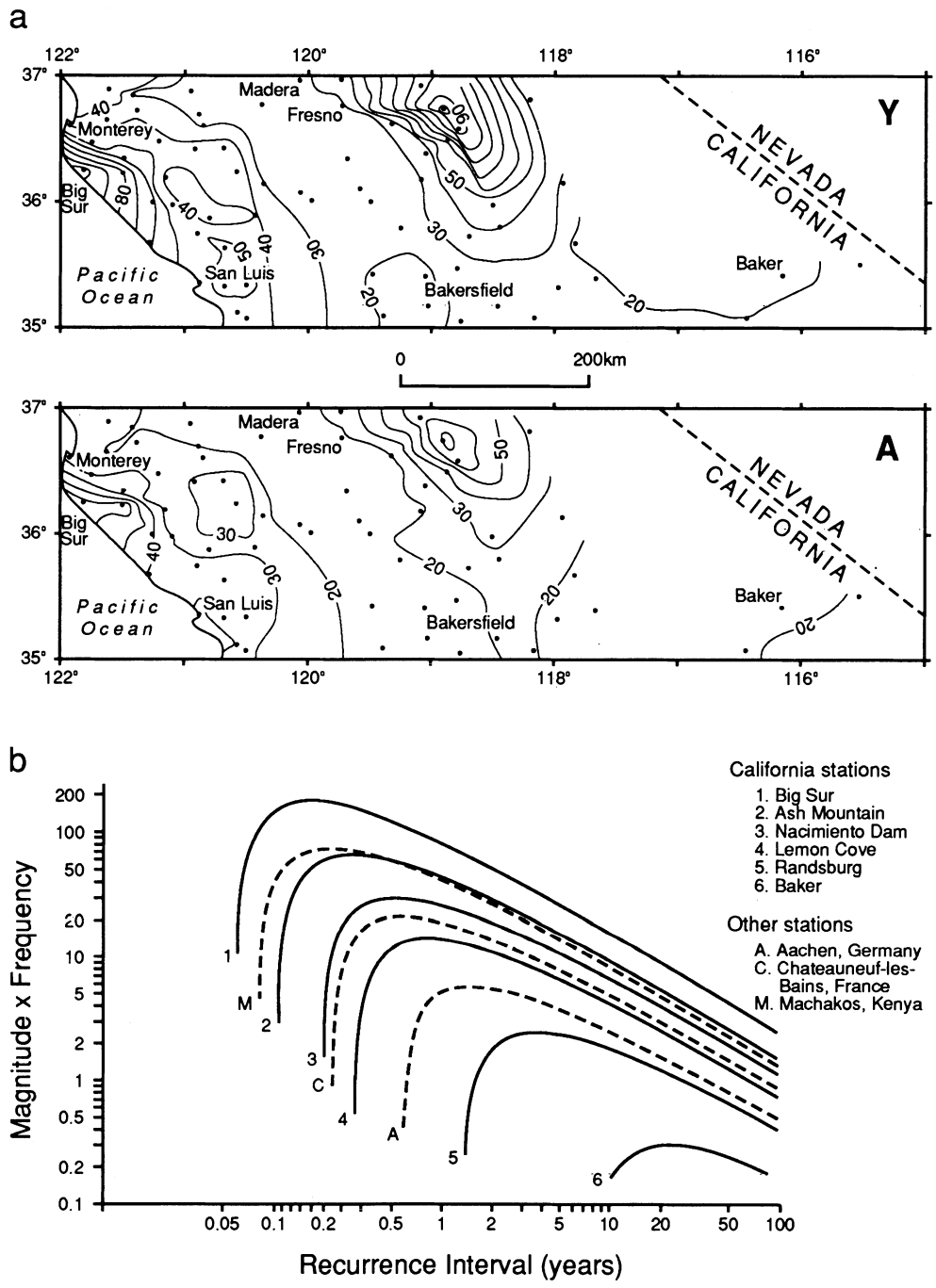

Figure 11.4 Frequency and magnitude distribution of rainfall (after Ahnert 1987). (a) Regional distribution of values of *A* and *Y* in California. (b) The product of magnitude and frequency for a variety of stations.

day. It provides the key parameter for providing the exponential distribution of rainfall magnitudes and deriving the excess above a critical threshold value (Thornes 1976). It is sensitive to the definition of rain day, but generally a figure of 0.2 mm is taken as the threshold. Average figures for desert areas are between 5 and 10 mm, and these tend to increase to the margins. These figures do not differ greatly from temperate areas and are generally less in the extreme deserts.

While mean rainfall per rain day is a useful index when only daily rainfall amounts are available (which is the case for large parts of the Earth and especially desert regions), the absolute intensity ($mm\ h^{-1}$) generally increases as shorter periods are considered. Although record intensities occur in humid tropical areas, intensities for arid areas are generally higher than those of temperate regions. For example, Dhar and Rakhecha (1979), working in the Thar Desert of India where average annual rainfall is 310 mm, found that one-day point rainfalls of the order of 50 to 120 mm have a recurrence interval of 2 years and that rainfalls associated with monsoon depressions can be from 250 to 500 mm in a single day. The peak daily rainfall can be several times the annual average. Berndtsson (1987), for example, observed that on 25 September 1969, 400 mm of rain fell at Gabes, central Tunisia, which is about five times the mean annual rainfall. In semi-arid south-eastern Spain the storms of 18–19 October 1973 produced rainfalls equal to the mean annual amount (300 mm) in a period of about 10 hours. In this semi-arid environment rainfall intensities of 70 mm typically recur about every 5 years.

Using the 1-hour duration and 2-year return period, Bell (1979) obtained figures typically of the order of 10 to 20 mm for central desert areas and 20 to 50 mm along desert margins. Again, this suggests that it is the desert margins where runoff effects are most likely to be geomorphologically important. He estimated the 'maximum probable' 1-hour rainfalls for the Australian arid region to be of the order of 180 mm at the poleward edge to 280 at the equatorwards margin. Similar figures have been estimated for the desert areas of the United States by Herschfield (1962), and Bell (1979) believed that they are probably typical of the arid zone in other parts of the world. Typically the 2-year 1-hour value has an intensity about ten times that of the 2-year 24-hour rainfall.

TEMPORAL VARIABILITY

For geomorphic purposes most data are of relatively short duration. Typically 40 to 50 years of daily rainfall records are available for the arid areas of the world. Autographic data, from which storm profiles can be constructed, are even rarer. For developing models of the impact of rainfall series it is therefore sometimes necessary to simulate series which have the same characteristics as the actual data. The problem is that small sample sizes preclude normal forcasting techniques and the variability of total rainfall in an event is quite high.

Within individual storm events there are often significant variations in intensity. Figure 11.5 illustrates a storm profile for the semi-arid Cuenca area of central Spain. The total rainfall for the storm was

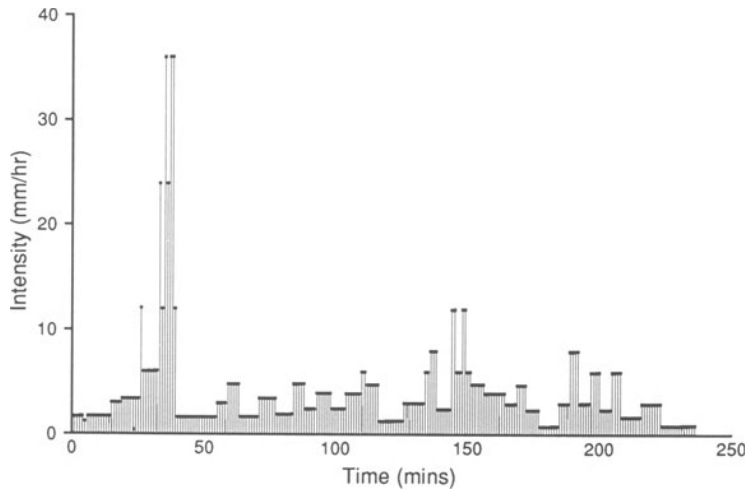

Figure 11.5 Rainfall storm profile for an autumn storm in Cuenca, Spain.

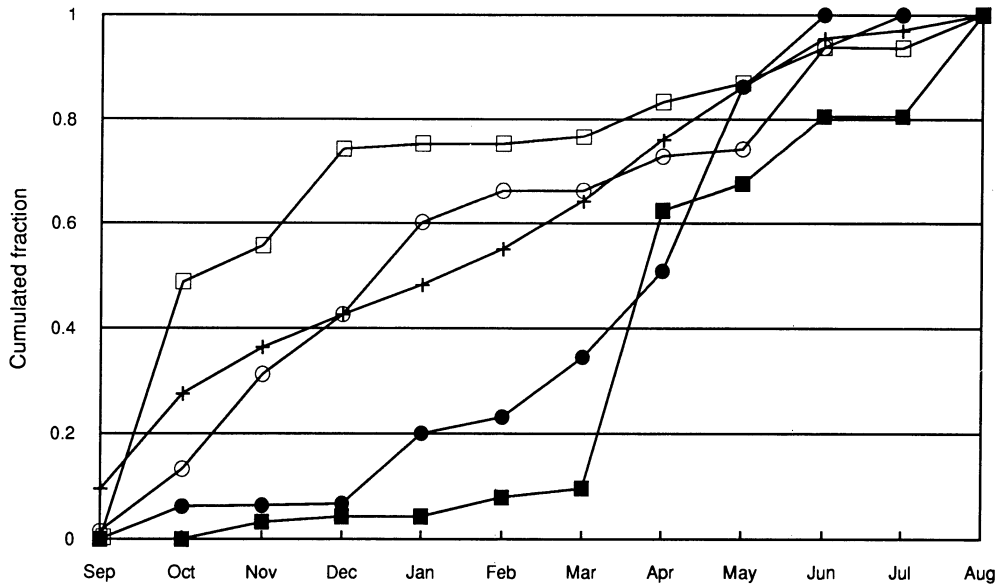

Figure 11.6 Seasonal variations in the annual distribution of rainfall for the province of Murcia, Spain. Key: □ = 1961; ○ = 1979; + = mean; ■ = 1981; ● = 1982.

24 mm, with an average intensity of 6 mm h^{-1} while the high burst in minutes 35 to 39 produced an intensity of 36 mm h^{-1}. Within-storm rainfall has been modelled by Jacobs *et al.* (1988) and a description of their approach is found below.

The distribution of events is reflected in the seasonal distribution of cumulative rainfall totals and these have a strong effect on plant growth in dry areas. For example Figure 11.6 shows the contrasts in rainfall patterns within the year for normal (1981), exceptionally wet (1961) and exceptionally dry years (1979, 1982) in south-east Spain. Lack of autumn rains inhibits the germination of seedlings, whereas lack of soil moisture in spring limits plant growth.

The seasonal distribution of event magnitudes and durations is also important from a runoff and infiltration point of view. Generally event magnitudes and durations reflect prevailing weather types, with cyclonic storms often giving long-duration, low-intensity rainfalls and convective (summer) storms giving short-duration, high-intensity rainfalls.

A simple seasonal model is provided by the Markov chain, in which sequences of rain and no-rain days and the rainfall magnitudes for these days are generated. Thornes and Brandt (in press) have provided a synthetic generator for the semi-arid regions of south-east Spain using this principle. The sequence of rain or non-rain days is obtained from a Markov probability matrix of transitions from rain–rain, rain–dry, dry–rain, and dry–dry days derived from the historical records on a seasonal basis. The magnitudes are then obtained from a two-parameter gamma distribution, again with seasonal parameters. Both the transition matrices and the gamma parameters were found to be stable over time in this environment.

A more sophisticated model was used by Duckstein *et al.* (1979) to investigate and simulate the structure of daily series. They define an event as a day having a precipitation greater than a constant amount, say 0.2 mm. The statistics of interest are then the number of events per unit time, the time between events, the depth of precipitation, the duration of precipitation, and the maximum intensity of rainfall in an event. A sequence is a number of rainfall events separated by three or fewer days. Then the dry spell duration is a run of days without rain, and the average seasonal maximum of the run of dry days defines extreme droughts. Finally, inter-arrival time is the time between the beginning of one sequence and the beginning of the next; in statistical terminology it is the renewal time.

For convective storms occurring in summer the events are independent and short (cf. Smith and Schreiber 1973). The probability of n events of j days duration is then given by the Poisson mass function

$$f_n(j) = \exp(-m)m_j/j! \qquad (11.2)$$

where m is the mean number of events per season.

The probability that the interarrival time T is t days is given by

$$f_T(t) = u\exp(-ut) \qquad (11.3)$$

where u is estimated from $1/\bar{T}$, with $\bar{T}$ the mean interarrival time between events. For Tucson, Arizona, u is estimated to be 0.27. Under some conditions, especially where the storms are more frequent (e.g. where a cyclonic element prevails), interarrival times may be better described by a gamma rather than an exponential distribution. Finally, the event magnitudes are also independent. For example in Granada province, southern Spain, Scoging (1989) found that 90% of summer storm rainfall lasted less than an hour and that the magnitude of the rainfall in an event is independent of its duration. Under these circumstances, which are most common for convective thunderstorms, the gamma distribution again provides a suitable model for rainfall magnitudes.

The amounts, intensities, and durations of storms are also found to vary significantly in the long term in dry as they do in temperate areas, and interest in these fluctuations has been heightened in recent years as the result of the potential implications of global warming for already dry areas.

Berndtsson (1987), for example, found that in Tunis from 1890 to 1930 there was a massive fall in mean annual rainfall and that after 1925 there was an oscillation of durations of 10 to 15 years. Similar phenomena have been recorded in other statistical analyses. Conte *et al.* (1989) demonstrated that oscillations in rainfall in the Western Mediterranean in the period after 1950 could be related to the Mediterranean Oscillation in barometric pressure. Thornes (1990) also observed both the steep decline in rainfall in the period 1890–1934 and oscillations in rainfall anomalies in the post-1950 period in the southern Iberian Peninsula. The rainfall decline, at $3\,\mathrm{mm\,y^{-1}}$, is of the order of magnitude currently predicted for climatic changes over the next 60 years by climatologists from general circulation models. The rainfall anomaly oscillations are in phase with those recorded by Conte *et al.* and almost exactly out of phase with those described for the Sahel.

SPATIAL VARIABILITY

If arid zone rainfall is difficult to predict in time, it is almost as difficult to predict in space. The spatial distribution of storms tends to be random in subtropical deserts. There is usually a poor correlation of rainfall amounts at stations only 5 km apart. It is rare for a single station to experience more than one storm in a day, and the spacing between concurrent storms is typically 50 to 60 km.

The development of rainfall in convective storms is quite complex and accounts for much of the locally highly concentrated rainfall amounts and intensities that accompany desert storms. Well-defined storm cells are born and then decay, and the cellular structure can give rise to well-defined rates of attenuation of rainfall with distance from the cell centres. Jacobs *et al.* (1988) examined summer data from a network of 102 gauges distributed over a $154\,\mathrm{km^2}$ area in Walnut Gulch Experimental Watershed, Arizona for the period 1970–1977, and they attempted to model the intensity and cumulative depth over temporal realizations of the process or for a particular event over space. The procedure assumes that a storm is born at maximum intensity and then decays exponentially through time, with the initial intensity being an independent exponentially distributed random variable. The spatial distribution of storm centres is modelled as a Poisson process, and the time of birth of each cell relative to storm outset is taken to be exponential. From these assumptions the variance and covariance structures of rainfall intensity and depth are derived analytically and appear to provide a reasonable representation of the structure of the storm patterns observed.

In comparison with the Walnut Gulch data, one of the best sets of rainfall data in a desert area in the world, the storm depths modelled by Jacobs *et al.* were found to be more homogeneous and isotropic over time. Zawadeski (1973) had already shown that storms are typically isotropic under about 10 km but increasingly anisotropic over larger distances.

INTERCEPTION

Our understanding of surface hydrological processes is very largely in terms of specific surfaces, such as bare soils, plants of various species and architecture, and more recently in terms of stone cover. In fact, desert surfaces usually comprise complex mixtures of these different types, just as satellite images represent complex mosaics of land use (Fig. 11.7). This means that both the understanding and modelling of such surfaces tend to be difficult. Moreover the very nature of desert soils with their chemical crusts, concentrated aggregates, complex surface roughness, and particular plant types means that hillslope hydrology (as opposed to hydraulics) of such regions is still in its relative infancy. Earlier treatises on desert hydrology, for example, have tended to simply reiterate the received wisdom from

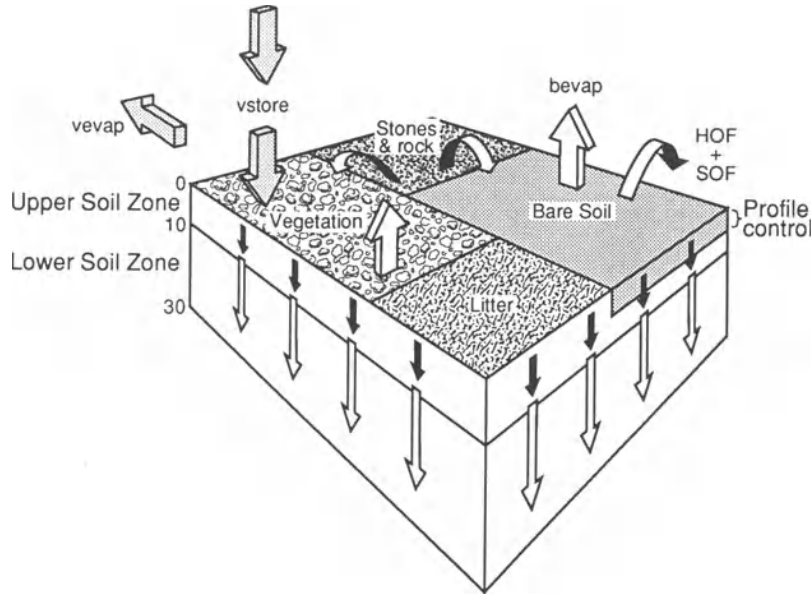

Figure 11.7 Compound character of surfaces in semi-arid and arid environments, showing major fluxes of evaporation (vevap, bevap), transpiration (trans), interception (vstore) and Hortonian and saturated overland flow (HOF, SOF).

temperate soils, which is, in reality, completely inappropriate.

Desert plants are structurally rather different from temperate and humid tropical plants in their life forms. They often have low leaf areas, especially adapted leaves and stems, and wide spacing (see below). The morphologies of several rangeland species of shrubs and grasses (e.g. *Cassia* sp., *Stipa tenacissima*) are designed to intercept rainfall and channel the water down as stemflow. This water infiltrates adjacent to the tree bole and produces enhanced water storage at depth. Slatyer (1965) showed that with mulga scrub once the interception store of 2 to 3 mm has been filled, stemflow accounts for up to 40% of the rain falling on the canopy, and falls of 15 to 20 mm of rain can cause about 100 litres of stemflow from adult trees. Stemflow equal to 30 to 40% of intercepted rain has also been found in semi-arid environments in the Zaragoza area of Spain by Gonzalez-Hidalgo (1991).

Evans *et al.* (1976), on the other hand, reported that about 90% of rainfall was converted into throughfall for creosote bush and about 65% for bursage. However, the percentage for different storms ranged from 67% to greater than 100% and from 26% to greater than 100% for creosote bush and bursage, respectively. Generally, in rangeland, losses from the canopy through the direct evaporation of intercepted water are thought to be unimportant (Johns *et al.* 1984). However, though the total loss to gross interception may be small, its role in redirecting water to the concentrated root zone below the stem may be very significant. The concentration of nutrients in the root zone is partly a testimony to this concentration of wash from the canopy itself. De Ploey (1982) has attempted to provide a simple model to estimate the interception properties of plant cover on the basis of stem density and stem angle and has simulated the behaviour of stems in the laboratory with a reasonable degree of success.

Stone cover is also important in determining the interception of water, but the picture is somewhat confused for two reasons. First, losses to runoff are estimated as the residual between water rate application by sprinkler and runoff from experimental micro-plots. Second, the loss rate is influenced by whether the stones are lying on the surface or embedded within it (Poesen *et al.* 1990). Our field experiments indicate that stones may intercept and store considerable volumes of water depending on their surface characteristics. Therefore, they probably account for much of the losses attributed to infiltration in sprinkler experiments. This question is further discussed below. The same is true of crusting. As yet we do not know the relative proportions attributable to interception, infiltration, and evaporation in determining the residual sum available for runoff.

UNSATURATED ZONE PROCESSES

Soils in deserts are as variable as, if not more variable than, their temperate counterparts. The effects of soil texture are emphasized, as profile control is dominant in the overall water balance. For example, Hillel and Tadmoor (1962), in a comparison of four desert soils in the Negev, showed that sandy soils wetted deeply, have the largest storage, the highest infiltration rates, and the lowest evaporation when compared with rocky slope soils and loessic and clay soils. The latter had very low storage as a result of surface crusting, poor absorption, and high evaporation rates. As a result, the plant growth capabilities were markedly different. Others too have shown that in sandy soils the upward movement of water vapour, facilitated by the open pore structure, may lead to condensation of water near the surface in winter-cold desert soils in amounts of the order of 15 to 25 mm.

A major driving force in desert soils is the high rate of near-surface evaporation. Water moves up through the soil as a result of the thermal gradient mainly through vapour transfer (Jurey *et al.* 1981). With available moisture the near-surface potential rates may reach 1500 to 2000 mm y^{-1}, at 2 m the rates are about 100 mm y^{-1}, and at 3 to 4 m they are practically negligible. As a result of this steep gradient, upward movement of water and, if available, salts is the dominant process in summer months, as in the *takyr* soils of Turkmenistan.

The stone content of desert soils generally increases with depth, though such soils may also have surface armouring induced by a variety of processes (Chapter 4). Field bulk density may be quite high for stoney soils, typically of the order of 1.8 compared with values of 1.0–1.4 for non-stoney soils. Mehuys *et al.* (1975) found little difference between stoney and non-stoney soils in the relationship between conductivity and soil tension, but strong differences in the relationship between conductivity and soil moisture. In two out of three cases the conductivity is higher in stoney than in non-stoney soils with similar soil moistures.

INFILTRATION

Infiltration rates on bare weathered soils in dry environments are often relatively high when surfaces are not compacted, especially where vegetation or a heavy surface litter occurs. Runoff is often critically determined by the controls of infiltration, especially vegetation at plot scales (Francis and Thornes 1990). In experiments using a simple sprinkler system at rates of 55 mm h^{-1}, with an expected recurrence interval of about 10 years, infiltration rates may be as high as 50 mm h^{-1} with runoff accounting for as little as 2 to 3% of the rainfall. However, under all circumstances the infiltration rates are highly variable.

In general, infiltration rates increase with litter and organic matter content of soils. One of the earliest investigations, by Lyford and Qashu (1969), showed that infiltration rates decreased with radial distance from shrub stems due to lower bulk density and higher organic matter content under the shrubs. Later investigations by Blackburn (1975) on semi-arid rangeland in Nevada examined the effects of coppice dunes (i.e. vegetation bumps) on infiltration, runoff, and sediment production. Using a sprinkler simulator at 75 mm h^{-1} on small plots, he analysed the average infiltration rates at the end of 30 min and found that the coppice dune rate was three to four times that for the dune interspace areas. The soil characteristics of the interspaces were most important in determining runoff rates, and infiltration rates were strongly negatively correlated with percentage bare ground. Similarly, Swanson and Buckhouse (1986), in a comparison of three subspecies of big sagebrush (*Artemisia tridentata*, *A. wyomingensis*, and *A. vaseyana*) occupying three different biotopes in Oregon, found no significant differences in final infiltrability between habitat type and climax understorey species. However, infiltration in shrub canopy zones had generally higher rates than shrub interspaces, confirming the results obtained by Lyford and Qashu (1969) and Blackburn (1975).

There is often an interaction between infiltration capacity, vegetation cover and aspect in dry environments. For example, Faulkner (1990), examining infiltration rates on sodic soils in Colorado, has found that aspect has a strong influence on infiltration rates through vegetation cover, though some caution needs to be exercised here because of the role of piping in infiltration rate and runoff control in the bare badland areas.

Gifford *et al.* (1986) examined the infiltrability of soils under grazed and ungrazed (20 years) crested wheatgrass (*Agropyron desertorum*) in Utah using both sprinkling and ring infiltrometers. They found that infiltration rates measured by the ring infiltrometer were 2.3 to 3.2 times higher than those measured by the sprinkling infiltrometer (cf. Scoging and Thornes 1979) and that season and grazing/non-grazing were the main sources of variation. The spring infiltrability values were double the summer values, and the ungrazed were three times the grazed values.

Infiltration rates are generally reduced by crusting, which may result from algal growth, rainfall compaction, and precipitate development. Thin algal crusts have an important role in stabilizing the soil surface, though there seems to be some disagreement as to its hydrological significance. Some workers claim that the crust, by limiting the impact of raindrops on a bare soil, actually prevents the development of a true rainbeat crust and thus the algae increase infiltration. A contrary view, however, is that the biological crusts have a strong water repellency and so increase runoff. Alexander and Calvo (1990) and Yair (1990) have investigated the organic crusting and attest to its significance in controlling surface runoff. Alexander and Calvo found that lichens provide crusting on north-facing but not on south-facing slopes and that lichens produce more rapid ponding and runoff but not more erosion. Yair reported that removal of the crust from sandy dune soils produced a dramatic increase in the time to runoff and that the runoff coefficient was an order of magnitude lower, largely due to reinfiltration.

On the other hand, compaction by raindrop impact leading to sealing significantly reduces infiltration (Morin and Benyami 1977). Roo and Riezebos (1992) have attempted to provide a model for the impact of crust development on infiltration amounts.

Finally, stones control the infiltration rates into soils to some extent. The general conclusion of the many field and laboratory studies on infiltration rates under a rock cover indicates a generally positive correlation between infiltration and stone cover, but Poesen *et al.* (1990) argued that this depends on whether the rocks are partially buried or resting on the surface. In the former case there tends to be a negative correlation because the stones intercept the rainfall and lead to higher evaporation and runoff rates, whereas in the latter case they tend to inhibit crusting and so encourage infiltration. Working on shrub lands, both Tromble *et al.* (1974) and Wilcox *et al.* (1988) obtained negative correlations between infiltration and stone cover, but the latter accounted for this in terms of the reduced opportunity for plant cover development, which enhances infiltration as noted above. In a recent field experiment Abrahams and Parsons (1991) also obtained a negative correlation between stone cover and infiltration rate and again explained this in terms of the higher infiltration rates under bushes where stones were generally absent (see Fig. 8.5). They concluded that, at least for shrub covered pediments, inverse relations between infiltration and stone cover could be used in modelling.

EVAPORATION FROM SURFACES AND TRANSPIRATION FROM PLANTS

Most literature for dry environments suggests that there is a high correlation between evapotranspiration and rainfall (Scholl 1974) and that in general the total annual evapotranspiration for desert environments is equal to the cumulative annual infiltration into the soil for the year. This is more or less equal to the annual precipitation minus the annual runoff. Moreover, at least once per year the soil moisture becomes more or less negligible and deep drainage is more or less negligible relative to total annual evapotranspiration. Therefore, the principal interest is in the temporal distribution of evapotranspiration during the year.

Actual estimates of the relative balance of the various components give a clear idea of the importance of evapotranspiration in the overall water budget. Renard (1969) suggested that evaporation and evapotranspiration from Walnut Gulch is about 85 to 90% of the incoming rainfall, and in the study by Floret *et al.* (1978) in Tunisia evaporation from bare soil alone was calculated to be between 40 and 70% of the total depending on the year. Evans *et al.*'s (1981) comparative analysis of bare soil and different plant species (creosote, mesquite, and sagebrush) revealed no significant differences between the bare soil and the vegetated sites for any extended period of time. Nor were there any differences between plant species, and most of the evapotranspiration took place in periods immediately following rainfall. Then the rates varied between 2.3 and 10 mm d^{-1}, with rates of 1 mm d^{-1} for extended periods of time between rainfall events and rates of less than 0.1 mm d^{-1} for the driest parts of the year.

These results emphasize the ability of desert plants to exist at high water stresses. Final water contents correspond to suctions of -10 to -50 bars. Typically the plant stress is uniformly distributed throughout the plant at dawn and in equilibrium with the soil suction. As the day develops the plant stresses increase so that for *Larrea tridentata* stresses of 40 to 65 bars are reached, and in *Ceratoides lanata*, for example, 120 bars potential is not uncommon.

The evapotranspiration process is clearly crucially important for dry environments, even when vegetation cover is small, and exercises a significant control on the total water budget. Since this budget is controlled by the plant cover, which also plays a major role in the hydrology and hydraulics of overland flow, we return to the vegetation cover next.

A general classification of xerophytic plants is

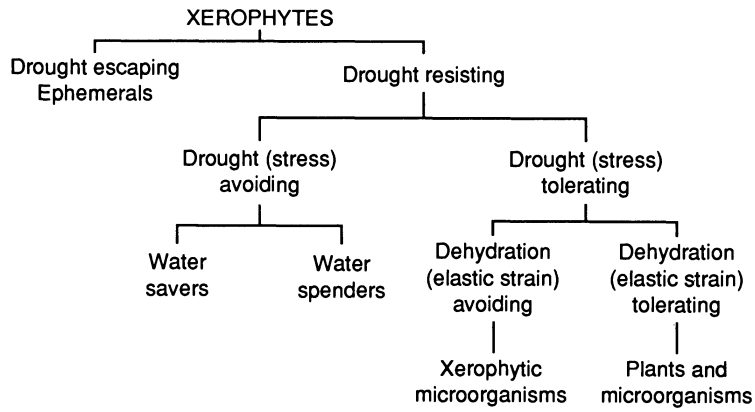

Figure 11.8 Structure of xerophytic plant types (after Levitt 1972).

given in Figure 11.8 (Levitt 1972). Xerophytic plants can escape drought seasons by an ephemeral habit or resist drought either by avoiding it by reducing water consumption or by using the maximum possible when it is available. The latter strategy is a characteristic especially of phreatophytes, such as mesquite and tamarisk. Other plants are able to tolerate drought by mechanical means. Mosses and lichens, for example, can expand again after dehydration. Such poikilohydrous plants have the capacity to take up water instantaneously and survive extreme and prolonged desertification.

Specific observations on desert vegetation have been made by Nobel (1981) in the Sonoran Desert. He investigated the desert grass *Hilaria rigida*, which is a clump grass of the C4 type and has amongst the highest photosynthetic rates so far reported. In this species, clumps of increasing size tend to be further from a random point and further from their nearest neighbour of the same species. This larger spacing suggests pre-emption of groundwater. This conclusion is partly borne out by the fact that leaves on small clumps (less than 10 culms) have a threefold higher rate of transpiration per unit leaf area than do leaves on larger clumps (over 200 culms), indicating that the water transpired does not vary much with clump size. Given that the amount of CO_2 fixed per unit ground area does not differ much with clump size, the pattern of large and small clumps can be quite stable. This may also be indicated by the low interdigitation of root systems for different clumps. This high level of adjustment suggests that clump life could be quite long. Somewhat similar conclusions were reached by Phillips and McMahon (1981).

Some species are evergreen, while others are facultatively drought deciduous. Several studies have indicated that the leaf area index (LAI) declines as water potential declines, and Woodward (1987) has developed a model which predicts LAI in terms of a cumulated water deficit, arguing that when the water deficit falls below −80 mm abscission begins (Fig. 11.9).

In addition to changes of leaf shape and plant structure, other special plant physiological adaptations occur which give desert plants more efficient water use. For example, succulent plants possess pathways for the fixation of CO_2 that enable assimilation to proceed with the stomata open only at night, when potential for evaporation from cladodes and leaves is minimal (Fuchs 1979).

The plant cover and biomass is a function of the production and distribution of the photosynthetic production, and this is usually controlled by the evapotranspiration rate. In modelling the impact of climatic change on erosion in which the plant cover is a most critical variable, the key issue in arid and semi-arid areas is the plant water balance and its impact on net production (i.e. the difference between the plant material produced by photosynthesis and that consumed for maintenance). It is generally assumed that the plant biomass comes into equilibrium with the available water (cf. Eagleson 1979, Thornes 1990, and see below).

Lane *et al.* (1984) demonstrated for the Mojave Desert that the best predictors of annual plant productivity were linear relations with mean annual precipitation ($r^2 = 0.51$), seasonal precipitation (January–May, $r^2 = 0.74$), annual transpiration ($r^2 = 0.84$), and seasonal transpiration ($r^2 = 0.90$).

Net plant productivity in the south Tunisian steppe is approximately 1000 kg ha^{-1} y^{-1} of dry matter or approximately 5.5 kg ha^{-1} mm^{-1} of rainfall.

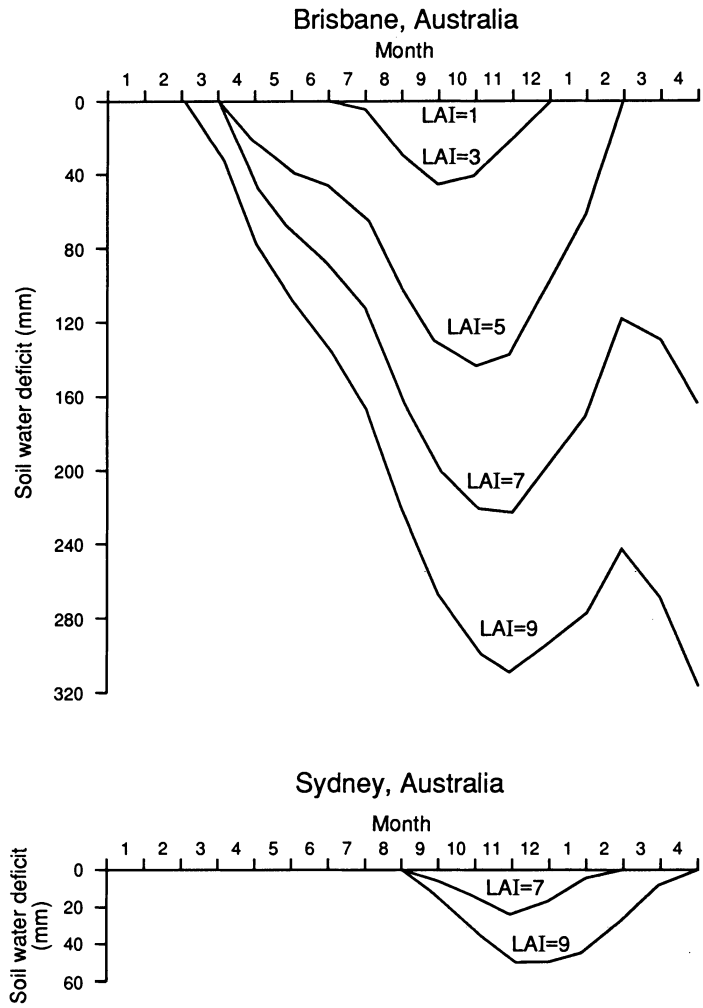

Figure 11.9 Predicted monthly soil-water deficit for soils at two sites in Australia in accordance with Woodward's (1987) model. LAI = leaf area index (after Woodward 1987).

Wet years produced 1550 kg of dry matter per hectare and dry years about 1060. The difference is due to the distribution of rainfall. This distribution is especially important when the annuals and perennials occur at different times of the year. Floret *et al.* (1978) found that annuals peak in May, while perennials peak in June and July. For maximum production of annuals, rainfall should be regularly distributed between autumn and the end of spring, while bushes do better if the deep soil layers are still wet in mid-May.

Modelling vegetation growth and water consumption for sparse vegetation can be illustrated by the ARFEQ model of Floret *et al.* (1978). These authors modelled primary production and water use in a south Tunisian steppe, comprising dominantly *Rhatherium suaveolus*. This is a zone of typically 170 to 180 mm y^{-1} rainfall, falling mainly in September and March. The soil is a gypsous sandy clay with an organic matter content of the order of 0.4 to 0.7%. The cover of perennial species is about 35% *Stipa* sp., *Aristida* sp., and *Plantago albicans*. *Rantherium* accounts for a further 30% with about 26 500 tussocks ha^{-1}. The surfaces typically have 1600 kg ha^{-1} of above-ground phytomass and 50 to 80 kg ha^{-1} of litter on the soil.

In the ARFEQ model bare soil drainage is an inverse function of the storage above field capacity; potential evapotranspiration is calculated as a function of the measured Piche evaporation; and actual

evapotranspiration is related to potential through the dimensionless water content of the water content of the upper horizon. For the plant cover, total transpiration is obtained from a comparison of the atmospheric demand and the soil-water stress. The atmospheric demand is expressed in terms of LAI, stomatal conductance, and Piche evaporation. The soil-water resistance is obtained from the difference between soil-water stress and leaf stress mediated by a root resistance, which is inversely proportional to the amount of root mass in a given soil layer. Leaf-water potential is then assumed to meet the requirement that there is an equilibrium between the atmospheric demand and the root extraction. This is a common assumption for water-limited plant covers (i.e. that the plant water use is in equilibrium with the applied stress). In practice this assumption may often be doubtful given the high interannual and longer-term variability. Below we examine how changes in water availability and redistribution lead to vegetation cover extinction and, hence, to changes in the hydrological regime over the longer term.

From these hydrological considerations, gross photosynthesis is assumed to be a function of water status, LAI, and incoming solar radiation (Feddes 1971), and the photosynthetic rate less respiration and senescence is used to determine dry matter production. The results of the model suggest that approximately 0.26 to 0.54 g of dry matter are produced per kilogram of H_2O, rising in spring to 1.26 for annuals and 1.39 for perennials.

While still in the domain of unsaturated control, it is worth noting that there have been significant new developments in estimating the impact of large areas of bare surface on the now widely accepted Penman–Monteith equation (Monteith 1981), though the developments are still largely restricted to agricultural crops, such as millet. The Penman–Monteith model is based on the estimation of potential evapotranspiration controlled by atmospheric demand through the resistances of plant stomata (stomatal resistance), the canopy overall, and the atmosphere above the canopy to water vapour transport. However, it has been observed recently that a substantial amount of water is lost from the surface by evaporation from dry soils. For example, Gregory (1991) reported that as much as 75%, and commonly of the order of 35%, is lost by evaporation from bare soil surfaces between row crops. There seem to be two possible approaches to dealing with this problem: the first is to have separate estimators for crops and bare areas; and the second it to have a combined model which takes both into account. With regard to the first approach, Ritchie (1972) developed a model which assumed that after rain, soil evaporation is determined by net radiation at the soil surface. However, following this initial phase, evaporation from the bare soil becomes increasingly limited by the ability of water to diffuse through the drying soil surface. In this second phase, Ritchie set cumulative soil evaporation to be inversely proportional to the square root of time. Many observations of desert soils have empirically supported the use of this proportionality even though this model allows no interaction between the soil and the canopy. Two particular models are important in the second approach: ENWATBAL developed by Lascano *et al.* (1987) and the sparse crop model of Shuttleworth and Wallace (1985). In the latter the near-surface layer is comprised (Fig. 11.10) of an upper layer, which loses moisture directly from the canopy, and an interactive soil substrate, which has its own surface resistance and an aerodynamic resistance between the soil and the canopy. The combined evapotranspiration is then set up as:

$$LE_c + LE_s = C_c PM_c + C_s PM_s \qquad (11.4)$$

in which L is the latent heat of vaporization, E_c the canopy transpiration, E_s the bare soil evaporation, and PM_c and PM_s the respective Penman–Monteith estimates. The coefficients C_c and C_s are then empirical coefficients which are functions of the aerodynamic resistance and bulk stomatal resistance of the crop and the soil (Wallace 1991).

PHREATOPHYTES

It was argued in the 1960s that phreatophytes in the American South-west were major consumers of water and that the elimination of phreatophyte vegetation might be considered as a suitable method of water harvesting. Bouwer (1975) considered that potentially 6.4 million hectares of phreatophytes could be consuming $30 \times 10^9\ m^3$ of water. The uptake of groundwater by plant roots varies diurnally and seasonally, but fundamentally the evapotranspiration rate appears to be related to the depth of water table. Bouwer (1975) has modelled it as such on the assumption that the system is in steady state. The deeper the roots the greater the water table can sink and still maintain essentially potential evapotranspiration rates. Because roughness and total leaf area tend to increase with increasing plant height, and trees and shrubs are generally deeper rooted than grasses, potential evapotranspiration for deep-rooting vegetation is higher than that for

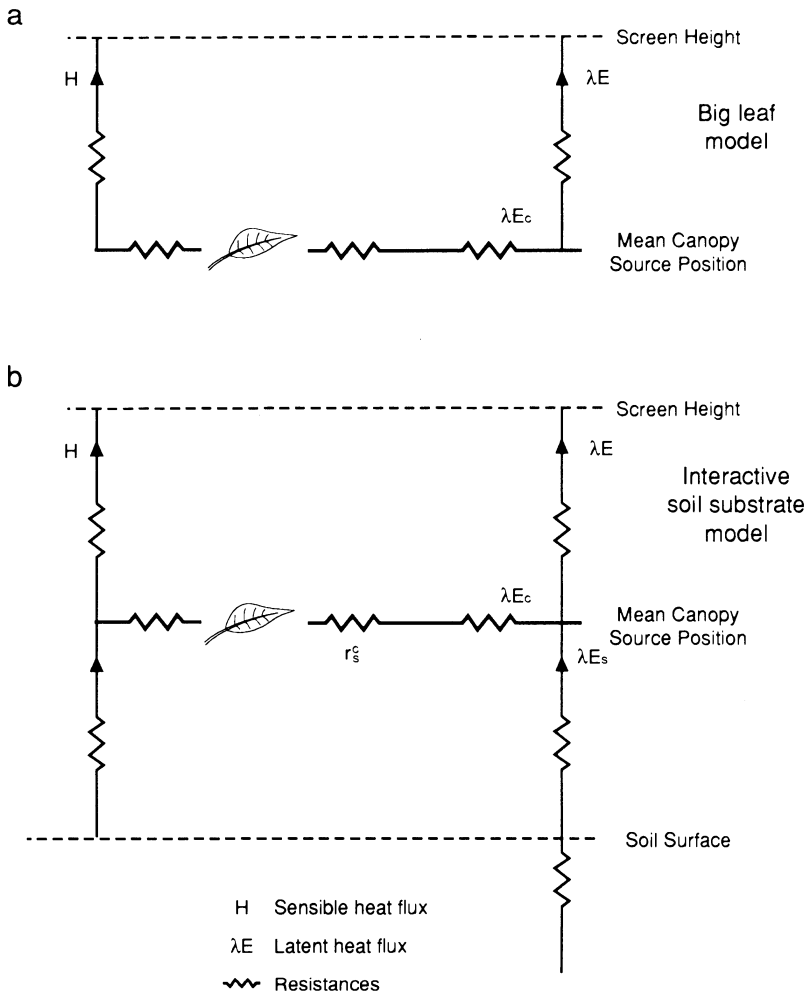

Figure 11.10 The Shuttleworth and Wallace (1985) model of canopy and bare soil: (a) classical 'big leaf' model, (b) interactive soil substrate model. *E* is total latent heat flux, with subscripts c and s representing canopy and bare ground, respectively, and *r* is the canopy resistance.

shallow-rooting plants, and higher still than that for bare soil.

Van Hylckama (1975) has estimated the water loss with and without salt cedar cover in the lower Gila valley, Arizona (Fig. 11.11). His analysis suggests that with salt cedar the surface groundwater rate would yield about 2.5 m y^{-1} of water loss with trees and 2.0 m y^{-1} without. This difference increases sharply as the water table falls. Bouwer, however, noted that the reduction in channel seepage due to phreatophyte control increases and the actual amount of water which can be saved decreases as distance from the channel decreases.

HILLSLOPE RUNOFF

In drylands overland flow is patchy in occurrence, reticular in character, and often terminates before reaching the channel by reinfiltrating on the hillslope (Yair and Lavee 1985). Its characteristics are largely determined by the disposition of stones, vegetation, and macroscale roughness. Conversely, it plays an important role in the location of plant activity at the drier margins, and there may be a complex interaction between overland flow, reinfiltration, plant cover, and erosion. This reticular flow has been the subject of much recent research, since

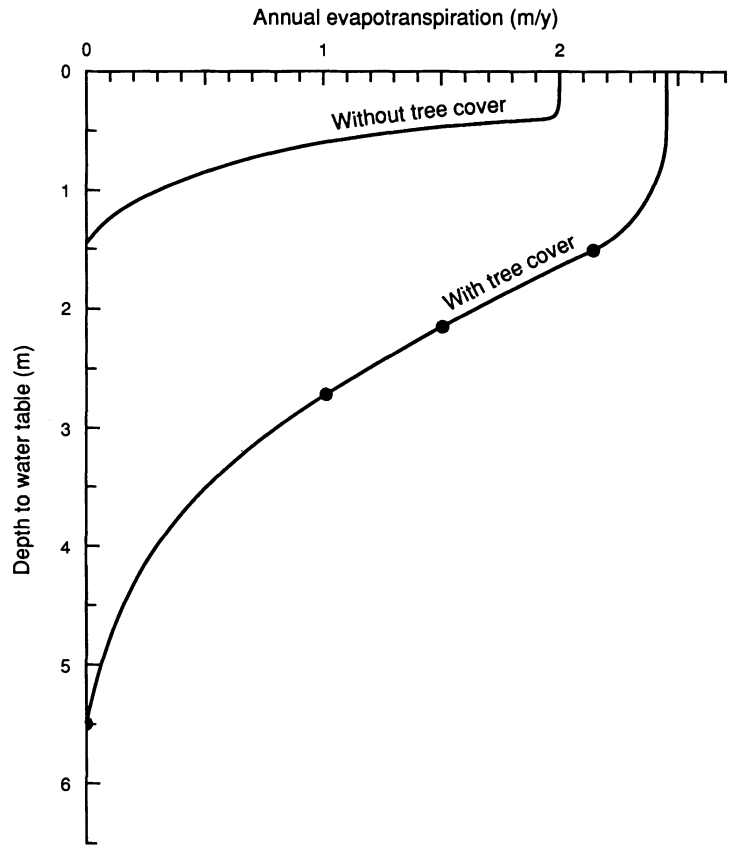

Figure 11.11 Gila valley phreatophytes water loss by evapotranspiration over depth, with (solid lines with circles) and (hypothetically) without salt cedar cover.

the important observations of Emmett (1970). Abrahams *et al.* (1986), Thornes *et al.* (1990), Dunne *et al.* (1991), and Baird *et al.* (1992) have all drawn attention to the impact of surface topographic stones and vegetation in concentrating the flow into rills and eventually gullies. Reticular flow contrasts significantly with sheet flow. In the past overland flow has often been modelled as sheet flow by means of the kinematic cascade model, which assumes that an overland flow of uniform depth is propagated down a hillslope comprising a series of smooth planes. The significance of reticular flow lies in the restriction of flow-induced infiltration and wash erosion to the actual flow-wetted area at the surface, which in turn has important implications for a wide range of processes. In Chapter 8 the generation and propagation of reticular runoff in hydraulic terms is discussed in detail. Here we restrict ourselves to the main controls on the quantity and timing of slope runoff in terms of the water reaching the channel system.

On slopes mantled with coarse debris, the stone content exerts a substantial control on hillslope runoff process. Yair and Lavee (1974) examined runoff from coarse scree slopes using rainfall simulators at three intensities: 60 mm h^{-1} for 10 minutes, 30 mm h^{-1} for 10 minutes, and 15 mm h^{-1} for 20 minutes. In these experiments the runoff was generated mainly in the lower areas (i.e. within the gullies). The explanation given was that the larger blocks (15 to 20 cm) in these areas yield more runoff and concentrate the water on small underlying patches of fine-grained materials, thus exceeding the infiltration rates in these fine-grained receiving areas.

Stones, like vegetation (Fig. 11.12), concentrate the flow so that velocities are higher, infiltration localized, and scour restricted in space. Baird *et al.* (1992) have modelled this process following the free volume concept of Thornes *et al.* (1990). In their model the rainfall is assumed to be distributed

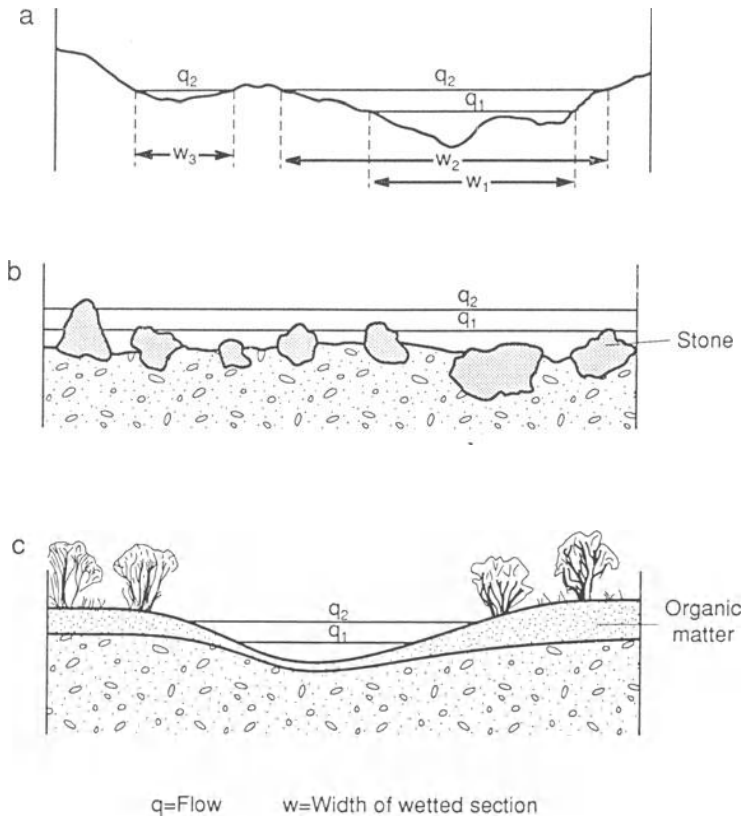

Figure 11.12 Diagrams illustrating roughness elements. In (a) rills provide different flow depths and widths. In (b) the roughness elements are formed by surface rocks. In (c) the roughness elements are created by bushes and generate different infiltration amounts according to the thickness and disposition of organic matter.

across the entire surface but water entering a slope section is allowed to fill the hollows to a depth equivalent to its volume. Assuming a normally distributed ground roughness, they avoid describing the detailed topography in each cell and generate a distribution of flow velocities on the basis of depth and slope distributions for the wetted areas. As the flow increases in depth, it drowns surfaces of different infiltration properties and infiltration rates evolve dynamically for different flow conditions. Results of the operation of this model show significant changes in the hydrograph and in sediment yields when compared with unrilled slopes (Fig. 11.13).

At the hillslope scale, Yair and Lavee (1985) demonstrated a complex interaction between runoff generation, slope properties, and vegetation cover on slopes in the northern Negev at Sede Boquer. They observed that flow from bare upper-slope rock surfaces passes on to lower slopes with increasing amounts of colluvium. There is a progressive diminution of water availability to plants further downslope, resulting in a change in species composition as well as plant cover density. In the upper part of the colluvium, perennial species are dominated by Mediterranean species, whereas lower down Saharo-Arabian species with a lower water demand dominate.

The distribution of species according to water availability and erosion competition was modelled by Thornes (1990) on the assumption of a wedge-shaped colluvium of increasing thickness downslope. This model yields an accumulation of water with increasing distance downslope, common in more humid Mediterranean environments, so that plants with a lower water use efficiency are located at the base of the slope (Fig. 11.14). Kirkby (1990), on the other hand, modelled the actual runon and reinfiltration conditions at Sede Boquer using a digital simulation model. Here the microtopography

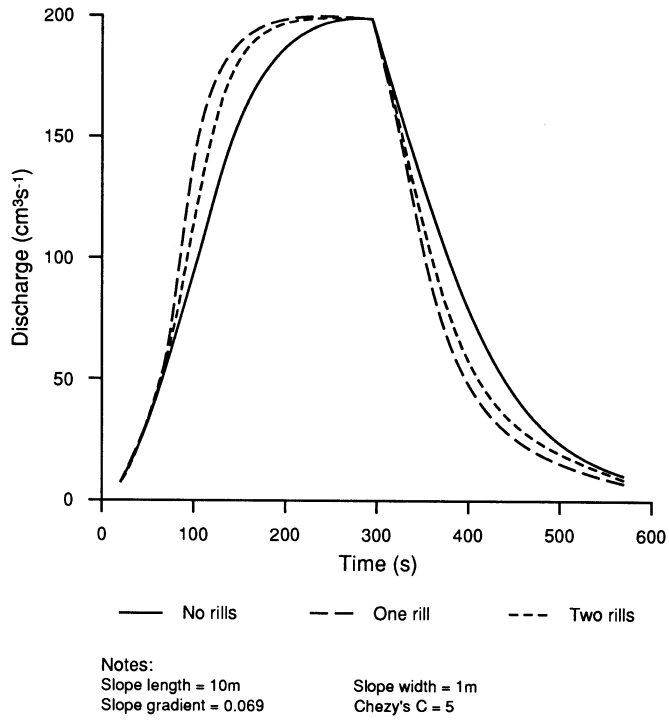

Figure 11.13 Results from the RETIC model showing that the existence of rilling tends to steepen-up both the rising and receding limbs of the hydrograph.

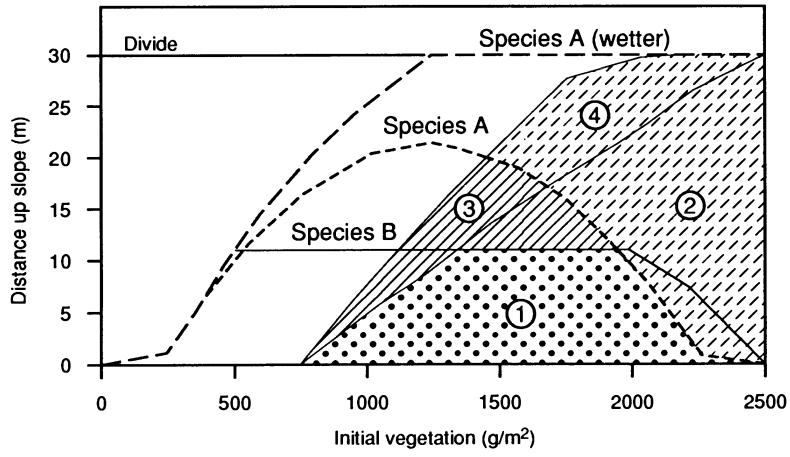

Figure 11.14 The distribution of two species competing for water on a slope as a function of the initial vegetation cover. Species B is restricted to the lower part of the slope (below 12 m) almost regardless of the initial conditions. Species A can extend further upslope and under wet conditions can reach the divide, provided that the initial vegetation exceeds about 1200 g m^{-2}. In zone 1 both species are unchanging in biomass. In zone 3 (with diagonal hatching) species A is stable under dry conditions but species B will decrease. In zones 2 and 4 species A is stable and of unchanging biomass under wet conditions, but unstable and decreasing under dry conditions (after Thornes 1990).

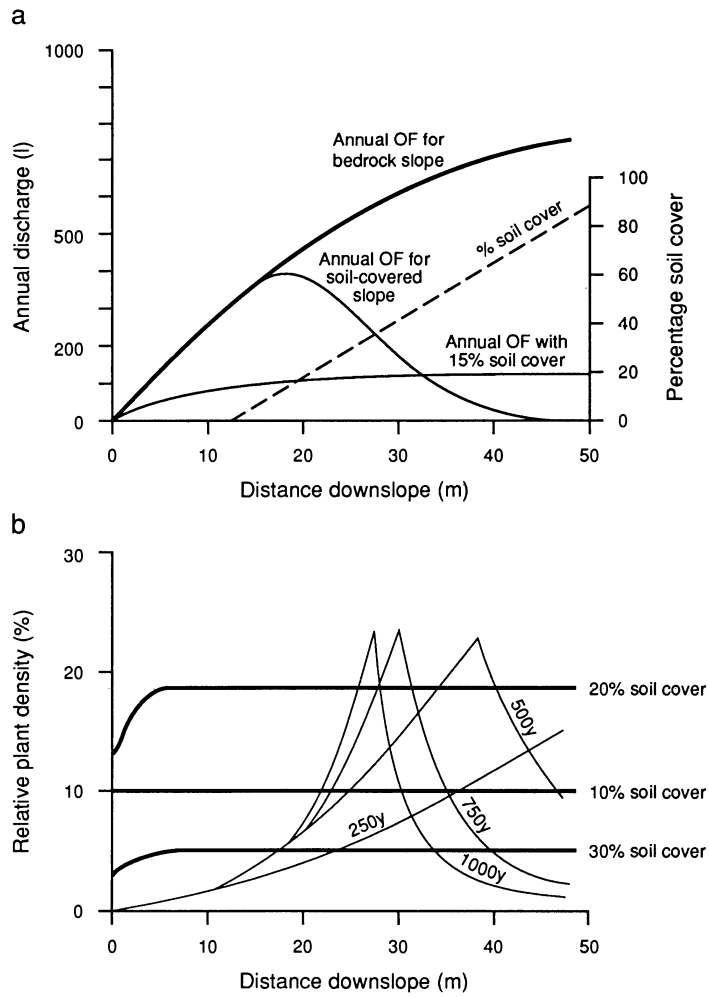

Figure 11.15 Kirkby prediction of overland flow (OF) and vegetation density: (a) annual runoff on bedrock and on a colluvial slope with increasing colluvium in a downslope direction; (b) estimated plant cover and its evolution as erosion and deposition take place through runon from bedrock to a colluvial surface (after Kirkby 1990).

is generated by an exponential distribution, infiltration and evaporation follow storage-controlled laws, and water is routed kinematically. Some typical results are shown in Figure 11.15a, giving the simulated overland flow for the bedrock surface and soil-covered sections and illustrating the pronounced effects of reinfiltration in the latter. The effects of redeposition are also felt so that the peak of erosion is in mid-slope, the net effect being to sweep the sediment in a downslope direction through time, leading to a redistribution of the whole complex of evaporation, recharge, and plant growth in that direction, which is offset only by the deposition of loess on the slope. The effects of the progressive movement of the system downslope are illustrated by the changes in the estimated relative plant densities through time shown in Figure 11.15b. After 100 years the peak densities are predicted at about 28 m and by 500 years at about 42 m. At a given time the rise in plant cover continues downslope to a peak until no more water is available for evapotranspiration, after which it falls again dramatically in a downslope direction (Fig. 11.15b). The effect of this sweeping of sediment is to concentrate the vegetation in a narrow band in the zone of maximum infiltration losses. This peak vegetation cover actually moves slightly upslope through time. This complex interaction between vegetation, infiltration, and

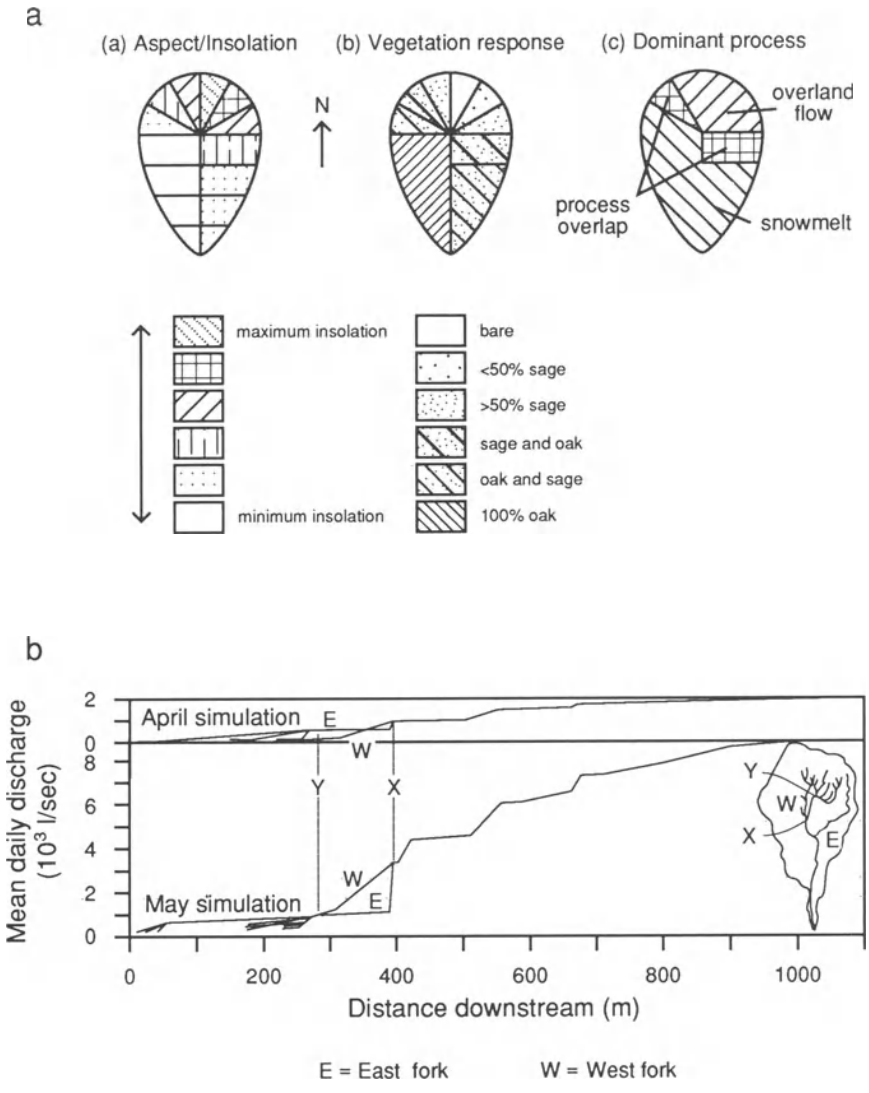

Figure 11.16 (a) Hypothetical process domains in a mountain semi-arid snowmelt-dominated mountain catchment. (b) Simulated downstream changes in mean daily discharges in the pre-melt and melt seasons in Alkali Creek, Colorado (after Faulkner 1987).

erosion at the hillslope scale is thought to replicate the actual conditions described for Sede Boquer quite well.

Much of the observation and modelling of dryland processes has been at the point, plot, or hillslope scale, and the problem of scaling up these observations and models to a regional scale has hardly been mentioned. An exception to this is the work of Pickup (1988) in Australia. Although this work is essentially directed at the problem of grazing-induced erosion, through the idea of scour–transport–fill (STF) sequences, the approach is essentially hydrological in character. The spatial organization of runoff controls was also examined in a semi-arid mountain catchment by Faulkner (1987). This work also serves to remind us of the importance of snowmelt in semi-arid mountains as well as cold deserts. The hypothetical model of domains is shown in Figure 11.16a, where the relative dominance of different processes is dependent on aspect and vegetation response. Faulkner proceeded to simulate the runoff production from the different

surfaces in terms of snowmelt and rainfall runoff generation using established techniques. Figure 11.16b shows not only the importance of snowmelt on the hydrograph but also the different spatial impact its contribution has on the pattern of channel runoff.

At the regional scale the measured runoff redistribution of rainfall represents a complex range of factors. The various sources of losses to the surface affect the nature and timing of runoff in semi-arid environments on the hillslopes as well as in the channels. Pilgrim *et al.* (1979) estimated for the Fowler's Gap Arid Zone Research Station site in New South Wales initial losses prior to runoff of 5.35 mm with a continuing loss of typically 2 mm h^{-1}. However, as Wheater and Bell (1983) point out, catchment losses vary according to the scale of the runoff processes. In this regard, Shanen and Schick (1980) showed that in the Middle East initial loss estimates are 2.5 mm for small plots, 5.5 mm for 1 to 7 ha catchments, and 7 to 8 mm for a 3.45 km^2 catchment. This is a reflection of the general law that percentage runoff decreases with size of catchment, but in dry lands the losses are generally more acute. There is a mixture here too of direct losses from the catchment surface and channel transmission losses. The latter become particularly important with the development of an infiltrating channel fill (see below).

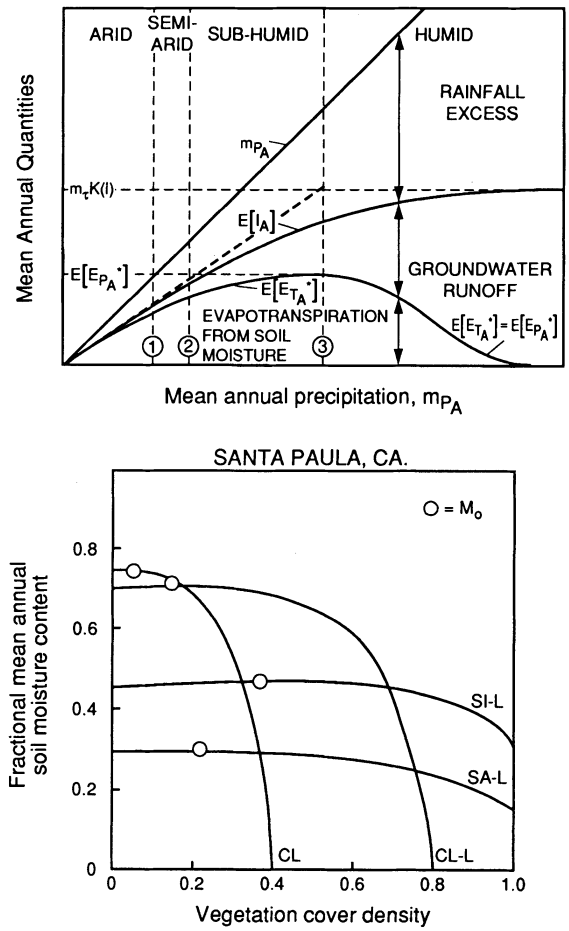

Figure 11.17 (a) The hydrological components and classification of hydrological regimes according to Eagleson's model. (b) The relationship between plant cover density, soil type, and soil moisture in the same model.

OVERALL WATER BALANCE

Accepting that these complexities arise in runoff regimes and that they have strong distributed patterns at the local scale, there is nevertheless an important role for a general model of the overall water balance, especially in the light of attempts to connect general circulation models to models of surface change. One of the most significant developments in this respect has been Eagleson's (1979) attempt to provide a hydrological model for the principal hydrological balance components in the overall annual hydrological cycle. This complex model rests on a statistical dynamic formulation of the vertical (point) water budget through equations expressing the infiltration, exfiltration, transpiration, percolation, and capillary rise from the water table both during and between storms. By asserting that the vegetation growth is in equilibrium and never in a stressed condition, Eagleson derives the expectation of the annual evapotranspiration and the optimal vegetation cover density for any location for which the required parameters are available. Typically the overall partition of the water budget and its division into climatic regimes are shown in Figure 11.17a as a function of rainfall m_{P_A}. The E outside the brackets indicates that the values are the statistically expected values. The solid lines indicate the major controls. Actual evapotranspiration $E_{T_A}^*$ increases with rainfall to a maximum when it equals potential evapotranspiration $E_{P_A}^*$. Infiltration I_A increases with rainfall until it is limited by saturated percolation to groundwater, which is a function of the mean duration of the rainy season m_τ and the saturated hydraulic conductivity $K(1)$. The uppermost, straight, solid line is the line through which mean annual rainfall m_{P_A} is equal to mean annual potential evapotranspiration $E_{P_A}^*$, so to the right of this line there is always excess water.

The vertical dashed lines associated with numbers just above the horizontal axis define climatic zones. The lower bound of the semi-arid zone (1) occurs when the mean annual rainfall is greater than the mean actual annual evapotranspiration, recalling that the latter includes the effects of seasonality, vegetation cover, soil type, and so on. The upper bound of this zone (2) separates the semi-arid from the subhumid regimes. In the former, infiltration and evapotranspiration are profile- (soil-) controlled, whereas in the latter evapotranspiration is climate-controlled. Above this (above rainfall at 3) infiltration is greater than actual evapotranspiration and the soil will be fully humid. Figure 11.17(b) shows the response of vegetation cover to soil moisture for different soil types (silt-loam, sandy loam, clay-loam, and clay). The point marked M_o is the optimum vegetation cover for the prevailing soil characteristics and soil moisture in an unstressed condition in Santa Paula, California (Eagleson 1979).

GROUNDWATER

Although deep percolation from rainfalls is generally small and, therefore, groundwater is generally relatively unimportant from a geomorphic point of view, this is not true of suballuvial aquifers. Here the aquifer is recharged from transmission losses from channel flow and, therefore, it has important implications for runoff and transporting capacity. Moreover, the suballuvial rockhead configuration may lead to groundwater resurgence and availability of water to phreatophytes. Figure 11.18a shows the configuration of the alluvial fill of the Mojave River, California. It can be seen from this diagram that the suballuvial aquifer thins and shallows in the vicinity of Victorville, to the south of Bell Mountain, and again near Barstow. These subsurface 'narrows' force the water near to the surface, causing a significant growth of phreatophytes, which have a significant effect on channel behaviour and morphology. Figure 11.18b shows the pattern of precipitation at Lake Arrowhead and the resulting flow at Victorville and Barstow for the spring of 1969. By the time the flow had reached Barstow, the transmission losses to the bed had eliminated the lower flows. Finally, Figure 11.18c shows the evolution of ground water in the suballuvial aquifer. This graph indicates the remarkable recovery of levels by recharge in the 1969 and 1978 floods. Buono and Lang (1980) reported that by the time the flow had reached Victorville 43% of it had been lost, and that 50% had been lost by the time it reached Barstow.

In another study of a much smaller channel system, Butcher and Thornes (1978) attempted to model the impact of transmission losses on channel flow and the survival of flow to the main channel. They showed that coupled with the transmission losses, the propensity for flows to survive in smaller channels and reach the main channel flow system also depended on the contributions of yet smaller channels to the system in question. The pattern of contributions of smaller subcatchments, called the area increment function, determined the likelihood that a flow would survive as far as the next tributary input. Butcher and Thornes modelled flows using a kinematic cascade routing model (KINGEN) developed by Woolhiser (1976) coupled with a transmission loss model for reaches between major tributaries based on a simple Kostiakov-type equation and the opportunity time for flow permitted by the passage of the flood wave. Smaller infiltration rates were found to produce disproportionately greater survival lengths. This application to a specific channel was generalized by Thornes (1977), who combined three principles – a differential equation for channel losses developed from Burkham's (1970) model, the hydraulic geometry of ephemeral channels (Leopold and Miller, 1956), and an area increment function based on Shreve (1974) – to solve the equations for the probability of survival downstream given various parameters derived from field studies. The general spatial scheme is shown in Figure 11.19, together with typical theoretically derived survival curves. The implications of this model for geomorphic phenomena are illustrated in the next chapter. An excellent summary of the modelling of transmission losses was given by Lane (1980), and Lane (1982) developed a semi-empirical approach to transmission losses in the context of distributed modelling for small semi-arid watersheds.

CHANNEL FLOW

McMahon (1979) summarized the characteristics of runoff in desert environments on the basis of an examination of 70 annual flow records and peak discharge series from six desert zones. He found that runoff in desert channels was more varied than in humid channels, a fact confirmed by McMahon *et al.* (1987). Examining global runoff variations, these authors found that as runoff decreases, variability (defined as the standard deviation/mean annual runoff) increases. Consequently, extrapolation from humid zones is not acceptable. In testing the carry-over effect, it was found that in desert channels the first-order serial correlation between annual flows

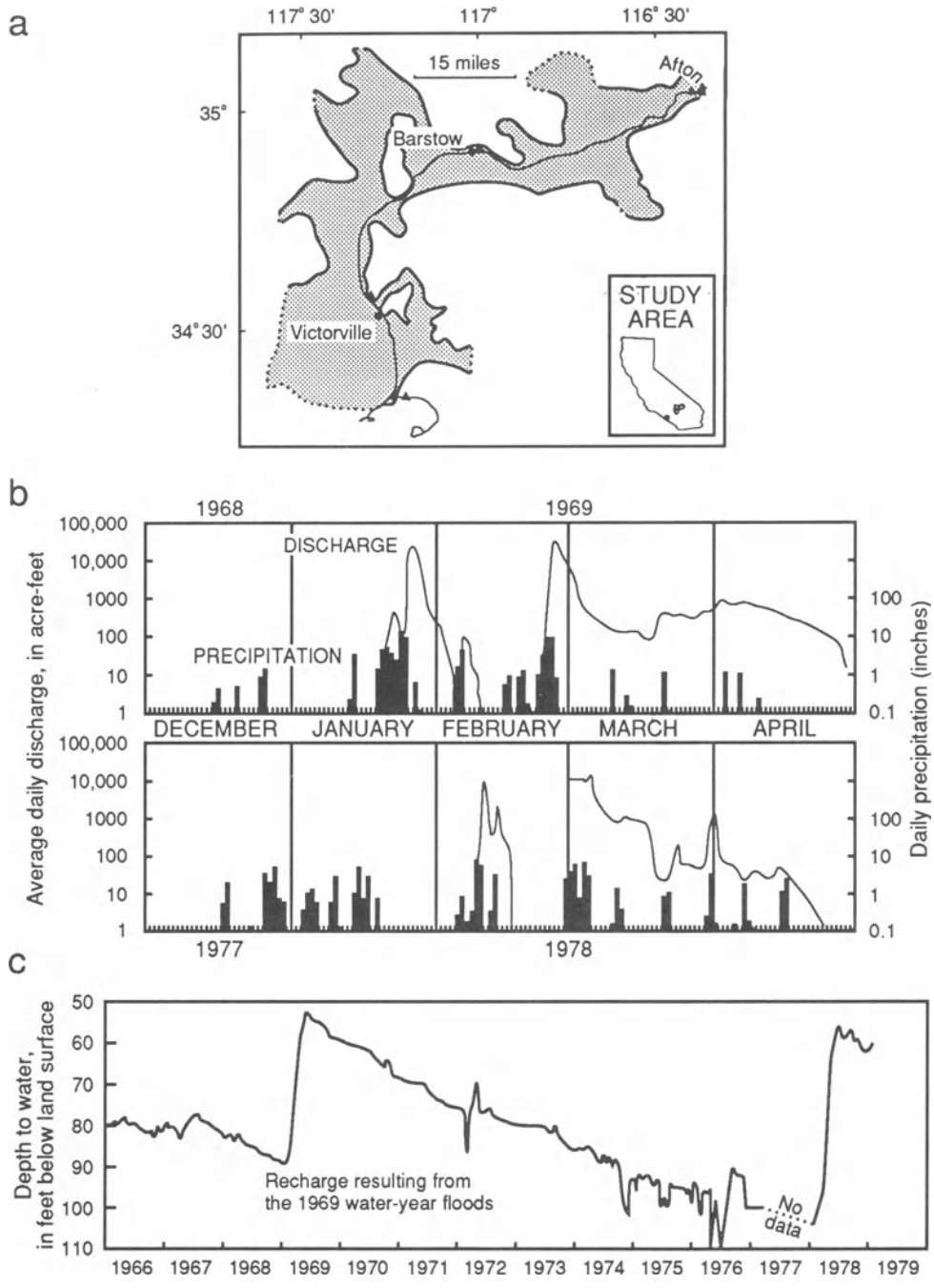

Figure 11.18 Transmission losses in the Mojave River, California (after Buono and Lang 1980). (a) General location map showing alluvial fill. (b) Precipitation and flow for the floods of 1969 and 1978. (c) Changes in the water level below the surface at Baker.

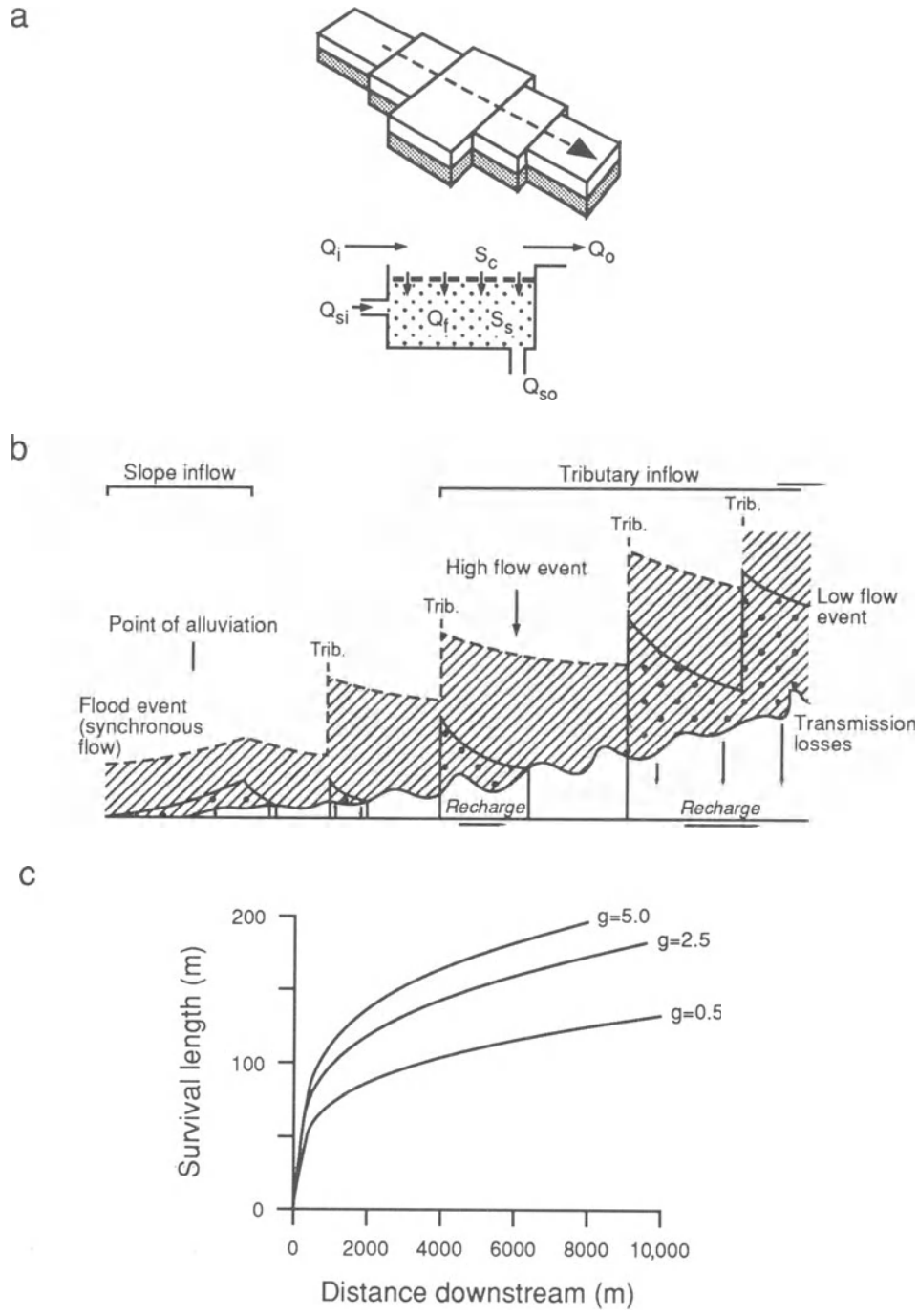

Figure 11.19 (a) The effects of transmission losses on flow (after Thornes 1977). Q is surface discharge, Q_s is subsurface discharge, Q_f is transmission losses, S_c is channel sediment discharge and S_s is subsurface sediment discharge. The subscripts i and o denote inflow and outflow, respectively. (b) Hypothetical pattern of flows for two flood events. (c) Distribution of survival lengths with variation in the parameter g, which is the rate of change of discharge with area.

(for 50 records) is 0.01. McMahon summarized the situation as follows:

(a) flood events are irregular and of short duration;
(b) data from gauging records are extremely poor;
(c) high stream velocities (4 m s^{-1}) are common;
(d) high debris loads occur during the passage of flood waves;
(e) gauging station controls are sandy and unstable;
(f) drainage boundaries are indefinite;
(g) overbank flows occur frequently;
(h) underflow is often a large part of flood events.

These conclusions are borne out by a few examples. Costa (1987) itemized the 12 largest floods ever measured in the United States. All occurred in semi-arid to arid areas, with mean annual rainfalls ranging from 114 to 676 mm; 10 had mean annual rainfalls less than 400 mm. This finding conflicts with the results of Wolman and Gerson (1978) who concluded that differences in maximum possible runoff from a single severe storm in different physiographic regions and climatic regimes appear to be insignificant. However, the United States experience does not suggest that these floods were due simply to high rainfall intensity. Rather it indicates that for a given intensity, rains in semi-arid and arid environments produce more runoff per unit area than they do in temperate environments. This finding reflects the whole panoply of surface infiltration and runoff controls dealt with earlier in the chapter. Mean velocity in these floods ranged from 3.47 to 9.97 m s^{-1}, and shear stresses and unit stream powers were several hundred times greater than those produced in larger rivers.

The analysis of more individual extreme events is even more perplexing. Wheater and Bell (1983) found that problems with data are severe and that flood hydrology in arid zones was (and still is) largely unquantified. They exemplify the difficulties involved with reference to Wadi Adai in Oman where their reconstruction of a specific major flood depended heavily on a mixture of modelling and parameter estimation from sparse data. The wadi has a catchment area of 370 km^2, channel slopes of 0.13 to 0.50, and a channel width of 50 to 150 m. On the basis of intermittent flood records stretching back to 1873, the flood of 3 May 1981 had a recurrence interval of 100 to 300 years. The main flood peak arrived at 0300 hours, the recession started at 0530 hours, and there was hardly any flow by 1700 hours. Flow velocities were estimated to be 3.6 to 4.5 m s^{-1}.

Descriptions abound of the characteristic features of flow in ephemeral channels, though the number of well-documented sites at which they have been properly investigated is still quite small. Among these the best are the Walnut Gulch Experimental Watershed, Arizona (Renard 1970) and the Nahal Yael Watershed, Israel (Schick 1986). The events in ephemeral channels, separated by zero flows, are often asynchronous across the channel network and are sometimes accompanied by well-developed bores and periodic surges in flow. Moreover, the recession limbs are usually very steep. All these features have been modelled, sometimes in combination, and Lane (1982) has considered their application to Walnut Gulch. We now consider the modelling of some of the components. The geomorphic impact of these phenomena is considered in the following chapter.

The development of a steep bore at the front of ephemeral channel flow is caused by a combination of intense storms, rapid translation of the water under conditions of high drainage density, and the interaction of wave movement and transmission losses. The second of these is addressed in Chapter 12. The development of a bore is analogous to the release of water in an irrigation ditch or in a dam burst. At the front edge of the wave the water is initially shallow and the bed friction high. This is compounded by the exhaust of air from the bed as infiltration forces it out, sometimes trapping it between the advancing subsurface wetting front and the groundwater.

Smith (1972) modelled these effects using the kinematic wave approach, which assumes that consideration of the momentum of the flow can be neglected. He predicted the advance rate, surface profiles, and modifications with time to kinematic wave flow over an initially dry infiltrating plane. Although the kinematic wave approach has been the subject of much recent criticism, it appears to be appropriate for small catchments, where it is possible to resolve the physical detail without compromising the deterministic nature of the model (Ponce 1991). Smith's approach was to set up the continuity equation to take account of the transmission losses – that is

$$\mathrm{d}h/\mathrm{d}t + \mathrm{d}(uh)/\mathrm{d}x = q(x,t) \qquad (11.5)$$

where h is flow depth, u the local velocity, x the distance along the channel, t is time, and $q(x,t)$ the local inflow (e.g. from tributaries or valley-side walls) or outflow (i.e. transmission losses). Figure 11.20a shows the basic setup of his model. A sharp fronted flood wave is advancing from left to right across an inclined channel bed. Beneath the bed the graphs show that infiltration rate is greatest near the

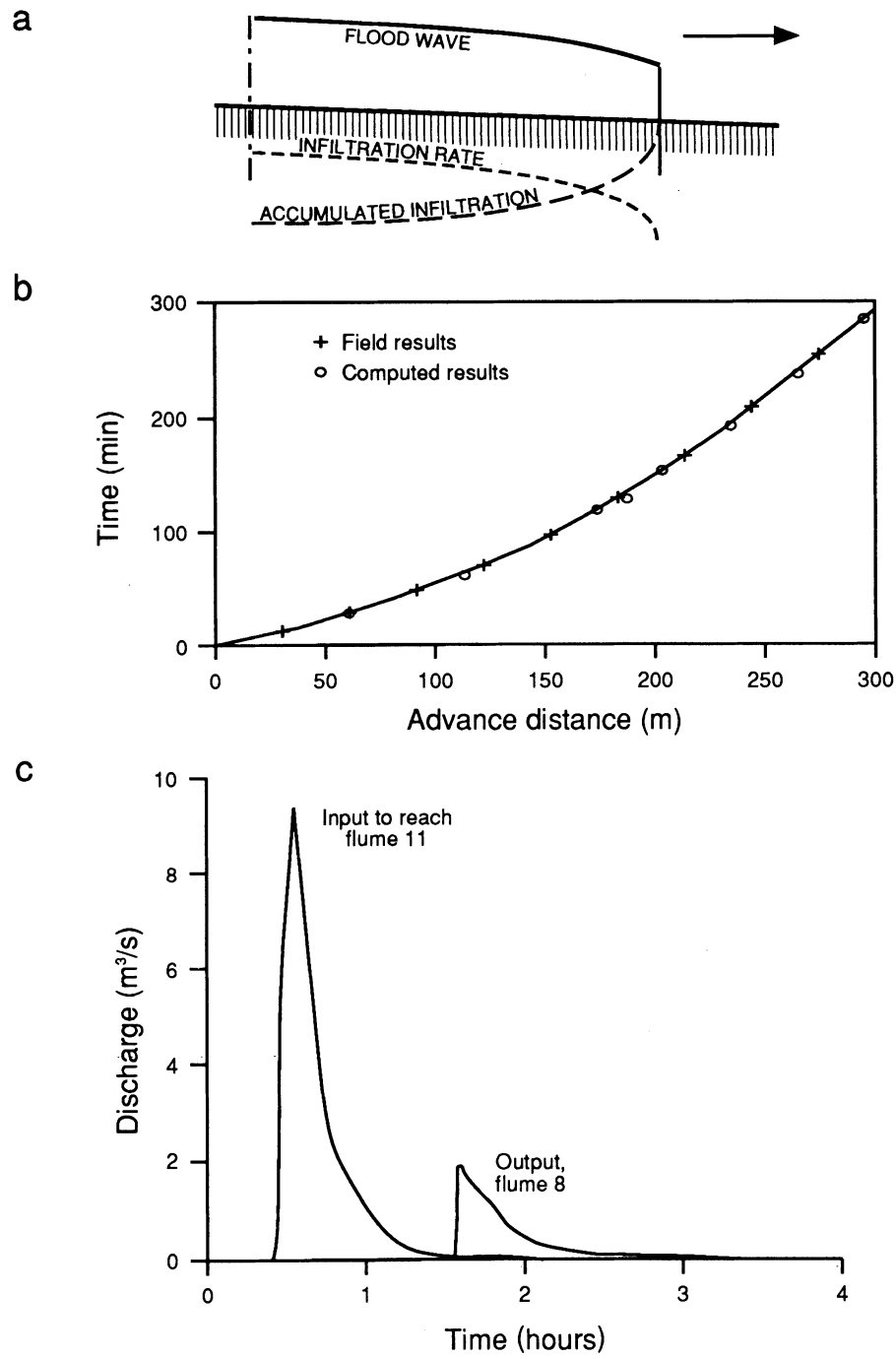

Figure 11.20 Smith's (1972) model of wave front propagation in an infiltrating channel: (a) general set up of model, (b) downstream progress of flood wave compared with field data, and (c) actual propagation of a flood wave in Walnut Gulch between two stations.

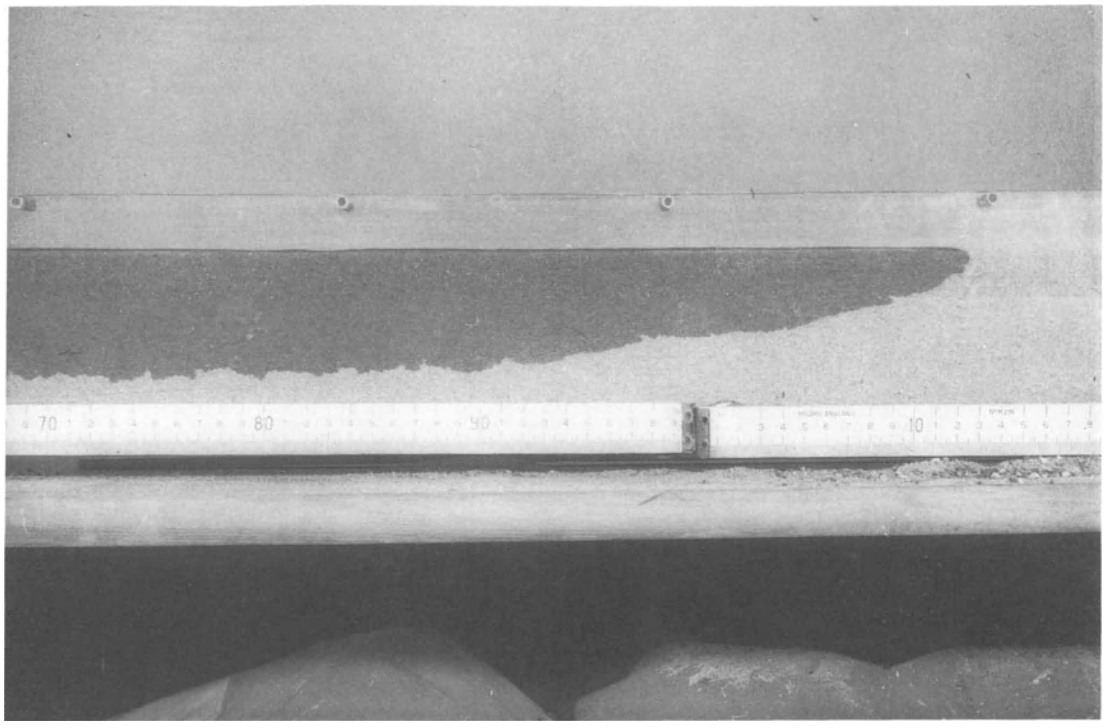

Figure 11.21 Infiltration through transmission losses in a laboratory channel. The surface flow is moving from left to right across the flume and the depth of the wetting front is shown by the darker area in the sand.

front of the advancing wave and that the cumulative infiltration increases away from the advancing front. The latter can be compared with Figure 11.21, which is based on laboratory experiments of advancing fronts by Thornes (1979). The kinematic approximation is given by the stage-discharge equation

$$Q = \alpha \cdot h^{m+1} \tag{11.6}$$

in which α and m are constants. The wave front itself is assumed to move as a kinematic shock. For infiltration, Smith set

$$-q(x) = K(T)^{-a} + f_0 \tag{11.7}$$

in which $q(x)$ is the infiltration rate at x, T is the time since surface ponding, K and a are coefficients related to the characteristics of the channel bed materials, and f_0 is the long-term transmission loss rate. This is essentially the Kostiakov equation. Typical advance rates of the front are shown for the model (which replicated field data of Criddle (1956) very well) in Figure 11.20b. The curve suggests that the velocity of the wave front (the gradient of the line) increases with time, the average rate over this period being about 1 m min^{-1} in this particular case. Typical figures in semi-arid channels seem to be of the order of 1 to 3 km h^{-1} (as illustrated for Walnut Gulch in Figure 11.20c), and the model replicates well the steepening of the wave front downstream. Behind the peak flow of the hydrograph, which comes almost immediately after the wave front, the deeper water provides a relatively lower roughness and a higher velocity, and so the wave front grows.

Infiltration also takes its toll on the recession limbs of ephemeral channel flood waves, which are also usually steeper than in temperate channels. The recession limb can be imagined as a wedge-shaped reservoir moving down channel, with the tail of the flow catching up with the front as transmission losses draw in the shallower water of the recession limb, as has been modelled by Peebles (1975).

Not all rising limbs are associated with a single wave of water, and Foley (1978) described the onset of flow to be a series of translatory waves of small amplitude building up to flood depth. Periodic surges are also a characteristic of steady ephemeral channel flow, especially in larger channels. These appear as sudden increases in stage and may move as waves faster than the actual flow of the water itself, usually, but not always in a downstream direction. They can be responsible for extensive damage and

also for some special sediment transport and depositional effects exclusive to this kind of flow. Leopold and Miller (1956) provided an excellent description of such a flow in which they observed a series of bores each 0.15 to 0.30 m high and between 0.5 and 1 minute apart. One possible explanation is that the waves represent asynchronous contributions from different parts of the channel network. However, Leopold and Miller (1956) ascribed them to a type of momentum wave associated with the hydraulics of the channel itself. Such surges have also been simulated in the laboratory by Brock (1969), and R.J. Heggen (unpublished data 1986) described changes in width and velocity as well as height in these phenomena. Generally, under Green's Law, the elevation of a sinusoidal wave decreases as channel width increases, so the surges tend generally to attenuate downstream.

CONCLUSION

From this chapter it is evident that while the essential controls of arid and semi-arid hydrology are much the same as those of temperate environments, it is the time–space intensity of the hydrological processes which leads to significant differences in the corresponding geomorphic processes. Above all it is the time and space distribution of precipitation which leads to a much less ordered patterning of processes and the resulting forms. Even in arid environments, and certainly in semi-arid environments, the spatio-temporal diversity of rainfall leads to a distinctive pattern of plant water use, plant growth, and the resulting biological activity, both on hillslopes and, to a lesser extent, in channels. These two interrelated elements, water and biological growth, are the key to understanding past, present, and future deserts.

REFERENCES

Abrahams, A.D. and A.J. Parsons 1991. Relation between infiltration and stone cover on a semiarid hillslope, southern Arizona. *Journal of Hydrology* **122**, 49–59.

Abrahams, A.D., A.J. Parsons and S.H. Luk 1986. Resistance to overland flow on desert slopes. *Journal of Hydrology* **88**, 343–63.

Ahnert, F. 1987. An approach to the identification of morphoclimates. In *International geomorphology 1986*, Volume II, V. Gardiner (ed.), 159–88. Chichester: Wiley.

Alexander, R.W. and A. Calvo 1990. The influence of lichens on slope processes in some Spanish badlands. In *Vegetation and erosion*, J.B. Thornes (ed.), 385–98. Chichester: Wiley.

Baird, A., J.B. Thornes and G. Watts 1992. Extending overland flow models to problems of slope evolution and the representation of complex slope surface topographies. In *Overland flow: hydraulics and erosion mechanics*, A.J. Parsons and A.D. Abrahams (eds), 199–211. London: University College Press.

Bell, F.C. 1979. Precipitation. In *Arid land ecosystems*, Volume I, D.W. Goodall and R.A. Perry (eds), 373–93. Cambridge: Cambridge University Press.

Berndtsson, R. 1987. Spatial and temporal variability of rainfall and potential evapotranspiration in Tunisia. *International Association of Scientific Hydrology Publication* 168, 91–100.

Blackburn, W.H. 1975. Factors influencing infiltration and sediment production of semi-arid rangeland in Nevada. *Water Resources Research* **11**, 929–37.

Bouwer, H. 1975. Predicting reduction in water losses from open channels by phreatophyte control. *Water resources Research* **11**, 96–101.

Brock, R.R. 1969. Development of roll-wave trains in open channels. *Journal Hydraulics Division, Proceedings of the American Society of Civil Engineers* **95**, 1401–27.

Buono, A. and D.J. Lang 1980. Aquifer recharge from the 1969 and 1978 floods in the Mojave River basin, California. In *Water Resources Investigations Open File Report 80-207*. Washington, DC: U.S. Government Printing Office, U.S. Geological Survey.

Burkham, D.E. 1970. A method for relating infiltration rates to stream flow rates in perched streams. *U.S. Geological Survey Professional Paper* 700-D, 226–71.

Butcher, G.C. and J.B. Thornes 1978. Spatial variability in runoff processes in an ephemeral channel. *Zeitschrift für Geomorphologie Supplement Band* **29**, 83–92.

Carson, M.A. and M.J. Kirkby 1971. *Hillslope form and process*. Cambridge: Cambridge University Press.

Conte, M., A. Giuffrida and S. Tedesco 1989. The Mediterranean oscillation. In *Conference on climate and water*, L. Huttunen (ed.), 121–38. Helsinki: Government of Finland Printing House.

Costa, 1987. Hydraulics and basin morphology of the largest flash floods in the conterminous United States. *Journal of Hydrology*, **93**, 313–38.

Criddle, C.L. 1956. Methods for evaluating irrigation systems. In *Agricultural Handbook* 82. Washington, DC: U.S. Department of Agriculture.

De Ploey, J. 1982. A stemflow equation for grasses and similar vegetation. *Catena* 9, 139–52.

De Ploey, J., M.J. Kirkby and F. Ahnert 1991. Hillslope erosion by rainstorms – a magnitude and frequency analysis. *Earth Surface Processes and Landforms* 16, 399–410.

Dhar, O.N. and P.R. Rakhecha 1979. Incidence of heavy rainfall in the Indian desert region. *International Association for Scientific Hydrology Publication* 128, 13-8.

Duckstein, L., M. Fogel and I. Bogardi 1979. Event based models of precipitation. *International Association of Scientific Hydrology Publication* 128, 51–64.

Dunne, T., W. Zhang and B.F. Aubry 1991. Effects of rainfall, vegetation and microtopography on infiltration and runoff. *Water Resources Research* 27, 2271–87.

Eagleson, P.S. 1979. Climate, soil and vegetation. *Water Resources Research* 14, 705–77.

Emmett, W.W. 1970. The hydraulics of overland flow on hillslopes. *U.S. Geological Survey Professional Paper* 662-A.

Evans, D.D., T.W. Sammnis and B. Asher 1976. Plant growth and water transfer interactive processes under

desert conditions. *US/IBP Desert Biome Research Memoir* 75-44. Logan, UT: Utah State University.

Evans, D.D., T.W. Sammnis and D.R. Cable 1981. Actual evapotranspiration under desert conditions. In *Water in desert ecosystems*, D.D. Evans and J.L. Thames (eds), 195–219. Stroudsburg, PA: Dowden, Hutchinson and Ross.

Faulkner, H. 1987. Gully evolution in response to flash flood erosion, western Colorado. In *International geomorphology 1986*, Volume I, V. Gardiner (ed.), 947–73. Chichester: Wiley.

Faulkner, H. 1990. Vegetation cover density variations and infiltration patterns on piped alkali sodic soils. Implications for modelling overland flow in semi-arid areas. In *Vegetation and erosion*, J.B. Thornes (ed.), 317–46. Chichester: Wiley.

Feddes, R.A. 1971. Water, heat and crop growth. Thesis, Agricultural University of Wageningen.

Floret, C., R. Pontanier and S. Rambal 1978. Measurement and modelling of primary production and water use in a south Tunisian steppe. *Journal of Arid Environments*, 82, 77–90.

Foley, M.G. 1978. Scour and fill in steep sand-bed ephemeral streams. *Bulletin of the Geological Society of America* **89**, 559–70.

Fournier, F. 1960 *Climat et erosion*. Paris: Presses Universitaire.

Francis, C.F. and J.B. Thornes 1990. Runoff hydrographs from three Mediterranean vegetation cover types. In *Vegetation and erosion*, J.B. Thornes (ed.) 363–84. Chichester: Wiley.

Fuchs, M. 1979. Atmospheric transport processes above arid land vegetation. In *Arid land ecosystems*, Volume 1, D.W. Goodall and R.A. Perry (eds), 393–433. Cambridge: Cambridge University Press.

Gifford, G.F., M. Merzougi and M. Achouri 1986. Spatial variability characteristics of infiltration rates on a seeded rangeland site in Utah, USA. In *Rangeland: a resource under siege*, P.J. Joss, P.W. Lynch and O.B. Williams (eds), 46–7. Canberra: Australian Academy of Sciences.

Gonzalez-Hidalgo, C. 1991. Aspect, vegetation and erosion on slopes in the Violada area, Zaragosa. Unpublished Ph.D. thesis, University of Zaragosa.

Gregory, P.J. 1991. Soil and plant factors affecting the estimation of water extraction by crops. *International Association for Scientific Hydrology Publication* 199, 261–73.

Herschfield, D.M. 1962. Extreme rainfall relationships. *Journal of Hydraulics Division, Proceedings of the American Society of Civil Engineers* **88**, 73–92.

Hillel, D. and N. Tadmoor 1962. Water regime and vegetation in the central Negev Highlands of Israel. *Ecology* 43, 33–41.

Jacobs, B.L., I. Rodriguez-Iturbe and P. Eagleson 1988. Evaluation of homogenous point process description of Arizona thunderstorm rainfall. *Water Resources Research* 24, 1174–86.

Johns, G.G., D.J. Tongway and G. Pickup 1984. Land and water processes. In *Management of Australia's rangelands*, G.N. Harrington, A.D. Wilson and M.D. Young (eds), 25–40. Canberra: Commonwealth Scientific and Industrial Research Organization.

Jury, W.A., J. Letey and L.H. Stolzy 1981. Flow of water and energy under desert conditions. In *Water in desert ecosystems*, D.D. Evans and J.L. Thames (eds), 92–113. Stroudsburg, PA: Dowden, Hutchinson and Ross.

Kirkby, M.J. and R.H. Neale 1987. A soil erosion model incorporating seasonal factors. In *International geomorphology 1986*, Volume II, V. Gardiner (ed.), 189–210. Chichester: Wiley.

Kirkby, M.J. 1990. A simulation model for desert runoff and erosion. *International Association for Scientific Hydrology Publication* 129, 87–104.

Lane, L.J. 1980. Transmission losses. *National engineering handbook*, Section 4, Chapter 19. Washington, DC: U.S. Printing Office, U.S. Department of Agriculture, Soil Conservation Service.

Lane, L.J. 1982. Distributed model for small semi-arid watersheds. *Journal Hydraulics Division. Proceedings of the American Society of Civil Engineers* **108**, 1114–31.

Lane, L.J., E.M. Romney and T.E. Hakenson 1984. Water balance calculations and net production of perennial vegetation in the northern Mojave desert. *Journal Range Management* **37**, 12–18.

Langbein, W.B. and S.A. Schumm 1958. Yield of sediment in relation to mean annual precipitation. *Transactions of the American Geophysical Union* **39**, 1076–84.

Lascano, R.J., C.H.M. van Bavel, J.L. Hatfield and D.R. Upchurch 1987. Energy and water balance of a sparse crop: simulated and measured soil evaporation. *Soil Science Society of America Journal* 51, 1113–21.

Le Houerou, N. 1979. North Africa. In *Arid land ecosystems*, Volume 1, D.W. Goodall and R.A. Perry (eds), 83–107. Cambridge: Cambridge University Press.

Leith, H. and R.H. Whittaker 1975. *The primary productivity of the biosphere*, Ecological Studies 14. New York: Springer.

Leopold, L.B. and J.P. Miller, 1956. Ephemeral streams – hydraulic factors and their relationship to the drainage net. *U.S. Geological Survey Professional Paper* 282-A.

Levitt, J. 1972. *Responses of plants to environmental stress*. New York: Academic Press.

Lyford, F.P. and H.K. Qashu 1969. Infiltration rates as affected by desert vegetation. *Water Resources Research* **5**, 1373–6.

McMahon, T.A. 1979. Hydrological characteristics of arid zones. *International Association of Scientific Hydrology Publication* 128, 105–23.

McMahon, T.A., B.L. Finlayson and R. Srikanthan 1987. Runoff variability: a global perspective. *International Association of Scientific Hydrology Publication* 168, 3–12.

Mehuys, G.R., L.H. Stolzy, J. Letey and L.V. Weeks 1975. Effect of stones on the hydraulic conductivity of relatively dry desert soils. *Soil Science Society of America Proceedings* **39**, 37–42.

Monteith, J. 1981. Evaporation and surface temperature. *Quarterly Journal of the Royal Meteorological Society* **107**, 1–27.

Morin, J. and Y. Benyami 1977. Rainfall infiltration into bare soils. *Water Resources Research* **13**, 813–7.

Nobel, P.S. 1981. Spacing and transpiration of various sized clumps of a desert grass *Hilaria rigida*. *Journal of Ecology* **69**, 735–42.

Peebles, R.W. 1975. Flow recession in the ephemeral stream. Unpublished Ph.D. thesis, University of Arizona, Tucson.

Peltier, L.C. 1950. The geographical cycle in periglacial

regions. *Annals of the Association of American Geographers* **50**, 214–36.

Phillips, D.L. and J.A. McMahon, 1981. Competition and spacing patterns in desert shrubs. *Journal of Ecology* **69**, 97–115.

Pickup, G. 1988. Modelling arid zone soil erosion at the regional scale. In *Essays in Australian fluvial geomorphology*, R.F. Warner (ed.), 1–18. Canberra: Academic Press.

Pilgrim, D.H., I. Cordery and D.G. Doran 1979. Assessment of runoff characteristics in arid western New South Wales. *International Association for Scientific Hydrology Publication* 128, 141–50.

Poesen, J., F. Ingelmo-Sanchez and H. Mucher 1990. The hydrological response of soil surfaces to rainfall as affected by cover and position of rock fragments in the top layer. *Earth Surface Processes and Landforms*, **15**, 653–72.

Ponce, V.M. 1991. The kinematic wave controversy. *Journal of Hydraulic Engineering* **117**, 511–25.

Renard, K.J. 1969. Evaporation from an ephemeral stream bed: discussion. *Journal of the Hydraulics Division, Proceedings of the American Society of Civil Engineers* **95**, 2200–4.

Renard, K.J. 1970. The hydrology of semi-arid rangeland watersheds. *U.S. Department of Agriculture, Agricultural Research Service*, 41–162. Washington, DC: U.S. Government Printing Office.

Ritchie, J.T. 1972. Model for predicting evaporation from a row crop with incomplete cover. *Water Resources Research* **8**, 1204–13.

Roo, A.P.J. and H. Th. Riezebos 1992. Infiltration experiments on loess soils and their implications for modelling surface runoff and soil erosion. *Catena* **19**, 221–41.

Schick, A.P. 1986. Hydrologic aspects of floods in extreme arid climates. In *Flood geomorphology*, V.R. Baker, R.C. Kochel, R.C. and P.C. Patton (eds), 189–203. Wiley: New York.

Scholl, D.G. 1974. Soil moisture flux and evapotranspiration determined from soil hydraulic properties in a chaparral stand. *Soil Science Society America Journal* **40**, 14–18.

Scoging, H. 1989. Run-off generation and sediment mobilisation by water. In *Arid zone geomorphology*, D.S.G. Thomas (ed.) 87–116. London: Belhaven.

Scoging, H.M. 1990. 'A theoretical and empirical investigation of soil erosion in a semi-arid environment.' Unpublished Ph.D. thesis, University of London.

Scoging, H. and J.B. Thornes 1979. Infiltration characteristics in a semi-arid environment. *International Association Scientific Hydrology Publication* 128, 159–68.

Shanen, L. and A.P. Schick 1980. A hydrological model for the Negev Desert Highlands – effects of infiltration, runoff and ancient agriculture. *Hydrological Sciences Bulletin* 25, 269–82.

Shmida, A. 1985. Biogeography of desert flora. In *Ecosystems of the world*, Volume 12A, *Hot desert and arid shrublands*, Evenari, M., I. Noy-Meir and D.W. Goodall (eds) 23–77. Amsterdam: Elsevier.

Shmida, A., M. Evenari and I. Noy-Meir 1986. Hot desert ecosystems an integrated view. In *Ecosystems of the World*, Volume 12B, *Hot deserts and arid shrublands*, M. Evenari, I. Noy-Meir and D.W. Goodall (eds), 379–88. Amsterdam: Elsevier.

Shreve, R.L. 1974 Variations of main stream length with basin area in river networks. *Water Resources Research* **10**, 1167–77.

Shuttleworth, W.J. and J.S. Wallace 1985. Evaporation from sparse crops – an energy combination theory. *Quarterly Journal Royal Meteorological Society* **111**, 839–55.

Slatyer, R.O. 1965. Measurements of precipitation interception by an arid zone plant community (*Acacia aneura*). *UNESCO Arid Zone Research* **25**, 181–92.

Smith, R.E. 1972. Border irrigation advance and ephemeral flood waves. *Proceedings American Society of Civil Engineers*, 98(IR2), 289–307.

Smith R.E. and H.A. Schreiber 1973. Point processes of seasonal thunderstorm rainfall 1. Distribution of rainfall events. *Water Resources Research* **9**, 871–84.

Swanson, S.R. and J.C. Buckhouse 1986. Infiltration on Oregon lands occupied by three subspecies of big sagebrush *Artemisia*. *U.S. Department of Agriculture, Agricultural Research Service* INT-200, 286–91. Washington, DC: U.S. Government Printing Office.

Thornes, J.B. 1976. *Semi-arid erosional systems*, Geography Research Papers No. 7. London: London School of Economics.

Thornes, J.B. 1977. Channel changes in ephemeral streams, observations, problems and models. In *River channel changes*, K.J. Gregory (ed.), 317–55. Chichester: Wiley.

Thornes, J.B. 1979. Fluvial Processes. In *Process in geomorphology*, C.E. Embleton and J.B. Thornes (eds), 213–72. London: Arnold.

Thornes, J.B. 1990. The interaction of erosional and vegetational dynamics in land degradation: spatial outcomes. In *Vegetation and erosion*, Thornes, J.B. (ed.) 41–53. Chichester: Wiley.

Thornes, J.B. 1991. Environmental change and hydrology. In *El Agua en Andalucia III*, V. Giraldez (ed.), 555–70. Cordoba: University of Cordoba.

Thornes, J.B. and J.C. Brandt in press. Erosion–vegetation competition in a stochastic environment undergoing climatic change. In *Environmental change in drylands*, A.C. Millington and K. Pye (eds). Chichester: Wiley.

Thornes, J.B., C.F. Francis, F. Lopez-Bermudez and A. Romero-Diaz 1990. Reticular overland flow with coarse particles and vegetation roughness under Mediterranean conditions. In *Strategies to control desertification in Mediterranean Europe*, Rubio, J.L. and J. Rickson (eds), 228–43. Brussels: European Community.

Tromble, J.M., K.G. Renard and A.P. Thatcher 1974. Infiltration for three rangeland soil-vegetation complexes. *Journal Range Management* **41**, 197–206.

Van Hylckama, T.E.A. 1975. Water use by salt cedar in the lower Gila River valley (Arizona) *U.S. Geological Survey Professional Paper* 491-E.

Wallace, J.S. 1991. Measurement and modelling of evaporation from a semi-arid system. *International Association Scientific Hydrology Publication* 199, 131–48.

Walter, H. 1971. *Ecology of tropical and subtropical vegetation*. Edinburgh: Oliver and Boyd.

Wheater, H.S. and N.C. Bell 1983. Northern Oman flood study. *Proceedings of the Institute of Civil Engineers* **75**, 453–73.

Whittaker, R.H. and W.A. Niering 1964. The vegetation of the Santa Catalina Mountains, Arizona. 1. Ecological

classification and distribution of species. *Journal of the Arizonian Academy of Science* **3**, 9–34.

Wilcox, B.P., M.K. Wood and J.M. Tromble 1988. Factors influencing infiltrability of semiarid mountain slopes. *Journal of Range Management* **41**, 197–206.

Wolman, M.G. and R. Gerson 1978. Relative scales of time and effectiveness of climate in watershed geomorphology. *Earth Surface Processes* **3**, 189–208.

Wolman, M.G. and J.P. Miller 1960. Magnitude and frequency of forces in geomorphic processes. *Journal Geology* **68**, 54–74.

Woodward, F.I. 1987. *Climate and plant distribution*. Cambridge: Cambridge University Press.

Woolhiser, D.A. 1976. Overland flow. In *Unsteady open channel flow*. K. Mahmood and V. Yevjevich (eds), 485–508. Fort Collins, CO: Water Resources Publications.

Yair, A. 1990. Runoff generation in a sandy area – the Nizzana Sands, Western Negev, Israel. *Earth Surface Processes and Landforms* **15**, 597–609.

Yair, A. and H. Lavee 1974. Areal contribution to runoff on scree slopes in an extreme arid environment – a simulated rainfall experiment. *Zeitschrift für Geomorphologie Supplement Band* **21**, 106–21.

Yair, A. and H. Lavee 1985. Runoff generation in arid and semi-arid environments. In *Hydrological forecasting*, M.G. Anderson and T. Burt (eds), 183–220. Chichester: Wiley.

Zawadeski, I.I. 1973. Statistical properties of precipitation patterns. *Journal of Applied Meteorology* **12**, 459–71.

CHANNEL PROCESSES, EVOLUTION, AND HISTORY

12

John B. Thornes

INTRODUCTION

The development of river channels and related fluvial landforms has probably been studied more than any other aspect of geomorphology in arid and semi-arid areas. This is due largely to the originality, forcefulness, and intellectual background of American geomorphologists developed during and sustained long after the exploration of the American West. The strong sense of field observation and experiment coupled with a deep historical perspective, both derived from a geological training, led to some of the most formative contributions to the subject. So much so perhaps that, despite the major endeavours by Europeans in denudation chronology, in climatic and glacial geomorphology, and later in hillslope and channel geomorphology, the conceptual basis of the subject at the end of the 20th century still bears a heavy imprint from the American source. In the Old World, only the Israelis, under A. Schick, have been able to maintain such a strong contribution to desert fluvial geomorphology.

The leaders of this paradigm, G.K. Gilbert, K. Bryan, S.A. Schumm, L.B. Leopold, A. Schick, and most recently W.L. Graf, have left a legacy which is impossible to overestimate. Because of the significance of this work it has been the subject of quite frequent reviews, of which three have particular importance, *Fluvial Processes in Geomorphology* by L.B. Leopold, M.G. Wolman, and J.P. Miller in 1964, *The Fluvial System* by S.A. Schumm in 1977, and *Fluvial Processes in Dry Land Rivers* by W.L. Graf in 1987. The first laid the foundations for modern fluvial geomorphology; the second demonstrated the success of a mixture of sound conceptual advances coupled with field and laboratory experimental techniques; and the third provided an excellent state of the art report at the end of the 1980s.

In this chapter the more limited objective is to bring out the distinctiveness of arid and semi-arid rivers rather than to present them as models for all rivers or to assume that they encapsulate all fluvial processes. Moreover, I attempt to separate out processes, evolution, history, and place, which tend to become intertwined in a way that makes it difficult to see the channels for the pebbles or the evolution for the individual floods. Some fluvial processes are treated in other chapters. For example alluvial fans, which are a logical endpoint to the dryland channel experiencing excessive transmission losses and conforming to the same behaviour, are dealt with in Chapter 14.

All landforms result from the tendency to equilibrium between force and resistance. The applications of these forces are *processes*, and the particular processes and especially their rate of application depend on the prevailing tectonic, topographic, and climatic domains. The landforming response to these processes may follow a predictable trajectory through time and space determined by the intrinsic dynamics of the system. This is landform *evolution*. Often, especially in arid and semi-arid environments, this trajectory is not completed before other external forces come into play or before there is a change of rate of the application of the forces. The actual trajectory of forms through time, the landform *history*, is therefore much more complex than the intrinsic evolution of specific forms and we can expect to gain only a partial understanding of landform evolution by studying landform history. Alternatively we may use that history, in conjunction with external forcing, to validate the theoretical

Geomorphology of Desert Environments. Edited by Athol D. Abrahams and Anthony J. Parsons. Published in 1994 by Chapman & Hall, London. ISBN 978-94-015-8256-8

mechanisms of landform evolution, although this process is also beset with many difficulties.

PROCESSES

The fundamental processes in channels are those caused by running water, the most important of which are scour, transport, and deposition. Other processes of importance are seepage from groundwater, bank failure, and vegetative growth. Less important processes include weathering of material in the channel, chemical precipitation, and subsurface particulate movement.

The essential features of the hydrology of arid and semi-arid channels were outlined in Chapter 11. These are:

(a) The flows are ephemeral – that is, the channel is dry for some period between the arrivals of runoff-producing storms.
(b) Dryland channels experience transmission losses of water to their beds – that is, the discharge may decrease or even dry up completely in a downchannel direction.
(c) The flow may be asynchronous – that is, the flow from different tributary systems may reach the trunk stream at different times, sometimes when the main channel is dry either before or after a flow has passed through.
(d) The flow is almost always unsteady in time and non-uniform in space and is often supercritical.

In general, flows in ephemeral channels are characterized by high sediment concentrations and large sediment yields. The classical works of Langbein and Schumm (1958) and Fournier (1960) indicated that semi-arid environments, especially those with high relief, have exceptional yields. These observations have been confirmed many times since and link exceptional amounts of geomorphic work to extreme events, indicating that magnitude and frequency relationships are here different to those of temperate channels (Schick 1977).

SCOUR

These hydrologic processes determine the nature and rate of channel-forming processes, the most important of which is scour. Scour is determined by the uptake of sediments and/or regolith from the bed and results in a lowering of the bed surface. In the sedimentation literature scour is also called entrainment. It can be determined by the use of scour chains anchored vertically into the channel bed (Emmett and Leopold 1965). As entrainment of particles occurs the part of the vertical chain exposed comes to lie horizontally on the bed and can be re-excavated to indicate the depth of scour and subsequent deposition. The depth of scouring may also be estimated from the burial depth of identifiable particles. Hubbell and Sayre (1964) first used radioactive tracers to determine the movement and scour depth of sand in sand-bed streams, and recently Hassan (1990) has used magnetically tagged pebbles. He describes several mechanisms for the burial of particles: (a) advancing bedforms, especially in sand-bed channels; (b) depositional movement of small grains through the interstices of large clasts; (c) scouring around large pebbles embedded in finer sediment, leading to lowering and subsequent burial; (d) covering the particles with later-deposited ones; and (e) embodiment and sinking in a moving traction carpet.

In his comparison of two ephemeral streams in Israel, both subject to medium-sized flows during the period of observation, Hassan found (a) that burial depths, which were greater under bars than in the thalweg, varied significantly over very short distances, indicating a higher variability of scour than suggested by the scour chains, and (b) that burial depths changed between events, between sections, and between bedforms. He attributed the burial to subsequent deposition during the storm and therefore concluded that tracer particles provided a good indicator of the depths of scour and subsequent fill.

Actual depths of scour in this study were estimated to be of the order of 14 to 16 cm for the largest storms, with shear stresses of 5.5 and 10.6 $N\,m^{-2}$. These differed significantly from depths estimated using the predictive equations of Leopold *et al.* (1966) ($D = 10q^{0.5}$, where D is scour depth in feet and q is discharge per foot width of the channel in cubic feet per second) and Carling (1987) ($D = 43.2q^{0.27}$ where D is scour depth in millimetres and q is discharge per metre width of channel in cubic metres per second). In the Salt River, a tributary to the Gila in Arizona, Graf (1983a) recorded depths of scour of 7 m with a flood discharge of about 500 $m^3\,s^{-1}$ and of 8.2 m at congested bridge piers. Leopold *et al.* (1966) recorded depths of 38 m at the site of the Hoover Dam on the Lower Colorado. Lateral changes are also strongly affected by scour and more easily recorded, though not necessarily more prevalent. Thornes (1974) mapped changes in channel width resulting from a single exceptional storm. These changes had a periodic character comparable to the pool and riffle sequence recorded in temperate channels. Some sections

underwent more lateral and others more vertical scour. Similarly Scott (1973) observed substantial lateral scour in Tujunga Wash, southern California, in a large storm in 1969. Lateral scour magnitudes of up to 40 m were recorded resulting in doubling of the flooded channel cross-section.

The spatial variability of scour was also recorded by Foley (1978) in ephemeral sand-bed channels in California. He defined mean bed scour as scour occurring simultaneously over a stream segment length comparable to the flood crest length, whereas local scour and fill are limited to a reach whose length is comparable to channel width. Local scour and fill does not necessarily occur over the whole transverse section and may occur several times at the same location in an individual flood. This seems to be caused by the migration of antidunes, which normally occupy less than the total channel width. A train of slowly moving antidunes reworks the stream bed along the axis of the train. If antidunes are the largest bedforms during a flood, then greatest bedform scour and fill occur where antidunes are largest and a scour-fill trough results. Both field and laboratory observations by Foley appear to confirm this process. Figure 12.1 shows the location of maximum scour for a December flood in Quatal Creek, Ventura County, which has a gradient of 2.3%. The predominant scour zone (90 cm depth) occurred in a narrow belt, occupying about one-third the channel width and, as is commonly the case, the net change was small compared with the total scour depth during the event. During this flood there was a single antidune train passing through the reach, but there may be as many as three or four in ephemeral channels. For channels behaving in this fashion it is expected that scour-chain data will show a threshold discharge below which little scour and fill are evident. This is because antidune amplitude has to be greater than the maximum dune troughs, otherwise the former would be obliterated by recession limb bedforms.

It is suggested by Foley that maximum scour in steep sand-bed streams can be estimated from the antidune equations (Foley 1977), which provide the maximum possible antidune amplitudes, assuming bankfull discharge and breaking stationary waves. Application of the equations to the Arroyo Frijoles data obtained by Leopold *et al.* (1966) indicated that the results were not in conflict with the hypothesis that all bed reworking in the Arroyo Frijoles was by bedforms.

The scouring process is related to the competence of the flow to pick up the available material and the capacity (maximum possible bedload transport rate per unit width) of the flow to transport it away from the site. The competence of the flow is determined by the ability of the flow to lift or drag the particles up into the water and sediment mix. In arid rivers supplying a mixture of sediment sizes this is increased by the hyperconcentrated nature of the flows (i.e. sediment concentrations in excess of 40% by weight) and decreased by the concentration of coarse particles at the bed surface by selective removal of the fines. The ability to entrain particles of a given size is often estimated using the Shields (1936) entrainment function, which defines the critical bed shear stress required to move a particle of a given size, or using one of the many variants reviewed by Maizels (1983).

The process of entrainment is complicated by armouring, which is the development of a coarse bed surface layer. Armouring is common in most rivers where there is a wide range of available particle sizes and is usually attributed to selective scour. Formation of an armoured bed in temperate channels requires low bed transport rates and a reasonably long period of constant flow (Sutherland and Williman 1977). This selective scouring may arise when the capacity for transport is greater than the available supply. Dietrich *et al.* (1989) suggested that surface coarsening develops in gravel-bed rivers when local bedload supply from upstream is less than the ability of the flow to transport the load. This supply reduction causes changes in bedforms and progressive confinement of the active bedload transport to a narrow finer bed surface bordered by a coarse, less active bed. Although these results were obtained under conditions of perennial flow in a flume, the forms described are quite common in desert channels with a mixed bedload, and the mechanism is almost certainly important in ephemeral channels, where transverse variations in sediment size are quite common and can be very important. The variations in supply were accompanied by quite significant changes in bedforms, with cross-channel bedload concentrations (waves of coarse sediment) due to congestion being replaced by lateral sorting. This switch can be observed in ephemeral channels when there is a long tail to the hydrograph before flow ceases.

Armouring appears to be less effective as the flow becomes deeper and more concentrated in time – in other words as the flow becomes more unsteady. This means that in ephemeral channels, where flow is generally very unsteady, the development of an armoured layer is generally less effective. Nouh (1990) found that the effectiveness of armouring P decreased significantly as the ratio $P = (D/T)(1/u_*)$

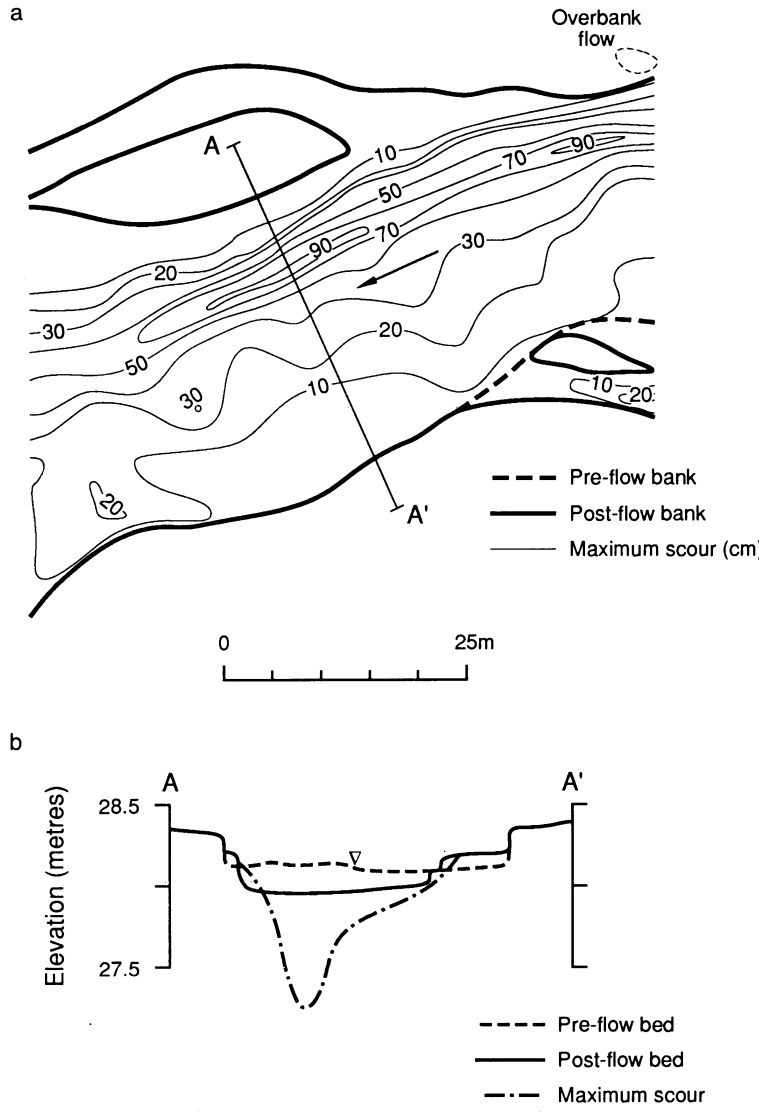

Figure 12.1 (a) Maximum scour map for Quantal creek, Ventura County, California in a single flood in December 1974 and (b) corresponding cross-section (after Foley 1978).

becomes larger, where D is flow depth, T is flow duration, and u_* is shear velocity. Typically desert streams have very short hydrograph durations. Figure 12.2 shows the effect of unsteadiness of flow in producing a strongly bimodal sediment size distribution, which is commonly found in ephemeral channels.

Entrainment may be inhibited in the very earliest stages of hydrograph rise and during small flows by a strongly bonded and sometimes cemented clay layer. This layer consists of suspended or even wash load sediment that would be carried off in perennial channels, but in ephemeral streams is deposited in the final stages of recession as the flow approaches zero. It is often colonized by algae which form algal mats, and these again resist entrainment at very low discharges. The fineness of the sediments and the algae development together can also significantly reduce transmission losses.

An attempt was made by Schick *et al.* (1987) to provide a general model for the relative role of burial and excavation of coarse particles. They assumed a

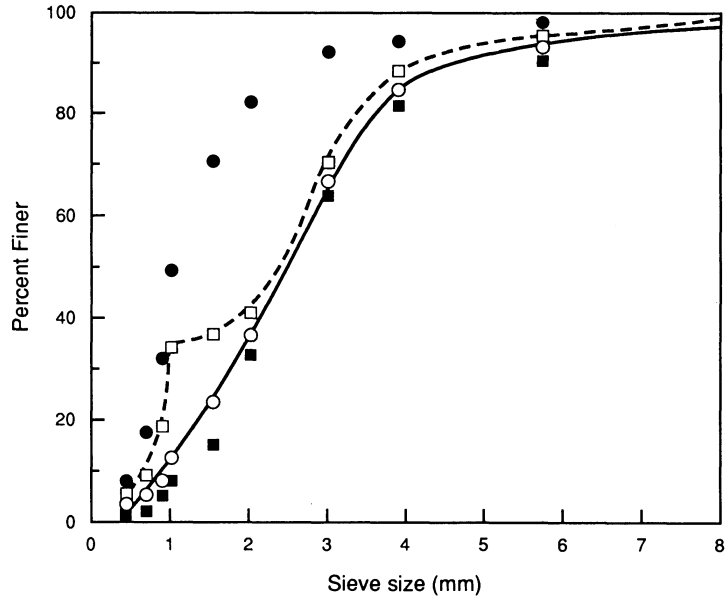

Figure 12.2 Plot of original and armoured size distributions for different flow conditions. The initial mean particle size = 1.00 mm; the initial geometric standard deviation = 2.00 mm (after Nouh 1990). ● = original; ■ = armour; steady flow; ○ = armour, $P = 0.004$; □ = armour, $P = 0.016$.

constant proportion of initially surficial tracer particles which are buried b_r and a constant ratio of buried tracer pebbles which are excavated e_r and obtained the equilibrium long-term number of buried particles S_i and the long-term number of buried tracer particles B_i:

$$S_i = [e_r/(b_r + e_r)]\,S_0 \qquad (12.1)$$

$$B_i = [b_r/(b_r + e_r)]\,S_0 \qquad (12.2)$$

where S_0 is the initial number of tracer particles at the surface, assuming none at depth. This is of course a simple first-order Markov chain, in which b_r and e_r represent the transitional probabilities of a shift from unburied to buried states and buried to unburied states, respectively. From this one could estimate the number of events to the equilibrium vector of the proportions present in both states. Schick *et al.* (1987) found that tracers in their experiments in the Negev Desert had about 70% burial and 30% exposure, which might imply about 50% probability of burial and 20% probability of re-excavation. They argued that e_r is likely to be greater in perennial flows of low intensity leading to an armoured surface layer, whereas in ephemeral channels flash flooding, mixing, and associated tendencies to burial appear more likely, leading to less likelihood of armouring. They suggested that, in general, the equilibrium proportions of buried and unburied tracers will reflect the dominant flows, and these are likely to occur with an average recurrence of about once every two years. They also showed that to get close to the equilibrium values under the conditions of the model (i.e. with stationary values of the transitional probabilities) would usually need at least five events. Their field observations suggested that between 6 and 14 events might have been required to reach the present distributions of their marked particles.

Markov process theory offers some interesting possibilities of extending the model defined by the authors, for example using mean residence times in the different states (buried and unburied) which are themselves flow dependent (e.g. Morley and Thornes 1972).

TRANSPORT

The transporting capacity of the stream depends on the energy available for transport, and this in turn depends on the proportion of energy expended on other consumptive uses such as frictional losses. This issue has been widely discussed in the literature. There are basically three approaches. The first expresses the total load capacity as a function of the stream power and views the transport phenomenon

as a moving carpet of decreasing density upwards, with dilation providing lift and slope providing the forward motion. This approach estimates transport rate through the Bagnold (1966) formula as

$$i_b = \omega[(e_b)/(\tan\alpha) + 0.01(u/v)] \qquad (12.3)$$

where i_b is total transport rate for immersed sediment, ω is unit stream power which equals γqs, γ is the specific weight of water, q is the discharge per unit width of bed, s is the energy slope, e_b is the efficiency of bedload transport, $\tan\alpha$ is the dynamic friction coefficient, u is the mean flow velocity, and v is the effective fall velocity of the suspended sediment.

The second approach typically attempts to provide a transporting capacity for each size fraction available in the channel bed as a function of the available shear stress and the critical shear stress required to entrain particles of that size. If this entrainment is a function of the actual availability of material in the bed, then the approach can accommodate armouring. Some success in estimating ephemeral channel flow transport has been obtained through the use of Laursen's (1958) equations based on this basic approach. Reid and Frostick (1984), for example, found excellent correlations between observed sand-size fraction concentrations and the values predicted by Laursen's (1958) formula. In addition, the formula has been applied successfully to the Walnut Gulch data by Lane (1982) coupled with a suspended load fraction transport equation based on Bagnold (1966). Laursen obtained bedload sediment transport for a particle size fraction d_i from

$$q_{sb}(d_i) = \varepsilon f_i \beta_s(d_i) \cdot \tau[\tau - \tau_{c(d_i)}] \qquad (12.4)$$

in which q_{sb} is bedload transport rate for dry sediment, ε is a weighting factor to ensure the sum of the individual transport capacities equals the total transport capacity computed using the median particle size, f_i is the proportion of particles in size class i and $\beta_s(d_i)$ is a transport coefficient. The critical bed shear stress is $\tau_{c(d_i)}$. The total bedload discharge is then obtained by summing the particle size fractions. In fact, Frostick *et al.* (1983) found that silt and clay concentrations could not be well predicted by Laursen's equation because the sources of these size fractions are the valley slopes with their variable soils and complicated patterns of sediment delivery.

A third approach is to consider the average travel distance of bedload material and this is often done using painted stones. Leopold *et al.* (1966) found that the average travel distance of particles ranging in mass from 200 to 13 000 g is linearly related to maximum discharge and poorly related to size. In general, they found that the small particles did not travel materially farther than large ones, and nearly half the flows include examples of large particles moving farther than small ones. There is thus no neat inverse relation between transport distance and particle size, at least in ephemeral streams.

The pattern of sediment transport through ephemeral channel hydrographs is often marked by a 7-shaped sedigraph (i.e. graph of sediment concentration against time). Sediment concentration rises almost instantaneously to high values and then falls through time as the discharge peak passes and recession sets in. This behaviour is also mirrored by particle size because the dominant particle size also declines through time, as illustrated by the sedigraphs shown in Figure 12.3.

Thornes (1980) observed that besides the rapid rise in sediment transport, with rapid recession there may be almost instantaneous deposition of large particles which is usually spatially discontinuous. Moreover, in a succession of flows, the behaviour of sediment transport changes as availability of materials of different sizes changes. After a very large flood many more coarse particles are available for transport, and often there is a greater sediment mixture. This leads to a catastrophe model of sediment uptake and deposition in which the common assumption that sediment is being transported at a capacity rate according to stream power has to be relaxed. This in part explains why Bagnold (1977) found $(\omega - \omega_c)$ a better predictor of sediment transport than stream power ω, where ω_c is critical stream power required to entrain sediment. If a wide range of sediment sizes is available, then saturated (i.e. capacity) transport can occur. If the distribution has a single mode at a large particle size, then nothing can be transported until that size is reached, and the flow is undersaturated to that point. Progressive armouring, caused by a sequence of flows with low competence, often gives rise to this situation in ephemeral channels. An exceptional flow is then required to disrupt the armour and make the finer bed sediment available for transport. From Yalin's (1977) fourth-power law of shear velocity for competence a set of equilibria in flow adjustments to sediment transport (and vice versa) can be derived. This set of equilibria can be represented by a cubic surface in shear velocity with stream power and sediment availability as parameters in the control space, as shown in Figure 12.4a. D^* is the ratio of mean to the standard deviation of particle size in the stream bed, T^* is the available power, and i_b is Bagnold's sediment transport rate.

The manifold in Figure 12.4a represents the 'fast

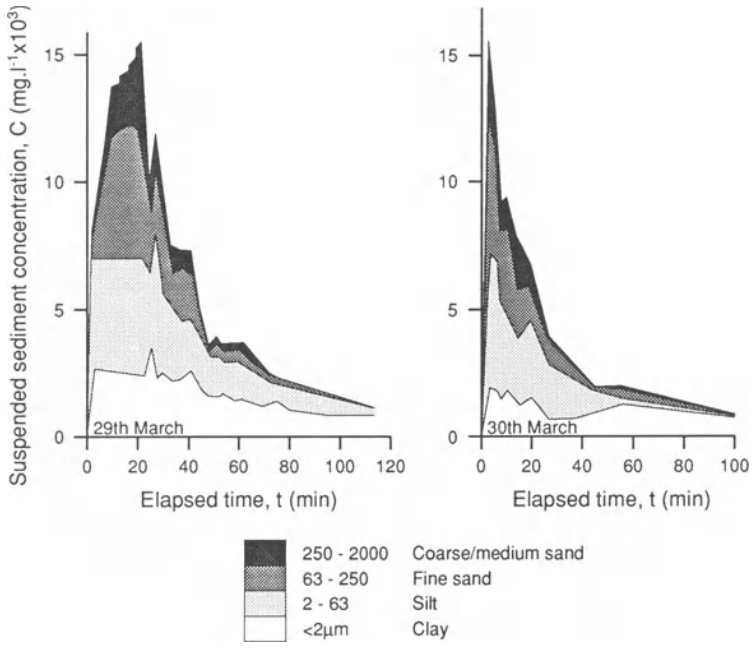

Figure 12.3 Concentration of suspended sediment by size fraction through three flash floods in the Il Kimere catchment, Kenya (after Frostick *et al.* 1983).

dynamic' of the sediment transport system. At *f*, there is a smooth increase in transport with power because a range of particles is available for transport, as shown in Figure 12.4c. At *g* the distribution function is narrower and particles larger so that very rapid entrainment occurs only at the point a_{2^*} on the surface. Less power is required to transport sediment already in motion, so there is a hysteresis and rapid deposition occurs at a_{1^*}.

The 'slow dynamic' of the system is provided by trajectories across the D^*–T^* control plane as these control parameters vary through time. The inherent structural instabilities (threshold in Schumm's (1979) terms) are provided by the manifold. In an ephemeral channel the rise and fall of the hydrograph carries the system across the horizontal D^*–T^* control plane. The stream power for the threshold of final motion is significantly lower than that required for initiation (cf. the experimental results of Reid *et al.* 1985). In the long term the supply of material to the floodplain also varies as a result of a variety of smaller flows producing armouring and the deposition of fine sediments brought in by asynchronous tributary flows. The model is also responsive to channel width variations. These are critical in ephemeral channels because they are often much greater than the actual flow and because they vary widely in space. Sudden changes in sediment transport capacity occur when the channel widens suddenly. As the depth/width ratio increases, the shear increases, and transporting power can increase. However, there comes a point when a further increase causes breakdown of sediment transport, carrying the system back across the cusp. A similar explanation was provided by Reid and Frostick (1984) for rapid spatial variations in transporting capacity. Downstream distance and local changes in channel width account for 77% of the variance in particle-size of flood deposits. Carling (1989) found evidence from a gravel-bed river of a catastrophic break in sediment transport related to threshold powers in excess of $15\,W\,m^{-2}$ at which framework gravels are transported. As this fraction is taken up, the transport process reaches its maximum efficiency of about 1%. Carling suggested that instead of a cusp-type catastrophe, a critical size/sorting ratio gives rise to a simple two-dimensional bifurcation.

When bedload transport rates are measured in ephemeral channels they are commonly found to exhibit wave-like behaviour that is independent of stream power (e.g. Lekach and Schick 1983). These waves are sometimes attributed to kinematic behaviour akin to traffic flow (Langbein and Leopold 1968), but in ephemeral channels seem to arise from

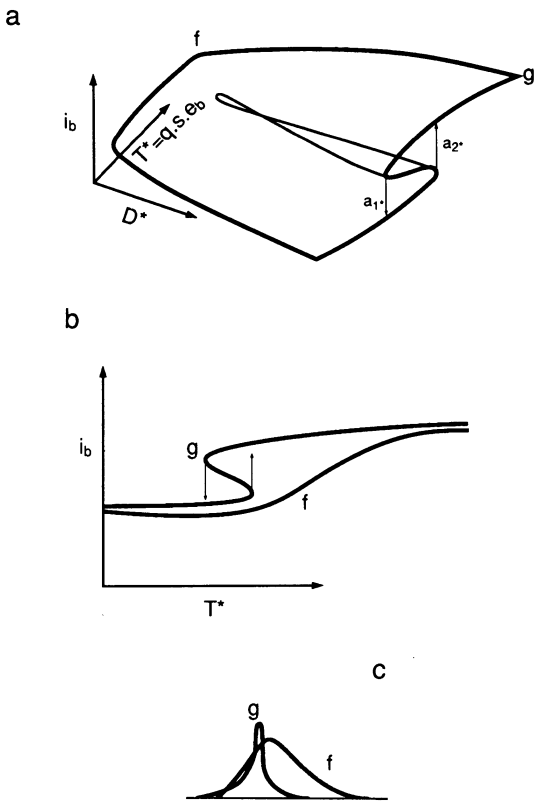

Figure 12.4 Cusp catastrophe model of sediment transport in ephemeral channels: (a,b) the structural instability; (c) size distributions for low and high values of D^*.

discontinuities in the channel area increment function and its relation to channel slope, as noted by Thornes (1974).

There have been two recent developments in sediment transport theory. The first has been the attempt to accommodate variations in the availability of sediment for transport. Most bedload transport equations tend to assume uniform availability of material for transport. The catastrophe model above assumes that available material is controlled by bed particle size, but it may also be constrained by what is available upstream from a sediment transport monitoring station. For example, van Sickle and Beschta (1983) incorporated variable sediment supply in their suspended sediment transport model. At the simplest level, suspended sediment concentration $C(t)$ at time t is given as a function of discharge $Q(t)$ and total available suspendable sediment stored within the stream channel $S(t)$:

$$C(t) = aQ(t)^b \cdot g[S(t)] \qquad (12.5)$$

with a and b as parameters of the sediment rating curve and $g(S)$ a function to express the relative changes in concentration due to changes in supply given by

$$g(S) = p \cdot \exp(rS/S_0) \qquad (12.6)$$

where S_0 is the initial available sediment at the beginning of the rainy season (i.e., the model run). Parameters a and b are related to properties of the channel system such as hydraulic geometry, channel morphology, and gradient. The parameter r can be interpreted as an index of sediment availability. For large r concentrations are sensitive to small decreases in $S(t)$, so r is likely to be a function of bed composition. p is another empirically determined parameter.

In this model the sediment availability is lumped into a single variable $S(t)$. In a later paper Beschta (1987) suggested that the sediment available for transport is distributed among several storage compartments and that the compartments may be depleted during an event and according to stage (lower stores more often depleted). During a rising limb, new compartments are progressively depleted at higher stages. On the falling limb the reverse occurs. This is somewhat similar to the compartment model of Moore (1984) wherein sediment variability over time is a function of availability, a sediment removal function (availability and storm magnitude), and sediment translation.

The second recent development in sediment transport theory has been the modelling of sediment transport as a travelling wave which is attenuated downstream by dispersive processes. Although such a model has not been applied to dryland river channels as far as we know, Pickup *et al.* (1983) have undertaken such an exercise for the Kawerong River, Papua New Guinea, which received heavy loads of mining sediments. The predicted rates of supply at the downstream end of the system appear to have been reasonably approximated by this model, and there seem to be good prospects for applying the methodology for the downstream propagation of tributary fans.

DEPOSITION

The previous discussion has already strayed to some extent into deposition. Net deposition is called aggradation. Depositional features are important in ephemeral channels because they dominate the morphology for long periods and cause serious economic losses throughout the drylands of the world. In sequences of scour and fill, the channel frequently

fills with sediment to levels close to that prevailing before a particular flow event, and the effects of scour may be buried. Depositional features also control transmission losses, determine scour sequences for subsequent lower flows, and provide clues to the sequences of flows. Baker *et al.* (1979) have pioneered the use of slackwater deposits in determining the magnitude of past flows and have shown how such deposits may be employed to estimate the frequency and magnitude of rare events. Slackwater deposits are formed in the dead zone where tributary water is backed up by the main channel flow. They are particularly important in arid environments where the potential for erosion of the deposits between floods is reduced once they have become vegetated and where tributary channels are often small and do not produce enough flow to remove the deposited material. Moreover, when there is a flood it is likely to be a large one and the effects on channels are likely to be long-lasting, even though many rivers in arid lands do not have usable slackwater deposits.

Frostick and Reid (1979) initiated the investigation of the drainage net control on channel fill sequences under flash flood conditions from a sedimentological point of view. By examining depositional sequences and their composition they were able to show the sequence of contributions from different tributaries operating out of phase. Marcus (1987), too, has recently demonstrated that a mixing model for heavy mineral concentration dilution by sediment yield from tributaries can go some way to quantifying sediment deposition in ephemeral channels. Specific departures from the model then give indications of asynchronous flow and deposition in the channel. The capture of sediment by in-channel vegetation also explains some of the patterns he found. The study of these phenomena is as yet still poorly advanced.

Just as in perennial channels, deposition in ephemeral channels results from loss of power to transport. But differences between perennial and ephemeral channels occur in the locations of deposition which reflect both the asynchroneity of flow in the network and the transmission losses in ephemeral channels. In the absence of flow in the main channel, the former gives rise to fan development at tributary junctions. Even when there is flow in the main channel, it may be insufficient to transport the material from the tributary junction. Finley and Gustavson (1983) described such features in a small catchment in the Texas Panhandle produced in a single 10-year event. At one location a 16-m-long boulder-to-cobble gravel bar containing minor amounts of sand was built out into a channel itself only 12 to 15 m wide. These are asymmetrical junctions in which the usual scour (Mosley 1972, 1976) is replaced by deposition due to asynchroneity of flow and thus matches more closely the cases cited by Burkham (1972) and Kennedy (1982). Thornes (1991) simulated this effect using both digital and hardware simulation (Fig. 12.5). He found for the flume experiments that the total sediment volume deposited in the main channel is largely a function of the transmission losses in the main channel and the relative magnitudes of the two flows, though the total deposited volume also increases with the total combined flow.

The effect of junction deposition may cause movement of the main channel across valley to undercut the opposite bank, may provide slugs of sediment which are propagated downstream as waves under larger flows, and may even cause damming of the main channel itself. Finally, we may note that similar features occur in perennial channels subject to extreme flood events, especially when carrying large volumes of boulder- and cobble-sized materials, and for the same reasons.

Transmission losses tend to cause lobes of sieve deposits in the main channel whose position and permanency relate to the frequency and magnitude of flow survivals, and the location of such deposits has been modelled by Thornes (1977). The banks of channels may also be buried in sandy desert areas by wind-blown sand, as reported by Burke *et al.* (1970).

BRAIDING

In single thread channels the processes of scour and deposition give rise to channel forms which are quite well adjusted to dominant flows through the mechanics of the channel boundary (as reviewed by Thornes 1979). This all pervading unity of river channels, revealed by the hydraulic geometry, has also been found applicable to ephemeral channels, as reviewed by Graf (1987a). In both sand- and gravel-bed channels, the process of braiding, involving interplay of both scour and deposition, produces much more complex channel geometries, which appear chaotic both in the common sense of the word (Ergenzinger 1987) and in the special use of the terms implying non-linear dynamic behaviour (Thornes and Gregory 1991). According to Davies (1987), variability is the essence of the problem, implying that simple averaging of overall flow quantities such as depth and width over space and/or time is meaningless in the context of predicting river

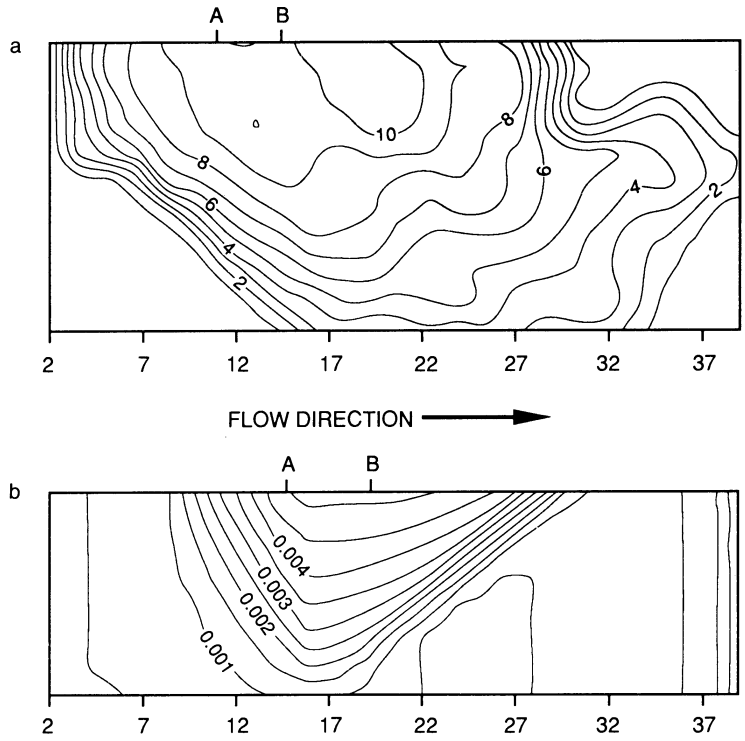

Figure 12.5 Computer simulation (a) and hardware model (b) of depositional contours at a channel junction with the entrance angle at 45° (after C. Thornes 1991).

behaviour. Braided rivers in their natural states typically have large width/depth ratios (in excess of 20), steep gradients (of the order of 0.01) and have widely varying bed material sizes. Only relatively rare events occupy the bed completely, and the number of individual channels can vary from 1 to more than 20.

The investigation of braiding as a plan form characteristic was pioneered by Lane (1937), Leopold and Wolman (1957), and Fahnestock (1963). Leopold and Wolman (1957) established a discriminant function between braided and non-braided channels related to slope and discharge. More recently Parker (1976) has redefined the discrimination in terms of slope/Froude number and Thornes (1980) and Graf (1987b) expressed the problem in terms of a cusp catastrophe.

The detailed investigation of braided rivers has proved much more difficult and problematic, as Ergenzinger's (1987) synthesis of the work carried out in the Butramo catchment in Calabria has demonstrated. Our own observations on the Rambla Seca in south-east Spain show that channels can shift between braiding and meandering within a short distance, giving a pseudo-oscillatory channel width pattern (Thornes 1977), and over a short time. Typically on the steep rising limb of a hydrograph, braiding is induced by prior channel morphology. At peak flow the bed may have a planar form. While on the falling limb there is a sequence through braided to meandering channels as the flow conditions change. In the Butramo, Ergenzinger (1987) observed flows of $10\,m\,s^{-1}$, with suspended load transport of about $710\,kg\,s^{-1}$ and a maximum yield of about $23\,kg\,s^{-1}\,km^{-2}$. Width/depth ratios had a modal class between 25 and 35 during peak flows, and the ratios appeared to increase during recession, when after the flood crest the flow is still using over-sized old braids. The investigation indicated that there is great stability of braid form during different discharges, though no simple relationship was observed between width/depth ratios and the number of braids. Above 60 there is a tendency to three braids and above 100 a tendency to four, but for every width/depth ratio there is always the possibility of a two-braid system,

which is most likely during the first half of the flood wave. Ergenzinger found a weak tendency for the friction factor of the total braids to diminish with increasing discharge, whereas shear stress grew at approximately the same rate as width and depth. The actual values are close to the theoretical values under the minimum variance hypothesis of Langbein (1965) and suggest that there is a high degree of self-regulation by braids, related to bankfull geometry, even during times of great variation of discharge. According to these results the braided forms are adjusted to allow the water to discharge as efficiently as possible.

Not all recent workers have found that braided channels perform so well in accordance with general minimization principles. After thousands of measurements Mosley (1983) concluded that scientifically defensible, quantitative prediction of the impact of discharge change on the ecologically significant aspects of a braided river was impossible. This does not mean that generalities about processes are not possible, and the confluence–scour–bar collection of processes is regarded as the essential building block for braided channels according to Davies (1987) and has been modelled by Ashmore (1982).

Again, pulse-like transport of sediment occurs in braided systems. Ashmore (1987) reported laboratory experiments on braided channels whose transport rates show periodic behaviour. Comparing the yield data with time-lapse photography, many of the larger pulses could be identified with zones of increased braiding activity and more abundant migratory unit bars. These observations are consistent with Griffith's (1979) model of bed waves but might also imply a bifurcation between alternative stable states, wide and shallow or narrow and deep, as suggested by Thornes (1980).

CHANNEL INITIATION

Although Leopold *et al.* (1966) found that sheetwash was the most important contributor to erosion in their classic study of Arroyo de los Frijoles, many authors have demonstrated the unquestionable influence of channels and channel development on both morphological change and on sediment yield from arid and semi-arid channels. In addition to major ephemeral channels, gullies are especially common in arid and semi-arid environments. There are essentially two general modes of formation: (a) the Hortonian mode of formation involving concentration of overland flow and abstraction of larger by smaller gullies in the network to produce a regular channel system, and (b) the non-Hortonian mode involving headward extension and bifurcation. In the second type the dominant mechanisms appear to be overfall, mechanical collapse, spring sapping from resurgent ground water, and piping.

Hortonian Channel Development

Gullies are sometimes identified as either continuous or discontinuous. Continuous gullies begin their downstream course with many small rills, while discontinuous gullies start with an abrupt headcut and terminate in a lobe on the hillside where the channel slope intersects the hillslope (Leopold and Miller 1966). Ireland *et al.* (1939) suggested that almost all gullies result from either an increase in runoff or an acceleration of flow. Flow acceleration may result from (a) random convergence of the flow around vegetation or other surface roughness elements, (b) local disturbance of the surface which reduces its resistance to shear, such as localized grazing or burrowing (Heede 1974), or (c) particular hydrodynamic conditions of flow which may be empirically identified by the Froude number (Savat 1977, Boon and Savat 1980). According to these mechanisms, channels form because the flow applies a shear stress to the underlying soil sufficient to overcome its resistance to shear. This is the threshold concept of channel initiation.

Begin and Schumm (1979) suggested a criterion for assessing the threshold instability of valley floors in alluvial fills. This criterion is the ratio between the applied flow shear stress T_0 and a threshold shear stress T_{th}, in which T_0 is $A^{rf}S$, A is the catchment area, S is the valley floor slope, f is the hydraulic geometry exponent of the power relation between flow depth and discharge, and r is the exponent of the power relation between discharge for a given return period and catchment area. The value of T_{th} is set equal to the minimum value of T_0 for gullied valley floors. Figure 12.6 shows the probability of valley floor entrenchment as a function of T_0/T_{th}.

The effect of slope on Hortonian drainage patterns has been examined experimentally by Phillips (1988). Eight experiments were conducted in a flume with different ground slopes under simulated rainfall on a homogeneous mixture of sand, silt, and clay. Incremental base level lowering accomplished maximum drainage density, just as Parker (1977) found. In this process channel generations (groups of morphologically similar channels that evolve at different times during the development of a drainage network) formed during all the experiments, and there was a definite change in network pattern from

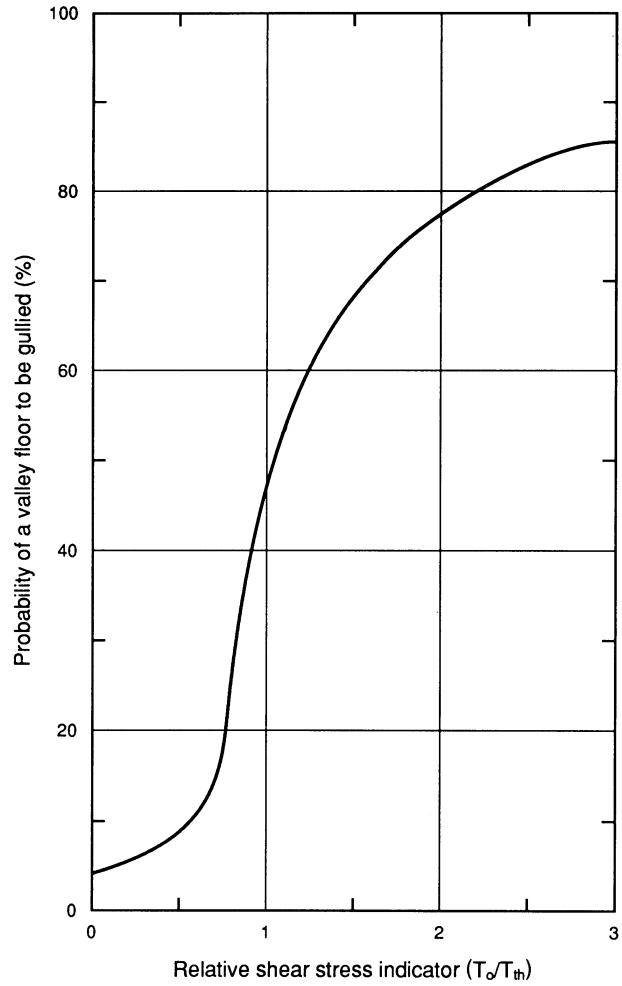

Figure 12.6 The schematic relationship between probability of incision of a valley floor and the ratio T_0/T_{th} according to Begin and Schumm (1979).

dendritic to subdendritic to subparallel to parallel as slope increased from 0.0106 to ⩾0.05.

In addition to the threshold mechanism there is a general instability mechanism for Hortonian channel development proposed by Smith and Bretherton (1972). They suggested that channel development could occur from a random perturbation on a hillside if the rate of increase in the capacity to transport sediment exceeds the rate of production of sediment to be transported. This criterion has been used by Kirkby (1980) to develop a theory of network extension capable of predicting drainage density under different climatic conditions and under various assumptions of land-use change. Recently this theory has been further developed to merge the threshold and dynamic instability approaches, as described below.

Non-Hortonian Channel Development

Incision is not the only mechanism whereby drainage channels may be initiated. Other mechanisms include piping (Harvey 1982, Gerits *et al.* 1987), liquefaction and microslumping (Savat and De Ploey 1982), mass failure (Thornes 1974, Dietrich *et al.* 1986), throughflow or groundwater seepage, called spring sapping in the older literature (Dunne 1980, Higgins 1984), and deflation (Mosley 1972).

The exact role played by piping in gully initiation is still a matter of debate. The pipes themselves form

in homogeneous, sodic-rich materials usually in response to steep hydraulic gradients. But only where these gradients match surface gradients do pipes offer an obvious mechanism for gully initiation except by collapse of the roof of a pipe.

The evolution of the drainage network by headward knickpoint growth has been demonstrated experimentally by Parker (1977). A laboratory prototype with a pre-existing network developed on a mixture of sand, silt, and clay was subjected to two treatments: one with steeper slopes but no base level lowering, and the other with less steep slopes and base level lowering. Lowering the base level produces a network that develops fully as it grows headward. The knickpoint migrates upstream, and the channels grow and bifurcate to produce a fully developed network in which little internal growth occurs. Without lowering, long tributaries develop, and the area between these tributaries is later filled in by additional tributary growth. Network development due to base level lowering produces the higher drainage density. Moreover, during this style of network development the first-order streams show a regular length, implying a regularity in length before bifurcation. In fact, this length becomes smaller as the space became saturated. This is a similar result to that expected by Thornes (1988) from a competition model of gully headward growth. The model posits a logistic growth model for headward extension constrained by both area and by vegetation cover in the upslope ungullied area.

The generation of channels by groundwater sapping, initially recognized by Leopold *et al.* (1964), was examined in detail by Howard (1988a). He identified the following characteristics of channels formed by sapping: theatre-shaped valley headwalls, strong structural controls, hanging tributary valleys, long main valleys with short stubby tributaries, irregular angles of channel junctions, and valley widths nearly constant in a downstream direction. This process appears to require large volumes of water and is most efficient in unconsolidated layered sediments where the limiting factor is simply the transporting capacity of spring-fed flows. Experiments in homogeneous unconsolidated sediments even with small percentages of silt and clay indicate that very high hydraulic gradients are required to initiate erosion, and then viscous mudflows become the most important mechanism. Three-dimensional experiments have been conducted on sapping using essentially homogeneous isotropic sand mixtures in a laboratory model (Howard 1988b). The experimental setup is shown in Figure 12.7, and experiments were conducted with and without a downstream scarp in non-cohesive and slightly cohesive sand. As suggested by Dunne (1980), the channels with a more advanced headcut cause convergence of flow lines and resultant capture of ground water from adjacent channel headcuts. Similar competitive behaviour was advocated by Faulkner (1974) for gullies developed in the Red Deer Plateau in Alberta, though here the mechanism is one of capture of overland flow. As the channels extend headward and flow convergence increases discharge, erosion rates increase. Thus behaviour is logistic, as modelled by Thornes (1988). This was offset to some extent in the experiment by decreasing the head in the reservoir. Bifurcation was caused by three factors: (a) widening of the valley head, (b) slight variations in permeability, and (c) headwall slumps. Howard's (1988b) mathematical model of network evolution is discussed below.

HEADCUT PROPAGATION

Because flow is non-steady and non-uniform, sediment removal is substantial, and weathering relatively limited, topographic discontinuities are much more common in ephemeral than in perennial channels. These discontinuities tend to take two forms. The first is a sharp increase in channel slope produced by either erosional history (base level lowering) or resistant bedrock layers. These features, which are here called knickpoints, have channels upstream and downstream. The second is the switch-over from unchannelled hillslope to channelized flow, herein called gully heads. In the former the processes are those of differential entrainment and transport; in the latter mass failure is usually involved.

Knickpoint Migration

Knickpoint migration has been recorded by many authors, and knickpoints are common features in ephemeral channels. Where there are intercalated weak and resistant materials, knickpoints are often multiple in character and lead to a valley-in-valley form, such as those simulated in the laboratory by Holland and Pickup (1976). The general morphology is shown in Figure 12.8. The knickpoint lip is the break of slope where the channel bottom becomes markedly steepened, and it makes an angle with the knickpoint face. The drawdown is the reach just above the knickpoint lip where the water surface is steepened as a result of the drawdown over the knickpoint lip. Often in a channel there will be several knickpoints in succession. Schumm *et al.*

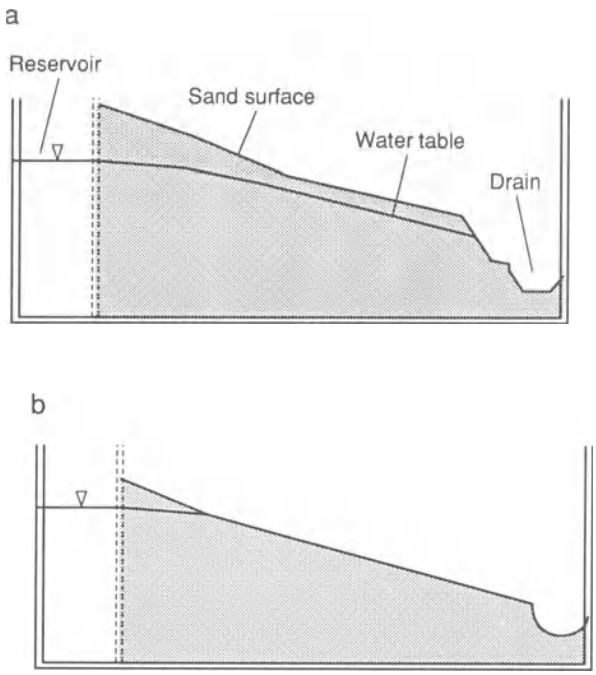

Figure 12.7 Howard's (1988b) experimental sapping chamber setup with (a) and without (b) a downstream scarp in the sediment.

(1987) described these as precursor, primary, and secondary knickpoints. These features may merge into a knickpoint zone, an area of steeper channel separating two less steep sections.

The role of overland flow in headcut migration has been studied both in the field and in the laboratory. Field studies by Bradford and Piest (1977) showed that the rate of migration of headcuts can be explained statistically by discharge over the lip. Gardner (1983), in an extensive series of laboratory experiments, created artificial knickpoints by base level lowering in a laboratory flume. Immediately after the drop in base level, drawdown over the knickpoint lip caused oversteepening of the water surface profile. The drawdown zone extended nearly 7 cm upstream from the knickpoint, and average flow velocity doubled over the lip. Erosion was most intense along the centre line in the zone of highest velocity, and a V-shaped notch occurred at the lip. In the incised reach below the knickpoint, width increased, but velocity and depth decreased to stable values. Maximum velocity, near maximum depth and minimum width, consistently occurred at the knickpoint lip, and therefore maximum erosion occurred at the lip, gradually decreasing away from the lip in both upstream and downstream directions. This distribution of erosional intensity was maintained along the knickpoint reach until the knickpoint had evolved into a uniformly inclined slope. The erosion took place in two components: the incision of the channel in the drawdown reach above the lip and the progressive reduction in the face slope during migration. No net aggradation occurred within the bedrock channel below the knickpoint for any of the experimental runs.

Obviously, since all knickpoints do not die out, there must be some process capable of sustaining the form. Plunge pool action is clearly one of the mechanisms involved and especially in conditions of vertical inhomogeneity, as noted by Gardner (1983).

Gully Headcuts

When headcuts are propagating into unchannelled surfaces they are called gully headcuts. Headcuts

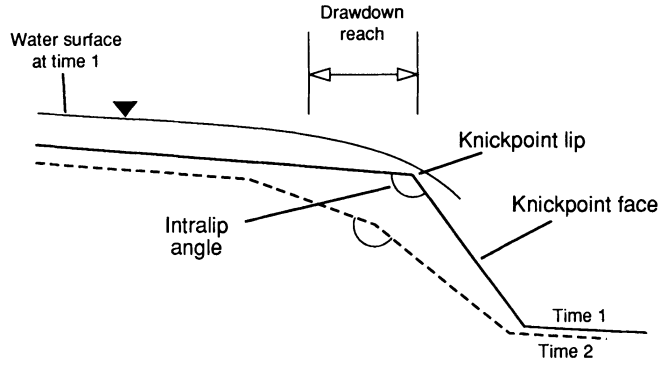

Figure 12.8 Terminology of a knickpoint, based on Gardner (1983).

may also occur, however, along the floors of broad alluvial fills, such as the arroyos of the American South-west. There are basically three processes involved, scour of the boundary and the plunge pool (where it exists), mass failure engendered in a variety of ways, and transport of sediment away from the headcut.

Erosion of the lip operates under the normal conditions of scour and is presumed to be proportional to the tractive force of the flowing water. The velocity at this boundary is determined by the upstream approach velocity, which is dependent on the discharge per unit width of flow, and the depth of the free fall after detachment. There is some empirical evidence to support this model of gully growth by headcut recession. For example, Beer and Johnson (1965) in an analysis of data from western Iowa correlated gully growth positively with surface runoff and negatively with gully length and its distance from the divide. Similarly, Piest *et al.* (1975) showed that gully growth is strongly correlated with discharge. Mitchell and Bubenzer (1980) summarized empirical equations that have been proposed for headcut recession in the United States.

Some care is needed, however, in drawing the conclusion that gully growth is due to boundary scour. As outlined below, scour pool development and mass failure are also clearly related to discharge, and the two processes are sometimes confounded. In general, the inability to separate these two processes underlies both Seginer's (1966) simple formula, in which gully head retreat is a power function of catchment area, and Thornes' (1984) use of distance from the divide for modelling gully growth. Moreover, Heede (1974) argued that sediment loads from gullies are often more related to time and duration of flows than to flow magnitude, again reflecting the variety of processes involved.

Failure due to mass movement is the result of undercutting by a scour pool or by groundwater suffusion. The processes of erosion below free-trajectory jets have been studied by Mason (1984) in the context of the discharge of flood waters downstream from dams. It is the erosive characteristics of the jets which are least well known. In large dams the effects can be severe. For example, in the Picote dam in Portugal after a flood in 1962 a pit 20 m deep was formed in granite causing a 15-m-high bar of eroded material downstream, and in the Kariba dam from 1962 to 1967 a 50-m-deep plunge pool was excavated. Although little is understood about cavitation by a free jet in rock and soil materials, the plunge pool often takes on a regular and predictable geometry. Depending on the point of attachment, the scour potential of the falling water combines with the hydraulics of the water in the pool to determine the pool's shape. The point of attachment is determined by the trajectory of the falling water and the height of fall. Thus height of the headcut plays a triple role: first it determines the velocity at the lip, second the energy at the point of attachment, and third the stability conditions of the headcut. For these reasons many workers have proposed that the depth of scour D under a jet is a function of unit flow q, head drop H, flow depth at the lip h, particle size of the bed material d, and the acceleration of gravity g. Then, the general relationship is assumed to be:

$$D = c(q^e H^f h^j)/g^m d^n \qquad (12.7)$$

On the basis of 26 data sets from prototypes and another 47 from hydraulic models Mason (1984) concluded that the following empirical values of the coefficients provide a good fit to the prototypes and models: $c = 6.42 - 3{\cdot}1H^{0.1}$, $m = 0.3$, $j = 0.15$, $e = 0.6 - H/300$, $f = 0.05 + H/200$, and $n = 0.1$. Equation 12.7 has a coefficient of variation of the observed to predicted values of 25%.

Laursen (1953) seems to have been among the first to find that scour patterns formed by jets are similar in shape. Van der Poel and Schwab (1988) developed dimensionless empirical predictive equations for the depth, length, width, and volume of plunge pools from experimental work. In these experiments, scour holes were initially wide and shallow and reached a more constant shape during the erosion process so that depth to length ratio settled to 0.5. Formation of the plunge pool at the base of the gully headwall increased the effective height of the wall and, consequently, decreased the stability. Using the Morgenstern–Price method of stability analysis, van der Poel and Schwab found that the selected failure surfaces intersected the surface with an angle of 90°. The highest reductions in the safety factor occurred for long scour times, materials of low shear strength, and low tailwater levels. Moreover, for equal total discharges, the conditions with the lower discharge rates for longer periods of time caused greater reductions in the factor of safety. An increase in the slope upstream from the headcut had little influence on plunge pool dimensions. The main effect of increased slope was to shift the point of reattachment further from the headwall.

Bradford *et al.* (1973) also carried out stability analyses of headcuts based on the Simplified Bishop Method of Slices. The results of the analyses indicate that water table height has the greatest effect on gully wall stability. By contrast, tension cracks have

a negligible effect. However, in our own experiments with gully head stability in a clay soil, cracks perform an important role in inducing infiltration, and it may be through this role that failure can occur in gully heads where ephemeral flow conditions prevail. Experiments in field conditions in semi-arid Spain show no indications that soils were ever near saturation before runoff events. Consequently, a more likely mechanism is the loading of already cracked soil by water leading to toppling failure. Bradford *et al.* (1973) calculated that rainfalls of 140 mm h^{-1} would be required to induce failure in the case they studied. However, their calculation assumes Darcian flow. Crack-induced macropore infiltration and transmission losses, especially for headcuts within the channel, may provide sufficient pore water to reduce effective stress sufficient for failure to occur long before that due to Darcian seepage and at lower rainfall intensities.

CHANNEL WIDENING AND BIFURCATION

Debris is supplied not only from the headcut but also from the side walls of gullies and channels. Channel widening and downcutting in gullies are less commonly described than headward extension, though the balance between them is probably critical in determining whether a gully will propagate headward or diffuse laterally and disappear. Thornes (1984) likened the headward growth of gullies to an aeroplane moving through still air. When headward propagation is more rapid than lateral diffusion (as in cohesive soils) long narrow gullies with few bifurcations occur. When widening is more important (especially in non-cohesive materials) dendritic drainage networks with frequent bifurcations develop. Widening occurs by both erosion by running water and mass failure. The fluting described by Veness (1980) consists of vertically elongated grooves, generally tapering at the top, that furrow into the wall of the gully. They are formed by concentrated flow over the edge of a gully. Bank sloughing and even rotational failure, on the other hand, may cause collapse of gully walls, especially where undercutting has occurred.

VEGETATION EFFECTS

A characteristic feature of arid and semi-arid channels is that they are often the site of vegetation growth. The suballuvial moisture provides sustenance for phreatophytic plants and for seasonal herbs and grasses. As a result, both erosional and sedimentational processes are modified. In gullies and upland channels, vegetation typically occupies the floor of the channel sometimes as a dense brush. In larger channels, bars are usually colonized first, since they provide easier sites for successional changes to occur. With full vegetation development the channel is hemmed in by thick groves of trees, usually in large wide channels where there is considerable groundwater replenishment. Whole systems can be transformed if the vegetation is removed, and there is clearly a cycle of colonization, destruction, and recolonization with events of great magnitude. Consequently, vegetative growth in the channel environment can provide strong clues to channel history. The establishment of a species depends not only on ecological amplitude but also on a variety of chance factors, including factors such as time of year of flooding, stem-sprouting ability of species, and the number of viable seeds deposited at the site. Once established, the interaction between species for light, water, and nutrients does not seem to change the composition much. What is more important is the capacity to survive torrential flows (Campbell and Green 1968).

In Sycamore Creek, Arizona, Fisher *et al.* (1982) observed the effects of three floods in rapid succession which obliterated 98% of the standing crop of cottonwood (*Populus freemontii*), walnut (*Juglans major*), sycamore (*Palatanus wrightii*), and ash (*Fraxinus velutina*). Within 63 days of these events the stream decreased by 28% in width, 22% in depth, and 34% in mean velocity. Schumm and Lichty (1963) also reported the progressive reinvasion of a floodplain environment by woody vegetation along the Cimarron River. Beginning with a major flood in 1914 and continuing until 1942 the river widened to an average of about 400 m. During the period 1943 to 1954 floodplain construction occurred due to increased rainfall and better conditions for tree growth. Although floods once again increased, channel widening was constrained by the trees. This situation contrasted with that earlier in the century when the floodplain was colonized by grasses. The constraining effects of vegetation on hydraulic geometry have also been documented by Zimmerman *et al.* (1967) for temperate channels and by Thornes (1970) for tropical rainforest environments.

Relatively little is known about the conditions giving rise to vegetation removal. Bull (1979) suggested that for gully headcuts progressive headward growth may lead to dewatering of the area upslope of the headcut and death or reduced fitness of the vegetation. This, it is suggested, allows the headcut to grow further in a kind of positive feedback mechanism (see Thornes 1988). A more coherent

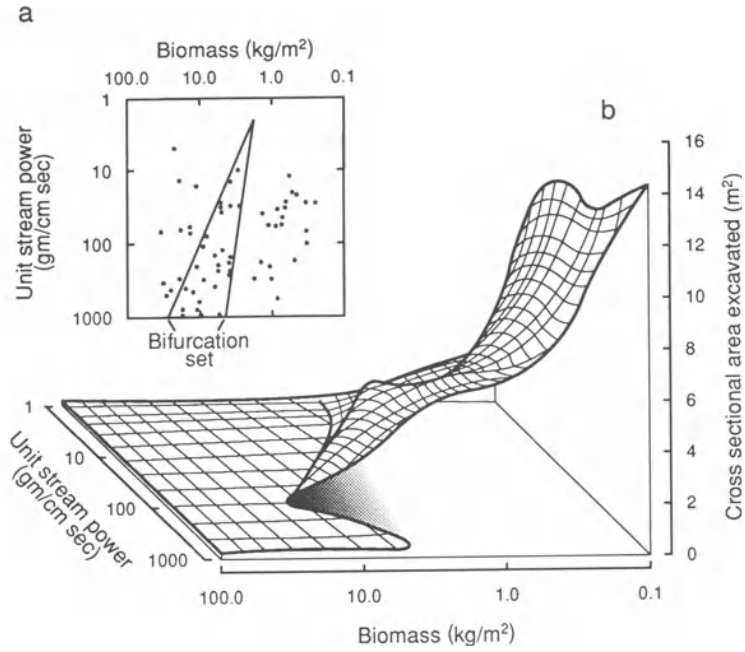

Figure 12.9 The cusp catastrophe model of arroyo development according to Graf (1979): (a) the distribution of sampled sites in the control plane; (b) the catastrophe surface. Major trenching occurs in and to the right of the bifurcation set.

attack on the problem has been made by Graf (1979). He attempted to provide a model for scour as a function of stream power and channel resistance expressed as vegetation density through biomass. He used hydrologic equations to convert field and remotely sensed data into the force of flowing water, expressed as unit stream power at a variety of sites in the central Front Range, Colorado. Previous analysis of the systematic covariation among force, resistance, and amount of material excavated led to the expectation that as force increased and resistance decreased, scour would be significantly increased. In fact, a three-dimensional plot of the variables showed that this did not occur. Figure 12.9 shows a reinterpretation of these data with a cusp catastrophe formulation. The left-hand edge of the fold represents a threshold corresponding to the equation $\tau = 0.45B_v^{2.33}$, where τ is the tractive force of the 10-year flood and B_v is the biomass on the valley floor. If $\tau > B_v$, then channel entrenchment results. If $B_v > \tau$, then the channel is stable. In fact in the overlap (between the two bifurcation sets) either condition may occur, but entrenchment is the more likely.

EVOLUTION

By evolution of landforms we refer to the development of forms according to a particular set of processes. Evolution describes the development of landforms regardless of a particular place or time. It is an abstract construction because hardly ever in nature is the evolutionary trajectory worked through to completion. One of the earliest and, at its time, most persuasive evolutionary models was Davis' cycle of erosion. Many contemporary models of evolution are still qualitative or based on an idealization of an actual historical series.

CHANNEL INITIATION

The general stability approach to channel development examines the conditions under which a small perturbation will grow or disappear according to whether the hillslope is stable or unstable. Smith and Bretherton (1972) suggested that the hillslope is unstable if sediment transport capacity increases more than linearly with water discharge because then where flow converges in a hollow the ability of

the flow to transport sediment increases more rapidly than the inflow of sediment. The flow therefore erodes in an effort to make up the sediment deficit. This mechanism will hereafter be referred to as the S-B instability.

The threshold approach defines erosional thresholds by an excess of tractive stress over resistance. The tractive stress is then defined through process laws based on the generalized qs product, where q is the unit discharge and s is the slope (e.g. Willgoose *et al.* 1990). Kirkby (1993) suggested that there is a progressive shift from behaviour controlled by S-B instability conditions, which dominates in semi-arid environments, to one in which threshold criteria dominate in temperate environments.

Kirkby (1993) approached the problem through an evolutionary model which has hydrological and erosional components. The former component is a slope routing model which allows for equilibrium overland flow, partial overland flow due to infiltration losses, and throughflow. The latter component is a sediment transport model which involves rainsplash driven by rainfall intensity and gradient and wash processes driven by the square of overland flow discharge in excess of a threshold of sediment detachment. These two components can be combined with the hydrological model and daily rainfall parameters to derive the relative dominance of threshold instability (rills occur by exceeding the material strength) and S-B instability (hollows or gullies occur through sediment transport capacity increasing faster than water discharge).

This leads to the development of two zones whose significance varies according to the threshold value and the storm size. The first zone has well-developed headcuts combined with rilling, where the morphology is sharp and there is no diffusion out of the headcut. In semi-arid environments this is the gully zone. Upslope of the gully zone is a second zone where threshold behaviour dominates before S-B instability sets in. Rill wash is actively eroding and transporting material, but hollow enlargement is prevented in moderate storms by active splash infilling. For large storms rill erosion can dominate, but their banks tend to be diffuse. Farther upslope out of the channels is a belt of instability but without rilling, comparable to Horton's belt of no erosion.

This pattern of a sharp headcut, a fuzzy rilling zone, and an unstable but unrilled zone are commonly found in semi-arid environments. Where thresholds are very low, gradients steep, and vegetation sparse, the headcut zone extends almost to the divide and badlands prevail.

HEADCUT PROPAGATION

There is considerable historical evidence that intense dissection, high drainage density, and badlands develop by the headward movement of waves of dissection and the consequent extension of channel systems. Such conclusions were drawn by Schumm (1956) at Perth Amboy, by Seginer (1966) in southern Israel, by Howard (1971) in the Henry Mountains, and by Thornes and Gilman (1983) in south-east Spain. Moreover, Parker (1977) demonstrated in the laboratory that channel network extension by headward growth succeeded base level lowering. Headcut migration may also lead to the fusion of several spatially discontinuous gullies (Heede 1974).

A variety of models has been developed for drainage network evolution. In any network half the channel links are first-order streams and, therefore, half the total channel length lies in the headwater areas. It follows that factors which control the stream heads are important in controlling drainage density. Thus, for example, Howard (1971) simulated network growth by adding new links at the edge of the network at random. Channels grow headward and bifurcate, producing a 'wave of dissection' at the sources of the first-order channels and Euclidian topologically random networks. A more recent model of headward growth was proposed by Stark (1991) in which stream heads branch and propagate at a rate which is proportional to the strength of the substrate – a process known in physics as invasive percolation – with the added requirement of self-avoidance (i.e. loops cannot occur). Variations in lithology, structure, diagenesis, groundwater hydrology, soil development, and vegetation cover lead to variations in substrate strength. This means that stream head propagating across a catchment boundary is more probable at some points than others. By making the assumption that the next point to give way on the margin will be the weakest, the model of headward growth and branching becomes invasive percolation. This model is consistent with the fractal scaling of streams implicit in Hack's (1957) scaling exponent for main channel length against drainage basin length and with Horton's laws.

One way to generate the rule that headward growth follows water would be to make the substrate in the invasive percolation model sensitive to throughflow distribution and, consequently, to potential mass failure (Dietrich *et al.* 1986) or to relate it to topography in areas where overland flow is dominant using a spatial convergence criterion such as the TOPMODEL convergence index applied to the surface (Bevan and Kirkby 1979).

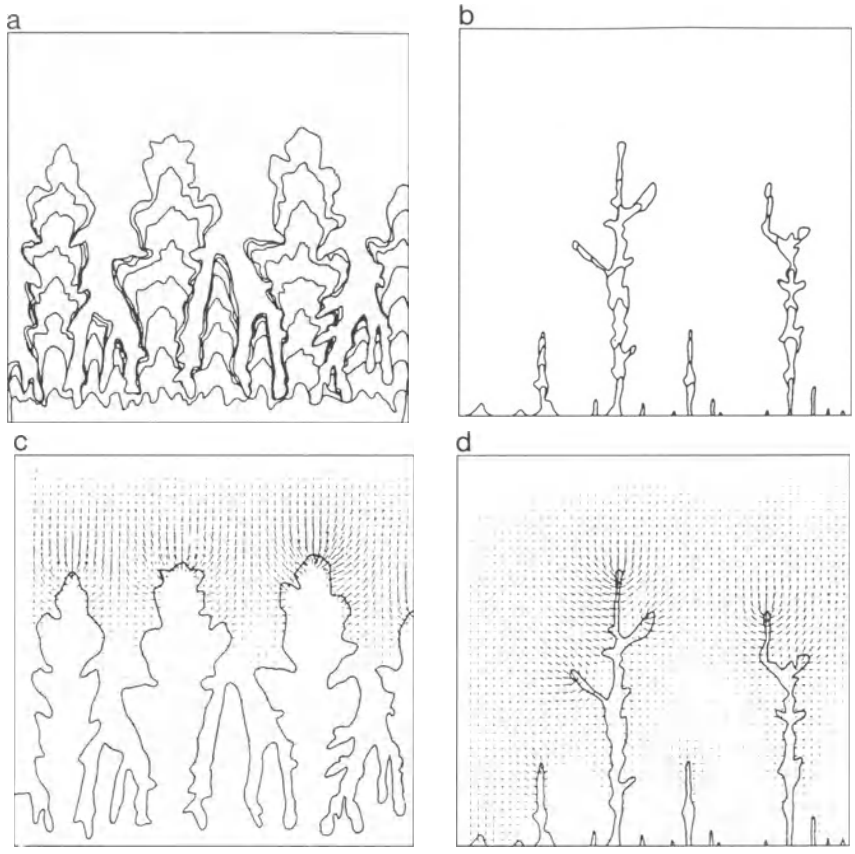

Figure 12.10 Plan view of a simulated valley network of sapping heads according to Howard (1988b). (a) shows the model run for a critical discharge of zero and (b) with a high critical discharge; (c) and (d) show the corresponding flow vectors.

The subsurface flow and emergence of groundwater has been used by Howard (1988b) to model the evolution of headcuts by spring sapping. This model assumes a planar caprock aquifer (that may be tilted) with uniform areal recharge and self-similar variation in permeability. The rate of sapping backwasting E is then assumed to depend upon the amount by which the linear discharge rate at the scarp face q exceeds a critical discharge q_c:

$$E = w(q - q_c)^z \qquad (12.8)$$

where w and z are coefficients. Headcut erosion is simulated by solving for the groundwater flow, eroding the scarp by a small amount, and then reiterating. Valleys simulated in this fashion (Fig. 12.10) tend to have linear or crudely dendritic patterns, with nearly constant width and blunt rather than sharp terminations.

Thornes (1984) suggested a model for bifurcation in which bifurcation occurred when the maximum erosion caused by boundary overfall shifted away from the centreline of the gully head. It was assumed that erosion is a function of discharge per unit width along the boundary. This was shown analytically to occur when the semi-curve of the boundary was quartic (Fig. 12.11). Marchington (1987) modelled this process using a digital simulation of the boundary overfall with realistic soil conditions and a validated overland flow model. However, we were not able to produce significant bifurcation in laboratory hardware experiments by this mechanism alone.

KNICKPOINT MIGRATION

Earlier in this chapter we divided headcuts and knickpoints on the basis of the nature of the upslope condition. Thornes (1988) attempted to model gully headcut development and migration into a non-eroded area. The model assumes a logistic growth of

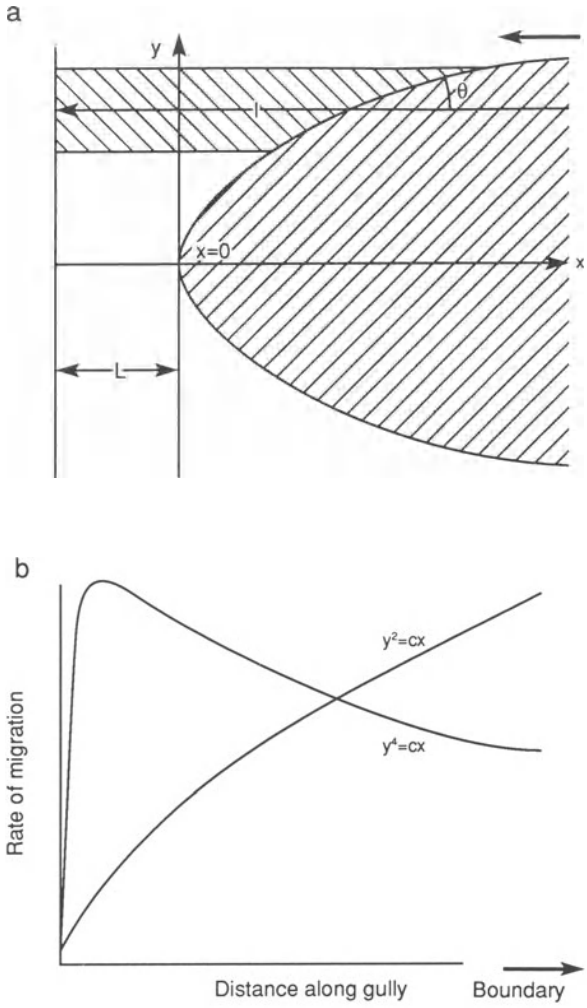

Figure 12.11 Thornes' (1984) model for gully head bifurcation analysis: (a) the geometrical resolution of flow strips about the headcut for a simple parabolic geometry; (b) the distribution of rate of upslope migration around the headcut for two different initial headcut forms, parabolic and quartic. For the first the form diffuses out because maximum erosion is further down the gully boundary. For the second the maximum erosion occurs to the left or right of the centreline of the headcut.

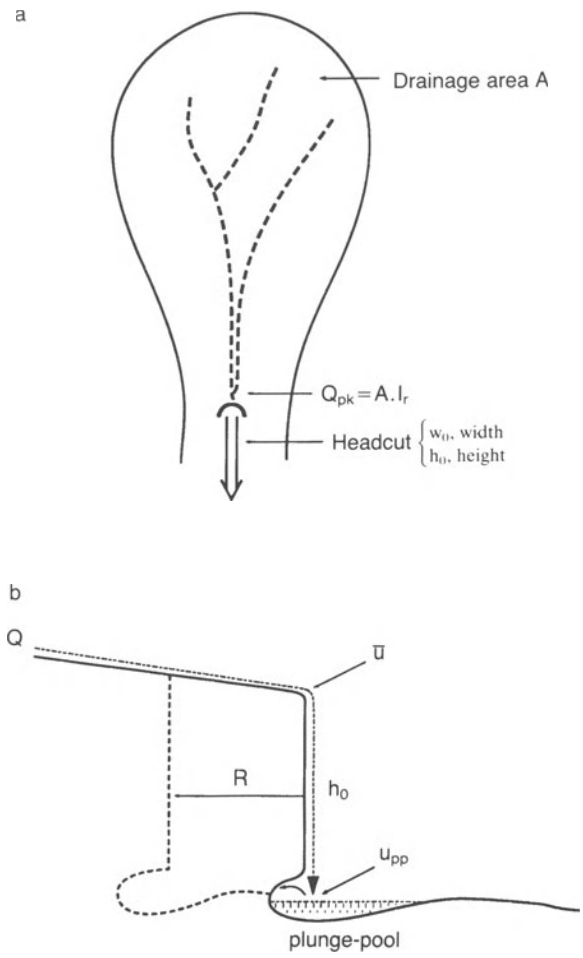

Figure 12.12 De Ploey's (1989) notation for a model of plunge pool controlled headcut retreat: (a) drainage area; (b) headcut.

gullies – that is, the gully growth rate is a function of gully size up to some limit set by the constant of channel maintenance and, hence, catchment area. In this model, as the gully progressively consumes its own catchment, it interacts with the vegetation cover in the uneroded area to eventually stabilize.

The migration of headcuts within existing channel networks is better documented. De Ploey (1989) considered a headcut migration for a single storm event generating a discharge from a drainage area A (Fig. 12.12). From fluid mechanics he derived the kinetic energy of the falling water, from soil mechanics the critical wall height, and from geometry the volume eroded. Setting the velocity proportional to the energy expended this derivation yielded an expression for the velocity:

$$U_R = \frac{E_R Q(g + u^2/2h_o)}{w_o} \qquad (12.9)$$

in which Q is the discharge, w_o is the width of the overfall, g is the acceleration due to gravity, h_o is the height of the overfall, u is the velocity of the stream at the head of the overfall, $E_R = Fv_w/c'$, v_w is the bulk density of the material forming the headcut cliff

and c' is its cohesion, and F is an erodibility factor which has to be empirically determined. In large headcuts the term u/h_o is expected to be small and behaviour is controlled by $E_R Qg$ and so has some elements in common with the empirical analysis of Mason (1984) outlined earlier. In rills the second term becomes important, implying that small steps migrate more rapidly than large ones. De Ploey interpreted this to indicate that in rills small headcuts would catch up to large headcuts, thereby increasing the size of the larger ones and hence their stability. From experiments E_R has been observed to be of the order of 10^{-6} to 10^{-5} s^2 cm^{-2} and U_R of the order of 1 cm min^{-1} for rills of width about 10 cm on low slopes. For gullies with low slopes the expression reduces further to $U_R = E_R Qg/w$ – that is, U_R is proportional to discharge per unit width – in line with the empirical observations of Piest *et al.* (1975) but independent of the height of the headcut. The proportionality with unit discharge brings headcut migration into the general class of erosional processes indicated by Willgoose *et al.* (1990) and the general model for headcut migration of Thornes (1984) based on boundary scour.

Finally, in this section we turn to a more general model of headcut evolution proposed by Begin (1983). This model starts with the development of an approximate equation for sediment discharge q_s as a linear function of channel gradient dy/dx:

$$q_s = b_d k(dy/dx)$$

in which k is a constant at constant water discharge and b_d is bulk density. This yields

$$\frac{\partial q_s}{\partial x} = b_d k \frac{\partial^2 y}{\partial x^2} \qquad (12.10)$$

which when substituted into the continuity equation

$$\frac{\partial y}{\partial t} = \frac{1}{b_d} \frac{\partial q_s}{\partial x} + B \qquad (12.11)$$

results in

$$\frac{\partial y}{\partial t} = k \frac{\partial^2 y}{\partial x^2} + B \qquad (12.12)$$

in which B is the lateral inflow of sediment per unit time t per unit flow width per unit length of channel. This is analogous to a diffusion equation with k as the 'diffusion' coefficient.

Assuming a simple linear channel gradient and no lateral sediment influx ($B = 0$), base level is subject to a fixed amount of lowering and the evolution of the channel gradient in adjusting to the new base level can be determined through time and space in the manner described by Culling (1960). The same reasoning can be used to obtain the velocity of propagation of a disturbance through the system. Migration curves for disturbances of different magnitudes are shown in Figure 12.13. Smaller disturbances are seen to propagate at faster rates (i.e. the curves are steeper).

Further assuming that a new channel bifurcates from the main channel at a fixed depth below the surface (the rationale for this is not entirely clear), then the distance travelled for a disturbance of that magnitude to reach the headwater can be obtained, as can the distance to the source of the first-order stream (which is again defined by a depth below the initial surface). Comparing these two lengths provides the length of first-order channels in the system. This is shown to be proportional to $t^{0.5}$ – that is, the length of first-order tributaries increases in proportion to the square root of time. This behaviour is generally similar to that observed by Parker (1977) in his laboratory experiment, although in this experiment the exponent of time was 0.32. This evolutionary model still seems to suffer from the subjective nature of the definition of the stream head and of the conditions of bifurcation, which seem rather arbitrary. The questionable assumption that $B = 0$ can be relaxed (Begin *et al.* 1981), although the analysis is more cumbersome. The advantage of the approach is that it provides the time–space trajectory of the propagation of the disturbance.

HISTORY

At any location the successive operation of even the same processes and the same historical rainfall sequence operating on different boundary and initial conditions can, and usually does, produce a specific and particular history of development of landforms or a particular and specific sequence of sediment yields.

Moreover, a given sequence of conditions can produce a lagged response in time across the catchment which is a function of the specific catchment conditions. According to Bull (1990), in arid and semi-arid regions available power typically is small and amounts of bedload large. He argued that such conditions severely limit the rates at which streams respond to either climatic or tectonic perturbations, and that large variations occur in times of onset of aggradation. In particular with diachronous response, the onset of aggradation may be progressively later with distance upstream.

As the channel characteristics also vary, the nature

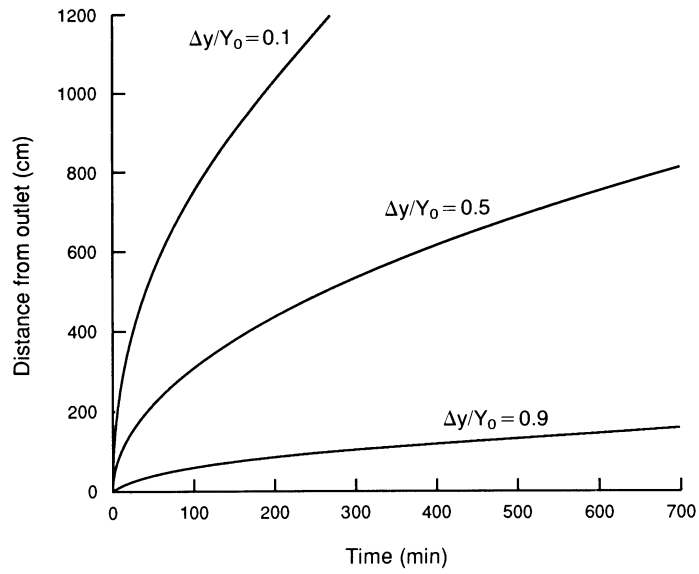

Figure 12.13 Migration curves for propagation of disturbances of different magnitudes $\Delta y/Y_o$ according to Begin's (1983) model.

of the response will probably be complex rather than simple. Even with synchronous response the different behaviour of hillslope and channel processes in different parts of the system are likely to produce a complex response (Schumm 1973).

Finally, we note that the same channel exposed to a different magnitude and frequency of rainfall events can be expected to produce a different fluvial landform assemblage. This last point is of course the basis of much inferential work in climatic geomorphology, especially in semi-arid and arid regions, where the earlier literature is replete with climatic sequences for arid and semi-arid landscapes based on alluvial sequences (e.g. Vita Finzi 1969, Barsch and Royse 1972).

Wolman and Gerson (1978) assert that the geomorphic effectiveness of an event is governed not only by the absolute magnitude of the force or energy which it brings to bear but by the frequency with which it recurs, the processes during intervening intervals, and the work performed during such intervals. In addition, because of the variety of possible combinations of processes and earth materials, similar or convergent landforms may result from different combinations or sequences of processes acting on different materials. In other words, there is a problem of equifinality.

This chapter ends with three examples of historical studies. All three indicate the major difficulties in using history to infer past climates from palaeohydrology in dry lands. These difficulties stem from (a) the dependence of a specific response on initial conditions, (b) the role of extreme events in a complicated series of perturbations, and (c) the relatively long relaxation times of the systems if left for some time without another major event. In addition the second study illustrates the need for a thorough appreciation of the mutual interaction between vegetational and channel evolution – a phenomenon which still awaits detailed study in all geomorphic, but especially semi-arid and arid, environments.

SHORT-TERM HISTORY: INHERITANCE OF PAST FORMS

The first study is Graf's (1983b) investigation of the sedimentational history of Walnut Gulch, Arizona, one of the best instrumented semi-arid catchments in the world. He poses three questions:

(a) How has sediment transport varied through time?
(b) What has been the spatial distribution of removal during the last episode of erosion when arroyo development occurred?
(c) What has that erosion implied for continued sediment transport?

Like most of the arid South-west (Cooke and Reeves 1976), the stream channels of Walnut Gulch

were mainly narrow and shallow in the late 1800s and meandered across the upper surface of the alluvial fill. Beginning in about 1930 entire drainage basins were entrenched and the grassy bottom lands (cienagas) were destroyed. The entrenched channels remained in 1981 with small amounts of refilling, as observed elsewhere in the American South-west. Graf examined the volumetric sediment differences between the pre-erosion and post-erosion channels on the basis of a series of surveyed sections and under a series of clearly specified assumptions. From this analysis he found that the total amount of sediment removed was enough to cover the entire catchment (150 km^2) to a depth of 4 cm. Most of this was removed from the highest order channels (83% from seventh-order channel). In a downstream direction, the volume removed from the main channel first increased and then decreased reflecting sediment supply, tractive force, and total stream power. The amount of material available in the upper part of the network is relatively small because flow is small. In the middle of the basin, tractive force (competence) is sufficient to entrain material, and the channel is wide enough to permit high values of total power (capacity), so large amounts of material were lost. In the lowest reaches the channel became so wide that depth of flow and tractive force declined and limited the amount of material lost by erosion. Local structural controls also affected the distribution of erosion, as shown in Figure 12.14.

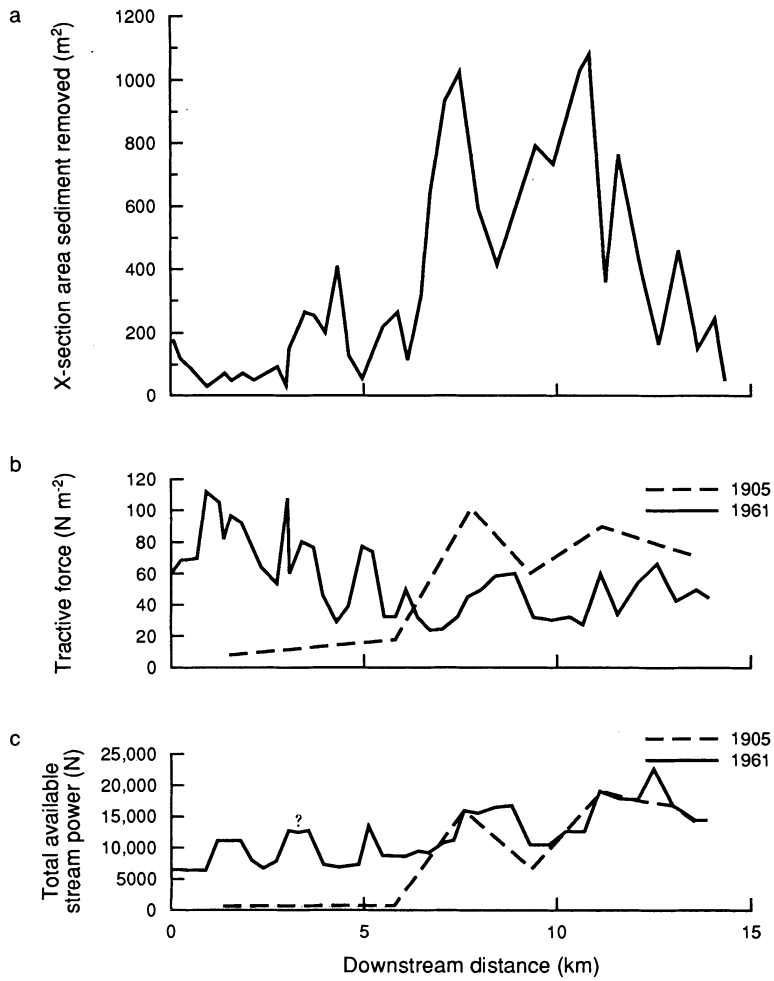

Figure 12.14 (a) Downstream distribution of areas of channel cross-section excavated by erosion on the main stream of Walnut Gulch between 1905 and 1961; (b) and (c) changes in tractive force and total stream power as a result of this event (after Graf 1983b).

The volume removed (estimated at 6.2×10^6 m^3) is a relatively small amount of the total sediment in storage, but the rate of removal during the episode was nevertheless about 18 times greater than recent rates.

Because there is still plenty of sediment available for removal, tractive force and total stream power represent reasonable indicators of the ability of the channel to transport sediment. What Graf's study shows is that as a result of this historic episode, the distribution of tractive force and total stream power changed during the event, mainly through increases in width (Fig. 12.14). An erratic but general downstream decline in tractive force replaced a strong increase. Now the largest particles can be transported in the upstream reaches. Stream power now increases downstream at a slower rate than before the erosional event. This study reaffirms the view expressed earlier that in ephemeral channel systems the *history* of events provides an important new set of boundary conditions for subsequent processes. Predictions based on models of processes or empirical values from measurements are sensitive to history in any particular case.

This message is repeated many times in the specific histories of semi-arid rivers. Yi Fu Tuan (1966, p. 583) asserted of gullies in the American South-west that

> 'Notwithstanding the use of biological and other supportive evidence, the cause of gullying and deposition during even the last 100 years defies agreement on generalities.'

MEDIUM-TERM HISTORY: CHANNEL DEVELOPMENT AND VEGETATION COVER

Burkham (1972) provided a history of fluvial activity between 1846 and 1970 in the Gila River in Safford Valley, Arizona. This study illustrates the variability and complexity of response in relation to vegetation cover. The Safford Valley is about 15 km wide and about 100 km long and is filled with more than 350 m of sand, silt, and gravel alluvium. Burkham studied a reach about 72 km long with a floodplain 300 to 1700 m wide, a contemporary channel of 20 to 170 m wide, and a slope of 0.002. The floodplain in 1970 was densely covered with saltcedar, willow, and mesquite, except in areas where vegetation had been removed by humans. The climate is semi-arid with a mean annual rainfall of 217 mm and a range of 75 to 430 mm. The rainfall is frontal in winter and convective in summer.

Until 1904 the Gila River was probably less than 50 m wide and 3 m deep at bankfull, and it meandered through a willow-, cottonwood-, and mesquite-covered floodplain. Widening began in 1905 and continued until 1917 (Fig. 12.15), during which period most of the vegetation was destroyed, most of it prior to 1909. Redevelopment of the floodplain occurred in the period 1918 to 1970; the stream became progressively wider, the channel meandered again, and the vegetation cover in the floodplain became more dense, except for minor stream widening in 1941 and 1965–7. Vegetation recovery was promoted by the introduction of saltcedar from the Mediterranean in the early 1920s. The species found

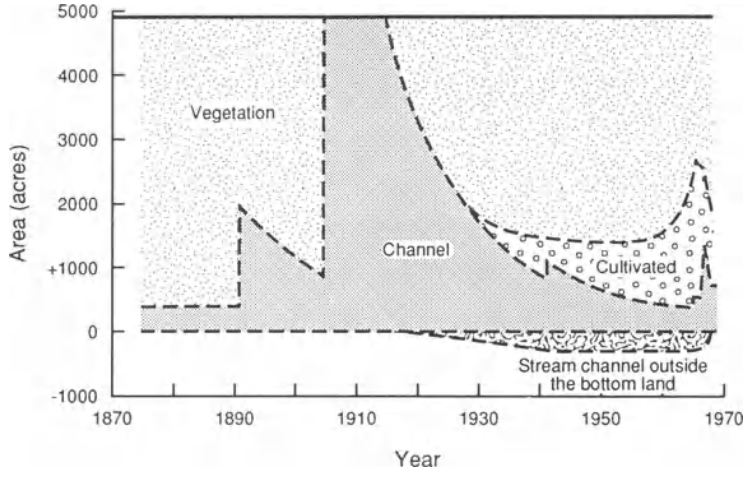

Figure 12.15 History of widening of the Gila channel according to Burkham (1972).

conditions of growth especially conducive, and it thrived until it started to be cut down extensively after 1955. During the same period the sinuosity increased from about 1.0 in 1918 to about 1.2 in 1964.

Major floods were the primary cause of widening, perhaps because the river was undersaturated with respect to transport capacity when it reached the Safford Valley. Grazing played a relatively unimportant role in channel widening, and trees are thought to have had a minor influence, except through their influence as transported debris. As the stream channel widened, it straightened, and its gradient increased by about 20%. This led to propagation of erosion into the tributary channels. Reconstruction was achieved almost entirely by sediment accretion in five ways: (a) by the development of islands in the stream channel, whose stability was enhanced by vegetation growth; (b) by direct deposition on the floodplain; (c) by deposition in the stream channels along the banks; (d) by the formation of natural levees; and (e) by deposition on alluvial fans at the mouths of tributary streams. Burkham argued that increased accretion was more important in the lower than in the upper part of the valley due to transmission losses to the bed.

The significance of this case study is that it illustrates the strong interaction between channel history on the one hand and vegetation destruction and recovery on the other. This is important not only for contemporary rivers but also for understanding the impact of individual events in older sequences used in palaeohydrology. The specific event in 1906 which caused the major changes was probably the largest flood in 130 years and possibly in 300 years. Recovery took of the order of 50 years, reiterating the need to understand extreme events in the reconstruction of fluvial histories and providing valuable information for the validation of models of fluvial evolution.

LONG-TERM HISTORY: SEDIMENT AVAILABILITY

The impact of sediment availability on runoff and sediment yield has been investigated by Yair and Enzel (1987) in the Negev. They point out that the usual assumption, based on Langbein and Schumm (1958), that runoff and sediment yield decrease as the climate becomes more arid, is flawed when large amounts of bare rock are exposed. Under these conditions runoff may actually increase. In the Negev, the channels formed before the Upper–Middle Palaeolithic are in a landscape with no palaeosols, significant bare rock, and high runoff rates. Following extensive loess deposition, channels were choked by fine sand, silt, and clay particles (Fig. 12.16) and drainage densities were dramatically lowered. When the environmental conditions changed again later at the beginning of the Holocene, these valleys had lower runoff, erosion, and transportation rates, and they responded quite differently and less actively to those with significant areas of bare rock.

What this example forcibly illustrates is that climatic changes of a global magnitude are played out on a spatially variable stage, so that predictions based on simple (or even complicated) models of the impact of global change may prove fallacious unless the initial conditions are adequately described in time and space. With their astonishing variety of surfaces and forms, the arid and semi-arid environments are likely to prove particularly problematic in this respect.

CONCLUDING REMARKS

At the beginning of this chapter we set out to identify those characteristics of desert river channel processes that are distinctive. From a process point of view it is primarily the selective transport, burial and re-excavation of materials under episodic flow that is most important. This characteristic seems largely to reflect the fact that the falling limb of ephemeral flows falls to zero, so that all strong deposition takes place over earlier materials. A secondary important characteristic relates to the significance of in-channel vegetation. A third is the importance of transmission losses and the resulting asynchroneity of flow leading to particular depositional forms.

The evolution of channel behaviour is dominated by the same complex intrinsic thresholds that occur in perennial channels, but in ephemeral channels headward growth and bifurcation through gullying are more prominent as overland flow plays a much greater role. In the channels themselves the organization of plan form is probably also a threshold feature. The characteristic coarse materials and high bedloads lead to a high frequency of braided channel patterns.

At any instant, ephemeral channels, like their perennial counterparts, reflect the past history of events. The only real difference appears to be in the extent to which the effects of high magnitude events are preserved, often over great periods of time. This has often led to the belief that in ephemeral channels the history of the past is more readily deciphered. In reality, the problems in such channels are much more difficult than in perennial ones because of the

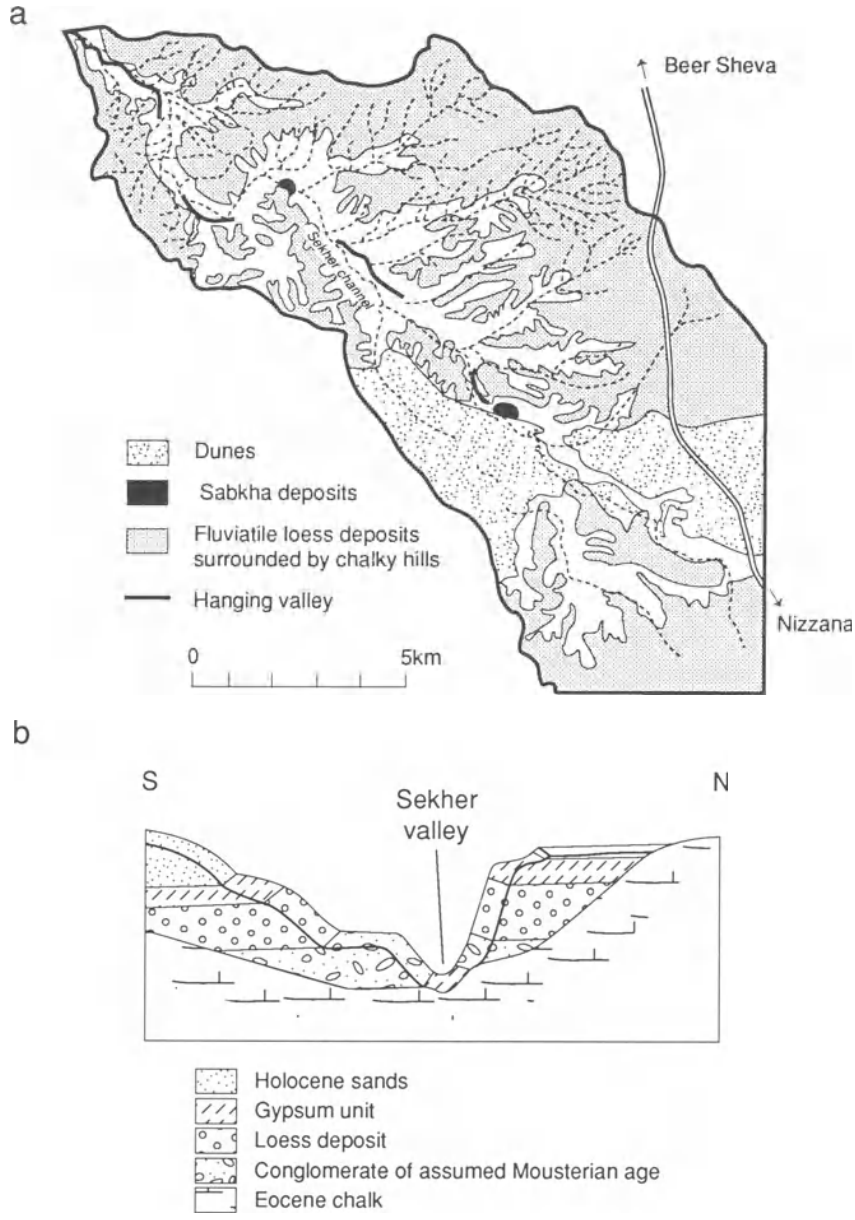

Figure 12.16 (a) Low drainage density in the loess area and high drainage density in the rocky area, Beer Sheva depression; (b) stratigraphic section in the southern part of the depression (after Yair and Enzel 1987).

lack of synchroneity of flow throughout the channel system. There are still too many unknowns to be resolved before the present can be usefully regarded as the key to the past.

REFERENCES

Ashmore, P.E. 1982. Laboratory modelling of gravel braided stream channel morphology. *Earth Surface Processes and Landforms* **7**, 202–25.

Ashmore, P.E. 1987. Discussion of bedload transport in braided gravel-bed rivers. In *Sediment transport in gravel bed streams*, C.R. Thorne, J.C. Bathurst and R.D. Hey (eds) 811–20. Chichester: Wiley.

Bagnold, R.A. 1966. An approach to the sediment transport problem from general physics. *U.S. Geological Survey Professional Paper* 422-I.

Bagnold, R.A. 1977. Bed load transport by natural rivers. *Water Resources Research* **13**, 303–12.

Baker, V.R., R.C. Kochel and P.C. Patton 1979. Long term flood frequency analysis using geological data. *Inter-*

national Association of Hydrological Sciences Publication 128, 3–9.

Barsch, D. and C.F. Royse 1972. A model for the development of Quaternary terraces and piedmont-terraces in the southwestern United States. *Zeitschrift für Geomorphologie* **16**, 54–75.

Beer, C.E. and H.P. Johnson 1965. Factors relating to gully growth in the deep loess area of Western Iowa. Proceedings of the Second Federal Inter-Agency Commission on Sedimentation. *U.S. Department of Agriculture Miscellaneous Publication* 970, 37–43.

Begin, Z.B. 1983. Application of 'diffusion' degradation to some aspects of drainage net development. In *Badland geomorphology and piping*, R. Bryan and A. Yair (eds), 169–81. Norwich: Geobooks.

Begin, Z.B. and S.A. Schumm 1979. Instability of alluvial floors: a method for its assessment. *Transactions of the American Society of Agricultural Engineers* **22**, 347–50.

Begin, Z.B., D.F. Meyer and S.A. Schumm 1981. Development of longitudinal profiles of alluvial channels in response to base level lowering. *Earth Surface Processes and Landforms* **6**, 49–68.

Beschta, R.L. 1987. Conceptual models of sediment transport in streams. In *Sediment transport in gravel bed streams*, C.R. Thorne, J.C. Bathurst and R.D. Hey (eds) 387–420. Chichester: Wiley.

Bevan, K. and M.J. Kirkby 1979. A physically based, variable contributing area model of basin hydrology. *Hydrological Sciences Bulletin* 24, 43–69.

Boon, W. and J. Savat 1980. A nomogram for the prediction of rill erosion. In *Soil conservation*, R.P.C. Morgan (ed.), 303–18. Chichester: Wiley.

Bradford, J.M. and R.F. Piest 1977. Gully wall stability in loess derived alluvium. *Soil Science Society of America Journal* **41**, 115–22.

Bradford, J.M., D.A. Farell and W.E. Larson 1973. Mathematical evaluation of factors affecting gully stability. *Soil Science Society of America Proceedings* **37**, 103–7.

Bull, W.B. 1979. Water in deserts. In *Water in desert ecosystems*, D.D. Evans and J.L. Thames (eds), 1–22. Stroudsburg, PA: Dowden, Hutchinson, and Ross.

Bull, W.B. 1990. Stream terrace genesis: implications for soil development. *Geomorphology* **3**, 351–67.

Burkham, D.E. 1972. Channel changes of the Gila River in Safford Valley, Arizona. *U.S. Geological Survey, Professional Paper* 655-J.

Burke, J.D., R.G. Brereton and P.M. Muller 1970. Desert stream channels resembling lunar sinuous rills. *Nature* **225**, 1234–6.

Campbell, C.J. and W. Green 1980. Perpetual succession of a stream-channel vegetation in a semi-arid region. *Journal of the Arizona Academy of Science* **5**, 87–93.

Carling, P.A. 1987. Bed stability in gravel stream, with reference to stream regulation and ecology. In *River channels: environment and process*, K. Richards (ed.), 321–47. Oxford: Blackwell.

Carling, P.A. 1989. Bedload transport in two gravel-bedded streams. *Earth Surface Processes and Landforms* **14**, 27–41.

Cooke, R.U. and R.W. Reeves 1976. *Arroyos and environmental change in the American South-west*. Oxford: Clarendon.

Culling, W.E.H. 1960. Analytical theory of erosion. *Journal of Geology* **69**, 336–44.

Davies, T.R.H. 1987. Bed load transport in braided gravel-bed rivers. In *Sediment transport in gravel bed streams*, C.R. Thorne, J.C. Bathurst and R.D. Hey (eds), 793–811. Chichester: Wiley.

De Ploey, J. 1989. A model for headcut retreat in rills and gullies. *Catena Supplement* **14**, 81–6.

Dietrich, W.E., C.J. Wilson and S.L. Reneau 1986. Hollows, colluvium, and landslides in soil-mantled landscapes. In *Hillslope processes*, A.D. Abrahams (ed.), 361–88. Boston: Allen and Unwin.

Dietrich, W.E., J.W. Kirchner, H. Ikeda and F. Iseya 1989. Sediment supply and the development of the coarse surface layer in gravel-bedded rivers. *Nature* **340**, 215–17.

Dunne, T. 1980. Formation and control of channel networks. *Progress in Physical Geography* **4**, 211–39.

Emmett, W.W. and L.B. Leopold 1965. Downstream pattern of river bed scour and fill. Proceedings of the Second Federal Interagency Conference on Sedimentation. *U.S. Department of Agriculture Miscellaneous Publication* 970, 399–409.

Ergenzinger, P. 1987. Chaos and order: the channel geometry of gravel-bed braided rivers. *Catena Supplement* **10**, 85–98.

Fahnestock, R.K. 1963. Morphology and hydrology of a glacial stream. *U.S. Geological Survey Professional Paper* 422-A.

Faulkner, H. 1974. An allometric growth model for competitive gullies. *Zeitschrift für Geomorphologie Supplement Band* **21**, 76–87.

Finley, R.J. and T.C. Gustavson 1983. Geomorphic effects of a 10-year storm on a small drainage basin in the Texas Panhandle. *Earth Surface Processes and Landforms* **8**, 63–79.

Fisher, G.S., M.L.J. Gray, N.B. Grimm and D.E. Busch 1982. Temporal succession in a desert stream ecosystem. *Ecological Monographs* **53**, 93–110.

Foley, M.G. 1977. Gravel lens formation in antidune regime flow – a quantitative hydrodynamic indicator. *Journal Sedimentary Petrology* **47**, 738–46.

Foley, M.G. 1978. Scour and fill in steep sand-bed ephemeral streams. *Bulletin of the Geological Society of America* **89**, 559–70.

Fournier, F. 1960. *Climat et erosion*. Paris: Presses Universitaires Français.

Frostick, L.E. and I. Reid 1979. Drainage net control of sedimentary parameters in sand-bed ephemeral streams. In *Geographical approaches to fluvial processes*, A.F. Pitty (ed.), 173–201. Norwich: Geobooks.

Frostick, L.E., I. Reid and J.T. Layman 1983. Changing size-distribution of suspended sediment in arid-zone flash floods. *International Association of Sedimentologists Special Publication* 6, 97–106.

Gardner, T.W. 1983. Experimental study of knickpoint behaviour and longitudinal profile evolution in cohesive, homogenous material. *Bulletin of the Geological Society of America* **94**, 664–72.

Gerits, J., A.C. Imeson, J.M. Verstraten and R.B. Bryan 1987. Rill development and badland regolith properties. *Catena Supplement* **8**, 141–80.

Graf, W.L. 1979. The development of montane arroyos and gullies. *Earth Surface Processes* **4**, 1–14.

Graf, W.L. 1983a. Flood related channel changes in an arid-region river. *Earth Surface Processes and Landforms* **8**, 125–41.

Graf, W.L. 1983b. Variability in sediment removal in a semi-arid watershed. *Water Resources Research* **19**, 643–52.

Graf, W.L. 1987a. *Fluvial processes in dryland rivers*. Berlin: Springer-Verlag.

Graf, W.L. 1987b. Definition of floodplains along arid-region rivers. In *Flood geomorphology*, V.R. Baker, R.C. Kochel and P.C. Patton (eds), 234–49. New York: Wiley.

Griffiths, G.A. 1979. Recent sedimentation history of the Waimakiriri River, New Zealand. *Journal of Hydrology (N.Z.)* **18**, 6–28.

Hack, J.T. 1957. Studies of the longitudinal stream profiles in Virginia and Maryland. *U.S. Geological Survey Professional Paper* 294-B.

Harvey, A. 1982. The role of piping in the development of badlands and gully systems in south-east Spain. In *Badland geomorphology and piping*, R.B. Bryan and A. Yair (eds), 317–36. Norwich: Geobooks.

Hassan, M.A. 1990. Scour, fill and burial depth of coarse material in gravel bed streams. *Earth Surface Processes and Landforms* **15**, 341–56.

Heede, B.H. 1974. Stages of development of gullies in the Western United States of America. *Zeitschrift für Geomorphologie* **18**, 260–71.

Higgins, C.G. 1984. Piping and sapping: development of land forms by groundwater outflow. In *Groundwater as a geomorphic agent*, R.G. LaFleur (ed.), 18–58. Boston: Allen and Unwin.

Holland, W.N. and G. Pickup 1976. Flume study of knickpoint development in stratified sediment. *Geological Society of America Bulletin* **87**, 76–82.

Howard, A.D. 1971. Simulation of stream networks by headward growth and branching. *Geographical Analysis* **3**, 59–68.

Howard, A.D. 1988a. Groundwater sapping on Mars and Earth. In *Sapping features of the Colorado Plateau: a comparative planetary guide*, A.D. Howard, R.C. Kochel and H.E. Holt (eds), 1–5. Washington, DC: National Aeronautics and Space Administration, NASA SP-491.

Howard, A.D. 1988b. Groundwater sapping experiments and modelling. In *Sapping features of the Colorado Plateau: a comparative planetary guide*, A.D. Howard, R.C. Kochel and H.E. Holt (eds), 71–83. Washington, DC: National Aeronautics and Space Administration, NASA SP-491.

Hubbell, D.W. and W.W. Sayre 1964. Sand transport studies with radioactive tracers. *Journal Hydraulics Division, Proceedings of the American Society of Civil Engineers* **90** (HY1) 39–68.

Ireland, H.A., C.F.C. Sharp and D.H. Eargle 1939. Principles of gully erosion in the Piedmont of South Carolina. *U.S. Department of Agriculture Bulletin* 63.

Kennedy, B.A. 1982. On Playfair's Law of accordant junctions. *Earth Surface Processes and Landforms* **9**, 135–63.

Kirkby, M.J. 1980. The stream head as a significant geomorphological threshold. In *Threshold in geomorphology*, D.R. Coates and J.D. Vitek (eds), 57–73. Boston: Allen and Unwin.

Kirkby, M.J. 1993. Thresholds and instability in stream head hollows. In *Channel network hydrology*, K.J. Bevan and M.J. Kirkby (eds), 255–93. Wiley: Chichester.

Lane, E.W. 1937. Stable channels in erodible materials. *Transactions American Society of Civil Engineers* **102**, 123–94.

Lane, L.J. 1982. Development of a procedure to estimate runoff and sediment transport in ephemeral streams. *International Association of Hydrologic Sciences Publication* 137, 275–82.

Langbein, W.B. 1965. Geometry of river channels: closure of discussion. *Journal of Hydraulics Division, Proceedings of the American Society of Civil Engineers*, **91** (HY3), 297–313.

Langbein, W.B. and L.B. Leopold 1968. River channels, bars and dunes – theory of kinematic waves. *U.S. Geological Survey Professional Paper* 422-L.

Langbein, W.B. and S.A. Schumm 1958. Yields of sediment in relation to mean annual precipitation. *Transactions of American Geophysical Union* **39**, 1076–84.

Laursen, E.M. 1953. Observations on the nature of scour. *Iowa State University, Studies in Engineering Bulletin* 34, 179–97.

Laursen, E.M. 1958. Total sediment load of stream. *Journal Hydraulics Division, Proceedings of American Society of Civil Engineers* **84** (HY1), 1531–6.

Lekach, J. and A.P. Schick 1983. Bedload transport in waves. *Catena* **10**, 267–79.

Leopold, L.B. and J.P. Miller 1956. Ephemeral streams – hydraulic factors and their relation to the drainage net. *U.S. Geological Survey Professional Paper* 282-A.

Leopold, L.B. and M.G. Wolman 1957. River channel patterns: braided, meandering, and straight. *U.S. Geological Survey Professional Paper* 282-B.

Leopold, L.B., M.G. Wolman and J.P. Miller 1964. *Fluvial processes in geomorphology*, San Francisco: Freeman.

Leopold, L.B., W.W. Emmett and R.M. Myrick 1966. Channel and hillslope processes in a semi-arid area, New Mexico. *U.S. Geological Survey Professional Paper* 352-G.

Maizels, J.K. 1983. Palaeovelocity and palaeodischarge determination for coarse gravel deposits. In *Background to palaeohydrology*, K.J. Gregory (ed.) 101–39. New York: Wiley.

Marchington, A. 1987. Development of a dynamic model of gully growth. Unpublished Ph.D. Thesis, University of Bristol.

Marcus, W.A. 1987. Copper dispersion in ephemeral stream sediments. *Earth Surface Processes and Landforms* **12**, 217–29.

Mason, P.J. 1984. Erosion of plunge pools downstream of dams due to the action of free-trajectory jets. *Proceedings of the Institution of Civil Engineers, Part 1*, **76**, 523–37.

Mitchell, J.K. and G.D. Bubenzer 1980. Soil loss estimation. In *Soil erosion*, M.J. Kirkby and R.P.C. Morgan (eds), 17–62. Chichester: Wiley.

Moore, R.J. 1984. A dynamic model of basin sediment yield. *Water Resources Research* **20**, 89–105.

Morley, D. and J.B. Thornes 1972. Markov decision networks. *Geographical Analysis* **4**, 180–93.

Mosley, M.P. 1972. Evolution of a discontinuous gully system. *Annals of the Association of American Geographers* **62**, 655–63.

Mosley, M.P. 1976. An experimental study of channel confluences. *Journal of Geology* **84**, 535–62.

Mosley, M.P. 1983. Response of braided rivers to changing discharge. *Journal of Hydrology (N.Z.)* **22**, 18–64.

Nouh, M. 1990. The self-armouring process under unsteady flow conditions. *Earth Surface Processes and Landforms* **15**, 357–64.

Parker, G. 1976. On the cause and characteristic scales of

meandering and braiding in rivers. *Journal of Fluid Mechanics* **76**, 459–80.

Parker, R.S. 1977. Study of drainage basin evolution and its hydrological implications. Unpublished Ph.D. Dissertation, Colorado State University, Fort Collins, CO.

Phillips, L. 1988. The effect of slope on experimental drainage patterns: possible application to Mars. In *Sapping features of the Colorado Plateau: a comparative planetary guide*, A.D. Howard, R.C. Kochel and H.E. Holt (eds), 107. Washington, DC: National Aeronautics and Space Administration, NASA SP-491.

Pickup, G., Higgins, R.J. and I. Grant 1983. Modelling sediment transport as a moving wave – the transfer and deposition of mining waste. *Journal of Hydrology* **60**, 281–301.

Piest, R.F., J.M. Bradford and R.G. Spomer 1975. Mechanisms of erosion and sediment movement from gullies. In *Present and prospective technology for predicting sediment yields and sources*, Agricultural Research Service Report ARS-S-40, 162–76. Oxford, MS: U.S. Department of Agriculture.

Reid, I. and Frostick, L. 1984. Flash flood hydraulics and sediments in the arid zone of northern Kenya. Universita Firenze, Departimento di ingegneria civile, *Sezione gelogia applicata* 3/84.

Reid, I., Frostick, L.E. and J.T. Layman 1985. The incidence and nature of bedload transport during flood flows in coarse-drained alluvial channels. *Earth Surface Processes and Landforms* **10**, 33–44.

Savat, J. 1977. The hydraulics of sheet flow on a smooth surface and the effects of simulated rainfall. *Earth Surface Processes* **2**, 125–40.

Savat, J. and J. De Ploey 1982. Sheetwash and rill development by surface flow. In *Badland geomorphology and piping*, R.B. Bryan and A. Yair (eds), 113–26. Norwich: Geobooks.

Schick, A. 1977. Study of sediment generation, transport and deposition in semi-arid zones. *Hydrological Sciences Bulletin* **4**, 535–42.

Schick, A., M.A. Hassan and J. Lekach 1987. A vertical exchange model for coarse bedload movement: numerical considerations. *Catena Supplement* **10**, 73–83.

Schumm, S.A. 1956. Evolution of drainage systems and slopes at Perth Amboy, New Jersey. *Bulletin of the Geological Society of America* **67**, 597–646.

Schumm, S.A. 1973. Geomorphic thresholds and complex response. In *Fluvial geomorphology*, M. Morisawa (ed.), 299–310. Binghamton, NY: Publications in Geomorphology.

Schumm, S.A. 1977. *The fluvial system*. New York: Wiley-Interscience.

Schumm, S.A. 1979. Geomorphic thresholds: the concept and its applications. *Transactions of the Institute of British Geographers* **4**, 485–515.

Schumm, S.A. and R.W. Lichty 1963. Channel widening and flood plain construction along the Cimarron River in southwestern Kansas. *U.S. Geological Survey Professional Paper* 352-D.

Schumm, S.A., P.M. Mosley and W.E. Weaver 1987. *Experimental fluvial geomorphology*. New York: Wiley.

Scott, K.M. 1973. Scour and fill in Tujunga Wash: a fan head valley in urban southern California. *U.S. Geological Survey Professional Paper* 750-B, B1–B28.

Seginer, I. 1966. Gully development and sediment yield. *Journal of Hydrology* **4**, 236–53.

Shields, A. 1936. Andwendung der Ahnlichkeitsmechanik und der Turbulenzforschung auf die Geschiebebewegung. *Mitteilungen der Preussischen Versuchsanstalt für Wasserbau und Schiffbau*, Heft 26, Berlin. English translation by W.P. Ott and J.C. van Uchelen, *California Institute of Technology, Hydrodynamics Laboratory Publication* 167.

Smith, T.R. and F.P. Bretherton 1972. Stability and the conservation of mass in drainage basin evolution. *Water Resources Research* **8**, 1506–29.

Stark, C.P. 1991. An invasion percolation model of drainage network evolution. *Nature* **352**, 423–5.

Sutherland, A.J. and E.B. Williman 1977. Development of armoured surfaces in alluvial channels. *Proceedings 6th Australasian Hydraulics and Fluid Mechanics Conference*, Adelaide, 5–9 December 1977, 126–30.

Thornes, C. 1991. Ephemeral stream confluences in a semi-arid environment: an experimental and stream study. Unpublished Dissertation, Hertford College, University of Oxford.

Thornes, J.B. 1970. The hydraulic geometry of stream channels in the Xingu-Araguaia headwaters. *Geographical Journal* **136**, 87–96.

Thornes, J.B. 1974. Semi-arid erosional systems. *London School of Economics Geographical Paper* 7.

Thornes, J.B. 1977. Channel changes in ephemeral streams: observations, problems and models. In *River channel changes*, K.J. Gregory (ed.), 318–35. Chichester: Wiley.

Thornes, J.B. 1979. Fluvial processes. In *Process in geomorphology*, C.E. Embleton and J.B. Thornes, 213–71. London: Allen and Unwin.

Thornes, J.B. 1980. Structural instability and ephemeral channel behaviour. *Zeitschrift für Geomorphologie Supplement Band* **36**, 233–44.

Thornes, J.B. 1984. Gully growth and bifurcation. In *Erosional control – man and nature*, Proceedings of the XV Conference of the International Erosion Control Association, Denver, 131–40.

Thornes, J.B. 1988. Erosional equilibria under grazing. In *Conceptual issues in environmental archaeology*. J. Bintliff, D.A. Davidson and E.G. Grant (eds), 193–211. Edinburgh: Edinburgh University Press.

Thornes, J.B. and A. Gilman 1983. Potential and actual erosion around archaeological sites in south-east Spain. *Catena Supplement* **41**, 91–114.

Thornes, J.B. and K.J. Gregory 1991. Unfinished business: a continuing agenda. In *Temperate zone palaeohydrology*, L. Starkel, K.J. Gregory and J.B. Thornes (eds), 430–8. Chichester: Wiley.

Tuan, Y.F. 1962. Structure, climate and basin landforms in Arizona and New Mexico. *Annals of the Association of American Geographers* **52**, 51–68.

Van der Poel, P. and G.O. Schwab 1988. Plunge pool erosion in cohesive channels below a free overfall. *Transactions of the American Society of Agricultural Engineers* **31**, 1148–53.

Van Sickle, J. and R.L. Beschta 1983. Supply-based models of suspended sediment transport in streams. *Water Resources Research* **19**, 768–78.

Veness, J.A. 1980. The role of fluting in gully extension. *Journal of Soil Conservation New South Wales* **36**, 100–7.

Vita-Finzi, C. 1969. *The Mediterranean valleys*, Cambridge: Cambridge University Press.

Willgoose, G.R., R.L. Bras and I. Rodriguez-Iturbe 1990. A coupled channel network growth and hillslope evolution model. 1. Theory. *Water Resources Research* **27**, 1671–84.

Wolman, M.G. and R. Gerson 1978. Relative scales of time and effectiveness of climate in watershed geomorphology. *Earth Surface Processes* **3**, 189–208.

Yair, A. and Y. Enzel 1987. The relationship between annual rainfall and sediment yield in arid and semi-arid areas. The case of the northern Negev. *Catena Supplement* **10**, 121–35.

Yalin, M.S. 1977. *The mechanics of sediment transport*, 2nd edn. Oxford: Pergamon Press.

Zimmerman, R.C., J.C. Goodlett and G.H. Cromer 1967. The influence of vegetation on channel form of small streams. *International Association of Hydrological Sciences Publication* 75, 255–75.

PART FIVE

PIEDMONTS

PEDIMENTS IN ARID ENVIRONMENTS 13

John C. Dohrenwend

INTRODUCTION

Pediments, gently sloping erosional surfaces of low relief developed on bedrock, occur in a wide variety of lithologic, neotectonic, and climatic settings. Reported on six continents, their distribution spans the range of subpolar latitudes from the Arctic to the Antarctic and the range of climate from hyperarid to humid tropical (Whitaker 1979). On the Cape York Peninsula in tropical north-east Queensland, a tectonically quiescent region of Precambrian granitic and metamorphic rocks overlain by gently dipping Mesozoic and Cenozoic sediments, pediments are a dominant landscape component occurring as fringing piedmonts and strath valleys of the crystalline rocks and as broad erosional plains on the sedimentary rocks (Smart *et al.* 1980). In the Gran Sabana of south-east Venezuela, a broadly upwarped region of gently dipping early Proterozoic strata, pediments comprise the floors of broad subsequent valleys developed within less resistant parts of the section (Dohrenwend *et al.* 1994b). In the late Tertiary and Quaternary landscape of the Basin and Range geomorphic province of the south-west United States, pediments (developed within a variety of neotectonic settings and on a broad range of igneous, metamorphic, and sedimentary lithologies) occupy piedmont slopes, mountain passes, and broad topographic domes (Hadley 1967, Oberlander 1972, Cooke and Warren 1973, Moss 1977, Dohrenwend 1987a). Clearly, pediments are azonal, worldwide phenomena that tend to form under conditions of relative geomorphic stability where processes of erosion and deposition are locally balanced over the long term such that mass transport and general surface regrading dominate landscape evolution. However, pediments are most conspicuous in arid and semi-arid environments where vegetation densities are low and deep weathering is limited. Hence, they have been studied most intensively in these regions and are generally perceived as an arid land phenomenon.

Pediments have long been the subject of geomorphological scrutiny. Unfortunately, the net result of this long history of study is not altogether clear or cogent and has not produced a clear understanding of the processes responsible for pediment development. 'The origin of these landforms has been controversial since Gilbert (1877) first recognized and described them' (Tator 1952, p. 294). Indeed, 'pediments have attracted more study and controversy, and have sparked the imagination of more geomorphologists, than most other landforms in deserts' (Cooke and Warren 1973, p. 188). This attention and controversy stem from a variety of factors which are inherent in the very nature of these landforms.

(a) Pediments are counter-intuitive landforms. To many, it is intuitive that uplands should be erosional features underlain by resistant bedrock, whereas the adjacent piedmont plains should be depositional features underlain by sedimentary deposits derived from the uplands. To others, it is intuitive that most landscapes should be adjusted such that variations in lithology/structure and form are highly correlated. In reality, most pediments are, at least in part, surfaces of erosion and transportation where the underlying lithology/structure may be the same as or very similar to that of the adjacent uplands.

(b) As defined in geomorphology, a pediment is a nearly planar surface of mass transport and/or laterally uniform erosion which functions as a zone of transition between a degrading upland and a stable base level or slowly aggrading lowland. As such, pediments comprise a fairly general class of landforms that occur within many different climatic regimes and geomorphic settings. They are the product of a variety of processes, and the relative significance of these

Geomorphology of Desert Environments. Edited by Athol D. Abrahams and Anthony J. Parsons. Published in 1994 by Chapman & Hall, London. ISBN 978-94-015-8256-8

processes varies from one climatic–geomorphic setting to another.

(c) Within any particular climatic–geomorphic setting, the processes which act to form and maintain the pediment operate both non-linearly and discontinuously. It follows, therefore, that both the distribution of form and the operation of process will probably be chaotic (in the true mathematical sense) within the zone of transition represented by the pediment. Such systems cannot be clearly and comprehensively described by linear models of cause and effect.

(d) As transitional landforms, pediments are partly active, partly inactive, partly dissected, and partly buried. Their boundaries are irregular, gradational, and poorly defined. In most cases, they are at least partly obscured by discontinuous veneers of alluvial deposits and/or deeply weathered bedrock; indeed, many actively forming pediments undoubtedly lie unrecognized beneath continuous mantles of such materials. These characteristics commonly frustrate attempts of measurement, description, and analysis.

DEFINITIONS

The confusion and controversy which pervades the study of pediments encompasses even the basic definition of the term. Originally used as an architectural term, pediment refers to the vertically oriented triangular termination (or gable) of a gently pitched ridge roof (Dinsmoor 1975, p. 394, Janson 1969, p. 90). When borrowed from architecture and used in the field of geomorphology, however, the term quickly acquired an entirely different meaning (i.e. a gently sloping erosional surface of low relief). Morphologically, the gently sloping erosion surface of geomorphology corresponds much more closely to a gently pitched roof than to the vertical termination of that roof.

Of more fundamental significance, however, is the fact that pediments are morphologically complex landforms that form within a wide variety of geomorphic environments. It is hardly surprising, therefore, that the variability in pediment definition is nearly as great as the variability in pediments themselves (Tator 1953, Cooke and Warren 1973, p. 188, Whitaker 1979, Oberlander 1989).

Only the most general definitions can accommodate the broad range of form and wide variety of geomorphic environments associated with pediments. The definition proposed by Whitaker (1979, p. 432) is a case in point. 'A pediment is a terrestrial erosional footslope surface inclined at a low angle and lacking significant relief. . . . It usually meets the hillslope at an angular nickline, and may be covered by transported material'. Unfortunately, such definitions are so broad that they limit the utility of the term as a basis for meaningful geomorphic inquiry and comparison. Qualifying modifiers such as those suggested by Tator (1953, p. 53) partly overcome this problem. 'The term pediment should be retained for the broad (but individually distinct) degradational surface produced by subaerial processes (including running water) in dry regions. Qualifications as to physiographic location may be expressed by the use of mountain, piedmont, or flat-land . . . Additional terminology should include the words suballuvial, for alluviated erosion levels, and subaerial, for non-alluviated levels'. However, the problem of describing pediments in a consistent and scientifically productive manner remains.

Other definitions increase precision but at the expense of general applicability. Consider for example, two definitions that apply specifically to piedmont pediments in the south-western United States:

> 'The term pediment may be restricted to that portion of the surface of degradation at the foot of a receding slope, which (1) is underlain by rocks of the upland and which is either bare or mantled by a layer of alluvium not exceeding in thickness the depth of stream scour during flood, (2) is essentially a surface of transportation, experiencing neither marked vertical downcutting nor excessive deposition, and (3) displays a longitudinal profile normally concave, but which may be convex at its head in later stages of development' (Howard 1942, p. 8).
>
> '. . . pediments are composed of surfaces eroded across bedrock or alluvium, are usually discordant to structure, have longitudinal profiles usually either concave upward or rectilinear, slope at less than 11°, and are thinly and discontinuously veneered with rock debris. The upper limits of pediments are usually mountain/piedmont junctions, although pediments may meet along watersheds; pediments are generally masked downslope by alluvium, and their lower boundaries are the lines at which the alluvial covers become continuous' (Cooke 1970, p. 28).

These definitions are useful general descriptions of piedmonts; however, they are not entirely satisfactory when applied to pediment domes and terrace pediments in the same region. Moreover, although generally similar, they are not in complete agree-

ment. Cooke placed the downslope boundary of the pediment where alluvial cover becomes continuous, whereas Howard defined it as the point where the thickness of cover equals the depth of effective stream scour. Tator (1953) concurred that the thickness of alluvial cover commonly approximates the depth of scour. However, Bull (1977) suggested that the downslope limit be defined where the thickness of alluvial cover exceeds one percent of the piedmont length. Such wide definitional disparities obstruct comparative analysis and synthesis of the pediment literature.

For the purposes of the present discussion, a pediment is descriptively defined as a gently sloping erosional surface developed on bedrock or older unconsolidated deposits. This erosion surface may be subaerially exposed or covered by a discontinuous to continuous veneer of alluvial deposits. Its downslope limit may be defined (following the suggestion of Bull, 1977) as that point where the deposit thickness exceeds a small fraction of the pediment length (e.g. 0.5 to 1.0%) or some arbitrarily defined maximum thickness (e.g. 25 to 30 m), whichever is less. The bedrock may include essentially any lithologic type with any structural attitude. An erosional surface developed on piedmont or basin fill deposits is no different genetically from an erosional surface developed on plutonic or metamorphic rocks. Indeed, at least some pediment surfaces extend without interruption across high-angle contacts between crystalline bedrock and partly indurated alluvium (Dohrenwend *et al.* 1986). (Of course, where the underlying sediments are neither indurated nor deformed, discrimination between pediment and alluviated piedmont may be difficult.)

CLASSIFICATION

That pediments are highly variable landforms is further illustrated by the variety of schemes that have been proposed to classify them. Cooke and Warren (1973) offered a classification based on general geomorphic environment: (a) an apron pediment is located between watershed and base level, usually between an upland and a depositional plain; (b) a pediment dome occurs on upland slopes (and crests) that are not surmounted by a mountain mass; and (c) a terrace pediment is developed adjacent to a relatively stable base level such as a through-flowing stream. Twidale (1983) presented a morphogenic classification based on relations between surface material and underlying lithology which are used to infer pediment forming processes: (a) a mantled pediment occurs where crystalline bedrock is veneered by a residual weathering mantle and which is inferred to have been formed by subsurface weathering of the crystalline bedrock and wash removal of the resulting debris; (b) a rock pediment forms where crystalline bedrock is exposed at the surface and which is inferred to respresent the exposed weathering front of a formerly mantled pediment; and (c) a covered pediment is characterized by a veneer of coarse debris covering an erosional surface that cuts discordantly across sedimentary strata. Oberlander (1989) advocated a two-part classification based on the relations between the pediment, its adjacent upland, and the underlying lithology and structure: (a) a glacis pediment (*glacis d'erosion en roches tendres*; Dresch 1957, Tricart 1972) is an erosional surface that bevels less resistant materials but does not extend into adjacent uplands underlain by materials of greater resistance, whereas (b) a rock pediment occurs where there is no change in lithology between the erosional surface and the adjacent upland. These various schemes provide general conceptual frameworks for the study and analysis of pediments; however, they tend to be somewhat parochial in perspective and are not entirely consistent or compatible with one another.

THE PEDIMENT ASSOCIATION

Geomorphically, the pediment is only part of an open erosional-depositional system termed the pediment association by Cooke (1970). This system includes the pediment, the upland area tributary to it, and the alluvial plain to which it is tributary (Fig. 13.1). Johnson (1932b, p. 399) conceptualized the system as 'three concentric zones in each of which the dominant action of streams differs from that in the other two: (1) an inner zone, the zone of degradation, corresponding closely to the mountainous highland, in which vertical down-cutting of the streams reaches its maximum importance; (2) An intermediate zone, the zone of lateral corrasion, surrounding the mountain base, in which the lateral cutting by streams attains its maximum relative importance. This is the zone of pediment formation. (3) An outer zone, the zone of aggradation, where upbuilding by deposition of alluvium has its maximum relative importance'.

Morphologically, the pediment is the most stable component of this open system. As surfaces of fluvial transport (in arid and semi-arid environments, at least) which operate over long periods of time at or very close to the threshold for critical power in streams, pediments preserve little evidence

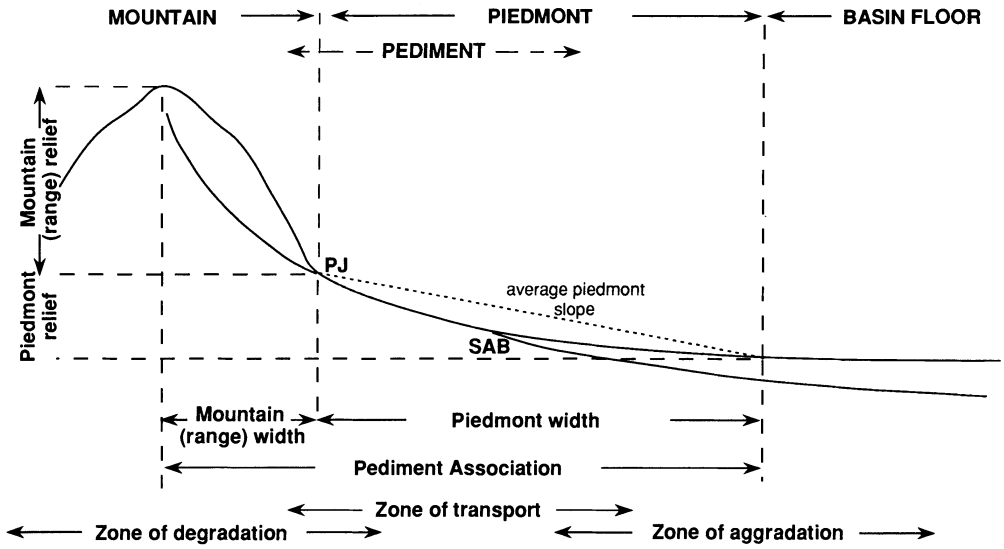

Figure 13.1 The pediment association 'includes the pediment, the mountain drainage basins tributary to it, and the alluviated plain to which it is tributary' (Cooke 1970, p. 28). PJ = piedmont junction; SAB = subaerial alluvial boundary.

of their own evolutionary history. Consequently, relatively little can be learned regarding pediment formation from the pediment surface itself. With the exception of those few places where relict pediment surfaces are preserved beneath lava flows, or other similar caprock materials that can be precisely dated (Oberlander 1972, Dohrenwend *et al.* 1985, 1986), geologic evidence of pediment formation is best preserved within other components of the pediment association: the geomorphic record preserved in relic upland landforms, the stratigraphic record contained within deposits of the alluvial plain, and the ongoing process/landform transition of the piedmont junction. Thus, analysis of pediment formation is best approached, in most cases, through study of the entire pediment association.

PEDIMENT MORPHOLOGY

Certainly one of the most remarkable physical attributes of any pediment is the generally planar and featureless character of most (or at least part of) its surface (Figs 13.2 & 13.3). Consider, for example, this description of the pediments fringing the Sacaton Mountains of southern Arizona: 'The surface which encircles the mountains is remarkably smooth, being scarred only by faint channels rarely more than a foot deep. Near the mountains it has a slope of 200 to 250 feet per mile but at a distance of a few miles it is so flat that films of water cover broad areas after heavy rains' (Howard 1942, p. 16). Despite this general simplicity, detailed examination of pediment morphology commonly reveals substantial complexity; '. . . a pediment which is a clean, smooth bedrock surface is rare indeed' (Cook and Warren 1973, p. 196). In many instances, the proximal pediment surface is characterized by an irregular mosaic of exposed bedrock and veneers of thin alluvial cover and (or) residual regolith. On active pediments, exposed bedrock areas may be shallowly dissected and gently undulating with several metres of local relief, whereas mantled areas are typically only slightly dissected to undissected with generally less than 1 to 2 m of local relief. Either type of surface may be interrupted by isolated knobs, hills, and ridges of bedrock that stand above the general level of the surrounding erosional plain.

Significant aspects of pediment morphology include: (a) the character and form of pediment boundaries including the upslope limit (piedmont junction) and downslope limit (upslope limit of alluvial cover); (b) characteristic surface profiles, both longitudinal and transverse; (c) patterns of surface drainage and drainage dissection; (d) the form and distribution of major surface irregularities including inselbergs and tors; and (e) the character and distribution of the associated regolith. These morphologic characteristics are determined, at least in part, by a variety of influences including lithology and structure, relative size and shape of the piedmont

Figure 13.2 The broad, gently sloping, largely undissected surface of Cima Dome. One of the largest pediments in the eastern Mojave Desert, Cima Dome is approximately 16 km across and 600 m high. Aerial view is south-east.

Figure 13.3 Partly alluviated pediment surface on metamorphic rocks (including gneiss, granitoid rocks, diabase dykes, schist, marble, and quartzite), west piedmont of the Chemeheuevi Mountains. Aerial view is south across Chemeheuevi Valley, eastern Mojave Desert.

and its associated upland, tectonic history, and climate. Consequently, they may vary widely even within the limits of an individual pediment.

FORM AND CHARACTER OF THE MOUNTAIN FRONT

The boundary between an upland area, mountain or mountain range, and its associated piedmont is commonly termed the mountain front. However, 'mountain front is an unfortunate term inasmuch as it suggests an almost linear and continuously outfacing boundary between the mountain mass and the pediment, whereas virtually all mountain fronts are indented to some degree by embayments' (Parsons and Abrahams 1984, p. 256). These embayments are, for the most part, widened valley floors that tend to form along the mountain front whenever the rate of erosional retreat of the valley sides exceeds the rate of incision of the valley floor. Such conditions are common where the mountain mass is no longer undergoing rapid uplift and local base level is either stable or rising. Consequently, the sinuosity (degree of embayment) of a tectonically inactive mountain front tends to increase with time (Bull and McFadden 1977).

The embayed nature of inactive mountain fronts has been recognized by many workers, and its significance relative to the formation and expansion of pediments is well established (e.g. Bryan 1922, Johnson 1932a, Sharp 1940, Howard 1942, Parsons and Abrahams 1984). Indeed, Lawson (1915, p. 42) was among the first to describe the general progression of embayment development. 'The contour of the subaerial [mountain] front for the greater part of the time of its recession is not in reality a straight, or even a gently sinuous line, but is actually indentate. At the indentations are cañons or gullies and from these emerge the greater part of the detritus which forms the embankment [alluvial plain] and which is distributed radially from an apex in, or at the mouth of, every cañon or gully. . . . The identations may be slight in the early stages of front recession, is most pronounced in the middle stages and becomes less intricate in the later stages.' Parsons and Abrahams (1984, p. 258) further define the process as follows, 'For a particular mountain mass during a particular period of time, the relative effectiveness of divide removal [between embayments] and mountain front retreat in extending a piedmont will depend on the relative rates of migration of piedmont junctions in embayments and along mountain fronts and the relative lengths of embayments and mountain fronts'.

FORM AND CHARACTER OF THE PIEDMONT JUNCTION

The junction of the mountain slope and piedmont is commonly termed the piedmont junction. In many areas, this boundary is marked by an abrupt and pronounced break in slope. It may be particularly abrupt and well-defined where (a) an active fault bounds the mountain front, (b) marginal streams flow along the base of the upland slope, (c) slopes are capped with resistant caprock, (d) slopes are coincident with bedrock structure (dykes, joints, fault line, steep-dipping to vertical beds, etc.), or (e) a pronounced contrast exists between debris sizes on the hillslope and on the piedmont surface. In other areas, particularly along the dipslope flanks of tilted range blocks, piedmont surfaces may merge smoothly, almost imperceptibly, with the range slope and, in the case of gentle asymmetric tilting, may even extend up to and be truncated by the range crest. In yet other areas, particularly where a proximal pediment is pervasively dissected, the piedmont junction may be represented by a diffuse transition zone as much as several hundred metres wide and highly irregular both in plan and in profile. In such locations, the junction may be so irregular that it cannot be mapped as a discrete boundary. Indeed, even in those areas where the junction appears to be relatively well-defined when viewed from a distance, closer examination commonly reveals considerable complexity in both plan and profile.

The local character of the piedmont junction is determined in part by the nature of the transition from relatively diffuse erosional processes on the hillslope to somewhat more concentrated fluvial processes on the piedmont surface. As Bryan (1922, pp. 54–5) observed '. . . the angle of slope of the mountain is controlled by the resistance of the rock to the dislodgement of joint blocks and the rate at which these blocks disintegrate. . . . Fine rock debris is moved down the mountain slope by rainwash and carried away from the foot of the slope by rivulets and streams that form through the concentration of the rainwash. . . . The angle of slope of the pediment, however, is due to corrasion by the streams, and this corrasion is controlled by the ability of the water to transport debris . . . . The sharpness of the angle between the mountain slope and the pediment is one of the most remarkable results of the division of labor between rainwash on the mountain slopes and streams on the pediment'. Where this transition is profound, the piedmont junction is abrupt; where the transition is more gradual, the junction is typically less well defined. In those areas where the

junction separates hillslope from piedmont interfluve the abruptness of the transition appears to be related to hillslope lithology and structure. 'In quartz monzonite areas there is often a marked contrast between debris sizes on mountain fronts and on pediments, which may account for the distinct break of slope between the two landforms in these areas; on other rock types, where the particle-size contrast is less marked, the change in slope is less abrupt' (Cooke and Warren 1973, p. 195).

In the extreme case where no transition in process occurs, there is no piedmont junction. 'The "sharp break in slope" between the pediment surface and the mountain front . . . exists only in interfluvial areas. . . . The course of any master stream channel from a given drainage basin in the mountains onto the pediment surface and thence to the basin floor below has no sharp break in slope. In the absence of constraints, such as recent structural disturbances, any stream channel will exhibit a relatively smooth, concave upward, longitudinal profile that accords with the local hydraulic geometry . . . . The interfluvial areas, however, generally do exhibit a marked change in slope . . . . The reason for the existence of such a zone is precisely that it is an interfluvial area; the dominant process that operates on the mountain front is not fluvial' (Lustig 1969, p. D67).

THE ALLUVIAL BOUNDARY AND THE SUBALLUVIAL SURFACE

The transition between exposed bedrock and alluvial cover on pediments is not well documented. The very nature of this boundary impedes detailed mapping, measurement or quantitative description. The few general descriptions available show that the subaerial alluvial boundary is gradational, discontinuous, and highly irregular (e.g. Sharp 1957, Tuan 1959, Dohrenwend *et al.* 1986). Several factors contribute to this complexity. (a) The suballuvial bedrock surface (termed the suballuvial bench by Lawson, 1915) subparallels the surface of the alluvial mantle; its longitudinal profile is nearly rectilinear and its average slope is only very slightly steeper than the average slope of the subaerial surface (Cooke and Mason 1973). (b) On many pediments in the Mojave and Sonoran deserts, alluvial thicknesses of a few metres or less are typical for distances of at least 1 km downslope from exposed bedrock surfaces (Howard 1942, Tuan 1959, Cooke and Mason 1973, Dohrenwend unpublished data). (c) The subaerial alluvial boundary appears to be highly transient, migrating up and downslope across the piedmont in response to long-term changes in stream power and sediment load. Upslope migration is documented by buried palaeochannels of similar dimensions to active surface channels (Cooke and Mason 1973, Dohrenwend unpublished data), whereas downslope migration and proximal exhumation are suggested by the pervasive dissection of exposed bedrock surfaces (Cooke and Mason 1973).

LONGITUDINAL SLOPE

The longitudinal slope of pediments typically ranges between 0.5° and 11° (Tator 1952, Cooke and Warren 1973, p. 193, Thomas 1974, p. 217). Slopes in excess of 6° are uncommon except in proximal areas. In the south-west United States, average longitudinal slopes typically range between 2° and 4° and rarely exceed 6° (Table 13.1).

There is general agreement that the characteristic form of the longitudinal profile of most pediments is concave-upward (e.g. Bryan 1922, Johnson 1932b, Lustig 1969, p. D67, Thomas 1974, p. 217). Although Davis (1933), Gilluly (1937) and Howard (1942) described convex-upward profiles for the crestal areas of pediment passes and pediment domes; rectilinear to concave longitudinal profiles typify most slopes on these landforms except in the immediate vicinity of the crest (Sharp 1957, Dohrenwend unpublished data; Fig. 13.2). The pediments of arid and semi-arid regions are generally considered to be graded surfaces of fluvial transport where the surface slope is adjusted to the discharge and load of the upland/piedmont drainage, and the characteristic concave longitudinal profile is the result of this adjustment to fluvial processes. Systematic relations between pediment slope and stream size clearly demonstrate this adjustment. In proximal areas, for example, pediment slope is steeper immediately downslope from intercanyon areas than downstream from valley mouths (Bryan 1922). Also, as Gilluly (1937, p. 332) observed in the Little Ajo Mountains of south-west Arizona, 'the pediment is, for the most part, concave upward in profile, generally more steeply along the smaller stream courses [3.25°], less steeply along the larger streams [0.75°]'. Local variations in pediment slope that are closely related to lithologic variations also testify to this adjustment. 'The longitudinal profile (concave) should not be assumed to be a smooth curve in all cases. It is rather, similar to the average stream profile, segmented, the smoother portions being developed across areas of homogeneous rock. Across heterogeneous rocks the profile is segmental, steeper on the more resistant and gentler on the less resistant types' (Tator 1952, p. 302).

The influences of lithology and climate on pedi-

Table 13.1 Representative pediment slope data (degrees), south-western United States

Area	*Range of longitudinal slopes*	*Mean longitudinal slope*	*Number of pediments*	*Reference*
Western Mojave Desert (granitic)	0.5–5.37	2.5	37	Cooke (1970)
Western Mojave Desert (non-granitic)	0.75–5.15	2.8	16	Cooke (1970)
Eastern Mojave Desert (granitic)	0.8–5.3	2.0	5	Dohrenwend (unpublished data)
Eastern Mojave Desert (granitic domes)	1.0–6.0	3.4	9	Dohrenwend (unpublished data)
Eastern Mojave Desert (non-granitic)	0.7–4.4	1.9	5	Dohrenwend (unpublished data)
Mojave Desert (granitic)	1.6–8.6*	3.4	17	Mammerickx (1964)
Sonoran Desert (granitic)	1.95–5.0*	3.5	4	Mammerickx (1964)
Mojave and Sonoran deserts (non-granitic)	1.25–4.4*	2.8	5	Mammerickx (1964)
South-eastern Arizona	0.5–2.2	–	–	Bryan (1922)
	0.5–3.3	–	–	Gilluly (1937)
Ruby–East Humboldt Mountains, Nevada (west flank)	0.8–3.8	–	–	Sharp (1940)
Ruby–East Humboldt Mountains, Nevada (east flank)	4.3–5.4	–	–	Sharp (1940)

*Range of mean values.

ment slope are not well defined; however, they appear to be relatively insignificant. On the basis of a morphometric analysis, Mammerickx (1964) concluded that bedrock is not a significant factor in determining average pediment slopes in the Sonoran and Mojave Deserts. She supported this conclusion by documenting the apparently random asymmetry of a number of pediment domes in the region. 'On any dome it is difficult to imagine that the amount of rain or debris supplied to the different slopes is different, yet they are asymmetrical. The asymmetry further is not systematic in any particular direction' (Mammerickx 1964, p. 423). Comparison of slope means and ranges for granitic versus non-granitic pediments in the south-west United States (Table 13.1) also suggests the validity of this conclusion. The influence of climate on pediment slope also appears to be relatively insignificant. The typical range of longitudinal slopes appears to be essentially the same in wet–dry tropical environments as it is in arid and semi-arid environments (Thomas 1974, p. 223–4).

The influence of tectonism on pediment slope is similarly ill-defined but may be considerably more significant. Cooke (1970) documented a significant positive correlation between the relief:length ratio of the pediment association and pediment slope for 53 pediment associations in the western Mojave Desert. Because the relief:length ratio of the pediment association is very likely at least partly determined within this region by the local history and character of tectonic movement, the possibility of an indirect influence of tectonism on the slope of these pediments is indicated by this correlation. This tentative conclusion is supported by a comparative analysis of the general morphometric characteristics of several diverse neotectonic domains within the south-west Basin and Range province (Dohrenwend 1987b). Average values of piedmont slope for each of these domains show a strong positive correlation with average values of range relief, which in turn show a strong positive correlation with a morphometric index of relative vertical tectonic activity (Table 13.2). This suggests that average piedmont slope is largely determined by the general morphometric character of each domain (e.g. initial range relief, range width and spacing, etc.) which in turn is largely determined by the style, character, and timing of local tectonism.

TRANSVERSE SURFACE PROFILE

Although the longitudinal pediment profile is, for the most part, slightly concave-upward, the form of the pediment surface transverse to slope may assume any one of several general forms; convex-upward or fan-shaped (Johnson 1932b, Rich 1935, Howard 1942), concave-upward or valley-shaped (Bryan 1936, Gilluly 1937, Howard 1942), or essentially rectilinear (Tator 1952, Dohrenwend unpublished data). These general transverse forms are usually better developed in proximal areas of the

Table 13.2 Morphometric summary of the west-central Basin and Range province average range and piedmont dimensions

Tectonic domain	*Average range relief, Rr* (km)*	*Average piedmont relief, Pr (km)*	*Average range width, Rw (km)*	*Average piedmont width, Pw (km)*	*Average slope of piedmont association (Rr + Pr)/(Rw + Pw)*	*Averagae piedmont slope† (Pr/Pw)*
Central Great Basin	0.73	0.21	6.20	5.90	0.077	0.034
South-east Great Basin	0.63	0.24	3.15	6.00	0.095	0.040
South-west Great Basin	1.38	0.29	6.90	4.90	0.142	0.059
Northern Mojave Desert	0.49	0.30	2.85	8.20	0.072	0.037
Walker Lane Belt						
North-west Goldfield Block	0.64	0.27	3.30	6.10	0.096	0.044
North-east Goldfield Block	0.49	0.24	3.25	7.70	0.066	0.031
Spring Mountains Block	1.19	0.51	9.25	11.9	0.080	0.043

*Average range relief $Rr = 0.15Ti + 0.16$, where the index of relative vertical tectonic activity $Ti = (Rr/Pr) + (Rw/Pw)$; $r = 0.767$, $p = 0.044$.
†Average piedmont slope $(Pr/Pw) = 0.022Rr + 0.024$; $r = 0.829$, $p = 0.021$.

pediment (Tator 1952). However, undulating surfaces displaying irregular combinations of convex, concave, and rectilinear slope elements superimposed on one or more of these general forms are also characteristic where proximal areas are pervasively dissected. Undissected distal areas approach a gently undulating to nearly level transverse form (Tator 1952).

Arguments based on the presence or absence of a particular transverse surface form have been used to advocate various conceptual models of pediment development. For example, Johnson (1932b) considered rock fans (a proximal pediment with a general fan shape in plan and a convex-up transverse profile) to be compelling evidence of lateral planation by streams; whereas, Rich (1935) argued that such forms may also be produced by repeated stream capture induced by unequal incision of drainage with upland sources as compared to drainage without upland sources. Howard (1942) suggested that the transverse profiles of pediment embayments may be either convex, concave, or a combination of these forms depending on the relative activity of trunk and tributary streams within the embayment. As these and other models suggest, the tendency for water flow to channelize and then to concentrate via the intersection of channels acts to produce a variety and complexity of transverse surface forms.

PATTERNS OF DRAINAGE AND DRAINAGE DISSECTION

According to Cooke and Warren (1973, p. 197), the general pattern of drainage on pediments is essentially identical to the characteristic drainage patterns of alluvial fans and bajadas. Three interrelated types of drainage commonly develop: (a) distributary networks which radiate from proximal areas to gradually dissipate in medial and/or distal parts of the piedmont; (b) frequently changing, complexly anastomosing networks of shallow washes and rills in medial piedmont areas (Fig. 13.4); and (c) in areas of falling base level, integrated subparallel networks which are generally most deeply incised in distal areas of the alluviated piedmont plain. The transitions between these various drainage types are typically gradational and diffuse.

Detailed examination of pediment drainage, however, reveals a somewhat more complex situation than that portrayed by this generalized model (Fig. 13.5). Although many large pediments are generally smooth and regular with less than a few metres of local relief, a more complex morphology occurs where shallow drainageways locally incise the pediment surface into irregular patchworks of dissected and undissected topography. The undissected areas are mostly flat with shallow, ill-defined, discontinuous to anastomosing drainageways and low indistinct interfluves, whereas dissected areas are typically scored by well-defined subparallel drainageways that form shallow regularly spaced valleys separated by rounded interfluves (Dohrenwend *et al.* 1986, p. 1051). 'If the dissection is not deep (less than 3 feet), the ground surface of the pediment is undulatory and the stream pattern is braided. If the pediment is deeply dissected (more than 3 feet) the stream pattern is essentially parallel, weakly integrated, and not braided' (Mammerickx 1964, p. 423). In the specific case of Cima Dome in the eastern Mojave Desert, 'dissection has been greatest on the east and southeast slopes . . . . Other

Figure 13.4 The west flank of the Granite Springs pediment dome (eastern Mojave Desert) has been dissected into a washboard of low rounded interfluves by a fine-textured network of shallow, subparallel to complexly interconnecting washes. Aerial view is north.

Figure 13.5 'Chaotic' patchwork of dissected and undissected bedrock surfaces on Cretaceous monzogranite, west flank of the Granite Springs pediment dome, eastern Mojave Desert. Pliocene lava flows of the Cima volcanic field cap the deeply embayed erosional escarpment in the background.

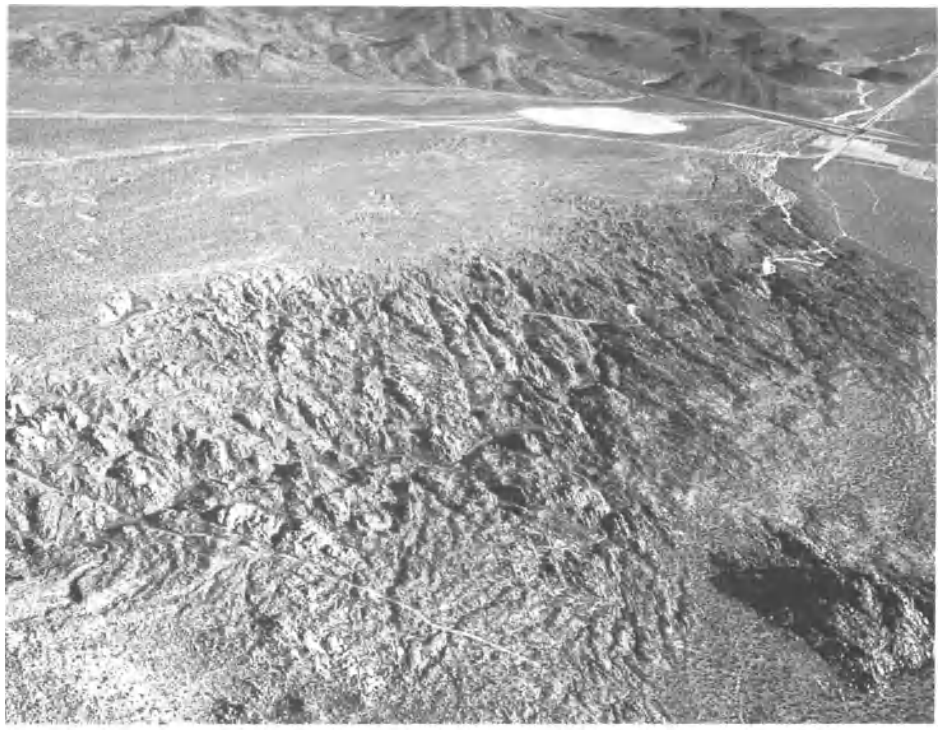

Figure 13.6 Localized dissection of a proximal pediment surface cut on Mesozoic monzogranite. 'Sediment-starvation' has lowered the critical power threshold of this piedmont-sourced drainage system causing intense dissection (of as much as 20 m) of the pediment surface. Adjacent undissected areas are traversed by sediment-satiated streams fed by large drainage basins in the adjacent uplands. Aerial view is south-east across the south piedmont of the Granite Mountains, eastern Mojave Desert.

parts of the dome, particularly the upper slopes and lower south flank, have washes between residual knobs and ridges. These are discontinuous and seemingly due to channelization of runoff between the residuals. . . . Some of the lowermost smooth alluvial slopes have small channels as much as 1 foot deep, 2–3 feet wide, and 100–200 feet long that start abruptly and end in a lobate tongue of loose grus. . .' (Sharp 1957, p. 277).

One of the more noteworthy features of pediment drainage, at least within the desert regions of western North America, is the characteristic tendency for dissection of proximal areas (Fig. 13.6). On some pediments, proximal dissection is largely restricted to small isolated areas long the mountain front; on others, particularly those surrounding small residual mountain masses, it forms broad continuous zones of intricately scored topography that extend as much as 2 or 3 km downslope from the mountain front. This dissection likely results from several diverse influences including short-term climate change (Bryan 1922) and the tendency for differential incision of drainage with upland sources as compared with drainage where sources are limited to the piedmont (Rich 1935, Denny 1967). However, regrading of proximal piedmont areas in response to evolutionary reduction of the associated mountain mass may be the dominant influence, particularly where a broad continuous pediment surrounds a small upland mass (Johnson 1932a,b, Howard 1942, Cooke and Mason 1973). 'As the mountains dwindle in size, precipitation and the volume of sediment available for streams decrease. The decrease in load more than compensates for the loss of water, so that the dwindling waters are gradually rejuvenated. They thus lower their gradients, but the lowering is greatest in their headwater regions because farther down the slope the load is increased by pediment debris' (Howard 1942, p. 135). The occurrence of proximal dissection on many pediments indicates that pediment regrading does not necessarily proceed via uniform downwearing of the proximal surface but rather may proceed via shallow incision by a diffuse network of small stream channels.

Figure 13.7 Numerous widely scattered tors and small inselbergs (developed on Mesozoic monzogranite) interrupt the otherwise gently sloping pediment plain which forms the east piedmont of the Granite Mountains in the eastern Mojave Desert.

INSELBERGS

Inselbergs are isolated hills that stand above a surrounding erosional plain (Fig. 13.7). They vary widely in abundance and size from one pediment to another. Inselbergs as tall as 180 m have been described in the Mojave and Sonoran Deserts (e.g. Sharp 1957, Moss 1977); however, heights of 10 to 50 m appear to be much more common in this region (e.g. Tuan 1959). Kesel (1977) reported that inselbergs of the Sonoran Desert have convex-concave slopes where the basal concavity comprises from 50 to 70% and the crestal convexity from 15 to 50% of the profile. One of the more significant characteristics of inselbergs relative to pediment formation is their distribution relative to the pediment surface. They commonly occur as extensions of major range front interfluves, and their size and number tend to decrease with increasing distance from the mountain front (Cooke and Warren 1973, p. 196).

REGOLITH

The regolith associated with pediment surfaces is, of course, widely variable. Transported regolith, predominantly wash and channelized flow deposits, also includes colluvial deposits within and adjacent to interfluvial piedmont junctions and thin deposits of desert loess on some inactive surface remnants. Residual regolith is mostly *in situ* weathered bedrock. The maximum thickness of transported regolith on pediments is, as discussed previously, a matter of definition. However, average thicknesses in many proximal to medial areas are limited to a few metres (Gilluly 1937, Tator 1952, Mabbutt 1966, Cooke and Mason 1973). As discussed above, these deposits commonly form thin discontinuous to continuous mantles across the bedrock surface, and surface relief is typically very similar in both form and magnitude to that of the underlying bedrock. Channels as much as 1 to 2 m deep and 10 m wide are common on both surfaces; however, both are mostly planar and relatively featureless. The thickness of residual regolith of most pediments is difficult to measure but appears to be quite variable (Oberlander 1974, Moss 1977). At least several tens of metres of saprolitic bedrock typically underlie the surfaces of many of the granitic piedmonts in the south-west Basin and Range province (Oberlander 1972, 1974, Moss 1977, Dohrenwend *et al.* 1986).

INFLUENCES ON PEDIMENT DEVELOPMENT

LITHOLOGIC AND STRUCTURAL INFLUENCES

It has long been recognized that local lithologic and structural variations strongly influence pediment development (Gilbert 1877, p. 127–8, Davis 1933,

Figure 13.8 Dissected *glacis d'erosion* cut across late Tertiary alluvial and lacustrine strata, Stewart Valley, Nevada. Aerial view is south.

Bryan and McCann 1936, Tator 1952, Warnke 1969). On the piedmonts flanking the Henry Mountains of southern Utah, for example, Gilbert (1877, p. 128) observed that in 'sandstones flat-bottomed cañons are excavated, but in the great shale beds broad valleys are opened, and the flood plains of adjacent streams coalesce to form continuous plains. The broadest plains are as a rule carved from the thickest beds of shale'. Gilluly (1937, pp. 341–2) reported a similar relation in the Little Ajo Mountains of south-western Arizona. 'The development of pediments is apparently conditioned by the lithology of the terrane, the softer and more readily disintegrated rocks forming more extensive pediments than do the harder and more resistant rocks. . .. They are commonly better developed on [weathered] granitic rocks and soft sediments than on other rocks.'

Among the most conspicuous expressions of local lithologic/structural influence are the inselbergs, tors and other positive surface irregularities that so commonly interrupt the pediment plain (Tuan 1959, Kesel 1977). These erosional remnants are characteristically associated with rocks that, by virtue of their lithology, texture, and/or structure, are more resistant to weathering and erosion than those underlying the adjacent pediment. Such relations are particularly well expressed on Cima Dome in the eastern Mojave Desert where '. . . major knobs and hillocks rising 50 to 450 feet above the slopes of [the dome] are underlain by rocks other than the pervasive quartz monzonite. . . . At scattered places, dikes and silicified zones in the quartz monzonite form linear ridges or abrupt risers a few to 25 feet high . . .. On upper parts of the dome are numerous knobs and hillocks as much as 35 feet high composed of exceptionally massive quartz monzonite' (Sharp 1957, p. 277).

On a more regional scale, numerous reports from the literature suggest that although pediments occur on many different rock types in arid regions of the south-west United States, the more extensive pediments may be preferentially developed on less resistant lithologies. In the Mojave and Sonoran Deserts, extensive bedrock pediments bevel deeply weathered, coarse-crystalline granitic rocks in many areas (Davis 1933, Gilluly 1937, Tuan 1959, Mammerickx 1964, Warnke 1969, Cooke 1970, Oberlander 1972, 1974, Moss 1977, Dohrenwend *et al.* 1986) (Figs 13.2, 13.4 and 13.7). In the west-central Great Basin (Gilbert and Reynolds 1973, Dohrenwend 1982a,b), pediments occur primarily on middle to upper Cenozoic terrigenous sedimentary rocks (predominantly partly indurated fluvial and lacustrine deposits, Fig. 13.8) and on less resistant volcanic rocks (predominantly lahars and non-welded ash flow tuffs, Fig. 13.9). Pediments also bevel upper Cenozoic terrigenous sediments along the Ruby and East Humboldt ranges of north-east Nevada (Sharp 1940),

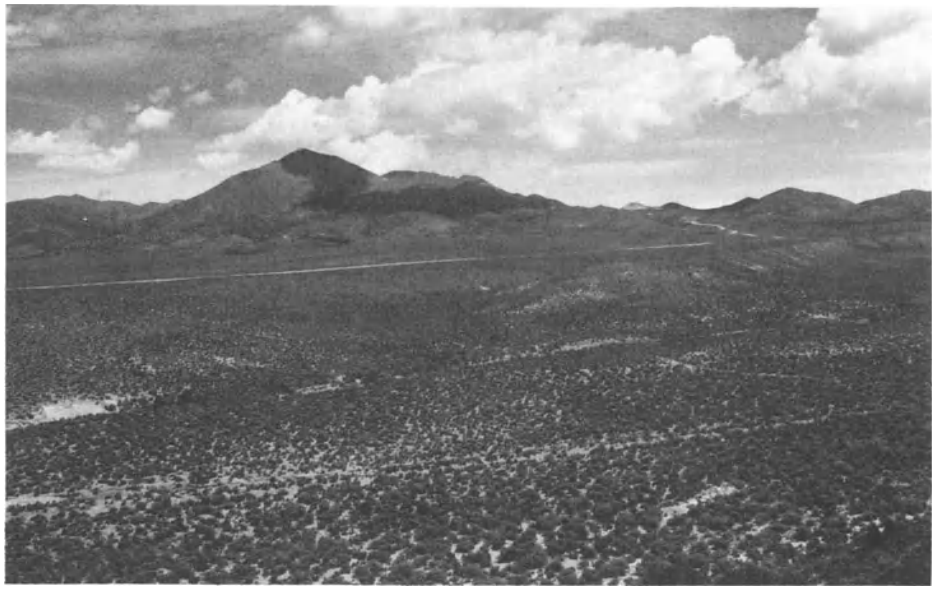

Figure 13.9 Dissected remnants of a rock pediment and *glacis d'erosion* cut across Mesozoic granitic rocks, Tertiary volcanic rocks, and Tertiary terrigenous sediments on the back-tilted flank of the Wassuk Range, west-central Nevada. View is north-east towards Lucky Boy Pass (elevation *c.* 8000 ft) and Corey Peak (elevation 10 520 ft).

in the Furnace Creek area of Death Valley (Denny 1967), in the San Pedro, Sonoita, and Canada del Oro basins of south-east Arizona (Melton 1965, Menges and McFadden 1981), along the lower valley of the Colorado River (Wilshire and Reneau 1992), and along the valley of the Rio Grande (Denny 1967).

In many other areas, however, extensive pediments cut across a variety of more resistant sedimentary, volcanic and metamorphic rocks (Tuan 1959, Mammerickx 1964, Cooke and Reeves 1972, Dohrenwend 1987a). Moreover, regional mapping and analysis of the general distribution of pediments within the tectonically active central and western Great Basin (Dohrenwend *et al.* 1994a) indicates that, within this region at least, pediment development is not clearly related to the distribution of more easily erodible rock types. Rather, the relative extent of rock types exposed on bedrock pediments accords well with the relative extent of those same rock types within the adjacent ranges (Fig. 13.10). This suggests that local tectonic stability may be the dominant control of pediment development in this tectonically active region.

TECTONIC INFLUENCES

The bedrock pediments of the south-west United States are located, for the most part, within stable or quasi-stable geomorphic environments where erosional and depositional processes have been approximately balanced for relatively long periods of time. Although pediments have not been systematically mapped or correlated with tectonic environment across the entire region, a clear correspondence between tectonic stability and pediment development is apparent.

General geomorphic analyses of the Basin and Range province document a variety of regional morphometric and geomorphic variations (including the distribution of pediments versus alluvial fans) that are clearly related to variations in the distribution and style of Quaternary faulting (Lustig 1969, p. D68, Bull 1977, Bull and McFadden 1977). For example, Lustig's (1969) morphometric and statistical analysis of Basin and Range morphology concludes that pediments are more abundant in areas characterized by low average values of range relief, height, width, length, and volume, whereas alluvial fans are more abundant where these values are large. This conclusion is generally supported by a regional neotectonic evaluation of the south-west Basin and Range province based on a geomorphic classification of the relative tectonic activity of mountain fronts (Bull 1977, Bull and McFadden 1977). This study documents several distinct regions of contrasting neotoctonic activity that may be distinguished,

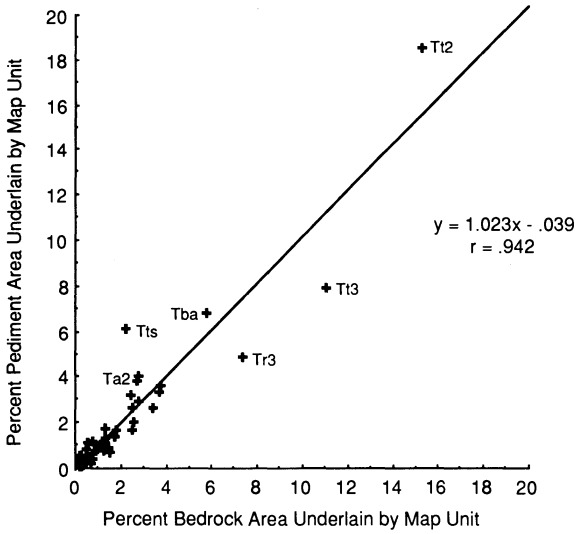

Figure 13.10 Graph comparing the relative extent of exposed bedrock pediments versus the relative abundance of bedrock in upland areas for each bedrock unit (with total surface exposures greater than 100 km^2) on the geologic map of Nevada (Stewart and Carlson 1977). In essentially all cases, the relative abundance of exposed bedrock pediments underlain by a specific rock type accords well with the relative abundance of that same rock type within the upland areas of the region. Thus, it would appear that pediment development in Nevada has not been strongly influenced by lithologic distribution (from Dohrenwend *et al.* 1994a). **Ta2** = Tertiary andesite flows and breccias and related rocks of intermediate composition (17 to 34 Ma); **Tba** = Tertiary basalt and andesite flows (6 to 17 Ma); **Tr3** = Tertiary rhyolite flows and shallow intrusive rocks (6 to 17 Ma); **Tts** = Tertiary ash-flow tuffs and tuffaceous sedimentary rocks (6 to 17 Ma); **Tt2** = Tertiary welded and non-welded silicic ash-flow tuffs (17 to 34 Ma); **Tt3** = Tertiary welded and non-welded silicic ash-flow tuffs (6 to 17 Ma).

in part, by a relative lack or abundance of pediments. Active and moderately active range fronts (with large alluvial fans, few if any pediments, steep hillslopes on all rock types, elongate drainage basins, and low mountain front sinuosities) define a region of pronounced dip-slip faulting between the Sierra Nevada and Death Valley in the south-west Great Basin; and moderately active to slightly active range fronts (with both fans and pediments, relatively equant drainage basins, broader valleys, and moderate mountain front sinuosities) characterize a region of strike-slip faulting in the south-central Mojave Desert. In contrast, inactive range fronts (with broad mountain front pediments, large embayments, and high mountain front sinuosities) distinguish regions of post-middle Miocene tectonic stability in the western and eastern parts of the Mojave Desert (Bull, 1977, Dohrenwend *et al.* 1991). Thus, the pediments of the Basin and Range province are generally larger and more continuous in areas of greater vertical tectonic stability.

This strong relation between tectonic stability and pediment development is also reflected throughout the south-west Basin and Range province by a general spatial association between extensive pediments and many areas of shallow Miocene detachment faulting (Dohrenwend 1987a). Morphometric comparisons of basin and range morphology (Dohrenwend 1987b), range front morphology (Bull 1977, Bull and McFadden 1977), and the regional distribution of young faults (Dohrenwend *et al.* 1994c) indicate significantly less post-detachment vertical tectonism in areas with extensive pediments than in other parts of the province. Moreover, a generally low local topographic relief (*c.* 100 to 250 m?) has been inferred for areas of shallow deformation along closely spaced listric normal faults in this region (Zoback *et al.* 1981). This combination of relative tectonic stability and relatively low initial tectonic relief has permitted the formation of numerous pediments that typically encircle their associated uplands and extend downslope as much as 5 to 10 km from the mountain front.

Regional mapping of pediments throughout the state of Nevada (which includes many of the more tectonically active regions of the Basin and Range province) indicates that pediment development there also has been controlled primarily by spatial and temporal variations in late Cenozoic tectonic activity (Dohrenwend *et al.* 1994a). Pediment areas with exposed bedrock or thin alluvial cover occupy approximately 15% of the intermontane piedmonts and basins of the region. The more extensive and continuous of these pediments are located in the south-central and western parts of the state in areas of relatively shallow Miocene detachment faulting that apparently have undergone relatively little post-Miocene vertical tectonic movement (see above). Typically, these areas are characterized by a relatively subdued topography consisting of low narrow ranges, broad piedmonts, and small shallow basins. Conversely, pediments are smaller and less abundant within the more tectonically active areas of the state. Included within these tectonically active areas are the longest, most continuous, and most active dip-slip fault zones; the longest and widest ranges; and the largest, deepest, and most continuous Cenozoic basins in the Great Basin.

Within tectonically active areas, pediments are

largely confined to local settings of relative geomorphic stability. Exposed bedrock pediments typically occupy proximal piedmont areas immediately adjacent to the range front; however, in some cases pediments may extend from range front to basin axis. Particularly favourable settings include range embayments and both low broad passes within and narrow gaps between ranges. Such settings are especially well suited for pediment development if they are also situated on the backtilted flanks of large asymmetric range blocks or gently upwarped structural highs. Smaller pediments occur on the tilted flanks of small blocks along major strike-slip faults, on upfaulted piedmont segments, and within small embayments adjacent to active fault-bounded range fronts (Dohrenwend 1982c).

Although all of these diverse geomorphic settings are related by a common condition of relative long-term stability, they are quite different in many other respects. Hence, the pediments formed within each of these local geomorphic environments are morphologically distinct. Comparison of the pediments on the east and west flanks of the Ruby–East Humboldt Range in north-eastern Nevada illustrates this relation between pediment morphology and local neotectonic–geomorphic environment (Sharp 1940). The east flank of this asymmetrically west-tilted range is bounded by a major range front fault system. Thus the drainage basins and piedmonts of the east flank are smaller and steeper than those of the west flank, and Pleistocene glaciation was less extensive on the east flank than on the west flank. Consequently, the large pediments of the west flank extend across the backtilted flank of the range, whereas the smaller pediments of the east flank are confined to embayments upslope from the range-bounding fault. Seven surfaces (pediments and partial pediments) occur on the west flank of the range, and these pediments are cut mostly on soft basin deposits. In contrast, the pediments of the east flank are, with one exception, cut entirely on the hard rocks of the mountain block. 'Remnants of pediments on the west flank extend as far as 5 miles from the foot of the mountain slope, and the undissected surfaces were probably even more extensive. The east flank pediments are narrower, at least as exposed, and seldom extend more than 1.5 miles from the mountains. The west flank pediments have gentler gradients and are more nearly smooth than those of the east side. The pediments of the west side are mantled by a comparatively uniform cover of stream gravel; those of the east side have only local patches of stream gravel . . .' (Sharp 1940, pp. 362–3).

CLIMATIC INFLUENCES

The influence of climate on pediment development has not been systematically studied and, therefore, is not very well documented or understood. Pediments occur within the broad range of climates from subpolar to humid tropical. They are particularly abundant and well developed, however, in arid/semi-arid and tropical wet–dry regimes. Indeed pediments are so characteristic of these two rather disparate regimes that they represent somewhat of an embarrassment to advocates of climatic geomorphology (Chorley *et al.* 1984, p. 486). Descriptive reports in the literature indicate that the pediments of most climatic realms are generally similar in form and landscape position. For example, 'broad, gently sloping [erosional] surfaces which extend from the base of hillslopes, and which in some cases pass beneath alluvial accumulations and in others terminate at a break in slope leading down to the river channel or floodplain, undeniably exist in the tropics' (Thomas 1974, p. 218). These tropical pediments are characterized by generally smooth, concave-up longitudinal profiles with declivities ranging between 1° and 9°. Also they are most commonly interpreted to function as surfaces of transport between hillslope and riverine plain. These similarities of form, position, and function notwithstanding, it is not at all clear that the processes of mass transport which maintain these surfaces are at all similar from one climatic regime to another. However, it is apparent that these surfaces are for the most part typically associated with either local or regional settings of long-term geomorphic stability.

Because long-term geomorphic stability appears to be a general requirement for pediment formation, it is very likely that the development of many pediments, particularly larger ones, may transgress periods of unidirectional climate change and that such changes may profoundly affect pediment development. For example, several lines of evidence indicate that the granitic pediments of the Mojave and Sonoran Deserts were fully developed by late Miocene time and since that time have been modified primarily by partial stripping of a thick saprolitic regolith (Oberlander 1972, 1974, Moss 1977). According to Oberlander, the late Miocene Mojave–Sonoran region was probably an open woodland interspersed with grassy plains that extended across extensive cut and fill surfaces of low relief surmounted by steep-sided hills. Pediment formation within this landscape appears to have involved an approximate balance between regolith erosion (probably by slope wash, rill wash and channelized flow

processes) and regolith renewal (by chemical breakdown of granitic rock along a subsurface weathering front). This balance was apparently upset by increasing aridity resulting in a loss of vegetative cover which triggered regolith stripping and concomitant formation of the relatively smooth pediment surfaces that characterize the modern landscape. Evidence supporting this general scenario includes saprolite remnants preserved beneath late Tertiary lava flows, the elevated positions of these lava-capped palaeosurfaces above present erosion surfaces, continuity between the relic saprolite and boulder mantles on hillslopes, and general grusification as much as 40 m below present pediment surfaces. Interestingly enough, it is generally agreed that the pediments of many tropical and subtropical areas have also developed across pre-weathered materials or have been significantly modified, at least, by erosional stripping of deeply weathered materials (Mabbutt 1966, Twidale 1967, Thomas 1974, p. 218–20).

PEDIMENT DEVELOPMENT AND TIME

It is generally perceived that extensive pediments are a characteristic feature of old landscapes (Lawson 1915, Bryan 1922, Davis 1933, Howard 1942) and that their formation requires a condition of general landscapes stability wherein erosional and depositional processes are approximately balanced over long periods of time (cyclic time of Schumm and Lichty 1965). There is little doubt that the more extensive pediments of the Basin and Range province are, at least in part, relics of considerable age. Throughout this region, local burial of piedmonts and pediments by late Cenozoic lava flows provides convincing evidence of their long-term morphologic stability, even in regions of neotectonic activity (Figs 13.11 and 13.12, Table 13.3). Moreover, ubiquitous deep weathering beneath extensive pediments in the Mojave and Sonoran Deserts indicates at least pre-Quaternary ages for the original surfaces of these pediments (Oberlander 1972, 1974, Moss 1977).

Average rates of downwearing and backwearing.

One of the more reliable approaches for estimating average erosion rates in the Basin and Range province involves the documentation and analysis of erosion surfaces capped by Tertiary and Quaternary basaltic lava flows. Average downwearing rates can be estimated by measuring the average vertical distance between an erosional palaeosurface capped by a lava flow and the adjacent modern erosion surface, then dividing this height difference by the K/Ar age of the lava flow. Using this approach, average downwearing rates have been estimated for several widely separated upland and piedmont areas within the Great Basin and Mojave Desert. For upland areas, these estimates range between 8 and 47 m per million years for periods of 0.85 to 10.8 m.y. (Table 13.3a); whereas for proximal piedmont areas, the estimates range from less than 2 to 13 m per million years for periods of 1.08 to 8.9 m.y. (Table 13.3b). During similar time periods, medial piedmont areas have remained largely unchanged (Table 13.3c). These data document a general evolutionary scenario of upland downwearing and proximal piedmont regrading which has been regulated in part by the long-term stability of the medial piedmont which serves as a local base level for the upper part of the pediment association (Figs. 13.11 and 13.12).

Average rates of backwearing or slope retreat can be estimated in a similar manner by measuring the average horizontal distance between the maximum possible original extent of a lava flow which caps an erosional palaeosurface and the present eroded margin of that flow, then dividing this horizontal distance by the K/Ar age of the lava flow. Estimated rates of slope retreat determined by this method range between 37 and 365 m per million years (Tables 13.3a and b). Of course, these estimates of average backwearing should be used only as general approximations. The armouring effect of blocky basalt talus inhibits the backwearing of basalt capped hillslopes; moreover, substantial uncertainties are inherent in determining the original extent of most lava flows. However, these average backwearing rates are comparable with the 0.1 to 1-km-per-million-year rates of range front retreat and pediment formation that have been previously estimated or assumed for diverse areas of the Basin and Range province (Wallace 1978, Mayer *et al.* 1981, Menges and McFadden 1981, Saunders and Young 1983).

If one assumes that the estimated rates of downwearing and backwearing compiled in Table 13.3 are, in fact, representative of erosion rates in arid regions of the south-western United States, then a typical upland in this region has probably undergone from as little as 50 m to as much as 250 m of downwearing and from 0.2 to 2 km of backwearing since late-Miocene time. During this period, the medial areas of the piedmont fringing this typical upland would have experienced little morphologic change. Hence, it is very likely that many of the larger pediments of the Mojave and Sonoran Deserts (which typically are at least several kilometres wide)

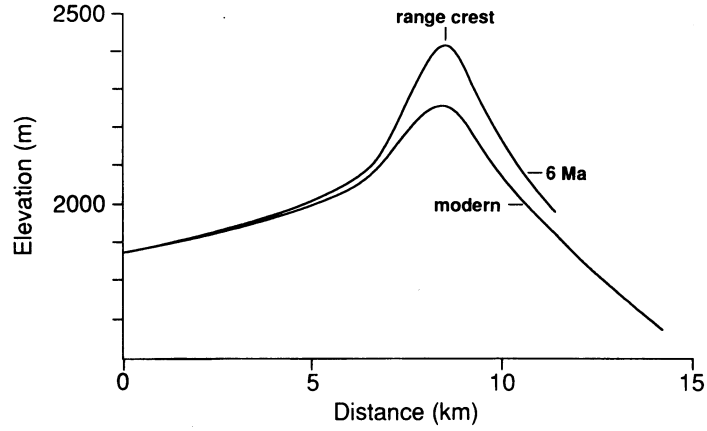

Figure 13.11 Longitudinal profiles comparing modern and late Miocene erosional surfaces on the west flank of the Reveille Range. Since latest Miocene time, rates of incision and downwearing have ranged between 20 and 35 m per million years in crestal and upper flank areas and between 5 and 20 m per million years in lower flank and proximal piedmont areas. Medial and distal piedmont areas have undergone less than 5 m of net downwearing.

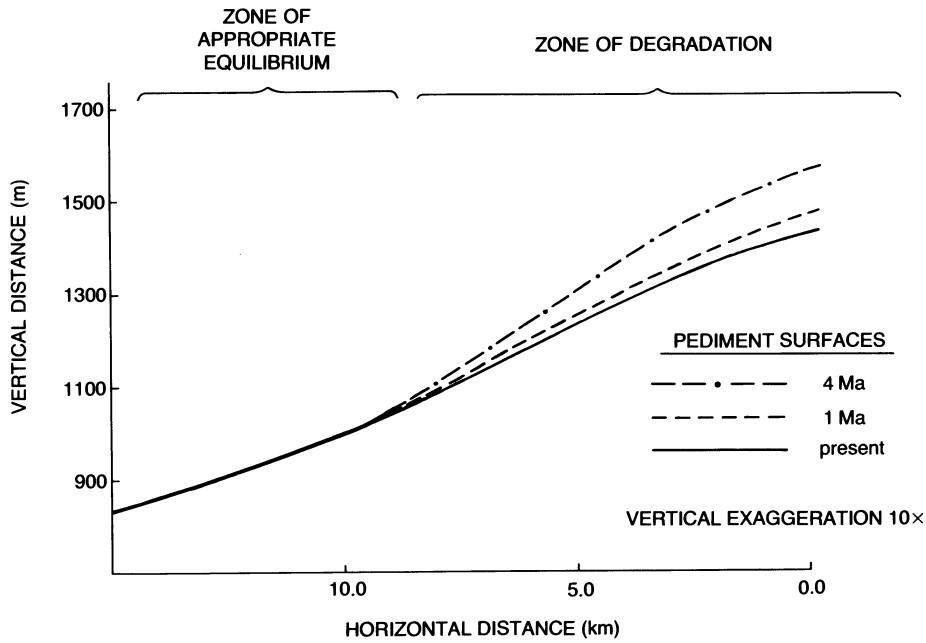

Figure 13.12 Empirical model of pediment dome evolution in the eastern Mojave Desert based on a compilation of elevation differences between active pediment surfaces and relict surfaces capped by dated lava flows. The 1 Ma and 4 Ma surfaces were reconstructed using a smoothed plot of average downwearing rates versus distance from dome summits. Upper flank areas have been eroded, midflank areas have remained in a state of approximate equilibrium, and lower flank areas (not shown) have probably aggraded. Horizontal distance is measured from the dome summit (from Dohrenwend *et al.* 1986).

Table 13.3 (a) Erosion rates in upland areas of the south-west Basin and Range province inferred from comparisons between active and basalt-capped relic erosion surfaces

Location	*Minimum age of relic surface (Ma)*	*Maximum average downwearing rate (m per m.y.)*	*Maximum average rate of slope retreat (m per m.y.)*	*Reference*
Fry Mountains, southern Mojave Desert	8.90 ± 0.9	8	–	Oberlander (1972)
Cima volcanic field, eastern Mojave Desert	4.48 ± 0.15	11	290	Dohrenwend *et al.* (1986) Turrin *et al.* (1985)
Cima volcanic field, eastern Mojave Desert	3.85 ± 0.12	29	365	Dohrenwend *et al.* (1986) Turrin *et al.* (1985)
Cima volcanic field, eastern Mojave Desert	0.85 ± 0.05	30	320	Dohrenwend *et al.* (1986) Turrin *et al.* (1985)
White Mountains, south-west Great Basin	10.8	24	–	Marchand (1971)
Buckboard Mesa, southern Great Basin	2.82	47	–	Carr (1984)
Columbus Salt Marsh, central Great Basin	3.04 ± 0.2	21	37	Dohrenwend (unpublished data)
Reveille Range, central Great Basin	5.70 ± 0.20	34	230	Ekren *et al.* (1973)
Reveille Range, central Great Basin	3.79 ± 0.34	20	200	Dohrenwend *et al.* (1985, unpublished data)

Table 13.3 (b) Erosion rates in proximal piedmont areas of the south-west Basin and Range province inferred from comparisons between active and basalt-capped relic erosion surfaces

Location	*Minimum age of relict surface (Ma)*	*Maximum average downwearing rate (m per m.y.)*	*Maximum average rate of slope retreat (m per m.y.)*	*Reference*
Fry Mountains, southern Mojave Desert	8.90 ± 0.90	<2	–	Oberlander (1972)
Cima volcanic field, eastern Mojave Desert	3.64 ± 0.16	11	85	Dohrenwend *et al.* (1986)
Reveille Range, central Great Basin	5.76 ± 0.32	8	230	Dohrenwend *et al.* (1985, unpublished data)
Reveille Range, central Great Basin	5.58 ± 0.30	2.5	190	Dohrenwend *et al.* (1985, unpublished data)
Lunar Crater volcanic field, central Great Basin	2.93 ± 0.30	9	–	Turrin and Dohrenwend (1984, unpublished data)
Lunar Crater volcanic field, central Great Basin	1.08 ± 0.14	13	–	Turrin and Dohrenwend (1984, unpublished data)
Quinn Canyon Range, central Great Basin	8.5 ± 0.7	15	–	Dohrenwend (unpublished data)
Columbus Salt Marsh, central Great Basin	3.04 ± 0.2	13	50	Dohrenwend (unpublished data)

Table 13.3 (c) Late Cenozoic basaltic volcanic fields on piedmonts in the south-west Basin and Range province where net vertical erosion/deposition has been low (generally less than 5 m in most medial and/or distal piedmont areas) since lava flow emplacement

Area	*Latitude*	*Longitude*	*Age range (Ma)*	*Reference*
Buffalo Valley, northern Great Basin	40.35°N	117.3°W	0.9–3.0	Dohrenwend (1990a)
Reveille Range, central Great Basin	38.1°N	116.2°W	3.8–5.8	Dohrenwend *et al.* (1985) Dohrenwend (1990b)
Lunar Crater volcanic field, central Great Basin	38.25°N	116.05°W	*c.* 0.1–2.9	Turrin and Dohrenwend (1984) Dohrenwend (1990c)
Quinn Canyon Range, central Great Basin	37.9°N	115.95°W	7.8–9.2	Dohrenwend (unpublished data)
Clayton Valley, western Great Basin	37.8°N	117.65°W	0.2–0.5	Dohrenwend (1990d)
Columbus Salt Marsh, central Great Basin	38.1°N	118.05°W	2.8–3.2	Dohrenwend (unpublished data)
Crater Flat, southern Great Basin	37.1°N	116.5°W	*c.* 0.1–3.7	Carr (1984), Turrin *et al.* (1991)
Big Pine, south-west Great Basin	37.05°N	118.25°W	<0.1–1.2	Gillespie (1990)
Saline Valley, south-west Great Basin	36.85°N	117.7°W	0.5–0.7	Dohrenwend (unpublished data)
Cima volcanic field, eastern Mojave Desert	35.25°N	115.75°W	*c.* 0.1–1.1	Dohrenwend *et al.* (1986) Dohrenwend (1990e)

have been forming since at least late Miocene time. This pattern of landscape evolution is particularly well documented on the slopes and piedmonts of the Reveille Range in south-central Nevada (Fig. 13.11). Since latest Miocene time, denudation rates along the crest and upper flanks of the Reveille Range have ranged between 20 and 35 m per million years. Downwearing of lower flank and upper-piedmont areas has ranged between 5 and 20 m per million years; and most middle and lower piedmont areas have remained in a state of approximate erosional equilibrium (Dohrenwend *et al.* 1985, 1986).

Direct evidence of pediment age.

The local burial of Tertiary pediments remnants by late Miocene and Pliocene basalt flows provides convincing evidence for a long history of pediment evolution (Oberlander 1972, 1974, Dohrenwend *et al.* 1985, 1986). North of the San Bernardino Mountains in the south-western Mojave Desert, late Miocene lava flows cover pediment remnants cut across saprolitic weathering profiles. These remnants now stand as much as 60 m above adjacent pediment surfaces (Oberlander 1972). In the vicinity of Cima dome in the north-eastern Mojave Desert, Pliocene lava flows bury remnants of ancient pediments cut across less intensely weathered materials (Fig. 13.13); and flows younger than 1.0 Ma bury pediment remnants locally capped by soils similar to those developed on adjacent Quaternary surfaces (Fig. 13.14). In this area, differences in height between buried surface remnants and adjacent active pediment surfaces are systematically related to the ages of the overlying lava flows (i.e. at equal distances downslope from the crest of the pediment dome, the older the buried remnant the greater its height above the adjacent active surface). Moreover, the ubiquitous presence of deep weathering profiles underlying other extensive granitic pediments in the Mojave and Sonoran Deserts suggests at least pre-Quaternary ages for the original pediment surfaces (Oberlander 1972, 1974, Moss 1977). These relations indicate that, since late Miocene time, pediment surfaces cut across deeply weathered granitic rocks have evolved more or less continuously by progressive stripping of a thick late Tertiary weathering mantle (Oberlander 1972, 1974, Moss 1977, Dohrenwend *et al.* 1986). Hence, these pediments are, at least in part, ancient forms of late Miocene age.

PEDIMENT PROCESSES

As Cooke and Warren (1973, p. 203) aptly pointed out, attempts to deduce the formation of an existing landform from observation of the processes presently operating on that landform are often unsuccessful because this approach commonly confuses cause

Figure 13.13 Early Pliocene basaltic lava flows of the Cima volcanic field preserve remnants of a large Miocene pediment dome cut across deeply weathered monzogranite and Tertiary terrigenous sedimentary rocks. Aerial view north-east towards the 80 to 120-m-high erosional scarp which bounds the western edge of the Pliocene flows. A continually evolving pediment surface extends downslope from the base of this deeply embayed escarpment. This modern pediment is pervasively dissected by a finely textured, subparallel network of shallow (<3 m deep) washes.

Figure 13.14 Quaternary basaltic lava flows (*c.* 0.1 to 1.0 Ma) of the Cima volcanic field veneer remnants of a continually evolving pediment surface formed on Cretaceous monzogranite and middle Tertiary terrigenous sediments. Deep incision of a *c.* 1.0 Ma flow complex (left foreground) reflects the delicate erosional–depositional balance of this active pediment surface. Aerial view is north-west.

and effect. Mere spatial association does not establish a cause and effect relation between form and process. Indeed, such relations are particularly unlikely in the case of long-lived landforms (such as pediments) that have evolved through complex histories of tectonic and climate change. The various processes operating on such landforms and the relative effectiveness of these processes undoubtedly has changed dramatically through time. Even when a cause and effect relation between form and process does exist, such a relation may well be unidirectional (i.e. the form determines the process, but the process did not produce the form). For example, sheetflood erosion cannot produce a planar pediment surface because a planar surface is necessary for sheetflooding to occur (Paige 1912, Cooke and Warren 1973, p. 203). Similarly, weathering and subsequent removal of the weathered debris are unlikely to produce a pediment surface but will act to maintain a pre-existing surface if these processes are uniformly applied (Lustig 1969, p. D67). Thus, the assumption that the processes presently operating to maintain or modify pediment form are the same as those responsible for pediment formation is not justified.

PROCESSES ON PEDIMENT SURFACES

In the desert regions of western North America, pediments serve as integral parts of the piedmont, and the processes operating on pediment surfaces are much the same as those operating on other parts of the piedmont plain (Dohrenwend 1987a). Processes which act to maintain or modify pediment surfaces include surface and subsurface weathering, unchannelized flow (sheet flow, sheetflooding, rill wash), and channelized flow (gully wash, debris flow, and stream flow). In most cases, the relatively diffuse processes of weathering and unchannelized flow will tend to be more uniformly distributed in space than the more concentrated processes of channelized flow. Where the combined effect of these processes acts uniformly over the entire pediment surface, the surface will be maintained as an active pediment. Where the combined effect is not uniformly applied, however, incision will occur most likely in response to decreases in stream sediment load (Fig. 13.6) and/or increases in stream discharge. Surfaces abandoned by fluvial action as a result of incision form isolated islands of relative stability where the processes of subsurface and surface weathering (particularly salt weathering), soil formation, desert loess accumulation, and stone pavement development are locally dominant.

Under conditions of tectonic and base level stability, the piedmont surface is divisible into three general process zones: an upper zone of erosion, an intermediate zone of transportation, and a lower zone of aggradation (Johnson 1932a,b, Cooke and Warren 1973, p. 197, Dohrenwend *et al.* 1986). These zones shift upslope and downslope across the piedmont in response to changes in the overall upland/piedmont drainage system, and the boundaries between zones are both gradational and complex. Their precise position at any given time is determined by the relative rates of debris supply and removal across the piedmont plain. If the rate of debris supply to the piedmont increases or the rate of removal decreases, these zones tend to migrate upslope; conversely, if the rate of supply decreases or the rate of removal increases, they tend to migrate downslope (Cooke and Mason 1973). On most piedmonts in arid and semi-arid environments, the rates of debris supply and removal are largely determined by channelized flow processes; thus the relative extent and position of each general process zone reflects the average location, over time, of the threshold of critical power for each component of the piedmont drainage system. On average, stream power exceeds critical power in the zone of erosion, approximately equals critical power in the zone of transportation, and falls short of critical power in the zone of aggradation (Bull 1979). This general scenario is supported by (a) regional patterns of proximal piedmont dissection in the Mojave and Sonoran Deserts; (b) long-term trends of piedmont and pediment erosion documented by spatial relations between volcanic landforms and active piedmont surfaces (Dohrenwend *et al.* 1985, 1986, Dohrenwend 1990a, 1990c); and (c) morpho-stratigraphic relations in the Apple Valley area of the western Mojave Desert (Cooke and Mason 1973).

In the zone of erosion, channelized flow processes typically dominate and commonly result in shallow to moderate dissection of the proximal piedmont. However, surface regrading may also proceed without significant incision via the operation of unchannelized flow and lateral shifting of channelized flow. In the zone of transportation, stream power and critical power are essentially balanced over the long term such that net surface erosion is nearly undetectable. Surface processes in this zone are probably dominated by lateral shifting of channelized flow in shallow anastomosing gullies and washes (Rahn 1967, Cooke and Mason 1973, Dohrenwend *et al.* 1986).

SUBSURFACE WEATHERING

Subsurface weathering processes have strongly influenced pediment development in many regions, particularly in humid tropical, tropical wet–dry, and semi-arid environments (Ruxton 1958, Mabbutt 1966, Thomas 1974, p. 218–26, Oberlander 1989). Such processes are critical to the formation or modification of many pediments, particularly those developed on crystalline bedrock (Oberlander 1974, 1989, Moss 1977). Clearly, weathered and disaggregated bedrock can be much more readily loosened, entrained, and eroded by wash and stream action than unweathered bedrock. Indeed, the apparent predilection of pediments for areas underlain by granitic rocks is due, in large measure, to the susceptibility of these rocks to subsurface weathering and to the particular mechanical characteristics of the residual grus. This well-sorted, sand-sized, non-cohesive material forms non-resistant channel banks that are highly susceptible to erosion by laterally shifting channelized flow. Hence, granitic pediments possess a highly effective mechanism of self-regulation which tends to suppress fluvial incision. Wherever the threshold of critical power is exceeded by stream flow, erosion of the channel banks rapidly increases sediment load and raises the critical power threshold to the level of available stream power. The profound contrast in surface morphology between granitic and metamorphic piedmonts in the Mojave Desert serves as a graphic illustration of this phenomenon. Granitic piedmonts are, in most cases, essentially undissected and relatively featureless plains of active transport, whereas metamorphic piedmonts are more commonly dissected into intricately nested surfaces of diverse age.

Controlled largely by the availability of moisture, the rates and distribution of subsurface weathering processes are closely related to local geomorphic setting and to shallow subsurface form and structure. Conditions favouring moisture accumulation and retention will typically intensify weathering processes. On arid and semi-arid piedmonts, moisture accumulation and retention commonly occurs (a) beneath footslopes within the piedmont junction, (b) along the alluvium–colluvium and bedrock interface, (c) along buried bedrock channels, and (d) in areas of intersecting bedrock fractures. Hence, the surface described by the subsurface weathering front is typically highly irregular, and stripping of the residual regolith in areas of proximal dissection commonly reveals complex and intricate etching of the bedrock surface.

PIEDMONT MODIFICATION BY SUBSURFACE WEATHERING AND REGRADING

Subsurface weathering and the subsequent erosional modification of piedmonts or other surfaces of low relief has played a central role in the expansion and/or regrading of many pediments (Mabbutt 1966, Oberlander 1972, 1974, 1989, Moss 1977, Dohrenwend *et al.* 1986). In the Flinders Ranges of South Australia, for example, 'the abrupt change in slope in the piedmont zone (junction) is caused principally . . . by differential weathering at the foot of the scarp. . . . The bedrock 1.5 km from the scarp is weathered only to a moderate degree . . .. Close under the scarp, however, similar strata are much more intensely altered. Kaolin is abundant, bedding only vaguely discernable, and the rock has lost much of its strength . . .. Runoff from the often bare hillslopes percolates into the rock strata where it reaches the plain, causing [this] intense weathering' (Twidale 1967, p. 113). Also in central Australia, '. . . grading on . . . granitic and schist pediments has largely acted through the mantles, whereby the smoothness of the depositional profiles has been transmitted to suballuvial and part-subaerial pediments. . . . On granitic pediments . . . suballuvial notching and levelling proceed through weathering in the moist subsurface of the mantle. On schist pediments control of levelling by the mantle is less direct in that its upper surface is the plane of activity of ground-level sapping and of erosion by rainwash and sheetflow. . . . [These processes] are most active near the hill foot, where mantling and stripping alternate more frequently; the lower parts of both schist and granitic pediments . . . appear to be largely and more permanently suballuvial . . .' (Mabbutt 1966, pp. 90–1). Although subsurface weathering processes have strongly influenced pediment development in many areas and profoundly modified pediment surfaces in many others, it would appear unlikely that these processes actually 'control' pediment development, at least in arid and semi-arid environments. The preservation of tens of metres of intensely weathered bedrock beneath active granitic pediments demonstrates that these landforms are transport-limited (not weathering- or detachment-limited). The present form of the active surface is the product of fluvial erosion and transport; it is not closely related to either the position or the form of the subsurface weathering front. Moreover, even though stripping of the proximal areas of many pediments has exposed the intricately etched (weathering-limited) surfaces of formerly

buried weathering fronts, deeply weathered regolith remains beneath adjacent mantled surfaces of fluvial transport. Thus even this pediment regrading is primarily controlled by fluvial processes; only the detailed form of the proximal pediment has been significantly influenced by the position of the weathering front.

MODELS OF PEDIMENT FORMATION

Within the general context of the pediment association (i.e. degrading upland, aggrading alluvial plain, and intervening zone of transition and transport), pediment development can be usefully perceived as the necessary result of upland degradation (Lustig 1969, p. D67). As the pediment association evolves and mass is transferred from the upland to the alluvial plain, the diminishing upland is replaced by an expanding surface of transportation, the pediment. Hence, most models of pediment development implicitly link upland degradation and pediment development; and the major differences between these models centre primarily on the issues of mountain front (or piedmont junction) retreat and upland degradation. Accordingly, the various models that have been presented in the literature can be grouped according to the dominant style of upland degradation proposed. These styles are

(a) range front retreat where channelized fluvial processes (mainly lateral planation) predominate (Gilbert 1877, p. 127–9, Paige 1912, Blackwelder 1931, Johnson 1931, 1932a,b, Field 1935, Howard 1942);
(b) range front retreat where diffuse hillslope and piedmont processes predominate (Lawson 1915, Rich 1935, Kesel 1977);
(c) range front retreat assisted by valley development where the relative dominance of diffuse hillslope and piedmont processes versus channelized flow varies according to general geomorphic environment (Bryan 1922, 1936, Gilluly 1937, Sharp 1940);
(d) range degradation dominated by drainage basin development (valley deepening and widening, embayment formation and enlargement) (Lustig 1969, p. D67, Wallace 1978, Bull 1979, 1984, Parsons and Abrahams 1984).

This trend in dominant styles of upland degradation clearly shows a progressive maturation of Gilbert's original (1877) model. Thus, as Parsons and Abrahams (1984) point out, these models are not mutually exclusive; indeed, they are more complementary than contradictory.

RANGE FRONT RETREAT BY LATERAL PLANATION

Models of lateral planation emphasize the importance of channelized fluvial processes. Erosion of the mountain mass and retreat of the mountain front is considered to be effected primarily by the lateral shifting of debris-laden streams issuing from within the mountains. The diffuse action of weathering, slopewash, and rill wash on hillslopes is acknowledged but is not considered essential to pediment formation. The resulting pediment surface is continually regraded by the lateral shifting of these streams across the piedmont.

> 'Whenever the load [of a stream] reduces the downward corrasion to little or nothing, lateral corrasion becomes relatively and actually of importance. . . . The process of carving away the rock so as to produce an even surface, and at the same time covering it with an alluvial deposit, is the process of planation. . . . The streams . . . accomplish their work by a continual shifting of their channels; and where the plains are best developed they employ another method of shifting . . .. The supply of detritus derived from erosion . . . is not entirely constant. . . . It results from this irregularity that the channels are sometimes choked by debris and . . . turned aside to seek new courses upon the general plain. . . . Where a series of streams emerge from the adjacent mountain gorges upon a common plain, their shiftings bring about frequent unions and separations, and produce a variety of combinations' (Gilbert 1877, pp. 127–9).

> '. . . the essence of the theory lies in the broader conception that rock planes of arid regions are the product of stream erosion rather than in any particular belief as to the relative proportions of lateral and vertical corrasion. . . . Every stream is, in all its parts, engaged in the three processes of (a) vertical downcutting or degrading, (b) upbuilding or aggrading, and (c) lateral cutting or planation. . . . The gathering ground of streams in the mountains, where greater precipitation occurs, will normally be the region where vertical cutting is at its maximum. . . . Far out from the mountain mass conditions are reversed. Each stream must distribute its water and its load over an ever-widening sector of country. The water disappears, whether by evaporation or by sinking into the accumulating alluvium. Aggradation is at its maximum . . .. Between . . .[these regions]. . . there must be a belt or zone where the streams are essentially at grade. . . . Thus from the center

outward are (1) the zone of degradation, (2) the zone of lateral corrasion, and (3) the zone of aggradation. Heavily laden streams issuing from the mountainous zone of degradation are from time to time deflected against the mountain front. This action combined with the removal of peripheral portions of the interstream divides by lateral corrasion just within the valley mouths, insures a gradual recession of the face or faces of the range. Such recession will be aided by weathering as well as by rain and rill wash; but it must occur even where these processes are of negligible importance' (Johnson 1932a, pp. 657–8).

'. . .lateral planation may be carried on by streams of all sizes, by distributaries as well as by tributaries, by individual channels of a braided stream, and by sheetfloods' (Howard 1942, p. 107).

RANGE FRONT RETREAT BY DIFFUSE HILLSLOPE AND PIEDMONT PROCESSES

A second group of models identifies diffuse hillslope processes (mainly weathering, slopewash, and rill wash) coupled with removal of the resultant debris from the piedmont junction by sheetwash and rill wash as the dominant mechanism of mountain front retreat and pediment extension. Lateral planation by mountain streams is acknowledged as locally significant but is not considered to be an essential process. Sheetflooding is considered to be the dominant process of pediment surface regrading.

'If we examine a typical region in an old age stage of the arid cycle, where scattered residuals of former mountain masses stand on broad rock pediments . . .. Obviously the mountains are wasting away by weathering, and just as obviously the weathered products must be carried away over a gradient steep enough to permit them to be moved. The rock, though weathered, cannot be removed below the line of this gradient. Consequently as the mountains waste away, a sloping rock plain, representing the lower limit of wasting, must encroach upon them from all sides. . . . The gradient of this rock plain must be that necessary for the removal of the waste material – no more and no less – therefore, the rock will be covered by only a thin and discontinuous veneer of waste in transit' (Rich 1935, p. 1020).

'The prevailing conditions of stream load force the desert streams to *corrade laterally*, as Johnson has pointed out, and in many places such corrasion contributes actively to the formation of pediments, especially along the sides of canyons debouching from the desert mountains. Nevertheless, lateral corrasion need be only a contributing, and not an essential factor in the formation of pediments, and a very minor factor in the retreat of mountain fronts' (Rich 1935, p. 1021).

RANGE FRONT RETREAT ASSISTED BY VALLEY DEVELOPMENT

A third group of models builds on the complementary nature of the previous models and accommodates their differences in emphasis by recognizing that the relative importance of weathering, unchannelized flow, or channelized flow processes varies according to specific geomorphic setting.

'The conclusions reached as to the formation of pediments under the various geological, topographic, and climatic conditions of the Ruby–East Humboldt region are as follows:
(1) Pediments are formed by lateral planation, weathering, rill wash, and rain wash. The relative efficacy of these various processes is different under geologic, topographic, and climatic conditions.
(2) Lateral planation is most effective along large permanent streams and in areas of soft rocks.
(3) Weathering, rill wash, and rain wash are most effective in areas of ephemeral streams, hard rocks, and a low mountain mass.
(4) All variations from pediments cut entirely by lateral planation to those formed entirely by the other processes are theoretically possible, although in this area the end members of the series were not observed and perhaps do not actually exist in nature' (Sharp 1940, p. 368).

RANGE DEGRADATION BY DRAINAGE BASIN DEVELOPMENT

The first three groups of models focus on the evolutionary retreat of the mountain front. In contrast, the models of this group address the broader issue of the overall degradation of the mountain mass. Their emphasis is on the evolutionary development of upland valleys through non-uniform erosion of the mountain mass by the concentrated action of channelized streamflow. It is significant to note that these models do not require parallel retreat of the mountain front as the primary mode of pediment expansion. These more comprehensive models emphasize the dominant role of fluvial erosion in the degradational evolution of the entire

pediment association, and they illustrate the increasing sophistication of geomorphic theory as applied to the analysis of landscape evolution.

'The many discussions of pediment surfaces have focused on the wrong landform . . .. There is no question that the processes of subaerial and suballuvial weathering occur on pediment today, nor that fluvial erosion also occurs. A pediment must exist prior to the onset of these processes, however, and in this sense the origin of the pediments resides in the adjacent mountain mass and its reduction through time. . . . Given stability for a sufficient period of time, the consequences of mountain reduction must inevitably include the production of a pediment, whether in arid or nonarid regions. The nature of the surface produced may vary, and it may be mantled by, or free of, alluvium. However, it simply represents an area that was formerly occupied by a mountain. . .. The only real "pediment problem" is how the reduction or elimination of the mountain mass occurs' (Lustig 1969, p. D67).

'. . . it is obvious that the pediment grows most rapidly along the major streams. In every indentation in the mountain front and in places where streams emerge from the canyons onto the plains the rate of formation of the pediment is rapid, and consequently extensions of the pediment into the mountains are common. . . . The erosion of the mountains at the headwaters of many streams is much faster than in the lower portions of the same streams . . .. Consequently the headwater slopes may recede more rapidly than the side walls of the valleys' (Bryan 1992, pp. 57–8).

'The rates of mountain front retreat are basically unknown, but by any reasonable assessment they are slow in relation to rates of processes that are operative in drainage basins. This is clearly true because the headwater region of any given drainage basin also consists of steep walls that are virtually identical to those of the mountain front in interfluvial areas. In these headwater regions the same processes of weathering and removal of debris occur. Hence, the rates of retreat of the bounding walls in the headwaters of drainage basins must be at least as great as the rate of retreat of the mountain front in interfluvial areas. Also, however, the drainage basins represent the only parts of any mountain range that are subjected to concentration of flow and to its erosional effects, and these basins must therefore be the principal loci of mountain mass reduction' (Lustig 1969, p. D67).

'During the valley downcutting that occurs after mountain-front uplift, the width of the valley floor will approximate stream width at high discharges. Valley-floor width decreases upstream from the front because of the decrease in the size of the contributing watershed. . .. With the passage of geologic time, the stream will widen its valley as it approaches the threshold of critical power. As lateral cutting becomes progressively more important, the stream will not spread over the entire valley floor during high discharges. The approximation of a threshold condition migrates gradually upstream as the upstream reaches downcut. . . . The configurations of the . . . pediment embayments . . . are functions of the rates of lateral cutting and/or hillslope retreat along the stream and the time elapsed since lateral erosion became predominant at various points along the valley. More than a million years may be needed to form pediment embayments' (Bull 1979, pp. 459–60).

'. . . it seems likely that, where a significant proportion of the piedmont junction occurs within embayments, the actual rate of piedmont formation will be much greater than that achieved by mountain front retreat alone. In embayments the rate of piedmont formation will depend upon the length of the embayments as well as upon the rate of piedmont junction migration' (Parsons and Abrahams 1984, p. 258).

GENERAL MODEL OF PEDIMENT FORMATION

FUNDAMENTAL CONCEPTS

A number of fundamental geomorphological concepts provide insights useful for developing a comprehensive understanding of pediments and their formation.

(a) Analysis of a geomorphic system is in large part determined by the temporal and spatial limits that are used to define the system (Schumm and Lichty 1965). For example, the concept of dynamic equilibrium provides useful insights concerning the tendency for adjustment of slope declivity to lithology and/or structure within an upland area: however, the concept is less useful when applied to the problem of upland degradation over 'cyclic time' (unless mass continues to be added to the system through uplift). Depending on the time and space perspective of the analysis, processes may appear to be steady or fluctuating, continuous or discontinuous, and

forms may appear to be stable, unstable, or quasi-stable. When considering the evolution of a landscape or the interrelations among its components, it is essential to define the system within those scales of space and time that are appropriate to the problem at hand. Regarding the specific problem of pediment formation, the appropriate spatial scale is very likely the pediment association (Cooke 1970) and the appropriate temporal scale is cyclic time (Schumm and Lichty 1965). Viewed from this perspective, emphasis is placed on interdependent changes between landscape components and processes in a changing open system (Bull 1975).

(b) Most geomorphic systems are multivariate and operate both non-linearly and discontinuously; therefore, these systems may respond complexly to mass and energy inputs (whether these inputs are non-linear or linear, continuous or discontinuous). 'When the influence of external variables such as isostatic uplift is combined with the effects of complex response and geomorphic thresholds, it is clear that denudation, at least during the early stage of the geomorphic cycle, cannot be a progressive process. Rather, it should be comprised of episodes of erosion separated by periods of relative stability, a complicated sequence of events' (Schumm 1975, p. 76).

(c) Process transitions and thresholds further complicate the operation of most geomorphic systems; and the behaviour of such systems may be particularly complex at or near these transitions. In the specific case of pediments, the locus of pediment formation is generally considered to be the piedmont junction, a zone of abrupt transition for both morphology and process. Moreover, the pediment itself serves as the transition between range and alluvial plain, and over the long term, pediment drainage operates at or very close to the threshold of critical power in streams. 'In the western Mojave Desert, evidence for the movement of the upper limits of alluvium across piedmont plains is provided by such features as channels buried beneath alluvium downslope of the limits, and upslope of the limits by the truncation of soil and weathering profiles and the presence of alluvial outliers. Movement of the boundary need not be accompanied by dissection of the plain, but this is frequently the case' (Cooke 1970, p. 37). Like many boundary zones in non-linear systems, this continuously shifting transition is both complex and chaotic. Hence, the timing and duration of periods of erosion, transport, or aggradation at any point in the system may very well be indeterminant, particularly where fluvial components of the system are operating at or are approaching the threshold of critical power.

(d) Form and process are closely interrelated within the pediment association. At any point in time, form is an initial constraint on process. As the distribution of form changes through time in response to process, the distribution of process changes accordingly. For example, '. . .the relative importance of divide removal [between embayments] and mountain front retreat. . . is strongly dependent on the size and relief of the associated mountain mass, and hence . . . it is likely to change in a systematic way as the mountain mass diminishes in size through time. Specifically . . . as a mountain mass diminished in size there is a tendency for . . . divide removal to become progressively less important relative to mountain front retreat' (Parsons and Abrahams 1984, p. 265). Similarly, the relative importance of lateral planation very likely also diminishes with time. 'In an arid or desert region, flow over a long time and detrital load are most likely to exist where an ephemeral stream emerges from a canyon having a considerable length and a fairly large drainage basin within a mountain area. Such conditions prevail in the cycle of the erosion from youth to postmaturity. In old age, however, the detrital load is small, the dissection of the original mountain mass is far advanced, and the streams are easily diverted out of their channels. All of these factors tend to minimize lateral planation' (Bryan 1936, p. 775). Thus within the pediment association, different processes operate at different rates and times in different parts of the system and the distribution of these processes changes in space through time.

(e) As an open geomorphic system, the pediment association is 'a complex multivariate phenomenon which responds at different rates to different external variables such that it need not be in equilibrium with all variables at once' (Palmquist 1975, p. 155). Thus, the various components of the pediment association are not necessarily adjusted to one another or to the system as a whole. Rather, as interdependent components of an evolving open system, the progressively degrading uplands and aggrading alluvial plains of the pediment association are examples of landforms that are not necessarily attracted toward a steady state. 'For many land-

forms, height, volume, or other dimensions change progressively with time instead of tending toward a time-independent size or configuration' (Bull 1975, p. 112).

(f) Pediments may be formed by many different combinations of processes operating within and constrained by a variety of tectonic, climatic, and lithologic/structural environments. Moreover, as slowly developing long-lived landforms, pediments may be subjected to substantial changes in these environmental factors as they develop. Thus many pediments may be, in part at least, forms inherited from former conditions. This possibility severely limits the profitable application of morphometric analysis to the question of pediment development. Unless a high degree of similarity of initial size and shape and of subsequent morphogenetic history can be demonstrated, morphological differences between pediments or their associated uplands cannot be used to develop general inferences about range degradation or pediment formation.

FACTORS AFFECTING PEDIMENT FORMATION AND EXPANSION

A model of pediment development which applies equally well to all possible geomorphic situations is likely to be either oversimplified with respect to any specific situation or unmanageably complex if all possible situations are analysed in detail; consequently, the following summary focuses on piedmont pediments in arid and semi-arid environments.

(a) As piedmont surfaces, pediments serve as zones of transition (and transport) between uplands and alluvial plains. In arid and semi-arid regions, the redistribution of mass between the degrading upland (where stream power generally exceeds critical power) and the aggrading alluvial plain (where stream power is generally less than critical power) proceeds mainly by physical processes. Erosion within the upland is driven primarily by the action of concentrated water flow, development of integrated drainage networks from rills to rivers and the concomitant formation and expansion of valleys and embayments (Lustig 1969, p. D67, Wallace 1978, Bull 1979). The more diffuse and uniformly distributed processes of hillslope weathering and erosion operate within this general geomorphic framework of fluvially carved valleys and embayments. Moreover, the great bulk of material removed from the mountain mass is transported via streamflow, and debris transport across the pediment surface as well as deposition on the alluvial plain are likewise dominated by fluvial action.

(b) Long-term geomorphic stability appears to be a fundamental requirement for the formation and maintenance of extensive bedrock pediments. Within the south-western United States, pediments are larger and more abundant in areas of low vertical tectonic activity where base level is either stable or slowly rising. Such conditions facilitate the approximate long-term balance between erosional and depositional processes on piedmonts that is essential for pediment development. 'The pediment, instead of being abnormal and restricted to certain localities, is widespread throughout . . . [the desert regions of western North America] and is the type of plain normally developed during quiescent periods. Alluvial fans on the other hand, probably cannot be made under static conditions. They are built where normal gradients have been changed by faulting, warping, lateral erosion, or other special causes' (Blackwelder 1929, p. 168).

(c) Pediment formation is unidirectional through time. 'When tectonic stability exists, a geomorphic system is partially closed to materials . . .. Thus the [general] behavior of the system during denudation becomes predictable; a continued decrease in relief must occur. Therefore, a dynamic equilibrium within a drainage basin or a hillslope as a whole cannot exist for material flux except when the rate of uplift equals the rate of denudation . . .. The imbalance in material flux means that changes in the size, elevation or form of the system must occur' (Palmquist 1975, pp. 155–6). Although individual components of the pediment association (e.g. hillslopes, valley bottoms, stream channels, piedmont junctions, etc.) may be generally adjusted to lithology and process over the short term; each component and its relations to the other components change systematically and asymmetrically over the long term. As a fluvially dominated open system, the pediment association is attracted towards a stationary state; it is 'indeed directed through time' (Montgomery 1989, p. 51).

(d) Pediment formation (expansion, maintenance, and modification) varies in time and space, both non-linearly and discontinuously. At any point in time, processes of pediment formation vary in space (Sharp 1940). For example, as a pediment develops and expands along a mountain front, it

is also maintained as a surface of transportation in more distal areas. Expansion involves fluvial processes (in channels, valleys, and embayments) and hillslope processes (on valley and embayment sideslopes and on mountain front interfluves). Maintenance involves weathering, sheet flow, and streamflow processes on the piedmont. Moreover, the relative significance of these processes also changes over time (Bryan 1936). Initially when the mountains are large and the piedmonts narrow, upland degradation predominates; eventually as the mountains become smaller and the piedmonts broader, pediment maintenance and regrading dominate. The rates at which these processes operate also vary (both in time and space). Degradation in response to uplift is initially rapid and gradually slows (Morisawa 1975). Other factors being equal, larger streams generally erode more rapidly and, therefore, occupy larger deeper valleys with lower gradients than do smaller streams (Bull 1979). Consequently, the effects of fluvial action are seldom distributed uniformly along the mountain front. The mountain front is distinctly non-linear in plan (Lawson 1915) and, in most instances, does not retreat parallel to itself (Parsons and Abrahams 1984).

(e) The retreat of mountain front spurs appears to be less important with regard to the evolution of mountain fronts (and pediment development) than fluvial downwearing and embayment development (Lustig 1969, p. D67, Bull 1984). In the absence of significant fluvial erosion, tectonically inactive mountain fronts may remain relatively unchanged over periods of as much as several million years (Dohrenwend *et al.* 1985, Mayer 1986, Harrington and Whitney 1991). Strongly asymmetric ranges clearly illustrate the dominance of fluvial erosion on mountain front degradation. The small subparallel drainages along the scarp flank erode relatively slowly inducing little change; whereas the large integrated drainages of the backtilted flank erode rapidly inducing drainage basin development, valley widening, embayment enlargement, valley sideslope convergence and spur decline. The presence of deeply dissected, partly stripped remnants of older, higher, and more steeply sloping relic surfaces along many mountain fronts also argues against general mountain front retreat as a primary mode of mountain mass reduction.

(f) Medial piedmonts are very stable and often persist with little dissection or regrading over periods of several million years (Dohrenwend *et al.* 1985, 1986). Although the threshold of critical power in streams may be crossed abruptly, a generally long-term balance between stream power and critical power appears to be maintained across a considerable breath of many piedmont surfaces. Where a drainage system is able to adjust channel form and roughness in response to limited variations in discharge and sediment load, it may accommodate such changes while at the same time continuing to operate at the critical power threshold. Also where the piedmont is broad, changes in discharge or load can be accommodated, at least in part, by upslope or downslope migration of the erosion–transport and transport–deposition limits of the critical power threshold (Cooke and Mason 1970). The stability of the medial piedmont implies that it is the local base level for mountain degradation, proximal piedmont dissection, and pediment formation.

(g) The critical requirement for pediment formation (and maintenance) is that all piedmont drainage must operate, on average, at or very close to the threshold of critical power across a broad zone of transition between upland and lowland. Within this zone, episodes of dissection and aggradation must be limited in both time and space. Because pediment formation is a slow process that is largely concentrated along the junction between upland and piedmont, pediment formation and maintenance must proceed simultaneously in different parts of the system. Upland slopes may retreat and/or decline by a variety of processes, but conditions must be maintained such that an expanding pediment replaces the shrinking mountain mass. Embayment formation and expansion, inselberg development, pediment formation and maintenance all result from the erosional–depositional balance of the medial piedmont.

(h) Although long-term change is relatively uniformly distributed across the pediment; short-term changes may be non-uniformly and 'chaotically' distributed. The precise character of these short-term changes is determined in part by the system's ability to 'self regulate' responses to short-term variations in discharge or sediment load. This self regulation is significantly influenced by the availability of readily erodible and transportable materials. If such materials are abundant and uniformly distributed across the piedmont, the tendency for lateral erosion usually exceeds the tendency for vertical incision and

the system will regrade uniformly in space without significant dissection. However, if these materials are not abundant and/or are not uniformly distributed, the tendency for vertical incision may equal or exceed the tendency for lateral erosion and the system will very likely regrade locally and discontinuously.

(i) Proximal dissection is a common characteristic of both pediments and alluviated piedmonts. This regrading occurs in response to a sustained increase in stream power (duration and/or intensity of flow) or a sustained decrease in critical power (amount and/or calibre of available load). Possible causes include short-term climate changes (Bryan 1922), long-term undirectional climate change, tectonic tilting of the piedmont, complex response of the upland–proximal-piedmont drainage system (Rich 1935, Denny 1967), and isostatic adjustment of the piedmont association (Howard 1942, Cooke and Mason 1973). Over the long term, however, the most likely cause would appear to be the redistribution of mass within the pediment association. Regrading is constrained by the stability of the medial piedmont; if the medial piedmont is undissected and morphologically stable then proximal dissection must be the result of change within the adjacent upland. As uplands diminish in size, both stream discharge and sediment load decrease but the effect of the decrease in load appears to predominate.

It is a general misconception that most alluviated piedmonts are primarly if not entirely depositional landforms. In fact after initial formation, even bajadas may be as much zones of regrading and transport as they are loci of deposition. Proximal dissection is common on both pediments and bajadas, and the tendency for dissection by piedmont drainage underscores the delicate erosional–depositional balance of many proximal and medial piedmont areas. Field measurement of badlands dissection (Schumm 1956, 1962) and comparison of the relative positions of adjacent modern and relict piedmont surfaces capped by late Tertiary lava flows (Dohrenwend *et al.* 1985, 1986) also document the erosional predilection of proximal piedmont areas.

(j) Subsurface weathering undoubtedly facilitates pediment formation via conversion of resistant bedrock into non-resistant regolith that can be disaggregated into readily loosened and easily transported detritus. However, it would appear unlikely that the operation of sursurface weathering processes actually controls pediment development in those situations where the overall mode of landscape evolution proceeds via upland retreat and replacement by expanding piedmonts (e.g. Bryan 1922, Johnson 1932b, Lustig 1969, p. D67, Parsons and Abrahams 1984). As the preservation of tens of metres of intensely weathered bedrock beneath granitic pediments in the south-western United States clearly demonstrates, many pediment surfaces are not closely related to either the position or the form of the subsurface weathering front. Rather, the existence of an alluviated piedmont, pediment, or similar surface of low relief would seem to be a required precondition for development of a quasi-planar weathering front and for subsequent planation of its deeply weathered regolith mantle. Hence, exhumation of the weathering front, mantle-controlled planation, and other similar processes are probably most effective where the overall mode of landscape change is one of stepwise weathering and stripping in a region of low relief (e.g. Mabbutt 1966).

REFERENCES

Blackwelder, E. 1929. Origin of the piedmont plains of the Great Basin, *Bulletin of the Geological Society of America* **40**, 168–9.

Blackwelder, E. 1931. Desert plains. *Journal of Geology* **39**, 133–40.

Bryan, K. 1922. Erosion and sedimentation in the Papago country, Arizona. *US Geological Survey Bulletin* 730, 19–90.

Bryan, K. 1936. The formation of pediments. *16th International Geological Congress Report*, Washington, DC (1933), 765–75.

Bryan, K. and F.T. McCann 1936. Successive pediments and terraces of the upper Rio Puerco in New Mexico. *Journal of Geology* **44**, 145–72.

Bull, W.B. 1975. Landforms that do not tend toward a steady state. In *Theories of landform development*, W.N. Melhorn and R.C. Flemal (eds), 111–28. Binghamton, NY: Publications in Geomorphology.

Bull, W.B. 1977. The alluvial fan environment. *Progress in Physical Geography* **1**, 222–70.

Bull, W.B. 1979. Threshold of critical power in streams. *Bulletin of the Geological Society of America Part I* **90**, 453–64.

Bull, W.B. 1984. Tectonic geomorphology. *Journal of Geological Education* **32**, 310–24.

Bull, W.B. and L.D. McFadden 1977. Tectonic geomorphology north and south of the Garlock fault, California. In *Geomorphology in arid regions*, D.C. Doehring (ed.), 115–37. Binghamton, NY: Publications in Geomorphology.

Carr, W.J. 1984. Regional structural setting of Yucca Mountain, southwestern Nevada, and late Cenozoic rates of tectonic activity in part of the southwestern Great Basin, Nevada and California. *US Geological Survey*

Open-File Report, OFR-84-854.
Chorley, R.J., S.A. Schumm and D.E. Sugden 1984. *Geomorphology*. London: Methuen.
Cooke, R.U. 1970. Morphometric analysis of pediments and associated landforms in the western Mojave Desert, California. *American Journal of Science* **269**, 26–38.
Cooke, R.U. and P. Mason 1973. Desert Knolls pediment and associated landforms in the Mojave Desert, California. *Revue de Geomorphologie Dynamique* **20**, 71–8.
Cooke, R.U. and R.W. Reeves 1972. Relations between debris size and the slope of mountain fronts and pediments in the Mojave Desert, California. *Zeitschrift für Geomorphologie* **16**, 76–82.
Cooke, R.U. and A. Warren 1973. *Geomorphology in deserts*. Berkeley, CA: University of California Press.
Davis, W.M. 1933. Granitic domes in the Mohave Desert, California. *San Diego Society of Natural History Transactions* **7**, 211–58.
Denny, C.S. 1967. Fans and pediments. *American Journal of Science* **265**, 81–105.
Dinsmoor, W.B. 1975. *The architecture of Ancient Greece, an account of its historic development*. New York: Norton.
Dohrenwend, J.C. 1982a. Surficial geology, Walker Lake 1° by 2° quadrangle, Nevada–California. *US Geological Survey Miscellaneous Field Studies Map*, MF-1382-C, scale 1:250,000.
Dohrenwend, J.C. 1982b. Late Cenozoic faults, Walker Lake 1° by 2° quadrangle, Nevada–California. *US Geological Survey Miscellaneous Field Studies Map*, MF-1382-D, scale 1:250,000.
Dohrenwend, J.C. 1982c. Tectonic control of pediment distribution in western Great Basin. *Geological Society of America Abstracts with Programs* **14**, 161.
Dohrenwend, J.C. 1987a. The Basin and Range. In *Geomorphic systems of North America*, W. Graf (ed.) 303–42. Boulder, CO.: Geological Society of America, The Geology of North America, Centennial Special Volume 2.
Dohrenwend, J.C. 1987b. Morphometric comparison of tectonically defined areas within the west-central Basin and Range. *US Geological Survey Open-File Report* 87–83.
Dohrenwend, J.C. 1990a. Buffalo Valley volcanic field, Nevada. In *Volcanoes of North America*, C.A. Wood and J. Kienle (eds), 256–7. Cambridge: Cambridge University Press.
Dohrenwend, J.C. 1990b. Cima, California. In *Volcanoes of North America*, C.A. Wood and J. Kienle (eds), 240–1. Cambridge: Cambridge University Press.
Dohrenwend, J.C. 1990c. Clayton Valley, Nevada. In *Volcanoes of North America*, C.A. Wood and J. Kienle (eds), 261. Cambridge: Cambridge University Press.
Dohrenwend, J.C. 1990d Lunar Crater, Nevada. In *Volcanoes of North America*, C.A. Wood and J. Kienle (eds), 258–9. Cambridge: Cambridge University Press.
Dohrenwend, J.C. 1990e. Reveille Range, Nevada. In *Volcanoes of North America*, C.A. Wood and J. Kienle (eds), 260–1. Cambridge: Cambridge University Press.
Dohrenwend, J.C., B.D. Turrin and M.F. Diggles 1985. Topographic distribution of dated basaltic lava flows in the Reveille Range, Nye County, Nevada: implications for late Cenozoic erosion of upland areas in the Great Basin. *Geological Society of America Abstracts with Programs* **17**, 351.
Dohrenwend, J.C., S.G. Wells, L.D. McFadden and B.D. Turrin 1986. Pediment dome evolution in the eastern Mojave Desert, California. In *International geomorphology*, V. Gardiner (ed.), 1047–62. Chichester: Wiley.
Dohrenwend, J.C., W.B. Bull, L.D. McFadden, G.I. Smith *et al.* 1991. Quaternary Geology of the Basin and Range province in California. In *Quaternary nonglacial geology: conterminous United States*, Morrison, R.B. (ed.), 321–52. Boulder, CO.: Geological Society of America, The Geology of North America, K-2.
Dohrenwend, J.C., R.C. Jachens and B.C. Moring 1994a. Map showing indicators of subsurface basin geometry in Nevada. *US Geological Survey Miscellaneous Investigations Map*, scale 1:1,000,000, in press.
Dohrenwend, J.C., G. Yanez and G. Lowry 1994b. Cenozoic landscape evolution of La Gran Sabana Sur, southeast Venezuela: implications for the occurrence of gold and diamond placers. *US Geological Survey Bulletin*, in press.
Dohrenwend, J.C., B.A. Schell, C.M. Menges, B.C. Moring, *et al.* 1994c. Reconnaissance photogeologic map of young (Quarternary and late Tertiary) faults in Nevada. *US Geological Survey Miscellaneous Investigations Map*, scale 1:1,000,000, in press.
Dresch, J. 1957. Pediments et glacis d'erosion, pediplains et inselbergs. *Information Géographique*, **21**, 183–96.
Ekren, E.B., C.L. Rogers and G.L. Dixon 1973. Geologic and Bouguer gravity map of the Reveille Quadrangle, Nye County, Nevada. *US Geological Survey Miscellaneous Geologic Investigations Map* I-806, scale 1:48,000.
Field, R. 1935. Stream carved slopes and plains in desert mountains. *American Journal of Science* **29**, 313–22.
Gilbert, C.M. and M.W. Reynolds 1973. Character and chronology of basin development, western margin of the Basin and Range province. *Bulletin of the Geological Society of America* **84**, 2489–510.
Gilbert, G.K. 1877. *Report on the geology of the Henry Mountains*. US Geographical and Geological Survey of the Rocky Mountain Region. Washington, DC: U.S. Department of the Interior.
Gillespie, A.R. 1990. Big Pine, California. In *Volcanoes of North America*, C.A. Wood and J. Kienle (eds), 236–7. Cambridge: Cambridge University Press.
Gilluly, J. 1937. Physiography of the Ajo region, Arizona. *Bulletin of the Geological Society of America* **48**, 323–48.
Hadley, R.F. 1967. Pediments and pediment-forming processes. *Journal of Geological Education* **15**, 83–9.
Harrington, C.D. and J.W. Whitney 1991. Quaternary erosion rates on hillslopes in the Yucca Mountain region, Nevada. *Geological Society of America Abstracts with Programs* **23**, A118.
Howard, A.D. 1942. Pediment passes and the pediment problem. *Journal of Geomorphology* **5**, 3–32, 95–136.
Janson, H.W. 1969. *History of art: a survey of the major visual arts from the dawn of history to the present day*. Englewood Cliffs, NJ: Prentice-Hall.
Johnson, D.W. 1931. Planes of lateral corrasion. *Science* **73**, 174–7.
Johnson, D.W. 1932a. Rock planes of arid regions. *Geographical Review* **22**, 656–65.
Johnson, D.W. 1932b. Rock fans of arid regions. *American Journal of Science* **23**, 389–416.

Kesel, R.H. 1977. Some aspects of the geomorphology of inselbergs in central Arizona, USA. *Zeitschrift für Geomorphologie* **21**, 119–46.

Lawson, A.C. 1915. The epigene profiles of the desert. *University of California Department of Geology Bulletin* **9**, 23–48.

Lustig, L.K. 1969. Trend surface analysis of the Basin and Range province, and some geomorphic implications. *US Geological Survey Professional Paper* 500-D.

Mabbutt, J.A. 1966. Mantle-controlled planation of pediments. *American Journal of Science* **264**, 78–91.

Mammerickx, J. 1964. Quantitative observations on pediments in the Mojave and Sonoran deserts (Southwestern United States). *American Journal of Science* **262**, 417–35.

Marchand, D.E. 1971. Rates and modes of denudation, White Mountains, eastern California. *American Journal of Science* **270**, 109–35.

Mayer, L. 1986. Tectonic geomorphology of escarpments and mountain fronts. In *Active tectonics*, R.E. Wallace (ed.), 125–35. Washington, DC: National Academy Press.

Mayer, L., M. Mergner-Keefer and C.M. Wentworth 1981. Probability models and computer simulation of landscape evolution. *US Geological Survey Open-File Report* 81-656.

Melton, M.A. 1965. The geomorphic and paleoclimatic significance of alluvial deposits in southern Arizona. *Journal of Geology* **73**, 1–38.

Menges, C.M. and L.D. McFadden 1981. Evidence for a latest Miocene to Pliocene transition from Basin-Range tectonic to post-tectonic landscape evolution in southeastern Arizona. *Arizona Geological Society Digest* **13**, 151–60.

Montgomery, K. 1989. Concepts of equilibrium and evolution in geomorphology: the model of branch systems. *Progress in Physical Geography* **13**, 47–66.

Morisawa, M. 1975. Tectonics and geomorphic models. In *Theories of landform development*, W.N. Melhorn and R.C. Flemal (eds), 199–216. Binghamton, NY: Publications in Geomorphology.

Moss, J.H. 1977. Formation of pediments: scarp backwearing of surface downwasting? In *Geomorphology in arid regions*, D.O. Doehring (ed.), 51–78. Binghamton, NY: Publications in Geomorphology.

Oberlander, T.M. 1972. Morphogenesis of granitic boulder slopes in the Mojave Desert, California. *Journal of Geology* **80**, 1–20.

Oberlander, T.M. 1974. Landscape inheritance and the pediment problem in the Mojave Desert of southern California. *American Journal of Science* **274**, 849–75.

Oberlander, T.M. 1989. Slope and pediment systems. In *Arid zone geomorphology*, D.S.G. Thomas (ed.), 56–84. London: Belhaven.

Paige, S. 1912. Rock-cut surfaces in the desert regions. *Journal of Geology* **20**, 442–50.

Palmquist, R.C. 1975. The compatibility of structure, lithology and geomorphic models. In *Theories of landform development*, W.N. Melhorn and R.C. Flemal (eds), 145–68. Binghamton, NY: Publications in Geomorphology.

Parsons, A.J. and A.D. Abrahams 1984. Mountain mass denudation and piedmont formation in the Mojave and Sonoran Deserts. *American Journal of Science* **284**, 255–71.

Rahn, P.H. 1967. Sheetfloods, streamfloods, and the formation of pediments. *Annals of the Association of American Geographers* **57**, 593–604.

Rich, J.L. 1935. Origin and evolution of rock fans and pediments. *Bulletin of the Geological Society of America* **46**, 999–1024.

Ruxton, B.P. 1958. Weathering and sub-surface erosion in granites at the piedmont angle, Balos, Sudan. *Geological Magazine* **95**, 353–77.

Saunders, I. and A. Young 1983. Rates of surface processes on slopes, slope retreat and denudation. *Earth Surface Processes and Landforms* **8**, 473–501.

Schumm, S.A. 1956. The role of creep and rainwash on the retreat of badland slopes. *American Journal of Science* **254**, 693–706.

Schumm, S.A. 1962. Erosion on miniature pediments in Badlands National Monument, South Dakota. *Bulletin of the Geological Society of America* **73**, 719–24.

Schumm, S.A. 1975. Episodic erosion: a modification of the geomorphic cycle. In *Theories of landform development*, W.N. Melhorn and R.C. Flemal (eds), 69–86. Binghamton, NY: Publications in Geomorphology.

Schumm, S.A. and R.W. Lichty 1965. Time, space and causality in geomorphology. *American Journal of Science* **263**, 110–9.

Sharp, R.P. 1940. Geomorphology of the Ruby–East Humboldt Range, Nevada. *Bulletin of the Geological Society of America* **51**, 337–72.

Sharp, R.P. 1957. Geomorphology of Cima Dome, Mojave Desert, California. *Bulletin of the Geological Society of America* **68**, 273–90.

Smart, J., K.G. Grimes, H.F. Doutch and J. Pinchin 1980. The Carpentaria and Karumba Basins, north Queensland. *Australian Bureau of Mineral Resources, Geology and Geophysics Bulletin* 202.

Stewart, J.H. and J.E. Carlson 1977. Geologic map of Nevada. *Nevada Bureau of Mines and Geology Map* 57, scale 1:500,000.

Tator, B.A. 1952. Pediment characteristics and terminology (part I). *Annals of the Association of American Geographers* **42**, 295–317.

Tator, B.A. 1953. Pediment characteristics and terminology (part II). *Annals of the Association of American Geographers* **43**, 47–53.

Thomas, M.F. 1974. *Tropical geomorphology*. New York: Wiley.

Tricart, J. 1972. *Landforms of the humid tropics, forests and savannas*. London: Longman.

Tuan, Yi-Fu 1959. Pediments in southeastern Arizona. *University of California Publications in Geography* 13.

Turrin, B.D. and J.C. Dohrenwend 1984. K-Ar ages of basaltic volcanism in the Lunar Crater volcanic field, northern Nye County, Nevada: implications for Quaternary tectonism in the central Great Basin. *Geological Society of America Abstracts with Programs* **16**, 679.

Turrin, B.D., J.C. Dohrenwend, R.E. Drake and G.H. Curtis 1985. Potassium–argon ages from the Cima volcanic field, eastern Mojave Desert, California. *Isochron West* **44**, 9–16.

Turrin, B.D., D. Champion and R.J. Fleck 1991. $^{40}Ar/^{39}Ar$ age of Lathrop Wells volcanic center, Yucca Mountain, Nevada. *Science* **253**, 654–7.

Twidale, C.R. 1967. Hillslopes and pediments in the

Flinders Ranges, South Australia. In *Landform studies from Australia and New Guinea*, J.N. Jennings and J.A. Mabbutt (eds), 95–117. Cambridge: Cambridge University Press.

Twidale, C.R. 1983. Pediments, peniplains, and ultiplains. *Revue de Geomorphologie Dynamique* **32**, 1–35.

Wallace, R.E. 1978. Geometry and rates of change of fault-generated range fronts, north-central Nevada. *US Geological Survey Journal of Research* **6**, 637–50.

Warnke, D.A. 1969. Pediment evolution in the Halloran Hills, central Mojave Desert, California. *Zeitschrift für Geomorphologie* **13**, 357–89.

Whitaker, C.R. 1979. The use of the term 'pediment' and related terminology. *Zeitschrift für Geomorphologie* **23**, 427–39.

Wilshire, H.G. and S.L. Reneau 1992. Geomorphic surfaces and underlying deposits of the Mohave Mountains piedmont, lower Colorado River, Arizona. *Zeitschrift für Geomorphologie* **36**, 207–26.

Zoback, M.L., R.E. Anderson and G.A. Thompson 1981. Cenozoic evolution of the state of stress and style of tectonism of the Basin and Range province of western United States. *Philosophical Transactions of the Royal Society of London, Series A* **300**, 407–34.

ALLUVIAL FAN PROCESSES AND FORMS

14

TERENCE C. BLAIR and JOHN G. McPHERSON

INTRODUCTION

Alluvial fans are a prominent landform type commonly present where a channel emerges from mountainous uplands to an adjoining valley. Although occurring in perhaps all global climatic regimes, fans in deserts traditionally have been the most studied due to their excellent exposure and ease of access. This chapter attempts to (a) provide an up-to-date synthesis of the literature on alluvial fans in desert settings, and (b) introduce a framework for their understanding based on concepts that have emerged during the last 120 years of scientific research. This synthesis emphasizes recent developments in fan studies as well as published and unpublished results from our own work in the south-western United States. The conceptual framework developed in this chapter, despite being exemplified by fans from deserts, is also applicable to fans forming under other climatic conditions.

Alluvial fans are sedimentary deposits with a form that resembles the segment of a cone radiating downslope from a point where a channel emerges from an upland (Bull 1977) (Figs 14.1 and 14.2). Fans commonly have a semi-circular or pie-piece plan-view shape (Figs 14.1 and 14.3), whereas cross-profiles display a plano-convex geometry (Fig. 14.4). Radial profiles either exhibit a constant slope like that of a cone (Fig. 14.5), or have half of a concave-upwards geometry. Fan radii typically extend from 0.5 to 10.0 km from the mountain front (Fig. 14.3) (Anstey 1965, 1966). Fan deposits either radiate unabated in a 180° arc (Fig. 14.1d) or are laterally restricted by and coalesce with neighbouring fans to form a bajada (Fig. 14.1a and 14.1c).

The construction of alluvial fans results from the accumulation of sediment where a stream exits an upland area and the transporting medium loses its power and thereby its carrying capacity. Alluvial fans almost invariably consist of coarse-grained, poorly sorted deposits due to (a) the relatively short transport distance of the sediment from its source, (b) the involvement of mass wasting processes instigated by high relief, and (c) the rapid loss of carrying capacity of the flow. A more progressive loss of flow power downslope, particularly on larger fans, results ideally in coarse-grained (boulder) sediment deposition in the proximal area and relatively finer-grained (cobble, pebble and sand) sediment more distally (e.g. Lawson 1913, Blissenbach 1954). Downslope, fans are bordered by aeolian, fluvial, lacustrine, or marine environments (Fig. 14.3). They are easily differentiated from the neighbouring fluvial environments by the characterisistic fan morphology, including radial slope values of 2 to 20° (e.g. Anstey 1966), which contrast with $\leq 0.5°$ slope values for gravelly fluvial systems (McPherson *et al.* 1987).

Fans comprise one element of a spectrum of relatively high-sloping deposits found in the piedmont (foot of mountain) zone. Steeply inclined, mountain-flanking alluvial deposits lacking distinctive individual fans have been termed alluvial slopes (Hawley and Wilson 1965), whereas high-sloping subaerial deposits rimming volcanic centres are called volcanic aprons. Windblown deposits that steeply mantle mountain fronts are termed aeolian sandsheet ramps. Glacial moraines may also border fans of desert settings (e.g. Derbyshire and Owen 1990). Continental deposits with low slopes, such as those of longitudinal fluvial systems or lacustrine systems (Fig. 14.1), also can lie interspersed with alluvial fans in the piedmont zone (e.g. Hunt and Mabey 1966, Hunt *et al.* 1966).

Geomorphology of Desert Environments. Edited by Athol D. Abrahams and Anthony J. Parsons. Published in 1994 by Chapman & Hall, London. ISBN 978-94-015-8256-8

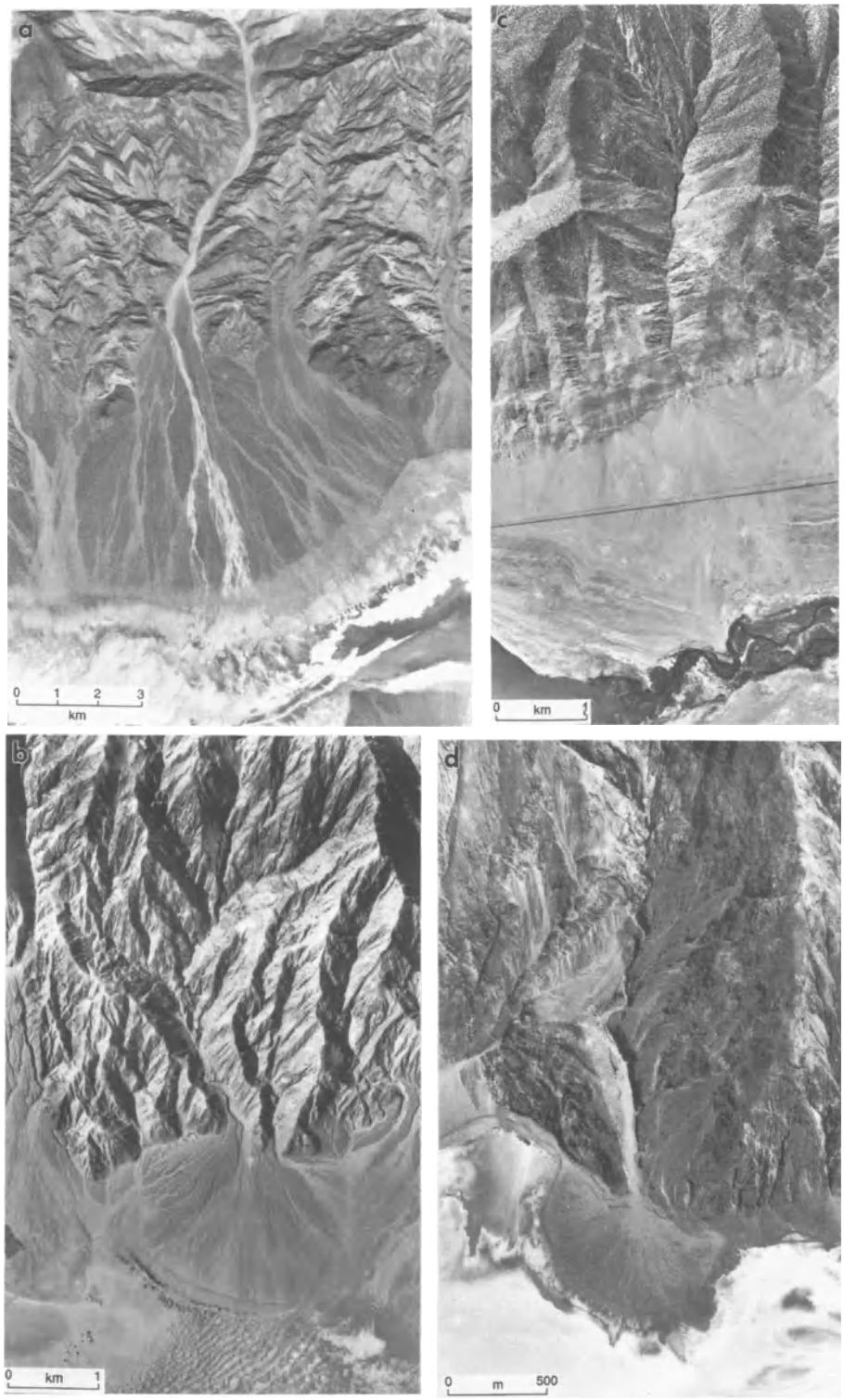

Figure 14.1 Aerial photographs of selected alluvial fans: (a) Trail Canyon fan of south-western Death Valley, California, (b) Grotto Canyon fan in northern Death Valley, (c) Deadman Canyon fan near Walker Lake, Nevada, and (d) South Badwater fan in south-eastern Death Valley.

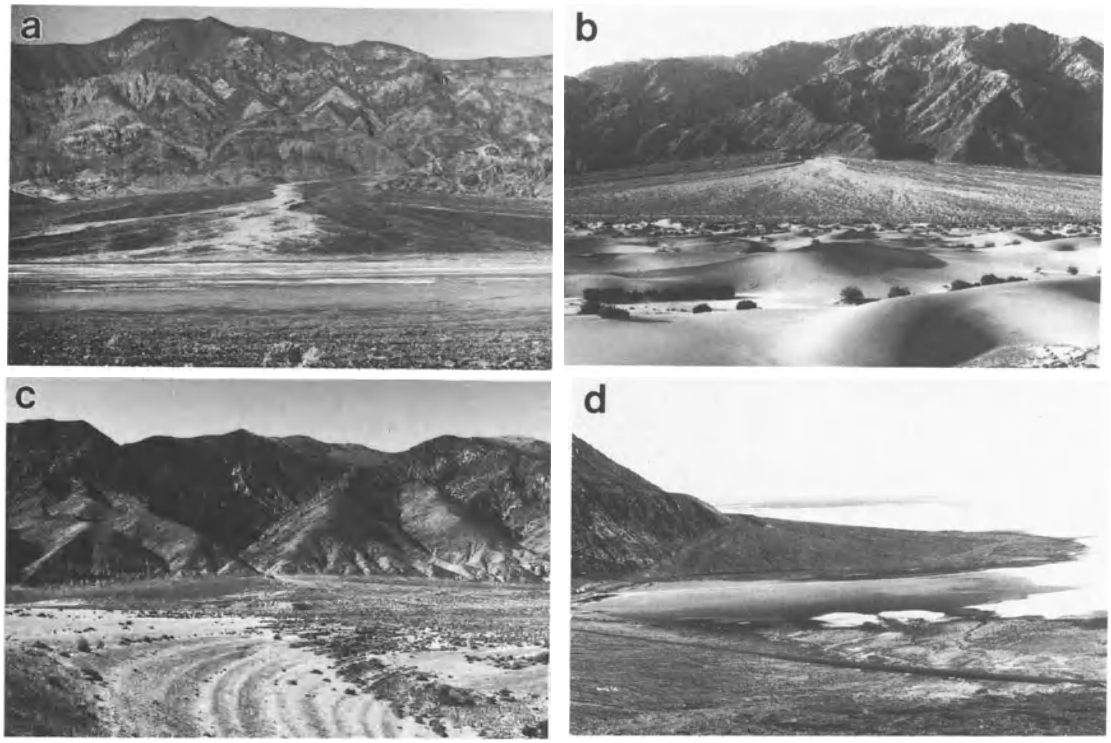

Figure 14.2 Ground-level photographs of alluvial fans illustrated in Figure 14.1: (a) Trail Canyon, (b) Grotto Canyon, (c) Deadman Canyon, and (d) South Badwater. The Trail Canyon and South Badwater fans are bordered distally by playas, whereas the Stovepipe Wells aeolian erg bounds the Grotto Canyon fan. Linear ridges along the margin of the Deadman Canyon fan are former lake shorelines.

The major morphologic features of the alluvial fan system are the drainage basin, feeder channel, apex, incised channel, distributary channels, intersection point, active depositional lobe, and headward-eroding gullies (Fig. 14.3). The drainage basin constitutes the upland area from which sediment and water discharge are derived. Alluvial fan drainage basins in desert settings typically are characterized by steep slopes and short first, second, or up to fifth-order ephemeral channels (Fig. 14.3). The highest-order stream in the drainage basin that leads to the fan is called the feeder channel. Usually only one prominent channel is present, although some fans may have multiple feeders (e.g. Fig. 14.3b). The apex of a fan is the point at the mountain front where the feeder channel emerges from the highlands (Drew 1873). This point represents the most proximal, and usually the highest, part of the fan. The apex is obvious where the mountain front is sharp (Fig. 14.3c and d), but is less distinctive where the feeder channels have carved large embayments (Fig. 14.3a).

The incised channel is a downslope extension of the feeder channel on the fan (Fig. 14.3a). It may comprise a singular trunk stream or one that divides downslope into several distributary channels. Incised channels are commonly, although not always, present (Fig. 14.3), occurring most typically on fans with longer radii. Incised channels usually terminate in the upper or medial part of the fan, but may also extend completely to the distal margin. The downfan position where an incised channel ends by merging with the fan slope is called the intersection point (Hooke 1967). Flows depart from the incised channel on to the fan surface at this point and laterally expand. The fan segment downslope from the intersection point typically is the site of sediment aggradation in an area termed the active depositional lobe (Fig. 14.3). The arc length of the active depositional lobe is a function of the radius of the lobe and the maximum angle of flow expansion, or the lobe expansion angle. Lobe expansion angles may be 180° on small fans but more typically are between 15° and 90° on larger ones (Fig. 14.3). Headward-eroding gullies are common features on the distal parts of fans (e.g. Denny 1967), particularly in older, temporarily inactive areas away from the

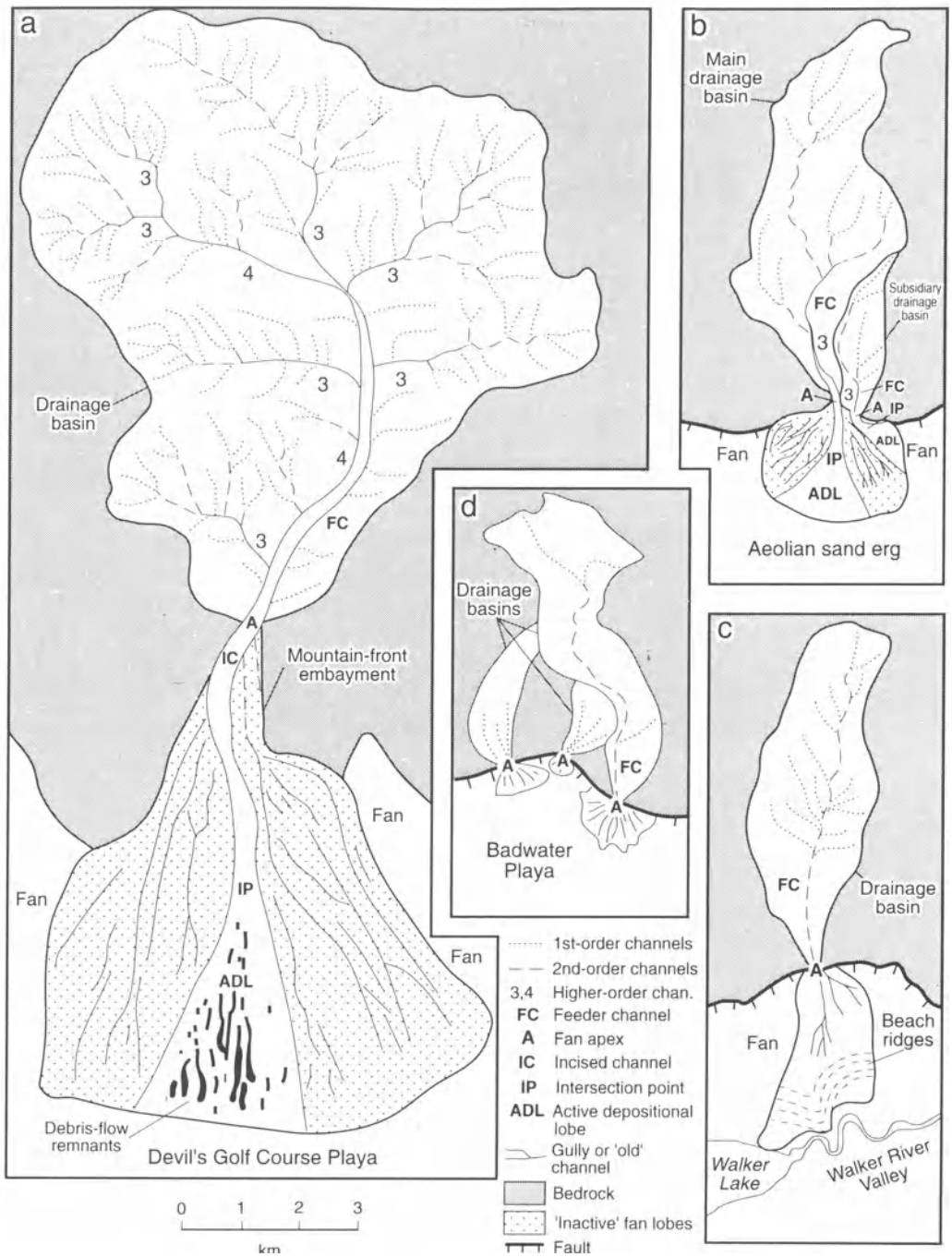

Figure 14.3 Planview line sketches based on topographic maps and aerial photographs of the fans and drainage basins illustrated in Figure 14.1: (a) Trail Canyon, (b) Grotto Canyon, (c) Deadman Canyon, and (d) Badwater fans.

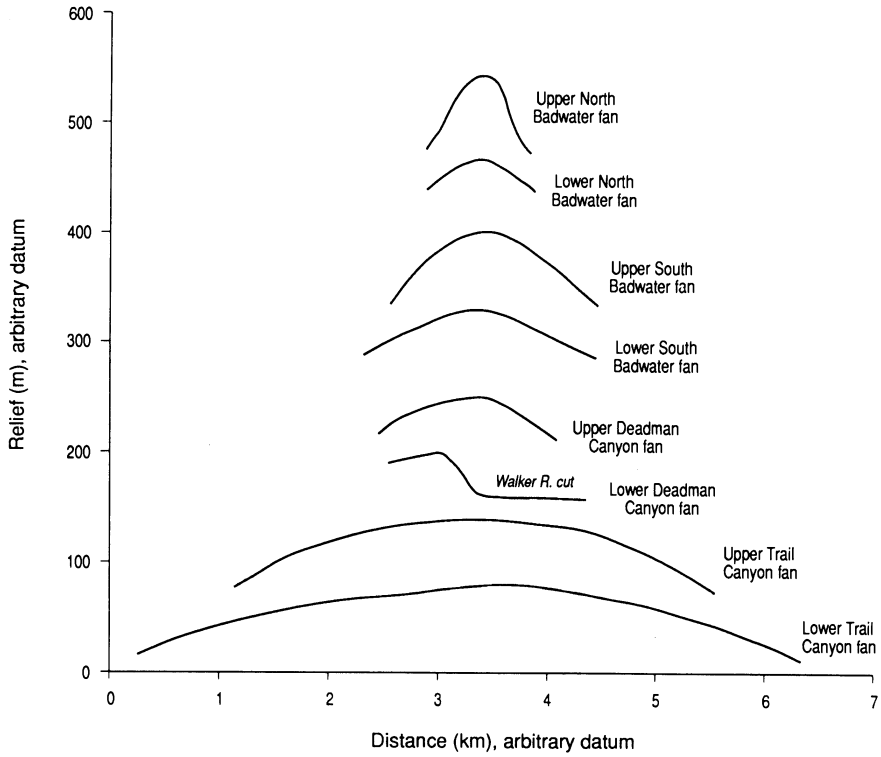

Figure 14.4 Cross profiles of fans illustrated in Figure 14.1. The cavity in the lower Deadman Canyon fan profile results from the imbalanced distribution of fan deltaic deposits and from erosion by the impinging Walker River. Vertical exaggeration is 10.

active depositional lobe (Fig. 14.3). Headward erosion by these gullies may eventually progress sufficiently upslope to intersect the incised channel, causing the position of the active depositional lobe to switch in an autocyclic manner to another part of the fan (Denny 1967).

HISTORICAL BACKGROUND

F. Drew (1873), working in the upper reaches of the Indus River in the western Himalaya of India, provided perhaps the earliest scientific description of arid-zone alluvial fans (pp. 445–7):

> 'The accumulations to which I give this name [alluvial fans] are of great prevalence in Ladakh, and are among the most conspicuous forms of superficial deposits. They are found at the mouths of side-ravines, where they debouch into the plain of a wider valley . . . . The radii of the fan are about a mile long; the slope of the ground along these radii (which are each in the direction of greatest slope) is five or six degrees. The fan is properly a flat cone, having its apex at the mouth of the ravine . . . .
>
> The mode of formation of this fan is not difficult to trace. Granting the stream of the side-ravine to be carrying down such an amount of detritus as to cause it to be accumulating, rather than a denuding stream, and there being such a relation between the carrying power of the water and the size of the material as to allow of this remaining at a marked slope, we have before us all of the conditions necessary.'

Scientific publications on desert alluvial fans predating 1960 are few in number and, with the exception of that by Drew (1873), are based on studies in the south-western United States. Fan research greatly increased during the 1960s, led by work in the south-western United States (Fig. 14.6). This research was in response to the growing need to identify water resources and geological hazards to accommodate the region's expanding population. The resulting studies began to reflect advances in the related fields of soil science, fluid dynamics,

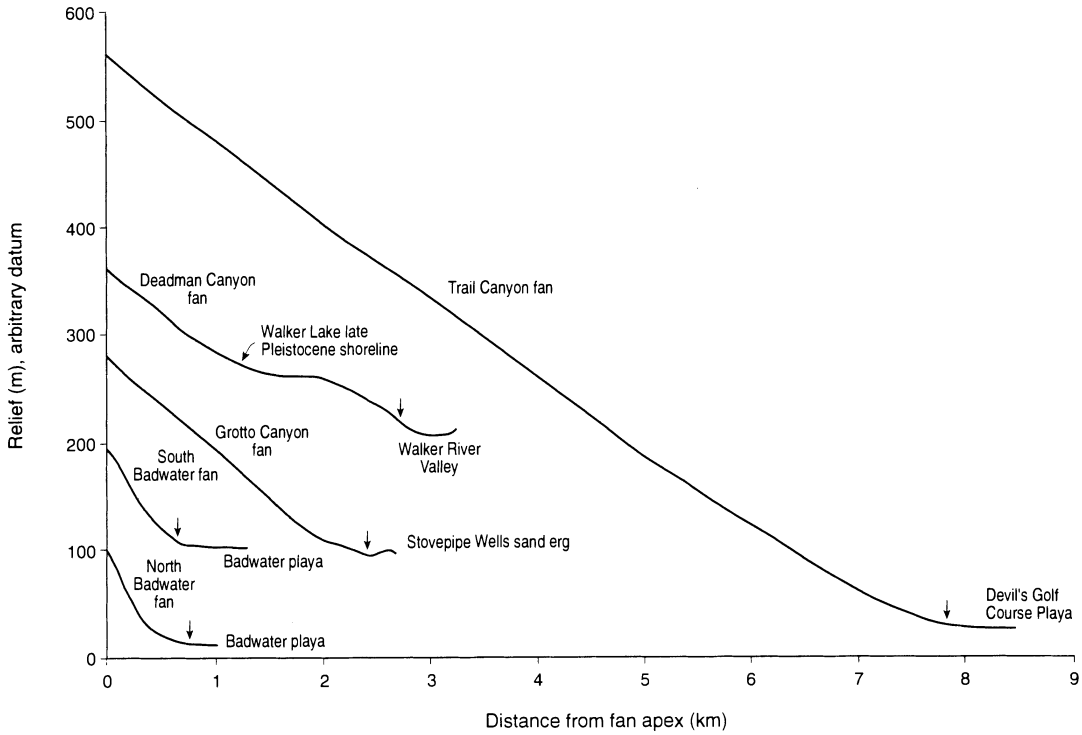

Figure 14.5 Radial profiles of fans illustrated in Figure 14.1 including, downslope, the adjoining part of their neighbouring environments. Vertical arrows denote boundaries between the fans and the neighbouring environments. Vertical exaggeration is 10.

transport mechanics, petrology, quantitative geomorphology, and aerial imagery.

The number of published papers on desert alluvial fans increased exponentially during the 1970s and 1980s, with the easily accessible and spectacular fans of the south-western United States continuing to be the dominant focus of research (Fig. 14.6). The proportion of papers dealing with fans in other desert regions also expanded during these two decades but still represents only about 20% of the total. These papers concern fans in Spain, Italy, the Middle East, Africa, Iran, Pakistan, India, Argentina, and Chile. The rapid growth of fan research from the 1970s to the present (Fig. 14.6) has been stimulated by the practical need for knowledge for geological hazards identification and mitigation (neotectonics, slope stability, flood control, urban planning, contaminated groundwater cleanup, careful selection of hazardous waste disposal sites), civil engineering (construction of highways, dams and other infrastructures), petroleum geology (predictive stratigraphy, palaeogeography, basin studies, diagenesis, and reservoir distribution and quality), mining geology (including the economic extraction of aggregate, gold, uranium, diamond, and platinum deposits), groundwater characterization (for agricultural and urban needs), archaeological studies, and continued basic research in geomorphology, process sedimentology, hydrogeology, and engineering geology.

CONDITIONS FOR ALLUVIAL FAN DEVELOPMENT

Three conditions are necessary for optimal alluvial fan development: (a) a topographic setting where a channel becomes unconfined by emerging from an upland drainage basin on to a relatively flat lowland; (b) sufficient sediment production in the drainage basin for fan construction; and (c) infrequent intense precipitation to create high water discharge needed to transport the sediment from the drainage basin to the fan site. The most typical topographic setting for alluvial fans is marginal to uplifted structural blocks bounded by faults with significant dip-slip. An example of this setting is in the Basin and Range province of the south-western United States, where

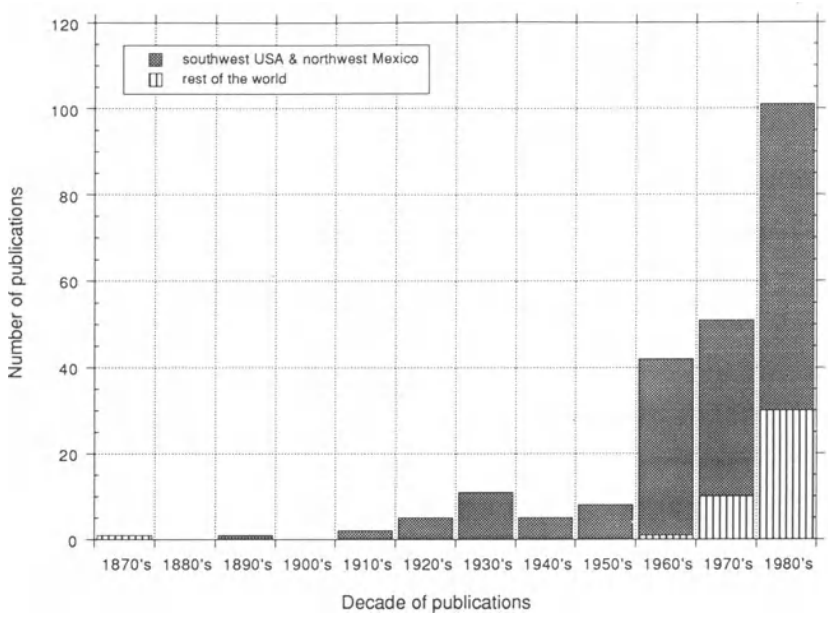

Figure 14.6 Plot of the number of publications on desert alluvial fans by decades since 1870. The numbers are based on an extensive survey of the geological literature.

an upland with adjoining lowland configuration is tectonically developed and maintained. Other topographic settings conducive to the development of alluvial fans are (a) where tributary channels enter an incised river valley, such as along the Grand Canyon of the Colorado River in Arizona (e.g. Webb *et al.* 1987), (b) where streams enter deglaciated, commonly moraine-rimmed valleys (e.g. Rust and Koster 1984, Blair 1987a), or (c) where bedrock exposures possessing topographic relief form by differential erosion (e.g. Sorriso-Valvo 1988, Harvey 1990).

Sediment production in the drainage basin, the second condition necessary for fan development, usually is met given adequate time. The common achievement of this condition is due to the presence of relief and the incessant weathering of rocks under Earth's surface conditions. Sediment yield in a drainage basin is highly dependent upon the presence of relief, increasing exponentially as relief increases due to the effects of gravity on slope erosion (Schumm 1963, 1977, Ahnert 1970). The types of rock-weathering in desert drainage basins that produce sediment are (a) physical disintegration, including sheeting, fracturing, exfoliation, ice or salt crystal growth in voids, and root penetration; and (b) chemical decomposition, encompassing reactions such as hydrolysis, dissolution, and oxidation (e.g. Ritter 1978, pp. 79–167). Weathering is greatly promoted along structurally controlled mountain fronts because of tectonic fracturing, which exposes significantly more rock surface area to alteration than in unfractured situations. Thus, the drainage basins of alluvial fans along mountain front fault zones are efficient sediment producers due both to their location on a structural block where relief is maintained and to their position coincident with the zone of maximum tectonic fracturing and, hence, zone of maximum weathering.

In contrast, drainage basins in non-tectonic settings, such as along paraglacial valleys or incised river valleys, commonly have previously deposited glacial or fluvial sediment available for recycling to the fan, although this sediment has a finite volume that will become depleted (e.g. Ryder 1971). Drainage basins developed on bedrock spurs created by variable resistance to erosion, or from compressional tectonism that has ceased, may also generate fans for which a relatively limited sediment supply is available (e.g. Sorriso-Valvo 1988, Harvey 1990). Although fans from these non-tectonic settings traditionally are assumed to be identical to ones formed in tectonic settings in terms of processes, their evolutionary scenarios may be quite different due to the lack of maintenance of relief and sediment supply.

The third condition necessary for fan development is a mechanism for moving the generated sediment

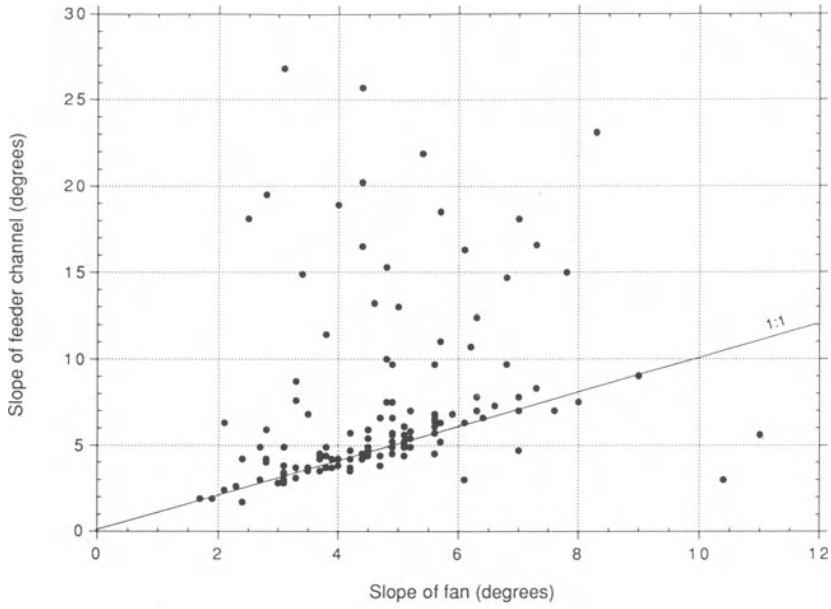

Figure 14.7 Plot of the slope of the 1-km-long segment of the feeder channel upslope from the fan apex versus the corresponding slope of the 1-km-long upper fan segment for 132 Death Valley fans. These slope values are similar (±1°) in just 56% of the cases.

from the drainage basin to the fan site. The most prominent processes known to achieve this transport are catastrophic stream discharge and mass wasting events, including flashfloods, rockfalls, rock avalanches, gravity slides, and debris flows. All of these processes require, or are greatly promoted by flood conditions manifested either as (a) short-term flashy discharge from a high precipitation event such as a thunderstorm (e.g. McGee 1897, Beaty 1963), (b) significant precipitation following sustained antecedent rainfall or snowmelt (e.g. Caine 1980, Cannon and Ellen 1985, Wieczorek 1987), (c) rapid icemelt or snowmelt events (Leggett *et al.* 1966, Beaty 1990), or (d) combinations of the above. Although drainage basins in desert settings are prone to flashy discharge, flooding of this type is by no means restricted to these climatic zones. In fact, all non-polar Earth climates contain atmospheric mechanisms that produce extensive flooding (Hayden 1988).

The topography and shape of alluvial fan drainage basins make them particularly prone to generating catastrophic floods. Mountainous topography induces precipitation in both barotropic or baroclinic atmospheric regimes by enhancing the vertical airflow that triggers condensation (Hayden 1988). Additionally, precipitation that falls in these drainage basins is quickly funnelled into the feeder channel (e.g. Fig. 14.3a), giving rise to flows with the potential to move extremely coarse sediment (French 1987). Flashflood potential is highest in drainage basins with high relief, multiple feeders, and a rotund shape (Strahler 1957).

Net fan aggradation from drainage basin discharge events requires that the floods lose some of their ability to transport sediment upon exiting the drainage basin. This loss of competency and capacity is a function of decreases in both flow depth and velocity resulting primarily from (a) the lateral expansion of flows either at the fan apex or intersection point as a result of the loss of the confining channel walls, and (b) a lessening of slope as the flow reaches the fan site. Although Bull (1977) has demonstrated that there is not always a break in slope between the feeder channel and the upper fan, deposition is instigated on many fans by pronounced slope changes (e.g. Trowbridge 1911, Beaty 1963). This relationship is illustrated by a data set of 132 fans in Death Valley, California (Fig. 14.7). The slope of the 1-km-long segment of the feeder channel adjoining the fan apex is significantly greater (>1°) than the slope of the 1-km-long segment of the incised channel or upper fan immediately below the apex in 40% of these fans. There is no appreciable difference

in slope (within ±1°) in 56% of the cases, and in 4% the slope of the fan is actually significantly steeper than the slope of the feeder channel.

Not all channels issuing from mountain fronts construct alluvial fans. Perennial rivers with highly integrated drainage basins, such as the Kern River and San Joaquin River of southern California, the Feather River of northern California, and the Arkansas River and Platte River of Colorado, are capable of maintaining channel banks and flow competency. Thus, these rivers do not form alluvial fans upon emergence from their respective uplands. Instead, they maintain bedload-dominated fluvial tracts.

In conclusion, mountainous deserts commonly provide the optimal conditions necessary for alluvial fan development. They have the necessary topography to induce rainfall and catastrophic runoff, enhance sediment production, and trigger mass wasting events. Additionally, the fact that the most favourable topographic configuration for fan development is in zones of structurally controlled block faulting, where mountain fronts are tectonically maintained, makes extensional terranes such as the American Basin and Range province or the East African–Red Sea rift zones the most optimal structural setting for the deposition of widespread, well-developed fans.

PRIMARY PROCESSES ON ALLUVIAL FANS

Sedimentary processes active on alluvial fans are of two types, primary and secondary. Primary processes are herein defined as those responsible for transporting sediment from the drainage basin to the fan. These processes include rockfalls, rock avalanches, gravity slides, debris flows, sheetfloods, and incised-channel floods (Fig. 14.8). Primary processes generally result in fan construction or aggradation and act concomitantly with the enlargement of the drainage basin due to sediment removal. Primary sedimentary events generally are triggered by rare and catastrophic flashfloods or earthquakes. They therefore are of short duration but high impact with regard to fan construction. In contrast, secondary processes are those events that cause the remobilization or modification of sediment that previously had been deposited on the fan by any of the primary processes. Included in this category are overland flow, wind erosion, bioturbation, soil development, sediment weathering, faulting, and case hardening (Fig. 14.8). Secondary processes most commonly result in fan erosion or degradation and, except for faulting and some overland flows, are associated with normal or non-catastrophic conditions. Although they may have minimal influence on fan construction, secondary processes usually dominate the surface features of a fan except in areas recently affected by a primary depositional event (Blair 1987a).

The primary processes common on alluvial fans or in their drainage basins are divided into two classes: fluid-gravity flows and sediment-gravity flows. Sediment transportation and deposition in fluid-gravity flows, or the synonymous term water flows, are caused by the downslope movement of water in response to the force of gravity. Transportation in these flows is accomplished by the force of moving water acting on the sedimentary particles. In contrast, downslope transportation in sediment-gravity flows is caused by the force of gravity acting directly on the sedimentary particles, which causes the movement of any contained fluids (Middleton and Hampton 1976). Sediment-gravity events encompass a collection of processes termed mass wasting or mass movements due to the fact that they entail the slow to rapid downslope transfer of large volumes of rock or its overlying sedimentary cover (Varnes 1978).

Prior to Blackwelder's (1928) article on the occurrence of debris flow activity on the bajadas of southern California, fans were believed to be built entirely by fluid-gravity flows. This misconception arose due to the configuration of the drainage net, feeder channel,and incised channel, leading to the term alluvial in alluvial fan. A recent study by Derbyshire and Owen (1990) of fans along the Karakoram Mountains of north-western India, where Drew (1873) coined the term alluvial fan, has demonstrated that sediment-gravity processes also are important on these fans in addition to the water-flow processes recognized by Drew. The term alluvial is maintained today when discussing continental fans despite this history, although it is now well established and widely recognized that fluid-gravity flows are only one of several sedimentary processes responsible for alluvial fan construction.

SEDIMENT-GRAVITY PROCESSES

Sediment-gravity processes are fundamental to the formation of all alluvial fans. Almost all sediment reaching a fan is at least partially transported by some kind of sediment-gravity mechanism active in the drainage basin. In many fans, particularly those with small drainage basins, these processes are capable of depositing sediment directly at the fan site.

The initiation of all sediment-gravity processes in

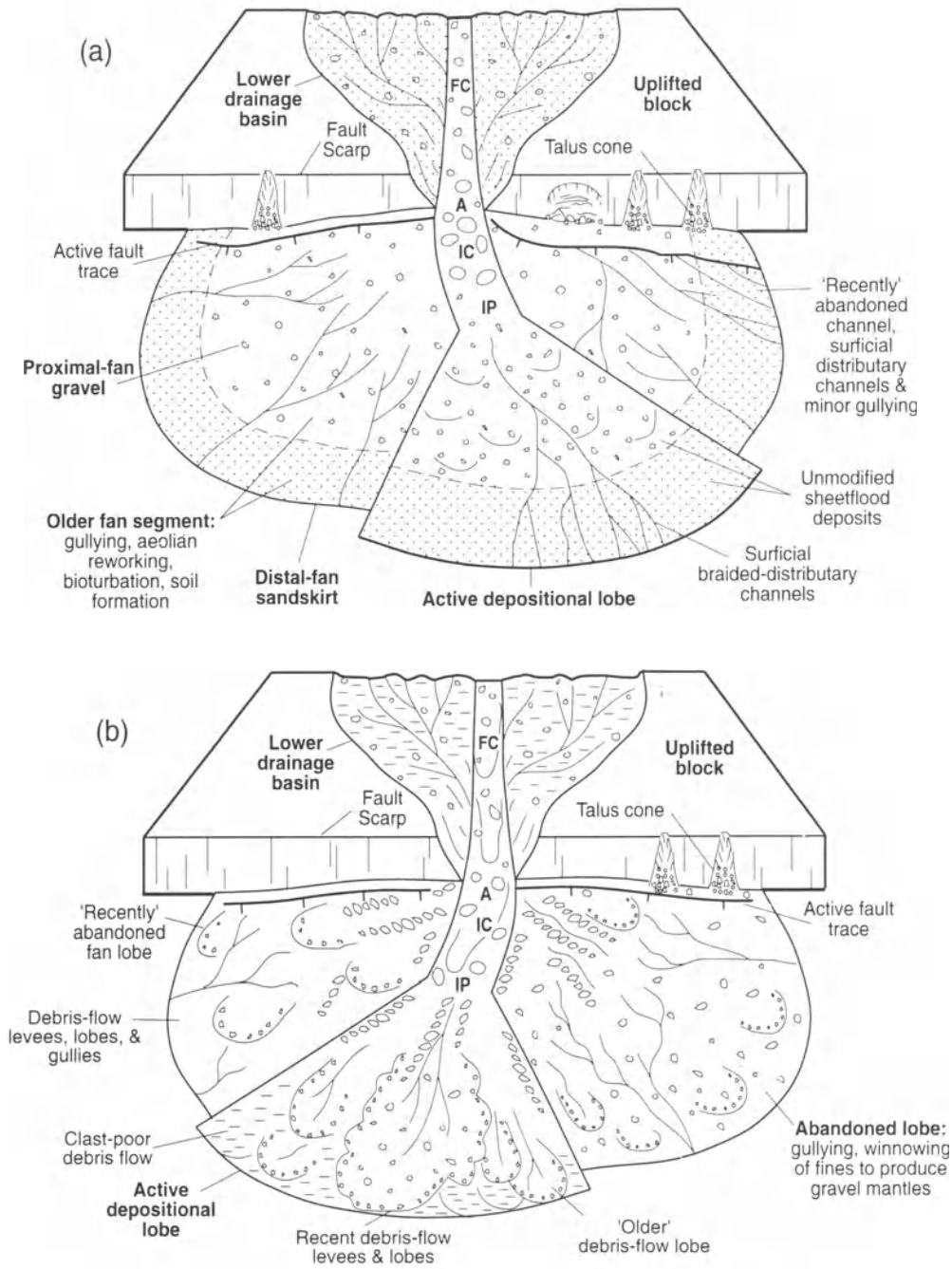

Figure 14.8 Schematic diagrams of the common primary and secondary processes on alluvial fans, including (a) those on fans dominated by water flows, and (b) those on fans dominated by debris flows. These diagrams are based on numerous fans studied by the authors. Abbreviations are A = fan apex, FC = drainage basin feeder channel, IC = incised channel on fan, IP = fan intersection point.

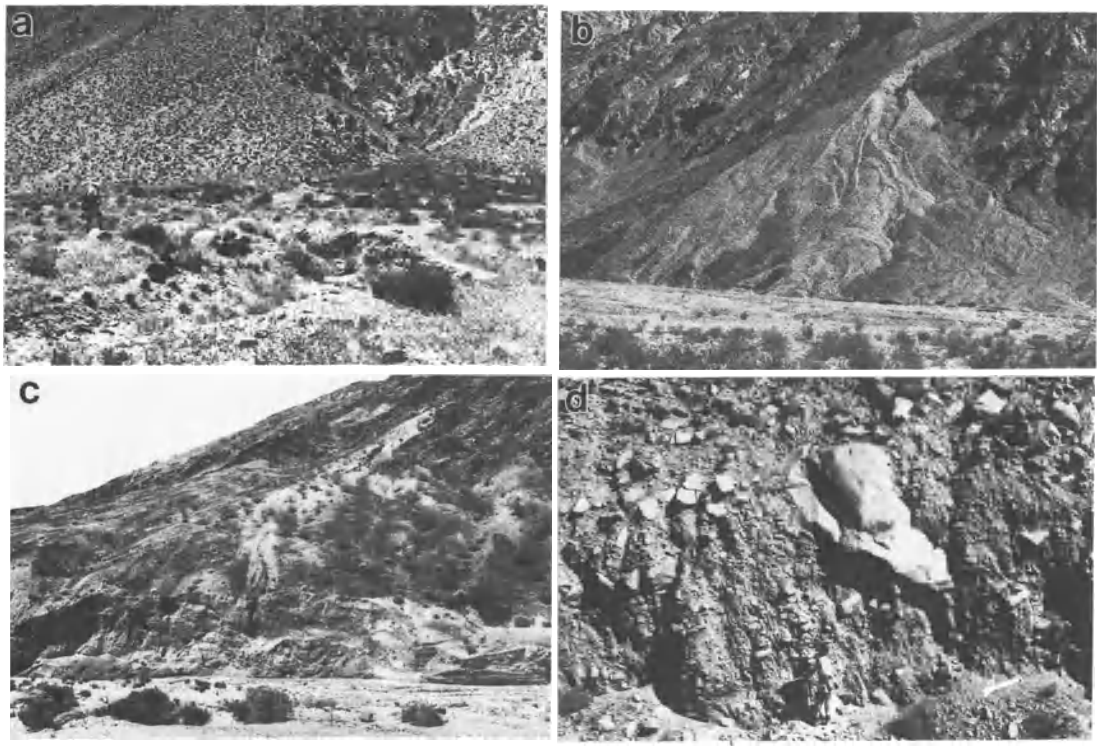

Figure 14.9 Photographs of rockfall accumulations. (a) High-sloping colluvial deposits continuously mantle the mountain front near the proximal Rifle Range fan, Hawthorne, Nevada. Geologist (left-centre) for scale. (b) View of a colluvial cone with prevalent avalanche chutes located near Morman Point in Death Valley. Rock varnish more extensively darkens the progressively older clasts on this cone. (c) View of a colluvial cone near the apex of the Cucamonga fan in Eureka Valley, California. The vertical cut reveals a scallop-shaped stratigraphy resulting from the accumulation of sediment in distinctive avalanche chutes. (d) Vertical cut through very poorly sorted colluvial sediment that accumulated by freefall at the head of the Copper Canyon fan, Walker Lake, Nevada. Geologist (lower-centre) for scale.

a drainage basin results from a reduction of the resisting forces relative to the gravity forces imposed upon the slope materials. The resisting forces may be reduced and drainage-basin slopes destabilized by several factors, including (a) bedrock fracturing and weathering, which lowers the rock's internal friction and shear strength, (b) oversteepening of the slope by toe erosion caused through either human or natural activity, (c) earthquake-caused ground motion, which can provide the initial kinetic energy for downslope movement, (d) the addition of water or gas, which increases the sediment pore pressure and shear load, causing a reduction of the effective normal stress, or (e) combinations of the above (e.g. Ritter 1978, Keefer 1984, Cotecchia 1987, Hencher 1987). Four end-member classes encompassing the continuum of sediment-gravity processes that are active in alluvial fan drainage basins and result in sediment transport to the fan are rockfalls, rock avalanches, gravity slides, and debris flows.

Rockfalls

Rockfall is the downward movement of bedrock blocks that drop from cliffs under the force of their own weight (Chapter 8). These blocks either roll or bounce towards the valley, or accumulate at the base of the cliff in near-angle-of-repose (30° to 40°) mantles called talus, colluvium, or scree deposits (Figs 14.9) (Drew 1873, Sharpe 1938, Rapp and Fairbridge 1968, Rahn 1986). Rockfall blocks initially are shaped by tectonic jointing, fracturing, or shearing; or by the release along other geological discontinuities such as lithologic boundaries, bedding planes, sheeting or cooling joints, slaty cleavage, and schistosity horizons (Hencher 1987). Blocks eventually become loosened and detached along these discontinuities with the aid of weathering and groundwater. The downward movement of unstable blocks typically is triggered by heavy rainfall, freeze–thaw action, or by the shaking motion of earthquakes (Keefer 1984,

Statham and Francis 1986, Cotecchia 1987, Beaty and DePolo 1989).

Rockfall accumulations are common in alluvial fan drainage basins, and may extend outwards from the mountain front on to the proximal fan (Fig. 14.9a and b) (Beaty 1989). These deposits either continuously mantle cliff faces (Fig. 14.9a) or more commonly develop a conical shape due to the concentration of the free-falling material through a notch in the bedrock (Fig. 14.9b and c). The conical deposits, called talus cones or colluvial cones, form close to the base of a cliff mainly through numerous small rockfalls or avalanches (Drew 1873, Rapp and Fairbridge 1968). Talus cones typically are composed of angular, poorly sorted gravel (pebbles to boulders), with or without interclast sand or mud matrix (Fig. 14.9d). The matrix may be added by infiltration subsequent to clast deposition.

Rock Avalanches

The rapid fall of a large, extensively fractured or jointed bedrock mass may cause it to quickly disintegrate into boulder- to clay-sized fragments as it moves downslope and transforms into a granular flow termed a rockfall avalanche (Mudge 1965), sturzstrom (Hsu 1975), dry avalanche (Fauque and Strecker 1988), or, as used herein, a rock avalanche (Chapter 8). The sources of energy in rock avalanches, which may move at speeds exceeding 100 km h^{-1}, are the kinetic energy of the initial fall and the potential energy acquired during downslope movement from gravity (Mudge 1965, Hsu 1975, Melosh 1987, Yarnold and Lombard 1989). An important support mechanism for the clasts in such a dry flow is vibrational or acoustic energy caused by high-frequency pressure fluctuations produced by random motion of groups of fragments of debris organized into elastic waves (Melosh 1987). This process overcomes the internal friction in the flow, allowing rock avalanches to travel significant distances from the mountain front relative to other sediment-gravity flow types and even to move for short distances in an upslope direction. Most rock avalanches have runout distances of ≤10 km (Hart 1991, Topping 1991), with the unobstructed expansion of the debris mass commonly encountered at alluvial fan sites especially detrimental to flow continuation (Nicoletti and Sorriso-Valvo 1991).

Rock avalanche events that resulted in the accumulation of sediment on fans along the Sierras Pampeanas in north-western Argentina were described by Fauque and Strecker (1988). The rock avalanche deposits on these fans have a lobate form 3 to 4 km long, 0.5 to 1.5 km wide, and are characterized by an 8 to 10-m-high frontal rim with lateral levees. Surface area per avalanche deposit varies from 1.0 to 7.5 km^2, and volume from 5 to 65×10^6 m^3. Older fan deposits are exposed in the internal part of the lobes. This form suggests that the rock avalanche moved as a non-Newtonian viscous flow across the piedmont after falling from a high source region as much as 7 km upslope in the drainage basin. Down-fan movement of the rock avalanche was most extensive along the axial part of the flow. The resulting deposits are inversely graded, with boulders as large as 2 to 20 m across present at the top of the levees, and small boulders to silt-sized material occurring in the lower parts.

Rock avalanching also is a common process along the piedmont zones of southern California and Arizona (Burchfiel 1966, Yarnold and Lombard 1989, Hart 1991). The deposits of these rock avalanches, called megabreccias, commonly are 20 to 120 m thick and have runout distances of several kilometres. These deposits are typified by a matrix-rich lower layer that may be overlain by an upper layer consisting of highly fractured but relatively intact rock debris possessing crackle-breccia or jigsaw breccia fabrics. These zones developed due to variations in the internal motion of the avalanche materials. The formation of the matrix-rich lower layer is attributed to the pulverization of the rock mass as it moved due to shearing coupled with the weight of the overlying material, whereas the upper zone fabrics developed by the rigid deformation of the bedrock mass as it moved downslope. The deposits of the rock avalanches studied in Arizona and southern California contrast with those described by Fauque and Strecker (1988) in Argentina in that the former possess a tabular or mounded geometry and the latter have a levee and snout morphology.

Gravity Slides

Gravity slides (cf. landslides, rockslides, sediment slides, landslips, debris slides, or slumps) constitute a family of mass movements characterized by distinctive bodies of bedrock or colluvium initially positioned high on an unstable slope and moved either slowly or rapidly downward along well-defined basal surfaces called glide planes (Sharpe 1938, Varnes 1978). Gravity slides are differentiated from other types of sediment-gravity flows, such as rock avalanches, by the movement of the material as a coherent mass rather than as a granular flow of individual particles. Movement in a gravity slide occurs over the planar or gently curved glide hori-

zon, and the sliding mass is essentially undeformed except possibly for partial disintegration of brittle rock (Ritter 1978). The glide plane may be shallow and parallel to the ground surface or it may constitute the boundary between the sedimentary cover and the underlying bedrock. The gap left behind in the slope from which the slide material detaches is called the slide scar. Slide scars typically are spoon-shaped as a result of the rotational movement of the detached material (Varnes 1978). Gravity slide processes are important in fan drainage basins by moving sediment from the slopes to the feeder channel or even directly out to the fan. In addition, first-order channels in the drainage basin commonly develop during gravity slide events (Patton 1988, Sorriso-Valvo 1988).

Both bedrock and colluvial gravity slides can be initiated by coseismic ground motions. Keefer (1984), who studied the relationship between historical gravity slides and earthquakes, found that slopes consisting of either weakly cemented bedrock, bedrock with abundant discontinuities, or colluvial material are most susceptible to seismically induced sliding. He noted that slides with shallow glide planes are triggered in proximity to epicentres by only weak ground motions (Richter-scale magnitudes of 4.0 to 5.0), whereas progressively thicker slides required progressively greater motions to initiate the movement. Keefer also concluded that both the size of a slide and its distance of transport have a positive correlation with the magnitude of the earthquake and proximity to the epicentre.

Colluvial slides most often are triggered by the addition of water to the slope materials, which increases pore pressure and decreases shear strength, making them susceptible to failure (Costa 1988, Mathewson *et al.* 1990). Water within the colluvium also serves as a lubricant that reduces glide plane friction. The accumulation of water in the sediment pores above the glide plane further enhances slope instability by increasing the shear load of the mass due to the added water weight (Hencher 1987). A common location for colluvial landslides to develop is in sediment-filled bedrock hollows of the upper slopes of the drainage basin where colluvium accumulates most rapidly, and where overland flows are concentrated by the funnelling action created by the converging topography (Reneau *et al.* 1984, 1986, 1990). The mobilization of water-saturated colluvium typically results in the transformation of the colluvial slide into a debris flow due to the granular content of the colluvium and to the entrainment of the pore water into the flow as it moves (e.g. Reneau *et al.* 1984, 1990, Costa 1988).

Debris Flows

Debris flows are a type of sediment-gravity flow characterized by a mixture of granular solids (gravel, sand, clay, tree limbs, etc.) and small amounts of entrained water and air that move downslope under the force of gravity (Varnes 1978, Johnson 1984) (Chapter 8). Debris flow is the most significant sediment-gravity process in terms of the volume of material deposited directly on alluvial fans. This sediment-gravity flow type differs from the others inasmuch as water and air are irreversibly entrained with the sedimentary particles, moving together at the same velocity as a viscoplastic body (Johnson 1970). Unlike water flows, the solid and fluid phases of a debris flow do not separate upon deposition except for slight dewatering (Costa 1988).

Debris flows are initiated by two mechanisms. The most widespread mechanism involves the transformation of a wet colluvial slide into a debris flow by the entrainment of air and water through the jostling, deformation, and loss of individuality of the particles as it moves downslope (Johnson and Rahn 1970, Johnson 1984, Reneau *et al.* 1984, 1990, Costa 1988). This transformation requires the presence of water in the colluvium and, therefore, is most apt to occur during or immediately after excessive rainfall or snowmelt when the pores are saturated (e.g. Sharp 1942, Fryxell and Horberg 1943, Sharp and Nobles 1953, Beaty 1963, 1990, Johnson 1970, Campbell 1975, Hooke 1987, Mathewson *et al.* 1990). Clay, even in amounts of just a few percent by volume, is extremely important in initiating debris flows from colluvial slides by providing strength to the interstitial fluid phase and by lowering permeability. Permeability reduction hinders the dissipation of pore fluids, causing an increase in pore pressure and a lowering of the internal friction, giving mobility to the flow. The transformation from a colluvial slide to a debris flow is due most likely to liquefaction or dilatancy (Ellen and Fleming 1987). This transformation is promoted by poor sorting, which limits the interlocking of particles and subsequent internal friction (Rodine and Johnson 1976).

The second scenario by which debris flows can be initiated is where fast-moving water intersects an area mantled by abundant sediment. The ensuing reaction, in which the water dissipates its energy by dispersing clasts through churning, tossing, and mixing, can result in the rapid entrainment of the sediment, air, and water to produce a debris flow (Johnson 1970, 1984). Johnson termed this type of initiation process the firehose effect.

The generation of debris flows by either triggering mechanism occurs most optimally where flashflood

discharge crosses or infiltrates steep slopes mantled by abundant sediment. Slopes that promote debris flow initiation typically have a 27 to 56° dip (Campbell 1975). Slopes greater than 56° commonly are too steep to maintain a mantle of colluvium whereas slopes of less than 27° have a diminished propensity for failure by gravity-induced mechanisms. Because flashfloods are relatively infrequent, and because the sediment accumulation sufficient to produce a debris flow requires time, the recurrence interval of debris flows is relatively long, varying from 300 to 10 000 years (Costa 1988, Hubert and Filipov 1989). Locally, where conditions are abnormally ideal for their generation, they are more frequent (e.g. Jian and Defu 1981, Jian and Jingrung 1986).

Investigations of active debris flows illustrate that they move in surges, with boulders concentrated either at the front or on top of the flow (e.g. Blackwelder 1928, Fryxell and Horberg 1943, Sharp and Nobles 1953, Johnson 1970, 1984). The surges are caused by the addition of new material by intermittent slope failure, bank failure and sloughing, or the development and breaching of temporary dams caused by the interaction of clasts and channel constrictions. Sedimentary particles in moving debris flows are supported by the high density and strength of the flow caused by cohesive, dispersive, buoyant, and locally turbulent forces (Middleton and Hampton 1976, Costa 1984, 1988). Cohesive strength is provided by the contained clay, whereas buoyancy is promoted by high concentrations of coarse grains. The differential response of boulders to buoyant and dispersive forces, caused by small differences in density between them and the rest of the material, results in the concentration of boulders at the top and front (Middleton 1970, Fisher 1971). Debris flows generally move with laminar character (Johnson 1970, Rodine and Johnson 1976). The lack of turbulence compels debris flows to be generally non-erosive despite the fact that they are capable of transporting boulders weighing several hundred tons (Rodine and Johnson 1976).

Debris flow movement downslope is sustained until its shear strength increases sufficiently to overcome gravity forces. Flow cessation ultimately results from the thinning of the flow to the point where the plastic yield strength equals the shear stress. This process may be aided by dewatering, which leads to increased frictional contact between grains. Debris flows containing boulders and cobbles may also be halted before critical thinning or dewatering has occurred by the damming effect of the coarse clasts at the frontal and lateral margins (Pierson 1985), or by their jamming against obstacles in the flow path such as upright trees or protruding boulders of older deposits (Blair 1987a).

Three types of debris flows active on alluvial fans can be differentiated. Two types, called clast-rich debris flows and clast-poor debris flows, can be distinguished on the basis of the volume of gravel (Fig. 14.10). The term rubbly debris flow has been used as a synonym for the clast-rich variety, whereas mudflow equates to the clast-poor type. The amount of gravel in a debris flow is a function of the availability of gravel in the source sediment rather than a reflection of variations in flow strength. Therefore, the clast-rich and clast-poor terms are recommended inasmuch as the processes involved in them are identical (e.g. Johnson 1984). Additionally, a single event may produce both clast-rich and clast-poor debris flows.

The third type of debris flow, called non-cohesive debris flow, is a specialized clast-rich type generated where clay is absent (Jarrett and Costa 1986, Blair 1987a). The absence of clay results in the lack of cohesive strength in the flow; instead sediment is supported by dispersive, turbulent, buoyant, and structural-grain forces. In general, the resultant deposits of cohesive and non-cohesive clast-rich debris flows are similar, although those of the non-cohesive variety are more vulnerable to erosion due to the lack of cohesive bonding between grains. In addition, the runout distance of a cohesive debris flow is likely higher than a non-cohesive one because the clay serves to reduce the effective normal stresses between the clasts, hindering frictional locking (Rodine and Johnson 1976).

Clast-rich debris flows of either the cohesive or non-cohesive variety typically occur on fans as lobes and levees present within the incised channel or directly on the fan surface (Fig. 14.10). Pre-existing topographic irregularities such as gullies commonly are filled by the passing debris flow. Clast-rich debris flows of the proximal fan generally consist of levee deposits, whereas relatively thin but more widespread lobes characterize deposits distally (Fig. 14.10a). Debris flow levees are produced by the lateral displacement of the coarse sediment from the snout of the moving flow and by the high internal friction in the zone of shearing at the flow margins (Sharp 1942, Johnson 1970, 1984). The levees represent parallel ridges of sediment left behind after the flow has waned and most of the debris has moved out into the lobes at the end of the flow path (Fig. 14.10). Flow surging commonly produces stacked beds in the debris-flow lobes (Fig. 14.10a and e). Falling-stage of a debris-flow event may result in the production of a clast-poor phase (Fig. 14.10e). Waning-stage water discharge also will commonly erode

and winnow the surface of the newly deposited debris flow (Fig. 14.10e) (Beaty 1963, Johnson and Rahn 1970). This winnowing process can result from high subsequent drainage basin discharge caused by the release of stored groundwater tapped by the slope failure that initiated the debris flow activity (Mathewson *et al.* 1990).

Clast-poor debris flow deposits differ from their clast-rich counterparts by not forming levees and by having lobes that are more extensively thinned before deposition. The resultant deposits are lobes that smoothen pre-existing topography and have planar surfaces due to the lack of protruding clasts (Fig. 14.10f and h). Clasts and tree branches that may be present are concentrated along the lobe margins (Fig. 14.10g). Desiccation cracks are common in clast-poor debris flows due to the high clay content (Fig. 14.10f). These debris flows, like their clast-rich counterparts, are susceptible to erosion by falling-stage or subsequent water flows (Fig. 14.10f and h).

FLUID-GRAVITY PROCESSES

Fluid-gravity flows are Newtonian fluids characterized by the lack of shear or yield strength and by the fact that sediment and water remain in separate phases during transport (Costa 1988). The sediment-support mechanism in this flow type is fluid turbulence. Transport results either from suspension or from the rolling and saltating of sediment along the base of the flow by the transfer of energy from moving water to the individual particles. Sediment concentration in water flows typically is $\leq$ 20% by volume, with flows containing 20 to 47% sediment being termed hyperconcentrated (Costa 1988). Hyperconcentrated flows may achieve low shear stress values but, as in water flows, and in contrast to debris flows, sediment and water remain in separate phases and turbulence is the major support mechanism (Beverage and Culbertson 1964, Costa 1988). As hyperconcentration develops, sediment fall velocities decrease and buoyant or dispersive stresses aid sediment support.

Two types of fluid-gravity flow processes are operative on alluvial fans: sheetfloods (unchannelized or unconfined flows on the fan lobes) and incised channel flows. Both flow types result from the rapid concentration in the drainage basin of runoff from snowmelt or rainfall, leading to catastrophic discharge downslope. Sediment mantling the slopes or valleys of the drainage basin may be eroded by flow turbulence and carried to the fan site. Both sheetfloods and channelized flows can have sediment concentrations ranging from low to hyperconcentrated, depending on the intensity of the flow and the availability of sediment in the flow path.

Sheetfloods

A sheetflood is a broad expanse of unconfined runoff moving downslope (McGee 1897). The flow event is of relatively low frequency and high magnitude (Hogg 1982), while the flow itself is generally shallow and short-lived and has a limited travel distance. Sheetflooding is produced by catastrophic discharge, most commonly from high-intensity rainfall, combined with the absence of channelized drainage.

The characteristics of sheetflooding are well illustrated by a catastrophic event that occurred on the Roaring River fan in Rocky Mountain National Park, Colorado (Blair 1987a). This sheetflood event was caused by the failure in the upper drainage basin of a human-enlarged natural dam containing a cirque lake. An aerial photograph of the active sheetflood demonstrates it to be continuous over the entire

Figure 14.10 Photographs of clast-rich and clast-poor debris flow deposits. (a) Overview of the deposits from a 1984 debris flow event on a 1.5-km-long fan near Dolomite in Owens Valley, California. The flow divided downslope into numerous lobes. (b) Side view of matrix-supported boulder deposits constituting the recent debris flow levees on the Dolomite fan. Army shovel for scale. (c) Lobes spilled laterally from a breach in the levee of the Dolomite fan debris flow. Geologist for scale (arrow). (d) Oblique perspective of the recent clast-rich, interdigitate lobe margins of the Dolomite fan debris flow. Army shovel for scale. (e) Overview of the downfan lobe on the Dolomite fan in which clast-poor debris flow deposits accumulated above the clast-rich ones. Both of the flows were winnowed in their central area by water discharge that immediately followed debris flow deposition. (f) Overlapping clast-poor debris flows on the Copper Canyon fan, Walker Lake, Nevada. The lower flow (foreground) occurred in 1982, the upper one (middle ground) in 1990. Winnowing and slight dissection of the lower flow occurred during the intervening eight years. Geologist (upper-right) for scale. (g) Close-up of the 1990 Copper Canyon fan clast-poor debris flow. Note that the flow delicately divided around the desert plants despite the concentration there of gravel clasts. Desiccation cracks are present on the surface of the flow. (h) Waning-stage water flows during the 1990 Copper Canyon event winnowed fines from the central part of the debris flow deposits (photograph centre). Note the winnowed, darkened, and sparsely vegetated surface on the 1982 clast-poor debris flow (foreground).


a
b
c
d
e
f
g
h

Figure 14.11 Photographs of alluvial fan sheetflood deposits. (a) Vertical trench exposure of alternating cobble–pebble gravel and laminated granular sand produced by the 15 July 1982 Roaring River sheetflood. The dark horizon near the top of the trench was deposited ten months after the flood. (b) Up-fan view of Roaring River fan sheetflood deposits immediately after flood cessation. A prominent sandskirt occurs in the foreground. The gravelly sheetflood surface is locally modified by a channel carved during falling flood stage. (c) View of the relatively smooth and sloping sheetflood surface on the Roaring River fan not modified by falling stage channel incision. (d) Oblique aerial photograph of fans in western Arizona displaying transverse ribs of sediment-deficient sheetflood origin (road for scale). (Photo provided courtesy of S.G. Wells.)

320-m-long active depositional lobe, which had an expansion angle of 120°. Hydraulic reconstructions indicate that this sheetflood had an average depth of 0.5 m, a velocity of 4.4 m s^{-1}, and a maximum water discharge value of 45.6 $m^3 s^{-1}$. Supercritical flow generated up-fan migrating transverse waves on the water surface with antidune bedforms on the sediment surface below, similar to the sheetflood features described nearly a century earlier by McGee.

As much as 5 m of stratified sand- to boulder-sized sediment was deposited on the Roaring River fan by this sheetflood (Blair 1987a). The deposits include laminated pebbly sand interbedded with pebble or cobble gravel in couplets 5 to 20 cm thick and oriented at an angle of 4°, parallel to the fan slope (Fig. 14.11a). Gravel deposition occurred during the wash-out phase of the antidune train, whereas the granular sand was deposited during fall-out of the suspended load after antidune destruction. Repetition of antidune development and destruction resulted in the stacking of up to 15 couplets of gravel and pebbly granular sand throughout the sheetflood deposit. A skirt of planar-bedded granular sand accumulated down-fan from the gravelly couplets (Fig. 14.11b). The surface of the deposits produced during the sheetflood was partly incised during the flood falling-stage, producing two channels 4 to 5 m across and 0.4 m deep (Fig. 14.11b). The smoothly dipping surface of the sheetflood was preserved elsewhere on the lobe not carved during falling-stage (Fig. 14.11c). The presence of the diagnostic gravel and sand couplets and planar-bedded sand-skirt deposits on fans throughout the south-western United States suggests that sediment-laden sheetflooding is an important, but poorly recognized, fan-building process.

Wells and Dohrenwend (1985) have reconstructed

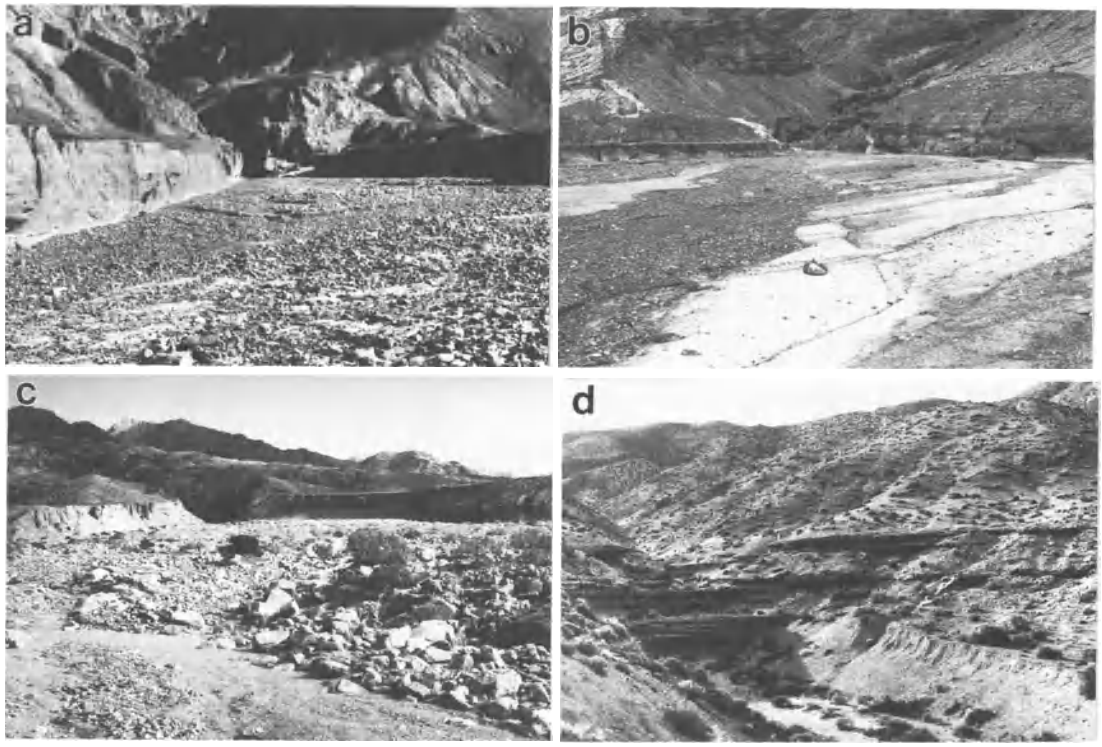

Fig. 14.12 Photographs of incised channels. (a) Up-fan perspective of an incised channel of a fan from Death Valley. Note the vertical, 3-m-high channel walls and the relatively flat floor consisting of cobbles and unwinnowed debris flows. (b) View of the proximal part of the incised channel of the Mosaic Canyon fan, Death Valley. Winnowed pebbles and smooth-surfaced, clast-poor debris flows occur on the channel bottom. (c) Incised channel of a fan derived from the Smith Mountains granitic pluton, Death Valley. The channel floor contains a coarse mantle of boulders lateral to which finer gravelly and sandy sediment was deposited. (d) Terraced fine-grained deposits (lower-right) occur in the incised channel of this fan located north of Copper Canyon, Walker Lake, Nevada.

latest Pleistocene to middle Holocene sheetflood events on alluvial fans in the Mojave Desert of California and Arizona based on the presence of transversely oriented bedforms consisting of sand, granules, and pebbles. These features, called transverse ribs, resemble starved ripples (Fig. 14.11d). They have wavelengths of 2 to 6 m and indicate that multiple, sediment-deficient sheetfloods with estimated flow velocities of 0.3 to 0.6 m s^{-1} occurred on these fans.

Incised Channel Flows

Incised channels serve as conduits for catastrophic flows on the upper fan, facilitating the transfer of sediment-gravity flows or sheetfloods downslope. Confining walls in these channels usually are 1 to ≥4 m high (Fig. 14.12). Channel floors may be nearly flat or display low-relief erosional or depositional forms (Fig. 14.12). Water flows travelling through incised channels may deposit only the coarsest sediment fraction due to higher flow competency created by the channel wall confinement (Fig. 14.12c). Finer-grained sediment, including terraces (Fig. 14.12d), may accumulate on or lateral to these deposits during the waning flood stage or during smaller discharge events. Incised channels also will accommodate the passage of sediment-gravity flows, the falling-stage fraction of which may also be deposited in the channel (Fig. 14.12b). Winnowing of fines from the deposits left by the passage of these flows may leave a flat bed of cobbles and boulders (Fig. 14.12a).

SECONDARY PROCESSES ON ALLUVIAL FANS

The long periods of time between successive primary depositional episodes on alluvial fans expose the

surficial sediment to modifications by the secondary processes. These processes include reworking by water, aeolian activity, bioturbation, groundwater activity, particle weathering, and pedogenesis. The deposits may also be modified by neotectonic action such as faulting, tilting, or folding.

SURFICIAL REWORKING BY WATER

Discharge from rainfall or snowmelt in a fan drainage basin only infrequently produces a primary depositional event. On most occasions water discharge to the fan, whether of gentle or catastrophic character, is sediment-deficient. These discharge events, called overland flows (Horton 1945), may be capable of winnowing fine sediment from the surface of previous primary deposits (Fig. 14.13). Overland flows can occur in incised fan channels and on either active or inactive depositional lobes. The winnowed sediment typically is sand and clay but can range in size to pebbles and cobbles (e.g. Beaumont and Oberlander 1971). This sediment is moved farther down-fan, possibly even to neighbouring environments off the fan. The reworking of the surface of primary deposits on the fan by overland flows is the most widespread and active secondary process.

Erosive overland flows also result in the production of rills and headward-eroding gullies on the fan surface. Rills are initiated by the convergence of overland flow across the fan as a result of slight topographic or textural variations. They range from shallow features to channels with walls 10 to 50 cm high (Fig. 14.13e and f). A more advanced state of dissection produces gullies, which commonly occur on the distal fan and lengthen by eroding on their upslope end (Fig. 14.13f and g) (Denny 1967). The height of the gully walls may exceed 1 m (Denny 1965). A lag of the coarsest sediment fraction present in the primary deposit from which the fines have been removed typically covers the bottoms of the rills or gullies (Fig. 14.13b and c). Gullies or rills typically attain a distributary pattern that radiates down-fan either from the apex or the intersection point.

Calcite cementation of channel and gully walls or floors of a fan may result from the passage of water saturated with respect to calcium and carbonate. Precipitation from these waters can produce a hard, layered calcite cement termed case hardening. Lattman and Simonberg (1971) concluded from studies of fans near Las Vegas, Nevada, that case hardening occurs most commonly on fans derived from drainage basins underlain by carbonate or basic igneous bedrock, the weathering of which supplies abundant calcium ions, carbonate ions, and calcite-rich dust. This process can occur at a very fast rate, tightly cementing freshly exposed deposits in as little as 1 to 2 years (Lattman 1973).

AEOLIAN ACTIVITY

Exposed sand, silt, and clay on the fan surface are susceptible to erosion by wind, as demonstrated by the immense dust plumes visible in the atmosphere over deserts on windy days (Fig. 14.13f). One effect of this aeolian activity is to winnow the fine fraction until the fan surface is fortified by an immovable gravel layer called desert pavement, which protects the underlying material from further wind erosion (Fig. 14.13c and h) (Tolman 1909, Denny 1965, 1967, Hunt and Mabey 1966). The exposed gravel may be carved into ventifacts by abrasion from the passage of wind-carried sand (Fig. 14.13h).

A second effect of wind on a fan is the deposition of sand and silt as coppice dunes around plants, as isolated deposits upon the irregular fan surface (Fig. 14.13e), or as sandsheet deposits initiated by the effect of irregular topography on the windflow patterns. Aeolian deposits on alluvial fans may occur as thin accumulations of sand leeward of topographic irregularities or as relatively thick, laterally

Figure 14.13 Photographs of secondary processes on alluvial fans. (a) Surficial fine-fraction winnowing of a mud-cracked, clast-poor debris flow by subsequent overland water flows and wind erosion has left a lag of dispersed granules and fine pebbles. Furnace Creek fan, Death Valley. (b) View across an incised channel of a fan showing a 2-m-high vertical exposure of bouldery clast-rich debris-flow deposits. The deposit surface has had the fines removed by overland flow. Water flows in the channel (foreground) likewise have removed fines, leaving a bed of clast-supported gravel previously contained in the matrix-supported debris flows. North Badwater fan, Death Valley. (c) Side view of a gully on the Rose Creek fan, Hawthorne, Nevada, displaying debris flow deposits that have been winnowed at the surface by overland flow and wind. An incipient desert pavement resulted. (d) Extensive winnowing of bouldery debris flow deposits of the Shadow Rock fan, Deep Springs Valley, California, has produced a varnished, surficial boulder mantle. (e) Aeolian sand transported as wind ripples occurs in this rill on the Furnace Creek fan, Death Valley. (f) Gullies are prominent on the distal part of this fan near Titus Canyon, Death Valley. Note the dust plume in the valley centre generated by strong northerly winds achieving gusts of 80 km h^{-1}. (g) View of headward-eroding gullies (centre) on a fan in Death Valley. (h) Surface view of pebbly pavement created by wind erosion of the Bat Canyon fan, Amargosa Valley, California.

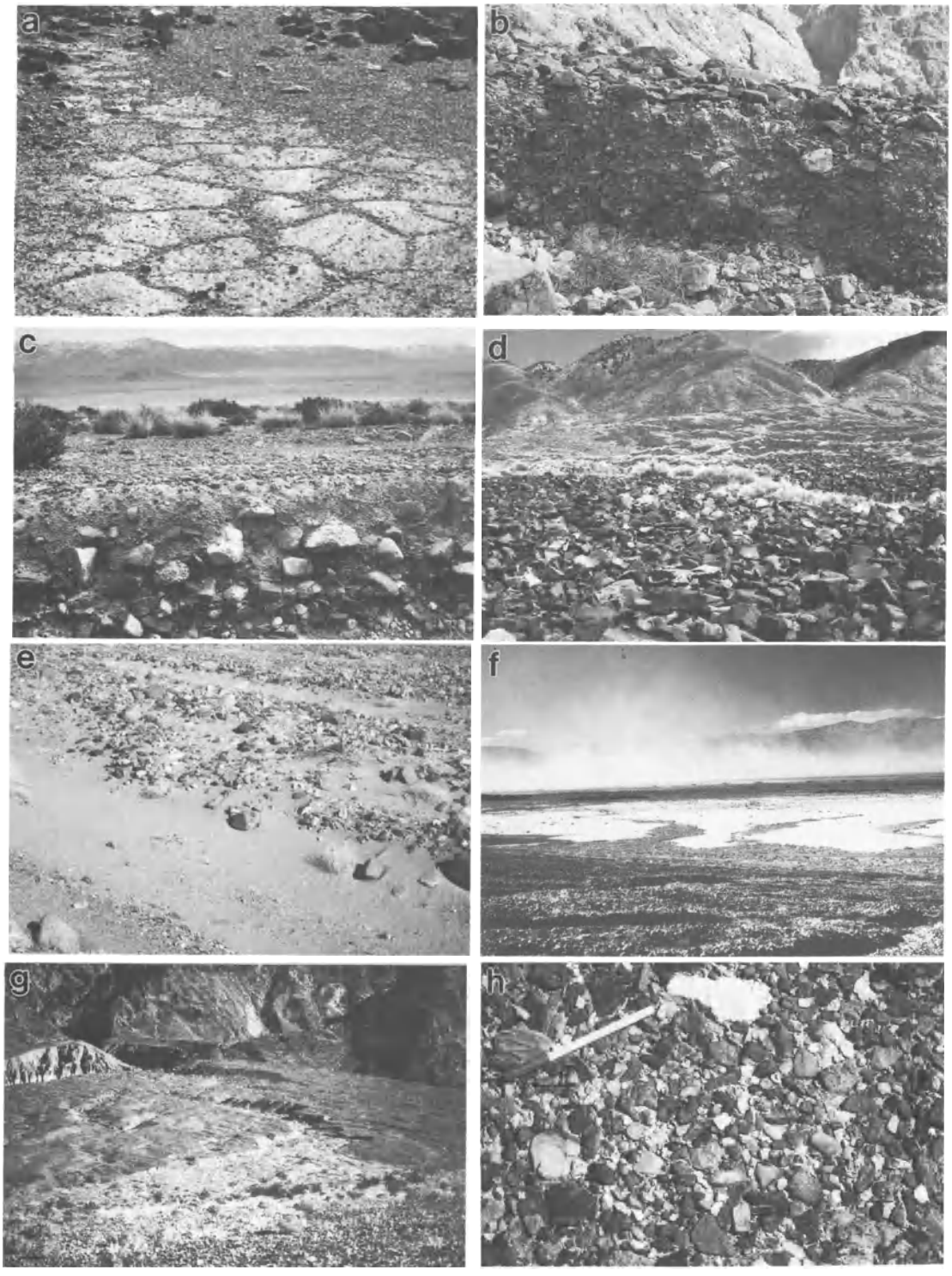
a
b
c
d
e
f
g
h

continuous sand blankets that disrupt or overwhelm fan sedimentation (e.g. Blair *et al.* 1990). In the most extreme case, aeolian sand dune complexes can migrate on to and cover the fan (Anderson and Anderson 1990).

BIOTURBATION

Plants and burrowing insects, arthropods, or rodents are common in surficial alluvial fan deposits in even the most arid deserts (Fig. 14.14a and b). Plant life commonly is sustained by shallow groundwater that is present in the fan sediment. Plant roots may extend for a metre or more into the fan sediment, disrupting the original primary stratification and homogenizing the deposits (Fig. 14.14a). The desert plants also provide a habitat for animals. Colonies of rodents amid desert plants on fans may significantly alter the deposits of the primary processes by disrupting stratification and dispersing sediment (Fig. 14.14b). Burrowers may also disturb the desert pavement, exposing previously protected sediment to wind erosion.

GROUNDWATER ACTIVITY

Alluvial fans serve as important aquifers for groundwater movement from the mountains to the valley floor, affecting the deposits in several ways. Groundwater discharge or flow near the surface of the distal fan can give rise to conditions conducive for plant growth. The slow movement of groundwater rich in dissolved solids may also result in the precipitation of cements such as calcite in the sediment pores (e.g. Bogoch and Cook 1974, Jacka 1974, Alexander and Coppola 1989). Travertine can precipitate on the fan where groundwater issues to the surface at springs (Hunt and Mabey 1966). The distal parts of fans in proximity to saline water bodies such as playas or marine embayments also may be cemented or disrupted by evaporite crystal growth in pores due to the evaporative draw of these fluids through the sediment. Groundwater flow may also destabilize slopes such as channel walls or fault scarps, instigating slumping (e.g. Alexander and Coppola 1989).

NEOTECTONICS

Inasmuch as alluvial fans optimally form along tectonically active mountain fronts, the deposits commonly are disrupted by seismic events. The most conspicuous result is vertical offset of fan sediment, creating scarps 0.5 to 40.0 m high (Fig. 14.14c). These scarps usually occur near and trend parallel to the mountain fronts, but also can be oriented obliquely to them and cut the distal fan (Wallace 1984a, Beehner 1990, Reheis and McKee 1991). The scarps create unstable, high-angle slopes that will degrade by creep, slumping, and freefall to produce fault-slope colluvial wedges (e.g. Wallace 1978, Nash 1986, Berry 1990). Faulting may disrupt groundwater flow through the fan sediment, possibly creating springs that may induce slumping along the scarp (Alexander and Coppola 1989). Scarps also readily instigate the development of headward-eroding gullies (Fig 14.14c).

Other types of neotectonic modification of fan sediment have been documented. Alexander and Coppola (1989) described 1-m-deep fissures in the proximal fan formed by seismic ground shaking. Mountain front faults with a strike-slip component, such as the San Andreas fault of southern California, cause folding of fan sediment (e.g. Butler *et al.* 1988, Rockwell 1988) or significant lateral offset of the fan from its drainage basin (e.g. Harden and Matti 1989) in a process referred to as beheading. Rotational tilting of fan deposits also is a common feature caused by dip-slip along listric mountain front faults (e.g. Rockwell 1988).

WEATHERING AND SOIL DEVELOPMENT

Many types of mechanical and chemical weathering modify alluvial fan sediment, including crystal growth in voids or mineral hydration along planes of weakness (Fig. 14.14d) (Hunt and Mabey 1966, Goudie and Day 1980). Fan sediment in the vicinity of caustic evaporite playas undergoes grain size reduction by salt crystal growth (Fig. 14.14e). Another common product of weathering includes the precipitation on clasts of thin hydrous manganese oxide coatings termed rock varnish (Fig. 14.14b and d) (Chapter 6). The thickness of the varnish and its darkness have been successfully used to differentiate the relative ages of various fan lobes (e.g. Hooke 1967, Dorn and Oberlander 1981, Slate 1991). Radiocarbon dating of this varnish also provides potential for obtaining absolute ages of fan surfaces (e.g. Dorn *et al.* 1989), although problems with this new method remain (e.g. Bierman and Gillespie 1991a, b, Bierman *et al.* 1991, Reneau *et al.* 1991). Alteration of the fan deposits by weathering also occurs immediately below the fan surface. Unstable grains such as ferromagnesium minerals or feldspars alter to finer-sized products through hydrolysis and oxidation (Walker 1967, Walker and Honea 1969). Clay-sized particles also are mechani-

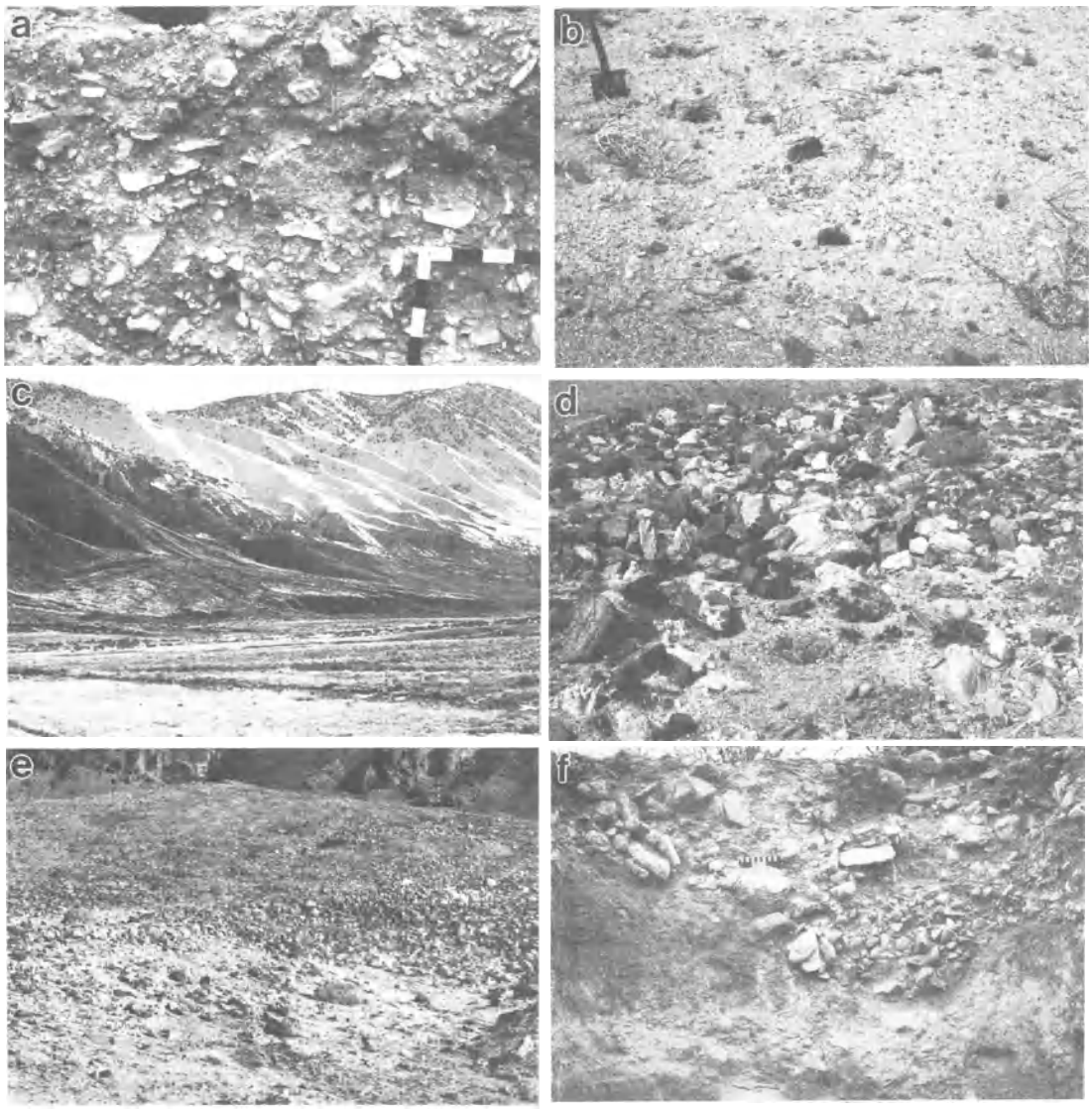

Figure 14.14 Photographs of secondary processes active on fans. (a) Gully cut of a proximal fan along the western Jarilla Mountains, south-central New Mexico. Gravelly fan and sandy aeolian deposits have been intermixed by plant root activity, resulting in the destruction of primary stratification. Reddened Bt (argillic) and white Btk (argillic and calcic) soil horizons are developed in this sediment. Pedogenic carbonate (white) extensively coats the gravel clasts. Scale bar increments are 10 cm. (b) Overview of a rodent colony comprising numerous burrows in near-surface fan sediment, Walker Lake, Nevada. Army shovel (upper left) for scale. (c) Three fault scarps ranging from 1 to 4 m high offset this fan in Deep Springs Valley, California. (d) Close-up of metamorphic cobbles located on the distal North Badwater fan in Death Valley. The clasts have been split by the growth of salt crystals along the foliation planes. (e) Overview of the distal North Badwater fan demonstrating the effect of grain size reduction due to salt weathering in proximity to the Badwater playa. (f) Vertical trench revealing well-developed carbonate soil horizons in a fan along the western Jarilla Mountains, New Mexico. Cobbles and pebbles of a filled gully are visible in the upper half of the photograph. Scale bar is 15 cm long.

cally added to sediment pores as the result of transportation by infiltrating water (Walker *et al.* 1978).

The long periods of time between successive depositional episodes makes the fan sediment, particularly in the inactive lobes, parent material for developing soils. Soil types found in desert fans result from the accumulation of horizons of clay, carbonate, silica, or evaporites such as gypsum (Fig. 14.14a and f). Carbonate and clay horizons are the most common soil horizon types encountered in the desert fans of south-western United States and south-eastern Spain (Gile and Hawley 1966, Gile *et al.* 1981, Christenson and Purcell 1985, Machette 1985, Harvey 1987, Wells *et al.* 1987, Mayer *et al.* 1988, Reheis *et al.* 1989, Berry 1990, Blair *et al.* 1990, Harden *et al.* 1991, Slate 1991). Gypsiferous and siliceous soils are less commonly documented in fan sediments (Reheis 1986, Al-Sarawi 1988, Harden *et al.* 1991). The extent of soil profile development in fan sediment is a function of time, the aeolian flux of the materials from which the horizon is composed, and the amount of precipitation (Machette 1985, Reheis 1986, Mayer *et al.* 1988). The presence of plant roots in the sediment also serves to instigate the accumulation of soil horizons produced by downward movement of percolating waters, including clay, carbonate, and gypsum. The extent of development of soil horizons in a given area, therefore, is useful for determining the relative age and correlation of fan deposits (e.g. Wells *et al.* 1987, Slate 1991).

Well-developed or tightly cemented soil B horizons, such as petrocalcic horizons that have become exhumed by erosion, serve to armour the fan from further secondary erosion (Lattman 1973, Gile *et al.* 1981, Van Arsdale 1982, Wells *et al.* 1987, Harvey 1990). These layers also expedite the downslope movement of overland flow by reducing the permeability of the surficial deposits.

SIGNIFICANCE OF DISTINGUISHING PRIMARY AND SECONDARY PROCESSES

Although the differences between primary and secondary sedimentary processes on alluvial fans were clearly illustrated decades ago (e.g. Beaty 1963, Denny 1967), most fan articles are written without an obvious appreciation of this distinction. One consequence has been the acceptance of the assumption that secondary processes, which usually dominate the fan surface, are the principal ones constructing the fan, rather than serving merely to remould and mask the primary processes (Blair 1987a). Two major problems arising from this assumption are the reality of sieve lobes and braided distributary channels on fans. A further complication has been introduced by those trying to equate fan activity to climatic or tectonic influences on the basis of the apparent process type without considering the ramifications of the intrinsic primary versus secondary sedimentary modes.

SIEVE LOBES ON ALLUVIAL FANS

The idea of sieve-lobe deposition on alluvial fans was proposed by Hooke (1967) based on laboratory studies of small-scale (radii ≤1-m-long) features constructed of granules and sand that morphologically resembled fans. Hooke identified in these modelling experiments a surficial deposit formed by the rapid infiltration of sediment-laden water discharged from the drainage basin. A lobate deposit, termed a sieve lobe, accumulated at the point where the water was unable to effect further transport due to complete infiltration into the permeable sandy substrate. This term was applied because the permeable laboratory sediment acted as a strainer or sieve that permitted water to pass while holding back the coarse material in transport. These deposits in the laboratory simulations had the coarsest materials (granules) at the front of the lobe, and were backfilled upslope by finer (sand-sized) sediment.

Although acknowledging that his laboratory studies may have no significance to real fan processes, Hooke concluded that sieve deposits like those observed in the laboratory comprise extensive facies on seven natural fans in south-eastern California. Four of these fans were identified, including the Trollheim and Shadow Rock fans in Deep Springs Valley, the Gorak Shep fan in Eureka Valley, and the North Badwater fan in Death Valley. These fans were reported to be constructed of material derived from drainage basins underlain by bedrock that did not weather to produce permeability-reducing fine-grained sediment such as clay. Based on Hooke's work, the sieve lobe mechanism has become established as one of the major processes operative on alluvial fans (e.g. Bull 1972, 1977, Dohrenwend 1987).

Our evaluations of the exposed stratigraphy of the four natural fans identified by Hooke as possessing sieve lobes revealed that the principal primary process by which these fans have been built is, without exception, debris flows (Fig. 14.15a and b). The drainage basin bedrock has weathered to produce abundant clay in all four of these cases. As a result, the fan deposits are rich in matrix fines (Fig. 14.15b)

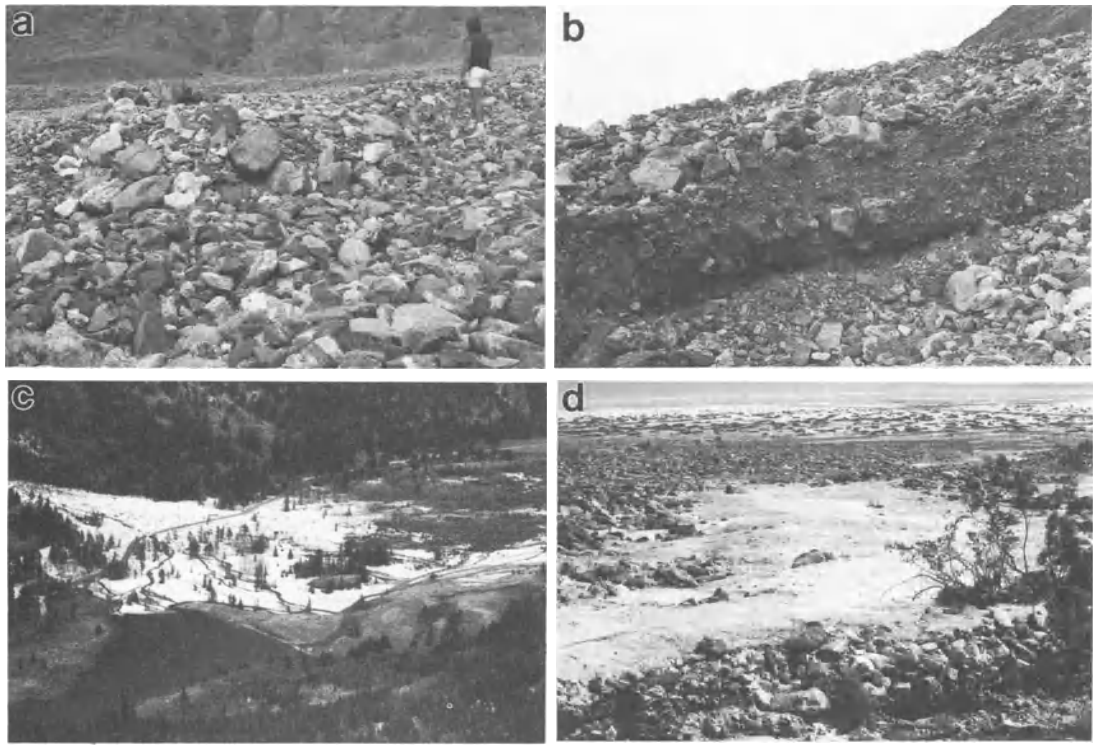

Figure 14.15 Photographs of purported sieve lobes, braided distributary channels, and masked sheetfloods. (a) Oblique view of one of the type sieve lobes (photograph centre), North Badwater fan, Death Valley. (b) View of vertical cut 1.5-m-high in a channel wall in the vicinity of Figure 14.15a. This view reveals matrix-rich debris flow deposits below a zone containing the identified sieve lobe. The fines have been removed from the surficial part of the debris flow lobes on this fan by overland flow, leaving an arcuate mass of winnowed gravel erroneously identified as a sieve lobe. (c) Overview of the Roaring River fan, Colorado. Braided distributary channels were carved into the fan surface underlain solely by sheetflood deposits. (d) View of light-coloured, clast-poor debris flows on the Trail Canyon fan, Death Valley. The presence of these flows within shallow channels gives a misleading braided distributary appearance to the fan (Figs 14.1a and 14.2a) when viewed from the distance (e.g. Nummedal and Boothroyd 1976).

and have low permeabilities, conditions that conflict with those listed by Hooke as necessary for sieve lobe development. Based on our examination of the identified sieve lobes on these natural fans, we alternatively conclude that these clast-supported, matrix-free lobate masses are the surficial part of clast-rich debris flow lobes from which the matrix has been removed by secondary overland flows. The lobate forms described by Hooke and observed on these fans are identical to the clast-rich debris flow lobe margins. Our interpretation is further substantiated by the presence at depth of matrix-supported debris flow deposits which have not been subjected to surficial winnowing and that still contain abundant interclast matrix (Fig. 14.15b). The existence of the sieve-lobe process on alluvial fans, therefore, remains only a hypothetical consideration.

BRAIDED DISTRIBUTARY CHANNELS ON ALLUVIAL FANS

Perhaps the greatest misconception concerning alluvial fans is the belief that they are constructed from braided distributary channel systems. This view results from the common presence of shallow channels with a distributary pattern on many fan surfaces. The idea especially was popularized by Bull (1972) who wrote (p. 66):

> 'Most of the water-laid sediments [of alluvial fans] consist of sheets of sand, silt, and gravel deposited by a network of braided distributary channels . . .. The shallow distributary channels rapidly fill with sediment and then shift a short distance to another location. The resulting deposit commonly is a sheetlike deposit of sand, or gravel,

that is traversed by shallow channels that repeatedly divide and rejoin . . .. In general, they [the deposits] may be crossbedded, laminated, or massive. The characteristics of sediments deposited by braided streams are described in detail by Doeglas (1962).'

Our analysis of the stratigraphic sequence of numerous fans displaying braided distributary channels reveals that these features invariably are surficial and formed either by incision during waning flood stage or through secondary winnowing and remoulding of primary deposits, including debris flows (Figs 14.13b, c, f, and 14.15b) and sheetfloods (Figs 14.11b, c, and 14.15c) (Blair 1987a). Furthermore, stratotypes described by Doeglas (1962) for braided streams, such as planar and trough crossbedding, are not found in vertical cuts of sediments associated with these braided distributary channels.

Other evidence commonly cited as support for the assumption that braided fluvial systems are responsible for fan construction includes the vivid depiction of braided distributary channels on aerial or oblique photographs of fans. An example of a fan reported to be built by braided distributary channel activity on the basis of this type of evidence is the Trail Canyon fan of Death Valley (Fig. 14.1a and 14.2a) (e.g. Nummedal and Boothroyd 1976). A field examination of this fan, however, reveals that the apparent light-coloured distributary channels present on photographs are shallow surficial features cut into the tops of debris flows by secondary processes, and that these channels are filled by clast-poor debris flows (Fig. 14.15d). An extreme consequence of the common misidentification of secondary channels as primary fan-building processes has been the reduction of alluvial fans to just a type of braided stream system (Miall 1978, p. 33).

Conversely, a failure to isolate the braided distributary channel features on alluvial fans as a secondary process has resulted in the inability of many researchers to clearly recognize the major constructive processes, such as sheetfloods and debris flows. This problem ensues despite the fact that the surficial carving of debris flow and sheetflood deposits is now well established (e.g. Beaty 1963, Lustig 1965, Johnson 1970, Blair 1987a). The surficial reworking of these primary deposits, combined with their long recurrence intervals, is probably why it was not until Blackwelder's (1928) paper that the importance of debris flows in fan construction was recognized (Costa 1984). Similarly, the masking of sheetfloods by surficial remoulding was concluded by Blair (1987a) to be the reason that sheetflooding, to this day, is not a more widely recognized fan-building process.

IMPLICATIONS FOR CLIMATIC AND TECTONIC EFFECTS ON FAN DEVELOPMENT

The enlargement of the incised channels on alluvial fans by downcutting (i.e. fanhead trenching) and the dissection of the fan surface by gullying have been attributed by many researchers to be a consequence of climatic change (e.g. Dohrenwend 1987). The fan sequences upon which dissection is occurring are believed to have accumulated during periods of different, usually more moist, past climates (e.g. Blissenbach 1954, Lustig 1965, Melton 1965, Williams 1973, Nilsen 1982, l985, Harvey 1984a, b, 1987, 1988, Dorn *et al.* 1987, Dorn 1988). Although the scientific validity of this oversimplified climate-response hypothesis has been questioned (e.g. Rachocki 1981), and the difficulty of establishing time stratigraphy and climate-sensitivity parameters remains, this hypothesis has been widely accepted. It is based on the idea that different, generally more moist, past climates resulted in greater sediment production in the drainage basin, and that aggradation concurrently took place as a result of the expedient transfer of this sediment to the fan. As a corollary, sediment production in the drainage basin is considered in this model to be retarded during periods of usually more arid climates, causing water flows to depart the drainage basin without sediment. The lack of sediment in these departing flows makes them highly erosive as they cross the fan, resulting in incised channel downcutting and gully formation.

Harvey (1984a, b, 1987, 1988), for example, noted that gullying of the fan surface and downcutting in the incised channels in his Spanish study area occurred upon older surficial deposits constructed by debris flows or sheetfloods. The change from active fan aggradation, indicated by debris flow or sheetflood accumulation, to the present state of dissection, as indicated by gullying and incised channel enlargement, was attributed to a reduction in sediment availability in the drainage basin triggered by climatic change from the middle Pleistocene to the present. This relationship, however, might more simply be interpreted as an intrinsic sedimentological process resulting from the surficial reworking by secondary processes of deposits from primary processes with low recurrence intervals. The largely non-tectonic setting of these Spanish fans and the relatively low relief of their drainage basins would suggest that the recurrence interval of catastrophic primary events is low, and that secon-

dary processes predictably would dominate the fan surfaces.

Another site where the activity of secondary processes has been proposed to be climatically induced is the Hanaupah and Johnson Canyon fans in Death Valley (Dorn *et al.* 1987, Dorn 1988). These fans currently exist under hyperarid conditions (Hunt *et al.* 1966). Dorn *et al.* (1987) proposed on the basis of carbon isotope data from rock varnish that aggradation probably occurred under semi-arid or even humid intervals of the Quaternary. Channel incision and gullying, it is suggested, took place during shifts towards aridity, including during the present arid cycle. This interpretation is based on at least three questionable assumptions. The first is that channel incision and gully development are not products of intrinsic sedimentological events on the fan, including falling-stage erosion or secondary surficial reworking by overland flows. A second assumption is that the fan drainage basins are completely devoid of sediment during relatively drier conditions. The presence of sediment within the drainage basins of the Hanaupah and Johnson Canyon fans and the common historical occurrence of debris flow events on fans in Death Valley, including one on the Trail Canyon fan (Fig. 14.3a), a neighbour of the Hanaupah fan, directly counter this assumption. In fact, active sedimentation on fans by primary processes throughout the south-western United States is strong evidence that they are dynamic features, not fossil forms inherited from wetter pasts (Beaty 1974). A third assumption by Dorn *et al.* (1987) is that climate shifts were drastic during the Quaternary, swinging in Death Valley between hyperarid and semi-arid, or even to humid. This conclusion is not supported by other investigators. For example, a runoff-response model by Mifflin and Wheat (1979) suggests that the widespread late Pleistocene pluvial lakes of the western Basin and Range province could have been generated and maintained by an increase in annual precipitation of 68% above the present and a 10% decrease in annual evaporation. This model predicts that hyperarid conditions would have persisted in Death Valley even during the more wet and cool late Pleistocene period. In conclusion, and as forewarned by Tolman (1909), our understanding of climatic change probably is too poorly understood at present to unequivocally attribute certain processes or stratigraphic sequences on alluvial fans to it, particularly when these features can more simply be explained by the intrinsic sedimentological processes of fan building.

Tectonic tilting of the proximal fans of Death Valley also has been proposed as an origin of incised channels (Hooke 1972), extending a hypothesis previously suggested by Eckis (1928) and Bull (1964a). Paradoxically, the fans used as examples by Hooke for tectonic arguments include the same two fans used by Dorn *et al.* (1987) for climate arguments. Although uplift of the proximal part of a fan would likely induce downcutting as proposed in Hooke's model, the cited fans in Death Valley do not show evidence that such deformation has occurred.

CONTROLS ON FAN PROCESSES

At least five key factors control or strongly influence the major sedimentary processes and deposits of alluvial fans: (a) the lithology and splitting properties of the bedrock underlying the drainage basin, (b) the shape and evolution of the drainage basin, (c) neighbouring environments, (d) climate, and (e) tectonism. These variables form a system of interacting feedback relationships that are exceedingly difficult to analyse or quantify due to their complexity and to their general lack of detailed study. The impact of each of these variables, however, can be demonstrated.

DRAINAGE BASIN BEDROCK LITHOLOGY

The type of bedrock in drainage basins from which sediment is derived has a significant impact on the primary alluvial fan process types. Rocks of differing lithology give rise to different sediment suites and volumes due to their variable response to weathering. Bedrock in desert settings optimal for fan development, especially tectonically maintained mountain fronts, produces sediment in varying sizes and amount depending upon (a) the style of fracturing in proximity to faults, (b) the presence or absence of internal discontinuities such as bedding planes or foliation planes, and (c) the reaction to chemical weathering and non-tectonic types of physical weathering. These variations are not fully understood and usually are seriously underestimated with respect to fan development. Their importance can be illustrated by a survey of sediment types found in fan drainage basins of the south-western United States underlain by differing bedrock lithologies.

Granitic plutons and gneissic rocks break into particles varying from sand to very coarse boulders in response to tectonically induced jointing and fracturing, exfoliation, and granular disintegration. The equidimensional and coarse grain-size of sediment on fans derived from granite results from the uniform joint pattern commonly developed in this

rock type due to its homogeneous, coarse-grained fabric. By contrast, gneissic rocks typically yield more tabular boulders due to the anisotropy imposed by the metamorphic foliation. Boulders from both of these lithologies are either angular, reflecting the joint pattern, or are more rounded depending upon the degree of chemical weathering along the edges of the joint blocks. Granules and sand-sized sediment (grus) also are a common product of the physical weathering of the granitic or gneissic rocks. In contrast, clay and silt-sized sediment usually are only minor products due to the low intensity of chemical weathering in deserts.

Bedrock consisting of tightly cemented dense sedimentary rocks such as quartzite undergoes significant brittle fracture in proximity to mountain-front faults, producing angular pebbles, cobbles, and boulders. Little sand, silt, or clay is produced in this situation due to the effective cementation of the matrix grains. Dense carbonate rocks also succumb to tectonism in a brittle fashion, producing gravel-sized angular blocks. If present, interstratified soft sedimentary rocks such as shale cause the intervening brittle rocks to fracture and weather to produce tabular gravel-sized clasts as well as a prominent clay fraction.

Finer-grained drainage basin bedrock lithologies such as pelitic metamorphic rocks, shale, mudstone, or volcanic rocks commonly weather to yield sediment varying in size from boulders to clay, with an abundance of the finer grain sizes and a deficiency of sand. Thickly mantled colluvial slopes comprising cobbles, pebbles, and clay are commonly developed on bedrock of this type.

The different reactions of the various lithologies in the drainage basin to physical and chemical weathering lead to different styles of erosion and transport of the liberated sediment. Colluvial landslides and cohesive debris flows are favoured by steep slopes and sediment containing significant clay. Debris flows, therefore, are very common on fans with drainage basins established in shale, mudstone, volcanic rocks, or pelitic metamorphic rocks. By contrast, debris flows are much less common in desert fans with drainage basins developed in non-clay-producing lithologies, such as granites or quartzites. Slopes in these latter lithologies are more apt to produce rock avalanches, rockfalls, non-cohesive debris flows, and sheetfloods. The desert fans of Spain studied by Harvey (1984b, 1988, 1990) illustrate the point. Fans derived from drainage basins underlain by high-grade metamorphic bedrock rarely contain debris flow deposits, whereas neighbouring fans derived from basins set in sedimentary or low-grade metamorphic rocks consist primarily of debris flow deposits.

The above examples represent the idealized condition where the drainage basin is underlain by one rock type. More complicated scenarios develop in the case of multiple drainage basin bedrock types. These complexities could result in interspersed and mixed process types based on which part of the drainage basin is eroding at any given time. Differing bedrock lithologies can also affect the rate of denudation of the colluvial cover of respective lithologies, as exemplified by the Nahal Yael drainage basin in Israel. Bull and Schick (1979) found that the grusy colluvial cover of the granitic rocks in this drainage basin has been completely stripped, whereas areas underlain by amphibolite have been only partly stripped due to the greater cohesion of the clayey colluvial mantle.

DRAINAGE BASIN SHAPE

The overall shape and evolution of the shape of an alluvial fan drainage basin can have a major impact on the operative sedimentary processes of the fan system. Basin shape affects slope values, feeder channel profile characteristics, relief, propensity for flashflood promotion, and storage capacity. Knowledge of the impact of these factors on fan construction is in its infancy (Fraser and Suttner 1986). Slope angles in concert with lithology type may determine whether rockfalls, rock avalanches, gravity slides, debris flows, or flashfloods are promoted in a drainage basin. The presence or absence of storage capacity in the drainage basin dictates how and when the sediment is delivered to the fan site. Relief may determine the size of sediment-gravity events that can be generated, whereas the elevation of the upper drainage basin may determine the chances of receiving significant precipitation via either rainfall or snowfall. The orientation of the drainage basin with respect to sunlight or the track of the major storms may also influence weathering, erosion, and transport activity, and thereby fan aggradation.

The ability of drainage basins to rapidly transmit or store sediment varies significantly with their areal size, which can range from a fraction of a square kilometre to hundreds of square kilometres. The smallest drainage basins may consist of only a single valley carved along a fracture in bedrock, with any collected discharge or dislodged clasts rapidly transferred to the fan. Feeder-channel incision and widening can proceed with time, allowing limited storage of primary deposits such as debris flows or colluvium. Progressively greater storage occurs with

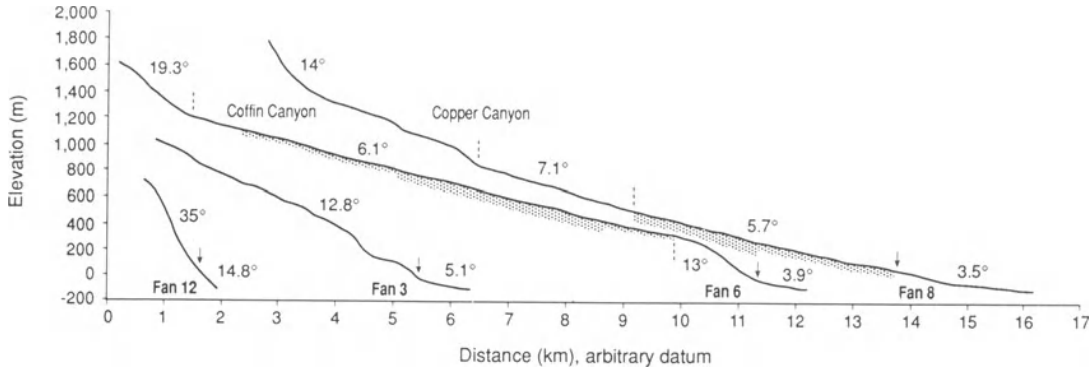

Figure 14.16 Long profiles of the feeder channels for four fans in the vicinity of Copper Canyon, Death Valley (see Fig. 14.17 for planview locations). Average slopes of the feeder channel or segments thereof are labelled. The stippled pattern denotes segments containing stored sediment. Zones of greatest sediment storage are denoted by the thickest pattern. Vertical exaggeration is 2.5. Vertical datum is mean sea level.

drainage basin enlargement because sediment can be maintained either as side-sloping colluvium or as deposits on the feeder-channel floor. The principal effects of sediment storage in the feeder channel are lower fan sedimentation rates and, in the extreme case, the trapping of sediment-gravity flows that do not have the runout capability to continue past the lower-gradient zones to the fan site. This selective trapping of sediment-gravity deposits increases the volume of fluid-gravity deposits at the fan site inasmuch as they can readily bypass the lower-gradient zones.

The volume of material stored in a feeder channel is variable, depending upon the long profile characteristics and the width of the reaches conducive to storage. Feeder channel long profiles can range from consistently steep to step-like (Fig. 14.16). The reaches of reduced slope in stepped feeder channel profiles may be sufficiently gentle to instigate deposition from catastrophic flows. The volume of material that can accumulate in these gently sloping reaches increases with increasing channel width. Two examples of feeder channels that have stepped profiles containing zones of sediment storage are the Coffin Canyon and Copper Canyon fans of Death Valley. Feeder channel erosion appears to be dominant in the reaches of these channels with slopes of greater than 7°, whereas at least some sediment aggradation has occurred in reaches with lesser slopes (Fig. 14.16).

The ability of the feeder channel to store sediment commonly increases with increasing drainage basin size, probably reflecting structural complexities in the underlying bedrock. This relationship is illustrated by the 14 neighbouring fans and cones located in the vicinity of Copper Canyon in south-eastern Death Valley. The drainage basins of these features vary in area from $<0.5\,km^2$ to $10\,km^2$ (Fig. 14.17). The two largest fans, Copper Canyon and Coffin Canyon, have relatively large drainage basins characterized by third- and fourth-order feeder channels (Fig. 14.17). Second-order channels make up the feeder channels in the four intermediate-sized drainage basins (numbers 1, 3, 4, and 9 of Fig. 14.17). The eight small fans or cones have equally small drainage basins containing just first-order channels (Fig. 14.17). Essentially all stored sediment in this region occurs in the two largest drainage basins (Copper and Coffin Canyons) and is concentrated in their highest-order channels (Fig. 14.17).

The initial shape of a fan's drainage basin and the basin's subsequent evolution are largely a product of (a) inherited local and regional structures and discontinuities such as faults, joints, and geological contacts, (b) newly imposed structural discontinuities, and (c) bedrock lithology. In general, fractured zones or other forms of geological discontinuities, whether inherited or newly created, become the locus of drainage basin development because these zones erode more quickly relative to adjoining ones. The significance of these variables, though poorly understood, can be demonstrated by the example from Death Valley. A comparison of the bedrock and structural geology in the drainage basins of the 14 fans and cones in the vicinity of Copper Canyon illustrates important interrelationships between fan and drainage basin evolution (Figs 14.17 and 14.18). One common relationship is the location of feeder channels, particularly in the area immediately upslope from the fan apex, directly along faults that trend at a high angle to the main mountain front faults (note fans 1, 2, 3, 4, 6, 7, and 9

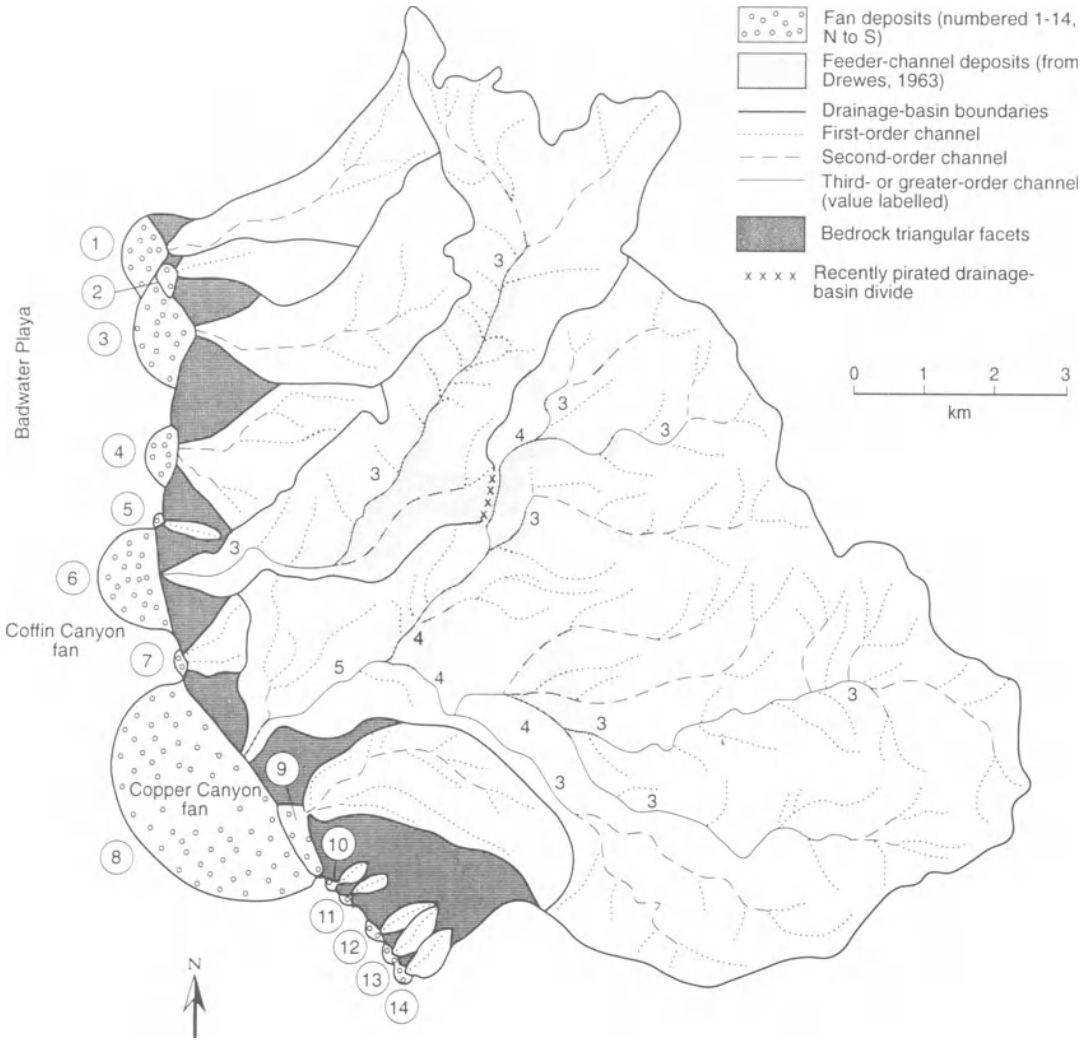

Figure 14.17 Channel distribution in the drainage basins of 14 alluvial fans and cones in the vicinity of Copper Canyon, south-eastern Death Valley. Uncircled numbers denote channel order, whereas patterned areas identify alluviated reaches of the feeder channels according to Drewes (1963). Circled numbers identify each of the 14 fans or cones.

in Figs 14.17 and 14.18). This relationship is caused by and illustrates the promotion of weathering and erosion along fracture zones. These zones likely represent structural discontinuities established prior to the onset of the present tectonic setting in which fan deposition is occurring. Another example of how inherited structures affect drainage basin and fan development is the Copper Canyon system. This basin is centred on a major down-dropped block, the surficial part of which is composed of relatively soft Miocene and Pliocene sedimentary rocks (fan 8, Figs 14.17 and 14.18). The resultant high sediment yield in this drainage basin has produced the largest fan in this sector of Death Valley. By contrast, fans or cones 5, 10, 11, 12, 13, and 14 (Figs 14.17 and 14.18) are relatively small, in large part because their drainage basins are developed along relatively unfractured anticlinal structures in Precambrian metasedimentary rocks. The lack of fracturing, relative youth of the structures, and low erodibility have resulted in, at most, only incipient fan and drainage development.

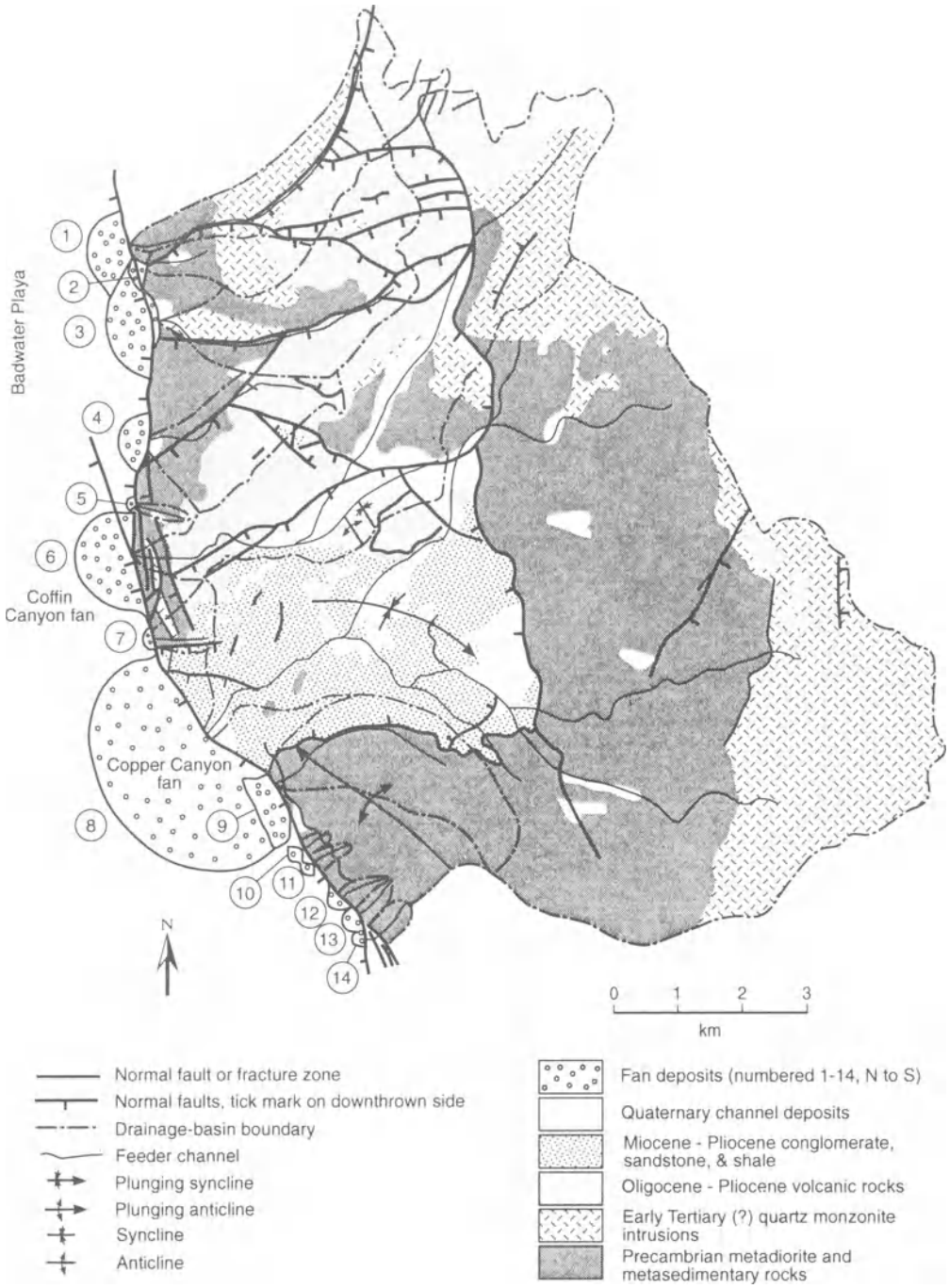

Figure 14.18 Bedrock and structural geology of the drainage basins of 14 alluvial fans and cones in the vicinity of Copper Canyon, Death Valley (after Drewes 1963). Fan feeder channels also are denoted.

EFFECTS OF NEIGHBOURING ENVIRONMENTS

Aeolian, fluvial, volcanic, lacustrine, or marine environments that border alluvial fans can impact the operative fan processes by modifying the conditions of deposition at the fan site. Aeolian activity can be detrimental where windblown deposits interfere with the fan processes. Aeolian sandsheet or dune complexes along the toes of fans commonly limit the runout distance of water flows or debris flows, inducing deposition in ponds (Fig. 14.19a). Aeolian deposits may migrate on to the medial or proximal fan, more seriously disrupting the primary depositional processes. The migration of a sand erg to the proximal part of the fans in northern Panamint Valley, California, for example, has caused debris flows to become impounded in the proximal zone, increasing the aggradation rate there at the expense of the distal region (Anderson and Anderson 1990).

Aeolian fine sand and silt also have greatly modified the primary processes active on alluvial fans in the Alamogordo area of south-central New Mexico. An influx of aeolian sediment during the middle Holocene has caused the sedimentary processes on the Alamogordo fan, located along the front of the Sacramento Mountains, to change from principally sheetflood to channelized flow (Fig. 14.19b). This change resulted from the cohesive strength of the invading silty aeolian sediment which led to bank stability, thereby favouring channelized flows rather than sheetfloods. In another case on the nearby western Jarilla Mountain piedmont, aeolian sandsheet deposition has been so high relative to fan activity that fan sedimentation has been reduced to just minor alluvial activity in isolated arroyos cut into the aeolian deposits (Blair *et al.* 1990).

Fluvial environments, usually in the form of longitudinally oriented ephemeral or perennial rivers, may alter fan processes by eroding their distal margins and steepening the overall slope. An example is where Death Valley wash has incised the toes of converging fans in northern Death Valley (Fig. 14.19c). Another example is from near Schurz, Nevada, where the Walker River has eroded part of the distal Deadman Canyon fan, distributing the sediment into the river's floodplain (Figs 14.1 and 14.19d).

The occurrence of either lacustrine or oceanic water bodies marginal to fans can have a profound effect on the fan processes. Subaerial fan flows quickly transform into other features, such as Gilbert-delta foresets, upon reaching a shoreline (Fig. 14.19e) (Sneh 1979, McPherson *et al.* 1987). This situation limits the runout distance of fan processes, causing aggradation higher on the fan than normally would occur. The slopes of the distal fan inundated by either lake or marine waters may be significantly steepened as the result of concentrated proximal fan aggradation or from erosion by waves or longshore currents (Fig. 14.19g). Subsequent drops in water level can expose oversteepened lower slopes, across which subaerial primary flows accelerate instead of the more common deceleration that occurs in the distal fan (Fig. 14.19h). Beach, longshore drift, or shoreface accumulations on these eroded margins (e.g. Link *et al.* 1985, Beckvar and Kidwell 1988, Newton and Grossman 1988), alternatively, may create benches or ridges that can locally impound the primary flows. Flat-lying evaporitic peritidal or playa environments may develop in the distal fan area (e.g. Hayward 1985, Purser 1987), inducing particle weathering and inciting primary fan flows to undergo deposition due to a pronounced slope reduction (Fig. 14.19h).

Volcanism may strongly affect fan processes by depositing ash either in the drainage basins or

Figure 14.19 Effects of neighbouring environments on alluvial fans. (a) Aeolian sandsheet deposits flanking the distal margins of the Shadow Rock and Trollheim fans, Deep Springs Valley. (b) Quarry cut 5-m-high in upper Holocene deposits of the medial Alamogordo Canyon fan, south-central New Mexico. An influx of aeolian sediment (light grey) changed the transportational processes of the fan gravels (dark grey) from sheetflooding in the lower part to channels in the upper part. This change was caused by the higher resistance of the loess to erosion, resulting in the maintenance of channel walls. (c) View of eroded toes (dark vertical walls, photograph centre) of converging fans in northern Death Valley. Erosion has been caused by the concentration of discharge in the longitudinally oriented Death Valley wash. (d) Erosion into the distal Deadman Canyon fan (vertical wall) resulted from the lateral migration of Walker River, near Schurz, Nevada. Geologist (upper centre) for scale. (e) Gilbert foresets approximately 3 m thick on the distal part of the Rose Creek fan near Hawthorne, Nevada. These foresets resulted from the transformation of debris flows upon their passage into the lake below a past shoreline. (f) View of fan along the Inyo Mountains in central Owens Valley that is completely covered by rugged Holocene basalt flows (black). (g) Extensive erosion by waves and longshore currents has occurred on the fans adjoining Walker Lake, Nevada. Vehicle (lower left) for scale. The now-exposed lower segments of these fans have a much greater slope than the upper segment due to this erosion. (h) Aerial view of the Coffin Canyon fan prograding into the flat Badwater playa in Death Valley. Individual debris flows (tongues extending from the distal margin) reaching this playa undergo deposition due to the rapid lowering of slope. Van (upper centre) for scale.

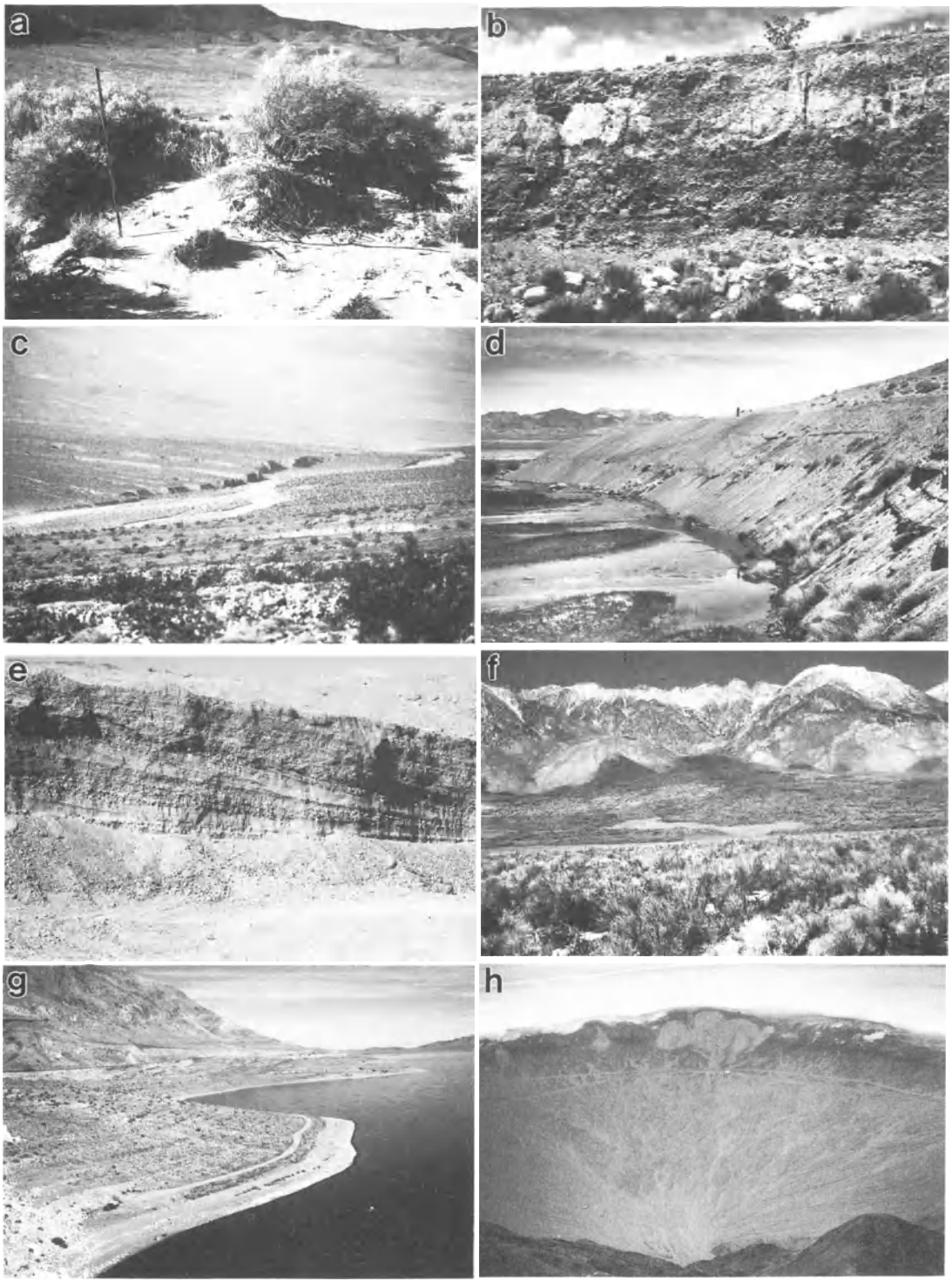
a
b
c
d
e
f
g
h

directly on the fan, causing an interference of flows at the fan site, and potentially instigating debris flows on steep drainage basin slopes (McPherson *et al.* 1985). Volcanic flows emanating from mountain front faults may also cause barriers to sediment transport on the fan surface, in extreme cases armouring the entire fan with almost unerodible basalt (Fig. 14.19f).

CLIMATIC EFFECTS

Climate is widely considered to be a major control on the types of sedimentary processes found on alluvial fans on the basis of net water availability, which affects bedrock weathering and sediment generation, potential sediment transport mechanisms, and vegetation cover. Research on the interaction between climatic variables and their effect on alluvial fan development remains in its infancy due to the complexities of this interaction and the overall lack of study. Two directions of research have emerged. One deals with the specific effects of climatic variables on sediment yield such as precipitation patterns, temperature, and vegetation. The second involves the relationships between fan processes and more broad climatic regimes of deserts versus non-deserts.

Effects of Climatic Variables on Fan Development

Three interrelated, climatically controlled variables that have received some assessment with regard to fans are precipitation amounts and patterns, temperature, and vegetation. All of these variables are relevant to fans inasmuch as they affect bedrock weathering rates, sediment yield, and the recurrence interval of catastrophic sediment transport from the drainage basin. The most basic aspect of precipitation is the mean annual amount, which affects weathering rates, vegetation, and transportational rates. Without rainfall, weathering and transportational events would be inoperative, and vegetation extremely sparse. However, even with minimal precipitation weathering and fan aggradation will take place, as exemplified by Death Valley with its very low 43 mm of annual precipitation.

Two other, and perhaps more significant, aspects of precipitation are the intensity of individual events and their frequency (e.g. Leopold 1951, Caine 1980). Both of these variables affect the infiltration capacity in the drainage basins, which must be exceeded before overland flow and potential sediment transport can commence. Infiltration capacity is exceeded and discharge events generated either by intense rainfall or by relatively normal rainfall following adequate antecedent precipitation (Ritter 1978, Cannon and Ellen 1985, Wieczorek 1987). Discharge is generated in the latter case if the infiltration capacity is unable to return to its original high value by slow percolation or evaporation. The effects that these aspects of precipitation may have on fan construction are profound. For example, areas of low precipitation, such as Death Valley, potentially can have more active fan accumulation than significantly more moist deserts because precipitation characteristically occurs in the more effective, high-intensity thunderstorm style. Alternatively, the sediment production rate in the drainage basin will likely be higher in more moist deserts (e.g. Langbein and Schumm 1958), making more sediment available for potential transport.

The effect that temperature has on fans is more poorly understood. It is likely significant, however, due to the fact that the rates of bedrock weathering reactions increase exponentially with temperature. Temperature gradients caused by the orographic conditions in a drainage basin may result in an initial decrease in weathering rates upslope due to decreasing temperature followed by an increase in weathering rates at higher altitudes as freeze–thaw processes become important. This trend may be complicated by the tendency for weathering rates to increase as precipitation increases with altitude.

Vegetation has long been considered an important control on sediment yield from a drainage basin. Inasmuch as vegetation reflects the climate, it is usually described as a climatic variable. One effect attributed to plant cover is an increase in the production of clay in the drainage basin due to the enhanced chemical weathering caused by organic acids in the vicinity of roots, and due to the greater preservation of soil moisture (e.g. Lustig 1965). Vegetation also affects sediment slope stability by strengthening its resistance to gravity as a result of the increased shear strength caused by rooting (Greenway 1987, Terwilliger and Waldron 1991). Differing plant types will have a variable effect on slopes due to the multitude of styles and depth of root penetration, and to the density of the ground cover (Terwilliger and Waldron 1991). Alternatively, plants may serve to produce long-term slope instability by causing the slopes to become steeper than they would be if the plant cover did not exist. This effect is illustrated by the common failure of slopes after vegetation is disturbed, such as after natural fires or from human-caused activities like agriculture (e.g. Wells 1987).

Relationships Between Fans and Broad Climatic Zones: the Question of 'Wet' and 'Dry' Fans

A second research direction with regard to the climatic control of fan development is characterized by attempts to associate the prevalence of certain process types operative on fans within the broad desert (dry) versus non-desert (wet) climate classification. The central point of discussion in this realm of research is the idea that debris flow processes are most prevalent on fans of arid and semi-arid climates, and water-flow processes in climates with greater rainfall. This hypothesis can be traced back at least to Blackwelder (1928), who attributed the lack of vegetation on drainage basin slopes, a feature best met in desert settings, as one of the criteria needed to optimize debris flow generation. A plethora of scientific articles has since negated this concept by clearly demonstrating the common occurrence of debris flows in non-desert settings around the globe (see Costa 1984 for a review). In fact, debris flows may be more common in the temperate and wet climates than in desert climates due to the greater production of clay from bedrock resulting from higher chemical weathering rates. Additionally, and as previously discussed, the presence or absence of debris flows on fans primarily is a function of the bedrock lithology and morphology of the drainage basin rather than of climate.

Unfortunately, there has been a rekindling of the notion of a climatic classification of alluvial fans during the last 15 years on the basis of assuming that certain processes are only effective under certain climatic conditions. For example, the adjectival terms 'dry' and 'mudflow' were introduced for fans 'formed by ephemeral stream flow', and 'wet' for fans 'formed by perennial stream flow' (Schumm 1977, p. 246). This relationship incorrectly assumes that fans traversed by perennial rivers cannot be dominated by debris flows, and that those traversed by ephemeral channels cannot be dominated by water flows. Further, the wet fan example provided by Schumm is the Kosi River of north-eastern India, a perennial river on an alluvial plain that lacks fan morphology and has an imperceptible slope of 0.02°. The geomorphologic and sedimentologic characteristics of the Kosi River are of a low-gradient river system that bears no resemblance to an alluvial fan (Rust and Koster 1984).

Subsequently, dry (debris flow) fans were classified as those formed in arid or semi-arid regions, and wet (or fluvial) fans as those formed in humid regions (McGowen 1979, p. 43). This association fails to acknowledge the presence of debris flows and water flows on fans in desert and non-desert settings alike. Like Schumm, McGowen envisaged wet fans as those dominated by fluvial deposits. However, the examples given, namely the Kosi River of north-eastern India and the braided proglacial streams of south-eastern Alaska (Boothroyd 1972), are simple fluvial systems unrelated to alluvial fans as either originally defined or in basic sedimentologic and morphologic character. The classification of the expanding reaches of the Alaskan proglacial braided river channels having average slopes of $<0.5°$ as fluvially dominated humid climate alluvial fans was made solely on the basis of a comparable planview braided distributary channel pattern. A marriage between Bull's (1972) 'braided distributary fan' concept and that of a fluvial-dominated, wet fan type (Boothroyd and Nummedal 1978, McGowen 1979) resulted. This fluvial or wet fan model is flawed in three respects: (a) the braided distributary channel pattern displayed on fans is a secondary rather than primary process, (b) the almost imperceptible slopes of proglacial braided rivers are readily distinguishable from their high-sloping alluvial fan counterparts, and (c) the principally lower-flow-regime conditions and resultant sedimentary structures of braided rivers, including trough and planar crossbedding, are easily differentiated from those occurring on fans, where deposition is mostly by catastrophic sediment-gravity processes or by fluid-gravity processes characterized by upper-flow-regime conditions. These fundamental differences in process and product between fans and fluvial systems are a direct reflection of the higher slope values of fans (2–20°) relative to fluvial systems ($<0.5°$).

TECTONIC EFFECTS

The most common and favourable conditions for the development and long-term preservation (especially with regard to the rock record) of alluvial fans exist in tectonically active zones that juxtapose mountainous uplands and lowland valleys. The creation and maintenance of relief by tectonism has an exponential effect on sediment yield by creating relief (Schumm 1963, 1977, Ahnert 1970). Without continued tectonism to maintain relief, fans may be minor and short-lived features, ultimately characterized by substantial secondary reworking. A possible example of well-studied fans of this style includes those in Spain developed adjacent to topographically expressed compressional structures formed prior to the middle Miocene (e.g. Harvey 1984a, 1988). This scenario contrasts with an active tectonic setting such as an extensional basin, where relief and the mountain-to-valley topographic configuration can be

maintained for ≥50 million years, and where individual fans may be active sites of net aggradation for 1 to 7 million years (e.g. Blair 1987b, Blair and Bilodeau 1988). Extensional and translational tectonic settings are most conducive to sustaining the optimal conditions for fan development, including the maintenance of relief and the stabilization of both the mountain front boundary and the fan site. The laterally moving structures of compressional tectonic regimes are much less conducive to fan development due to the unstable position of the mountain fronts, which, through time, result in the destruction of fan sites.

The more detailed characteristics of tectonism, including rates and occurrence of uplift, downthrow, and lateral displacement, will greatly influence the overall form and development of the fan and to a lesser degree the nature of the fan processes and deposits. Even within a singular tectonic regime, such as the extensional Basin and Range province, variations in tectonism at all scales can be reflected in the alluvial fans. Examples of fans reflecting small-scale variations in tectonism are those that have developed along the active range front fault in south-eastern Death Valley in the vicinity of Coffin Canyon (Figs 14.17 and 14.18). Subsidiary structures and inherited structures there have had an important effect on sediment yield and drainage basin development as demonstrated by the major variations in fan and drainage basin size. A larger-scale example of tectonic variation in the Basin and Range province that may affect fan development is provided by a map plotting the coeval ages of most recent faulting (Thenhaus and Wentworth 1982, Wallace 1984b). This map demonstrates numerous subprovinces differentiated on the basis of the age of the most recent fault activity, including those characterized by historical, pre-historical Holocene, late Quaternary, or pre-late Quaternary faulting. The map also illustrates the dynamic character of tectonism in a setting like the Basin and Range province.

Tectonism is also a major control on fan processes and deposits through the indirect and often complex influence it has on climate and vegetation in the drainage basin. For example, changing uplift rates may adjust elevation and, in turn, the climate and vegetation of the drainage basin, possibly causing changes in weathering or erodibility of the bedrock. As a result, the important fan variables of sediment supply rate, sediment calibre, and the water-to-sediment ratio may be altered, and these alterations may affect the primary sediment transport mechanisms.

ALLUVIAL FAN FORMS

Two classes of alluvial fan forms, constituent and composite, can be differentiated on the basis of origin and scale. Constituent forms are herein defined as morphological features that have resulted directly from the primary and secondary processes building and modifying the fan or from external effects such as faulting or interactions with neighbouring environments. The scale of the constituent forms is small, usually only a fraction of the size of the whole fan. These features contrast with the overall fan morphology, or the composite form, which represents the consequential or resultant shape of all of the constituent forms.

CONSTITUENT MORPHOLOGY

The most prominent constituent form on an alluvial fan usually is the incised channel, which may range from 2 to 150 m in width and have nearly vertical walls 1 to 20 m high (Figs 14.12 and 14.15b). The incised channel can extend down-fan from the apex for tens to hundreds of metres. Smaller forms may be present within incised channels, including terraces or debris flow plugs with relief of 0.5 to 1.5 m (Fig. 14.12d). Smaller-scale (≤0.5 m high) erosional forms such as rills or boulder deposits usually are present in this channel (Figs 14.12 and 14.13b). Clast-poor debris flows may also be present, producing a smoothed channel floor (Fig. 14.12b).

Many constituent morphological features on a fan have less than 2 m of relief and a lateral extent of several tens of metres. Rock avalanche tongues and clast-rich debris flow lobes and levees produce an irregular morphology, particularly in the proximal fan, with relief commonly of 0.5 m to 1.5 m (Fig. 14.10). Individual lobes may be 2 to 10 m across and extend tens to hundreds of metres in a down-fan direction (Fig. 14.10a). Jams of sheetflood boulders may also have a relief of 0.5 to 1.5 m and extend laterally for hundreds of metres. Erosive secondary forms, including gullies (Figs 14.10e and f, 14.11b, 14.13c, f, and g, 14.15c, and 14.19c) and winnowed mantles (Fig. 14.13d), may also produce features with this scale of relief and may extend laterally for several metres. In contrast, near-vertical fault scarps, developed as a result of offset of the fan sediment, can create walls up to 40 m high typically oriented parallel to and commonly occurring near the mountain front (Fig. 14.14c).

Lower-relief forms (≤0.5 m high) that extend laterally for tens to hundreds of metres also are common on fans. Rills produced by secondary erosion typical-

ly have a relief of less than 25 cm (Figs 14.13e and 14.15d). Rodent colonies may create mounds of sediment ≤50 cm high and several metres across (Fig. 14.14b). Sediment-deficient sheetfloods can produce transverse ribs 20 cm high distributed over whole fan lobes (Fig. 14.11d). Sediment-laden sheetflood and clast-poor debris flows may produce nearly smooth areas on the fan that can extend laterally for tens to hundreds of metres (Figs 14.10g, 14.11c and 14.13a). Smooth fan surfaces also can be formed by overland flow and aeolian winnowing (Fig. 14.13c and d).

Neighbouring environments may create externally induced constituent forms on the fans. For example, viscous volcanic flows such as basalt may irregularly cover fans, creating relief 0.1 to 3.0 m high and elongated parallel to fan slope (Fig. 14.19f). Aeolian sand-dune or sandsheet deposits 1 to 30 m high may migrate on to the fan, significantly altering its form (Fig. 14.19a). Coppice dunes create mounds 1 to 10 m across and 0.5 to 4.0 m high. Lateral migration by rivers may result in the erosion of distal fan sediment, leaving cuts 1 to 10 m high extending along the edge of the fan (Fig. 14.19d). Lake or marine water bodies impinging on the fan can also cause significant erosion of the fan margins or deposit shore-linear features such as spits, bars, and beach ridges (Figs 14.2c and 14.19g).

Constituent forms generally are not studied or portrayed in cross-fan or radial fan profiles because their relief (usually ≤2 m) is less than the contour interval commonly used on conventional topographic maps in mountainous terrain (typically 10 m). Constituent features such as incised channels, levees, and lobe boundaries, may be readily discernible if detailed maps with 1-m-interval contours are available (e.g. Fig. 14.20).

COMPOSITE MORPHOLOGY

The overall fan form, or composite morphology, is characterized by planview shape, the presence or absence of an incised channel, and radial and cross-fan profiles. Composite fan forms have been the subject of more study than the constituent forms because they can be identified using conventional topographic maps combined with aerial imagery.

Planview Shape and Incised Channels

The planview shape of an alluvial fan where it ideally is allowed to aggrade without lateral constrictions is semi-circular (Fig. 14.1d). Lateral constriction, however, usually occurs due to the presence of neighbouring fans, which cause the fan radii to become elongated perpendicular to the mountain front (Fig. 14.1b and c). Radial growth may also be limited by perennial lakes, marine embayments, aeolian sandsheets, or rivers that erode or overtop the distal fan. These distal environments can result in a preferential shortening of the fan radii perpendicular to the mountain front (Fig. 14.19g).

The presence or absence of a prominent incised channel on the proximal part of the fan is another important feature of the composite fan morphology. Such channels extend the fan's radial length by acting as conduits for water flows and sediment-gravity flows, positioning the active depositional lobe farther from the mountain front than on fans lacking incised channels. Their presence results in greater travel distances for primary processes, promoting fan extension by lobe progradation. Incised channels, therefore, are more likely to be present and have greater length on fans with progressively longer radii.

Radial Profiles

The radial fan profile is probably the most significant feature of the composite morphology inasmuch as it is a measure of the slope affecting sedimentary flows down the fan surface. The two main factors controlling the average slope and variations in slope along the radial profile are (a) the dominant processes operative on the fan and (b) the sediment size available for fan construction. The composite radial profile reflects the types of processes that build the fan inasmuch as differences in the physical properties of each process gives rise to deposits with varying slopes (Blissenbach 1954). Freefall accumulations such as talus form the steepest slopes, typically between 30 and 40° (Fig. 14.21). Freefall material mixed with other sediment-gravity flow types such as debris flows, rock avalanches, and gravity slides, create fan slopes ranging from 10 to 30° (Fig. 14.21). Clast-rich debris flows or bouldery sheetflood deposits more typically build fans with slopes between 5 and 15°, whereas fans dominated by sandy, pebbly, and cobbly sheetflooding or clast-poor debris flows have the lowest slopes, about 2 to 6° (Fig. 14.21). Distal accumulations such as sandskirts decrease the average fan slope, as do incised channels that promote aggradation in a progressively more distal direction (e.g. Drew 1873).

Another important factor in determining a fan's radial slope is the size of the sediment used to construct the fan (Tolman 1909, Blissenbach 1952). A direct relation exists between fan slope and gravel

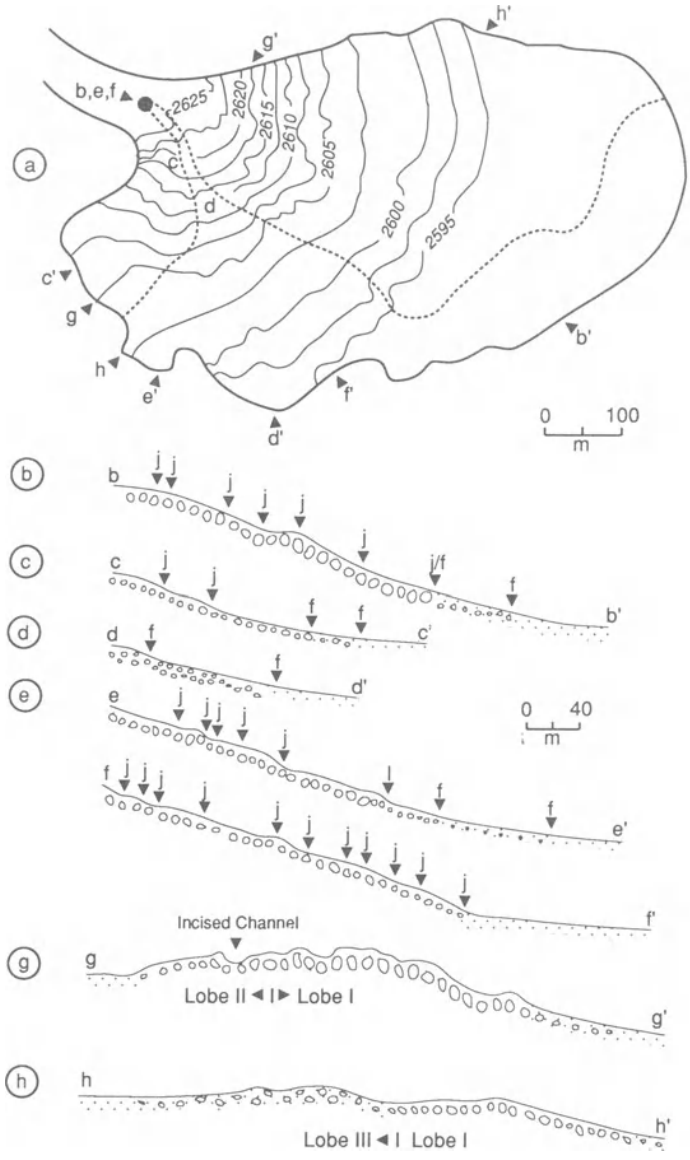

Figure 14.20 Radial and cross-profiles of lobes and transects of the Roaring River alluvial fan, with some constituent forms labelled (after Blair 1987a). Arrows point to segment boundaries, which are caused by boulder-log jams (j), facies changes (f), or lobe boundaries (l). Vertical exaggeration of the profiles is 2.5.

size, with fan slope increasing as grain size increases. The depositional slope of a fan sector underlain by boulder deposits, therefore, is greater than that of a fan sector underlain by pebbles or sand. An example of this relation is the sheetflood deposits of the Roaring River fan (Blair 1987a). The slope of this fan is 6 to 10° where underlain by boulders, 4 to 6° where fine boulders and cobbles are present, 2 to 4° in the sandy pebble gravel sector, and 1.4 to 2.0° in the distal sandskirt region (Fig. 14.20).

The radial fan profile also can be modified by erosional or depositional processes related to adjacent environments. Shoreface erosion by Walker Lake, for example, has steepened the distal part of some of the fans in this valley from 3.6° to 7.8° (Fig. 14.19g). In contrast, deposits by shoreline processes on parts of the neighbouring fans have lowered the

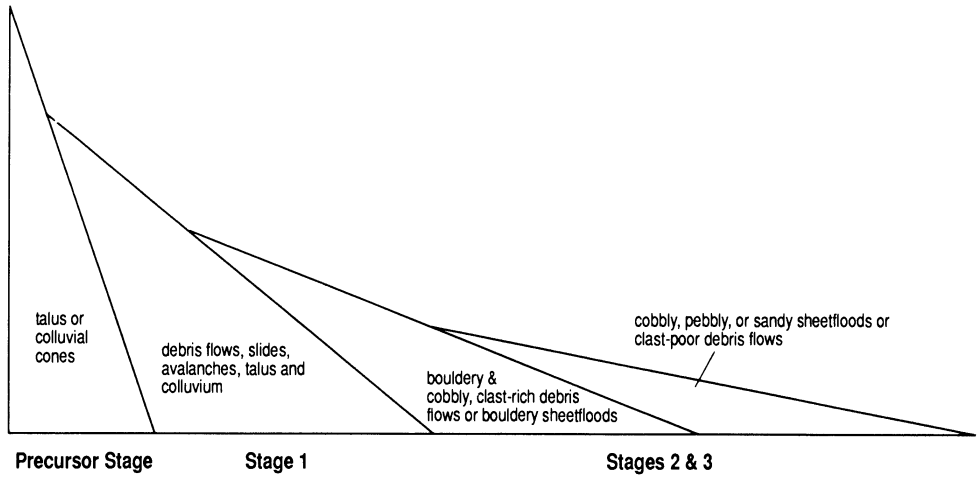

Figure 14.21 Schematic diagram of the slopes, drawn with a 2× vertical exaggeration, of various associations of primary processes commonly operative on alluvial fans. Depositional slopes increase towards the left, fan radii lengthen towards the right, and knickpoints decrease in elevation towards the right. Stages refer to the common depositional and morphological evolutionary schemes that fans ideally follow as they increase in size.

average fan radial slope or made it more irregular.

The radial profile of a fan not modified by neighbouring environments displays one of the following three styles: (a) a relatively constant slope, (b) a distally decreasing slope, which gives rise to a concave-upwards geometry, or (c) a segmented slope (Figs 14.5 and 14.20). Constant slopes are typical of fans in which only one primary process type is operative and where there is no marked decrease in grain size down-fan. The debris flow dominated fans of Death Valley demonstrate this relationship (Fig. 14.5). In contrast, fans with pronounced downslope decreases in grain size, such as from boulders to sand, are characterized by radial profiles with a concave-upwards geometry associated with distally decreasing slope values. The profile may be accentuated by radial variations in process type, such as from rock avalanche deposits in the proximal fan to sheetflood deposits in the distal fan.

Segmented fans are those with radial profiles characterized by two or more sectors, each with a constant slope angle, but with values that differ from the adjoining sectors, decreasing down fan (Bull 1964a). This profile type is similar to a distally decreasing one except that slopes change in value at inflection points rather than in an exponential fashion. Development of segmented profiles has been attributed to either a change in slope of the feeder channel caused by rapid and intermittent tectonic uplift of the mountains, base level change, or climate change (Bull 1964a). In the case of the western Fresno County fans, Bull (1962) favoured a change in channel slope due to uplift of the drainage basin. In contrast, segmentation of the radial profiles of fans in Death Valley has been attributed to tectonic rotation of the fans themselves (Hooke 1972). Blair (1987a), who was able to construct radial profiles of the Roaring River fan with the constituent forms identified, demonstrated that radial profile segmentation on this fan resulted from intrinsic causes, including (a) simply crossing from one fan lobe to the next along profile, (b) crossing from one constituent form to another along profile, or (c) from inflections in slope caused by sharp, down-fan changes in sediment size (Fig. 14.20). The same types of intrinsic sedimentological causes of segmentation present on the Roaring River fan may also have created this pattern on other fans where it has been attributed to the extrinsic effects of climate or tectonism (Blair 1987a).

Cross-fan Profiles

Cross-fan profiles, in contrast to radial profiles, are a poorly studied characteristic of the composite fan morphology. They generally have an overall plano-convex geometry, although variations exist. Cross-profiles from the upper part of the fan, for example, have greater amplitude than those from the lower fan (Fig. 14.4). The height of the cross-profiles may vary between fans due to differences in relief caused by changes in the grain size or the operative

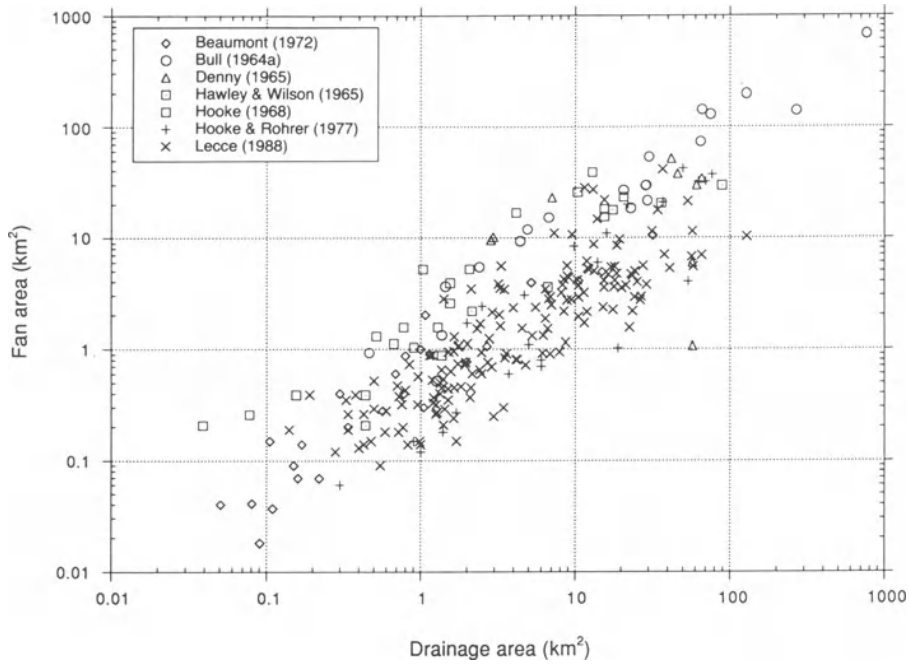

Figure 14.22 Log–log plot of drainage basin area versus fan area based on a compilation of data from published sources.

depositional process. Irregularities also may be caused by constrictive or erosive lateral environments (Fig. 14.4). Although essentially unstudied, cross-profiles also differ between fans as a result of the variable distribution of the constituent forms. On the Roaring River fan, for example, cross-profiles are asymmetric due to the spatial distribution of the lobes (Fig. 14.20). Variations in texture within individual lobes on this fan, such as in Lobe I, also cause irregularities in this cross-profile, as does the position of the incised channel.

MORPHOMETRIC RELATIONSHIPS BETWEEN ALLUVIAL FANS AND THEIR DRAINAGE BASINS

RELATIONSHIP BETWEEN FAN AREA AND DRAINAGE BASIN AREA

The most widely compared features of the composite fan and its drainage basin are their respective planview areas, which have a positive correlation (Fig. 14.22) (Bull 1962, 1964a, 1977, Denny 1965, Hawley and Wilson 1965, Hooke 1968, Beaumont 1972, Hooke and Rohrer 1977, French 1987, Lecce 1988, 1991). The association of small fans with small drainage basins and large fans with large drainage basins is intuitively obvious since the movement of sediment from the drainage basin to the fan serves to increase both the size of the fan and the size of the drainage basin. The relationship usually is given quantitatively as

$$A_f = cA_d^n$$

where A_f is the area of the fan, A_d is the area of the drainage basin, and c and n are empirically determined constants. The exponent n varies from 0.7 to 1.1, whereas c is even more erratic, ranging from 0.1 to 2.2 (Harvey 1990). Attempts also have been made to isolate the effect of variables on this relationship, usually with conflicting results. For example, Bull (1964a, b) concluded in his study of western Fresno County fans that drainage basins underlain by erodible lithologies such as shale produce larger fans per unit of drainage basin area than basins underlain by more resistant sandstone. In contrast, Lecce (1988, 1991) found that fans along the nearby western White Mountain front have greatest area per unit of drainage basin area where derived from very resistant bedrock such as quartzite.

It is clear from the data plotted in Fig. 14.22 that there is a general trend of increasing fan area with

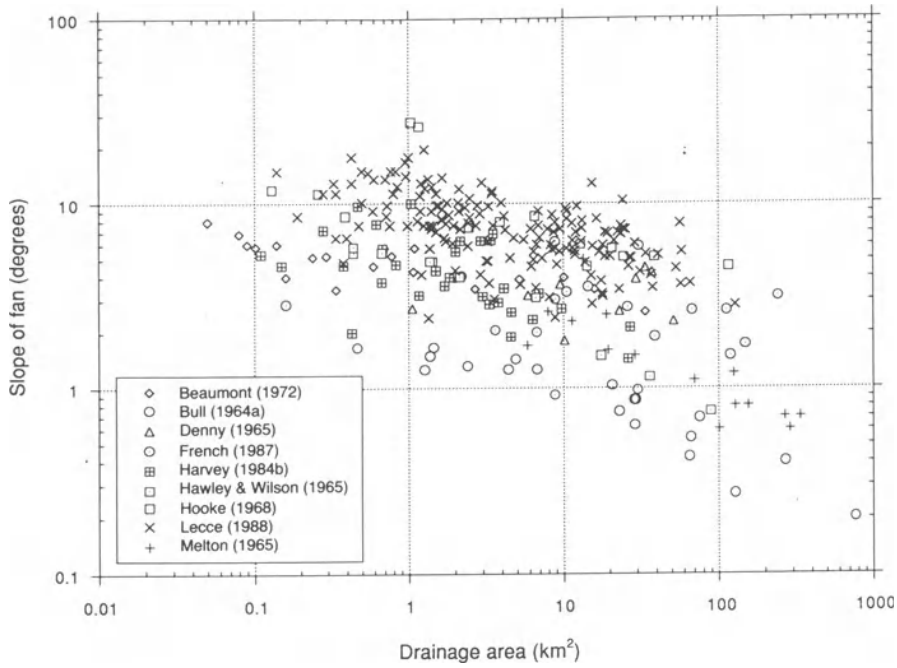

Figure 14.23 Log–log plot of average fan slope versus drainage basin area based on a compilation of data from published sources.

drainage basin area. The wide scatter of the data, however, indicates that this relationship is exceedingly more complex than has been suggested. First, there is an obvious problem of whether the assumption of comparing only the planview areas of three-dimensional features has mathematical merit (Lustig 1965). Second, it should not be surprising that this relationship is more complex than portrayed when the multitude of variables affecting the fan area and drainage basin area are considered. Variables such as drainage basin relief and altitude, fan relief and depth, stream piracy in the drainage basin, tectonic beheading of fans, the operative sedimentological processes, the effects of inherited and local structures or geological discontinuities, the drainage basin bedrock lithology, the degree of aerial constriction of the fans, and the interplay of environments that border the fans all combine to greatly influence fan area and drainage basin area.

FAN GRADIENT VERSUS DRAINAGE BASIN SIZE

Drew (1873) observed that fans with relatively large drainage basins had lower average slopes than those with smaller drainage basins. This relation has been quantified by others during the last 30 years (e.g. Bull 1962, 1964a, Denny 1965, Hawley and Wilson 1965, Melton 1965, Hooke 1968, Beaumont 1972, French 1987, Harvey 1987, Lecce 1988, 1991) and is demonstrated by a plot of the average fan slope versus the drainage basin area (Fig. 14.23). This relationship reflects the greater storage capacity of larger drainage basins and its effect on primary process types active on the fan. Also, fans with progressively longer radii have progressively lower slopes due to the distal progradation of active depositional lobes via a progressively elongating incised channel. The wide scatter of the compiled data (Fig. 14.23) reveals, however, that there are other variables not accounted for in this plot. As previously discussed, drainage basin area is not a good proxy for the volume of the material eroded from the drainage basin. Moreover, the multitude of variables such as bedrock geology and the relief in the drainage basin can have an important impact on the operative primary processes and size of liberated sediment, and these factors directly affect average fan slope. Thus, like the fan area versus drainage basin area plot, the average fan slope versus drainage basin area plot serves to demonstrate an obvious trend but does not account for the details of the system.

GENERAL FAN TYPES

Despite the inherent complexities, alluvial fans can be grouped into two types on the basis of the dominant operative primary processes and the resultant constituent and composite fan morphologies. Each of these two types can further be subdivided based on the relevance of secondary reworking by overland flows.

TYPE I ALLUVIAL FANS

Type I fans are constructed principally of cohesive clast-rich and clast-poor debris flows, which may or may not have an active incised channel in their upper segment (Fig. 14.8b). Colluvial slides, bedrock slides, rock avalanches, and rockfalls may also be active primary processes. The main constituent forms include lobes and levees of clast-rich debris flows and smoothed surfaces of clast-poor debris flows. Lobate or irregular masses from gravity slides, rock avalanches, or rockfalls may be present locally. The average slope of these fans varies from 5 to 15°, with radial profiles most commonly maintaining a constant slope. More steeply dipping colluvial cones are present in the proximal fan area.

Due to the low recurrence interval of the debris flow activity on Type I fans, surfaces away from the active depositional lobe and even the active depositional lobe itself widely display the effects of secondary processes. Dominating the secondary processes are the surficial winnowing of the exposed debris flow tops by overland flow and wind to produce gullies, rills, or a hummocky gravel mantle. Gullies and rills are present if the maximum clast size is cobbles or pebbles; a hummocky mantle of winnowed deposits results if boulders are present. A braided distributary pattern commonly results from this secondary erosion.

Type I fans are produced in deserts from drainage basins underlain by bedrock that weathers to produce sufficient matrix clay. Such bedrock includes pelitic metamorphic rocks, sedimentary rocks containing shale interbeds, and most volcanic rock types. Weathering of these lithologies under desert conditions also produces boulders, cobbles, pebbles, silt, and clay, but little sand. Distal sandskirts, therefore, usually are not present and sand interbeds in the proximal part of the fan are absent. Boulders are relatively small unless interbeds of more brittle clasts such as carbonate or quartzite are present in the drainage basin. Drainage basins are relatively steep and mantled by colluvium. Examples of this fan type are the South Badwater fan in Death Valley and the Dolomite fan in Owens Valley, California (Figs 14.1d and 14.10). Sand may locally be present in minor amounts in the debris flows of Type I fans where granitic plutons have intruded the low-grade metamorphic, volcanic, or shaley terranes. An example of this scenario is the Deadman Canyon fan of Walker Lake, Nevada (Fig. 14.1c).

The extent of secondary reworking of the debris flows in a Type I fan typically is minor, resulting in a stratigraphic record characterized dominantly of stacked debris flows separated by minor winnowed gravel lags produced mainly by rill or gully erosion. The drainage basin conditions of some debris flow dominated fans, in contrast, are conducive to the production of minor to catastrophic, sediment-deficient overland flows capable of extensively winnowing previously deposited debris flows, particularly in proximity to the fan apex or intersection point. This scenario develops where fan drainage basins are especially large, or where clay production in the drainage basin is retarded due to the bedrock lithology. The resultant effect at the fan site is the extensive winnowing of fine sediment from the primary debris flows by secondary overland flows, creating a stratigraphy characterized by interbedded debris flows, coarse, non-sorted gravel lags with common outsized clasts, and bedded granules and pebbles. Examples of this fan type are the Furnace Creek, Trail Canyon, and Hanaupah fans of Death Valley, California (Fig. 14.1a). This distinctive debris flow dominated fan type is designated Type IB, in contrast to debris flow dominated fans characterized by minimal secondary reworking and designated Type IA.

TYPE II ALLUVIAL FANS

Fluid-gravity flows and their waterlain deposits are dominant on Type II fans (Fig. 14.8a). Hyperconcentrated sheetfloods and incised channel flows are common, whereas rockfall, rock avalanche, and non-cohesive debris flow deposits may be present locally. Incised channels typically contain cobbles and boulders, whereas sheetflood deposits vary in grain size from boulders to sand in a down-fan direction. Sandy interbeds are common in the gravelly sheetflood deposits. A prominent sandskirt rims the lower part of the fan where neighbouring environments detrimental to its preservation are not present. Primary constituent forms in the proximal fan include the incised channel and non-cohesive debris flow or rock avalanche levees. The fan surface in general is relatively smooth, especially in contrast to Type I fans. The average slope of the Type II fan is between 2 and 8°, with a progressive down-fan

lessening of slope corresponding to a reduction down-fan in grain size. The resultant radial pattern is either concave-upwards or segmented.

Secondary processes are dominant on Type II fans due to the relative ease of erosion of the surficial sediment and the infrequency of catastrophic primary events. The carving of rills and gullies with a braided distributary pattern by non-catastrophic overland flows is the most prevalent result of secondary erosion. Other secondary modifications include aeolian winnowing or deposition, bioturbation, soil development, and particle weathering. As with its Type I counterparts, the degree of secondary winnowing by overland flows may vary from minimal to extensive. A Type IIA designation is given to the minimal reworking case; a Type IIB designation is applied to the extensive reworking case. Unlike their Type I counterparts, this subdivision is less easy to make due to a similarity in the resulting facies types.

Type II fans are most commonly produced in deserts where the drainage basins are underlain by fractured and jointed granitic plutons and gneiss or by friable gravelly sandstone. Weathering of these rock types under desert conditions liberates sediment of all sizes ranging from coarse boulders to very fine sand. Silt and clay, however, are produced in amounts so small that debris flows are not easily generated. Drainage basin slopes are either mantled by pebbles and sand or contain partially dislodged boulders and cobbles. Flashflood or snowmelt events produce catastrophic water flows and non-cohesive debris flows from the diverse calibre of available sediment. Examples of Type II fans are the Roaring River fan in Colorado, fans derived from the Sierra Nevada in Owens Valley, California, and the fans derived from the Smith Mountains in Death Valley (Figs 14.11 and 14.12c).

ALLUVIAL FAN EVOLUTIONARY SCENARIOS

Given the considerations reviewed in this chapter and a freshly formed topographic setting conducive to fan development, such as an active normal fault along an extensional basin, the following idealized four-stage evolutionary scenario for fan development through time can be envisaged. This scenario reflects the progressive enlargement of the fan and the concomitant evolution of its drainage basin.

PRECURSOR FAN STAGE: TALUS CONE FORMATION

The first accumulations at the base of a newly created, sharp valley margin are talus or colluvial cones. Sediment is funnelled through a V-shaped fault-controlled crook that may enlarge to become a fan drainage basin. The talus cones are steep (commonly 30 to 40°) and do not extend far from the mountain front (Figs 14.9b and 14.21). Examples of this stage are the cones present along the active fault zone in south-eastern Death Valley (Fig. 14.9b). Not all talus cones will be succeeded by the development of alluvial fans; probably most will not. However, those positioned at the mountain front where sediment continues to be focused evolve to become part of an incipient fan (Fig. 14.24a).

STAGE 1: DEVELOPMENT OF THE FAN FOUNDATION (INCIPIENT FANS)

Incipient fans differ from talus cones by containing deposits of clast-rich debris flows, rock avalanches, or gravity slides in addition to the freefall material. They also bear a more fan-like shape. The slopes of incipient fans are still relatively steep (10 to 25°), but have lower slopes than those of talus cones (Fig. 14.21). A marked contrast (knickpoint) in slope angles is exhibited where the incipient fan has breached a precursor-stage cone (Fig. 14.24a). Incipient fans also extend significantly farther outward (commonly 0.5 km) from the mountain front than do the precursor talus cones (Fig. 14.24a).

A Stage 1 fan consists of debris flow and winnowed debris flow deposits with mixtures of other sediment-gravity deposits where the drainage basin bedrock weathers to produce ample clay (Type I incipient fan) (Fig. 14.24a). In contrast, where bedrock weathering produces clay-deficient sediment, the deposits consist of rock avalanche, non-cohesive debris-flow, sheetflood, and minor debris flow deposits (Type II incipient fan) (Fig. 14.24b). In either case, these deposits create the ramp-like foundation necessary for the subsequent development of fans with more common composite morphologies.

STAGE 2: DEVELOPMENT OF COMMON COMPOSITE FAN MORPHOLOGY

Stage 2 of development of either Type I or Type II alluvial fans is characterized by the creation of more gentle average radial slopes (3 to 15°) resulting from a reduced input by all mass wasting processes except debris flows. Fan construction occurs primarily as debris flows on Type I fans and sheetfloods with admixtures of non-cohesive debris flows in Type II fans (Figs 14.21 and 14.24c). Primary flows from the drainage basin issue on to the active depositional lobe either directly at or near the fan apex. The primary deposits commonly are subjected to secon-

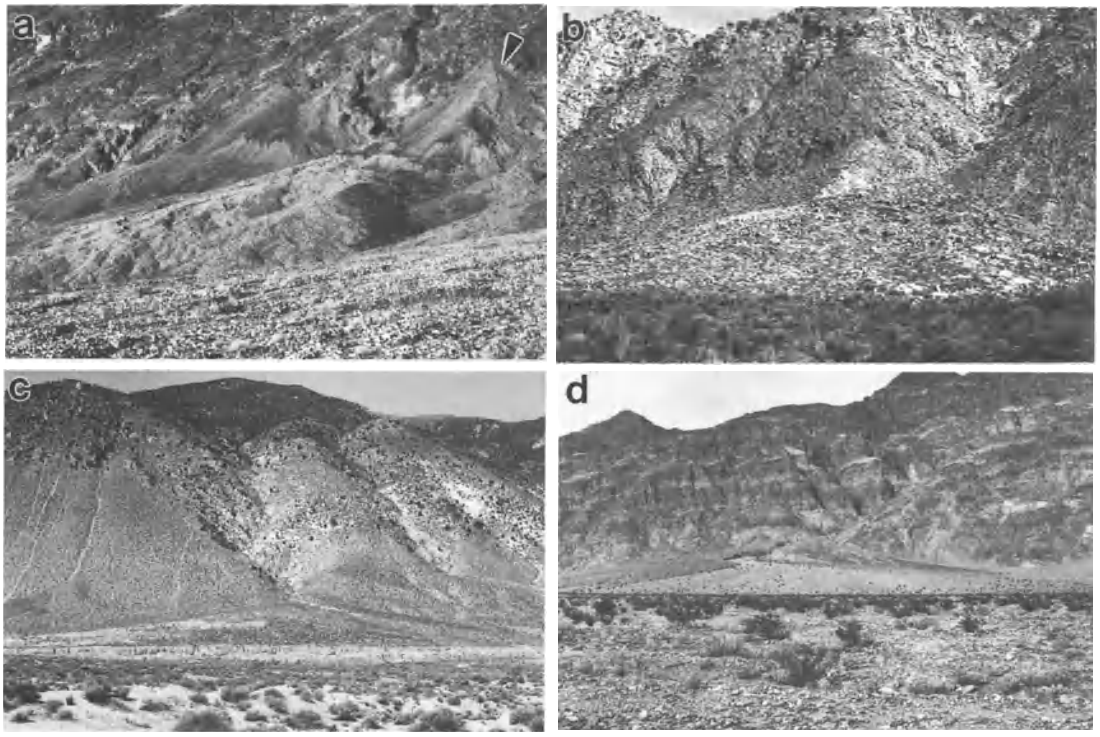

Figure 14.24 Photographs illustrating the stages of fan development. (a) View of a Stage 1 fan from Death Valley. A precursor colluvial cone (arrow) was breached during the development of this incipient fan. (b) Development of Stage 1 fan in eastern Deep Springs Valley by rock avalanche and non-cohesive debris-flow transportation from the fractured and jointed granitic bedrock of the drainage basin. (c) View of the Rifle Range fan, Hawthorne, Nevada, displaying Stage 2 development. (d) Example of Stage 3 fan development characterized by a prominent incised channel; Titus Canyon fan, Death Valley. This fan is prograding by progressive downslope movement of the active depositional lobe (light coloured).

dary processes, especially rill erosion and gullying that carve surficial braided distributary channels. Radial lengths of Stage 2 fans are greater than those of Stage 1 fans but are still relatively short, commonly less than 3 km (Fig. 14.24c).

STAGE 3: FAN PROGRADATION SCENARIOS

The third stage of development of both Type I and Type II fans is characterized by radial enlargement from the progradation of active depositional lobes outward from a progressively lengthening incised channel (Fig. 14.24d). The radii of fans in this stage are commonly 2 to 10 km long. The major primary and secondary processes operative during Stage 2 remain the same for Stage 3, including debris flows (Type I fans) and sheetfloods (Type II fans). The unique feature of Stage 3 is the development of a prominent incised channel that extends a significant distance (≥1 km) below the fan apex. This feature causes debris flows or water flows to remain confined on the upper fan, allowing for their accumulation in more distal settings. Average fan slopes are lowered to 2 to 8° due to the down-fan movement of the locus of deposition (Figs 14.21 and 14.24d).

BASIN VARIATIONS IN FAN EVOLUTION

The rate of progression through the three stages of development varies from one fan to another. The achieved stage of even neighbouring fans may differ due to variations in drainage basin features such as fracture density and relief. An example from the vicinity of Titus Canyon in northern Death Valley has adjacent fans displaying all three stages of evolution. The largest and most advanced (Stage 3) is the Titus Canyon fan (Fig. 14.24d). This fan has a drainage basin built around a very prominent structure oriented perpendicular to the mountain front (Reynolds 1974). This drainage basin also contains

numerous other geological discontinuities that induce weathering and the generation of flows that transport material to the fan, rapidly enlarging the drainage basin. In contrast, neighbouring fans display developmental Stages 1 or 2 depending on the position of their drainage basins with respect to minor discontinuities in the uplifted block. The fans in the vicinity of Copper Canyon in Death Valley also exemplify this scenario (Fig. 14.18). The largest and most developed (Stage 2) fans have the largest and most structurally complex drainage basins from which significant sediment is produced. The smallest fans in this area, in contrast, have small and unstructured drainage basins and have reached only Stage 1 in their evolution.

The typical fan stage does bear consistency along basin margins. For example, the fans in southeastern Death Valley exhibit Stages 1 or 2 of development, whereas the fans across the valley along the Panamint Mountains all have reached Stage 3 (e.g. Fig. 14.3a and d). This relationship is caused by active and recent offset along the mountain-front fault on the eastern side of the basin, which has caused lacustrine transgression and burial of fans, initiating a new tectonic cycle (Blair 1985, 1987b). In contrast, the Stage 3 fans along the Panamint Mountains have been developing for a significantly longer period of time due to their position along the inactive side of the asymmetric Death Valley half graben.

CONCLUSIONS

Alluvial fans are common landforms of deserts, occurring where a channel emerges from an upland drainage basin to a tectonically controlled mountain front and valley. Primary processes that construct fans are rockfalls, rock avalanches, gravity slides, debris flows, and confined or unconfined flashfloods, all of which are most commonly instigated by sporadic and catastrophic heavy rainfall or snowmelt. The types of processes active on a fan are dictated by precipitation characteristics, drainage basin bedrock geology, morphology and enlargement history of the drainage basin, and the effect of neighbouring environments on the fan site. Fan sediment is surficially modified under more normal conditions by secondary processes, including overland water flows, wind erosion, soil development, particle weathering, bioturbation, and groundwater movement. The fan sediment may also be faulted or tilted due to tectonic activity.

The constituent morphology of a fan is a direct result of the operative primary and secondary processes. Constituent forms include debris flow lobes and levees, incised channels, smooth surfaces, rills, and gullies. The overall fan form, or composite morphology, represents the sum of all of the constituent forms. Composite morphology is characterized by a fan-shaped planview, convex cross-profiles, and radial profiles that have either a consistent slope or down-fan decreasing slope that produces a concave-upwards geometry. Fan slopes depend upon grain size variations and the types of processes operative on fans, both of which are primarily dictated by the characteristics of the drainage basin.

Desert fans are divided into two general types. Type I fans are constructed principally of clast-rich and clast-poor cohesive debris flows and may also have an incised channel. They commonly are produced by drainage basins underlain by volcanic, clayey sedimentary, or pelitic metamorphic rocks that weather to produce significant clay. Type II fans are built mostly by fluid-gravity flows, including incised channel flows and sheetfloods, along with rock avalanches or non-cohesive debris flows. They are the more common product of drainage basins yielding little clay, such as granitic terranes. Secondary reworking of the Type I or II alluvial fans ranges from minor to extensive. A Type IA or IIA designation is given where the reworking is minor; a Type IB or IIB designation is given where the reworking of the primary processes by overland flows is extensive.

Drainage basin enlargement through time results in a predictable three-stage evolutionary scenario for alluvial fans, which follows a precursor stage. The precursor stage entails the accumulation of a talus or colluvial cone at the base of a bedrock notch. If a drainage basin becomes established by the enlargement of this notch, processes such as rock avalanches, debris flows, and gravity slides may occur in addition to rockfalls, leading to an incipient or Stage 1 alluvial fan. The ramp-like foundation upon which the more common composite fan morphologies form is produced during this stage. Debris flows and sheetflooding dominate the construction of fans during Stages 2 and 3, leading to decreased average slopes. Incised channels are not present or are very short in Stage 2 fans, whereas they are prominent and characterize Stage 3 fans. The presence of well-developed incised channels is a result of the progressive growth of the fan through lobe progradation. This overall evolutionary scenario results in fans that both lengthen and decrease in slope through time in concert with their drainage basin enlargement.

REFERENCES

Ahnert, F. 1970. Functional relationships between denudation, relief, and uplift in large mid-latitude drainage basins. *American Journal of Science* **268**, 243–63.

Alexander, D. and L. Coppola 1989. Structural geology and dissection of alluvial fan sediments by mass movements: an example from the southern Italian Apennines. *Geomorphology* **2**, 341–61.

Al-Sarawi, M. 1988. Morphology and facies of alluvial fans in Kadhmah Bay, Kuwait. *Journal of Sedimentary Petrology* **58**, 902–7.

Anderson, S.P. and R.S. Anderson 1990. Debris-flow benches: dune-contact deposits record paleo-sand dune positions in north Panamint Valley, Inyo County, California. *Geology* **18**, 524–7.

Anstey R.L. 1965. *Physical characteristics of alluvial fans.* Natick, MA: Army Natick Laboratory, Technical Report ES-20.

Anstey, R.L. 1966. A comparison of alluvial fans in west Pakistan and the United States. *Pakistan Geographical Review* **21**, 14–20.

Beaty, C.B. 1963. Origin of alluvial fans, White Mountains, California and Nevada. *Annals of the Association of American Geographers* **53**, 516–35.

Beaty, C.B. 1974. Debris flows, alluvial fans, and revitalized catastrophism. *Zeitschrift für Geomorphologie* **21**, 39–51.

Beaty, C.B. 1989. Great boulders I have known. *Geology* **17**, 349–52.

Beaty, C.B. 1990. Anatomy of a White Mountain debris-flow – the making of an alluvial fan. In *Alluvial fans – a field approach.* A.H. Rachocki and M. Church (eds), 69–90. New York: Wiley.

Beaty C.B. and C.M. DePolo 1989. Energetic earthquakes and boulders on alluvial fans: Is there a connection? *Bulletin of the Seismological Society of America* **79**, 219–24.

Beaumont, P. 1972. Alluvial fans along the foothills of the Elburz Mountains, Iran. *Palaeogeography, Palaeoclimatology, Palaeoecology* **12**, 251–73.

Beaumont, P. and T.M. Oberlander 1971. Observations on stream discharge and competence at Mosaic Canyon, Death Valley, California. *Bulletin of the Geological Society of America* **82**, 1695–8.

Beckvar, N. and S.M. Kidwell 1988. Hiatal shell concentrations, sequence analysis, and sealevel history of a Pleistocene alluvial fan, Punta Chueca, Sonora. *Lethaia* **21**, 257–70.

Beehner, T.S. 1990. Burial of fault scarps along the Organ Mountains fault, south-central New Mexico. *Bulletin of the Association of Engineering Geologists* **27**, 1–9.

Berry, M.E. 1990. Soil catena development on fault scarps of different ages, eastern escarpment of the Sierra Nevada, California. *Geomorphology* **3**, 333–50.

Beverage, J.P. and J.K. Culbertson 1964. Hyperconcentrations of suspended sediment. *Proceedings of the American Society of Civil Engineers, Journal of the Hydraulics Division,* **90**(HY6), 117–28.

Bierman, P. and A. Gillespie 1991a. Range fires: Accuracy of rock-varnish chemical analyses: implications for cation-ratio dating. *Geology* **19**, 196–9.

Bierman, P. and A. Gillespie 1991b. Range fires: a significant factor in exposure-age determination and geomorphic surface evolution. *Geology* **19**, 641–4.

Bierman, P., A. Gillespie and S. Huehner 1991. Precision of rock-varnish chemical analyses and cation-ratio ages. *Geology* **19**,135–8.

Blackwelder, E. 1928. Mudflow as a geologic agent in semi-arid mountains. *Bulletin of the Geological Society of America* **39**, 465–84.

Blair, T.C. 1985. Nonmarine sedimentological response to tectonism in rift basins: a comparison of the Jurassic Todos Santos Formation, Chiapas, Mexico, with Quaternary deposits in Death Valley, California. Golden, CO: *Society of Economic Paleontologists and Mineralogists Annual Midyear Meeting* **II**, 11–12.

Blair, T.C. 1987a. Sedimentary processes, vertical stratification sequences, and geomorphology of the Roaring River alluvial fan, Rocky Mountain National Park, Colorado. *Journal of Sedimentary Petrology* **57**, 1–18.

Blair, T.C. 1987b. Tectonic and hydrologic controls on cyclic alluvial fan, fluvial, and lacustrine rift-basin sedimentation, Jurassic–lowermost Cretaceous Todos Santos Formation, Chiapas, Mexico. *Journal of Sedimentary Petrology* **57**, 845–62.

Blair, T.C. and W.L. Bilodeau 1988. Development of tectonic cyclothems in rift, pull-apart, and foreland basins: sedimentary response to episodic tectonism. *Geology* **16**, 517–20.

Blair, T.C., J.C. Clark and S.G. Wells 1990. Quaternary stratigraphy, landscape evolution, and application to archeology; Jarilla piedmont and basin floor, White Sands Missile Range, New Mexico. *Bulletin of the Geological Society of America* **102**, 749–59.

Blissenbach, E. 1952. Relation of surface angle distribution to particle size distribution on alluvial fans. *Journal of Sedimentary Petrology* **22**, 25–8.

Blissenbach, E. 1954. Geology of alluvial fans in semi-arid regions. *Bulletin of the Geological Society of America* **65**, 175–90.

Bogoch, R. and P. Cook 1974. Calcite cementation of a Quaternary conglomerate in southern Sinai. *Journal of Sedimentary Petrology* **44**, 917–20.

Boothroyd, J.C. 1972. Coarse-grained sedimentation on a braided outwash fan, northeast Gulf of Alaska. *University of South Carolina Coastal Research Division Technical Report* 6-CRD.

Boothroyd, J.C. and D. Nummedal 1978. Proglacial braided outwash: a model for humid alluvial fan deposits. In *Fluvial sedimentology*, A.D. Miall (ed.), 641–68, Calgary: Canadian Association of Petroleum Geologists Memoir 5.

Bull, W.B. 1962. Relations of alluvial fan size and slope to drainage basin size and lithology in western Fresno County, California. *U.S. Geological Survey Professional Paper* 450-B.

Bull W.B. 1964a. Geomorphology of segmented alluvial fans in western Fresno County, California. *U.S. Geological Survey Professional Paper* 352-E.

Bull, W.B. 1964b. History and causes of channel trenching in western Fresno County, California. *American Journal of Science* **262**, 249–58.

Bull, W.B. 1972. Recognition of alluvial fan deposits in the stratigraphic record. In *Recognition of ancient sedimentary environments*, J.K. Rigby and W.K. Hamblin (eds), 63–83. Tulsa: Society of Economic Paleontologists and Mineralogists Special Publication 16.

Bull, W.B. 1977. The alluvial fan environment. *Progress in*

Physical Geography **1**, 222–70.

Bull, W.B. and A.P. Schick 1979. Impact of climatic change on an arid watershed: Nahal Yael, southern Israel. *Quaternary Research* **11**, 153–71.

Burchfiel, B.C. 1966. Tin Mountain landslide, south-eastern California, and the origin of megabreccia. *Bulletin of the Geological Society of America* **77**, 95–100.

Butler, P.R., B.W. Troxel and K.L. Verosub 1988. Late Cenozoic history and styles of deformation along the southern Death Valley fault zone, California. *Bulletin of the Geological Society of America* **100**, 402–10.

Caine, N. 1980. The rainfall intensity – duration control of shallow landslides and debris flows. *Geografiska Annaler* **62A**, 23–7.

Campbell, R.H. 1975. Soil slips, debris flows, and rainstorms in the Santa Monica Mountains and vicinity, southern California. *U.S. Geological Survey Professional Paper* 851.

Cannon, S.H. and S. Ellen 1985. Abundant debris avalanches, San Francisco Bay region, California. *California Geology*. December, 267–72.

Christenson, G.E. and C. Purcell 1985. Correlation and age of Quaternary alluvial-fan sequences, Basin and Range province, southwestern United States. In *Soils and Quaternary geology of the southwestern United States*, D.L. Weide (ed.), 115–22. Boulder: Geological Society of America Special Paper 203.

Costa, J.E. 1984. Physical geomorphology of debris flows. In *Developments and applications of geomorphology*, J.E. Costa and P.J. Fleisher (eds), 268–317. Berlin: Springer.

Costa, J.E. 1988. Rheologic, geomorphic, and sedimentologic differentiation of water floods, hyperconcentrated flows, and debris flows. In *Flood geomorphology*, V.R. Baker, R.C. Kochel and P.C. Patton (eds), 113–22. New York: Wiley.

Cotecchia, V. 1987. Earthquake-prone environments. In *Slope stability*, M.G. Anderson and K.S. Richards (eds), 287–330. Chichester: Wiley.

Denny, C.S. 1965. Alluvial fans in the Death Valley region, California and Nevada. *U.S. Geological Survey Professional Paper* 466.

Denny, C.S. 1967. Fans and pediment. *American Journal of Science* **265**, 81–105.

Derbyshire, E. and L.A. Owen 1990. Quaternary alluvial fans in the Karakoram Mountains. In *Alluvial fans – A field approach*, A.H. Rachocki and M. Church (eds), 27–54. New York: Wiley.

Doeglas, D.J. 1962. The structure of sedimentary deposits of braided rivers. *Sedimentology* **1**, 167–93.

Dohrenwend, J.C. 1987. Basin and Range. In *Geomorphic systems of North America*, W.L. Graf (ed.), 303–42. Boulder: Geological Society of America Centennial Special Volume 2.

Dorn, R.I. 1988. A rock-varnish interpretation of alluvial-fan development in Death Valley, California. *National Geographic Research* **4**, 56–73.

Dorn, R.I. and T.M. Oberlander 1981. Rock varnish origin, characteristics, and usage. *Zeitschrift für Geomorphologie* **25**, 420–36.

Dorn, R.I., M.J. DeNiro and H.O. Ajie 1987. Isotopic evidence for climatic influence of alluvial-fan development in Death Valley, California. *Geology* **15**, 108–10.

Dorn, R.I., A.J.T. Jull, D.J. Donahue, T.W. Linick, *et al.* 1989. Accelerator mass spectrometry radiocarbon dating of rock varnish. *Bulletin of the Geological Society of America* **101**, 1363–72.

Drew, F. 1873. Alluvial and lacustrine deposits and glacial records of the Upper Indus Basin. *Geological Society of London Quarterly Journal* **29**, 441–71.

Drewes, H. 1963. Geology of the Funeral Peak Quadrangle, California, on the east flank of Death Valley. *U.S. Geological Survey Professional Paper* 413.

Eckis, R. 1928. Alluvial fans in the Cucamonga district, southern California. *Journal of Geology* **36**, 111–41.

Ellen, S.D. and R.W. Fleming 1987. Mobilization of debris flows from soil slips, San Francisco Bay region, California. In *Debris flows/avalanches: process, recognition, and mitigation*. J.E. Costa and G.F. Wieczorek (eds), 31–40. Boulder: Geological Society of America Reviews in Engineering Geology 7.

Fauque, L. and M.R. Strecker 1988. Large rock avalanche deposits (Strurzstrome, sturzstroms) at Sierra Aconquija, northern Sierras Pampeanas, Argentina. *Ecologae Geologae Helvetae* **81**, 579–92.

Fisher, R.V. 1971. Features of coarse-grained, high-concentration fluids and their deposits. *Journal of Sedimentary Petrology* **41**, 916–27.

Fraser, G.S. and L. Suttner 1986. *Alluvial fans and fan deltas*. Boston: International Human Resources Development Corporation.

French, R.H. 1987. *Hydraulic processes on alluvial fans*. Amsterdam: Elsevier.

Fryxell, F.M. and L. Horberg 1943. Alpine mudflows in Grand Teton National Park, Wyoming. *Bulletin of the Geological Society of America* **54**, 457–72.

Gile, L.H. and J.W. Hawley 1966. Periodic sedimentation and soil formation on an alluvial-fan piedmont in southern New Mexico. *Soil Science Society of America Proceedings* **30**, 261–8.

Gile, L.H., J.W. Hawley and R.B. Grossman 1981. Soils and geomorphology in the Basin and Range area of southern New Mexico – guidebook to the Desert Project. *New Mexico Bureau of Mines and Mineral Resources Memoir* 39.

Goudie, A.S. and M.J. Day 1980. Disintegration of fan sediments in Death Valley, California by salt weathering. *Physical Geography* **1**, 126–37.

Greenway, D.R. 1987. Vegetation and slope stability. In *Slope stability*, M.G. Anderson and K.S. Richards (eds), 187–230. Chichester: Wiley.

Harden, J.W. and J.C. Matti 1989. Holocene and late Pleistocene slip rates on the San Andreas fault in Yucaipa, California, using displaced alluvial-fan deposits and soil chronology. *Bulletin of the Geological Society of America* **101**, 1107–17.

Harden, J.W., J.L. Slate, P. Lamothe, O.A. Chadwick, *et al.* 1991. Soil formation on the Trail Canyon alluvial fan. *U.S. Geological Survey Open-File Report* 91-296.

Hart, M.W. 1991. Landslides in the Peninsular Ranges, southern California. In: *Geological excursions in southern California and Mexico*, M.J. Walawender and B.B. Hanan (eds), 349–71. San Diego: Geological Society of America annual meeting field guidebook.

Harvey, A.M. 1984a. Aggradation and dissection sequences on Spanish alluvial fans: influence on morphological development. *Catena* **11**, 289–304.

Harvey, A.M. 1984b. Debris flow and fluvial deposits in Spanish Quaternary alluvial fans: implications for fan morphology. In: *Sedimentology of gravels and conglomerate*, E.H. Koster and R.J. Steel (eds), 123–32. Calgary: Canadian Society of Petroleum Geologists Memoir 10.

Harvey, A.M. 1987. Alluvial fan dissection: relationship between morphology and sedimentation. In *Desert sediments: ancient and modern*, L. Frostick and I. Reid (eds), 87–103. London: Geological Society of London Special Publication 35.

Harvey, A.M. 1988. Controls of alluvial fan development: the alluvial fans of the Sierra de Carrascoy, Murcia, Spain. *Catena Supplement* **13**, 123–37.

Harvey, A.M. 1990. Factors influencing Quaternary fan development in southeast Spain. In *Alluvial fans – a field approach*, A.H. Rachocki and M. Church (eds), 247–70. New York: Wiley.

Hawley, J.W. and W.E. Wilson 1965. Quaternary geology of the Winnemucca area, Nevada. *University of Nevada Desert Research Institute Technical Report* 5.

Hayden, B.P. 1988. Flood climates. In *Flood geomorphology*, V.R. Baker, R.C. Kochel and P.C. Patton (eds), 13–26. New York: Wiley.

Hayward, A.B. 1985. Coastal alluvial fans (fan deltas) of the Gulf of Aqaba (Gulf of Eilat), Red Sea. *Sedimentary Geology* **43**, 241–60.

Hencher, S.R. 1987. The implications of joints and structures for slope stability. In *Slope stability*, M.G. Anderson and K.S. Richards (eds), 145–86. Chichester: Wiley.

Hogg, S.E. 1982. Sheetfloods, sheetwash, sheetflow, or . . .?. *Earth Science Reviews* **18**, 59–76.

Hooke, R.L. 1967. Processes on arid-region alluvial fans. *Journal of Geology* **75**, 438–60.

Hooke, R.L. 1968. Steady-state relationships of arid-region alluvial fans in closed basins. *American Journal of Science* **266**, 609–29.

Hooke, R.L. 1972. Geomorphic evidence for late Wisconsin and Holocene tectonic deformation, Death Valley, California. *Bulletin of the Geological Society of America* **83**, 2073–98.

Hooke, R.L. 1987. Mass movement in semi-arid environments and the morphology of alluvial fans. In *Slope stability*, M.G. Anderson and K.S. Richards (eds), 505–29. Chichester: Wiley.

Hooke, R.L. and W.L. Rohrer 1977. Relative erodibility of source-area rock types, as determined from second-order variations in alluvial-fan size. *Bulletin of the Geological Society of America* **88**, 1177–82.

Horton, R.E. 1945. Erosional development of streams and their drainage basins; hydrophysical approach to quantitative morphology. *Bulletin of the Geological Society of America* **56**, 275–370.

Hsu, K.J. 1975. Catastrophic debris streams (Sturzstroms) generated by rockfalls. *Bulletin of the Geological Society of America* **86**, 129–40.

Hubert, J.F. and A.J. Filipov 1989. Debris-flow deposits in alluvial fans on the west flank of the White Mountains, Owens Valley, California. *Sedimentary Geology* **61**, 177–205.

Hunt, C.B. and D.R. Mabey 1966. Stratigraphy and structure, Death Valley, California. *U.S. Geological Survey Professional Paper* 494-A.

Hunt, C.B., T.W. Robinson, W.A. Bowles, and A.L. Washburn 1966. Hydrologic basin, Death Valley, California. *U.S. Geological Survey Professional Paper* 494-B.

Jacka, A.D. 1974. Differential cementation of a Pleistocene carbonate fanglomerate, Guadalupe Mountains. *Journal of Sedimentary Petrology* **44**, 85–92.

Jarrett, R.D. and J.E. Costa 1986. Hydrology, geomorphology, and dam-break modeling of the July 15, 1982 Lawn Lake and Cascade Lake dam failures, Larimer County, Colorado. *U.S. Geological Survey Professional Paper* 1369.

Jian, L. and L. Defu 1981. The formation and characteristics of mudflow and flood in the mountain area of the Dachao River and its prevention. *Zeitschrift für Geomorphologie* **25**, 470–84.

Jian, L. and W. Jingrung 1986. The mudflows in Xiaojiang Basin. *Zeitschrift für Geomorphologie Supplement Band* **58**, 155–64.

Johnson, A.M. 1970. *Physical processes in geology*. San Francisco: Freeman-Cooper.

Johnson, A.M. 1984. Debris flow. In *Slope instability*, D. Brunsden and D.B. Prior (eds), 257–361. New York: Wiley.

Johnson, A.M. and P.H. Rahn 1970. Mobilization of debris flows. *Zeitschrift für Geomorphologie Supplement Band* **9**, 168–86.

Keefer, D.K. 1984. Landslides caused by earthquakes. *Bulletin of the Geological Society of America* **95**, 406–21.

Langbein, W.B. and S.A. Schumm 1958. Yield of sediment in relation to mean annual precipitation. *Transactions of the American Geophysical Union* **30**, 1076–84.

Lattman, L.H. 1973. Calcium carbonate cementation of alluvial fans in southern Nevada. *Bulletin of the Geological Society of America* **84**, 3013–28.

Lattman, L.H. and E.M. Simonberg 1971. Case-hardening of carbonate alluvium and colluvium, Spring Mountains, Nevada. *Journal of Sedimentary Petrology* **41**, 274–81.

Lawson, A.C. 1913. The petrographic designation of alluvial fan formations. *University of California Publications in Geology* **7**, 325–34.

Lecce, S.A. 1988. Influence of lithology on alluvial fan morphometry, White and Inyo Mountains, California and Nevada. Unpublished M.A. thesis. Tempe: Arizona State University.

Lecce, S.A. 1991. Influence of lithologic erodibility on alluvial fan area, western White Mountains, California and Nevada. *Earth Surface Processes and Landforms* **16**, 11–18.

Leggett, R.F., R.J.E. Brown and G.H. Johnson 1966. Alluvial fan formation near Aklavik, Northwest Territories, Canada. *Bulletin of the Geological Society of America* **77**, 15–30.

Leopold, L.B. 1951. Rainfall frequency: an aspect of climate variation. *Transactions of the American Geophysical Union* **32**, 347–57.

Link, M.H., M.T. Roberts and M.S. Newton 1985. Walker Lake Basin, Nevada: an example of late Tertiary(?) to recent sedimentation in a basin adjacent to an active strike-slip fault. In *Strike-slip deformation, basin formation, and sedimentation*, K.T. Biddle and N. Christie-Blick (eds), 105–25. Tulsa: Society of Economic Paleontologists and Mineralogists Special Publication 37.

Lustig, L.K. 1965. Clastic sedimentation in Deep Springs Valley, California. *U.S. Geological Survey Professional Paper* 352-F.

Machette, M.N. 1985. Calcic soils of the southwestern United States. In *Soils and Quaternary geology of the southwestern United States*, D.L. Weide (ed.), 115–22. Boulder: Geological Society of America Special Paper 203.

Mathewson, C.C., J.R. Keaton and P.M. Santi 1990. Role of bedrock ground water in the initiation of debris flows and sustained post-flow stream discharge. *Bulletin of the Association of Engineering Geologists* **27**, 73–83.

Mayer, L., L.D. McFadden and J.W. Harden 1988. Distribution of calcium carbonate in desert soils: a model. *Geology* **16**, 303–6.

McGee, W.J. 1897. Sheetflood erosion. *Bulletin of the Geological Society of America* **8**, 87–112.

McGowen, J.H. 1979. Alluvial fan systems. In *Depositional and groundwater flow systems in the exploration for uranium*, W.E. Galloway, C.W. Kreitler and J.H. McGowen (eds), 43–79. Austin: Texas Bureau of Economic Geology Research Colloquium.

McPherson, J.G., D.B. Waresback and J.R. Flannery 1985. Rift-controlled volcanogenic alluvial-fan sedimentation, northern Rio Grande, New Mexico. *Third International Fluvial Sedimentology Abstracts Volume*, 28–9.

McPherson, J.G., G. Shanmugam and R.J. Moiola 1987. Fan deltas and braid deltas: Varieties of coarse-grained deltas. *Bulletin of the Geological Society of America* **99**, 331–40.

Melosh, H.J. 1987. The mechanics of large avalanches. In *Debris flows/avalanches: process, recognition, and mitigation*, J.E. Costa and G.F. Wieczorek (eds), 41–50. Boulder: Geological Society of America Reviews in Engineering Geology 7.

Melton, 1965. The geomorphic and paleoclimatic significance of alluvial deposits in southern Arizona. *Journal of Geology* **73**, 1–38.

Miall, A.D. 1978. Fluvial sedimentology: A historical review. In *Fluvial sedimentology*, A.D. Miall (ed.), 1–47. Calgary: Canadian Society of Petroleum Geologists Memoir 5.

Middleton, G.V. 1970. Experimental studies related to the problems of flysch sedimentation. *Geological Association of Canada Special Paper* 7, 253–72.

Middleton, G.V. and M.A. Hampton 1976. Subaqueous sediment transport and deposition by sediment gravity flows. In *Marine sediment transport and environmental management*, D.J. Stanley and D.J.P. Swift (eds), 197–218. New York: Wiley.

Mifflin, M.D. and M.M. Wheat 1979. Pluvial lakes and estimated pluvial climates of Nevada. *Nevada Bureau of Mines and Geology Bulletin* 94.

Mudge, M.R. 1965. Rockfall-avalanche and rockslide-avalanche deposits at Sawtooth Ridge, Montana. *Bulletin of the Geological Society of America* **76**, 1003–14.

Nash, D.B. 1986. Morphologic dating and modeling degradation of fault scarps. In *Active tectonics: studies in geophysics*, 181–94. Washington, DC: National Academy Press.

Newton, M.S. and E.L. Grossman 1988. Late Quaternary chronology of tufa deposits, Walker Lake, Nevada. *Journal of Geology* **96**, 417–33.

Nicoletti, P.G. and M. Sorriso-Valvo 1991. Geomorphic controls of the shape and mobility of rock avalanches. *Bulletin of the Geological Society of America* **103**, 1365–73.

Nilsen, T.H. 1982. Alluvial fan deposits. In *Sandstone depositional environments*, P. Scholle and D. Spearing (eds), 49–86. Tulsa: American Association of Petroleum Geologists Memoir 31.

Nilsen, T.H. 1985. Introduction and Editor's comments. In *Modern and ancient alluvial fan deposits*, T.H. Nilsen (ed.), 1–29. New York: Van Nostrand Reinhold.

Nummedal, D. and J.C. Boothroyd 1976. Morphology and hydrodynamic characteristics of terrestrial fan environments. *University of South Carolina Coastal Research Division Technical Report* 10-CRD.

Patton, P.C. 1988. Drainage basin morphometry and floods. In *Flood geomorphology*, V.R. Baker, R.C. Kochel and P.C. Patton (eds), 51–64. New York: Wiley.

Pierson, T.C. 1985. How debris flows stop. *Geological Society of America Abstracts with Programs* **17**, 623.

Purser, B.H. 1987. Carbonate, evaporite, and siliciclastic transitions in Quaternary rift sediments of the northwestern Red Sea. *Sedimentary Geology* **53**, 247–67.

Rachocki, A. 1981. *Alluvial fans*. Chichester: Wiley.

Rahn, P.H. 1986. *Engineering geology*. New York: Elsevier.

Rapp, A. and R.W. Fairbridge 1968. Talus fan or cone; scree and cliff debris. In *Encyclopedia of geomorphology* 1106–9. New York: Reinhold.

Reheis, M.C. 1986. Gypsic soils on the Kane alluvial fans, Big Horn County, Wyoming. *U.S. Geological Survey Professional Paper* 1590-C.

Reheis, M.C., J.W. Harden, L.D. McFadden and R.R. Shroba 1989. Development rates of late Quaternary soils, Silver Lake playa, California. *Soil Science Society of America Proceedings* **53**, 1127–40.

Reheis, M.C. and E.H. McKee 1991. Late Cenozoic history of slip on the Fish Lake Valley fault zone, Nevada and California. *U.S. Geological Survey Open-File Report* 91-290.

Reneau, S., W.E. Dietrich, C.J. Wilson and J.D. Rogers 1984. Colluvial deposits and associated landslides in the northern San Francisco Bay area, California, U.S.A. In *Proceedings of the 4th International Symposium on Landslides*, 425–30. Toronto: International Society for Soil Mechancis and Foundation Engineering.

Reneau, S., W.E. Dietrich, R.I. Dorn, C.R. Berger, *et al.* 1986. Geomorphic and paleoclimatic implications of latest Pleistocene radiocarbon dates from colluvium-mantled hollows, California. *Geology* **14**, 655–8.

Reneau, S., W.E. Dietrich, D.J. Donahue, A.J.T. Jull, *et al.* 1990. Late Quaternary history of colluvial deposition and erosion in hollows, central California Coastal Ranges. *Bulletin of the Geological Society of America* **102**, 969–82.

Reneau, S.L., T.M. Oberlander and C.D. Harrington 1991. Accelerator mass spectrometry radiometric dating of rock varnish: discussion. *Bulletin of the Geological Society of America* **103**, 310–11.

Reynolds, M.W. 1974. Geology of the Grapevine Mountains, Death Valley, California. In *Guidebook to the Death Valley region, California and Nevada*, 92–9. Boulder: Geological Society of America Cordilleran Section Field Trip 1.

Ritter, D.F. 1978. *Process geomorphology*. Dubuque, IA: William C. Brown.

Rockwell, T. 1988. Neotectonics of the San Cayetano fault, Transverse Ranges, California. *Bulletin of the Geological Society of America* **100**, 500–13.

Rodine, J.D. and A.M. Johnson 1976. The ability of debris heavily freighted with coarse clastic materials to flow on gentle slopes. *Sedimentology* **23**, 213–34.

Rust, B.R. and E.H. Koster 1984. Coarse alluvial deposits. In *Facies models*, 2nd edn, R.G. Walker (ed.), 53–69. Toronto: Geological Association of Canada.

Ryder, J.M. 1971. Some aspects of the morphometry of paraglacial alluvial fans in south-central British Columbia. *Canadian Journal of Earth Sciences* **8**, 1252–64.

Schumm, S.A. 1963. The disparity between the present rates of denudation and orogeny. *U.S. Geological Survey Professional Paper* 454-H.

Schumm, S.A. 1977. *The fluvial system*. New York: Wiley.

Sharp, R.P. 1942. Mudflow levees. *Journal of Geomorphology* **5**, 222–7.

Sharp, R.P. and L.H. Nobles 1953. Mudflow of 1941 at Wrightwood, southern California. *Bulletin of the Geological Society of America* **64**, 547–60.

Sharpe, C.F.S. 1938. *Landslides and related phenomena: a study of mass movements of soil and rock*. New York: Columbia University Press.

Slate, J.L. 1991. Quaternary stratigraphy, geomorphology, and ages of alluvial fans in Fish Lake Valley. In *Pacific Cell Friends of the Pleistocene Guidebook to Fish Lake Valley, Nevada and California* 1991, 94–113.

Sneh, A. 1979. Late Pleistocene fan-deltas along the Dead Sea rift. *Journal of Sedimentary Petrology* **49**, 541–52.

Sorriso-Valvo, R. 1988. Landslide-related fans in Calabria. *Catena Supplement* **13**, 109–21.

Statham, I. and S.C. Francis 1986. Influence of scree accumulation and weathering on the development of steep mountain slopes. In: *Hillslope processes*, A.D. Abrahams (ed.), 245–68. Boston: Allen & Unwin.

Strahler, A.N. 1957. Quantitative analysis of watershed geomorphology. *Transactions of the American Geophysical Union* **38**, 913–20.

Terwilliger, V.J. and L.J. Waldron 1991. Effects of root reinforcement on soil-slip patterns in the Transverse Ranges of southern California. *Bulletin of the Geological Society of America* **103**, 775–85.

Thenhaus, P.C. and C.M. Wentworth 1982. Map showing zones of similar ages of surface faulting and estimated maximum earthquake size in the Basin and Range province and selected adjacent areas. *U.S. Geological Survey Open-File Report* 82-742.

Tolman, C.F. 1909. Erosion and deposition in the southern Arizona bolson region. *Journal of Geology* **17**, 136–63.

Topping, D.J. 1991. The deposits of large catastrophic landslides as paleogeographic tools: an example from Death Valley, California. *Geological Society of America Abstracts with Programs* **23**, A82.

Trowbridge, A.C. 1911. The terrestrial deposits of Owens Valley, California. *Journal of Geology* **19**, 706–47.

Van Arsdale, R. 1982. Influence of calcrete on the geometry of arroyos near Buckeye, Arizona. *Bulletin of the Geological Society of America* **93**, 20–6.

Varnes, D.J. 1978. Slope movement types and processes. In *Landslides, analysis and control*, R.L. Schuster and R.J. Krizek (eds), 11–33. Washington, DC: Transportation Research Board, National Academy of Sciences, Special Report 176.

Walker, T.R. 1967. Formation of red beds in modern and ancient deserts. *Bulletin of the Geological Society of America* **67**, 353–68.

Walker, T.R. and R.M. Honea 1969. Iron content of modern deposits in the Sonoran Desert: a contribution to the origin of red beds. *Bulletin of the Geological Society of America* **80**, 535–44.

Walker, T.R., B. Waugh and A.J. Crone 1978. Diagenesis in first-cycle desert alluvium of Cenozoic age, southwestern United States and northwestern Mexico. *Bulletin of the Geological Society of America* **89**, 19–32.

Wallace, R.E. 1978. Geometry and rates of change of fault-generated range-fronts, north-central Nevada. *U.S. Geological Survey Research Journal* **6**, 637–50.

Wallace, R.E. 1984a. Fault scarps formed during the earthquakes of October 2, 1915, in Pleasant Valley, Nevada, and some tectonic implications. *U.S. Geological Survey Professional Paper* 1274-A.

Wallace, R.E. 1984b. Patterns and timing of late Quaternary faulting in the Great Basin Province and relation to some regional tectonic features: *Journal of Geophysical Research* **89**, 5763–9.

Webb, R.H., P.T. Pringle and G.R. Rink 1987. Debris flows from tributaries of the Colorado River, Grand Canyon National Park, Arizona. *U.S. Geological Survey Open-File Report* 87-118.

Wells, S.G. and J.C. Dohrenwend 1985. Relict sheetflood bedforms on late Quaternary alluvial fan surfaces in the southwestern United States. *Geology* **13**, 512–6.

Wells, S.G., L.D. McFadden and J.C. Dohrenwend 1987. Influence of late Quaternary climatic changes on geomorphic and pedogenic processes on a desert piedmont, eastern Mohave Desert, California. *Quaternary Research* **27**, 130–46.

Wells, W.G. 1987. The effects of fire on the generation of debris flows in southern California. In *Debris flows/avalanches: process, recognition, and mitigation*, J.E. Costa and G.F. Wieczorek (eds), 105–14. Boulder: Geological Society of America Reviews in Engineering Geology 7.

Wieczorek, G.F. 1987. Effect of rainfall intensity and duration on debris flows in central Santa Cruz Mountains, California. In *Debris flows/avalanches: process, recognition, and mitigation*, J.E. Costa and G.F. Wieczorek (eds), 93–104. Boulder: Geological Society of America Reviews in Engineering Geology 7.

Williams, G.E. 1973. Late Quaternary piedmont sedimentation, soil formation and paleoclimates in arid South Australia. *Zeitschrift für Geomorphologie* **17**, 102–25.

Yarnold, J.C. and J.P. Lombard 1989. Facies model for large block avalanche deposits formed in dry climates. In *Conglomerates in basin analysis*, I.P. Colburn, P.L. Abbott and J. Minch (eds), 9–32. Los Angeles: Pacific Section Society of Economic Paleontologists and Mineralogists Symposium Book 62.

PART SIX

LAKE BASINS

HEMIARID LAKE BASINS: HYDROGRAPHIC PATTERNS

15

Donald R. Currey

'The Great Basin [of western North America]: . . . contents almost unknown, but believed to be filled with rivers and lakes which have no communication with the sea . . .'

Brevet Capt. J.C. Frémont, Corps of Topographical Engineers (1845).

INTRODUCTION

Lakes and other mappable bodies of standing water occur at the atmosphere–lithosphere interface. Over short time intervals, water body configurations (hydrography) are directly responsive to atmospheric (hydroclimatic) forcing. Over longer intervals, hydrography also reflects lithospheric (tectonic and volcanic) forcing. In turn, hydrographic patterns in lake basins strongly influence and even control many geomorphic and stratigraphic patterns (e.g. Mabbutt 1977, pp. 180–214). These linked patterns (hydroclimatic + tectonic → hydrographic → geomorphic + stratigraphic) make lakes and kindred water bodies superb instruments for gauging environmental change and recording palaeoenvironmental history.

Large quantities of lacustrine hydrographic and geomorphic information reside in spatial and temporal patterns, several of which are summarized in this and the following chapter. Although it is often convenient to view water bodies and associated features two-dimensionally (e.g. in plan or cross-section), lacustrine spatial patterns are inherently three-dimensional (Fig. 15.1). Similarly, lacustrine temporal patterns that derive from changing spatial patterns are inherently four-dimensional. Therefore, X (easting), Y (northing), and Z (altitude) coordinates obtained by georeferencing technologies such as GPS (global positioning system), together with ages measured by chronoreferencing technologies such as AMS (accelerator mass spectrometer) analysis of cosmogenic isotopes and OSL (optically stimulated luminescence) analysis of clastic sediments, are essential elements of hydrographic and geomorphic patterns.

HEMIARID LAKE BASINS

Hydrographic and topographic closure are fundamental, and quite distinct, aspects of surface water distribution in all drainage basins. By definition, every lake basin has topographic closure, or containment, but only those that have 'no communication with the sea' (Frémont 1845) also possess hydrographic closure (Fig. 15.2). Basins that are closed both topographically and hydrographically and also contain or have contained bodies of standing water are hemiarid lake basins, the subjects of this and the following chapter.

Hemiarid lake basins have dual hydroclimates (Fig. 15.3). Highlands are non-arid, with cumulative water balance surpluses (annual precipitation greater than annual evapotranspiration). Lowlands are arid (semi-arid, arid, hyperarid) with cumulative water balance deficits (annual precipitation less than annual potential evapotranspiration). Highlands are in varying degrees runoff producers – that is, they are sources of water for stream discharge and groundwater recharge in lowlands. Lowlands are mainly runoff collectors and evaporators – that is, they are consumers of surface and subsurface water from highlands. Water bodies in hemiarid lake basins tend to be classic examples of self-regulating, climate-driven systems (Thorn 1988, pp. 164–92). That is, by undergoing sometimes dramatic size

Geomorphology of Desert Environments. Edited by Athol D. Abrahams and Anthony J. Parsons. Published in 1994 by Chapman & Hall, London. ISBN 978-94-015-8256-8

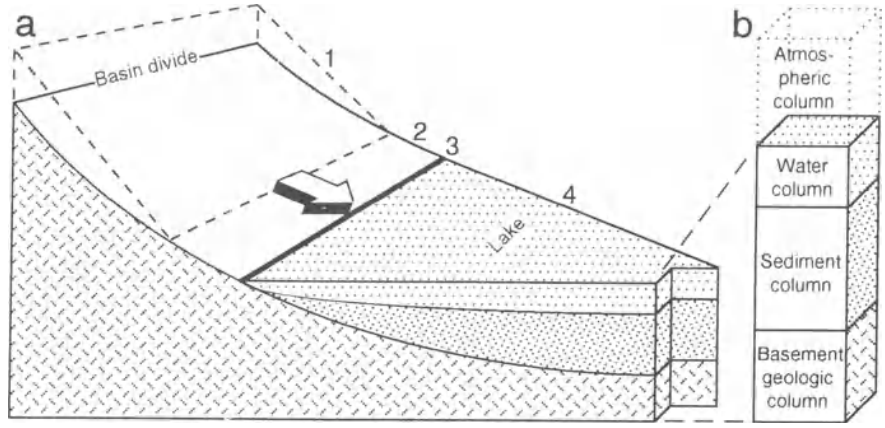

Figure 15.1 Block diagram of a narrow sector in a hypothetical lake basin showing (a) water and sediment transfer from (1) the zone of net runoff and net denudation, through (2) the zone of maximum water and sediment transfer, to (3) the shoreline, and into (4) the zone of water body equilibration and net sedimentation, and (b) four-tired environmental/palaeoenvironmental column in the basin.

(surface area) changes in response to climate changes, they tend to keep their water losses (mainly surface evaporation) and gains (mainly runoff from land, plus direct precipitation) in dynamic equilibrium (e.g. Mifflin and Wheat 1979, pp. 8–10, Street-Perrott and Harrison 1985). The negative feedback role of surface area in water-body self-regulation is illustrated in Figure 15.4.

Hydroclimatic zonation within hemiarid lake basins is mainly a function of altitude and slope direction, but the areal extent of each zone is planimetric (Fig. 15.3). The water-surplus higher 'half' of a hemiarid lake basin has an area that can be expressed dimensionlessly by the surplus area ratio (SAR), where SAR is water-surplus area as a fraction of total basin area. The lower limit of the water-surplus zone (and upper limit of the water-deficit zone) is the hydroclimate equilibrium line altitude (HELA), which is the average altitude above sea level at which annual precipitation and evapotranspiration are equal. The water-deficit lower 'half' of a hemiarid lake basin has an area that can be expressed by the deficit area ratio (DAR), where DAR + SAR = 1. Water-deficit subzones (Fig. 15.3) include dry lowlands, wet lowlands (except lakes and ponds), and open water (lakes and ponds). The area of open water can be expressed dimensionlessly by the water area ratio (WAR), where WAR is the area of open water as a fraction of total basin area.

	Hydrographically open basin	Hydrographically closed basin
Topographically open basin	Uncontained and externally drained basin	Uncontained and internally drained basin
Topographically closed basin	Contained and externally drained lake basin	Contained and internally drained hemiarid lake basin

Figure 15.2 Hemiarid lake basins (lower right) are closed both topographically and hydrographically – that is, they have both containment and internal drainage.

Hydroclimatic zones (and hydrographic features) in hemiarid lake basins are always subject to change. In Figure 15.5, possible hydroclimatic change is viewed in terms of five annual outcomes (in nine cells at lower right) that can be produced by 81 seasonal scenarios (combinations of lettered cells at upper right and numbered cells at lower left). For example, a 'G3' seasonal scenario would be expected to produce a 'much wetter' annual outcome. Furthermore, if the example is a subtropical desert, a G3 scenario would probably involve significant intensification of summer monsoon circulation.

Hydrographic features that have been referred to as alkali lakes, alkaline lakes, arid lakes, arid-land lakes, athalassic salt lakes, bad waters, bitter lakes, bolson lakes, brackish lakes, brine lakes, closed lakes, closed-basin lakes, dead lakes, dead seas, depression lakes, desert lakes, desertic lakes, dry lakes, endoreic lakes, ephemeral lakes, exotic lakes, hydrographically closed lakes, hypersaline lakes, impermanent lakes, inland salt lakes, inland seas, interior-drainage lakes, intermittent lakes, landlocked lakes, lost lakes, mud lakes, oasis lakes, pan

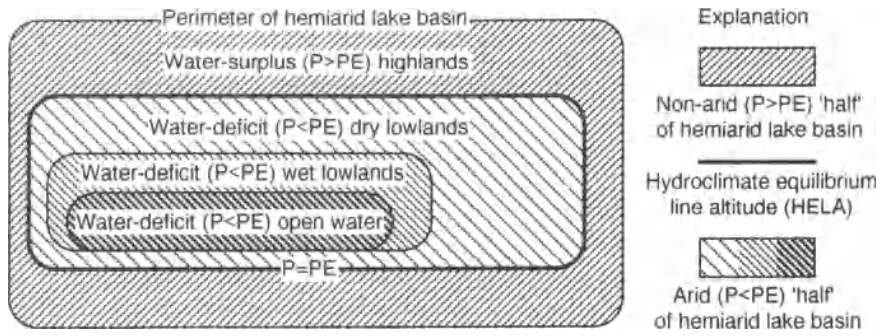

Figure 15.3 Schematic plan of a hypothetical hemiarid lake basin showing water-surplus (non-arid) and water-deficit (arid) hydroclimatic zones; P = annual precipitation and PE = annual potential evapotranspiration (Mather 1978, p. 8). This basin has a surplus area ratio (SAR) of one-half and a water area ratio (WAR) of one-tenth.

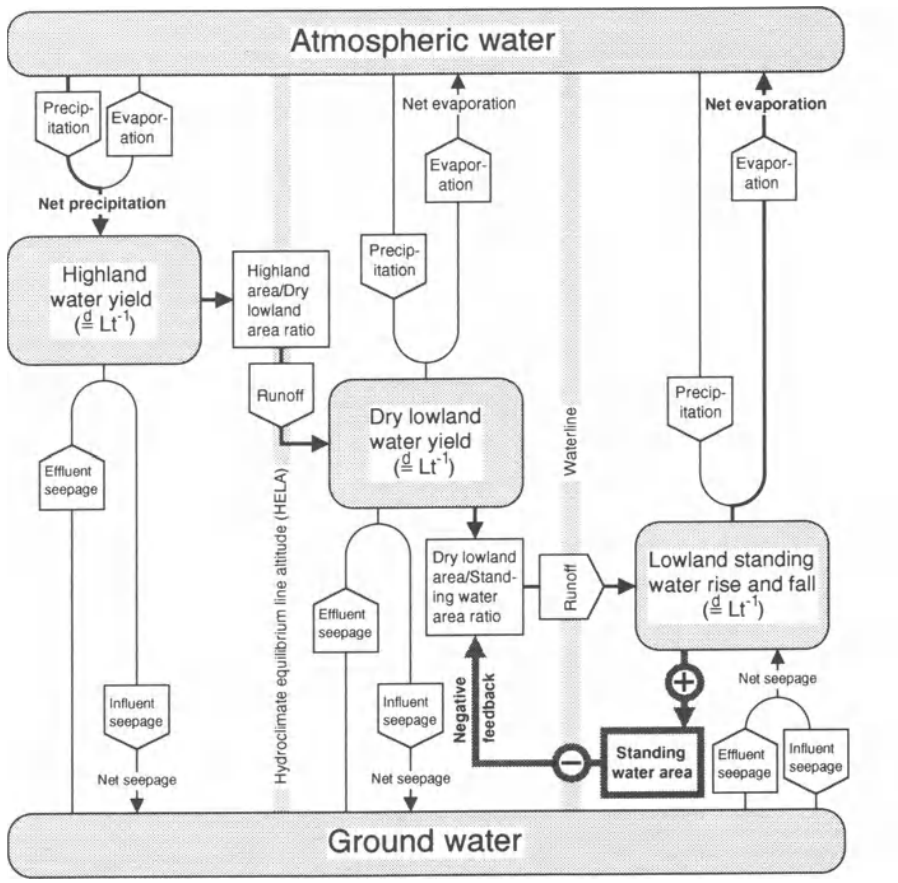

Figure 15.4 Water balance transfers in hemiarid lake basins, where runoff originates in non-arid highlands (upper left), passes through water-deficit dry uplands and lowlands (middle), and terminates in hydroclimatically arid lowlands with standing water (lower right). Transfers are dimensionally equal to length (depth of water) per unit time. Negative feedback regulates runoff per unit area of lowland standing water, keeping inputs (mainly runoff) to standing water and output (evaporation) from standing water in dynamic equilibrium.

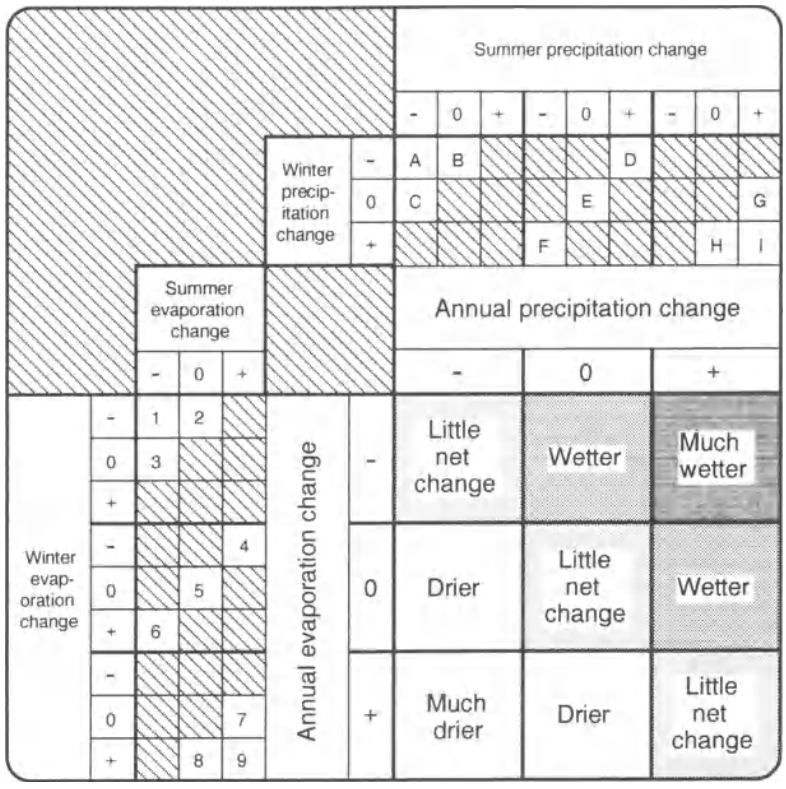

Figure 15.5 Hydroclimatic change in hemiarid lake basins, with five annual outcomes (lower right) produced by 81 seasonal scenarios (upper right and lower left). Symbols: − = decrease, 0 = no change, and + = increase annually or seasonally; see text for explanation.

lakes, playa lakes, saline lakes, salt lakes, salt marsh lakes, salt seas, salton seas, semi-arid lakes, semi-desert lakes, sink lakes, sinking lakes, soda lakes, temporary lakes, terminal lakes, undrained lakes, etc. often connote hemiarid lake basins. Excluding sites fed mainly by sea water or ground water, water bodies below sea level indicate hemiarid lake basins.

Many so-called pluvial lakes of Quaternary age (e.g. Morrison 1968, Reeves 1968, pp. 119–31, Smith and Street-Perrott 1983) occurred in what were and still are hemiarid lake basins, although the sites of some pluvial lakes have been breached and dissected by through-flowing drainage (e.g. Meek 1989). Completely non-arid basins (SAR = 1.0) with topographic closure invariably lack hydrographic closure – that is, they contain externally drained bodies of fresh water. Completely arid basins (DAR = 1.0) seldom contain water bodies larger than groundwater-fed brine pools.

BASIN ORIGINS

Hemiarid lake basins occur in regions where aridity and tectonic activity coincide (Fig. 15.6). Tectonic activity, with or without syntectonic volcanism, generally is the underlying cause of topographic closure (e.g. Thornbury 1965, pp. 471–505, Eaton 1982). Geomorphic processes, which can both enhance and degrade topographic closure, commonly are important secondary causes.

Tectonism and volcanism cause topographic closure in two ways: (a) by blocking basin outlets and (b) by lowering basin floors (Table 15.1). The greatest depths of topographic closure typically result from block faulting in regions of extensional tectonics and from subsidence due to partial emptying of magma chambers beneath volcanic terranes.

Geomorphic processes also cause topographic closure by blocking basin outlets and lowering basin floors (Table 15.2). Geomorphic contributions to

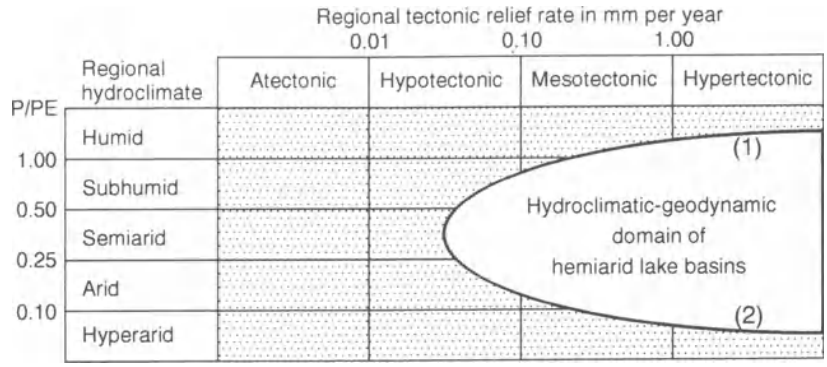

Figure 15.6 Hemiarid lake basins occur in regions where aridity and tectonic activity coincide; P and PE as in Figure 15.3. Hypertectonism extends the domain of hemiarid lake basins by causing (1) intrazonal rainshadows in humid zones and (2) intrazonal orographic precipitation in hyperarid zones.

Table 15.1 Structural (tectonic and volcanic) origins of lake containment basins,* where underlying causes of topographic closure are structural blockage (B) of basin outlets and structural lowering (L) of basin floors. Very shallow (1), shallow (2), moderately deep (3), and deep (4) topographic closure depths are typical of occurrences in North American deserts and semi-deserts

Structural causes of topographic closure	*Typical closure depths*			
	(1)	*(2)*	*(3)*	*(4)*
Tectonic lake containment basins:				
major half-grabens (L)			●	●
major grabens (L)			●	●
transcurrent faulting sag ponds (B)	●	●		
transcurrent-faulting-blocked valleys (B)	●	●		
horst-dammed valleys (B)			●	
anticline-dammed valleys (B)			●	
diapir-dammed valleys (B)		●	●	
doubly plunging syncline basins (L)			●	
ring-fracture-bounded basins (L)		●	●	
volcano-tectonic collapse basins (L)			●	●
Volcanic lake containment basins:				
calderas (L)			●	●
craters (L)		●	●	
maars (L)		●	●	
volcano-dammed valleys (B)			●	
lahar-dammed valleys (B)		●	●	
ash-flow-dammed valleys (B)			●	
lava-flow-dammed valleys (B)		●	●	
collapsed lava tubes (L)	●	●		

*Compiled from Hutchinson (1957, pp. 156–63).

topographic closure are usually limited to low-relief embellishments of pre-existing structural basins. Some geomorphic embellishments cause structural basins and systems of interconnecting structural basins to become segmented into shallow, topographically closed sub-basins (e.g. Hunt *et al.* 1966, pl. 1, Peterson 1981, p. 35). Large alluvial fans and compound barrier beaches are particularly important as sills between sub-basins (e.g. Russell 1885, pl. XVIII, Benson and Thompson 1987).

Table 15.2 Geomorphic origins of lake containment basins,* where immediate causes of topographic closure are geomorphic blockage (B) of basin outlets or geomorphic lowering (L) of basin floors. Very shallow (1), shallow (2), moderately deep (3), and deep (4) topographic closure depths are typical of occurrences in North American deserts and semi-deserts

Geomorphic causes of topographic closure†	*Typical closure depths*			
	(1)	*(2)*	*(3)*	*(4)*
Mass-wasting lake containment basins:				
landslide-dammed basins (B)	•	•	•	
slump rotation basins (L)	•	•		
Glacial lake containment basins:				
ice-dammed basins (B)				
moraine-dammed basins (B)	•	•	•	
glacially scoured basins (L)				
kettles (L)	•	•		
Periglacial lake containment basins:				
cryofluction-dammed basins (B)				
thermokarst basins (L)				
nivation hollows (L)	•			
Solution lake containment basins:				
travertine- and sinter-rimmed pools (B)	•	•		
sinkholes (L)	•	•		
cavern pools (L)	•	•		
Fluvial lake containment basins:				
natural-levee-dammed basins (B)	•	•		
alluvial-fan-dammed basins (B)	•	•	•	•
delta-dammed basins (B)	•	•	•	
abandoned waterfall plunge pools (L)	•	•		
abandoned channels (L)	•	•		
flood-scoured pools (L)	•	•		
Aeolian lake containment basins				
interdune swales (B)	•	•		
dune-dammed basins (B)	•	•		
blowouts (L)	•	•		
deflation basins (L)	•	•	•	
Seashore lake containment basins				
barrier-beach-enclosed lagoons (B)				
barrier-reef-enclosed lagoons (B)				
shore platform tide pools (L)				
Lakeshore lake containment basins				
barrier-beach-enclosed lagoons (B)	•	•		
barrier-complex-dammed sub-basins (B)	•	•	•	•
Phytogenic lake containment basins				
bog-rimmed pools (B)	•			
Zoogenic lake containment basins				
beaver ponds (B)	•	•		
animal wallows (L)	•			
Cosmogenic lake containment basins				
meteorite impact craters (L)	•	•	•	

*Compiled from Hutchinson (1957, pp. 156–63).
†The absence of any indication of closure depth adjacent to a particular lake type signifies that that lake type is not found in deserts.

BASIN CHANGES

A hemiarid lake basin can contain lakes up to a maximum size (basin capacity) that is controlled by the height of the basin threshold, and it can contain shallow water bodies that are identifiable as lakes down to a minimum size (basin capability) that is controlled by the shape of the basin floor. Basin capacity and basin capability are affected by many geomorphic and structural factors. Eventually, as

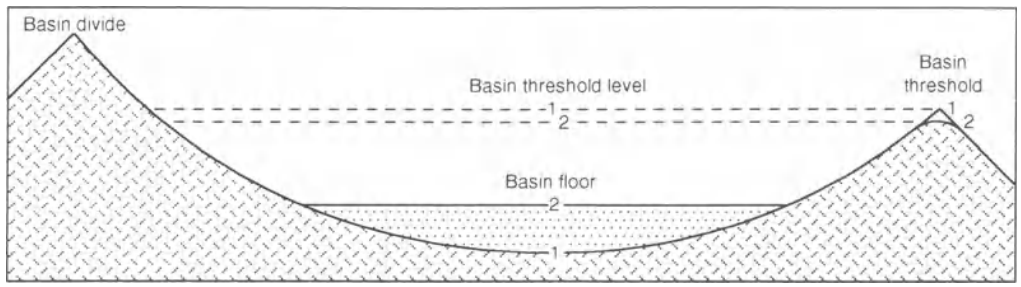

Figure 15.7 Schematic cross-section of a hypothetical lake basin showing basin threshold and basin floor changes produced by geomorphic and structural activity (Tables 15.3 and 15.4) through time (1 = earlier and 2 = later). Basin fill sediments overlie basin $floor_1$ and underlie basin $floor_2$. Topographic closure decreased from (threshold $level_1$–$floor_1$) to (threshold $level_2$–$floor_2$).

Table 15.3 Basin threshold morphodynamics*

Causes of basin threshold change	*Threshold height change*†
Geomorphic causes	
fan toe accretion	+
loess accretion	+
aeolian sand accretion	+
aeolian deflation and abrasion	−
cryptoluvial piping and sapping	−
surface overflow incision	−
surface overflow headward erosion	−
hydraulic failure of threshold	−
flood channel scouring	−
flood channel kolk overdeepening	−
flood-triggered landsliding	+
palaeochannel alluviation	+
palaeochannel colluviation	+
Structural (tectonic and volcanic) causes	
far-field isostatic deflection	+ or −
near-field hydro-isostatic deflection	+ or −
near-field litho-isostatic deflection	−
near-field glacio-isostatic deflection	0
extensional seismotectonic displacement	+ or −
transcurrent seismotectonic displacement	+ or −
compressional seismotectonic displacement	+ or −
volcanic flow emplacement	+ or −
cinder cone construction	+
tephra deposition	+

*Adapted from Currey (1990).
†Symbols: + = threshold raised; 0 = insignificant in most hemiarid lake basins; and − = threshold lowered.

basin thresholds undergo denudation and basin floors undergo widening and flattening by aggradation (Fig. 15.7), some basins lose part or all of their capacity to contain large lakes and many become incapable of containing small lakes. That is, as capacity and capability tend to degrade with time, the range of lake sizes that basins can hold becomes narrower. Similarly, the range of hydroclimatic variation that hemiarid lake basins can record geomorphically and stratigraphically tends to diminish with time.

Basin threshold height, which ultimately controls basin capacity, is subject to change from a variety of geomorphic and structural causes (Table 15.3). The greatest change in threshold height is likely to occur the first time a lake transgresses to its basin threshold. In that situation, observations from several hemiarid lake basins in western North America

Table 15.4 Basin floor morphodynamics*

Causes of basin floor change	*Height change*†	*Breadth change*‡
Geomorphic causes		
proluvial (fan toe sandflat) deposition	+	−
deltoid (Mabbutt 1977) deposition	+	0 or −
deltaic deposition	+	0 or −
offshore deposition	+	0
lakeshore erosion	+	0 or +
lakeshore deposition	+	0 or −
evaporite deposition	+	0 or +
evaporite dissolution	−	0 or −
spring bog deposition	+	0
spring mound deposition	+	0
hydroaeolian planation	+	+
aeolian erosion	−	0 or +
aeolian deposition	+	0 or −
Structural (tectonic and volcanic) causes		
far-field isostatic deflection	+ or −	−
near-field isostatic deflection	+ or −	−
seismotectonic displacement	+ or −	−
salt diapir doming	+	−
magma chamber inflation or deflation	+ or −	−
volcanic flow emplacement	+	−
volcano accretion	+	−
volcano tectonic subsidence	−	−
tephra deposition	+	0

*Adapted from Currey (1990).
†Symbols: + = basin floor raised; 0 = level of basin floor unchanged; and − = basin floor lowered.
‡Symbols: + = basin floor enlarged; 0 = area of basin floor unchanged; and − = basin floor reduced in size.

suggest the following sequence of geomorphic events (in order of occurrence): (1) piping and sapping by pre-flood subsurface overflow beneath and downstream from the threshold, (2) channel incision by pre-flood surface overflow downstream from the threshold, (3) headward erosion of the pre-flood overflow channel, (4) hydraulic failure when headward erosion reaches the threshold, (5) scouring of the flood path into a deep flood channel upstream and downstream from the threshold, (6) scouring an overdeepened kolk in the flood channel floor near the site of the former threshold, (7) landsliding along the flanks of the flood channel, (8) alluviation of the flood channel by waning-flood and post-flood overflow, (9) segmentation of the flood palaeochannel by small alluvial fans that build from either side, and (10) colluviation of the flood palaeochannel by slopewash that includes reworked loess.

Basin-floor height and breadth, which also are subject to change from a variety of geomorphic and structural causes (Table 15.4), tend to increase as basin fill sediments aggrade through time. As a result, the capability of many hemiarid lake basins to accommodate small lakes gradually decreases. In theory, decreasing basin capability should be offset by processes such as faulting and volcanism that create new basin-floor relief. In practice, however, aggrading sediments are readily distributed over very low gradients on basin floors that alternate between subaqueous and subaerial conditions (see hydroaeolian planation in next chapter). This repeatedly restores and enlarges basin-floor horizontality in many hemiarid lake basins, and repeatedly flattens many sites that might otherwise contain small lakes.

BASIN HYDROGRAPHIC CONNECTIONS

Intrabasin hydrographic connections (waterways) involve movement of water, solutes, and sediments from one area to another within a hemiarid lake basin. Interbasin hydrographic connections (cascades) involve movement of water, solutes, and

Table 15.5 Intrabasin waterways, with extant-lake and palaeolake examples from hemiarid lake basins in North America*

Input waterways	*Throughput waterways*	
	Lakes without connected arm(s) or sub-basin(s)	*Lakes with connected arm(s) and/or sub-basin(s)*
Lakes without inflow from major river(s)	Simple lakes: Summer Lake, Oregon† Palaeolakes common	Compound lakes: Extant lakes rare Lake Chewaucan, Oregon‡
Lakes with inflow from major river(s)	Complex lakes: Sevier Lake, Utah† Owens Lake, California† Lake Manix, California‡ Lake Thatcher, Idaho‡	Compound-complex lakes: Great Salt Lake, Utah† Lake Searles, California‡ Lake Bonneville, Utah‡ Lake Lahontan, Nevada‡

*Adapted from Currey (1990).
†Extant lake.
‡Palaeolake.

sediments from one hemiarid lake basin to another. It is common for two or more basins to be connected by subsurface cascades (e.g. Harrill *et al.* 1988), but by definition it is uncommon for two or more hemiarid lake basins to be connected by surface cascades (e.g. Hubbs *et al.* 1974, p. 4, Mifflin and Wheat 1979, pl. 1, Williams and Bedinger 1984). Indeed, surface cascades occur only (a) infrequently, when threshold-controlled 'minipluvial' highstands occur in basins with shallow topographic closure, (b) rarely, when threshold-controlled 'plenipluvial' highstands occur in basins with deep topographic closure, or (c) extrinsically, when runoff acquired through drainage diversion or stream capture leads to threshold control.

Intrabasin waterways are of two kinds (Table 15.5): (a) input waterways which act as conduits of basin runoff to lakes, and (b) throughput waterways which form links between distinct morphological subdivisions within lakes. In dichotomous terms, input waterways involve the presence or absence of rivers with perennial or intermittent discharge into lakes. Similarly, throughput waterways involve the presence or absence of strait-connected arms and/or sill-connected closed sub-basins in lakes. Intrabasin waterways influence lacustrine geomorphic patterns strongly in compound-complex lakes like former Lake Lahontan (Benson and Thompson 1987), which also tend to be large lakes, and weakly in simple lakes (Table 15.5).

At a very general level, all hemiarid lake basins occupy one of four possible cascade positions (Fig. 15.8) and many basins have attributes that reflect their cascade position. For example, cascade-head basins are typically low-salinity environments, whereas cascade-terminus basins often contain brines and saline sediments.

In surface cascades, water, solutes, and usually sediments move from one basin to another at comparatively high, even torrential, rates for comparatively brief periods. In subsurface cascades, water and solutes, but not sediments, move from basin to basin at low rates, sometimes moistening and salinizing basin floors from beneath, for extended periods. As they enter, cross, and leave hemiarid lake basins, surface and subsurface cascades interact with basin morphology in distinctive cascade patterns (Fig. 15.9).

Certain cascade patterns are repeated spatially and temporally in many hemiarid lake basins. Spatially, five patterns prevail in near-terminal and terminal basins (Fig. 15.9, right-hand column), which seldom have completely dry surfaces and which commonly store solute and sediment yields from large upstream regions. Temporally, five stages of cascade evolution are common in upstream basins (Fig. 15.9, middle column): (1) tectonically young basins commonly store sediments and spill mainly water and solutes; (2) with geomorphically reduced topographic closure, basins increasingly pass sediments downstream as well; (3) with deepening threshold incision, stored materials are released at rates that range from gradual to catastrophic; (4) some basins are eventually opened completely by through-flowing surface drainage; and (5) when stream discharge wanes, through-flowing drainage can be limited to groundwater and solutes in the subsurface. Regional cascades of water, solutes, and sediments that are typical of hemiarid lake basins are illustrated in Figure 15.10.

Relative to cascade terminus	Relative to cascade head: Most headward basin **H**	Relative to cascade head: Basin downstream from head **h**
Basin upstream from terminus **t**	Cascade-head basin **Ht**	Mid-cascade basin **ht**
Terminal basin **T**	Cascade with one basin **HT**	Cascade-terminus basin **hT**

Figure 15.8 Basin positions in regional cascades of water, solutes, and sediments.

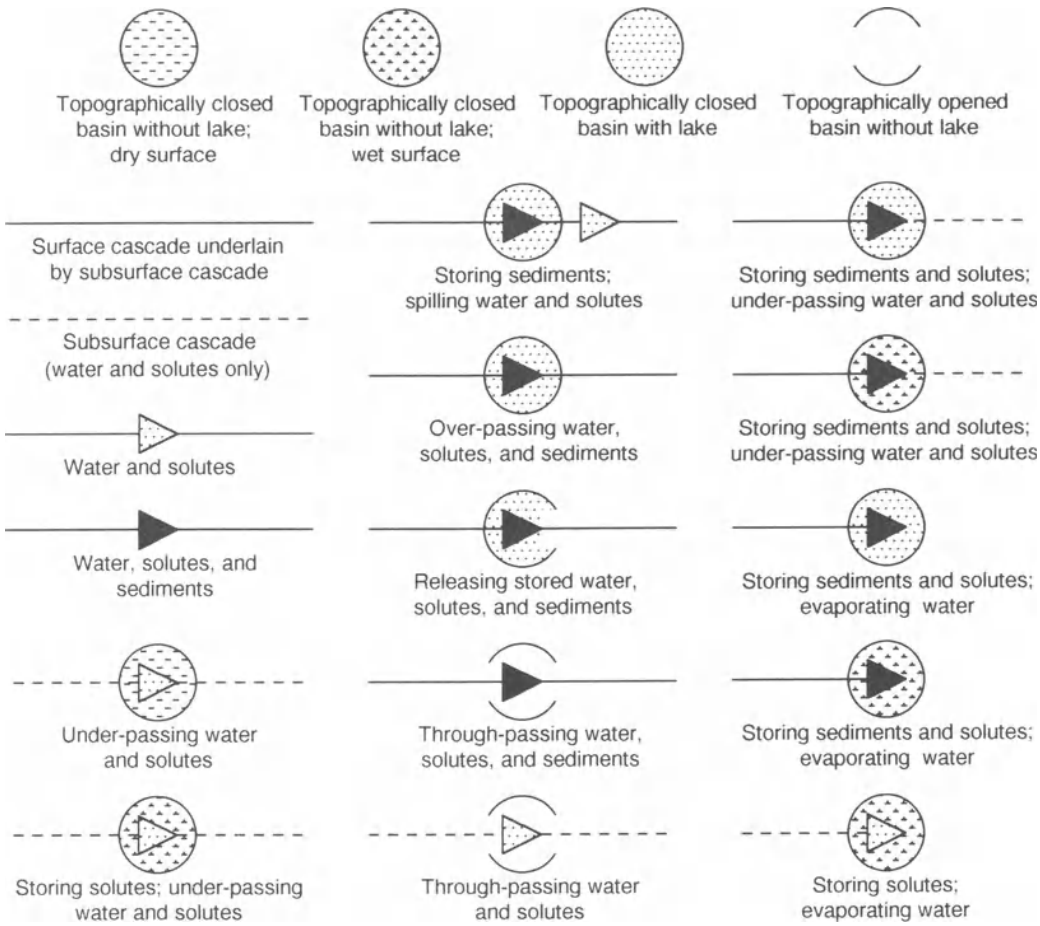

Figure 15.9 Plan view symbols depicting cascades of water, solutes, and sediments in hemiarid lake basins. Direction of flow (indicated by triangles) is left to right.

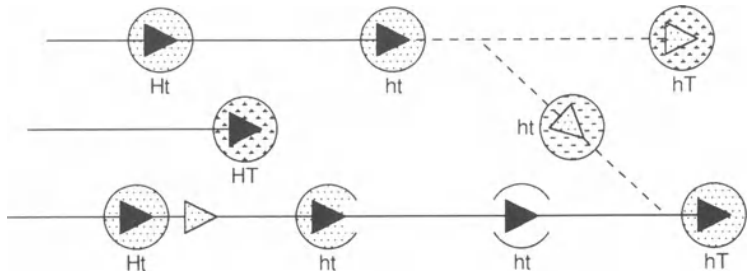

Figure 15.10 Schematic plan of two hypothetical regional cascades – that is, a one-basin cascade (HT) and an eight-basin cascade with two terminal basins (hT).

HYDROGRAPHIC CONTINUUM

Despite water's long-term regional scarcity, its occurrences are remarkably varied on the floors of hemiarid lake basins (e.g. Langbein 1961, p. 18, Houghton 1986, pp. 17–251). Those occurrences belong to a hydrographic continuum that can be subdivided into several definable but intergradational hydrographic realms and subrealms (Table 15.6). In essence, megalakes, lakes, and ponds are runoff-collecting and runoff-evaporating water bodies. Aquatic wetlands, saturated wetlands, and unsaturated wetlands are groundwater-discharging and groundwater-evaporating basin floors. Playas and microplayas are stormwater-wetted, stormwater-infiltrating, and stormwater-evaporating basin floors.

Ecologically, lacustrine habitats are limited mainly to water bodies with depths greater than 2 m; shallower water bodies are the realm of palustrine habitats (Cowardin *et al.* 1979, p. 12). Geomorphically, well-developed evidence of lacustrine processes is limited mainly to water bodies with depths greater than 4 m. In shallower water bodies (a) aerodynamic turbulence causes frequent mixing of the water column and vigorous hydrodynamic stirring of the offshore sediment record, and (b) gently shelving topography suppresses onshore propagation of waves in other than low energy bands of the wave spectrum, which effectively limits onshore and longshore transport of beach-forming sediments.

In low-lying areas that contain little or no standing water much of the time, as well as in low-lying areas that are adjacent to lakes, mixed wetlands form complex mosaics on the floors of many hemiarid lake basins. In order of increasing salinity, mixed wetlands commonly range from spring-fed aquatic marshes, to seep-fed muddy marshes, to alkali meadows, to saline mudflats, and ultimately to phreatic saltflats (Table 15.6).

HYDROGRAPHIC CHANGE

Hydrographic change is the hallmark of hemiarid lake basins (e.g. Street and Grove 1979). It takes many forms and has many causes. For example, transgression, stillstand, or regression can occur at any lakeshore locality, and each of these net changes can have several causes (Fig. 15.11). Spatial, temporal, and kinematic analysis of net hydrographic change and its components is fundamental to lacustrine geomorphology. Therefore, hydrographic change is viewed from basin-wide spatial, temporal, and spatio-temporal perspectives here before proceeding to geomorphic evidence of hydrographic change in the next chapter.

Hydrographic change occurs within spatial limits that are set by basin morphometry (Fig. 15.12). As described in the section on basin changes, the upper limit of potential hydrographic change (basin capacity) is threshold controlled and the lower limit (basin capability) is basin-floor controlled. Large ranges of uninterrupted hydrographic change are possible only in hemiarid lake basins with deep topographic closure and small basin floors.

Hydrographic responsiveness expresses the vertical (surface altitude) change that a water body undergoes in response to a given hydrologic (surface area) change. Steep-sided basins (e.g. Fig. 15.12) are responsive to hydroclimatic change, while flat-sided basins are relatively unresponsive – that is, hydrographic responsiveness is a direct function of basin slope.

Hydrographic fitness expresses how well late Pleistocene and Holocene highstands and lowstands in hemiarid lake basins fit their containment basins (Fig. 15.13). Full geomorphic and stratigraphic records of hydrographic change are found in continuously fit basins (e.g. Lake Lahontan basin in Nevada and California). Less than complete records

Table 15.6 Hydrographic realms and subrealms on the floors of hemiarid lake basins have characteristic surface water and groundwater hydrology, and characteristic geomorphic and geodynamic features

Hydrographic realms and subrealms	*Surface water and groundwater hydrology*	*Geomorphic and geodynamic features*
Lakes:		
Megalakes	Permanent* bodies of open standing water; static water surfaces >100 m above basin floors over large areas (>1000 km^2); total areas >10 000 km^2; far-flung tributary networks, usually with surface runoff from more than one climatic region and several highland life zones	Well-developed evidence of shore (backshore, foreshore, nearshore) and offshore sedimentation; tributary networks usually derive terrigenous sediments from several geologic terranes; measurable evidence of near-field hydro-isostatic deflection; possible evidence of litho-isostatic deflection near depocentres
Lakes	Persistent* or permanent bodies of open standing water; static water surfaces >4 m above basin floors; usually with surface runoff from more than one life zone	Well-developed evidence of shore sedimentation; commonly evidence of offshore sedimentation; terrigenous sediments commonly from more than one geologic terrane; little evidence of near-field isostatic deflection, but possible evidence of far-field deflection
Quasi-lakes:		
Ponds	Transient* or persistent bodies of open standing water; static water surfaces 1 to 4 m above basin floors; standing water mostly from surface runoff	Too shallow for well-developed evidence of shore sedimentation; too shallow for unreworked evidence of offshore sedimentation; hydroaeolian planation and, in shallow basins, brim-full sedimentation tend to transform ponds into wetlands and playas; evaporite ponds floored with soluble salts occur in sub-basins where evaporating brines are replaced by saline surface waters, sometimes from adjacent water bodies by restricted inflow across low barriers
Wetlands:		
Aquatic	Ground surfaces covered by transient layers of local standing water <1 m deep; standing water mostly from groundwater discharge	Range from biotically productive aquatic marshes dominated by emergent hydrophytes to clear evaporite pools floored with soluble salts and saline pools floored with saline muds
Saturated	Surficial materials water saturated; groundwater tables that coincide with basin floors discharge water and solutes	Range from muddy marshes and spring bogs dominated by hydrophytes to non-vegetated phreatic saltflats (= saltpans, etc.) where perennial evaporite pavements are renewed or enlarged by recurring precipitation of soluble salts from saline groundwaters that saturate basin floors; unless renewed as phreatic saltflats, limnogenous saltflats (evaporite pavements formed by desiccation of antecedent lakes) undergo dissolution into saline mudflats or playas, or burial by younger muds
Unsaturated	Surficial materials damp, but usually drier than field capacity; groundwater tables that underlie basin floors discharge capillary water and solutes through evaporative pumping, also termed the wick effect	Range from alkali meadows dominated by salt-tolerant grasses and shrubs to sparsely vegetated saline mudflats; undergo precipitation of efflorescent salts during seasons of strong evaporative pumping, followed by dissolution of efflorescent salts during seasons of surface wetting

Table 15.6

Hydrographic realms and subrealms	*Surface water and groundwater hydrology*	*Geomorphic and geodynamic features*
Drylands		
Playas	Surficial materials usually drier than wilting point; water tables much below basin floors; capillary fringes do not intercept basin floors; wetted briefly by rain or snowmelt, and flooded occasionally by stormwater runoff from surrounding piedmont and upland source areas	Relatively salt-free, fine-grained surfaces (= non-saline mudflats, claypans, etc.) where stormwater runoff events spread suspended sediments widely and dump coarser sediments locally; in absence of effective effluent seepage or evaporative pumping, occasional influent seepage effectively leaches soluble salts from playa surfaces
Microplayas	Very small playas, usually with areas $<1\ km^2$	Playas that develop in local depressions such as blowouts and former lagoons, rather than on basin floors of more general extent

*See Figure 15.14.

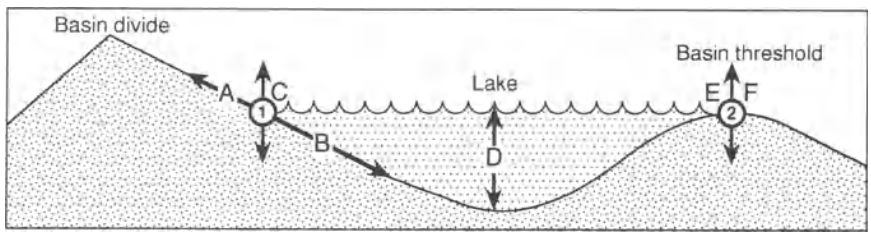

Figure 15.11 Schematic profile through a lake basin, showing possible net hydrographic change (A = transgression and B = regression) at a shoreline locality (1) due to possible combinations of upward or downward neotectonic deformation (C), hydrologic change of the lake (D), and geomorphic change (E) or neotectonic deformation (F) of the lake threshold (2).

of hydrographic change are found in overfit basins (e.g. Lake Bonneville–Great Salt Lake basin in Utah and adjacent states, and Lake Russell–Mono Lake basin in California). Far from complete records of hydrographic change are found in misfit basins (e.g. Lake Mojave and Lake Searles basins, California) and in underfit basins (e.g. Death Valley, California). In addition to hydrographic fitness, lakeshore configuration and sediment supply (reviewed in the next chapter) are important factors in the geomorphic recording of hydrographic change.

Temporal measures of hydrographic change in hemiarid lake basins include persistence and recurrence of open standing water (Fig. 15.14). Water bodies vary greatly in their persistence and recurrence, which are particularly important as factors in the geomorphic development of basin floors. Transient lake–playa regimes with relatively short inundation and subaerial periods (high- to medium-frequency cycles of lake–playa alternation, Fig. 15.14) strongly favour geomorphic processes that tend to flatten and widen basin floors and thus reduce the capability of such basins to contain small lakes.

Temporal domains of hydrographic change in hemiarid lake basins include historic (written records of change), protohistoric (archaeological evidence related to change), and prehistoric (change prior to human habitation). In all three temporal domains, the basic tool for storing, correlating, and displaying basin-wide spatio-temporal information about hydrographic change is the hydrograph (e.g. Fig. 15.15). Hydrographs have spatio-temporal coordinate systems, typically with y-axis water levels, areas, or volumes plotted as functions of x-axis time. Figure 15.15 spans historic, protohistoric, and latest prehistoric time.

Hypsographs have spatial coordinate systems and can also display selected spatio-temporal information (e.g. Fig. 15.16). Dimensionless spatial coordin-

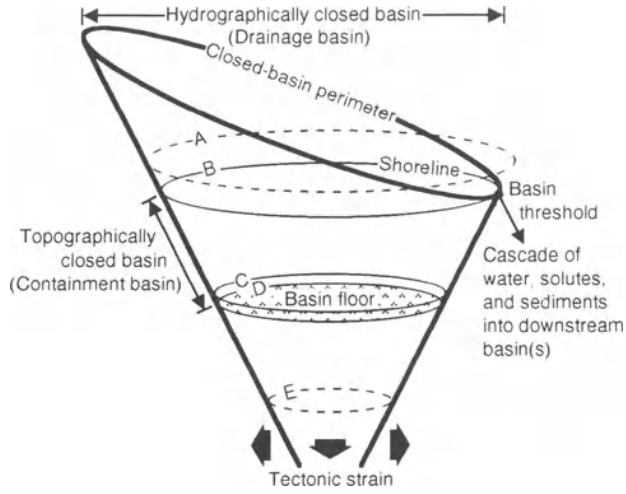

Figure 15.12 'Dixie cup' ('conical graben') model of a hypothetical hemiarid lake basin showing (A) off-scale highstand inferred by extrapolating from geomorphically recorded hydrographic history, (B) threshold-controlled shoreline, (B–C) hydrographically fit lake stages, (C) low-water limit of lacustrine processes, (C–D) ponds and aquatic wetlands, (D) saturated and unsaturated wetlands on basin floor, and (E) off-scale lowstand inferred by extrapolating from geomorphically recorded hydrographic history (after Currey 1990).

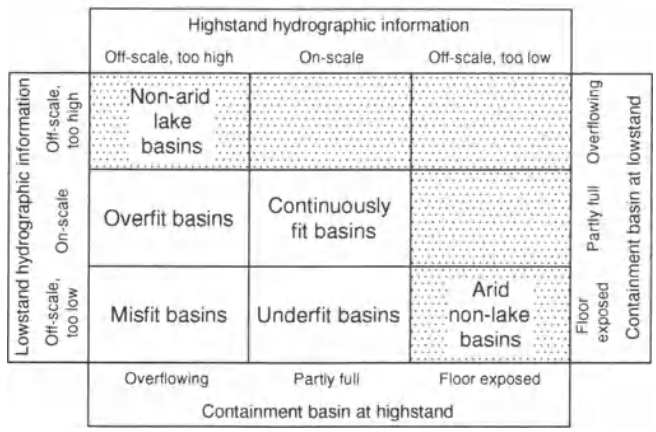

Figure 15.13 Hydrographic fitness defined in terms of late Quaternary highstands and lowstands (after Currey 1990); hemiarid lake basin cells not stippled.

ates, using indices of comparative water body morphometry, can facilitate direct size comparisons of present and past water bodies in one or more basins. Two such indices are the palaeolake height index (PHI), where ϕ is a water body's depth at a particular time as a fraction of its greatest late Quaternary depth, and the palaeolake surface index (PSI), where ψ is a water body's area at a particular time as a fraction of its greatest late Quaternary area (Currey 1988). Figure 15.16 spans a greater spatio-temporal range than, and provides a basin-wide frame of reference for, Figure 15.15.

Diagrams of hydrographic change in hemiarid lake basins have tended to possess auras of authority, certitude, and spatio-temporal order that have beguiled workers in many sciences, including palaeoclimatology, archaeology, and tectonophysics. Clearly, however, the reliability of those diagrams can be no better than the quality of the geomorphic information (see following chapter) on which they are based.

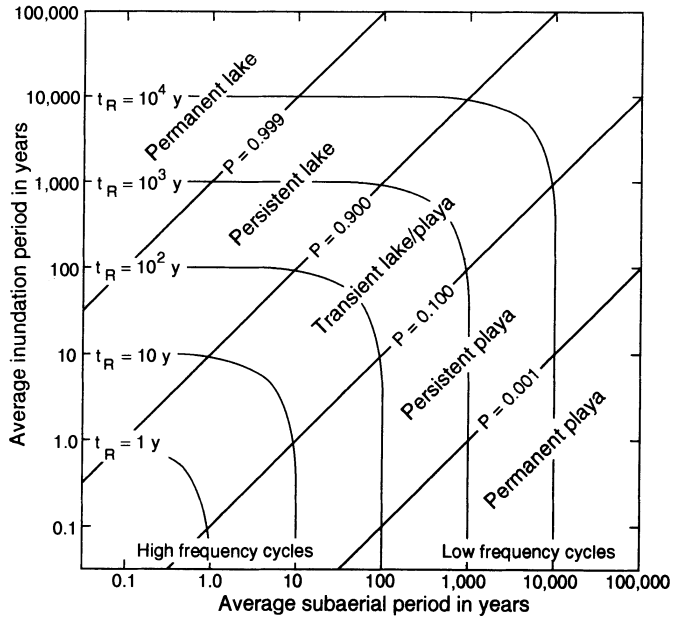

Figure 15.14 Persistance (P) of standing water on floors of lake basins is a dimensionless number from 0.0 to 1.0 that expresses average inundation period in years as a fraction of recurrence. Recurrence (t_R) is time in years of average inundation period plus average subaerial period (after Currey 1990). Frequencies of episodic inundation range from ultra-high to ultra-low.

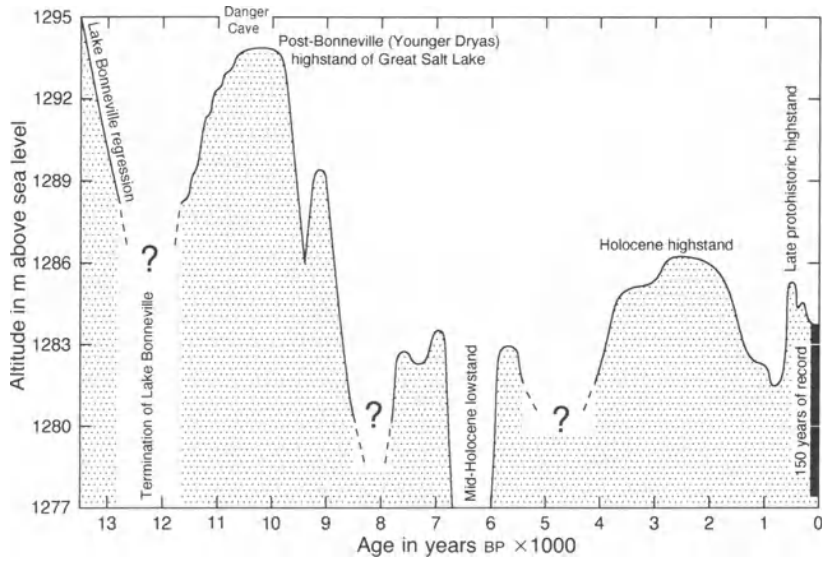

Figure 15.15 Hydrograph showing upper envelope of lake levels (upper limit of static water at high stages) in the basin of Great Salt Lake, Utah, during the last 13 000 years (after Murchison 1989, p. 128). Lower envelope, delimiting low stages during that time, is poorly known. Earliest known human habitation in the basin occurred between 11 and 10 ka at Danger Cave (1314 m; Jennings 1957, fig. 38). Historic hydrologic record has been summarized by Arnow and Stephens (1990, p. 4).

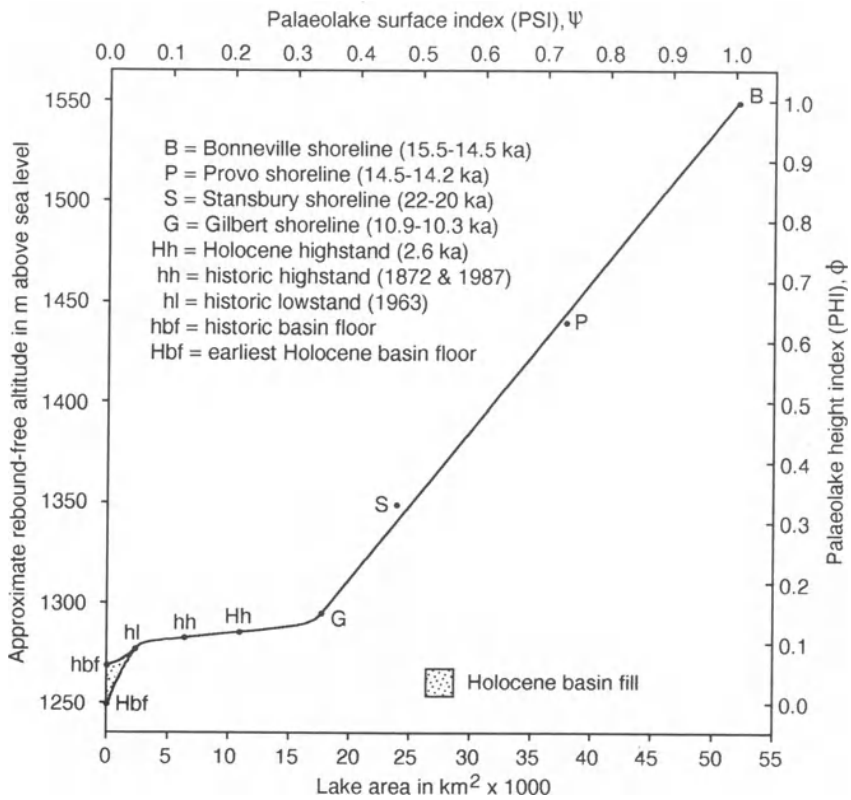

Figure 15.16 Hypsograph showing containment basin topography (sloping line) and selected late Pleistocene and Holocene lake levels (dots) in the Lake Bonneville basin, western USA (after Currey 1990); chronology from Currey and Burr (1988), Oviatt (1988), Oviatt *et al.* (1990), and Benson *et al.* (1992). Estimated rebound-free altitudes (Currey and Oviatt 1985) simplify basin-wide studies. In this example, PHI is scaled from 0.0 on the terminal Pleistocene basin floor to 1.0 at the highest late Quaternary (threshold-controlled Bonneville) shoreline; PSI is scaled from 0.0 at no standing water, which is unlikely in this basin, to 1.0 at the Bonneville shoreline.

ACKNOWLEDGEMENTS

Much of the research on which this chapter is based was supported by NSF grant EAR-8721114. Many of the ideas expressed here have taken shape during more than a decade of fruitful association with University of Utah graduate students and faculty, and with esteemed colleagues in archaeology, geodynamics, geotechnical engineering, soils, the Utah Geological Survey, and the U.S. Geological Survey.

REFERENCES

Arnow, T. and D. Stephens 1990. Hydrologic characteristics of the Great Salt Lake, Utah: 1847–1986. *U.S. Geological Survey Water-Supply Paper* 2332.

Benson, L.V. and R.S. Thompson 1987. Lake-level variation in the Lahontan basin for the past 50,000 years. *Quaternary Research* **28**, 69–85.

Benson, L., D. Currey, Y. Lao and S. Hostetler 1992. Lake-size variations in the Lahontan and Bonneville basins between 13,000 and 9000 ^{14}C yr B.P. *Palaeogeography, Palaeoclimatology, Palaeoecology* **95**, 19–32.

Cowardin, L.M., V. Carter, F.C. Golet and E.T. LaRoe 1979. Classification of wetlands and deepwater habitats of the United States. *U.S. Fish and Wildlife Service* FWS/OBS-79/31.

Currey, D.R. 1988. Isochronism of final Pleistocene shallow lakes in the Great Salt Lake and Carson Desert regions of the Great Basin. *American Quaternary Association Program with Abstracts* **10**, 117.

Currey, D.R. 1990. Quaternary palaeolakes in the evolution of semidesert basins, with special emphasis on Lake Bonneville and the Great Basin, U.S.A. *Palaeogeography, Palaeoclimatology, Palaeoecology* **76**, 189–214.

Currey, D.R. and T.N. Burr 1988. Linear model of threshold-controlled shorelines of Lake Bonneville. In *In the footsteps of G.K. Gilbert – Lake Bonneville and neotectonics of the eastern Basin and Range province*, M.N. Machette (ed.), 104–10. Utah Geological and Mineral Survey Miscellaneous Publication 88-1.

Currey, D.R. and C.G. Oviatt 1985. Durations, average rates, and probable causes of Lake Bonneville expansions, stillstands, and contractions during the last deep-lake cycle, 32,000 to 10,000 years ago. *Geographical Journal of Korea* **10**, 1085–99.

Eaton, G.P. 1982. The Basin and Range province: origin and tectonic significance. *Annual Review of Earth and Planetary Science* **10**, 409–40.

Frémont, J.C. 1845. Map of an exploring expedition to the Rocky Mountains in the year 1842 and to Oregon & North California in the years 1843–44. In *The expeditions of John Charles Frémont – map portfolio*, D. Jackson and M.L. Spence (eds) 1970, map 3. Urbana: University of Illinois Press.

Harrill, J.R., J.S. Gates and J.M. Thomas 1988. Major ground-water flow systems in the Great Basin region of Nevada, Utah, and adjacent states. *U.S. Geological Survey Hydrologic Investigations Atlas* HA-694-C.

Houghton, S.G. 1986. *A trace of desert waters – the Great Basin story*. Salt Lake City: Howe.

Hubbs, C.L., R.R. Miller and L.C. Hubbs 1974. Hydrographic history and relict fishes of the north-central Great Basin. *California Academy of Science Memoir* 7.

Hunt, C.B., T.W. Robinson, W.A. Bowles and A.L. Washburn 1966. Hydrologic basin, Death Valley, California. *U.S. Geological Survey Professional Paper* 494-B.

Hutchinson, G.E. 1957. *A treatise on limnology, volume 1: geography, physics, and chemistry*. New York: Wiley.

Jennings, J.D. 1957. Danger Cave. *University of Utah Anthropological Paper* 27. Salt Lake City: University of Utah Press.

Langbein, W.B. 1961. Salinity and hydrology of closed lakes. *U.S. Geological Survey Professional Paper* 412.

Mabbutt, J.A. 1977. *Desert landforms*. Cambridge, MA: MIT Press.

Mather, J.R. 1978. *The climatic water budget in environmental analysis*. Lexington, KY: Lexington Books (D.C. Heath).

Meek, N. 1989. Geomorphic and hydrologic implications of the rapid incision of Afton Canyon, Mojave Desert, California. *Geology* **17**, 7–10.

Mifflin, M.D. and M.M. Wheat 1979. Pluvial lakes and estimated pluvial climates of Nevada. *Nevada Bureau of Mines and Geology Bulletin* 94.

Morrison, R.B. 1968. Pluvial lakes. In *The encyclopedia of geomorphology*, R.W. Fairbridge (ed.), 873–83. New York: Reinhold.

Murchison, S.B. 1989. Fluctuation history of Great Salt Lake, Utah, during the last 13,000 years. Ph.D. dissertation, University of Utah, Salt Lake City.

Oviatt, C.G. 1988. Late Pleistocene and Holocene lake fluctuations in the Sevier Lake basin, Utah, U.S.A. *Journal of Paleolimnology* **1**, 9–21.

Oviatt, C.G., D.R. Currey and D.M. Miller 1990. Age and paleoclimatic significance of the Stansbury shoreline of Lake Bonneville, northeastern Great Basin. *Quaternary Research* **33**, 291–305.

Peterson, F.F. 1981. Landforms of the Basin and Range province defined for soil survey. *Nevada Agricultural Experiment Station Technical Bulletin* 28.

Reeves, C.C. 1968. *Introduction to paleolimnology*. Amsterdam: Elsevier.

Russell, I.C. 1885. Geological history of Lake Lahontan: a Quaternary lake of northwestern Nevada. *U.S. Geological Survey Monograph* 11.

Smith, G.I. and F.A. Street-Perrott 1983. Pluvial lakes of the western United States. In *Late Quaternary environments of the United States, volume 1: the late Pleistocene*, H.E. Wright and S.C. Porter (eds), 190–212. Minneapolis: University of Minnesota Press.

Street, F.A. and A.T. Grove 1979. Global maps of lake-level fluctuations since 30,000 yr B.P. *Quaternary Research* **12**, 83–118.

Street-Perrott, F.A. and S.P. Harrison 1985. Lake levels and climate reconstruction. In *Paleoclimate analysis and modelling*, A.D. Hecht (ed.), 291–340. New York: Wiley.

Thorn, C.E. 1988. *Introduction to theoretical geomorphology*. London: Unwin Hyman.

Thornbury, W.D. 1965. *Regional geomorphology of the United States*. New York: Wiley.

Williams, T.R. and M.S. Bedinger 1984. Selected geologic and hydrologic characteristics of the Basin and Range province, western United States. *U.S. Geological Survey Miscellaneous Investigations Series Map* I-1522-D.

HEMIARID LAKE BASINS: GEOMORPHIC PATTERNS

16

Donald R. Currey

'When the lakes of arid regions become extinct, either by reason of evaporation or sedimentation, evidence of their former existence remains inscribed on the inner slopes of their basins or concealed in the strata deposited over their bottoms. These records as a rule are much more lasting than those left by lakes in humid lands . . . '

Israel C. Russell (1895, pp. 94–5).

INTRODUCTION

Geomorphic and stratigraphic patterns, which in lacustrine geoscience differ more in etymology than substance, are the evidence by which hydrographic patterns and underlying hydroclimatic and tectonic patterns are reconstructed in hemiarid lake basins. Regional and local geomorphic patterns are equally important: regional geomorphic patterns are the predictive basis for making local geomorphic observations, and local patterns are the observational basis for building and testing regional models.

Figure 16.1 illustrates the importance of regional and local geomorphic patterns (and underlying tectonic, hydrographic, and hydrologic patterns) in two substantially different hypothetical basins. The hypertectonic hemiarid lake basin (Fig. 16.1, A–A') has highlands that are likely to yield significant runoff, lowlands that are likely to be segmented into closed sub-basins by active alluvial fans, and sub-basin floors that are likely to be locally depressed by active faulting. In contrast, the hypotectonic arid basin (Fig. 16.1, B–B') has inselberg uplands that are unlikely to yield significant runoff, lowlands in which sub-basins have long been aggraded and arroyo-integrated, and a basin floor that in all likelihood is large and essentially flat. The occurrence of a lake or the geomorphic evidence of one or more Quaternary palaeolakes, large or small, has a substantially higher probability in the hypertectonic basin than in the hypotectonic basin.

LAKEBEDS

From their greatest depths to their highest surges, lakes are in continuous to occasional contact with sublacustrine materials. Portions of lake–substrate interfaces have been termed beds, bottoms, floors, shores, mudlines, etc. In this review, all lake–substrate interfaces of specified ages in hemiarid basins are termed lakebeds. Conceptually, lakebeds are the desktops on which lakes encode and inscribe information about their environments, including their morphometry (e.g. Håkanson 1981, p. 72), energy fluxes, material fluxes, and sedimentology (Sly 1978; Håkanson and Jansson 1983). Information regarding lakebed depth (bathymetry), deposition–erosion net balance (Håkanson and Jansson 1983, pp. 177–212), sediment size, mineralogy (Jones and Bowser 1978), and geochemistry is of prime importance geomorphically.

A regional geomorphic model that can be applied to lakebeds in many hemiarid basins consists of topologically concentric bathymetric environment zones (Table 16.1). Each isochronic lakebed that marks a successive stage in a lacustrine sequence is a special case of the general model. In each case, the nearshore, foreshore, and backshore zones form a geomorphically dynamic lakeshore (Fig. 16.2). Lakebed sediment sizes, which are characteristically well sorted according to turbulent energies, typically increase from the deepest part of the offshore zone to the middle of the foreshore zone.

Several spatial and temporal threads run through lakebed geomorphic patterns. Given adequately

Geomorphology of Desert Environments. Edited by Athol D. Abrahams and Anthony J. Parsons. Published in 1994 by Chapman & Hall, London. ISBN 978-94-015-8256-8

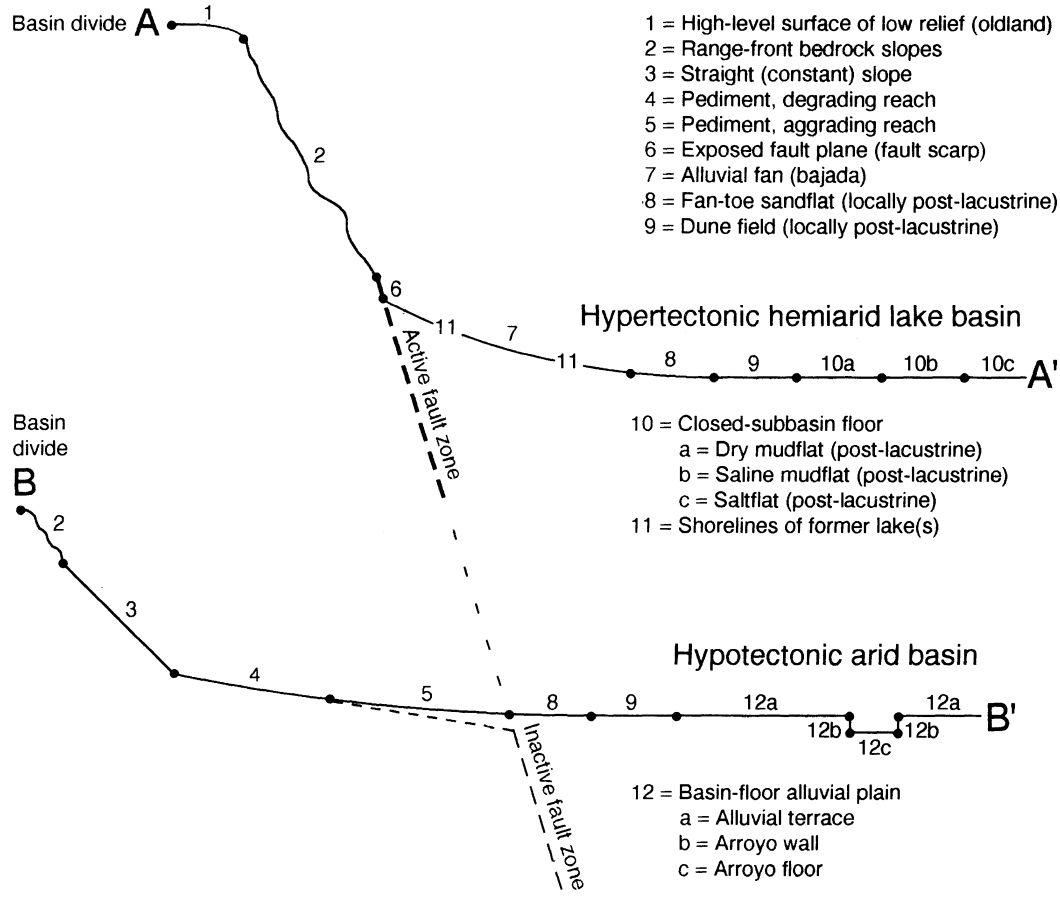

Figure 16.1 Schematic profiles showing regional (A–A′ and B–B′) and local (1–12) geomorphic patterns that are typical of hypertectonic hemiarid lake basins and hypotectonic arid basins.

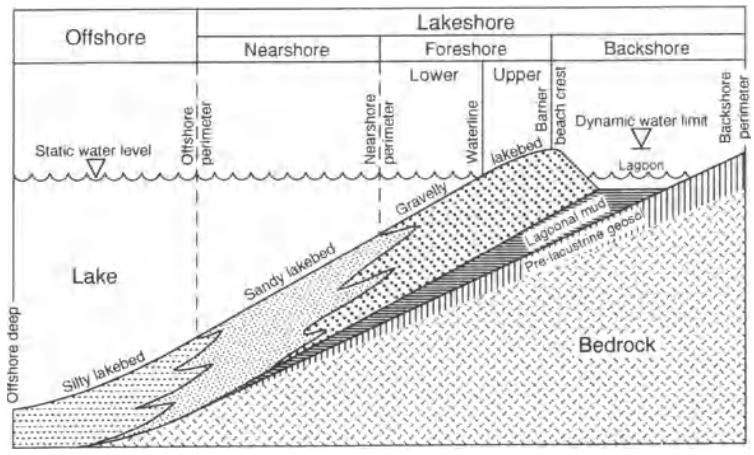

Figure 16.2 Schematic cross-section of lakebed in hemiarid lake basin, showing bathymetric environment zones in and near an idealized barrier beach lakeshore. See Table 16.1 for details.

Table 16.1 Offshore, nearshore, foreshore, backshore, and rearshore bathymetric environment zones in and adjacent to lakeshores in hemiarid lake basins*

Zones and zone transitions	*Typical environments*
Offshore deep	Deepest places in lakes; lakebeds commonly anoxic and fetid, with sediments commonly >1% plankton residues
Offshore zone	Depths typically >6 m; gently sloping lakebeds blanketed by marls (carbonate micrite muds), diatomaceous marls, terrigenous silts and clays, or volcanic ashes; soluble salts can precipitate offshore during major regressions
Offshore perimeter	Landward transition from low to moderate turbulence and from muddy to sandy lakebeds; basinward limit of lakeshore
Nearshore zone	Depths typically 2–6 m; low-gradient, basinward-sloping aprons of fine clastic sands, charaliths, or mats and heads of algoid tufa; commonly ooid-producing; soluble salts can precipitate nearshore from cold, high-salinity waters
Nearshore perimeter	Landward transition from moderate-energy sandy lakebeds to high-energy gravelly lakebeds
Lower foreshore zone	Depths typically <2 m; moderately steep, basinward-sloping, surf-constructed subaqueous beach faces of medium to coarse sands and gravels; commonly bouldery; lithoid and algaloid tufas locally abundant as beach matrix and as coatings on rocky lakeshores; soluble salts can precipitate on lower foreshore from cold, high-salinity waters
Lower foreshore perimeter	Waterline; landward limit of open water under static water conditions, i.e. basinward edge of land
Upper foreshore zone	Heights typically <2 m above static water level; swash-constructed subaerial beach faces are landward extensions of subaqueous beach faces; locally bouldery
Upper foreshore perimeter	Crests of basinward-sloping, backset-stratified beach faces; landward limit of swash
Backshore zone	Inland-sloping foreset-stratified washover beach slopes, lagoons, primary dunes (foredunes), deltaic lowlands, mudflats, saltflats, and marshes directly impacted by overwash processes and episodic onshore surges
Backshore perimeter	Inland transition from direct to indirect lacustrine geomorphic impacts, i.e. inland limit of foredune accretion and flooding by onshore surges; inland limit of lakeshore
Rearshore zone	Secondary dunes derived from foredunes; floodplains and groundwater tables affected by fluctuations of lacustrine base levels
Rearshore perimeter	Inland limit of indirect lacustrine geomorphic impacts, i.e. inland limit of secondary dunes and base level effects

*See Figure 16.2.

georeferenced and chronoreferenced databases, individual (isochronic) lakebeds can be resolved into sets of linear patterns (e.g. mappable source-to-sink sediment pathways) and areal patterns (mappable polygons); successions of lakebeds can be resolved into volumetric patterns (mappable polyhedrons). Although minimal spatio-temporal resolution can be sufficient to distinguish among pre-lacustrine, co-lacustrine, and post-lacustrine geomorphic features, high spatio-temporal resolution is required to quantify the kinematics of geomorphic and hydrographic change (e.g. Currey and Burr 1988).

LAKEBED SEDIMENT SOURCES

Lakebeds are surfaces underlain by lacustrine sediments that range in thickness from greater than 1 m in many offshore and lakeshore areas of net deposition, to shallow veneers on erosional platforms, to practically nil on steeply sloping bedrock headlands. Lacustrine sediments are of three types: (a) those that originate outside the water column, (b) those that originate in the water column, and (c) those that originate in fluid-filled pores under the water column. The three types are commonly referred to as allogenic, endogenic, and authigenic, although the latter two are sometimes grouped together because of their common links to lake biochemistry (Jones and Bowser 1978). In this review, sediments that have their origins on land are termed terrigenous (following usage in marine geology) and those that have their origins in and under lakes are termed limnogenous.

Terrigenous lacustrine sediments (Table 16.2) comprise all clastic materials that are transported into lakes by geomorphic agents, as well as those that lakes acquire by lakeshore erosion. Fluviolacustrine materials are commonly the dominant terrigenous sediments on the lakebeds of hemiarid basins with major streams. Away from the deltas of major

Table 16.2 Terrigenous lacustrine sediments of importance in hemiarid basins are supplied by lakeshore erosion (E) or by short- to long-distance transportation (T)

Sediment types	*Sediment origins*
Litholacustrine	(E) Clastic sediments that lakes acquire by eroding cliffs (free faces) in resistant bedrock and bluffs (straight slopes) in non-resistant bedrock; includes clasts acquired by rockfalls and rockslides from cliffs and bluffs
Colluviolacustrine	(E) Clastic sediments that lakes acquire by stripping unconsolidated colluvial materials off slopes that are underlain by bedrock and consolidated sediments
Alluviolacustrine	(E) Clastic sediments that lakes acquire by eroding bluffs in alluvial fans and bajadas; includes clasts acquired by mass wasting of bluffs
Retrolacustrine	(E) Clastic sediments (intraclasts) that lakes acquire by reworking and redepositing terrigenous and limnogenous sediments of earlier lakebeds
Fluviolacustrine	(T) Clastic sediments, including glacial outwash, that are introduced into lakes by drainage networks of many sizes; partly dispersed offshore and partly localized inshore (in low-gradient, suspended-load deltas, bedload fan deltas, sandy underflow fans, and aggraded–prograded estuaries)
Aerolacustrine	(T) Airborne mineral dusts (silts and clays), biodusts (palynomorphs and humic matter), organic ashes, volcanic ashes, and salts that settle out of the atmospheric column on to lake surfaces; insoluble dusts settle out of the water column on to lakebeds
Cryolacustrine	(T) Ice-rafted dropstones (commonly pebbles and cobbles) that are released during spring breakup of shore-fast lake and river ice; ice-shoved beach deposits
Anthropolacustrine	(T) Materials (structures and refuse) that are placed in lakes by people
Glaciolacustrine	Sediments that are carried into lakes by glacier ice are rare or non-existent in hemiarid lake basins

streams and in hemiarid lake basins without major streams, alluviolacustrine materials are commonly the dominant terrigenous sediments, particularly in lakeshore deposits.

Limnogenous sediments (Table 16.3) comprise all materials that originate physico-chemically or biochemically at the top of, within, at the bottom of, or under the water column in hemiarid lake basins, regardless of water depth. Of the lacustrine chemical sediments (Eugster and Kelts 1983), carbonates are the most ubiquitous in hemiarid lake basins, far exceeding organic matter and typically equalling or exceeding soluble salts. Micritic marls, with amounts and sizes of admixed terrigenous fines that reflect proximity to land-based sediment sources, are the most common offshore carbonate sediments (e.g. Galat and Jacobsen 1985). Various forms of tufa (e.g. Morrison 1964, pp. 44–57) and ooidal sands (e.g. Eardley 1966) are common carbonate sediments in lakeshore zones.

Algaloid tufas (Table 16.3), which in many hemiarid lake basins are among the more intriguing and varied surficial materials, are laminated calcite, aragonite, and calcite–aragonite mixtures that form on algae-colonized substrates in sunlit, wave-agitated, calcium-bicarbonate-saturated waters. Large algaloid tufa forms include mounds, domes, and pinnacles, as well as extensive mats (hardgrounds) on soft sediments. Smaller forms include cauliform discs and heads, radiating (dendritic) discs and heads, polyp clusters, smooth rinds and rippled rinds on bedrock and detached rocks, rinds enveloping metre-size pods of gravel, bun-shaped oncoids, and pearl-like pisolites.

LAKESHORE SEDIMENT PATHWAYS

Most limnogenous sediments are deposited beneath or at their point of origin in the formative water column. Most terrigenous sediments (and coarse limnogenous sediments such as ooidal sands) are transported significant distances before undergoing long-term deposition. The finer terrigenous sediments (mainly fluviolacustrine clays, silts, and fine sands) are commonly transported by runoff that discharges directly into offshore waters by hypopycnal flow (near-surface suspensions of clays and silts) and hyperpycnal underflow (near-bottom density currents laden with mixtures of clay, silt, and fine sand). The coarser terrigenous sediments (mainly alluviolacustrine and litholacustrine gravels and coarse sands) and coarse limnogenous sediments occur mostly in lakeshore (nearshore, foreshore, and backshore) zones. There they are reworked and redeposited many times as they move from sediment sources to sediment traps along lakeshore pathways.

The four basic lakeshore sediment pathways (Fig.

Table 16.3 Limnogenous sediments of importance in hemiarid lake basins

Sediment types	*Sediment origins*
Micrites	Silt-size carbonate crystals that form in calcium-bicarbonate-saturated surface waters, and settle out as marl in the summer, when CO_2 is depleted by phytoplankton (mainly algal) photosynthesis and thermal degassing; calcite micrites (and tufas) tend to precipitate in low-salinity hard waters and aragonite micrites (and tufas) tend to precipitate at higher salinities
Plankton residues	Organic matter (sapropel or proto-kerogen) that results from anaerobic decay of settled-out plankton (mainly algae); common in fine-grained sediments on poorly oxygenated lakebeds
Microfossils*	Opaline frustules of diatoms can be particularly abundant, with sediments ranging from diatomaceous muds and marls to pure diatomites; pollen grains are commonly preserved in water-saturated sediments
Macrofossils*	Mollusca shells are common in the deposits of fresh-to-brackish shallow waters; charaliths (diminutive straw-like calcified filaments of macrophyte algae, particularly of the genus *Chara*) are commonly washed into nearshore deposits from foreshore substrates; ostracod shells are common in fine-grained sediments on well-oxygenated lakebeds; fish bones and scales are less common, but occur widely in the deposits of fresh-to-brackish waters
Ooids	Spheroidal ooids (aragonite-encapsulated sand grains) and cylindrical ooids (aragonite-encapsulated fecal pellets, e.g. of the brine shrimp *Artemia*) that form in gently shoaling calcium-bicarbonate-saturated nearshore waters; commonly wash onshore to form beaches and dunes
Algaloid† tufas	Phycolites (general name for all algaloid structures) comprise (a) spongiostromes (laminated structures formed by algae growing in smooth mats), including stromatolites (attached to substrate) and oncolites (unattached, free to roll), and (b) dendrolites (arborescent or near-arborescent structures formed by algae growing in tufted mats), including dendritic, cellular, and 'coralline' tufa
Tufacretes	Conglomerate- or concrete-like, calcite- and aragonite-cemented gravels and coarse sands that form in shallow, calcium-bicarbonate-saturated waters where moderate (not copious) supplies of coarse clasts are available and where breaking waves accelerate warm-season degassing of CO_2; tufacrete landforms include platform pavements and ledges, slope-draping slabs, and foreshore beachrock
Salt beds	Offshore and nearshore beds of soluble salts that settle out after crystallizing in seasonally supersaturated surface waters, e.g. halite (NaCl) when evaporation is high and mirabilite ($Na_2SO_4 \cdot 10H_2O$) when temperatures are low; foreshore salt beds include mirabilite that washes onshore and is preserved in the interstices of more stable beach materials; backshore salt beds include halite that precipitates on lake-fringing saltflats

*Including subfossils of late Quaternary age.
†Richard Rezak's classification (Morrison 1964, p. 48).

16.3) in hemiarid lake basins trend (a) landward from the foreshore zone to the backshore zone and sometimes beyond (inland transport), (b) landward from the nearshore zone to the foreshore zone (onshore transport), (c) basinward from the foreshore zone to the nearshore or offshore zone (offshore transport), and (d) in the direction of net littoral drift within the foreshore and nearshore zones (longshore transport).

It is common for lakeshore sediment pathways in hemiarid lake basins to be well defined geomorphically. In inland transport, foreshore medium sands are carried into lagoons by overwash and on to accreting foredunes by saltation. In onshore transport, nearshore ooids and fragments of tufa and beachrock commonly are carried on to foreshore beach faces by the onshore component of breaking waves (swash). In offshore transport, foreshore fines are winnowed into deeper water by breaking waves, and foreshore sands and gravels pass into deeper water on the up-drift sides of groin-like headlands and at the ends of spits and cuspate barriers. In longshore transport, foreshore sands and gravels can be carried several kilometres by the longshore component of breaking waves (littoral drift), without benefit of topographic gradient. Longshore transport has moved large (128 to 256 mm) cobbles at least 2 km on high-energy beaches in the Great Basin.

It is also common for geomorphic conditions to vary greatly from one lakeshore sector to another. In all but the smallest hemiarid lake basins, this produces distinctive basin-wide and local patterns of lakeshore segmentation (Fig. 16.4a and b). Lakeshore segments are distinguished by two

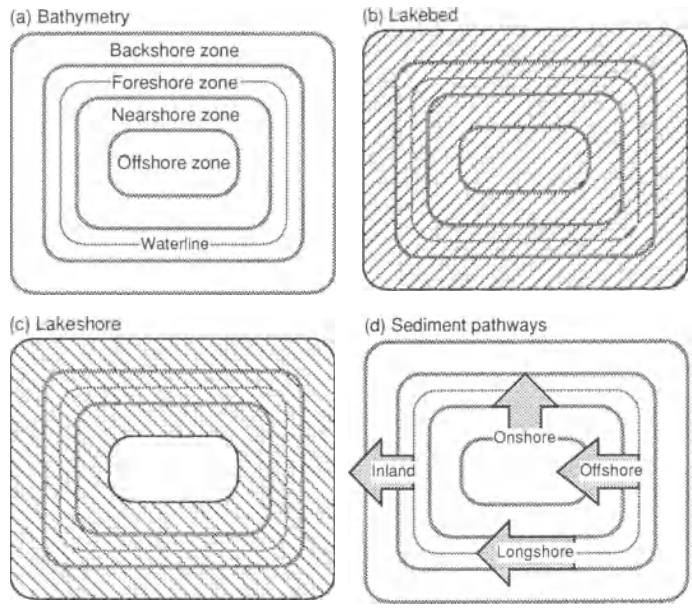

Figure 16.3 Schematic plans of (a) bathymetric zones (Table 16.1 and Fig. 16.2), showing (b) lakebed and (c) lakeshore areas of (d) inland, onshore, offshore, and longshore sediment movement.

criteria: their longshore transport directions and longshore sediment budgets. Lakeshore segments join at segment boundaries (nodes), which are points where (a) longshore transport directions reverse or (b) longshore sediment budgets change algebraic sign (from net erosion to net deposition or *vice versa*). Erosional lakeshore segments have deficit longshore sediment budgets, in which total longshore outputs exceed total longshore inputs and the difference is equal to sediments entrained by lakeshore erosion. Depositional lakeshore segments have surplus longshore sediment budgets, in which total sediment inputs exceed total longshore outputs and the difference is equal to sediments stored in beaches and deltas.

Lakeshore segment boundaries (Fig. 16.4b, longshore nodes) occur where longshore transport directions diverge or converge (divergent and convergent nodes), where longshore transport budgets change from deposition to erosion (revergent nodes), and where longshore transport budgets change from erosion or steady state to deposition (provergent nodes). In addition to the longshore criteria that are used to define lakeshore segmentation, features such as lithology and geomorphic expression (original geomorphic development together with subsequent geomorphic preservation) can be noteworthy features of lakeshore segments and subsegments (e.g. Fig. 16.4b).

LAKEBED SEDIMENT SINKS

The marine geomorphic literature (e.g. Davies 1980, pp. 126–33) sometimes distinguishes among coastal sediments that reside in (a) stores (temporary sediment storage in active beaches), (b) traps (long-term sediment storage in beaches at re-entrants and salients), and (c) sinks (permanent sediment losses from beaches on to land and into deep water). Similar distinctions can sometimes be made in hemiarid lake basins, although relatively steep geomorphic (stream and slopewash) gradients tend to limit post-lacustrine residence times of lake sediments in beaches and, most notably, in blanket deposits above basin floors. However, the corollary (that the residence times of lake sediments, including ubiquitous reworked sediments, in basin-floor sinks are essentially unlimited) does not necessarily follow, because the floors of many hemiarid lake basins (a) are prone to vigorous subaqueous and aeolian scour during lowstands, and (b) eventually undergo tectonic rejuvenation by tilting and/or faulting.

Long-term sediment sinks in hemiarid lake basins can be viewed from several perspectives. For example, physiography is widely used as a basis for differentiating depositional subenvironments. Alluvial fans, fan-toe sandflats, dry mudflats, saline mudflats, salt pans, perennial saline lakes, aeolian

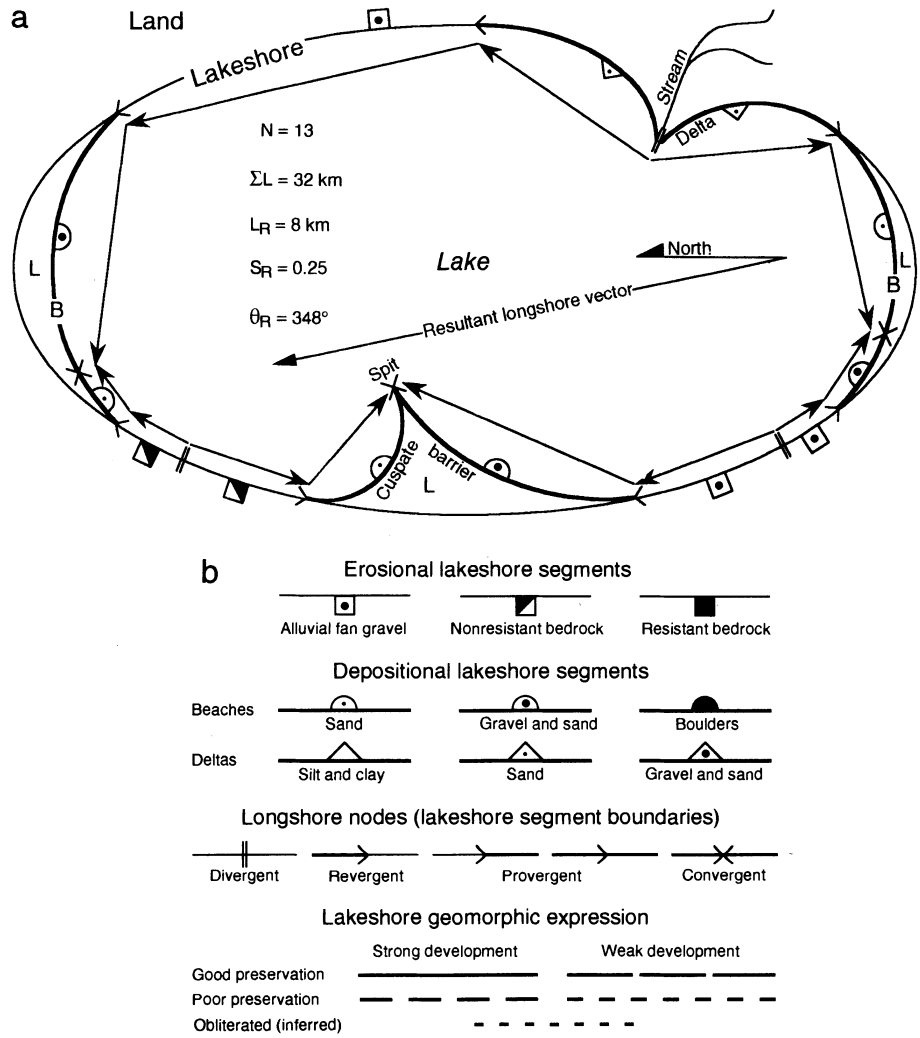

Figure 16.4 (a) Map of hypothetical lakeshore showing longshore pathways from sediment sources to depositional sites. L = lagoon and B = barrier beach; see (b) for explanation of lakeshore segmentation symbols. Longshore vector polygon and resultant longshore vector are plotted within lake area. N = number of lakeshore segments (= number of longshore vectors), ΣL = total length of longshore vectors, L_R = length of resultant longshore vector, S_R = strength of resultant longshore vector (L_R as fraction of ΣL), and θ_R = azimuth of resultant longshore vector. (b) Explanation of lakeshore segmentation symbols used in (a). Erosional flags project landward and depositional pennants project lakeward.

dunes, perennial streams, ephemeral streams, springs, spring-fed ponds, and shorelines are important depositional environments in saline lake basins (Hardie *et al.* 1978; Eugster and Kelts 1983). Distributary-channel deltoids (Mabbutt 1977, p. 162) are important in some desert lowlands (e.g. where the terminal reach of the Amargosa River intermittently aggrades Badwater Basin, on the floor of Death Valley, California: Hunt *et al.* 1966, pl. 2). Two perspectives that focus on lakebed sediment sinks are outlined here.

The zone-sector-polygon subenvironment model (Table 16.4 and Fig. 16.5) rationalizes the continuum of lakebed sediment sinks in terms of two orthogonal spatial patterns: (a) topologically concentric bathymetric zones and (b) topologically radial sediment budget sectors. In this model, the four bathymetric environment zones outlined previously (Fig. 16.2 and Table 16.1) intersect 12 (or more) longshore sediment budget sectors to define 48 (or more) depositional subenvironment polygons. The structure of this model lends itself to geographic in-

Table 16.4 Zone-sector-polygon model of lacustrine depositional subenvironments, in which 48 subenvironment polygons are defined by the intersections (Fig. 16.5) of four bathymetric environment zones (Fig. 16.2 and Table 16.1) and 12 longshore environment (sediment dynamics) sectors. Paired upper case letters denote typically strong linkages between depositional subenvironments and longshore sediment dynamics; lower case letters denote typically weak linkages

Longshore environment (sediment dynamics) sectors	*Bathymetric environment zones:*			
	Offshore (O)	*Nearshore (N)*	*Foreshore (F)*	*Backshore (B)*
	Depositional subenvironment polygons			
Sediment source (net output) sectors:				
non-resistant bedrock (N)	on	NN	FN	BN
earlier lakebeds (E)	oe	NE	FE	BE
alluvial fan gravels (A)	oa	NA	FA	BA
stream mouth gravels (S)	OS	NS	FS	BS
river mouth sands and silts (R)	OR	NR	FR	BR
ooid-supplied shore (O)	oo	NO	FO	BO
Sediment transfer (steady state) sector:				
longshore transport (L)	ol	NL	FL	BL
Sediment sink (net input) sectors:				
beach accretion sink (B)	ob	NB	FB	BB
inland aeolian sink (I)	oi	NI	FI	BI
deep water sink (D)	OD	ND	FD	bd
Energy- and sediment-starved sectors:				
wave-starved shallows (W)	ow	nw	FW	BW
clast-starved resistant bedrock (C)	oc	nc	FC	BC

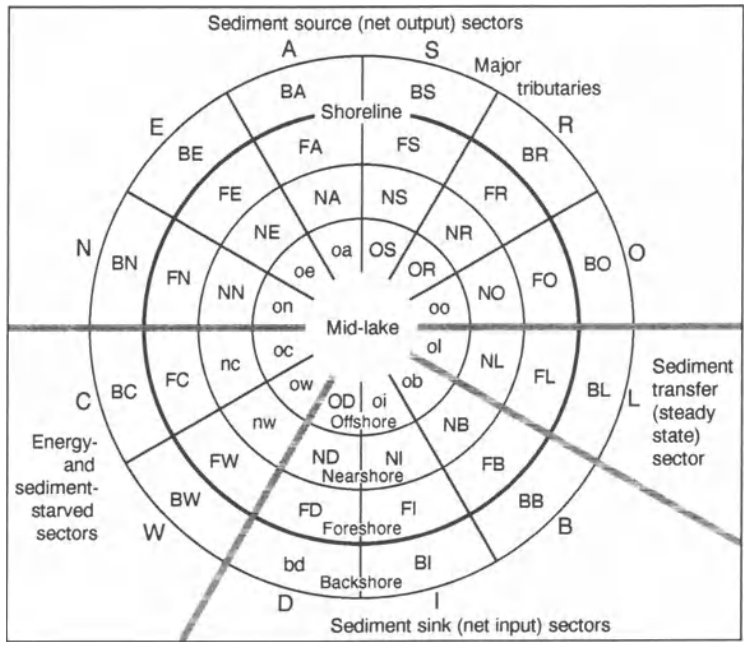

Figure 16.5 Zone-sector-polygon model of lacustrine depositional subenvironments arrayed in conceptual plan, with 48 subenvironment polygons defined by intersections of four concentric zones (bathymetric environment zones, Table 16.1 and Fig. 16.2) and 12 radial sectors (longshore sediment dynamics sectors). See Table 16.4 for explanation of symbols.

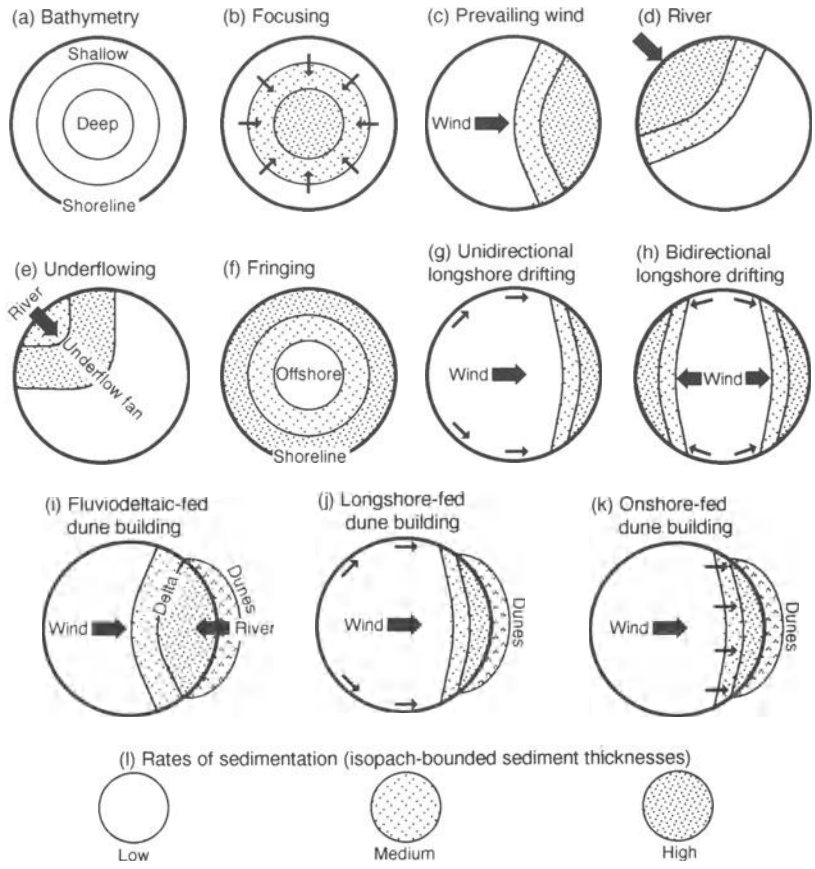

Figure 16.6 'Bubble' models showing areal patterns of sediment redistribution in lacustrine depocentres; (a)–(d) are after Longmore (1986) and (e)–(k) are additional patterns observed in south-western North America.

formation system (GIS) applications, including geomorphic mapping, in hemiarid lake basins.

'Bubble models' of depocentres highlight major patterns of lakebed sediment sinks. Models (e) through to (k) in Figure 16.6 are based on observations in North American hemiarid lake basins: (e) underflow depocentres (e.g. Oviatt 1987) occur offshore from river mouths with sediment-laden hyperpycnal flow; (f) fringing-beach depocentres occur mainly in small basins with easily eroded piedmont gravels; (g and j) depocentres fed by wind-driven longshore drift occur in almost every hemiarid lake basin, often as major beaches at gravel-dominated sites and beach-fed dunes at sandy sites; (h) major beaches have formed at the north and south ends of many Great Basin lakes due to orographically channelled southerly and northerly winds; (i) at least one major dune field is constructed of sand from the front of a windward-projecting late Pleistocene delta (Sack 1987); and (k) ooidal beaches and beach-fed dunes of Holocene age are widespread in gently shelving, mainly west-facing sectors of Great Salt Lake (Currey 1980).

In many hemiarid basins, lakebed geomorphic and stratigraphic features are regionally mantled and locally buried by post-lacustrine aeolian, colluvial, and pedogenic surficial materials. Aeolian deposits, including loess (ubiquitous in at least minor quantities), mud-pellet dunettes (often anchored aerodynamically to shrubs) and lunettes (around downwind margins of playas), and secondary sand dunes and sand sheets reworked from beach-fed primary dunes (Davies 1980, p. 157), commonly date from lake regressions and lowstands. Colluvial deposits, including coverhead that accumulates on erosional shorelines (Sharp 1978, pp. 13–4) and cover-beds that accrete basin-wide during waning-ice-age intervals (Kleber 1990), are poorly sorted, loess-enriched surficial materials emplaced by creep and slopewash. Aeolian and colluvial surficial deposits

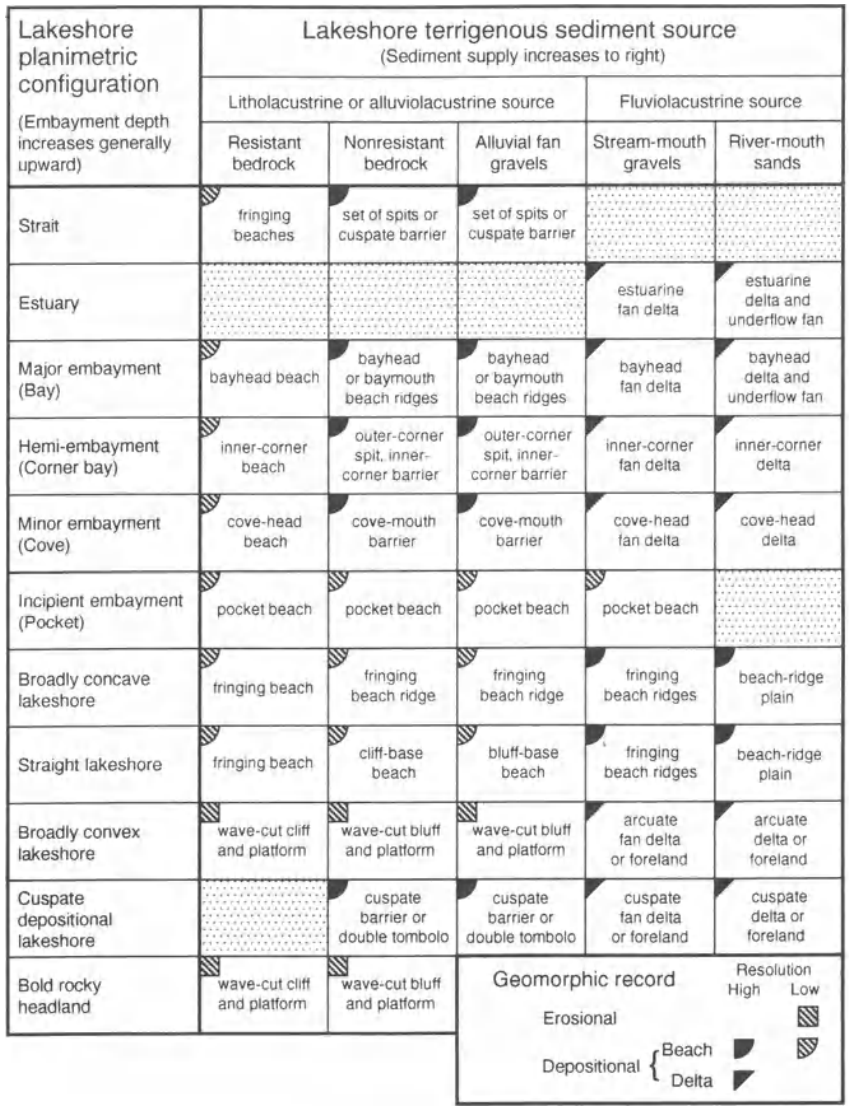

Figure 16.7 Forty-five common lakeshore geomorphic environments, arrayed in order of increasing terrigenous sediment supply and embayment depth; uncommon or null sets are stippled. Geomorphic resolution of lakeshore history is largely a function of sediment supply and embayment depth. Lakeshore geomorphic environments merge laterally in many combinations: for example, headland environments are commonly flanked by hemi-embayment environments.

commonly contain pedogenic carbonates and translocated clays (e.g. Birkeland *et al.* 1991, pp. 22–4), particularly where steppe vegetation has restricted geomorphic activity and contributed to pedogenesis.

LAKEBED LANDFORMS

Sediment sources, pathways, and sinks in hemiarid lake basins are embodied in landforms that record pre-lacustrine, co-lacustrine, and post-lacustrine geomorphic history. Lakebed landforms can be viewed in many ways; here they are viewed as modules in planimetric and stratigraphic patterns, and as indicators of post-lacustrine change.

Lacustrine geomorphic information is recorded mainly in lakeshore landforms, particularly depositional landforms. Geomorphic resolution of lake history tends to increase with increasing supplies of lakeshore terrigenous sediments (and ooidal sands) and increasing planimetric depth of lakeshore embayments (Fig. 16.7). Straits are important sites of geomorphic information (e.g. Burr and Currey 1992)

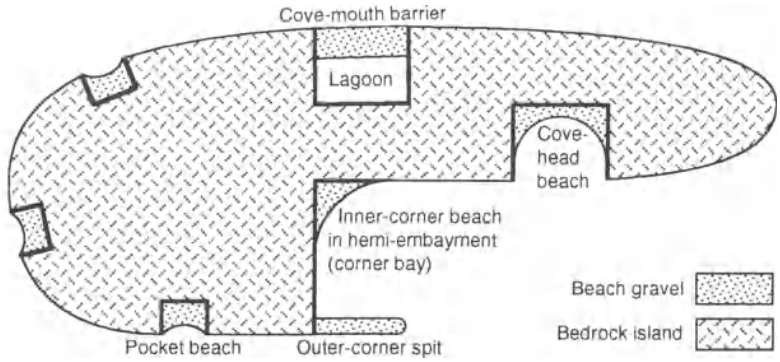

Figure 16.8 Map of hypothetical island with one hemi-embayment (corner bay), two minor embayments (coves), and three incipient embayments (with pocket beaches).

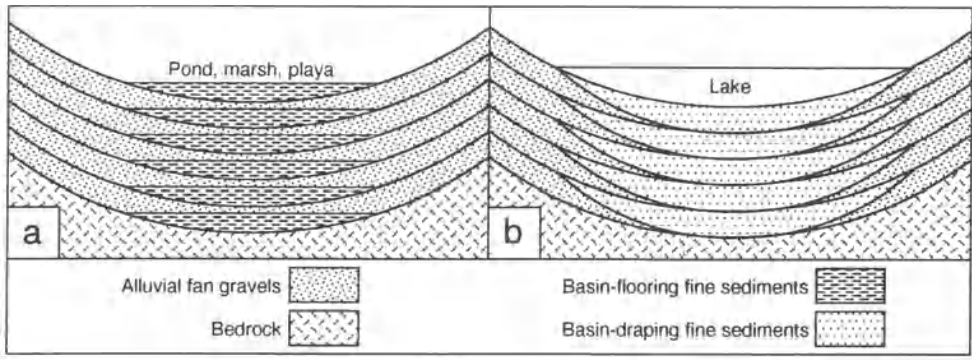

Figure 16.9 Schematic cross-sections of hemiarid lake basins with depositional sequences produced by recurring (a) shallow-water and (b) deep-lake cycles (after Currey 1990).

in large hemiarid lake basins; major embayments, including the concave ends of elongate lakes, are important in most basins; corner bays, coves, and pockets are important in most basins and on islands (Fig. 16.8). Two exceptions to the geomorphic importance of lakeshore embayments and terrigenous sediment supply should be noted: it has long been recognized that (a) cuspate progradation (e.g. Gilbert 1885, Zenkovich 1967, pp. 514–26, Carter 1988, pp. 192–6) commonly produces detailed geomorphic records in lakeshore sectors that are straight or even convex lakeward and (b) tufa accretion (e.g. Russell 1895, pp. 110–3, Morrison 1964, pp. 44–8, Benson *et al.* 1992) commonly produces detailed lakeshore geomorphic records during biogeochemically favourable intervals.

Stratigraphic sequences in hemiarid lake basins can be viewed as dominated by two geomorphic end members (Fig. 16.9), which alternate in basins with large lake-size variation. In the shallow-water geomorphic pattern (Fig. 16.9a), basin floors undergo progressive enlargement and overall flattening by hydroaeolian planation, in which six phases of geomorphic activity occur repeatedly as conditions alternate between shallow (typically less than 2 m) inundation and subaerial exposure (Merola *et al.* 1989; Currey 1990): (1) wind-driven bodies of shallow standing water entrain suspended sediment by subaqueous and circumaqueous (lateral) scour; (2) deposition of suspended sediment occurs as settling in still water and stranding in evaporating water; (3) subaerial desiccation reduces newly deposited suspended sediment to clasts of curled and cracked dry mud; (4) aeolian erosion deflates mud clasts and abrades desiccated surfaces; (5) aeolian deposition of mud clasts occurs on foredunes, upwind-opening lunettes that partially encircle deflated areas, and downwind-opening antilunettes that are largely encircled by deflated areas; and (6) post-aeolian diagenesis sinters and cements aeolian mud clasts.

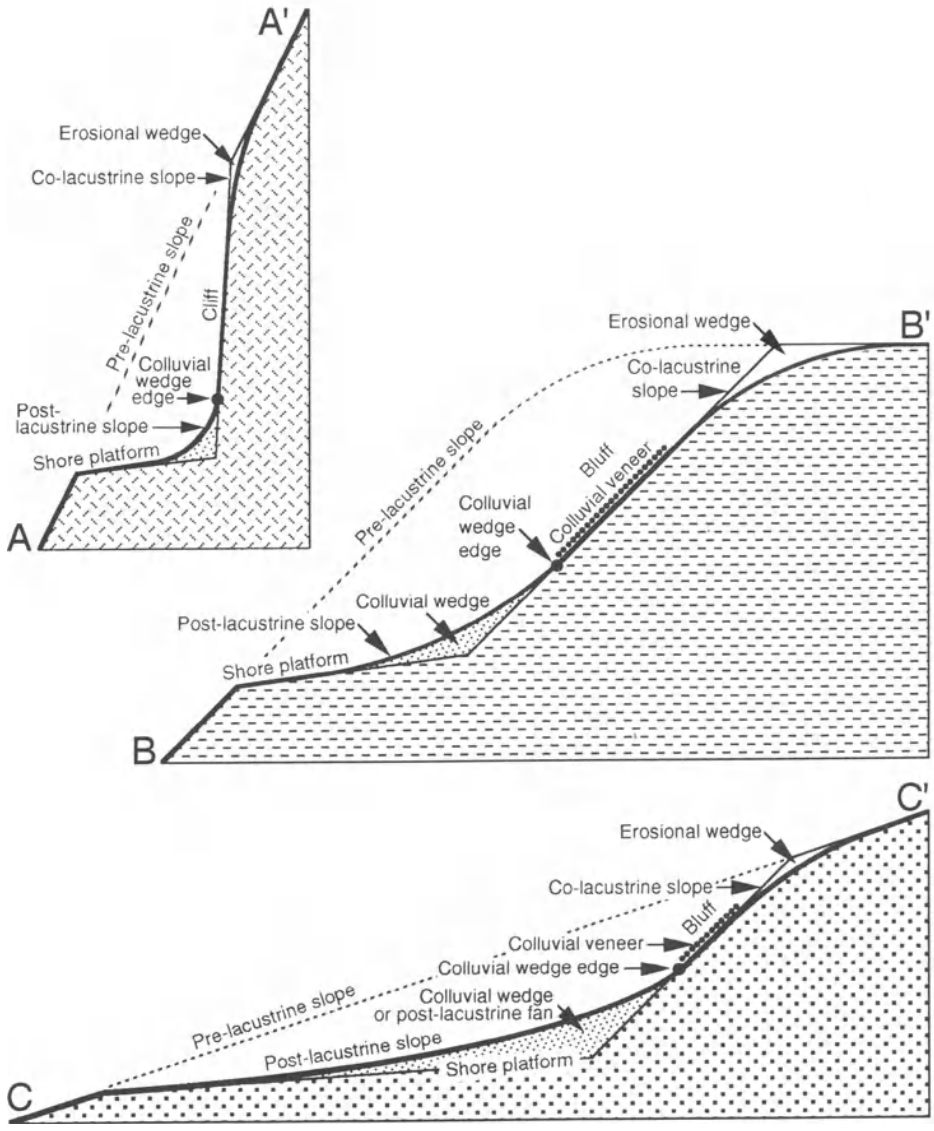

Figure 16.10 Schematic cross-sections showing post-lacustrine modification of co-lacustrine slopes, with patterns that are typical of erosional shorelines in resistant bedrock (A–A'), non-resistant bedrock (B–B'), and alluvial fan gravels (C–C'). Colluvial wedge edge (large dot = upper limit of positive colluvium mass balance) migrates upslope toward middle of co-lacustrine cliff or bluff as a function of post-lacustrine time.

Materials in (5) and (6) are reworked by repetitions of (1) through to (4). In the deep-water geomorphic pattern (Fig. 16.9b), basin-floor planation is eclipsed by lakebed differentiation into offshore, nearshore, foreshore, and backshore bathymetric zones (Table 16.1 and Fig. 16.2).

Co-lacustrine, as well as pre-lacustrine, lakeshore landforms undergo post-lacustrine geomorphic change that is perceptible across a wide range of spatial scales. At the local end of the scale spectrum, in surveyed profiles and cross-sections, geomorphic modification is time-dependent change in which post-lacustrine colluvial and alluvial wedges grow at the expense of buried midslopes and waning upper slopes, as in the erosional shoreline examples of Figure 16.10. Regionally, in maps and imagery, geomorphic decay is time-dependent change in which post-lacustrine geomorphic activity (common-

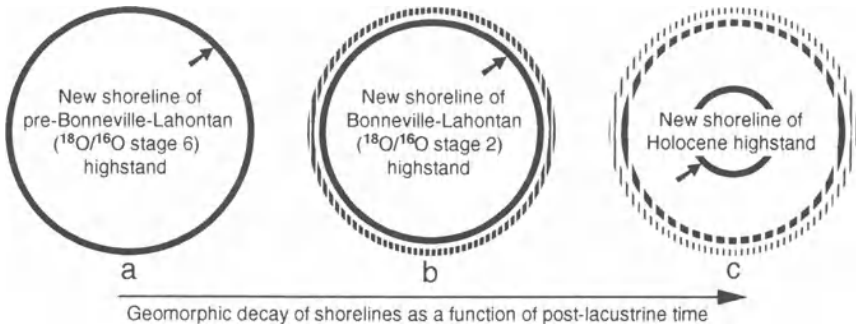

Figure 16.11 Schematic plans showing post-lacustrine decay of successively younger concentric shorelines. Patterned after late Quaternary shorelines in Nevada (e.g. Mifflin and Wheat 1979). Shoreline (a) probably formed about 140 ka, (b) about 15 ka, and (c) about 2.6 ka. The shoreline preservation index (π_s) for these shorelines is typically <0.1, 0.8, and >0.9, from oldest to youngest.

ly alluvial fan activity) gradually obliterates lakeshore form, as in the generalized shoreline examples of Figure 16.11. A useful gauge of geomorphic decay is given by the expression $1 - \pi_s$, where π_s is the shoreline preservation index, a dimensionless number from 0 to 1 that expresses visible shoreline length as a fraction of reconstructed total shoreline length (e.g. Fig. 16.11).

PALAEOLAKE STUDIES

Palaeolake studies draw on paradigms and techniques of the geosciences and biological sciences (e.g. Eardley *et al.* 1973, Spencer *et al.* 1984, Benson *et al.* 1990) and have applications that relate to many science questions and public policy issues. The goals of palaeolake studies are to reconstruct palaeolake histories and to constrain reconstructions of regional and global change. Selected aspects of palaeolake studies that are relevant to geomorphology are outlined here and are discussed at greater length in Chapter 24.

Palaeolake histories, and the histories of hemiarid lake basins generally, are reconstructed from lacustrine and non-lacustrine material evidence (bold rectangular boxes in Fig. 16.12). Much of this evidence is contained in depositional landforms – that is, in morpho-stratigraphic records. Morpho-stratigraphy, in which the methods of geomorphology and stratigraphy are employed interactively, is fundamental to successful research design in geomorphic studies of palaeolakes and their basins (Fig. 16.13). Morpho-stratigraphy is particularly useful in palaeolake studies that stress shoreline history as a basis for reconstructing hydrographic and tectonic history.

Basin-wide palaeolimnology, as illustrated by the idealized Great Basin palaeolake in Figure 16.14, provides a unifying framework for reconstructing individual stages of palaeolake history. In qualitative terms, the proximal (P), medial (M), and distal (D) reaches of palaeolakes like the one in Figure 16.14 tend to have distinctive patterns of hydrology, circulation, sedimentation, and lithofacies (Table 16.5) that help to explain geomorphic and stratigraphic patterns. In more quantitative terms, the proximal, medial, and distal reaches of many palaeolakes, including the one in Figure 16.14, can be viewed as loci in ternary fields that depict relationships among palaeolimnology variables, including inputs to the lacustrine water balance (Fig. 16.15a), origins of net horizontal motion in the epilimnion (Fig. 16.15b), and origins of sediment at the bottom of the water column (Fig. 16.15c).

Basin-wide (or sub-basin-wide) stratigraphy, as illustrated by the idealized Great Basin graben in Figure 16.16, provides the framework for reconstructing long intervals of palaeolake history. The large variations in water body size that are so characteristic of hemiarid lake basins result in depositional sequences with complex lateral and vertical changes of lithofacies, biofacies, and chemical facies. This complexity tends to be cyclical, which lends itself to what the *North American Stratigraphic Code* (NACSN 1983) terms allostratigraphic classification. In Figure 16.16, four allostratigraphic units of alloformation rank, each including two or three lithofacies, can be differentiated on the basis of laterally traceable discontinuities, in this case buried soils and disconformities (NACSN 1983). Stratigraphic markers, including regional discontinuities that generally date from palaeolake lowstands,

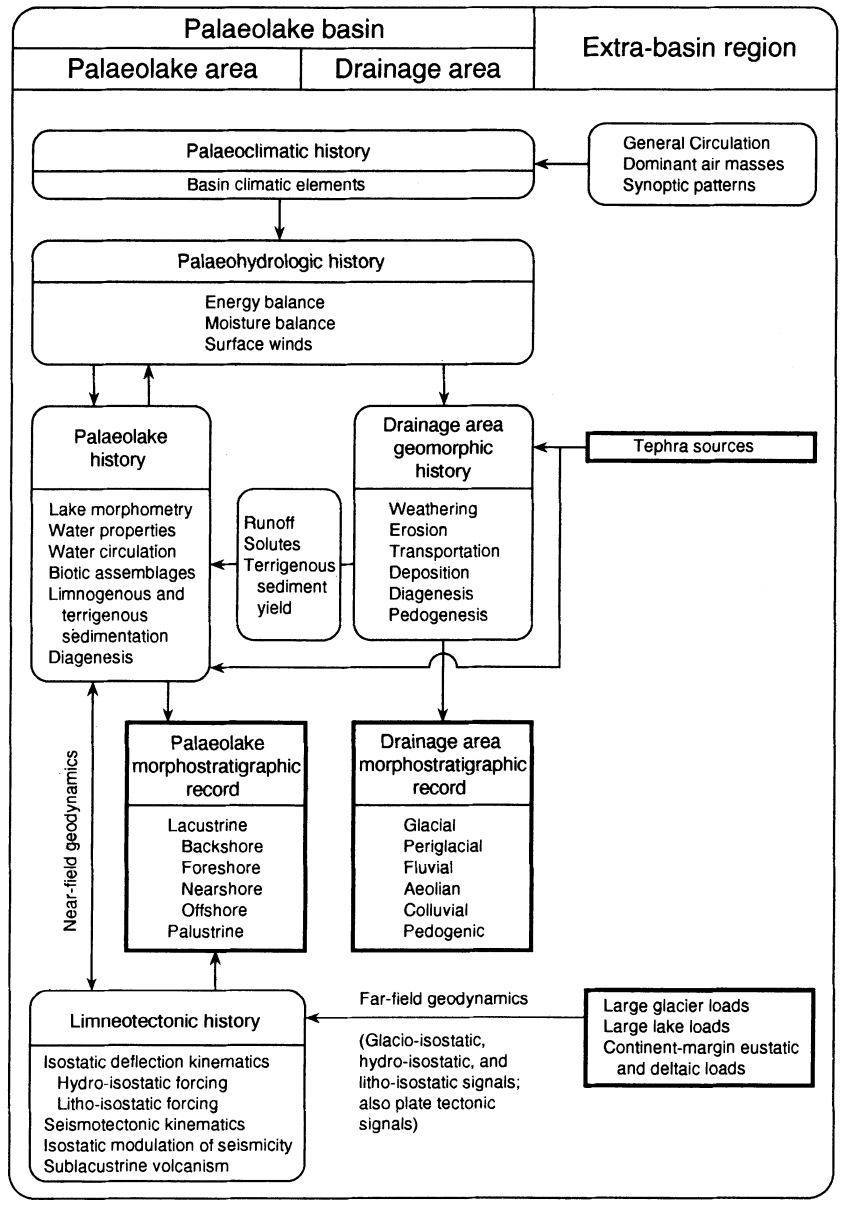

Figure 16.12 Flowchart showing elements of palaeolake history (rounded boxes), which are reconstructed from the geologic and geomorphic records (bold rectangular boxes) in lake basins and surrounding regions by response-process inference that is essentially counter to process→response causality (after Currey 1990).

assume great importance in hemiarid lake basins (e.g. Table 16.6) for two reasons: (a) in some cases they are the lower and upper boundaries of alloformations and (b) in many other cases they are indispensable tools for correlating intra-alloformation events within individual basins and from one basin to another.

Advances in palaeolake studies have closely paralleled refinements in geochronology (e.g. Easterbrook 1988, Forman 1989, Sack 1989, Birkeland *et al.* 1991). Particularly in the last decade, increasing spatio-temporal resolution has made hemiarid lake basins prime venues for studies of geomorphic kinematics (time rates of past landform changes),

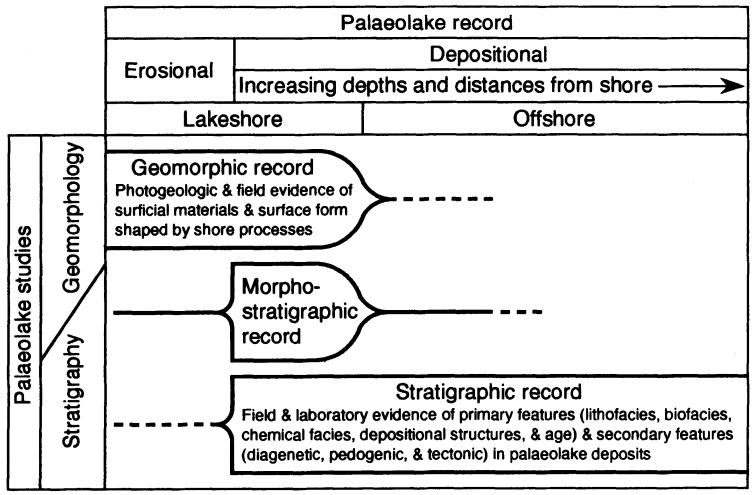

Figure 16.13 Morpho-stratigraphy combines the methods of geomorphology and stratigraphy in studies of palaeolake depositional landforms (after Currey and Burr 1988).

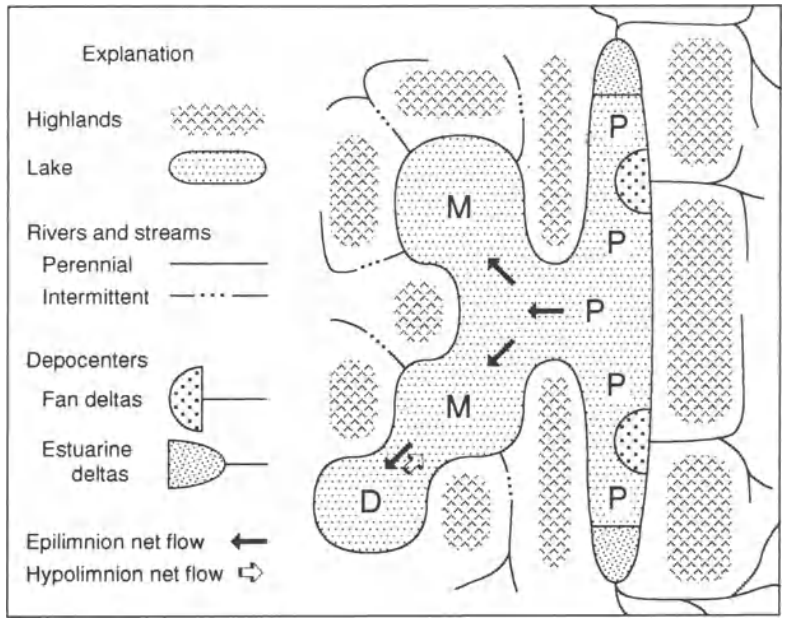

Figure 16.14 Map of hypothetical palaeolake in hemiarid basin, showing proximal (P), medial (M), and distal (D) reaches (after Currey 1990). Arrows show general directions of net flow (see Table 16.5 and Fig. 16.15).

hydrographic kinematics (time rates of past waterbody changes), and crustal–upper mantle geodynamics. Because radiocarbon dating is such an important tool in late Quaternary palaeolake studies (e.g. Table 16.7), refinements of that technology are noteworthy. The current shift from β-decay counting to accelerator mass spectrometry (AMS) measurement of ^{14}C allows ages of good precision to be obtained from samples containing milligram quantities of carbon. Applications include AMS ^{14}C dating of organic carbon traces in lake sediments (e.g. Thompson *et al.* 1990) and in lakeshore rock varnish (e.g. Dorn *et al.* 1990). As calendaric calibration of ^{14}C ages improves (e.g. Bard *et al.* 1990), so does precision in studies of palaeolake kinematics and geodynamics.

Table 16.5 Conditions typical of proximal, medial, and distal reaches in closed-basin lakes*

	Proximal reach	*Medial reach*	*Distal reach*
Hydrology	Local runoff dominant source of water-balance input; epilimnion salinity relatively low	Transbasin flow important source of water-balance input	Transbasin flow dominant source of water-balance input; epilimnion salinity relatively high
Circulation	Water-balance-driven net outflow in epilimnion	Water-balance-driven net throughflow in epilimnion	Water-balance-driven net inflow in epilimnion
Sedimentation	High rates of terrigenous and very low rates of limnogenous sedimentation	Low rates of terrigenous and limnogenous sedimentation	Low rates of limnogenous and very low rates of terrigenous sedimentation
Lithofacies	Fluviodeltaic clastics prevalent	Offshore micrite (typically calcite) and lakeshore clastics	Offshore micrite (typically aragonite) and lakeshore carbonates

*Adapted from Currey (1990). See Figures 16.14 and 16.15.

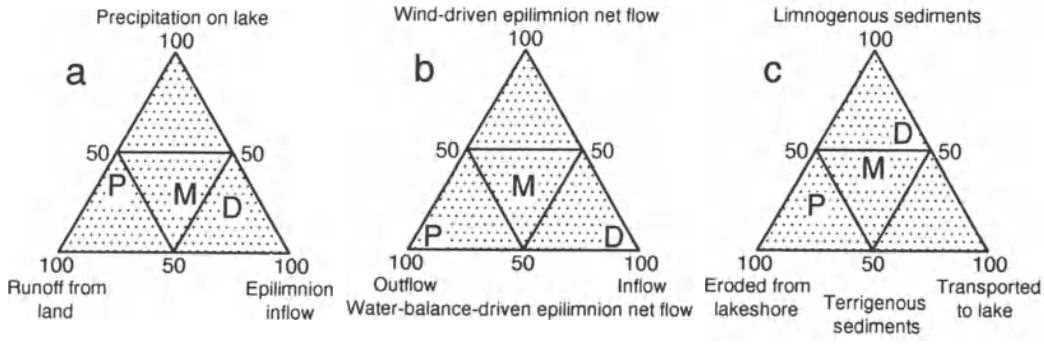

Figure 16.15 Loci of proximal (P), medial (M), and distal (D) reaches of hypothetical palaeolake (Fig. 16.14 and Table 16.5) in ternary fields depicting lake dynamics: (a) water balance inputs as a percentage of long-term receipts, (b) sources of net horizontal motion in epilimnion as a percentage of long-term net epilimnion flow, and (c) sources of sediments at bottom of water column as a percentage of long-term sedimentation (after Currey 1990).

Other geochronology advances that hold promise for palaeolake studies include optically stimulated luminescence (OSL) dating of quartz grains (e.g. Smith *et al.* 1990), which improves on thermoluminescence (TL) dating, and geochronometry using cosmogenic isotopes other than ^{14}C. For example, cosmogenic helium (^{3}He) and chlorine (^{36}Cl) have seen successful experimental use in dating basalt erosion and halite deposition, respectively, in the Lake Bonneville region.

Within-basin and between-basin comparisons of isotopic ages of possibly synchronic (coeval) features are commonly of interest in palaeolake studies. A dimensionless basis for comparing paired ages – that is, the ages before present of two samples from one palaeolake basin or of one sample from each of two palaeolake basins – is the index of temporal accordance ι. This index ranges from 0 where paired ages are completely dissimilar (discordant) to 1 where paired ages are identical (accordant). In Table 16.8, $\iota = 1 - [(\text{older age} - \text{younger age})/(\text{older age} + \text{younger age})]$.

Beginning with the work of Russell (1885) and Gilbert (1890), late Quaternary hydrographic change in hemiarid lake basins has traditionally been portrayed by hydrographs in which surface elevation, maximum depth, average depth, area, volume, or mass of standing water is plotted as a function of relative or absolute time. With increasing spatiotemporal resolution of lakeshore morpho-stratigraphy have come increasingly detailed palaeolake histories, often with several temporal wavelengths and spatial amplitudes of hydrographic change appearing as cycles within cycles (e.g. Fig. 16.17). First- and second-order temporal wavelengths, sometimes termed episodes and phases (e.g. Fig.

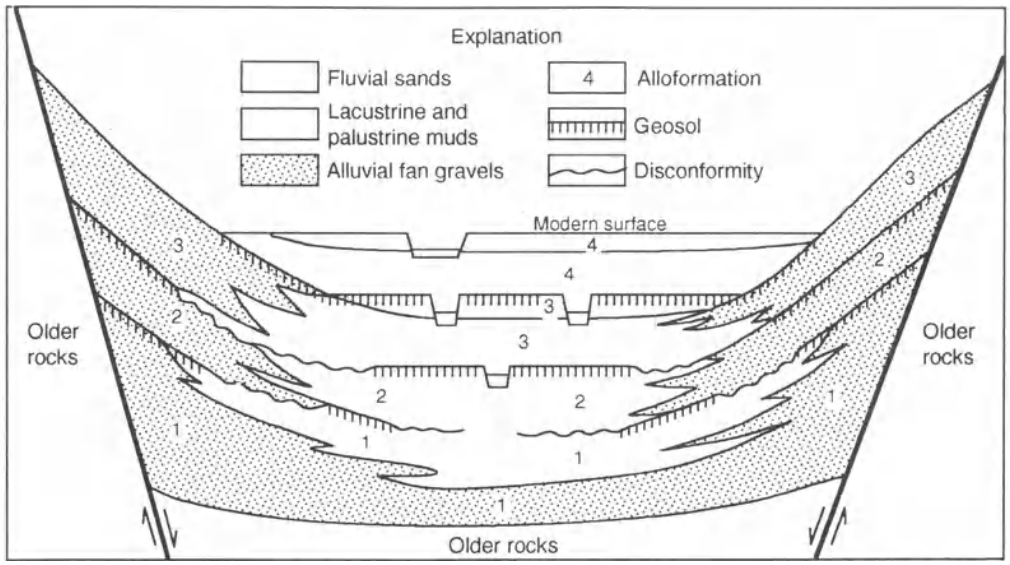

Figure 16.16 Schematic cross-section illustrating allostratigraphic classification of lacustrine muds and other sediments in a graben (after NACSN 1983). Patterned after Cache Valley, Utah, in the Lake Bonneville basin (Williams 1962, p. 136).

16.17; NACSN 1983), are measured in millennia. Third- and fourth-order temporal wavelengths, sometimes termed oscillations (e.g. Currey 1990) and stands, are mostly measured in centuries and decades (e.g. Currey and Burr 1988). 'Instantaneous' singularities in palaeolake history are commonly referred to as events, with some of the more notable being seismic, pyroclastic, and catastrophic flood (e.g. Jarrett and Malde 1987) events.

Geomorphic and palaeoenvironmental change that may not be evident in traditional hydrographs can often be represented explicitly in geomorphically annotated hydrographs. In Figure 16.17, annotations highlight several hypothetical but plausible features: ooid beaches (O) indicate saline stages, possibly with brine shrimp; prominent gravel beaches (B) mark transgressive stages, when pre-lacustrine alluvial fans and colluvium-mantled slopes were initially reworked into beaches; tufa-cemented stonelines (S and T) mark regressive stages, when water hardness increased and older beach gravels were locally reworked and cemented; intrenched and prograded deltas (D) indicate a falling local base level – that is, a regression; a salinity crisis near the close of the lacustral episode is marked by fetid, organic-rich sediments that accumulated offshore when freshwater plankton populations were annihilated by (and pickled in) increasingly concentrated brines; red beds mark emergence of the basin floor at the close of the lacustral episode, when previously anoxic hypolimnion sediments were reddened by oxidation of Fe^{+2}-sulphides to Fe^{+3}-oxides; and salt beds are former dissolved solids forced from solution by volumetric reduction at the close of the lacustral episode (e.g. in its 2000-year transition to hypersaline Great Salt Lake, the volume of freshwater Lake Bonneville was reduced by three orders of magnitude).

APPLIED PALAEOLAKE STUDIES

Palaeolake studies have applications in many fields, including climatology, hydrogeology, wetlands and shorelands management, mineral industries, and limneotectonics. Many of these applications are based on the principle of converse uniformitarianism (conformitarianism), which states that the past is the key to the present and future. The importance of palaeolakes as sources of proxy climate data in atmospheric research, including global change studies and general circulation models, is well documented (e.g. Street-Perrott and Harrison 1985, Benson and Paillet 1989, Chapter 24). In the western United States, studies of Quaternary lakes provide crucial information in hydrogeologic evaluations of potential sites for long-term storage of high-level nuclear waste (e.g. Williams and Bedinger 1984, Sargent and Bedinger 1985).

Table 16.6 Stratigraphic markers of regional importance in Lake Bonneville studies: B = marker beds (distinctive sediment layers), H = marker horizons (distinctive surfaces between sediment layers), and P = marker profiles (sediment layers imprinted by subaerial palaeoenvironments or palaeoseismicity)

Stratigraphic markers	*B*	*H*	*P*	*Examples*
Offshore micrites:				Oviatt 1987
white marl	•			
with abundant dropstones	•			
Coquinas:				Oviatt 1987
gastropod	•			
ostracod	•			
Tephra:				Oviatt and Nash 1989
silicic	•			
basaltic	•			
Evaporites:				Eugster and Hardie 1978
mirabilite	•			Eardley 1962
halite	•			
Stonelines:				
foreshore	•			
fluviolacustrine	•			
buried desert pavement	•	•		Currey 1990
Tufa:				
tufacrete ledges	•	•	•	
heads and mounds	•	•		Carozzi 1962
beachrock and hardground	•			Spencer *et al.* 1984
Transgressive basal layers:				
gravels on truncated geosols	•	•	•	
basal organics (muck and wood)	•			Scott *et al.* 1983
Oolitic sand layers	•			Eardley *et al.* 1973
Buried aeolian deposits:				
loessal colluvium	•	•	•	
aeolian sand	•	•		
Discontinuities:				NACSN 1983
erosional unconformities		•		
non-depositional unconformities		•		
Red beds:				
in situ		•	•	
transported	•			Currey 1990
Soils:				Birkeland *et al.* 1991
buried soils (geosols)		•	•	Eardley *et al.* 1973
relict (residual) soils		•	•	
K horizons (caliche)		•	•	Machette 1985
natric horizons		•	•	
Root tubules (rhizoliths)		•	•	Eardley *et al.* 1973
Desiccation cracks		•	•	Currey 1990
Seismically convoluted bedding			•	

Wetlands management in hemiarid lake basins seeks to minimize the adverse effects that hydrographic fluctuations can have on vital aquatic environments, including those that support waterfowl, recreation and tourism, and saline industries (e.g. Fig. 16.18). Shorelands management in hemiarid lake basins seeks to minimize (by measures such as planning, zoning, dyking, and pumping) the potential impacts of rising lake levels on transportation and communication networks, public utilities, industrial development, and urban sprawl (e.g. Fig. 16.18). Increasingly, wetlands and shorelands management strategies are founded on base line information from palaeolake studies.

Many hemiarid lake basins contain significant mineral resources, chiefly potash, soda ash, sodium chloride, borates, nitrates, magnesium, lithium, uranium, sand and gravel, volcanics, zeolites, diato-

Table 16.7 Organic carbon (O) and carbonate carbon (A = aragonite, C = calcite, D = dolomite) materials yielding radiocarbon ages of relevance to Lake Bonneville studies

Material	*O*	*A*	*C*	*D*
Wood fragments	•			
Charcoal flecks	•			
Spring bog peat	•			
Marsh muck	•			
Seeds	•			
Geosol humates	•			
Biodust in rock varnish	•			
Bone collagen	•			
Neotoma excreta	•			
Mollusca, shell proteins	•			
Mollusca, snail shells		•		
Mollusca, clam shells		•		
Ostracods, shells		•		
Ostracods, shell proteins	•			
Ooids		•		
Artemia faeces in ooids	•			
Marl, *Chara* phytoliths		•	•	
Marl, micrite		•	•	
Plankton residues in mud	•			
Tufa, algaloid		•	•	
Algal residues in tufa	•			
Tufacrete matrix		•	•	
Travertine, cave			•	
Travertine, spring			•	
Caliche			•	
Root tubule rhizoliths			•	
Saline mudflat carbonate				•

Table 16.8 Index of temporal accordance (IOTA)

Temporal accordance	*IOTA* (ι)
High (paired ages plausibly synchronous)	$1.00 \geq \iota > 0.99$
Problematic (paired ages possibly synchronous)	$0.99 > \iota > 0.90$
Low (paired ages doubtfully synchronous)	$0.90 > \iota \geq 0$

mite, and fossil fuels (e.g. Reeves 1978). Palaeolake studies and mineral industries tend to be mutually supportive, with the former providing information that often is of value in assessing mineral reserves and development options, and the latter contributing to the corpus of palaeolake knowledge by making available subsurface information that frequently has been obtained at great expense (e.g. Smith 1979, pp. 6–8, Smith *et al.* 1983, p. 3).

Limneotectonics (lacustrine neotectonics) is the use of palaeolake levels (PLLs) as long-base-line tiltmeters and palaeolake beds (PLBs) as local slip-meters to measure co- and post-lacustrine rates of crustal motion, particularly vertical motion (Currey 1988). A PLL is the originally horizontal upper bounding surface (atmosphere–lake interface) of a palaeolake stage of known age, as reconstructed from lakeshore morpho-stratigraphic evidence that is analogous to the raised shorelines (e.g. Rose 1981) of many sea coasts. A PLB is the lower bounding surface (lake–substrate interface) of a palaeolake stage of known age, as observed in the lakebed stratigraphic record.

In many hemiarid lake basins, total neotectonic vertical deformation is the algebraic sum of (a) seismotectonic vertical displacement caused by faulting and (b) one or more (near-field, far-field, hydro-, glacio-, litho-) isostatic vertical deflection signals generated by crustal loading and/or unloading. An important goal of limneotectonics is to assess the contribution made by each of these sources of crustal motion (e.g. Fig. 16.19).

Palaeolakebeds that have been displaced by faulting are common in hemiarid lake basins that owe their existence to hypertectonism (Figs 15.4 and 16.1), as does the basin of Lake Bonneville–Great Salt Lake. Beneath Great Salt Lake, seismic reflection surveys (Mikulich and Smith 1974) and many boreholes have helped to define the geometry of sub-bottom PLBs and, thereby, the late Cenozoic kinematics of sub-bottom tectonic blocks (e.g. Pechmann *et al.* 1987). In backhoe trenches across post-lacustrine fault scarps at many localities in the Lake Bonneville–Great Salt Lake region, detailed studies of offset PLBs (and of scarp-burying colluvial wedges) are providing insights into the magnitudes and recurrence intervals of late Quaternary seismic events (e.g. Machette *et al.* 1991).

At several sites in the Lake Bonneville–Great Salt region, maximum late Quaternary seismicity and maximum late Quaternary isostatic rebound seem to have coincided in time, particularly where the orientation of seismotectonic extension coincided with the orientation of isostatic deflection radii (Fig. 16.17b). This suggests a pattern in which the tempo of seismotectonic displacement is modulated by the vertical direction and tempo of hydro-isostatic deflection. Specifically, where the traces of active extensional (normal) faults are tangent to isolines (isobases) of near-field hydro-isostatic deflection, seismicity may be (1) suppressed during times of sustained isostatic subsidence and (2) enhanced during subsequent times of maximum isostatic rebound.

Palaeolake levels that have undergone near-field

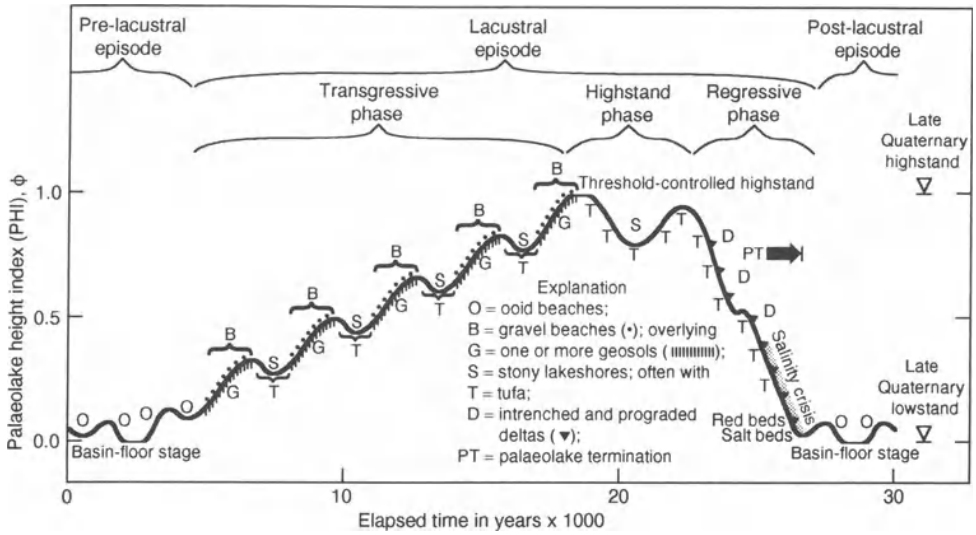

Figure 16.17 Geomorphically annotated hydrograph (heavy line) of a hypothetical palaeolake cycle in a hydrographically closed basin. Patterned in part after Lake Bonneville (e.g. Currey *et al.* 1984). Hydrograph depicts decamillennium-scale change (lacustral episode and phases) and millennium-scale oscillations (subphases); century-scale fluctuations are not shown except as implied by beach dots; decade-scale variation is within the hydrograph line width.

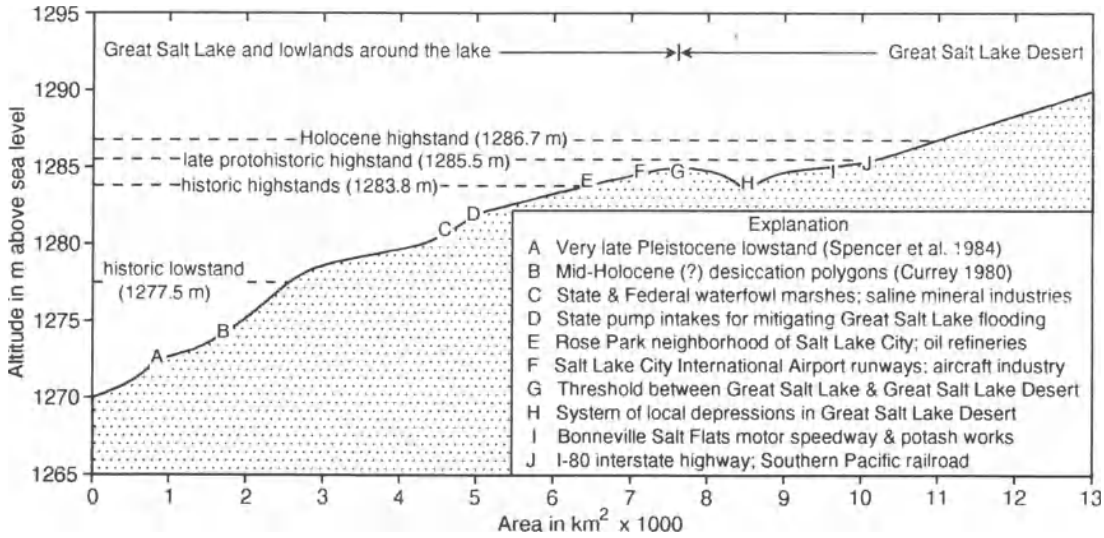

Figure 16.18 Geomorphically annotated hypsograph showing singular levels in the lowest part of the Great Salt Lake basin, Utah (after Currey 1990). Average gradient across area depicted is only 0.0002. See Figure 15.16 for basin-wide context.

hydro-isostatic deflection occur in hemiarid lake basins with histories of large water load changes, as in the Lake Lahontan (Mifflin and Wheat 1971) and Lake Bonneville (Crittenden 1963, p. E9, Currey 1982) regions of the Great Basin. Subsequent to Lake Bonneville's highstand about 15 ka, when the lake had a depth of over 370 m and a volume of almost 10 000 km^3, about 74 m of differential uplift occurred within the near-field area (52 000 km^2) enclosed by the highest shoreline (Currey 1990). About 16 m of additional differential uplift can be detected as far-field effects in small lake basins up to 120 km outside the highest Bonneville shoreline (e.g. Bills and Currey 1988). Post-Bonneville rebound has total-

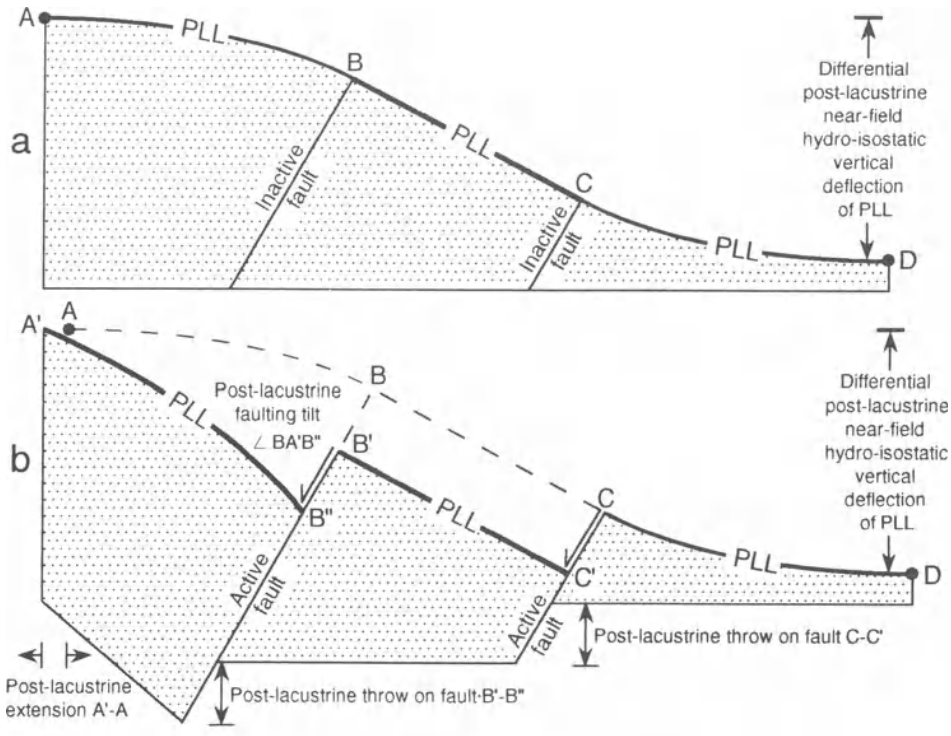

Figure 16.19 Schematic profiles (not to scale) of regional and subregional deformation of an originally horizontal palaeolake level (PLL) of known age (after Currey 1990). A–D is regional trend of a hydro-isostatically deflected PLL. A and D are PLL localities of maximum and minimum observed isostatic rebound – that is, A is the isostatic deflection centroid and D is a distal point on an isostatic deflection radius. (a) Total post-lacustrine neotectonic deformation comprises only near-field hydro-isostatic deflection. (b) Total post-lacustrine neotectonic deformation comprises regional isostatic deflection (dashed) overprinted with subregional seismotectonic displacement, including rotational displacement of tectonic block A'–B" and translational displacement of tectonic block B'–C'.

led less than 1 m since 2.6 ka, as gauged by the essentially horizontal shoreline that marks the Holocene highstand of Great Salt Lake.

The maximum rate of hydro-isostatic vertical deflection in the Bonneville basin is estimated to have been -7.3 cm y^{-1} about 15 ka (Currey and Burr 1988). This is somewhat less than maximum rates of glacio-isostatic rebound in Fennoscandia and Canada, where regional crustal uplift exceeded 10 cm y^{-1} in very late Pleistocene and early Holocene time (Lajoie 1986). Where (a) known water loading and unloading histories have acted on (b) unknown Earth rheologies to produce (c) known hydro-isostatic deflection histories, limneotectonics can be a powerful tool in Earth rheology modelling (Bills and May 1987) – that is, limneotectonics can be a rich source of insight into the thickness and flexural rigidity of the Earth's crust and the viscosity layering of the upper mantle.

ACKNOWLEDGEMENTS

Much of the research on which this chapter is based was supported by NSF grant EAR-8721114. A large debt is owed to supportive colleagues, including G. Atwood, M. Berry, B. Bills, J. Czarnomski, B. Everitt, B. Haslam, M. Isgreen, J. Keaton, G. King, M. Lee, K. Lillquist, D. Madsen, S. Murchison, J. Oviatt, J. Petersen, A. Reesman, D. Sack, G. Tackman, and G. Williams.

REFERENCES

Bard, E., B. Hamelin, R.G. Fairbanks and A. Zindler 1990. Calibration of the ^{14}C timescale over the past 30,000 years using mass spectrometric U–Th ages from Barbados corals. *Nature* **345**, 405–10.

Benson, L.V. and F.L. Paillet 1989. The use of total lake-surface area as an indicator of climatic change: examples from the Lahontan basin. *Quaternary Research* **32**, 262–75.

Benson, L.V., D.R. Currey, R.I. Dorn, K.R. Lajoie, *et al.* 1990. Variation in size of four Great Basin lake systems during the past 35,000 years. *Palaeogeography, Palaeoclimatology, Palaeoecology* **78**, 241–86.

Benson, L., D. Currey, Y. Lao and S. Hostetler 1992. Lake-size variations in the Lahontan and Bonneville basins between 13,000 and 9000 ^{14}C yr B.P. *Palaeogeography, Palaeoclimatology, Palaeoecology* **95**, 19–32.

Bills, B.G. and D.R. Currey 1988. Lake Bonneville: Earth rheology inferences from shoreline deflections. *EOS* **69**, 1454.

Bills, B.G. and G.M. May 1987. Lake Bonneville: constraints on lithospheric thickness and upper mantle viscosity from isostatic warping of Bonneville, Provo, and Gilbert stage shorelines. *Journal of Geophysical Research* **92**, 11493–508.

Birkeland, P.W., M.N. Machette and K.M. Haller 1991. Soils as a tool for applied Quaternary geology. *Utah Geological and Mineral Survey Miscellaneous Publication* 91-3.

Burr, T. and D.R. Currey 1992. Hydrographic modelling at the Stockton Bar. In *Field guide to geologic excursions in Utah and adjacent areas of Nevada, Idaho, and Wyoming*, J.R. Wilson (ed.) 207–19. Utah Geological Survey Miscellaneous Publications 92-3.

Carozzi, A.V. 1962. Observations of algal biostromes in the Great Salt Lake, Utah. *Journal of Geology* **70**, 246–52.

Carter, R.W.G. 1988. *Coastal environments*. London: Academic Press.

Crittenden, M.D. 1963. New data on the isostatic deformation of Lake Bonneville. *U.S. Geological Survey Professional Paper* 454-E.

Currey, D.R. 1980. Coastal geomorphology of Great Salt Lake and vicinity. In *Great Salt Lake: a scientific, historical, and economic overview*, J.W. Gwynn (ed.), 69–82. Utah Geological and Mineral Survey Bulletin 116.

Currey, D.R. 1982. Lake Bonneville: selected features of relevance to neotectonic analysis. *U.S. Geological Survey Open-file Report* 82-1070.

Currey, D.R. 1988. Seismotectonic kinematics inferred from Quaternary paleolake datums, Salt Lake City seismopolitan region, Utah. In *National earthquake hazards reduction program, summaries of technical reports volume xxvii*, 457–61. U.S. Geological Survey Open-file Report 88-673.

Currey, D.R. 1990. Quaternary palaeolakes in the evolution of semidesert basins, with special emphasis on Lake Bonneville and the Great Basin, U.S.A. *Palaeogeography, Palaeoclimatology, Palaeoecology* **76**, 189–214.

Currey, D.R. and T.N. Burr 1988. Linear model of threshold-controlled shorelines of Lake Bonneville. In *In the footsteps of G.K. Gilbert – Lake Bonneville and neotectonics of the eastern Basin and Range Province*, M.N. Machette (ed.), 104–10. Utah Geological and Mineral Survey Miscellaneous Publication 88-1.

Currey, D.R., G. Atwood and D.R. Mabey 1984. Major levels of Great Salt Lake and Lake Bonneville. *Utah Geological and Mineral Survey Map* 73.

Davies, J.L. 1980. *Geographical variation in coastal development*, 2nd edn. London: Longman.

Dorn, R.I., A.J.T. Jull, D.J. Donahue, T.W. Linick, *et al.* 1990. Latest Pleistocene lake shorelines and glacial chronology in the western Basin and Range Province, U.S.A.: insights from AMS radiocarbon dating of rock varnish and paleoclimatic implications. *Palaeogeography, Palaeoclimatology, Palaeoecology* **78**, 315–31.

Eardley, A.J. 1962. Glauber's salt bed west of Promontory Point, Great Salt Lake. *Utah Geological and Mineral Survey Special Studies* 1.

Eardley, A.J. 1966. Sediments of Great Salt Lake. In *The Great Salt Lake*, W.L. Stokes (ed.), 105–20. Utah Geological Society Guidebook 20.

Eardley, A.J., R.T. Shuey, V. Gvosdetsky, W.P. Nash, *et al.* 1973. Lake cycles in the Bonneville basin, Utah. *Bulletin of the Geological Society of America* **84**, 211–6.

Easterbrook, D.J. (ed.) 1988. Dating Quaternary sediments. *Geological Society of America Special Paper* 227.

Eugster, H.P. and L.A. Hardie 1978. Saline lakes. In *Lakes: chemistry, geology, physics*, A. Lerman (ed.), 237–93. New York: Springer.

Eugster, H.P. and K. Kelts 1983. Lacustrine chemical sediments. In *Chemical sediments and geomorphology*, A.S. Goudie and K. Pye (eds), 321–68. London: Academic Press.

Forman, S.L. (ed.) 1989. Dating methods applicable to Quaternary geologic studies in the western United States. *Utah Geological and Mineral Survey Miscellaneous Publication* 89-7.

Galat, D.L. and R.L. Jacobsen 1985. Recurrent aragonite precipitation in saline-alkaline Pyramid Lake, Nevada. *Archiv. für Hydrobiologie* **105**, 137–59.

Gilbert, G.K. 1885. The topographic features of lake shores. *U.S. Geological Survey 5th Annual Report*, 69–123.

Gilbert, G.K. 1890. *Lake Bonneville*. U.S. Geological Survey Monograph 1.

Håkanson, L. 1981. *A manual of lake morphometry*. Berlin: Springer.

Håkanson, L. and M. Jansson 1983. *Principles of lake sedimentology*. Berlin: Springer.

Hardie, L.A., J.P. Smoot and H.P. Eugster 1978. Saline lakes and their deposits: a sedimentological approach. In *Modern and ancient lake sediments*. A. Matter and M.E. Tucker (eds), 7–41. Oxford: Blackwell Scientific.

Hunt, C.B., T.W. Robinson, W.A. Bowles and A.L. Washburn 1966. Hydrologic basin, Death Valley, California. *U.S. Geological Survey Professional Paper* 494-B.

Jarrett, R.D. and H.E. Malde 1987. Paleodischarge of the late Pleistocene Bonneville Flood, Snake River, Idaho, computed from new evidence. *Bulletin of the Geological Society of America* **99**, 127–34.

Jones, B.F. and C.J. Bowser 1978. The mineralogy and related chemistry of lake sediments. In *Lakes: chemistry, geology, physics*, A. Lerman (ed.), 179–235. New York: Springer.

Kleber, A. 1990. Upper Quaternary sediments and soils in the Great Salt Lake area, U.S.A. *Zeitschrift für Geomorphologie* **34**, 271–81.

Lajoie, K.R. 1986. Coastal tectonics. In *Active tectonics*, 95–124. Washington: National Academy Press.

Longmore, M.E. 1986. Modern and ancient sediments – data base for management of aquatic ecosystems and their catchments. In *Limnology in Australia*, P. De Deckker and W.D. Williams (eds), 509–22. Dordrecht: W. Junk.

Mabbutt, J.A. 1977. *Desert landforms*. Cambridge, MA: MIT Press.

Machette, M.N. 1985. Calcic soils of the southwestern United States. In *Soils and Quaternary geology of the*

southwestern United States, D.L. Weide (ed.), 1–21. Geological Society of America Special Paper 203.

Machette, M.N., S.F. Personius, A.R. Nelson, D.P. Schwartz, *et al.* 1991. The Wasatch fault zone, Utah – segmentation and history of Holocene earthquakes. *Journal of Structural Geology* **13**, 137–49.

Merola, J.A., D.R. Currey and M.K. Ridd 1989. Thematic mapper–laser profile resolution of Holocene lake limit, Great Salt Lake Desert, Utah. *Remote Sensing of Environment* **27**, 229–40.

Mifflin, M.D. and M.M. Wheat 1971. Isostatic rebound in the Lahontan basin, northwestern Great Basin. *Geological Society of America Abstracts with Program* **3**, 647.

Mifflin, M.D. and M.M. Wheat 1979. Pluvial lakes and estimated pluvial climates of Nevada. *Nevada Bureau of Mines & Geology Bulletin* 94.

Mikulich, M.J. and R.B. Smith 1974. Seismic reflection and aeromagnetic surveys of the Great Salt Lake, Utah. *Bulletin of the Geological Society of America* **85**, 991–1002.

Morrison, R.B. 1964. Lake Lahontan: geology of the southern Carson Desert, Nevada. *U.S. Geological Survey Professional Paper* 401.

(NACSN) North American Commission on Stratigraphic Nomenclature 1982. North American stratigraphic code. *American Association of Petroleum Geologists Bulletin* **67**, 842–75.

Oviatt, C.G. 1987. Lake Bonneville stratigraphy at the Old River Bed, Utah. *American Journal of Science* **287**, 383–98.

Oviatt, C.G. and W.P. Nash 1989. Late Pleistocene basaltic ash and volcanic eruptions in the Bonneville basin, Utah. *Bulletin of the Geological Society of America* **101**, 292–303.

Pechmann, J.C., W.P. Nash, J.J. Viveiros and R.B. Smith 1987. Slip rate and earthquake potential of the East Great Salt Lake fault, Utah. *EOS* **68**, 1369.

Reeves, C.C. 1978. Economic significance of playa lake deposits. In *Modern and ancient lake sediments*, A. Matter and M.E. Tucker (eds), 279–90. Oxford: Blackwell Scientific.

Rose, J. 1981. Raised shorelines. In *Geomorphological techniques*, A. Goudie (ed.), 327–41. London: Allen & Unwin.

Russell, I.C. 1885. Geological history of Lake Lahontan: a Quaternary lake of northwestern Nevada. *U.S. Geological Survey Monograph* 11.

Russell, I.C. 1895. *Lakes of North America*. Boston: Ginn.

Sack, D. 1987. Geomorphology of the Lynndyl Dunes, west-central Utah. In *Cenozoic geology of western Utah*, R.S. Kopp and R.E. Cohenour (eds), 291–9. Utah Geological Association Publication 16.

Sack, D. 1989. Reconstructing the chronology of Lake Bonneville. In *History of geomorphology*, K.J. Tinkler (ed.), 223–56. London: Unwin Hyman.

Sargent, K.A. and M.S. Bedinger 1985. Geologic and hydrologic characterization and evaluation of the Basin and Range province relative to the disposal of high-level radioactive waste – Part II, Geologic and hydrologic characterization. *U.S. Geological Survey Circular* 904-B.

Scott, W.E., W.D. McCoy, R.R. Shroba and M. Rubin 1983. Reinterpretation of the exposed record of the last two cycles of Lake Bonneville, western United States. *Quaternary Research* **20**, 261–85.

Sharp, R.P. 1978. *Coastal southern California*. Dubuque, IA: Kendall/Hunt.

Sly, P.G. 1978. Sedimentary processes in lakes. In *Lakes: chemistry, geology, physics*, A. Lerman (ed.), 65–89. New York: Springer.

Smith, B.W., E.J. Rhodes, S. Stokes, N.A. Spooner, *et al.* 1990. Optical dating of sediments: initial quartz results from Oxford. *Archaeometry* **32**, 19–31.

Smith, G.I. 1979. Subsurface stratigraphy and geochemistry of late Quaternary evaporites, Searles Lake, California. *U.S. Geological Survey Professional Paper* 1043.

Smith, G.I., V.J. Barczak, G.F. Moulton and J.C. Liddicoat 1983. Core KM-3, a surface-to-bedrock record of late Cenozoic sedimentation in Searles Valley, California. *U.S. Geological Survey Professional Paper* 1256.

Spencer, R.J., M.J. Baedecker, H.P. Eugster, R.M. Forester, *et al.* 1984. Great Salt Lake and precursors, Utah: the last 30,000 years. *Contributions to Mineralogy and Petrology* **86**, 321–34.

Street-Perrott, F.A. and S.P. Harrison 1985. Lake levels and climate reconstruction. In *Paleoclimate analysis and modelling*, A.D. Hecht (ed.), 291–340. New York: Wiley.

Thompson, R.S., L.J. Toolin, R.M. Forester and R.J. Spencer 1990. Accelerator-mass spectrometer (AMS) radiocarbon dating of Pleistocene lake sediments in the Great Basin. *Palaeogeography, Palaeoclimatology, Palaeoecology* **78**, 301–13.

Williams, J.S. 1962. Lake Bonneville – Geology of southern Cache Valley, Utah. *U.S. Geological Survey Professional Paper* 257-C.

Williams, T.R. and M.S. Bedinger 1984. Selected geologic and hydrologic characteristics of the Basin and Range Province, western United States. *U.S. Geological Survey Miscellaneous Investigations Series Map* I-1522-D.

Zenkovich, V.P. 1967. *Processes of coastal development*. New York: John Wiley.

PART SEVEN

AEOLIAN SURFACES

AEOLIAN SEDIMENT TRANSPORT 17

Nicholas Lancaster and William G. Nickling

INTRODUCTION

Aeolian processes, involving the entrainment, transport, and deposition of sediment by the wind, are an important component of the spectrum of geomorphic processes in arid regions. This chapter along with Chapters 18, 19, and 25 form an integrated unit that discusses the fundamentals of aeolian sediment entrainment and transport, wind erosion processes and landforms, dune morphology and dynamics, and palaeoclimatic interpretations of aeolian sediments and landforms.

Aeolian processes involve interactions between the wind and the ground surface. Understanding their operation requires a knowledge of relevant surface characteristics (e.g. texture, vegetation cover, degree of cohesion and crusting) as well as the dynamics of airflow over the surface. Two major components of the aeolian sediment transport system can be identified: (a) material of sand size (>50 μm); and (b) silt- and clay-sized particles (<50 μm) or dust. There are major differences in the processes by which these two types of aeolian sediment are transported and deposited, although entrainment processes are governed by very similar variables.

In recent years, important advances have been made in our understanding of the processes of aeolian sediment transport. The field is however still dominated by the classical work of R.A. Bagnold, especially in regard to the transport of sand. The recognition that aeolian processes occur on Mars provided a stimulus for studies that helped to sharpen concepts of the fundamentals of sediment transport. Increasing concern over desertification of arid and semi-arid lands has stimulated research into dust transport processes. Whereas sand transport studies have tended to be carried out in academia, many of the major advances in dust transport studies have come from agricultural engineers and have had a strong applied focus. Recent advances have come by a combination of careful wind tunnel and field experiments and numerical modelling of processes.

TRANSPORT MODES

There are three distinct modes of aeolian transport (Fig. 17.1). These depend primarily on the grain size of the available sediment (Bagnold 1941). Very small particles (<60–70 μm) are transported in suspension and kept aloft for relatively long distances by turbulent eddies in the wind. Larger particles (approximately 60–1000 μm) move downwind by saltation. The impact of saltating particles with the surface may cause short-distance movement of adjacent grains (reptation). Larger (> 500 μm) or less exposed particles may be pushed or rolled along the surface by the impact of saltating grains in surface creep.

True suspension occurs when the particle settling velocity U_f is very small in relation to the shear velocity of the wind. Pure saltation occurs when the turbulent vertical component of velocity has no significant effect on the particle trajectories. No sharp distinction exists between true suspension and saltation. Instead, there is a transitional state, termed modified saltation, that is characterized by semi-random particle trajectories influenced by both inertia and settling velocity (Hunt and Nalpanis 1985, Nalpanis 1985). Tsoar and Pye (1987) also distinguished between suspended grains that remain aloft for long periods of time (long-term suspension) and those which settle back to the surface relatively quickly (short-term suspension).

THE SURFACE WIND

Most naturally occurring airflow is turbulent and consists of eddies of different sizes that move with different speeds and directions. In these conditions

Geomorphology of Desert Environments. Edited by Athol D. Abrahams and Anthony J. Parsons. Published in 1994 by Chapman & Hall, London. ISBN 978-94-015-8256-8

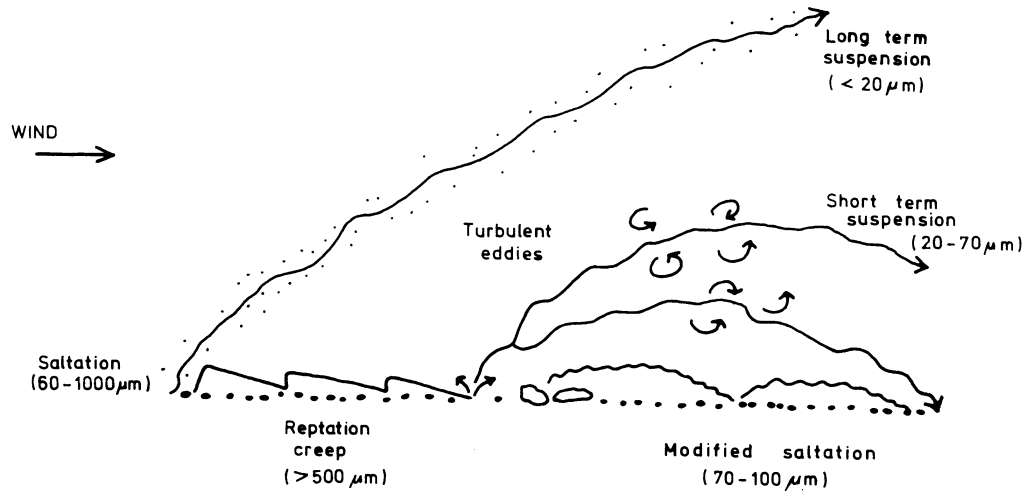

Figure 17.1 Modes of aeolian sediment transport (after Pye 1987).

the flow can only be characterized by time-averaged parameters. Turbulent eddies transfer momentum from one 'layer' to another such that each 'layer' has a different average velocity and direction. This process is known as 'turbulent mixing' and the definition of wind profiles in this way is known as the mixing length model (Prandtl 1935). As a result of frictional effects, the wind speed near the bed is retarded. If the surface is composed of very fine particles (<80 μm) the surface is aerodynamically smooth (particle friction Reynolds number $Re_p \leq 5$). A very thin laminar flow sublayer, usually less than 1 mm thick, develops adjacent to the bed even for flows in which most of the boundary layer is turbulent. By contrast, when surface particles or other roughness elements are relatively large the surface is aerodynamically rough $Re_p \geq 70$). The laminar sublayer ceases to exist and is replaced by a viscous sublayer for which the velocity profile is not well understood (Middleton and Southard 1984). Under conditions of neutral atmospheric stability, the velocity profile above the viscous sublayer for aerodynamically rough surfaces is characterized by the Prandtl–von Karman equation

$$u/u_* = 1/\kappa \ln(z/z_0) \qquad (17.1)$$

where u is the velocity at height z, z_0 is the aerodynamic roughness length of the surface, u_* is the shear velocity and κ is von Karman's constant (≈ 0.4). In these conditions, the wind profile plots as a straight line on semi-logarithmic axes with the intercept on the ordinate axis representing z_0 (Fig. 17.2). No matter how strong the wind blows all the velocity profiles tend to converge to the same intercept or z_0 value (Fig. 17.3). Thus u_* increases with increasing wind speed at a given height (z) above the surface.

For sand surfaces, z_0 is approximately 1/30 the mean particle diameter, but also varies with the shape and distance between individual particles or other roughness elements (Fig. 17.4). The value of z_0 increases to a maximum of about 1/8 particle diameter when the roughness elements are spaced about two times their diameter (Greeley and Iversen 1985). Typical values of z_0 for desert surfaces are shown in Table 17.1. The exact nature of the relationship between z_0 and surface roughness and particle size is, however, poorly understood (Lancaster *et al.* 1991).

Where the surface is covered by tall vegetation or high densities of other large roughness elements (e.g. lava flows), the wind velocity profile is displaced upwards from the surface to a new reference plane which is a function of the height, density, porosity, and flexibility of the roughness elements (Oke 1978). The upward displacement is termed the

Table 17.1 Typical values of aerodynamic roughness (z_0) for desert surfaces (from Lancaster *et al.* 1991)

Surface type	*Aerodynamic roughness (m)*
Playas	0.00013–0.00015
Alluvial fans	0.00084–0.00167
Desert pavements	0.00035
Lava flows	0.01480–0.02860

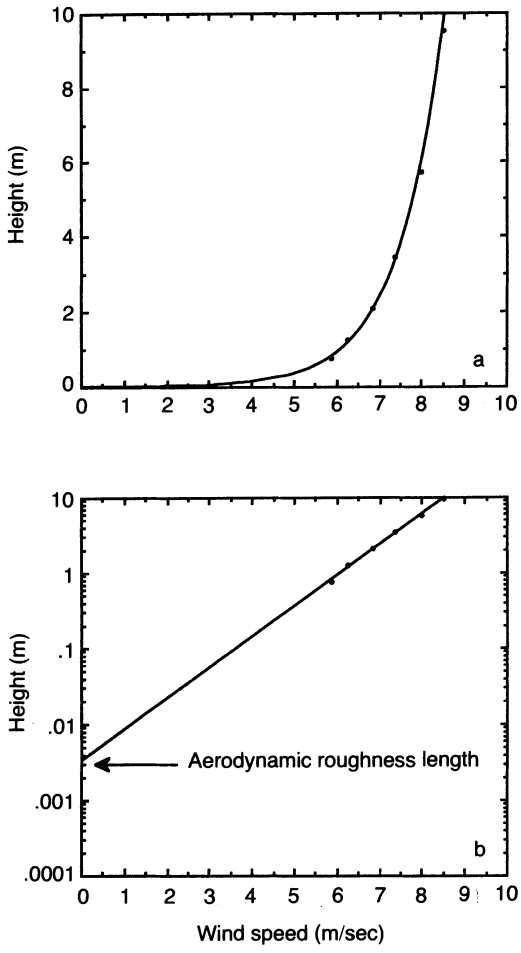

Figure 17.2 Boundary-layer wind profiles over the surface of an alluvial fan in Death Valley. (a) linear scale, (b) logarithmic scale for height. Intercept is the aerodynamic roughness length.

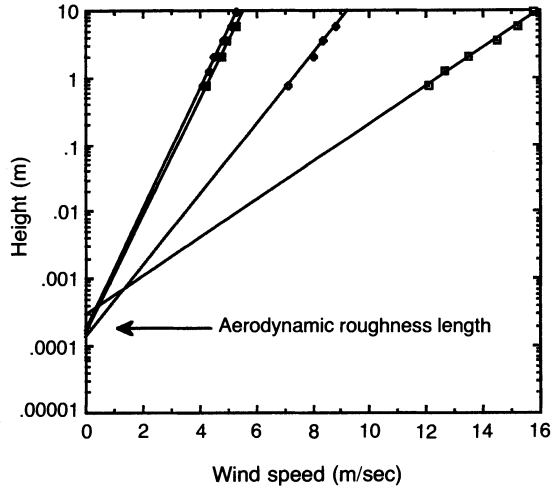

Figure 17.3 Changes in boundary-layer wind profiles over the surface of an alluvial fan in Death Valley with different wind speeds (measured at the highest anemometer). Note that the roughness length remains the same although wind speed at a given height increases.

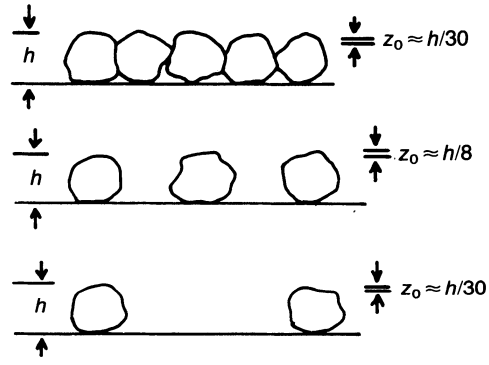

Figure 17.4 Relationship between aerodynamic roughness length z_0 and non-erodible roughness element spacing (after Greeley and Iversen 1985).

zero plane displacement height (d_0). The wind profile equation then becomes

$$u/u_* = 1/\kappa \ln[(z - d_0)/z_0] \qquad (17.2)$$

The shear velocity (u_*) is proportional to the slope of the wind velocity profile when plotted on a logarithmic height scale (Fig. 17.2) and is related to the shear stress τ at the bed and the air density ρ by

$$u_* = (\tau\rho)^{1/2} \qquad (17.3)$$

When the wind shear velocity is great enough to move sand particles the near-surface wind velocity profile is altered because momentum is extracted from the wind near the surface by the saltating sand grains. The velocity distributions with height remain as a straight line but tend to converge to a focus z' at a point 0.2 to 0.4 cm above the surface. Below this the wind profile is non-logarithmic, and wind speed in this zone may actually decrease as u_* increases (Bagnold 1941). The focus z' may represent the mean saltation height of uniformly sized grains (Bagnold 1941) and is approximately ten times the mean grain diameter of the bed (Zingg 1953). The apparent bed roughness z_0' is dependent on u_* during sediment transport (Owen 1964). Thus

$$z_0' = a(u_*^2/2g) \qquad (17.4)$$

where $a = 0.02$ and g is the acceleration of gravity.

Owen believed that the effective bed roughness scaled with the height of the saltation layer. However, wind tunnel studies by White and Schultz (1977) and Gerety and Slingerland (1983) show that there is a wide range of saltation trajectories. The parameter $u_*^2/2g$ is not a good predictor of saltation layer thickness, although it may be useful as an index of effective roughness height (Gerety 1985).

ENTRAINMENT OF SEDIMENT BY THE WIND

THE THRESHOLD OF MOTION

Grains will be moved by the wind when the fluid forces (lift, drag, moment) exceed the effects of the weight of the particle and cohesion between adjacent particles (Fig. 17.5). The drag and lift forces as well as the resultant moment are caused by the fluid flow around and over the exposed particles. The lift force results from the decreased fluid static pressure at the top of the grain as well as the steep velocity gradient near the grain surface (Bernoulli effect). The weight and cohesive forces are related to physical properties of the surface particles including their size, density, mineralogy, shape, packing, moisture content, and the presence or absence of bonding agents such as soluble salts.

As drag and lift on the particle increase, there is a critical value of u_* when grain movement is initiated. This is the fluid threshold shear velocity or u_{*t} (Bagnold 1941):

$$u_{*t} = A\{[(\rho_p - \rho)/\rho]gd\}^{1/2} \qquad (17.5)$$

where A is an empirical coefficient dependent on grain characteristics, ρ_p is the grain density, and d is the grain diameter. The value of A is approximately 0.1 for particle friction Reynolds numbers $Re_p > 3.5$.

During the downwind saltation of grains their velocity and momentum increase before they fall back to the surface. On striking the surface, the moving particles may bounce off other grains and become re-entrained into the airstream or embedded in the surface. In both cases, momentum is transferred to the surface in the disturbance of one or more stationary grains. As a result of the impact of saltating grains, particles are ejected into the airstream at shear velocities lower than that required to move a stationary grain by direct fluid pressure. This new lower threshold required to move stationary grains after the initial movement of a few particles is the dynamic or impact threshold (Bagnold 1941). The dynamic or impact threshold for a given sediment follows the same relationship as the fluid threshold (equation 17.5) but with a lower coefficient A of 0.08 (Fig. 17.6).

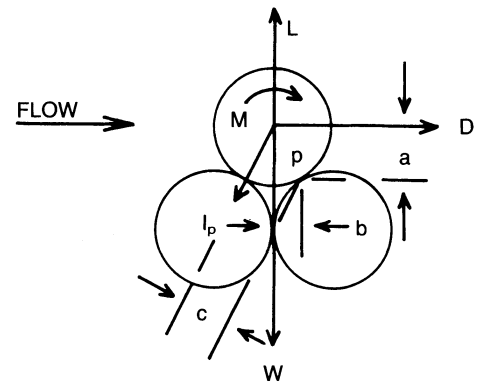

Figure 17.5 Schematic view of forces on a spherical particle at rest: D = aerodynamic drag, L = lift, M = moment, I_p = interparticle force, and W = weight. Moment arms about a point p given by a, b, c (after Greeley and Iversen 1985).

PROCESSES OF SEDIMENT ENTRAINMENT

Bagnold (1941) suggested that once the critical threshold shear velocity is reached, stationary surface grains begin to roll or slide along the surface by the direct pressure of the wind. Once particles begin to gain speed they start to bounce off the surface into the air stream and initiate saltation. More recent work (e.g. Chepil 1959, Iversen and White 1982) indicates that particles moving into saltation do not usually roll or slide along the surface prior to upward movement into the air stream. Initial movement into saltation is caused by instantaneous air pressure differences near the surface which act as lift forces. As wind velocity is increased, particles begin to vibrate with increasing intensity and at some critical point leave the surface instantaneously. Lyles and Krauss (1971) observed that the vibrations were seldom steady and occurred in flurries of three to five vibrations (1.8 ± 0.3 Hz for sand grains of 0.59 to 0.84 mm) before the particles instantaneously leave the bed. It appears therefore that microscale turbulence may play a role in threshold processes. Williams *et al.* (1990) suggest that fluid threshold is dependent on the turbulent structure of the boundary layer, and that initial disturbance is related spatially and temporally to semi-organized flurries of activity. The flurries appear to be associated with sweep and burst sequences that are well known in boundary layers. Grains dislodged by sweeps of

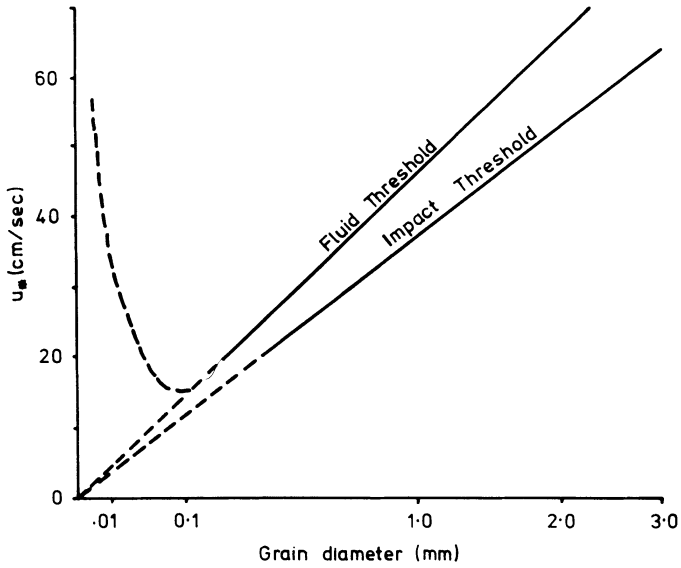

Figure 17.6 Relationship between fluid and impact threshold shear velocity and particle size (after Bagnold 1941).

movement are likely to become the agents for further dislodgements by collision.

Wind tunnel experiments to detect initial grain motions and count individual grain movements show that when velocity is slowly increased over the sediment surface, the smaller or more exposed grains are first entrained by fluid drag and lift forces in either surface creep or saltation (Nickling 1988). As the velocity continues to rise, larger or less exposed grains are also moved by fluid forces. Saltating grains rebound from the surface and may eject one or more stationary grains at shear velocities lower than that required to entrain them by direct fluid pressures and lift forces. The newly ejected particles move downwind and impact the surface, displacing an even larger number of stationary grains. As a result, there is a cascade effect with a few grains of varying sizes and shapes being entrained primarily by drag and lift forces. These grains set in motion a rapidly increasing number of grains by saltation impact. This progression from fluid to dynamic threshold based on number of grain movements is characterized by the relationship between the number of grain movements and u_* measured in the wind tunnel tests (Fig. 17.7). The shear velocity associated with the minimum radius of curvature on the grain count plots closely approximates the fluid threshold determined from Bagnold's threshold equation.

It is clear that the threshold process is a complex one, involving localized near-bed turbulent features that dislodge grains which act as 'seeds' for downwind ejections of further grains. Initiation of widespread grain motion involves a cascading effect, such that the number of grains in motion increases exponentially. Interactions between the developing saltation cloud and the wind result in extraction of momentum from the near-surface wind and a reduction in the near-bed wind speed so that the saltating grains are accelerated less and impact with less energy. As a result, the number of grains dislodged at the bed decreases, and the transport rate approaches a dynamic equilibrium value termed 'steady state saltation' by Anderson and Haff (1988) or 'equilibrium saltation' by Owen (1964). Equilibrium appears to be reached very rapidly, with a characteristic time period of 1 to 2 s (Fig. 17.8).

EFFECTS OF SURFACE CONDITIONS ON ENTRAINMENT

Although fluid threshold can be closely defined for a uniform sediment size greater than approximately 0.1 mm, it cannot be defined for most natural sediments because they usually contain a range of grain sizes and shapes which vary in grain density and packing. As a result, fluid and dynamic thresholds should be viewed as threshold ranges that are a function of the size, shape, sorting, and packing of the surface sediments.

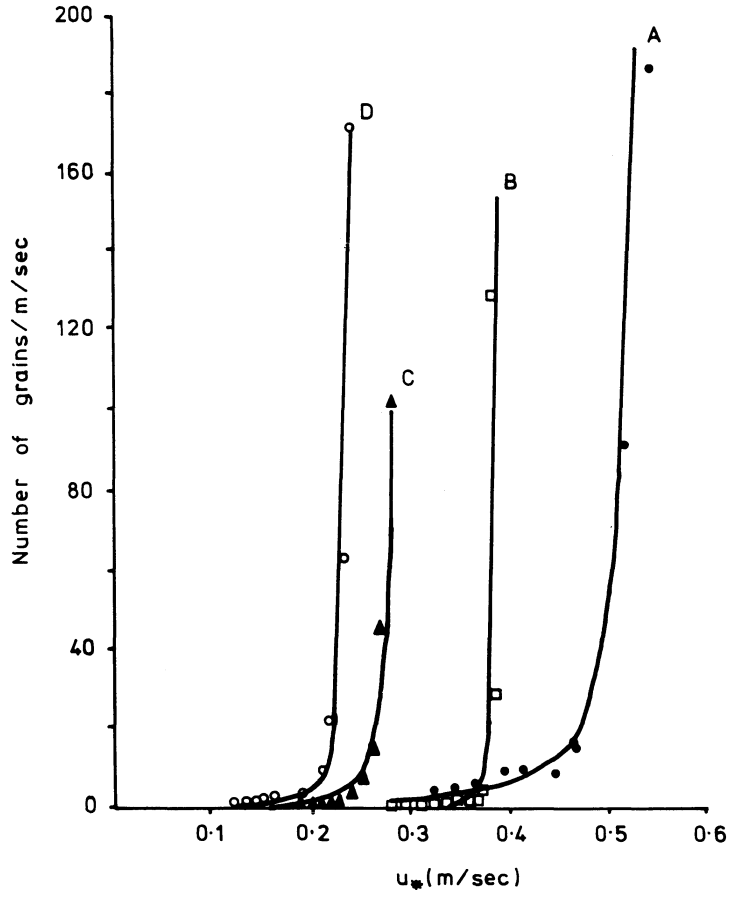

Figure 17.7 Increase in number of grain entrainments with increasing shear velocity for four sands measured with a laser particle counting system. Sands A to D have different mean sizes (77 μm to 19 μm) and sorting characteristics that are reflected in the shape and relative positions of the grain count curves (after Nickling 1988).

Grain Size Effects

The relationship between threshold shear velocity and particle diameter based on equation 17.5 (Fig. 17.6) shows that for a particle friction Reynolds number $Re_p > 3.5$ (grain diameter $>80\,\mu$m) u_{*t} increases with the square root of grain diameter. In this case, the grains protrude into the airflow and are therefore aerodynamically 'rough' so that the drag acts directly on the grains. For $Re_p < 3.5$, the grains lie within the laminar sublayer. The drag is distributed more evenly over the surface which is aerodynamically 'smooth', and the value of the threshold parameter A rises rapidly. As a result u_{*t} is no longer proportional to the square root of grain diameter but is dependent on the value of A. Wind tunnel studies (e.g. Bagnold 1941, Chepil 1945a) confirm that very high wind speeds are required to entrain fine-grained materials.

Iversen *et al.* (1976), Greeley *et al.* (1976), and Iversen and White (1982) have questioned the assumption that the coefficient A in the Bagnold threshold model is a unique function of particle friction Reynolds number. The threshold equation can be rewritten in a dimensionless form (Iversen and White 1982) as

$$A = u_{*t}/[(\rho/\rho_p)gd]^{1/2} \qquad (17.6)$$

where A is the dimensionless threshold shear velocity.

In a series of detailed theoretical and wind tunnel investigations with a wide range of particle sizes and densities, Greeley and his co-workers were able to show that A is nearly constant for larger particles, but increases rapidly for small particles (Fig. 17.9). This suggests that A is not solely a function of particle diameter for grains less than about 80 μm in

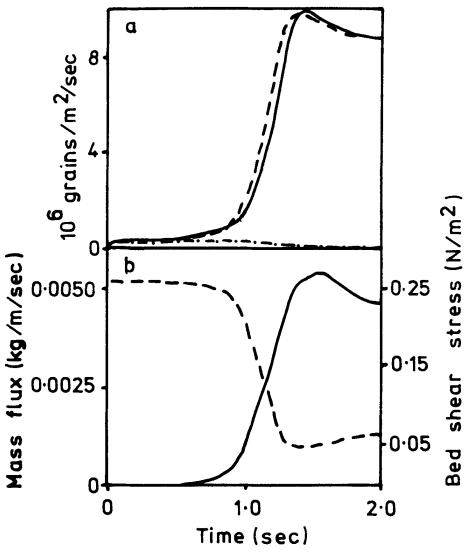

Figure 17.8 Computer simulations of saltation for 25-μm grains. (a) Numbers of grains impacting (dashed line), being ejected (rebound and splash, solid line), and being entrained (dot-dashed) as a function of time. Note that equilibrium is reached in a very short time (about 2 s). (b) Corresponding history of total mass flux (solid) and shear stress at the bed (dashed) (after Anderson and Haff 1988).

diameter. For very small grains interparticle forces such as electrostatic charges and moisture films appear to be important. The general form of the threshold equation can therefore be defined by

$$A = A_1 f(Re_p)[(1 + K_1)/(\rho_p g d^n)]^{1/2} \qquad (17.7)$$

where f is the Coriolis parameter, K_1 and n are the interparticle force coefficient and exponent, respectively, and A_1 is the cohesionless threshold coefficient. This expression is a generalization of equation 17.6 in terms of Re_p and assumes that the interparticle force is proportional to particle diameter to the power $3 - n$.

Regression analyses of the wind tunnel data enabled Iversen and White (1982) to estimate values for A_1, K_1 and n for a wide range of Re_p values, giving the following threshold equations:

$$A = 0.2[(1 + 0.006)/(\rho_p g d^{2.5})]^{1/2}/(1 + 2.5Re_p)^{1/2} \quad \text{for } 0.03 \leq Re_p \leq 0.3 \qquad (17.8)$$

$$A = 0.129[(1 + 0.006)/(\rho_p g d^{2.5})]^{1/2}/(1.928Re_p^{0.092} - 1)^{1/2} \quad \text{for } 0.3 \leq Re_p \leq 10 \qquad (17.9)$$

$$A = 0.120[(1 + 0.006)/(\rho_p g d^{2.5})]^{1/2}\{1 - 0.0858\exp[-0.0617(Re_p - 10)]\} \quad \text{for } Re_p \geq 10 \qquad (17.10)$$

Local Bed Slope

The local bed slope may influence threshold shear velocity through the effects of gravity acting via the angle of internal friction of the sediment. Howard (1977) produced a theoretical expression for the effect of local slope on threshold shear velocity:

$$u_{*t} = F^2 d[(\tan^2\alpha\cos^2\theta - \sin^2\chi\sin^2\theta)^{1/2} - \cos\chi\sin\theta] \qquad (17.11)$$

where $F = B[g(\rho_p - \rho)/\rho]^{1/2}$, B is a dimensionless constant with a value of 0.31, α is the angle of internal friction of the sediment, θ is the local slope, and χ is the angle between the local wind direction and the direction normal to the maximum local slope.

Hardisty and Whitehouse (1988) used a portable wind tunnel on Saharan sand dunes to investigate the effects of slope on threshold shear velocity. They found that threshold increases slightly with slope for positive slope angles, and decreases significantly for negative slopes, in close accordance with theoretical models (Fig. 17.10).

Entrainment of Fine-grained Sediments

Particles with grain diameters less than approximately 80 μm are inherently resistant to entrainment by wind, yet major dust storms are common occurrences in many parts of the world. This is because dust particles (silt and clay size) are frequently ejected by the impact of saltating sand grains (Chepil and Woodruff 1963), and not by direct fluid pressures and lift forces (Chepil 1945b, Gillette 1974, Nickling and Gillies 1989). Abrasion by saltating particles breaks up surface crusts and aggregates, releasing fine particulates into the air stream (Chepil 1945c, Gillette *et al.* 1974, Nickling 1978, Hagen 1984). The vertical emission of small particulates, expressed as a ratio of the amount of soil moved in saltation and creep, is proportional to approximately u_*^4 (Gillette 1977, Nickling and Gillies 1989). Sand-sized aggregates of silt and clay may also be transported in saltation but tend to break up or abrade during transport, providing fines which are carried away in suspension (Gillette and Goodwin 1974, Gillette 1977, Nickling 1978, Hagen 1984).

Moisture Content

Field observations and wind tunnel studies have shown that surface moisture content is an extremely important variable controlling both the entrainment and flux of sediment by the wind. Experiments by

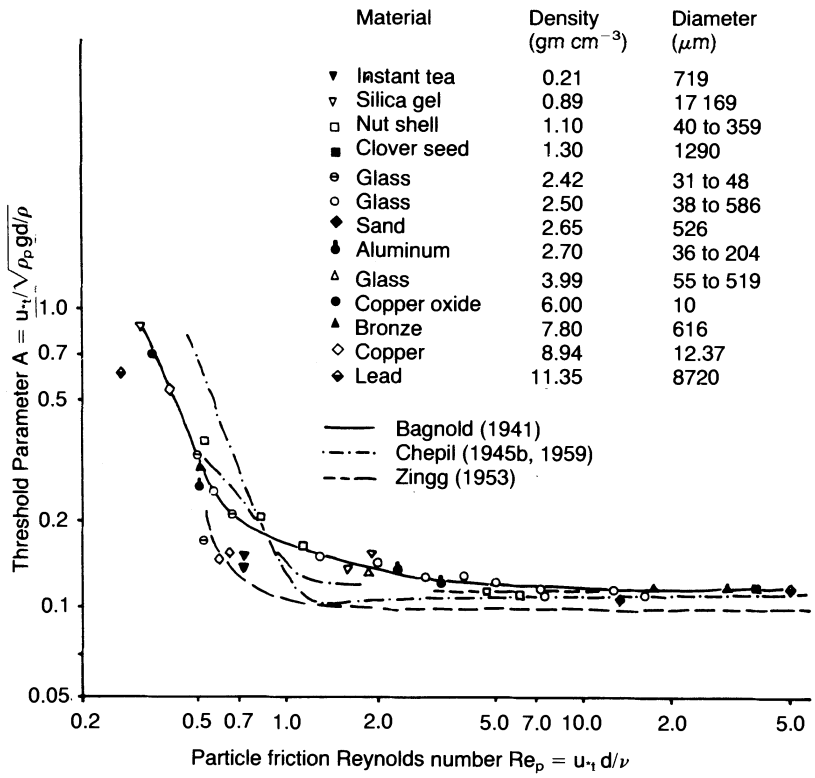

Figure 17.9 Relationships between threshold shear velocity parameter and particle friction Reynolds number. Data from Bagnold (1941), Chepil (1945b, 1959), and Zingg (1953) (after Greeley and Iversen 1985).

Belly (1964) show that gravimetric moisture contents of approximately 0.6% can more than double the threshold velocity of medium-sized sands. Above approximately 5% gravimetric moisture content, sand-sized material is inherently resistant to entrainment by most natural winds. Wind tunnel experiments on agricultural soils showed an exponential relationship between the increase in moisture content and threshold velocity (Azizov 1977).

In an attempt to develop a more generally applicable relationship, McKenna-Neuman and Nickling (1989) have derived and tested a theoretical moisture model based on capillary forces developed at interparticle contacts surrounded by isolated wedges of water. The capillary forces F_c are inversely proportional to moisture tension and directly proportional to the geometric properties of the contacts. The capillary force at the contact can be defined by

$$F_c = \pi T_s^2 G_c / P \qquad (17.12)$$

where T_s is the surface tension of water, G_c is a dimensionless geometric coefficient describing the shape of the contacts between grains, and P is the moisture tension developed in the water wedge at the grain contact.

Equation 17.12 can be expressed as a capillary force moment for grains with either open or closed packing arrangements which can be incorporated into Bagnold's (1941) threshold equation providing a general expression for the threshold velocity of a moist surface:

$$u_{*tw} = A[(\rho_p - \rho)/\rho)^{1/2}\{(6 \sin 2\alpha)/ [\pi d^3(\rho_p - \rho)g \sin \alpha]F_c + 1\}^{1/2} \qquad (17.13)$$

where α is the angle of internal friction and d is the grain diameter. Results from wind tunnel tests compare well with those predicted by equation 17.13 (Fig. 17.11).

Bonding Agents

Particles at the surface may be bound together by silt and clay, organic matter, or precipitated soluble salts to produce erosion-resistant structural units or more continuous surface crusts. The effectiveness of silt and clay as bonding agents depends on their relative proportion in relation to the quantity of sand-sized material. Soils with 20 to 30% clay, 40 to 50% silt,

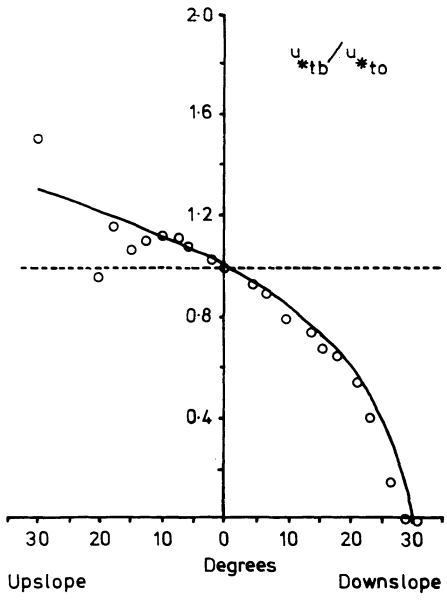

Figure 17.10 Relationship between threshold velocity u_{*t} and bed slope. Circles are values from field experiments, solid line is theoretical relationship determined by Dyer (1986). u_{*tb}/u_{*to} is the ratio between threshold velocity on a sloping bed and a flat bed (equal to unity on a flat bed) (after Hardisty and Whitehouse 1988).

and 20 to 40% sand are least affected by abrasion (Chepil and Woodruff 1963). The presence of organic matter increases the ability of particles to form aggregates that are less susceptible to entrainment by wind than the individual grains (Chepil 1951), but very high organic contents in dry soils increase erosion potential because of the very loose soil structure.

Even low concentrations of soluble salts can significantly increase threshold velocity by the formation of cement-like bonds between individual particles (Nickling 1978, Nickling 1984, Nickling and Ecclestone 1981). Sodium chloride is more effective than magnesium and calcium chloride in reducing soil movement because sodium tends to produce a surface crust that protects the underlying soils (Lyles and Schrandt 1972).

Surface Crusts

Surface crusts formed by various processes can also increase the threshold velocity. Crusts can be formed by raindrop impact on bare soils (Chen *et al.* 1980), algae and fungi (Foster and Nicolson 1980, Van den Anker *et al.* 1985), or precipitation of soluble salts (Nickling 1978, Pye 1980, Gillette *et al.* 1980, 1982).

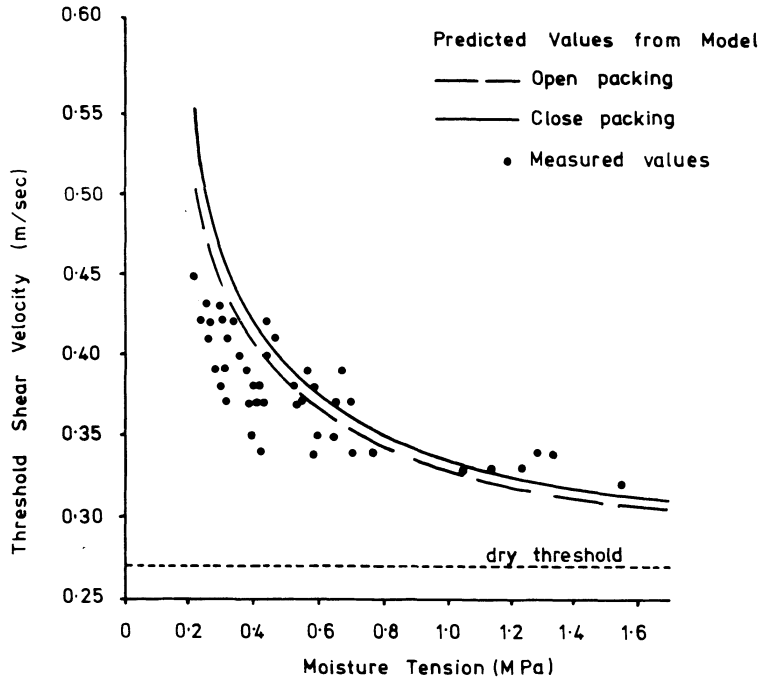

Figure 17.11 Comparison of theoretical and observed threshold velocities with increases in soil moisture tension (decrease in gravimetric moisture content). Theoretical curves for open and closed packing arrangements computed using equation 17.13 (after McKenna-Neuman and Nickling 1989).

For undisturbed soils, even weak crusts (modulus of rupture <0.07 MPa) will significantly increase the threshold velocity for Mojave Desert surfaces (Gillette *et al.* 1980, 1982). Disturbance of the surface by off-road vehicles and cattle trampling breaks crusts and decreases threshold velocities (Nickling and Gillies 1989).

Surface Roughness

The presence of vegetation, gravel lag deposits or other non-erodible roughness elements is important to both the entrainment and transport of sediment by wind. When the wind blows over a smooth unobstructed surface, the total force of the wind F is imparted more or less uniformly across the entire surface. The shear stress τ per unit area A_s of the surface is defined by

$$\tau = F/A_s \tag{17.14}$$

When non-erodible roughness elements are present the shear stress is not uniformly distributed: a proportion of the shear stress or momentum flux is absorbed by the elements protecting the underlying erodible surface. The degree of protection is a function of the size, geometry, and spacing of the elements (Marshall 1971, Lyles *et al.* 1974, Gillette and Stockton 1989, Musick and Gillette 1990). In the absence of large roughness elements, the shear stress at the surface can be determined from the shear velocity (u_*) using the log–linear wind profile (equation 17.1) by

$$\tau_s = \rho u_*^2 \tag{17.15}$$

where τ_s is the shear stress at the surface.

In the case of surfaces covered with large roughness elements, the situation is more complex since the logarithmic wind profile does not extend down between the roughness elements, making the direct computation of the surface shear stress from the wind profile impossible. In these situations the total force imparted to the surface is equal to the sum of the forces on the roughness elements F_r and the intervening surface F_g (Schlicting 1936) so that

$$F = F_r + F_g \tag{17.16}$$

Similarly, the total shear stress on a surface covered with roughness elements can be partitioned between the elements and the intervening surface

$$\begin{aligned}\tau &= F_r/A_s + (F_g/A_g)(A_g/A_s) \\ &= F_r/A_s + \tau_g(A_g/A_s)\end{aligned} \tag{17.17}$$

where F_r is the force exerted on the roughness elements, A_g is the ground area not covered by roughness elements and τ_g is the shear stress on the intervening ground surface.

Although this concept is relatively straightforward, the direct measurement of the shear stress applied to the elements or the surface is difficult, especially in field situations where the size and distribution of roughness elements can vary greatly. Bradley (1969a, b) designed a type of drag plate to measure the force of the wind on the surface in field situations and used this instrument to measure the change in shear stress as wind passed from a smooth to a rough surface. Despite this work, no direct measurements of shear stress partitioning have been made in areas covered by sparse vegetation or other large-scale roughness elements in natural environments.

In order to overcome the difficulties associated with direct measurements, several authors have used indirect methods to determine shear stress partitioning between the surface and roughness elements (e.g. Marshall 1971, Lyles *et al.* 1974, Gillette and Stockton 1989, Musick and Gillette 1990, Stockton and Gillette 1990).

Stockton and Gillette (1990), for example, derived an indirect method for the partitioning of shear stress on sparsely vegetated surfaces that is based on the threshold shear velocities of the vegetated surface and the bare soil for a similar but unvegetated surface. Threshold shear velocities for vegetated surfaces were determined in the field using a newly designed instrument that detects the erosion threshold in locations where erosion events are widely spaced in time. The determination of the erosion threshold for the bare soils was carried out in a laboratory wind tunnel or in the field on specially prepared plots.

As indicated above, the total shear stress imparted to a vegetated surface is defined by equation 17.17 and is related to the logarithmic wind profile above the vegetation canopy. At the threshold of particle motion the shear stress on the bare soil and the vegetated surface can be defined by

$$\tau = \rho u_{*tv}^2 \text{ and } \tau_g = \rho u_{*t}^2 \tag{17.18}$$

where u_{*tv} and u_{*t} are the shear velocities at the threshold of particle motion on the vegetated and bare soil surfaces determined from the logarithmic wind profiles above the respective surfaces. The threshold shear velocity with plants or roughness elements on the surface may be expressed as

$$\tau = (F_r/A_s) + \tau_g(A_g/A_s) = \rho u_{*tv}^2 \tag{17.19}$$

The fraction of the total force (momentum flux)

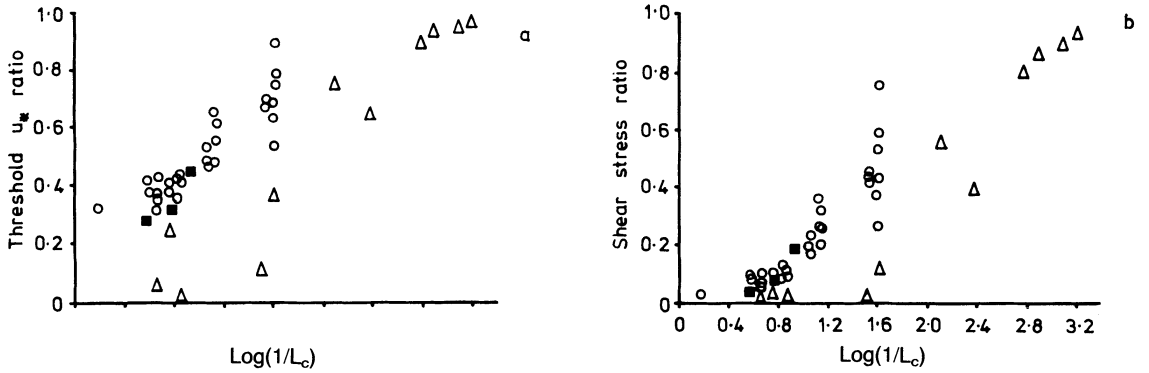

Figure 17.12 (a) Relationship between threshold shear velocity ratio u_*/u_{*t} and L_c (ratio of total frontal silhouette area to total floor area), and (b) relationship between shear stress ratio $1 - [F_r/(A_s\tau)]$ and L_c for different arrays of roughness elements. Squares = natural vegetation, triangles = wind tunnel experiments by Marshall (1971), and open circles = wind tunnel experiments by Gillette and Stockton (1989) (after Musick and Gillette 1990).

going to the erodible surface (shear stress partitioning) is

$$1 - [F_r/(A_s\tau)] = (\tau_g/\tau)(A_g/A_s) \qquad (17.20)$$

which can be rewritten as a shear stress ratio defined by

$$1 - [F_r/(A_s\tau)] = R^2(A_g/A_s) \qquad (17.21)$$

where R is the threshold velocity ratio (u_{*t}/u_{*tv}) (Musick and Gillette 1990). The two parameters expressing the stress partitioning in this equation are R, the ratio of threshold shear velocity without vegetation to the threshold shear velocity with vegetation, and A_g/A_s, a geometric factor describing the proportion of surface area covered by the erodible soil.

Using a significantly different approach, Marshall (1971) also derived a shear stress partitioning parameter

$$1 - [F_r/(A_s\tau)]^{1/2} = b_1 \log_{10}(1/L_c) + a_1 \qquad (17.22)$$

when τ_g is finite and where b_1 and a_1 are empirically derived regression constants that depend on the diameter to height ratio of the roughness elements, and L_c is the roughness element concentration. This parameter has, however, been criticized by Gillette and Stockton (1989) because it is not equivalent to any force or ratio of forces at the surface. Rather, it was chosen by Marshall to indicate the critical point at which the concentration of non-erodible elements would inhibit erosion. The concentration or protection provided by the roughness elements is described by L_c, the ratio of the frontal area of non-erodible roughness elements to the total surface areas (Marshall 1971).

Musick and Gillette (1990) used their threshold shear velocity ratio to estimate the percentage of vegetative cover required to protect soils from erosion (Fig. 17.12). They suggest that since the shear velocity of natural winds infrequently exceeds 100 cm s^{-1}, this value could be taken as the lower boundary of u_{*tv} which would provide total protection against wind erosion for almost all soils. For example, in the case of sandy soils which have a u_{*t} of approximately 30 cm s^{-1}, the critical shear velocity ratio would be 0.3 corresponding to an L_c of approximately 0.25 to provide total protection. Similarly, finer-textured and crusted soils would have higher u_{*t} values and lower critical L_c values (Fig. 17.12).

Although the percentage of coverage provided by the non-erodible elements is important to the degree of erosion in the intervening areas, the size, shape, and distribution of the elements also have significant effects on the erodibility of the intervening areas. Wind tunnel tests by Logie (1982) indicate that low densities of roughness elements (glass spheres and gravel particles) tend to reduce the threshold velocity of the surface and cause increased erosion around the elements because of the development and shedding of eddies. By contrast, higher densities of roughness elements tend to increase the threshold velocity of the surface. In general, for any size and shape of roughness element a particular cover density exists where the influence changes from activation of erosion to protection of the surface. On the basis of wind tunnel tests and field measurements, Gillette and Stockton (1989) and Musick and Gillette (1990) also suggest that for the same percentage of surface cover (L_c), large widely spaced non-erodible elements provide less protec-

tion than do more uniformly spaced, smaller elements.

SAND TRANSPORT BY THE WIND

The process of sand transport by the wind can be viewed as a cloud of grains saltating along a sand bed, with grains regaining from the wind the momentum lost by impacts with the bed. These high-energy grains rebound from the bed with nearly a unit probability in a process termed 'successive saltation' (Rumpel 1985). Impacts between the saltating grains and the bed transfer momentum to other grains, which move a short distance. The motion of these low-energy ejected gains is termed reptation (Ungar and Haff 1987). The number and velocity distribution of grains ejected in this way is described statistically by the 'splash function' (Ungar and Haff 1987, Werner 1988). Experiments (Mitha *et al.* 1985, Willetts and Rice 1986) and numerical solutions (Anderson and Haff 1988) suggest that the saltating grains rebound with about 50 to 60% of their original velocity. However, the ejected grains reach a maximum of only about 10% the speed of the impacting grain. In addition, rearrangement of the bed by saltation impacts leads to movement of grains that remain in contact with the bed at all times (surface creep) (Anderson *et al.* 1990).

Using data on grain bed interactions from experimental and numerical simulations, Anderson and Haff (1988) developed a full model for saltation from inception to steady state. They assumed a simple linear relationship between aerodynamic entrainment of grains and shear stress above the fluid threshold

$$N_a = \alpha_s(\tau_a - \tau_c) \qquad (17.23)$$

where N_a is the number of entrained grains per unit area, τ_a is the mean shear stress, τ_c is the critical threshold shear stress, and α_s is a constant. Feedback effects between the wind and the developing saltation cloud were modelled after Ungar and Haff (1987). The model appears to simulate most of the main features of aeolian saltation, including the decline in mass flux and grain concentration with height. The system reaches a steady state characterized by an equal number of impacting and ejected grains and a stationary wind profile in about 1 to 2 s (Fig. 17.8). The mass flux of particles behaves in a non-linear fashion as a cubic power function of u_* and is within the range of experimental measurements of mass flux. An alternative model for saltation (Werner 1988) uses a splash function developed from experimental data. In this model the transport rate q is defined as

$$q \approx (u_*^2 - u_{*s}^2)^{1.2} \qquad (17.24)$$

where u_{*s} is the shear velocity calculated from the airborne shear stress at the surface.

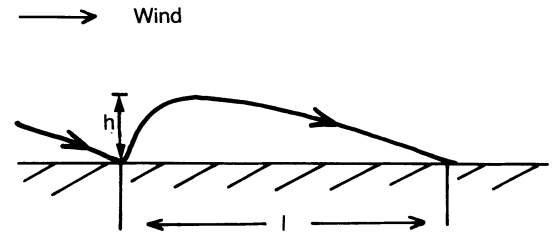

Figure 17.13 Schematic view of a typical saltation trajectory. h = saltation height and l = saltation path length.

SALTATION TRAJECTORIES

Sand particles moving in saltation are characterized by trajectories with an initial steep vertical ascent followed by a parabolic path such that they return to the bed with relatively small impact angles (Fig. 17.13). For an idealized case assuming that the initial take-off speed is in the same order as the shear velocity, the trajectory height h is 0.81 u_*^2/g and the length l is 10.3 u_*^2/g (Owen 1964). Lift-off angles of 75° to 90° were measured by Bagnold (1941) and Chepil (1945a), but White and Schultz (1977) determined the average ejection angle to be about 50° for particles 586 μm in diameter for a shear velocity of 40 cm s^{-1}. White and Shultz (1977) also observed that particle trajectories were higher than those predicted by theoretical equations of motion. This occurs because of a lift force that is generated by the spinning of the grain as it moves through the air (the Magnus effect) which is related to the rate of spinning (350 to 400 r.p.s.) and the steep velocity gradient adjacent to the particle surface (White 1982). When the Magnus effect is included in the equations of motion, theoretical trajectories are in much better agreement with those observed in wind tunnel experiments (White and Shultz 1977).

Because the near-surface wind velocity gradient is steep, the higher the saltating particles rise from the surface, the greater is the velocity at which they are carried in the air stream and the longer are saltation path lengths. Once particles have attained their maximum height they descend approximately linearly to impact with the surface at incidence angles of 10° to 16° (Bagnold 1941), or from 4° to 28° with an

average angle 13.9° (White and Schultz 1977). The impact angle of a saltating particle tends to decrease with increases in wind velocity and decrease with particle size (Jensen and Sørensen 1986).

Grain shape has a pronounced effect on the saltation path and the nature of the bed collisions. Platy sands tend to saltate in longer, lower trajectories compared with more spherical particles (Willetts 1983). In wind tunnel tests of two sands with similar mean size but different particle shapes (compact and platy), Willetts and Rice (1986) found that collision was a more efficient mechanism for maintaining saltation in the compact quartz particles than for the platy sands. Platy sand loses less forward momentum on impact than the more compact quartz grains and undergoes a much smaller change of vertical momentum so that collision impacts can maintain a larger load of compact particles than platy particles.

THE SALTATION LAYER

Wind tunnel and field studies as well as numerical models of the cloud of saltating and reptating grains show that most sediment is transported close to the ground, with an exponential decline in sediment and mass flux concentration with height (Bagnold 1941, Sharp 1964, Williams 1964, Nickling 1978, Nickling 1983, Anderson and Hallett 1986). Over sand surfaces in the wind tunnel most grains travel within the lower 1 to 2 cm (Bagnold 1941, Williams 1964). Sharp (1964) found that 50% by weight of sediment transported across an alluvial surface in the Coachella Valley travelled within 13 cm of the ground, and 90% below 60 cm. There is no clear upper limit to the saltation layer, but most studies suggest that it is approximately ten times the mean saltation height. As observed by Bagnold (1941) and Sharp (1964), saltating grains are found at much greater heights over hard gravel or pebble surfaces. Williams (1964) and Gerety (1985) also observed a decline in average grain size with height. However, the size of sediment transported at a given height tends to increase with u_*.

SAND TRANSPORT EQUATIONS

The seminal work of Bagnold (1941) relating the quantity of sand transported as a function of the shear stress exerted by wind forms the basic theoretical background and supporting empirical evidence for almost all research on aeolian sand transport rates. Using theoretical considerations in conjunction with field and wind tunnel observations Bagnold found that the sediment transport mass flux in saltation and creep (q) could be defined by:

$$q = C(d/D)^{1/2}(\rho/g)u_*^3 \qquad (17.25)$$

where D is the size of a 'standard' 0.25-mm sand. The coefficient C is a sorting coefficient with values of 1.5 for nearly uniform sand, 1.8 for naturally graded sand, 2.8 for poorly sorted sand, and 3.5 for a pebbly surface. For a given value of u_* the sediment flux q increases from a minimum for nearly uniform sand to somewhat higher values for more poorly sorted sands and reaches a maximum value over a pebble surface. The effect of impacts from larger saltating grains is probably greater for poorly sorted sands, whereas for pebbly surfaces sand grains saltate more effectively and further because of more perfect rebound.

Following Bagnold's (1941) work, other investigations have developed both theoretical and empirical equations to describe the transport of sediment by wind (for a review see Sarre 1989). These equations, although frequently derived in different ways and from different points of view, are similar in general form to that initially proposed by Bagnold (1941). For example, Zingg (1953) modified the Bagnold equation to

$$q = C(d/D)^{0.75}(\rho/g)u_*^3 \qquad (17.26)$$

A fundamental problem with both the Bagnold and Zingg equations is that they do not include a threshold term and thus predict sediment transport at shear velocities below that required to initiate particle movement. Kawamura (1951) proposed a somewhat different equation that included a threshold shear velocity (u_{*t}) term:

$$q = k(\rho/g)(u_* - u_{*t})(u_* - u_{*t})^2 \qquad (17.27)$$

where k is an empirical coefficient which is a function of the textural characteristics of the sediment ($k = 2.78$ for moderately well-sorted sand with a mean diameter of 0.25 mm). A threshold shear velocity term was also included in the transport equation derived by Lettau and Lettau (1978):

$$q = C(d/D)^r \rho u_*^2(u_* - u_{*t}) \qquad (17.28)$$

where the exponent r has values ranging from 0.5 to 0.75.

Comparison of sediment flux predicted by different transport equations with increasing shear velocity for similar particle sizes (Fig. 17.14) shows that despite the rather similar form of the equations and similar mean particle diameters used in the calculations, the equations give significantly different results. However, accurate data on sediment fluxes are

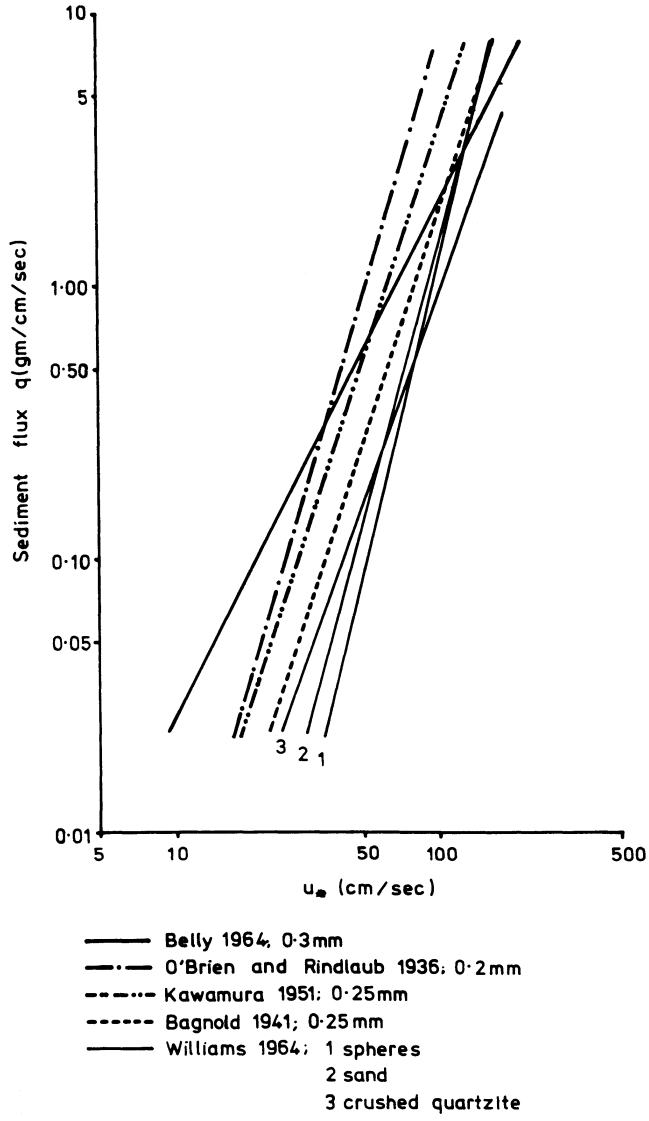

Figure 17.14 Comparison between different sand-sized sediment flux equations.

difficult to obtain due to less than perfect trap efficiencies and the non-stationary nature of the bed in wind tunnel experiments (Rasmussen and Mikkelsen 1991).

TEXTURAL CONTROLS ON SAND TRANSPORT

Most sediment transport equations contain various empirically derived coefficients which are a function of the grain size and sorting characteristics of the sediments. Differences in the sediment flux predicted by these equations may be related to undocumented textural differences, especially the grain shape of the test sands used in the experiments (Williams 1964, Willetts *et al.* 1982).

Wind tunnel tests show the effects of particle shape on the sediment transport rate (Williams 1964, Willetts *et al.* 1982, Willett 1983, Finlan 1987). Sediment flux q varies as a power function of shear velocity u_* but with exponents considerably different than the value of 3 suggested by Bagnold (1941) and others. The value of the exponent and thus the flux of sediment increase with the sphericity of the sediment from 2.76 for crushed quartzite to 3.42 for

natural sand, and 4.10 for glass spheres (Williams 1964). Williams (1964) also showed that at low shear velocities ($u_* < 75$ cm s^{-1}) there is a tendency for sediment transport rate to increase as particle shape becomes more irregular.

DUST TRANSPORT BY THE WIND

Small particulates (dust: <20 μm diameter) are usually transported by the wind in suspension. Although these particles can be entrained into the air stream by direct fluid pressure and lift forces, they are frequently ejected by the impact of saltating sand grains. In other cases they are released by abrasion, either during transport in saltation and creep of sand-sized aggregates of silt and clay or by the bombardment of larger stationary aggregates by saltating grains. The small particulates, once entrained, are carried by turbulent eddies in the air stream and have the potential to be transported to great heights and for long distances.

MODELS OF DUST TRANSPORT

Once entrained, the length of time particles remain in suspension and the distance that they are transported is a function of (a) the settling velocity of the particles, and (b) the velocity and turbulence of the airflow (Tsoar and Pye 1987). The settling velocity of particles is defined by Stokes' Law as

$$U_f = Kd^2 \qquad (17.29)$$

where U_f is the particle settling velocity, $K = \rho_p g / 18\mu$, and μ is the dynamic viscosity of the air.

At a given instant, a turbulent wind can be viewed as having a horizontal velocity component u and a vertical velocity component w (Tsoar and Pye 1987). For a given time interval the mean values for the velocity components are designated $\bar{u}$ and $\bar{w}$. Fluctuations in the vertical velocity component are given by $w' = \bar{w} - w$. Under neutral stability conditions near the surface the fluctuating vertical velocities have a normal distribution and a mean of zero. The force opposing the tendency for small particles to settle out of the air stream is defined by the standard deviation of the vertical fluctuating velocity distribution $\sigma = (w'^2)^{1/2}$. The rate at which small particles tend to settle out of the air stream is dependent on the settling velocity of the particles, U_f (equation 17.29). Consequently, a small particle should remain in suspension if $(w'^2)^{1/2} > U_f$. The standard deviation of the fluctuating vertical velocities is related to the shear velocity by

$$cu_*^2 = (w'^2)^{1/2} \qquad (17.30)$$

where c is a constant with a range of approximately 0.7 to 1.4 and a mean of about 1.0 (Lumley and Panofsky 1964). As a result, grains will remain in suspension when the ratio $U_f/u_* < 1.0$ (Rouse 1937, Chepil and Woodruff 1957, Gillette 1974). However, the difference between saltation and suspension is not distinct, as both the turbulent structure of the wind and the textural characteristics of the sediment influence the settling velocity. Tsoar and Pye (1987) suggested an arbitrary upper limit for pure suspension of $U_f/u_* = 0.7$.

For particles to be suspended for long periods and distances, they must be kept aloft by the upward velocity fluctuations of the wind. Particles with $U_f/u_* = 0.4$ have a ratio of upward to downward movements of 0.5 in air with a normal vertical velocity distribution (Gillette 1974, 1977). The probability that a particle of this size would be carried to any great height or for any great distance is therefore low. The settling velocity of particles smaller than 20 μm is less than 0.1 u_* for almost all strong winds, and so they will remain in suspension to great heights and/or over long distances. Tsoar and Pye (1987) used the ratio $U_f/u_* = 0.1$ to differentiate between long-term and short-term suspension. They show that when u_* is 0.2 to 0.6 m s^{-1}, medium and coarse silt grains, which make up most loess deposits, are transported mostly in short-term suspension and modified saltation (Fig. 17.15).

The vertical and horizontal transport of small particulates in suspension is related to the coefficient of turbulent exchange or the eddy diffusion coefficient. The maximum likely distance and time travelled by a dust particle is inversely proportional to the fourth power of the particle diameter (Tsoar and Pye 1987) and can be estimated by

$$L = U^2 \varepsilon / K^2 d^4 \qquad (17.31)$$

where L is the distance travelled by the suspended particle, ε is the eddy diffusion coefficient, U is the mean wind velocity, and $K = \rho_p g / 18\mu$. Tsoar and Pye (1987) indicated that during moderate dust storms, particles coarser than 20 μm are unlikely to travel more than about 30 km from the source, whereas those finer than 20 μm in diameter may be dispersed over a distance of approximately 500 km when $\varepsilon = 10^4$ m s^{-1}. For values of $\varepsilon = 10^6$ m s^{-1} particles 20 to 30 μm in diameter could be transported as much as 3000 km.

Rouse (1937) showed that the relative concentration of suspended particulates of a particular size at a given height is given by

$$C_p/C_z = [(H-y)/y] - [z/(H-z)]^m \qquad (17.32)$$

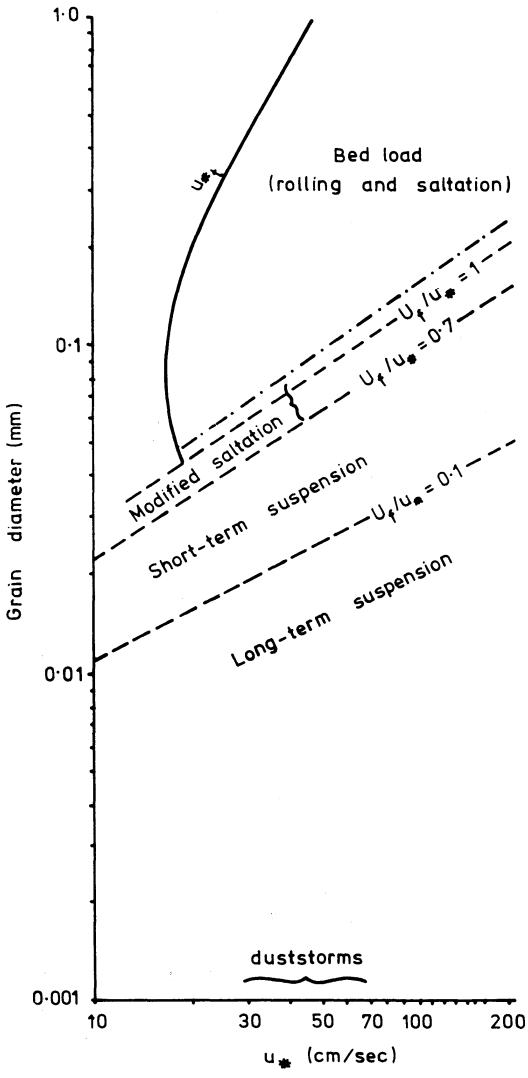

Figure 17.15 Modes of transport for quartz spheres of different diameters at different wind shear velocities (after Tsoar and Pye 1987).

where C_p/C_z is the relative concentration (number of particles per cm^3) at any level y referenced to an arbitrary elevation z above the surface (where $z < y$), and H is the elevation at which the particle concentration is zero. For the lower atmosphere, $H \gg y$ and equation 17.23 can be simplified to

$$C_p/C_z = (z/y)^m \qquad (17.33)$$

where $m = U_f/Ku_* = 2.5(U_f/u_*)$. In the case of small particles that obey Stokes' Law, equation 17.33 can be modified by solving for the particle settling velocity (U_f) to obtain:

$$C_p/C_z = \exp[2.5(Kd^2/u_*)\ln(z/y)] \qquad (17.34)$$

Tsoar and Pye (1987) used this expression to compute the relative concentration above the surface for spherical quartz particles of different sizes, assuming a shear velocity of 70 cm s^{-1}. Particles coarser than 20 μm are carried only a few metres above the ground and are much more likely to be trapped by vegetation and other surface roughness elements, whereas those finer than 20 μm are distributed almost evenly with height up to at least 100 m and will travel for long distances.

The quantity of dust transported in suspension is directly related to the rate at which grains are ejected into the air stream from the surface. Gillette *et al.* (1972) suggested that the vertical particle flux G can be determined from the particle concentration profile by

$$G = \varepsilon(\partial C_p/\partial y) \qquad (17.35)$$

where G is the vertical particle flux (g cm^{-2} s^{-1}), ε is the eddy diffusion coefficient, and C_p is the particle concentration at height y. Under neutral stability conditions

$$\varepsilon = u_* \kappa y \qquad (17.36)$$

OBSERVATIONS OF DUST FLUX AND CONCENTRATION PROFILES

Models for the vertical profile of dust concentration in the lower atmosphere have been verified by field observations by Chepil and Woodruff (1957), Gillette *et al.* (1972, 1974), Goossens (1985), and Nickling (1978, 1983). Suspended sediment concentrations decrease exponentially with height above the surface (Fig. 17.16), but there is considerable variability in the vertical profile from one dust event to another as a result of variations in atmospheric turbulence (Nickling 1978). As in the saltation layer, there is an exponential decrease in mean grain size with height during dust storms (Chepil and Woodruff 1957, Gillette *et al.* 1974, Goossens 1985). Goossens (1985) found suspended sediment to be stratified by particle size, with coarse silt moving mostly near the bottom of the dust cloud, whereas finer silt is transported at both top and bottom. However, studies by Nickling (1983) show that there is considerable storm to storm variation in the decrease of mean size with height because of differences in the degree of turbulent mixing and the range of grain sizes supplied to the air stream. Suspended sedi-

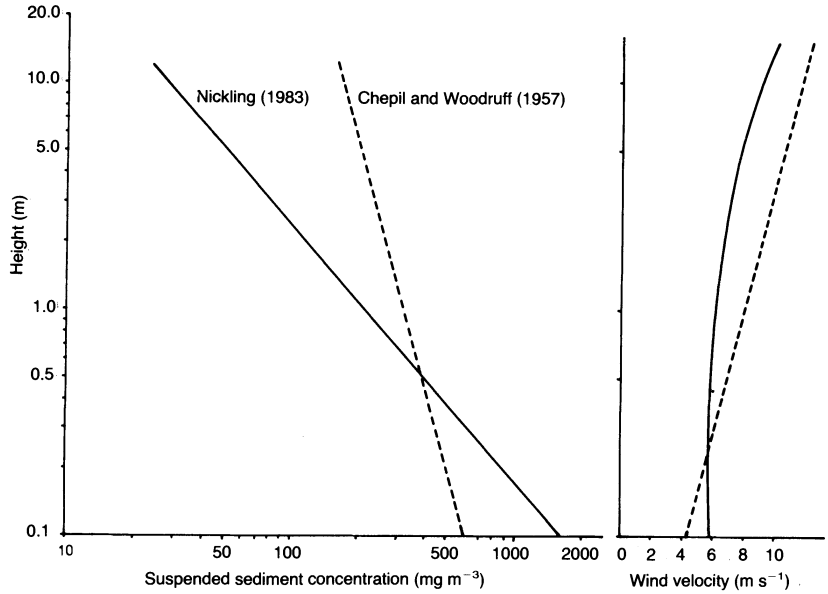

Figure 17.16 Variation in the concentration of suspended sediment with height above the surface. Data from Nickling (1978) and Chepil and Woodruff (1957).

ment tends to improve in sorting from the surface up to 1.5 m, above which it is increasingly more poorly sorted (Nickling 1983). The improvement in sorting up to 1.5 m may result from the selective removal of relatively coarse grains in modified saltation as height increases. Above 1.5 m all particles are relatively small and have a tendency to become more uniformly mixed by the turbulent eddies.

Gillette (1977) provided the most detailed vertical particulate flux data available for natural surfaces. The relationship between observed particle fluxes and wind shear velocity (Fig. 17.17) indicates that sandy soils show a fairly uniform trend of increasing vertical particle flux with shear velocity. In contrast, loamy soils show a greater scatter in particle flux, most likely because of their widely different dry aggregate structures. The relatively low values of vertical particle flux associated with the clay soil results from a high threshold shear velocity and the resistance to break-up of aggregates containing montmorillinitic clay.

Nickling and Gillies (1989) have investigated the relative vertical particle fluxes from different surface types in southern Arizona using a portable field wind tunnel. There is a general increase in vertical particulate flux with increasing shear velocity (Fig. 17.18) that compares favourably with the results of Gillette (1977). The strength of the relationship is improved if the data set is partitioned on the basis of textural and surface characteristics. Strong linear relationships were found between G and u_* for loamy soils (silt and clay contents greater than 25%) and soils with sand contents greater than 85%. For a given shear velocity, particle emissions are greater for loamy soils than sandy soils. The highest emission rates are associated with loamy textured soils that have been heavily distributed by vehicular traffic (e.g. construction sites and off-road vehicle tracks). Surface roughness can also have a significant effect on the vertical particulate flux. The presence of roughness elements such as standing vegetation, clods, or pebbles tends to decrease the emission of particulates on similar textured soils at approximately the same shear velocities because of a shielding effect.

WIND EROSION PREDICTION

The pioneer work of W.S. Chepil (summarized in Chepil and Woodruff 1963) and R.A. Bagnold (1941) provided both the theoretical background and empirical observations on the primary variables that influence the erosion of soils by wind. Chepil's work on the wind erosion of agricultural soils culminated in the development of the U.S. Department of Agriculture Wind Erosion Equation (Woodruff and Siddoway 1965) for which a computer solution was developed by Skidmore *et al.* (1970).

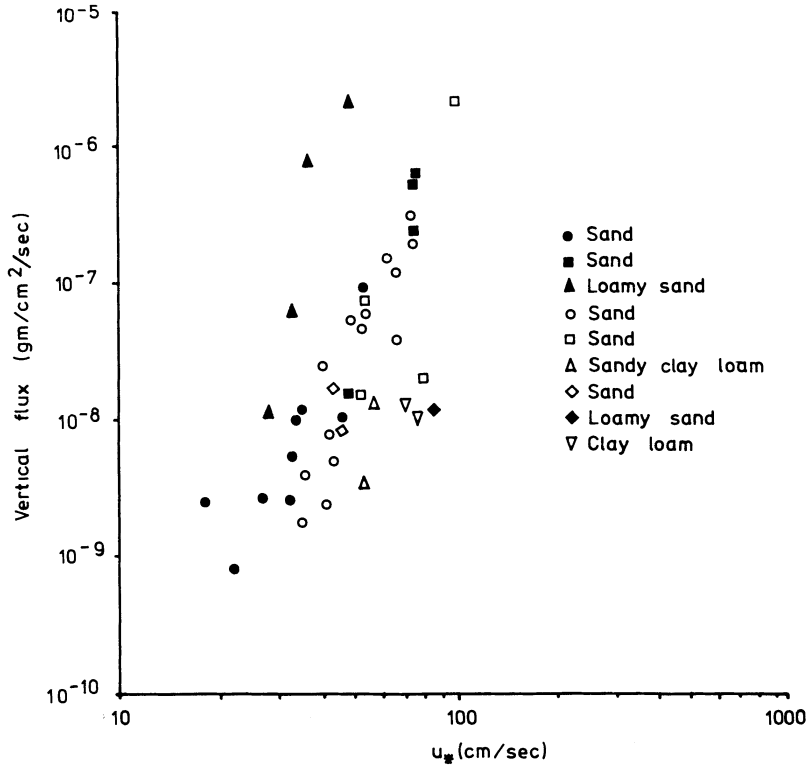

Figure 17.17 Relationship between vertical particulate flux and wind shear velocity for different soils in Texas (after Gillette 1977).

This empirical model allows for determination of annual soil losses by wind from a given field based on eleven field and climatic variables which can be grouped into five principal factors. Several versions of the original model are in use which combine the factors in several ways. The general equation can be expressed in the following functional form:

$$E = f(I, Cl, R, L_f, V) \qquad (17.37)$$

where E is annual soil loss, I is a soil erodibility index, Cl is a local wind erosion climatic factor, R = a soil ridge roughness factor, L_f is equivalent field width (the maximum unsheltered distance across the field along the prevailing wind direction), and V is an equivalent quantity of vegetation cover factor.

Although the general form of the equation is relatively straightforward, its application is complicated by the interactions between the individual factors that are actually functions of other variables. As a result, the equation is not a simple, single multiplicative function as in the case of the Universal Soil Loss Equation. Moreover the time frame for the equation is yearly, based on long-term climatic conditions for a given site, standardized to long-term climatic records at Garden City, Kansas. Solutions for the Wind Erosion Equation for periods of less than one year or by event are difficult to obtain because of the general format of the model and the nature of the original input data used to derive the primary factors.

The functioning of the Wind Erosion Equation has been criticized by several authors (e.g. Cole 1984a, b Gillette 1986, Nickling 1989) because of its inherent weaknesses and unreliability in predicting realistic soil losses, especially in locations with climatic conditions which vary significantly from the Mid-West of the United States. In recognition of the inherent problems associated with the Wind Erosion Equation, the U.S. Department of Agriculture has undertaken a major research effort to develop a Wind Erosion Prediction System (WEPS) that uses a physically based model incorporating climatic, soil, crop, and tillage parameters and submodels (Hagen 1991).

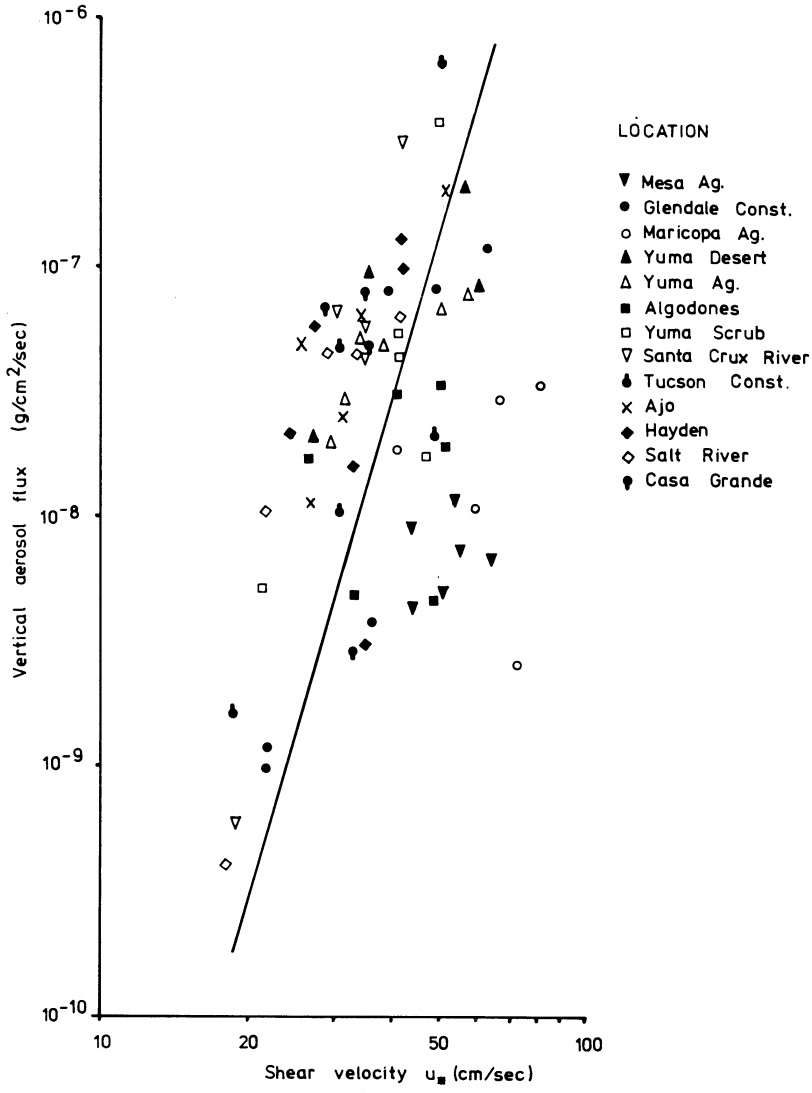

Figure 17.18 Relationship between vertical particulate flux and wind shear velocity measured over different soils in Arizona using a portable field wind tunnel (after Nickling and Gillies 1989).

Gillette (1986) and Gillette and Passi (1988) have also developed a physically based model which closely follows the aerodynamics and physics of the wind erosion process. The model is based on an expectation integral approach that predicts horizontal soil mass flux at the downwind edge of an eroding field as a function of wind shear velocity in relation to a probability density function of wind velocities (two-parameter Weibull distribution) and the threshold shear velocity at which wind erosion starts. Soil losses E for a given location and time period ΔT are computed by

$$E = C_2 \sum_{i=1}^{n} R_i g(L_f) A_s \Delta T \int_{u_{ti}}^{\infty} G(u) p_i(u) \mathrm{d}U \tag{17.38}$$

where C_2 is a constant determined by calibration, i is the index of summation over n different erodible areas in the region of interest, R_i is the effect of soil roughness, $g(L_f)$ is the effect of field length, A_s is the land area being considered, $G(u)$ is the vertical mass flux of dust as a function of wind speed, $p_i(u)$ is the probability density function of wind speed during the period, and u_{ti} is the threshold wind speed for dust emission. This model was used by Gillette (1986) to evaluate four of the five factors in the Wind Erosion Equation and to model dust emissions caused by wind erosion in the United States as a part of the National Acid Precipitation Assessment Program (Gillette and Passi 1988). Nickling (1989) and Nickling and Satterfield (in press) have modified the original model to predict short-term soil losses on agricultural fields (Guelph Wind Erosion and Assessment Model, GWEAM). This model differentiates between soil movement (erosion) within the field and soil lost beyond pre-defined field boundaries as well as predicting the amount of fine-grained material (dust) lost in suspension. The model also has the capability to aid in the design and placement of windbreaks.

REGIONAL SCALE TRANSPORT OF AEOLIAN SEDIMENTS

Aeolian geomorphic systems can be viewed as an interrelated set of processes and landforms in which sediment is transported by the wind from source areas to depositional sinks via transport pathways. Source and sinks for sediment are linked by a cascade of energy and materials which can be viewed in terms of sediment inputs and outputs, transfers, and storages (Chorley and Kennedy 1971, Cooke and Warren 1973).

Major sources for aeolian sediments (Fig. 17.19) are subtropical deserts and semi-arid and subhumid areas where soil is exposed seasonally to strong winds (Pye 1987). Bare, loose sediments containing sand and silt, but little clay (which promotes crusting and cementation of particles) are favourable surfaces for dust production. Major sources for dust storms are ephemeral river flood plains, dry lakes, coastal sabkhas, alluvial fans, and loess deposits (Pye 1987). Estimates of dust production have a wide range but reliable data are sparse (Table 17.2). For example, Middleton *et al.* (1986) note that in 1934 dust storms removed 300×10^6 tons of sediment from the Great Plains, and that a 6-h storm in West Africa resulted in soil loss of 4×10^5 tons. Up to 1 m of topsoil was removed from parts of the Texas High Plains in the February 1977 dust storm (McCauley *et al.* 1981).

Most aeolian sand is derived from material which has been transported by some other medium. Fluvial, alluvial, and deltaic deposits are important sources of windblown sand in North America, Arabia, India, and Australia (Sharp 1966, Glennie 1970, Wasson 1983). Playas contribute sand for dunefields such as White Sands, New Mexico (McKee 1966), and beaches are sources of sand in the Namib (Lancaster and Ollier 1983). Some sand seas have internal sources from deflation of inter-

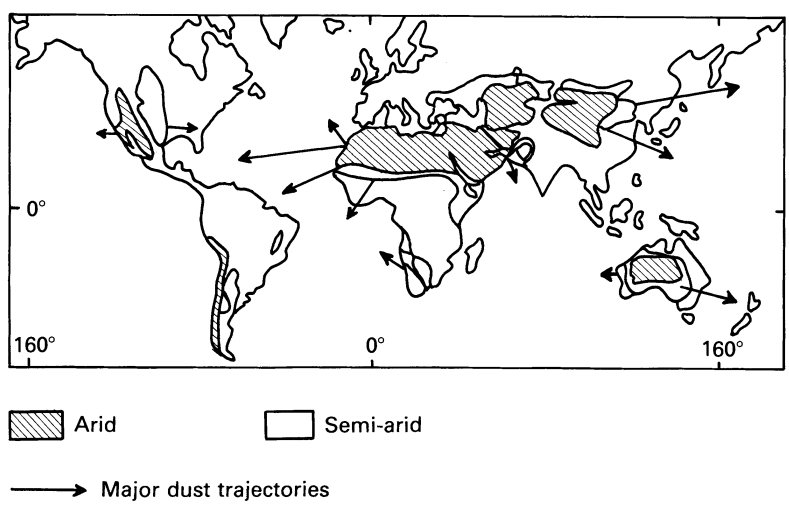

Figure 17.19 Location of major dust source areas and major trajectories of suspended sediment.

Table 17.2 Estimates of dust production (after Goudie 1983)

Location	*Annual quantity (millions of tons)*
World	128 ± 64 to 5000
Sahara	300
Aral Sea area (former USSR)	75
Southern Mediterranean	20–30
South-western USA	4
Mediterranean	3.2 ± 1.6

Table 17.3 Dustfall deposition rates (after Goudie 1983)

Location	*Rate (tonnes km^{-2} y^{-1})*
Kuwait	55
Bulgaria	44.5
Arizona	54
Negev (Israel)	50–200
Mexico City	<10 to >50
Caspian Sea	39.5
Kansas, USA	56
Northern Nigeria	137–181

dunes and reactivation of older dunes (Wasson 1983, Lancaster 1988). There are few data on sand erosion rates. In Algeria, Williams (1970) estimated 1 to 4 m of deflation in 2000 years; Lettau and Lettau (1969) inferred that 0.2 m of sand was eroded in 100 years in Peru; Wilson (1971) suggested that sand deflation rates increase by several orders of magnitude from bajadas to beaches and river bars. In mixed sediments, deflation ceases once a protective lag of coarse particles is developed, so that most sources of aeolian sand are also areas of active sediment renewal by fluvial or other processes (Sharp 1980).

Spacecraft images and data on atmospheric dust deposition show that dust storms can transport large quantities of material over long distances (Goudie 1983). Major dust plumes from the Sahara have been identified over the eastern Atlantic Ocean (Schütz 1980), and dust from central Asia reaches the Pacific north-west in concentrations of up to 60 mg m^{-3} (Pye 1987). The frequency of dust storms in which visibility is reduced to less than 1 km also gives an indication of the flux of dust. Dust storms occur most frequently in the Sahara, the Arabian Peninsula, the Seistan Basin of Iran, the Indus Plain, former Soviet central Asia, and the Tarim Basin of China (Goudie 1983, Middleton *et al.* 1986).

Aeolian sand transport systems may be of regional or subcontinental extent. Such systems have been inferred from wind data for the Sahara (e.g. Dubief 1952, Wilson 1971); Australia (Brookfield 1970, Wasson *et al.* 1988), and the Namib (Lancaster 1985), and confirmed by satellite images on which sand transport paths can be traced by zones of high albedo and features such as sand-choked river valleys, sand sheets and streaks, barchans, shadow dunes and shrub coppice dunes (e.g. Mainguet 1984, Zimbelman and Williams 1990).

Dust deposition may occur when wind velocity is reduced or particles are trapped by vegetation or rough surfaces. Alternatively, dust particles may aggregate or be precipitated by rain. Although deposition rates as high as 150 tonnes km^{-2} y^{-1} can occur (Table 17.3), much dust is remobilized by subsequent storms. Most medium and coarse dust is deposited in desert margin areas. Extensive desert loess was deposited during glacial stages when wind speeds and silt production were higher (Tsoar and Pye 1987). Much fine dust is deposited in ocean sediments downwind of arid regions (e.g. Kolla *et al.* 1979, Sarnthein *et al.* 1981).

Major sand seas in the Sahara, Arabia, central Asia, Australia, and southern Africa cover as much as 45% of the arid areas. Sand is deposited when transport rates are reduced by topography or, more commonly, by changes in climate which lead to lower wind velocities or winds that are more variable in direction, thus reducing net sand flux (Fryberger and Ahlbrandt 1979). Most sand seas occur where transport rates are low or where sand transport paths converge. The same winds which transport sand to the sand sea can also remove it, causing the sand sea to migrate downwind (Wilson 1971, Mainguet 1984).

DUST-TRANSPORTING WIND SYSTEMS

The most dramatic manifestation of dust transport by wind is the occurrence of dust storms, internationally defined as meteorological events in which visibility at eye level is reduced to less than 1000 m by dust raised from the surface. The frequency of dust storms at selected localities (Table 17.4) shows that the highest reported frequency of dust storms is in the Seistan Basin of Iran where dust storms are encountered on average 80.7 d y^{-1} (Middleton *et al.* 1986). A fundamental control on the distribution of dust storms in space and time is the occurrence of meteorological conditions that produce winds of sufficient velocity to entrain and transport dust. There are five major types of meteorological conditions which produce major dust storms (Middleton *et al.* 1986, Pye 1987): (a) the passage of cold fronts

Table 17.4 Dust storm frequencies per year of dust storms creating visibilities of less than 1000 m for selected locations (after Goudie 1983)

Location	*Frequency*
Abadan, Iran	13
Amritsar	10
Allahabad, India	8
New Delhi, India	8
Ganganagar, India	17
Pathankot, India	8
Paotou, China	19
Paoting, China	18.5
Baghdad, Iraq	21.5
Basra, Iraq	14.7
Aqaba, Jordan	10.7
H4, Jordan	16.3
Al Hummar, Jordan	7.0
Kano, Nigeria	23.0
Maidiguri, Nigeria	23.0
Nguru, Nigeria	26.0
Mexico City, Mexico	68
Kazakhstan, former USSR	60
Kantse, China	35
Hami, China	33
Beersheva, Israel	27
Shaibah, Iraq	37.6
Hinaidi, Iraq	33.2
Diwaniyah, Iraq	35.0
Kuwait Airport, Kuwait	27.1
Abu Kamal, Syria	9.7
Mersa Matruh, Egypt	9.6
Riyadh, Saudi Arabia	12.7
Daharan, Saudi Arabia	11.3
Tabouk, Saudi Arabia	10.8
Khartoum, Sudan	24

associated with depressions, (b) low pressure systems with intense baroclinal pressure gradients, (c) the convergence zone between cold and warm air masses in regions of monsoonal air flow, (d) downdraughts associated with intense convectional activity, and (e) katabatic drainage. On a more localized scale, intense dust devils caused by strong heating of the surface can also eject large quantities of dust into the air. There are many local variations on the major dust-generating wind conditions listed above, as discussed by Goudie (1983), Middleton *et al.* (1986), and Pye (1987).

The most important cause of dust storms is the passage of cold fronts associated with mid-latitude depressions (Pye 1987). Strong winds preceding or following the fronts are responsible for dust-transporting winds in China and central Asia (Ing 1969), Israel and Egypt (Yaalon and Ganor 1966), the High Plains and south-west United States (McCauley *et al.* 1981, Brazel 1989), and southern Australia (Garratt 1984). Dust-transporting winds associated with very steep regional pressure gradients are characterized by the Shamal winds of the Persian Gulf region (Khalaf and al-Hasash 1983), and the Santa Ana winds of California (Nakata *et al.* 1976). On a more localized scale, dust storms associated with strong downdraughts from convection cells (downdraught haboobs) are common in the Sudan (Idso 1967), the Gobi Desert (Middleton *et al.* 1986), the Thar Desert (Joseph *et al.* 1980), and the Phoenix area of Arizona, where 50% of all dust storms are of this type (Idso *et al.* 1972, Brazel and Nickling 1986). Katabatic winds generate dust storms in semi-arid western Canada (Coote *et al.* 1981), Iran, and northern India and Pakistan (Middleton *et al.* 1986).

On a global scale, the most important dust-transporting winds are associated with the passage of low pressure fronts across the southern Sahara and the Sahel region of Africa (Fig. 17.20). Sixty percent of the global production of dust is believed to come from the Sahara and is transported by the Harmattan winds (Junge 1979). In winter, the Harmattan winds affect a large part of west Africa south of latitude 15°N. During this season, dust is derived from the north-eastern Sahara in the alluvial plain of Bilma in Niger and Faya Largeau in Chad (Goudie 1983) and transported in a south-westerly direction towards the Gulf of Guinea, reaching northern Nigeria in 24 to 48 h (MacTanish 1982).

During the Northern Hemisphere summer, dust storms are frequent in the southern Sahara and Sahel. At this time the Inter Tropical Convergence Zone (ITCZ), which separates hot dry Saharan air from moister tropical air to the south, lies across the northern Sahel. Squall lines, with strong dust-raising winds, develop several degrees of latitude south of the monsoon front. They usually occur between 10°N and 15°N and move from east to west. The squalls are usually short lived, with only a few reaching the west African coast. However, during summer Saharan dust is transported westward over the Atlantic in association with waves developed in the mid-tropospheric easterly flow. Dust associated with these outbreaks has been traced as far west as the Caribbean, Florida, and eastern South America (Prospero *et al.* 1981).

CONCLUSIONS AND FUTURE RESEARCH NEEDS

Although the past decade has brought significant advances in our understanding of the complex processes of sediment transport by the wind, there remain many challenging problems for the future. In

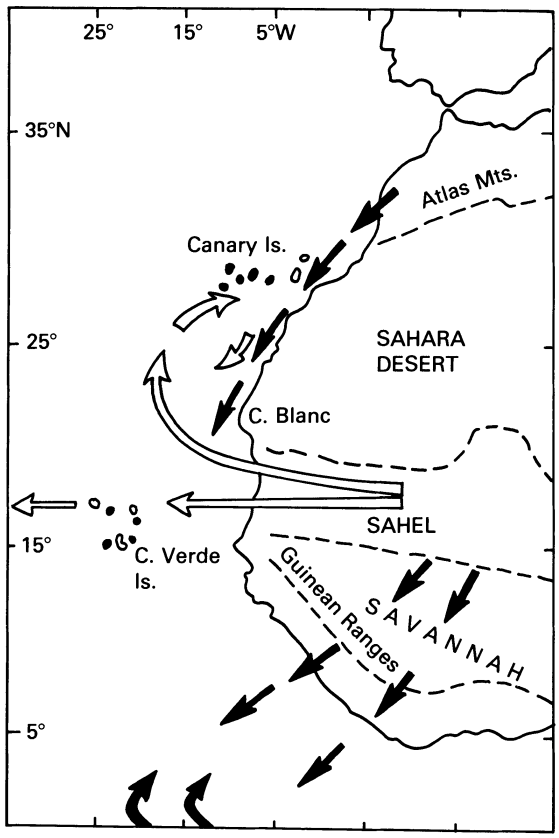

Figure 17.20 Airflow patterns and dust-transporting winds in north-western Africa. Solid arrows = trade winds and open arrows = mid-tropospheric winds (after Pye 1987).

order to reduce the conceptual and experimental complexities to manageable proportions, most theoretical and empirical research to date has focused on very simple systems in which sediments are assumed to be composed of a single grain size, and the wind is assumed to be blowing with a steady velocity. Important questions, such as the formation of small-scale stratification types (e.g. wind ripple laminae), and the ejection of dust from desert surfaces, require knowledge about grain behaviour in mixed grain size beds. This will include studies of saltation with a wide range of grain trajectories and consideration of the development of the bed in space and time (e.g. armouring and the development of wind ripples). It is clear that the surface wind is not steady in time and space and that saltation responds rapidly to changes in wind velocity. When coupled with the strongly non-linear relationship between sediment flux and wind shear velocity, calculation of long-term transport rates requires that much more detailed information on the high frequency nature of wind velocity fluctuations is required. These problems present important challenges to the aeolian research community. Whereas increased computing power will enable more realistic simulations of aeolian processes, there are extreme difficulties to be overcome in the experimental and field techniques required to verify and parameterize these models. As Anderson *et al.* (1991) note, theory has caught up with wind tunnel and field experimental techniques in many areas. More cooperation between theoretical and experimental approaches is clearly indicated for the next generation of aeolian transport studies.

NOTATION

A	threshold coefficient
A_g	ground area not covered by roughness elements
A_s	unit surface area
A_1	cohesionless threshold coefficient
a	empirical constant
a_1	empirical regression constant
b_1	empirical regression constant
C	sorting coefficient in mass flux equations
C_p	particle concentration at height y
C_z	particle concentration at height z
c	constant
c_2	empirical constant
D	reference grain diameter (0.25 mm)
d	grain diameter
d_0	zero plane displacement height
E	soil loss for specified time period
F	total force of the wind
F_c	capillary force on grain contact
F_r	wind force on roughness elements
F_g	wind force on ground surface
f	Coriolis parameter
G	vertical particle flux
G_c	shape of the contacts between grains
$G(u)$	vertical mass flux of dust as a function of wind speed (u)
g	acceleration of gravity
$g(L_f)$	field length effect parameter
H	height at which particle concentration is zero
h	saltation trajectory height
I	soil erodibility index
i	index of summation
K	settling velocity coefficient
K_1	interparticle force coefficient
k	sand texture coefficient

L	maximum travel distance for a suspended particle
L_c	ratio of total frontal silhouette area of roughness elements to total surface area
L_f	equivalent field width
l	saltation path length
P	moisture tension at grain contact
$p_i(u)$	probability density function of wind speed
q	sand transport rate (mass flux)
m	exponent
N_a	number of entrained grains per unit area
n	interparticle force exponent
R	soil ridge roughness factor
Re_p	particle friction Reynolds number
R_i	soil roughness index
r	exponent
T_s	surface tension of water
U	mean wind speed
U_f	particle settling velocity
u	horizontal component of wind velocity
u_*	wind shear velocity or friction speed
u_{*s}	shear velocity calculated from the airborne shear stress at the surface
u_{*t}	threshold shear velocity
u_{*tb}	threshold shear velocity for sloping surface
u_{*ti}	threshold shear velocity for dust emissions
u_{*to}	threshold shear velocity for flat surface
u_{*tv}	threshold shear velocity for vegetated surface
u_{*tw}	threshold shear velocity for moist surface
V	vegetation cover factor
w	vertical component of wind velocity
w'	fluctuations in vertical wind velocity
y	height of measurement of suspended sediment
z	height above the surface
z_0	aerodynamic roughness length
α	angle of internal friction
α_s	constant
ΔT	time period
ε	eddy diffusion coefficient
θ	local slope angle
κ	von Karman's constant (≈ 0.4)
μ	dynamic viscosity of air
ρ	air density
ρ_p	particle density
σ	standard deviation of the vertical fluctuating velocity distribution
τ	shear stress
τ_a	mean shear stress
τ_c	critical threshold shear stress
τ_g	shear stress on the ground surface between roughness elements
χ	angle between local slope and wind direction

REFERENCES

Anderson, R.S. and P.K. Haff 1988. Simulation of eolian saltation. *Science* **241**, 820–23.

Anderson, R.S. and B. Hallett 1986. Sediment transport by wind: toward a general model. *Bulletin of the Geological Society of America* **97**, 523–35.

Anderson, R.S., M. Sørensen and B.B. Willetts 1991. A review of recent progress in our understanding of aeolian sediment transport. *Acta Mechanica Supplement* **1**, 1–19.

Azizov, A. 1977. Influence of soil moisture on the resistance of soil to wind erosion. *Soviet Soil Science* **9**, 105–8.

Bagnold, R.A. 1941. *The physics of blown sand and desert dunes*. London: Chapman & Hall.

Belly, Y. 1964. Sand movement by wind. *U.S. Army Corps of Engineers, Coastal Engineering Research Center, Technical Memo* 1, Addendum III, 24 pp.

Bradley, E.F. 1969a. A micrometeorological study of velocity profiles and surface drag in the region modified by a change in surface roughness. *Quarterly Journal of the Royal Meteorological Society* **96**, 361–9.

Bradley, E.F. 1969b. A shearing stress meter for micrometeorological studies. *Quarterly Journal of the Royal Meteorological Society* **94**, 380–7.

Brazel, A.J. 1989. Dust and climate in the American Southwest. In *Palaeoclimatology and palaeometeorology: modern and past patterns of global atmospheric transport*, M. Leinen and M. Sarthein (eds), 65–96. Dordrecht: Kluwer.

Brazel, A.J. and W.G. Nickling 1986. The relationship of weather types to dust storm generation in Arizona (1965–1980). *Journal of Climatology* **6**, 255–75.

Brookfield, M. 1970. Dune trends and wind regime in Central Australia. *Zeitschrift für Geomorphologie Supplement Band* **10**, 121–58.

Chen, Y., J. Tarchitzky, J. Brouwer, J. Morin, *et al.* 1980. Scanning electron microscope observations on soil crusts and their formation. *Soil Science* **130**, 49–55.

Chepil, W.S. 1945a. Dynamics of wind erosion: I. Nature of movement of soil by wind. *Soil Science* **60**, 305–20.

Chepil, W.S. 1945b. Dynamics of wind erosion: II. Initiation of soil movement. *Soil Science* **60**, 397–411.

Chepil, W.S. 1945c. Dynamics of wind erosion: IV. The translocating and abrasive action of the wind. *Soil Science* **61**, 169–77.

Chepil, W.S. 1951. Properties of soil which influence wind erosion: I. The governing principle of surface roughness. *Soil Science* **69**, 149–62.

Chepil, W.S. 1959. Equilibrium of soil grains at the threshold of movement by wind. *Proceedings of the Soil Science Society of America* **23**, 422–8.

Chepil, W.S. and N.P. Woodruff 1957. Sedimentary characteristics of dust storms. II. Visibility and dust concentration. *American Journal of Science* **255**, 104–14.

Chepil, W.S. and N.P. Woodruff 1963. The physics of wind erosion and its control. *Advances in Agronomy* **15**, 211–302.

Chorley, R.J. and B.A. Kennedy 1971. *Physical geography: a systems approach*. London: Prentice Hall.

Cole, G.W. 1984a. A method for determining wind erosion rates from wind tunnel-derived functions. *Transactions of the American Society of Agricultural Engineers* **27**, 110–26.

Cole, G.W. 1984b. A stochastic formulation of soil erosion caused by wind. *Transactions of the American Society of Agricultural Engineers* **27**, 1405–10.

Cooke, R.U. and A. Warren 1973. *Geomorphology in deserts*. London: Batsford.

Coote, D.R., J. Dumanski and J.F. Ramsey 1981. *An assessment of the degradation of agricultural lands in Canada*. Agricultural Land Resource Research Institute, Contribution 118.

Dubief, J. 1952. Le vent et la deplacement du sable du Sahara. *Travaux de la Institute de Recherches Sahariennes* **8**, 123–64.

Dyer, K. 1986. *Coastal and estuarine sediment dynamics*. Chichester: Wiley.

Finlan, C.A. 1987. The effects of particle shape and size on the entrainment and transport of sediment by wind. M.S. Thesis, University of Guelph.

Foster, S.M. and T.H. Nicolson 1980. Microbial aggregation of sand in the maritime dune succession. *Soil Biology and Biochemistry* **13**, 205–8.

Fryberger, S.G. and T.S. Ahlbrandt 1979. Mechanisms for the formation of aeolian sand seas. *Zeitschrift für Geomorphologie* **23**, 440–60.

Garratt, J.R. 1984. Cold fronts and dust storms during the Australian summer 1982/3. *Weather* **39**, 98–103.

Gerety, K.M. 1985. Problems with determination of u_* from wind-velocity profiles measured in experiments with saltation. In *Proceedings of International Workshop on the Physics of Blown Sand*, O.E. Barndorff-Nielsen, J.T. Møller, K.R. Rasmussen and B.B. Willetts (eds), 271–300. Aarhus: University of Aarhus.

Gerety, K.M. and R. Slingerland 1983. Nature of the saltating population in wind tunnel experiments with heterogeneous size-density sands. In *Eolian sediments and processes*, M.E. Brookfield and T.S. Ahlbrandt (ed.), 115–31. Amsterdam: Elsevier.

Gillette, D.A. 1974. On the production of soil wind erosion aerosols having the potential for long-term transport. *Journal of Atmospheric Research* **8**, 735–44.

Gillette, D.A. 1977. Fine particulate emissions due to wind erosion. *Transactions of the American Society of Agricultural Engineers* **20**, 890–7.

Gillette, D.A. 1986. Wind Erosion. In *Soil conservation: assessing the national resource inventory*, 129–58. Washington, DC: National Academy Press.

Gillette, D. and P.A. Goodwin 1974. Microscale transport of sand-sized soil aggregates eroded by wind. *Journal of Geophysical Research* **79**, 4080–4.

Gillette, D.A. and R. Passi 1988. Modelling dust emission caused by wind erosion. *Journal of Geophysical Research* **93**, 14 233–42.

Gillette, D.A. and P.H. Stockton 1989. The effect of nonerodible particles on the wind erosion of erodible surfaces. *Journal of Geophysical Research* **94**, 12 885–93.

Gillette, D.A., I.H. Blifford and C.R. Fenster 1972. Measurements of aerosol-size distributions and vertical fluxes of aerosols on land subject to wind erosion. *Journal of Applied Meteorology* **11**, 977–87.

Gillette, D.A., I.H. Blifford Jr and D.W. Fryrear 1974. The influence of wind velocity on the size distributions of aerosols generated by the wind erosion of soils. *Journal of Geophysical Research* **79**, 4068–75.

Gillette, D.A., J. Adams, A. Endo and D. Smith 1980. Threshold velocities for the input of soil particles into the air by desert soils. *Journal of Geophysical Research* **85**, 5621–30.

Gillette, D.A., J. Adams, D. Muhs and R. Kihl 1982. Threshold friction velocities and rupture moduli for crusted desert soils for the input of soil particles in the air. *Journal of Geophysical Research* **87**, 9003–15.

Glennie, K.W. 1970 *Desert sedimentary environments*. Amsterdam: Elsevier.

Goossens, D. 1985. The granulometric characteristics of a slowly-moving dust cloud. *Earth Surface Processes and Landforms* **10**, 353–62.

Goudie, A.S. 1983. Dust storms in space and time. *Progress in Physical Geography* **7**, 502–29.

Greeley, R. and J.D. Iversen 1985. *Wind as a geological process*. Cambridge: Cambridge University Press.

Greeley, R., B. White, R. Leach, J. Iversen *et al.* 1976. Mars: wind friction speeds for particle movement. *Geophysical Research Letters* **3**, 417.

Hagen, L. 1984. Soil aggregate abrasion by impacting sand and soil particles. *Transactions of the American Society of Agricultural Engineers* **27**, 805–8.

Hagen, L.J. 1991. A wind erosion prediction system to meet user needs. *Journal of Soil and Water Conservation* **46**, 106–11.

Hardisty, J. and R.J.S. Whitehouse 1988. Effect of bedslope on desert sand transport. *Nature* **334**, 302.

Howard, A.D. 1977. Effect of slope on the threshold of motion and its application to orientation of wind ripples. *Bulletin of the Geological Society of America* **88**, 853–6.

Hunt, J.C.R. and P. Nalpanis 1985. Saltating and suspended particles over flat and sloping surfaces, I. Modelling concepts. In *Proceedings of international workshop on the physics of blown sand*, O.E. Barndorff-Nielsen, J.T. Møller, K.R. Rasmussen and B.B. Willetts (eds), 9–36. Aarhus: University of Aarhus.

Idso, S.B. 1967. Dust storms. *Scientific American* **235**, 108–14.

Idso, S.B., R.S. Ingram and J.M. Pritchard 1972. An American haboob. *American Meteorological Society Bulletin* **53**, 930–55.

Ing, G.K.T. 1969. A dust storm over central China. *Weather* **27**, 136–45.

Iversen, J.D. and B.R. White 1982. Saltation threshold on Earth, Mars and Venus. *Sedimentology* **29**, 111–9.

Iversen, J.D., J.B. Pollack, G.R. and B.R. White 1976. Saltation threshold on Mars: the effect of interparticle force, surface roughness, and low atmospheric density. *Icarus* **29**, 383–93.

Jensen, J.L. and M. Sørensen 1986. Simulation of some aeolian saltation transport parameters: a re-analysis of William's data. In *Proceedings of the international workshop on the physics of blown sand*, O.E. Barndorff-Nielsen, J.T. Møller, K.R. Rasmussen and B.B. Willetts (eds), Aarhus: University of Aarhus.

Joseph, P.W., D.K. Raipal and S.N. Deka 1980. 'Andhi'; the convective dust storm of northwest India. *Mausam* **31**, 431–2.

Junge, C.E. 1979. The importance of mineral dust as an atmospheric constituent in the atmosphere. In *Saharan dust*, C. Morales (ed.) 49–60. New York: Wiley.

Kawamura, R. 1951. Study of sand movement by wind. *Institute of Science and Technology, Tokyo, Report* **5**(3-4), Tokyo, Japan, 95–112.

Khalaf, F.I. and M. al-Hasash 1983. Aeolian sediments in the northwestern part of the Arabian Gulf. *Journal of Arid Environments* **6**, 319–32.

Kolla, V., P.E. Biscaye and A.F. Hanley 1979. Distribution of quartz in late Quaternary Atlantic sediments in relation to climate. *Quaternary Research* **11**, 261–77.

Lancaster, N. 1985. Winds and sand movements in the Namib sand sea. *Earth Surface Processes and Landforms* **10**, 607–19.

Lancaster, N. 1988. Development of linear dunes in the southwestern Kalahari, southern Africa. *Journal of Arid Environments* **14**, 233–44.

Lancaster, N. and C.D. Ollier 1983. Sources of sand for the Namib Sand Sea. *Zeitschrift für Geomorphologie Supplement Band* **45**, 71–83.

Lancaster, N., R. Greeley and K.R. Rasmussen 1991. Interaction between unvegetated desert surfaces and the atmospheric boundary layer: a preliminary assessment. *Acta Mechanica Supplement* **2**, 89–102.

Lettau, H. and K. Lettau 1969. Bulk transport of sand by the barchans of Pampa La Joya in southern Peru. *Zeitschrift für Geomorphologie* **13**, 183–95.

Lettau, K. and H.H. Lettau 1978. Experimental and micrometeorological field studies on dune migration. In *Exploring the world's driest climate*, K. Lettau and H.H. Lettau (eds), 110–47. Madison, WI: University of Wisconsin, Institute for Environmental Studies.

Logie, M. 1982. Influence of roughness elements and soil moisture of sand to wind erosion. *Catena* **1**, 161–73.

Lumley, J.L. and H.A. Panofsky 1964. *The structure of atmospheric turbulence*. New York: Wiley.

Lyles, L. and R.K. Krauss 1971. Threshold velocities and initial particle motion as influenced by air turbulence. *Transactions of the American Society of Agricultural Engineers* **14**, 563–6.

Lyles, L. and R.L. Schrandt 1972. Wind erodibility as influenced by rainfall and soil salinity. *Soil Science* **114**, 367–72.

Lyles, L., R.L. Schrandt and N.F. Schneidler 1974. How aerodynamic roughness elements control sand movement. *Transactions of the American Society of Agricultural Engineers* **17**, 134–9.

MacTanish, G.H. 1982. Nature and distribution of Harmattan dust. *Zeitschrift für Geomorphologie* **26**, 417–35.

Mainguet, M. 1984. Space observations of Saharan aeolian dynamics. In *Deserts and arid lands*, F. El Baz (ed.), 59–77. The Hague: Nyhoff.

Marshall, J.K. 1971. Drag measurements in roughness arrays of varying densities and distribution. *Agricultural Meteorology* **8**, 269–92.

McCauley, J.F., C.S. Breed, M.J. Grolier and D.J. MacKinnon 1981. The U.S. dust storm of February, 1977. In *Desert dust: origin, characteristics, and effect on Man*, T.L. Pewe (ed.). Geological Society of America Special Paper 186.

McKee, E.D. 1966. Structures of dunes at White Sands National Monument, New Mexico (and a comparison with structures of dunes from other selected areas). *Sedimentology* **7**, 1–69.

McKenna-Neuman, C. and W.G. Nickling 1989. A theoretical and wind tunnel investigation of the effect of capillary water on the entrainment of sediment by wind. *Canadian Journal of Soil Science* **69**, 79–96.

Middleton, G.V. and J.B. Southard 1984. *Mechanics of sediment movement*. Tulsa, OK: Society of Economic Paleontologists and Mineralogists.

Middleton, N.J., A.S. Goudie and G.L. Wells 1986. The frequency and source areas of dust storms. In *Aeolian geomorphology*, W.G. Nickling (ed.), 237–59. London: Allen & Unwin.

Mitha, S., M.Q. Tran, B.T. Werner and P.K. Haff 1985. The grain-bed impact process in aeolian saltation. *Brown bag preprint series in basic and applied science* BB-36. Pasadena, CA: Department of Physics, California Institute of Technology.

Musick, H.B. and D.A. Gillette 1990. Field evaluation of reltionships between a vegetation structural parameter and sheltering against wind erosion. *Land degradation and rehabilitation* **2**, 87–94.

Nakata, J.K., H.G. Wilshire and G.G. Barnes 1976. Origin of Mojave Desert dust plumes photographed from space. *Geology* **4**, 644–8.

Nalpanis, P. 1985. Saltating and suspended particles over flat and sloping surfaces, II. Experiments and numerical simulations. In *Proceedings of international workshop on the physics of blown sand*, O.E. Barndorff-Nielsen, J.T. Møller, K.R. Rasmussen and B.B. Willetts (eds), 37–66. Aarhus: University of Aarhus.

Nickling, W.G. 1978. Eolian sediment transport during dust storms: Slims River Valley, Yukon Territory. *Canadian Journal of Earth Science* **15**, 1069–84.

Nickling, W.G. 1983. Grain-size characteristics of sediment transported during dust storms. *Journal of Sedimentary Petrology* **53**, 1011–24.

Nickling, W.G. 1984. The stabilizing role of bonding agents on the entrainment of sediment by wind. *Sedimentology* **31**, 111–7.

Nickling, W.G. 1988. Initiation of particle movement by wind. *Sedimentology* **35**, 499–512.

Nickling, W.G. 1989. Prediction of soil loss by wind. In *Land conservation for future generations*, S. Rimwanich (ed.), 75–94. Bangkok: Ministry of Agriculture.

Nickling, W.G. and M. Ecclestone 1981. The effects of soluble salts on the threshold shear velocity of fine sand. *Sedimentology* **28**, 505–10.

Nickling, W.G. and J.A. Gillies 1989. Emission of fine-grained particles from desert soils. In *Palaeoclimatology and palaeometeorology: modern and past patterns of global atmospheric transport*, M. Leinen and M. Sarnthein (eds), 133–65. Amsterdam: Kluwer.

O'Brien, M.P. and B.D. Rindlaub 1936. The transportation of sand by wind. *Civil Engineering* **6**, 325–7.

Oke, T.R. 1978. *Boundary layer climates*. New York: Methuen.

Owen, P.R. 1964. Saltation of uniform grains in air. *Journal of Fluid Mechanics* **20**, 225–42.

Prandtl, L. 1935. The mechanics of viscous fluids. In *Aerodynamic theory*, Volume III, F. Durand (ed.), 57–109. Berlin: Springer.

Prospero, J.M., R.A. Glaccum and R.T. Nees 1981. Atmospheric transport of soil dust from Africa to South America. *Nature* **289**, 570–2.

Pye, K. 1980. Beach salcrete and eolian sand transport:

evidence from North Queensland. *Journal of Sedimentary Petrology* **50**, 257–61.

Pye, K. 1987. *Aeolian dust and dust deposits*. London: Academic Press.

Rasmussen, K.R. and H. Mikkelsen 1991. Wind tunnel observations of aeolian transport rates. *Acta Mechanica Supplement* **1**, 135–44.

Rouse, H. 1937. Modern conceptions of the mechanics of fluid turbulence. *Transactions of the American Society of Civil Engineers* **102**, 403–543.

Rumpel, D.A. 1985. Successive aeolian saltation: studies of idealized collisions. *Sedimentology* **32**, 267–80.

Sarnthein, M., G. Tetzlaff, B. Koopmann, K. Wolter and U. Pilaumann 1981. Glacial and interglacial wind regimes over the eastern subtropical Atlantic and North-West Africa. *Nature* **293**, 193–6.

Sarre, R.D. 1989. Aeolian sand transport. *Progress in Physical Geography* **11**, 157–82.

Schlicting, H. 1936. Experimentle untersuchungen zum rauhigkeitsproblem. *Ingeniew-Archiv* **7**, 1–34. (English Translation: NACA Technical Memorandum 823, 1936.)

Schütz, L. 1980. Long range transport of desert dust with special emphasis on the Sahara. *Annals of the New York Academy of Sciences* **338**, 515–32.

Sharp, R.P. 1964. Wind-driven sand in Coachella Valley, California. *Bulletin of the Geological Society of America* **75**, 785–804.

Sharp, R.P. 1966. Kelso Dunes, Mohave Desert, California. *Bulletin of the Geological Society of America* **77**, 1045–74.

Sharp, R.P. 1980. Wind driven sand in the Coachella Valley, California: further data. *Bulletin of the Geological Society of America* **91**, 724–30.

Skidmore, E.L, P.S. Fisher and N.P. Woodruff 1970. Wind erosion equation: computer solution and application. *Proceedings of the Soil Science Society of America* **34**, 931–5.

Stockton, P.H. and D.A. Gillette 1990. Field measurements of the sheltering effect of vegetation on erodible land surfaces. *Land Degradation and Rehabilitation* **2**, 77–86.

Tsoar, H. and K. Pye 1987. Dust transport and the question of desert loess formation. *Sedimentology* **34**, 139–54.

Ungar, J.E. and P.K. Haff 1987. Steady-state saltation in air. *Sedimentology* **34**, 289–99.

Van den Anker, J.A.M., P.D. Jungerius and L.R. Muir 1985. The role of algae in the stabilization of coastal dune blowouts. *Earth Surface Processes and Landforms* **10**, 189–92.

Wasson, R.J. 1983. Dune sediment types, sand colour, sediment provenance and hydrology in the Strzelecki-Simpson Dunefield, Australia. In *Eolian sediments and processes*, M.E. Brookfield and T.S. Ahlbrandt (eds), 165–95. Amsterdam: Elsevier.

Wasson, R.J., K. Fitchett, B. Mackey and R. Hyde 1988. Large-scale patterns of dune type, spacing, and orientation in the Australian continental dunefield. *Australian Geographer* **19**, 89–104.

Werner, B.T. 1988. A steady-state model of wind-blown sand transport. *The Office of Naval Technology, The Naval Weapons Center*, 1.

White, B.R. 1982. Two-phase measurements of saltating turbulent boundary layer flow. *International Journal of Multiphase Flow* **9**, 459–73.

White, B.R. and J.C. Schultz 1977. Magnus effect in saltation. *Journal of Fluid Mechanics* **81**, 497–512.

Willetts, B.B. 1983. Transport by wind of granular materials of different grain shapes and densities. *Sedimentology* **30**, 669–79.

Willetts, B.B. and M.A. Rice 1986. Collision in aeolian transport: the saltation/creep link. In *Aeolian geomorphology*, W.G. Nickling (ed.), 1–18. London: Allen & Unwin.

Willetts, B.B., M.A. Rice and S.E. Swaine 1982. Shape effects in aeolian grain transport. *Sedimentology* **29**, 409–17.

Williams, G. 1964. Some aspects of the eolian saltation load. *Sedimentology* **3**, 257–87.

Williams, G.E. 1970. Piedmont sedimentation and late Quaternary chronology in the Biskra region of the northern Sahara. *Zeitschrift für Geomorphologie* **10**, 40–63.

Williams, J.J., G.R. Butterfield and D.G. Clark 1990. Rates of aerodynamic entrainment in a developing boundary layer. *Sedimentology* **37**, 1039–48.

Wilson, I.G. 1971. Desert sandflow basins and a model for the development of ergs. *Geographical Journal* **137**, 180–99.

Woodruff, N.P. and F.H. Siddoway 1965. A wind erosion equation. *Proceedings of the Soil Science Society of America* **34**, 931–5.

Yaalon, D.H. and E. Ganor 1966. The climatic factor of wind erodibility and dust blowing in Israel. *Israel Journal of Earth-Sciences* **15**, 27–32.

Zimbelman, J.R. and S.H. Williams 1990. Interbasin transport of aeolian sand, Mojave Desert, California. *Eos* **71**, 1245.

Zingg, A.W. 1953. Wind tunnel studies of the movement of sedimentary material. In *Proceedings of the Fifth Hydraulic Conference. Studies in Engineering*, Bulletin 34, 111–35. Iowa City: University of Iowa.

DUNE MORPHOLOGY AND DYNAMICS 18

Nicholas Lancaster

INTRODUCTION

Quartz sand dominates aeolian deposits in arid regions, as dust-sized particles are carried out of the desert entirely or are trapped by vegetation or rough surfaces on desert margins (Tsoar and Pye 1987). Most (>95%) sand occurs in accumulations known as sand seas or ergs (Wilson 1973) that comprise areas of dunes of varying morphological types and sizes as well as areas of sand sheets. Smaller dune areas are known informally as dunefields. Major sand seas occur in the old world deserts of the Sahara, Arabia, central Asia, Australia, and southern Africa, where sand seas cover between 20 and 45% of the area classified as arid (Fig. 18.1). In North and South America there are no large sand seas, and dunes cover less than 1% of the arid zone.

In recent years, the focus of studies of dunes has changed radically. Despite the variety of different dune types and the multiplicity of local names that have been used to refer to them (see summary in Breed *et al.* 1979), satellite images of desert sand seas show that dunes of essentially similar form occur in widely separated sand seas (Breed and Grow 1979, McKee 1979). Detailed field studies of dune morphology and dynamics (e.g. Howard *et al.* 1978, Tsoar 1983, Livingstone 1986, Lancaster 1989a) have done much to end decades of speculation about the formative processes for dunes. This combination of the regional perspective of remote sensing data and detailed field studies has resulted in a new set of paradigms that emphasize studies of processes on different temporal and spatial scales, in contrast to the descriptive approach used by many earlier workers (Cooke and Warren 1973).

Dunes are created by interactions between granular material (sand) and shearing flow (the atmospheric boundary layer). The resulting landforms are bedforms that are dynamically similar to those developed in subaqueous shearing flows (e.g. rivers, tidal currents). Their forms reflect the characteristics of the sediment (primarily its grain size) and the surface wind (surface shear stress or friction speed and directional variability). In some areas vegetation may be a significant factor. As the bedform grows upwards into the boundary layer, the primary air flow is modified by interactions between the form and the flow which create secondary flow circulations. These play a major role in determining dune morphology.

In all sand seas, there is a hierarchical system of aeolian bedforms superimposed on one another (Wilson 1972, Lancaster 1988). Three orders of aeolian bedforms can be identified (Fig. 18.2), although only the first two occur in all sand seas: (a) wind ripples (spacing 0.1 to 1 m), (b) individual simple dunes or superimposed dunes on compound and complex dunes (spacing 50 to 500 m), and (c) compound and complex dunes or draa (spacing greater than 500 m). Each element of the hierarchy responds to the dynamics of a component of the wind regime in an area and possesses a characteristic time period, termed the relaxation or reconstitution time (Allen 1974), over which it will adjust to changed conditions. This increases from minutes in the case of wind ripples to millennia for draas. Change in bedforms involves the movement of sediment. Thus an increasing spatial scale is also involved at each level of the hierarchy.

Dune-forming processes operate at three main spatial and temporal scales (Warren and Knott 1983) which correspond approximately to the steady, graded and cyclic timescales of Schumm and Lichty (1965). Processes operating at the steady scale, which involves very short or even instantaneous amounts of time and small areas, include the formation of wind ripples. The graded scale involves periods of 1 to 100 years, and particularly concerns

Geomorphology of Desert Environments. Edited by Athol D. Abrahams and Anthony J. Parsons. Published in 1994 by Chapman & Hall, London. ISBN 978-94-015-8256-8

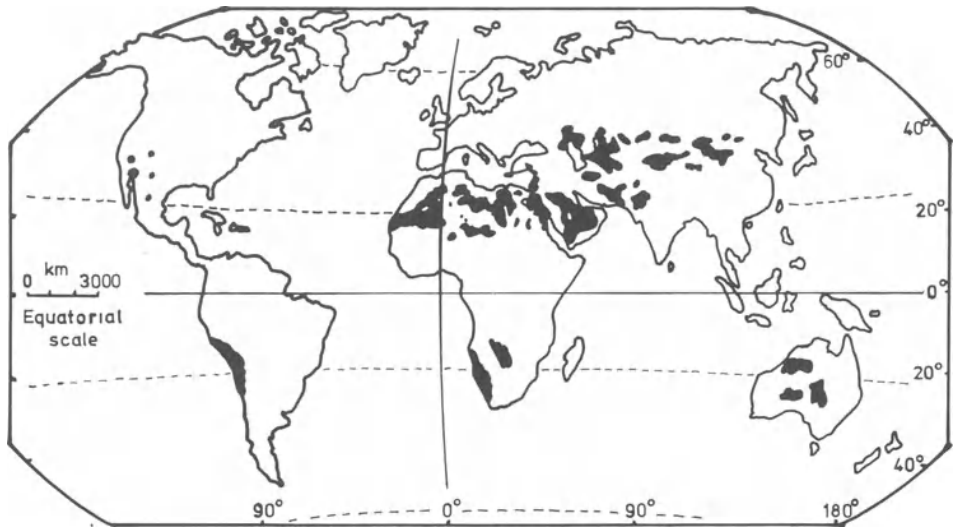

Figure 18.1 Location of major low latitude sand seas and dunefields.

the dynamics and morphology of dunes, which tend towards an actual or partial equilibrium with respect to rates and directions of sand movements generated by surface winds. Form–flow interactions and feedback processes are important at this scale, which is probably the most important in determining the morphology and dynamics of dunes. The cyclic timescale involves periods of 10^3 to 10^6 years and a spatial scale corresponding to that of sand seas and their regional physiographic and tectonic setting. Processes at this scale involve those responsible for the accumulation of sand seas as sedimentary bodies.

The following discussion of dune morphology and dynamics will proceed up this temporal and spatial hierarchy of aeolian sand deposits, with an emphasis on the fundamental processes operating at each scale.

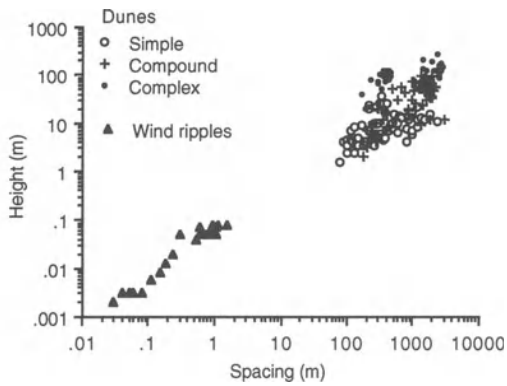

Figure 18.2 The hierarchy of aeolian bedforms, as expressed by the relationship between bedform height and spacing. Note clear separation between wind ripples and dunes, but overlap of height-spacing relationships for simple, compound, and complex dunes. Data from Lancaster (1988) and many other sources.

WIND RIPPLES

Wind ripples (Fig. 18.3) are ubiquitous on all sand surfaces except those undergoing very rapid deposition. They are the initial response of sand surfaces to sand transport by the wind, and form because flat sand surfaces over which transport by saltation and reptation takes place are dynamically unstable (Bagnold 1941). The formation and movement of wind ripples are therefore closely linked to the processes of saltation and reptation.

Wind ripples trend perpendicular to the sand-transporting winds, although Howard (1977) has emphasized the effects of slope on ripple orientation. Because they can be reformed within minutes, wind ripples provide an almost instantaneous indication of local sediment transport and wind directions. Typical wind ripples have a wavelength of 50 to 200 mm and an amplitude of 0.005 to 0.010 m (Bagnold 1941, Sharp 1963). Much longer wavelength (0.5 to 2 m) ripples with an amplitude of 0.1 m or more are composed of coarse sand or granules (1 to 4 mm median grain size) and are termed 'granule ripples' by Sharp and 'megaripples'

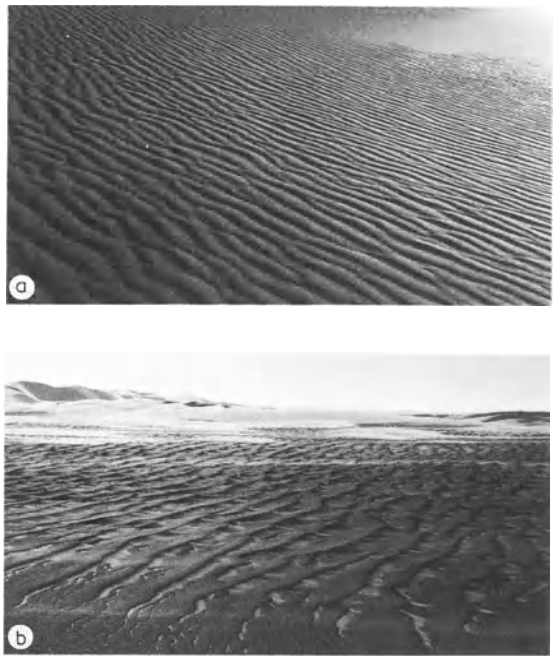

Figure 18.3 Wind ripples: (a) ripples in medium–fine sand in the Namib sand sea, and (b) granule ripples on the Skeleton Coast, Namibia.

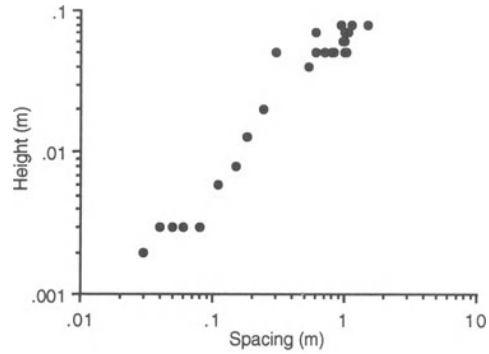

Figure 18.4 Wind ripple morphometry. Note that there is a continuum of ripple wavelength from 'normal' wind ripples to granule ripples. Data from Sharp (1963), Walker (1981), and author's field observations.

by Greeley and Iversen (1985). Ellwood *et al.* (1975) showed that granule ripples are not distinct forms, and form one end of a continuum of wind ripple dimensions (Fig. 18.4). Ripple wavelength is a function of both particle size and sorting and wind speed so that ripples in coarse sands have a greater spacing than those in fine sands (Sharp 1963). For sands of a given size, ripple wavelength increases with wind friction speed (Seppälä and Linde 1978). Most wind ripples are asymmetric in cross-section with a slightly convex stoss slope at an angle of 8 to 10° and a lee slope that varies between 20 and 30° (Sharp 1963). In all cases the crest of the ripple is composed of grains that are coarse relative to the mean size of the surface sand.

Several models have been put forward to explain the formation and characteristic wavelength of ripples. Bagnold (1941) pointed to the close correspondence between calculated saltation path lengths and observed ripple wavelengths in wind tunnel experiments. Chance irregularities in 'flat' sand surfaces give rise to variations in the intensity of saltation impacts (Fig. 18.5a) creating zones that would be preferentially eroded or protected. Grains from the zone of more intense impacts (A–B) would land downwind at a distance equal to the average saltation pathlength such that a zone of more intense saltation impacts would propagate downwind. In addition, variations in surface slope and saltation impact intensity cause variations in the reptation rate. Bagnold argued that interactions between the developing surface microtopography and the saltating and reptating grains would soon lead to a coincidence between the characteristic saltation pathlength and the ripple wavelength (Fig. 18.5b). Wilson (1972) and Ellwood *et al.* (1975) extended Bagnold's hypothesis to show that even the wavelengths of granule ripples were related to the mean saltation pathlength of one grain size off another.

Bagnold's concept of the formation of wind ripples was first challenged by Sharp (1963) who argued that grains in ripples are moved mostly by reptation. Irregularities in the bed and interactions between grains moving at different speeds give rise to local increases in bed elevation. These 'proto-ripples' begin as short-wavelength, low-amplitude forms and grow to their steady state dimensions by the growth of larger forms at the expense of smaller. Each developing ripple creates a 'shadow zone' in its lee (Fig. 18.5c), with a width proportional to ripple wavelength and impact angle. The size of the shadow zone determines the position of the next ripple downwind. Sharp argued that the controls of ripple wavelength are impact angle and ripple amplitude, both of which are dependent on grain size and wind speed, but he could see no obvious reason why ripple wavelength should be dependent on the mean saltation pathlength. His observations on ripple development to an equilibrium size and spacing have been confirmed experimentally by the wind tunnel experiments of Seppälä and Linde (1978) and

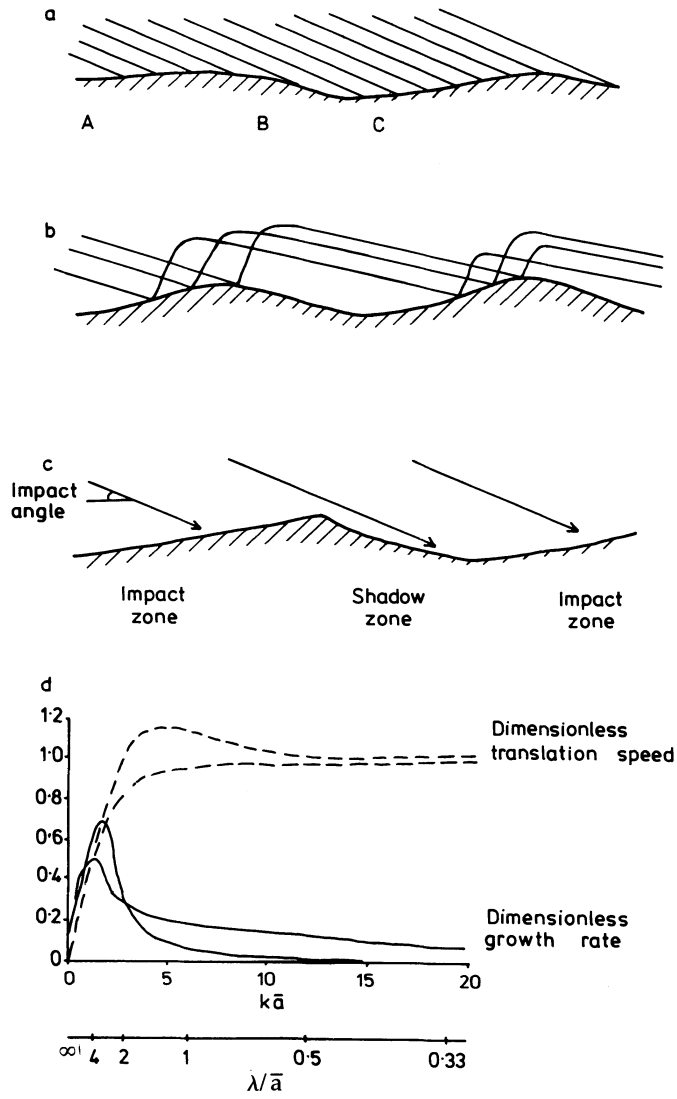

Figure 18.5 Models for wind ripple formation. (a, b) Variation in impact intensity over a perturbation in the bed (after Bagnold 1941). Note higher impact intensity in zone A–B compared with B–C. (c) Alternation of impact and shadow zones on a developing wind ripple (after Sharp 1963). (d) Growth and movement of developing bed perturbations that evolve to wind ripples (after Anderson 1987).

Walker (1981) and by computer simulations of sediment surfaces (Werner 1988).

Anderson (1987) has provided a rigorous model for ripple development based on experimental data and numerical simulations of sand beds. Recent experimental and theoretical work on aeolian saltation (see Chapter 17) has demonstrated that saltating sand consists of two populations: (a) long trajectory, high impact energy 'successive saltations' and (b) short trajectory, low impact energy 'reptations'. There is a wide distribution of saltation trajectories with typical pathlengths that are much longer than ripple wavelengths, and a low range (1 to 2°) of impact angles. This suggests that the high impact energy grains do not contribute directly to ripple formation, as Bagnold hypothesized, but drive the reptation process. Using a simplified model of aeolian saltation, Anderson (1987) was able to show that a flat bed is unstable to infinitesimal variations in bed elevation, giving rise to spatial variations in the mass flux of reptating grains. Convergence and divergence of mass flux rates result in the growth of

ripples, with the fastest growing ripples having a wavelength about six times the mean reptation distance (Fig. 18.5d). As reptation lengths increase with wind friction speed, ripple wavelength should increase as well. This is in good agreement with the wind tunnel data of Seppälä and Linde (1978) and Walker (1981).

Ripple wavelengths therefore appear to scale with grain transport distance, but it is the reptation length rather than saltation pathlength that is the relevant parameter. However, Werner (1988) has suggested that the self-organization of sand surfaces into ripples is not dependent on a transport length scale. Rather, it results from merging of smaller and larger ripples promoted by statistical fluctuations in the mass flux of reptating grains. A quasi-stable wavelength emerges that is the effect of the sharply decreasing rate of ripple mergers with increasing ripple size.

New models for ripple development indicate that their formation and characteristic dimensions are not related directly to the movement of grains in successive saltation, as Bagnold (1941) hypothesized. Rather, wind ripples are initiated by statistical fluctuations in the flux of reptating grains driven by impacts from a uniform distribution of saltating grains. Once the initial nucleii of the ripple pattern are set up, then the effects of local bed slope on impact intensity and the local reptation mass flux become important, as shown by the wind tunnel experiments of Willetts and Rice (1986), and the pattern becomes self-organizing, probably through merging of ripples in the manner suggested by Werner (1988).

DUNES

DUNE MORPHOLOGY AND MORPHOMETRY

Dunes occur in a variety of morphologic types, each of which displays a range of sizes (height, width, and spacing). Most dune patterns are quite regular, as evidenced by the close correlations that exist between dune height and spacing (Fig. 18.6).

Many different classifications of dune types have been proposed (see Mainguet 1983, 1984 for a list of different schemes). They fall into two groups: (a) those based on the external morphology of the dunes (morphological classifications), and (b) those that imply some relationship of dune type to formative winds or sediment supply (morphodynamic classifications).

The morphological classification of McKee and his co-workers (McKee 1979) groups dunes on the basis of their shape and number of slip faces into five major types: crescentic, linear, reversing, star, and parabolic (Fig. 18.7). In turn, three varieties of each dune type can occur: simple, compound, and complex. Simple dunes are the basic form of each dune type. Compound dunes are characterized by superimposition or juxtaposition of dunes of the same morphological type (e.g. superimposition of smaller crescentic dunes on the stoss side of large crescentic dunes). Complex dunes occur where dunes of two types are superimposed or merged (e.g. crescentic dunes on the flanks of larger linear or star dunes, or linear dunes with star dune peaks). Compound and

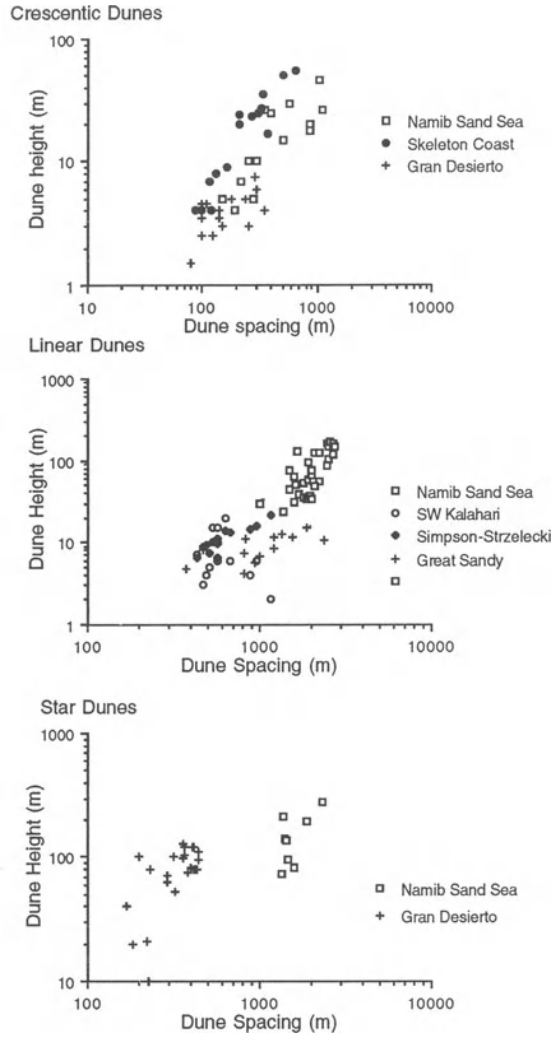

Figure 18.6 Relations between dune height and spacing. Data from author's measurements and Wasson and Hyde (1983b).

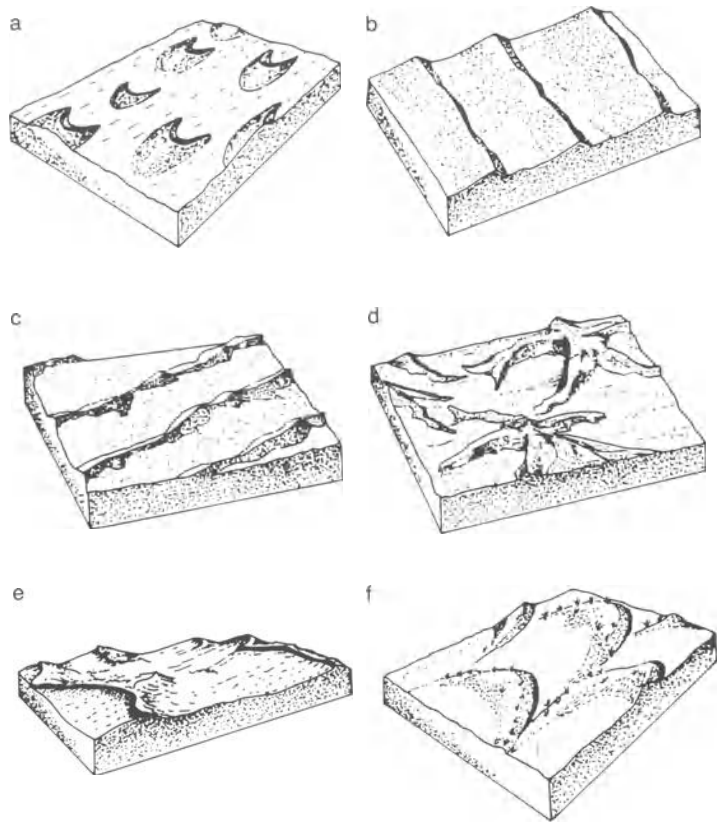

Figure 18.7 Morphologic classification of dunes (modified after McKee 1979): (a) barchans, (b) crescentic ridges, (c) linear, (d) star, (e) reversing, and (f) parabolic.

complex dunes are equivalent to the draa of Wilson (1972), and this term has been applied to all large dunes with superimposed bedforms (Kocurek 1981).

There are many morphodynamic classifications in which dunes are classified by their morphology and relationship to formative winds, especially their alignment relative to the dominant or resultant (vector sum) sand transport direction (e.g. Aufrère 1928, Clos-Arceduc 1971, Wilson 1972, Hunter *et al.* 1983). Thus dunes may be classified as transverse, longitudinal, or oblique, yet studies of dune dynamics (e.g. Tsoar 1983, Lancaster 1989a) show that different parts of the same dune may be simultaneously transverse, oblique, or longitudinal to the transport direction. Other workers (e.g. Mainguet 1983, 1984) have attempted to order dunes by including aspects of their mobility and relationship to sediment budgets and distinguish between erosional types (parabolic dunes, sand ridges) and purely depositional forms (barchanic edifices, transverse chains, linear dunes, and star dunes). One problem with all morphodynamic systems of dune classifications is that they assume a knowledge of how dunes form. As will be seen below, that knowledge is at best incomplete. The subsequent discussion will therefore follow a morphologic classification of dune types.

Crescentic Dunes

The simplest dune types and patterns are those that form in wind regimes characterized by a narrow range of wind directions. In the absence of vegetation, crescentic dunes are the dominant form. Hunter *et al.* (1983) and Tsoar (1986) indicate that this dune type is stable where the directional variability is 15° or less about a mean value. Isolated crescentic dunes or barchans occur in areas of limited sand availability. As sand supply increases, barchans coalesce laterally to form crescentic or barchanoid ridges that consist of a series of connected crescents in plan view (McKee 1966, Kocurek *et al.* 1992).

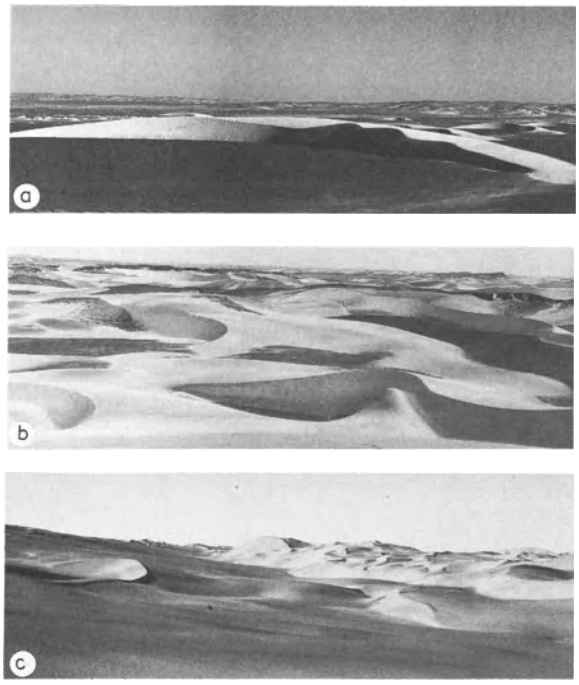

Figure 18.8 Crescentic dunes: (a) barchans on the upwind margin of the Skeleton Coast dunefield, Namibia; (b) simple crescentic dunes, Skeleton Coast dunefield, Namibia; and (c) compound crescentic dunes, Namib sand sea – note two orders of dune spacing, primary dunes and superimposed dunes.

Larger forms with superimposed dunes are termed compound crescentic dunes (e.g. Breed and Grow 1979, Havholm and Kocurek 1988, Lancaster 1989b).

Barchans (Fig. 18.8a) appear to be a stable form in areas of limited sand supply and unidirectional winds, as demonstrated by their ability to migrate long distances with only minor changes of form (e.g. Long and Sharp 1964, Haynes 1989, Hastenrath 1987). They tend to occur in two main areas: (a) on the margins of sand seas (e.g. Smith 1980, Sweet *et al.* 1988), and (b) in sand transport corridors linking sand source zones with depositional areas (e.g. Bagnold 1941, Embabi 1982). Barchans are characterized by an ellipsoidal shape in plan view, with a concave slip face and 'horns' extending downwind. Dune height is typically about one-tenth of the dune width (Finkel 1959, Hastenrath 1967, Embabi 1982). Strongly elongated horns and asymmetric development of barchan plan shapes occur in some areas (e.g. Hastenrath 1967, Lancaster 1982a), and have been attributed to asymmetry in the wind regime or sand supply. In some areas, barchans of this type are transitional to linear dunes (Lancaster 1980, Tsoar 1984).

Crescentic dunes of simple and compound varieties occupy some 10% of the area of sand seas world-wide (Fryberger and Goudie 1981) and occur in all desert regions. The patterns of most crescentic dunes are quite regular, as indicated by the close correlations that exist between dune height and spacing (Fig. 18.6). Most simple crescentic and barchanoid ridges (Fig. 18.8b) are between 3 and 10 m high, with a spacing of 100 to 400 m. Typical areas of simple crescentic ridges occur at White Sands, New Mexico (McKee 1966), Guererro Negro, Baja California (Inman *et al.* 1966), and in the Skeleton Coast dunefield in the northern Namib (Lancaster 1982a).

Compound crescentic dunes (Fig. 18.8c) occupy some 20% of the area of sand seas world-wide. They usually consist of a main dune ridge 20 to 50 m high with a spacing of 800 to 1200 m. Smaller crescentic ridges 2 to 5 m high and 50 to 100 m apart are superimposed on their upper stoss slopes and crestal areas. Compound crescentic dunes are typified by those along the western edge of the Namib sand sea (Lancaster 1989b), and the Algodones Dunes of California (Norris and Norris 1961, Havholm and Kocurek 1988). Other major areas of this dune type occur in the United Arab Emirates, the Takla Makan, Tunisia, KaraKum, and the Gran Desierto (Breed *et al.* 1979).

Linear Dunes

Linear dunes are characterized by their length (often more than 20 km) straightness, parallelism, and regular spacing, and high ratio of dune to interdune areas. Lancaster (1982b) estimated that 50% of all dunes are of linear form, with the percentage varying between 85 and 90% for areas of the Kalahari and Simpson–Strzelecki Deserts to 1 to 2% for the Ala Shan and Gran Desierto sand seas. Linear dunes are the dominant form in sand seas in the Southern Hemisphere and in the southern and western Sahara.

Many linear dunes consist of a lower gently sloping plinth, often partly vegetated, and an upper crestal area where sand movement is more active. Slip faces develop on the upper part of the dune, their orientation depending on the winds of the season. The average form of the dune may be symmetrical with an approximately triangular profile, but in each season its profile tends to an asymmetric form with a convex stoss slope and a well-developed lee face (Tsoar 1985). Several

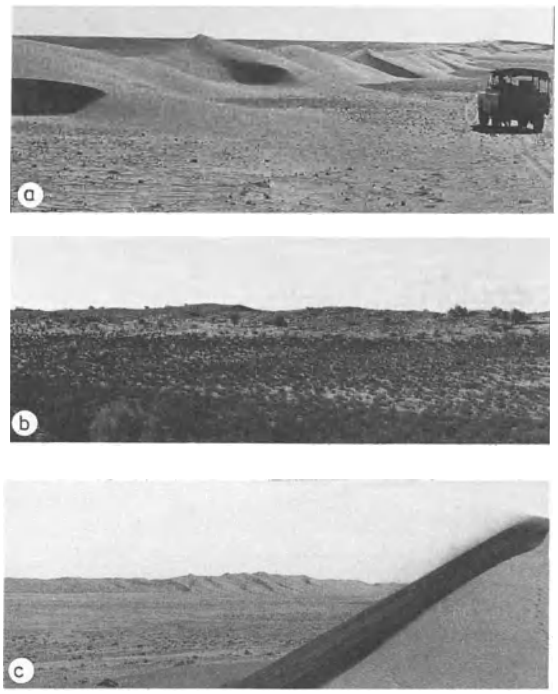

Figure 18.9 Linear dunes: (a) simple linear dunes, Namib sand sea, showing regularly repeated peaks and saddles; (b) vegetated simple linear dunes, south-western Kalahari; and (c) complex linear dunes, Namib sand sea.

varieties of linear dunes are recognized (Fig. 18.9). Simple linear dunes are of two types: the long, narrow, straight, partly vegetated linear dunes of the Simpson and Kalahari Deserts (the vegetated linear dunes of Tsoar 1989), and the more sinuous seif-type dunes found in Sinai (Tsoar 1983), parts of the eastern Sahara, and along the west edge of the Algodones dunefield. Compound linear dunes consist of two to four seif-like ridges on a broad plinth and are typified by those in the southern Namib sand sea (Lancaster 1983). Large (50 to 150 m high, 1 to 2 km spacing) complex linear dunes with a single sinuous main crestline with distinct star-form peaks and crescentic dunes on their flanks (Lancaster 1983) occur in the Namib and Rub al Khali sand seas. Wide (1 to 2 km) complex linear dunes with crescentic dunes superimposed on their crests occur in the eastern Namib, parts of the Wahiba Sands (Warren 1988), and the Akchar sand sea of Mauritania (Kocurek *et al.* 1992).

The origins of linear dunes and their relationship to formative wind directions have been the subject of considerable controversy, as reviewed by Lancaster (1982b) and Tsoar (1989). A widely held view is that linear dunes form parallel to prevailing or dominant wind directions (e.g. Folk 1970, Glennie 1970, Wilson 1972). Their parallelism and straightness are believed to result from roller vortices in which helicoidal flow sweeps sand from interdune areas to dunes (e.g. Hanna 1969, Wilson 1972). However, there are inconsistencies between the spacing of many dunes and the reported dimensions and stability of helical roll vortices (Lancaster 1982b, Livingstone 1986), which would have to be positioned at exactly the same place at successive wind episodes in order to allow dunes to grow and extend (Greeley and Iversen 1985). The only observational evidence for helical roll vortices in dune areas comes from studies of tethered kites in the Simpson Desert, Australia (Tseo 1990).

There is, however, a substantial body of empirical evidence that indicates that linear dunes form in bidirectional wind regimes and extend approximately parallel to the resultant direction of sand transport. Correlations between dune types and wind regimes (e.g. Fryberger 1979), studies of internal structures (McKee and Tibbitts 1964, McKee 1982) and detailed process studies on linear dunes (Tsoar 1983, Livingstone 1986, 1989) support such a view.

Star Dunes

Star dunes (Fig. 18.10) are the largest dunes in many sand seas and may reach heights of more than 300 m. They contain a greater volume of sand than any other dune type (Wasson and Hyde 1983a) and appear to occur in areas that represent depositional centres in many sand seas (Mainguet and Callot 1978, Brookfield 1983, Lancaster 1983). Star and related reversing dunes comprise 9 to 12% of all dunes in the Namib, Gran Desierto, and central Asian sand seas. They are absent from the Australian deserts, from the Kalahari, and from India, but comprise 40% of dunes in the Grand Erg Oriental.

Star dunes are characterized by a pyramidal shape, with three or four arms radiating from a central peak and multiple avalanche faces. Each arm has a sharp sinuous crest, with avalanche faces that alternate in aspect as wind directions change. The arms may not all be equally developed and many star dunes have dominant or primary arms on a preferred orientation. The upper parts of many star dunes are very steep with slopes at angles of 15 to 30°; the lower parts consist of a broad, gently sloping (5 to 10°) plinth or apron. Small crescentic or reversing dunes may be superimposed on the lower flank and upper plinth areas of star dunes.

Star dunes have been hypothesized to form at the

Figure 18.10 Star dunes, Gran Desierto sand sea. Note preferred east–west orientation of major dune arms and small reversing dunes in middle distance.

centres of convection cells, at the nodes of stationary waves in oscillating flows, above rock hills, or at the nodal points of complex dune alignment patterns created by crossing or converging sand transport paths (Lancaster 1989a). Comparisons between the distribution of star dunes and wind regimes suggest that they form in multidirectional or complex wind regimes (Fryberger 1979). A strong association between the occurrence of star dunes and topographic barriers has also been noted (Breed and Grow 1979). Topography may modify regional wind regimes to increase their directional variability, as in the Erg Fachi Bilma and Namib (Mainguet and Callot 1978, McKee 1982, Lancaster 1983), or create traps for sand transport, as at Kelso Dunes (Sharp 1966) and Great Sand Dunes (Andrews 1981).

Parabolic Dunes

Parabolic dunes (Fig. 18.11), common in many coastal dunefields, have a restricted distribution in arid region sand seas. The only major sand sea with significant areas of this dune type is in the Thar Desert of India (Verstappen 1968, Breed and Grow 1979, Wasson *et al.* 1983). Small areas of parabolic dunes occur in the south-western Kalahari, Saudi Arabia (Anton and Vincent 1986), north-east Arizona (Hack 1941), and at White Sands (McKee 1966).

Parabolic dunes are characterized by a U shape with trailing partly vegetated parallel arms 1 to 2 km long and an unvegetated active 'nose' or dune front 10 to 70 m high that advances by avalanching. In the Thar Desert, compound parabolic dunes with shared arms occur in some areas and result from merging or shingling of several generations of dunes with different migration rates (Wasson *et al.* 1983). The conditions under which parabolic dunes form are not well known. They seem to be associated with the presence of a moderately developed vegetation cover, and with unidirectional wind regimes. Downwind, some parabolic dunes are transitional to crescentic dunes (Anton and Vincent 1986).

Zibars and Sand Sheets

Not all aeolian sand accumulations are characterized by dunes. Low relief sand surfaces such as sand sheets are common in many sand seas and occupy from as little 5% of the area of the Namib sand sea to as much as 70% of the area of Gran Desierto

Figure 18.11 Parabolic dunes, St Anthony dunefield, Snake River Plains Idaho. Photography by R. Greeley.

(Lancaster *et al.* 1987). Fryberger and Goudie (1981) estimate that 38% of aeolian deposits are of this type. Many sand sheets and interdune areas between linear and star dunes are organized into low rolling dunes, without slipfaces, known as zibars (Holm 1960, Warren 1972, Tsoar 1983, Nielson and Kocurek 1986) with a spacing of 50 to 400 m and a maximum relief of 10 m. Typically zibars are composed of coarse sand, and occur on the upwind margins of sand seas.

Sand sheets develop in conditions unfavourable to dune formation (Kocurek and Nielson 1986). These may include a high water table, periodic flooding, surface cementation, coarse-grained sands, and presence of a vegetation cover all of which act to limit sand supply for dune building. Coarse grains armour the surface of sand sheets in the eastern Sahara (Bagnold 1941, Breed *et al.* 1987). Sand sheets in the north-western Gran Desierto have developed in conditions of a sparse vegetation cover which is insufficient to prevent sand transport taking place, but sufficient to cause divergence and convergence of airflow around individual plants in the manner suggested by Ash and Wasson (1983) and Fryberger *et al.* (1979) giving rise to localized deposition by wind ripples and shadow dunes.

DUNE DYNAMICS

The initiation, growth, and equilibrium morphology of all dunes are determined by their sediment budget, defined as the balance between local erosion and deposition, summed for the dune as a whole. Principles of sediment continuity require that the mass or volume of sediment is conserved (Middleton and Southard 1984) so that

$$\partial h/\partial t = -\partial q/\partial x \qquad (18.1)$$

where h is the local bed elevation, q is the local volumetric sediment transport rate in the direction x and t is time. Changes in sand transport rates in time or space therefore control dune morphology. In turn, the developing bedforms exert a strong control on local transport rates through form–flow interactions and secondary flow circulations, leading to a dynamic equilibrium between dune morphology and local airflow.

Dune Initiation

Dune initiation is poorly understood and little studied but is of major importance in understanding how dunes and dune patterns develop. It involves localized deposition leading to bedform nucleation, which will then fix a pattern that can propagate downwind (Wilson 1972). Reductions in the local sediment transport rate can occur through convergence of streamlines, by changes in surface roughness (e.g. vegetation, increased surface particle size) that decrease local shear stress, or by variations in microtopography (slope changes, relict bedforms).

Wind tunnel experiments (Bagnold 1941) suggest that surfaces of mixed grain size (sand and 4-mm pebbles) act as reservoirs in which sand is stored during periods when winds are just above the threshold shear velocity u_{*t}, but is removed by stronger winds. Bagnold observed that a sand patch thins and extends downwind in gentle winds ($1.1u_{*t}$), but thickens and extends upwind in strong winds ($4u_{*t}$) provided that a sufficient supply of sand is available. He explained his observations in terms of differences in aerodynamic roughness z_0 and u_{*t} between the surfaces. During periods of gentle winds shear velocity u_* is less than u_{*t} for pebbles but greater than that for sand because z_0 for the pebble surface is greater than z_0 for a sand surface. Transport is therefore possible only on the sand surface. On the lee side of the sand patch, the increase in z_0 as the surface changes from sand to pebbles gives rise to deposition, and the sand patch extends downwind. During periods of strong winds u_* exceeds u_{*t} for pebbles and u_{*t} for sand, so material is eroded from the rough surface. However, the increased quantity of sand in saltation extracts momentum from the wind such that deposition occurs on the sand patch and at its upwind margin, extending it upwind and increasing its thickness. Bagnold (1941) also observed that a strong sand-transporting wind has a transverse instability such that sand tends to deposit in longitudinal strips 1 to 3 m wide and 1 to 2 cm thick. He suggested that

these strips could be the nuclei for the initiation of linear dunes.

Recent work by Greeley and Iversen (1987) has shown that for winds of a given speed at height z, values of u_* are greater on aerodynamically rougher surfaces. Transport rates may be larger or smaller on the rougher surface, depending on the relative values of u_*, the ratio of u_{*t} for the smooth surface to u_{*t} for the rough surface, and the ratio between particle diameter and z_0. They suggested that transport takes place only on smoother surfaces at low wind speeds; at intermediate speeds transport occurs on both surfaces, with greater transport on the smooth surface. However, at high wind speeds, transport rates are higher on the rough surface, implying that sand patches will erode at low and intermediate wind speeds, but accrete at high wind speeds. This is an alternative explanation for the phenomena observed by Bagnold, but Greeley and Iversen do not take into account the increase in z_0 that occurs when saltation takes place (saltation roughness), and they deal with surfaces that are much rougher (alluvial fans and lava flows) than those typical of areas in which dunes are initiated.

When winds pass from surfaces with one roughness to surfaces with another roughness, the wind profile changes and requires some distance to reach equilibrium with the new surface (Blom and Wartena 1969). An internal boundary layer develops downwind from the edge of the change in roughness and gradually diffuses up into the pre-existing boundary layer. The leading edge of a sand patch will therefore be a zone of fluctuating flow and zones of alternate erosion and deposition. Bagnold (1941) observed in the wind tunnel that this zone extended for 4 to 6 m, which he suggested was the minimum size for a true dune.

Field studies of the initiation and early development of dunes are rare. Cooper (1958) and Jäkel (1980) described the development of barchans and transverse ridges from thin sand patches with no flow separation in their lee to small dunes with lee-side flow separation, but they did not document how these forms were initiated. Kocurek *et al.* (1992) have documented in great detail the initiation and growth of dunes at Padre Island, Texas. Nucleation of bedforms takes place where wind speeds are reduced by 37 to 86% of upwind values due to changes in aerodynamic roughness or microtopography as a result of patches of grass, erosional depressions, relict dune topography, or vegetated sand ridges (coppice dunes). Not all sites of initial deposition develop into dunes, but growth is favoured by a greater initial amount of deposition and enhanced local sand supply. They recognized five stages of dune initiation and development (Fig. 18.12) with a progressive evolution of the lee face and bedform-induced secondary flow expansion and separation: (a) irregular patches of dry sand a few centimetres high, (b) 0.1 to 0.35-m-high protodunes with wind ripples on all surfaces, (c) 0.25 to 0.40-cm protodunes with grainfall on lee slopes, (d) 1 to 1.5-m-high barchans with grainflow, and (e) 1 to 2-m-high crescentic ridges. The developing dunes were characterized by a reverse asymmetry (steeper stoss slope) in stage (b) similar to that noted by Cooper (1958). The change from flow expansion to flow separation came as lee slopes exceeded 22°. Subsequent evolution of the dunefield mainly takes place by repeated mergings, splittings, lateral linking, and cannibalization of dunes. Dune growth is at the expense of interdune areas and the pattern evolves so that the height:spacing ratio tends toward 1:20, a figure that is common in many areas of crescentic dunes.

Airflow Over Dunes

As dunes grow, they project into the atmospheric boundary layer, resulting in compression of streamlines at the crest and a corresponding increase in wind speed and shear stress (Fig. 18.13). This is of fundamental importance in understanding the morphology of all dunes. In multidirectional wind regimes, the nature of interactions between dune form and airflow changes as winds vary direction seasonally, and major lee-side secondary flow patterns become important in determining dune morphology and dynamics.

Increases in wind velocity on the stoss slopes of dunes were predicted by Bagnold (1941) and Wilson (1972) and measured but not commented upon by Howard *et al.* (1978). Studies by Lancaster (1985, 1987), Tsoar (1985) and Mulligan (1988) have shown that the magnitude of the velocity increase is represented by the speed-up ratio Δs or amplification factor Az represented by U_2/U_1 where U_2 is the velocity at the dune crest and U_1 is the velocity at the upwind base of the dune. Typical values for Az range between 1.1 and 2.0 and vary with dune height and aspect ratio (Lancaster 1985, Tsoar 1985) (Fig. 18.14). On Namib linear dunes, amplification factors also vary directly with wind direction, being greatest when the winds are blowing perpendicular to the dunes. Similar velocity increases have been measured over small hills (see Taylor *et al.* 1987 for a recent review). The rate of velocity increase on the stoss slope is not linear (Fig. 18.15a) and follows the

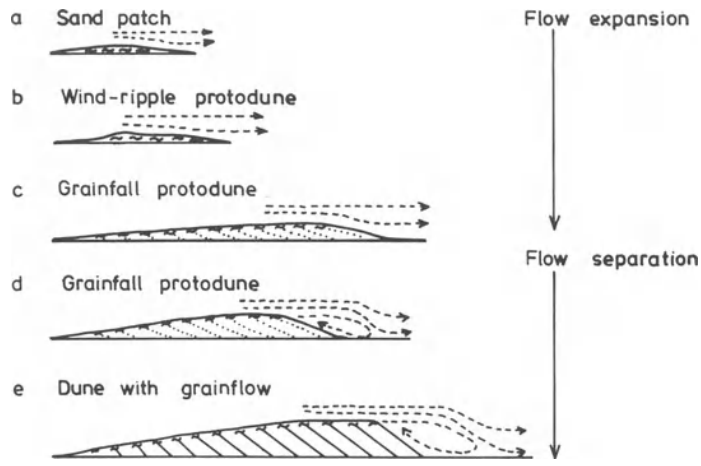

Figure 18.12 Stages of dune development at Padre Island, Texas (after Kocurek *et al.* 1992).

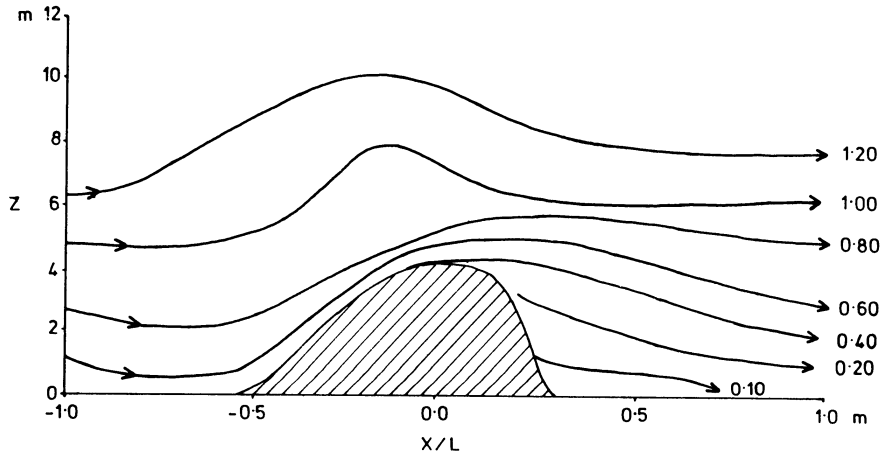

Figure 18.13 Airflow over an isolated barchan dune, Salton Sea, California. Stream line wind speeds are normalized with respect to an anemometer at 5 m height upwind of the dune. Note flow compression on upper stoss slope and flow expansion in lee.

slope of the dune closely, decreasing toward the crest (Tsoar 1985, Mulligan 1988).

As Bagnold (1941) and Watson (1987) have pointed out, the equilibrium morphology of dunes is controlled by the pattern of wind shear velocity or friction speed u_* over the dune because it is u_* that determines transport rates. Velocity profiles measured on the stoss slopes of dunes are not logarithmic, so rigorous derivation of u_* from profile parameters is not possible. Estimates of u_* by Mulligan (1988) and Lancaster (1987) show that values of friction speed increase by a factor of three from upwind of the dune to a maximum on the upper stoss slope of the dune (Fig. 18.15b). This confirms the model predictions and experimental data of Lai and Wu (1978) and McLean and Smith (1986) that indicate a shear stress maximum on the upper stoss slope. The magnitude of local friction speed appears to be related to the overall wind speed and to local slope (Lancaster 1987), such that on star and linear dunes u_* values decrease as the dune form comes into equilibrium with a new wind season.

Increases in wind velocity and friction speed on the stoss slopes of dunes lead to an increase in

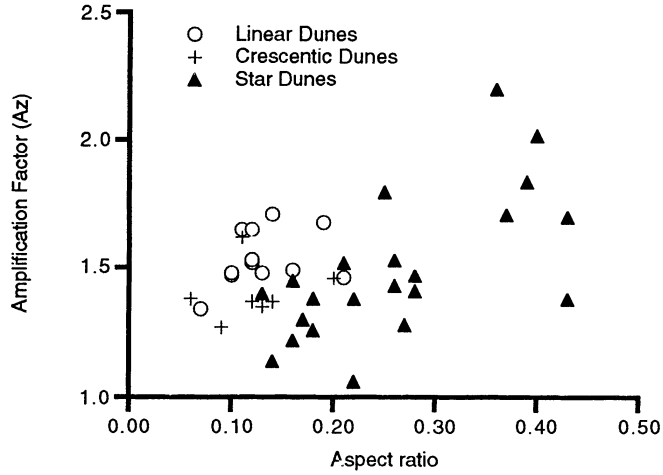

Figure 18.14 Relations between velocity increase (amplification factor) and dune aspect ratio *h*/*L*. Data from Namibian and Gran Desierto dunes.

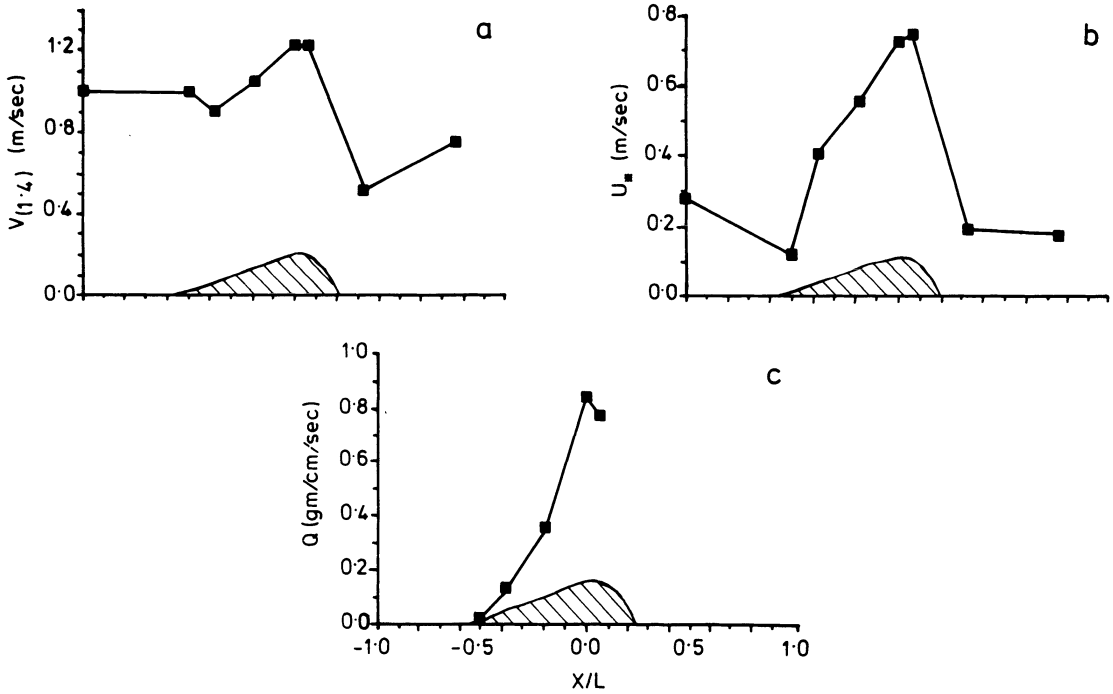

Figure 18.15 Patterns of (a) wind speed (normalized with respect to upwind anemometer); (b) estimated friction speed u_*; and (c) potential sand transport rate (calculated using Bagnold formula) over an isolated barchan dune, Salton Sea, California.

transport rates toward the crest. Differences between sand transport rates at the base and crest of the stoss slope are at a maximum when incident winds are just above threshold velocity and decrease as the overall wind speed increases (Fig. 18.16) (Lancaster 1985). Preliminary studies by Lancaster (1987) show an exponential increase in sediment transport rates on the stoss slope of an isolated barchan in a period of strong winds (Fig. 18.15c). In periods of low wind speeds, sand transport occurs only in crestal areas, whereas in periods of strong winds all of the dune is mobile. This phenomenon is

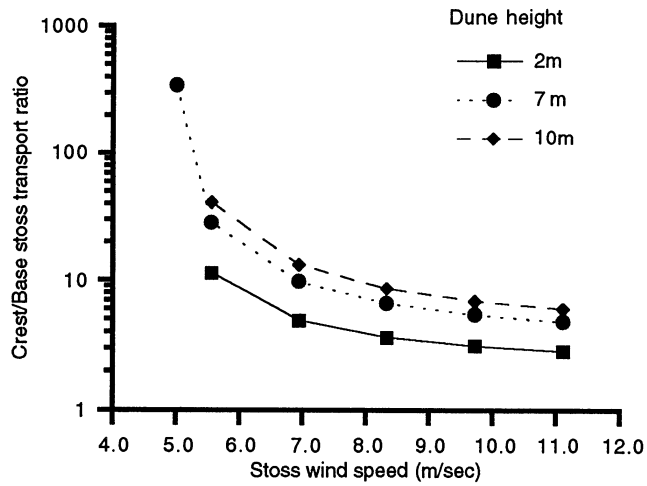

Figure 18.16 Ratio between calculated potential sand transport rate (calculated using Bagnold formula) at the base and crest of stoss slopes of 2-, 7-, and 10-m-high crescentic dunes (after Lancaster 1985).

particularly important for large dunes and suggests that the dunes may be lowered in periods of low wind speeds but grow in periods of stronger winds.

In the lee of the crest, wind velocities and transport rates decrease rapidly as a result of flow expansion between the crest and brink, and flow separation occurs on the avalanche face. All sand transported over the crest of crescentic dunes is deposited, so that they are typically 'sand trapping' bedforms (Wilson 1972). As a result, their movement can be described by the equation

$$c = Q/yh \qquad (18.2)$$

where c is the migration rate, Q is the bulk volumetric sand transport rate, y is the bulk density of sand, and h is dune height (Bagnold 1941). An inverse relationship between dune height and migration rate (Fig. 18.17) has been determined by numerous investigators (e.g. Finkel 1959, Long and Sharp 1964, Hastenrath 1967, Tsoar 1974, Endrody-Younga 1982, Embabi 1982, Slattery 1990).

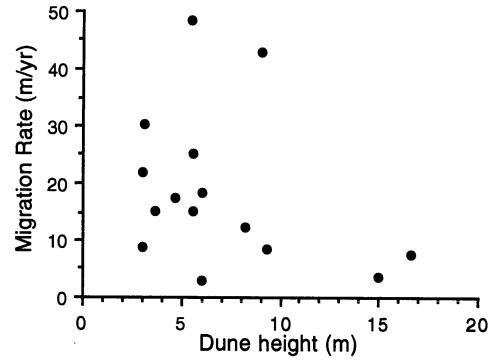

Figure 18.17 Relations between crescentic dune migration rate and dune height. Scatter in points in y direction is a function of the overall wind energy at the different localities. Data are mean values calculated from Finkel (1959), Long and Sharp (1964), Hastenrath (1967), Tsoar (1974), Embabi (1982), Endrody-Younga (1982), Haynes (1989), and Slattery (1990).

Sweet and Kocurek (1990) suggested that there are three types of flow in the lee of dunes: (a) separated, (b) attached, and (c) attached deflected. The nature of lee-side flow is controlled by the dune shape (aspect ratio), the incidence angle between the primary wind and the crestline, and the stability of the atmosphere (Fig. 18.18). Wind speeds in the lee of crescentic dunes are typically very variable and only 0.3 to 0.9 of those at adjacent crests. The existence of eddies and reversed flow directions is controversial, due in part to the considerable problems of visualizing such flows. They were discounted by Cooper (1958) and Sharp (1966), but observations by Hoyt (1965), Warren and Knott (1983) and Sweet and Kocurek (1990) support their existence. Relatively high lee-side wind velocities are associated with low aspect ratio dunes and oblique primary winds. The degree of wind deflection is in all cases a cosine function of the incidence angle between the crestline and the primary wind. High aspect ratio dunes and transverse flows result in true flow separation and a weak back eddy. The width of the separation zone for dunes that are truly transverse to the flow is controlled by the wind speed at

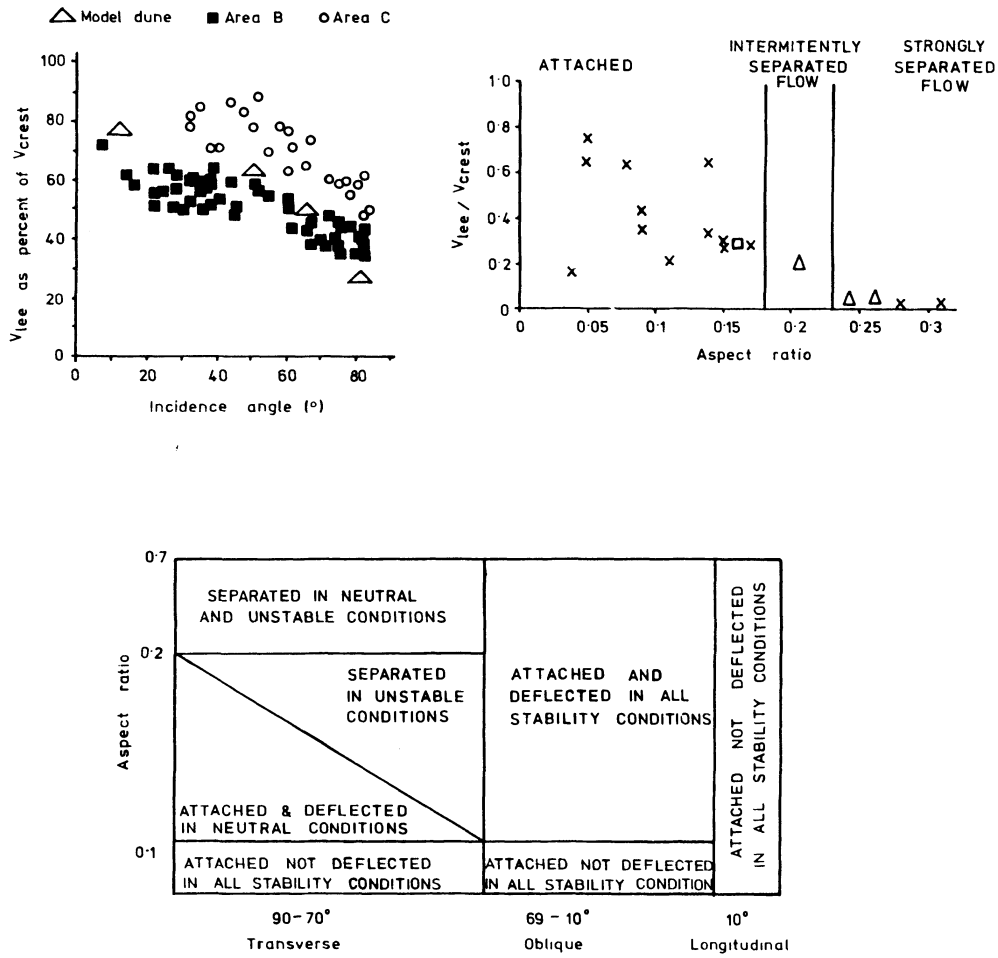

Figure 18.18 Relations between lee-side flow speed, incidence angle, and aspect ratio for crescentic dunes (after Sweet and Kocurek 1990).

the crest, dune aspect ratio, and atmospheric stability, but never exceeds two dune heights (Sweet and Kocurek 1990). However, Lancaster (1987, 1989b) noted that wind velocities in the lee of isolated crescentic dunes do not recover to upwind values before 10 to 15 dune heights.

Airflow in the lee of linear and star dunes is complex, especially where the crestline is sinuous. Flow separation occurs at the crest, but when the flow is oblique to the crestline a helical eddy develops on the lee side and transports sand along the dune (Tsoar 1983). This eddy covers the whole of the lee side on simple (5 to 10 m high) linear dunes, but extends for only 10 to 20% of the height of large (50 to 150 m high) complex linear dunes (Livingstone 1986) and of 40-m-high star dunes in the Gran Desierto (Lancaster 1989a) (Fig. 18.19). The oblique flow is deflected along the lee slope parallel to the dune crest (Figs 18.19 and 18.20), with the degree of deflection being inversely proportional to the incidence angle between the crestline and the primary wind. When the angle between the dune and the wind is less than 40° the velocity of the deflected wind is greater than that at the crest and sand is transported along the dune (Tsoar 1983, Nielson and Kocurek 1987, Lancaster 1989a). When winds are at more than 40° to the crestline the velocity of the deflected wind is reduced, giving rise to lee-side deposition. Changes in the local incidence angle between primary winds and a sinuous dune crest result in a spatially varying pattern of deposition and erosion (Fig. 18.21). Deposition dominates where winds cross the crestline at angles approaching 90°, and erosion or along-dune trans-

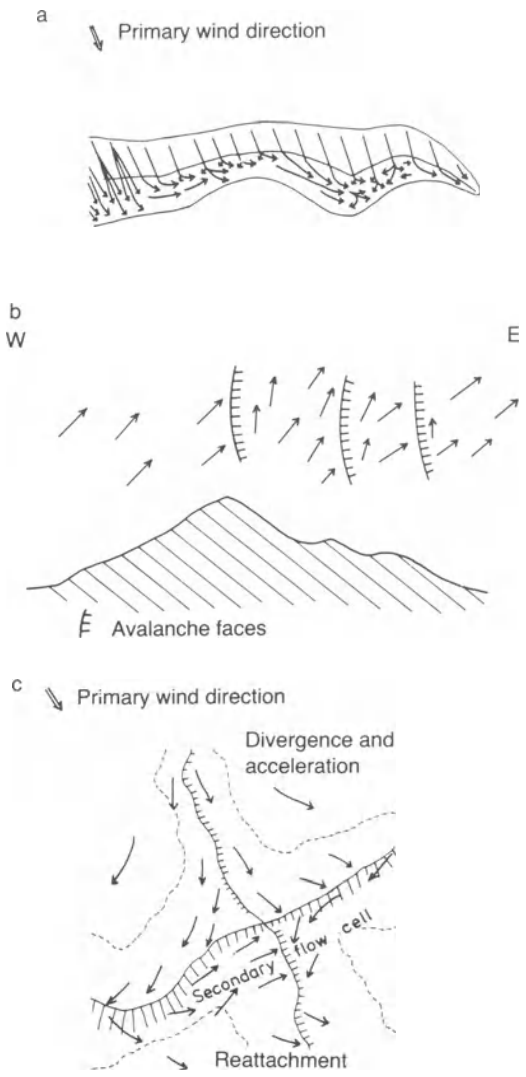

Figure 18.19 Patterns of wind direction on (a) simple linear dune (after Tsoar 1983), (b) complex linear dune (after Lancaster 1989b), and (c) star dune (after Lancaster 1989a).

port occurs where incidence angles are less than 40° (Tsoar 1983). Interactions between winds from different directions and the pre-existing dune form give rise to a series of peaks and saddles that migrate down the dune (Tsoar 1983). On large linear and star dunes (Fig. 18.19), lee slope airflow reverts to the primary direction on the plinth (Livingstone 1986, Nielson and Kocurek 1987, Lancaster 1989a). Its velocity, however, may continue to decrease so that sand is transported from Namib linear dunes only in very strong winds (Lancaster 1989b).

Figure 18.20 Along-dune transport on lee of star dune.

Models and field observations of subaqueous bedforms (McLean and Smith 1986) indicate that the redevelopment of an attached boundary layer in the lee of dunes may be a major control of dune spacing. At the point of flow reattachment, wind speed and shear stress (and hence sand transport rates) are at a minimum. Downwind from this point, an internal boundary layer develops below the wake region created by flow separation at the crest (Fig. 18.22). This internal boundary layer adjusts to the velocity of the wake region, which increases downwind due to the transfer of momentum from the flow above it. In the absence of another dune downwind, the shear stress at the bed, and hence transport rate, increases asymptotically to an equilibrium value downwind of the reattachment zone (Fig. 18.23). McLean and Smith (1986) suggest that the point at which the shear stress maximum is reached defines the position of the next bedform downwind. If this model is correct, and comparisons with field data suggest that it does represent flow over subaqueous bedforms accurately, then dune spacing may be determined by some combination of average wind speed conditions and overall bedform size (and hence sand supply). No field verification of the model has been carried out for an aeolian dune. Such an investigation would appear to offer considerable promise for understanding the fundamentals of aeolian dune spacing.

Erosion and Deposition Patterns on Dunes

Bagnold (1941) and Allen (1968) have argued that the amount of erosion and deposition occurring on a dune surface is proportional to the slope angle and the rate of advance of that part of the dune. Thus

$$\partial q/\partial x = yc\tan\alpha \qquad (18.3)$$

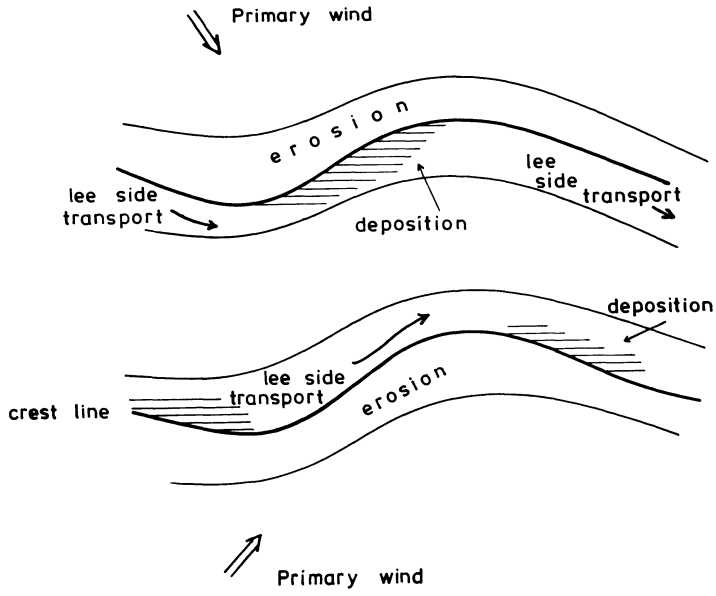

Figure 18.21 Patterns of erosion and deposition on a sinuous linear dune (after Tsoar 1983).

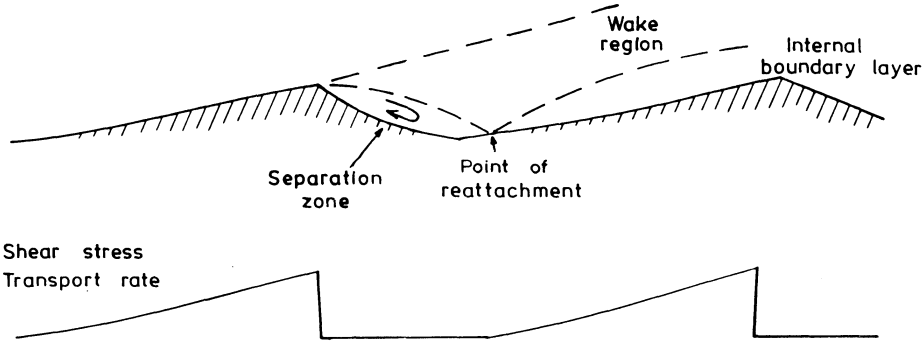

Figure 18.22 Airflow and shear stress patterns in the lee of a transverse dune (after McLean and Smith 1986).

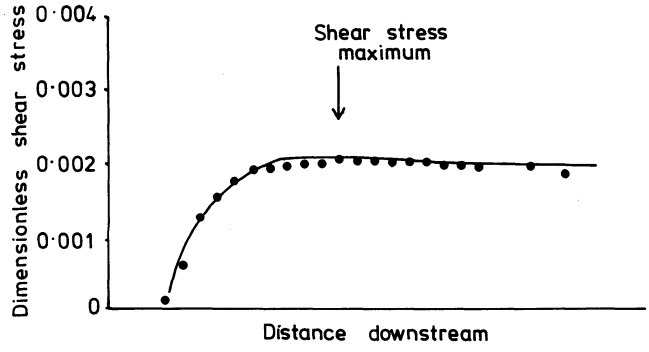

Figure 18.23 Shear stress maximum down-current from an isolated step (after McLean and Smith 1986). Next bedform may develop as shear stress and transport rates decrease after this position.

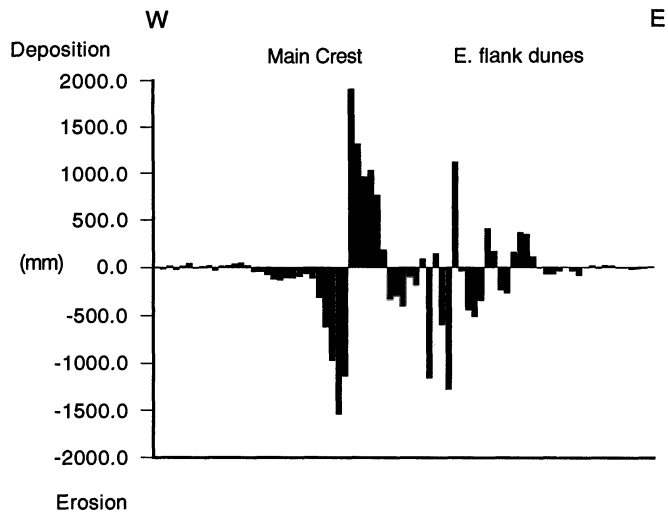

Figure 18.24 Patterns of annual net erosion and deposition across a Namib complex linear dune. Primary wind is oblique to the dune from the south-south-west to the south-west.

where $\partial q/\partial x$ is the rate of sand removal or deposition per unit area at any point, y is the bulk density of dune sand, c is the rate of advance of the dune, and α is the slope angle. Thus there will be no erosion at the dune crest; and when $\tan\alpha$ is negative, as on lee slopes, $\partial q/\partial x$ is also negative and thus deposition will occur. However, this relationship is a purely geometric one, and does not consider the effects of changing wind velocities and sand transport rates over the bedform on erosion or deposition rates or on the rate of advance of the dunes.

Following the requirements of sediment continuity, increases in shear stress and transport rates toward the crest indicate that the stoss slopes of all crescentic dunes are erosional. Downwind, the wind has to transport an increasing amount of sand eroded from the dune slope. This in turn requires that wind velocities and surface shear stress should change to increase transport rates proportionately. If the amount of sand in transport exceeds the capacity of the wind to transport it, deposition will occur, leading to adjustment of dune form (increasing dune steepness) and, hence, of local wind speed and transport rates. There is thus a high degree of interaction between the shape of the dune, the amount of change in wind velocities and sand transport rates and the rate and pattern of erosion or deposition (Tsoar 1985, Lancaster 1985, 1987). The shape of the stoss profiles of dunes thus appears to be adjusted to maintain a dynamic equilibrium between the rate of erosion and the increase in velocity required to keep an ever increasing amount of sand in transport. The shape of simple dunes in unidirectional winds can be evaluated using the sediment continuity equation (Fredsoe 1982):

$$\partial h/\partial t = -\partial q/\partial x \qquad (18.1)$$

Each dune is migrating at a rate Q_B given by

$$Q_B = q_c/H \qquad (18.4)$$

where q_c is the volumetric sediment transport rate at the dune crest and H is the height of the dune. Combining equations 18.1 and 18.4 (Fredsoe 1982) gives

$$h/H = q/q_c$$

It is possible to estimate q for any point on the dune using the data on velocity amplification, and from this to evaluate the shape of transverse bedforms which will be in equilibrium with a given wind velocity. Lancaster (1985) suggested that at low wind velocities dunes tend to develop rather steeper profiles compared with those developed at high velocities. Transverse dune ridges become broader and more rounded as wind velocities increase, in a similar manner to subaqueous bedforms (Fredsoe 1982).

Measurements of erosion and deposition on linear, reversing, and star dunes show that they consist of a crestal area where erosion and deposition rates are high and a plinth zone in which there is little surface change but considerable throughput of sand (Sharp 1966, Lancaster 1989b, Livingstone 1989) (Fig. 18.24). On Namib linear dunes and Gran

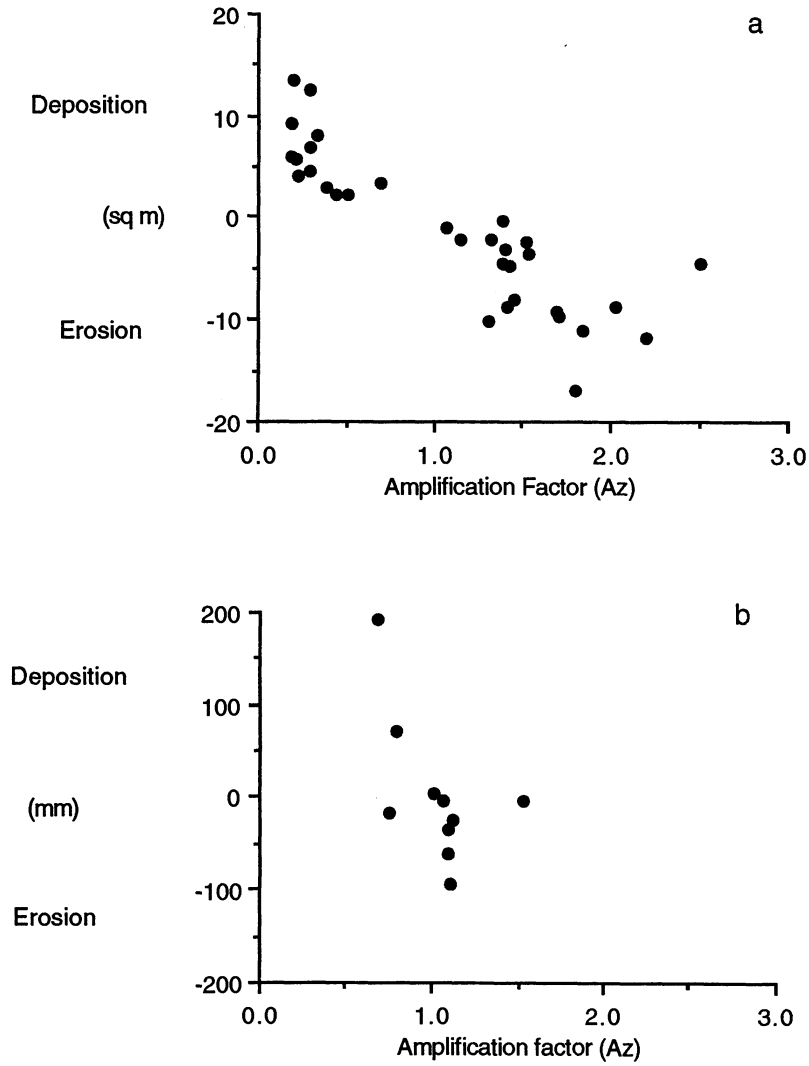

Figure 18.25 Relations between erosion and deposition and amplification factors for (a) Gran Desierto star dunes (erosion and deposition expressed as change in cross-sectional area of that part of the dune), and (b) Namib linear dunes.

Desierto star dunes, over half the total amount of erosion and deposition takes place in the crestal zone (Lancaster 1989a, b, Livingstone 1989), as the position of the crestline varies seasonally over a distance of 3 to 10 m. The observed patterns of erosion and deposition follow changes in wind speed over the dunes and are directly related to the magnitude of velocity and transport rate amplification on dune slopes (Fig. 18.25) through the requirements of sediment continuity. This does not lead to a lowering of the dune crest because this zone is reworked from season to season, and there is very little net change in the position of the crestline. Time-series of erosion and deposition show that the greatest amount of change occurs when winds change direction seasonally. This is the result of winds encountering a dune form that is out of equilibrium with a new wind direction. Field observations and models show that the crestal profiles of linear and star dunes tend toward a convex form similar to that of transverse dunes (Tsoar 1985) and erosion and deposition rates near the crest decline as the dune comes into equilibrium with a new wind direction.

CONTROLS OF DUNE MORPHOLOGY

Sediment Characteristics

There appears to be no evidence for a genetic relationship between the grain size and sorting character of sands and dune type, except that sand sheets and zibar are often composed of coarse, poorly sorted, often bimodal, sands (e.g. Bagnold 1941, Warren 1972, Lancaster 1982a, Kocurek and Nielson 1986, Nielson and Kocurek 1986, Tsoar 1986, Maxwell and Haynes 1989).

Similarly there appears to be no relationship between dune alignment and sediment characteristics, despite the suggestions of Wilson (1972) and Cooke and Warren (1973). In most cases differences in the grain size and sorting characteristics between dune types in the same sand sea can be explained by different source areas and histories (Blount and Lancaster 1990), the relation of dunes to transport pathways, and the nature of sand transport on the dunes themselves (Lancaster 1983).

Wind Regimes

The association of dunes of different morphological types with wind regimes which have different characteristics, especially of directional variability, has been noted by many investigators. Recent work has recognized that the directional variability of the wind regime is a major determinant of dune type. Wind speed, grain size, and vegetation play subordinate roles. The effects of sand supply are uncertain (Wasson and Hyde 1983a, Rubin 1984).

Fryberger (1979) compared the occurrence of each major dune type (crescentic, linear, star) on Landsat images of sand seas with data on local wind regimes, using the ratio between total (DP) and resultant sand flow (RDP) as an index of directional variability. High RDP/DP ratios characterize near unimodal wind regimes, whereas low ratios indicate complex wind regimes. Fryberger (1979) found that the directional variability or complexity of the wind regime increases from environments in which crescentic dunes are found to those where star dunes occur (Fig. 18.26). Crescentic dunes occur in areas where RDP/DP ratios exceed 0.50 (mean RDP/DP ratio 0.68) and frequently occur in unimodal wind regimes, often of high or moderate energy. Linear dunes develop in wind regimes with a much greater degree of directional variability and commonly form in wide unimodal or bimodal wind regimes with mean RDP/DP ratios of 0.45. The trend of linear dunes was observed to be approximately parallel to the resultant direction of sand transport.

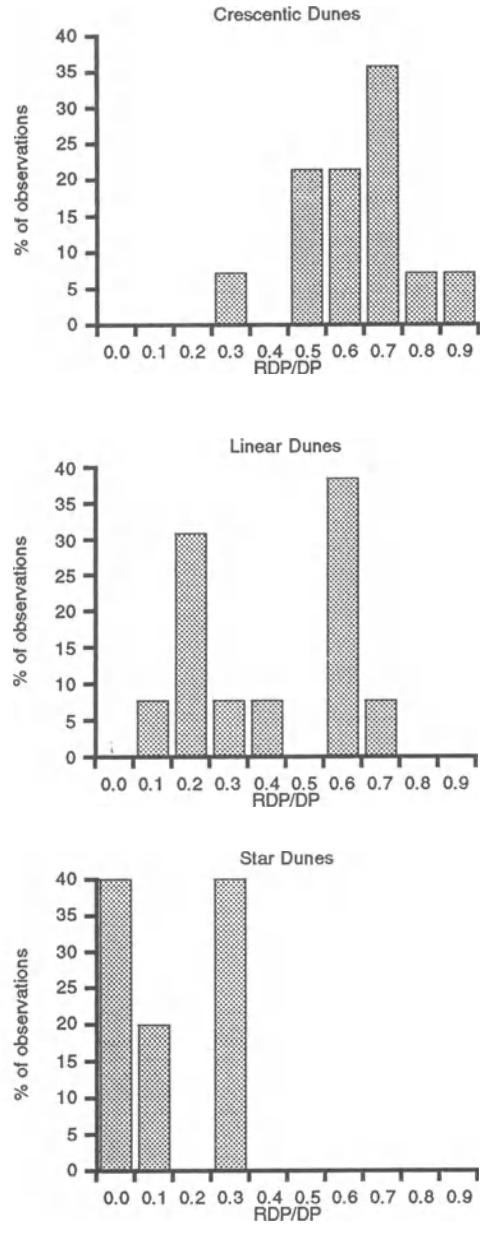

Figure 18.26 Relations between dune type and RDP/DP ratios (data from Fryberger 1979).

Star dunes occur in areas of complex wind regimes with RDP/DP ratios less than 0.35 (mean = 0.19).

Comparison of the distribution of dunes of different morphological types in the Namib sand sea with the information on sand-moving wind regimes (Lancaster 1983, 1989b) tends to confirm Fryberger's hypothesis that there is an increase in the directional

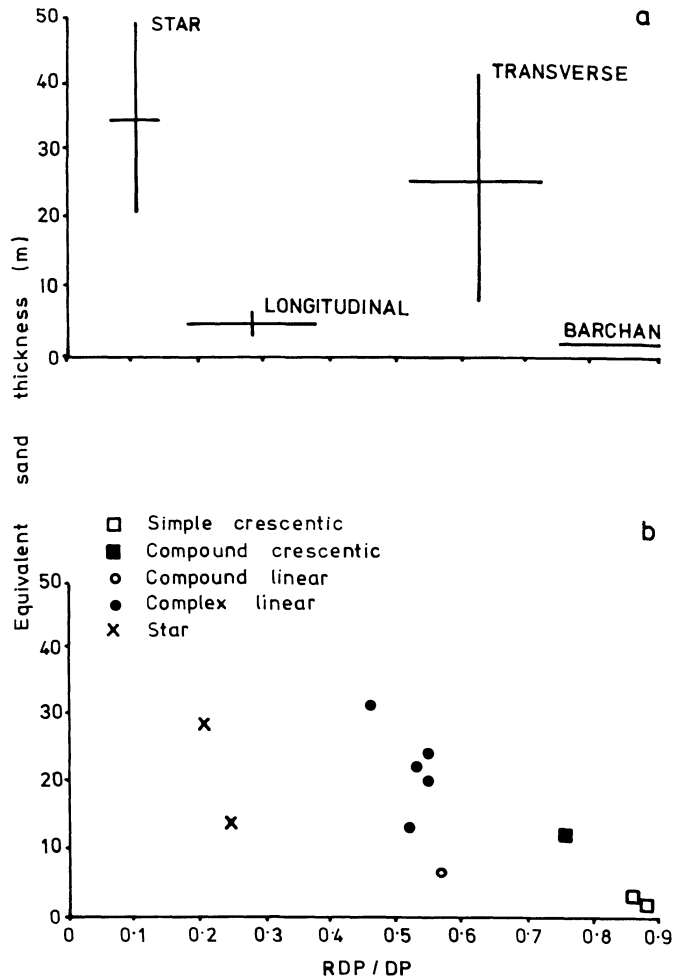

Figure 18.27 Relations between dune type and equivalent sand thickness (EST) for (a) a global sample of dunes (after Wasson and Hyde 1983a) and (b) the Namib sand sea. Note that linear dunes in the Namib occur in less variable wind regimes than those in Wasson and Hyde's sample.

variability of the sand-moving wind regime from crescentic to star dunes. However, the overall directional variability of wind regimes in the Namib sand sea is less than that in Fryberger's global sample (Fig. 18.27b).

Process studies give some indications as to why dunes of different types should occur in different wind regimes. The primary response of sand surfaces to the wind is to form an asymmetric transverse dune with a convex stoss slope. This is the most common dune form in unidirectional wind regimes. In multidirectional wind regimes, profiles of the crestal areas of linear and star dunes tend toward this form in each wind season. As dunes grow, the cross-sectional area increases exponentially and their reconstitution time increases by one or two orders of magnitude. Because of their size, they can no longer be remodelled in each season, so form–flow interactions become significant, and they develop a morphology that is controlled by more than one wind direction. There are many examples of dunes of different types occurring together in the same wind regime: the small dunes are almost always crescentic forms because they can be reformed entirely in each wind season; large dunes tend to be linear or star types. Star, and probably linear, dunes are therefore not primary dune types: they are developed by the modification of other dunes as they migrate into areas of different wind regimes (Tsoar 1974, Lancaster 1989a).

The essential mechanism for linear dune formation is the deflection of winds that approach at an oblique angle to the crest to flow parallel to the lee side and transport sand along the dune. Thus any winds from a 180° sector centred on the dune will be diverted in this manner and cause the dune to elongate downwind. This will not necessarily take place in a direction parallel to resultant direction of sand transport, but most probably at an angle of 20 to 30° to the most persistent sand-transporting wind direction. Linear dunes are not stable in a unidirectional wind regime because erosion and deposition are concentrated at the same localities, resulting in their eventual break-up (Tsoar 1983). Thus a seasonal change in wind direction is necessary to maintain the dune and its triangular profile.

In bimodal wind regimes, deflection of oblique winds on the lee side will tend to elongate the form, producing a linear dune. The effects of each wind direction will be controlled by their direction relative to the dune. If a high percentage of winds are at optimal angles for lee-side deflection, then the dune will extend strongly, and such dunes will tend to be long and relatively low. If winds blow at higher angles to the dune, then longitudinal movements of sand will be replaced by deposition on lee-side avalanche faces. Sand will tend to stay on the dune and increase its height. A limiting case will occur when winds are perpendicular to the crest, producing a reversing dune. Such dunes tend to accrete vertically and develop major lee-side secondary flow cells that move sand toward the centre of the dune, leading to the formation of star dunes.

The development of star dunes is strongly influenced by the high degree of form–flow interaction, which occurs as a result of seasonal changes in wind direction, and the existence of a major lee-side secondary circulation. The pattern of winds on star dunes indicates that most of the resultant erosion and deposition involves the reworking of deposits laid down in the previous wind season. Sand, once transported to the dune, tends to stay there and add to its bulk. This is a result of the high deposition rates on lee faces and the fact that wind velocity and sand transport rates decrease away from the central part of the dune. The prominent lee-side secondary flows also tend to move sand towards the centre of the dune and promote the development of the arms.

Sand Supply

The availability of sand for dune building has long been considered a factor influencing dune morphology (Hack 1941, Wilson 1972). Using a sample of dunes of different types from sand seas in all major desert areas, Wasson and Hyde (1983a) established that the mean equivalent or spread-out thickness (EST) of dune sand in a given area for all dune types was statistically identical and concluded that although sediment availability was a significant variable determining dune type, it was not the only one.

However, by plotting EST against Fryberger's RDP/DP ratio, a clear discrimination of dune types was achieved (Fig. 18.27a), leading to the conclusion that barchans occur where there is very little sand and almost unidirectional winds; transverse dunes are located where sand is abundant and winds variable; linear dunes develop where sand supply is small, but winds are more variable; and star dunes form in complex wind regimes with abundant sand supply. Similar relationships are evident in the Namib sand sea, although the range of directional variability is less (Fig. 18.27b).

However, EST is not a measure of sand supply, but of the volume of sand contained in the dunes and may be a reflection of dune type with the dune type being influenced by the other factors, especially the wind regime (Rubin 1984). In the Namib sand sea it is possible to clearly discriminate between dune types on the basis of their relationships with wind regimes. The EST data merely suggest that there is more sand in complex linear and star dunes than in compound linear and all types of crescentic dunes.

Vegetation

The effects of vegetation on sand transport rates and nucleation of dunes have been discussed in earlier sections. Sand is an excellent medium for plant growth in deserts, because of its high moisture-holding capacity (Bowers 1982). Many dunes, even in hyperarid regions like the Namib, are vegetated to some extent, mostly in the plinth areas of linear and star dunes where relatively little surface change occurs (Thomas and Tsoar 1990).

The direct effects of vegetation on dune form are not well understood. Hack (1941) suggested that in north-eastern Arizona there was a transition from crescentic to parabolic dunes with increased vegetation cover, and that linear dunes occurred in areas with less sand and vegetation than parabolic dunes (Fig. 18.28). Tsoar (1989) has distinguished between straight 'vegetated linear dunes' (widespread in Australia and the Kalahari) and sinuous crested 'seif'-type linear dunes. He argues that straight linear dunes form in the presence of a significant vegetation cover as lee dunes developing downwind

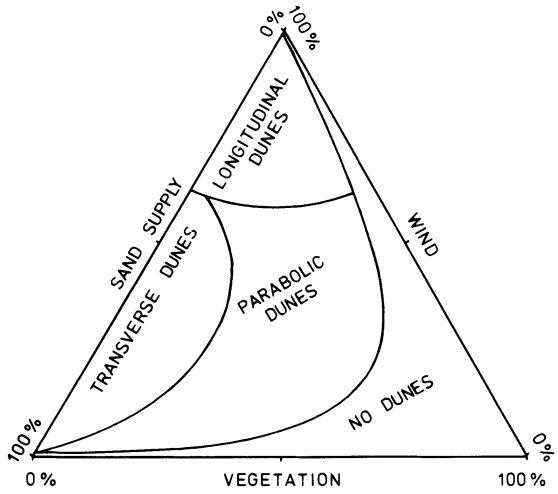

Figure 18.28 Relations between dune type, sand supply, wind strength, and vegetation cover (after Hack 1941).

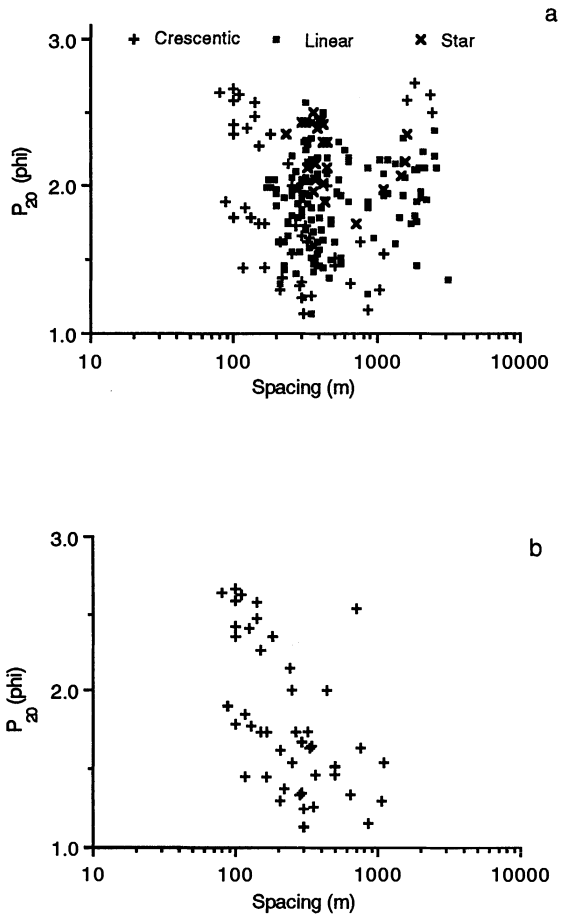

Figure 18.29 Relations between dune spacing and size of coarse 20th percentile of dune sand for (a) crescentic, linear, and star dunes (after Lancaster 1988), and (b) crescentic dunes in Namibian and Gran Desierto sand seas.

from vegetated mounds (coppice dunes). However, stratigraphic evidence (e.g. Wasson 1983a) shows that many linear dunes of this type were originally formed during the late Pleistocene and have since become stabilized by vegetation in more humid and/or less windy conditions. The form is therefore not the result of current processes. Where dunes are still active in these regions (or have been reactivated by vegetation disturbance), their form is similar to that of other linear dunes with a sinuous sharp crestline.

CONTROLS OF DUNE SIZE AND SPACING

Effects of Grain Size

Wilson (1972) found a clear relation between dune and draa spacing and the grain size of the coarse twentieth percentile of dune crest sands (P_{20}) in three northern Saharan sand seas. However, data for dunefields and sand seas in the Namib, the south-western Kalahari, and the Gran Desierto of Mexico (Fig. 18.29a) show that there is no general relation between dune spacing and grain size in these areas. Similarly, recent data from Australia (Wasson and Hyde 1983b) show no relation between P_{20} and linear dune spacing. These data suggest that Wilson's hypothesis of a grain size control of dune spacing is not generally applicable. In a given sand sea, the spacing of some dune types is apparently correlated with P_{20}, whereas other types show no relation. The spacing of complex and star dunes in the Namib and Gran Desierto sand seas is unrelated to P_{20}. However, data for simple and compound crescentic dunes show that their spacing tends to increase with a coarsening of P_{20} (Fig. 18.29b). One possible explanation is that crescentic dunes composed of coarse sands tend to have broad rounded crests (Tsoar 1986), so that they have a greater crest-to-crest spacing than crescentic dunes with narrow, sharp crests.

Effects of Wind Regimes

Several workers have suggested that dune size and spacing increase as wind speed and sand transport rates increase (Glennie 1970, Wilson 1972, Besler 1980). By analogy with subaqueous bedforms (Allen

1968, Rubin and Hunter 1982), it might be expected that dune size is related to mean sand transport rates, so that larger dunes are located where sand transport rates are high, and small dunes occur where transport rates are low. However, for 100-km^2 areas of dunes in the Namib sand sea the opposite situation occurs: large dunes are found in areas where annual potential sand transport rates are low and small dunes occur in areas of high potential sand transport rates (Fig. 18.30a). Similar patterns appear in Saharan sand seas.

However, when the height of crescentic dunes superimposed on the flanks of individual complex linear dunes in the Namib sand sea is compared with measured wind speeds (Fig. 18.30b), it is found that they scale directly with wind velocities and potential sand transport rates, as also observed by Rubin and Hunter (1982) and Havholm and Kocurek (1988). These observations suggest that superimposed dunes and draas are formed by two different scales of airflow variability and can coexist in the same flow in a similar manner to the subaqueous bedforms studied by Smith and McLean (1977) and Rubin and McCulloch (1980). The morphology of superimposed dunes on complex and compound dunes is controlled by secondary air flows created by the major dune which is formed by the primary air flow. The size of compound and complex dunes appears to be the result of long-continued growth in wind regimes that give rise to deposition on the dune, and their occurrence in a sand sea reflects regional sand transport patterns in which sand is transported from areas of high transport rates and deposited in areas of low or decreasing transport rates (Lancaster 1988).

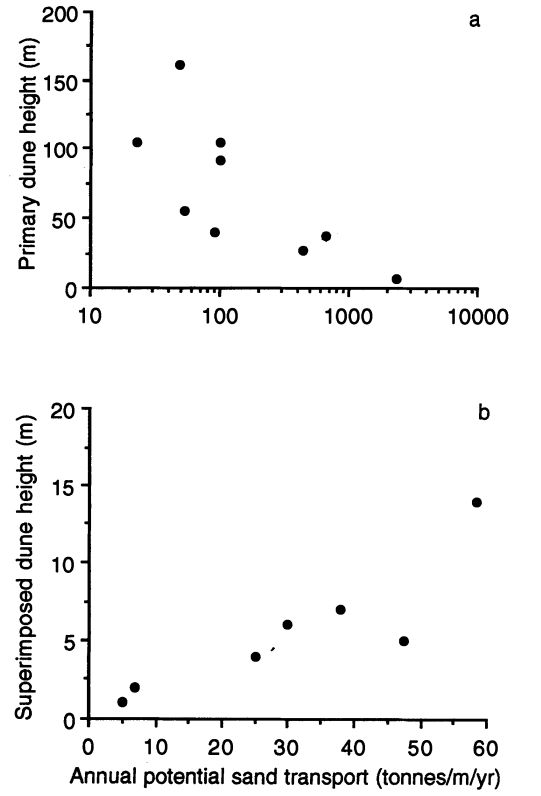

Figure 18.30 Relations between dune height and annual potential sand transport (after Lancaster 1988) for (a) primary dunes in the Namib sand sea and (b) crescentic dunes superimposed on the lee side of Namib complex linear dunes.

Given sufficient sand supply, ripples and dunes will be formed on flat desert surfaces. In the same way, the slopes of large dunes will present an effectively planar surface on which sand transport takes place. Therefore, variations in sand transport rates on compound or complex dunes in time or space (Lancaster 1985) will lead to the formation of superimposed dunes if the major dune is sufficiently large. This suggests that there is a minimum size for compound and complex dunes. Although the sample size is small, data on the width and spacing of simple, compound, and complex crescentic and linear dunes (Breed and Grow 1979) indicate that the mean sizes of simple, compound, and complex dunes are statistically significantly different from one another, suggesting that a minimum dune size must be reached before superimposed dunes can develop. In the Namib sand sea, simple crescentic dunes have a spacing of less than 500 m, whereas compound dunes are all more than 500 m apart. There is, however, a continuum of the height and spacing of the major bedform from simple to compound and complex types (Fig. 18.2). This suggests that, given sufficient sand supply and time, simple dunes will grow into compound and complex forms.

It appears, therefore, that dunes of different types develop in different ways, and there are no generally applicable relations between dune size or spacing and grain size or wind regime characteristics. The relations between dune size and potential sand transport rates indicate that the size of superimposed dunes increases with transport rate, whereas complex dune size decreases with transport rate. Thus, it appears that the factors that control dune size and spacing are determined in part by the character of the dunes themselves. First, this is a result of the nature of dune dynamics. As the dune grows, it projects into the boundary layer and

creates secondary patterns of air flow on and around itself. These secondary flows play a major role in the development of dunes by their control of patterns of erosion and deposition and the dynamics of superimposed dunes. Second, dunes of different sizes behave in different ways as a result of variations in reconstitution time. This can be represented by the time taken for the bedform to migrate one wavelength in the direction of net transport. In the Namib sand sea, typical complex linear dunes have a spacing of 2100 m and migrate at a rate of $0.05\,m\,y^{-1}$. The reconstitution time for these dunes is therefore 42 000 years. Crescentic dunes superimposed on the flanks of the linear dunes have a mean spacing of 90 m and migrate at a rate of $3\,m\,y^{-1}$, giving a reconstitution time of 30 years. Reconstitution time therefore increases by several orders of magnitude from simple to complex dunes. This implies that the morphology of simple dunes and superimposed dunes is governed principally by annual or seasonal patterns of wind speed and direction and by spatial changes in wind speed over draas. The lifespan of these dunes is about 10 to 100 years. Compound and complex dunes are relatively insensitive to seasonal changes in local air flow conditions and may persist for 1000 to 100 000 years. Their size is not a direct function of grain size or sand transport rates but is the result of long-continued growth in conditions of abundant sand supply. The distribution of compound and complex dunes in sand seas is controlled by regional-scale patterns of winds and sand transport rates. The Algodones dunes, California, are an excellent example of these principles. The compound crescentic dunes are approximately transverse to the mean annual resultant sand transport direction, whereas the superimposed dunes change their orientation in response to seasonal changes in wind direction (Havholm and Kocurek 1988).

The differences in scale between the elements of the aeolian bedform hierarchy suggest that the factors which control the size and spacing of simple dunes should be considered separately from those that influence the size and spacing of draas. Variations in winds and sand transport rates at different temporal and spatial scales appear to be the most important control of aeolian dune size and spacing. Whereas the height and spacing of individual simple and superimposed dunes in active sand seas probably tend toward an equilibrium with respect to contemporary sand transport rates and directions, the size and spacing of compound and complex dunes are functions of the long-term pattern of accumulation of sand in certain areas of the sand sea determined by regional-scale patterns of winds and sand transport rates.

SAND SEAS

Sand seas are dynamic sedimentary bodies that form part of regional-scale sand transport systems in which sand is moved by the wind from source zones to depositional sinks. The most important sediment sources are fluvial and deltaic sediments (e.g. Andrews 1981, Lancaster and Ollier 1983, Wasson 1983a). Other sources include beaches (e.g. Inman *et al.* 1966, Lancaster 1982a), Pleistocene palaeolakes, playas, and sabkhas (e.g. McKee 1966, Besler 1982, Wasson 1983b). Some sand seas have internal sediment sources as a result of the deflation of interdunes and reactivation of older dunes (Wasson 1983b, Lancaster 1988). In the Sahara and Arabia, many sand seas receive inputs of sand from adjacent sand bodies (Fryberger and Ahlbrandt 1979, Mainguet 1984) along well-defined sediment transport corridors that are clearly visible on satellite images (Wilson 1971, Fryberger and Ahlbrandt 1979, Mainguet 1984).

DUNE PATTERNS IN SAND SEAS

Many sand seas show a clear spatial patterning of dune types (Fig. 18.31), dune size and spacing, and sediment thickness (Breed *et al.* 1979, Lancaster *et al.* 1987, Sweet *et al.* 1988, Wasson *et al.* 1988, Lancaster 1989b). Upwind, the near-source areas are characterized by sand sheets and zibars and areas of low crescentic dunes. Sediment thickness is low. The central areas of the sand sea are occupied by large compound and complex dunes that represent the major area of sediment accumulation. Downwind, the leading edge of the sand sea is an area of thin sediment accumulation with small, often crescentic, dunes and prograding sand sheets and streaks. In parallel with changes in dune types, there are distinct trends in dune sediments (e.g. Sweet *et al.* 1988, Lancaster 1989b). Sands in upwind areas tend to be coarser and less well sorted than those in the depositional centres of sand seas.

Spatial variations in dune types have been documented from many sand seas (e.g. Breed *et al.* 1979, Lancaster 1983, Wasson 1983b, Lancaster *et al.* 1987, Warren 1988). In some sand seas (e.g. the Namib) these changes can be related to regional changes in wind regimes, but sharp transitions between dune types and differences in their sedimentary characteristics (e.g. in the Simpson–Strzelecki, the Wahiba Sands, and the Gran Desierto)

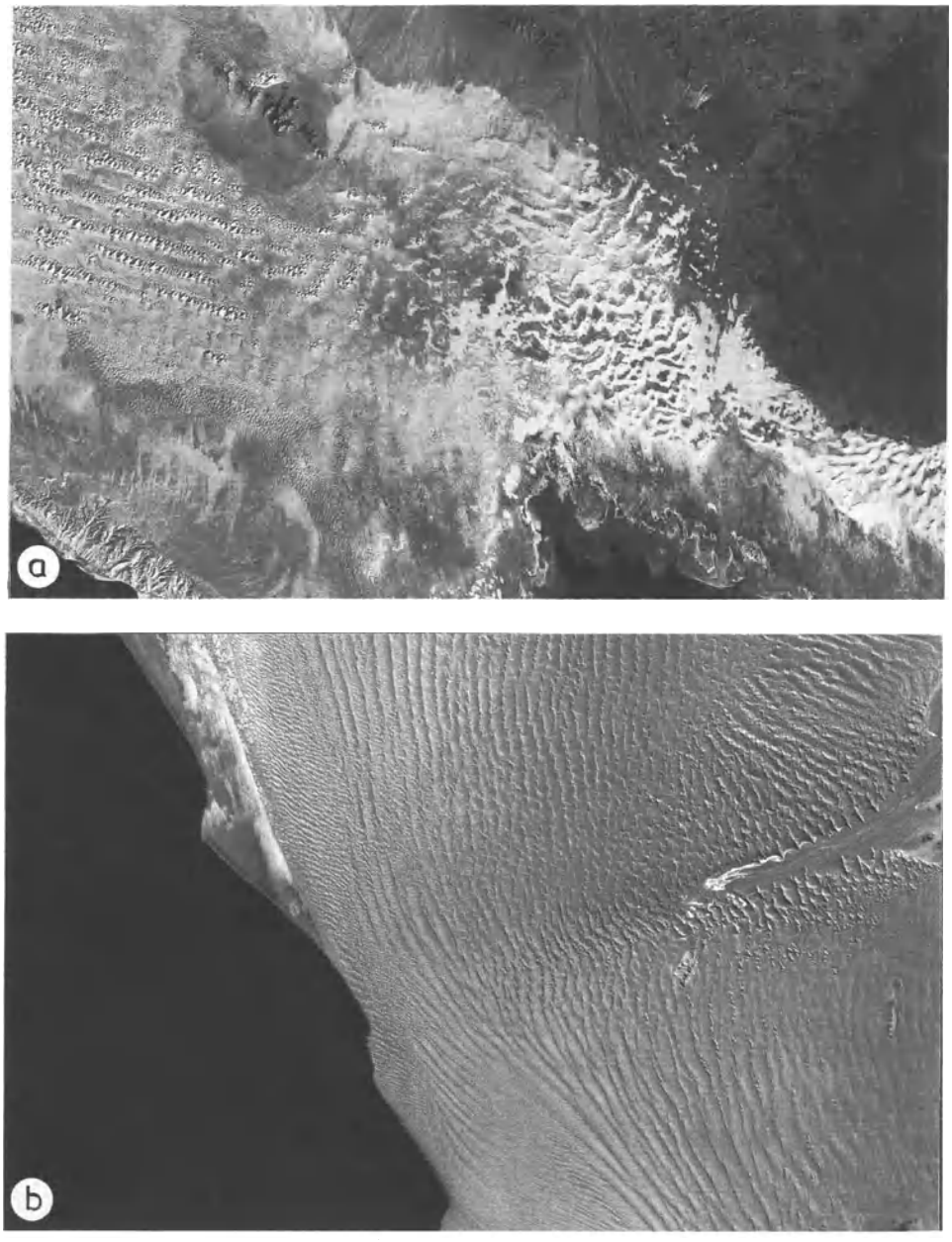

Figure 18.31 Spatial variations in dune types in sand seas for (a) the central part of the Namib sand sea and (b) the Gran Desierto sand sea. Note that the Namib sand sea forms an integrated system of dunes, although compound crescentic dunes along the coast may be younger than linear dunes inland, whereas the Gran Desierto consists of isolated depositional centres, each with a distinct dune morphology and sediment characteristics.

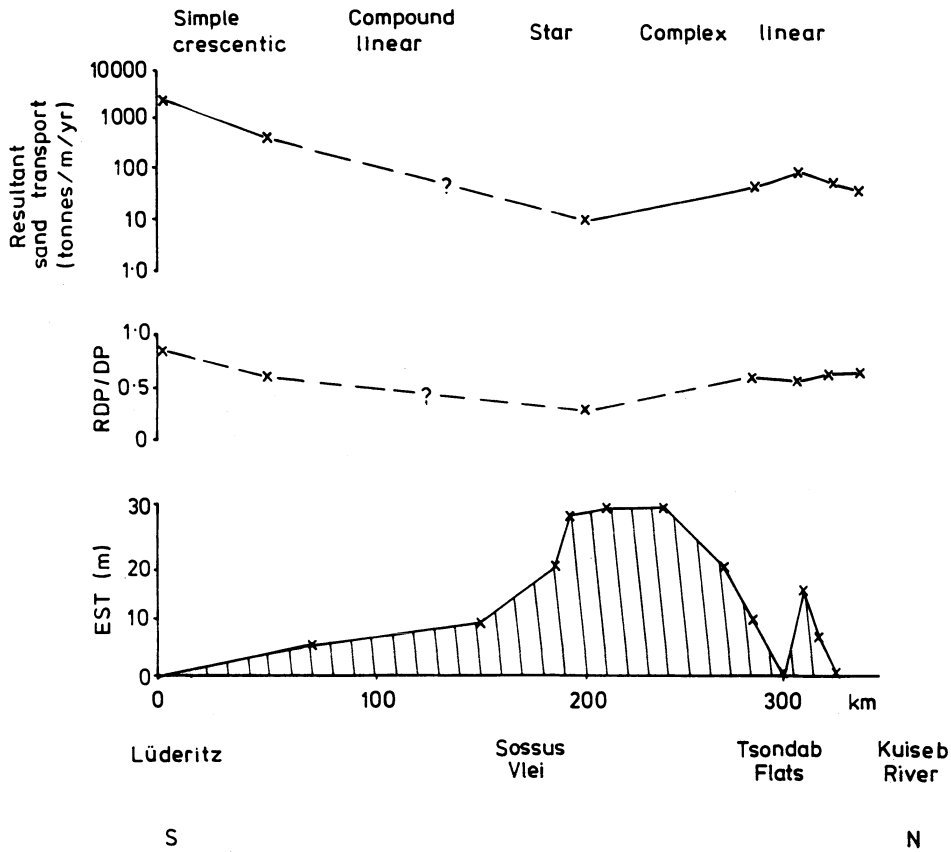

Figure 18.32 Relations between dune type, RDP/DP ratio, and equivalent sediment thickness (EST) along a south–north traverse across the Namib sand sea. Note that the thickest sand accumulations occur in the area of lowest wind energy and maximum directional variability of the wind regime.

suggest that many sand seas are composed of different generations of dunes, each with a distinct morphology and sediment source.

MODELS FOR SAND SEA ACCUMULATION

Concepts of sediment budgets can be applied to sand seas in a similar way to dunes. Deposition of sand and the accumulation of sand seas occur downwind of source zones wherever sand transport rates are reduced as a result of changes in climate or topography. Compilations of wind data together with information from aerial photographs and satellite images (Wilson 1971, Fryberger and Ahlbrandt 1979, Mainguet 1984) show that long-distance transport of sand by the wind occurs in the Namib, Sahara, and Arabian Deserts. However, Australian sand seas and many North American dunefields receive sand from local sources (Wasson *et al.* 1988, Blount and Lancaster 1990). Some sand seas accumulate where sand transport pathways converge in the lee of topographic obstacles (e.g. Fachi-Bilma Erg) or in areas of low elevation (Wilson 1971, Mainguet and Callot 1978, Wasson *et al.* 1988). Others occur where winds are checked by topographic barriers (e.g. Grand Erg Oriental, Kelso Dunes, Great Sand Dunes).

Decelerating winds and reduced potential sand transport rates may be the result of changes in regional circulation patterns that decrease wind speeds and/or increase their directional variability. Sand seas and dunefields in the western and southern Sahara, Saudi Arabia, the eastern Mojave and Sonoran Deserts, and the Namib (Fig. 18.32) occur in areas of low total or net sand transport compared with areas without sand sea development (Fryberger and Ahlbrandt 1979, Fryberger *et al.* 1984, Mainguet 1984, Smith 1984, Lancaster 1989b). Many sand seas (e.g. the Akchar and Makteir sand seas in Mauritania and the Nafud of Saudi Arabia) are crossed by

sand flows. The same winds that transport sand to the sand sea can also remove it at the downwind end. These are the 'flow crossed' sand seas of Wilson (1971).

Within the sand sea there are three main depositional mechanisms (Mader and Yardley 1985): (a) dune migration with declining transport rates downwind resulting in bedform climbing; (b) modification of dunes by winds from directions other than those which produced bedform migration leading to concentration of sand in growing bedforms (e.g. star dunes); and (c) merging, in which dunes coalesce with negligible erosion, as migration is slowed by topographic barriers or regional climatic changes.

EFFECTS OF CLIMATIC, TECTONIC, AND EUSTATIC CHANGES

Many sand seas incorporate large volumes of sediment and have clearly accumulated over a long period of time, during which Quaternary climatic and eustatic changes have had a major influence on sand supply and dune mobility. The important effects of Quaternary events on sand sea and even dune formation are only just being recognized, partly in response to the realization that many ancient aeolian sandstones have accumulated episodically and consist of genetically independent sand bodies separated by major regional-scale bounding surfaces (Kocurek 1988). Enhanced sand supply and dune formation has been favoured by periods of geomorphic instability and fluvial sediment production (Wasson 1984, Wells and McFadden 1987), and littoral sands exposed during periods of low glacial sea level provided a sediment source for sand seas in Arabia, the Namib, and southern Australia. Increased wind speeds and more vigorous circulation patterns in glacial periods gave rise to more active sand transport in many areas. This may have been sufficient to have reactivated currently stabilized dunes in many areas of Australia and the Sahel (Talbot 1984, Wasson 1984). In contrast, interdune pond and marsh sediments have been reported from sand seas in the Sahara (e.g. Rognon 1987), the Namib (Lancaster and Teller 1988), and Saudi Arabia (Whitney *et al.* 1983), providing evidence for intervals of substantially increased moisture availability, most notably in the periods 40 000 to 25 000 years BP and (in the Sahara and Arabia) 9000 to 4500 years BP. Many areas of dunes were most likely stabilized by vegetation during these times.

Detailed studies of dune and interdune sediments in the Akchar Sand Sea of Mauritania by Kocurek *et al.* (1992) show that it represents the amalgamation of Late Pleistocene and Holocene deposits. The prominent large complex linear dunes are composite features. Their core consists of sand deposited during the period 20 000 to 13 000 years BP. This was stabilized by vegetation during a period of increased rainfall 11 000 to 4500 years BP, when pedogenesis altered dune sediments and lakes formed in interdune areas. Further periods of dune formation after 4000 years BP cannibalized existing aeolian deposits on the upwind margin of the sand sea. The currently active cap of crescentic dunes superimposed on the linear dunes dates to the past 30 years. Similar sequences of dune deposits have been recognized in the Sahel (Talbot 1985) and southern Sahara (Vökel and Grunert 1990). In the Rub al Khali, Nafud and Wahiba sand seas of the Arabian Peninsula aridity and dune formation occurred between 20 000 and 9000 years BP (McClure 1978, Whitney *et al.* 1983, Warren 1988). These dunes were stabilized by vegetation with weak pedogenesis and lakes in interdune areas from 9000 to 6000 years BP. The morphology of the modern dune system may be less than 2000 years old (Fig. 18.33). Episodic dune formation has also been indicated for the Australian and Thar deserts (Wasson 1983b, Wasson *et al.* 1983).

In North America, the Gran Desierto sand sea has accumulated episodically (Blount and Lancaster 1990). Evidence from dune morphology and sediments indicates that there are three major sand populations which represent three pulses of sediment input. The oldest sands were derived from the ancestral Colorado River floodplain and delta before tectonic movements caused an avulsion of the river to the west. Later inputs of sand came from the modern Colorado River floodplain and coastal areas south of the sand sea in periods of low sea levels. Relatively brief periods of aeolian deposition were separated by long intervals of geomorphic stability during which existing sand populations were reworked and pedogenic alteration and/or deflation of existing dune areas and sand sheets occurred in many areas of the sand sea. Laterally extensive bounding surfaces in sand sheets north-west of the sand sea provide evidence for dune stabilization by vegetation in wetter climates, and extensive deflation of sand sheets when sand supply from the Colorado River was terminated, possibly by incision related to sea level regressions.

Stratigraphic evidence from major sand seas suggests that their accumulation has been episodic, with long periods of stability being interrupted by relatively brief episodes of sediment input and dune

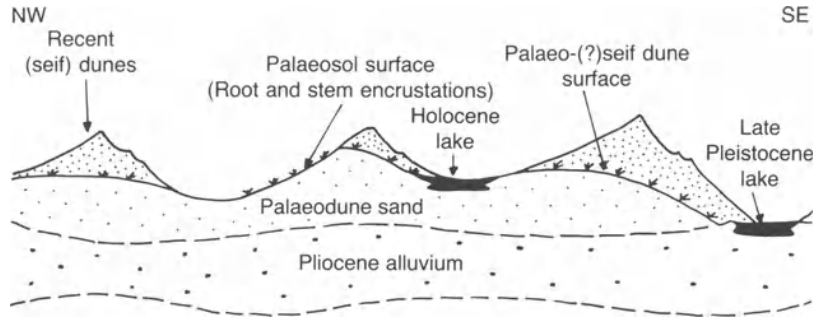

Figure 18.33 Sediments and tentative stratigraphy of the Rub al Khali, Saudi Arabia (after McClure 1978).

formation. Within the past 30 000 years dunes in many sand seas appear to have been actively accumulating for only 25 to 33% of the time (Lancaster 1990). Current aeolian activity in many areas is merely reworking and/or cannibalizing existing sediments leading to increasing complexity of the dune patterns (Warren 1988). These changes appear to have been most prominent in sand seas in currently semi-arid areas such as the Kalahari and Australia, but they also affected hyperarid areas such as the eastern Sahara (Haynes 1982).

CONCLUSIONS AND FUTURE RESEARCH DIRECTIONS

Major advances in our knowledge of the dynamics of dunes and sand seas have occurred since the early 1970s. There is now a general understanding of the processes that form or at least maintain most major dune types. The importance of scale effects is recognized, so that the processes that form wind ripples or simple dunes need to be considered at different temporal and spatial scales from those that form compound and complex dunes and sand seas. Recent advances in the study of ancient aeolian sandstones have emphasized the importance of climatic and eustatic changes in sand sea, and probably complex dune, development.

Despite considerable recent progress, many unresolved questions remain. At the dune scale, we still know little or nothing about the pattern of actual sand transport rates on dunes and their relationship to winds and dune topography, the mechanisms by which dunes grow, and the controls on dune spacing (and therefore mesoscale airflow at the dune–interdune scale). At the regional scale, the vertical sequence of deposits and the history of many sand seas in relation to climatic and eustatic changes is unknown.

In the recent past, the most important developments have come from detailed field studies of aeolian processes at different scales. Despite the promise of simulation models of dunes, it is clear that in the near future progress in understanding dune dynamics and morphology will rely heavily on carefully conducted field studies.

REFERENCES

Allen, J.R.L. 1968. *Current ripples*. Amsterdam: Elsevier.

Allen, J.R.L. 1974. Reaction, relaxation and lag in natural sedimentary systems: general principles, examples and lessons. *Earth Science Reviews* **10**, 263–342.

Anderson, R.S. 1987. A theoretical model for aeolian impact ripples. *Sedimentology* **34**, 943–56.

Andrews, S. 1981. Sedimentology of Great Sand Dunes, Colorado. *Society of Economic Paleontologists and Mineralogists Special Publication* **31**, 279–91.

Anton, D. and P. Vincent 1986. Parabolic dunes of the Jafurah Desert, Eastern Province, Saudi Arabia. *Journal of Arid Environments* **11**, 187–98.

Ash, J.E. and R.J. Wasson 1983. Vegetation and sand mobility in the Australian desert dunefield. *Zeitschrift für Geomorphologie Supplement Band* **45**, 7–25.

Aufrère, L. 1928. L'orientation des dunes et la direction des vents. *Academie des Sciences, Paris, Comptes Rendues* **187**, 833–5.

Bagnold, R.A. 1941. *The physics of blown sand and desert dunes*. London: Chapman & Hall.

Besler, H. 1980. Die Dunen-Namib: entstehung und dynamik eines ergs. *Stuttgarter Geographische Studien* **96**.

Besler, H. 1982. A contribution to the aeolian history of the Tanezrouft. *Bulletin de la Association de Geographes Francais* **484**, 55–60.

Blom, J. and L. Wartena 1969. The influence of changes in surface roughness on the development of the turbulent boundary layer in the lower layers of the atmosphere. *Journal of Atmospheric Science* **26**, 255–65.

Blount, G. and N. Lancaster 1990. Development of the Gran Desierto sand sea. *Geology* **18**, 724–8.

Bowers, J. 1982. The plant ecology of inland dunes in western North America. *Journal of Arid Environments* **5**, 199–220.

Breed, C.S. and T. Grow 1979. Morphology and distribution of dunes in sand seas observed by remote sensing. In *A study of global sand seas*, E.D. McKee (ed.), 253–304. United States Geological Survey Professional Paper 1052.

Breed, C.S., S.G. Fryberger, S. Andrews, C. McCauley, *et al.* 1979. Regional studies of sand seas using LANDSAT (ERTS) imagery. In *A study of global sand seas*, E.D. McKee (ed.), 305–98. United States Geological Survey Professional Paper 1052.

Breed, C.S., J.F. McCauley and P.A. Davis 1987. Sand sheets of the eastern Sahara and ripple blankets on Mars. In *Desert sediments: ancient and modern*, L.E. Frostick and I. Reid (eds), 337–59. Oxford: Blackwell Scientific.

Brookfield, M. 1983. Aeolian sands. In *Facies models*, R.G. Walker (ed.), 91–103. Geoscience Canada Reprint Series 1.

Clos-Arceduc, A. 1971. Typologie des dunes vives. *Travaux de la Institute de Géographie de Reims* **6**, 63–72.

Cooke, R.U. and A. Warren 1973. *Geomorphology in deserts*. London: Batsford.

Cooper, W.S. 1958. Coastal sand dunes of Oregon and Washington. *Geological Society of America Memoir* **72**.

Ellwood, J.M., P.D. Evans and I.G. Wilson 1975. Small scale aeolian bedforms. *Journal of Sedimentary Petrology* **45**, 554–61.

Embabi, N.S. 1982. Barchans of the Kharga Depression. In *Desert landforms of Egypt: a basis for comparison with Mars*, NASA CR-3611, F. El-Baz and T.A. Maxwell (eds), 141–56. Washington, DC: NASA.

Endrody-Younga, S. 1982. Dispersion and translocation of dune specialist tenebrionids in the Namib area. *Cimbebasia (A)* **5**, 257–71.

Finkel, H.J. 1959. The barchans of southern Peru. *Journal of Geology* **67**, 614–47.

Folk, R. 1970. Longitudinal dunes of the northwestern edge of the Simpson Desert, Northern Territory, Australia, 1. Geomorphology and grain size relationships. *Sedimentology* **16**, 5–54.

Fredsoe, J. 1982. Shape and dimension of stationary dunes in rivers. *Journal of Hydraulics Division, Proceedings of the American Society of Civil Engineers* **108**, 932–47.

Fryberger, S.G. 1979. Dune forms and wind regimes. In *A study of global sand seas*, E.D. McKee (ed.) 137–40. United States Geological Survey Professional Paper 1052.

Fryberger, S.G. and T.S. Ahlbrandt 1979. Mechanisms for the formation of aeolian sand seas. *Zeitschrift für Geomorphologie* **23**, 440–60.

Fryberger, S. and A.S. Goudie 1981. Arid geomorphology. *Progress in Physical Geography* **5**, 420–8.

Fryberger, S., T. Ahlbrandt and S. Andrews 1979. Origin, sedimentary features, and significance of low-angle aeolian 'sand sheet' deposits, Great Sand Dunes National Monument and vicinity, Colorado. *Journal of Sedimentary Petrology* **49**, 733–46.

Fryberger, S.G., A.M. Al-Sari, T.J. Clisham, S.A.R. Rizoi, *et al.* 1984. Wind sedimentation in the Jafurah sand sea, Saudi Arabia. *Sedimentology* **31**, 413–31.

Glennie, K.W. 1970. *Desert sedimentary environments*. Amsterdam: Elsevier.

Greeley, R. and J.D. Iversen 1985. *Wind as a geological process*. Cambridge: Cambridge University Press.

Greeley, R. and J.D. Iversen 1987. Measurements of wind friction speeds over lava surfaces and assessment of sediment transport. *Geophysical Research Letters* **14**, 925–8.

Hack, J.T. 1941. Dunes of the western Navajo Country. *Geographical Review* **31**, 240–63.

Hanna, S.R. 1969. The formation of longitudinal sand dunes by large helical eddies in the atmosphere. *Journal of Applied Meteorology* **8**, 874–83.

Hastenrath, S.L. 1967. The barchans of the Arequipa region, southern Peru. *Zeitschrift für Geomorphologie* **11**, 300–11.

Hastenrath, S.L. 1987. The barchan dunes of southern Peru revisited. *Zeitschrift für Geomorphologie* **31**, 167–78.

Havholm, K. and G. Kocurek 1988. A preliminary study of the dynamics of a modern draa, Algodones, southeastern California, USA. *Sedimentology* **35**, 649–69.

Haynes, C.V. 1982. Great Sand Sea and Selima Sand Sheet, eastern Sahara: geochronology of desertification. *Science* **217**, 629–33.

Haynes, C.V. 1989. Bagnold's barchan: a 57-yr record of dune movement in the eastern Sahara and implications for dune origin and palaeoclimate since Neolithic times. *Quaternary Research* **32**, 153–67.

Holm, D.A. 1960. Desert geomorphology in the Arabian Peninsula. *Science* **123**, 1369–79.

Howard, A.D. 1977. Effect of slope on the threshold of motion and its application to orientation of wind ripples. *Bulletin of the Geological Society of America* **88**, 853–6.

Howard, A.D., J.B. Morton, M. Gad-el-Hak and D.B. Pierce 1978. Sand transport model of barchan dune equilibrium. *Sedimentology* **25**, 307–38.

Hoyt, J. 1965. Air and sand movements to the lee of dunes. *Sedimentology* **7**, 137–43.

Hunter, R.E., B.M. Richmond and T.R. Alpha 1983. Storm-controlled oblique dunes of the Oregon Coast. *Bulletin of the Geological Society of America* **94**, 1450–65.

Inman, D.L., G.C. Ewing and J.B. Corliss 1966. Coastal sand dunes of Guerrero Negro, Baja California, Mexico. *Bulletin of the Geological Society of America* **77**, 787–802.

Jäkel, D. 1980. Die bildung von barchanen in Faya-Largeau/Rep. du Tchad. *Zeitschrift für Geomorphologie* **24**, 141–59.

Kocurek, G. 1981. Significance of interdune deposits and bounding surfaces in aeolian dune sands. *Sedimentology* **28**, 753–80.

Kocurek, G. 1988. First order and super bounding surfaces in aeolian sequences – Bounding surfaces revisited. *Sedimentary Geology* **56**, 193–206.

Kocurek, G. and J. Nielson 1986. Conditions favourable for the formation of warm-climate aeolian sand sheets. *Sedimentology* **33**, 795–816.

Kocurek, G., M. Townsley, E. Yeh, K. Havholm, *et al.* 1992. Dune and dunefield development stages on Padre Island, Texas: effects of lee airflow and sand saturation levels and implications for interdune deposition. *Journal of Sedimentary Petrology* **62**, 622–35.

Lai, R.J. and J. Wu 1978. *Wind erosion and deposition along a coastal sand dune*, University of Delaware Sea Grant Program, DEL-SG-10-78.

Lancaster, N. 1980. The formation of seif dunes from barchans – supporting evidence for Bagnold's hypothesis from the Namib Desert. *Zeitschrift für Geomorphologie* **24**, 160–7.

Lancaster, N. 1982a. Dunes on the Skeleton Coast, SWA/

Namibia: geomorphology and grain size relationships. *Earth Surface Processes and Landforms* **7**, 575–87.

Lancaster, N. 1982b. Linear dunes. *Progress in Physical Geography* **6**, 476–504.

Lancaster, N. 1983. Controls of dune morphology in the Namib sand sea. In *Aeolian sediments and processes*, T.S. Ahlbrandt and M.E. Brookfield (eds), 261–89. Amsterdam: Elsevier.

Lancaster, N. 1985. Variations in wind velocity and sand transport rates on the windward flanks of desert sand dunes. *Sedimentology* **32**, 581–93.

Lancaster, N. 1987. Variations in surface shear stress over aeolian dunes. *Geological Society of America, Abstracts with Programs* **19**, 738.

Lancaster, N. 1988. Controls of aeolian dune size and spacing. *Geology* **16**, 972–5.

Lancaster, N. 1989a. The dynamics of star dunes: an example from the Gran Desierto, Mexico. *Sedimentology* **36**, 273–89.

Lancaster, N. 1989b. *The Namib sand sea: dune forms, processes, and sediments*. Rotterdam: A.A. Balkema.

Lancaster, N. 1990. Palaeoclimatic evidence from sand seas. *Palaeogeography, Palaeoclimatology, Palaeoecology* **76**, 279–90.

Lancaster, N. and C.D. Ollier 1983. Sources of sand for the Namib Sand Sea. *Zeitschrift für Geomorphologie Supplement Band* **45**, 71–83.

Lancaster, N. and J.T. Teller 1988. Interdune deposits of the Namib Sand Sea. *Sedimentary Geology* **55**, 91–107.

Lancaster, N., R. Greeley and P.R. Christensen 1987. Dunes of the Gran Desierto Sand Sea, Sonora, Mexico. *Earth Surface Processes and Landforms* **12**, 277–88.

Livingstone, I. 1986. Geomorphological significance of wind flow patterns over a Namib linear dune. In *Aeolian geomorphology*, W.G. Nickling (ed.), 97–112. Allen & Unwin: Boston.

Livingstone, I. 1989. Monitoring surface change on a Namib linear dune. *Earth Surface Processes and Landforms* **14**, 317–32.

Long, J.T. and R.P. Sharp 1964. Barchan dune movement in Imperial Valley, California. *Bulletin of the Geological Society of America* **75**, 149–56.

Mader, D. and M.J. Yardley 1985. Migration, modification and merging in aeolian systems and the significance of the depositional mechanisms in Permian and Triassic dune sands of Europe and North America. *Sedimentary Geology* **43**, 85–218.

Mainguet, M. 1983. Dunes vives, dunes fixées, dunes vêtues: une classification selon le bilan d'alimentation, le régime éolien et la dynamique des édifices sableux. *Zeitschrift für Geomorphologie Supplement Band* **45**, 265–85.

Mainguet, M. 1984. A classification of dunes based on aeolian dynamics and the sand budget. In *Deserts and arid lands*, F. El-Baz (ed.), 31–58. The Hague: Martinus Nijhoff.

Mainguet, M. and Y.I. Callot 1978. L'erg de Fachi-Bilma (Tchad-Niger). *Mémoires et Documents CNRS* **18**, 178.

Maxwell, T.A. and C.V. Haynes Jr 1989. Large-scale, low-amplitude bedforms (chevrons) in the Selima sand sheet, Egypt. *Science* **243**, 1179–82.

McClure, H.A. 1978. Ar Rub' al Khali. In *Quaternary Period in Saudi Arabia. 1: Sedimentological, hydrochemical, geomorphological investigations in central and eastern Saudi Arabia*, S.S. Al-Sayari and J. G. Zötl (ed.), 252–63. Vienna, New York: Springer.

McKee, E.D. 1966. Structures of dunes at White Sands National Monument, New Mexico (and a comparison with structures of dunes from other selected areas). *Sedimentology* **7**, 1–69.

McKee, E.D. 1979. Introduction to a study of global sand seas. In *A study of global sand seas*, E.D. McKee (ed.), 3–19. United States Geological Survey Professional Paper 1052.

McKee, E. 1982. Sedimentary structures in dunes of the Namib Desert, South West Africa. *Geological Society of America Special Paper* 188.

McKee, E. and G.C. Tibbitts Jr 1964. Primary structures of a seif dune and associated deposits in Libya. *Journal of Sedimentary Petrology* **34**, 5–17.

McLean, S.R. and J.D. Smith 1986. A model for flow over two-dimensional bedforms. *Journal of Hydraulic Engineering* **112**, 300–17.

Middleton, G.V. and J.B. Southard 1984. *Mechanics of sediment movement*. Tulsa, OK: Society of Economic Paleontologists and Mineralogists.

Mulligan, K.R. 1988. Velocity profiles measured on the windward slope of a transverse dune. *Earth Surface Processes and Landforms* **13**, 573–82.

Nielson, J. and G. Kocurek 1986. Climbing zibars of the Algodones. *Sedimentary Geology* **48**, 1–15.

Nielson, J. and G. Kocurek 1987. Development, processes, migration and deposits of star dunes, Dumont, California. *Bulletin of the Geological Society of America* **99**, 177–86.

Norris, R.M. and K.S. Norris 1961. Algodones dunes of southeastern California. *Bulletin of the Geological Society of America* **72**, 605–20.

Rognon, P. 1987. Late Quaternary climatic reconstruction for the Maghreb (North Africa). *Palaeogeography, Palaeoclimatology, Palaeoecology* **58**, 11–34.

Rubin, D.M. 1984. Factors determining desert dune type: discussion. *Nature* **309**, 91–2.

Rubin, D.M. and R.E. Hunter 1982. Bedform climbing in theory and nature. *Sedimentology* **29**, 121–38.

Rubin, D.M. and D.S. McCulloch 1980. Single and superimposed bedforms: a synthesis of San Francisco Bay and flume observations. *Sedimentary Geology* **26**, 207–31.

Schumm, S.A. and R.W. Lichty 1965. Time, space, and causality in geomorphology. *American Journal of Science* **263**, 110–19.

Seppälä, M. and K. Linde 1978. Wind tunnel studies of ripple formation. *Geografiska Annaler* **60**, 29–42.

Sharp, R.P. 1963. Wind ripples. *Journal of Geology* **71**, 617–36.

Sharp, R.P. 1966. Kelso Dunes, Mohave Desert, California. *Bulletin of the Geological Society of America* **77**, 1045–74.

Slattery, M.C. 1990. Barchan migration on the Kuiseb River Delta, Namibia. *South African Geographical Journal* **72**, 5–10.

Smith, J.D. and S.R. McLean 1977. Spatially averaged flow over a wavy surface. *Journal of Geophysical Research* **82**, 1735–46.

Smith, R.S.U. 1980. Maintenance of barchan size in the southern Algodones dune chain. Imperial County, California. National Aeronautics and Space Administration, Reports of the Planetary Geology Program, *NASA Technical Memorandum* 81776, 253–4.

Smith, R.S.U. 1984. Aeolian geomorphology of the Devils Playground, Kelso Dunes and Silurian Valley, California. In *Surficial geology of the eastern Mojave Desert, California*, J.C. Dohrenwend (ed.), 162–73. Boulder, CO: Geological Society of America.

Sweet, M.L. and G. Kocurek 1990. An empirical model of aeolian dune lee-face airflow. *Sedimentology* **37**, 1023–38.

Sweet, M.L., J. Nielson, K. Havholm and J. Farralley 1988. Algodones dune field of southeastern California: case history of a migrating modern dune field. *Sedimentology* **35**, 939–52.

Talbot, M.R. 1984. Late Pleistocene dune building and rainfall in the Sahel. *Palaeoecology of Africa* **16**, 203–14.

Talbot, M.R. 1985. Major bounding surfaces in aeolian sandstones: a climatic model. *Sedimentology* **32**, 257–66.

Taylor, P.A., P.J. Mason and E.F. Bradley 1987. Boundary-layer flow over low hills. *Boundary-layer meteorology* **39**, 107–32.

Thomas, D.S.G. and H. Tsoar 1990. The geomorphological role of vegetation in desert dune systems. In *Vegetation and erosion*, J.B. Thornes (ed.), 471–89. Chichester: Wiley.

Tseo, G. 1990. Reconnaissance of the dynamic characteristics of an active Strzelecki Desert longitudinal dune, southcentral Australia. *Zeitschrift für Geomorphologie* **34**, 19–35.

Tsoar, H. 1974. Desert dunes morphology and dynamics, El Arish (northern Sinai). *Zeitschrift für Geomorphologie Supplement Band* **20**, 41–61.

Tsoar, H. 1983. Dynamic processes acting on a longitudinal (seif) dune. *Sedimentology* **30**, 567–78.

Tsoar, H. 1984. The formation of seif dunes from barchans – a discussion. *Zeitschrift für Geomorphologie* **28**, 99–103.

Tsoar, H. 1985. Profile analysis of sand dunes and their steady state significance. *Geografiska Annaler* **67A**, 47–59.

Tsoar, H. 1986. Two-dimensional analysis of dune profile and the effect of grain size on sand dune morphology. In *Physics of desertification*, F. El-Baz and M.H.A. Hassan (eds), 94–108. The Hague: Martinus Nyhoff.

Tsoar, H. 1989. Linear dunes – forms and formation. *Progress in Physical Geography* **13**, 507–28.

Tsoar, H. and K. Pye 1987. Dust transport and the question of desert loess formation. *Sedimentology* **34**, 139–54.

Verstappen, H.T. 1968. On the origin of longitudinal (seif) dunes. *Zeitschrift für Geomorphologie* **12**, 200–20.

Vökel, J. and J. Grunert 1990. To the problem of dune formation and dune weathering during the Late Pleistocene and Holocene in the southern Sahara and Sahel. *Zeitschrift für Geomorphologie* **34**, 1–17.

Walker, D.J. 1981. An experimental study of wind ripples. M.S. Thesis, Massachusetts Institute of Technology.

Warren, A. 1972. Observations on dunes and bimodal sands in the Tenere desert. *Sedimentology* **19**, 37–44.

Warren, A. 1988. The dunes of the Wahiba Sands. In *Scientific Results of the Royal Geographical Society's Oman Wahiba Sands Project 1985–1987*, R.W. Dutton (ed.), 131–60. Muscat, Oman: Journal of Oman Studies, Special Report 3.

Warren, A. and P. Knott 1983. Desert dunes: a short review of needs in desert dune research and a recent study of micro-meteorological dune initiation mechanisms. In *Aeolian sediments and processes*, M.E. Brookfield and T.S. Ahlbrandt (ed.), 343–52. Amsterdam: Elsevier.

Wasson, R.J. 1983a. The Cainozoic history of the Strzelecki and Simpson dunefields (Australia), and the origin of the desert dunes. *Zeitschrift für Geomorphologie Supplement Band* **45**, 85–115.

Wasson, R.J. 1983b. Dune sediment types, sand colour, sediment provenance and hydrology in the Strzelecki-Simpson Dunefield, Australia. In *Aeolian sediments and processes*, M.E. Brookfield and T.S. Ahlbrandt (eds), 165–95. Amsterdam: Elsevier.

Wasson, R.J. 1984. Late Quaternary environments in the desert dunefields of Australia. In *Late Cainozoic palaeoclimates of the Southern Hemisphere*, J.C. Vogel (ed.), 419–32. Rotterdam: A.A. Balkema.

Wasson, R.J. and R. Hyde 1983a. Factors determining desert dune type. *Nature* **304**, 337–9.

Wasson, R.J. and R. Hyde 1983b. A test of granulometric control of desert dune geometry. *Earth Surface Processes and Landforms* **8**, 301–12.

Wasson, R.J., S.N. Rajaguru, V.N. Misra, D.P. Agrawal, *et al.* 1983. Geomorphology, late Quaternary stratigraphy and palaeoclimatology of the Thar dunefield. *Zeitschrift für Geomorphologie Supplement Band* **45**, 117–51.

Wasson, R.J., K. Fitchett, B. Mackey and R. Hyde 1988. Large-scale patterns of dune type, spacing, and orientation in the Australian continental dunefield. *Australian Geographer* **19**, 89–104.

Watson, A. 1987. Variations in wind velocity and sand transport rates on the windward flanks of desert sand dunes: comment. *Sedimentology* **34**, 511–15.

Wells, S.G. and L.D. McFadden 1987. Influence of Late Quaternary climatic changes on geomorphic processes on a desert pavement, eastern Mojave Desert, California. *Quaternary Research* 130–46.

Werner, B.T. 1988. A steady-state model of wind-blown sand transport. *Journal of Geology* **98**, 1–17.

Whitney, J.W., D.J. Faulkender and M. Rubin 1983. The environmental history and present condition of the northern sand seas of Saudi Arabia. *United States Geological Survey Open File Report* OF-03-95.

Willetts, B.B. and M.A. Rice 1986. Collision in aeolian transport: the saltation/creep link. In *Aeolian geomorphology*, W.G. Nickling (ed.), 1–18. London: Allen & Unwin.

Wilson, I.G. 1971. Desert sandflow basins and a model for the development of ergs. *Geographical Journal* **137**, 180–99.

Wilson, I.G. 1972. Aeolian bedforms – their development and origins. *Sedimentology* **19**, 173–210.

Wilson, I.G. 1973. Ergs. *Sedimentary Geology* **10**, 77–106.

LANDFORMS OF AEOLIAN EROSION 19

Julie E. Laity

INTRODUCTION

Aeolian erosion develops through two principal processes: deflation (removal of loosened material and its transport as fine grains in atmospheric suspension) and abrasion (mechanical wear of coherent material). The relative significance of each of these processes appears to be a function of the properties of surface materials and the availability of abrasive particles. The landforms that result from aeolian erosion include ventifacts, ridge and swale systems, yardangs, desert depressions, and inverted relief.

The significance of wind erosion as a geomorphological process has been debated throughout this century. A summary of changing perspectives on the role of wind erosion in deserts is found in Goudie (1989). In recent years, the availability of remote sensing images of terrestrial deserts and of Mars has been an important stimulus for research and has provided information on the extent of large-scale erosion systems as well as on the timing, frequency, and size of dust storms. Improved methods of radiocarbon dating rock varnishes may allow ventifacts to be of value in the reconstruction of palaeowind circulation.

Despite these advances, comparatively little is known about the formation of erosional landforms in deserts. Most papers provide only general observations on form, materials, and environment and, with few exceptions, short- or long-term measurements of process or detailed environmental analyses have not been made. Consequently, landform age, processes and rates of formation, and evolutionary history are poorly understood.

VENTIFACTS

Published work dealing with ventifacts dates back to the mid-19th century. The first recognition of aeolian erosion was by Blake (1855) who described ventifacts from the Salton Sea region of California. Faceting of stones by wind abrasion was documented by Travers (1870), and further discussion on wind erosion was provided by Gilbert (1875). Evans (1911) proposed that 'ventifact' encompass the multiple and compound terms (wind-grooved stones, wind-faceted stones, etc.) then in use. Bryan (1931) published a bibliography of 258 titles on ventifacts, including a useful discussion on terminology and an overview of theories concerning the formation of ventifacts. An area of early debate concerned whether faceted pebbles are shaped by monodirectional winds, winds from two opposing directions, or winds from variable directions. In addition, the factors that control the final shape of ventifacts were in contention. Woodworth (1894) indicated that a rock of moderate size will have a facet cut at right angles to the wind, with new facets formed as a result of accidental overturning or rotation. However, researchers in Europe proposed a final form primarily conditioned by (a) the shape of the original base (a square base would yield a pyramid of four faces), (b) winds that split along the ground and impinge upon the rock from variable directions, or (c) the original size and shape of the rock. The view of Woodworth (1894) was subsequently supported by Sharp (1949, 1964, 1980) and appears to represent the present majority opinion. In the recent literature, differences of opinion exist with regard to the relative importance of saltating and suspended grains in the formation of ventifacts.

The term ventifact, although widely applied, is ill-defined. It is used to describe wind-eroded forms of varying size, form, and material composition. Although facets are often regarded as fundamental characteristics of ventifacts (Sharp and Malin 1984), they are often poorly developed on large boulders and rock outcrops, where the presence of pits, flutes, and grooves may be indicative of wind

Geomorphology of Desert Environments. Edited by Athol D. Abrahams and Anthony J. Parsons. Published in 1994 by Chapman & Hall, London. ISBN 978-94-015-8256-8

Figure 19.1 Wind abraded outcrop near a hill crest. Extensive planation and grooving of a marble outcrop in the Mojave Desert by wind driven sand (note dune sand in lower left corner of photograph). Upslope acceleration and passage of wind through a saddle results in maximum erosion near the crest.

erosion. On lava flows and bedrock outcrops, individual abraded rocks may be found in association with extensively eroded semi-planar surfaces (Fig. 19.1). The material that forms ventifacts may not be stone at all: over short time periods playa ventifacts have been observed to form in cohesive sediments (Williams and Greeley 1981). Although field evidence suggests that most ventifacts result from sand-blasting, dust and snow have also been proposed as agents of erosion.

Ventifacts have some value as criteria of past climatic conditions. The presence of wind-worn stones in ancient formations (Precambrian, Cambrian, Devonian, Permian, Jurassic, Triassic, Cretaceous, Tertiary, and Pleistocene) has been used as evidence of more arid conditions (Bryan 1931). Although ventifacts are indicative of intense wind activity, they do not necessarily signify aridity, as they also form in temperate regions along ocean or lake margins, and in periglacial settings. Aspects of ventifact form (facets, grooves, flutes, and pits) enable a determination of palaeowind direction, and the presence of ventifacts provides clues to the relative abundance of abrasive materials and vegetation cover in earlier environments. Although it is recognized that many ventifacts are no longer forming ('relict' or 'fossil' forms), the actual age of most ventifacts is unknown.

ENVIRONMENTS OF VENTIFACT FORMATION

Ventifacts form in environments characterized by (a) a supply of an abrasive material, (b) lack of complete vegetative cover, (c) relatively strong winds, (d) a topographic situation that allows the free sweep of wind or that locally accelerates wind, and (e) ground surface stability. Ventifacts are found in desert, periglacial, and coastal environments on Earth and are believed to occur on Mars. Many of the ventifacts are fossil in nature: a change in any of the factors listed above will diminish or cease wind erosion. In so far as there has been relatively little research on ventifacts in warm deserts and the processes of ventifact formation in coastal and periglacial settings are similar to those of the desert, these latter environments will be briefly reviewed and the research results incorporated into the discussion.

Ventifacts have been recorded from a number of present-day periglacial environments, including northern Canada (McKenna-Neuman and Gilbert 1986), Antarctica (Hall 1989, Lindsay 1973, Miotke 1982), Iceland (Antevs 1928, Greeley and Iversen 1985), Greenland, higher elevations in South America (Czajka 1972), as well as regions of North America (Blackwelder 1929, Powers 1936) and Europe that have experienced such conditions in the past. Ventifacts found along the eastern base of the Sierra Nevada, California exceed a metre in height and are abraded extensively across their windward surface with pits 5 to 10 mm in diameter and 10 to 25 mm in depth, and long grooves 5 to 15 mm in width (Blackwelder 1929). These ventifacts are clearly fossil in nature, as evidenced by the partly exfoliated condition of the rock surfaces and the growth of vegetation that shelters the rock outcrops. Powers (1936) described 60-cm-long grooves in crystalline boulders strewn on the sandy Lake Wisconsin plain. Such grooves were apparently carved by high velocity winds during periglacial periods when vegetation was absent. In Antarctic dry valleys, very high wind speeds (up to 300 km h^{-1}) result in medium sand, granules, and pebbles abrading rocks (Hall 1989). Wind tunnel experiments suggest that with such intense winds the yearly abrasion rates average a few millimetres and ventifacts form within a few decades or, at most, a few centuries (Miotke 1982).

Ventifacts occur in coastal locations where winds are strong and drifts of sand provide an effective abrading agent (Travers 1870, King 1936). A number of ventifact locations along the Massachusetts coast are listed in Wentworth and Dickey (1935). Few ventifacts have been reported for moist temperate climates outside of the coastal zone. In Nova Scotia they occur as a result of highly permeable sediments that result in locally dry surface conditions (Hickox 1959).

Although ventifacts appear to be fairly common in warm deserts and semi-arid environments, there has been relatively little substantive field research on their formation, with the exception of Sharp's (1964, 1980) experimental plots. The spatial distribution of ventifacts in deserts is largely unknown, because such small features cannot be identified from aerial imagery, and our knowledge of ventifact sites thereby depends on fortuitous discovery by individuals who recognize ventifacts and who furthermore publish their observations. High altitude photography has proven useful in locating ventifacts in the Mojave Desert, California, because their occurrence is often coincident with deposits of active and stabilized sand, with wind streaks, and with regions where the air is locally accelerated, either by topographic constrictions or by passing over a hill (Laity 1987). Most researchers have assumed that the abrading agent in deserts is wind-blown sand, but few have provided specific information as to grain size, shape, or lithology. Sediment analyses by Sharp (1964), Greeley and Iversen (1986) and Laity (unpublished data) suggest that fine to medium-sized sand dominates in the formation of ventifacts in California.

MORPHOLOGY OF VENTIFACTS

Lithology and Size of the Original Rock

Ventifacts develop in a wide range of rock types, ranging from exceptionally hard quartzite to softer limestone and marble. Although almost all lithologies develop characteristic faceting, fluting, or grooves, rocks such as schist or gneiss are particularly prone to linear erosion features and to etching, particularly where foliation is parallel to the wind (Sharp 1949, Lancaster 1984). Polishing and smoothing of rock surfaces have been observed on all lithologies. For any given environment, the occurrence and long-term preservation of ventifacts in different rock types are in large part affected by weathering processes that destroy surface features. Owing to the efficacy of solution, no evidence of wind-cutting was found in limestone or dolomite in Wyoming, although ventifacts of this composition are common elsewhere (Sharp 1949). In desert regions, granites do not preserve grooving as well as other materials, owing to granular disintegration and exfoliation (Lancaster 1984, Laity 1991). Likewise schists and pegmatites of the Namib Desert (Selby 1977, Lancaster 1984) and andesite in the Mojave Desert (Laity 1991) were found to weather too rapidly to preserve significant evidence of abrasion.

The size of the original material appears to be a strong control on the ultimate form of the ventifact. If the original rock is small, with a diameter of only a few centimetres, the ventifacts are more likely to be the classic faceted types (with planar faces and smooth surfaces) that lack lineations (Schoewe 1932, Wentworth and Dickey 1935, King 1936, Needham 1937, Maxson 1940, Glennie 1970, Czajka 1972, Whitney and Dietrich 1973, Babikir and Jackson 1985, Nero 1988). Schoewe (1932) suggested that the ratio of the height of a faceted ventifact to the height

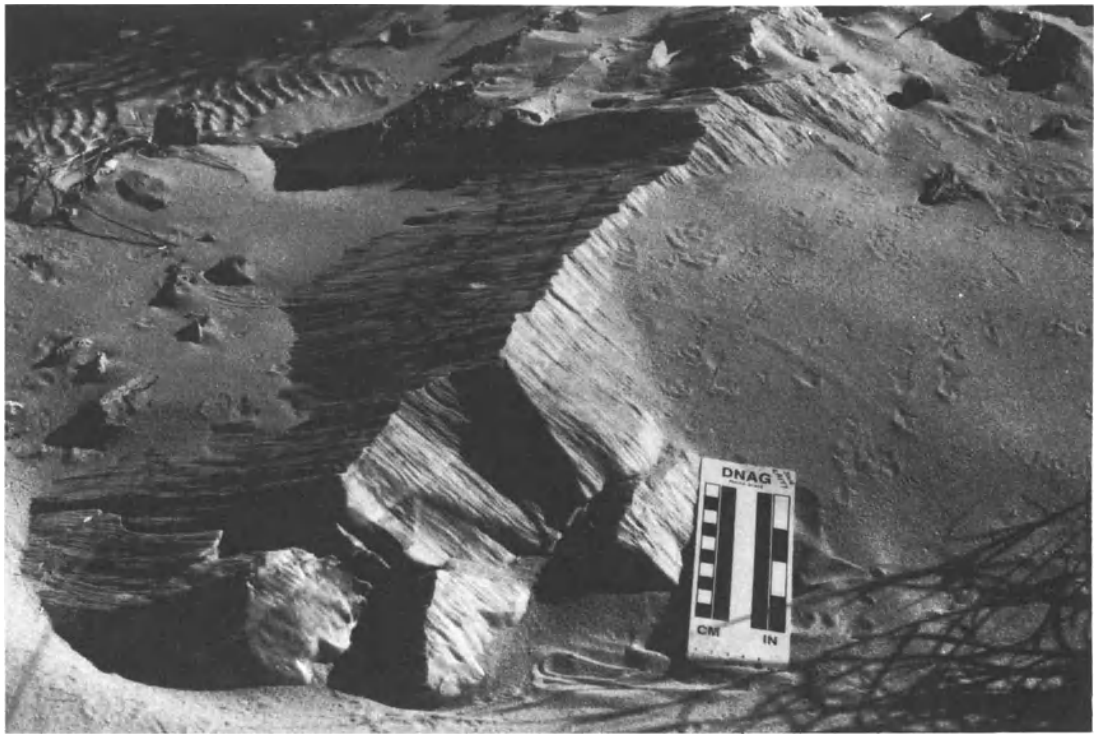

Figure 19.2 Wind eroded rock formed in a bidirectional flow regime on a hill crest in the Little Cowhole Mountains, Mojave Desert, California. Wind directions are from the north and south, producing two facets, each facing the impinging winds. Material surrounding the ventifacts is active aeolian sand. Many such ventifacts become partially or completely buried by sand and are re-excavated by changes in the wind regime.

of the sand-laden current should not exceed 1:8. Thus, if the zone of saltation extends to 64 cm, the diameter of the largest fragment faceted would be 8 cm. Maxson (1940) noted that faceted ventifacts in Death Valley, California, did not exceed a height of 8 cm, and that larger fragments were striated and polished but not faceted. He inferred that larger fragments split the wind and led to more complex flow, causing fluting and grooving but no faceting.

Given sufficient time for erosion, moderate-sized boulders may develop a semi-planar face, or two, if the wind is bidirectional (Fig. 19.2); these faces are invariably fluted or grooved on the windward exposure (Powers 1936, Sharp 1949, Czajka 1972, Laity 1987). Owing to their great mass, facets usually do not develop on large abraded boulders exceeding 1 m in diameter, although some bevelling may be apparent (Fig. 19.3). Powers (1936) noted grooves and fluting on a crystalline boulder 4.5 m in diameter. Outcrop ledges may show evidence of planation and be pitted or grooved.

Erosional Forms

Smoothing and Polishing of Rock Surfaces

Smoothing and polishing of rock surfaces is perhaps the most common feature reported for ventifacts. Polish occurs both on smooth facets and within flutes and grooves (Maxson 1940). According to Tremblay (1961), ventifact surfaces in Canada exhibit a high gloss that exceeds that of polish due to glacial action.

Facets

King (1936) and Sharp (1949) used the term facet to describe a relatively plane surface which has been cut at right angles to the wind, regardless of the original shape of the stone, and the term face to describe the original surface of the rock fragment. Facets commonly join along a sharp ridge or keel (Figs 19.2 and 19.4), and the number of keels (kante) is used to describe the stones as einkante, zweikanter,

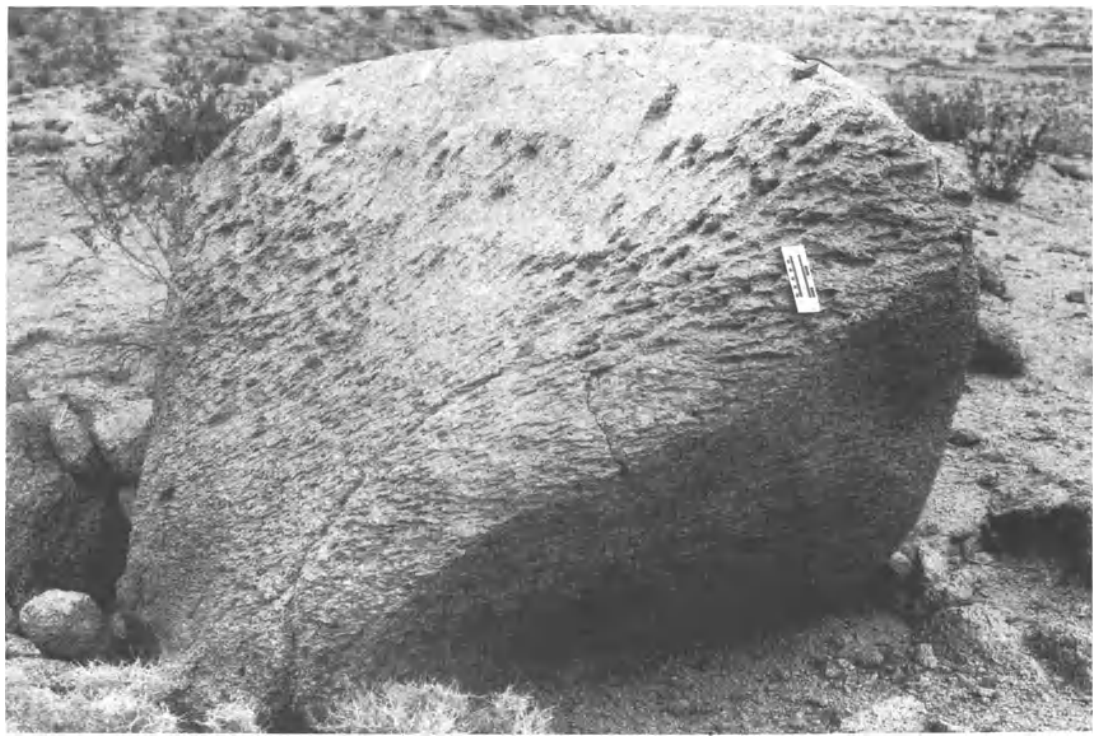

Figure 19.3 Abraded granite boulder approximately 1 m high located on a hill crest in the Mojave Desert. Varnish within grooves was dated by Dorn (1986) to 5500 ± 200 years BP, and provides a minimum limiting age for the cessation of abrasion in this region. While most granites in desert regions do not retain evidence of ventifaction, the grooves in this boulder are preserved owing to their considerable depth.

dreikanter (one-, two-, three-ridged), etc. (Bryan 1931). Much effort has been expended on the morphological classification of ventifacts (Bryan 1931, King 1936, Czajka 1972), particularly for small faceted forms.

The multiple facets that develop on ventifacts have been attributed to (a) the original shape of the stone, (b) splitting of the wind around the rock, (c) winds from different directions, and (d) shifting of ventifacts owing to undermining by wind scour, and overturning by wind, frost action, rain wash, and animal disturbance. In cold environments, frost shifting may be a particularly effective mechanism, as discussed by Sharp (1949) and Lindsay (1973).

Pits

A pitted surface is one indented by closed depressions, often of irregular shape. Whitney (1978, 1979), McCauley *et al.* (1979), and Garvin (1982) showed that wind is capable of producing pits on the surface of dense, homogeneous stones. However, Sharp and Malin (1984) emphasized that pitting is not an inevitable by-product of aeolian erosion, as material such as chert and limestone may develop facets, flutes, and grooves but no pits. It is probably easier for the wind to modify pre-existing pits, such as vesicles in basalt, by enlargement or integration (Fig. 19.5).

Pits occur on surfaces that are inclined at high angles to the wind (55 to 90°) and thereby indicate the windward side of boulders. As the angle between the face and the wind decreases, a transition from pits to deep flutes with overhanging ends occurs (Sharp 1949).

A fretted surface, although irregularly pitted, is characterized by projecting points, knobs, and ridges that form a particularly rough surface (Sharp and Malin 1984). In some cases a visible inclusion at the tips of the projections is visible (Figs 19.4 and 19.6).

Flutes

Flutes are scoop-shaped in plan, open at one end and closed at the other and broadly U-shaped in cross-section. Most flutes open downwind. They

Figure 19.4 Small marble ventifact with two facets joined along a sharp keel. The finger-like projections extending from the ventifact result from visible inclusions of resistant material.

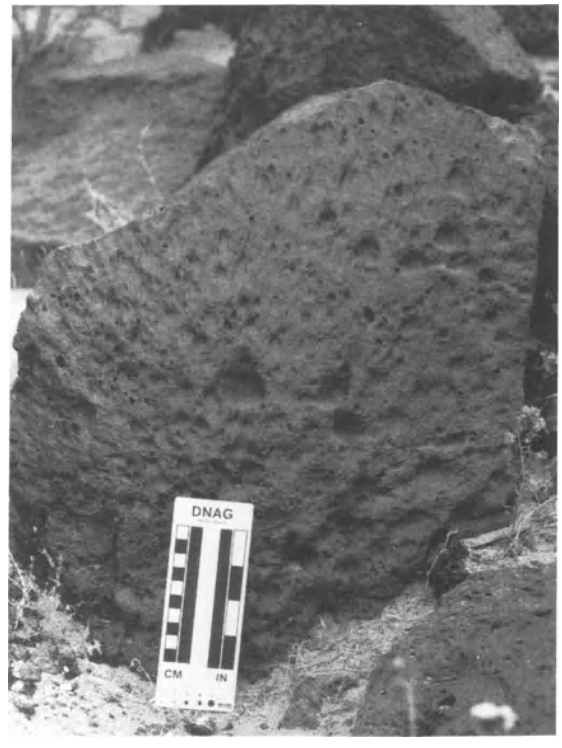

Figure 19.5 Pits developed on high-angle windward face in basalt. These features are relatively common in basalt and probably result from enlargement and integration of pre-existing vesicles. Rock varnish in grooves of surrounding ventifacts suggests that abrasion ceased approximately 5600 years BP (Laity 1991).

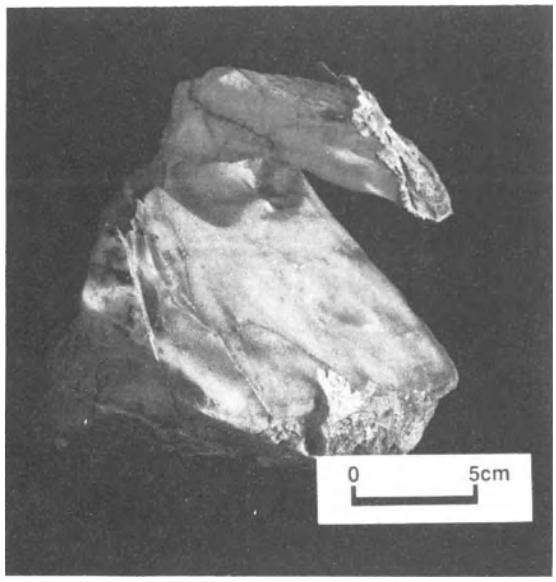

Figure 19.6 Large handle-like projection, 12 cm in length, extending from a marble ventifact. Thin veins of more resistant material in marble give rise to differential erosion. Direction of wind flow was from right to left.

may be so small as to be nearly indiscernible to the naked eye. Flutes form on surfaces that are horizontal or inclined at low angles (less than 40°) to the wind; flutes become shorter and deeper as the inclination of the surface steepens (Maxson 1940, Sharp 1949). They form independently of material hardness, composition, or rock structure. In the Namib Desert, larger and deeper flutes are associated with coarse-grained rocks, such as granites, and closely spaced flutes with fine-grained rocks, such as dolomites and volcanics (Lancaster 1984).

Flute development by aeolian processes is not understood. Maxson (1940) proposed that flutes are cut beneath vortices of fine sand, and Whitney (1978) argued that vortex pits may coalesce into flute pits and pit chains. Small pits were observed in the bottom of some flutes in the Namib Desert (Lancaster 1984). However, such features are not recorded elsewhere in the literature, and most flutes exhibit smooth interior surfaces that lack pits.

Grooves

Grooves are longer than flutes and open at both ends. They are best developed on surfaces gently

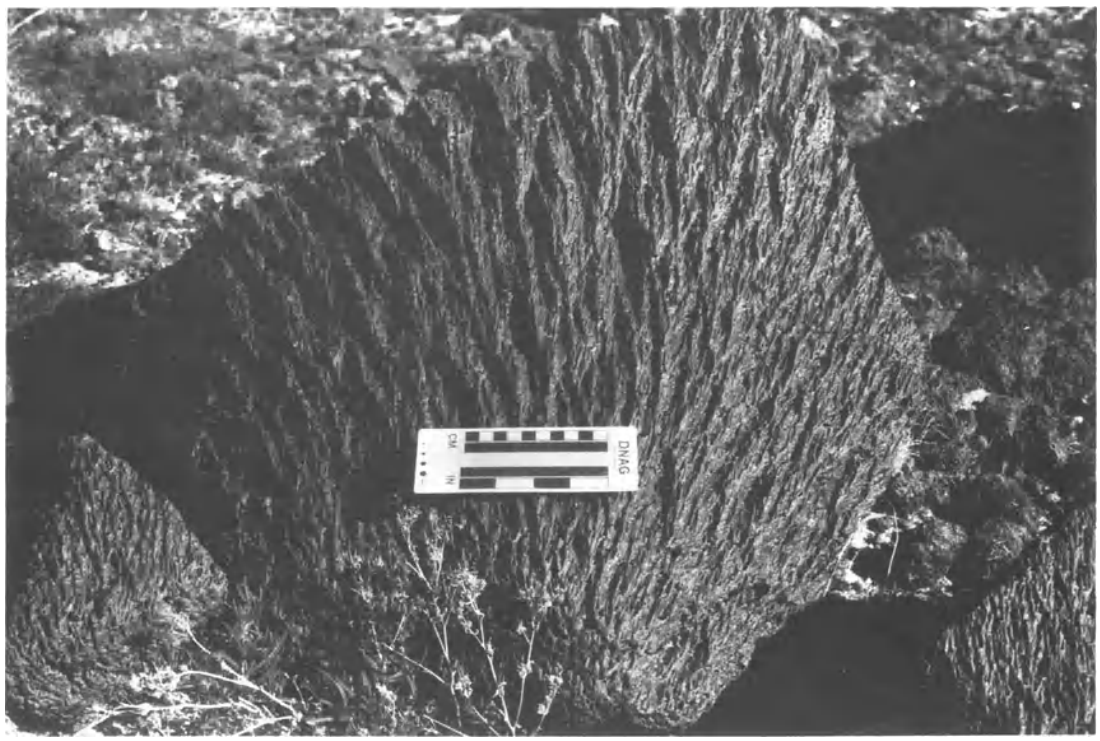

Figure 19.7 Ventifact formed in basalt boulder 0.6 m in diameter. The flutes and grooves radiate outward from a central area.

Figure 19.8 Detail of abrasion in marble. Two scales of grooves are found on this boulder face: fine striae with a wavelength measured in millimetres occur in association with larger grooves approximately 3 cm in width, 2 cm in depth, and 15 to 25 cm long. Fine aeolian sands are seen in the lower right-hand corner of the picture and in the larger grooves.

inclined or parallel to the wind and, like flutes, may cut indiscriminately across mineral grains and rock structures. Ventifact groove and flute trends are remarkably parallel on near-horizontal surfaces and reflect the flow direction of the highest velocity winds in an area (Laity 1987). On large curved surfaces facing the wind, the flutes or grooves radiate outward from a central pitted area (Fig. 19.7). Sharp (1949) observed that flutes and grooves are not mutually exclusive, for the surfaces of large grooves are often fluted on a small scale.

Tremblay (1961) characterized three scales of groove development based on his observations in northern Canada: striae are fine lineations (Fig. 19.8), grooves are of intermediate scale, and channels attain several centimetres in depth (up to 13 cm deep in his study area). None of the lineations exceeds a metre in length, and most are considerably shorter. Whereas fine striae appear to cross a whole outcrop, in detail each comprises a succession of short scoop-like depressions a few centimetres long.

As in the case of flutes, there is little understanding of the formation of grooves. According to Maxson (1940), grooves suggest vortices descending along the rock surface in the wind direction; once formed, the grooves may be modified by saltating grains at air velocities below those critical in the generation of vortices. Schoewe (1932) discovered that sand grains impinging at low angles on hard, smooth surfaces skid instead of rebounding directly into the air and proposed that this action may be related to the development of flutes and grooves.

Etching

Etching occurs when the composition of a rock mass is not homogeneous, and the wind selectively erodes less resistant strata or foliations. In contrast to flutes and grooves, the patterns formed on the rock are irregular in nature.

Helical Forms

Helical forms are not commonly recorded. They are particularly well developed in marble in the Mojave Desert, California. In form, they begin as shallow grooves, deepen and spiral in a downwind direction, and terminate in a sharp point (Figs 19.9 and

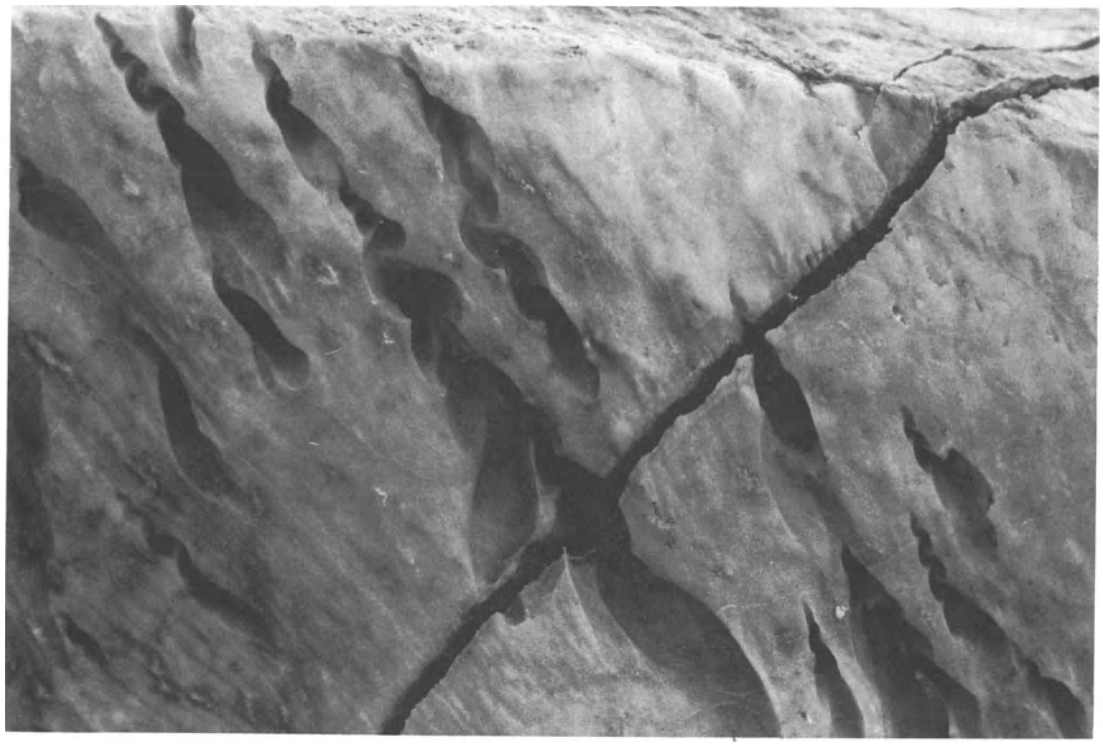

Figure 19.9 Helical forms developed in marble. These features occur at scales up to 20 cm in length and several centimetres in width and depth. The abrading agent is sand, some of which can be seen trapped within the large helical form bisected by a rock fracture.

19.10). They range from several millimetres to several centimetres in width and depth, appearing to maintain a consistent form as their scale increases. Helical forms may be found in association with flutes (Fig. 19.10). Their development is not understood, but preliminary observations suggest that they occur where wind velocities are very high, such as within topographic saddles near hill crests.

Processes of Rock Destruction

Three processes have been identified as having the potential for rock destruction in an aeolian regime: abrasion, deflation, and rock wedging. Abrasion results from the impact of particles either in saltation or suspension. Most rock abrasion is apparently accomplished by sand-sized (about 60 to 2000 μm in diameter) grains transported in saltation (Greeley *et al.* 1984). Finer material (Whitney and Dietrich 1973) and even the wind alone (Whitney 1979) have been shown in laboratory experiments to erode rock mass. The latter results primarily from deflation, the removal of previously weathered rock material by strong winds. As no ventifacts have yet been recorded from a region of pure air flow alone, and as particulate material is generally abundant, the efficacy of erosion by pure air need not be an issue. In some environments the apparent absence of sand has led to a consideration of snow as an abrasive (Teichert 1939, Dietrich 1977b, Schlyter 1989). However, experiments conducted on Baffin Island, Canada, by McKenna-Neuman and Gilbert (1986) showed that poles covered with eight coats of exterior enamel were rapidly stripped and eroded by aeolian sands, but remained perfectly preserved when subject to blowing snow and ice. These observations agree with those of other researchers (Blackwelder 1929, Tremblay 1961, Miotke 1982, Nero 1988), and indicate that sand is the most important agent of abrasion in cold climates. Recent observations by Hall (1989) in Antarctica suggest that wind-blown particles (sand, granules, and small pebbles) may cause rock breakdown by wedging. Grains moving at high velocity are packed into cracks, and succeeding particles impact grains that are already wedged. This process has yet to be recorded in warm deserts. Solution processes may play a role in enlarging or initiating pits or in

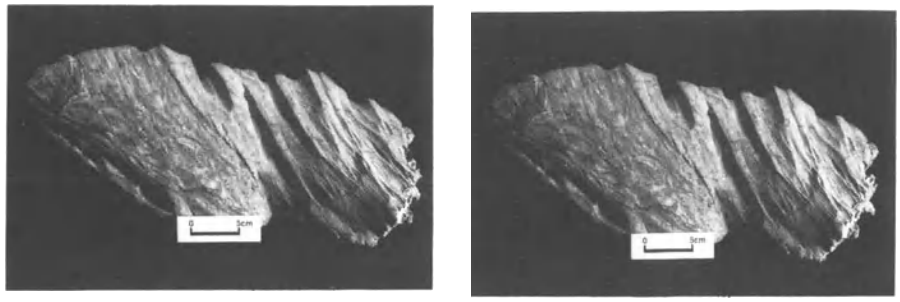

Figure 19.10 Stereo pair of a ventifact formed of marble. This ventifact shows deep grooves, helical scores, a smooth burnished surface, and a surface that slopes away from the prevailing wind. The back (leeward) side of the ventifact is rough and shows no evidence of wind erosion.

forming rills, but these processes appear subordinate to wind erosion (McCauley *et al.* 1980).

Nature of Abradant

Dust

Although most researchers attribute the formation of ventifacts to a sandblast action, dust has also been invoked to explain the formation of finely detailed features such as flutes and to explain the polish commonly observed. Higgins (1956) suggested that dust in suspension was the abrasive agent for small multifaceted pebbles embedded in bedrock but later concluded that the stones were probably not ventifacts (Higgins, personal communication 1988). Sharp (1949) considered that polish on ventifacts may result from material finer than sand. In the Namib Desert, Lancaster (1984) suggested that dust particles are probably more important than sand in creating smooth polished rock surfaces, flutes, and grooves, as the effects of sand laden winds would be akin to the destructive effects of industrial sand blasting processes. None the less, sand was abundant around the ventifacts he described and could be seen blowing across wind-eroded features. Maxson (1940) and Whitney (1978) attributed flutes or lineations to cutting by particles fine enough to follow vortex currents; most sand grains travelling by saltation probably pass through small vortices without much change of path.

Wind tunnel experiments by Dietrich (1977a) indicate that wind-blown materials which are relatively soft or small in particle diameter can produce some erosion. Dust was blown against blocks of low hardness (halite and sylvite) and against synthetic periclase continuously for 455 days. At the end of the experiment, the materials showed a change in surface microtexture, becoming rougher, but had no measurable loss in weight. As most natural materials are harder than those tested, and as dust storms are not common, averaging approximately 22 per year in warm deserts of Africa and the Middle East and less than 5 per year in North America (Middleton 1989), a very long period of time would be necessary to remove the mass essential for the development of ventifacts.

In a recent review of ventifact formation, Breed *et al.* (1989) summarized arguments for the role of dust abrasion as follows:

(a) Sandblasting is capable of abrading flattened surfaces seen on many faceted stones, but cannot account for the erosional markings (pits, flutes or grooves, helical scores) which may occur on all surfaces of ventifacts, and which appear too small and delicately textured to have been made by the impact of sand-sized grains. Ventifacts situated entirely within the saltation zone lack fine detail such as fluting on their windward faces.

(b) Ventifacts are rarely seen in or near fields of sand dunes, but are common on the stony surfaces of sand-poor regions.

(c) Sand blasting cannot explain the tapered forms of ventifacts, which typically have more rock mass eroded from their lee areas than from their windward.

(d) Very finely textured pits and flutes develop when materials are subject to dust erosion in the laboratory. Dust abrasion experiments conducted by Whitney (1979) generated micropitted surfaces, but pitting was rare on the windward surfaces. Some pits were aligned in chains and believed to be precursors to U-shaped flutes. A bubble-generating device was used to simulate the behaviour of low-speed suspended particles around a ventifact. The negative flow observed to the lee of a ventifact led McCauley *et al.* (1979) to conclude that pits and flutes on all sides of

rocks could be explained by wind from a single direction.

These points will be discussed further in the following section.

Sand

Despite laboratory evidence that dust is capable of abrading rock over long time periods, it is likely that sand is the most effective agent of abrasion in ventifact formation. Areas where sand has been identified as an agent of erosion include coastal environments (King 1936), periglacial regions (Powers 1936, Tremblay 1961, Miotke 1982, McKenna-Neuman and Gilbert 1986, Nero 1988), and desert regions (Sharp 1964, 1980, Sugden 1964, Selby 1977, Smith 1984, Laity 1991).

The following arguments may be made for the significant role of sand in aeolian erosion.

(a) Sand is a much more effective agent of erosion than dust. The mass of material lost per particle impact is directly proportional to the kinetic energy of impacting grains (Greeley *et al.* 1984, Anderson 1986). Particle size is a critical factor determining the susceptibility to abrasion of rocks S_a. Abrasion experiments using particles ranging in size from 75 to 160 μm (Greeley *et al.* 1982, 1984) show that S_a varies with particle diameter D to approximately the third power.

(b) Experiments also show that the amount of abrasion incurred by a ventifact impacted by particles less than 90 μm in diameter decreases much more rapidly with decreasing particle size and velocity than predicted by kinetic energy considerations or experiments using larger sized particles (Stewart *et al.* 1981). Two factors account for this. First, where clay particles are present in the entrained material, these particles are transferred to the surface of the target, sheltering it from subsequent abrasion by larger particles (a cushioning effect). Second, there is an apparent kinetic energy threshold for impact fracture, suggesting that the abrasion mechanisms change with kinetic energy.

(c) For suspended grains ($D \leq 0.31$ mm), Anderson (1986) showed that particle deflection by the air flow around the ventifact leads to a reduction in the delivery of kinetic energy to the surface. Thus, large particles are more likely to impact the surface than small particles. Sharp (1980) showed that the cutting rate increased coincident with the increased flux of windborne sand, and Tremblay (1961) related the amount of erosion by the wind to the availability of sand.

(d) The present-day absence of sand from a region does not preclude it from consideration as the primary abrasive agent. Mainguet (1972) and Sharp and Malin (1984) emphasized that the movement of sand in aeolian corridors tends to be episodic, so that sites which have been traversed by large quantities of saltating grains now harbour only small accumulations. Also, many ventifacts are relict, and the abrasive sand that carved them may have been deposited elsewhere.

(e) In some areas, the distribution of ventifacts is clearly associated with the presence of sand (King 1936, Tremblay 1961, Smith 1984, Laity 1991). In the eastern Mojave Desert fossil forms occur in association with deposits of stabilized sand or in aeolian corridors where sand has travelled to nearby sites of deposition. Actively forming ventifacts occur in rock outcrops presently being traversed by fine-grained sands (Figs 19.2, 19.8, and 19.11). Ventifacts are not found in areas subject to dust influx alone. More than a metre of silt has been deposited in some areas of the Cima volcanic field (Dohrenwend 1987), yet despite long exposure to dust, there is no evidence of abrasion on rock surfaces.

(f) Actively forming ventifacts lying within the saltation zone clearly demonstrate fine details on their surfaces (Figs 19.2, 19.8, 19.9, and 19.10). Sharp (1964) described the formation of flutes on bricks in a wind-driven sand environment. In the Little Cowhole Mountains, Mojave Desert, fine sands are seasonally redistributed by the winds, alternately burying and exposing rocks (Laity, unpublished data). All of the marble within the vicinity shows considerable mass removal and planation as well as sharply defined erosional markings (flutes, grooves, or helical forms) (Figs 19.9 and 19.10). Some of the striations are only 1 mm across, separated in parallel arrays by sharp ridges (Fig. 19.8). If sand is not responsible for the creation of these microfeatures, it could be argued that they would be destroyed by the protracted impact of saltating grains.

Saltating sand grains are also carried across the Amboy (Greeley and Iversen 1986) and Pisgah (Laity 1987) lava fields of the Mojave Desert. The flutes and grooves that occur on the subhorizontal flow surfaces are developed by saltating grains on a descending path. Near the surface, where wind velocity approaches zero, dust would be an ineffective agent of abrasion (Anderson 1986).

Figure 19.11 Marble ventifacts illustrate that maximum erosion occurs on the windward face. Direction of wind flow is from left to right, transporting fine- to medium-grained sand, shown surrounding the rocks. As a consequence of an increase in abrasion with height above the surface, ventifacts develop semi-planar faces, with the upper part receding more rapidly than the lower.

(g) Polished surfaces can result from sand abrasion. Ventifacts of the Pisgah lava flow demonstrate a high degree of sheen and are macroscopically smooth. Under a microscope there is abundant sand visible within the cavities and, at higher magnifications, scanning electron micrographs of flute interiors show considerable topographic roughness indicative of repeated chipping (Fig. 19.12). Occasional large impact structures have fresh cleavage facets that show no loss in definition at high magnifications (Laity 1991).

(h) Most ventifacts show significant erosion on their windward faces and no erosion on their lee surfaces (Blackwelder 1929, Sharp 1964). Indeed, this relationship, in addition to the development of diagnostic features such as facets and pits, has allowed the use of ventifacts in the reconstruction of palaeowinds and palaeoenvironments. Windward erosion is best observed on large boulders, which are not subject to the movement and overturning that allow successive faces to experience abrasion. In Blackwelder's (1929) study of boulders of about 1 m in height, the windward surfaces were found to be strongly grooved and drilled, whereas on the leeward face 'no such markings were found, but on the contrary the rocks are merely cracked and exfoliated in the ordinary manner' (p. 256). McKenna-Neuman and Gilbert (1986) observed that well-polished flutes and grooves developed on the windward face of ventifacts, whereas the lee face was typically covered in lichen and showed no evidence of abrasion. Regardless of rock lithology, ventifacts throughout the Mojave Desert clearly show the anticipated relationship between maximum abrasion on the windward face, and a facet that slopes away from the wind (Figs 19.11 and 19.13).

(i) Pits are generally considered to be diagnostic of high-angle impact by sand grains on windward faces (Sharp 1949). Studies of pitted surfaces and wind flow in the Mojave Desert confirm this relationship. Pits are not developed equally on all sides of rocks, but are limited to high-angle windward surfaces (Fig. 19.4) (Laity 1987, 1991, Smith 1984).

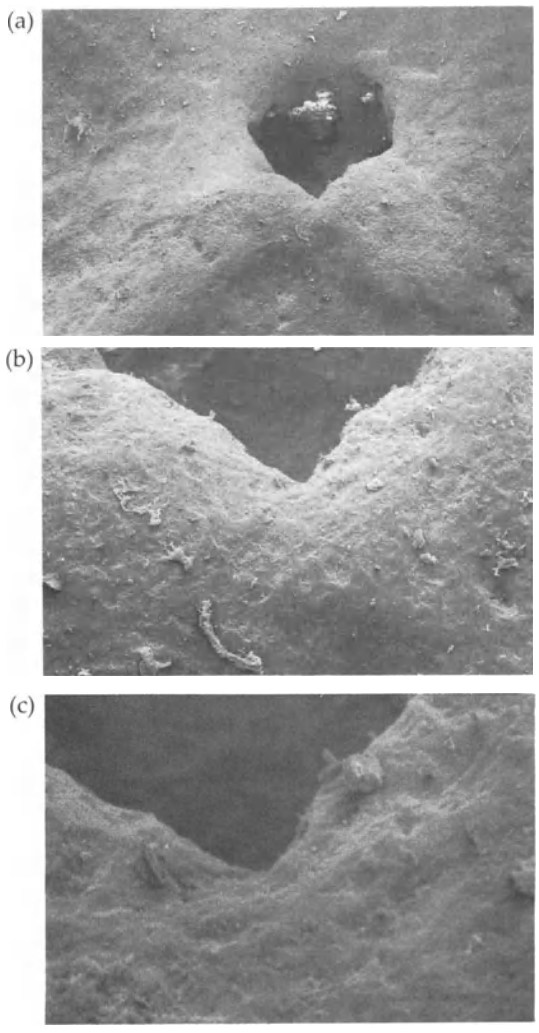

Figure 19.12 Three scanning electron micrographs of a basalt ventifact surface. (a) At low magnifications (50×) and when examined visually, the surface appears smooth and polished. Successively higher magnifications (at 260× and 1200×, (b) and (c) respectively) illustrate the chipped nature of the surface resulting from sand grain impact.

In summary, laboratory experiments have shown that dust is capable of changing the surface micromorphology of rocks but, in contrast to sand abrasion, mass removal is generally too small to be measured. To date, no actively forming ventifacts have been identified that develop in an environment dominated by dust. Dust has been invoked primarily as an agent in the formation of fossil ventifacts when a sand source is not evident, and to explain the polish and fine flutes and grooves that develop on ventifact surfaces. However, lack of sand in the immediate vicinity of ventifacts is not conclusive, as the movement of sand across landscapes is commonly episodic. Furthermore, ventifacts with polished surfaces and fine features are shown to occur in regions where sand dominates the flux of particles. In order to resolve the relative significance of dust and sand, further field work focusing on actively forming ventifacts must address questions of the nature and abundance of particles impacting the rock, the mechanism and rates of abrasion, and the evolution of specific features.

FORMATION OF VENTIFACTS

The formation of ventifacts has been assessed analytically, by wind tunnel experiments, and by field examination. Early wind tunnel experiments are discussed in Schoewe (1932). Laboratory experiments have sought to examine the nature of the abradant, the target material, and the wind on ventifact formation. Most studies have attempted to address questions concerning rates of abrasion. Many were conducted in tunnels which were too small to allow natural conditions of grain bounce and which did not replicate natural surface conditions. The abradant varied greatly in grain size (Schoewe 1932, Kuenen 1960, Whitney and Dietrich 1973, Dietrich 1977a) and in angularity (Miotke 1982), and little attempt was made to collect material that represented the size, shape, or sorting characteristics of material abrading ventifacts in the field. Owing to their slow rate of abrasion, natural rocks were seldom used as the target material. On the whole, laboratory studies have yielded little information on the long-term genesis of ventifacts and the development of specific microfeatures. However, wind abrasion in the field is extremely complex aerodynamically and it is impossible to completely reproduce such conditions in the laboratory.

With the exception of the pioneering work of Sharp (1964, 1980), field studies have not been process-oriented but have concentrated on aspects of ventifact morphology and on the use of ventifacts in palaeoclimatic interpretations. Anderson (1986) used a model of aeolian sediment transport to provide insight into the gross morphology of ventifacts, relating calculated kinetic energy fluxes of saltating particles to observed patterns of abrasion.

Magnitude of Erosion

The magnitude of ventifact erosion is dependent on the susceptibility of the rock to erosion, S_a (as determined by density, hardness, fracture–mecha-

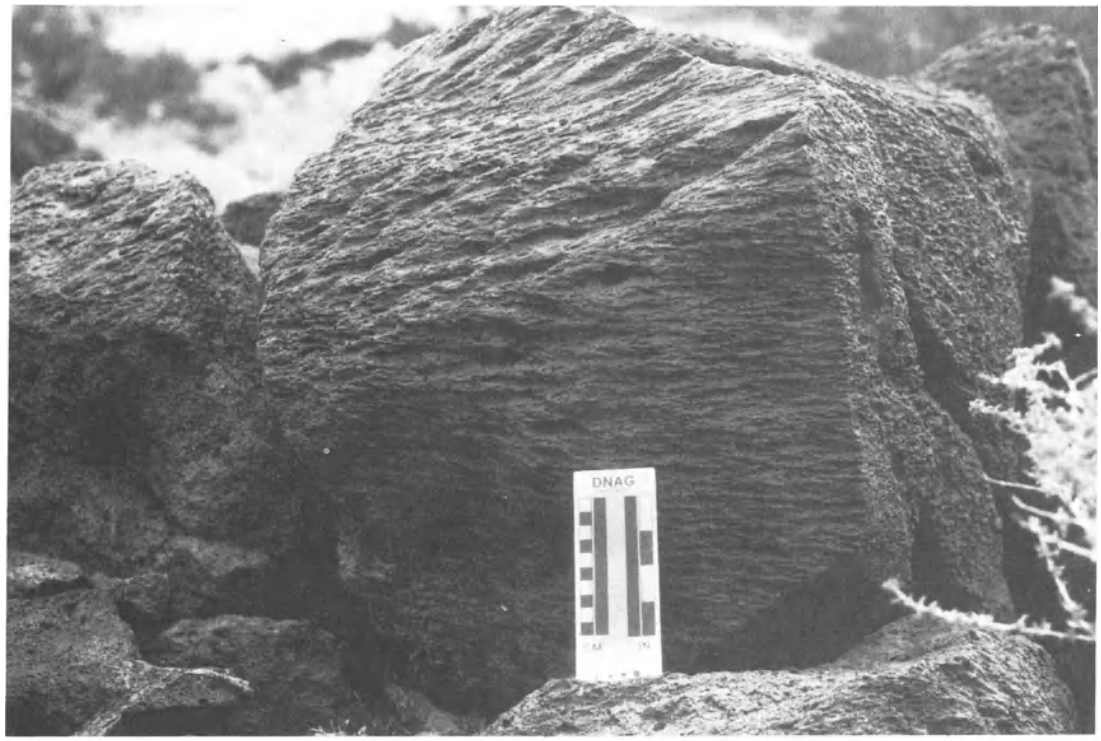

Figure 19.13 Ventifact formed of basalt. This photograph illustrates significant erosion on the windward face of the ventifact and the absence of erosion on the leeward face. Airflow and sand transport across basalt boulder fields results in complex patterns of erosion.

nical properties, and shape of the rock) and on properties of the impacting particle, such as particle diameter D, density ρ_p, speed V, and angle of incidence α (90° = perpendicular impact) (Greeley *et al.* 1984, Anderson 1986). The mass of material lost per impact, A (Scattergood and Routbort 1983) is

$$A = S_a \rho_p (V \sin\alpha - V_0)^n (D - D_0)^m \qquad (19.1)$$

where V_0 and D_0 are the threshold particle speed and diameter that will initiate erosion. Abrasion experiments indicate values of $n = 2$ and $m = 3$ (Anderson 1986). The mass of material removed per impact is roughly proportional to the kinetic energy of the impact.

Height of Abrasion and Development of the Erosion Profile

Ventifacts develop within the curtain of saltating sand grains, and their shape and development is dependent on particle fluxes within this zone. Saltating grains follow a path termed the saltation trajectory. Grain velocity increases throughout the path, reaching 50% of maximum velocity near the peak of the trajectory. In general, particles travelling at greater heights have higher velocities, owing to an increase in wind speed above the ground and the longer saltation paths that allow more time for them to be accelerated by the wind (Greeley *et al.* 1984). Calculated kinetic energy fluxes of saltating particles are greater where liftoff velocities are increased by grain bounce on elastic surfaces rather than mobile beds (Anderson 1986). In deserts, harder surfaces that promote grain bounce include extensive areas of stone pavement, boulder-strewn slopes, surfaces impregnated by late stage calcium carbonate, and exposed bedrock areas, including basalt flows. Such settings are subject to more vigorous erosion (Greeley and Iversen 1985, Laity 1987).

The range of effective sand abrasion rarely exceeds 1 m above the surface. Hobbs (1917) observed this limit on a variety of materials in Egypt, including cast-iron telegraph poles, thick adobe walls, and granite knobs, where a lower polished zone intersected the remaining weathered rock along a fairly sharp boundary. 'Pedestal rocks' develop as a result of concentrated erosion near the rock base, as shown in Figure 19.14. Ventifacts 1 m in height

Figure 19.14 Pedestal rock, approximately 5 m in height, resulting from aeolian abrasion at the base (photo courtesy of H. Hagedorn).

show sand blast effects to their upper surfaces (Fig. 19.3).

Within this general zone of abrasion, erosion profiles develop with distinct maxima of mass removal (Sharp 1964, 1980, Wilshire *et al.* 1981, Anderson 1986). The pattern of erosion is similar for all materials, although the magnitude depends on material properties. The height of maximum erosion is influenced by such parameters as wind speed and the degree of grain bounce. Sharp (1964, 1980) recorded erosion maxima 0.10 to 0.12 m above the surface in Lucite rods exposed to the wind for 15 years. Fence posts eroded during a 24-hour California storm showed maxima at an average elevation of 0.28 m on the upwind side of roads. Elevated heights of erosion resulted from higher grain bounce on road pavement, so that on the downwind side average maxima were recorded at an elevation of 0.43 m (Wilshire *et al.* 1981).

As a consequence of the increase in abrasion up to the maximum level, many ventifacts ultimately develop semi-planar faces, with the upper part of the abrasion face receding more rapidly than the lower part (Figs 19.2, 19.5, 19.10, and 19.11). Very large ventifacts may also exhibit a surface that slopes away from the prevailing wind (Fig. 19.3), but owing to the greater height and mass of the rock, to a limited time of exposure to abrasion, and to variable rock resistance, such features are usually less well developed than those of smaller ventifacts.

Friction with the ground results in wind speed that is minimal near the surface. A sill of uneroded material at ground level developed on bricks and hydrocal blocks in an experimental plot (Sharp 1964). Owing to the complexity of interactions between topography, wind flow, and shifting sands, such a sill is not always observed in nature. On subhorizontal surfaces such as lava flows, saltating grains on a descending path erode flutes and grooves.

Characteristics of the Particle

As discussed earlier, the composition, shape, size and quantity of windblown materials all affect the abrasion of rock. Greeley *et al.* (1984) showed that there is little difference in abrasion by quartz and basalt particles, that ash is less efficient in erosion, and that aggregates may be plastered on to the target, forming a protective coating, and thereby lessening erosion. Laboratory experiments have shown that abrasion increases with particle diameter and with angularity, but field studies have rarely assessed these characteristics. Greeley and Iversen (1986) collected and analysed samples of windblown material on Amboy lava field, California. In general, these samples were typical aeolian sands, consisting of fine- to medium-sized sand and being moderately well sorted. Additionally, Miotke (1982) observed that the sharp-edged weathering particles that develop in polar areas are particularly abrasive.

Sharp (1949, p. 185) characterized the amount of sand necessary for ventifact formation as being 'adequate but not too abundant'. He demonstrated a direct correlation between rates of erosion at his experimental plot and the influx of grains (Sharp 1964, 1980). Laboratory experiments show that where blowing sand concentrations are great, rebound effects from the target rock interfere with incoming grains and lessen the abrasion (Suzuki and Takahashi 1981). Furthermore, too great a supply of sand results in burial of ventifacts.

The role of the angle of incidence of the incoming grain to the target has been assessed primarily through wind tunnel experiments. Several studies have indicated that maximum abrasion occurs on faces inclined at angles of about 60° to the wind. Schoewe (1932) showed that the rate of abrasion on faces sloping at 30° is about one-third as great as on faces inclined at 60°. Thus, rates of abrasion change through time, becoming progressively less as the facet becomes more inclined. Rock faces pointing at higher angles into the wind abrade more slowly because rebounding grains hit incoming grains, slow

them, and result in lower impact energies (Greeley *et al.* 1982).

Needham (1937) measured the facet angle with the horizontal for very small ventifacts (up to 1 cm in diameter). Most (63%) fell within the range 45 to 69°, 22% had high angle faces (70 to 89°), whereas very few (15%) had low angle faces (25 to 44°). No ventifacts were measured with facet angles less than 25°.

Susceptibility to Abrasion of the Target Materials

The erodibility of different materials has been assessed experimentally by controlling for impact velocity, impact angle, and impacting particle size and type (Greeley and Iversen 1985). The bond strength of the rock appears more important than its hardness in predicting abrasion (Dietrich 1977a, Suzuki and Takahashi 1981). Experiments by Greeley *et al.* (1982) indicate that glassy materials such as obsidian will erode quickly for surfaces perpendicular to the wind, whereas crystalline materials such as granite and basalt erode more quickly when surfaces are subparallel to the wind.

Rate of Abrasion

Natural rates of abrasion are difficult to determine and are probably highly variable through time owing to the many different controlling factors that influence ventifact formation. Wind velocities are not constant, but vary according to season, time of day, and the passage of fronts. Most of the abrasion occurs during periods of high velocity winds, which occur for only a small percentage of the time. Abrasion rates also change because, as erosion progresses, the rocks gradually wear, changing the angle of incidence of the impacting grain. If abrasion is episodic through time, weathering of the rock between erosional episodes may prepare it for abrasion and increase subsequent rates of surface wear. Weathered material may also be partially removed by deflation.

Time-dependent particle flux also determines abrasion rates. Even when sand is available, it may move intermittently through an area. A 15-year study of abrasion by Sharp (1980) showed an annual rate of wear 15 times greater during the last 3-year interval than in preceding years owing to an increased flux of windborne material derived from nearby fluvial flooding debris. Megascopically visible effects (polish, pitting, and incipient fluting) developed within 10 months during periods of intense erosion characterized by an abundance of windborne particulate material (Sharp 1980). Ventifacts may be buried by sand for short periods of time and be protected. Over longer time periods, the availability of particles may decline through time owing to climatic change.

Greeley *et al.* (1984) summarized rates of abrasion inferred from various ventifact sites. They range from approximately 10^{-5} to 10^{-1} cm y^{-1}. Sharp (1964, 1980) concluded that ventifact formation in the Coachella Valley, California, would have required dozens or hundreds of years. In the central Namib Desert the faceting of boulders 10 to 50 cm in diameter is thought to have taken thousands of years to complete (Selby 1977). Abrasion rates appear much higher in Antarctica, primarily owing to higher wind speeds. Miotke (1982) suggested an erosion rate of 5 to 20 mm y^{-1}, based on laboratory simulations, and concluded that the rate of ventifact formation is largely dependent on wind velocity. Ventifacts are thought to develop in a number of days to months along storm-exposed coastlines, and in a number of hours with extremely high winds (Kuenen 1960). The significance of wind speed is supported by observations in the Mojave Desert, where one of the most important predictors of abrasion intensity is wind speed, as determined by topographic position of the ventifacts.

Attempts to correlate laboratory experiments on abrasion with field conditions have not been successful owing to the artificial conditions imposed by most wind tunnel experiments and the lack of wind frequency data and particle flux information for field sites.

Topographic Influences on the Development and Spatial Distribution of Ventifacts

Local and regional topography affect wind velocity, sand flux, and the direction of wind flow, and thereby influence the location of ventifacts, the orientation of flutes, grooves and facets, and the magnitude of erosion. Two topographic situations that commonly affect ventifact development are (a) wind speed increase through topographic constrictions, and (b) wind acceleration up the windward flanks of hills. At large scales, wind acceleration through constrictions may involve passage through a valley, and at a small scale, through a saddle or dip in an outcrop. A series of eight 100-m transects laid out at 2-km intervals in a topographic constriction in a structurally controlled valley in the Mojave Desert, California, showed that faceting and grooving affected 70 to 90 percent of all exposed cobbles and boulders. In the area downwind of the constric-

tion velocity generally declines as streamlines spread out, and ventifacts are absent (Laity 1987).

Wind also accelerates as it moves up the windward flanks of hills. This has recently been widely noted by meteorologists and has been considered with regard to dune development (Ash and Wasson 1983, Lancaster 1985). As wind moves over an isolated hill there is a compression of streamlines in the boundary layer that causes the wind to accelerate towards the crest of the slope and then to decelerate on the downwind side. This is important geomorphologically because the increase in wind speed over the surface of the hill produces increased sand transport as well as additional surface shear stress (Jackson and Hunt 1975, Lancaster 1985). Mason (1986) determined wind speed and direction at heights of 8 m measured continuously at ten sites around a smooth, nearly circular hill that rises 70 m above the surrounding terrain. Mean velocity $u(8)$ was reduced to a minimum of $0.8\,u(8)$ at the base of the upstream face and flow over the summit increased to $2.0\,u(8)$. These observations suggest that flow is reduced on the uphill face, increases on the sides and summit of the hill, and separates on the lee slope. The actual acceleration of wind depends on the height of the hill and the angle of the incident flow. The largest shear stress values, pressure changes, form drags, and wind velocities are recorded when the near-surface wind approaches approximately normal to the topography. The effect of velocity speed-up increases with the height of the topographic obstacle.

The threshold velocity for the movement of sand may be reached as a consequence of this acceleration of wind near the crest. Therefore, an increase in sand transport at higher elevations is anticipated. This effect is particularly marked because the rate of sand transport is proportional to the cube of the excess of wind velocity over the threshold velocity for sand movement (Bagnold 1941). Lancaster (1985) reported that with a $6.5\ \mathrm{m\ s^{-1}}$ wind, sand movement at the crest of a transverse dune is 19.5 times greater than at its base if the dune is 5 m high, and 121 times greater if the dune is 20 m high.

Wentworth and Dickey (1935), in their survey of ventifact localities in the United States, noted that many ventifacts occur on the surfaces or margins of mesas where pebbles are exposed to strong, persistent winds from adjacent areas of lower elevation. Field mapping of ventifacts in the Mojave Desert showed that upper hill slopes and crests are favourable sites for ventifact formation and that, in many cases, the intensity of abrasion, as measured by pit diameter and groove width and length, often increases with elevation up the slope (Laity 1987). Local topographically enhanced velocity increase may allow winds of moderate velocity to be effective in abrasion (McKenna-Neuman and Gilbert 1986). Where regional winds are of higher velocity, deep grooving and pitting may occur, particularly on large boulders that present high-angle faces to winds.

USE OF VENTIFACTS IN DETERMINING AN AEOLIAN REGIONAL HISTORY AND PALAEOCIRCULATION

Numerous investigators have shown that wind direction may be determined by reference to the position of the sharpest bounding edge of a facet, by pitting on the face, or by the direction of grooving and fluting (Maxson 1940, Selby 1977, McCauley *et al.* 1980, Laity 1987, Nero 1988). For faceted ventifacts, the keel is oriented in a large majority of cases at right angles to the wind (Maxson 1940): in the central Namib Desert 93% of ventifacts have facets indicating a dominant wind from the north-east (Selby 1977).

Fossil ventifacts provide an excellent record for palaeocirculation reconstruction. As small ventifacts can change their orientation through time, large stable boulders and outcrops are the best choice for mapping. The relict nature of ventifacts is often indicated by the weathered, dulled and partly exfoliated condition of the rock surfaces (Blackwelder 1929, Smith 1967, Smith 1984) and by the presence of rock varnish (Dorn 1986). Grooves and fluting may not cover the entire surface of the boulder, but rather occur in patches where weathering has failed to remove them (Powers 1936). The growth of vegetation surrounding ventifacts, the lack of any apparent wind-blown material, or the stabilization and incipient soil development of aeolian deposits also indicates the fossil nature of ventifacts.

Powers (1936) inferred palaeowind direction on fossil ventifacts in South Park, Colorado, using grooves on rock ledges. Sharp (1949) demonstrated that there were at least four separate periods of wind-cutting at four levels along the eastern base of the Big Horn Mountains, Wyoming. Pleistocene wind directions were measured by reference to wind-cut faces, flutes, grooves, and pits on large stable boulders. Ventifacts of the Athabasca sand dunes, north-western Saskatchewan, Canada, show sandblast features (facets, polishing) on both the north-west and south-east facing sides of boulders and cobbles, the former developed by present-day north-westerly winds and the latter by prevailing winds from the south-east during the mid- to early Holocene (Nero 1988). Tremblay (1961) also

observed that large areas of northern Saskatchewan and Alberta are marked by striations on outcrops and erratics indicating palaeowind flow from the south-south-east.

In the east-central Mojave Desert, California, three principal flow directions – westerly, northerly, and southerly – were identified from the analysis of mapped grooves (Smith 1984, Laity 1991). Relative ages of ventifacts were assessed by field relationships and an examination of the surface micromorphology of ventifacts. Numerical ages were determined from rock varnish that forms in rock grooves following the cessation of abrasion (Dorn 1986, Laity 1991). The results of the mapping and age-dating suggest that aeolian activity was probably greatest in the early to mid-Holocene and greatly diminished in the late Holocene. The widespread cessation of abrasion in the mid-Holocene is marked by weathering of the micro-impact structures in grooves and flutes, by the formation of rock varnish, and by the stabilization of sands in the immediate vicinity of ventifacts. Whereas the time of cessation of abrasion can be determined by varnish dating, it is more difficult to determine the onset of ventifaction and the time required for the ventifacts to form, as rates of abrasion depend on both material and climatic conditions that are largely unknown.

Problems in reconstructing surface palaeowinds by ventifact mapping occur when there has been more than one pulse of erosion and high velocity wind emanated from different directions in succeeding episodes. The most recent winds may erase the imprint of earlier activity, although in rare cases cross-grooves are discernible. Multiple episodes of erosion are best preserved in hilly or mountainous regions, because erosion by earlier winds may be preserved on topographically protected (leeward) slopes.

RIDGE AND SWALE SYSTEMS AND YARDANGS

Ridge and swale systems and yardangs are closely related features of aeolian erosion. Whereas yardangs have been reported from all deserts except those of Australia, ridge systems appear to be limited to the Saharan Desert of Africa.

RIDGE AND SWALE SYSTEMS OF THE SAHARA

Mainguet *et al.* (1980) considered the Sahara a single vast aeolian unit, with wind being the most active geomorphic agent. The region is divided into sectors where either sand transport or deposition dominates. Sand seas or ergs represent the depositional sector. Zones of sand transport are characterized by landforms of erosion, including wind-abraded ridge and swale systems, yardangs, and zones of deflation.

Figure 19.15 Space Shuttle image of ridges following, in an arc, the deflection of the trade winds around the Tibesti Mountains. The system crosses the Aorounga Crater, Chad, near the centre of the photograph.

Ridges and swales are best demonstrated by vast systems that occur in a zone bordering the Tibesti Mountains to the east, south, and west. On satellite and aerial images the ridges appear dark, owing to the well-developed patina of rock varnish, and the corridors show as lighter-coloured lineations. In orbital views, the systems appear to be continuous for hundreds of kilometres, sweeping in a broad arc around the mountains (Fig. 19.15). On aerial photographs (1:50 000), the discontinuous nature of the systems is evident, with the largest ridges not longer than 4 km (Mainguet 1972). In the Bembéché region, which lies to the north-east of Faya-Largeau, the ridges are very wide (up to 1 km) in proportion to their height (Fig. 19.16).

There are three factors that account for the development of these remarkable features in this region: (a) extensive exposures of sandstone, (b) a dense network of joints that allows the wind to be channelized, and (c) a monodirectional wind, charged with sand. The cover of Palaeozoic and Mesozoic sandstones is largely preserved on the southern flank of the mountains, whereas on the northern flank only isolated patches persist (Hagedorn 1980). The sandstone appears particularly sus-

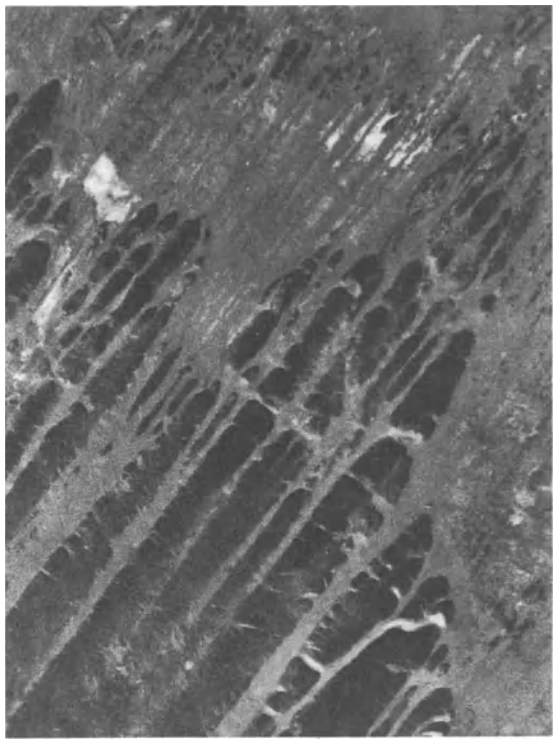

Figure 19.16 Ridge and swale systems of the Sahara. Scale 1:50 000. Vast systems occur in a zone bordering the Tibesti Mountains to the east, south, and west. On aerial images the ridges appear dark owing to rock varnish, and the swales show as lighter coloured. In the Bembéché region of Chad, illustrated here, the ridges are very wide (up to 1 km) in proportion to their height (Cliché Institut National Géographique, Paris).

ceptible to erosion, and forms of this type do not appear in basalts, crystalline bedrock, schists or siltstones (Mainguet 1972). In diatomites the ridges have a scale of development ten times less than that of sandstone.

The circum-Tibesti region is deformed and fractured along two major axes, NE–SW and NW–SE. Wind exploited the fracture system most closely aligned with its own direction, gradually enlarging corridors, the size of which is a function of the deviation between the wind direction and joint trends. Where the coincidence is best, the corridors are, with respect to the ridges, the least enlarged and the most regular in form. Fractures that run counter to the ridge trends are often exploited to form the fronts of ridges or yardings, these appearing to line up in a row.

The general direction of the wind is determined by trade wind circulation, except where it is diverted

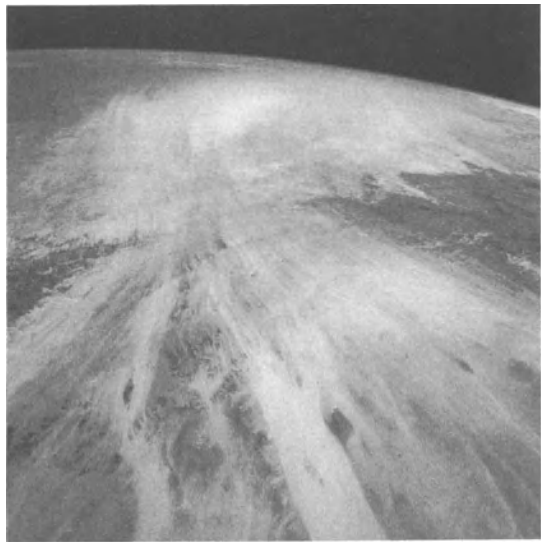

Figure 19.17 High oblique Space Shuttle view of an April sandstorm to the south of the Tibesti Mountains, Chad.

around major topographic obstacles such as the Tibesti Mountains. Northern Chad, to the east of the Tibesti, is characterized by the constancy of sand-laden winds that blow 8 months out of 12 from the north-east (Fig. 19.17). Maximum velocities are reached during the daytime, when sand is transported at velocities of 6 to 8 m s^{-1} or greater. The ridges follow, in an arc, the deflection of the wind.

The amount of sand in the corridors is variable, with some being totally engulfed. Sand abrasion acts preferentially in the corridors and is ineffective on the middle and upper slopes of ridges, which are marked by a deep patina above the basal fringe area of eroded rock. There is no evidence that deflation plays a significant role. Wider swales may be occupied by barchans, whose axes parallel those of the ridge systems and the resultant winds (Mainguet 1972) (Fig. 19.18). The barchans are indicative of sand transport through the region.

The channelized topography has a wavelength that, in cross-section, appears to be relatively constant for any given group of ridges and swales (Mainguet 1970). The periodicity is determined to some degree by the fracture density, but topography and wind strength also appear to play a role, with the largest ridges found on the more elevated parts of the terrain, and the smaller forms in the lowest. Abrupt changes in scale may occur as an escarpment is surmounted by the wind (Mainguet 1972). In some areas, two families of ridges and corridors may develop, with the larger system being the most

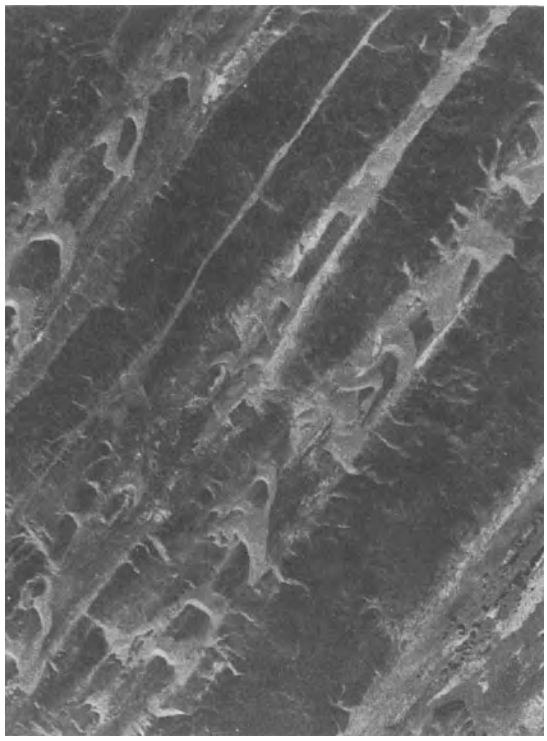

Figure 19.18 Sand transport through large ridge and swale systems. Scale 1:50 000. The swales are occupied by barchan dunes, whose axes parallel those of the ridge systems and the resultant winds (Cliché Institut National Géographique, Paris).

elevated and the longest, and the smaller superimposed within the corridors.

An interplay through time between fluvial and aeolian processes is evident. Lacustrine sediments occur in the largest aeolian corridors, apparently emplaced after the initial cutting of the ridges. Deposition was followed by a renewed phase of aeolian excavation. Lacustrine deposits, as well as ravines developed on the slopes of some ridges, suggest alternating wind and water dominance. Fluvial action may also have etched and enlarged many of the joints in the sandstone, thereby allowing wind channelization to occur. At the present time, wind action is dominant, and acts to erase most traces of fluvial activity.

YARDANGS

In contrast to ridge systems, yardangs are more streamlined and aerodynamic in form. They are often described as resembling an inverted ship's hull, although in many cases the yardangs are

Figure 19.19 Yardang in lacustrine sediments formed at the southern rim of the Lut Desert, Iran (photo courtesy of H. Hagedorn).

flat-topped. The windward face of the yardang is typically blunt-ended, steep and high, whereas the leeward end declines in elevation and tapers to a point (Fig. 19.19). It should be noted, however, that yardangs take on many forms (Figs 19.20 and 19.21) (Whitney 1983, Halimov and Fezer 1989). Measurements of yardang length:width ratios commonly average 3:1 or greater. This elongate form minimizes the drag or resistance to the wind. Yardangs form parallel to one another, typically occurring as extensive fields (Fig. 19.22), and they are oriented into the strongest regional winds. They may occur as tight arrays, separated from one another by either U-shaped or flat-bottomed troughs, or as widely spaced, highly streamlined features on wind-bevelled plains.

Yardangs have received attention as curiosities and geological oddities since the late 1800s. Stapff (1887) gave an account of 'aerodynamic landforms' sculpted out of bedrock in the Kuiseb valley of the Namib Desert of south-west Africa, and yardangs were described by Walther (1891, 1912) in Egypt and by Kozlov (1899) east of Lop Nor. The term yardang was introduced by Hedin (1903, volume 1, p. 350) to describe a labyrinth of clay 'terraces' in the Lop Nor (Nur) (Mongolian *nur* means lake) region at the eastern edge of the Taklimakan Desert in China which the natives of the area called yardang. Hedin (volume 2, p. 139) attributed their formation to initial erosion by running water, and subsequent resculpturing by the wind. More recent interest in yardangs was fostered by the discovery of large yardang fields on Mars (Ward 1979) and by the availability of aerial photography and satellite imagery (Mainguet 1972, Ward 1979, Halimov and Fezer 1989).

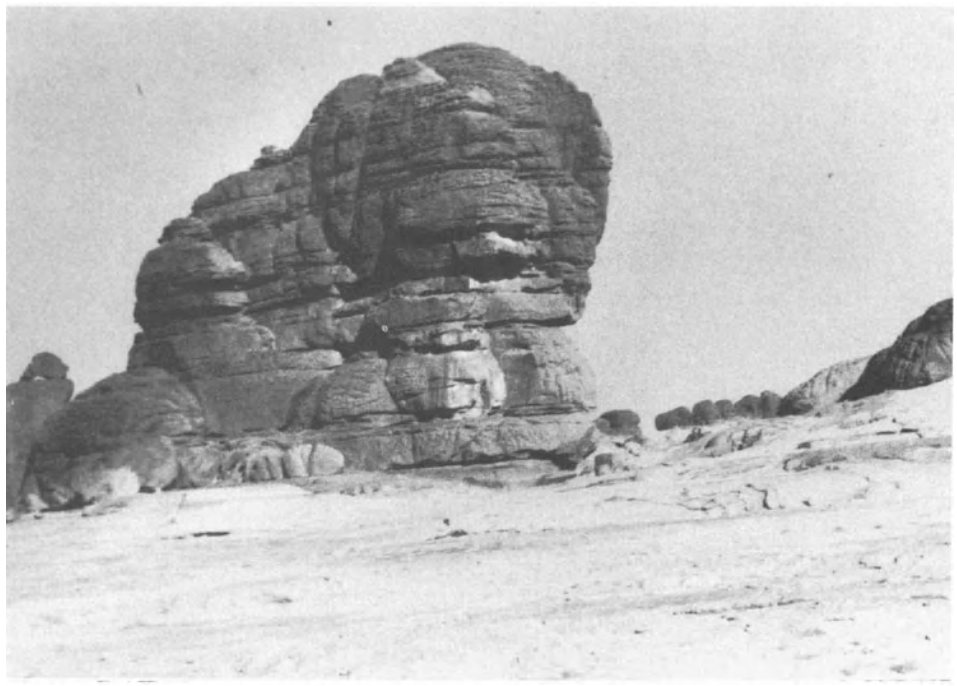

Figure 19.20 Large (more than 20 m high) yardang in sandstone of Cambrian age in the southern foreland of the Tibesti Mountains, Chad (photo courtesty of H. Hagedorn).

Figure 19.21 Yardangs in sandstone of Cambrian–Ordovician age in the foreland of the Djado Plateau, Niger, near the border with Libya. Note persons standing on top of the yardang for scale (photo courtesy of H. Hagedorn).

Figure 19.22 Oblique aerial photograph of wind erosion in the southern Borkou Highlands, Chad. Joints in the yardangs form blocks that are at right angles to the trend of the ridges. The upper limit of wind corrasion follows the transition from lighter to darker colours (photo courtesy of H. Hagedorn).

Like ventifacts, yardangs have not been studied in detail, and much remains to be determined about their formation. There is little meteorological information available for most yardang fields. Although it is apparent that most form in association with monodirectional wind regimes, the velocity of winds within the corridors and the frequency of sand-transporting winds are not known. Nor is there any knowledge of the interplay between wind and topography in major yardang and ridge systems. Our understanding of wind flow around individual yardangs is based primarily on laboratory and theoretical determinations (Ward and Greeley 1984, Whitney 1985), rather than instrumentation. The long-term evolutionary development of yardang fields, the role of fluvial erosion and jointing in initial channelization of winds, and the rates of formation are poorly understood. The role of abrasion and deflation in determining the ultimate form of yardangs also remains uncertain, and probably varies according to the rock type.

Factors Affecting the Distribution of Yardangs

Yardangs occur in desert regions on all continents except Australia. They occupy only a very small part of the Earth's surface, as they require conditions of great aridity, nearly unidirectional winds, and, in some cases, a favourable material and some assistance from weathering to form. None the less, aerial photography and satellite imagery show that many yardang fields are of great areal extent. McCauley *et al.* (1977) provide a comprehensive discussion of the Earth's major yardang fields. In Africa, yardangs occur in the Arabian Peninsula, Egypt, Libya, Chad, Niger, the Namib Desert of southern Africa, and possibly along the coast of Mauritania. Asia has several yardang fields, including those of the Taklimakan Desert in the Tarim Basin described by Hedin (1903), the Qaidam depression of Central Asia, and the large yardangs of the north-western part of the Lut Desert, Iran. Yardangs are found along the coastal desert of Peru in South America and a small group occurs in the Mojave Desert of North America.

Yardangs develop where wind processes dominate over fluvial processes, and are thereby limited to extremely arid deserts. In order for the wind to be effective, plant cover and soil development are generally minimal. In the Borkou region of Chad, no vegetation occurs expect where subsurface oasis water is within the reach of plant roots. Many

yardang fields develop where strong unidirectional winds occur throughout much of the year (Hobbs 1917, McCauley *et al.* 1977), but others, such as that of the Lut Desert, develop in regions of opposing winds that reverse direction seasonally. In areas of reversing winds, it appears that one wind is usually dominant and the opposing wind is lighter and less frequent.

Yardangs form in a broad range of geologic materials, including sandstones, limestones, claystones, granites, gneisses, schists, and lacustrine sediments. The lithologies of major yardang fields are summarized in Goudie (1989).

The role of topography in the development of yardangs has not been explored. A number of yardang fields, including those of Lop Nur and the Lut Desert, occur in topographic depresssions or are surrounded by mountain ranges that rise to considerable heights above the desert floor. Hagedorn (1980) observed that around the Tibesti Mountains there is an altitudinal zonation of geomorphic processes, with aeolian corrasion dominant at the lowest elevations, decreasing in intensity up to an altitude of 800 m. The modification of wind flow as it passes through the inter-yardang corridors is of considerable interest but has not been studied.

Form and Scale Relationships

Wind tunnel experiments and measurement of mature, streamlined yardangs suggest an ideal length-to-width ratio of 4:1 (Ward and Greeley 1984) independent of scale. Not all yardangs will achieve this form, however, owing to variations in lithology, wind strength and direction, and the length of time the yardangs have been in existence. The ideal proportions are probably approached only after a long period of erosion. In Peru, well-developed streamlined yardangs have ratios ranging from 3:1 to 10:1 (McCauley *et al.* 1977). Although usually of dimensions measured in a few metres, some yardangs can attain heights of as much as 200 m and be several kilometres long (Mainguet 1968).

The inter-yardang spaces have been variously termed troughs, couloirs, corridors, swales, and boulevards. Where the inter-yarding space is narrow, troughs appear to be U-shaped; as they widen their bottoms become flattened (Blackwelder 1934). In some cases, this latter development may be due to a resistant stratum, such as a hard clay layer. Although attention is often focused on the yardang, most of the geomorphic activity creating yardang fields appears to be concentrated in the troughs themselves. The troughs may be totally engulfed in sand, or be only partially sand covered (Mainguet 1972), show low transverse ridges of fine gravel (Blackwelder 1934) or ripple trains that diverge at the head and converge in the downwind direction around the yardang flanks (McCauley *et al.* 1977). Pebble-covered lag surfaces may develop around yardangs (Mainguet 1972). Corridors are commonly occupied by migrating barchan dunes whose major axes parallel those of the ridges and the resultant winds (Gabriel 1938, Hagedorn 1971, Mainguet *et al.* 1980). The rocks in the corridors often carry numerous marks of aeolian erosion, including longitudinal striations, and shallow erosional basins, metres or tens of metres in length, that occur either as isolated forms or in groups (Mainguet 1972).

Processes of Yardang Field Formation

Yardangs are probably produced by a combination of abrasion and deflation and are further modified by fluvial erosion and mass movement. The significance of each of these processes in determining the ultimate form varies according to yardang lithology and structure and the climatic history of the region.

Abrasion

In many yardang fields the passages are filled with aeolian sand (Grolier *et al.* 1980, Halimov and Fezer 1989) or gravel (Blackwelder 1934). Mainguet (1972) and Hagedorn (1971) emphasize the episodic nature of sand transport, so that yardang fields may be temporarily free of drifting sand even within a wind-corrasion landscape.

The role of abrasion in the formation of yardangs is evident in the overall shape and colour of the lower slopes. The windward end and lateral slopes are commonly polished and fluted by sand blasting to a height of one or two metres (Hobbs 1917, Hagedorn 1971, Grolier *et al.* 1980). In materials such as sandstone, the upper surface of the yardang is rough and unshaped by the wind and covered by a dark weathered crust, whereas the lower slopes are smoothed and appear white in colour (Fig. 19.22) (Hagedorn 1971, Mainguet 1972). Abrasion leads to undercutting of the steep windward face and lateral slopes (Fig. 19.23). Although most researchers have considered the fluting on lower slopes indicative of abrasion, Whitney (1984) believed that if sandblasting was significant these forms would be destroyed, and envisaged subsidiary flows that transport vortices and bring suspensates such as silt and fine sand into contact with the rock. This problem of

Figure 19.23 Rockshelter formed by wind at the foot of a sandstone yardang, Djado Plateau, Niger. Other yardangs are visible in the background (photo courtesy of H. Hagedorn).

interpretation is akin to that surrounding the formation of flutes and grooves on ventifacts.

Deflation

The significance of deflation in yardang evolution probably varies according to material induration. The dark patina of sandstone yardangs in the Sahara indicates that there is little active removal of material from the ridge summits, and indeed the varnish probably aids in cementing the grains and protecting them from deflation. Similarly, limestone yardangs of Egypt commonly have flat tops that are irregular in form and retain some of the weathered surface that pre-dates erosion (El-Baz *et al.* 1979), suggesting that deflation has been insignificant.

Deflation may be important in the evolution of yardangs found in less indurated lacustrine material. Formed in fine-bedded white siltstones, yardangs 30 to 50 m high and up to 1.5 km long on the Pampa de la Averia, Peru, possess smooth, streamlined shapes from base to crest (McCauley *et al.* 1977). The aerodynamic form is the primary evidence to support the role of deflation. However, there have been no field studies as yet to confirm that erosion and modification of yardangs take place by this process.

Researchers differ in their opinion as to the relative importance of abrasion and deflation in forming yardangs, even in a small yardang field such as that at Rogers Lake, California. These yardangs are carved in moderately consolidated deposits containing beds of fine gravel, sand, silt, and clay (Ward and Greeley 1984). McCauley *et al.* (1977) felt that the major process by which yardangs attain their streamlined shape and smooth ridge crests is deflation, as evidenced by the lack of small-scale grooving and scouring, and the winnowed appearance of the rocks caused by quartz grains and clay that are swept away in suspension. Abrasion is considered to play a minor role, causing some undercutting of the windward end and flanks and contributing to lowering of the troughs. On the other hand, Ward and Greeley (1984) considered abrasion to be the most important process in the development of the Rogers Lake yardangs, dominating trough formation and initial sculpting of the ridges. Thereafter, deflation increases in importance as it combines with abrasion to maintain the aerodynamic shape. Blackwelder (1934) also considered that the rounded form of low yardangs at Rogers Lake results from abrasion by saltating grains that flow both around and over the forms.

Fluvial Erosion

Running water acts in several ways to aid in yardang field development. At the outset, yardang fields may be initiated along stream courses that are enlarged and modified by the wind. Subsequently, the inter-yardang troughs may be fluvially eroded and the yardang slopes gullied. Proximity to piedmont slopes and their periodic streamflow was considered to be critical to the dissection of yardangs in the Lut Desert (Krinsley 1970). However, yardangs probably cannot persist in an increasingly humid climate, as more frequent fluvial erosion destroys the yardang form, and vegetation limits wind erosion.

Gullies develop on yardangs composed of relatively soft deposits, such as lakebed silts and clays. Ward and Greeley (1984) observed that intense aeolian abrasion destroys evidence of fluvial erosion at the windward ends of yardangs at Rogers Lake, that the more stable mid-sections harbour the largest gullies, and that at the leeward end gully development is hampered by deposition of a porous mantle of aeolian sediment. Small alluvial cones deposited at the base of the gullies are destroyed by sand blasting (Blackwelder 1934). Ward and Greeley (1984) suggested that the concave-upward form of yardang flanks at Rogers Lake results from sheetwash and gullying. They note that in more arid regions, such as coastal Peru, streamlined yardangs have broader crestlines and convex-upward flanks.

Intense gullying, earthflows, and solution on the flanks and summits characterize the yardangs of the Lut Desert of Iran (Krinsley 1970). These 60-m-high yardangs formed in playa sediments exhibit upper slopes well above the range of effective abrasion. Deflation is too slow a process to remove evidence of fluvial dissection. The gullies deepen during the winter rainy season, whereas aeolian processes dominate during the rest of the year.

In some cases, the gullies observed on the flanks of the yardangs may be relics of earlier wetter climates and be associated with lacustrine deposits in the inter-yardang corridors. In areas of the Sahara studied by Mainguet (1972), erosion of the deposits and the filling of the gullies by sand indicate that wind is now the dominant process.

Mass Movement

Mass movement has received little attention as a modifying process, although the presence of slump blocks alongside yardangs appears to be quite common, particularly where the nose of the yardang has been undercut or where the yardang is formed of strongly jointed materials such as sandstone.

Models of Yardang Development

Yardang fields may be initiated in gullies and fractures that are aligned parallel to the direction of the prevailing wind and become enlarged by this wind (Hedin 1903, Blackwelder 1934, Ward and Greeley 1984). As air enters the passage, the streamlines are compressed and the wind accelerates. Sand that is carried through the passage abrades the bottom and sides of the trough, causing the slopes to become progressively steeper (Blackwelder 1934). During the early stages of formation, wind and occasional fluvial erosion erode the passages more rapidly than the yardangs, causing the passages to deepen and the yardangs to grow (Halimov and Fezer 1989). The effects of abrasion are most evident within a metre of the floor of the trough, decreasing in intensity on the upper slopes of the yardang. The low levels to which abrasion is effective account for the commonly ragged appearance of the crests of yardang ridges.

Blackwelder (1934) suggested that yardang troughs are initially elongate and somewhat sinuous in form, become wider with time, and finally breach the ridges at places of weakness. As abrasion is more intense at the prows of the yardangs, the ridges become shorter and smaller, eventually developing into conical hills, mesas, and pyramids (Halimov and Fezer 1989). Blackwelder (1934) likened the processes that destroy the windward ends of yardangs to those which affect ventifacts or wind-abraded outcrops.

When the yardangs are lowered to approximately 1 m (Rogers Dry Lake) or 2 to 3 m (Qaidam Basin) in height, sand blasting affects the entire form, and the crests become more rounded and streamlined. In some cases, the hills vanish, leaving wide interspaces. Halimov and Fezer (1989) noted that only the streamlined whalebacks, which appear to be the most aerodynamically adjusted forms, survive for a long period. These progressive changes are slowed by two processes: the development of a wind-resistant lag material on aeolian sands, and the cementation of yardang walls by crusts variously composed of sand grains, loess, and salt.

Variations in the evolutionary form of yardangs occur because of material differences. Where the wind erodes horizontally layered rocks of varying resistances, tabular forms with protruding shelves or stair-step profiles are formed. On the other hand, inclined or vertically layered sediments will be eroded into ridges characterized by grooves and fins (Blackwelder 1934). Yardangs sometimes develop at angles to the structural grain of the rock. Joints and faults cross wind-shaped forms in the Sahara, and

differential erosion in schists may result in a structural grain that runs obliquely to the form of the yardang (Hagedorn 1971).

According to Halimov and Fezer (1989), the Qaidam depression of central Asia is the site of the largest yardang field on Earth. They used the morphologies of the large number of yardangs in this area as the basis of a classification system and considered that the form of the yardangs was indicative of the stage of development. Yardangs were classified into eight types: (a) mesas; (b) saw-toothed ridges where rocks offer variable resistance to erosion; (c) conical yardangs when the saw teeth become deeply eroded; (d) pyramidal forms that may resemble miniature Matterhorns ('the most frequent, variable and curious type' (pp. 210–1)) and include the largest yardangs; (e) very long ridges, measuring up to 5 km in length and parallel to one another; (f) hogbacks, a form that is more elongate than cones and pyramids, with some edges preserved despite a rounded form; (g) whalebacks with a rounded surface that may be entirely subject to sandblasting when lowered to about 2 m; and (h) low, streamlined whalebacks, varying in height from 0.5 to 3 m, with interspaces from 100 to 500 m. For this last type of yardang, the length : width : height ratio attains 10 : 2 : 1, the surface becomes rounded, and there is little drag. This type apparently forms under conditions of high wind speeds that result from a long fetch.

The rate of formation and modification of yardang fields is not known. Yardangs at Rogers Lake, Mojave Desert, appear to be eroding by abrasion of the headward end at a rate of $2\,cm\,y^{-1}$, and by lateral erosion caused by both abrasion and deflation at $0.5\,cm\,y^{-1}$. The attachment of some yardangs to the original shoreline deposits suggests that this small yardang field is still evolving. Halimov and Fezer (1989) calculated that small yardangs form in less than 1500 to 2000 years, based on dated pottery in the silt sediment. The Western Desert of Egypt has a very long history of wind excavation with erosion documented in the late Miocene or early Pliocene (El-Baz *et al.* 1979). A pronounced feature of this region is the almost complete absence of drainage lines, despite recurrent episodes less arid than the present.

Wind Tunnel Simulations of Yardang Development

Ward and Greeley (1984) conducted wind tunnel experiments to simulate yardang development. Natural rock samples require an impractical duration of exposure to abrasion before significant erosion occurs, and therefore synthetic sediments were used, and soap bubbles substituted for sand. Several forms (such as mounds and cubes) were moulded and subjected to uniform winds. The samples evolved in a common sequential order, which resulted in final length-to-width ratios of about 4 : 1. Erosion proceeded from the windward corners, to the front slope and crestline, to the leeward corners, and finally to the leeward slope. Abrasion dominated at the windward end of the yardang, whereas deflation and reverse flow were more important near the middle and at the leeward end. Rates of erosion were greatest at the beginning of the experiment and diminished as the form became more streamlined.

Streamlined shapes are developed by modification of the original form. Where the original form is broad, erosion decreases its width, and elongation may occur by deposition of a tail. If the original form is more elongate, the dominant change will be a decrease in length.

SMALL-SCALE AEOLIAN GROOVING

Small-scale channelling is a feature less often mentioned in the literature. Worrall (1974) described channelling on nearly horizontal surfaces in the Faya district of Chad. The grooves are remarkably parallel and regularly spaced, but shallow (a few centimetres in depth and width) and discontinuous. They occur in homogeneous diatomite and on saline crusts and are formed by saltating sand grains.

DESERT DEPRESSIONS

The role of wind erosion in the excavation of both small- and large-scale desert depressions is difficult to determine, as closed depressions may form by a number of different mechanisms, often acting in combination. These include (a) block faulting, (b) broad shallow warping, (c) crater lake development in volcanic areas, (d) chemical weathering and solution, (e) zoogenic processes, and (f) wind erosion.

The origin of very large enclosed basins, such as the noteworthy depressions of the Western Desert of Egypt (Siwa, Qattara, Baharia, Farafra, Dakhla, and Kargha), has been subject to several interpretations. Depressions occur along the boundaries of northward-dipping strata and are bounded to the north by escarpments and to the south have gently rising valley floors. The depressions are often cited as textbook examples of deflation, with the depth of erosion limited by the groundwater table which forms a base level (Ball 1927). Knetsch and Yallouze (1955) invoked tectonic action in their models of depression formation. Said (1960) excluded the pos-

sibility of a tectonic origin, noting the absence of faults in the regions, which indicates that uplift was not accompanied by any significant tensional stresses. The role of wind action is suggested by the conformity of depression locations with areas of thinner and more easily breached limestone capping. Recent work on the palaeoclimates of Egypt (Said 1981, 1983) has shown that the southern part of the Western Desert experienced a wet climate through most of the Tertiary and Quaternary, punctuated by brief episodes of aridity. Albritton *et al.* (1990) proposed that the Qattara Depression was originally excavated as a stream valley, subsequently modified by karstic activity, and further deepened and extended by mass wasting, deflation, and fluviatile processes. Thus, the depressions probably had a polygenetic origin, with wind erosion playing a major role only during arid phases of the Quaternary.

Debate over the origin of smaller depressions also indicates that a single mode of genesis is unlikely, and that several processes have probably contributed to their development. Remote sensing has revealed the widespread nature of such small-scale forms, termed pans. Deflation is often cited as a contributor to pan development in many arid or formerly arid environments. Pan initiation and growth appear to depend on materials that are susceptible to deflation, developing preferentially in poorly consolidated sediments, shales, and fine-grained sandstones. Pans may occur in interdunal basins, as palaeodrainage depressions aligned along former river courses, and by excavation on the floors of former pluvial lakes. The role of aeolian processes is evidenced by the widespread occurrence of lunette dunes to the lee of the pans and of clay pellets in downwind dunes, and by the analysis of Space Shuttle photography which shows that pans are source regions for dust storms (Middleton *et al.* 1986).

Aridity is important for pan development, in so far as lack of vegetation enhances wind flow and permits deflation of sediments made more susceptible as a result of salt weathering which produces fine-grained debris (Haynes 1982, Goudie 1989). As the depressions are enlarged, they become more attractive to grazing animals which further disrupt the surface, rendering it more prone to erosion (Goudie 1989).

CONCLUSIONS

Landforms of aeolian erosion vary greatly in size from vast systems of ridges several kilometres in length and up to one kilometre in width to small grooves only millimetres in amplitude. None the less, they exhibit many forms in common. Small faceted ventifacts exhibit shallow grooves; as ventifacts increase in size the grooves and flutes become more fully developed and dominate the form; outcrops in the immediate vicinity may be similarly abraded, as are the lower slopes of some yardangs; near-horizontal surfaces may be fluted and grooved; and ultimately small-scale aeolian grooving (Worrall 1974) may be transitional to yardangs and ridge and swale systems.

The two primary mechanisms of aeolian erosion are deflation and abrasion. Deflation contributes to the formation of large-scale features such as depressions and streamlined yardangs composed of easily erodible materials and may be instrumental in pavement formation. Abrasion is the primary process by which ventifacts form and is a major contributor to the development of yardangs and ridge systems in indurated material. Abrasion results from impact by either saltating or suspended material. Mass removal is greatest when large saltating grains impact a surface. Erosion by suspended grains is a much slower process, with particles commonly swept around an obstacle rather than striking it directly.

The origin of features such as flutes and grooves on the surfaces of ventifacts and yardangs is a matter of contention. It has been suggested that suspended materials are necessary to create fine detail on ventifact surfaces. Nevertheless, such features are commonly recorded in the saltation zone and are not damaged or destroyed by action of sand blasting, indicating that sand grains are primarily responsible for their formation.

Landforms of wind erosion have received much less attention than those of deposition and are as yet poorly understood. Fundamental questions as to the relative role of abrasion and deflation in the formation of yardangs, the nature of the abrasive agent and the mechanism of microfeature formation on yardangs and ventifacts, the interaction of yardang and ridge systems and wind flow, and the age, evolutionary history and rates of formation of erosional landforms remain unanswered and await further process-oriented research. Such studies will provide an improved basis for understanding the climatic and geomorphic history of arid regions.

REFERENCES

Albritton, C.C., J.E. Brooks, B. Issawi and A. Swedan 1990. Origin of the Qattara Depression, Egypt. *Bulletin of the Geological Society of America* **102**, 952–60.

Anderson, R.S. 1986. Erosion profiles due to particles entrained by wind: application of an aeolian sediment-transport model. *Bulletin of the Geological Society of America* **97**, 1270–8.

Antevs, E. 1928. Wind deserts in Iceland. *Geographical Review* **18**, 675–6.

Ash, J.E. and R.J. Wasson 1983. Vegetation and sand mobility in the Australian desert dunefield. *Zeitschrift für Geomorphologie Supplement Band* **45**, 7–25.

Babikir, A.A.A. and C.C.E. Jackson 1985. Ventifacts distribution in Qatar. *Earth Surfaces Processes and Landforms* **10**, 3–15.

Bagnold, R.A. 1941. *The physics of blown sand and desert dunes*. London: Chapman & Hall.

Ball, J. 1927. Problems of the Libyan Desert. *Geographical Journal* **70**, 209–24.

Blackwelder, E. 1929. Sandblast action in relation to the glaciers of the Sierra Nevada. *Journal of Geology* **37**, 256–60.

Blackwelder, E. 1934. Yardangs. *Bulletin of the Geological Society of America* **45**, 159–65.

Blake, W.P. 1855. On the grooving and polishing of hard rocks and minerals by dry sand. *American Journal of Science* **20**, 178–81.

Breed, C.S., J.F. McCauley and M.I. Whitney 1989. Wind erosion forms. In *Arid zone geomorphology*, D.S.G. Thomas (ed.), 284–307. New York: Wiley.

Bryan, K. 1931. Wind-worn stones or ventifacts – a discussion and bibliography. Washington, DC: *National Research Council Circular* 98, Report of the Committee on Sedimentation, 1929–1930, 29–50.

Czajka, W. 1972. Windschliffe als Landschaftmerkmal. *Zeitschrift für Geomorphologie* **16**, 27–53.

Dietrich, R.V. 1977a. Impact abrasion of harder by softer materials. *Journal of Geology* **85**, 242–6.

Dietrich, R.V. 1977b. Wind erosion by snow. *Journal of Glaciology* **18**(78), 148–9.

Dohrenwend, J.C. 1987. Basin and Range. In *Geomorphic systems of North America*, W.L. Graf (ed.), 303–42. Boulder, CO: Geological Society of America, Centennial Special Volume 2.

Dorn, R. 1986. Rock varnish as an indicator of aeolian environmental change. In *Aeolian geomorphology*, W.G. Nickling (ed.), 291–307. Boston: Allen & Unwin.

El-Baz, F., C.S. Breed, M.J. Grolier and J.F. McCauley 1979. Eolian features in the Western Desert of Egypt and some applications to Mars. *Journal of Geophysical Research* **84**, 8205–21.

Evans, J.W. 1911. Dreikanter. *Geological Magazine* **8**, 334–5.

Gabriel, A. 1938. The southern Lut and Iranian Baluchistan. *Geographical Journal* **92**, 193–210.

Garvin, J.B. 1982. Characteristics of rock populations in the western desert and comparison with Mars. In *Desert landforms of southwest Egypt: a basis for comparison with Mars*. F. El-Baz and T.A. Maxwell (eds), 261–80. Washington, DC: National Aeronautics and Space Administration, Contractor Report 3611.

Gilbert, G.K. 1875. Report on the Geology of Portions of Nevada, Utah, California, and Arizona. *Geographical and Geological Surveys West of the 100th Meridian*, 3.

Glennie, K.W. 1970. *Desert sedimentary environments*. Developments in Sedimentology, No. 14. Amsterdam: Elsevier.

Goudie, A.S. 1989. Wind erosion in deserts. *Proceedings of the Geologists' Association* **100**, 89–92.

Greeley, R. and J.D. Iversen 1985. *Wind as a geological process*. Cambridge: Cambridge University Press.

Greeley, R. and J.D. Iversen 1986. Aeolian processes and features at Amboy Lava field, California. In *Physics of desertification*, F. El-Baz and M. Hassan (eds), 210–40. Dordrecht: Martinus Nijhoff.

Greeley, R., R.N. Leach, S.H. Williams, B.R. White *et al.* 1982. Rate of wind abrasion on Mars. *Journal of Geophysical Research* **87**, B12, 10 009–14.

Greeley, R., S.H. Williams, B.R. White, J.B. Pollack, *et al.* 1984. Wind abrasion on Earth and Mars. In *Models in geomorphology*, M.J. Woldenberg (ed.), 373–422. Boston: Allen & Unwin.

Grolier, M.J., J.F. McCauley, C.S. Breed and N.S. Embabi 1980. Yardangs of the Western Desert. *Geographical Journal* **146**, 86–7.

Hagedorn, H. 1971. Untersuchungen über Relieftypen arider Räume an Beispielen aus dem Tibesti-Gebirge und seiner Umgebung. *Zeitschrift für Geomorphologie Supplement Band* **11**, 1–251.

Hagedorn, H. 1980. Geological and geomorphological observations on the northern slope of the Tibesti Mountains, central Sahara. In *The geology of Libya*, Volume III, M.J. Salem and M.T. Busrewil (eds), 823–35. London: Academic Press.

Halimov, M. and F. Fezer 1989. Eight yardang types in central Asia. *Zeitschrift für Geomorphologie* **33**, 205–17.

Hall, K. 1989. Wind blown particles as weathering agents? An Antarctic example. *Geomorphology* **2**, 405–10.

Haynes, C.V. 1982. The Darb El-Arba'in desert: a product of Quaternary climatic change. In *Desert landforms of southwest Egypt: a basis for comparison with Mars*. F. El-Baz and T.A. Maxwell (eds), 91–117. Washington, DC: National Aeronautics and Space Administration, Contractor Report 3611.

Hedin, S. 1903. *Central Asia and Tibet*. New York: Greenwood Press.

Hickox, C.F. 1959. Formation of ventifacts in a moist, temperate climate. *Bulletin of the Geological Society of America* **70**, 1489–90.

Higgins, C.G., Jr 1956. Formation of small ventifacts. *Journal of Geology* **64**, 506–16.

Hobbs, W.H. 1917. The erosional and degradational processes of deserts, with especial reference to the origin of desert depressions. *Annals of the Association of American Geographers* **7**, 25–60.

Jackson, P.S. and J.C.R. Hunt 1975. Turbulent flow over a low hill. *Quarterly Journal of Royal Meteorological Society* **101**, 929–55.

King, L.C. 1936. Wind-faceted stones from Marlborough, New Zealand. *Journal of Geology* **44**, 201–13.

Knetsch, G. and M. Yallouze 1955. Remarks on the origin of the Egyptian oasis depressions. *Bulletin Societe Géographique Egypte* **28**, 21–33.

Kozlov, R.K. 1899. *Otschet pomoshnika nachaunica expedici*. Moskva.

Krinsley, D.B. 1970. A geomorphological and palaeoclimatological study of the playas of Iran. *U.S. Geological Survey Final Report*, Contract No. PRO CP 70-800.

Kuenen, P.H. 1960. Experimental abrasion 4: eolian action. *Journal of Geology* **68**, 427–49.

Laity, J.E. 1987. Topographic effects on ventifact development, Mojave Desert, California. *Physical Geography* **8**, 113–32.

Laity, J.E. 1991. Ventifact evidence for Holocene wind patterns in the east-central Mojave Desert. *Zeitschrift für Geomorphologie, Supplement Band* **84**, 1–16.

Lancaster, N. 1984. Characteristics and occurrence of wind erosion features in the Namib Desert. *Earth Surfaces Processes and Landforms* **9**, 469–78.

Lancaster, N. 1985. Variations in wind velocity and sand transport on the windward flanks of desert sand dunes. *Sedimentology* **32**, 581–93.

Lindsay, J.F. 1973. Ventifact evolution in Wright Valley, Antarctica. *Bulletin of the Geological Society of America* **84**, 1791–8.

Mainguet, M. 1968. Le Bourkou – Aspects d'un modelé éolien. *Annales de Géographie* **77**, 296–322.

Mainguet, M. 1970. Un étonnant paysage: les cannelures gréseuses du Bembéché (N. du Tchad). Essai d'explication géomorphologique. *Annales de Géographie* **79**, 58–66.

Mainguet, M. 1972. *Le modelé des grès*. Paris: Institute Geographie National.

Mainguet, M., L. Canon and M.C. Chemin 1980. Le Sahara: géomorphologie et paléogéomorphologie éoliennes. In *The Sahara and the Nile; Quaternary environments and prehistoric occupation in northern Africa*, M.A.J. Williams and H. Faure (eds), 17–35.

Mason, P.J. 1986. Flow over the summit of an isolated hill. *Boundary-Layer Meteorology* **37**(4), 385–405.

Maxson, J.H. 1940. Fluting and faceting of rock fragments. *Journal of Geology* **48**, 717–51.

McCauley, J.F., C.S. Breed and M.J. Grolier 1977. Yardangs. In *Geomorphology in arid regions*. D.O. Doehring (ed.), 233–69. Boston: Allen & Unwin.

McCauley, J.F., C.S. Breed, M.J. Grolier and F. El-Baz, 1980. Pitted rocks and other ventifacts in the western desert. In *Journey to the Gulf Kebir and Uweinat*, F. El-Baz (ed.), *Geographical Journal* **146**, 84–5.

McCauley, J.F., C.S. Breed, F. El-Baz, M.I. Whitney, *et al.* 1979. Pitted and fluted rocks in the Western Desert of Egypt: Viking comparisons. *Journal of Geophysical Research* **84**, 8222–32.

McKenna-Neuman, C. and R. Gilbert 1986. Aeolian processes and landforms in glaciofluvial environments of southeastern Baffin Island, N.W.T., Canada. In *Aeolian geomorphology*, W.G. Nickling (ed.), 213–35. Boston: Allen & Unwin.

Middleton, N.J. 1989. Desert dust. In *Arid zone geomorphology*, D.S.G. Thomas (ed.), 262–83. New York: Wiley.

Middleton, N.J., A.S. Goudie and G.L. Wells 1986. The frequency and source areas of dust storms. In *Aeolian geomorphology*, W.G. Nickling (ed.), 237–59. Boston: Allen & Unwin.

Miotke, F. 1982. Formation and rate of formation of ventifacts in Victoria land. *Polar Geography and Geology* **6**, 98–113.

Needham, C.E. 1937. Ventifacts from New Mexico. *Journal of Sedimentary Petrology* **7**, 31–3.

Nero, R.W. 1988. The ventifacts of the Athabasca sand dunes. *The Musk Ox* **36**, 44–50.

Powers, W.E. 1936. The evidences of wind abrasion. *Journal of Geology* **44**, 214–19.

Said, R. 1960. New light on the origin of the Qattara depression. *Bulletin Societe Géographique Egypt* **33**, 37–44.

Said, R. 1981. *The geological evolution of the River Nile*. Berlin: Springer.

Said, R. 1983. Remarks on the origin of the landscape of the eastern Sahara. *Journal of African Earth Sciences*, 153–8.

Scattergood, R.O. and J.L. Routbort 1983. Velocity exponent in solid-particle erosion. *Journal of the American Ceramic Society* **66**, C184–6.

Schlyter, P. 1989. Periglacial ventifact formation by dust or snow, some south Swedish examples. Second International Conference on Geomorphology, Symposium No. 5 *'Polar Geomorphology'*, Bremen.

Schoewe, W.H. 1932. Experiments on the formation of wind-faceted pebbles. *American Journal of Science* **24**, 111–34.

Selby, M.J. 1977. Palaeowind directions in the central Namib Desert, as indicated by ventifacts, *Madoqua* **10**, 195–8.

Sharp, R.P. 1949. Pleistocene ventifacts east of the Big Horn Mountains, Wyoming. *Journal of Geology* **57**, 173–95.

Sharp, R.P. 1964. Wind-driven sand in Coachella Valley, California. *Bulletin of the Geological Society of America* **75**, 785–804.

Sharp, R.P. 1980. Wind-driven sand in Coachella Valley, California: further data. *Bulletin of the Geological Society of America* **91**, 724–30.

Sharp, R.P. and M.C. Malin 1984. Surface geology from Viking landers on Mars: a second look. *Bulletin of the Geological Society of America* **95**, 1398–412.

Smith, H.T.U. 1967. Past versus present wind action in the Mojave Desert region, California. *Air Force Cambridge Research Laboratories*, 67-0683, 1–26.

Smith, R.S.U. 1984. Eolian geomorphology of the Devils Playground, Kelso Dunes and Silurian Valley, California. In *Western geological excursions. Vol. 1: Geological Society of America 97th annual meeting field trip guidebook, Reno, Nevada*, J. Lintz (ed.), 239–51.

Stapff, F.M. 1887. Karte des unteren Khuisebtals. *Petermanns Geographische Mitteilungen* **33**, 202–14.

Stewart, G., D. Krinsley and J. Marshall 1981. An experimental study of the erosion of basalt, obsidian and quartz by fine sand, silt and clay. *National Aeronautics and Space Administration Technical Manual* 84211, 214–5.

Sugden, W. 1964. Origin of faceted pebbles in some recent desert sediments of southern Iraq. *Sedimentology* **3**, 65–74.

Suzuki, T. and K. Takahashi 1981. An experimental study of wind abrasion. *Journal of Geology* **89**, 23–36.

Teichert, C. 1939. Corrasion by wind-blown snow in polar regions. *American Journal of Science* **37**, 146–8.

Travers, W.T.L. 1870. On the sandworn stones of Evan's Bay. *Transactions of the New Zealand Institute* **2**, 247–8.

Tremblay, L.P. 1961. Wind striations in northern Alberta and Saskatchewan, Canada. *Bulletin of the Geological Society of America* **72**, 1561–4.

Walther, J. 1891. Die Denudation in der Wüste und ihre geologische Bedeutung. *Abhandlungen Sächsische Gesellschaft Wissenshaft* **16**, 345–570.

Walther, J. 1912. *Das Gesetz der Wüstenbildung in Gegenwart und Vorzeit*. Leipzig: Von Quelle und Meyer.

Ward, A.W. 1979. Yardangs on Mars: evidence of recent wind erosion. *Journal of Geophysical Research* **84**, B14 8147–63.

Ward, A.W. and R. Greeley 1984. Evolution of the yardangs at Rogers Lake, California. *Bulletin of the Geological Society of America* **95**, 829–37.

Wentworth, C.K. and R.I. Dickey 1935. Ventifact localities in the United States. *Journal of Geology* **43**, 97–104.

Whitney, M.I. 1978. The role of vorticity in developing lineation by wind erosion. *Bulletin of the Geological Society of America* **89**, 1–18.

Whitney, M.I. 1979. Electron micrography of mineral surfaces subject to wind-blast erosion. *Bulletin of the Geological Society of America* **90**, 917–34.

Whitney, M.I. 1983. Eolian features shaped by aerodynamic and vorticity processes. In *Eolian sediments and processes*, M.E. Brookfield and T.S. Ahlbrandt (eds), 223–45. Amsterdam: Elsevier.

Whitney, M.I. 1984. Comments on 'Shapes of streamlined islands on Earth and Mars: experiments and analyses of the minimum-drag form'. *Geology* **12**, 570–1.

Whitney, M.I. 1985. Yardangs. *Journal of Geological Education* **33**, 93–6.

Whitney, M.I. and R.V. Dietrich 1973. Ventifact sculpture by windblown dust. *Bulletin of the Geological Society of America* **84**, 2561–82.

Williams, S. and R. Greeley 1981. Formation and evolution of playa ventifacts, Amboy, California. *National Aeronautics and Space Administration Technical Memorandum* 84211, 197–9.

Wilshire, H.G., J.D. Nakata and B. Hallet 1981. Field observations of the December 1977 wind storm, San Joaquin Valley, California. In *Desert dust*, T.J. Péwé (ed.), 233–51. Geological Society of America Special Paper 186.

Woodworth, J.B. 1894. Post-glacial aeolian action in southern New England. *American Journal of Science* **47**, 63–71.

Worrall, G.A. 1974. Observations on some wind-formed features in the southern Sahara. *Zeitschrift für Geomorphologie* **18**, 291–302.

PART EIGHT

CLIMATIC CHANGE

ROCK VARNISH AS EVIDENCE OF CLIMATIC CHANGE

20

Ronald I. Dorn

INTRODUCTION

Rock varnish is a paper-thin coating of up to about 70% clay minerals cemented to the underlying rock by oxides of iron and manganese (Potter and Rossman 1977, 1979). The distribution, characteristics, and origin of rock varnish are reviewed by Dorn (1991). This chapter presents a review of how rock varnish may be used to reconstruct palaeoenvironmental fluctuations in alkalinity (Dorn 1984, 1990), dust (Dorn 1986), and stable carbon isotopes (Dorn and DeNiro 1985). Possible new methods are also proposed for reconstructing past geomorphic environments by using fluctuations in lead and erosional unconformities within varnish.

Rock varnish has three properties that make its investigation as a palaeoenvironmental indicator worth while. First, it is ubiquitous in deserts. Second, the length of the varnish record can be quite long; varnish on older landforms can record hundreds of thousands of years of environmental fluctuations. Third, varnish contains unique palaeoenvironmental information not available from other sources, such as concentration of airborne dust being deposited, alkalinity, and stable carbon isotope values of plants adjacent to varnish.

A basic premise of this chapter is that the nature of rock varnish is influenced by the surrounding environment. As the environment changes, so do certain textural and microchemical characteristics of varnish. Five conditions must be met before palaeoenvironmental data can be successfully extracted from rock varnish.

(a) *The environmental signal in rock varnish forms as a synsedimentary deposit.* Deposition of the signal inherent in varnish must be continuous, without erosional episodes. Figure 20.1 presents varnishes that meet this condition, while Figure 20.2 illustrates varnishes that are inappropriate for palaeoenvironmental analysis due to erosional unconformities.

(b) *The rock varnish investigated is exposed only to the atmosphere.* Rock varnishes do frequently form in the subsurface (Dorn and Oberlander 1982, Douglas 1987). Although they might be useful in assessing subsurface conditions, these types of varnishes have not been examined as possible palaeoclimatic research tools.

(c) *Manganese and iron in varnish are not reworked by solution after deposition.* Figure 20.3 shows examples of remobilization and redeposition of varnish constituents, in contrast to the even layering in Figure 20.1.

(d) *The palaeoenvironmental signal can be reproduced from spot to spot on a rock, from rock to rock at a site, and from site to site in a region.* The character of rock varnish at any given place reflects the microenvironment only at that particular site, and similarly the palaeoenvironment at that place. For a more regional environmental signal to be extracted from rock varnish, the results of any given profile must be reproduced to filter out 'noise' created by changes unique to specific microsites.

(e) *Some time control exists for the onset of varnishing.* A numerical age for exposure of the rock surface underlying the varnish may be a K/Ar date for a lava flow, a ^{14}C date on shells from an ancient beach ridge, ^{36}Cl or ^{3}He age on rock exposure, or varnish dating by ^{14}C, cation-ratio, or uranium-series dating. With continuous deposition and knowing the age of the base of the varnish, a sequence of palaeoenvironmental fluctuations can be reconstructed for that period of time.

Geomorphology of Desert Environments. Edited by Athol D. Abrahams and Anthony J. Parsons. Published in 1994 by Chapman & Hall, London. ISBN 978-94-015-8256-8

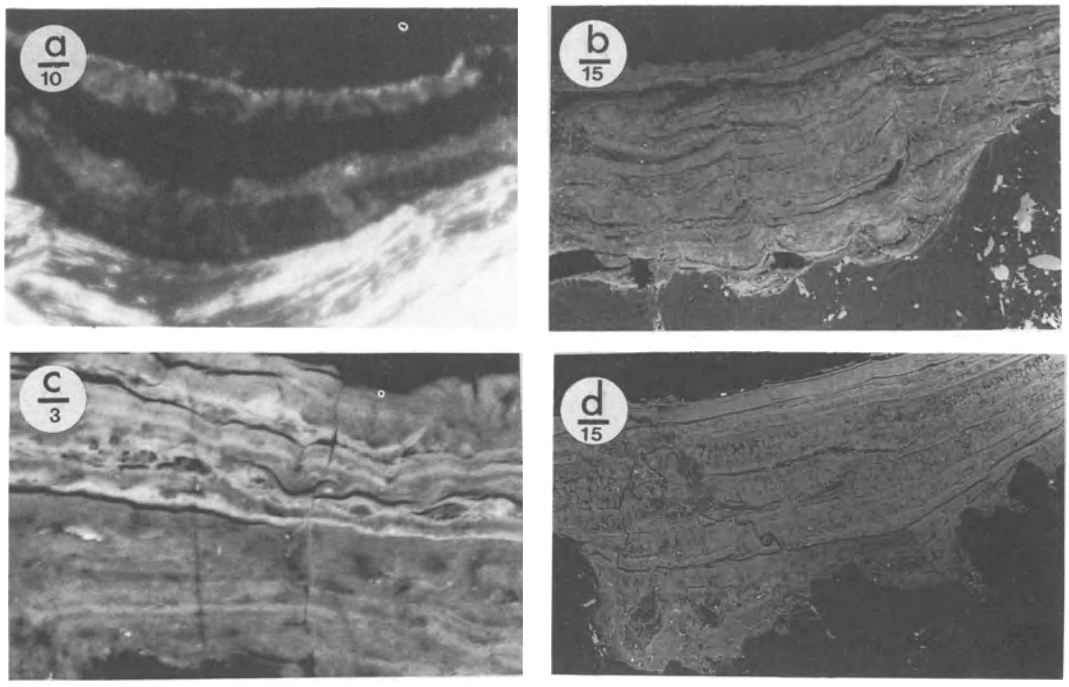

Figure 20.1 Views of varnish cross-sections that are appropriate for palaeoenvironmental analysis, where layering is even and consistent. Scale bars in micrometres. (a) Light microscope image of varnish on Hanaupah Canyon fan, Death Valley, California. The sequence of layering from top to bottom is light (Mn poor), dark (Mn rich), light (Mn poor), and dark (Mn rich), and lastly the light coloured rock. (b) Backscatter electron microscope image of varnish from Pampa San Jose, near Nasca, Peru. Brighter regions in backscatter images have a higher atomic number and in varnish usually more manganese and iron (Krinsley *et al.* 1990). (c) Backscatter image of varnish formed on Afton Bar of Lake Manix, California (Meek 1989). (d) Backscatter image of Mn-rich rock varnish from Marie Byrd Land, Antarctica. Sample collected by Mort Turner.

A serious limitation of rock varnish as a palaeoclimatic research tool is the inability to date layers within varnishes. Assumptions of linear rates of deposition might very well approximate reality in some circumstances, but such assumptions cannot be supported.

So far five signals have been identified in rock varnishes that record palaeoenvironmental fluctuations. Undoubtedly, future detailed studies will reveal other regularly fluctuating variables. The following discussion presents theory and examples of application for each palaeoenvironmental signal.

PALAEOALKALINITY SIGNAL

THEORY

Variations in manganese (Mn) and iron (Fe) abundance with depth were first noticed by Hooke *et al.* (1969). It was not until the research by Perry and Adams (1978), however, that these fluctuations were recognized as discrete depositional layers that might yield insights into palaeoclimate. Dorn and Oberlander (1982) argued that low Mn concentrations (low Mn/Fe ratios) would indicate conditions unfavourable for the microbial enhancement of manganese, in particular too much alkalinity. Dorn (1984) found that Mn/Fe ratios varied regularly on volcanics of the Coso Range.

Two competing theories to explain the concentration of manganese in varnish both explain Mn/Fe fluctuations by fluctuations in alkalinity. (a) The physico-chemical model of varnish formation (Elvidge and Iverson 1983, Whalley 1983, Smith and Whalley 1988) proposes that small pH–Eh fluctuations with acidic rain or dew release Mn but not Fe. The enhanced Mn and some of the Fe precipitates as water evaporates and pH increases. One explanation for layers of varnish poor in Mn follows this model. If the environment becomes too alkaline, Mn

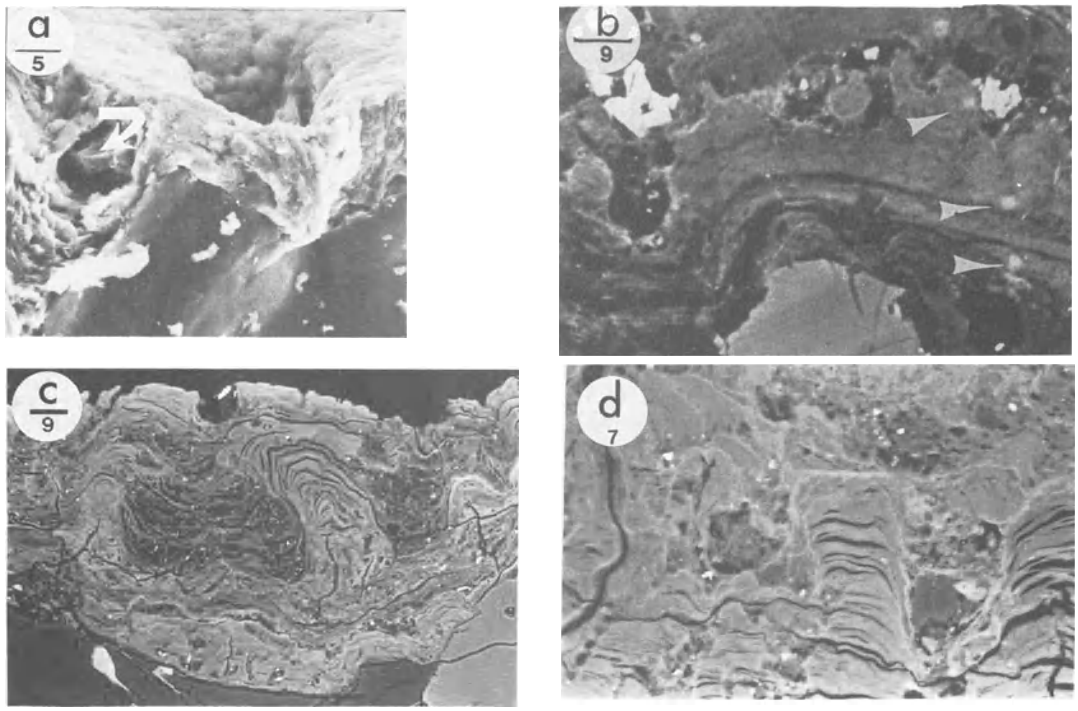

Figure 20.2 Views of past episodes of biogeochemical erosion within varnish. Scale bars in micrometres. (a) Secondary electron micrograph of varnish from Death Valley. The arrow identifies a piece of barium-rich detritus that has been deposited in the pit probably eroded by microcolonial fungi and is now covered over by younger varnish. A more recent erosional pit has formed to the right. (b) Backscatter image of the bottom layer of varnish formed on Coso Range volcanic 28, eastern California. Arrows identify electron microprobe burn marks. A textural change above the highest arrow is interpreted as a past surface of varnish erosion. Note the undulating surface with bright barium detritus stuck in the pits similar to Figure 20.2a. (c) Backscatter image of sample from Lathrop Wells, southern Nevada, illustrating several palaeoerosional pits that are only visible by examining cross-sections, and not by simply looking at the top of a rock varnish. (d) Palaeoerosional pits from varnish on Bishop Tuff, eastern California.

would not be reduced and the varnish would remain poor in Mn during this alkaline period. (b) The bacterial model of varnish formation (Dorn and Oberlander 1981, 1982, Palmer *et al.* 1985, Jones 1991) holds that extremely alkaline conditions are not favourable for the concentration of Mn by bacteria. In either model, alkalinity would inhibit Mn enhancement. As support, Dorn (1990) also presented a number of empirical correlations between Mn/Fe ratios and soil pH, varnish pH, two water balances, varnish $\delta^{13}C$ values, and altitude that indicate a strong empirical relationship between alkalinity and low Mn/Fe ratios in Holocene varnishes.

Jones (1991, p. 127) presented a modified model for Mn enhancement in rock varnish, the first experimental evidence on the physico-chemical precipitation of Mn, as well as new empirical evidence indicating the presence of manganese-oxidizing bacteria in Peru:

> 'During wetter times eolian clay minerals spend more time in contact with dew and fog, thus increasing the amount of Mn put into solution. At the same time, wetter soils, increased plant cover, and flooded playa lakes decrease the total amount of alkaline eolian material settling on varnish surfaces. Less alkaline surface conditions favor Mn precipitating bacteria . . . thus allowing them to take full advantage of the increased levels of dissolved Mn in the varnishing solutions. A reduction in circulation of eolian clays may also reduce the amount of clay minerals incorporated into the varnish, thus reducing the amount of Fe in the varnish as well. High Mn production and precipitation plus less Fe incorporation yields a

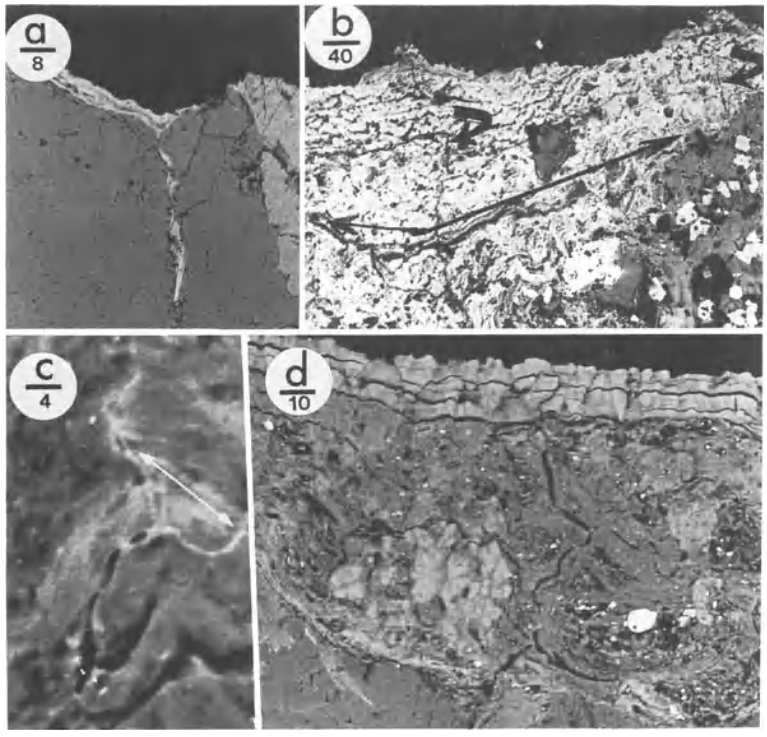

Figure 20.3 Backscatter electron micrographs exemplifying the mobility of manganese and iron in some samples. Scale bars in micrometres. (a) Penetration of bright 'crack' varnish into fractures beneath the surface. Sample from near the Marble Mountains, Mojave Desert, California (sample from D.H. Krinsley). (b) Varnish on Coso Range volcanic 28 with fractures from the surface to the bottom of the varnish (black curved arrows). The fractures have mounds at the surface. These are different from interlayer fractures (double headed black arrow) in that they are lined by remobilized manganese, as shown in (c). (c) The double headed white arrow points to remobilized Mn and Fe deposited in a fracture in varnish from Hanaupah Canyon alluvial fan, Death Valley, California. (d) This highly granular, detritus-rich texture is from water moving through rock varnish. Sample from Shoreline Butte, Manix Lake basin, California (Meek 1989).

> higher Mn:Fe ratio. Conversely, drier conditions reduce the contact time between clay minerals and varnishing solutions, inhibit Mn-precipitating bacteria through increased deposition of alkaline eolian materials, and increase the amount of Fe-bearing eolian clay minerals incorporated into varnish. A low Mn:Fe ratio results.'

Although the evidence continues to mount for a bacterial origin of enhanced Mn in rock varnish, all parties appear to concur that conditions of greater alkalinity should promote lower Mn/Fe ratios in varnish. The causes of alkalinity fluctuations probably relate to the vegetation cover over dryland soils and fluctuations in the area covered by endoreic lakes (Dorn 1990, Jones 1991).

Making and analysing cross-sections of rock varnish by light and electron microscopy is a relatively inexpensive means of reconstructing long-term variations in palaeoclimate. It is easier than coring lakes, for example. However, to investigate rock varnish reliably takes more than collecting just a few pieces of varnish. The circumstances of microsite collection must be controlled (Dorn 1989, Krinsley *et al.* 1990), and results must be replicated over a wide area before a palaeoclimatic interpretation can be attempted. It is necessary to work with continuous layers from multiple thin sections taken from several rock exposures and collected over a region. Potter (1979) noted that optical discontinuities in layers in varnish would prevent their use in dating or palaeoenvironmental interpretation. Also, Dorn and Krinsley (1991) stressed that all alkalinity profiles must be taken away from zones of leaching within varnish.

APPLICATIONS

Figure 20.4 displays representative palaeoalkalinity signals in rock varnishes from basalt flows with K/Ar

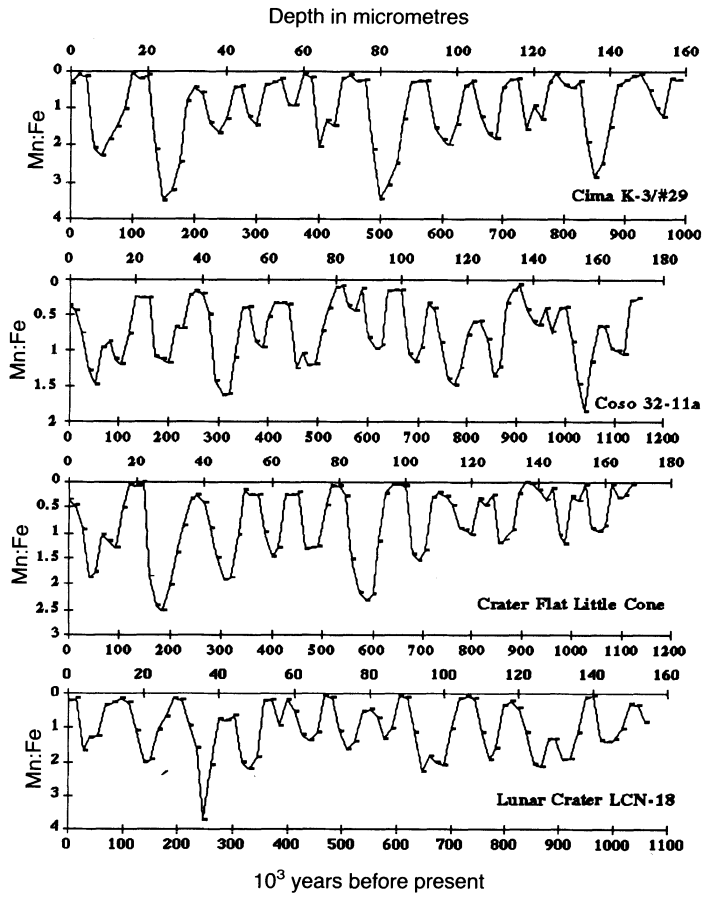

Figure 20.4 Microlaminations of Mn/Fe variations in varnishes formed on K/Ar dated lava flows from the western Basin and Range province, United States. An assumption of a linear rate of deposition is used to obtain the age scale, where the bottom of each varnish is assigned the K/Ar date and the top is assigned the present. K/Ar dates are from the Coso Range flow 32 in eastern California (Duffield *et al.* 1980), from the Cima volcanic field flow K-3/#29 in the Mojave Desert (Turrin *et al.* 1985), from Little Cone in the Crater Flat volcanic field of southern Nevada (Vaniman *et al.* 1982), and from LCN-18 in the Lunar Crater volcanic field of central Nevada (Turrin and Dorn, in preparation).

age control in the western Basin and Range province of the United States, Figure 20.5 from alluvial fan sequences in Death Valley, California, and Figure 20.7 from hillslope deposits in the Negev Desert, Israel. Each transect is representative of multiple microprobe profiles taken from layered varnishes from each site. For example, Dorn (1984, 1990) completed hundreds of electron microprobe transects of varnishes in the Coso volcanic field.

Figure 20.4 presents transects of rock varnishes collected from the surfaces of lava flows that should reflect the K/Ar age; photographs of textures of sampled constructional lava surfaces are presented by Dorn (1989, p. 585). The sampled sites in Figure 20.4 are adjacent to palaeolakes that have fluctuated throughout the Quaternary (Benson *et al.* 1990), changing the chemistry of aeolian fall-out. Full lakes contribute fewer alkaline aerosols (Baronne *et al.* 1981, Mayer and Anderson 1984, McFadden *et al.* 1986, Reheis 1988). Similarly, a greater vegetation cover associated with a more positive water balance should decrease deflation of aerosols in the surrounding uplands and probably lower the pH of the surface horizon.

Rock varnish is most sensitive to long-term fluctuations of the order of 10^4 to 10^5 years. About 12 to 13 events of reduced alkalinity are recorded in the western Basin and Range province over the last million years (Fig. 20.4). Since reduced alkalinity is probably equated to periods of greater moisture

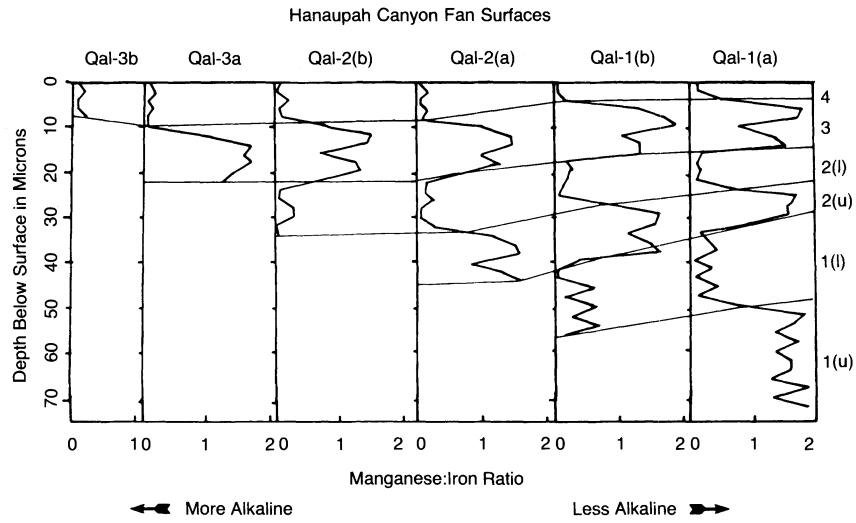

Figure 20.5 Mn/Fe variations on different surfaces of Hanaupah Canyon alluvial fan, Death Valley, California. The different Quaternary alluvium (Qal) surfaces are identified and discussed by Dorn (1988, Chapter 23). High Mn/Fe ratios indicate reduced alkalinity in semi-arid periods, and low ratios indicate high alkalinity in more arid periods.

effectiveness that produce higher Mn concentrations, these results indicate there were at least 12 to 13 periods of greater moisture availability in the region. I should stress that since internal age control is not available, the length of each period is uncertain. It is likely, however, that short-lived fluctuations occurred but have not been recorded in slowly formed rock varnishes.

Figure 20.5 presents a series of representative Mn/Fe profiles from Hanaupah Canyon alluvial fan on the Panamint Range bajada on the west side of southern Death Valley. Sequences of microchemical laminations on equivalent alluvial-fan surfaces are quite similar. The oldest unit has three 'cycles' of high and low Mn/Fe ratios near the fan head, but the basal layer of high Mn/Fe ratios is pinched out near the fan toe. The same pattern is repeated for two cycles on the second oldest unit. One complete cycle is revealed on the surface radiocarbon dated to be latest Pleistocene (Dorn *et al.* 1989), and only low Mn/Fe ratios are found on the Holocene unit. Chapter 23, Figure. 23.8 provides an aerial photograph of Hanaupah fan and a more detailed discussion of the geomorphic implications of these data.

Gerson (1982) proposed a climatic model for the development of talus flatirons in the Negev Desert of Israel. Gerson believed a talus cover forms during more humid periods and erodes during more arid phases. If base level is stable enough, some of the talus cover remains as a flatiron. Each successive humid–arid cycle has the potential to leave a talus flatiron remnant. Varnish was sampled from two sequences of talus flatirons, one near Paran in the Arava Valley and the other at Timna. A model of flatiron development at Timna is presented in Figure 20.6. Data in Figure 20.7 from Timna and from Paran (Dorn 1984) support Gerson's model.

PALAEODUST SIGNAL

THEORY

Perry and Adams (1978) first noted that rock varnish has a tendency to accrete at discrete centres. As these accreting nucleation points merge, a botryoidal micromorphology develops (Fig. 20.8a). Not all varnishes, however, have a texture resembling melted marbles. The majority of varnishes from deserts that I have studied have a lamellate micromorphology, a structure of subparallel platelets (Fig. 20.8b), or have textures intermediate between botryoidal and lamellete.

Dorn (1986) presented a model where the amount of dust on the surface of the varnish is a key factor controlling the micromorphology of varnishes exposed to the atmosphere. A botryoidal varnish forms when manganese enrichment occurs in a relatively dust-free environment that characteristically has a plant cover of over 40 to 50%. A lamellate

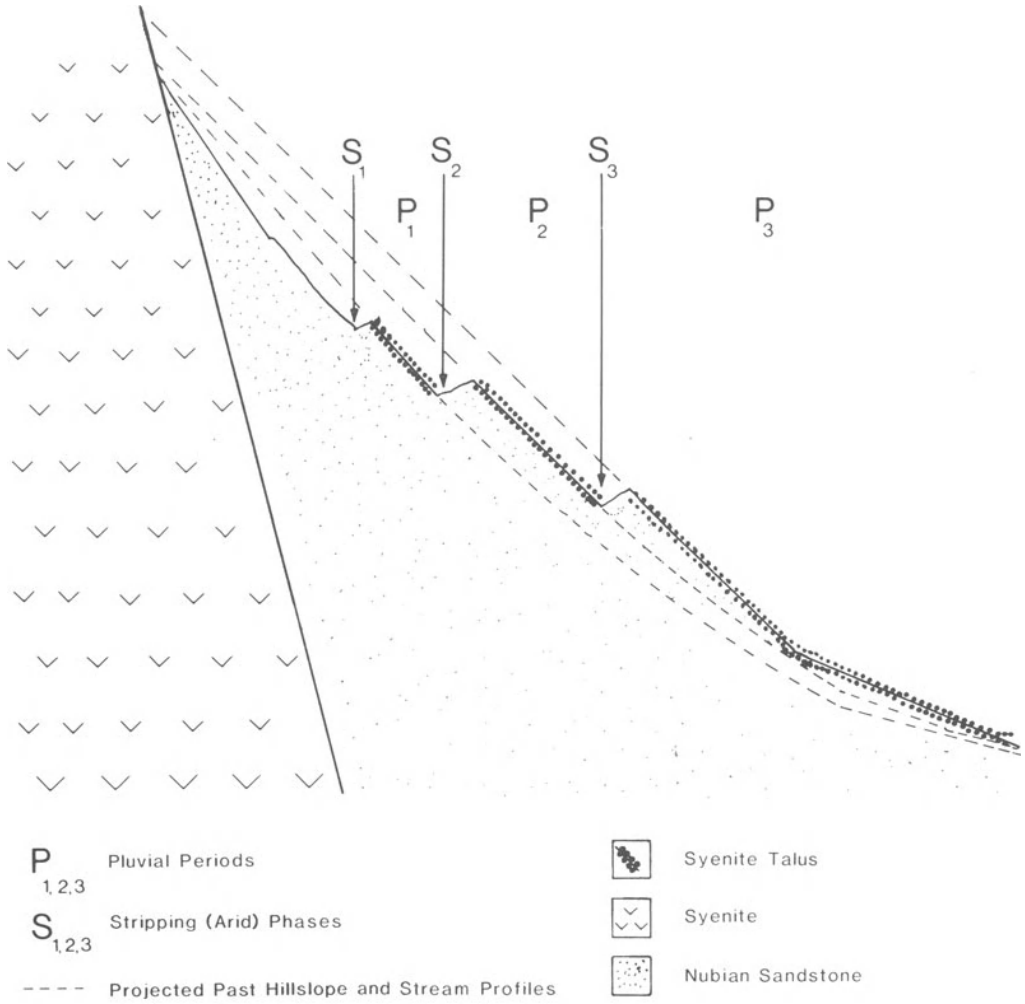

Figure 20.6 Talus flatirons from Timna, Negev Desert, Israel, are displayed in an idealized model modified from Gerson (1982). Subscripts 1, 2, and 3 represent successively older phases of flatiron development.

varnish develops, in contrast, when the environment is sparsely vegetated (less than 35% cover) and dusty. This model was supported by field and laboratory observations involving dust collection, vegetation transects, existing models of aeolian transport, and scanning electron microscopy (SEM) examination of replicate varnish cross-sections (Dorn 1986).

APPLICATION

It is possible to identify changes in the aeolian environment by changes in the micromorphology of varnish in a cross-section. Figure 20.8 (c and d) presents superimpositions of lamellate over botryoidal micromorphologies in situations where the surfaces are known to be late Pleistocene in age, and where the areas experienced less arid (and probably more dusty) conditions in the late Pleistocene followed by arid (and probably less dusty) conditions in the Holocene. Superimpositions of dissimilar textures are more common in south-western North America and Israel (Dorn 1986) than in Australia (Dorn and Dragovich 1990). The following case studies exemplify possible uses of micromorphological fluctuations in rock varnish.

Most deserts are regions that have experienced tremendous fluctuations in the aeolian environment, often corresponding to regional climatic changes. Feedback processes relate to source material, vegeta-

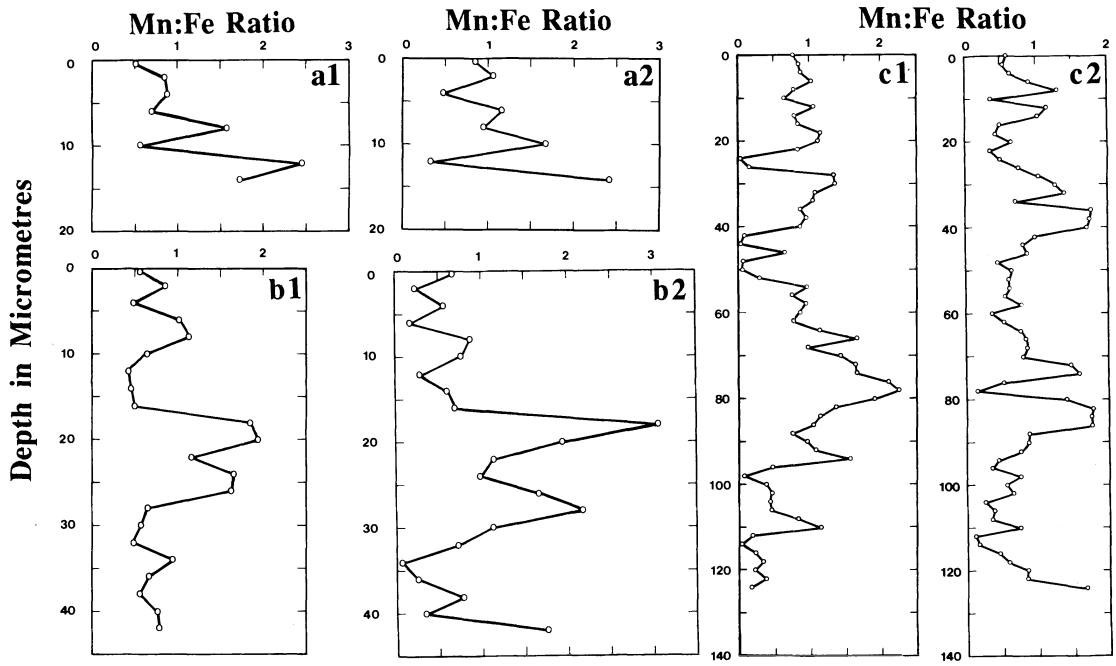

Figure 20.7 Microchemical laminations in rock varnishes collected from the flatiron sequence displayed in Figure 20.6: a1 and a2 from the youngest flatiron; b1 and b2 from the middle flatiron; and c1 and c2 from the oldest flatiron. Mostly alkaline conditions are recorded in a1 and a2. One major period of reduced alkalinity is evident in b1 (15–25 μm) and b2 (15–30 μm). Two major periods of reduced alkalinity are found in c1 and c2 (20–40 μm; 70–85 μm). Higher ratios at the base of varnishes in a1, a2, b2, and c2 may reflect the end of the more humid period of talus stability.

tion-related roughness, and changes in wind energy regime. Continuous records of fluctuations in aeolian activity are available from deep sea cores (Rea 1990) but not from desert areas. Rock varnish may allow a more direct correlation between aeolian activity in continental source regions and more distant proxy records.

The concept of core areas of desert during more humid times providing refugia for arid plants and animals is a recurrent theme in the palaeobotanical literature. By mapping the boundary between areas with subsurface botryoids and areas without, it might be possible to identify possible desert refugia. Such mapping efforts would be useful in testing palaeoclimatic models (Kutzbach 1987).

In an era of increasing awareness of the importance of climatic changes and with rapid population growth forcing the occupation of marginal drylands, there is a growing need for data on past boundaries of arid zones. It may be possible to map out regions that experienced intensified episodes of aridity in the past, perhaps finding lamellate varnishes in the subsurface where botryoidal varnishes grow now. One likely region to study this is the Sahel region of North Africa.

The micromorphological data gathered for Death Valley is consistent with the alkalinity signal presented in Figure 20.5. Rock varnish on alluvial fan units have Mn/Fe laminations corresponding with cycles of alternating botryoidal–lamellate variations (e.g. Fig. 20.8e). One complication in the study of micromorphological sequences is the gradual diagenesis over time (Dorn 1986) that appears to limit the frequency of finding varnishes with multiple cycles of alternating botryoidal and lamellate layers.

It is not possible to determine if the same environmental change that caused an Mn/Fe fluctuation resulted in a change in micromorphology. The polishing required for accurate and precise electron microprobe measurements usually does not preserve botryoidal structures in cross-sections (Fig. 20.8g). However, semi-quantitative energy-dispersive X-ray analysis of the non-polished cross-sections in Figure 20.8e suggests botryoidal layers are richer in Mn than the lamellate layers (Fig. 20.8f).

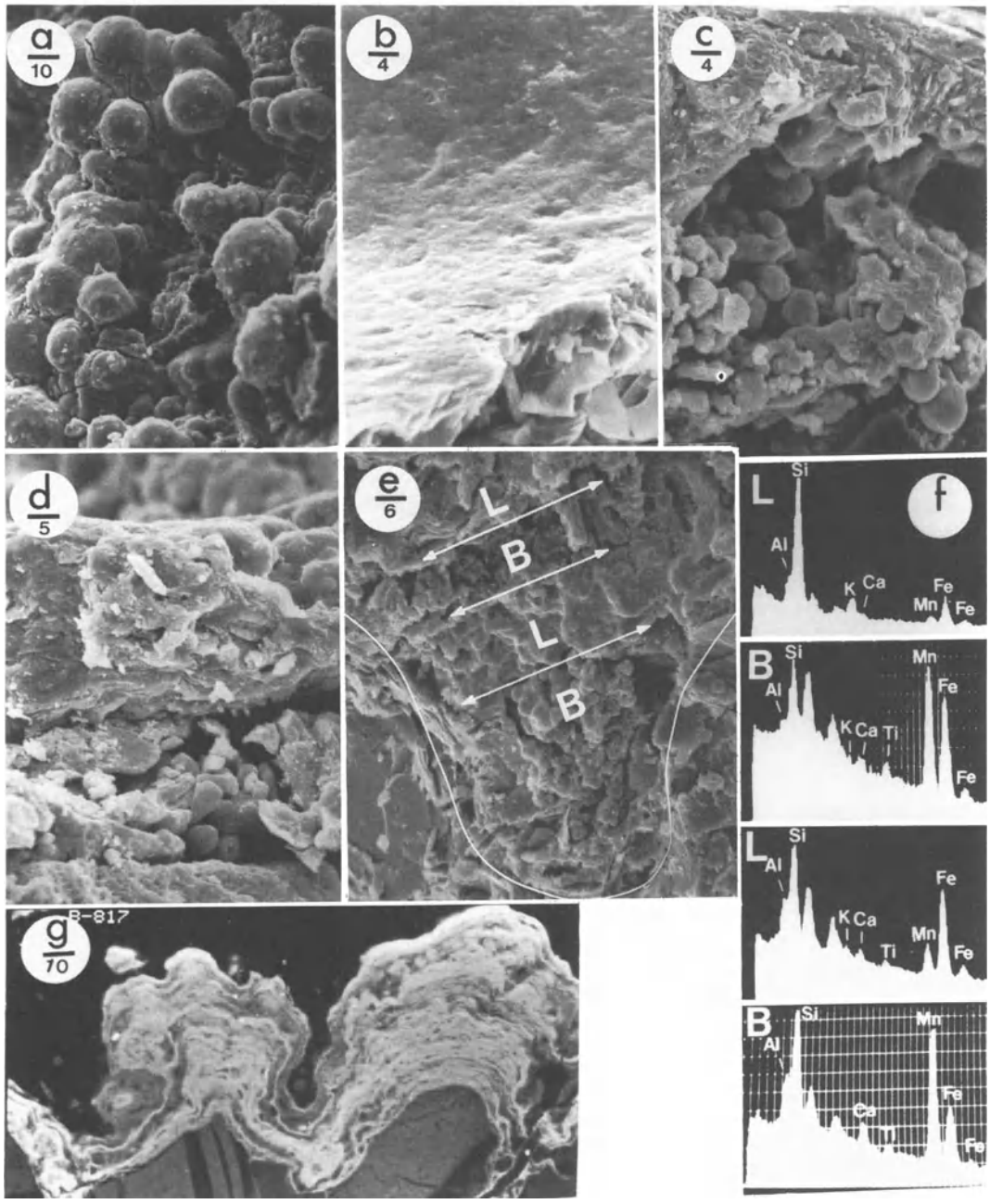

Figure 20.8 Varnish micromorphology. Scale bars in micrometres. (a) Botryoidal varnish from Kitt Peak, Arizona. (b) Lamellate varnish from Pampa San Jose, Peru. (c) Lamellate varnish formed on botryoidal varnish, from the −180 m full-glacial highstand of Lake Lisan, the precursor to the Dead Sea. (d) One cycle of lamellate on botryoidal varnish from a late Pleistocene (*c.* 23 ka) colluvial boulder line at Emigrant Pass, Death Valley, California. (e) Two cycles of lamellate (L) on botryoidal (B) varnish from the Q2a surface of Hanaupah Canyon alluvial fan, California. (f) Energy dispersive X-ray analyses of the different layers in (e). The upper analysis corresponds with the upper lamellate layer (L). The second analysis corresponds with the botryoidal layer (B) just beneath the surface, and so on. (g) The texture of subsurface botryoids is not usually preserved when polished thin sections are made. Some suggestion of botryoidal micromorphology, however, can be discerned in this backscatter micrograph from Kitt Peak, Arizona.

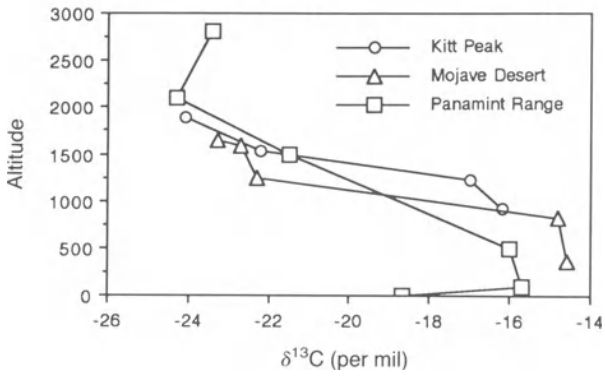

Figure 20.9 $\delta^{13}C$ variations of organic matter extracted from Holocene rock varnishes sampled from Kitt Peak, Arizona, central Mojave Desert, California, and Panamint Range, California, altitude transects. Kitt Peak and central Mojave transect data were presented by Dorn and DeNiro (1985). Death Valley data have not been published previously. More negative values in the lowest site of the Death Valley transect are probably due to the abundance of the C-3 plant *Larrea tridentata* (Creosote Bush).

STABLE CARBON ISOTOPE SIGNAL

Stable carbon isotope ratios of organic matter in the upper parts of rock varnishes of Holocene age show a strong association with environment. Organic matter resting on the surface of varnishes from arid regions typically has less negative $\delta^{13}C$ values, ranging from -11 to -19 per mil, whereas varnishes from semi-arid to humid regions have $\delta^{13}C$ values around -23 per mil (Dorn and DeNiro 1985). This isotopic variability reflects the abundance of plants with different photosynthetic pathways in adjacent vegetation. Figure 20.9 displays $\delta^{13}C$ variations of varnishes on Holocene surfaces in three altitude-climatic transects from western North America that reflect the trend identified in Dorn and DeNiro (1985).

Differences in the isotopic compositions of layers in rock varnishes occur on the alluvial fans of Death Valley (Fig. 20.10a). $\delta^{13}C$ variations appear to reflect the same sequence of environmental fluctuations that are recorded in Mn/Fe ratios (Fig. 20.5) and varnish textures (Fig. 20.8e). However, the significance of these results has been thrown into ques-

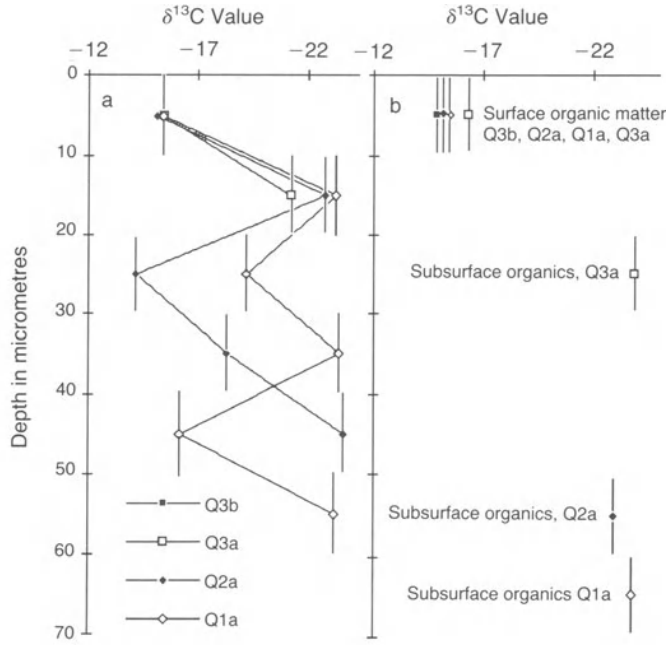

Figure 20.10 $\delta^{13}C$ variations in varnishes with depth from different Quaternary (Qal) surfaces of Hanaupah Canyon alluvial fan, Death Valley, California. The different Quaternary alluvial units (Qal) are discussed by Dorn (1988, Chapter 23). Less negative $\delta^{13}C$ values are interpreted to indicate varnish formation in an arid period, whereas more negative values formed in a semi-arid time. (a) Sampled from varnishes with intravarnish organic matter that has collected in erosional hollows. (b) Sampled from layered varnishes without intravarnish organic matter, where the organic detritus could be found only at the surface and underneath the varnish.

tion. Evenly layered varnish rarely has organic matter in the middle of the varnish – only at the surface and encapsulated beneath (Dorn *et al.* 1992). The intravarnish organic matter that is present is trapped as detritus in the hollows that are eroded into varnish (see Fig. 20.2). The intravarnish organic matter that was analysed (Fig. 20.10a), therefore, did not come from evenly layered varnish. When the work was conducted (Dorn 1988), much of the complexity of varnish textures and the importance of varnish layering was not fully realized. Whilst it is possible that the organics caught in intravarnish pockets represent a relative sequence of environmental changes for each alluvial unit in Figure 20.10a, this is not certain.

Figure 20.10b presents $\delta^{13}C$ values for organic detritus extracted from layered varnishes (like Fig. 20.1) collected from the same units as Figure 20.10a. Only surface and subvarnish organics were found and removed. The less negative $\delta^{13}C$ values of surface organics reflect the current aridity of the environment, while the more negative $\delta^{13}C$ values in subvarnish organic matter from Q3a, Q2a, and Q1a reflect a period of greater moisture abundance after the alluvial cobble was exposed to the atmosphere.

I now believe that $\delta^{13}C$ analysis will reach its full potential when a laser probe is used to sample varnish cross-sections for both ^{14}C and $\delta^{13}C$ measurements on the same material. That way, the internal pockets that catch organic detritus can be dated and the $\delta^{13}C$ values treated as an independently dated palaeoenvironmental indicator.

TRACE METAL FLUCTUATIONS

Boutron and Patterson (1986) identified substantial variations in lead concentration in ice cores from Antarctica across the Wisconsin–Holocene boundary. Wisconsin-age ice had much higher concentrations of lead that were thought to be from dust. Manganese-rich rock varnish collected (by Mort Turner) from an older moraine in upper Beacon Valley, Antarctica, was analysed by wavelength dispersive electron microprobe to assess any variations in lead concentration with depth.

Figure 20.11 presents two different electron microprobe transects from two different microdepressions on the same rock, showing substantial variations in lead concentrations. (The limit of detection for PbO is about 0.08% with a counting time of 200 s.) Although the age of the surface was not known, one quite speculative interpretation is that levels below the limit of detection in the upper 6 to 8 μm could possibly correlate with Boutron and Patterson's (1986) low levels of Holocene Pb fall-out, while higher levels at around 8 to 10 μm could correlate with higher Pb fall-out during the latest Pleistocene. An older PbO peak at around 20 μm could possibly represent a pre-late Wisconsin glaciation. Of course, for this type of analysis to have any significance, multiple transects on several varnishes of known age must be completed. However, these initial results indicate that it is feasible to profile Pb and other trace element variations in rock varnish, and that these profiles might yield a palaeoenvironmental signal.

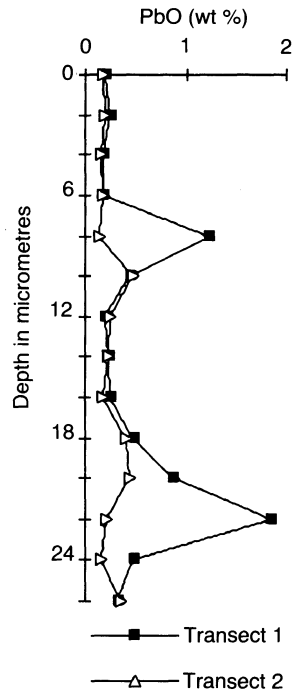

Figure 20.11 Variations in PbO with depth in rock varnish collected from morainal boulders of upper Beacon Valley, Victoria Land, Antarctica. Sample was collected by Mort Turner. Transect 1 and transect 2 were from layered varnishes in the centre of two different micropits.

EPISODES OF MINOR ABRASION

Mechanical abrasion readily removes rock varnish. Rock varnish has a hardness of $\leq$4.5 on Mohs' scale of abrasive resistance (Dorn and Oberlander 1982) and cannot withstand aeolian abrasion or fluvial transport. However, field examination of active desert washes and stones being actively abraded by dust and sand reveals pockets of varnish in protected microsites. These protected pockets pose

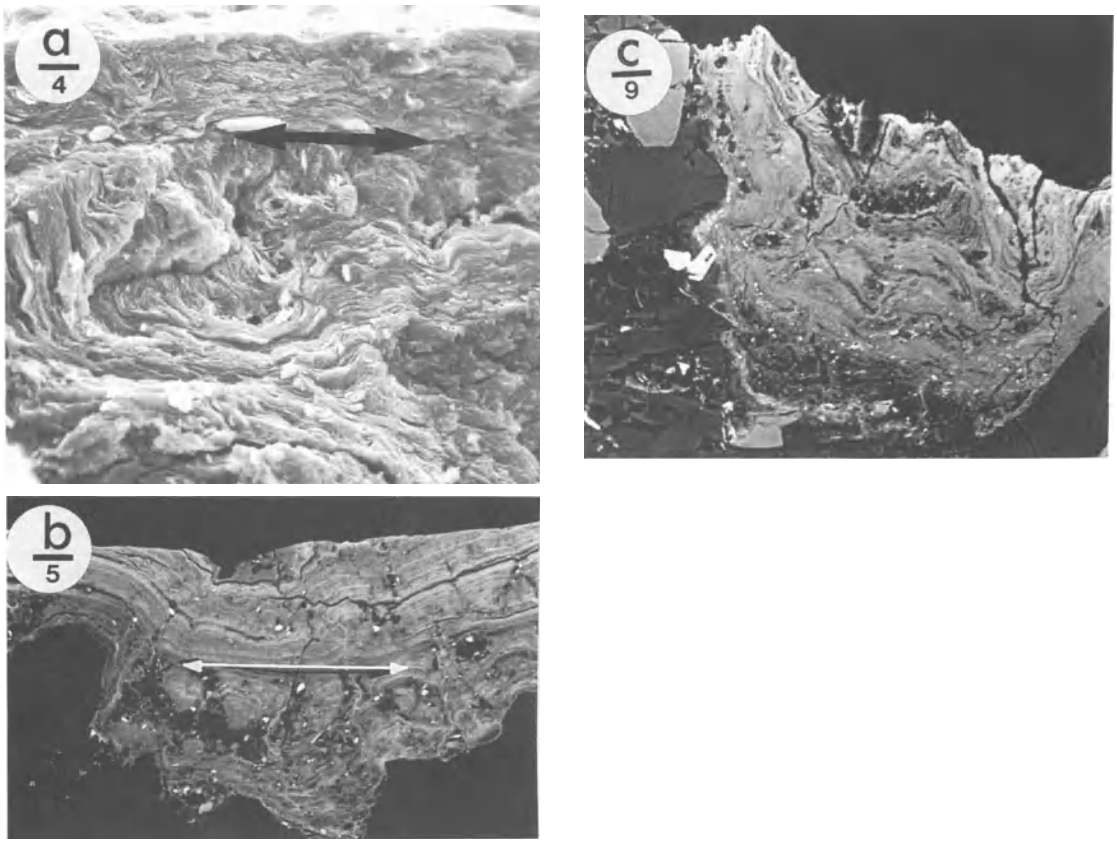

Figure 20.12 Erosional unconformities. Scale bars in micrometres. (a) Varnish sampled from a protected depression in a rock from the Cronese Basin, Mojave Desert, California. Three phases of varnish build-up and two (possibly three) phases of varnish erosion are recorded. First, the lower layer was deposited. Second, the area beneath the double arrow was eroded, most likely by the secretion of organic acids by fungi or lichens. Third, varnish filled in this depression. Fourth, aeolian abrasion truncated the varnish above the double arrow. Fifth, a newer layer of varnish was deposited above the double arrow. A possible sixth event is that some aeolian abrasion has occurred on top of the latest varnish layer. (b) The double arrow identifies an erosional unconformity in this backscatter image of rock varnish from Marie Byrd Land, Antarctica, that could represent aeolian abrasion from ice crystals. (c) Backscatter image of varnish collected from an active wash, Crater Flat, southern Nevada, that has been eroded by fluvial transport. There is not evidence of *in situ* varnish formation on this preserved pocket of older, inherited varnish.

serious problems for dating the timing of last abrasion and, hence, must be avoided. They also pose problems for palaeoenvironmental interpretations, and Krinsley *et al.* (1990) isolated this as one reason why varnishes must be selected very carefully for dating. Still, every cloud has a silver lining.

An unexplored geomorphological tool is the examination of varnish cross-sections for such episodes of partial mechanical abrasion, exemplified in Figure 20.12. One possible use in applied desert geomorphology is determining whether varnish on cobbles in washes represents *in situ* growth and hence some antiquity or is inherited from an older deposit and represents pockets of incomplete abrasion. Finding an erosional unconformity with newly deposited varnish would indicate antiquity. This is an important concern in arid regions, where housing is built on alluvial fans and the flooding history is often uncertain (Graf 1988). Another possible use would be in recording episodes of incomplete aeolian abrasion. There is no doubt, however, that this tool would be more powerful if it becomes possible to date layers in rock varnish.

SUMMARY

When rock varnishes are deposited in even layers, changes in chemistry and texture can reflect local

environmental fluctuations. With replicate sampling, regional variations can be determined for changes in the composition of airborne fall-out, namely alkalinity, dust concentration, and perhaps in the future stable carbon isotope composition. It may also be possible to correlate varnish to other records using trace element fluctuations such as lead. Lastly, analysing the texture of cross-sections can reveal episodes of minor mechanical abrasion useful in the interpretation of landscape evolution.

The key to the palaeoenvironmental analysis of rock varnish is careful selection of samples in the field, careful selection of samples in the laboratory, and replication of results. The rule of GIGO (garbage in, garbage out) applies to rock varnish just as well as to computers. It is not possible to grab a few samples in the field, cut them open, stick them under the microprobe, and expect good results.

ACKNOWLEDGEMENTS

This research was supported mostly by NSF PYI Award and NSF SES86-01937. The stable carbon isotope work was funded in part by donors of the Petroleum Research Fund administered by the American Chemical Society through PRF Grant 18016-GB2. The Death Valley research was funded by National Geographic Society. Thanks to M. Tamers and J. Stipp of Beta Analytic, G. Strathearn, J. Clark, P. Trusty, M. Turner, D.H. Krinsley, T. Liu, and D. Dorn for laboratory and field assistance and discussions.

REFERENCES

Baronne, J.B., L.L. Ashbaugh, B.H. Kusko and T.A. Cahill 1981. The effect of Owens Dry Lake on air quality in the Owens Valley with implications for the Mono Lake area. In *American Chemical Society Symposium Series No. 167. Atmospheric aerosol: source/air quality relationships*, E.S. Macias and P.K. Hopke (eds), 328–46. Washington, DC: American Chemical Society.

Benson, L.V., D.R. Currey, R.I. Dorn, K.R. Lajoie, *et al.* 1990. Chronology of expansion and contraction of four Great Basin lake systems during the past 35,000 years. *Palaeogeography, Palaeoclimatology, Palaeoecology* **78**, 241–86.

Boutron, C.F. and C. Patterson 1986. Lead concentration changes in Antarctic ice during the Wisconsin/Holocene transition. *Nature* **323**, 222–4.

Dorn, R.I. 1984. Cause and implications of rock varnish microchemical laminations. *Nature* **310**, 767–70.

Dorn, R.I. 1986. Rock varnish as an indicator of aeolian environmental change. In *Aeolian geomorphology*, W.G. Nickling (ed.) 291–307. London: Allen & Unwin.

Dorn, R.I. 1988. A rock varnish interpretation of alluvial-fan development in Death Valley, California. *National Geographic Research* **4**, 56–73.

Dorn, R.I. 1989. Cation-ratio dating of rock varnish: a geographical perspective. *Progress in Physical Geography* **13**, 559–96.

Dorn, R.I. 1990. Quaternary alkalinity fluctuations recorded in rock varnish microlaminations on western U.S.A. volcanics. *Palaeogeography, Palaeoclimatology, Palaeoecology* **76**, 291–310.

Dorn, R.I. 1991. Rock varnish. *American Scientist* **79**, 542–53.

Dorn, R.I. and M.J. DeNiro 1985. Stable carbon isotope ratios of rock varnish organic matter: a new paleoenvironmental indicator. *Science* **227**, 1472–4.

Dorn, R.I. and D. Dragovich 1990. Interpretation of rock varnish in Australia: case studies from the arid zone. *Australian Geographer* **21**, 18–32.

Dorn, R.I. and Krinsley, D.H. 1991. Cation leaching sites in rock varnish. *Geology* **19**, 1077–80.

Dorn, R.I. and T.M. Oberlander 1981. Microbial origin of desert varnish. *Science* **213**, 1245–7.

Dorn, R.I. and T.M. Oberlander 1982. Rock varnish. *Progress in Physical Geography* **6**, 317–67.

Dorn, R.I., A.J.T. Jull, D.J. Donahue, T.W. Linick, *et al.* 1989. Accelerator mass spectrometry radiocarbon dating of rock varnish. *Bulletin of the Geological Society America* **101**, 1363–72.

Dorn, R.I., P.B. Clarkson, M.F. Nobbs, L.L. Loendorf, *et al.* 1992. New approach to the radiocarbon dating of rock varnish, with examples from drylands. *Annals of the Association of American Geographers* **82**, 136–51.

Douglas, G.R. 1987. Manganese-rich rock coatings from Iceland. *Earth Surface Processes and Landforms* **12**, 301–10.

Duffield, W.A., C.R. Bacon and G.B. Dalrymple 1980. Late Cenozoic volcanism, geochronology, and structure of the Coso Range, Inyo County, California. *Journal Geophysical Research* **85**, 2381–404.

Elvidge, C.D. and R.M. Iverson 1983. Regeneration of desert pavement and varnish. In *Environmental effects of off-road vehicles*, R.H. Webb and H.G. Wilshire (eds), 225–43. New York: Springer.

Gerson, R. 1982. Talus relicts in deserts: a key to major climatic fluctuations. *Israel Journal Earth Science* **31**, 123–32.

Graf, W.L. 1988. *Fluvial processes in dryland rivers*, Berlin: Springer.

Hooke, R.L., H. Yang and P.W. Weiblen 1969. Desert varnish: an electron probe study. *Journal of Geology* **77**, 275–88.

Jones, C.E. 1991. Characteristics and origin of rock varnish from the hyperarid coastal deserts of northern Peru. *Quaternary Research* **35**, 116–29.

Krinsley, D., R.I. Dorn and S. Anderson 1990. Factors that may interfere with the dating of rock varnish. *Physical Geography* **11**, 97–119.

Kutzbach, J.E. 1987. Model simulations of the climatic patterns during the deglaciation of North America. In *North American and Adjacent Oceans During the Last Deglaciation*. Geology of North America, Geological Society of America Centennial Volume K-3, W.F. Ruddiman and H.E.J. Wright (eds), 425–46. Boulder, CO.: Geological Society of America.

Mayer, L. and M. Anderson 1984. Variations in carbonate dust flux in the southwestern United States – implica-

tions for rates of development of carbonate soil horizons. *Geological Society of America Abstracts with Programs* **16**, 586–7.

McFadden, L.D., S.G. Wells and J.C. Dohrenwend 1986. Influences of Quaternary climatic changes on processes of soil development on desert loess deposits of the Cima volcanic field, California. *Catena* **13**, 361–89.

Meek, N. 1989. Geomorphic and hydrologic implications of the rapid incision of Afton Canyon, Mojave Desert, California. *Geology* **17**, 7–10.

Palmer, F.E., J.T. Staley, R.G.E. Murray, T. Counsell, *et al.* 1985. Identification of manganese-oxidizing bacteria from desert varnish. *Geomicrobiology Journal* **4**, 343–60.

Perry, R.S. and J. Adams 1978. Desert varnish: evidence of cyclic deposition of manganese. *Nature* **276**, 489–91.

Potter, R.M. 1979. The tetravalent manganese oxides: clarification of their structural variations and relationships and characterization of their occurrence in the terrestrial weathering environment as desert varnish and other manganese oxides. Ph.D. Dissertation, California Institute of Technology.

Potter, R.M. and G.R. Rossman 1977. Desert varnish: the importance of clay minerals. *Science* **196**, 1446–8.

Potter, R.M. and G.R. Rossman 1979. The manganese- and iron-oxide mineralogy of desert varnish. *Chemical Geology* **25**, 79–94.

Rea, D.K. 1990. Aspects of atmospheric circulation: the late Pleistocene (0–950,000 yr) record of eolian deposition in the Pacific Ocean. *Palaeogeography, Palaeoclimatology, Palaeoecology* **78**, 217–27.

Reheis, M.C. 1988. Dust influx in southern Nevada and California: preliminary findings. *Geological Society of America Abstracts with Programs* **20**, A207.

Smith, B.J. and W.B. Whalley 1988. A note on the characteristics and possible origins of desert varnishes from southeast Morocco. *Earth Surface Processes and Landforms* **13**, 251–8.

Turrin, B.D., J.C. Dohrenwend, R.E. Drake and G.H. Curtiss 1985. K–Ar ages from the Cima volcanic field, eastern Mojave Desert, CA. *Isochron West* **44**, 9–16.

Vaniman, D.T., B.M. Crowe and E.S. Gladney 1982. Petrology and geochemistry of Hawaiite lavas from Crater Flat, Nevada. *Contributions to Mineralogy and Petrology* **80**, 341–57.

Whalley, W.B. 1983. Desert varnish. In *Chemical sediments and geomorphology: precipitates and residua in the near surface environment*, A.S. Goudie and K. Pye (eds), 197–226. London: Academic Press.

HILLSLOPES AS EVIDENCE OF CLIMATIC CHANGE

21

Karl-Heinz Schmidt

INTRODUCTION

Geomorphic systems disclose great differences in their sensitivity to climatic change, and the various relief units carry the imprints of past processes to dissimilar degrees. Fluvial systems are highly susceptible to climatically induced changes in process. Hillslopes, on the other hand, are generally regarded as being rather resistant to such changes. In addition to the sensitivity of relief units to climatic change, another point of crucial geomorphic interest is how long the legacies of past processes are preserved in the form elements. Unfortunately, sensitivity to change and the length of time of preservation of past changes are usually inversely correlated. This means that we have either a detailed record of short-term changes for a limited period of time or a relatively inaccurate record of only major changes for a longer timespan. However, even where a detailed record of past climatic changes has survived, because climatic changes are generally more frequent than landform changes, the record may not be complete, and the climatic changes may have occurred at the same time as the landform changes without having caused them (Ahmert 1990).

The critical factors rendering a process change geomorphologically significant are the intensity and magnitude of the climatic change as well as its direction and the duration of the new climatic regime. These factors are counteracted by the resistance of the geomorphic system to external change. It is this resistance to change which predominantly controls the relaxation time of a system. Relief units with very short relaxation times will only document legacies of former processes for the very recent past, and relief units with very long relaxation times will only document long-lasting and very intensive changes.

RESISTANCE TO CHANGE

With special regard to hillslopes the resistance of a relief unit to process change is dependent on a number of form, process, and lithological characteristics (Littmann and Schmidt 1989).

(a) Slope angle. A high slope angle leads to a low resistance to gravitational and hydraulic erosion on the slope units compared with pediment and planation surfaces or lithologically controlled stripped plateau surfaces. On free faces no legacies of past processes are preserved (Fig. 21.1).
(b) Lines of process concentration. If the relief unit is affected by lines of process concentration (e.g. valley floors, erosional gullies) which channel mass input, it becomes more susceptible to change. If a scarp is breached by a major river or if a river runs parallel to its foot (Fig. 21.2), resistance to change is reduced by the closer connection to base level fluctuations.
(c) Lithological characteristics of the surface material and substrate. This type of control is especially important in arid regions, where weathering and erosion processes operate in a highly selective manner in contrast to more humid regions which have greater moisture availability and an increase of chemical weathering. Outcrops of resistant bedrock layers on slopes, hillslope surfaces consisting of consolidated talus or gravels, and old pediment surfaces show a high resistance to erosion, whereas unconsolidated hillslope debris, particularly when consisting of fine-grained colluvial deposits, is easily rearranged by changing process regimes.

Taken overall, the effectiveness of a past geomorphic process E associated with a past climate in shaping a hillslope is proportional to the product of

Geomorphology of Desert Environments. Edited by Athol D. Abrahams and Anthony J. Parsons. Published in 1994 by Chapman & Hall, London. ISBN 978-94-015-8256-8

Figure 21.1 Free face in the Triassic Moenkopi Formation in the Capitol Reef area, Utah. The white caprock overlying the soft siltstones and sandstones is the Shinarump Conglomerate of the Chinle Formation. The main caprock of the complex scarp, the sandstones of the Glen Canyon Group, are visible in the background. No legacies of past processes are preserved on the Moenkopi slope.

the duration of the former process T_1 and its intensity I_1 divided by the resistance of the hillslope unit R.

$$E \propto \frac{T_1 I_1}{R} \tag{21.1}$$

On the other hand, the degree of preservation P of a past process on a hillslope is dependent on its resistance to change R divided by the duration T_2 and intensity I_2 of the present process.

$$P \propto \frac{R}{T_1 I_2} \tag{21.2}$$

If the resistance of a hillslope unit is considered to remain constant over time, the response of the system is mainly controlled by the duration and intensity of the processes involved. Only if the product of the duration and intensity of a past process is greater than the product of the duration and intensity of subsequent processes will the effects of the past process remain visible on the landform. With this general background, we will examine the suitability of desert hillslopes for the elucidation of past climatic changes.

INDICATOR POTENTIAL OF HILLSLOPES

In his textbook on slopes Young (1972, p. 18) stated that the form of present-day slopes has evolved mainly over the past million years or less and that climatic changes over this period have been on a scale sufficient to have a considerable effect on surface processes, particularly in the subtropical desert margins. The ages of hillslopes strongly depend on the strength of the material of which they are composed and the related denudational activity (Parsons 1988, p. 121). Consequently, the ages of hillslopes are decisively controlled by their resistance to change. When hillslopes or parts of them are old enough to have experienced the climatic changes of the Pleistocene, it is necessary to investigate

(a) whether the climatic changes were strong and long enough to shift form–process relationships from one state of equilibrium to a significantly different one (a change in principle), or
(b) whether they only enhanced or attenuated existing relationships (a change in degree), or
(c) whether they were too weak and short-lived to have caused any effect on the general trend of hillslope development (no morphological change).

Figure 21.2 Valley-side scarp in the Canyonlands section, Utah, of the Colorado Plateau. The Colorado River flows at the base of the scarp. The caprock consists of the sandstones of the Glen Canyon Group, whereas the lower slope is formed in the redbeds of the Chinle Formation. The lower slope is directly affected by base level fluctuations.

Only in the first case will truly independent climatogenetic landform elements in Büdel's (1982) sense have come into existence.

Slope systems are controlled by lateral backwearing, sometimes in combination with downwearing and slope angle reduction where processes of slope decline are involved. On bipartite cuesta scarps parallel retreat is the dominant mechanism. Slope denudation implies an inherent mechanism of surface destruction along the entire slope reach. This surface-destruction mechanism is a major drawback to the preservation of forms created by past climates.

The ability of hillslopes to bear clear testimony to distinct climatic phases is complicated by the fact that process change may not simply be expressed in a characteristic form assemblage of a slope system. The work of varying processes can also result in a uniform slope configuration, which represents a typical expression of a particular sequence of different climatic periods. The morphology of these slopes is due neither to present-day nor to past processes alone but has been shaped by a temporal succession of processes. Descriptions of hillslopes characterized by this type of development have been presented by Oberlander (1972) for the Mojave Desert and by Moss (1977) for southern Arizona. The term 'morphogenetic sequence' has been proposed by Mensching (1974) for the evolution of landforms, which owe their present shape to a combination of different processes. He has described a number of examples from North African arid and semi-arid areas (e.g. Mensching 1976).

As will be shown below, most legacies of former slope processes are found on bipartite slopes, where a hard caprock overlies an easily erodible formation. These hillslopes are generally called cuesta scarps. Homolithic slopes do not tend to furnish similar information. The indicator potential of the bipartite slopes can be explained by their specific composition. They normally consist of an upper steep slope in the resistant layer and a lower, moderately inclined slope in the less resistant beds. There is much confusion in the terminology of the different form elements of cuesta scarps (cf. Oberlander 1989). Terms such as subtalus slope (Koons 1955), footslope (Oberlander 1977), rampart (Howard and Kochel 1988) or substrate ramp (Oberlander 1989) have been utilized for the part of the scarp developed in soft rock below the caprock. The more neutral term lower scarp slope (Schmidt 1987a) will be used in this chapter. The caprock provides resistant talus which protects portions of the lower scarp slope from the slope's general fate of being destroyed by the backwearing processes. Mainly for this reason most studies dealing with evidence of past processes on desert hillslopes have chosen cuesta scarps as their research subject; so will this presentation.

Scarps may serve as useful indicators for major climatic fluctuations (Gerson 1982). The resistance to change and consequently the inertia is greater for hillslope systems than for rivers, floodplains, and alluvial fans. These fluvial systems are able to store a detailed record, but this record also includes some 'noisy' information. For the Colorado Plateau in the south-western United States the Holocene and late Pleistocene depositional and erosional history of the river systems is well known from the alluvial record (e.g. Hack 1942, Euler *et al.* 1979, Wells *et al.* 1982, Graf *et al.* 1987). There is, however, no comparable evidence of past climatic oscillations on the cuesta scarps (Schmidt 1988). Apparently the relaxation times are longer and thresholds for formative change are higher for the slopes. The base level fluctuations

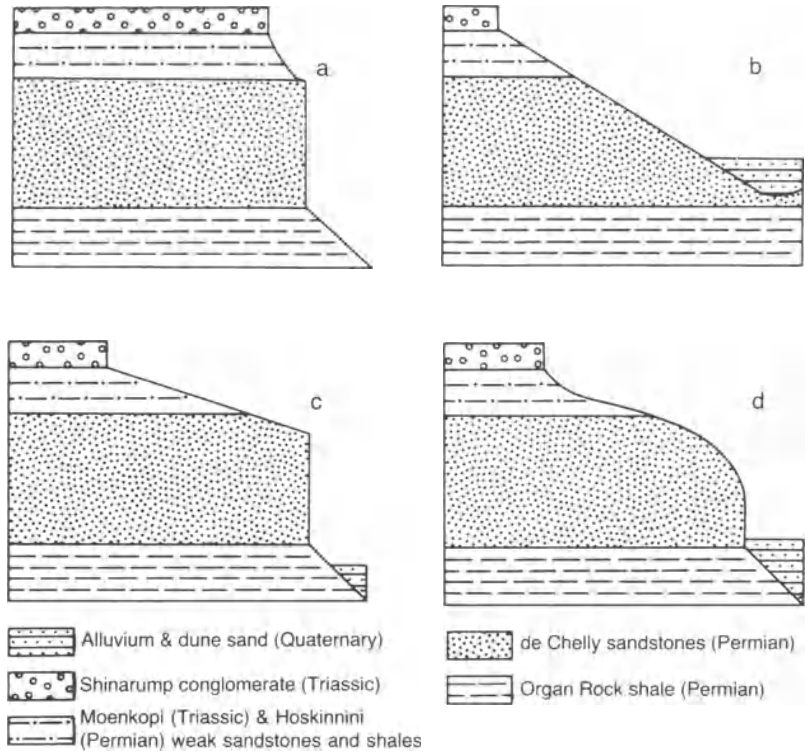

Figure 21.3 Schematic cross-sections through the four main scarp types occuring on de Chelly sandstone in Monument Valley (redrawn after Ahnert 1960). (a) Vertical cliff formed by predominance of pluvial sapping. Base of de Chelly sandstone is exposed above high lower scarp slope. (b) Bedrock slope formed by predominance of interpluvial surface wash. Base of de Chelly sandstone was never exposed. (c) Bedrock slope sharply truncated by vertical cliff. Predominance of surface wash followed by predominance of sapping. Base of de Chelly sandstone usually exposed above lower scarp slope. (d) Bedrock slope gradually leading into vertical cliff. Predominance of sapping followed by predominance of surface wash. Base of de Chelly sandstone usually covered by Quaternary alluvium and dune sand.

were neither long enough nor strong enough to be propagated upslope (Vanderpool 1982, Littmann and Schmidt 1989). On the hillslopes only former climates of long duration and characterized by highly effective processes have left their imprint. This makes these hillslopes a valuable indicator for the low frequency climatic periodicity of the Pleistocene. But not all desert cuesta scarps bear the imprint of former processes. A strong influence is exerted by the lithological and structural attributes of the caprock and substrate and other controlling factors (Gerson and Grossmann 1987, Schmidt 1989b). These factors will be discussed in a subsequent section.

STABILITY OR ACTIVITY IN DRY PERIODS

The question whether desert landforms remain more stable in dry (interpluvial) than in more humid (pluvial) conditions has for long been a matter of controversy. For desert washes (arroyos) in the American South-west the discussion about the influence of different hydrologic regimes including human interference has been summarized by Cooke and Reeves (1976), Graf (1983) and Karlstrom (1988). For cuesta scarps in the same region this controversy has been highlighted in the papers of Ahnert (1960) and Schumm and Chorley (1966). Ahnert (1960) argued that erosional processes, particularly slump block production and sapping processes supported by subterranean wash, were much more active during the pluvials, and that present-day landform modifications are only of minor importance. He derived a model of four main scarp types, formed by varying combinations of pluvial and interpluvial processes (Fig. 21.3). The greater moisture availability in the humid periods may well have enhanced groundwater flow and seepage above impervious beds. Howard and Kochel (1988) concluded from their detailed field observations in Navajo Sandstone

alcoves that present-day sapping activity and alcove development is much less than during a past pluvial climate. With respect to talus production, Schumm and Chorley (1966) maintained that the frequently observed lack of basal talus on the lower scarp slopes is not a consequence of slope stability but a result of effective weathering and a high rate of talus removal. Ahnert's (1960) climato-cyclic interpretation contrasts sharply with this equilibrium view of Schumm and Chorley (1966).

Presently inactive landslide material, slump blocks, and major rockfall accumulations on cuesta slopes have been interpreted as indicators of decreasing geomorphological activity from the last humid period to the present dry phase. Figure 21.4 shows the distribution of annual precipitation on the Colorado Plateau, the area to which most of the discussion in this section refers. The depositional features have been regarded as relict landforms inherited from past processes. Symptomatic for this kind of interpretation with regard to landslides is Hunt *et al.*'s (1953, p. 171) statement: 'They appear to have survived from a more humid climate when conditions were more conducive for weathering and recession of cliffs.' Landslides and large-scale rotational slumps as evidence of humid phase activity have been described from the Vermilion Cliffs and Echo Cliffs, Arizona (Strahler 1940, Phoenix 1963), from the Red House Cliffs, Utah (Mullens 1960), and the White Canyon area, Utah (Thaden *et al.* 1964) (Fig. 21.4). All of these sites are characterized by massive sandstones (Glen Canyon Group), overlying swelling bentonitic Chinle shale. These landslides are enormous in size, being up to 2 km long and 800 m wide (Thaden *et al.* 1964, p. 75). The absence of youthful slumps is taken as an indicator of present stability. The same line of reasoning was followed by Watson and Wright (1963) for the eastern flank of the Chuska Mountains, New Mexico, where extensive landslides occur in the differentially consolidated Chuska Sandstone, and by Reiche (1937) for the Black Mesa area, Arizona, where Mesa Verde sandstones overlie Mancos Shale (Fig. 21.4). Reiche, however, also reported two major young slumping events from 1870 and 1927.

Schumm and Chorley (1966) collected eyewitness accounts of active scarp retreat processes from the National Parks and National Monuments Services on the Colorado Plateau. These accounts make it clear that rockfalls of different magnitudes have frequently occurred in recent years. This conclusion is supported by descriptions of field geologists for different parts of the Colorado Plateau. Ford *et al.* (1976) gave a detailed account of rockfalls in the Grand Canyon area (Fig. 21.4). Cliff retreat is also a presently active process in the Montezuma Canyon area, Utah (Fig. 21.4), with isolated rockfalls occurring occasionally in the Dakota and Salt Wash sandstones (Huff and Lesure 1965). In the Slick Rock district, Colorado (Fig. 21.4) a number of slides were observed during field work in the years 1953 to 1956. The slides involved the Burro Canyon formation and the Salt Wash sandstone and occurred after heavy autumn rain (Shawe *et al.* 1968). Apparently present-day intensive precipitation events are well capable of triggering rockslides of resistant caprocks over water-saturated non-resistant lower-slope rocks.

Schumm and Chorley (1964) described a major rockfall event in Mesa Verde sandstones in the Chaco Canyon National Monument, New Mexico (Fig. 21.4), dating from 1941. They concluded (1966, p. 19): 'Although such contemporary occurrences of this magnitude may be rare, the fact that slumps have occurred during the past 100 years illustrates the need for caution in attributing all occurrences of an erosional phenomena [*sic*] to past climates greatly different from the present'. This quotation implies that the morphological features of cuesta scarps can be explained by presently active processes and that, if there have been changes at all, they have been only in the relative rates of processes. The continuity of large-scale cliff retreat processes has also been stressed by Davidson (1967) in the Circle Cliffs area, Utah (Fig. 21.4) and by Shawe *et al.* (1968) in the Slick Rock district, Colorado.

Any conclusion concerning activity or stability of geomorphic processes must try to avoid some potential hazards of misinterpretation. It is extremely hazardous to judge from a one- or two-year field investigation or even from a 100-year photographic record (Baars 1971, Shoemaker and Stephens 1975) whether a specific type of landform in a desert environment is stable or not. A period of 100 years covers not more than 1% of the Holocene. Geomorphological events on a hillslope are not only highly sporadic in time but also unevenly distributed in space in contrast to fluvial action. Gravitational events may be ordered according to the magnitude of the masses of material involved. They range from the fall of small grains through the fall of individual stones, slabs, and blocks, to rockfalls, rockslides, slumps, and landslides. Masses ranging from 10^{-3} g through 10^{8} g to 10^{12} g are transported by the different processes. Obviously the authors who deduce present-day morphological stability from their observations refer to giant landslides with lengths of several hundred metres or large slump blocks with lengths of 50 metres or more (e.g. Reiche 1937,

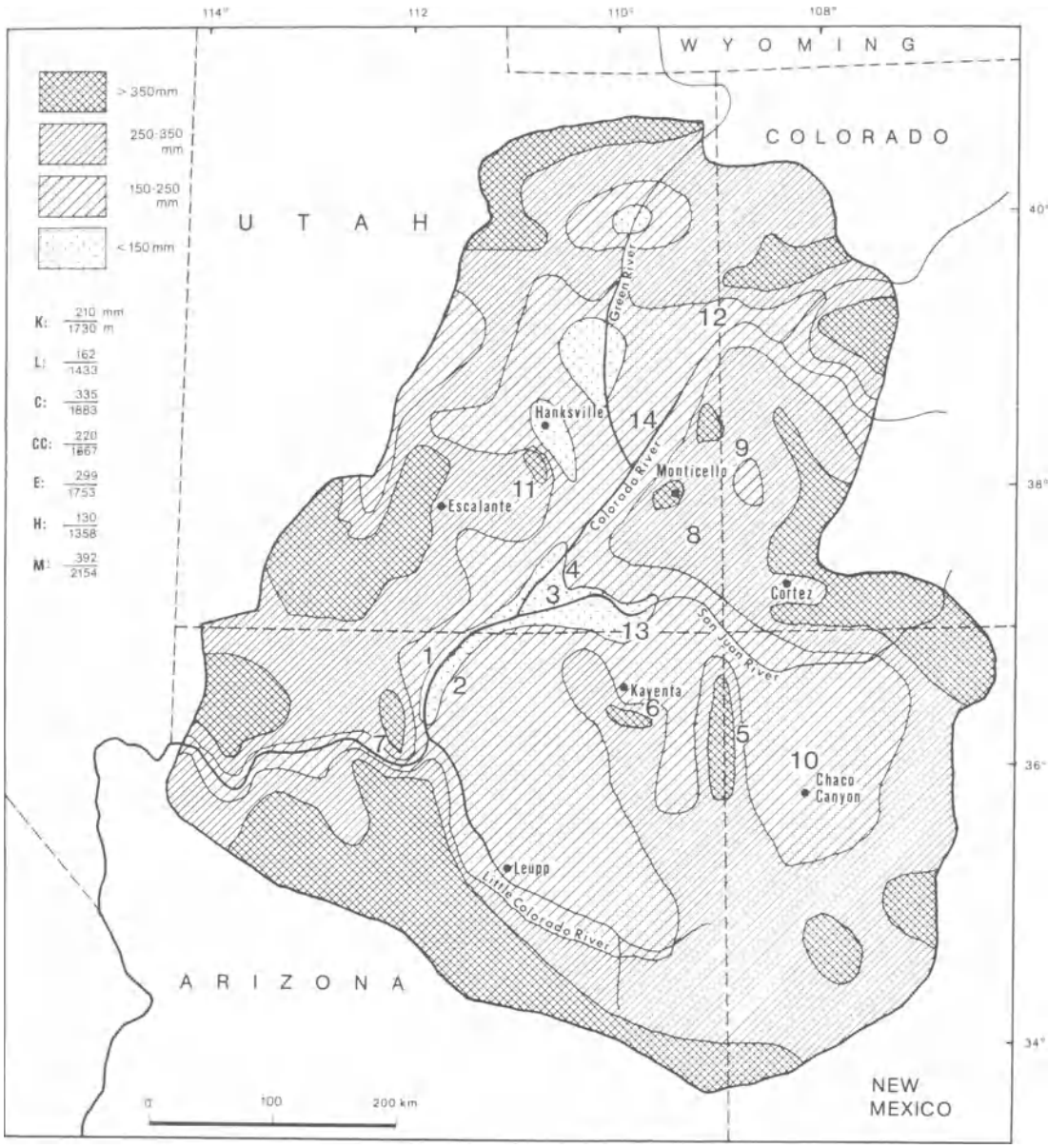

Figure 21.4 Distribution of mean annual precipitation on the Colorado Plateau. The initials below the legend refer to the stations shown on the map. The annual precipitation and the altitude of these stations are specified. The numbers on the map indicate locations mentioned in the text: (1) Vermillion Cliffs, (2) Echo Cliffs, (3) Red House Cliffs, (4) White Canyon, (5) Chuska Mountains, (6) Black Mesa, (7) Grand Canyon, (8) Montezuma Canyon, (9) Slick Rock district, (10) Chaco Canyon, (11) Circle Cliffs, (12) Book Cliffs, (13) Monument Valley, and (14) Canyonlands.

Strahler 1940, Mullens 1960, Watson and Wright 1963). Gravitational processes of smaller magnitude such as falls of individual rock fragments, minor rockfalls of a few cubic metres, and slab failures along joints or exfoliation structures have also been observed by authors, who otherwise deny the present-day activity of cuesta scarps (Strahler 1940). 'After severe summer rains and during early spring the Vermilion and Echo Cliffs sometimes resound with noise of falling rocks. The blocks that fall are

sometimes 15 or 20 feet in diameter' (Phoenix 1963, p. 40). The activity of processes has to be evaluated in the light of magnitude and frequency concepts. Moreover, on the scarp slopes the gravitational processes are spatially and temporally discontinuous. The variability in space and time increases with increasing process magnitudes. It is difficult to decide whether a particular type of high-magnitude process is really extinct or whether we just meet a cuesta slope in the interval between two such rare events.

When there are no signs of present-day high-magnitude events (rockfalls, slump blocks, or landslides) on a particular cuesta scarp section, this does not mean that there is a general state of morphodynamic stability. So the cuesta scarp section under consideration may well experience events of smaller magnitude, while at other scarp sections events of greater magnitude may happen at the same time (Fig. 21.5a and b). Only the chronological integration of processes of different magnitude and frequency and the spatial integration of all scarp sections will lead to a reliable evaluation of process activity in desert regions. A space-integrating argument in support of the view of present-day morphological activity is the current high rate of suspended sediment transport of the Colorado River and its tributaries (Smith *et al.* 1960), Iorns *et al.* 1965, Schmidt 1985). The overall denudation rate lies between 70 and 350 mm per 1000 years (Schmidt 1985), but it is difficult to determine how much material is eroded from the slopes and how much originates from the alluvial valley fills which have been dissected since the turn of the century. Erosion measurements on lower scarp slope rocks yield additional evidence for high process intensity. Colbert (1965) determined a denudation rate of 5.7 mm y^{-1} for steeper parts of the lower scarp slope of the Echo Cliffs, Arizona (Fig. 21.4), in the bentonitic shales of the Petrified Forest member of the Chinle Formation. Surface lowering in the easily erodible Mancos Shale at the foot of the Book Cliffs, Colorado (Fig. 21.4), varies between 0.2 and 2.2 mm y^{-1} and is a function of inclination and land use (Lusby 1979). In the same area a rate of denudation of 2.7 mm was measured in a single event (Hadley and Lusby 1967). Intensive lowering on Mancos Shale slopes (0.15 to 1.5 mm y^{-1}) was also determined by stake exposure measurements (Schumm 1964). The high erosion rates in the lower slope rocks are also indicative of the general activity of the cuesta scarps, because erosional backwearing is responsible for caprock undermining.

In Northern Africa, too, different views have been expressed concerning activity or stability of gravitational processes on cuesta scarps. The cuesta scarps in Nubian Sandstone on the margins of the Mourzouk basin have been investigated by Barth and Blume (1975) and Grunert (1983). Grunert stated that the landslides on the western flank of the basin are 'fossil' landforms dating from more humid periods in the middle Quaternary with annual precipitation amounts in excess of 400 mm (presently about 10 mm)! The landslides are presently destroyed by fluvial erosion. Barth and Blume (1975) take a broader view, pointing out that there are cuesta sections with extremely intensive denudational processes and others without any recent activity. The variations are explained by non-climatic controlling factors such as differences in resistance between caprock and lower slope rocks, differences in the thickness ratio, and differences in the elevation above base level. Apparently these controlling factors influence the cuesta scarps' resistance to change.

In a study of limestone scarps in the northwestern Sahara, Smith (1978) concluded that karstic and sapping processes and, consequently, cliff retreat are now stagnant. This view is again expressed in a more recent case study on Cenomanian–Turonian limestone scarps in south-eastern Morocco (Smith 1987). He deduced that the landforms are undergoing superficial modifications by weathering, but that the landscape as a whole has been essentially stable since mid to late Quaternary times (Tensiftien: about 1.3×10^5 years BP). He contended that undermining of the caprock is largely the product of spring sapping. The present author has also investigated the limestone cuesta scarps in Southern Morocco (Schmidt 1987b, 1989a). Certainly karst processes and sapping by karst water were much more efficient during humid periods than today. But rockfalls are not only caused by spring seepage and related alcove formation. Slope dissection and steepening are much more important for the destabilization of the caprock, and these mechanisms are also active in the present dry period. Limestone talus lies on and below the pediment level, which was formed in the last pluvial of the Pleistocene (Soltanien) (Schmidt 1989a) (Fig. 21.6a).

If we take the present variation in space as a substitute for the process variation in time caused by climatic change, there are some indications that the more arid areas show the greater erosional activity. In the upper Colorado River basin, where there is a great variety of different climatic regimes, the tributaries with the lowest precipitation and specific yield have the highest rates of mechanical denudation

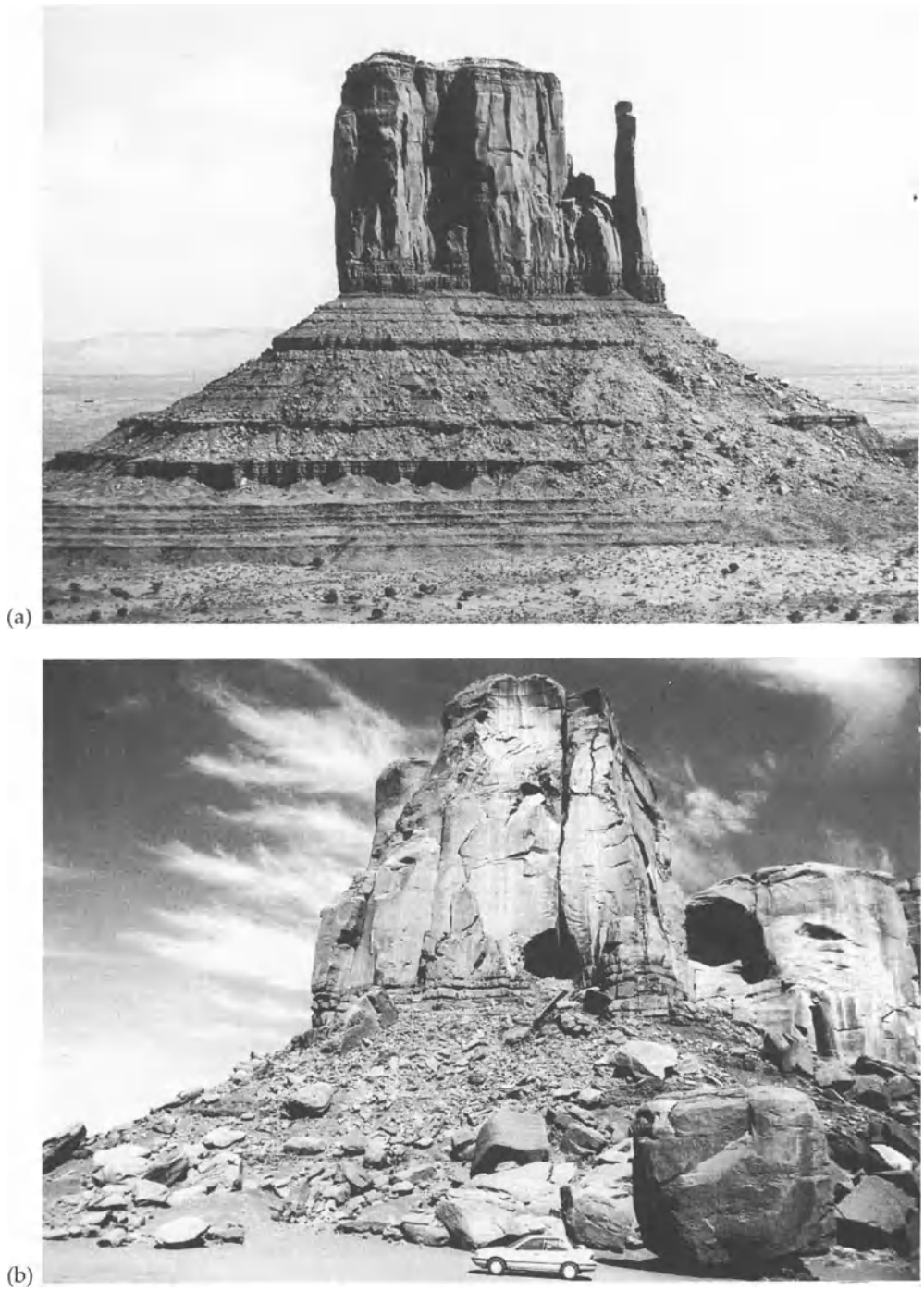

Figure 21.5 (a) West Mitten Butte in Monument Valley, Arizona. Vertical cliff is formed in de Chelly sandstone with Triassic layers on top (cf. Fig. 21.3), the lower slope is developed in the Organ Rock siltstones of the Cutler Formation. Note the intercalation of more resistant strata, which form ledges on the lower scarp slope. The lower slope is almost talus-free, which might lead the observer to assume general geomorphic stability. (b) Scarp of Spearhead Mesa, a nearby location in Monument Valley with the same stratigraphic setting. A fresh rockfall with large blocks covers the lower slope, which might lead the observer to assume geomorphic activity. Apparently, rockfalls can be triggered without pluvial sapping. A reliable evaluation of process activity or stability must use a time and space integrating survey.

(Schmidt 1985). Barth and Blume (1973) investigated cuesta scarps in several localities in the dry regions of the United States with different degrees of moisture availability from 165 mm annual precipitation with ten arid months on the central Colorado Plateau to 425 mm of annual precipitation with seven arid months in the Black Hills in Wyoming. The latter conditions might be representative of the situation in the last pluvial on the Colorado Plateau. Barth and Blume (1973) demonstrated that the cuesta scarps with the strongest morphological activity are found in the drier areas with precipitation amounts lower than 300 mm. In these areas the landform elements are interpreted as being in equilibrium with present-day processes and the authors rejected Ahnert's (1960) view of greater process activity in pluvial periods.

The preceding discussion shows that the question of alternating climates and of stable or unstable periods is difficult to resolve when the climatic changes only cause changes in degree in the process regime, and when different triggering processes (e.g. spring sapping, lower slope dissection) result in the same morphological response (e.g. rockfalls). Only landform elements which give evidence of significantly different processes of weathering and erosion will help to elucidate the effects of climatic change and the succession of different climatic regimes. Fortunately, there are cuesta scarp hillslopes which display multiphase assemblages of climato-genetic form elements.

TALUS AND PEDIMENT FLATIRONS

DESCRIPTION

Talus and pediment flatirons on the slopes of dryland cuesta scarps have a triangular to trapezoidal shape with their top directed towards the scarp (Figs 21.6 and 7). Talus flatirons are located on the scarp slope and pediment flatirons in the transition zone between scarp and foreland. In their distal parts, pediment flatirons may merge into river or lake basin terraces. Both the talus and pediment flatirons were parts of formerly active continuous slope systems, from which they received their debris cover. They have been detached from the presently active scarp by small rills running perpendicular to the general slope inclination, by slope steepening, and by cliff retreat. The inner slope of the flatirons is inclined towards the cuesta scarp and consists of the soft bedrock material of the lower portion of the scarp. The outer slope, which is inclined towards the scarp foreland with slope angles from 2 to 30°, is covered by a debris mantle consisting of resistant caprock talus protecting the soft lower slope rock from being eroded. The talus is generally not more than 5 m thick and has an average thickness of 2 m. In the proximal parts, however, the talus may contain blocks with *a*-axis diameters of more than 2 m which are remnants of rockfall debris.

MODELS OF FLATIRON FORMATION

Talus and pediment flatirons have been described from a variety of arid and semi-arid environments including the south-western United States (Koons 1955, Blume and Barth 1972, Barth and Blume 1973, Schmidt 1988), Spain (Sancho *et al.* 1988), the Saharan countries (Ergenzinger 1972, Grunert 1983), southern Morocco (Joly 1962, Dongus 1980, Schmidt 1987b, 1989a), Saudi Arabia (Barth 1976), Syria (Sakaguchi 1986), Cyprus (Everard 1963), and Israel (Gerson 1982, Gerson and Grossman 1987). In these publications different interpretations have been offered for the processes and climatic controls involved in the formation of these landforms. The debate has centred on the question of whether the flatirons are the product of climatically controlled distinct processes or whether they develop independently of climatic change. The respective conceptions of flatiron formation are called the climato-cyclic model and the non-cyclic model (Schmidt 1989b). Only in the former case can the flatirons be used as 'keys to major climatic fluctuations' (Gerson 1982, p. 123).

The non-cyclic model, which was first proposed by Koons (1955), is characterized by the sequence of events as depicted in Figure 21.8. No climatic change is needed for this sequence to occur. The successive stages of non-cyclic flatiron development from talus-free slopes to fresh talus cones and finally to complete separation of cones can be mapped in the field in close spatial proximity (Fig. 21.9).

The climato-cyclic model explains talus and pediment flatirons as consequences of climatically dependent alternations of significantly different processes on scarp slopes (Gerson 1982, Gerson and Grossman 1987, Schmidt 1987b, 1989a, b). In the more humid periods (pluvials) scarp slopes are controlled by debris flows and slopewash, which results in the formation of smooth, undissected concave slope profiles with only some gravitational activity in the proximal parts. When these conditions are replaced by more arid climatic regimes (interpluvials), dissection of the smooth debris slopes begins, bedrock is exposed in the rills, and gullying and rock collapse are the dominant processes. Parts of the formerly

Figure 21.6 (a) Cuesta scarp (Hamada de Meski, southern Morocco) capped by Cenomanian/Turonian limestones, which are underlain by soft continental redbeds. Climato-cyclic talus flatirons have developed on the scarp slope and pediment flatirons in the foreland. Different generations of flatirons can be discerned. Note the relatively fine-grained debris on the youngest (Soltanien = Würm) talus flatiron backslope in the right foreground. Below this 'pluvial' level we find coarse-grained rockfall material on the presently active slope. (b) Talus flatirons in the Negev, Israel, on a scarp with flints overlying chalks.

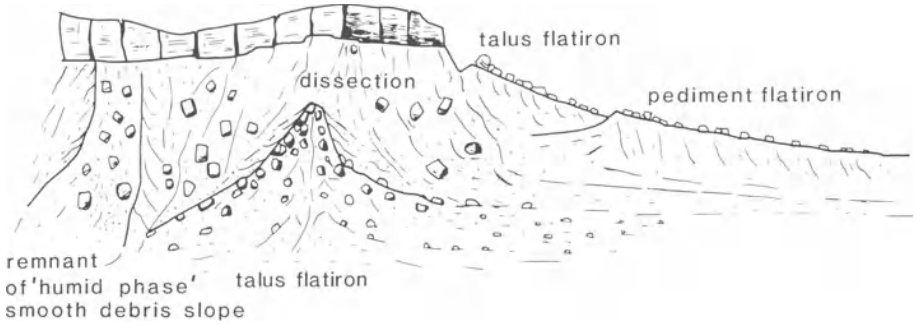

Figure 21.7 The climato-cyclic model of talus and pediment flatiron development (from Schmidt 1989b). A smooth concave debris-flow-controlled slope is formed in the more humid phase (pluvial). The slope is then dissected and steepened in the more arid phase (interpluvial). Parts of the debris slope are detached from the active scarp by dissection and scarp retreat, and talus and pediment flatirons originate.

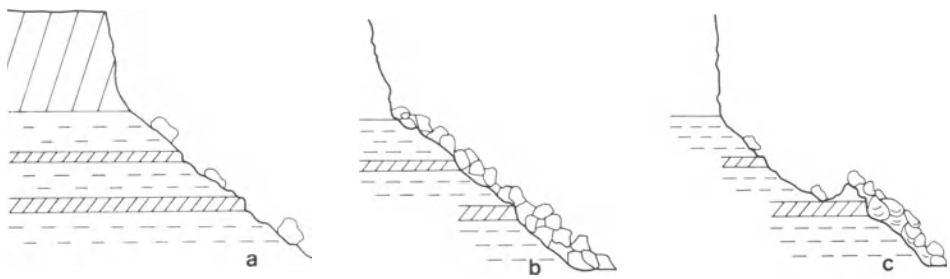

Figure 21.8 The non-cyclic model of talus flatiron development (from Schmidt 1989b). (a) The caprock is undermined and destabilized by dissection and steepening of the lower slope. (b) A rockfall is triggered, which covers the complete lower slope with a talus cone, at the same time reducing inclination of the lower slope. (c) The flanks of the talus cone are undermined by slope rills, the apex of the cone is detached from the scarp by tributaries to the major slope rills, and the talus cone becomes isolated from the scarp and a talus flatiron originates. After this succession of events the lower slope is again dissected and steepened, until a critical state of caprock destabilization is reached and a new rockfall is triggered.

continuous slope are separated from the active scarp, and talus and pediment flatirons begin to form, with the backslopes of the flatirons representing the remnants of the smooth debris slopes (Figs 21.6 and 21.7). In the current dry period, dissection of the smooth debris slopes and talus removal are ubiquitously observed processes on scarps in Northern Africa and the Middle East (Gerson 1982, Schmidt 1987b).

In these dry regions most talus relics are of climato-cyclic origin, whereas in the south-western United States, especially on the Colorado Plateau, most of the talus relics belong to the non-cyclic type. This difference is attributable to a number of lithological and structural controls essential to the formation of the two separate types of flatirons (Schmidt 1989b). Scarps with non-cyclic talus flatirons need to be fed with rockfall material which covers the complete lower slope with a talus cone. This continuous talus cone can only be supplied by thick caprocks and on scarp slopes where the thickness ratio between soft rock and caprock is not much greater than unity. The slope angle must be high enough to destabilize large parts of the caprock, and dissection of the lower scarp slope must not be so deep that the rockfall talus is trapped in the slope gullies. All of these conditions are met in the Colorado Plateau cuesta scarps formed by the Glen Canyon Group sandstones overlying the heterogeneous Chinle redbeds, where most of the non-cyclic flatirons are found (Fig. 21.9).

LITHOLOGICAL AND STRUCTURAL PREREQUISITES FOR THE FORMATION OF CLIMATO-CYCLIC TALUS AND PEDIMENT FLATIRONS

As the climato-cyclic talus relics attest to past climates and climatic change, the conditions necessary for their development are of particular interest.

Figure 21.9 Cuesta scarp with Glen Canyon sandstones overlying redbeds and bentonitic claystones (base of the scarp) of the Chinle Formation, Comb Ridge, Utah. Different stages of non-cyclic talus flatiron development can be observed along this reach of the Comb Ridge. From right to left: talus cone still connected with the vertical cliff; scarp section relatively free of talus; a talus cone undermined on its flanks; behind the gap in the scarp's crest two triangular talus flatirons with their apices separated from the scarp slope. Note the coarse-grained talus on the flatiron backslopes when compared with backslope material in Figure 21.6a and b.

(a) In the more humid phase, a smooth concave debris-flow-controlled slope profile must be formed as the initial stage of flatiron formation. This is only possible in thick lower slope rocks of relatively uniform resistance. In North Africa the continental redbeds below the Cretaceous limestones belong to this category of rock type (Fig. 21.6a), as does the Mancos Shale in the southwestern United States. Where the Mancos Shale crops out in the lower slope, some of the few instances of cyclic flatirons on the Colorado Plateau are found, such as on the slopes of Mesa Verde, Colorado (Fig. 21.10), on the Book Cliffs, Colorado and Utah (Fig. 21.4), and in the Henry Mountains basin west of Hanksville, Utah (Howard and Kochel 1988).

On lower scarp slopes with intercalated resistant layers, such as in the redbeds of the Chinle or Cutler Formations (Fig. 21.5a), the resistance to change is too great for smooth debris slopes to form and, consequently, for cyclic flatirons to develop (Schmidt 1988). Intensity and duration of the past process were not able to gain ascendancy over lithological form resistance (equation 21.1). On the other hand, free faces, as in the Moenkopi or Summerville Formations (Fig. 21.1) with their short relaxation times, are also not characterized by flatiron forms.

(b) The outer slopes of the talus and pediment flatirons need a highly protective talus cover to survive periods of cyclic duration. Only very resistant caprocks such as limestones, quartzites, or well-cemented sandstones and conglomerates can supply the lower slope with a sufficiently protective talus cover. The protective effect is enhanced when the talus becomes cemented by carbonates. Limestone and cemented sandstones and conglomerates can supply the slope debris with a lateral input of water containing carbonates in solution. In southern Morocco, for instance, the caprocks either guarantee the supply of carbonate cement (limestones, cemented conglomerates) or are very resistant (limestones, quartzites) (Schmidt 1987b, 1989b). Also the

Figure 21.10 Giant flatirons on the scarp of the Mesa Verde, Colorado. Mancos Shale is exposed on the flanks of the flatirons.

caprocks described from Israel (Gerson 1982) are very resistant (flints, limestones). On the Colorado Plateau, however, many of the caprocks are poorly cemented sandstones such as the Navajo, Entrada or de Chelly sandstones. There are no resistant limestone caprocks with the exception of the Kaibab Limestone (Schmidt 1988). If the flatirons carry a resistant backslope cover, their resistance to change and their tendency to be preserved increase. The intensity and duration of the subsequent processes are not competent to obliterate the legacies of the past processes (equation 21.2).

(c) The thickness ratio between soft rock and caprock is another important controlling factor. When the caprock is relatively thin and the thickness ratio in excess of 5, the mass of caprock material is not sufficient to cover and protect the complete lower slope with a talus apron, especially when the caprock is not very resistant. On the other hand, when the thickness ratio is less than unity, talus production exceeds talus transport and removal, the lower slope 'drowns' in debris and no smooth concave debris slope – the initial stage of flatiron formation – can develop. Additionally, great differences in resistance between caprock and soft rock promote cyclic flatiron formation.

(d) On complex scarps, where more than one caprock–soft-rock sequence is involved in scarp composition, the intercalated caprocks on the slopes impede the formation of a continuous concave debris slope and, hence, the development of talus or pediment flatirons.

(e) Undercutting rivers or washes at the foot of the scarp will steepen the basal part of the lower slope and preclude basal concavities from being formed. Also deeply incised canyons in the immediate scarp foreland with the resulting high vertical distance to base level make the evolution of cyclic flatirons impossible by decreasing the slope's resistance to change (Fig. 21.2).

Taken overall, conditions in Northern Africa and the Middle East are more suitable than in North America for cyclic flatiron generation. An investigation of about 100 Colorado Plateau cuesta scarps showed that most of the scarp slopes do not satisfy the above requirements, and lithological and structural constraints impede cyclic flatiron development (Schmidt 1989b).

CLIMATIC THRESHOLDS

In those areas where the smooth debris slopes are being destroyed, ubiquitous dissection is taking place, and a new generation of cyclic flatirons is being formed, the annual precipitation lies between 75 and 175 mm in southern Morocco (Schmidt 1987b) and between 150 and well below 100 mm in Israel (Gerson and Grossman 1987). In both areas high precipitation intensities with intensive gullying have been recorded. The question arises: what is the threshold precipitation at which slope dissection gives way to smooth debris slope formation, and vice versa? Gerson and Grossman (1987) specifiy that a change to a moderately arid (150 to 250 mm) or semi-arid (250 to 400 mm) climate will cause the onset of debris-flow-controlled processes. In a study of a cuesta scarp in the north-western Tibesti area, Ergenzinger (1972) came to the conclusion that annual precipitation amounts in excess of 200 mm are needed for the formation of a smooth debris slope (*Schwemmschutthang* in the German terminology).

Investigations of Cenomanian–Turonian limestone scarps in southern Morocco by the present author showed that, although flatiron development is extremely active on the southern margin of the High Atlas, no slope dissection nor flatiron formation occurs in its northern foreland. In this area mean annual precipitation exceeds 200 mm. The 200-mm isohyet seems to represent a critical threshold value for the formation of talus relics on scarps with limestone caprocks underlain by soft continental redbeds. Apparently the smooth undissected concave lower scarp slopes, which are more densely vegetated than the slopes south of the High Atlas, are in equilibrium with the processes operating under the current climatic regime. Also no flatirons are formed in the Middle Atlas where precipitation exceeds 400 mm. Caution is needed in spatially extrapolating this threshold precipitation value of 200 mm, which is defined only for a specific set of lithological and structural conditions. A smooth concave slope is presently being dissected on the Mesa Verde cuesta scarp (Fig. 21.10), while the mean annual precipitation at nearby Cortez, Colorado, lies close to 350 mm (Fig. 21.4). A detailed evaluation of the critical conditions initiating the dissection of smooth debris slopes under different lithological and structural controls is certainly needed. An important role will be played not only by precipitation but also by temperature with its influence on the frequency and intensity of frost action and on the formation of frozen ground during cold periods.

TIMESPANS REQUIRED FOR THE FORMATION OF CLIMATO-CYCLIC FLATIRON FORMS AND THE INTERPRETATION OF FLATIRON SEQUENCES

The resistance to change and the relaxation times of hillslopes (see above) strongly control the timespans needed for the climato-cyclic talus relics to develop. Short-term climatic changes of a few hundred years or less and individual events are generally not recorded on hillslopes (Gerson 1982, Vanderpool 1982, Gerson and Grossman 1987, Littmann and Schmidt 1989). Gerson (1982) gave a tentative minimum estimate of 25 000 to 50 000 years for a smooth debris slope to develop after dry-phase dissection. And several thousand years are required to convert a talus slope into a slope controlled by gullying and dissectional activity (Gerson and Grossman 1987). Dissection of smooth debris slopes during the late Holocene dry period is an example (Littmann and Schmidt 1989).

There is a general paucity of chronostratigraphic information for coarse-grained hillslope deposits, since they are mostly free of fossils, organic carbon remains, or archaeological evidence. With the present lack of absolute age determinations only some inferences about relative chronologies are possible. According to the model of climato-cyclic flatiron formation, the latest continuous smooth debris slope formed during the last wet period of at least several thousands years' duration. In Israel a talus relic has been dated by Mousterian artefacts to have originated during the early to middle Würm, which was a relatively wet period in the eastern Mediterranean region (Gerson and Grossman 1987). In southern Morocco many of the backslopes of the youngest flatiron generation merge into Soltanien (Würmian) terrace surfaces (Schmidt 1987b, Littmann and Schmidt 1989). Judging from the late Quaternary climatic record for the areas where climato-cyclic flatirons have developed (northern fringe of the Sahara, Middle East, eastern Mediterranean area), periods of greater moisture availability coincide with certain stages of the last glaciation (Gerson 1982, Schmidt 1987b). Littmann (1989) showed that the Atlas region remained wetter than today until the late glacial. More arid climates with slope dissection seem to have prevailed in interglacial times (such as the Holocene).

On the slopes and in the foreland of many cuesta scarps, sequences of talus and pediment flatirons are found, each flatiron backslope preserving the latest stage of a pluvial period (Figs 21.6a and 21.11). The inter-flatiron erosional gaps are the product of scarp recession during the dissection-controlled interpluvial and the subsequent debris-flow-controlled plu-

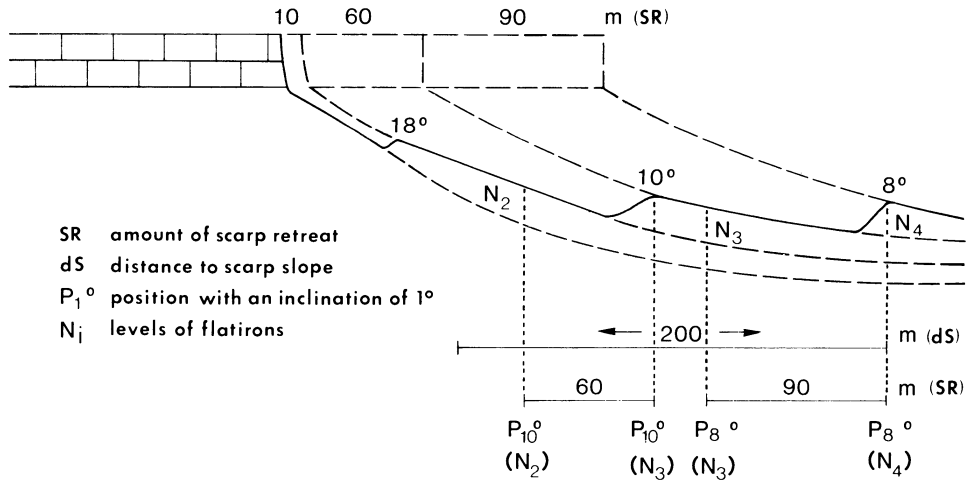

Figure 21.11 Sequence of flatirons on the slope of an erosional outlier capped by Eocene limestones (Gara Aferdou, southern Morocco). N_4 to N_2 are levels of talus and pediment flatirons. N_1 is the youngest (Holocene) terrace level. Amounts of scarp retreat can be obtained by measuring the distance from the top of the older flatiron (e.g. $P_{8°}$; N_4) to the point of equal inclination on the next younger flatiron backslope (e.g. $P_{8°}$; N_3). The amount of retreat in the example is 90 m. Measuring the distances between the tops of successive flatirons or the distances to scarp slope will overestimate the amount of scarp recession, because the inner slopes of the flatirons have also retreated after their formation. As the cycle from Amirien (Mindel) to Tensiftien (Riss) lasted about 2×10^5 years, a rate of retreat of about 0.45 m per 1000 years is obtained. Since the last pluvial (Soltanien) the scarp has retreated about 10 m. The average rate of retreat of the limestone scarps in southern Morocco is about 0.5 m per 1000 years (Schmidt 1987b).

vial periods. They represent the denudational activity of a complete interpluvial–pluvial cycle. This model is supported by cation-ratio relative dating methods of rock varnishes from flatiron surfaces in Israel (Dorn 1983, Gerson and Grossman 1987). Multicycle flatiron generations are best preserved on scarp spurs and on the flanks of erosional outliers, where the intensity of slope denudational processes is reduced. In southern Morocco up to four successive generations have been found on the limestone scarps (Schmidt 1987b). Six levels were mapped in the Makhtesh Ramon area in Israel (Gerson and Grossman 1987). The number of flatiron generations is an indication of the number of late and middle Quaternary pluvial periods, and the distance between two successive flatirons can be used for estimating scarp retreat during an interpluvial–pluvial cycle (Fig. 21.11) (Gerson 1982, Schmidt 1987b, 1989a, b). To estimate rates of retreat, the lengths of the cycles must be known, which is still a matter of speculation. The cycle Tensiftien (Riss) to Soltanien (Würm) lasted about 10^5 years, and the cycle Amirien (Mindel) to Tensiftien about 2×10^5 years. With these rough figures rates of retreat of about 0.5 m per 1000 years were calculated for the limestone scarps in southern Morocco (Schmidt 1987b, 1989a). Since the last pluvial, the scarps have retreated a mean distance of about 10 m (Fig. 21.11). Progress in dating techniques will certainly help to fit the cyclic flatiron sequences into the climatic pattern of the Quaternary and to use them for palaeoclimatic interpretations in a more detailed way than presently possible.

CONCLUSION

Desert hillslopes may serve as valuable indicators of the low-frequency climatic periodicity during the Quaternary because, owing to their relatively high resistance to change and their usually long relaxation times, they record changes of long duration and high process effectiveness. Particularly bipartite slopes (cuesta scarps) may bear clear testimony of climatic change. Yet many of the interpretations of climatic change derived from hillslope form and process evidence are based on inference. Although surveys of sediment yield (Schmidt 1985) and comparative investigations of cuesta scarps in areas of varying moisture availability (Barth and Blume 1973) strongly indicate that in the more arid regions denudational processes are in a state of high morphodynamic activity, the understanding of different

process combinations under changing climatic conditions remains fragmentary. With regard to gravitational processes on cuesta scarps, a promising field of research seems to be the association of the alluvial chronology with rockfalls and slope deposits to decide whether events have been more frequent during specific periods in the past.

Process alternations, which show not only changes of process rates but of process type, are of major interest for palaeoclimatic interpretations. Landform assemblages which give evidence of geomorphic processes of different character are the talus and pediment flatirons. Present possibilities of dating these landform successions are extremely unsatisfactory. But surface exposure dating may permit the dating of landforms in deserts previously thought to be undatable (Dorn and Philips 1991) and may help attain greater precision in the palaeoclimatic interpretation of hillslope form sequences. Climate, however, is only one of several factors controlling hillslope processes, and results obtained in one region cannot readily be transferred to other regions in different structural and lithological settings.

REFERENCES

Ahnert, F. 1960. The influence of Pleistocene climates upon the geomorphology of cuesta scarps on the Colorado Plateau. *Annals of the Association of American Geographers* **50**, 139–56.

Ahnert, F. 1990. Editorial: Some reflections on climatogenetic tropical geomorphology. *Tropical Geomorphology Newsletter* **9**, 1–2.

Baars, D.L. 1971. Rates of change, 1871–1968. In *Geology of Canyonlands and Cataract Canyon*, D.L. Baars and C.M. Molenaar (eds), 89–99. Durango, CO: Four Corners Geological Society.

Barth, H.K. 1976. Pedimentgenerationen und Reliefentwicklung im Schichtstufenland Saudi-Arabiens. *Zeitschrift für Geomorphologie Supplement Band* **24**, 111–9.

Barth, H.K. and H. Blume 1973. Zur Morphodynamik und Morphogenese von Schichtkamm- und Schichtstufenrelief in den Trockengebieten der Vereinigten Staaten. *Tübinger Geographische Studien* **53**, 1–102.

Barth, H.K. and H. Blume 1975. Die Schichtstufen in der Umrahmung des Murzuk-Beckens (libysche Zentralsahara). *Zeitschrift für Geomorphologie Supplement Band* **23**, 118–29.

Blume, H. and H.K. Barth 1972. Rampenstufen und Schuttrampen als Abtragungsformen in ariden Schichtstufenlandschaften. *Erdkunde* **26**, 108–16.

Büdel, J. 1982. *Climatic geomorphology*. Princeton, NJ: Princeton University Press.

Colbert, E.H. 1966. Rates of erosion in the Chinle Formation – ten years later. *Plateau* **38**, 68–74.

Cooke, R.U. and R.W. Reeves 1976. *Arroyos and environmental change in the American South-West*. Oxford: Oxford University Press.

Davidson, E.S. 1967. Geology of the Circle Cliffs area, Garfield and Kane Counties, Utah. *U.S. Geological Survey Bulletin* 1229.

Dongus, H. 1980. Rampenstufen und Fußflächenrampen. *Tübinger Geographische Studien* **80**, 73–8.

Dorn, R.I. 1983. Cation-ratio dating: a new rock varnish age-determination technique. *Quaternary Research* **20**, 49–73.

Dorn, R.I. and Philips, F.M. 1991. Surface exposure dating: review and critical evaluation. *Physical Geography* **12**, 303–33.

Ergenzinger, P. 1972. Reliefentwicklung an der Schichtstufe des Massif d'Abo (Nordwesttibesti). *Zeitschrift für Geomorphologie Supplement Band* **15**, 93–112.

Euler, R.C., G.C. Gumerman, T.N.V. Karlstrom, J.S. Dean, *et al.* 1979. The Colorado Plateaus: cultural dynamics and palaeoenvironment. *Science* **205**, 1089–101.

Everard, C.E. 1963. Contrasts in the form and evolution of hill-side slopes in central Cyprus. *Transactions of the Institute of British Geographers* **32**, 31–47.

Ford, T.D., P.W. Huntoon, W.J. Breed and G.H. Billingsley 1976. Rock movement and mass wastage in the Grand Canyon. In *Geology of the Grand Canyon*, W.J. Breed and E. Roat (eds), 116–28. Flagstaff, AZ: Museum of Northern Arizona.

Gerson, R. 1982. Talus relicts in deserts: a key to major climatic fluctuations. *Israel Journal of Earth Sciences* **31**, 123–32.

Gerson, R. and S. Grossman 1987. Geomorphic activity on escarpments and associated fluvial systems in hot deserts. In *Climate, history, periodicity, predictability*, R. Rampino, J.E. Sanders, W.S. Newman and L.K. Königsson (eds), 300–22. New York: Van Nostrand Reinhold.

Graf, W.L. 1983. The arroyo problem – palaeohydrology and palaeohydraulics in the short term. In *Background to palaeohydrology*, K.J. Gregory (ed.), 279–302, Chichester: Wiley.

Graf, W.L., R. Hereford, J. Laity and R.A. Young 1987. Colorado Plateau. In *Geomorphic systems of North America*, W.L. Graf (ed.), 259–302. Geological Society of America, Centennial Special Volume 2.

Grunert, J. 1983. Geomorphologie der Schichtstufen am Westrand des Murzuk-Beckens (Zentrale Sahara). *Relief, Boden, Paläoklima* **2**, 1–269.

Hack, J.T. 1942. The changing physical environment of the Hopi Indians of Arizona. *Peabody Museum Paper* **35**, 1–86.

Hadley, F.H. and G.C. Lusby 1967. Runoff and hillslope erosion resulting from high-intensity thunderstorms near Mack, Western Colorado. *Water Resources Research* **3**, 139–43.

Howard, A.D. and R.C. Kochel 1988. Introduction to cuesta landforms and sapping processes on the Colorado Plateau. In *Sapping features on the Colorado Plateau, a comparative planetary geology field guide*, A.D. Howard, R.C. Kochel and H.E. Holt (eds), 6–56. National Aeronautics and Space Administration Special Publication 491.

Huff, L.C. and F.G. Lesure 1965. Geology and uranium deposits of Montezuma Canyon area, San Juan County,

Utah. *U.S. Geological Survey Bulletin* 1190.

Hunt, C.B., P. Averitt and R.L. Miller 1953. Geology and geography of the Henry Mountains region, Utah. *U.S. Geological Survey Professional Paper* 228.

Iorns, W.V., C.H. Hembree and G.L. Oakland 1965. Water resources of the upper Colorado River basin, technical report. *U.S. Geological Survey Professional Paper* **441**.

Joly, F. 1962. Etudes sur le relief du Sud-est marocain. *Travaux de l'Institut Scientifique Chérifien, Série Géologie et Géographie Physique* **10**, 1–578.

Karlstrom, T.N.V. 1988. Alluvial chronology and hydrologic change of Black Mesas and nearby regions. In *The Anasazi in a changing environment*, G.J. Gumerman (ed.), 45–91. Cambridge: Cambridge University Press.

Koons, D. 1955. Cliff retreat in the southwestern United States. *American Journal of Science* **253**, 44–52.

Littmann, T. 1989. Spatial patterns and frequency distribution of late Quaternary water budget tendencies in Africa. *Catena* **16**, 163–88.

Littmann, T. and K.-H. Schmidt 1989. The response of different relief units to climatic change in arid environments (southern Morocco). *Catena* **16**, 343–55.

Lusby, G.C. 1979. Effects of converting sagebrush cover to grass on the hydrology of small watersheds at Boco Mountain, Colorado. *U.S. Geological Survey Water Supply Paper* 1532-J.

Mensching, H. 1974. Landforms as a dynamic expression of climatic factors in the Sahara and Sahel – a critical discussion. *Zeitschrift für Geomorphologie Supplement Band* **20**, 168–77.

Mensching, H. 1976. Fluviale und äolische Formungsprozesse arider Morphodynamik an Stufenrändern des saharischen Hamada-Reliefs. *Zeitschrift für Geomorphologie, Supplement Band* **24**, 120–7.

Moss, J.R. 1977. The formation of pediments: scarp backwearing or surface downwasting. In *Geomorphology in arid regions*, D.O. Doehring (ed.), 51–78. London: Allen & Unwin.

Mullens, T.E. 1960. Geology of the Clay Hills area, San Juan County, Utah. *U.S. Geological Survey Bulletin* 1087-H, 259–336.

Oberlander, T.M. 1972. Morphogenesis of granitic boulder slopes in the Mojave Desert, California. *Journal of Geology* **80**, 1–20.

Oberlander, T.M. 1977. Origin of segmented cliffs in massive sandstones in Southeastern Utah. In *Geomorphology in arid regions*, D.O. Doehring (ed.), 79–114. London: Allen & Unwin.

Oberlander, T.M. 1989. Slope and pediment systems. In *Arid zone geomorphology*, D.S.G. Thomas (ed.), 56–84. London: Belhaven Press.

Parsons, A.J. 1988. *Hillslope form*. London: Routledge.

Phoenix, D.A. 1963. Geology of the Lees Ferry area, Coconino County, Arizona. *U.S. Geological Survey Bulletin* 1137.

Reiche, P. 1937. The Toreva Block – a distinctive landslide type. *Journal of Geology* **45**, 538–48.

Sakaguchi, Y. 1986. Pediment – a glacial cycle topography? *Bulletin of the Department of Geography, University of Tokyo* **18**, 1–19.

Sancho, C., M. Gutierrez, J.L. Pena and F. Burillo 1988. A quantitative approach to scarp retreat starting from triangular slope facets, central Ebro basin, Spain. *Catena Supplement* **13**, 139–46.

Schmidt, K.-H. 1985. Regional variation of mechanical and chemical denudation, Upper Colorado River basin, USA. *Earth Surface Processes and Landforms* **10**, 497–508.

Schmidt, K.-H. 1987a. Factors influencing structural landforms dynamics on the Colorado Plateau – about the necessity of calibrating theoretical models by empirical data. *Catena Supplement* **10**, 51–66.

Schmidt, K.-H. 1987b. Das Schichtstufenrelief der präsaharischen Senke, Süd-Marokko. *Zeitschrift für Geomorphologie Supplement Band* **66**, 23–36.

Schmidt, K.-H. 1988. Die Reliefentwicklung des Colorado Plateaus. *Berliner Geographische Abhandlungen* **49**, 1–183.

Schmidt, K.-H. 1989a. Stufenhangabtragung und geomorphologische Entwicklung der Hamada de Meski, Südostmarokko. *Zeitschrift für Geomorphologie Supplement Band* **74**, 33–44.

Schmidt, K.-H. 1989b. Talus and pediment flatirons – erosional and depositional features on dryland cuesta scarps. *Catena Supplement* **14**, 107–18.

Schumm, S.A. 1964. Seasonal variations of erosion rates and processes on hillslopes in western Colorado. *Zeitschrift für Geomorphologie Supplement Band* **5**, 215–38.

Schumm, S.A. and R.J. Chorley 1964. The fall of Threatening Rock. *American Journal of Science* **262**, 1041–54.

Schumm, S.A. and R.J. Chorley 1966. Talus weathering and scarp recession in the Colorado Plateau. *Zeitschrift für Geomorphologie* **10**, 11–36.

Shawe, D.R., G.C. Simmons and N.L. Archbold 1968. Stratigraphy of Slick Rock District and vicinity, San Miguel and Dolores Counties, Colorado. *U.S. Geological Survey Professional Paper* 576-A.

Shoemaker, E.M. and H.G. Stephens 1975. First photographs of the Canyonlands. In *Canyonlands country*, J.E. Fassett (ed.), 111–22. Durango, CO: Four Corners Geology Society.

Smith, B.J. 1978. The origin and geomorphic implications of cliff foot recesses and tafoni on limestone hamadas in the north-west Sahara. *Zeitschrift für Geomorphologie* **22**, 21–43.

Smith, B.J. 1987. An integrated approach to the weathering of limestone in an arid area and its role in landscape evolution: a case study from Southeast Morocco. In *International Geomorphology. Part II*, V. Gardiner (ed.), 637–57. Chichester: Wiley.

Smith, W.O., C.P. Vetter and G.B. Cummings 1960. Comprehensive survey of sedimentation in Lake Mead, 1948–49. *U.S. Geological Survey Professional Paper* 295.

Strahler, A.N. 1940. Landslides of the Vermilion and Echo Cliffs, Northern Arizona. *Journal of Geomorphology* **3**, 285–301.

Thaden, R.E., A.F. Trites and T.L. Finell 1964. Geology and ore deposits of the White Canyon area, San Juan and Garfield Counties, Utah. *U.S. Geological Survey Bulletin* 1125.

Vanderpool, N.L. 1982. ERODE – a computer model of drainage basin development under changing baselevel conditions. In *Applied Geomorphology*, R. Craig and J. Craft (eds), 214–23. London: Allen & Unwin.

Watson, R.A. and H.E. Wright 1963. Landslides on the east flank of the Chuska Mountains, northwestern New Mexico. *American Journal of Science* **261**, 525–48.

Wells, S.G., T.F. Bullard and L.N. Smith 1982. Origin and evolution of deserts in the Basin and Range and the Colorado Plateau provinces of western North America. *Striae*, **17**, 101–11.

Young, A. 1972. *Slopes*. London: Longman.

RIVER LANDFORMS AND SEDIMENTS: EVIDENCE OF CLIMATIC CHANGE

22

Ian Reid

INTRODUCTION

Changes in the style of fluvial deposits have long been used by sedimentologists as an indication of broad changes in climate. Certainly, in traversing the globe from one environmental extreme to the other – from humid to arid regions – it is possible to discern substantial differences in the character of rivers, both from the point of view of the forms that they adopt and in the sediments that they carry (Schumm 1977, Wolman and Gerson 1978). However, rivers react to a number of stimuli, and it is often difficult to determine whether a change in character reflects tectonic or climatic influences, or both (Frostick and Reid 1989a). Attempts to attribute cause inevitably and ingeniously simplify the setting by choosing systems in areas where most factors are presumed to have remained more or less constant while, ideally, another varies monotonically. So, for example, location on a stable craton may allow an assessment of the impacts of climatic change on river systems without the additional complications that arise from tectonic instability (Schumm 1968). However, while this approach may be useful in deducing the response of rivers to recent shifts in climate – say, those of the late Pleistocene and Holocene – and may be instructive in indicating the direction and magnitude of likely changes to be expected in river systems during periods of environmental change, the sedimentary legacies are often too similar to those assumed to arise from tectonic influences to ascribe changes in sedimentary style confidently to either set of causes when stepping further back in time.

In fact, rivers are comparatively insensitive to changes in climate unless these changes are substantial. Moreover, it is likely that there is considerable hysteresis in the relationship between climate-driven change and river metamorphosis. Intuitively, it might be argued that the rate of change in a parameter such as channel sinuosity would be greater during a shift towards aridity because of the tendency to increased flashiness in the flood regime and, therefore, greater potential erosional damage. In contrast, channel change during a corresponding period of increasing humidity might depend upon sediment accretion at a time of progressively decreasing rates of sediment yield.

However, the sensitivity of rivers to climatic change is conditioned, in part, by the wide range in flood magnitude that is experienced under a singular climatic regime and by the erosional or depositional legacy of large events. Baker and his colleagues (Baker 1977, Baker *et al.* 1983, Patton *et al.* 1982) have drawn attention to the implications of very large floods having recurrence intervals of the order of 10^3 years in the Northern Territory of Australia and west Texas. Nanson (1986) has described what he calls floodplain stripping in the coastal valleys of New South Wales. Here, substantial quantities of accumulated sediment are removed periodically during the passage of rare high-magnitude floods, leaving channel dimensions that bear little relation to more frequent floods ordinarily thought to be channel-formative, and a floodplain topography that is difficult to interpret in the context of observed flows. Under a drier regime, Schumm and Lichty (1963) have collated historical records to show that the Cimarron River of south-western Kansas was widened dramatically from an average of 15 m to 200 m during a high-magnitude flood in 1914. During the next 25 years, channel width increased to an average value of 365 m with the passage of other damaging floods, after which it declined progressively to 183 m

Geomorphology of Desert Environments. Edited by Athol D. Abrahams and Anthony J. Parsons. Published in 1994 by Chapman & Hall, London. ISBN 978-94-015-8256-8

over a period of 21 years in sympathy with lower flood discharges. But the fact that at-a-point channel width can be shown to have had a 24-fold range during a period when climate did not change dramatically suggests that parameters such as these – so important as tools in palaeohydrology – may have only limited value in diagnosing climatic change, at least in arid zones.

The damaging impact of large floods highlights another problem in using channel dimensional parameters as diagnostic of climatic change. Schumm and Lichty's (1963) study of the Cimarron River suggested a relaxation period (the lag between infliction of the flood damage and a return to pre-flood conditions) of much more than 50 years in this semi-arid environment. This compares with a relaxation period of less than 20 years in a temperate humid environment where flood frequency and the prospects of channel reparation are higher (Gupta and Fox 1974). Wolman and Gerson (1978) have suggested from rather more casual observations made in Sinai that the lack of sediment-trapping riparian vegetation and the extreme infrequence of floods in arid zones removes almost entirely the potential for channel restoration. In this environment, the relaxation period is, to all intents and purposes, infinite. In these circumstances, and with the inevitability of poor or non-existent hydrological records in such drylands, it may be difficult to judge whether or not a channel and its sediments are anachronistic. In other words, it may be difficult to establish whether they represent the prevailing climate or one that is now past, even if only over a comparatively narrow range of annual effective precipitation.

Having cautioned that diagnosing climatic change from channel and sediment characteristics can be hazardous where extremes of weather inflict damage that is only slowly restored to reflect the prevailing climatic average, it has to be pointed out that rivers may not react entirely predictably to changing climate – at least as far as can be ascertained given that shifts in climate can rarely be defined precisely in terms of the consequences for runoff. One problem is that each drainage basin is a unique permutation of all those factors that encourage or discourage runoff and sediment transfer. Factors which act as regulators of change may be more important in one basin than in another. Despite this and the fact that the infrequence of runoff in deserts has deterred the collection of data relating to flood flows and sediment transport so that understanding of fluvial processes in such environments is undernourished, certain patterns of climate-induced behavioural change have emerged.

QUATERNARY CLIMATIC CHANGE AND CONTINENTAL DRAINAGE

The changing pattern of climate in middle and low latitudes has now been successfully documented, particularly for the last 30 000 years (Street and Grove 1979). Because of the equivocal nature of river response to subtle shifts in the character of water catchments, fluvial landforms and depositional legacies have usually been used to corroborate evidence derived from other sources – principally datable, lacustrine, strandline deposits – rather than acting as a primary source of information. Nevertheless, set against evaporation, changes in river regime are, and have been, an important determinant of lake levels; and nowhere has this been more significant than in dryland lake basins such as those of the East African Rift (Butzer *et al.* 1972), the Levant (Begin *et al.* 1974), Australasia (Bowler *et al.* 1976), and western North America (Benson 1978).

The water-balance curve of Lake Chad can be taken as a typical example of the changing relationship between runoff and evaporation in the period since the last glacial maximum (Fig. 22.1; Servant and Servant-Vildary 1980). Particularly noteworthy in this curve is the trend towards extreme desiccation between 20 and *c.* 13 ka. This pattern was widespread throughout low and middle latitude drylands and obviously had important implications for river systems. At a comparatively local scale, low base levels in internal drainage systems led to fluvial incision. This is not particularly well documented, if only because, although present lake levels are comparatively low, they are nevertheless higher than their late glacial minima. This means that evidence is either sublacustrine or buried by aggradation. So, for example, the surface of the Dead Sea is thought, on the basis of the geochemistry of evaporites, to have lain at about −700 m, some 300 m lower than at present (Katz *et al.* 1977), and hydrographic surveys have shown sublacustrine valleys running offshore as projections of present lines of drainage (Neev and Emery 1967). A subsurface seismic examination of small deltas on the shores of Lake Turkana in northern Kenya has revealed palaeochannels some 20 m below the present alluvial feeders. These buried palaeochannels have gradients about 1.5 times those of their modern counterparts, and were given an age of *c.* 17 ka, albeit on the flimsiest of arguments (i.e. through an assessment of the thickness of the alluvial wedge in the context of contemporary sedimentation rates and the questionable presumptions of uniformitarianism (Frostick and Reid 1986)).

On a broader geographical canvas, the compara-

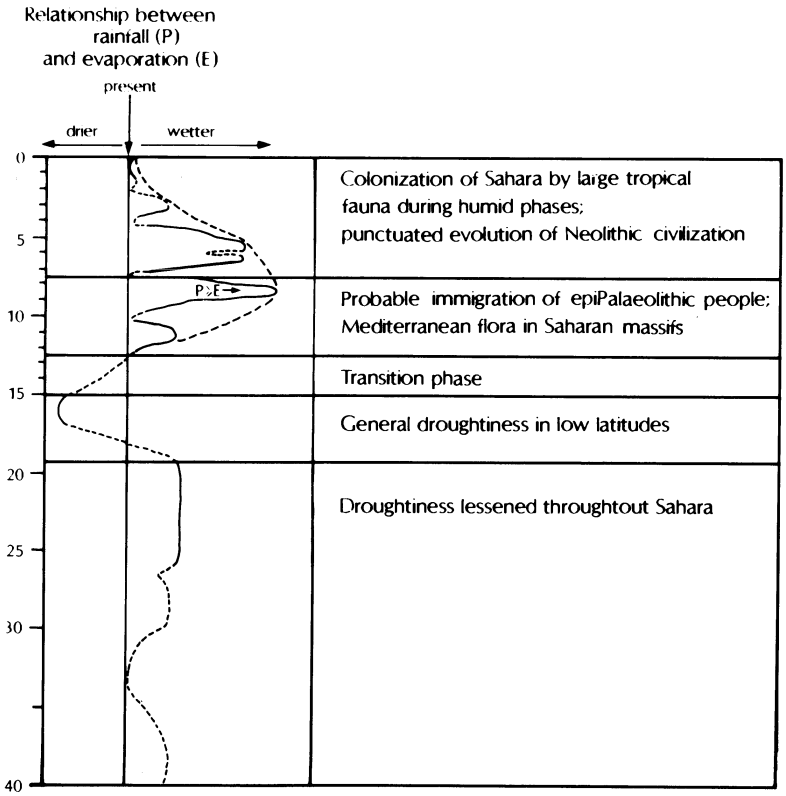

Figure 22.1 Climatic change in the Sahel over the last 40 000 years as inferred from strandline and other evidence in the Lake Megachad Basin (after Servant and Servant-Vildary 1980).

tive aridity of the last glacial maximum had considerable consequence for the nature and behaviour of the so-called exotic perennial rivers that traverse the world's drylands. Perhaps best known (in circumstances where information is always sparse, either because of the poor sedimentary preservation potential of desert environments or because information is being synthesized from a huge continental area) is that of the Nile (Adamson *et al.* 1980, Adamson 1982). There is inevitable controversy over the development of the integrated drainage that exists today. De Heinzelin and Paepe (1965) were of the view that the present river system is a product of the Upper Pleistocene and that previously there were a series of separate and unconnected basins. Butzer and Hansen (1968) acknowledged that the Blue Nile and other rivers rising in the highlands of Ethiopia had probably contributed to the trunk stream since the beginning of the Pleistocene, while Williams and Williams (1980) suggested that the Nile has had Ethiopian headwaters since Tertiary times. The history of the White Nile is even less certain. Kendall (1969) showed, from the evidence contained in lake-bottom cores, that Lake Victoria had no outlet during an undefined period prior to 12 ka, and Williams and Adamson (1974) have speculated that the White Nile was at best highly seasonal if not completely ephemeral during the hyperdesiccation of the terminal Pleistocene arid phase. The picture that emerges merely reinforces a view that the Nile system has, for various reasons and for some considerable time, defied the dendritic laws of drainage that help to describe large river systems on other relatively stable cratons.

The other notable element in the water balance of drylands in the recent past was the shift towards more humid conditions during the terminal Pleistocene and early Holocene (*c.* 12 to 5 ka; Fig. 22.1). The impact on rivers was as dramatic as was the preceding phase of desiccation and has to be understood if only to interpret the fluvial relics that litter the present arid landscape.

In the Sahel of West Africa, Talbot (1980) has drawn attention to the now defunct northern tributaries of the Niger, indicating that the contributing water catchment of the trunk stream was perhaps as

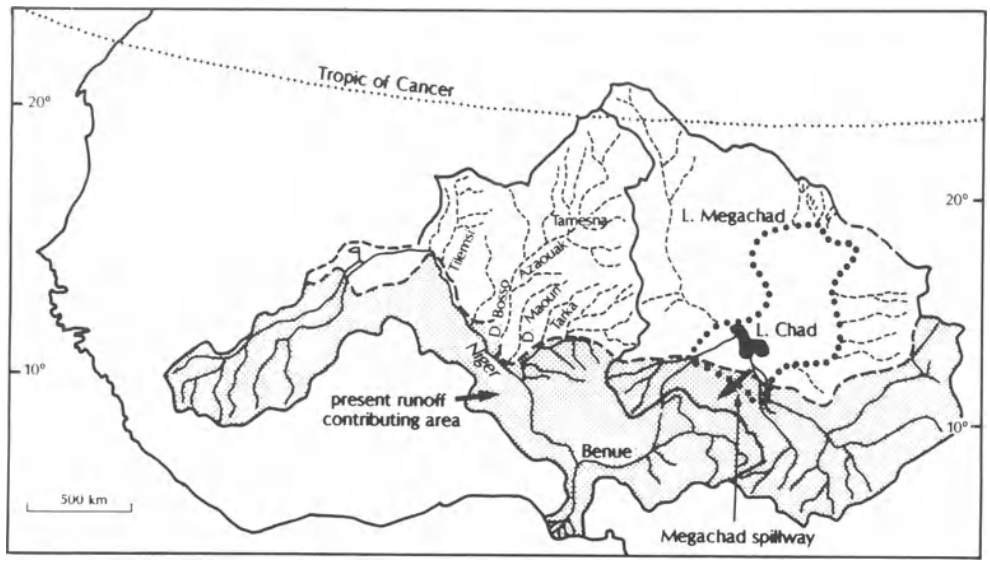

Figure 22.2 Water catchment of the Niger and Benue Rivers *c.* 9000 years BP and the present area contributing runoff to the lower Niger and to Lake Chad. The maximum extent of the palaeo-Lake Megachad and its overspill to the Benue are shown together with the largely relict drainage of the southern Sahara (after Talbot 1980).

much as 1.5 times that of the present day (Fig. 22.2). Indeed, he inferred, from a broad consideration of valley configuration, that the Dallol Bosso (now largely relict) may have been the trunk stream, and that the upper Niger might have been one of its right-bank tributaries. Further east, the contributing catchment of Lake Chad was enormous during this humid phase of the terminal Pleistocene, with the drainage focused on the thermally subsided Cretaceous Niger Rift, at the southern end of which lies the shrunken rump of the present lake. In fact, Lake Megachad, spreading into the Bodele Depression, occupied an area about six times that of present Lake Victoria and not far short of the area occupied by the modern Caspian Sea (Servant and Servant-Vildary 1980, Fig. 22.2). Apart from the now relict northern feeders of Megachad that, at this time, carried seasonal discharge down from the Tibesti Massif, the other element of the regional drainage that is of considerable interest (in part because it explains patterns of sedimentation beyond the present Chad catchment and outside the area of modern desert) lies well to the south of the modern lake. For a brief period around 9 ka, when the water balance favoured rainfall-runoff over evaporation, Megachad spilled into the Benue River and, from there, waters originating in the heart of the present Sahara reached the South Atlantic via the Niger (Servant and Servant-Vildary 1980, Grove 1985, Figs 22.1 and 22.2).

Neither was this the only large-scale integration of drainage at this time. In East Africa, a change in regional water balance led to a rise in lake levels within closed rift basins and in overspill from one to the other. In fact, it was at this time that the Nile catchment expanded enormously, if only for a brief period. Water from Lakes Chiamo and Abaya overspilled by way of the Sagan River into Chew Bahir which, in turn, overspilled through the Bakate Corridor to a much expanded Lake Turkana (Grove *et al.* 1975, Frostick and Reid 1989b, Fig. 22.3). To the south of Turkana, Lake Logipi overspilled to the Kerio River and thence to Turkana (Truckle 1976), while Turkana, already collecting the seasonal rains of a portion of the Ethiopian highlands through the Omo River, as it does today, overspilled to the north-west through the Alalibab Corridor. From here, the waters crossed the Lotogipi Swamps to enter the Pibor River, and then the River Sobat to join the White Nile (Harvey and Grove 1982; Fig. 22.3). With this temporary increase in contributing catchment, together with the overspill of Lake Victoria via the Falls at Jinja and the prevalence of relatively humid conditions across Equatoria, it is not surprising that the White Nile was three to four times the width of the present river (Adamson *et al.* 1982) and that Fairbridge (1963) was able to deduce a palaeodischarge three times that typical of the present day. Neither was this pattern of overspill unique to the early Holocene. For instance, Frostick

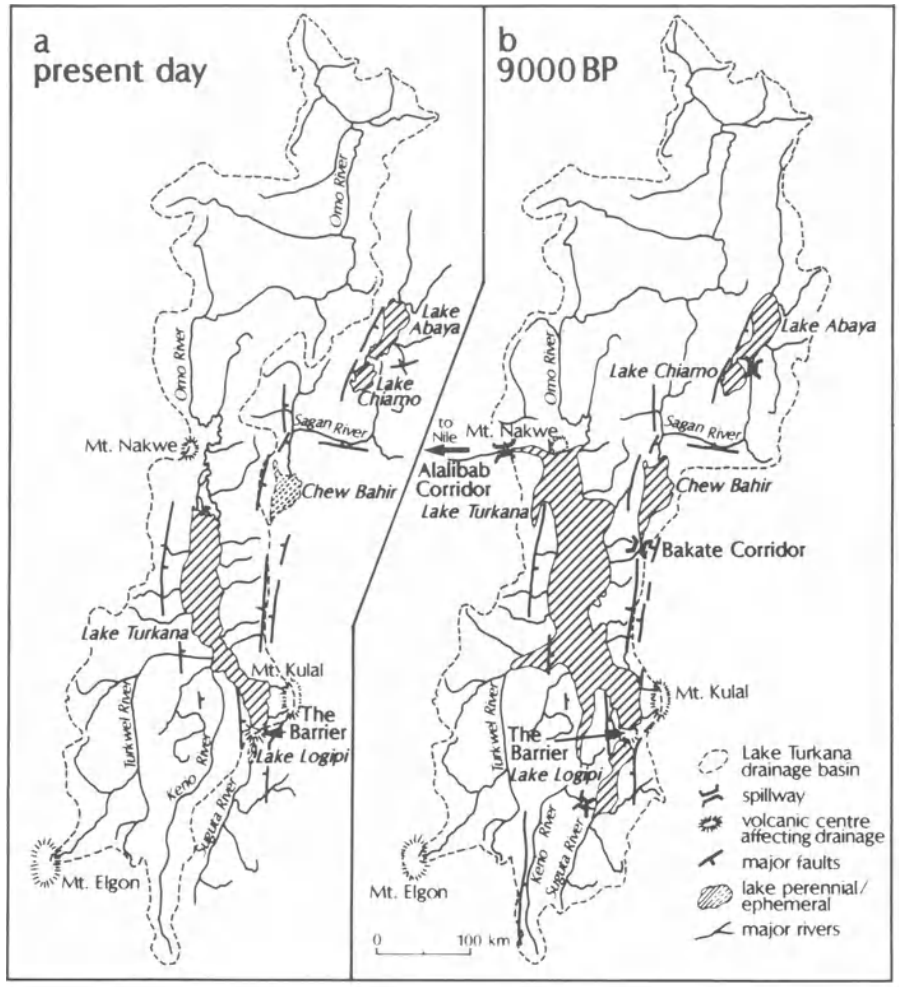

Figure 22.3 Water catchment of Lake Turkana in the northern section of the Gregory Rift of East Africa: (a) during the present phase of relative desiccation; and (b) during the early Holocene humid phase *c.* 9000 years BP, showing the swollen lakes and connecting spillways, and during the present phase of relative desiccation (after Frostick and Reid 1989b; Harvey and Grove 1982).

and Reid (1980) have drawn attention to a previous overspill from Chew Bahir to Lake Turkana, dated tentatively as older than 100 ka. This was responsible, in part, for deepening the Bakate Corridor (reused so conveniently in the Holocene) and for spreading the last and coarse-grained unit of the hominid-bearing Koobi Fora Formation in the East Turkana Basin.

FLUVIAL LANDFORM RECONSTRUCTION

Understanding this climate-driven sequence of events has been of considerable importance in arriving at an interpretation of the underfit or relict nature of drainage in present-day drylands. It has also provided the information and confidence necessary to reconstruct large erosional and aggradational landforms even where evidence is flimsy.

An interesting example comes from the hyperarid core of the Sahara, a region which has been used by the United States National Aeronautics and Space Administration as an Earthbound analogue of the Martian surface (El-Baz and Maxwell 1982). The Gilf Kebir plateau and surrounding area of south-western Egypt is currently dominated by aeolian processes that form, among other features, the giant

Selima Sandsheet (Breed *et al.* 1987). However, the area has not always been hyperarid. Peel (1939) advanced the view that the region bore the vestiges of a Tertiary landscape developed by fluvial processes, and this has been corroborated recently by surface-penetrating spaceborne imaging radar which has revealed broad alluvial valleys underlying features such as the Selima Sandsheet (McCauley *et al.* 1982b). Armed with this information, McCauley *et al.* (1982a) have reconstructed the Gilf Kebir landscape (Fig. 22.4a). Using the argument that vestigial knolls littering the present landscape represent mass wasted remnants of interfluves, they have drawn a best approximation of the former drainage net. This reconstruction has then been tested using stream-ordering rules. The regression coefficients that describe the relationship between number of streams and stream order are indistinguishable from those derived for modern drainage nets in less arid environments than prevail in the present-day Gilf Kebir (Fig. 224b).

Another case where knowledge of the climate-driven sequence of events during the late Pleistocene and early Holocene has allowed a confident interpretation of large fluvial landforms is that of the Gezira in Sudan (Williams and Adamson 1973, Adamson *et al.* 1982, Fig. 22.5). The Gezira is a large plain that lies between the White and Blue Niles. Superficially, it consists of clay. However, Williams and Adamson were able to establish conclusively that the plain is a relict low-angle fan of the Blue Nile, and that it is crossed by a number of defunct sand-filled distributaries. It is now clear that the distributaries were a product of the terminal Pleistocene desiccation phase, when flows from the Blue Nile were probably even more seasonal and somewhat more diminutive than at present, but when a change in land cover would have meant a higher and coarser specific sediment yield from the Ethiopian hinterland. Further upstream from the fan itself, the rivers Rahad, Dinder, and Blue Nile have been shown to have been elements in a complex of interconnected relatively shallow sandy channels (Fig. 22.5b$_1$) separated only by the silty clay of the floodplain that accumulated from frequent overbank spills. The more humid phase of the terminal Pleistocene and early Holocene was marked by incision of the Blue Nile, an abandonment of the Gezira, and clarification of the drainage pattern into a trunk stream and two substantial right-bank tributaries (Fig. 22.5b$_2$). As this occurred, silty clay continued to accrete on the floodplain, but the change in soil-water conditions brought about by fluvial incision and decreasing frequency of overbank flooding is

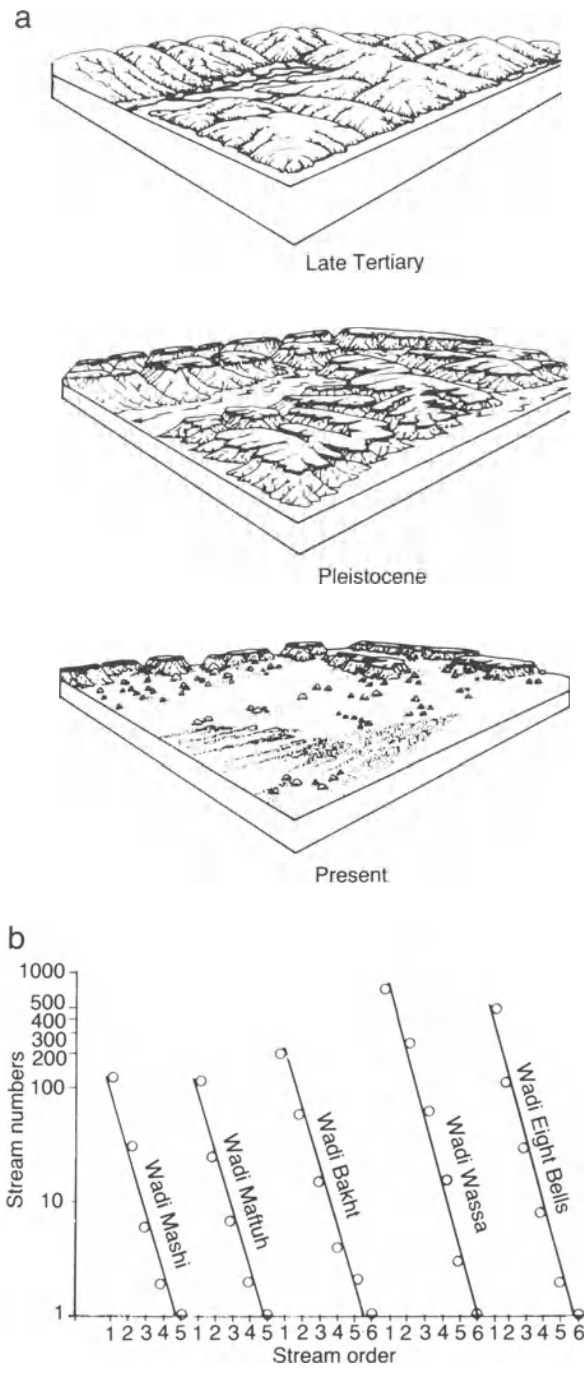

Figure 22.4 (a) Cartoons showing a reconstruction of the humid Tertiary and semi-arid Pleistocene landscapes of the Gilf Kebir plateau, which lies in the currently hyperarid core of the Sahara in south-western Egypt. (b) Stream-ordering of reconstructed Tertiary drainage systems in the Gilf Kebir plateau (after McCauley *et al.* 1982a).

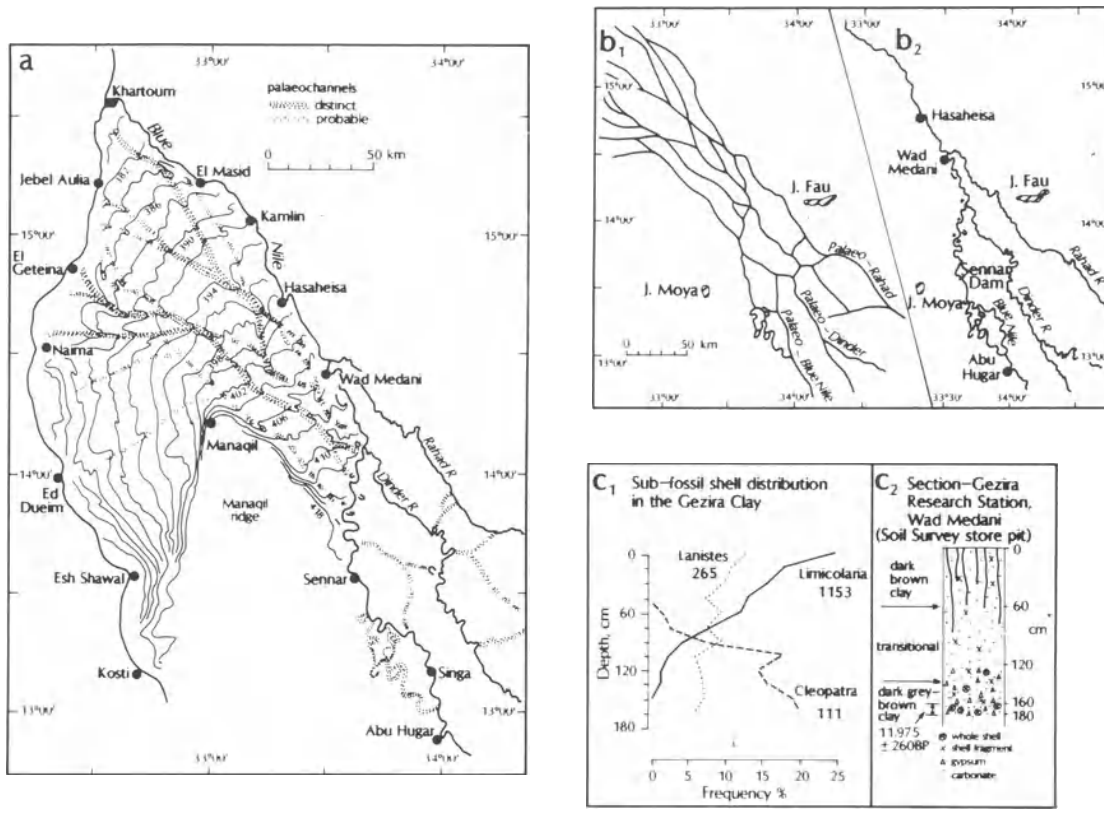

Figure 22.5 (a) Late Pleistocene low-angle alluvial fan of the Blue Nile, the Gezira, showing sandy distributary channels and contours. (b_1) Reconstructed channel complex of the Blue Nile, Rahad, and Dinder Rivers at the head of the Gezira fan during the arid phase of the terminal Pleistocene. (b_2) Present-day river planform following early Holocene incision of the Nile. (c_1) Changes in the abundance of three genera of molluscs with depth in the late-Pleistocene–Holocene floodplain muds of the Blue Nile at the head of the Gezira fan. *Cleopatra* is aquatic; *Lanistes* is amphibious; *Limicolaria* is terrestrial (c_2). Soil profile on floodplain of Blue Nile, showing ^{14}C date derived from shell material (after Adamson *et al.* 1982, mollusc data originally from Tothill 1946).

nicely recorded by the mollusc population (Fig. 22.5c). Aquatic genera such as *Cleopatra*, abundant during the early Holocene humid phase, rapidly died out as floodplain and slack-water pools became less common or non-existent; amphibious genera such as *Lanistes* were able to survive because the self-mulching properties of the crusted mud maintained a suitably moist subsoil environment for survival between successive flood inundations; terrestrial genera such as *Limicolaria* would have found conditions too wet during the early part of the Holocene humid phase, but obviously enjoyed conditions more and more as the floodplains became drier. Adamson *et al.* (1982) considered that this reorganization of the Blue Nile drainage from multi-thread to single-thread stream type had occurred somewhat before 5 ka.

CLIMATE AND CHANNEL PLANFORM

Changes in channel planform have long been thought of as indicative of climatic change, differences in the meander wavelengths of valleys and the rivers that flow through them being ascribed to changes in runoff volumes during the Quaternary. However, it was Dury (e.g. 1955, 1964, 1976) who honed ideas about cause and effect, and who showed that the meander geometry of single-thread rivers is functionally related to water discharge, among other things, at least in humid environments.

Dryland rivers tend to be wider and less sinuous than counterparts in humid regions (Schumm 1960, Wolman and Gerson 1978). Schumm (1961) ascribed this, in large part, to the nature of the material deposited from the transport load: the lower the

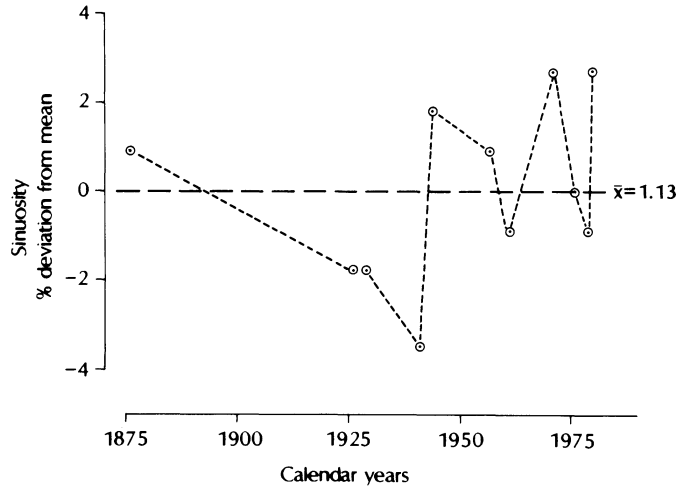

Figure 22.6 Percentage deviation of channel sinuosity from the 1868–1980 period mean on the Gila River between Monument Hill and Powers Butte, near Phoenix, Arizona (data from Graf 1981).

clay–silt content, the lower the bank cohesion and, consequently, the higher the width : depth ratio which, in turn, discourages the secondary currents associated with meandering (Reid and Frostick 1989).

Whether subtle changes in climate that are effective over short spans of time are able to bring about channel change is open to question. Graf (1981, 1984; Fig. 22.6) provided some insight through a collation of historical records for the Gila River and its tributaries in the North American South-west. The conclusions that can be drawn from these studies is that channel shifting is a frequent occurrence but that channel sinuosity has remained largely constant throughout a period characterized by changing rainfall intensity, if not by changes in annual total rainfall (Cooke 1974). In fact, sinuosity of the Gila River deviates by no more than ±3% from the mean value of 1.13 over a 104-year period.

Another archival study was conducted by Burkham (1972, 1976) along the same river but upstream (Fig. 22.7). Here, over the same period, a succession of large, damaging floods can be shown to have led to spasmodic straightening of the channel through the erosion of floodplain bottomland. Subsequent years saw the build-up of bars and their attachment to remnants of the pre-existing floodplain, so that sinuosity was eventually restored to pre-damage levels. Of incidental interest, but having important implications for sedimentation, is the fact that the increase in flow resistance and the decrease in channel gradient that accompanied the restoration process reduced the celerity of flood waves by about 60% as sinuosity increased from 1 to 1.2.

The lesson to be learnt from these two studies is that channels within a single semi-arid province (here, even the same river) can experience quite different planform changes over the same period. Burkham's study illustrates (as does Schumm and Lichty's study of channel width on the Cimarron River mentioned above) that any changes which might result from climatic alteration have to be viewed in the context of the dramatic changes brought about by individual high-magnitude floods. This suggests, again, that rivers are comparatively insensitive as indicators of more subtle shifts in climate, responding too readily, at least in arid environments, to unusual weather as much as reflecting the longer-term weather patterns that form an average condition – that is, climate.

These comments form a backcloth against which to judge the climatic implications of those studies that have revealed systematic changes in channel form over much longer periods.

Maizels (1987) provided an interesting example from the western Sharqiya of Oman (Fig. 22.8). The palaeochannels that she described hold added fascination because preferential cementation of the coarse-grained channel sediments has allowed them to resist the erosion and ablation that has affected the surrounding non-channel sediments. As a result, the channels are perched above the deflated plain by up to 30 m. In the most widespread sedimentary unit that was laid down in front of the Eastern

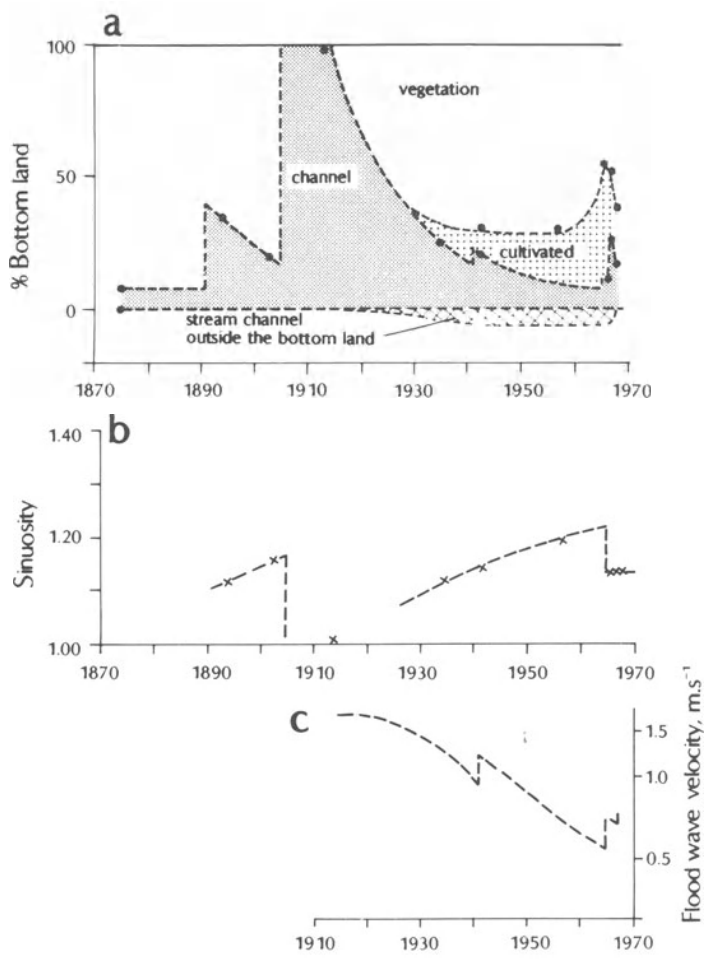

Figure 22.7 (a) Historical changes in the bottomland of the Gila River in Safford Valley, Arizona, as a result of high-magnitude floods in 1891, 1905–17, 1941, and 1967. (b) Changes in Gila River channel sinuosity in Safford Valley following floodplain damage and channel straightening during successive large flood events. (c) Changes in the average celerity of Gila River flood waves ranging in peak discharge between 283 and 566 $m^3 s^{-1}$ due to changes in flow resistance and channel sinuosity (a and b after Burkham 1972, c after Burkham 1976).

Oman Mountains, Fan I, Maizels identifies as many as five generations of palaeochannel. The oldest are most sinuous, with index values that are highly variable but generally exceed 1.5. The youngest are almost straight with a typical sinuosity index of 1.03. As for channel width, again there appears to be a progressive decrease with age from greater than 100 m to about 50 m. These changes may reflect a change in flow regime as much as a change in peak flood flows, since Maizels' exhaustive palaeohydraulic calculations show insignificant differences in peak channel discharge between the oldest and youngest generation of channels. She reasoned that the most sinuous channels would need at least seasonal flows to establish an equilibrium meandering form, which implies that the almost straight, youngest channels were formed under flashier, (?) ephemeral hydrographs.

In fact, Wolman and Gerson's (1978) compilation of data that compares flows in arid and humid regions may offer corroboration for the apparent contradiction between undifferentiated values of calculated peak flow and the very obvious change in channel planform. They have shown that flood peak discharges are indistinguishable from one environment to another, at least where water catchments range in area up to 100 km^2, even though the exponent relating total annual runoff to catchment

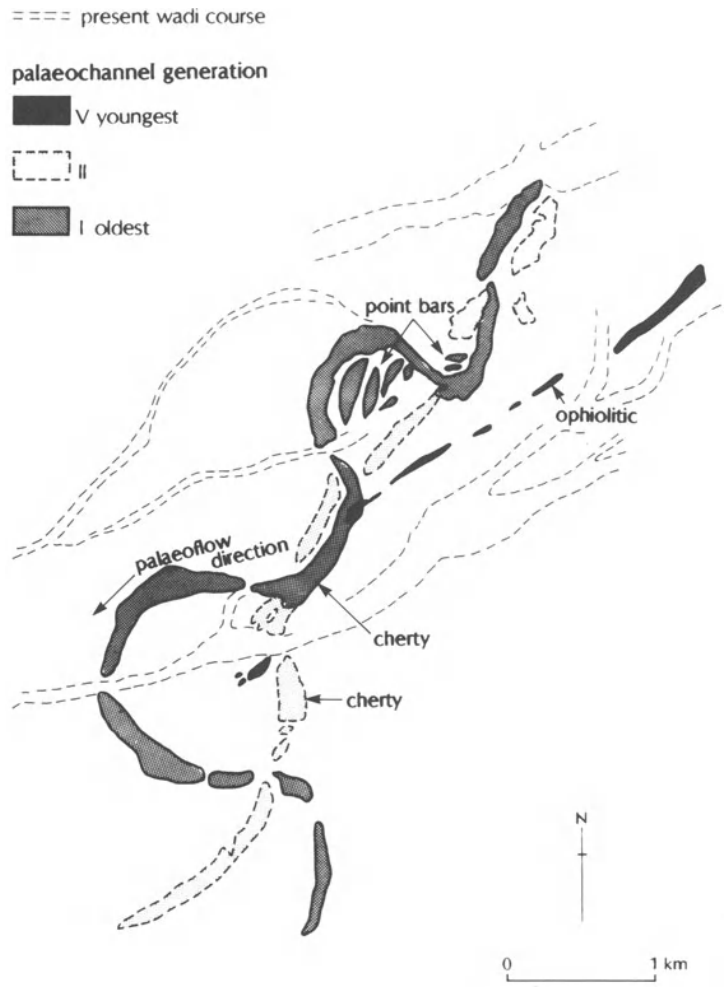

Figure 22.8 Plio-Pleistocene gravel-bed channel remnants of western Sharqiya, Oman, exhumed and left as bas-relief by erosion and deflation of surrounding non-channel sediments. Sinuosity and average width decrease progressively from the oldest to the youngest generation of channels. Reproduced by permission of the Geological Society from 'Plio-Pleistocene raised channel systems of the western Sharqiya (Wahiba), Oman' by J.K. Maizels in *Geological Society of London Special Publication* **35**, 1987.

area in humid environments is almost double its arid zone equivalent.

There are no dates attached to the Sharqiya palaeochannels, though they may be of Pliocene to early Pleistocene age. In any case, there are no other independent lines of evidence for climatic change. So the channels and their sediments become a valuable, if imprecise, guide to changing climate, as they do in even older desert settings (e.g. the reconstruction of Triassic landscape in a rift basin of the North Sea; Frostick *et al.* 1992).

Schumm (1968) offered a classic study of channel adjustments to climatic change, in this instance on the Riverine Plain of New South Wales (Fig. 22.9). Here, there are three generations of channels. The oldest had been called the Prior Streams by Butler (1950), while another group of palaeochannels, younger than the Prior Streams, was designated as the Ancestral Rivers (Pels 1964). Both of these have been superseded by the modern channels, among which the Murrumbidgee River was selected by Schumm for comparison with its predecessors.

The present-day Murrumbidgee is fairly sinuous, values of the sinuosity index lying in the region of 2. This is matched more or less by the Ancestral Rivers, although they had channel widths typically double

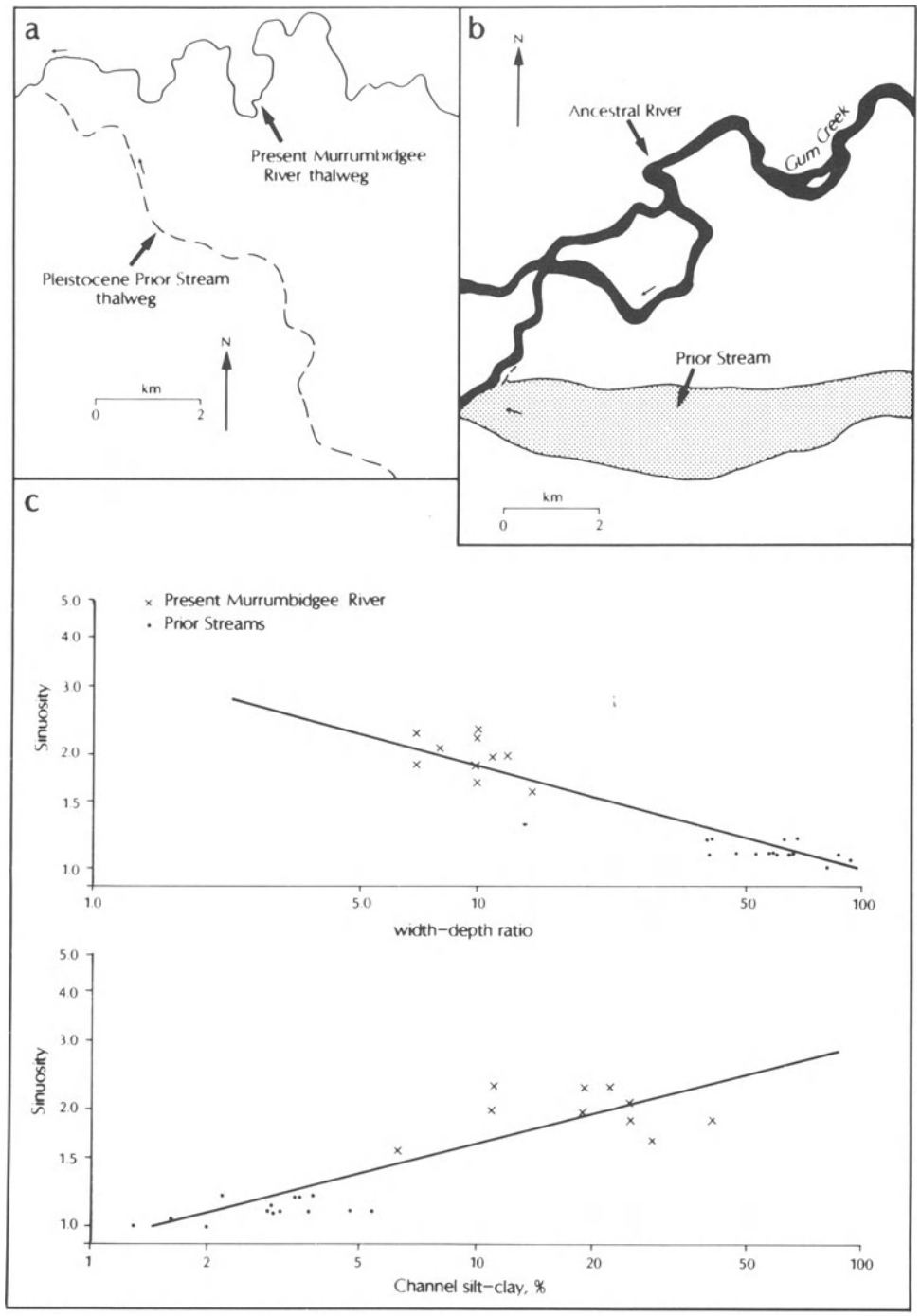

Figure 22.9 (a and b) Extracts from vertical aerial photographs of the Riverine Plain, New South Wales, which contrast the highly sinuous, muddy-banked, suspended-load channels of the modern Murrumbidgee River and Holocene Ancestral Rivers with the straight, sandy, bedload channels of the late Pleistocene Prior Streams. (c) Contrasts in sinuosity, channel width : depth ratio, and channel silt–clay percentage between the modern Murrumbidgee River which drains a subhumid to semi-arid catchment, and the Prior Streams, which were flash flood ephemerals draining semi-arid to arid catchments (after Schumm 1968).

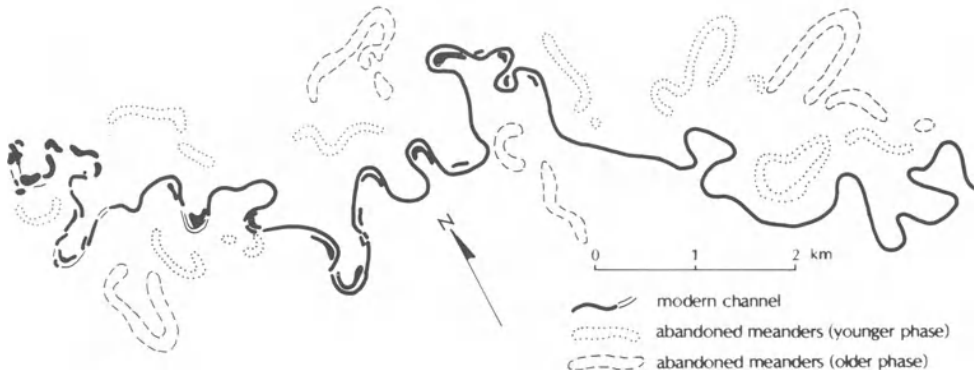

Figure 22.10 Osage-type underfit modern channels and remnants of wider precursors on the Gran Chaco of Argentina (after Baker 1978).

those of the Murrumbidgee and estimated bankfull discharges that were some five times those of the modern river. The Prior Streams had a completely different planform: the sinuosity index generally lay in the region just above unity, while channel width (as best as it can be defined) was as much as eight times that of the Murrumbidgee.

Schumm (1968) was able to draw on his previous analysis of channel form on the Great Plains of North America (Schumm 1963). In particular, he pointed to the important role of sediment in partly determining channel characteristics. Schumm (1960) had originally speculated that the inverse relationship between channel width : depth ratio and the silt–clay fraction of the channel perimeter reflected the cohesion of clays and the ability of clay-rich deposits to maintain a near-vertical sidewall. However, in his 1968 paper, he acknowledged the need to take account of the calibre of sediment presented to the river by hillslope processes and the adjustment of river form needed to maintain a measure of transport efficiency and avoid choking. In effect, a shift in sediment transport towards bedload (represented by the sand that dominates the bed material of the Prior Streams) was accommodated by a straightening and, therefore, steepening of the channel as well as by channel widening. The widening was facilitated by the lack of shear strength inherent in the sand forming a large fraction of the channel deposits. Using data from a number of American streams for which the calibre of transported sediment is known and can be rated against the silt–clay content of the channel perimeter material, Schumm estimated that the Prior Streams carried a sand load of about 22%, placing them in the so-called bedload channel category. This contrasts with the present-day, sinuous Murrumbidgee, which he estimated carries about 2% of its load as sand and which is a suspended-load channel.

Schumm was unable to place the different generations of Riverine Plain channels into a time frame with any great certainty, and, in any case, his interpretation of environmental change did not accord necessarily with those of others. Nevertheless, his arguments are powerful and point to a less vegetated landscape delivering coarser and higher sediment yields during the last glacial arid phase. River response to this can be seen in the wide, shallow and straight Prior Streams. A subsequent rise in humidity to levels higher than those of today increased the vegetation cover, decreased erosion rates, and led to the comparatively high and (?) perennial discharges of the Ancestral Rivers. A more recent decrease in humidity has been insufficient to alter significantly the character and quantity of sediment delivered to the river system, and so the present Murrumbidgee channel remains sinuous and has low width : depth ratios. Some corroboration of this late Holocene trend comes from channel planform changes on the Gran Chaco of northern Argentina, where channel widths have decreased in response to a reduction in runoff volume even though meander geometry has remained essentially unchanged (Baker 1978; Fig. 22.10). On the Riverine Plain, Schumm speculated that a further shift towards aridity might lead to changes in channel form that mimic those of the Prior Streams.

More recently, again on the Australian continent, speculative observations have helped to maintain the circumspection that surrounds the use of channel form as an indicator of climatic change. The sand-bed anastomosing channels of Cooper Creek, a major feeder of the Lake Eyre Basin, appear to be incised in a braid plain which has previously been

interpreted as a relic of a former flow regime. Nanson *et al.* (1986) have argued, albeit on the self-confessed basis of a paucity of hydrological records, that the braid plain is a contemporary feature, and that it is utilized as a floodway for very high discharges. The incised anastomosed channels are there to accommodate the flows of more moderate floods. The braids and braid bars are unusual in that they consist of sand-sized clay-rich aggregates. However, the contemporaneity of twin distinct channel types over such a large area and the suggestion that neither is anachronistic counsels the need for caution in making climatic inferences from apparent changes in channel form and deposits elsewhere and for earlier times.

THE ARROYO PROBLEM

Having examined the possibilities and problems of matching changes in the fluvial system to climatic change and vice versa on the grand scale, the moment has come to turn the spotlight on the intense debate that surrounded, and still surrounds, arroyo development in the American South-west.

Briefly, the end of the 19th century witnessed an apparently sudden, geographically widespread, progressive and deep incision of previously flat-floored alluvial bottomland. A comprehensive account is given by Cooke and Reeves (1976) who indicated that, while the exact timing of initial incision may vary, most of the trenching was accomplished between 1865 and 1915. Today, there is some suggestion that the process has been reversed and that net aggradation is occurring (Leopold 1976), despite reports that individual arroyos continue to grow by head-cutting (Malde and Scott 1977). In fact, rates of aggradation will be much lower than rates of incision, and Leopold *et al.* (1966) have advised that long-term monitoring of processes will be needed in order to achieve an understanding of the current direction that arroyo development is taking.

The controversy surrounding the initiation of arroyos was fuelled by the fact that not only were there some shifts in climate that might indirectly have brought about trenching, but that, simultaneously, land use of the area was fairly abruptly changed through the introduction of cattle by non-indigenes. Whatever the cause, it is generally agreed that runoff was encouraged through a depletion of vegetative ground cover. Bailey (1935), among others, blamed overgrazing and rejected the case for climatic change. Denevan (1967) sat on the fulcrum and argued that higher intensity summer storms had fallen on drought-weakened and overgrazed vegetation. Bryan (1941), in reviewing a longer period of time leading up to the events of the late 19th century and including the period of Pueblo Culture, was inclined to argue for increased runoff as a product of climatic change and a loss of vegetation. Leopold (1951) approached the changing climate problem from a more subtle point of view. He was able to show that the number of light raindays (thought to be vital to sustaining the herb and grass community as a partial ground cover) had been significantly lower in the last part of the 19th century (Fig. 22.11). He then speculated that this allowed the less frequent but higher magnitude runoff events to ravage valley bottomlands, so carving out the arroyos. His analyses of rainfall in New Mexico were later corroborated by Cooke's (1974) collation and analyses of records obtained at stations in Arizona.

Leopold's rainfall analysis suggests a mid-20th-century trend in storm intensity that would bring a return of rainfall patterns that characterized the period of arroyo cutting. In this circumstance, it should be possible to see signs of another epicycle of erosion. However, other factors have come to bear that complicate the picture. Graf (1978, Fig. 22.12a and b) has traced the spread of riparian tamarisk in the Colorado Plateau since its introduction from Europe in the late 1800s. In addition, he has drawn attention to the role of both riparian and channel vegetation in increasing flow resistance, showing that the amount of biomass on the floodway distinguishes entrenched and unentrenched channels, at least in upland Colorado (Graf 1979; Fig. 22.12c). These and other factors have complicated landform response to what are, after all, subtle changes in climatic variables, so that the cause of arroyo initiation still remains elusive.

Indeed, some believe that climatic change is unnecessary as an explanation for arroyo initiation (Patton and Schumm 1981). Schumm and Hadley (1957, Fig. 22.13) proposed a cycle of trenching and alluviation that they suggested accounts for the discontinuous nature of many arroyos. Transmission losses during flash flooding were thought to be responsible for encouraging localized deposition along a channel, which, in turn, produces equally localized steepening of the channel gradient and eventually encourages incision and knickpoint recession. The reduction of gradient downstream of the knick, together with erosional displacement of material from the knickpoint, brings about alluviation of the previously entrenched lower reaches, while arroyo development progresses upstream. In the fullness of time, renewed incision occurs at steeper

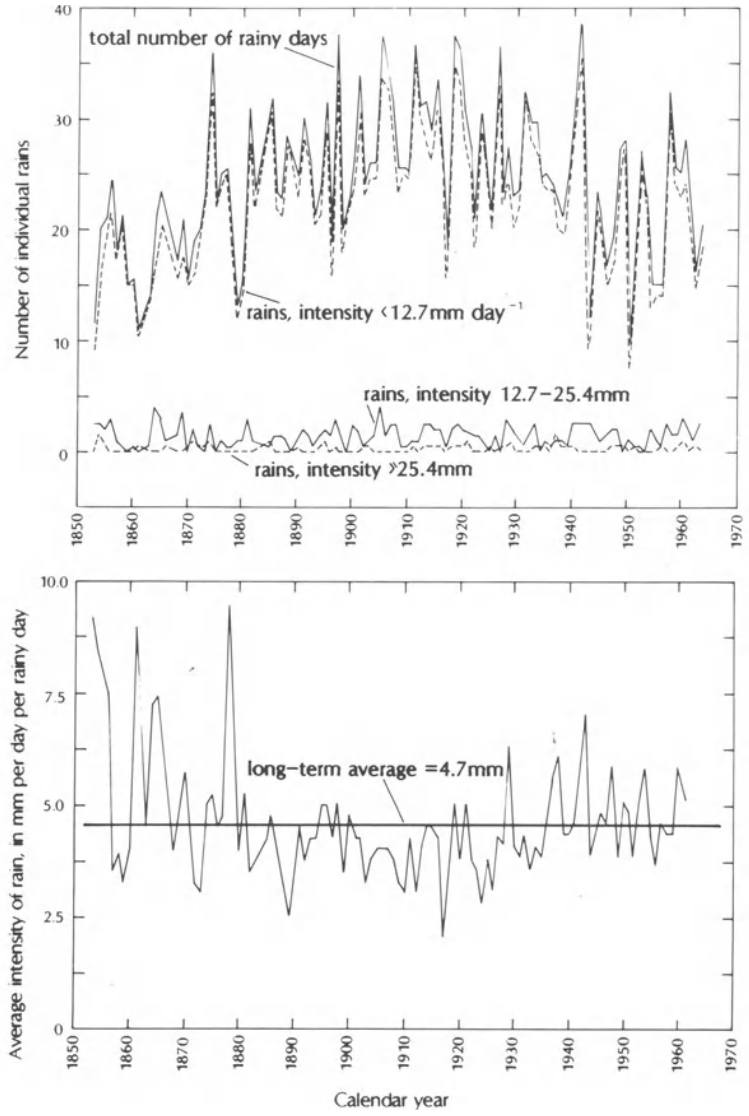

Figure 22.11 Frequency of non-summer (October–June) rainfalls by storm size and the average rainfall per rainy day at Santa Fe, New Mexico, covering the major period of arroyo incision (1865–1915) and subsequent developments (after Leopold *et al.* 1966).

sections in the alluvium that has been deposited in the trunk stream and a new knick moves progressively upstream in a new cycle.

A great deal of scientific enquiry has gone into the arroyo problem, yet the results remain equivocal. Perhaps as important an upshot of what at one time seemed a pressing problem in need of a solution has been the investment in obtaining a general understanding of fluvial processes, especially those of the world's drylands.

DRYLAND RIVER DEPOSITS

Dryland rivers differ from their perennial counterparts in the rate at which they convey sediment and, to some degree, in the character of their deposits (Reid and Frostick 1987, 1989). The reasons for such differences lie as much outside as within the river channel and are associated with protection of the ground by vegetation, the relative stability of topsoil structure, biopore control of soil hydraulic conduc-

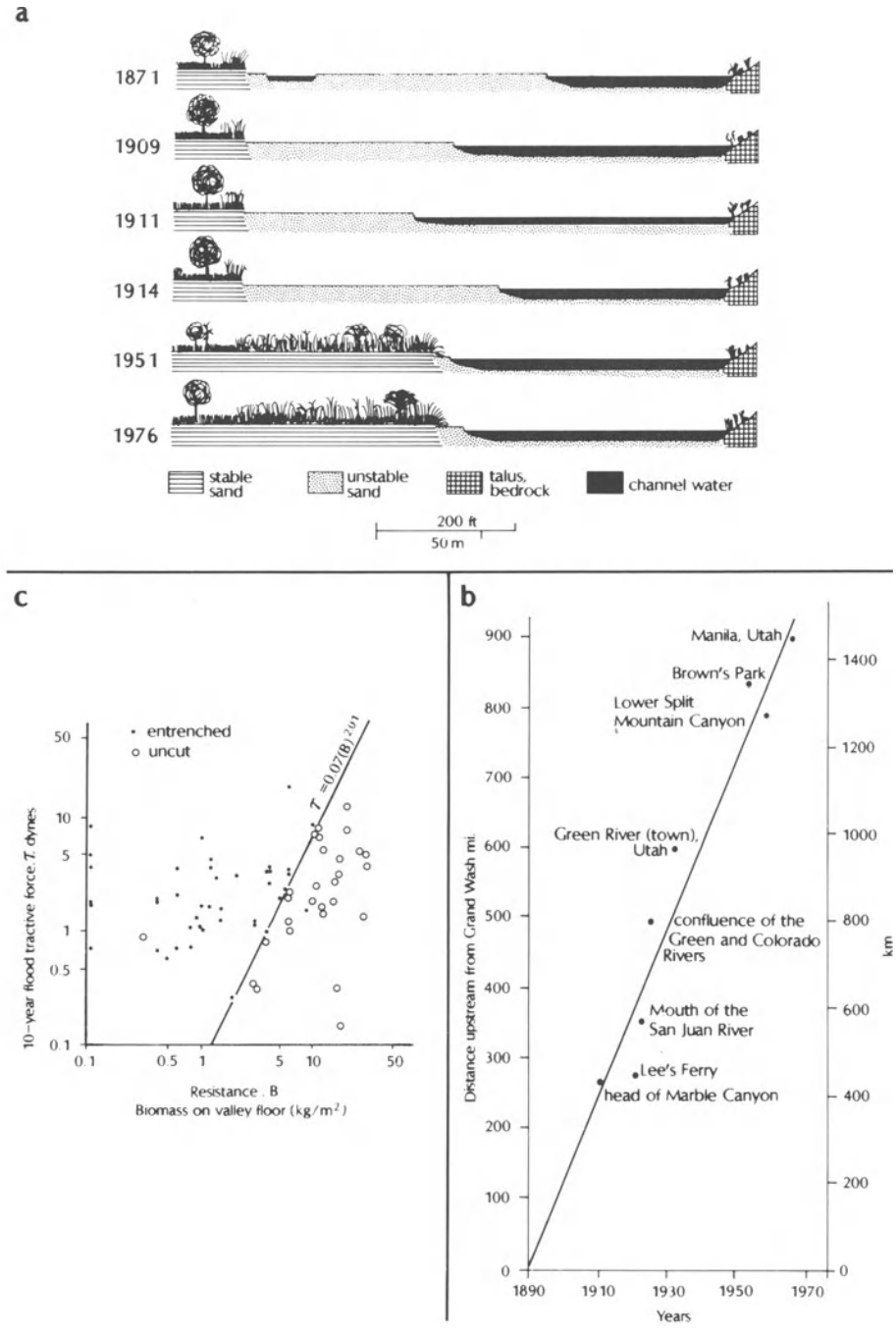

Figure 22.12 (a) Sketches of Green River cross-section at Bowknot Bend, Utah, derived from historical photographs and field survey before and after the arrival of tamarisk in the 1930s, showing the dramatic stabilization of alluvium, constriction of the low-water channel and increased flow resistance of the floodway. (b) Spread of tamarisk up the Colorado and Green Rivers – a rate of colonization averaging 20 km y^{-1} – after its introduction to North America from Europe in the 1880s. (c) Separation of entrenched and unentrenched valley bottomlands in upland Colorado as a function of biomass-induced flow resistance, allowing for the estimated average tractive force of the local 10-year flood at peak discharge. The line is a fitted disciminator and not a product of regresssion analysis (a and b after Graf 1978, c after Graf 1979).

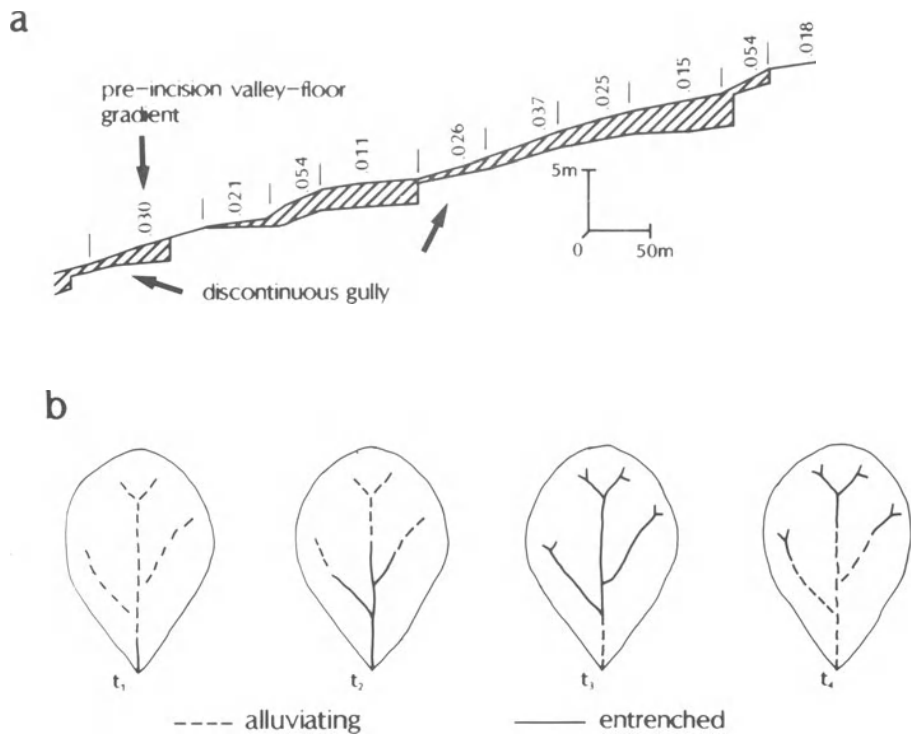

Figure 22.13 (a) Discontinuous gullies in Dam 17 Wash, near Cuba, New Mexico, showing knick points that have moved up-channel from oversteepened sections of the pre-incision alluvium. (b) Cycle of trenching and alluviation in semi-arid drainage basins (after Schumm and Hadley 1957).

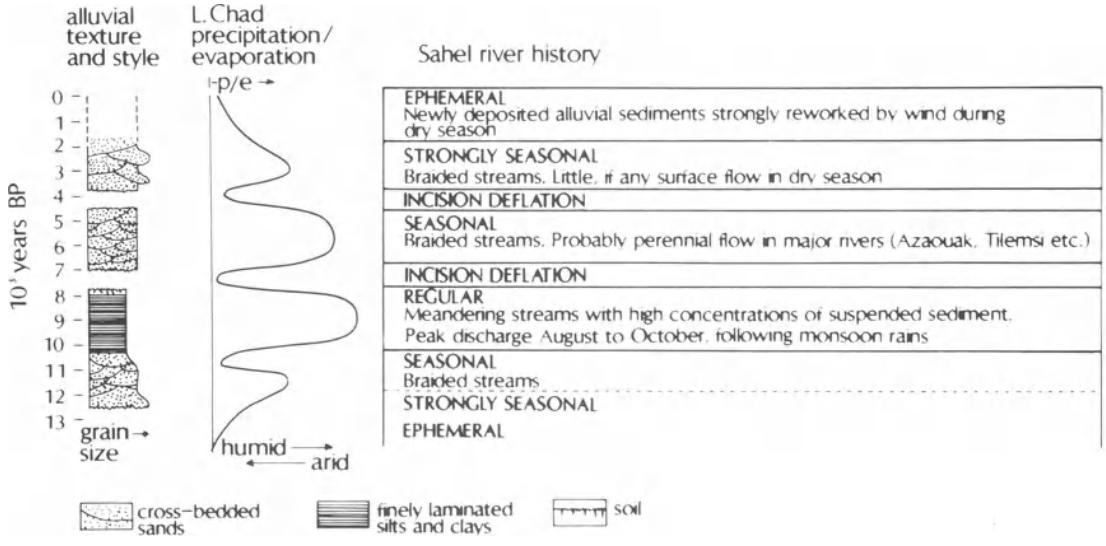

Figure 22.14 Schematic generalized sequence of sedimentation by West Sahel rivers during the terminal Pleistocene and Holocene set against the palaeoclimate curve derived from strandline and other evidence in the Lake Chad basin (after Talbot 1980).

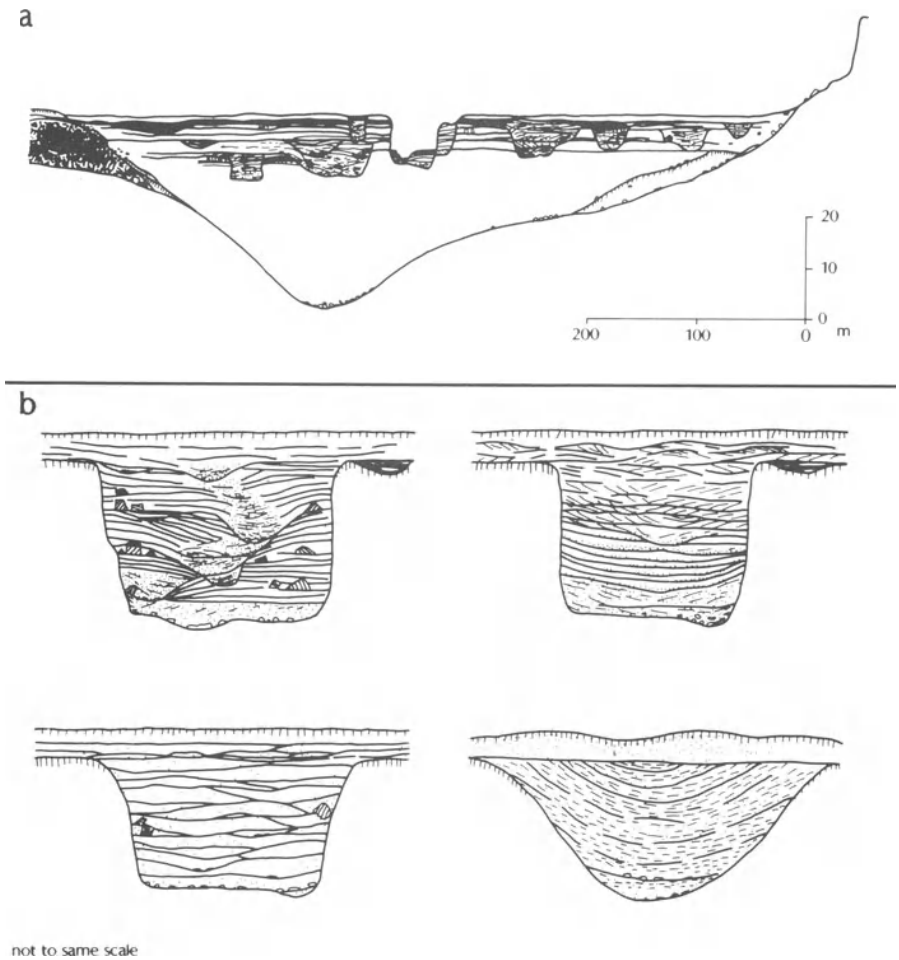

Figure 22.15 Styles of late Holocene channel-fills exposed in section by present-day arroyo development in Chaco Canyon, New Mexico (after Love 1982).

tivity and the incidence of surface ponding and overland flow, and so on – that is, all those factors that influence the availability and transfer of material from hillslopes. Within the river, the hydraulic feedback that results from the type and quantity of material with which it is presented leads not only to differences in channel plan and cross-sectional form, as discussed above, but also to differences in the architecture of the alluvium.

Talbot (1980) has given a schematic and regionally generalized sequence of river sediments that has arisen from shifts in climate in the western Sahel during the terminal Pleistocene and Holocene (Fig. 22.14). The sediment column is dominated by sand (which is derived in part from the reworking of southward driven Saharan dunes), but the period of maximum regional humidity that centres on 9 ka is characterized by a change towards suspended-load systems and indicates greater vegetation cover and soil development. These comparatively large changes in sediment calibre reflect what, for this region, have been end-members of the climatic spectrum and they are reminiscent of Schumm's (1968) findings on the Riverine Plain of New South Wales. However, there is no suggestion that the more subtle shifts in climate that are contemporaneous with the lesser risings of palaeo-Lake Chad are translated into depositional character.

Indeed, Love (1982) pointed to the equivocal relationship between fluvial deposition and climate using the mid- and late Holocene channel fills that are exposed by present-day incision within Chaco Canyon, New Mexico (Fig. 22.15). These palaeochannels range in size and, therefore, in their

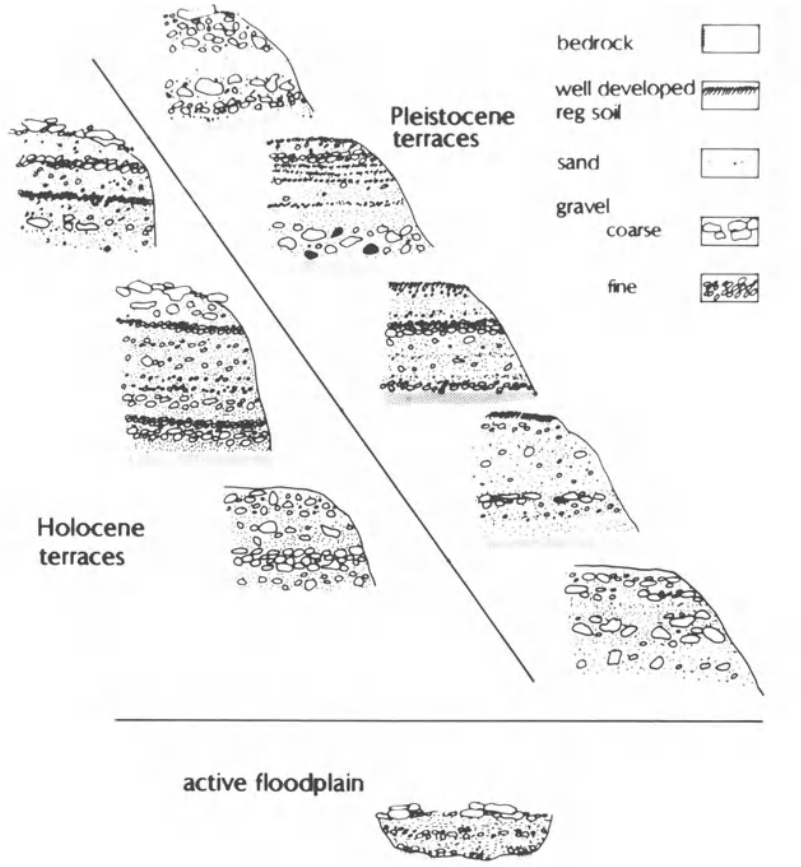

Figure 22.16 Differentiation of the largely fluviatile sediments of the Holocene terraces of the Timna Valley, southern Negev Desert, laid down by flash floods that punctuated extremely arid conditions, and those of Pleistocene age which consist in part of debris flow deposits and indicate a slightly ameliorated climate that produced moderately arid to semi-arid conditions. Reproduced by permission of the Geological Society from 'Fluviatile deposits and morphology of alluvial surfaces as indicators of Quaternary environmental changes in the southern Negev, Israel' by S. Grossman and R. Gerson in *Geological Society of London Special Publication* **35**, 1987.

probable role and importance as part of the contemporary drainage system. But they also range widely in the calibre and style of sedimentation, and include palaeochannels typical of ephemeral, flash-flood, bedload streams (Fig. 22.15b, lower left), those of mixed-load streams (upper left) as well as those of suspended-load streams (lower right). Yet, tree-ring and other sources of data show no dramatic shifts in climate during the period covering this episode of canyon filling. On the other hand, there are indications of phases of greater-than and less-than normal rainfall that may be reminiscent of the pattern established for the period of arroyo incision and possible refilling during the late 19th and 20th centuries. Although Love remains sceptical that these climatic wobbles can be used to explain differences in channel and channel-fill character, it suggests that a thorough examination of present-day arroyo fills might be useful in at least indicating the range of alluvial architecture that might be expected following known, subtle shifts in climate.

Having issued a cautionary note, it is possible to state that desert stream sediments may well carry tell-tale signs of relatively small changes in climate. Grossman and Gerson (1987) have drawn a distinction between Pleistocene and Holocene river terraces in the southern Negev Desert (Fig. 22.16). The older deposits are built partly by debris flows, and display a commensurately disorganized fabric, a wide range of clast size (up to 1.5 m), and a poor degree of stratification. The younger terrace deposits are fluviatile in origin, displaying a high degree of stratification, an ordered fabric, and so on. There are also differences in the reg soils that developed on

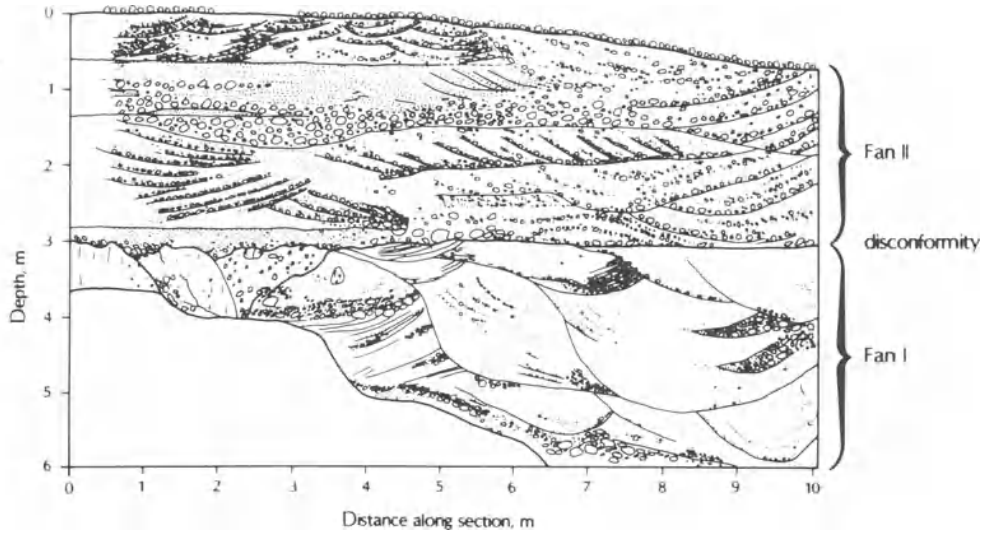

Figure 22.17 Deposits of the Plio-Pleistocene Wadi Andam Fan Complex of western Sharqiya, Oman. Fan I was laid by sinuous streams that probably had at least a seasonal discharge regime and indicate a wetter climate than Fan II which was a braid plain built by ephemeral flash floods. Reproduced by permission of the Geological Society from 'Plio-Pleistocene raised channel systems of the western Sharqiya (Wahiba), Oman' by J.K. Maizels in *Geological Society of London Special Publication* **35**, 1987.

the two sets of terraces. Those of Pleistocene origin show greater illuvial horizonation and a deeper profile. The inference is that the older terraces reflect a moderately arid to semi-arid climate in which rainfall was occasionally sufficient to encourage mass wasting of talus slopes in headwater reaches and so provide material of the right consistency for debris flows. At the same time, the rainfall regime, while not generous, nevertheless encouraged soil development. The Holocene terraces reflect the onset of the extreme aridity that characterizes the region at present. Debris flows were not a feature of the sediment transfer system and soil development was inhibited by the infrequency of rainfall.

Maizels (1987; Fig 22.17) offered another glimpse of the sedimentary legacy of changes in climate, albeit that it is the sediments and not independent lines of evidence that provide the clues, so that there is always the danger of circular argument. Notwithstanding this problem, the lowest unit of the Wadi Andam Fan complex (Fan I) exhibits a cut-and-fill structure that matches the meandering nature of the channels that drained from the Eastern Oman Mountains during the wetter conditions of the early Pleistocene. The beds of Fan II are, in contrast, thinner and more tabular, reflecting the flashier flood regime of the braided streams that developed in the region during arid phases of the mid- to late Pleistocene.

The examples discussed so far are, by and large, headwater or upper catchment deposits of small to moderate-sized drainage systems. However, the deposits of larger rivers also reflect shifts in climate. The patterns of change are not dissimilar to those already described except that the character of the sediment is governed by processes of comminution and selective entrainment that operate over the long transport distances that are involved. Adamson's (1982; Fig. 22.18) compilation of hydrological and sedimentological information for the Nile basin and adjacent areas provides a thoroughly researched example. In particular, the fine sediments deposited along the main Nile and in its delta are equated with the ameliorated climate of the period that preceded the last glacial maximum and of the early Holocene, while coarser sands are a product of the terminal Pleistocene and late Holocene arid phases. A similar pattern of events is drawn from analyses of the sediments of the Niger delta (Pastouret *et al.* 1978) and of those of the deep-sea fan that lies off the mouth of the Amazon (Damuth and Fairbridge 1970).

CONCLUSIONS

Desert rivers undoubtedly respond to those gross changes in climate that bring a shift in environment from arid to semi-arid or even subhumid conditions,

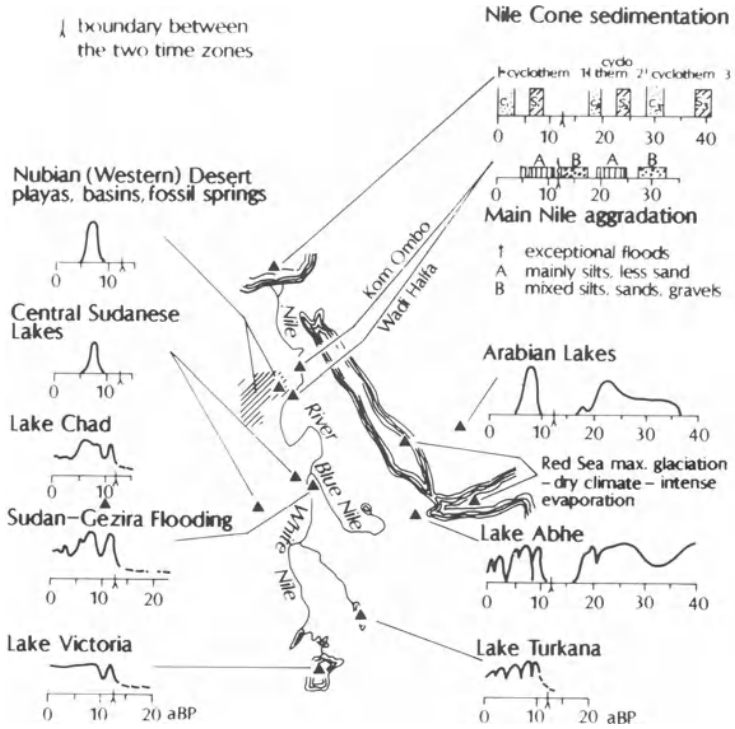

Figure 22.18 Summary of hydrological and sedimentological data for the greater Nile basin and adjacent areas during the late Pleistocene and Holocene (after Adamson 1982).

and vice versa. Perhaps this is not surprising given that Langbein and Schumm's (1958) celebrated curve relating present-day specific sediment yield to effective rainfall is at its steepest for the world's drylands. At finer resolution, it is still debatable whether river response reflects lesser changes in climate, if only because the alterations that occur in ground cover and soil and that affect the runoff process are stepped in character and do not vary continuously with increasing or decreasing rainfall. Besides this, the impact of occasional large floods undoubtedly tends to mask the gradual alteration of channel form that might be expected to accompany diminutive changes in climate.

However, despite the difficulties that are experienced in calibrating the fluvial measuring stick in terms of climate, river character is a valuable, and sometimes singular, guide to climate-induced environmental change, especially in deserts where biogenic evidence is often absent.

REFERENCES

Adamson, D.A. 1982. The integrated Nile. In *A land between two Niles*, M.A.J. Williams and D.A. Adamson (eds), 221–34. Rotterdam: Balkema.

Adamson, D.A., F. Gasse, F.A. Street and M.A.J. Williams 1980. Late Quaternary history of the Nile. *Nature* **288**, 50–5.

Adamson, D.A., M.A.J. Williams and R. Gillespie 1982. Palaeogeography of the Gezira and the lower Blue and White Nile valleys. In *A land between two Niles*, M.A.J. Williams and D.A. Adamson (eds), 165–219. Rotterdam: Balkema.

Bailey, R.W. 1935. Epicycles of erosion in the valleys of the Colorado Plateau province. *Journal of Geology* **43**, 337–55.

Baker, V.R. 1977. Stream-channel response to floods, with examples from central Texas. *Bulletin of the Geological Society America* **88**, 1057–71.

Baker, V.R. 1978. Adjustment of fluvial systems to climate and source terrain in tropical and subtropical environments. In *Fluvial sedimentology*, A.D. Miall (ed.), 211–30. Canadian Society Petroleum Geologists Memoir 5.

Baker, V.R., R.C. Kochel, P.C. Patton and G. Pickup 1983. Palaeohydrologic analysis of Holocene flood slack-water sediments. In *Modern and ancient fluvial systems*, J.D. Collinson and J. Lewin (eds), 229–39. Special Publication International Association Sedimentologists 6.

Begin, Z.B., A. Ehrlich and Y. Nathan 1974. Lake Lisan the Pleistocene precursor of the Dead Sea. *Geological Survey of Israel Bulletin* 63.

Benson, L.V. 1978. Fluctuations in the level of pluvial Lake Lohontan during the last 40 000 years. *Quaternary Research* **9**, 300–18.

Bowler, J.M., G.S. Hope, J.N. Jennings, G. Singh, *et al.*

1976. Late Quaternary climates of Australia and New Guinea. *Quaternary Research* **6**, 359–94.

Breed, C.S., J.F. McCauley and P.A. Davis 1987. Sand sheets of the eastern Sahara and ripple blankets on Mars. In *Desert sediments: ancient and modern*, L.E. Frostick and I. Reid (eds), 337–59. Geological Society of London Special Publication 35.

Bryan, K. 1941. Pre-Columbian agriculture in the Southwest, as conditioned by periods of alluviation. *Annals of the Association of American Geographers* **31**, 219–42.

Burkham, D.E. 1972. Channel changes of the Gila River in Safford Valley, Arizona 1846–1970. *U.S. Geological Survey Professional Paper* 655-G.

Burkham, D.E. 1976. Effects of changes in an alluvial channel on the timing, magnitude, and transformation of flood waves, southeastern Arizona. *U.S. Geological Survey Professional Paper* 655-K.

Butler, B.E. 1950. A theory of prior streams as a causal factor of soil occurrence in the Riverine Plain of southeastern Australia. *Australian Journal Agricultural Research* **1**, 231–52.

Butzer, K.W. and C.L. Hansen 1968. *Desert and river in Nubia: geomorphology and prehistoric environments at the Aswan Reservoir*. Madison, WI: University of Wisconsin Press.

Butzer, K.W., G.Ll. Isaac, J.L. Richardson and C. Washbourn-Kamau 1972. Radiocarbon dating of East African lake levels. *Science* **175**, 1069–76.

Cooke, R.U. 1974. The rainfall context of arroyo initiation in southern Arizona. *Zeitschrift für Geomorphologie Supplement Band* **21**, 63–75.

Cooke, R.U. and R.W. Reeves 1976. *Arroyos and environmental change in the American South-west*. Oxford, England: Clarendon Press.

Damuth, J.E. and R.W. Fairbridge 1970. Equatorial Atlantic deep-sea arkosic sands and ice-age aridity in tropical South America. *Bulletin of the Geological Society America* **81**, 189–206.

De Heinzelin, J. and R. Paepe 1965. The geological history of the Nile Valley in Sudanese Nubia. In *Contributions to the prehistory of Nubia*, F. Wendorf (ed.), 29–56. Dallas, Tex.: Southern Methodist University Press.

Deneven, W.M. 1967. Livestock numbers in Nineteenth-Century New Mexico, and the problem of gullying in the Southwest. *Annals of the Association of American Geographers* **57**, 691–703.

Dury, G.H. 1955. Bedwidth and wave-length in meandering valleys. *Nature* **176**, 31.

Dury, G.H. 1964. Principles of underfit streams. *U.S. Geological Survey Professional Paper* 452-A.

Dury, G.H. 1976. Discharge prediction, present and former, from channel dimensions. *Journal of Hydrology* **30**, 219–45.

El-Baz, F. and T.A. Maxwell (eds) 1982. *Desert landforms of southwest Egypt: a basis for comparison with Mars*. Washington, DC: National Aeronautics and Space Administration CR-3611.

Fairbridge, R.W. 1963. Nile sedimentation above Wadi Halfa during the last 20 000 years. *Kush* **11**, 96–107.

Frostick, L.E. and I. Reid 1980. Sorting mechanisms in coarse-grained alluvial sediments: fresh evidence from a basalt plateau gravel, Kenya. *Journal of the Geological Society of London* **137**, 431–41.

Frostick, L.E. and I. Reid 1986. Evolution and sedimentary character of lake deltas fed by ephemeral rivers in the Turkana basin, northern Kenya. In *Sedimentation in the African rifts*. L.E. Frostick, R.W. Renaut, I. Reid and J.-J. Tiercelin (eds), 113–25. Geological Society of London Special Publication 25.

Frostick, L.E. and I. Reid 1989a. Climatic versus tectonic controls of fan sequences: lessons from the Dead Sea, Israel. *Journal of the Geological Society of London* **146**, 527–38.

Frostick, L.E. and I. Reid 1989b. Is structure the main control of river drainage and sedimentation in rifts? *African Journal of Earth Sciences* **8**, 165–82.

Frostick, L.E., T.K. Linsey and I. Reid 1992. Tectonic and climatic control of Triassic sedimentation in the Beryl Basin, northern North Sea. *Journal of the Geological Society of London* **149**, 13–26.

Graf, W.L. 1978. Fluvial adjustments to the spread of tamarisk in the Colorado Plateau region. *Bulletin of the Geological Society America* **89**, 1491–1501.

Graf, W.L. 1979. The development of montane arroyos and gullies. *Earth Surface Processes* **4**, 1–14.

Graf, W.L. 1981. Channel instability in a braided, sand bed river. *Water Resources Research* **17**, 1087–94.

Graf, W.L. 1984. A probabilistic approach to the spatial assessment of river channel instability. *Water Resources Research* **20**, 953–62.

Grossman, S. and R. Gerson 1987. Fluviatile deposits and morphology of alluvial surfaces as indicators of Quaternary environmental changes in the southern Negev, Israel. In *Desert sediments: ancient and modern*. L.E. Frostick and I. Reid (eds), 17–29. Geological Society Special Publication 35.

Grove, A.T. 1985. *The Niger and its neighbours*. Rotterdam: Balkema.

Grove, A.T., F.A. Street and A.S. Goudie 1975. Former lake levels and climatic change in the rift valley of southern Ethiopia. *Geographical Journal* **141**, 171–202.

Gupta, A. and H. Fox 1974. Effects of high-magnitude floods on channel form: a case study in Maryland Piedmont. *Water Resources Research* **10**, 499–509.

Harvey, C.P.D. and A.T. Grove 1982. A prehistoric source of the Nile. *Geographical Journal* **148**, 327–36.

Katz, A., Y. Kolodny and A. Nissenbaum 1977. The geochemical evolution of the Pleistocene Lake Lisan–Dead Sea system. *Geochimica et Cosmochimica Acta* **41**, 1609–26.

Kendall, R.L. 1969. An ecological history of the Lake Victoria basin. *Ecological Monographs* **39**, 121–76.

Langbein, W.B. and S.A. Schumm 1958. Yield of sediment in relation to mean annual precipitation. *Transactions of the American Geophysical Union* **39**, 1076–84.

Leopold, L.B. 1951. Rainfall frequency, an aspect of climatic variation. *Transactions of the American Geophysical Union* **32**, 347–57.

Leopold, L.B. 1976. Reversal of erosion cycle and climatic change. *Quaternary Research* **6**, 557–62.

Leopold, L.B., W.W. Emmett and R.M. Myrick 1966. Channel and hillslope processes in a semiarid area New Mexico. *U.S. Geological Survey Professional Paper* 352-G.

Love, D.W. 1982. Quaternary fluvial geomorphic adjustments in Chaco Canyon, New Mexico. In *Adjustments of the fluvial system*, D.D. Rhodes and G.P. Williams (eds),

277–308. London: George, Allen & Unwin.
Maizels, J.K. 1987. Plio-Pleistocene raised channel systems of the western Sharqiya (Wahiba), Oman. In *Desert sediments: ancient and modern*, L.E. Frostick and I. Reid (eds), 31–50. Geological Society of London Special Publication 35.
Malde, H.E. and A.G. Scott 1977. Observations of contemporary arroyo cutting near Sante Fe, New Mexico, USA. *Earth Surface Processes* **2**, 39–54.
McCauley, J.F., C.S. Breed and M.J. Grolier 1982a. The interplay of fluvial, mass-wasting and eolian processes in the eastern Gilf Kebir region. In *Desert landforms of southwest Egypt: a basis for comparison with Mars*. F. El-Baz and T.A. Maxwell (eds), 207–39. Washington, DC: National Aeronautics and Space Administration CR-3611.
McCauley, J.F., G.G. Schaber, C.S. Breed, M.J. Grolier, *et al.* 1982b. Subsurface valleys and geoarchaeology of the eastern Sahara revealed by Shuttle Radar. *Science* **218**, 1004–20.
Nanson, G.C. 1986. Episodes of vertical accretion and catastrophic stripping: a model of disequilibrium floodplain development. *Bulletin of the Geological Society America* **97**, 1467–75.
Nanson, G.C., B.R. Rust and G. Taylor 1986. Coexistent mud braids and anastomosing channels in an arid-zone river: Cooper Creek, central Australia. *Geology* **14**, 175–8.
Neev, D. and K.O. Emery 1967. The Dead Sea. *Geological Survey of Israel Bulletin* 41.
Pastouret, L., H. Chamley, G. Delibrias, J.-C. Duplessy, *et al.* 1978. Late Quaternary climatic changes in western tropical Africa deduced from deep-sea sedimentation off the Niger Delta. *Oceanologica Acta* **1**, 217–32.
Patton, P.C. and S.A. Schumm 1981. Ephemeral-stream processes: implications for studies of Quaternary valley fills. *Quaternary Research* **15**, 24–43.
Patton, P.C., V.R. Baker and R.C. Kochel 1982. Slack-water deposits: a geomorphic technique for interpretation of fluvial paleohydrology. In *Adjustments of the fluvial system*. D.D. Rhodes and G.P. Williams (eds), 225–58. London: George, Allen & Unwin.
Peel, R.F. 1939. The Gilf Kebir. *Geographical Journal* **93**, 295–307.
Pels, S. 1964. The present and ancestral Murray River system. *Australian Geographical Studies* **2**, 111–9.
Reid, I. and L.E. Frostick 1987. Flow dynamics and suspended sediment properties in arid zone flash floods. *Hydrological Processes* **1**, 239–53.
Reid, I. and L.E. Frostick 1989. Channel form, flows and sediments in deserts. In *Arid zone geomorphology*, D.S.G. Thomas (ed.), 117–35. London: Belhaven Press.
Schumm, S.A. 1960. The shape of alluvial channels in relation to sediment type. *U.S. Geological Survey Professional Paper* 352-B.
Schumm, S.A. 1961. Effect of sediment characteristics on erosion and deposition in ephemeral stream channels. *U.S. Geological Survey Professional Paper* 352-C.
Schumm, S.A. 1963. Sinuosity of alluvial rivers on the Great Plains. *Bulletin of the Geological Society America* **74**, 1089–100.
Schumm, S.A. 1968. River adjustment to altered hydrologic regime – Murrumbidgee River and paleochannels, Australia. *U.S. Geological Survey Professional Paper* 598.
Schumm, S.A. 1977. *The fluvial system*. New York: Wiley-Interscience.
Schumm, S.A. and R.F. Hadley 1957. Arroyos and the semiarid cycle of erosion. *American Journal Science* **255**, 161–74.
Schumm, S.A. and R.W. Lichty 1963. Channel widening and flood-plain construction along Cimarron River in southwestern Kansas. *U.S. Geological Survey Professional Paper* 352-D.
Servant, M. and S. Servant-Vildary 1980. L'environment quaternaire de bassin du Tchad. In *The Sahara and the Nile*, M.A.J. Williams and H. Faure (eds), 133–62. Rotterdam: Balkema.
Street, F.A. and A.T. Grove 1979. Global maps of lake-level fluctuations since 30 000 yr BP. *Quaternary Research* **12**, 83–118.
Talbot, M.R. 1980. Environmental responses to climatic change in the West African Sahel over the past 20 000 years. In *The Sahara and the Nile*, M.A.J. Williams and H. Faure (eds), 37–62. Rotterdam: Balkema.
Tothill, J.D. 1946. The origin of the Sudan Gezira clay plain. *Sudan Notes and Records* **27**, 153–83.
Truckle, P.H. 1976. Geology and late Cainozoic lake sediments of the Suguta Trough, Kenya. *Nature* **263**, 380–3.
Williams, M.A.J. and D.A. Adamson 1973. The physiography of the central Sudan. *Geographical Journal* **139**, 498–508.
Williams, M.A.J. and D.A. Adamson 1974. Late Pleistocene desiccation along the White Nile. *Nature* **248**, 584–6.
Williams, M.A.J. and F.M. Williams 1980. Evolution of the Nile basin. In *The Sahara and the Nile*. M.A.J. Williams and H. Faure (eds), 207–24. Rotterdam: Balkema.
Wolman, M.G. and R. Gerson 1978. Relative scales of time and effectiveness of climate in watershed geomorphology. *Earth Surface Processes* **3**, 189–208.

THE ROLE OF CLIMATIC CHANGE IN ALLUVIAL FAN DEVELOPMENT

23

Ronald I. Dorn

This paper is dedicated to the memory of Ran Gerson, desert and climatic geomorphologist. We will miss his extraordinary insight.

INTRODUCTION

Alluvial fans are semi-conical landforms composed of stream deposits and debris flow materials where a canyon exits a mountain range. Alluvial fans are built in semi-arid, humid-temperate, and proglacial regions (Rachocki 1981, Nilsen and Moore 1984), but they have been studied more in deserts than in any other environment (Bull 1977, Graf 1988). Alluvial fans were worked on sparsely (e.g. Gilbert 1875, McGee 1897, Eckis 1928, Blissenbach 1954) until the 1960s when a flurry of papers brought them into vogue (e.g. Tuan 1962, Beaty 1963, Bull 1964, Denny 1965, 1967, Lustig 1965, Melton 1965, Hunt and Mabey 1966, Hooke 1967, 1968).

Alluvial fans have been used to support various conceptual geomorphic perspectives during the 20th century (Table 23.1). With the growth of quantitative methods, considerable effort has concentrated on quantifying morphometric parameters of fans and drainage basins, the sedimentology of modern and ancient fan deposits, contemporary processes of fan accretion, and such basic issues as why deposition occurs (Bull 1977, Nilsen and Moore 1984, Harvey 1989, Lecce 1991).

Alluvial fans interface with humans in a number of ways. A better understanding of alluvial fan geomorphology offers insights into management of urban environments in arid regions (Cooke *et al.* 1982). For example, much of Los Angeles and Phoenix is built on alluvial fans (Cooke 1984, Rhoads 1986). As urban growth continues in the United States sunbelt, managing the alluvial fan hazards of flooding, subsidence, and faulting becomes increasingly important (Bull 1977, Graf 1988, pp. 192–6, Baker *et al.* 1990). Alluvial fans are being considered for low-level nuclear waste sites in several American states. Archaeological artifacts and ground drawings (geoglyphs) are found on stable fan surfaces, comprising a cultural resource and posing barriers to development. A tremendous amount of research dollars has been and is being spent on understanding remote sensing characteristics of alluvial fan surfaces with one goal of correlating them with climatic changes (e.g. Schaber *et al.* 1976, Dailey *et al.* 1979, White 1990, 1991).

The focus of this paper is to review and assess current thought on the role of Quaternary climatic changes on alluvial fan development in regions that are now drylands. The first section reviews current thought. The second section presents case studies. The third section offers a critical assessment of climatic interpretations of alluvial fans.

CURRENT THOUGHT ON DESERT ALLUVIAL FANS AS INDICATORS OF CLIMATIC CHANGE

NATURE OF THE EVIDENCE

Evidence connecting alluvial fans to climatic change can be generalized into several categories: sedimentology unique to particular climate conditions; palaeoclimatic records incorporated directly into alluvial fan deposits or into post-depositional modification of fan deposits; correlation between ages of deposits and ages of existing palaeoclimatic data; and changes in aggradational and entrenchment history.

Comparatively little emphasis has been placed on correlating alluvial fan events to climate using stra-

Geomorphology of Desert Environments. Edited by Athol D. Abrahams and Anthony J. Parsons. Published in 1994 by Chapman & Hall, London. ISBN 978-94-015-8256-8

Table 23.1 Different geomorphological models used in alluvial fan research

Model	*Summary*
Evolutionary (Davis 1905)	Alluvial fans occur in a youthful stage in the arid lands cycle of erosion
Climatic (Tuan 1962, Melton 1965, Lustig 1965, Bull 1979, 1991, Wells *et al.* 1987, Dorn 1988)	Climatic changes influence the weathering, stream flow, mass movement, and sediment supply in the drainage basin above the fan. Climatic changes influence the base level of closed basins, gullying, weathering, and soil development on fan deposits
Dynamic equilibrium (Denny 1967)	Alluvial fans represent a dynamic equilibrium in the transportation of coarse debris from range to basin
Steady state (Hooke 1968)	The relationship of fan area A_f and drainage basin area A_d of $A_f = cA_d^n$ tends towards a steady state among coalescing fans in closed basins of similar lithology, tectonics and environment
Tectonic (Hooke 1972, Bull 1977, Rockwell *et al.* 1985)	Faulting influences the entrenchment and location of deposition on a fan, the preservation of older fan deposits, and morphometric parameters.
Complex response (Hawley and Wilson 1965, Schumm *et al.* 1987, White 1991)	Fan-head trenching and the shifting of depositional loci down-fan can be explained by a threshold response to oversteepening of the fan-head slope, or drainage basin ruggedness may also control fan incision
Allometry (Bull 1975, 1991)	Alluvial fans are not in a steady state. Boundary conditions of drainage basin, climate, and tectonism change over time

tigraphy and sedimentology, since the processes that produce alluvial fan sediments (water laid, debris flow, sieve flow) can exist in a variety of climates. Lustig (1965) argued that aggradation is associated with heavier precipitation, higher water : sediment ratios, and smaller tractive forces; fan dissection is associated with lower water : sediment ratios and mudflows with larger tractive forces. Bull (1977, p. 238) noted that the 'bedding of the deposits is one of the better methods of identifying the alluvial fan environment in the stratigraphic record.' Mayer *et al.* (1984), Grossman and Gerson (1987) and Bull (1991, pp. 55–62) have used sedimentology to infer the climate under which sediment transport occurred. Lake sediment–fan sediment interdigitation is relevant because as the size of a lake basin increases and decreases, constraints are placed on the geometry of fans entering the basin (Hooke 1968, 1972, Hooke and Dorn 1992, Hunt and Mabey 1966). A frequently used morphology indicator is whether the deposit has a gravel bar and channel morphology (often assumed to be) deposited during an arid Holocene climate, as opposed to a smooth pavement that is (often assumed to be) indicative of a late Pleistocene age (e.g. Hunt and Mabey 1966, Hooke 1972, Dorn *et al.* 1987a, Grossman and Gerson 1987, Wells *et al.* 1987, Bull 1991).

Palaeoclimatic indicators are rarely extracted from alluvial fan deposits. Charcoal and other organic material such as pollen are usually not preserved in older deposits in deserts. Even if they are found and their taxonomy identified or their geochemistry characterized, the investigator is uncertain of the source of the material (fan, lower drainage basin, or upper drainage basin). Probably the most utilized intrafan palaeoclimatic evidence would be palaeosols that can be used to indicate depositional hiatuses (e.g. Gile *et al.* 1981, Bull 1991). Advances are also being made in extracting climatic signals from dryland soils (Grossman and Gerson 1987, Reheis 1987, McFadden 1988, Cerling *et al.* 1989), and deposits of rock varnish found on the surfaces of fan units (see Chapter 20).

Correlating estimated ages of fan deposits with ages of existing palaeoclimatic data is a common approach used to infer a climatic signal (e.g. Shlemon 1978, Christenson and Purcell 1985, Ponti 1985, Wells *et al.* 1987, 1990, Dorn 1988, Blair *et al.* 1990, Harvey 1990, Bull 1991). Of course, correlation does not imply causation, and temporal correlations can only be used to disprove a climatic connection. Still, many investigators appear willing to accept this line of evidence to support a climatic model for alluvial fan development, especially if correlations are regional in extent.

Changes in the aggradational and entrenchment history of alluvial fans has also seen widespread use as a tool to make climatic interpretations as well as tectonic and intrinsic geomorphic interpretations (White 1991). Many believe that alluvial fans have received pulses of sediment in response to climatic events, although the particular climatic condition

responsible for deposition is under dispute. A major issue of disagreement is the cause(s) of variations in sediment supply from the drainage basin. While many have observed that fan aggradation has taken place during more humid periods (Lustig 1965, Coque and Jauzein 1967, Glennie 1970, Hötzl *et al.* 1978, Ponti 1985, Dorn *et al.* 1987a, Maizels 1987), others favour aggradation during climatic transitions to periods of greater aridity (Bull 1979, 1991, Bull and Schick 1979, Kale and Rajaguru 1987, Wells *et al.* 1987, 1990). Several have argued that both climatic conditions can result in aggradation (Tuan 1962, Williams 1973, Ponti 1985, Dorn 1988, Bull 1991, p. 55). The entire issue has been clouded by few actual ages on fan deposits and, therefore, the inability to correlate deposits with available palaeoenvironmental data, such as lake levels or palaeobiogeographic changes. Only a few studies have attempted to combine age control with palaeoenvironmental information (Williams 1973, Kale and Rajaguru 1987, Wells *et al.* 1987, 1990, Dorn 1988, Bull 1991, White 1991).

Some investigators have tried to infer a climatic signal from fan-head entrenchment, which can occur during periods of greater aridity (e.g. Lustig 1965, Coque and Jauzein 1967, Wells *et al.* 1987, Dorn 1988). Harvey (1987) argued that fan entrenchment is governed by surface crusting, discrepancies between fan and channel slopes, and channel morphology, while White (1991) concluded that drainage basin ruggedness is a key intrinsic control on dissection. Bull (1991, p. 273) maintained that entrenchment must be viewed as departure from equilibrium because 'with neither climatic nor tectonic perturbations, streams would cut down to only a single base level of erosion and few, if any, terraces would form.'

CLIMATIC GEOMORPHOLOGY MODELS OF ALLUVIAL FAN DEVELOPMENT

Four conceptual models have been proposed to relate climatic changes to alluvial fan development. The *transition-to-drier-climate* model has been the most popular in desert geomorphology research over the past decade. The *paraglacial* model has moved from its origins in British Columbia toward application elsewhere in western North America. There is also a group of authors who claim that *humid-period aggradation* occurs and is an important aspect of alluvial fan evolution in what are now deserts. Lastly, the *periglacial* model argues that periglacial activity during colder periods at higher elevations can produce abundant debris for transport to fans.

Transition-to-Drier-Climate Model

Since the research of Huntington (1907) and Eckis (1928) there has been a growing recognition of the importance of vegetation cover in influencing rates of erosion in drainage basins (Knox 1983), and Bull (1979, 1991) has proposed a general model of hillslope–fan response to climatic change (Fig. 23.1). Bull writes (1991, pp. 281, 284):

> 'Replenishment of the hillslope sediment reservoir is as important as erosion in the production of an aggradation event. Conditions that favor rapid and progressive increases in hillslope plant and soil cover may be infrequent or may require long time spans. . . . Aggradation of desert valleys occurred because of rapid stripping of a thin hillslope sediment reservoir after a change to markedly less vegetation cover or an increase in intense summer-type precipitation events, or both.'

Many authors have similarly stressed the importance of a reduction of vegetation cover in enhancing hillslope erosion and fan aggradation (e.g. Gile *et al.* 1981, Mayer *et al.* 1984, Kale and Rajaguru 1987, Wells *et al.* 1987, 1990, Dorn 1988, Blair *et al.* 1990, Harvey 1990).

Montgomery and Dietrich (1992, p. 829) offered a simple and elegant explanation for alternating periods of slow colluvium accumulation and relatively rapid stripping. The key is the location of the channel head on a slope. They argue that 'channels or rills may be carved into unchanneled valleys and hillslopes relatively quickly when the threshold for channel initiation is decreased, but significant time may be required to infill valleys when the threshold for channel initiation increases'. With climatic (or land-use) change to a decreased vegetation cover, the location of the channel moves upslope and excavates accumulated debris.

Paraglacial Model

Trowbridge (1911, p. 739) recognized the importance of glaciation on the development of alluvial fans:

> 'Glaciation has played a large part in the deposition of the [eastern] Sierra bajada [in the Owens Valley of California]. Glaciers prepared immense amounts of material in the mountain canyons for transportation by streams. At the same time they

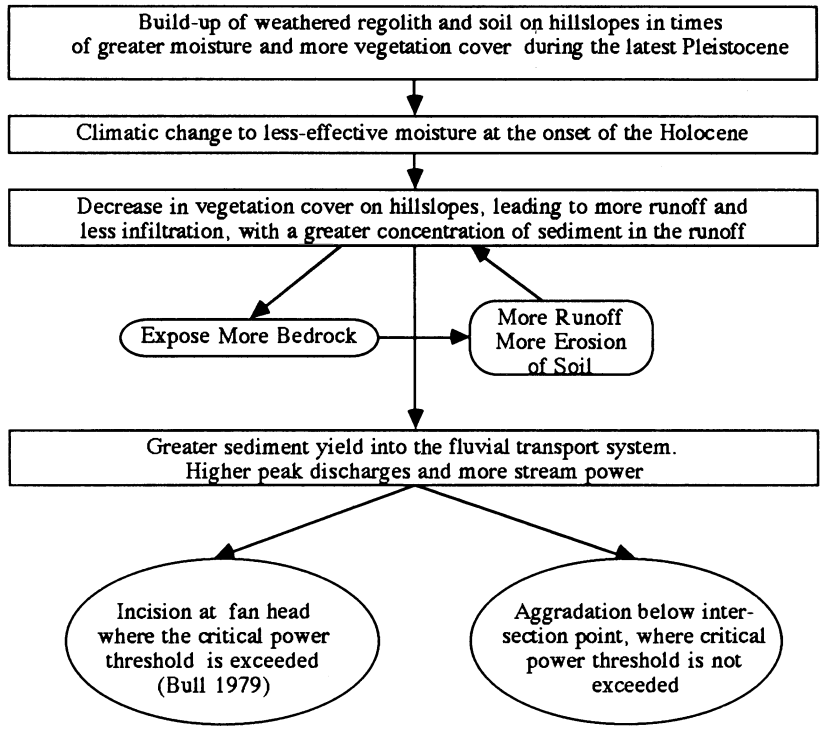

Figure 23.1 Model of alluvial fan aggradation during times of transition from more humid to more arid climates below a drainage not influenced by periglacial or glacial activity during the latest Pleistocene, modified from Bull (1979, 1991).

> furnished great volumes of water to act as the transporting agent during the melting-season.'

Sixty years later Ryder (1971) and Church and Ryder (1972, p. 3059) introduced the term 'paraglaciation' to mean

> '... nonglacial processes that are directly conditioned by glaciation. It refers both to proglacial processes, and to those occurring around and within the margins of a former glacier that are the direct result of the earlier presence of the ice. It is specifically contrasted with the term "periglacial", which does not imply the necessity of glacial events occurring.'

In relation to fans, glaciation produces major quantities of sediment that are introduced into the fluvial system, creating an imbalance for thousands of years after glaciation (Fig. 23.2). Originally applied to outwash deposits and alluvial fans in upland regions with relaxation times of a few thousand years, the paraglacial model of sediment redistribution can be felt over longer periods, where the 'major rivers [of glaciated British Columbia] are still redistributing sediment that was delivered to the valleys by glacial events more than 10 kyr ago' (Church and Slaymaker 1989, p. 454).

Where alluvial fans in arid and semi-arid lands are fed by drainage basins that have been glaciated, the paraglacial model must be considered. In western North America, for example, paraglaciation applies to such dryland fan systems as the bajada of the eastern Sierra Nevada (Trowbridge 1911), many ranges of the Great Basin (e.g. the White Mountains of California and Nevada: Beaty 1963, Elliott-Fisk 1987) and even ranges in the Rocky Mountains that abut semi-arid basins from Montana to New Mexico (e.g. the Sangre de Cristo Mountains: Pazzaglia and Wells 1989).

Humid-Period-Aggradation Model

The association between more moist climates and alluvial fan aggradation is a persistent theme in alluvial fan research. Lustig (1965, p. 185) felt deposition occurred from fan head to fan toe during more humid periods in Deep Springs Valley, eastern

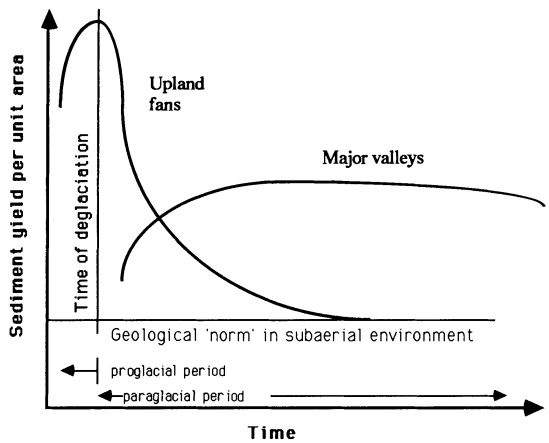

Figure 23.2 The paraglacial sedimentation model, modified from Church and Ryder (1972) and Church and Slaymayer (1989).

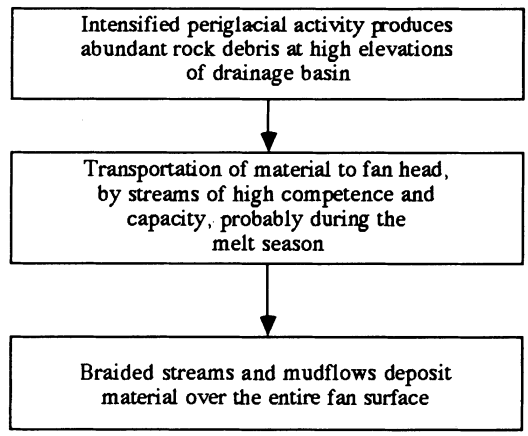

Figure 23.3 Model of alluvial fan aggradation at the base of a drainage exiting a high elevation range influenced by periglacial activity.

California. Tuan (1962), Barsch and Royse (1972), Mulhern (1982), Ponti (1985), Dorn *et al.* (1987a), and others concurred for different regions in North America. Even those who argue for the transition-to-drier-climate model have presented evidence of aggradational events during more moisture-effective humid periods (Mayer *et al.* 1984, Wells *et al.* 1987, Bull 1991, p. 55). Williams (1973) noted that aggradation occurred during more moisture-effective periods in South Australia. Working in North Africa, the Sinai Peninsula, and Saudi Arabia, Coque and Jauzein (1967), Hötzl *et al.* (1978), Talbot and Williams (1979), Goldberg (1984), Maizels (1987), Wilson (1990) and others argued that aggradation in dryland fan systems is best ascribed to periods of wetter (more moisture-effective) climate.

No single process-based explanation unifies these observations; however, there is the underlying realization that streams did not disappear during lengthy humid periods. Some explanations are based on chronological correlations with palaeoclimatic data indicating that aggradation occurred in more humid periods, such as 'average glacial conditions' (Bull 1991, p. 55). Others stress the importance of the start of a more humid period being able to transport material more effectively.

Periglacial Model

Another hypothesis involves the role of periglacial processes in producing sediment for delivery to alluvial fans (Williams 1973, Wasson 1977, Dorn 1988). During colder periods in the western United States, periglacial activity dominated many higher elevations (Péwé 1983, Dohrenwend 1984). The periglacial model is illustrated in Figure 23.3.

CASE STUDIES ON THE ROLE OF CLIMATIC CHANGE

In this section, I present some of my own studies which I have interpreted to support the above conceptual models. My approach here is to use conventional radiocarbon dating and rock varnish methods (radiocarbon dating: Dorn *et al.* 1989, 1992; cation-ratio dating: Dorn 1989, Dorn *et al.* 1990, Dorn and Krinsley 1991; palaeoenvironmental interpretation: Chapter 19) to correlate fan deposition with well-dated palaeoenvironmental records from the same local area, if not the same mountain range. Implicit in such correlations is the assumption that the deposit being studied is a product of the climatic state recorded by selected palaeoclimatic indicator(s) that correlates in time with the deposit.

An approach that correlates ages of alluvial fan units with climatic periods cannot be used to prove a climatic connection but only to suggest one. The correlation between a climatic state and the age of a fluvial event is problematic because long-term palaeoclimatic data (e.g. past vegetation, sea level, glacial, lacustrine, or insolation curves) at best only record the general climatic character of a period. Extreme climatic events within even a specific climatic period can lead to aggradation or entrenchment related to those extreme events (Graf 1988, Kochel and Ritter 1990) and not necessarily to the general climate state of the period. Lastly, the inherent

Figure 23.4 Alluvial fan sites discussed in the western Basin and Range province, United States.

uncertainties associated with all Quaternary dating methods will probably never allow us to know if a specific alluvial fan unit developed in response to a relatively short-lived climatic period, such as a 200-year-long dry phase that caused an upslope movement in channel heads in the midst of a 10 000-year period of more effective moisture.

Given these problems, why use a correlation approach? First, we often have little else to go on. Second, such correlations permit first-order deductions on relationships between climatic changes and fan aggradation that can be subjected to further testing. Lastly by looking at alluvial fan histories over a large area, regional generalizations can be made (e.g. Wells *et al.* 1990, Bull 1991).

The examples in this section will be limited to the last *c.* 40 000 years, the period of radiocarbon dating. Palaeovegetation information from *Neotoma* middens is vital to understanding slope processes in drainage basins (Bull 1991), and these middens have time control only for the period of radiocarbon dating. Most examples come from the western Basin and Range province of North America (Fig. 23.4), but results are also presented from alluvial fans in the drylands of Australia, Hawaii, and Peru.

SUPPORT FOR TRANSITION-TO-DRIER-CLIMATE MODEL

The Soda Mountains of the Mojave Desert, California (Fig. 23.4), crest at about 1100 m. They are subject to frontal winter precipitation and convective summer precipitation at present, and perhaps during the latest Pleistocene (Spaulding and Graumlich 1986, Bull 1991). There is no evidence to suggest that the Soda Mountains experienced glacial or periglacial activity during the late Wisconsin.

The nature of climatic changes in the Mojave Desert over the past 40 000 years is indicated by palaeovegetation records. Wells (1983), Spaulding and Graumlich (1986), Van Devender *et al.* (1987), Spaulding (1990), and others evaluated the palaeobiogeography of the region using place-specific *Neotoma*-gathered macrofossils. From before 40 000 to near 10 000 years BP, a dwarf conifer woodland was present below about 1500 m where only desert scrub species are now found.

Palaeolake changes also indicate a significantly more moisture-effective late Wisconsin environment. The Soda Mountains were surrounded by the Silver Lake arm of Pleistocene Lake Mojave on the east (Ore and Warren 1971, Brown *et al.* 1990) and the Cronese playas to the west. The Cronese playas have no clear Pleistocene shoreline record, because the Cronese basins have been inundated by about 27 m of sediment since the cutting of Afton Canyon about 14 000 years BP (Meek 1989).

Figure 23.5 depicts a small fan derived from an unnamed drainage in the Soda Mountains, called here Cronese-1 fan. Its surface was built mostly during the Holocene. The varnish radiocarbon (V/^{14}C) age of the early Holocene unit is 9700 ± 430 years (AA-937); this is best considered a minimum-limiting age for this unit. Varnish cation-ratio (CR)

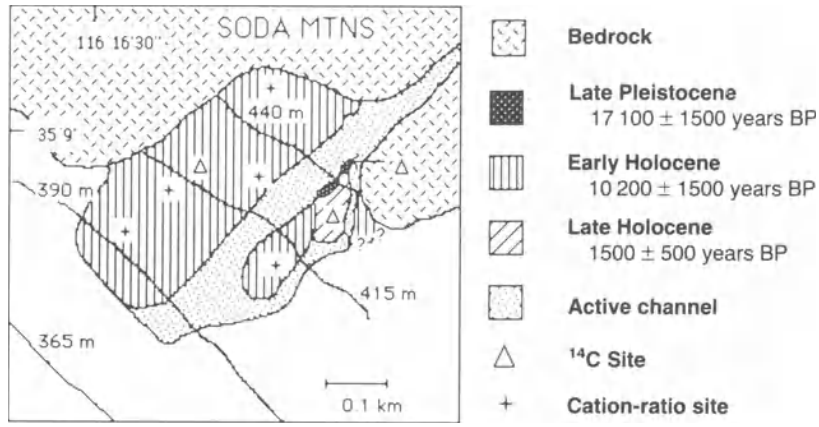

Figure 23.5 Cronese-1 alluvial fan of the Soda Mountains, Mojave Desert, California.

ages of five different boulders (sites identified on Fig. 23.5) sampled over this unit average 9800 ± 1200 years, using the calibration curve in Dorn *et al.* 1987b; this average age is consistent with the V/^{14}C age. The micromorphology of the rock varnish is lamellate all over this unit, consistent with a Holocene age (Dorn 1986, Chapter 20). The early Holocene unit represents the largest area of deposition on the Cronese-1 fan. Smaller depositional events did occur later in the Holocene (V/^{14}C age of 1370 ± 360 years; AA-938).

Hillslopes in the drainage above the Cronese-1 fan reveal a direct connection between geomorphic processes and fan deposition influenced by climatic changes. There are fossilized remnants of debris flow levees that have cation-ratio ages, for example, of 10 500 ± 1300, 10 500 ± 800, and 9400 ± 1300 years. These overlap the ages assigned to the early Holocene fan unit. Debris flows that deposited the early Holocene fan unit likely generated these levees. There are also areas of uneroded hillslope colluvium over bedrock. Cation-ratio ages on five different colluvial patches are 45 000 ± 4000, 36 000 ± 5000, 27 000 ± 3500, 21 500 ± 4000, and 15 500 ± 2000 years. These colluvial patches are interpreted as remnants of slopes once stabilized by the more extensive vegetation cover during the latest Pleistocene but not yet eroded. Exposed bedrock was also sampled for cation-ratio dating in eight places where the colluvial cover had been removed by erosion; all of these age estimates are Holocene: 9200 ± 600, 8900 ± 1800, 7800 ± 1200, 3700 ± 1100, 3000 ± 900, 1200 ± 600, <300, and <300 years.

There are also lines of colluvial boulders on the slopes above the fan, two of which have cation-ratio ages of 8600 ± 800 and 7900 ± 1100 years. They are linear troughs excavated by debris flows and then infilled by the downslope gravity transport of large boulders. Since overland flow converges on these lines, fine particles are removed, giving the appearance of a line of boulders parallel to the slope.

These results support the model of sediment generation during times of climate transition from more humid to more arid conditions in low-elevation ranges (Bull 1991, Fig. 23.1). During the late Pleistocene, a colluvial cover was present over bedrock above the Cronese-1 fan from 15 000 to 45 000 years BP. At the close of the Pleistocene period around 10 000 to 12 000 years BP, much of this colluvium was transported to the Cronese-1 fan by debris flows, as evidenced by the remnant levee deposits and boulder lines. Overland flow was undoubtedly important as well. Exposure of bedrock by erosion of the late Pleistocene colluvial cover has been an ongoing process during the Holocene, as evidenced by the range of Holocene cation-ratio dates on bedrock exposures.

Only a tiny remnant of latest Pleistocene deposition is preserved on the Cronese-1 fan (Fig. 23.5), with a minimum-limiting V/^{14}C age of 16 100 ± 800 years; AA-714). This late Pleistocene age is consistent with a varnish micromorphology of botryoidal under lamellate (cf. Dorn 1986, Chapter 20), the botryoidal layer forming during more humid conditions in the latest Pleistocene. The limited aerial extent of the late Pleistocene unit may be attributed to the burial of the distal fan margin by 27 m of Lake Manix flood deposits (Meek 1989). Fan-head burial of older deposits was undoubtedly influenced by the increased base level of the Cronese basins.

Results reported here for the Cronese-1 fan appear to be similar to those reported by Wells *et al.* (1987, 1990) for the region. However, the south-western side of the Soda Mountains bordering the Cronese playas is a different geomorphic environment than the Silver Lake side (Wells *et al.* 1987). The Cronese side has a different mix of metamorphic lithologies, steeper fan and drainage basin gradients, a strike-slip fault at its base, and was more heavily influenced by the aggradation of sediments excavated from Lake Manix (Meek 1989).

SUPPORT FOR THE PARAGLACIAL MODEL

Owens Valley is a deep graben situated between the high ranges of the Sierra Nevada and White–Inyo Mountains in eastern California (Fig. 23.4). Observations of Beaty (1963, 1970, 1974) and Lecce (1991) on alluvial fans entering the eastern side of the basin from the White–Inyo Mountains are an important part of the literature on dryland alluvial fans. The bajada on the western side of Owens Valley is even more extensive but has seen less study. Since Trowbridge's (1911) research, authors have assumed that this bajada was built from glacial outwash (e.g. Martel *et al.* 1987). Recent numerical age control has established that the eastern Sierra Nevada was extensively glaciated during the late Wisconsin with the maximum occurring at about 20 000 years BP but lasting until about 11 000 years BP (Mezger and Burbank 1986, Dorn *et al.* 1990, Phillips *et al.* 1990). Late Wisconsin glaciers (Tioga) reached their maximum extent at Pine Creek, which flows out of the eastern Sierra Nevada into Owens Valley (Fig. 23.6), about 20 000 years ago, receded to the mouth of Pine Creek by about 13 000 years BP, and retreated several kilometres up the canyon by 12 000 years BP (Dorn *et al.* 1990).

Alluvial fan deposits of Pine Creek (Fig. 23.4) were studied and collected for rock varnish dating in order to determine if there is a temporal, spatial, and sedimentological relationship with late Wisconsin glaciation in the drainage basin above the fan. Varnish cation-ratio dates on outwash boulders not spalled by fire events cluster into three groups. Cation-ratio ages from 6500 years to <300 years are on the Holocene unit mapped on Figure 23.6. These ages indicate that some fan aggradation has taken place during the post-glacial period, perhaps related to Holocene glacial advances or perhaps to non-glacial fluvial responses. Sixteen cation-ratio ages on the unit mapped on Figure 23.6 as latest Pleistocene range from about 9500 to 13 000 years BP. One boulder gave a varnish radiocarbon date of 12 700 ± 110 years BP (TO-1629). These data are consistent with a cessation of paraglacial aggradation at the end of the Tioga glaciation that was space and time transgressive, as in Figure 23.2.

Mauna Kea, Hawaii, was glaciated several times during the Pleistocene (Porter 1979). The last glaciation, Makanaka, reached its maximum extent about 20 000 years BP according to new varnish radiocarbon, varnish cation-ratio, ^{36}Cl, *in situ* ^{14}C, and silica glaze surface exposure dates (Dorn *et al.* 1991). As the Makanaka ice cap ablated, channelled outwash incised large gulches in the side of Mauna Kea, depositing alluvial fans in drylands at the base. One of these, Pohakaloa gulch fan, has a varnish radiocarbon date of 11 315 ± 95 years BP (ETH 5269; Beta 31069); considering lag effects, deposition on the fan ceased about 12 000 to 13 000 years BP. Varnish, ^{36}Cl, ^{3}He, and *in situ* ^{14}C surface dates on glacially polished rocks near the summit of Mauna Kea reveal that the top was ice free by about 15 000 years BP. Therefore, the 'relaxation time' (Church and Slaymaker 1989) of this small paraglacial system to finish transport of glacial materials was about 2000 to 3000 years.

SUPPORT FOR THE PERIGLACIAL MODEL

The Panamint Range of eastern California reaches elevations over 3300 m. The alluvial fans exiting the Panamint Range into Death Valley reach elevations below sea level (Figs 23.4 and 23.7). While no evidence has been found that glaciers formed during the Quaternary, the Panamint Range was high enough to have experienced considerable periglacial activity. Many of the ranges in the Great Basin have conspicuous fossil periglacial features (Péwé 1983), including Pleistocene nivation features in the Panamint Range (Dohrenwend 1984). Rock varnish on the larger, outer clasts of a stone garland in the Panamint Range above Hanaupah Canyon fan at about 3000 m has a minimum V/^{14}C age of 20 290 ± 220 years (AA-2322). This age probably reflects the onset of inactivity, perhaps indicating when sorting processes in the stone garland reached an equilibrium condition for the larger clasts. A boulder line of colluvium believed to be of a periglacial origin (Blackwelder 1935) has a V/^{14}C age indicating that stability was reached before about 27 100 ± 410 years BP (ETH 2809; Beta 19893).

It is a classic hypothesis that fan deposition is enhanced by frost-intensive conditions during glacial times (Melton 1965, Williams 1973, Wasson 1977). Periglacial activity produces sizeable debris loads (Clark 1987). Given the tremendous tectonically

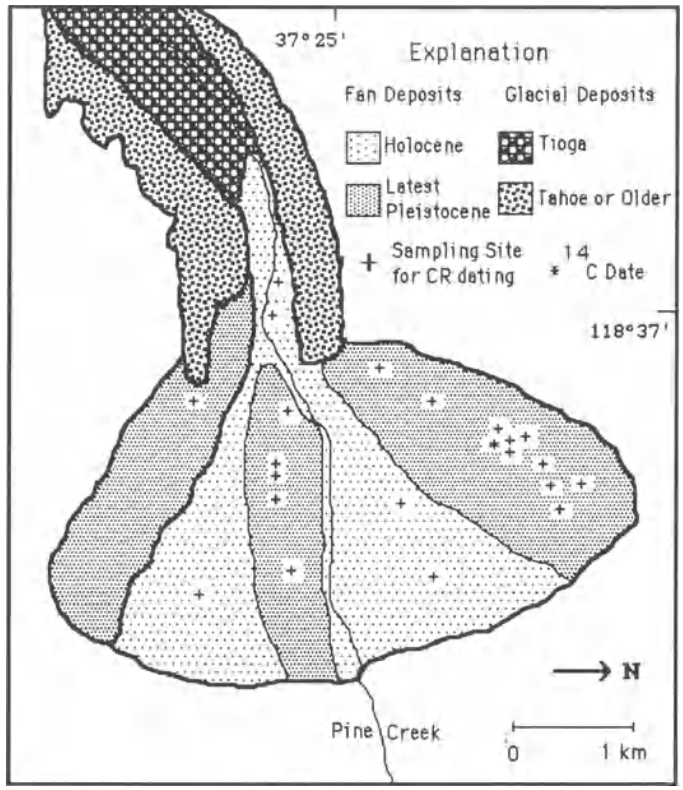

Figure 23.6 Alluvial fan and glacial moraines of Pine Creek, near Bishop, Owens Valley, California.

imposed relief from mountain crest to fan head in the Panamint Range of Death Valley (Hooke 1972, Hooke and Dorn 1992), this debris could readily be transported to the fan heads.

Palaeolake and palaeovegetation records indicate that the late Wisconsin was a time of greater moisture effectiveness in the Panamint Range and in Death Valley than during the Holocene. Based on interpretations of short cores in Death Valley, Hooke (1972) reported the last cycle of Pleistocene Lake Manly was present from before 26 000 to about 10 000 years BP. Dorn (1988) showed that highest stands reached by this cycle of Lake Manly were at about sea level, and that the high stand of this 80-m-plus-deep lake was abandoned about 13 000 years BP. Spaulding (1985) found that the region just to the east of Death Valley had a dwarf conifer woodland of *Juniperus osteosperma* at elevations below 1800 m from about 45 000 to 10 000 years BP. Wells and Woodcock (1985) report that from about 19 000 to 13 000 years BP, a *Yucca* semi-desert was present in Death Valley at 425 m, while *Juniperus osteosperma* woodland occurred on the lower slopes of the Panamint Range at an elevation of 1130 to 1280 m now occupied by creosote bush (*Larrea tridentata*). The vegetation of Death Valley changed to hot-desert scrub in a time-transgressive fashion from about 13 000 to 10 000 years BP.

The cause of greater moisture-effectiveness during the latest Pleistocene may be both cooler and moister conditions, but at different times. Cooler temperatures probably occurred from before 28 000 to 20 000 years BP because of the presence of fossilized periglacial remnants. More moist conditions are suggested for the period from about 19 000 to 13 000 years BP, based on Wells and Woodcock's (1985) and Spaulding's (1985) interpretation of the palaeovegetation record in the region.

Large areas of the Panamint fans experienced aggradation during the latest Pleistocene period of greater moisture effectiveness. V/^{14}C and cation-ratio ages, as well as a conventional ^{14}C age, support a latest Pleistocene age for this unit (Q3a in Dorn 1988, Hooke and Dorn 1992) at Galena Canyon fan (21 760

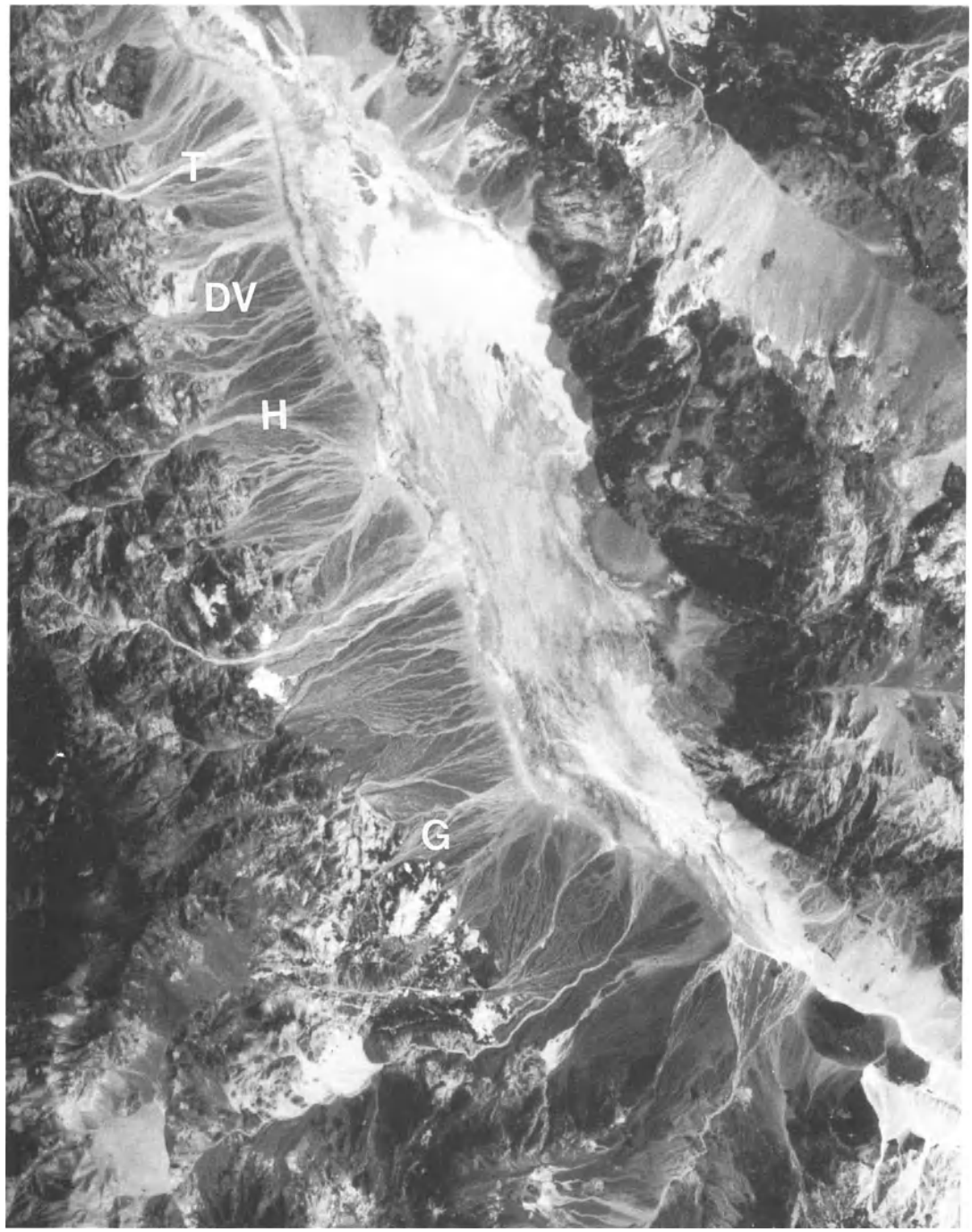

Figure 23.7 SPOT (Satellite Probatoire pour l'Observation de la Terre) satellite image of southern Death Valley, with the Panamint Range on the western side and Black Range on the eastern side. Alluvial fans referred to in the text are indicated by abbreviations: H = Hanaupah Canyon fan; DV = Death Valley Canyon fan; G = Galena Canyon fan; T = Trail Canyon fan.

± 280 years; AA-2130), Trail Canyon fan (19 960 ± 200 years; AA-1301), and Hanaupah Canyon fan (Fig. 23.7).

A gradual down-fan shift of deposition during the latest Pleistocene from about 50 000 to 14 000 years BP at Hanaupah Canyon fan (Fig. 23.8) likely occurred because of gradual tilting of the Panamint Range to the east (cf. Hooke 1972, Hooke and Dorn 1992). Microchemical, stable isotope, and micromorphological stratigraphies of varnishes on late Pleistocene units (Q3a in Dorn 1988, Chapter 20) indicate that deposition occurred during a more humid time corresponding to when periglacial activity and intensified frost weathering was more abundant in the upper elevations of the Panamint Range. Melton (1965, p. 30) recognized the dichotomy of debris-producing environments in the Panamint Range: 'the lower parts of the basins are hot and arid, with quite steep slopes, whereas the higher parts are subject to cold winters with frequent freeze–thaw cycles'. It is reasonable that the upper slopes supplied much of the sediment for fan building during the late Wisconsin through intensified periglacial activity.

The varnish evidence is also consistent with the transition-to-drier-climate model. There is a positive feedback, presented by Bull (1991), that is supported by my varnish data; as colluvium is eroded, the amount of bare rock is increased and this increases the amount of overland flow, in turn leading to increased erosion of the colluvium. For example, a low-elevation (<1000 m) slope above Death Valley Canyon fan had a cover of colluvium from at least 28 000 to 15 000 years BP (Fig. 23.9). With the change to hot-dry desert scrub starting about 13 000 years BP (Wells and Woodcock 1985), debris flows have been eroding the colluvial cover and transporting it to the fan below during at least three periods in the Holocene, at about 9000 to 8000 years BP, 4000 years BP, and <300 years BP. These are periods of enhanced erosion of this particular slope and enhanced deposition on the fan below. This information is provided by V/^{14}C and cation-ratio dating of varnish on debris flow deposits and levees (Fig. 23.9).

Figure 23.10 illustrates remnants of latest Pleistocene colluvium in Death Valley in the form of talus flatirons (cf. Gerson 1982). A V/^{14}C date of 13 520 ± 110 years BP (AA-1421) on broken surfaces of the talus probably indicates when talus deposition ceased. The separation of the talus from the present hillslope was accomplished by subsequent erosion under mostly dry, arid conditions with minimal vegetation to stabilize the hillslopes (see Chapter 21 for a more detailed discussion of the origin of talus flatirons).

Periglacial-related deposition from high-elevation sediment sources and arid-time deposition from low-elevation sediment sources can be seen in juxtaposition at the head of Hanaupah Canyon fan (Fig. 23.11). Varnish on the latest Pleistocene Q3a unit (Fig. 23.8) yields a V/^{14}C age of >43 000 years (AA-1416) at the head of the fan; the cation ratio age from this site is 50 000 ± 4000 years.

Deposited on top of this latest Pleistocene unit is an early Holocene/latest Pleistocene fan (Fig. 23.11). The source of this small fan is a tributary drainage basin just to the north of the main channel at the head of Hanaupah fan (Figs 23.8 and 23.11), which crests below 1000 m. This tributary fan was deposited after about 16 500 years BP according to a radiocarbon date on the *top layer* of buried varnish from the latest Pleistocene Q3a unit (16 570 ± 190 years BP; ETH 4482, Beta 27778). Deposition ceased by 12 000 ± 1500 years BP, according to cation-ratio dating on the surface of this tributary fan. Following Bull's (1991) model, the change in vegetation cover to desert scrub (Wells and Woodcock 1985) destabilized the colluvium formed throughout the more humid Wisconsin. Colluvium stripped from the tributary basin was deposited on the latest Pleistocene Q3a unit.

This entire discussion is not meant to imply that only lower-elevation slopes supplied sediment during the warm-arid Holocene and that only upper-elevation slopes supplied debris during the cooler-moisture late Pleistocene. However, the most likely mechanisms for producing most of the sediment probably alternated between upper and lower slopes during the last glacial and post-glacial. The reaction of the hillslope–fan-sediment transport system in Death Valley and the Soda Mountains to the climatic change at the termination of the last glacial period is somewhat analogous to Church and Slaymaker's (1989) paraglacial model (Fig. 23.2). Both deglaciation and devegetation leave abundant loose material for transport and the fluvial system. According to the evidence on hillslopes, lower elevation hillslopes started to shed abundant colluvium in response to reduction in vegetation cover, but the erosion of the Pleistocene colluvium has been ongoing throughout the Holocene (Figs 23.9 and 23.10). As in British Columbia, the formation of alluvial fans in Death Valley is tied to the history of sediment transport in the basins above the fans.

The fan-head trenching of Hanaupah Canyon may have taken place in two steps. Hooke and Dorn

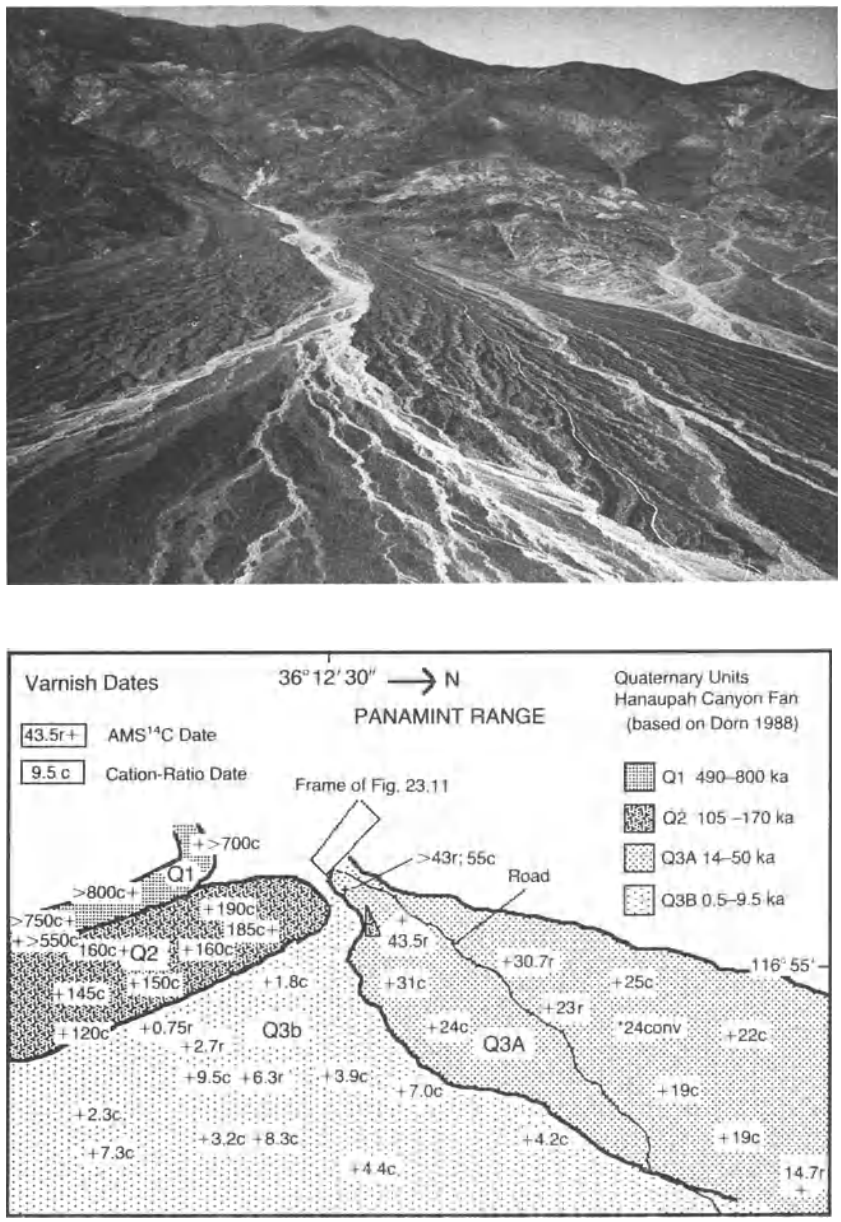

Figure 23.8 Oblique aerial photograph and corresponding map of Hanaupah Canyon alluvial fan, Death Valley. The symbol + indicates sampling sites for varnish dating. The associated number is the age estimate based on a cation-ratio date denoted by c or a varnish radiocarbon date denoted by r. The symbol * indicates one site where a conventional radiocarbon date was obtained on charcoal buried at a depth of 1.7 m (23 420 ± 550 years BP; Beta 28805). All ages are in 10^3 years. Alluvial units correspond to those used by Dorn (1988).

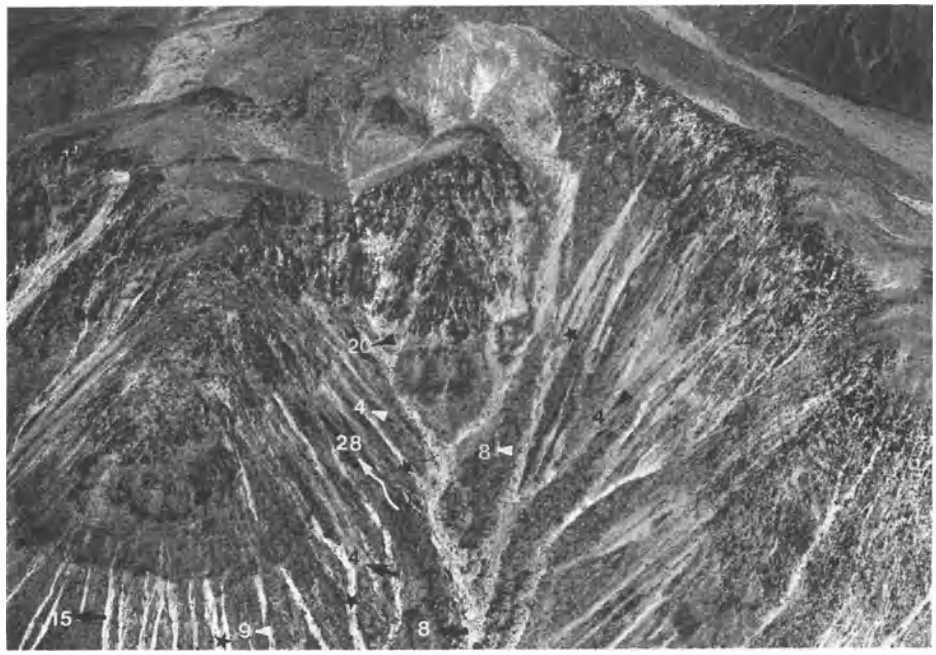

Figure 23.9 Hillslope just above Death Valley Canyon fan, Panamint Range. Varnishes on remnants of late Pleistocene colluvium date, by radiocarbon and cation-ratios, from 28 000 to 20 000 years BP. Three periods of debris flow erosion of this colluvium are indicated: about 9000 to 8000 years BP; about 4000 years BP; and <300 years BP. All ages are in 10^3 years.

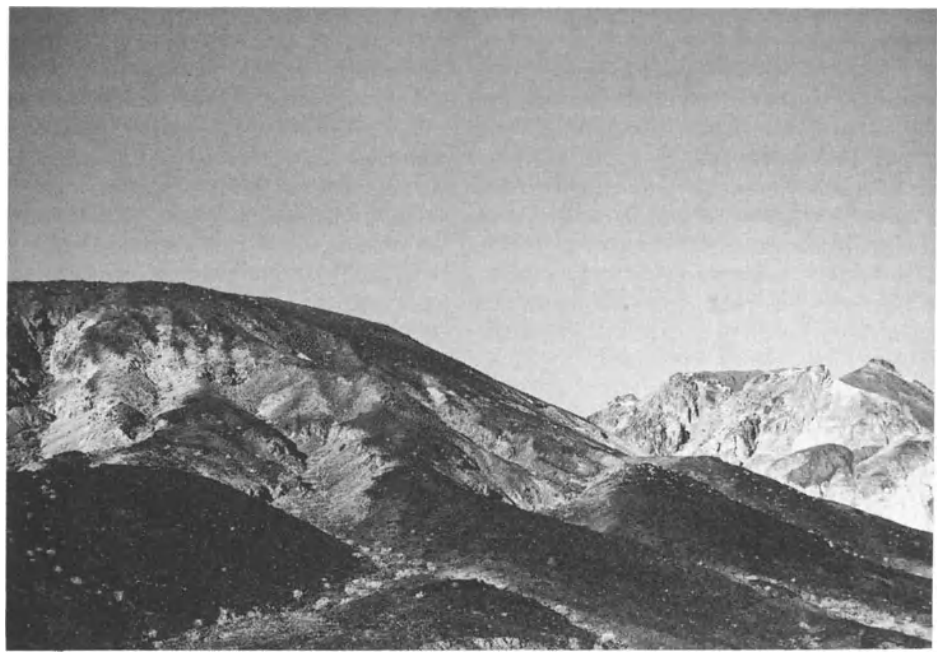

Figure 23.10 Remnants of Pleistocene hillslope colluvium at a low elevation site (<300 m) near Artists Drive in Death Valley, California. The darkened facets are well-varnished talus flatirons that were separated about 14 000 ^{14}C years ago from the talus source at the top of the hill. The cause of separation was probably increased hillslope erosion as vegetation cover was reduced at the close of the Pleistocene (Wells and Woodcock 1985), as proposed by Gerson (1982).

Figure 23.11 Incised alluvial fan on the north side at the head of Hanaupah Canyon alluvial fan, Death Valley. The approximate frame of this photo is shown in Figure 23.8, looking toward the north-west. The double-arrow line indicates the contact between the late Pleistocene–early Holocene tributary fan (above) and the Q3a deposit (*c.* 50 000 years BP) of the main drainage of Hanaupah fan. When the tributary fan was deposited, the main channel of Hanaupah Canyon was not deeply incised. As the main channel entrenched, so did the tributary fan. Creosote bushes (*Larrea tridentata*) 1 to 2 m high provide scale.

(1992) explored the first and better understood stage of entrenchment that started at the fan head during a more moist period. As evidenced by Figure 23.8, the main channel gradually incised deeply enough for the loci of deposition to migrate down-fan towards the toe from around 50 000 to 14 000 years BP. Laboratory experiments indicate that as the depth of entrenchment increases and the intersection point migrates down-fan, the new segment (down-fan of the intersection point) grows and its up-fan edge migrates up-fan. In trying to explain incision during a more moist period, Hooke and Dorn (1992) speculate that in an area of active tectonic extension, loading of the crust by the filling of Lake Manly with water may have been sufficient to trigger an episode of tectonic tilting.

The evidence for a second stage of entrenchment is less clear. It is found in the tributary fan (Fig. 23.11). The cessation of deposition on the tributary fan about 12 000 years BP indicates that sediment from the tributary basin was routed through a tributary fan-head trench after that time. Three possible explanations are offered. First, incision of the tributary fan could have been unrelated to a deepening of the main channel. Instead, it could have been due to widening of the main trench to the north; this would have simulated a sudden drop in base level, undercutting the tributary fan, and initiating the downcutting that routed sediment off the tributary fan. Second, F. Magilligan (pers. comm., 1992) suggested that progradation of the tributary fan from around 16 000 to 12 000 years BP could have constricted flow in the main channel. Such constriction would have increased stream power and caused further channel incision. Third, there must have been a time lag between the cessation of periglacial activity (during the full glacial period) supplying sediment from the upper basin slopes and the generation of sediment from lower basin slopes when devegetation started about 13 000 years BP. The packrat midden and palaeolake record reviewed earlier indicates that the terminal Pleistocene was a time of much more abundant moisture. A. Abrahams (pers. comm., 1992) suggested that the decrease in the supply of sediment from the upper basin would have given the relatively clear stream more power to incise into its bed.

An interesting contrast is provided by the Beltana

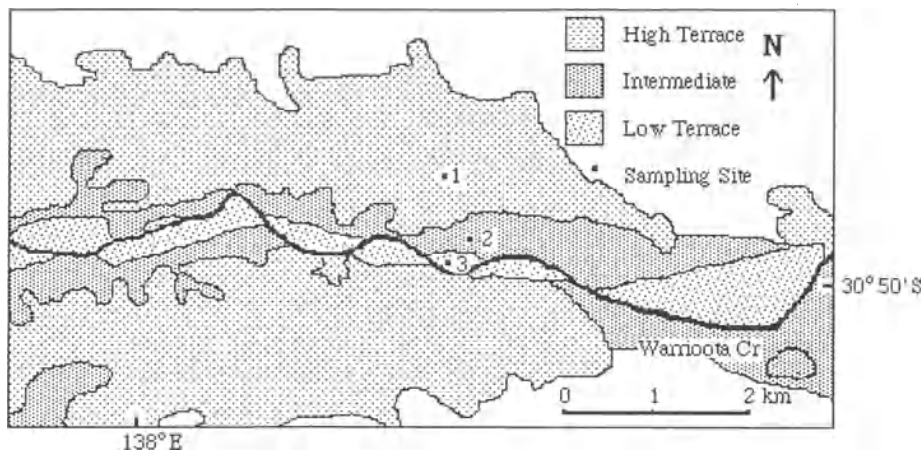

Figure 23.12 Map of alluvial units along the Warrioota Creek alluvial slope section of the Beltana alluvial complex, South Australia. Site numbers identify locations of sampling varnish for dating. Varnish collected from site 1 has a cation-ratio age of 45 000 to 40 000 years BP and was beyond the scope of radiocarbon dating. Site 2 has a varnish radiocarbon age of 7610 ± 75 years BP (ETH 5266; Beta 31066). Site 3 has a varnish cation-ratio age of 2700 ± 700 years BP.

piedmont of South Australia (Fig. 23.12). About 140 km north of Williams' (1973) Depot Creek and Wilkatana alluvial fans is an alluvial slope near Beltana, South Australia. Beltana is in a climate currently much more arid than Wilkatana, with about 100 mm less annual precipitation and with warmer temperatures (Bureau of Meteorology, Australia 1975). As Warrioota Creek exits from the Wilpena Group and Beltana Diapir on to the Beltana sub-basin, it has deposited an alluvial *Glacis d'erosion* (Twidale 1967).

Only a small portion of the Warrioota alluvial complex in the Beltana basin was studied. A sequence of three alluvial units above the active Warrioota channel was mapped and sampled for varnish dating. The locations of the samples are indicated in Figure 23.12. Only rounded fluvial gravels, unfractured by weathering, and larger than 50 cm in diameter were collected from desert pavements. The current channel had no observable varnish. The lowest terrace has a varnish cation-ratio age of 2700 ± 700 years. The middle terrace has a varnish radiocarbon age of 7610 ± 75 years (ETH 5266; Beta 31066). Varnish on gravels on the highest terrace was beyond the scope of radiocarbon dating (>38 000 years), but the cation ratios of these varnishes suggest the date of exposure was about 40 000 to 45 000 years BP.

These preliminary results from only one small portion of the Beltana alluvial complex are consistent with the findings of Williams (1973). The oldest unit coincides with Williams' Pooraka time of fan building which was characterized by a colder and drier periglacial climate. The inset terraces at about 7600 and 2700 years BP correlate in time with Williams' Eyre and Thompson Creek Formations, members 1 and 2, which were deposited during periods of greater precipitation.

According to these climatic interpretations, in both South Australia and Death Valley, aggradation can be caused by different types of climatic changes within the same drainage basin. This should not be surprising, since sediment transport does not start and stop with changes in climate.

CRITICAL PERSPECTIVE ON THE ROLE OF CLIMATIC CHANGE IN ALLUVIAL FAN DEVELOPMENT

It is an exciting time for climatic geomorphology. 'Multidisciplinary and diverse efforts by Quaternary scientists are continuing to reveal new and exciting pages of this important chapter of Earth's history' (Bull 1991, p. 121). There are new and improved sources of palaeoenvironmental data and new and improved dating methods. There is the growing realization that global change issues are important and that geomorphology has a significant role to play in assessing changing global climates.

However, it is a difficult task to separate climatic influences from tectonic, intrinsic, and other components of the geomorphic system. Before climatic models of alluvial fan development are adopted by geomorphologists, by remote sensing specialists examining fans, by climatic modellers, or by other

Table 23.2 Potential problems associated with climatic interpretations of alluvial fans

Issue	*Comment*	*References*
Range–piedmont feedbacks	Tributary streams and within-basin storage can play a critical role in fan development, as can fan geometry, lithology, scale, and basin morpometry. These effects can be misinterpreted as climatically induced effects	Hawley and Wilson 1965, MacArthur *et al.* 1990, Lecce 1991, White 1991
Tectonics	Long-term rates and the timing of specific events must be understood for each fan. It is especially critical to discover where the profile change occurred. Tectonically modified spatial variability in stream power could influence the location of incision, aggradation, and transportation	Hooke 1972, Rockwell *et al.* 1985, Bull 1991
Intrinsic geomorphic variables	Intrinsic variables can be short-term, forcing the loci of deposition to switch in a single storm. It can be longer term, where aggradation at fan head can enhance entrenchment (Fig. 22.11). Over the Quaternary period, headward incision of gullies led to drainage piracy redirecting the loci of fan deposition	Weaver, 1984, Schumm *et al.* 1987, Denny 1965, 1967
Palaeohydrology	Changes in stream power, competence, capacity, discharge, and changes in the abundance of debris flows must be understood for different periods, keeping in mind that deposition of fan material is not necessarily an equilibrium process (Bull 1991). Correlations of aggradational events with climatic changes must remain speculative until quantitative data on these and other critical variables are available for the palaeoflood events responsible for fan deposits	Ely and Baker 1990
Volume estimates	Volumes of alluvial units ascribed to a particular climate are critical to climatic intepretations, yet they are rarely available. Age control is needed in multiple stratigraphic positions over the length and width of the alluvial unit studied. Late Quaternary fan deposits are in some cases merely thin veneers on older gravels, while other units are thick wedges	Hunt and Mabey 1966, Hooke 1972, Bull 1991
Difficulty in correlating fan units with palaeoclimatic indicators	A *definitive* correlation of the age of a fan unit with a climatic period is problematic. (a) There is little evidence that global records, such as sea level curves or marine oxygen isotope, reflect local drainage basin conditions. (b) If local continental palaeoclimatic data are available, they may not be well dated, or the dating methods may not necessarily be readily comparable. (c) Typically, very little numerical age control exists for alluvial fan material. There are too many specific ages assigned to alluvial fan events in the published literature that have no basis in objective measurements. (d) If accurate numerical age control is available for fans, it is usually only precise enough to conclude that a particular aggradation event occurred during a lengthy climatic period of typically 10^3 to 10^4 years. Within such long periods, there are many climatic fluctuations	
Inability to falsify non-climatic hypothesis	Extreme storm events within even a specific climatic period can produce aggradational and entrenchment events that relate to that *extreme* climatic event, not necessarily to the general climate state of a given period	
Lag effects	Vegetation changes often lag behind climatic changes, sometimes for 10^2 to 10^3 years. This creates a complicated mismatch between the palaeoclimatic record and the geomorphic response	Bull 1991
Watersheds with large relief	A climatic change will be time- and elevation-transgressive, with sediment sources shifting up and down basin	Melton 1965
Palaeoclimatic data	Palaeoclimatic data do not come in a form useful for interpreting past geomorphological processes. For example, *Neotoma* packrat specialists have provided an outstanding data base that is specific to a site. However, these data cannot now be related to percentage plant cover, or percentage of plants rooted to a certain geomorphically effective depth. Until a strong, quantitative process–palaeoclimatic data link is forged, model evaluation will be limited to qualitative deduction	

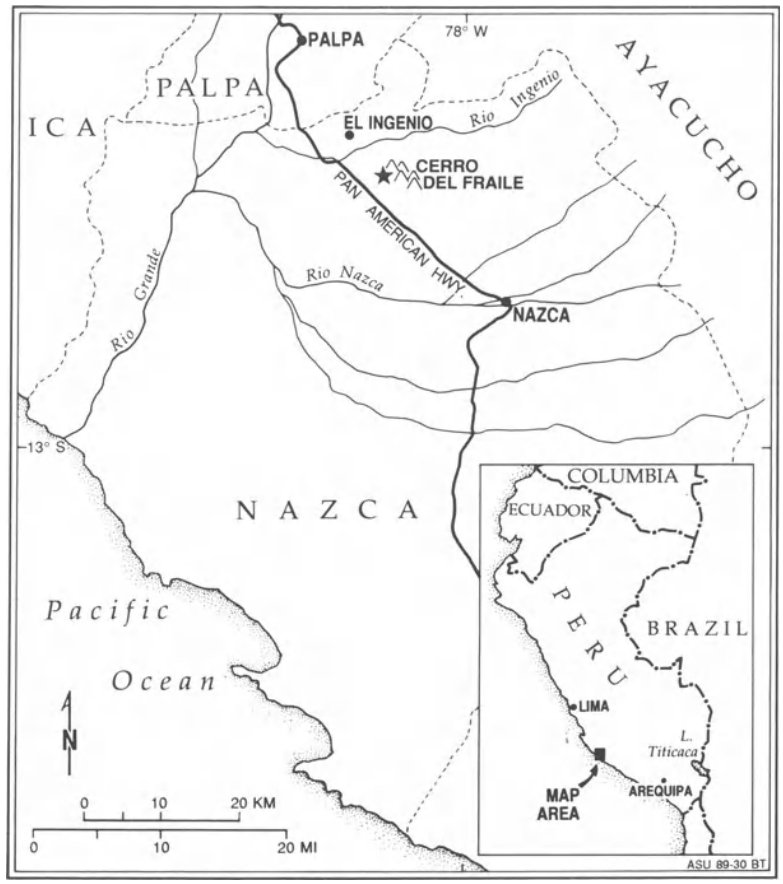

Figure 23.13 The Ingenio-1 fan exits the Cerro del Fraile range, near the town of Nazca, Peru.

disciplines interested in global changes, rigorous tests need to be conducted to control non-climatic components of the fan system.

Several potential problems with climatic interpretations are presented in Table 23.2. A few of these issues have been addressed in papers promoting climatic interpretations (Bull 1991), but this has been the exception rather than the rule. In all fairness, data on most of these issues are difficult to obtain, and researchers have used clever approaches to control factors influencing alluvial fans other than climate. For example, one way of separating the climatic change 'signal' from the tectonic 'noise' is to correlate alluvial fan events over different mountain ranges that likely have a similar climatic history but different tectonic histories. However, where alluvial fans also have different basin lithologies, basin and fan morphometries, basin reliefs, and scales, correlating climatically induced events on alluvial fans can become difficult. Certainly one of the greatest problems facing a climatic interpretation of alluvial fan research is developing quantitative relationships that incorporate the magnitude and frequency of fan-building events.

At present, no researcher has falsified the hypothesis that dryland alluvial fans are produced by high-magnitude (low-frequency) storms unrelated to any particular climatic regime. The importance of extreme climatic events may be found in the Nazca region of Peru where a small alluvial fan was sampled for varnish radiocarbon dating (Dorn *et al.* 1992). The Ingenio-1 fan exits a small drainage basin ($< 1\ km^2$) in the Cerro del Fraile range south of the town of Ingenio (Fig. 23.13). Radiocarbon dating of rock varnish indicates that alluvial units range in age from about 22 000 years to surfaces more recent than Nasca-age pottery (Dorn *et al.* 1992; Fig. 23.14).

The south coast of Peru is classified hyperarid, and would be viewed as arid by all palaeoclimatic indicators, whether lacustrine, soil, or palaeovegeta-

Figure 23.14 Oblique aerial photo and corresponding generalized map of Ingenio-1 alluvial fan. Ages are based on single varnish radiocarbon dates from the indicated sampling sites, with the ages in Dorn *et al.* (1992). The post-Nasca age for unit 5 is indicated by the lack of Nasca pottery found on its surface and the lack of Nasca pottery in the active channel. (Note that the 'Nazca' spelling is reserved for political units, whereas 'Nasca' denotes the prehistoric culture.)

Table 23.3 Comparison of alluvial fan chronologies in the Mojave Desert region of southern California and southern Nevada

Lower Colorado River region (Bull 1991, p. 86)	*Panamint Range entering Death Valley (Dorn 1988)*		*Cime Area, east-central Mojave (Wells* et al. *1990)*		*South Side San Gabriel Range (Bull 1991, p. 191)*	*Crater Flat Southern Nevada (Peterson* et al. *in preparation)*	
Q4b* 0†	Active channel		Active channel (Qf9)		T9 <1	Active channel	
Q4a 0.1–2	Q3b3	0.5–2.5	Qf8	<0.3–>0.7	T8 1–4	Crater Flat	<0.4–1.5
Q3c 2–4	Q3b2	2.0–4.5	Qf6,7	2–8	T7 4–7		
Q3a 8–12	Q3b1	6–11	Qf5	8–15	T6 7–12	Little Cone	7–11
Q2c 12–70	Q3a	13–50	Qf4	<34–>45	T5 12–20	Late Black Cone	17–30
Q2b 70–200	Q2b	110–130	Qf3	<47–>130	T4 50–60		
	Q2a	140–190	Qf2	<160–>320	T3 120–130	Early Black Cone	130–190
	Q1b	400–650			T2 700–790	Yucca	>370
Q1 >1200	Q1	>650–>800	Qf1	<3800	T1 >790	Solitario	>450–>740

*Surface designation.
†Age in thousands of years.

tion. Yet in this period of hyperaridity that has prevailed during the deposition of units 4, 5, and 6 (Fig. 23.14), extreme rainfall events have been required to generate the debris flow and braided stream deposits that are found on the fan (cf. Beaty 1963, 1974, Hooke 1967, 1987). Dorn *et al.* (1992) speculated that these were produced by strong El Niño–Southern Oscillation events, as in the north coast of Peru (Wells 1987). Regardless, the point is that high-magnitude, low-frequency, and extreme storm events built the fan. These could have occurred during virtually any general climatic period with the same fan-building events.

CONCLUSION

The role of climatic change in alluvial development has been somewhat of a Holy Grail for many desert geomorphologists. There has been an intuitive acceptance that the timescales of alluvial fans are long enough for fans to have experienced vastly different climatic states. Since casting out simple Davisian evolutionary models (Davis 1905), climatic interpretations have been an easy way of explaining difficult problems. This is not to say that so many have been so wrong. Yet the problems associated with making specific climatic-based interpretations of alluvial fan development are immense. Difficulties encountered are largely due to a lack of information on time, tectonism, palaeovegetation, paleoclimatology, and intrinsic geomorphic and palaeohydrology variables associated with aggradation events of unknown volume and timing and incision events of unknown cause and timing.

I believe that climatic changes are indeed critical for the understanding of alluvial fans in what are now deserts. The observations that led to the four climatic models presented earlier in this chapter are intuitively appealing, and the correlation of different alluvial units in Table 23.3 is plainly evident. Table 23.3 compares alluvial units in the Mojave Desert region of south-western North America. The compared deposits derive from ranges with very different tectonic histories. Some are active (Panamint Range into Death Valley and the San Gabriel Range), while others are less active (Cima region in the east-central Mojave Desert). Comparing Table 23.3 with Spaulding's (1985, 1990) *Neotoma* palaeovegetation record, an aerially extensive (volumes unknown) pulse of deposition occurred in the period of climatic transition from dwarf-conifer woodland to desert scrub (*c.* 10 000 ± 4000 years BP), as well as aggradation during a lengthy moist period when woodlands were ubiquitous (*c.* >45 000 to 12 000 years BP). I do not feel confident about correlating units beyond the range of radiocarbon dating. Older alluvial units incorporate very long chronological periods, and apparent correlations may simply represent overlap in age uncertainties, the inadvertent combination of different alluvial events that have a similar morphological expression, or both.

Lecce (1990) identified the 'alluvial fan problem' as the difficulty in generating a general model of alluvial fan development. Although general climatic models have been proposed (Table 23.1), there has also been a difficulty in proposing tests of these models. Geomorphologists are an individualistic breed. We are generally resistant to the mega-team projects favoured by climatologists. We like our

favourite sites and our pet conceptual models. However, there needs to be some coordination to systematically isolate tests of climatic hypotheses, or we will wander in the desert for yet another 40 years since destroying the golden idol of Davisian Geomorphology.

ACKNOWLEDGEMENTS

The research on which this chapter is based was funded mostly by an NSF PYI Award and NSF grant SES 86-01937. The Death Valley work was also supported by National Geographic Society grant 84-2961. Thanks to T. Cahill and T. Gill for PIXE measurements; A.J.T. Jull, D. Donahue, L. Toolin, and T. Linick of the University of Arizona accelerator, M. Tamers and J. Stipp of Beta Analytic, W. Wolfli of the Zurich accelerator, and Isotrace for AMS ^{14}C measurements; B. Trapido for graphic assistance; D. Dorn for field assistance; and W. Graf, R. Hooke, N. Meek, and W.B. Bull and many students for comments on various drafts.

REFERENCES

Baker, V.R., K.A. Demsey, L.L. Ely, J.E. Fuller, *et al.* 1990. Application of geological information to Arizona flood hazard assessment. Proceedings of International ASCE Symposium, *Hydraulics/Hydrology of Arid Lands*, San Diego, July 30–August 2, 621–6.

Barsch, D. and C.F.J. Royse 1972. A model for development of Quaternary terraces and pediment-terraces in the southwestern United States of America. *Zeitschrift für Geomorphologie* **16**, 54.

Beaty, C.B. 1963. Origin of alluvial fans, White Mountains, California and Nevada. *Annals of the Association American Geographers* **53**, 516–35.

Beaty, C.B. 1970. Age and estimated rate of accumulation of an alluvial fan, White Mountains, California, USA. *American Journal of Science* **268**, 50–70.

Beaty, C.B. 1974. Debris flow, alluvial fans and a revitalized catastrophism. *Zeitschrift für Geomorphologie Supplement Band* **21**, 39–51.

Blackwelder, E. 1935. Talus slopes in the Basin Range Province. *Proceedings of the Geological Society of America for 1934*, 317.

Blair, T.C., J.S. Clark and S.G. Wells 1990. Quaternary continental stratigraphy, landscape evolution, and application to archeology: Jarilla piedmont and Tularosa graben floor, White Sands Missile Range, New Mexico. *Bulletin of the Geological Society of America* **102**, 749–59.

Blissenbach, E. 1954. Geology of alluvial fans in semiarid regions. *Bulletin of the Geological Society of America* **65**, 175–90.

Brown, W.J., S.G. Wells, Y. Enzel, R.Y. Anderson, *et al.* 1990. The late Quaternary history of pluvial Lake Mojave – Silver Lake and Soda Lake basins, California. In *At the end of the Mojave: Quaternary studies in the eastern Mojave Desert*, R.E. Reynolds, S.G. Wells and R.J.I. Brady (eds), 55–72. Redlands: San Bernardino County Museum Association.

Bull, W.B. 1964. Geomorphology of segmented alluvial fans in Western Fresno County, California. *U.S. Geological Survey Professional Paper* 352-E, 89–128.

Bull, W.B. 1975. Allometric change of landforms. *Bulletin of the Geological Society of America* **86**, 1489–98.

Bull, W.B. 1977. The alluvial-fan environment. *Progress in Physical Geography* **1**, 222–70.

Bull, W.B. 1979. Thresholds of critical power in streams. *Bulletin of the Geological Society of America* **90**, 453–64.

Bull, W.B. 1991. *Geomorphic responses to climatic change*. Oxford: Oxford University Press.

Bull, W.B. and A.P. Schick 1979. Impact of climatic change on an arid watershed: Nahal Yael, southern Israel. *Quaternary Research* **11**, 153–71.

Bureau of Meteorology, Australia 1975. *Climatic Averages, Australia.*, Melbourne: Bureau of Meteorology.

Cerling, T.E., J. Quade, Y. Wang and J.R. Bowman 1989. Carbon isotopes in soils and palaeosols as ecology and palaeoecology indicators. *Nature* **341**, 138–9.

Christenson, G.E. and C. Purcell 1985. Correlation and age of Quaternary alluvial-fan sequences, Basin and Range province, southwestern United States. *Geological Society of America Special Paper* 203, 115–22.

Church, M. and J.M. Ryder 1972. Paraglacial sedimentation, a consideration of fluvial processes conditioned by glaciation. *Bulletin of the Geological Society of America* **83**, 3059–72.

Church, M. and O. Slaymaker 1989. Disequilibrium of Holocene sediment yield in glaciated British Columbia. *Nature* **337**, 452–4.

Clark, M.J. 1987. Geocryological inputs to the alpine sediment system. In *Glacio-fluvial sediment transfer*, A.M. Gurnell and M.J. Clark (eds), 33–58. New York: Wiley.

Coque, R. and A. Jauzein, 1967. The geomorphology and Quaternary geology of Tunisia. In *Guidebook to the geology and history of Tunisia*, L. Martin (ed.), Tripoli: Petroleum Exploration Society of Libya.

Cooke, R.U. 1984. *Geomorphological hazards in Los Angeles*. London: Allen & Unwin.

Cooke, R.U., D. Brunsden, J.C. Doornkamp and D. Jones 1982. *Urban geomorphology in drylands*. Oxford: Oxford University Press.

Dailey, M.I., T. Farr, C. Elachi and G. Schaber 1979. Geological interpretation from composited radar and Landsat imagery. *Photogrammetric Engineering and Remote Sensing* **45**, 1109–16.

Davis, W.M. 1905. The geographical cycle in arid climate. *Journal of Geology* **13**, 381–407.

Denny, C.S. 1965. Alluvial fans in the Death Valley region of California and Nevada. *U.S. Geological Survey Professional Paper* 466.

Denny, C.S. 1967. Fans and pediments. *American Journal Science* **265**, 81–105.

Dohrenwend, J.C. 1984. Nivation landforms in the western Great Basin and their paleoclimatic significance. *Quaternary Research* **22**, 275–88.

Dorn, R.I. 1986. Rock varnish as an indicator of aeolian environmental change. In *Aeolian geomorphology*, W.G. Nickling (eds), 291–307. London: Allen & Unwin.

Dorn, R.I. 1988. A rock varnish interpretation of alluvial fan development in Death Valley, California. *National Geographic Research* **4**, 56–73.

Dorn, R.I. 1989. Cation-ratio dating of rock varnish: a geographical perspective. *Progress in Physical Geography* **13**, 559–96.

Dorn, R.I. and D.H. Krinsley 1991. Cation-leaching sites in rock varnish. *Geology* **19**, 1077–80.

Dorn, R.I., M.J. DeNiro and H.O. Ajie 1987a. Isotopic evidence for climatic influence on alluvial-fan development in Death Valley, California. *Geology* **15**, 108–10.

Dorn, R.I., D.L. Tanner, B.D. Turrin and J.C. Dohrenwend 1987b. Cation-ratio dating of Quaternary materials in the east-central Mojave Desert, California. *Physical Geography* **8**, 72–81.

Dorn, R.I., A.J.T. Jull, D.J. Donahue, T.W. Linick, *et al.* 1989. Accelerator mass spectrometry radiocarbon dating of rock varnish. *Bulletin of the Geological Society of America* **101**, 1363–72.

Dorn, R.I., T.A. Cahill, R.A. Eldred, T.E. Gill, *et al.* 1990. Dating rock varnishes by the cation ratio method with PIXE, ICP, and the electron microprobe. *International Journal of PIXE* **1**, 157–95.

Dorn, R.I., F.M. Phillips, M.G. Zreda, E.W. Wolfe, *et al.* 1991. Glacial chronology of Mauna Kea, Hawaii, as constrained by surface-exposure dating. *National Geographic Research* **7**, 456–71.

Dorn, R.I., P.B. Clarkson, M.F. Nobbs, L.L. Loendorf, *et al.* 1992. New approach to the radiocarbon dating of rock varnish, with examples from drylands. *Annals of the Association of American Geographers* **82**, 136–51.

Eckis, R. 1928. Alluvial fans in the Cucamonga district, southern California. *Journal of Geology* **36**, 111–41.

Elliott-Fisk, D.L. 1987. Glacial geomorphology of the White Mountains, California and Nevada. *Physical Geography* **8**, 299–323.

Ely, L.L. and V.R. Baker 1990. Large floods and climate change in the southwestern United States. Proceedings of International ASCE Symposium, *Hydraulics/Hydrology of Arid Lands*. San Diego, July 30–August 2, 361–6.

Gerson, R. 1982. Talus relicts in deserts: a key to major climatic fluctuations. *Israel Journal of Earth Science* **31**, 123–32.

Gilbert, G.K. 1875. Report on the geology of portions of Nevada, Utah, California and Arizona, 1871–2. *Report of the U.S. Geographical and Geological Survey West of the 100th Meridian* **3**, 21–187.

Gile, L.H., J.W. Hawley and R.B. Grossman 1981. Soils and geomorphology in the Basin and Range area of southern New Mexico. Guidebook to the Desert Project. *New Mexico Bureau of Mines and Mineral Resources Memoir* **39**, 1–222.

Glennie, K.W. 1970. *Desert sedimentary environments*. Amsterdam: Elsevier.

Goldberg, P. 1984. Late Quaternary history of Quadesh Barnea, northeastern Sinai. *Zeitschrift für Geomorphologie* **28**, 193–217.

Graf, W.L. 1988. *Fluvial processes in dryland rivers*. Berlin: Springer.

Grossman, S. and R. Gerson 1987. Fluviatile deposits and morphology of alluvial surfaces as indicators of Quaternary environmental changes in the southern Negev, Israel. In *Desert sediments: ancient and modern*, L. Frostick and I. Reid (eds), 17–29. Geological Society of London Special Publication 35.

Harvey, A.M. 1987. Alluvial fan dissection: relationships between morphology and sedimentation. In *Desert sediments: ancient and modern*, L. Frostick and I. Reid (eds), 87–103. Geological Society of London Special Publication 35.

Harvey, A.M. 1989. The occurrence and role of arid zone alluvial fans. In *Arid zone geomorphology*, D.S.G. Thomas (eds), 136–58. London: Belhaven Press.

Harvey, A.M. 1990. Factors influencing Quaternary alluvial fan development in southeast Spain. In *Alluvial fans: a field approach*, A.H. Rachocki and M. Church (eds), 247–69. New York: Wiley.

Hawley, J.W. and W.E. Wilson 1965. Quaternary geology of the Winnemucca area, Nevada. *Desert Research Institute Technical Report* 5.

Hooke, R.L. 1967. Processes on arid region alluvial fans. *Journal Geology* **75**, 438–60.

Hooke, R.L. 1968. Steady-state relationships on arid-region alluvial fans in closed basins. *American Journal Science* **266**, 609–29.

Hooke, R.L. 1972. Geomorphic evidence for late Wisconsin and Holocene tectonic deformation, Death Valley, California. *Bulletin of the Geological Society of America* **83**, 2073–98.

Hooke, R.L. 1987. Mass movement in semi-arid environments and the morphology of alluvial fans. In *Slope stability*, M.G. Anderson and K.S. Richards (eds), 505–29. New York: Wiley.

Hooke, R. and R. Dorn 1992. Segmentation of alluvial fans in Death Valley, California: new insights from surface-exposure dating and laboratory modelling. *Earth Surface Processes and Landforms* **17**, 557–74.

Hötzl, H., F. Kramer and V. Maurin 1978. Quaternary sediments. In *Quaternary of Saudi Arabia. Vol.1*, S. al-Sayari and J. Zötl (eds), 264–301. Berlin: Springer.

Hunt, C.B. and D.R. Mabey 1966. Stratigraphy and structure, Death Valley, California. *U.S. Geological Survey Professional Paper* 494-A.

Huntington, E. 1907. Some characteristics of the glacial period in non-glaciated regions. *Bulletin of the Geological Society of America* **18**, 351–88.

Kale, V.S. and S.N. Rajaguru 1987. Late Quaternary alluvial history of the northwestern Deccas upland region. *Nature* **325**, 612–14.

Knox, J.C. 1983. Responses of river systems to Holocene climates. In *Late Quaternary environments of the United States*, Volume 2. *The Holocene*, H.E. Wright Jr (ed.), 26–41. Minneapolis: University of Minnesota Press.

Kochel, R.C. and D.F. Ritter 1990. Complex geomorphic response to minor climatic changes, San Diego County, CA. Proceedings of International ASCE Symposium, *Hydraulics/Hydrology of Arid Lands*, San Diego, July 30–August 2, 148–53.

Lecce, S.A. 1990. The alluvial fan problem. In *Alluvial fans: a field approach*. A.H. Rachocki and M. Church (eds), 3–24. New York: Wiley.

Lecce, S.A. 1991. Influence of lithologic erodibility on alluvial fan area, western White Mountains, California and Nevada. *Earth Surface Processes and Landforms* **16**, 11–8.

Lustig, L.K. 1965. Clastic sedimentation in Deep Springs

Valley, California. *U.S. Geological Survey Professional Paper* 352-F, 131–90.

MacArthur, R.C., M.D. Harvey and E.F. Sing 1990. Estimating sediment delivery and yield on alluvial fans. Proceedings of International ASCE Symposium, *Hydraulics/Hydrology of Arid Lands*, San Diego, July 30–August 2, 700–5.

Maizels, J.K. 1987. Plio-Pleistocene raised channel systems of the western Sharqiya (Wahiba), Oman. In *Desert sediments: ancient and modern*, L. Frostick and I. Reid (eds), 31–50. Geological Society of London Special Publication 35.

Martel, S.J., T.M. Harrison and A.R. Gillespie 1987. Late Quaternary vertical displacement rate across the Fish Springs Fault, Owen Valley Fault Zone, California. *Quaternary Research* **27**, 113–39.

Mayer, L., R. Gerson and W.B. Bull 1984. Alluvial gravel production and deposition – a useful indicator of Quaternary climatic changes in deserts (a case study in southwestern Arizona). *Catena Supplement* **5**, 137–51.

McFadden, L.D. 1988. Climatic influences on rates and processes of soil development in Quaternary deposits of southern California. *Geological Society of America Special Paper* 216, 153–78.

McGee, W.J. 1897. Sheetflood erosion. *Bulletin of the Geological Society America* **8**, 87–112.

Meek, N. 1989. Geomorphic and hydrologic implications of the rapid incision of Afton Canyon, Mojave Desert, California. *Geology* **17**, 7–10.

Melton, M.A. 1965. The geomorphic and paleoclimatic significance of alluvial deposits in southern Arizona. *Journal Geology* **73**, 1–38.

Mezger, L. and D. Burbank. 1986. The glacial history of the late Cottonwood Lakes area, southeastern Sierra Nevada. *Geological Society America Abstracts with Program* **18**, 157.

Montgomery, D.R. and W.E. Dietrich 1992. Channel initiation and the problem of landscape scale. *Science* **255**, 826–30.

Mulhern, M.E. 1982. Lacustrine, fluvial and fan sedimentation: a record of Quaternary climatic change and tectonism, Pine Valley, Nevada. *Zeitschrift für Geomorphologie Supplement Band* **42**, 117–33.

Nilsen, T.H. and T.E. Moore 1984. *Bibliography of alluvial-fan deposits*. Norwich: GeoBooks.

Ore, C.N. and C.N. Warren 1971. Late Pleistocene–early Holocene geomorphic history of Lake Mojave, California. *Bulletin of the Geological Society America* **82**, 2553–62.

Pazzaglia, F. and S.G. Wells 1989. Relative role of tectonism and climatic change on the evolution of Quaternary depositional landforms along a segmented range-front fault, Rio Grande Rift. *Geological Society of America Abstract with Programs* **21**, 269.

Peterson, F.F., J.B. Bell, A.R. Ramelli and R.I. Dorn 1992. Late Quaternary geomorphology and soils in Crater Flat, next to Yucca Mountain, southern Nevada, in preparation.

Péwé, T.L. 1983. The periglacial environment in North America during Wisconsin time. In *Late Quaternary environments of the United States*, Volume 1. *The late Pleistocene*, S.C. Porter (eds), 157–89. Minneapolis: University of Minnesota Press.

Phillips, F.M., M.G. Zreda, S.S. Smith, D. Elmore *et al.* 1990. A cosmogenic chlorine-36 chronology for glacial deposits at Bloody Canyon, eastern Sierra Nevada, California. *Science* **248**, 1529–32.

Ponti, D.J. 1985. The Quaternary alluvial sequence of the Antelope Valley, California. *Geological Society America Special Paper* **203**, 79–96.

Porter, S.C. 1979. Quaternary stratigraphy and chronology of Mauna Kea, Hawaii: a 380,000-yr record of mid-Pacific volcanism and ice-cap glaciation. *Bulletin of the Geological Society America, Part II* **90**, 980–1093.

Rachocki, A. 1981. *Alluvial fans. An attempt at an empirical approach*. Chichester: Wiley.

Reheis, M.C. 1987. Climatic implications of alternating clay and carbonate formation in semiarid soils of south-central Montana. *Quaternary Research* **27**, 270–82.

Rhoads, B.L. 1986. Flood hazard assessment for land-use planning near desert mountains. *Environmental Management* **10**, 97–106.

Rockwell, R.K., E.A. Keller and D.L. Johnson 1985. Tectonic geomorphology of alluvial fans and mountain fronts near Ventura, California. In *Tectonic geomorphology*, M. Morisawa and J.T. Hack (eds), 183–207. London: Allen & Unwin.

Ryder, J.M. 1971. Some aspects of the morphology of paraglacial alluvial fans in south-central British Columbia. *Canadian Journal of Earth Sciences* **8**, 1252–64.

Schaber, G.G., G.L. Berlin and W.E.J. Brown 1976. Variations in surface roughness within Death Valley, California: geologic evaluation of 25 cm wavelength radar images. *Bulletin of the Geological Society America* **87**, 29–41.

Schumm, S.A., M.P. Mosley and W.E. Weaver 1987. *Experimental fluvial geomorphology*. New York: Wiley.

Shlemon, R.J. 1978. Quaternary soil–geomorphic relationships, southeastern Mojave Desert, California and Arizona. In *Quaternary soils*, W.C. Mahaney (eds), 187–207. Norwich: GeoAbstracts.

Spaulding, W.G. 1985. Vegetation and climates of the last 45,000 years in the vicinity of the Nevada Test Site, south-central Nevada. *U.S. Geological Survey Professional Paper* 1329.

Spaulding, W.G. 1990. Vegetation and climatic development of the Mojave Desert: The last glacial maximum to the present. In *Packrat middens. the last 40,000 years of biotic change*, J.L. Betancourt, T.R. Van Devender and P.S. Martin (eds), 166–99. Tucson: University of Arizona Press.

Spaulding, W.G. and L.J. Graumlich 1986. The last pluvial climatic episodes in the deserts of southwestern North America. *Nature* **320**, 441–4.

Talbot, M.R. and M.A.J. Williams 1979. Cyclic alluvial fan sedimentation on the flanks of fixed dunes, Janjari, central Niger. *Catena* **6**, 43–62.

Trowbridge, A.C. 1911. The terrestrial deposits of Owens Valley, California. *Journal of Geology* **19**, 706–47.

Tuan, Y. 1962. Structure, climate and basin landforms in Arizona and New Mexico. *Annals of the Association American Geographers* **52**, 51–68.

Twidale, C.R. 1967. Hillslopes and pediments in the Flinders Range, South Australia. In *Landform studies from Australia and New Guinea*, J.N. Jennings and J.A. Mabbutt (eds), 95–117. Canberra: Australian National University Press.

Van Devender, T.R., R.S. Thompson and J.L. Betancourt

1987. Vegetation history of the deserts of southwestern North America; the nature and timing of the late Wisconsin–Holocene transition. In *North America and adjacent oceans during the last deglaciation*, W.F. Ruddiman and H.E.J. Wright (eds), 323–52. Boulder, CO: Geological Society America.

Wasson, R.J. 1977. Last-glacial alluvial fan sedimentation in the lower Derwent Valley, Tasmania. *Sedimentology* **24**, 781–99.

Weaver, W.E. 1984. Geomorphic thresholds and the evolution of alluvial fans. *Geological Society America Abstracts with Programs* **16**, 688.

Wells, L.E. 1987. An alluvial record of El-Nino events from northern coastal Peru. *Journal Geophysical Research* **92 (C13)**, 14 463–70.

Wells, P.V. 1983. Paleobiogeography of montane islands in the Great Basin since the last glaciopluvial. *Ecological Monographs* **53**, 341–82.

Wells, P.V. and D. Woodcock 1985. Full-glacial vegetation of Death Valley, California. Juniper woodland opening to *Yucca* semidesert. *Madrono* **32**, 11–23.

Wells, S.G., L.D. McFadden and J.C. Dohrenwend 1987. Influence of late Quaternary climatic changes on geomorphic and pedogenic processes on a desert piedmont, eastern Mojave Desert, California. *Quaternary Research* **27**, 130–46.

Wells, S.G., L.D. McFadden and J. Harden 1990. Preliminary results of age estimations and regional correlations of Quaternary alluvial fans within the Mojave Desert of Southern California. In *At the end of the Mojave: Quaternary studies in the eastern Mojave Desert*, R.E. Reynolds, S.G. Wells and R.J.I. Brady (eds), 45–53. Redlands: San Bernardino County Museum Association.

White, K. 1990. Spectral reflectance characteristics of rock varnish in arid areas. *School of Geography University of Oxford Research Paper* **46**, 1–38.

White, K. 1991. Geomorphological analysis of piedmont landforms in the Tunisian Southern Atlas using ground data and satellite imagery. *The Geographical Journal* **147**, 279–94.

Williams, G.E. 1973. Late Quaternary piedmont sedimentation, soil formation and paleoclimates in arid south Australia. *Zeitschrift für Geomorphologie* **17**, 102–25.

Wilson, M.C. 1990. Dating late Quaternary humid paleoclimatic episodes in the Sahel of West Africa from paleosol carbonate nodules. *Programme and Abstracts, First Joint Meeting, AMQUA and CANQUA, Waterloo, Canada*, 34.

GEOMORPHIC EVIDENCE OF CLIMATE CHANGE FROM DESERT-BASIN PALAEOLAKES

24

Dorothy Sack

INTRODUCTION

Hydrographically closed basins are numerous in arid regions largely for reasons related to climate (Langbein 1961). Whether desert basins originally formed by structural, volcanic, meteoritic, aeolian, fluvial, biologic, or other processes (Hutchinson 1957, Reeves 1968), they can generally be maintained for long periods if accumulation of surface water is insufficient in volume and duration to establish permanent overflow to externally drained fluvial systems. Other factors that can extend desert-basin longevity include high basin relief, continuance of depression-forming processes, and slow rates of sedimentation. As a result, closed desert basins are especially well developed in arid regions of active extensional tectonics, such as the Great Basin section of the Basin and Range physiographic province in western North America.

Surface-water accumulation insufficient for external drainage does not preclude formation of lakes in desert basins. Generally, large desert lakes are restricted to those few basins that have influent streams which either are exotic, as in the case of Salton Sea, California, or drain adjacent highlands, as in the case of Great Salt Lake, Utah (Fig. 24.1). Many other desert basins contain playa lakes or playas (Motts 1972, Mifflin and Wheat 1979, Smith and Street-Perrott 1983, Williams and Bedinger 1984). Desert water bodies of all kinds typically respond in a sensitive fashion to variations in effective moisture, as documented by historic records of changes in climate and lake size (Gilbert 1890, Peck and Richardson 1966, Arnow 1980).

Under sustained conditions of increasing effective moisture, desert-basin water bodies expand and eventually integrate with those in adjoining closed basins. As individual closed-basin lakes increase in area they decrease in number (Langbein 1961). Eventually they may attain open-basin status. Compared with their current hydrologic condition, many desert basins display geomorphic and stratigraphic evidence of having contained larger lakes, some with exterior drainage, during previous periods of greater effective moisture in the late Quaternary (Fig. 24.1) (Snyder *et al.* 1964, Mifflin and Wheat 1979, Williams and Bedinger 1984). These desert lake basins are storehouses of information regarding changes in the palaeohydrologic regime. This chapter focuses on the late Pleistocene palaeohydrologic evidence available from the geomorphic study of desert lake basins.

IMPORTANCE OF DESERT PALAEOLAKE STUDIES

Studies of palaeolake geomorphology, sedimentology, and stratigraphy contribute directly to each of those three individual fields (e.g. Gilbert 1890, Eardley 1938, Oviatt 1987). In addition, such studies are necessary for reconstructing lake-level chronologies, which have many applications. Age-controlled palaeolake shorelines and deposits are very useful for studying the nature, magnitude, and timing of geophysical and geomorphic phenomena in lake basins. For example, age control of major Lake Bonneville shorelines and deposits has enabled earth scientists to estimate relative ages of seismic events and to model isostatic compensation, isostatic response rate, upper mantle viscosity, and thickness

Geomorphology of Desert Environments. Edited by Athol D. Abrahams and Anthony J. Parsons. Published in 1994 by Chapman & Hall, London. ISBN 978-94-015-8256-8

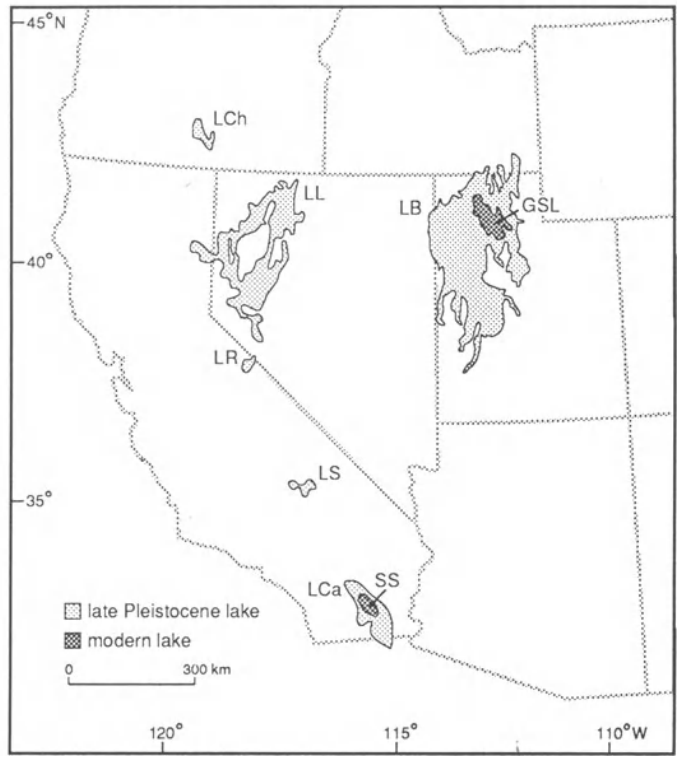

Figure 24.1 Location map of western North American late Pleistocene and modern lakes discussed in text. LB = Lake Bonneville, GSL = Great Salt Lake, SS = Salton Sea, LS = Lake Searles, LR = Lake Russell, LL = Lake Lahontan, LCh = Lake Chewaucan. The Salton Sea is shown in relation to Lake Cahuilla (LCa), which occupied that basin in the late Pleistocene.

of the lithosphere (Fig. 24.2) (Gilbert 1890, Crittenden 1963a, b, 1967, Walcott 1970, Passey 1981, Nakiboglu and Lambeck 1982, 1983, McCalpin 1986, Bills and May 1987, Personius 1988, Sack 1989). In addition, reliable lake-level chronologies play a vital role in reconstructing regional changes in effective moisture (e.g. Smith and Street-Perrott 1983, Benson *et al.* 1990), which in turn are affected by changes in palaeoclimatic variables. Each of these applications can only be as accurate as the reconstructed palaeolake chronology on which it is based.

Much scientific attention is currently directed toward constructing a theory of climate change (Flint 1974). Accurate modelling of future climate and the effects of human-induced perturbations of it may be crucial to providing sufficient food and water to regional subsets of the world's population. A large part of the data from which the explanatory theory of climate change is being constructed comes from the record of past climate change. An accurate history of past climates provides the observations which the successful theory of climate change must adequately explain (Gilbert 1886, Flint 1974).

Evidence relating to the climatic history of the Earth is stored in the geologic record. Sedimentary rocks, unconsolidated deposits, and ice provide palaeoenvironmental clues through their physical, chemical, isotopic, and biological components. For example, glacial till, saline playa deposits, oxygen-isotope ratios, and *in situ* fossils which have known climatic tolerance limits give some information on the palaeoclimate portion of the depositional environment. Age and duration of a palaeoenvironment are approximated with the various age-dating techniques appropriate to the material under investigation (e.g. Easterbrook 1988). Mapping the preserved areal extent of a sedimentary unit that represents a given palaeoenvironment provides data on the minimum spatial dimensions of that environment.

Accurate reconstruction of the climatic history of the Earth is complicated by several factors. The palaeoclimatic signal of the palaeoenvironmental evidence is usually not very specific. Evidence of a glaciation suggests cold conditions, but how cold? Interstratified playa and dune deposits imply arid

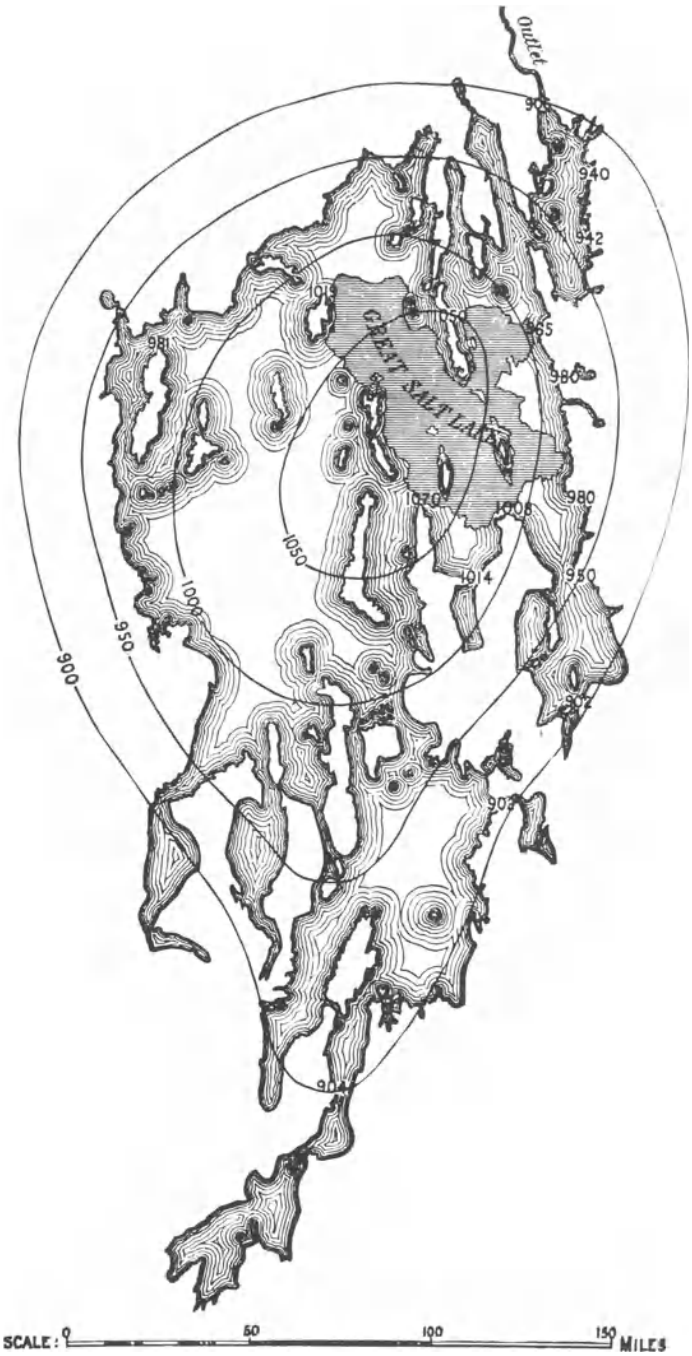

Figure 24.2 Theoretic curves of post-Bonneville deformation (Gilbert 1890 Plate L). The map depicts the general pattern of isostatic rebound of the highest shoreline of Lake Bonneville, which Gilbert named the Bonneville shoreline. Units are feet above Great Salt Lake. The location of Lake Bonneville is shown in Figure 24.1.

conditions, but how arid? Aquatic fossils directly reflect hydroenvironmental conditions which are only partially dependent on climate (Forester 1987). Alternatively, there are a few sources of palaeoenvironmental information, such as ice-wedge polygons, that do provide some definite climatic constraints (Washburn 1979). No doubt with continued study palaeoenvironmental researchers will improve the ability to glean specific climatic information from the palaeoenvironmental data. In the meantime, the focus of the palaeoclimatic signal can often be sharpened by combining multiple sources of palaeoenvironmental information (Street-Perrott and Harrison 1985).

Another difficulty in reconstructing palaeoclimate stems from the notion that the stratigraphic evidence produced by a change in climate may or may not depend strongly on what the climate was like before the change (Langbein and Schumm 1958, Hunt and Mabey 1966). For example, an increase in precipitation within an arid climate would probably result in greater erosion, but a precipitation increase within a moderately humid climate would result in decreased erosion (Langbein and Schumm 1958). On the other hand, a change from humid to semi-arid conditions would sufficiently reduce vegetation cover to allow an increase in sediment yield; sediment yield is also increased under a change from arid to semi-arid conditions (Langbein and Schumm 1958). Stratigraphic context is therefore very important in interpreting climate change from the sedimentary record.

Accurate reconstruction of the Earth's climatic history is further complicated by the facts that (a) multiple climatic environments exist on the Earth at any one time, (b) the geographic location of the sedimentary record for a climatic environment may change over geologic time, thereby divorcing it from its formative climate controls, and (c) palaeoenvironmental evidence from the sedimentary record is lost over time through disintegration, decomposition, reworking, diagenesis, and metamorphism. These complications are minimized by studying the most recent geological record, that of the Quaternary period. Within the Quaternary record, an enormous amount of palaeoenvironmental information is stored in desert palaeolake basins (Street-Perrott and Harrison 1985, Currey 1990).

PALAEOLAKE EVIDENCE OF CHANGES IN EFFECTIVE MOISTURE

GENERAL CONSIDERATIONS

Reconstructed palaeolake-level chronologies do not directly provide specific information on the magnitudes of palaeotemperature and palaeoprecipitation; instead, they indicate changes in effective moisture. Benson and Paillet (1989) argue that the lake-size attribute which responds most directly to variations in the hydrologic balance is total lake-surface area, rather than lake level or volume. It remains convenient, however, to portray fluctuations in palaeolake size in the manner established by the pioneers of palaeolake studies, I.C. Russell (1885) and G.K. Gilbert (1890), by plotting water-level elevation versus time (Fig. 24.3) (Morrison 1965, Scott *et al.* 1983, Spencer *et al.* 1984, Currey and Oviatt 1985, Benson and Paillet 1989, Benson *et al.* 1990). Moreover, for at least some lake basins, such as the Bonneville basin, lake level and surface area are linearly related (Currey and Oviatt 1985).

Numerous lines of evidence, including geomorphic, morphostratigraphic, and stratigraphic, are available and generally necessary for reconstructing the chronology of a desert-basin palaeolake (Fig. 24.4). Whether emphasis is placed on water-level elevation or surface area, the fluctuating size of a palaeolake is most directly recorded in its erosional and depositional shoreline geomorphic evidence, from which elevation and surface area may be derived (Figs 24.5 and 6) (Gilbert 1890, Currey 1982). Most well-developed coastal landforms are created by major water-level stillstands or oscillations. Such basin-margin geomorphic evidence for a particular stillstand or oscillation, however, may lack geochronometric control or may be obliterated by subsequent lacustrine or subaerial processes. Morphostratigraphy uses geomorphology and stratigraphy in conjunction in order to maximize the amount of information derived from assemblages of depositional landforms. From morphostratigraphic relationships found in exposures in basin-margin areas and locations transitional to the basin interior, the number and relative order of significant oscillations and stillstands can be interpreted (Scott *et al.* 1983, Currey and Oviatt 1985). The generally continuous sedimentary record of the basin interior may contain fossil, geochemical, isotopic, bedform, and other stratigraphic indicators of the hydrologic balance (Eardley *et al.* 1973, Spencer *et al.* 1984). In addition, temporal control from datable material and from tephrochronology is often easier to obtain there than at the shoreline. Unlike the geomorphic evidence from the shoreline, however, stratigraphic evidence from the basin interior does not provide a direct measure of lake size.

Some desert lake basins are more sensitive gauges of the palaeohydrologic balance than others. Desert lake basins in which groundwater accounts for a significant percentage of inflow or outflow may not

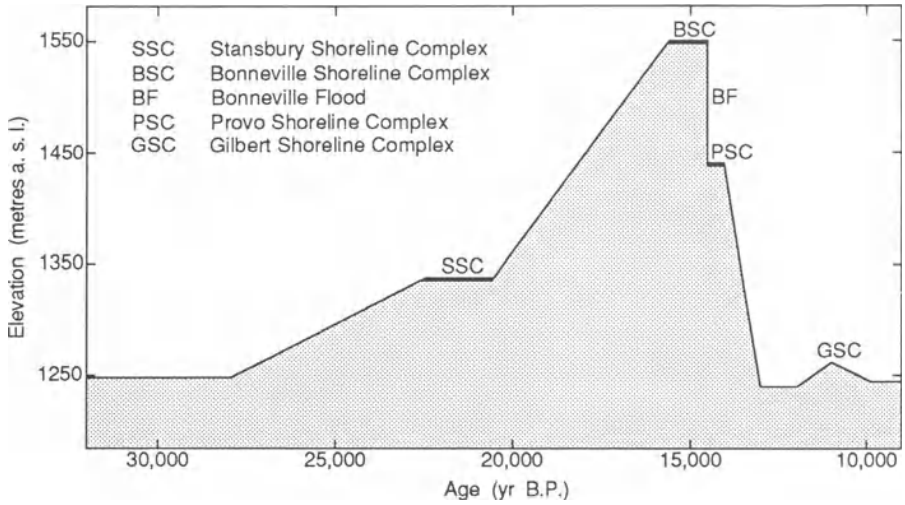

Figure 24.3 Schematic hydrograph of late Pleistocene Lake Bonneville showing its major lake levels (after Burr and Currey 1988).

have palaeolake-level chronologies that adequately reflect effective atmospheric moisture. For simplicity, the present discussion assumes palaeolakes of negligible groundwater transfer.

According to Street-Perrott and Harrison (1985), an amplifier lake is one that receives almost all of its input as surface runoff from the drainage basin, with only a small percentage of input derived from direct precipitation on to the lake. Moreover its output occurs mainly in the form of evaporation from the lake surface, rather than as surface overflow. Amplifier lakes that do not have exterior drainage are very sensitive to changes in the palaeohydrologic balance because short-term precipitation changes are amplified and cumulated. Street-Perrott and Harrison (1985) maintain that the best site to study palaeolakes is in basins of moderate steepness because the palaeolake shoreline record tends to be better preserved there than in basins of very steep relief and easier to interpret than in basins of low relief. Currey (1990) emphasizes that the fit between water-body morphometry and lake-basin morphometry is an important consideration in explaining the encoding and storing of the palaeolake record. Palaeohydrologic response is not adequately represented by the shoreline evidence for overfit stages – that is, when the water body achieves exterior drainage. Under threshold control the shoreline position is held approximately constant regardless of further increases in effective moisture. Likewise, palaeolake information is lost in underfit stages. Lacustrine processes are not recorded when water depths are below 2 to 4 m (Cowardin *et al.* 1979, Currey 1990) even if basin morphometry allows the shallow water body to occupy a large area. In summary, palaeohydrologic history is especially well documented by closed amplifier lakes contained in basins of moderate topographic relief (Street-Perrott and Harrison 1985) in which water-body morphometry is appropriate to – that is, fits – available basin morphometry at the lowest as well as the highest lake stages (Currey 1990).

GEOMORPHIC EVIDENCE OF PALAEOLAKE FLUCTUATIONS

The fundamental geomorphic evidence used to reconstruct palaeolake chronologies is shoreline evidence. Detailed mapping of principal lake levels is crucial in accurately determining the magnitude of changes in palaeolake surface area and elevation (Gilbert 1890, Currey *et al.* 1984a, Street-Perrott and Harrison 1985). Researchers use the ratio of lake surface area AL to basin tributary area AB, called the z ratio, as a quantitative index of the hydrologic response of a closed-basin lake to palaeoclimatic conditions (Snyder and Langbein 1962, Mifflin and Wheat 1979, Street-Perrott and Harrison 1985). Measurements of both variables are easy to obtain once the palaeodrainage basin and palaeolake level have been delineated.

Shoreline mapping involves intensive aerial

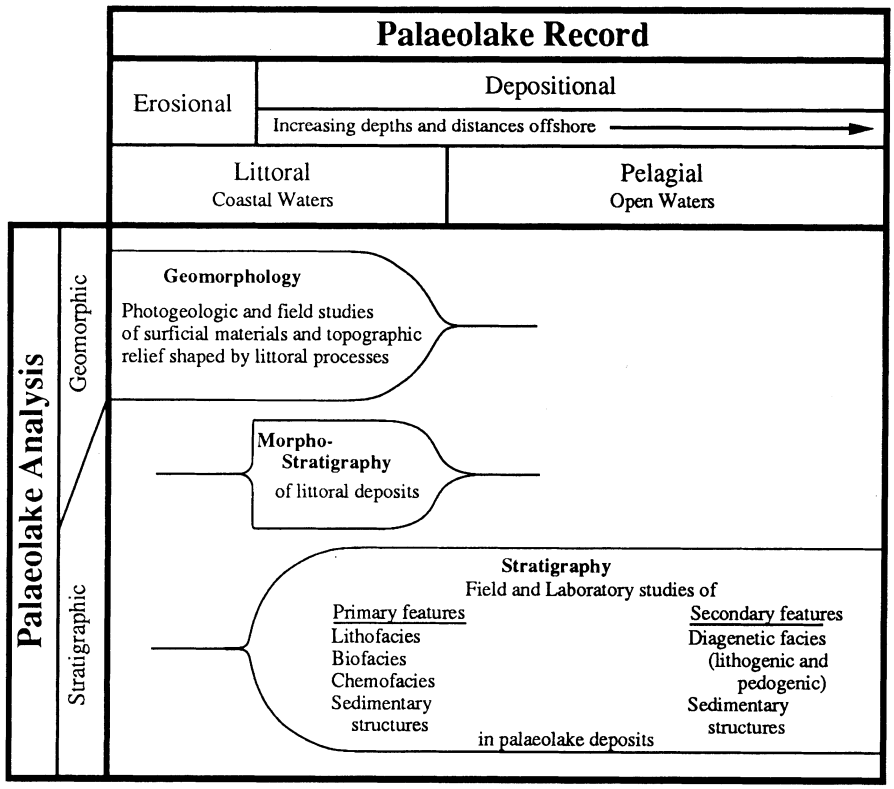

Figure 24.4 Diagram illustrating how geomorphology, morphostratigraphy, and stratigraphy are used in the study of the palaeolake record (Currey 1990, p. 200).

photograph interpretation and field study (Mifflin and Wheat 1979, Currey 1982, Sack 1990). It is facilitated by the quasi-horizontality of the evidence. Because of the sparse vegetative cover in desert lake basins, shoreline mapping is generally less difficult there than in humid areas. Mapping is hindered by alteration or obliteration of the shoreline evidence by later lacustrine processes or by post-lacustrine subaerial processes (Fig. 24.7). The close inspection of erosional and depositional coastal landforms on large- and intermediate-scale air photos that is required for mapping, aids in the recognition of stage-specific geomorphic signatures, which may reflect important components of the palaeolake's history (Sack 1990), and it helps in the identification of well-developed or well-exposed sites for field investigation.

Obtaining accurate measurements of shoreline elevation is an important component of shoreline mapping and of deciphering the palaeolake chronology. Measurements made at various points around a lake basin on a single palaeolake shoreline will show a range of modern elevations. Some of this variation is inherent in coastal geomorphic processes, such as the super-elevation of strongly developed coastal depositional features (Gilbert 1890, Currey 1982). Especially for large palaeolakes, this intrinsic variation in shoreline elevation is a small percentage of the maximum measured deviation (Currey 1982). The remainder is caused by isostatic and possibly neotectonic processes, which deform the shorelines from their original configuration (Fig. 24.2) (Gilbert 1890). Hydroisostatic rebound is caused by a decrease in water load and raises shorelines from their original positions by an amount dependent on the degree of unloading. The shallowest water, and therefore the smallest amount of unloading and rebound, will occur near the margin of a lake basin. The unrebounded elevation of a given palaeolake shoreline may be estimated from the lowest elevation found along that shoreline, provided tectonism has not affected the site.

Figure 24.5 The Provo shoreline of Lake Bonneville. This ground photograph provides an example of what the geomorphic evidence for palaeolakes can look like in what are now desert basins.

Other geomorphic characteristics of coastal landforms or landform assemblages provide clues to palaeolake history. Gilbert (1890) observed that size of lacustrine coastal depositional features depends on lake fetch, wind strength and duration, duration of the lake level, and sediment availability. Fetch and perhaps storm strength and duration increase with increasing lake area. Therefore, in Lake Bonneville, the existence of larger depositional features at the Provo shoreline than at the highest level, the Bonneville shoreline, led to the inference that the Provo shoreline lasted longer and had a greater supply of sediment than the Bonneville shoreline (Fig. 24.3) (Gilbert 1890, Currey 1980). Geomorphic characteristics may also provide clues to relative timing of a shoreline's formation. Shoreline deposits of calcium carbonate, such as tufa or ooids, seem to occur in greater concentrations at regressive-phase rather than transgressive-phase shorelines. Transgressive-phase shorelines of a major lake cycle may be larger than those of the regressive phase because transgressions are marked by maximum disequilibrium between form and process (Currey 1980). Because shoreline-forming stillstands and oscillations that occur with the regression impact topography already shaped by lacustrine processes, they have less geomorphic work to perform to bring the landscape into geomorphic equilibrium.

Geomorphic investigations are needed in order to distinguish those aspects of a palaeolake chronology that reflect hydrologic conditions from those that reflect hydrographic conditions. Thus far, this discussion has treated all fluctuations in palaeolake levels as though they were caused by climatically induced changes in effective moisture. Lake level, however, can also be affected by basin geomorphic considerations.

Outlet dynamics will affect the water level. The stabilizing effect of external drainage on lake level has already been noted. If exterior drainage is not recognized, the threshold-controlled shoreline will be attributed to a prolonged stability in effective moisture, which likely did not occur. Conversely, positive or negative changes in outlet elevation due to volcanism, tectonism, fluvial erosion, or mass movement can cause lake level to rise or fall without climate change. For example, the geomorphic event of threshold failure, and not a climatic event, caused Lake Bonneville to drop 104 m from the Bonneville to the Provo shoreline probably in less than a year

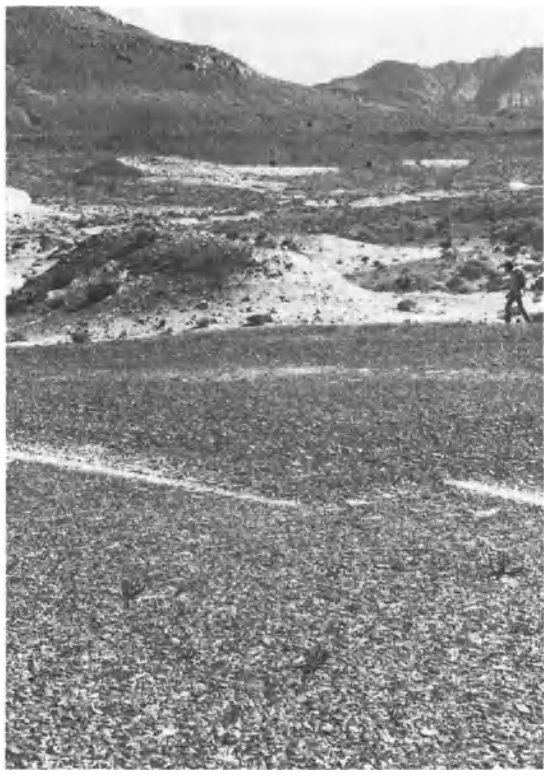

Figure 24.6 Lake Bonneville coastal and deeper water deposits. The photograph shows transgressive-phase coastal gravel in the foreground overlain by pelagic white marl. The Provo shoreline can be seen in the background.

(Fig. 24.3) (Gilbert 1890, Jarrett and Malde 1987, Burr and Currey 1988).

Isostatic effects produce changes of shoreline position that might be misinterpreted as climatic responses. The Bonneville shoreline of Lake Bonneville was formed as a result of an extended period of threshold control (Fig. 24.3). While at the Bonneville level, hydroisostatic loading caused the central portion of the large lake basin to subside relative to the outlet (Currey 1980, Currey *et al.* 1983, Burr and Currey 1988). As a result, in basin interior locations the lake underwent apparent transgressions as the water plane impinged on relatively higher portions of the landscape. These apparent transgressions appear in the morphostratigraphic record of the Bonneville shoreline zone (Fig. 24.8). A complicating factor in this example arises from the possible occurrence of a climatically induced, 45-m amplitude oscillation during the latter part of the Bonneville shoreline interval (Currey *et al.* 1983, 1984b, Oviatt 1984, Currey and Oviatt 1985, Burr and Currey 1988). Use of the term Bonneville shoreline complex is encouraged in order to emphasize the fact that the highest Lake Bonneville shoreline consists of several distinct geomorphic components, some of which are climatically induced and some of which are not (Currey *et al.* 1983, Burr and Currey 1988).

Sub-basin dynamics can play an important role in controlling palaeolake levels (Benson 1978, Benson and Mifflin 1985, Benson and Paillet 1989). Many palaeolakes, including for example Lakes Bonneville, Lahontan, and Chewaucan in western North America (Fig. 24.1), consisted of a collection of sub-basins separated from each other by interior thresholds (Fig. 24.9) (Eardley *et al.* 1957, Allison 1982, Benson and Thompson 1987). Each sub-basin was integrated with the main palaeolake for a different amount of time. Some sub-basins contained isolated, independent palaeolakes before and after their integration period (Currey 1980, Allison 1982, Sack 1990). During the transgressive phase of a lake cycle, the water level in one sub-basin will rise faster than in the others. When it reaches the elevation of the lowest interior threshold it will flow over that divide into the adjoining closed sub-basin. Unless there is significant erosion or slope failure at the interior threshold, the water level in the first sub-basin will be held approximately constant while the water level in the second sub-basin rises. A shoreline may form in the first sub-basin as the result of the stillstand, whereas the water level may rise too quickly in the second sub-basin to leave shoreline evidence (Sack 1990). The water level in the two sub-basins will eventually equilibrate. The sub-basin nature of a palaeolake must be thoroughly investigated so that stillstands and rapid rises in lake level caused by sub-basin dynamics are not given climatic interpretations. Large palaeolake basins, such as Lakes Bonneville and Lahontan, may have numerous sub-basins and complex sub-basin dynamics.

Drainage-basin dynamics can affect geomorphically induced fluctuations in palaeolake level. Geomorphic changes in the drainage basin area that can affect discharge may result from tectonism, volcanism, mass movement, or stream capture. Redirection of a major tributary into or out of the palaeolake's drainage basin may influence lake level without a change in climate and will alter the degree to which the lake responds to variations in effective moisture. The Bear River has been a principal tributary to Lake Bonneville and its Holocene remnant, Great Salt Lake, Utah, at least since the start of the Bonneville lake cycle more than 25 000 years ago (Bright 1963, Currey and Oviatt 1985, McCoy 1987). The latest

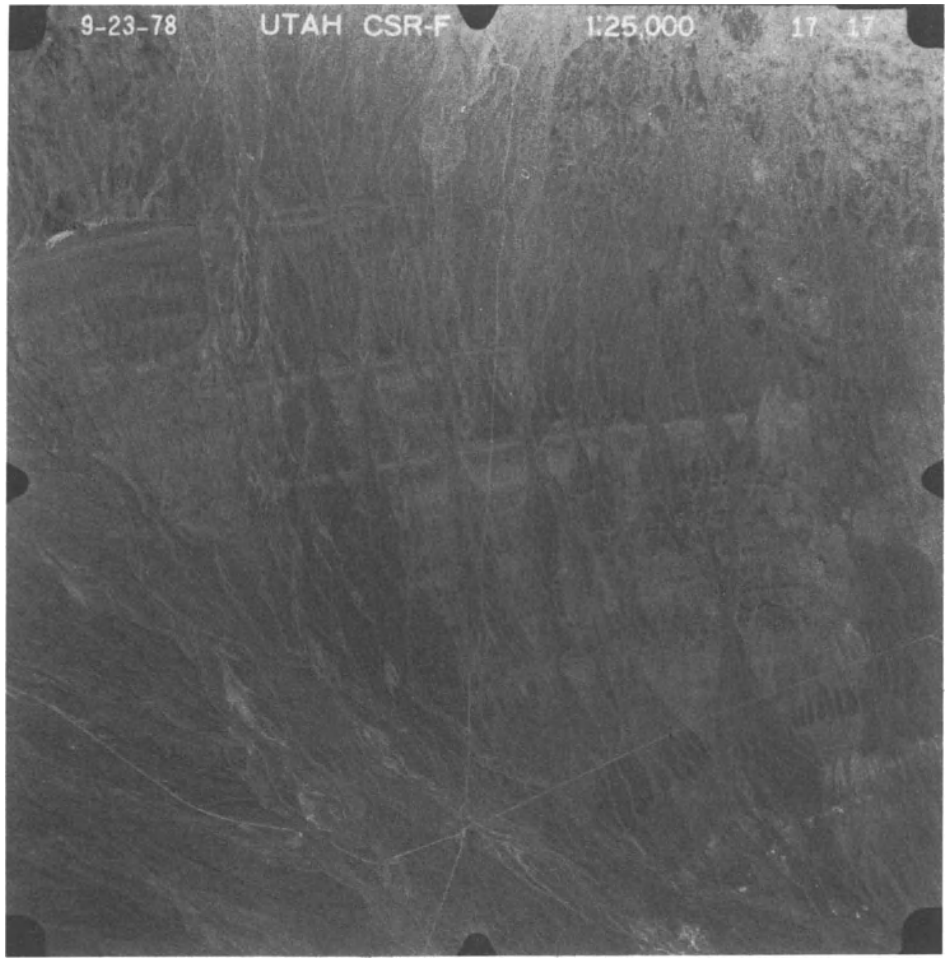

Figure 24.7 Vertical aerial photograph of Lake Bonneville shorelines (CSR-F 17-17). This photograph shows several shorelines which have been only partially obliterated by post-lacustrine subaerial processes.

deep-lake cycle in the Bonneville basin, the Bonneville lake cycle, lasted from approximately 28 000 to 13 000 years BP and occurred during marine oxygen-isotope stage 2 (Currey 1990). The penultimate Bonneville-basin deep-lake cycle, the Little Valley cycle, occurred late in marine oxygen-isotope stage 6, probably between about 150 000 and 90 000 years BP (Scott *et al.* 1983). According to deep-sea core data, the climatic minimum of isotope stage 6 may have been slightly more severe than that of isotope stage 2 (Shackleton and Opdyke 1973). Nevertheless, Lake Bonneville attained 1552 m elevation (Currey 1982) and exterior threshold control, whereas the highest exposure of the Little Valley cycle water body is approximately 1510 m (McCoy 1987). The large disparity in water level between these two Bonneville-basin lake cycles may be explained by the Bear River being tributary to Lake Bonneville but not to the Little Valley cycle lake (McCoy 1987).

NON-GEOMORPHIC EVIDENCE OF PALAEOLAKE FLUCTUATIONS

Geomorphology is a principal source of information concerning palaeolake fluctuations. That information, however, has its limitations. The geomorphic record is naturally weak for small palaeolakes, can consist of negative evidence for rapid changes in lake level, may be reworked by later water-level oscillations, and becomes increasingly obliterated by subaerial processes with increasing age (Gilbert 1890). Fortunately, other sources of palaeolake in-

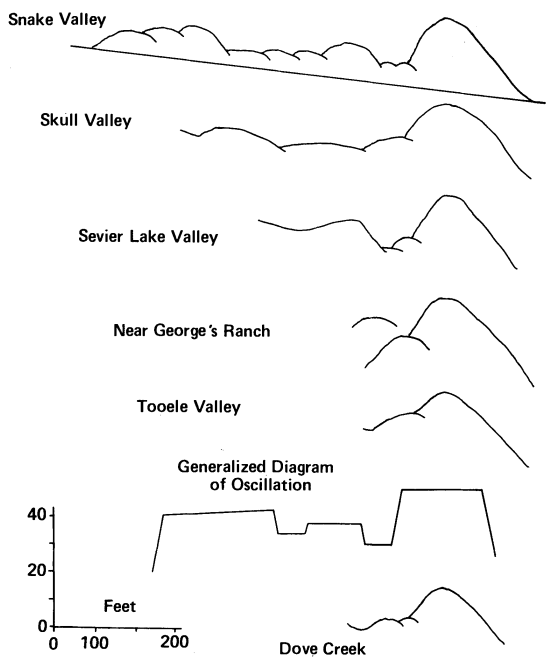

Figure 24.8 Profiles of barriers from the Bonneville shoreline complex (after Gilbert 1890, Plate XI) (Burr 1989, p. 11).

formation exist that can be combined with the geomorphic evidence to provide maximum resolution of a palaeolake chronology.

The basin-interior stratigraphic record does not provide specific measurements of lake size but has the advantage of potentially containing a continuous record of sedimentation that spans the entire lake cycle. Basin-interior evidence for palaeolake fluctuations is derived from core stratigraphy. Inferences concerning relative lake levels are made on the basis of core sedimentology, geochemistry, mineralogy, palaeontology, and palynology (Smith *et al.* 1983, Spencer *et al.* 1984). For example, within a Great Salt Lake core, the association of brine shrimp pellets and egg capsules with ripple laminae suggests the occurrence of a brine lake close to wave base, whereas freshwater ostracods, non-magnesium calcite, and light oxygen isotopes indicate deeper, fresher, and less evaporative conditions (Spencer *et al.* 1984). Temporal control attained for the core record from datable material and tephrochronology provides the basis for correlation between the basin-interior stratigraphic and basin-margin geomorphic evidence.

Morpho-stratigraphy combines information from the form of a feature with information concerning its internal composition to make inferences about the nature and timing of a depositional event. Morpho-stratigraphic techniques require sufficient stratigraphic exposure for the form of a depositional unit to be deduced. This is generally available to some degree for at least the larger late Quaternary desert-basin palaeolakes. In palaeolake studies, morpho-stratigraphy offers the advantages of both the direct link to lake size provided by geomorphology and the detailed sources of palaeoenvironmental information provided by stratigraphy.

Certainly palaeolake evidence is not the only source of palaeoenvironmental evidence in desert lake basins. The palaeolake data can be supplemented with whatever sources of information occur within the drainage basin (Street-Perrott and Harrison 1985). Examples of these other sources of palaeoenvironmental evidence include archaeology, periglacial phenomena, glaciers, bogs, streams, dunes, springs, pack-rat middens, and caves.

PALAEOCLIMATIC RECONSTRUCTIONS

Even after a palaeolake chronology has been reliably reconstructed and the influence of geomorphically induced hydrographic versus climatically induced hydrologic water-level changes has been identified, it is still difficult to deduce specific palaeoclimatic variables from the palaeohydrologic record. Assuming that only climatic influences were acting in a given palaeolake, a lake-level rise could be due to many factors including increased average annual precipitation, decreased average annual evapotranspiration, increased cool season precipitation, decreased warm season evapotranspiration, or combined changes in precipitation and evapotranspiration on an average annual or seasonal basis. Because an increase in precipitation would likely result in more vegetation, an increase in evapotranspiration would probably accompany a precipitation increase (Mifflin and Wheat 1979). Combined changes in both precipitation and evapotranspiration are most likely.

A link between the geomorphic evidence of lake size and specific climatic variables is found in the z ratio (Snyder and Langbein 1962, Mifflin and Wheat 1979, Street-Perrott and Harrison 1985), which was introduced previously as

$$z = AL/AB \qquad (24.1)$$

For a closed-basin lake which has insignificant groundwater transfer and in which annual input

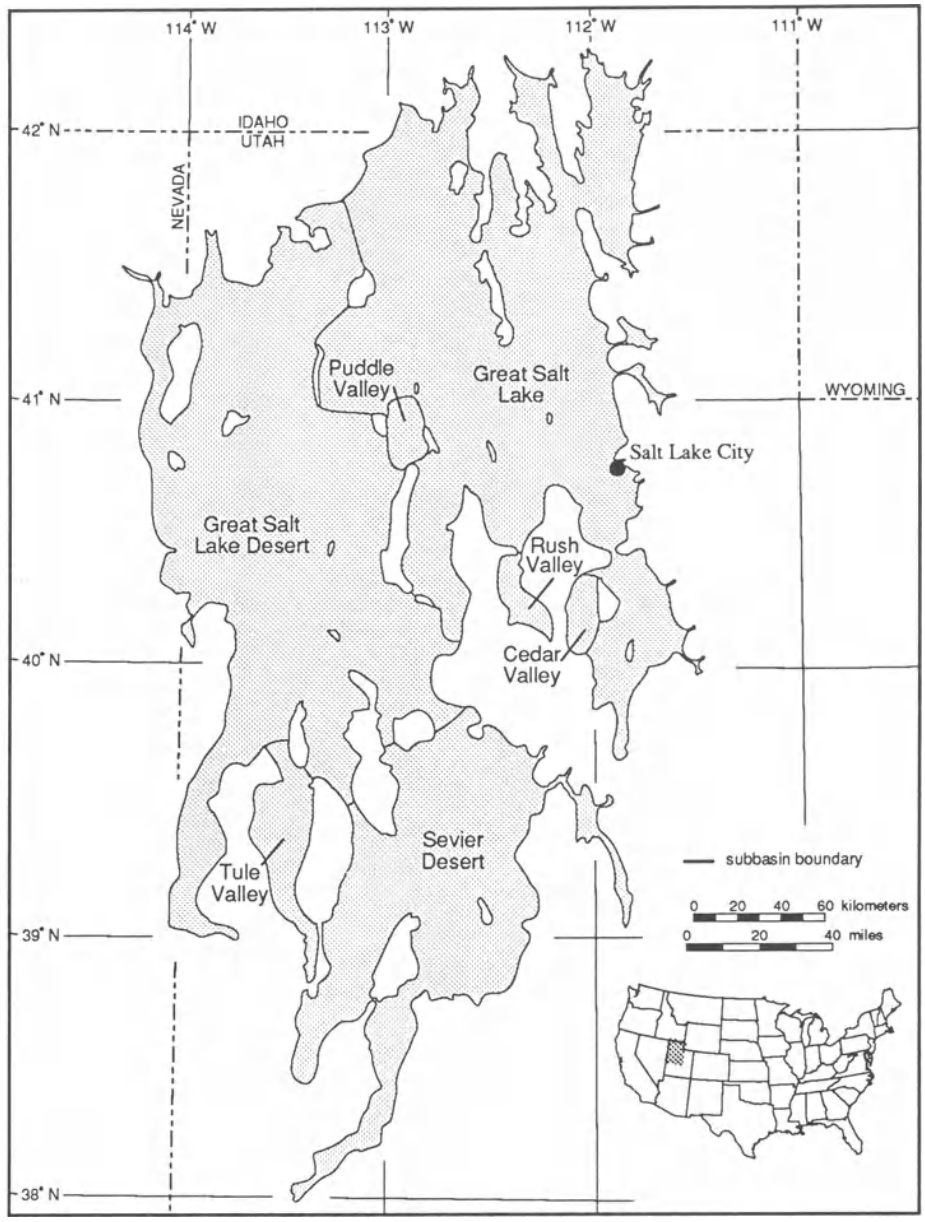

Figure 24.9 Major sub-basins of Lake Bonneville.

equals annual output, the water balance is represented by the equation

$$R + AL.PL = AL.EL \qquad (24.2)$$

where R is tributary runoff into the lake from the drainage basin, AL is area of the lake, PL is precipitation on to the lake, and EL is evaporation from the lake. Moreover, tributary runoff can be expressed in terms of drainage basin precipitation and evaporation:

$$R = AB(PB - EB) \qquad (24.3)$$

where AB is area of drainage basin tributary to the lake (excluding AL), PB is precipitation over the tributary drainage basin, and EB is evapotranspiration from the tributary drainage basin. By substitut-

ing for R, equation (24.2) becomes

$$AB(PB - EB) + AL(PL) = AL(EL) \quad (24.4a)$$

$$AB(PB - EB) = AL(EL - PL) \quad (24.4b)$$

$$AL/AB = (PB - EB)/(EL - PL) \quad (24.4c)$$

Therefore

$$z = AL/AB = (PB - EB)/(EL - PL) \quad (24.5)$$

Through the z ratio, the geomorphic evidence of lake area and basin area is related directly to the palaeoclimatic variables of precipitation and evaporation (Snyder and Langbein 1962, Mifflin and Wheat 1979, Street-Perrott and Harrison 1985). Variables AL and AB can be reconstructed from relict shoreline evidence of late Pleistocene palaeolakes, but determining values for the climatic variables is more difficult. Researchers have used modern relationships between mean annual temperature and precipitation to derive regional estimates of palaeoprecipitation for given palaeotemperatures (Mifflin and Wheat 1979). Palaeorunoff is then approximated from these estimates of palaeotemperature and palaeoprecipitation and also by use of modern empirical relationships among these variables (Langbein *et al.* 1949, Schumm 1965, Mifflin and Wheat 1979). Likewise, estimates of evaporation from a palaeolake are derived from recent data relating lake evaporation, altitude, and latitude (Mifflin and Wheat 1979). Iterations can be used until the z ratio calculated from the climatic variables approaches the z ratio attained from the geomorphic data, although more than one combination of values may be identified. Nevertheless, in this way, valuable estimates of palaeoclimatic variables can be made. For example, Mifflin and Wheat (1979) suggested that, compared with present values, the late Pleistocene palaeolakes in Nevada could have been maintained by a 5°F (2.8°C) lower mean annual temperature, 68% greater mean annual precipitation, and 10% lower mean annual lake evaporation.

Any discrepancies between geomorphically derived values of the z ratio and values derived by estimating palaeoclimatic variables may be due to (a) errors in determining AL and AB, (b) imprecision in the relationships established for modern data, or (c) the possibly incorrect assumption that the relationships among the palaeoclimatic variables can be adequately modelled by the relationships among the modern climatic variables (Mifflin and Wheat 1979, Benson and Thompson 1987). The first type of error can be avoided by careful mapping and fieldwork and by employing in calculations only those lake basins that have well-preserved geomorphic evidence which can be mapped with a high degree of confidence. In this regard, late Quaternary palaeolake basins in arid regions probably have the greatest potential. The second source of error will no doubt be minimized as geomorphologists and climatologists continue to investigate the modern empirical relationships among the relevant climatic and hydrologic variables. Validity of the assumption that the empirical relationships remain uniform over time can be checked by comparing palaeoclimatic inferences drawn from palaeolake data with inferences drawn from other sources of palaeoenvironmental evidence.

Potential error in reconstructing palaeoclimatic variables from palaeolake data may be minimized by using information from many basins to investigate regional or larger-scale trends instead of focusing on a single basin. Mifflin and Wheat's (1979) conclusions regarding the late Pleistocene climate of Nevada are based on their comparisons of geomorphically derived z ratios (equation 24.1) with climatically derived z ratios, for which they employed average regional values. Street and Grove (1979) and Street-Perrott and Harrison (1985) used data on numerous palaeolakes from all over the world. They employed a scheme of relative lake-level chronology, in which each lake's level over time was denoted only as high, intermediate, and low. Global maps showing the spatial patterns of relative lake size for various times in the late Quaternary led the researchers to inferences regarding changes in atmospheric circulation. Benson *et al.* (1990) studied four widely spaced late Quaternary palaeolakes in the Great Basin of western North America. Before comparing lake sizes, they normalized the data by dividing the maximum surface area of each palaeolake by its mean historical, reconstructed surface area (MHRSA) (Benson and Paillet 1989, Benson *et al.* 1990). In this way, they found that in the late Pleistocene, the two large northern lakes, Bonneville and Lahontan, had been ten times larger than their MHRSA values, whereas Lakes Russell and Searles had been only four to six times larger than their MHRSA values (Fig. 24.1). Benson *et al.* (1990) hypothesized that these observed differences may be explained by the position of the jetstream or by lake-effect precipitation impacting Lakes Bonneville and Lahontan.

Although specific values of palaeotemperature and palaeoprecipitation cannot yet be determined with certainty from the palaeohydrologic evidence of desert-basin palaeolakes, reasonable regional estimates have been made (e.g. Broecker and Orr 1958, Snyder and Langbein 1962, Mifflin and Wheat 1979).

In addition, regional and global patterns of palaeolake-level change have led to inferences regarding the atmospheric circulation of the past (e.g. Street and Grove 1979, Street-Perrott and Harrison 1985, Benson *et al.* 1990). Confidence in palaeoclimate estimates will improve as the modern empirical relationships among temperature, precipitation, evaporation, transpiration, and runoff are refined, assuming that these relationships are uniform over time. As the palaeoclimatic record is more accurately reconstructed, it will, in turn, contribute to predicting future climate. Geomorphic studies of desert-basin palaeolakes are an integral part of constructing a general theory of climate change because they provide field-based observations of past climate which the successful theory of climate change must adequately postdict. Maximum palaeoclimatic information for a region is derived by considering all sources of palaeoenvironmental evidence from a multidisciplinary perspective, but the desert-basin palaeolake evidence is a very important part of the palaeoenvironmental record.

REFERENCES

Allison, I.S. 1982. Geology of pluvial Lake Chewaucan, Lake County, Oregon. *Oregon State University Studies in Geology*, No. 11.

Arnow, T. 1980. Water budget and water-surface fluctuations of Great Salt Lake. *Utah Geological and Mineral Survey Bulletin* **116**, 255–63.

Benson, L.V. 1978. Fluctuation in the level of pluvial Lake Lahontan during the last 40,000 years. *Quaternary Research* **9**, 300–18.

Benson, L.V. and M.M. Mifflin 1985. Reconnaissance bathymetry of basins occupied by Pleistocene Lake Lahontan, Nevada and California. *U.S. Geological Survey Water-Resources Investigations Report* 85-4262.

Benson, L.V. and F.L. Paillet 1989. The use of total lake-surface area as an indicator of climatic change: examples from the Lahontan Basin. *Quaternary Research* **32**, 262–75.

Benson, L.V. and R.S. Thompson 1987. Lake-level variation in the Lahontan basin for the past 50,000 years. *Quaternary Research* **28**, 69–85.

Benson, L.V., D.R. Currey, R.I. Dorn, K.R. Lajoie, *et al.* 1990. Chronology of expansion and contraction of four Great Basin lake systems during the past 35,000 years. *Palaeogeography, Palaeoclimatology, Palaeoecology* **78**, 241–86.

Bills, B.G. and G.M. May 1987. Lake Bonneville – constraints on lithospheric thickness and upper mantle viscosity from isostatic warping of Bonneville, Provo, and Gilbert stage shorelines. *Journal of Geophysical Research* **92 (B11)**, 11493–508.

Bright, R.C. 1963. Pleistocene Lakes Thatcher and Bonneville southeastern Idaho. Ph.D. dissertation, University of Minnesota.

Broecker, W.S. and P.C. Orr 1958. Radiocarbon chronology of Lake Lahontan and Lake Bonneville. *Bulletin of the Geological Society of America* **69**, 1009–32.

Burr, T.N. 1989. Hydrographic isostatic modelling of threshold-controlled shorelines of Lake Bonneville. M.S. thesis, University of Utah.

Burr, T.N. and D.R. Currey 1988. The Stockton Bar. *Utah Geological and Mineral Survey Miscellaneous Publication* 88-1, 66–73.

Cowardin, L.M., V. Carter, F.C. Golet and E.T. LaRoe 1979. Classification of wetlands and deepwater habitats of the United States. *U.S. Fish and Wildlife Service* FWS/OBS-79/31.

Crittenden, M.D., Jr 1963a. Effective viscosity of the earth derived from isostatic loading of Pleistocene Lake Bonneville. *Journal of Geophysical Research* **68**, 5517–30.

Crittenden, M.D., Jr 1963b. New data on the isostatic deformation of Lake Bonneville. *U.S. Geological Survey Professional Paper* 454-E.

Crittenden, M.D., Jr 1967. Viscosity and finite strength of the mantle as determined from water and ice loads. *Geophysical Journal of the Royal Astronomical Society* **14**, 261–79.

Currey, D.R. 1980. Coastal geomorphology of Great Salt Lake and vicinity. *Utah Geological and Mineral Survey Bulletin* 116, 69–82.

Currey, D.R. 1982. Lake Bonneville: selected features of relevance to neotectonic analysis. *U.S. Geological Survey Open-File Report* 82-1070.

Currey, D.R. 1990. Quaternary palaeolakes in the evolution of semidesert basins, with special emphasis on Lake Bonneville and the Great Basin, U.S.A. *Palaeogeography, Palaeoclimatology, Palaeoecology* **76**, 189–214.

Currey, D.R. and C.G. Oviatt 1985. Durations, average rates, and probable causes of Lake Bonneville expansions, stillstands, and contractions during the last deep-lake cycle, 32,000 to 10,000 years ago. In *Problems of and prospects for predicting Great Salt Lake levels*, P.A. Kay and H.F. Diaz (eds), 9–24. Salt Lake City: University of Utah Center for Public Affairs and Administration.

Currey, D.R., C.G. Oviatt and G.B. Plyler 1983. Lake Bonneville stratigraphy, geomorphology, and isostatic deformation in west-central Utah. *Utah Geological and Mineral Survey Special Studies* **62**, 63–82.

Currey, D.R., G. Atwood and D.R. Mabey 1984a. Major levels of Great Salt Lake and Lake Bonneville. *Utah Geological and Mineral Survey Map* 73.

Currey, D.R., C.G. Oviatt and J.E. Czarnomski 1984b. Late Quaternary geology of Lake Bonneville and Lake Waring. *Utah Geological Association Publication* **13**, 227–37.

Eardley, A.J. 1938. Sediments of Great Salt Lake, Utah. *American Association of Petroleum Geologists Bulletin* **22**, 1305–411.

Eardley, A.J., V. Gvosdetsky and R.E. Marsell 1957. Hydrology of Lake Bonneville and sediments and soils of its basin. *Bulletin of the Geological Society of America* **68**, 1141–201.

Eardley, A.J., R.T. Shuey, V.M. Gvosdetsky, W.P. Nash, *et*

al. 1973. Lake cycles in the Bonneville basin, Utah. *Bulletin of the Geological Society of America* **84**, 211–6.

Easterbrook, D.J. (ed.) 1988. Dating Quaternary sediments. *Geological Society of America Special Paper* 227.

Flint, R.F. 1974. Three theories in time. *Quaternary Research* **4**, 1–8.

Forester, R.M. 1987. Late Quaternary paleoclimate records from lacustrine ostracodes. In *North America and adjacent oceans during the last deglaciation, The geology of North America*, Volume K-3, W.F. Ruddiman and H.E. Wright, Jr (eds), 261–76. Boulder, CO: Geological Society of America.

Gilbert, G.K. 1886. The inculcation of scientific method by example, with an illustration drawn from the Quaternary geology of Utah. *American Journal of Science* **31**, 284–99.

Gilbert, G.K. 1890. Lake Bonneville. *U.S. Geological Survey Monograph* 1.

Hunt, C.B. and D.R. Mabey 1966. Stratigraphy and structure, Death Valley, California. *U.S. Geological Survey Professional Paper* 494-A.

Hutchinson, G.E. 1957. *A treatise on limnology*, volume 1. *Geography, physics, and chemistry*. New York: Wiley.

Jarrett, R.D. and H.E. Malde 1987. Paleodischarge of the late Pleistocene Bonneville Flood, Snake River, Idaho, computed from new evidence. *Bulletin of the Geological Society of America* **99**, 127–34.

Langbein, W.B. 1961. Salinity and hydrology of closed lakes. *U.S. Geological Survey Professional Paper* 412.

Langbein, W.B. and S.A. Schumm 1958. Yield of sediment in relation to mean annual precipitation. *Transactions of the American Geophysical Union* **39**, 1076–84.

Langbein, W.B. *et al.* 1949. Annual runoff in the United States. *U.S. Geological Survey Circular* 52.

McCalpin, J. 1986. Thermoluminescence (TL) dating in seismic hazard evaluations – an example from the Bonneville basin, Utah. *Proceedings of the 22nd Symposium on Engineering Geology and Soils Engineering*, 156–76.

McCoy, W.D. 1987. Quaternary aminostratigraphy of the Bonneville basin, western United States. *Bulletin of the Geological Society of America* **98**, 99–112.

Mifflin, M.D. and M.M. Wheat 1979. Pluvial lakes and estimated pluvial climates of Nevada. *Nevada Bureau of Mines and Geology Bulletin* 94.

Morrison, R.B. 1965. New evidence on Lake Bonneville stratigraphy and history from southern Promontory Point, Utah. *U.S. Geological Survey Professional Paper* 525-C.

Motts, W.S. 1972. Some hydrologic and geologic processes influencing playa development in western United States. In *Playa Lake Symposium*, C.C. Reeves, Jr (ed.), 89–106. Lubbock: International Center for Arid and Semi-Arid Land Studies.

Nakiboglu, S.M. and K. Lambeck 1982. A study of the earth's response to surface loading with application to Lake Bonneville. *Geophysical Journal of the Royal Astronomical Society* **70**, 577–620.

Nakiboglu, S.M. and K. Lambeck 1983. A reevaluation of the isostatic rebound of Lake Bonneville. *Journal of Geophysical Research* **88**, 10439–47.

Oviatt, C.G. 1984. Lake Bonneville stratigraphy at the Old River Bed and Leamington, Utah. Ph.D. dissertation, University of Utah.

Oviatt, C.G. 1987. Lake Bonneville stratigraphy at the Old River Bed, Utah. *American Journal of Science* **287**, 383–98.

Passey, Q.R. 1981. Upper mantle viscosity derived from the difference in rebound of the Provo and Bonneville shorelines: Lake Bonneville basin, Utah. *Journal of Geophysical Research* **86**, 11701–8.

Peck, E.L. and E.A. Richardson 1966. Hydrology and climatology of Great Salt Lake. *Guidebook to the geology of Utah* 20, 121–34.

Personius, S.F. 1988. A brief summary of the surficial geology along the Brigham City segment of the Wasatch fault zone, Utah. *Utah Geological and Mineral Survey Miscellaneous Publication* 88-1, 27–32.

Reeves, C.C., Jr 1968. *Introduction to paleolimnology*. New York: Elsevier.

Russell, I.C. 1885. Geologic history of Lake Lahontan. *U.S. Geological Survey Monograph* 11.

Sack, D. 1989. Reconstructing the chronology of Lake Bonneville: a historical review. In *The history of geomorphology*, K.J. Tinkler (ed.), 223–56. London: Unwin Hyman.

Sack, D. 1990. Quaternary geology of Tule Valley, west-central Utah. *Utah Geological and Mineral Survey Map* 124.

Schumm, S.A. 1965. Quaternary paleohydrology. In *The Quaternary of the United States*, H.E. Wright, Jr and D.G. Frey (eds), 783–94. Princeton, NJ: Princeton University Press.

Scott, W.E., W.D. McCoy, R.R. Shroba and M. Rubin 1983. Reinterpretation of the exposed record of the last two cycles of Lake Bonneville, western United States. *Quaternary Research* **20**, 261–85.

Shackleton, N.J. and N.D. Opdyke 1973. Oxygen isotope and palaeomagnetic stratigraphy of Equatorial Pacific core V28–238: oxygen isotope temperature and ice volumes on a 10^{-5} to 10^{-6} year scale. *Quaternary Research* **3**, 39–52.

Smith, G.I. and F.A. Street-Perrott 1983. Pluvial lakes of the western United States. In *Late-Quaternary environments of the United States*, Volume 1. *The Late Pleistocene*, S.C. Porter (ed.), 190–212. Minneapolis: University of Minnesota Press.

Smith, G.I., V.J. Barczak, G.F. Moulton and J.C. Liddicoat 1983. Core KM-3, a surface-to-bedrock record of Late Cenozoic sedimentation in Searles Valley, California. *U.S. Geological Survey Professional Paper* 1256.

Snyder, C.T. and W.B. Langbein 1962. The Pleistocene lake in Spring Valley, Nevada, and its climatic implications. *Journal of Geophysical Research* **67**, 2385–94.

Snyder, C.T., G. Hardman and F.F. Zdenek 1964. Pleistocene lakes in the Great Basin. *U.S. Geological Survey Miscellaneous Geologic Investigations Map* I-416.

Spencer, R.J., M.J. Baedecker, H.P. Eugster, R.M. Forester, *et al.* 1984. Great Salt Lake, and precursors, Utah, the last 30,000 years. *Contributions to Mineralogy and Petrology* **86**, 321–34.

Street, F.A. and A.T. Grove 1979. Global maps of lake-level fluctuations since 30,000 yr B.P. *Quaternary Research* **12**, 83–118.

Street-Perrott, F.A. and S.P. Harrison 1985. Lake levels and climate reconstruction. In *Paleoclimate analysis and model-*

ing, A.D. Hecht (ed.), 291–340. New York: Wiley.
Walcott, R.I. 1970. Flexural rigidity, thickness, and viscosity of the lithosphere. *Journal of Geophysical Research* **75**, 3941–54.
Washburn, A.L. 1979. Permafrost features as evidence of climatic change. *Earth-Science Reviews* **15**, 327–402.
Williams, T.R. and M.S. Bedinger 1984. Selected geologic and hydrologic characteristics of the Basin and Range province, western United States. *U.S. Geological Survey Miscellaneous Investigations Map* I-1522-D.

PALAEOCLIMATIC INTERPRETATIONS FROM DESERT DUNES AND SEDIMENTS

25

Vatche P. Tchakerian

INTRODUCTION

During the Quaternary, the world's major deserts experienced dramatic changes in the nature and frequency of aeolian processes. Most ergs (sand seas) reveal evidence of repeated phases of dune formation. This paper presents a review of dune-building episodes during late Quaternary time and their palaeoclimatic significance. The emphasis of the paper is on African and North American sand seas. Although beyond the scope of this paper, an excellent synthesis for reconstructing ancient arid environments using aeolian, fluvial, and lacustrine evidence is presented by Thomas (1989).

In the continental tropical deserts of Africa, Australia, and Asia, peak dune deposition is believed to have been synchronous between hemispheres, and to have taken place after the glacial maximum at 18 ka (Williams 1975, Sarnthein 1978). However, there is mounting evidence to support the hypothesis of a late-glacial contraction of some of the southern African ergs (such as in the Kalahari and in adjacent areas in Botswana and Namibia) at the same time that their northern counterparts were experiencing dune-building phases and expansion (Lancaster 1979, 1981, Shaw and Cooke 1986, Thomas 1989). Thus even the synchroneity for dune deposition between the Northern and Southern Hemispheres in Africa still remains open to dispute. On the other hand, across Africa the period from 12 to 6 ka was characterized by high lake levels (Street-Perrott and Roberts 1983, COHMAP Members 1988) and greater effective moisture with no significant aeolian sedimentation.

During the glacial maximum, the deserts of the American South-west experienced increased effective moisture, high lake levels, and woodland expansions, owing largely to the southward displacement of the jet stream and the consequent storm tracks (COHMAP Members 1988, Benson *et al.* 1990). In the central Great Plains and the south-western deserts of the United States, peak dune activity seems to correspond with a drier, middle Holocene period from 8 to 5 ka (Dorn *et al.* 1989, Holliday 1989, Tchakerian 1989, Spaulding 1991).

Enhanced aeolian activity is recognized during major arid periods associated with climatic changes. However, major dune-building episodes are believed to be controlled primarily by wind frequency, magnitude, and persistence, as well as by sediment supply, basin geomorphology, and vegetation cover, rather than by hemispheric or regional changes in atmospheric pressure fields.

QUATERNARY AEOLIAN ACTIVITY FROM CONTINENTAL DESERTS

AFRICA

In the ergs of the African continent, the last Wisconsin cool substage most likely coincided with an arid episode as initially suggested by Grove and Warren (1968) and Grove (1969). Figure 25.1 represents a simplified chronology for late Quaternary dune-building episodes from the continental tropical and subtropical deserts of Africa, Asia, and Australia. This tropical aridity is believed to have been the result of high-latitude glaciations (Williams 1975, Sarnthein 1978). In North Africa, the evidence for late Wisconsin aridity comes in the form of extensive belts of fixed, fossil, or degraded dunes, which now extend from the Sahara south to latitude 10° to 12° N in the Sahel over a latitudinal distance of about

Geomorphology of Desert Environments. Edited by Athol D. Abrahams and Anthony J. Parsons. Published in 1994 by Chapman & Hall, London. ISBN 978-94-015-8256-8

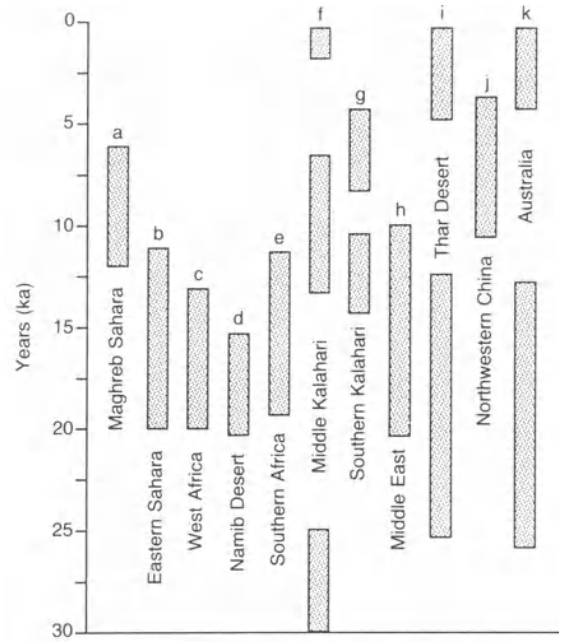

a: Rognon (1987)
b: Talbot (1980), Pachur *et al.* (1987)
c: Michel (1973), Grove (1985)
d: Deacon *et al.* (1984), Lancaster (1989)
e: Lancaster (1981)
f: Shaw and Cooke (1986)
g: Butzer *et al.* (1978)
h: Magaritz and Enzel (1990)
i: Wasson *et al.* (1983)
j: Sung-Chiao (1984)
k: Bowler and Wasson (1984)

Figure 25.1 A summary of late Quaternary dry periods for the tropical and subtropical continental deserts. Dune-building episodes most likely took place during the above periods. The histograms do not imply absolute ages since most dates do not come directly from dune deposits. More references are found in the text as well as in Thomas (1989).

5000 km (Grove and Warren 1968, Michel 1973, Williams 1975, 1985, Sarnthein 1978, Talbot 1980, 1984, Grove 1985, Rognon 1987, Thomas 1989). With the assistance of satellite imagery, it has become possible to identify fossil dunes in southern Africa as far north as 5° S in Zaire (Thomas and Goudie 1984). The majority of the North African and Sahelian dune systems are believed to have been formed between 20 and 12 ka, with several aeolian depositional phases (Rognon and Williams 1977, Bowler 1978, Williams and Faure 1980, Alimen 1982, Goudie 1983, Grove 1985, Thomas 1987, 1989). The period from 14 to 12.5 ka is characterized by hyper aridity, lake desiccation, and enhanced aeolian activity (Street-Perrott and Roberts 1983, Grove 1985).

In the Saharan ergs, aeolian activity was diminished owing to the incursions of moisture from the quasi-permanent low pressure cells associated with the colder conditions in Europe as well as the presence of glaciers in the higher latitudes (Nicholson and Flohn 1980, Rognon 1987). Based on concepts of atmospheric general circulation, Nicholson and Flohn (1980) proposed that the northern sections of the Sahara located in the Maghreb countries of North Africa, experienced relatively wet conditions between 20 and 14 ka. The Grand Erg Occidental and Erg Chech were inactive during the glacial maximum and resumed their dune-building activities only some time after 10 ka (Nicholson and Flohn 1980, Rognon 1987). Thus the majority of the northern Saharan ergs are believed to have been inactive during most of the late Pleistocene, while in the Sahel and other nearby areas, aridity was widespread with major dune-building episodes between 18 and 12 ka, with the driest period occurring sometime between 14 and 12.5 ka (Street-Perrott and Roberts 1983, Kutzbach and Street-Perrott 1985).

Additional evidence for glacial age aridity comes from ocean cores, in which significant concentrations of aeolian quartz grains have been found reflecting the enhanced trade-wind transport of dusts from arid regions (Sarnthein and Koopman 1980). Pokras and Mix (1985) presented evidence for high concentrations of aeolian biosiliceous particles in deep sea cores from the tropical Atlantic and attribute its presence to the deflation of diatomaceous deposits from dry lake beds beginning at about 20 ka. The proponents of cool-stage aridity in the tropics have also utilized information from meteoric groundwater. In the Sahara, Sonntag *et al.* (1980) indicated that very little discharge occurred from 20 to 14 ka, and suggest a period of substantially reduced hydrological activity during the last cold stage of the Wisconsin.

In the Kalahari Desert of southern Africa, both Lancaster (1981) and Thomas (1987) found three dune-building episodes primarily on the basis of dune orientations, with the alignment of the fixed linear dunes being out of synchroneity with the present dune-building winds. The authors suggested different circulation regimes for each of the dune systems and thus different ages of formation. Lancaster (1981) suggested that the dune-building episodes could have started as early as 19 ka with most aeolian activity diminishing by about 11 ka. At present, only sections of the Namib Desert experience aeolian erosion and deposition (Thomas and Goudie 1984, Lancaster 1989).

The available data from the southern African deserts suggest that late glacial aridity was not synchronous between the two desert regions (Thomas 1989). In the Middle Kalahari, wetter conditions are believed to have prevailed up until *c.* 15 ka

and to have been followed by arid conditions until well into the middle Holocene (Shaw and Cooke 1986, Thomas 1989). Additional evidence for late Pleistocene–early Holocene aeolian activity is also presented by Butzer *et al.* (1978) from the interior of South Africa.

AUSTRALIA

Fossil linear dunes are also found in the ergs of the Australian arid zone, outside the confines of the present deserts (Fig. 25.1). According to Wasson (1984), most of the dune systems were formed between *c.* 25 and 13 ka, with peak dune formation occurring between 20 and 16 ka and aeolian activity diminishing about 13 ka (Bowler 1976, Bowler *et al.* 1976, Rognon and Williams 1977, Langford-Smith 1982, Bowler and Wasson 1984). Wyrwoll and Milton (1976) proposed that aridity during glacial stages was widespread, especially in northwestern Australia, owing largely to increased anticyclonic activity. Based on thermoluminescence and radiocarbon dating, Gardner *et al.* (1987) proposed that the linear dunes in Western Australia could have begun to form as far back as 35 ka. Additional evidence for increased aeolian activity during this arid episode of the last glacial maximum comes from the submerged discordant dunes in Fitzroy Sound, dunes formed when sea level was lower (Jennings 1975). Renewed aeolian activity is evidenced by linear dune development in parts of the Australian arid interior during the Holocene (Bowler 1976, Wasson 1984). According to Wasson (1984), this renewed activity took place between 3 and 1 ka, when lake levels and temperatures fell from their high levels during the early Holocene.

ASIA

Data from the fossil sands in the Thar Desert of India indicate that the major dune-building episodes took place between 20 and 11 ka (Allchin *et al.* 1978, Wasson *et al.* 1983). In the deserts of the Arabian Peninsula, McClure (1976) found evidence for extensive aridity and dune building from 17 to 9 ka. There is evidence from Lake Lisan sediments in the Dead Sea and from the northern Sinai Desert for hyperaridity and increased rates of aeolian sedimentation from 26 to 15 ka (Gerson 1982). Based on radiocarbon dates from playa sediments, two dune-building episodes from 20.9 to 16 ka and 11.7 to 10.3 ka are recognized in the north-western Negev Desert of Israel (Magaritz and Enzel 1990). In the Al-Jafr basin of southern Jordan, there are indications of dune deposition after 26 ka (Huckreide and Weissmann 1968). Playa sediments from the Iranian Plateau also show evidence for increased concentrations of aeolian sands between 22 and 12 ka (Wright 1966). The evidence from the interior deserts of China and Mongolia is scant. From the eastern Mongolian deserts, three phases of dune deposition between 10 and 3 ka have been identified through radiocarbon dating on artifacts (Sung-Chiao and Xing 1982, Sung-Chiao 1984).

NORTH AMERICA

Great Plains

The majority of the evidence for late Quaternary aeolian activity comes from the study of stabilized sand dunes in north-eastern Colorado (Muhs 1985, Forman and Maat 1990), south-central Colorado, including the Great Sand Dunes (Fryberger *et al.* 1990), south-central Wyoming (Gaylord 1982, 1990, Ahlbrandt *et al.* 1983), south-western Nebraska, including the Sandhills (Smith 1965, Warren 1976, Ahlbrandt and Fryberger 1980, Ahlbrandt *et al.* 1983, Wright *et al.* 1985) and the Central Plains of Texas (Holliday *et al.* 1983, Holliday 1989). Figure 25.2 summarizes the major dune-building periods from the Great Plains. In the Sandhills of Nebraska, Ahlbrandt and Fryberger (1980) reported radiocarbon dates for regional dune formation from 8.5 to 7 and from 5 to 3 ka, with the latter constituting the major dune-building phase. Muhs (1985) also found that aeolian deposition occurred between 3 and 1.5 ka and corresponds with a period of glacier retreat in the Colorado Front Range. On the other hand, Wright *et al.* (1985) reported ^{14}C dates between 12 and 9 ka for organic sediments in basal layers of lake and marsh deposits from interdune depressions in the Nebraska Sandhills. These dates are older than those proposed by Ahlbrandt and Fryberger (1980) and Muhs (1985) and thus the exact timing of dune deposition is still unresolved. However, studies from surrounding regions suggest an early to mid-Holocene phase for dune deposition. Grigal *et al.* (1976) found two periods of dune formation between 8 and 5 ka from ^{14}C dates on lacustrine organics in north-central Minnesota. In the same vicinity, from the analysis of pollen and lacustrine sediments, Dean *et al.* (1984) found two periods of aridity between 8.5 and 4 ka. Based on radiocarbon and thermoluminescence age estimates for buried A horizons in aeolian sands from northern Colorado, Forman and Maat (1990) reported heightened dune reactivation and deposition some-

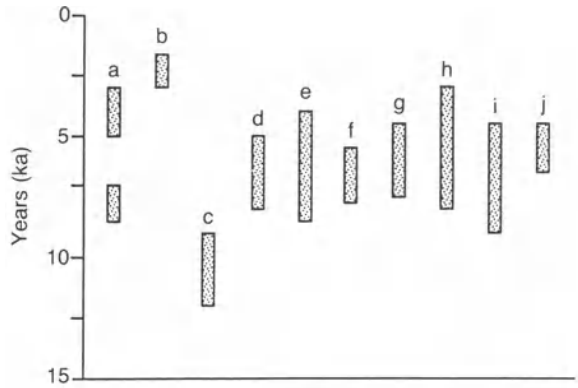

a: Nebraska Sand Hills (Ahlbrandt and Fryberger 1980)
b: Northeastern Colorado (Muhs 1985)
c: Nebraska Sand Hills (Wright *et al.* 1985)
d: North-Central Minnesota (Grigal *et al.* 1976)
e: North-Central Minnesota (Dean *et al.* 1984)
f: South-Central Wyoming (Gaylord 1982)
g: South-Central Wyoming (Gaylord 1990)
h: North Colorado (Forman and Maat 1990)
i: Central High Plains/Texas Panhandle (Holliday 1989)
j: Central High Plains (Holliday *et al.* 1983)

Figure 25.2 A summary of the late Quaternary dune-building episodes from the Great Plains, United States.

time between 9 and 7 ka. From the Ferris Dune Field in south-central Wyoming, Gaylord (1982) reported two periods of dune formation between 7.6 and 5.5 ka based on ^{14}C dates from organics. Using geomorphic and stratigraphic analysis of a 25-m-thick sequence of dune and interdune deposits at Clear Creek in south-central Wyoming, Gaylord (1990), found at least four episodes of increased aeolian sedimentation between 7.5 and 4.5 ka, with pronounced hyperaridity from 7.5 to 7 ka and 5.9 to 4.5 ka. From the southern High Plains in Texas, Holliday *et al.* (1983) and Holliday (1989) reported widespread aeolian activity beginning *c.* 9 ka with dune deposition between 6 and 4.5 ka, based primarily on geomorphic, stratigraphic, pedologic, and archaeological evidence from draws, dunes, lunettes, and playa sediments. It is apparent that the central High Plains experienced major aeolian depositional episodes between 12 and 5 ka, particularly between 7 and 5 ka (Fig. 25.2). Climatic simulations suggest a warmer, windier climate, and consequently reduced effective moisture for the continental interiors of the United States, such as in the Great Plains, between 8 and 5 ka (Kutzbach and Guetter 1986, COHMAP Members 1988, Holliday 1989). This concept of a middle Holocene dry period (Altithermal) in the southern High Plains (and the American South-west) was first proposed by Antevs (1955).

South-western Deserts

Compared with other continental deserts of the world, Quaternary aeolian deposits in the western United States have not been differentiated on the basis of age, probably because of the relative insignificance of large sand bodies in what are essentially gravel deserts. North American deserts are for the most part confined within the boundaries of two major geomorphic provinces, the Basin and Range of the western United States and Mexico and the Colorado Plateau of the south-western United States (Hunt 1983).

The few detailed studies from the Great Basin indicate late Quaternary dune-building episodes during early to mid-Holocene times (Sharp 1966, Smith 1967, Smith 1982, Tchakerian 1989, 1991, Lancaster 1990). Figure 25.3 presents a summary of the dune-building episodes from the Great Basin of the south-western United States. In Catlow Valley, south-east Oregon, two dune episodes overlie lake deposits between 7.5 and 4 ka (Mehringer and Wigand 1986). In the dissected badlands at Corn Creek Flat, 30 km north-west of Las Vegas, Nevada, Quade (1986) found evidence of increased aeolian sedimentation between 8 and 5 ka accompanied by a drop in the water table of at least 25 m. Renewed aeolian activity in the form of coppice dunes of up to 4 m high is believed to have started within the last 1000 years (Quade 1986). Additionally, renewed late Holocene activity commencing around 3 ka is also documented in the Tucson Mountains in southern Arizona based on ^{14}C dates from archaeological remains embedded in sand dunes (Brakenridge and Schuster 1986).

The majority of the aeolian sediments in the Mojave Desert, California are found as climbing and falling dunes and sand ramps, rather than as 'true' dunes (Smith 1984, Tchakerian 1989). These sand ramps are analogous to alluvial fans (in that they are formed primarily by episodic deposition of sands blown against mountains and subsequently reworked by hillslope runoff, talus deposits, and entrenched by dune wadis) and contain a plethora of geomorphological, sedimentological, and palaeoclimatic information (Tchakerian 1989, 1991). Quartz-surface micromorphologies, granulometric analysis, and soil-stratigraphic relationships for climbing and falling dunes in the Cronese Basin in the eastern Mojave Desert (Fig. 25.4) and for sand ramps at the Dale Lake area in the southern Mojave Desert reveal up to eight dune-building episodes during late Quaternary time (Tchakerian 1989, 1991). It is likely that at least four aeolian episodes have taken place

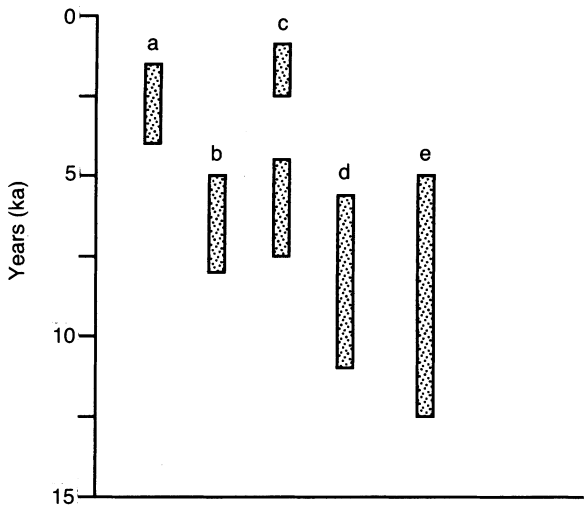

a: Southern Arizona (Mehringer and Wigand 1986)
b: Southern Nevada (Quade 1986)
c: Southern Oregon (Brakenridge and Schuster 1986)
d: Eastern Mojave Desert (Wells *et al.* 1987)
e: Southern Mojave Desert (Tchakerian 1989)

Figure 25.3 A summary of late Quaternary dune-building episodes from the south-western Great Basin, United States.

since 12 ka, with peak dune deposition during early to middle Holocene time (Tchakerian 1991). The last major episode probably occurred during the mid-Holocene, a period characterized by higher temperatures, lake desiccation, reduction in effective moisture and an increase in aeolian activity. Accelerator mass spectrometry (AMS) radiocarbon and cation-ratio dating performed on rock varnishes collected from ventifacts and stabilized talus deposits from the Cronese Basin in the eastern Mojave Desert indicates cessation in aeolian activity between 5.5 and 5 ka (Dorn 1986, Laity 1987, Dorn *et al.* 1989, Tchakerian 1989). The largest concentration of sand dunes in the Great Basin occurs in the Devil's Playground Erg in the central Mojave Desert, which includes the Kelso Dunes (Fig. 25.5), one of the largest dunefields in the Great Basin as well as one of the best studied (Sharp 1966, Smith 1967, Blom and Elachi 1981, Smith 1984, Tchakerian 1989, Lancaster 1990). Within the Kelso Dunes, three to four dune phases have been distinguished based primarily on different dune trends and morphologies, and they indicate significant oscillations in the dune-building wind directions as well as the episodic nature of aeolian activity (Sharp 1966, Tchakerian 1989, Lancaster 1990). Investigations of the late Quaternary history

Figure 25.4 A view of the Cronese Basin in the eastern Mojave Desert, California, showing the falling dunes that envelop the Cronese Mountains. The sands are veneered with talus from the mountains. Cation-ratio dating of rock varnishes on talus and ventifacts indicate cessation of aeolian activity around 5 ka (Dorn 1986, Dorn *et al.* 1989).

of Lake Manix in the western Mojave Desert indicate that the lake spilled and rapidly cut Afton Canyon sometime after 14 230 ± 1325 years BP (Meek 1989). The date of the Afton Canyon cut comes from radiocarbon age estimates on *Anodonta* found *in situ* on the highest shoreline (Meek 1989), and hence provides a maximum age for sand from the Mojave River Wash, which is considered the primary source for the active linear and transverse ridges of the Kelso Dunes (Sharp 1966, Tchakerian 1989). Further evidence for renewed Holocene aeolian activity starting around 3 ka comes from cation-ratio dates from ventifacts in the southern Mojave Desert (Laity 1987), and from lacustrine and aeolian studies from the Great Basin (Quade 1986, Brakenridge and Schuster 1986).

Whitney *et al.* (1985) concluded from studies of sand ramps at four localities in the northern Amargosa Desert in Nevada that the aeolian sediments were deposited during dry and windy Pleistocene climatic episodes as long ago as 750 ka. They noted the presence of up to 10 buried soils with Bishop Tuff, K/Ar dated at 740 ka, near the base of two of the four sand ramps studied. The palaeosols await further work and could provide, with adequate dating, important clues as to the nature of Quaternary aeolian activity.

Additional evidence for Quaternary aeolian activity in the Mojave Desert comes from alluvial stratigraphy (Wells *et al.* 1987), rock varnish microlaminations (Dorn 1984), and stages of soil development on dated lava flows of the Cima volcanic field (McFadden *et al.* 1986). Studies by Wells *et al.* (1987) on the late Quaternary geomorphic history of the Silver Lake in the eastern Mojave Desert have documented two aeolian depositional episodes based on stratigraphic relationships between alluvial fan deposits and ^{14}C dated high shoreline stands. These two episodes are believed to have occurred sometime between 10.5 and 8 ka.

Alternating Mn-rich and Mn-poor laminae in rock varnish on volcanic deposits in the Coso Range have also been interpreted as evidence for fluctuations in aeolian activity (Dorn 1984). According to this study, 25 laminations, and hence at least 13 oscillations in aeolian activity, have occurred during the last 1.1 m.y., with three main episodes during the past 100 000 years. Although it suggests a longer sequence of possible aeolian activity, at present the method is not sensitive enough to discern aeolian activity within the late Quaternary.

Indirect evidence for late Pleistocene aeolian activity is also recognized from buried soils within accretionary loess mantles on K/Ar dated basalt flows from the Cima volcanic field in the eastern Mojave Desert (Wells *et al.* 1985, McFadden *et al.* 1986). The youngest basalt flow, dated by cation-ratio methods at 16 000 ± 700 years BP, is overlain by several aeolian units (McFadden *et al.* 1986). A return to more alkaline (and thus arid) environmental conditions is also indicated by AMS ^{14}C dates on organics from rock varnishes formed on abandoned alluvial fan surfaces from the south-western flanks of the Soda Mountains in the Cronese Basin in the eastern Mojave Desert at 16 100 ± 1600 years BP (Dorn *et al.* 1987).

Figure 25.5 Kelso Dunes, Mojave Desert, California. View west from vegetation-stabilized dunes in the eastern part of the dunefield towards the Devil's Playground. Active dunes are in the middle distance and sand-ramp-covered hills to the right (photo courtesy of N. Lancaster).

Although the dunes of the Grand Desierto in the Sonoran Desert have been the focus of recent attention (Lancaster *et al.* 1987, Blount and Lancaster 1990), the late Quaternary aeolian activity as well as the relationships between climatic changes and dune-building episodes remain virtually unknown.

The foregoing discussion reveals a sharp contrast in the timing of major dune-building episodes between North America, where these episodes have a mid-Holocene date, and the deserts of Africa, Asia, and Australia (with the exception of sections of the Maghreb and some of the southern African ergs of the Kalahari and nearby areas), where dune deposition seems to have peaked between 20 and 12 ka (Fig. 25.1). In the next section the relationship between general atmospheric conditions and dune-building episodes will be discussed.

LATE QUATERNARY PALAEOCLIMATES AND AEOLIAN EPISODES

AFRICA, ASIA, AND AUSTRALIA

For the majority of the tropical and subtropical deserts of Africa, Asia, and Australia, the currently accepted paradigm equates the extension of the ergs to the development of high-latitude glaciations during the late Quaternary, with most of the major dune systems being formed on or just after the onset of maximum glacial conditions near 18 ka (Williams 1975, Sarnthein 1978). The general atmospheric characteristics associated with such a scenario are given by Nicholson and Flohn (1980) and Newell *et al.* (1981) and include the migration of the climatic belts towards the Equator and southwards, the increase in meridional (pole to Equator) atmospheric temperature gradients, the lessening of thermal contrasts between the two hemispheres, and an increase in wind speeds of the trades and mid-latitude westerlies. According to Harrison *et al.* (1984), during the glacial maximum at about 18 ka, the equatorial trough (including the Inter Tropical Convergence Zone (ITCZ)) and the subtropical high pressure belts were displaced equatorwards and are believed to have been instrumental in the development of the extensive belts of dunes in Africa (Lancaster 1979, Grove 1985, Thomas 1989). The intrusion of the ITCZ south of the Equator may explain why the southern African ergs were inactive or were contracting, and why they were thus out of phase with their northern counterparts in the Sahara (Fig. 25.1).

The reduction in temperature and precipitation patterns in conjunction with changes in wind regime also affected the overall vegetation characteristics (Talbot 1984, Pye and Tsoar 1990). According to Talbot (1984), in addition to an increase in the wind regime, precipitation had to have been 25 to 50% less than present values for the establishment of dunes in the Sahel between 20 and 13 ka. The presence of vegetated dunes does not, however, imply relict status because vegetation may very well be a normal component of certain dunes, such as the linear ridges of Australia and the Kalahari (Ash and Wasson 1983, Thomas and Shaw 1991).

According to Thomas and Shaw (1991), the use of vegetated fossil dunes as indicators of former arid conditions should be discarded or extensively revised. Vegetated linear dunes are preferred sites for plant anchorage and growth owing to the unique moisture-retaining capabilities of their sands, especially within interdune corridors and lower windward slopes (Tsoar and Møller 1986, Thomas and Shaw 1991). Additionally, aeolian transport has been documented from vegetated linear dunes with up to 35% plant cover (Ash and Wasson 1983), especially at the dune crests, where wind speeds tend to be accelerated and sediment transported at a much higher rate (Mulligan 1987). Throughout much of the Australian desert dunefields (where vegetation densities are below 10%), low wind velocities are thought to be responsible for the immobility of the sand bodies rather than the anchoring role of vegetation (Ash and Wasson 1983, Bowler and Wasson 1984, Wasson 1984). Thus enhanced aeolian activity and dune-building phases at the glacial maximum are thought to have resulted from strengthening of the anticyclonic winds, steeper meridional temperature gradients, and increased continentality owing to lower sea levels, as well as from lowered temperatures and precipitation (Bowler and Wasson 1984, Thomas and Goudie 1984, Wasson 1984).

Other environmental and morphological variables, such as the effects of decreased wind speeds on dune mobility (Thomas and Shaw 1991) and the nature of the dune form involved (Mabbutt 1977, Thomas 1989), should also be considered when analysing the relict status of dunes. Linear dunes are believed to be preferred sites for vegetation establishment (especially along the windward slopes) because of their migratory or extending forms (Thomas and Shaw 1991). On the other hand, transverse dunes (such as barchans) are too migratory to allow any form of vegetation foothold, while complex dunes exhibit vertical accretion and are usually found within ergs in hyperarid climates, and thus tend not to be conducive for vegetation establishment (Lancaster 1989, Thomas and Shaw 1991).

For the late Pleistocene, the picture that emerges is one of increased aeolian sedimentation in the southern Sahara and southwards (Sahel), with wetter and stable conditions in the northern Sahara and the Maghreb (Rognon 1987). In the southern African ergs, aeolian activity seems to have been limited to localized areas (such as in some sections of the Namib Desert), with relatively humid conditions prevalent throughout the Kalahari and adjacent deserts (Lancaster 1979, Thomas 1989).

During the late Pleistocene and the early Holocene, because of pronounced thermal differences between oceans and lands (owing to significant variations in solar insolation), a strong monsoonal flow developed from 12 to 6 ka with the majority of the Saharan lakes exhibiting high water stands (Williams 1982, Kutzbach and Street-Perrott 1985, Street-Perrott *et al.* 1985, COHMAP Members 1988, Zubakov and Borzenkova 1990). Lake

Megachad reached its highest level sometime between 9 and 6 ka (Maley 1977, Nicholson and Flohn 1980, Servant and Servant-Vildary 1980). In the Malian Sahara, two lacustrine phases are believed to have occurred, the first between 9.5 and 6.4 ka, and the second between 5.4 and 4 ka, with the period in between characterized by a dry episode (Petit-Maire and Riser 1983). Also, pollen samples from Holocene lacustrine sediments in north-west Sudan indicate a period of wetter conditions and high lakes between 9.5 and 4.5 ka (Ritchie and Haynes 1987). The lacustrine sediments are overlain by aeolian sands and are believed to represent the beginning of the arid conditions which still dominate the region (Ritchie and Haynes 1987). The early to middle Holocene moist periods are thought to have been instrumental for the development of the famous Neolithic cultures and rock art of the Sahara (Williams 1982, Zubakov and Borzenkova 1990). During the same period, lake levels were generally lower in the south-western basins of the United States (Smith and Street-Perrott 1983, Benson *et al.* 1990). Current arid conditions in the Sahara are thought to have begun sometime after 4 ka (Rognon 1987, COHMAP Members 1988).

NORTH AMERICA

During the glacial maximum, atmospheric conditions were dramatically different in the deserts of the American South-west. At the same time that the tropical and subtropical deserts were experiencing significant dune-building episodes, aeolian activity in the basins of the south-western deserts of the United States was at a minimum, with humid climatic conditions and desert basin lakes at high levels (Smith and Street-Perrott 1983, Benson and Thompson 1987, COHMAP Members 1988, Benson *et al.* 1990). According to general circulation models (Kutzbach 1987, COHMAP Members 1988), in the south-western deserts, temperatures were 2°C to 3°C lower than at present, while precipitation and potential evapotranspiration were higher. The changes reflected increased winter rains (associated with the southward shift of the storm track and jet), reduced evaporation (associated with lower temperatures), and stronger and more persistent winds (associated with the steep gradient in atmospheric pressure between glaciers in the mountains, such as the Sierra Nevada, and warmer land areas farther south, such as the Mojave Desert. Studies by Benson *et al.* (1990) and Dorn *et al.* (1990) indicate that the majority of closed-basin lakes in the south-western deserts of the United States were high from 16.5 to 12 ka, with some synchronous lake recessions exhibited by lakes Lahontan (Nevada), Bonneville (Utah), and Russell and Searles (California), from 14 to 13.5 ka. Small synchronous increases in lake water areas most likely took place in the above-mentioned four lake basins between *c.* 11.5 and 10 ka. This has also been interpreted as further support for the hemispheric occurrence of the Younger Dryas Event of Europe (Dorn *et al.* 1990).

It is generally suggested that the various aeolian sediments presently found within the basins of the south-western deserts of the United States have accumulated primarily in response to the lowering of lake basins and a consequent increase in the availability of fine sediment, as well as to changes in hillslope and alluvial geomorphic systems (Dohrenwend 1987, Wells *et al.* 1987, Tchakerian 1989, 1991). These changes are attributed to significant climatic oscillations (Wells *et al.* 1985, Dohrenwend 1987, Wells *et al.* 1987). Additionally, there is increasing evidence that winds were stronger in intensity and more persistent during the glacial maximum (Kutzbach 1987), and this, combined with falling lake levels, contributed to the formation of the sand dunes and sheets in the deserts of the American South-west (Wells 1983, Tchakerian 1989).

On the other hand, the Pleistocene to Holocene climatic transition was characterized by fluctuating environmental conditions and witnessed warmer temperatures, greater effective moisture (the latter both from winter precipitation and summer monsoonal rains), and brief high lake stands (Spaulding and Graumlich 1986) owing primarily to the northward displacement of the jet stream and its associated atmospheric phenomena (Kutzbach 1987, COHMAP Members 1988). Aeolian activity was sporadic with some basins showing dune-building episodes while others show no deposition at all (Tchakerian 1989).

Dune deposition in the basins of the south-western deserts of the United States is believed to have peaked in early to middle Holocene time, a period of aridity and drought from about 8 to 5 ka (Figs 25.2 and 25.3). This period was characterized by higher temperatures, drying of basin lakes, reduction in effective moisture, and an increase in aeolian activity (Dohrenwend 1987, Van Devender *et al.* 1987, Wells *et al.* 1987, Dorn *et al.* 1989, Tchakerian 1989, Spaulding 1991). Antevs (1955) first proposed such a climatic interval, which he labelled the Altithermal. Support for a middle Holocene aridity in the American South-west also comes from macrofossil records (radiocarbon-dated packrat middens) from the southern Mojave Desert (Spaulding 1991),

pollen-stratigraphic studies (Mehringer 1985, Hall 1985), geo-archaeological evidence (Waters 1989), soil chronosequences from the southern Great Basin (Hardin *et al.* 1991), radiocarbon and cation-ratio dating of varnished ventifacts (Dorn 1986, Laity 1987, Dorn *et al.* 1989), and global circulation models, which propose a peak in solar radiation about 10 to 9 ka, with a gradual warming associated with the changing orbital parameters (Manabe and Broccoli 1985, Kutzbach and Guetter 1986, Kutzbach 1987, COHMAP Members 1988).

During this time interval, most other continental deserts experienced humid conditions, high lake stands and an increase in effective moisture (Williams 1982, Goudie 1983, Street-Perrott and Roberts 1983, Bowler and Wasson 1984, Thomas and Goudie 1984, Rognon 1987, Thomas 1989). In contrast to the American South-west and the Great Plains, late Quaternary aeolian activity in most other deserts (the southern African ergs excluded) appears to have peaked between 20 and 12 ka (Fig. 25.1). However, the dune-building episodes from the western Great Basin (Fig. 25.3), correlate well with dune construction in the Great Plains (Fig. 25.2). The contemporaneity of earlier Holocene aeolian activity in different parts of western North America is probably owing to the re-establishment of arid conditions, previously displaced by a cooler moisture atmospheric circulation system around the margins of continental ice sheets farther north. In Eurasia, the continental deserts were farther removed from the effects of smaller ice sheets and deglaciation episodes to the north and responded instead to fluctuations in subtropical anticyclones. When these anticyclones weakened, for example between 8 and 5 ka, intrusive westerly and/or tropical airflows introduced moisture to such areas as the Sahara Desert (COHMAP Members 1988).

DISCUSSION

The concept of synchronous hemispheric tropical aridity and dune episodes (Williams 1975, Sarnthein 1978), needs to be refined to accommodate the complete nature of aeolian sedimentation and erosion. Dune-building episodes need not be correlated with aridity owing to the fact that aeolian deposition is most likely controlled by the type and amount of sediment supply, local and regional topographic and geomorphic controls, and the frequency, magnitude, and direction of the prevailing winds. Continental or regional scale changes in atmospheric phenomena and pressure fields are not alone sufficient for ultimately triggering dune deposition in desert basins, although major climatic transitions can produce significant changes in geomorphic processes which in turn influence the variables mentioned above (Pye and Tsoar 1987, Tchakerian 1989, Thomas 1989). As sediment transport varies with the cube of the shear velocity (Bagnold 1941), any increase in the speed and persistence of the wind (especially over longer timespans) can lead to an increase in sediment transport and thus dune deposition. Additionally, a decrease in surface roughness, such as the reduction in vegetation cover that took place during the glacial maximum over large areas in the subtropics (Rognon 1987), can lead to increases in boundary layer winds (Sud *et al.* 1988). Thus high wind speeds combined with lower vegetation densities (and reduced roughness) and ample sediment supply (from dry lake beds and surrounding piedmont areas) most likely constitute the key parameters that control the accumulation of vast amounts of aeolian sands and silts in most desert basins.

Because of the complex nature of aeolian depositional processes, a global systems approach need not necessarily be the correct paradigm through which to investigate the relationships between major dune-building episodes and global aridity associated with climatic changes in the deserts of the world. A more regional and systematic analysis of the aeolian deposits found in the basins of the major deserts should be accomplished before any generalizations can be made as to the global synchroneity of major atmospheric and climatic events and their likely effects on dune-building episodes.

The need to resist premature conclusions is made all the more important when we consider the recent interest in using palaeogeomorphic data from deserts as indicators of global warming. The complexity of the wind regime (magnitude, frequency, persistence), along with sediment type and supply, basin geomorphology, and vegetation cover, must be taken into account in global circulation models if any serious analysis between major arid intervals in the climatic record and dune-building episodes is to be attempted. For example, studies addressing global desertification causes, concerns, and remedies, need to incorporate the rather complex nature of the wind regime and aeolian sedimentation in their models and conclusions. With current refinements in thermoluminescence and rock varnish dating, a more accurate chronology for the timing of major dune-building episodes can be established, since most absolute dates do not come from aeolian deposits, owing to the paucity of organic carbon amenable to

radiometric dating in both dunes and other coevally deposited sediments.

ACKNOWLEDGEMENTS

I would like to thank R. Dorn, J. Laity, N. Lancaster, K. Mulligan, A. Orme and J. Smith for illuminating discussions on aeolian geomorphology.

REFERENCES

Ahlbrandt, T.S. and S.G. Fryberger 1980. Eolian deposits in the Nebraska Sand Hills. *U.S. Geological Survey Professional Paper* 1120.

Ahlbrandt, T.S., J.B. Swinehart and D.G. Maroney 1983. The dynamic Holocene dune fields of the Great Plains and Rocky Mountain Basins, USA. In *Eolian sediments and processes*, M.E. Brookfield and T.S. Ahlbrandt (eds), 379–406. New York: Elsevier.

Alimen, H.M. 1982. Le Sahara – grande zone desertiques Nord Africaine. In *The geological story of the world's deserts*, T.L. Smiley (ed.), 35–51. Uppsala: University of Uppsala Press.

Allchin, B.A., A.S. Goudie and K.T.M. Hegde 1978. *The prehistory and paleogeography of the great Indian Desert*. London: Academic Press.

Antevs, E.A. 1955. Geologic–climatic dating in the West. *American Antiquity* **20**, 317–35.

Ash, J.E. and R.J. Wasson 1983. Vegetation and sand mobility in the Australian desert dunefield. *Zeitschrift für Geomorphologie Supplement Band* **45**, 7–25.

Bagnold, R.A. 1941. *The physics of blown sand and desert dunes*. London: Methuen.

Benson, L.V. and R.S. Thompson 1987. The physical record of lakes in the Great Basin. In *North America and adjacent oceans during the last deglaciation*, Volume K-3, *Geology of North America*, W.F. Ruddiman and H.E. Wright Jr (eds), 241–60. Boulder, CO: Geological Society of America.

Benson, L.V., D.R. Currey, R.I. Dorn, K.R. Lajoie, *et al.* 1990. Chronology of expansion and contraction of four Great Basin systems during the past 35,000 years. *Palaeogeography, Palaeoclimatology, Palaeoecology* **78**, 241–86.

Blom, R. and C. Elachi 1981. Spaceborne and airborne imaging radar observations of sand dunes. *Journal of Geophysical Research* **86**, 3061–73.

Blount, G. and Lancaster, N. 1990. Development of the Gran Desierto sand sea, northwestern Mexico. *Geology* **18**, 724–8.

Bowler, J.M. 1976. Aridity in Australia: age, origins and expression in aeolian landforms and sediments. *Earth-Science Reviews* **12**, 279–312.

Bowler, J.M. 1978. Glacial age eolian events at high and low latitudes: a southern hemisphere perspective. In *Antarctic glacial history and world paleoenvironments*, E.M. van Zinderen Bakker (ed.), 149–72. Rotterdam: Balkema.

Bowler, J.M. and R.J. Wasson 1984. Glacial age environments of inland Australia. In *Late Cainozoic paleoclimates of the Southern Hemisphere*, J.C. Vogel (ed.), 183–208. Rotterdam: Balkema.

Bowler, J.M., G.S. Hope, J.N. Jennings, G. Singh, *et al.* 1976. Late Quaternary climates of Australia and New Guinea. *Quaternary Research* **6**, 359–94.

Brakenridge, G.R. and J. Schuster 1986. Late Quaternary geology and geomorphology in relation to archaeological site locations, southern Arizona. *Journal of Arid Environments* **10**, 225–39.

Butzer, K.W., R. Stuckenrath, A.J. Bruzewicz and D.M. Helgren 1978. Late Cenozoic paleoclimates of the Gaap Escarpment, Kalahari margin, South Africa. *Quaternary Research* **10**, 310–39.

COHMAP Members 1988. Climatic changes of the last 18,000 years: observations and model simulations. *Science* 241, 1043–52.

Deacon, J., N. Lancaster and L. Scott 1984. Evidence for late Quaternary climatic change in southern Africa. In *Late Cainozoic paleoclimates of the Southern Hemisphere*, J.C. Vogel (ed.), 21–34. Rotterdam: Balkema.

Dean, W.E., J.P. Bradbury, R.Y. Anderson and C.W. Barnosky 1984. The variability of Holocene climate change: evidence from varved lake sediments. *Science* **226**, 1191–4.

Dohrenwend, J.C. 1987. Basin and Range. In *Geomorphic systems of North America*, Volume 2, *Geology of North America*, W.L. Graf (ed.), 303–42. Boulder, CO: Geological Society of America.

Dorn, R.I. 1984. Cause and implications of rock varnish microchemical laminations. *Nature* **310**, 767–70.

Dorn, R.I. 1986. Rock varnish as an indicator of aeolian environmental change. In *Aeolian geomorphology*, W.G. Nickling (ed.), 291–307. Boston: Allen & Unwin.

Dorn, R.I., J.E. Laity and V.P. Tchakerian 1989. Holocene paleowinds in the Mojave Desert recorded by rock varnish dating of ventifacts: greenhouse analog? *Geological Society of America Abstracts with Programs* **21**, A343.

Dorn, R.I., D. Tanner, B.D. Turrin and J.C. Dohrenwend 1987. Cation-ratio dating of Quaternary materials in the east-central Mojave Desert, California. *Physical Geography* **8**, 72–81.

Dorn, R.I., A.J.T. Jull, D.J. Donahue, T.W. Linick, *et al.* 1990. Latest Pleistocene lake shorelines and glacial chronology in the western Basin and Range Province, USA: insights from AMS radiocarbon dating of rock varnish and paleoclimatic implications. *Palaeogeography, Palaeoclimatology, Palaeoecology* **78**, 315–31.

Forman, S.L. and Maat, P. 1990. Stratigraphic evidence for late Quaternary dune activity near Hudson on the Piedmont of northern Colorado. *Geology* **18**, 745–8.

Fryberger, S.G., L.F. Krystinik and C.J. Schenk 1990. *Modern and ancient eolian deposits: petroleum exploration and production*. Denver: Rocky Mountain Section, Society of Economic Paleontologists and Mineralogists.

Gardner, G.J., A.J. Mortlock, D.M Price, M.L. Readheas, *et al.* 1987. Thermoluminescence and radiocarbon dating of Australian desert dunes. *Australian Journal of Earth Sciences* **34**, 343–57.

Gaylord, D.R. 1982. Geologic history of the Ferris dune field, south-central Wyoming, in *Interpretation of Windflow Characteristics from Eolian Landforms*, R.W. Marrs and K.E. Kolm (eds), 65–82. Geological Society of America Special Paper 192.

Gaylord, D.R. 1990. Holocene paleoclimatic fluctuations

revealed from dune and interdune strata in Wyoming. *Journal of Arid Environments* **18**, 123–38.

Gerson, R. 1982. The Middle East: landform of a planetary desert through environmental changes. In *The geological story of the world's deserts*, T.L. Smiley (ed.), 52–78. Uppsala: University of Uppsala Press.

Goudie, A.S. 1983. The arid Earth. In *Mega-geomorphology*, R. Gardner and H. Scoging (eds), 152–71. Oxford: Clarendon Press.

Grigal, D.F., R.C. Severson and G.E. Goltz 1976. Evidence of eolian activity in north-central Minnesota 8,000 to 5,000 yr. ago. *Bulletin of the Geological Society of America* **87**, 1251–4.

Grove, A.T. 1969. Landforms and climatic change in the Kalahari and Ngamiland. *Geographical Journal* **134**, 192–212.

Grove, A.T. 1985. The physical evolution of the river basins. In *The Niger and its neighbours*, A.T. Grove (ed.), 2–60. Rotterdam: Balkema.

Grove, A.T. and A. Warren 1968. Quaternary landforms and climate on the south side of the Sahara. *Geographical Journal* **134**, 194–208.

Hall, S.A. 1985. Quaternary pollen analysis and vegetational history of the Southwest. In *Pollen records of late Quaternary North American Sediments*. V.M. Bryant Jr and R.C. Holloway (eds), 95–123. Dallas: American Association of Stratigraphic Palynologists Foundation.

Hardin, J.W., E.M. Taylor, C. Hill, R.K. Mark, *et al.* 1991. Rates of soil development from four soil chronosequences in the southern Great Basin. *Quaternary Research* **35**, 383–99.

Harrison, S.P., S.E. Metcalfe, F.A. Street-Perrott, A.B. Pittock, *et al.* 1984. In *Late Cainozoic paleoclimates of the Southern Hemisphere*, J.C. Vogel (ed.), 21–34. Rotterdam: Balkema.

Holliday, V.T. 1989. Middle Holocene drought on the southern High Plains. *Quaternary Research* **31**, 74–82.

Holliday, V.T., E. Johnson, H. Haas and R. Stuckenrath 1983. Radiocarbon ages from the Lubbock Lake site, 1950–1980. *Plains Anthropologist* **28**, 165–82.

Huckreide, R. and G. Weissmann 1968. Der JungPleistozane pluvialsee von Elgafr und Weitere daten zum Quartär Jordaniens. *Geologische Paleontologie* **2**, 13.

Hunt, C.B. 1983. Overview of our arid lands. In *Origin and evolution of North American deserts*, S.G. Wells and D. Hanigan (eds), 23–52. Albuquerque: University of New Mexico Press.

Jennings, J.N. 1975. Desert dunes and estuarine fill in the Fitzroy Estuary, north-western Australia. *Catena* **2**, 215–62.

Kutzbach, J.E. 1987. Model simulations of the climatic patterns during the glaciation of North America. In *North America and adjacent oceans during the last deglaciation*, Volume K-3, *Geology of North America*, W.F. Ruddiman and H.E. Jr Wright (eds), 425–46. Boulder, CO: Geological Society of America.

Kutzbach, J.E. and P.J. Guetter 1986. The influence of changing orbital parameters and surface boundary conditions on climate simulations for the past 18,000 years. *Journal of Atmospheric Sciences* **39**, 1177–88.

Kutzbach, J.E. and F.A. Street-Perrott 1985. Milankovitch forcing of fluctuations in the level of tropical lakes from 18 to 0 kyr BP. *Nature* **317**, 130–4.

Laity, J.E. 1987. Topographic effects on ventifact formation. Mojave Desert, California. *Physical Geography* **8**, 113–32.

Lancaster, N. 1979. Evidence for a widespread late Pleistocene humid period in southern Africa. *Nature* **279**, 145–6.

Lancaster, N. 1981. Paleoenvironmental implications of fixed dune systems in southern Africa. *Palaeogeography, Palaeoclimatology, Palaeoecology* **33**, 327–46.

Lancaster, N. 1989. *The Namib sand sea: dune forms, processes and sediments*. Rotterdam: Balkema.

Lancaster, N. 1990. Dune morphology and chronology, Kelso Dunes, Mojave Desert, California. *Geological Society of America Abstracts with Programs* **22**, A86.

Lancaster, N., R. Greeley and P.R. Christensen 1987. Dunes of the Gran Desierto sand sea, Sonora, Mexico. *Earth Surface Processes and Landforms* **12**, 277–88.

Langford-Smith, T. 1982. The geomorphic history of the Australian Deserts. In *The geological story of the world's deserts*, T.L. Smiley (ed.), 4–19. Uppsala: University of Uppsala Press.

Mabbutt, J.A. 1977. *Desert landforms*. Cambridge, MA: MIT Press.

Magaritz, M. and Y. Enzel 1990. Standing-water deposits as indicators of late Quaternary dune migration in the northwestern Negev, Israel. *Climatic Change* **16**, 307–18.

Maley, J. 1977. Paleoclimates of Central Sahara during the early Holocene. *Nature* **269**, 573–7.

Manabe, S. and A.J. Broccoli 1985. The influence of continental ice sheets on the climate of an ice age. *Journal of Geophysical Research* **90**, 2167–90.

McClure, H.A. 1976. Radiocarbon chronology of late Quaternary lakes in the Arabian Desert. *Nature* **263**, 755–6.

McFadden, J.C., S.G. Wells and J.C. Dohrenwend 1986. Cumulic soils formed in eolian parent materials on flows of the Cima volcanic field, Mojave Desert, California. *Catena* **13**, 361–89.

Meek, N. 1989. Geomorphic and hydrologic implications of the rapid incision of Afton Canyon, Mojave Desert, California. *Geology* **17**, 7–10.

Mehringer, P.J. Jr 1985. Late Quaternary pollen records from the interior Pacific Northwest and northern Great Basin of the United States. In *Pollen records of late Quaternary North American sediments*, V.M. Bryant Jr and R.C. Holloway (eds), 167–90. Dallas: American Association of Stratigraphic Palynologists Foundation.

Mehringer, P.J. Jr and P.E. Wigand 1986. Holocene history of Skull Creek dunes, Catlow Valley, southeastern Oregon, U.S.A. *Journal of Arid Environments* **11**, 117–38.

Michel, P. 1973. Les bassins des fleuvres Sénégal et Gambie: Etude géomorphologique. *Memoirs ORSTROM* 63 (3 volumes).

Muhs, D.R. 1985. Age and paleoclimatic significance of Holocene sand dunes in northeastern Colorado. *Annals of the Association of American Geographers* **75**, 566–82.

Mulligan, K.R. 1987. Velocity profiles measured on the windward slope of a transverse dune. *Earth Surface Processes and Landforms* **13**, 573–82.

Newell, R.E., S. Gould-Stewarts and J.C. Chung 1981. A possible interpretation of paleoclimatic reconstructions for 18,000 B.P. for the region 60°N to 60°S, 60°W to 100°E. *Paleoecology of Africa* **13**, 1–19.

Nicholson, S.E. and H. Flohn 1980. African environmental and climatic changes and the general atmospheric circulation in late Pleistocene and Holocene. *Climatic Change* **2**, 313–48.

Pachur, H.J., H.P. Röper, S. Kroplin and M. Goschin 1987. Late Quaternary hydrography of the eastern Sahara. *Berliner Geowissenschaften Abhandlungen* **75**, 331–84.

Petit-Maire, N. and J. Riser (eds) 1983. *Sahara ou Sahel? Quaternaire Recent du Bassin de Taoudenni, Mali.* Marseille: Imprimerie Lamy.

Pokras, E.M. and A.C. Mix 1985. Eolian evidence for spatial variability of late Quaternary climates in tropical Africa. *Quaternary Research* **24**, 137–49.

Pye, K. and H. Tsoar 1987. The mechanics and geological implications of dust transport and deposition in deserts with particular reference to loess formation and dune sand diagenesis in the northern Negev, Israel. In *Desert sediments: ancient and modern*, L. Frostick and I. Reid (eds), 139–56. Oxford: Blackwell, Geological Society of London Special Publication 35.

Pye, K. and H. Tsoar 1990. *Aeolian sand and sand dunes.* London: Unwin Hyman.

Quade, J. 1986. Late Quaternary environmental changes in the upper Las Vegas Valley, Nevada. *Quaternary Research* **26**, 340–57.

Ritchie, J.C. and C.V. Haynes 1987. Holocene vegetation zonation in the eastern Sahara. *Nature* **330**, 645–7.

Rognon, P. 1987. Late Quaternary climatic reconstruction for the Maghreb (North Africa). *Palaeogeography, Palaeoclimatology, Palaeoecology* **58**, 11–34.

Rognon, P. and M.A.J. Williams 1977. Late Quaternary climatic change in Australia and North Africa: a preliminary interpretation. *Palaeogeography, Palaeoclimatology, Palaeoecology* **21**, 285–327.

Sarnthein, M. 1978. Sand deserts during glacial maximum and climatic optimum. *Nature* **272**, 43–6.

Sarnthein, M. and B. Koopman 1980. Late Quaternary deep-sea record of northwest Africa: dust supply and wind direction. *Paleoecology of Africa* **12**, 239–53.

Servant, M. and S. Servant-Vildary 1980. L'environnement quaternaire du bassin du Tchad. In *The Sahara and the Nile*, M.A.J. Williams and H. Faure (eds), 133–62. Rotterdam: Balkema.

Sharp, R.P. 1966. Kelso Dunes, Mojave Desert, California. *Bulletin of the Geological Society of America* **77**, 1045–74.

Shaw, P.A. and H.J. Cooke 1986. Geomorphic evidence for the Late Quaternary paleoclimate of the Middle Kalahari of Northern Botswana. *Catena* **13**, 349–59.

Smith, G.I. and F.A. Street-Perrott 1983. Pluvial lakes of the western United States. In *Late Quaternary environments of the United States I. The late Pleistocene*, S.C. Porter (ed.), 190–211. Minneapolis: University of Minnesota Press.

Smith, H.T.U. 1965. Dune morphology and chronology in central and western Nebraska: *Journal of Geology* **73**, 557–78.

Smith, H.T.U. 1967. Past versus present wind action in the Mojave Desert region, California, *U.S. Air Force Cambridge Research Labs Publication* AFLCRL-67-0683.

Smith, R.S.U. 1982. Sand dunes in North American deserts. In *Reference handbook on the deserts of North America*, G.L. Bender (ed.), 481–526. Westport, CO: Greenwood Press.

Smith, R.S.U. 1984. Eolian geomorphology of the Devil's Playground, Kelso Dunes, and Silurian Valley, California. In *Surficial geology of the eastern Mojave Desert, California*, J.C. Dohrenwend (ed.), 162–74. Denver: Geological Society of America 1984 Annual Meeting Guidebook no. 14.

Sonntag, C., U. Thorweibe, J. Rudolph, E.P. Lohnert, *et al.* 1980. Isotope identification of Saharian groundwater. *Paleoecology of Africa* **12**, 159–71.

Spaulding, W.G. 1991. A middle Holocene vegetation record from the Mojave Desert of North America and its paleoclimatic significance. *Quaternary Research* **35**, 427–37.

Spaulding, W.G. and L.J. Graumlich 1986. The last pluvial climate episodes in the deserts of southwestern North America. *Nature* **320**, 441–4.

Street-Perrott, F.A. and N. Roberts 1983. Fluctuations in closed-basin lakes as an indicator of atmospheric circulation patterns. In *Variations in the global water budget*, F.A. Street-Perrott, M. Beran and R. Ratcliffe (eds), 331–45. Boston: Reidel.

Street-Perrott, F.A., N. Roberts and S. Metcalfe 1985. Geomorphic implications of late Quaternary hydrological and climatic changes in the Northern Hemisphere tropics. In *Environmental change and tropical geomorphology*, I. Douglas and T. Spencer (eds), 165–83. London: Allen & Unwin.

Sud, Y.C., J. Shukla and Y. Mintz 1988. Influence of land surface roughness on atmospheric circulation and precipitation: a sensitivity study with a general circulation model. *Journal of Applied Meteorology* **27**, 1036–54.

Sung-Chiao, C. 1984. The sandy deserts and the Gobi of China. In *Deserts and arid lands*, F. El-Baz (ed.), 95–113. The Hague: Martinus Nijhoff.

Sung-Chiao, C. and J. Xing 1982. Origin and development of the Shamo sand deserts and the Gobi stony deserts of China. In *The geological story of the world's deserts*, T.L. Smiley (ed.), 79–91. Uppsala: University of Uppsala Press.

Talbot, M.R. 1980. Environmental responses to climatic change in the West African Sahel over the past 20,000 years. In *The Sahara and the Nile*, M.A.J. Williams and H. Faure (eds), 37–62. Rotterdam: Balkema.

Talbot, M.R. 1984. Late Pleistocene dune building and rainfall in the Sahel. *Paleoecology of Africa* **16**, 203–14.

Tchakerian, V.P. 1989. Late Quaternary aeolian geomorphology, east-central Mojave Desert, California. Ph.D. Dissertation, University of California, Los Angeles.

Tchakerian, V.P. 1991. Late Quaternary aeolian geomorphology of the Dale Lake Sand Sheet, southern Mojave Desert, California. *Physical Geography* **12**, 347–69.

Thomas, D.S.G. 1987. Discrimination of depositional environments using sedimentary characteristics in the Mega Kalahari, central southern Africa. In *Desert sediments: ancient and modern*, L. Frostick and I. Reid (eds), 293–306. Oxford: Blackwell, Geological Society of London Special Publication 35.

Thomas, D.S.G. 1989. Reconstructing ancient arid environments. In *Arid zone geomorphology*, D.S.G. Thomas (ed.), 311–34. New York: Halsted Press.

Thomas, D.S.G. and A.S. Goudie 1984. Ancient ergs of the Southern Hemisphere. In *Late Cainozoic paleoclimates of the Southern Hemisphere*, J.C. Vogel (ed.), 407–18. Rotterdam: Balkema.

Thomas, D.S.G. and P.A. Shaw 1991. 'Relict' desert dune systems: interpretations and problems. *Journal of Arid Environments* **20**, 1–14.

Tsoar, H. and J.T. Møller 1986. The role of vegetation in the formation of linear sand dunes. In *Aeolian geomorphology*, W.G. Nickling (ed.), 75–95. Boston: Allen & Unwin.

Van Devender, T.R., R.S. Thompson and J.L. Betancourt 1987. Vegetation history of the deserts of southwestern North America: the nature and timing of the late Wisconsin–Holocene transition. In *North America and adjacent oceans during the last deglaciation*, Volume K-3, *Geology of North America*, W.F. Ruddiman and H.E. Wright Jr (eds), 323–52. Boulder, CO: Geological Society of America.

Warren, A. 1976. Morphology and sediments of the Nebraska Sand Hills in relation to Pleistocene winds and the development of aeolian bedforms. *Journal of Geology* **84**, 685–700.

Wasson, R.J. 1984. Late Quaternary paleoenvironments in the desert dunefields of Australia. In *Late Cainozoic paleoclimates of the Southern Hemisphere*, J.C. Vogel (ed.), 419–32. Rotterdam: Balkema.

Wasson, R.J., S.N. Rajagaru, V.N. Misra, D.P. Agrawal, *et al.* 1983. Geomorphology, late Quaternary stratigraphy and paleoclimatology of the Thar Desert. *Zeitschrift für Geomorphologie, Supplement Band* **45**, 117–52.

Waters, M.R. 1989. Late Quaternary lacustrine history and paleoclimatic significance of pluvial Lake Cochise, southeastern Arizona. *Quaternary Research* **32**, 1–11.

Wells, G.L. 1983. Late-glacial circulation over central North America revealed by aeolian features. In *Variations in the global water budget*, F.A. Street-Perrott, M. Beran and R. Ratcliffe (eds), 317–30. Boston: Reidel.

Wells, S.G., J.C. Dohrenwend, L.D. McFadden, B.D. Turrin, 1985. Late Cenozoic landscape evolution on lava flow surfaces of the Cima volcanic field, Mojave Desert, California. *Bulletin of the Geological Society of America* **96**, 1518–29.

Wells, S.G., L.D. McFadden and J.C. Dohrenwend 1987. Influence of the late Quaternary climatic changes on geomorphic and pedogenic processes on a desert piedmont, eastern Mojave Desert, California. *Quaternary Research* **27**, 130–46.

Whitney, J.W., W.C. Swadley and R.R. Shroba 1985. Middle Quaternary sand ramps in the southern Great Basin, California and Nevada. *Geological Society of America Abstracts with Programs* **17**, A750.

Williams, M.A.J. 1975. Late Quaternary tropical aridity synchronous in both hemispheres? *Nature* **253**, 617–8.

Williams, M.A.J. 1982. Quaternary environments in northern Africa. In *A land between two Niles*, M.A.J. Williams and D.A. Adamson (eds), 43–63. Rotterdam: Balkema.

Williams, M.A.J. 1985. Pleistocene aridity in tropical Africa, Australia and Asia. In *Environmental change and tropical geomorphology*, I. Douglas and T. Spencer (eds), 219–33. London: Allen & Unwin.

Williams, M.A.J. and H. Faure (eds) 1980. *The Sahara and the Nile*. Rotterdam: Balkema.

Wright, H.E., Jr 1966. Stratigraphy of lake sediments and the precision of the paleoclimatic record. In *World climate from 8,000 to 0 BC*, S.E. Soyer (ed.), 157–73. London: Royal Meteorological Society.

Wright, H.E., Jr, J.C. Almendinger and J. Gruger 1985. Pollen diagram from the Nebraska Sandhills and the age of the dunes. *Quaternary Research* **24**, 115–20.

Wyrwoll, K.H. and D. Milton 1976. Widespread late Quaternary aridity in Western Australia: *Nature* **264**, 429–30.

Zubakov, V.A. and I.I. Borzenkova 1990. *Global paleoclimate of the late Cenozoic*, Developments in Paleontology and Stratigraphy 12. Amsterdam: Elsevier.

CENOZOIC CLIMATIC CHANGES IN DESERTS: A SYNTHESIS

26

M.A.J. Williams

INTRODUCTION

Deserts are excellent geological, geomorphic, and archaeological museums. The very aridity to which they owe their existence has made them remarkable repositories of past depositional and erosional events (Frostick and Reid 1987). The fossil river valleys of the Sahara, the great salt lakes of Australia, China, and Patagonia, the dissected volcanic mountains of the Arabian peninsula and the Afar Desert – all are legacies of former tectonic, volcanic, and climatic episodes which ultimately gave rise to the deserts we see today. Each desert reflects its own individual geological inheritance and geomorphic history; each is unique in its assemblage of landforms; each ideally deserves detailed and separate study in its own right.

Two contrasting themes permeate the study of desert landscapes: timelessness and change (Williams 1984a, b). In many parts of the desert world, morphogenesis is virtually inactive, and relief is presently being conserved. In other more limited areas, recurrent dust storms and ever shifting dunes convey an impression of a dynamic and changing landscape. This latter impression is reinforced by the presence of now vegetated and stable dunefields located well beyond the present-day confines of active desert dunes, as well as by the occurrence of relict river and lake basins deep within the desert – silent witness to previously wetter climates. The paradox here is that deserts can be simultaneously both young and old, conserving as well as destroying relief, morphologically stable as well as geomorphically dynamic. In the deserts of Western Australia, for instance, late Quaternary dunefields occur cheek by jowl with valleys that have changed very little since the final separation of Australia from Antarctica over 50 m.y. ago. One intriguing outcome of the polygenetic nature of desert landscapes is therefore the frequent juxtaposition of very old elements of the landscape with others that are very new.

The aim of this chapter is to examine the role of past tectonic, volcanic, and climatic events in shaping the landscapes of our major deserts, focusing upon the Cenozoic legacy in particular, while noting that many aspects of desert geomorphology cannot be fully understood without an appreciation of much older tectonic and sedimentary events, many of them extending well back into Phanerozoic times, and some even into the Precambrian (Williams 1984a). We begin with a brief discussion of some characteristic desert landforms, followed by a concise analysis of the causes of present-day aridity. We then consider the geomorphic history of the North African and Australian deserts, and conclude with an evaluation of the impact of Cenozoic climatic fluctuations upon the evolution of desert landscapes.

CLIMATIC INTERPRETATION OF DESERT LANDFORMS

Is there a characteristic assemblage of landforms peculiar to and diagnostic of our present-day deserts? The published accounts of scientific explorers, geologists, and geomorphologists (e.g. Cooke and Warren 1973, Mabbutt 1977, Frostick and Reid 1987, Thomas 1989), our own observations in the deserts of Africa, Australia, India and the Middle East, and the increasingly informative imagery obtained by remote sensing, of which the volumes by Pesce (1968) and McKee (1978) were excellent early examples, all suggest that there is indeed a diagnostic suite of desert landforms, the relative proportions of

Geomorphology of Desert Environments. Edited by Athol D. Abrahams and Anthony J. Parsons. Published in 1994 by Chapman & Hall, London. ISBN 978-94-015-8256-8

which will vary from desert to desert, depending upon local and regional tectonic, volcanic, and climatic history (Williams 1984a, b, Williams *et al.* 1987).

As a very rough generalization, the major erosional landforms in deserts tend to be far older than many of the depositional landforms. Erosional landforms include desert mountains such as the Hoggar and Tibesti massifs of the Sahara, stony tablelands and plateaux such as the Mesozoic plateaux of central Australia, and denuded lowlands such as the shield deserts of Mauritania and Western Australia, which are located on tectonically stable Archaean and Proterozoic formations with a long history of subaerial erosion.

Depositional landforms include desert dunes, alluvial fans, and floodplains of varying complexity and size, and lacustrine features such as playa lakes. There is often a close relationship between alluvial, lacustrine, and aeolian features, typified by source-bordering dunes emanating from alluvial point-bar sands (Wasson 1976, Williams *et al.* 1991b) or by the clay dunes (lunettes) developed on the downwind margins of certain now dry or saline lakes in Algeria, Australia, and Siberia (Bowler 1973, 1976). The distinction between erosional and depositional landforms is often somewhat arbitrary, and will depend upon the temporal and spatial scale in which one is interested. A Holocene diatomite etched by wind erosion is evidence of lacustrine deposition during a less arid interval, as well as evidence of the efficiency of wind erosion during an ensuing drier phase (Williams 1971). The focus may be on the deposit (lacustrine diatomite) or on the landform (a series of yardangs eroded from the lake sediments). Alternatively, the emphasis may be on the origin of the lake basin (tectonic or deflationary?) in which the diatomites occur.

Many desert mountains and plateaux are flanked by rectilinear or gently concave rock-cut surfaces or pediments, which are usually mantled with a layer of sediment up to several metres thick (Mabbutt 1978a). Spectacular flights of staged pediments, in appearance somewhat reminiscent of the dissected flights of uplifted coral reefs in Barbados and New Guinea, are a feature of some of the piedmont slopes of the Atlas, Aurès, Hoggar, and Tibesti mountains in the Sahara (Coque 1962, Rognon 1967, Conrad 1969). In their distal sectors, the pediments may coalesce and become buried beneath alluvial fans and playa lakes. The larger fans and lake deposits often contain a fragmented but otherwise valuable record of late Tertiary and Quaternary depositional and hydrological fluctuations which may yield useful palaeoclimatic information (Williams and Faure 1980, Frostick and Reid 1987).

Before using the erosional and depositional landforms preserved in our deserts as evidence of past climatic changes, it is essential to distinguish between the effects of climate on the one hand, and those of geology on the other (Rognon 1989). The term geology here subsumes the influence of tectonic and volcanic processes as well as the more subtle controls exercised by lithology and rock structure.

Geomorphic evidence of climatic change is seldom unequivocal and leads too readily to circular argument (see discussion in Williams 1985 for details). Independent verification (or refutation) is vital if palaeoclimatology is to retain credibility. The appropriate question to ask is not whether or not there has been climatic change, but whether or not a particular climate is demanded by a particular suite of landforms (Cooke 1958, Flint 1959a, b). Since most erosional desert landforms can form in a variety of different ways, although the end-product, such as a pediment, may for all practical purposes have the same final appearance (Twidale 1978, Mabbutt 1978a), such features will not be usefully diagnostic of past climatic events. More helpful, because it is more sensitive, is the depositional legacy of former wetter and drier episodes, although here too great caution is needed when invoking climatic change.

Consider, for example, some late Cenozoic lakes in semi-arid Ethiopia. A lake may be created by lava damming a river and may vanish as a result of seismic disruption. Pliocene Lake Gadeb in the semi-arid south-eastern uplands of Ethiopia originated when a lava flow blocked the course of the ancestral Webi Shebele channel some 2.76 m.y. ago (Williams *et al.* 1979, Eberz *et al.* 1988). Earlier still, a vast lake occupied what is now the middle Awash valley of the southern Afar Desert and dried out shortly after 3.8 to 4.0 Ma during an intense phase of tectonic and volcanic activity (Williams *et al.* 1986). A final and more recent example will suffice to show the climatically ambiguous nature of some lake records. During the height of the recent prolonged drought in Ethiopia, when many Ethiopian rift lakes were shrinking, Lake Besaka, a graben lake lying at the foot of Fantale volcano, started to rise at a rate of $0.5\ m\ y^{-1}$ between 1974 and 1975 (M.A.J. Williams *et al.* 1981). A resurgence of hot spring activity along the fault scarps bordering the lake was the primary cause – possibly a precursor to a future eruption from the caldera, which last erupted about AD 1850. Within two years the brackish lake with its fauna of shrimp and flamingoes had become a freshwater

lake with a new fauna of freshwater fish and crocodiles.

Only by rigorous multidisciplinary study is it possible to differentiate between desert lakes formerly fed solely by surface runoff (whether local or far-travelled), or solely by groundwater, or by a combination of runoff and groundwater – a combination which will very likely have varied through time (Gasse 1975, Williams *et al.* 1987, 1991b, Street 1980, Abell and Williams 1989). It would be unprofitable to pursue this line of argument further until we have considered some of the causes of present-day aridity and some of the factors which control the distribution of our existing deserts.

CAUSES OF ARIDITY

Deserts are regions of rare and unreliable rainfall. They are not restricted to any particular latitude, but are especially extensive astride the two tropics, in latitudes characterized by more or less permanent high pressure cells and hot dry subsiding air. The two polar deserts are under the influence of semi-permanent anticyclones and of cold dry subsiding air. As air subsides and becomes compressed, it also becomes warmer, so that its relative humidity is decreased even though the absolute amount of water vapour held in desert air may be substantial and may become evident in the cold hours before dawn in the form of the evanescent desert dew. The anticyclonic deserts result from the global Hadley circulation, and have very little to do with the regional distribution of land and sea. Oceans in strictly tropical and high polar latitudes also receive minimal precipitation and are simply the oceanic extensions of the terrestrial deserts.

A second and very common cause of aridity on land is distance inland. Except for the equatorial zone, precipitation usually decreases rapidly away from the coast. The great temperate deserts of the continental interior of Asia are a prime example of such deserts, and the effects of continentality reinforce those of latitude in the hot tropical deserts of North Africa, Arabia, and Australia.

Two additional factors accentuate the aridity resulting from latitude and increasing distance from the nearest source of moist maritime air. One is the rain-shadow effect, and the other is the presence offshore of cold upwelling water or a cold ocean current. When warm moist maritime air reaches the land it frequently encounters mountain ranges, as in the case of the Andes, the Rockies, the Himalayas, the Ethiopian uplands, and the Eastern Highlands of Australia. The moist air rises and is cooled adiabatically, rapidly attaining vapour saturation, and shedding its precipitated water as rain or snow – hence such local names as Sierra Nevada and Snowy Mountains. If the coastal ranges are reasonably elevated relative to the interior, as is true of the Americas and Australia, there will be a pronounced rain-shadow effect inland of the ranges, with desiccation of the previously moist air accentuated as it flows downhill, becoming warmer and drier in the process. In extreme cases, the air may shed its moisture on mountains 2000 to 4000 m high, before descending to valleys lying close to or even below sea level, as in the Afar Depression and the Dead Sea Rift.

Deserts such as the Atacama and the Namib are flanked offshore by cold upwelling water. In fact, the western borders of all the Trade Wind or tropical deserts are washed by the cool waters of ocean currents generated by the gyres which flow clockwise in the Northern Hemisphere and anticlockwise in the Southern Hemisphere. The result is predictable: cool moist air from the ocean reaches land which is warmer than the adjacent cool ocean, so that the relative humidity of the air is reduced, and its capacity to absorb moisture rather than to shed it is increased. Such air masses therefore usually function as a desiccator rather than as a welcome source of moisture, leaving the plants and animals dependent on coastal fog for their survival. Erkowit, situated high in the Red Sea Hills of the eastern Sudan, is a good example of a mist oasis, receiving much of its precipitation from fog blowing off the Red Sea in winter while all around it is sweltering lowland desert.

Aridity should not be confused with desertification. Within the timescale of the last two million years the deserts have occupied essentially their present locations on the globe (Fig. 26.1). They are where they are for sound and relatively immutable geographical reasons. A combination of at least five major factors accounts for the distribution of modern deserts and for their low and erratic precipitation. These are the prevalence of dry subsiding air over the deserts (itself linked to latitude and to global atmospheric circulation), a vast land area, low inland relief and high coastal ranges, and the presence of cool ocean water close offshore. An additional factor is the presence aloft of a subtropical jetstream, the existence and course of which is partly controlled by the presence or absence of extensive areas of high elevation, such as the Tibetan Plateau immediately north of the Himalayas, which exerts a strong influence on the easterly jetstream which flows from Tibet across the Arabian peninsula towards Somalia

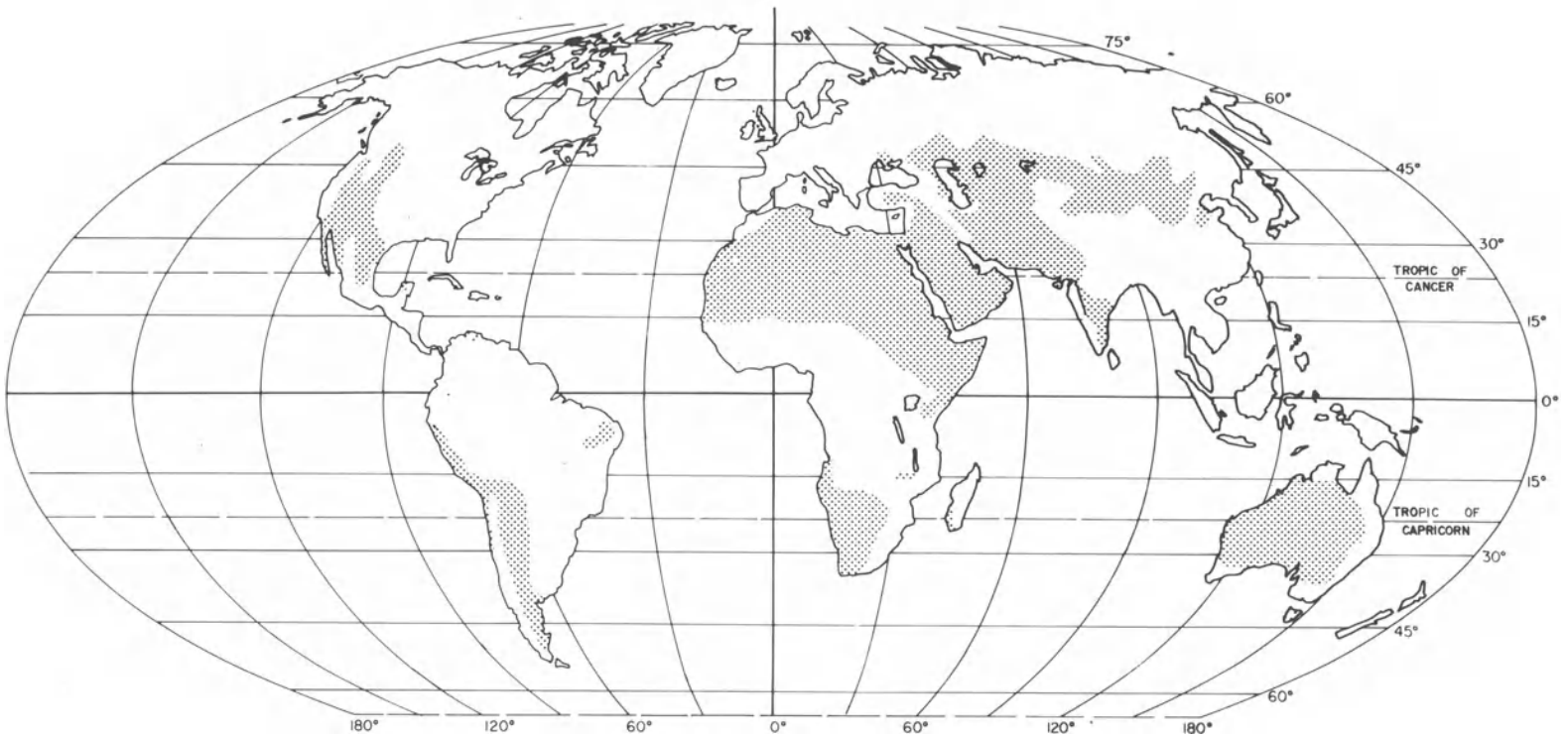

Figure 26.1 The semi-arid and arid regions of the world (after Crabb 1980, fig. 1).

(Rognon and Williams 1977, Flohn 1980), accentuating the aridity in those regions.

The previous discussion now requires some qualification, elaboration, and amendment. All of the 'relatively immutable' geographical controls over aridity alluded to in the previous paragraph are true only for the very late Cenozoic. Prior to that, lithospheric plate movements created a different and constantly changing distribution of land and sea, of warm and cold ocean currents, and of high and low terrestrial relief. We will discuss the climatic repercussions of Cenozoic plate tectonic movements in the final section of this chapter.

Even within the limited time frame of the Quaternary (*c.* 1.6 Ma), the sphere of influence of the deserts has waxed and waned from times of maximum expansion, such as from 18 to 12 ka, to times when Nile perch, crocodiles, and hippos swam in the lake-studded Sahara, such as from 11 to 7 ka. We will examine the causes and consequences of these Quaternary climatic fluctuations in the next two sections.

Finally, the role of prehistoric and historic human activities cannot be ignored. Trivial during Lower and Middle Palaeolithic times, when prehistoric world population was sparse, there are discernible signs of Upper Palaeolithic impact in many continents, especially through the widespread use of fire. The result was an increase in savanna at the expense of forest, and of grassland at the expense of woodland. With the onset of plant and animal domestication at the start of the Holocene, and the associated rapid increase in world population from roughly 10 million people at the start of the Neolithic (*c.* 10 ka) to roughly 100 million by 5 ka, increasing exponentially to a billion (10^9) by 2 ka (May 1978), the stage was set for unprecedented deforestation using polished stone axes and adzes initially, later to be replaced with bronze, iron, and steel.

Desertification is the general term used for a change to desert-like conditions in areas previously beyond the climatic limits of existing deserts (Mabbutt 1978b, 1985). It is brought about by a combination of poor land management (overgrazing, indiscriminate clearing of the vegetation cover, increased soil salinization) and prolonged local or regional intervals of drought. The result is a reduction in plant biomass, animal-carrying capacity, and overall ecological resilience and diversity, with occasionally catastrophic impacts on local pastoral and farming communities (Williams 1986, Glantz 1987). Despite eloquent but unsubstantiated claims to the contrary, there is no credible evidence that the deserts depicted on Figure 26.1 are the result of human action. Sweeping and apparently plausible assertions that the modern deserts are wholly or partly man-made (Ehrlich and Ehrlich 1970, p. 202) need to be placed in context. The expanding desert syndrome erupts after every severe drought, but the re-establishment of a modern plant cover along the desert margins during the wetter intervals between droughts is seldom mentioned. We return to this theme at the end of this chapter, after first examining the geomorphic history of our two largest tropical deserts: the Sahara and the arid inland of Australia.

GEOMORPHIC HISTORY OF THE SAHARA

PRECAMBRIAN TECTONIC LEGACY

The geomorphic history of the Sahara begins in the Precambrian, and the influence of the Precambrian tectonic and structural legacy is pervasive across North Africa and the Arabian Peninsula (Clifford and Gass 1970, Adamson and Williams 1980, 1987, Williams 1984a, Bowen and Jux 1987, El-Gaby and Greiling 1988). The Precambrian cover rocks are comparatively undeformed and unaltered, and appear to be of Middle and Upper Proterozoic age. They overlie the weakly to highly metamorphosed and strongly folded and faulted Archaean and Lower Proterozoic formations with a marked erosional unconformity and often form rugged plateaux, mesas, and monoclinal ridges of quartz arenite and conglomerate with intercalated dolerites and basalts. Other parts of Pangaea had a similar history of episodic Archaean and Lower Proterozoic metamorphism followed by prolonged intervals of widespread erosion and late Precambrian sedimentation. For example, the present-day landscapes of the Vindhyan Hills in north central India and the Arnhem Land Plateau in northern Australia differ from some of those in the western Sahara only in now being covered in savanna woodland.

Much of the Precambrian landscape is concealed beneath younger sedimentary and volcanic rocks in places up to 10 km thick, so that the real extent of outcropping Precambrian formations is limited to about 15% of the Sahara. Despite such limited outcrop, the influence of the ancient basement rocks of the Sahara is out of all proportion to their present surface distribution. In the past 20 years we have come to appreciate more and more that the patterns of Phanerozoic faulting, rifting, and volcanism, the emplacement of ring-complexes, and the distribution of major depocentres in arid northern Africa and

Arabia are a direct reflection of the pervading influence of geological structures which developed during the 650 to 550 Ma Pan-African orogenic event as well as during the 2000 to 1250 Ma Eburnean orogeny (Black and Girod 1970, Clifford and Gass 1970, Fabre 1974).

Later workers have shown how these early orogenic events have controlled the subsequent location of Phanerozoic uplands and sedimentary basins in the Sahara. Periodic reactivation of some of the major Precambrian structural trends has determined the location of Cenozoic faults, rifts, and volcanoes in northern Africa (UNESCO 1967, 1968, Vail 1972a, Adamson and Williams 1980, Williams 1984a, figure 3.6).

PALAEOZOIC AND MESOZOIC SEDIMENTATION

The Pan-African orogeny which reached its climax towards 550 Ma ago was followed by prolonged and widespread erosion which reduced much of the Sahara to a gently undulating plain. Renewed uplift towards 450 Ma heralded the late Ordovician glaciations of the Sahara (Beuf *et al.* 1971). Around the present Hoggar mountains some of the erosional evidence of these Ordovician ice caps is so well preserved that it almost appears to be Pleistocene. Melting of the Saharan ice caps was followed by the rapid and world-wide early Silurian rise in sea level, comparable to the glacio-eustatic sea level rise which followed melting of the late Pleistocene ice caps. Accumulation of Carboniferous mudstones, limestones and sandstones across the Sahara eventually gave way to Hercynian uplift in the western Sahara and Atlas associated with opening of the North Atlantic. Uplift and folding of the previously horizontal Palaeozoic sedimentary rocks triggered the Triassic and later erosion during which the woodlands of the northern Sahara were rapidly buried beneath the sandstones and mudstones laid down by Mesozoic rivers flowing from the south and east. Silicified tree-trunks, some still in upright positions of growth, are vivid indications of the speed and effectiveness of the Mesozoic fluvial aggradation. A hundred million years later, the prehistoric peoples of the Pleistocene Sahara were to use fragments of this silicified wood for stone toolmaking.

The early Mesozoic opening of the South Atlantic and the ensuing separation of the African and South American lithospheric plates resulted in a series of Mesozoic marine transgressions (Grove 1980). Much of the Sahara was relatively flat and low-lying at that time, and flanked by warm and shallow epi-continental seas. One such marine incursion flooded much of the central Sahara during the Upper Cenomanian and Lower Turonian (Raulais 1951), although the Hoggar uplands remained above sea level, as did much of the West African craton.

These Mesozoic marine and non-marine sedimentary formations comprise some of the greatest present-day aquifers in North Africa, and include the Nubian Sandstone Formation of the eastern Sahara and the Continental intercalaire (Kilian 1931) of the central Sahara. The more or less horizontal Mesozoic formations are scattered across the Sahara today in the form of extensive sandstone and limestone plateaux or hamada. Australia had a similar Mesozoic history, and there is little to distinguish the great stony tablelands and associated gibber plains of the present Australian desert from the vast gravel-strewn hamada and stony reg surfaces of the Sahara.

A classic example of a Saharan sandstone plateau or hamada is the Gilf Kebir in the now hyperarid desert of south-eastern Libya and south-western Egypt (Bagnold 1933, Sandford 1933, Peel 1939, 1941). The margins of the Gilf Kebir as well as those of other great sandstone plateaux in southern Libya, such as the three more recently explored hamada north-east of Tibesti (Williams and Hall 1965, Pesce 1968) are highly crenulated and deeply dissected by now inactive river valleys. Peel (1966) and many later observers have emphasized the former efficiency of such fluvial erosion, but perhaps the most eloquent testimony to these pluvial episodes – apart from the dry valleys themselves – are the great galleries of Upper Palaeolithic and Neolithic rock paintings and engravings of now vanished herds of elephants, giraffes, and domesticated cattle (Breuil 1928, Caporiacco and Graziosi 1934, Winkler 1939). More recently, Breed and her colleagues have made brilliant use of shuttle-imaging radar to identify Pleistocene and older river channels in the eastern Sahara (Breed *et al.* 1987). These now defunct watercourses flowed at least intermittently during the early to middle Pleistocene and at intervals thereafter, including the early to middle Holocene. During the early and middle Pleistocene, small bands of *Homo erectus* roamed the Sahara equipped with their all-purpose Acheulian toolkit of bifacially worked hand axes, cleavers and scrapers (Breed *et al.* 1987, McHugh *et al.* 1988). By Holocene times, the Palaeolithic hunters and gatherers had been replaced by Neolithic pastoralists who grazed their cattle throughout the Sahara (Williams and Faure 1980, Clark and Brandt 1984, McHugh *et al.* 1989).

CENOZOIC DEEP WEATHERING, UPLIFT, AND EROSION

Withdrawal of the shallow, equatorial Cretaceous seas from the Sahara was followed by a very long interval of intense early Tertiary weathering and leaching of the forested lowlands of the tectonically quiescent southern Sahara (Faure 1962). Near-surface solution and redeposition of iron and silica during the Palaeocene and Eocene gave rise to the resistant caprocks of ironstone or silicified rock which now protect many of the Mesozoic and Tertiary plateau summits from erosion. The present-day geomorphic outcome is a process of slow and episodic scarp retreat by undercutting of the less resistant mudstones and softer sandstones during wetter phases, followed by collapse of the resistant caprocks. The undercutting is effective even today, and is aided by seepage at the cliff base (Peel 1939, 1941), by salt weathering (Hume 1925) and by chemical weathering and deflation (Williams and Hall 1965). Similar processes of scarp retreat have been invoked to explain boulder-mantled debris slopes in the semi-arid north-west of South Australia (Jack 1915, Twidale 1960).

Post-Eocene uplift triggered a widespread phase of mid-Tertiary erosion within major massifs such as Tibesti and the Hoggar, as well as in more isolated ring-complexes such as Jebel Arkenu and Jebel 'Uweinat in south-east Libya or Adrar Bous in central Niger. The mid-Tertiary drainage system appears to have been a highly efficient and well-integrated system which kept pace with the various epeirogenic uplifts across the Sahara. The Nile cut down through Nubian Sandstone capping the Sabaloka ring complex to form the Sabaloka gorge north of Khartoum – one of the many instances of superimposed Cenozoic drainage in the Sahara (Grove 1980, Williams and Williams 1980). The early Tertiary mantle of deeply weathered rock was virtually removed from the uplands of the southern Sahara, leaving a bare and rugged landscape of gaunt rocky pinnacles and boulder-mantled slopes. Episodic deep weathering followed by episodic erosion and exhumation of the weathering front became the geomorphic norm of the later Cenozoic (Dresch 1959, Thorp 1969, Williams 1971). There seems little doubt that mid-Tertiary tectonic movements performed a dominant role in the initial pulse of erosion but the late Cenozoic climatic oscillations became increasingly important erosional pacemakers thereafter (Williams *et al.* 1987).

The sandy colluvial–alluvial debris eroded from the Saharan uplands was carried away from the mountains by the Tertiary and early Quaternary rivers to be in part deposited in late-Cenozoic marine deltas such as those of the Nile, the Niger, and the Senegal. However, a considerable proportion of the sediment began to accumulate in the closed interior basins created during the course of late Mesozoic and Cenozoic faulting, rifting and epeirogenic movements.

It was the unconsolidated Tertiary sediments laid down in large subsiding sedimentary basins such as the Kufra-Sirte basin in Libya, or the Chad basin, which provided the source material for the late Tertiary and Quaternary desert dunes. In the Chad basin, Servant (1973) identified wind-blown sands in a number of very late Tertiary stratigraphic sections. He concluded that the onset of aridity and the first appearance of desert dunes in this part of the southern Sahara was a late Tertiary phenomenon. Further north, in the Hoggar, some elements of the late Tertiary flora were already physiologically well adapted to aridity (Maley 1980a, b). If we accept the sedimentological evidence of Servant (1973) and the palynological evidence of Maley (1980a, b), then it follows that the onset of climatic desiccation and the ensuing disruption of the integrated mid-Tertiary Saharan drainage network was a feature of the very late Tertiary, long pre-dating the arrival of *Homo sapiens*. Before pursuing this topic in greater detail, we need to retrace our steps and examine the impact of Cenozoic volcanism, faulting, and rifting upon the Saharan landscape.

CENOZOIC VOLCANISM, UPLIFT, AND RIFTING

The basin and swell topography of the present-day Sahara (Fig. 26.2) is very largely a function of the Tertiary epeirogenic movements discussed earlier. An additional and extremely important factor was the massive extrusion of lava which accompanied and accentuated the late Cenozoic uplift of all the existing uplands, including the Ethopian Highlands, Jebel Marra, Tibesti, the Hoggar, and the Aïr.

An estimated 8000 km^3 of volcanic rock was erupted during the formation of Jebel Marra, and about half that amount (3000 km^3) during the eruptions which gave rise to Tibesti (Francis *et al.* 1973). The volcanic eruptions which helped to create Jebel Marra (elevation: 3088 m), Tibesti (3415 m) and the Hoggar (2918 m) were associated with significant uplift of the basement rocks which now lie beneath the late Cenozoic volcanic rocks. How much of this uplift took place during as opposed to before the eruptions is not known, but of the uplift itself there seems no doubt. Relative to the basement rocks on

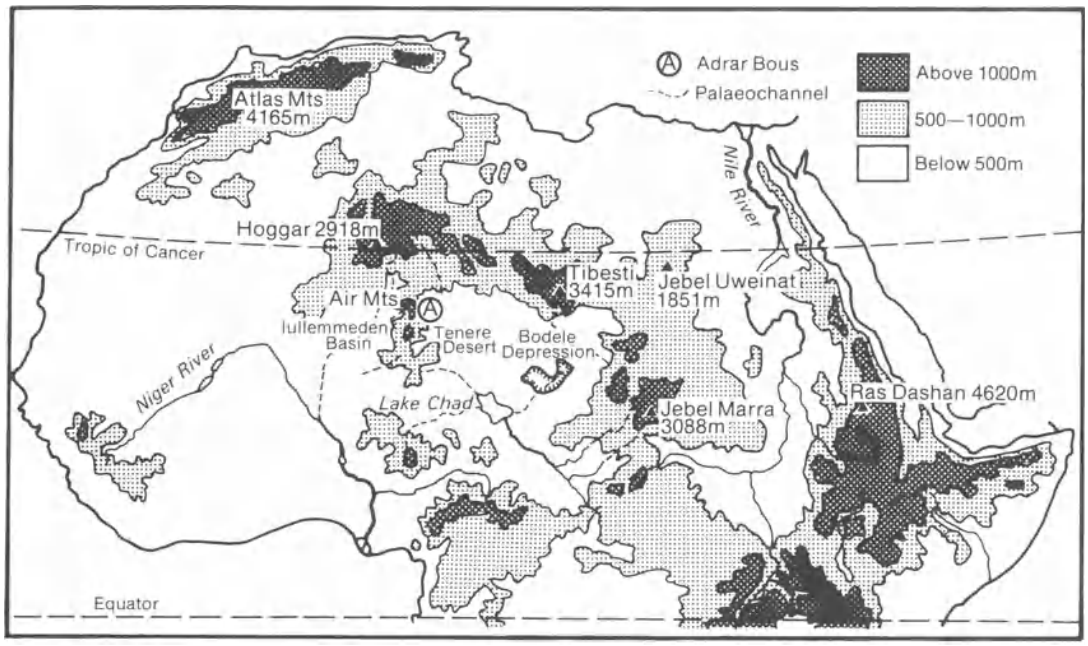

Figure 26.2 Relief map of northern Africa, showing distribution of major Saharan uplands and lowlands. Also shown is the locatioan of Adrar Bous ring-complex in the heart of the Sahara, immediately east of the northern Aïr massif, in the Tenere Desert of Niger (after Williams *et al.* 1987, fig. 1).

the adjacent plains, the basement rocks of Tibesti and the Hoggar have risen about 1000 m and those of Jebel Marra about 500 m (Bordet 1952, Vincent 1963, Vail 1972a, b). Much of the volcanic activity is of Miocene age and younger, and significant erosion of the crystalline basement rocks immediately preceded the volcanic activity and its erosional aftermath (Rognon 1967, Williams *et al.* 1980).

The timing of uplift in the Aïr massif is less well established (Williams *et al.* 1987), but the presence of possible Cretaceous sedimentary rocks at 1400 m on Tamgak granite plateau and very high (*c.* 1500 m) on the Goundai ring-complex (Vogt and Black 1963) suggests a possible 1000 to 2000 m of post-Cretaceous uplift. Given the late Cenozoic updoming of the Hoggar (Bordet 1952, Rognon 1967) and Jebel Marra (Vail 1972a, b) it seems likely that uplift of the Aïr is also of late Cenozoic age. The Mesozoic sedimentary formations south and west and Agadès all dip westwards away from the main Aïr massif and are again consistent with post-Cretaceous updoming of the massif.

Uplift of the Ethiopian Highlands is also a late Cenozoic event. Pollen grains characteristic of tropical lowland rainforests are abundant in Miocene lignites intercalated between basalt flows dated by K/Ar content at 8 Ma (Yemane *et al.* 1985). The basalts crop out at roughly 2000 m elevation near Gondar in the north-western Ethiopian uplands, suggesting roughly 2000 m of uplift in the past 8 m.y., or an average of 0.25 mm y^{-1}. The great depth and steepness of the Blue Nile gorge and the Tekazze gorge in central western Ethiopia is consistent with late Cenozoic uplift, and Faure has argued for an acceleration of uplift from Tertiary to Quaternary based on uplift rates of coral reefs along the Red Sea (Faure 1975). Since there is no necessary link between coastal uplift and uplift of the Ethiopian Highlands, the question is best left open. One thing is certain, however, and that is the enormous volume of rock eroded and removed from Ethiopia since extrusion of the Upper Oligocene and Miocene Trap Series basalts. The Blue Nile, the Tekazze, and their tributaries have removed about 100 000 to 200 000 km^3 of rock from the north-western Ethiopian uplands in the last 10 to 20 m.y., which is also equivalent to the volume of the Nile cone in the eastern Mediterranean (McDougall *et al.* 1975, Williams and Williams 1980). A comparison of modern rates of erosion in upland Ethiopia and mean geological rates of denudation persuaded Williams and Williams (1980) that uplift of the Ethiopian High-

lands was episodic, with prolonged intervals of relative stability between shorter intervals of rapid uplift. The abundance of montane forest podocarpus and juniper pollen in Pliocene sediments, which are now at low elevations in the lower Awash valley of the west-central Afar Desert (R. Bonnefille, pers. comm., 1991) also indicates that uplift of the Ethiopian uplands was accompanied by down-faulting and subsidence along the adjacent margins of the eastern Ethiopian escarpment (Adamson and Williams 1987).

The pattern of rifting in Ethiopia has created a very particular type of desert in the Afar Depression (Tiercelin 1987, Williams *et al.* 1986, Adamson and Williams 1987). The Afar is a lava desert and is one of the hottest and most forbidding deserts on Earth. Flanked by the mighty Ethiopian escarpment on the west, it descends over 150 m below sea level at Lake Asal, a salt lake now separated from the adjacent Red Sea by a puny Pleistocene lava dam.

Neogene fluviolacustrine sediments in southern Afar have yielded one of the longest, richest, and most complete records of fossil hominid evolution anywhere in Africa (Clark *et al.* 1984). Associated with these australopithecine hominid fossils are abundant superbly preserved Pliocene fossils of elephants, pigs, bovids, hippos, crocodiles, and sundry non-aquatic carnivores. The fauna is a savanna fauna, and most taxa belong to now extinct species. The presence of such fossils in parts of the Afar that do not now support much life, together with the presence of thick lacustrine deposits within the Neogene formations again raises the issue of possible late-Cenozoic climatic desiccation, a topic to which we now turn.

LATE CENOZOIC DESICCATION

Tertiary volcanism in the central and southern Sahara was preceded and accompanied by prolonged deep weathering. In central Niger kaolinitic and bauxitic weathering profiles up to 45 m thick are developed on rocks of Eocene to Precambrian age. Uplift in the mid-Tertiary resulted in a change from previously biogenic and chemical sedimentation in this region to dominantly clastic sedimentation (Faure 1962, Greigert and Pougnet 1967, p. 157). Rejuvenated rivers flowing down from the great watersheds of Tibesti, the Hoggar, and the Aïr deposited the fluvial gravels, sands, and clays of the 'Continental terminal' extensively around their parent uplands. Williams and co-workers have concluded that in Niger and adjacent areas 'the origin of the Sahara as a continental desert . . . may be said to stem from the Miocene Alpine orogeny and the subsequent stripping of the Eocene deep weathering profile' (Williams *et al.* 1987, p. 109). Apart from tectonic uplift, what other factors were responsible for this dramatic change from a landscape of lowland equatorial rainforest to one of bare rocky inselbergs and desert dunes?

A major influence, not mentioned so far, was the post-Palaeozoic northward drift of the African lithospheric plate. Triassic Africa was part of the Gondwana supercontinent, as were South America, Antarctica, Australia, and India. With the Jurassic and earlier separation of Gondwana into the two continents of West Gondwana (Africa and South America) and East Gondwana (Australia, Antarctica, and India) the stage was set for further break-up of these two large continents during the Cretaceous (Owen 1983).

The Cretaceous equator in Africa ran from southern Nigeria through central Chad and the northern Sudan into Arabia. During the late Mesozoic and Cenozoic, the African plate moved northward with a slow clockwise rotation (Habicht 1979). Early Cenozoic Africa was south of its present position by only a few degrees of latitude and came into contact with Europe as a result of a slight clockwise rotation during the Miocene and Pliocene. One outcome of the ensuing crustal deformation was the uplift of the Atlas, noted earlier, which was also coeval with volcanism and updoming of the Hoggar, Tibesti, Aïr and Jebel Marra uplands, creating the major elements of the topography depicted on Figure 26.2.

A further outcome of Africa's Mesozoic and Cenozoic northward drift and rotational movement was a corresponding southward shift of the equatorial rainforest. This zone once ran obliquely across the Sahara from Egypt and the northern Sudan southwestwards towards southern Nigeria. Aridity set in earlier in Morocco, Algeria, and Tunisia than in Egypt and the Sudan, as is evident from the abundance of Mesozoic and younger evaporite formations in the north-western Sahara, which by then had already reached dry tropical latitudes (Coque 1962, Conrad 1969, Williams 1980).

Three additional influences contributed to the late Cenozoic desiccation of the Sahara. These were the uplift of the Tibetan plateau, the build-up of continental ice in Antarctica and the Northern Hemisphere, and cooling of the world's oceans. We consider the possible causes of these phenomena in the final section of this chapter; our concern here is purely with their effects upon the Sahara.

Late Cenozoic uplift of the Himalayas and of the vast Tibetan plateau was associated with the inten-

sification (and perhaps the inception) of the easterly jet stream which today brings dry subsiding air to the deserts of Arabia and northern Africa. A major change in the flora and fauna of the Potwar plateau in the Siwalik foothills of Pakistan between 7.3 and 7.0 Ma may also be related to Himalayan uplift and is consistent with intensification of the Indian summer monsoon, if not with its origin at that time (Quade *et al.* 1989).

Accumulation of continental ice in Antarctica may seem somewhat remote from Saharan desiccation but was in fact of critical importance. Mountain glaciers were present on Antarctica early in the Oligocene, and a large ice cap was well established by 10 Ma (Shackleton and Kennett 1975). Continental ice was slower to form in the Northern Hemisphere but was present in high northern latitudes by 3 Ma, and possibly by 5 Ma, with a rapid increase in the rate of ice accumulation towards 2.5 to 2.4 Ma (Shackleton and Opdyke 1977, Shackleton *et al.* 1984). As temperatures declined over the poles, and sea surface temperatures at high latitudes grew colder, the temperature and pressure gradients between the Equator and the poles increased. There was a corresponding increase in Trade Wind velocities, and hence in the ability of these winds to mobilize and transport the alluvial sands of the Saharan depocentres and to fashion them into desert dunes. Higher wind velocities were also a feature of glacial maxima during the Pleistocene and were responsible for transporting Saharan desert dust far across the Atlantic (Parkin and Shackleton 1973, Parkin 1974, Williams 1975, Sarnthein 1978, Sarnthein *et al.* 1981). During the last glacial maximum at 25 to 18 ka, Australian desert dust was also blown as far as central Antarctica (Petit *et al.* 1981).

Late Cenozoic cooling of the ocean surface was also responsible for reducing intertropical precipitation. Galloway (1965) has noted that two-thirds of global precipitation now falls between latitudes 40°N and 40°S and depends upon effective evaporation from the warm tropical seas. The ocean surface cooling, which was linked to global cooling associated with high-latitude continental ice build up and enhanced cold bottom-water circulation, would help to reduce evaporation from the tropical seas, thereby reducing rainfall across North Africa.

The late Cenozoic desiccation which created the largest desert in the world was therefore a result of a number of factors. Northward drift of the African plate ultimately helped to disrupt the warm Tethys Sea with its abundant supply of moist maritime air. Northern Africa moved away from wet equatorial latitudes into the dry subtropics. Growth of the great continental ice sheets and cooling of the oceans saw a decrease in precipitation and an increase in the strength of the Trade Winds. At the start of the Oligocene there was a sharp drop in sea surface temperatures, with eventual global repercussions.

Sudano-Guinean woodland covered much of the Sahara during the Oligocene and early Miocene, having replaced the equatorial rainforest of Palaeocene and Eocene times. During the late Miocene and early Pliocene a xeric flora, well adapted to aridity, began to replace the earlier woodland, so that many elements of the present Saharan flora were already present during the late Pliocene, when aridity became even more severe across the Sahara and the Horn of Africa (Bonnefille 1976, 1980, 1983, Maley 1980b).

The combination of a reduction in plant cover and a trend towards more erratic rainfall had a profound impact on the late Cenozoic rivers of the Sahara. Big rivers capable of carving large valleys became seasonal or ephemeral. Integrated drainage systems became segmented and disorganized. Wind mobilized the sandy alluvium into mobile dunefields. Dunes formed barriers across river channels no longer competent to remove them. Dust storms left the desert topsoils depleted in clay, silt, and organic matter. The Sahara was now a true wilderness, as the Arabic word implies.

QUATERNARY CLIMATIC FLUCTUATIONS

Mid-Pliocene closure of the Panama isthmus towards 3.2 Ma paved the way for the rapid accumulation of continental ice sheets in high northern latitudes during the late Pliocene (Schnitker 1980, Loubere and Moss 1986, Prentice and Denton 1988). Oxygen isotope evidence from deep sea cores indicates that the onset of major Northern Hemisphere continental glaciations at 2.4 ± 0.1 Ma (Shackleton *et al.* 1984) also coincided with cooling in high southern latitudes (Kennett and Hodell 1986). The 2.3 to 2.5 Ma temperature drop is also evident in the south-eastern uplands of Ethiopia (Bonnefille 1983) and the dry northern interior of China, with the beginning of loess accumulation there now securely dated to 2.4 Ma (Heller and Liu 1982). In the north-western Mediterranean region, the presence of a Mediterranean vegetation adapted to winter rains and summer drought is already evident at 3.2 Ma, but it is not developed in its modern form until about 2.3 Ma (Suc 1984).

Magnetic susceptibility measurements of deep sea cores from the Arabian Sea and the eastern tropical Atlantic also reveal a change in the length of

astronomically controlled climatic cycles at this time. Prior to 2.4 Ma, the dominant cycles are the 23-ka and 19-ka precession cycles, but after 2.4 Ma, the 41-ka obliquity cycle becomes dominant (Bloemendal and de Menocal 1989).

Although the boundary between Pliocene and Pleistocene is now defined by the International Union of Geological Sciences as 1.6 Ma (Cowie and Bassett 1989), this somewhat arbitrary date should not obscure the fact that the continental glaciations characteristic of the Quaternary were ushered in by the dramatic fall in global temperatures towards 2.4 Ma.

There is now widespread recognition that the magnitude and frequency of the late Pliocene and Quaternary glaciations were strongly influenced by orbital perturbations. This recognition is thanks to the work of the brilliant Yugoslav astronomer and mathematician, Milutin Milankovitch, who was the first to persuade Quaternary scientists of the climatic importance of the Earth's orbital variations (Milankovitch 1920, 1930, Imbrie and Imbrie 1979, Berger 1981). The major cycles identified by Milankovitch, and for which he calculated the changes in insolation received on Earth at different seasons and latitudes for the successive stages of each cycle, are as follows. The 100-ka orbital eccentricity cycle is determined by the changing elliptical path of the Earth around the Sun. The changing tilt of the Earth's rotational axis gives the 41-ka obliquity cycle. The precession of the equinoxes varies with the changing distance between Earth and Sun and gives the 23-ka cycle.

Although the correlations between orbital perturbations, ice volume fluctuations, and glacio-eustatic sea level fluctuations are statistically significant and now well accepted (Chappell 1973, 1974, Hays *et al.* 1976), the relative influence of the various cycles has varied during the course of Quaternary time.

Scrutiny of oxygen isotope records from deep sea cores spanning the full duration of the Quaternary persuaded D.F. Williams *et al.* (1981) that the early Pleistocene from 1.8 to 0.9 Ma was subject to high-frequency but low-amplitude fluctuations in the oxygen isotope differences between glacial and interglacial maxima. In contrast, the last 0.9 Ma were characterized by high-amplitude but low-frequency fluctuations in oxygen isotopic composition (D.F. Williams *et al.* 1981). Since changes in the oxygen isotopic composition of benthic Foraminifera are very broadly a reflection of changes in global ice volume (Shackleton 1977, 1987), the changing pattern of glaciation during the Quaternary will also be reflected in variations in the severity and frequency of cycles of glacial aridity in the tropics.

Ruddiman and Raymo (1988) have recently demonstrated that the 100-ka orbital eccentricity cycle was dominant in North Atlantic cores during the last 735 000 years (i.e. during the Brunhes magnetic chron). Before then, during the Matuyama chron from 2.47 to 0.7 Ma, the 41-ka orbital cycle was dominant, reflected in more frequent but lower amplitude climatic fluctuations.

Given the powerful influence exerted by a cold North Atlantic upon both ice volume and precipitation in the Northern Hemisphere, certain palaeoclimatic inferences may be drawn with respect to the Pleistocene Sahara.

We have long known that the last glacial maximum in the Sahara was a time of accentuated aridity, with reactivation (or advance) of desert dunes up to 500 to 1000 km beyond their present southern limits (Grove 1958, Grove and Warren 1968, Talbot 1980, Williams 1975, 1985). During these times of glacial aridity and desert expansion, vast plumes of Saharan and Arabian desert dust were mobilized and blown far out to sea.

Over the past 0.6 m.y., maximum concentrations of Saharan desert dust in equatorial Atlantic deep sea cores coincide with times of low sea surface temperature or glacial maxima (Parmenter and Folger 1974, Bowles 1975). A similar pattern of glacial aridity is evident in the Red Sea and Gulf of Aden. Planktonic Foraminifera from deep sea cores collected in this region reveal through their changing isotopic composition that during the last 250 000 years, at least, glacial maxima were times of extreme aridity, with much increased sea surface salinity reflecting even higher local rates of evaporation than today (Deuser *et al.* 1976).

It would be misleading to portray all arid phases as coinciding with glacial maxima and all humid phases with peak interglacial times. The reality is both more complex and more interesting. Lake levels in Lake Chad (Servant 1973) and Lake Abhe (Gasse 1975) were high for at least 20 000 years before 18 ka when they fell rapidly. Lake Abhe remained dry until 12 ka, and Lake Chad intermittently dry until then, after which they both rose again rapidly, reaching peak levels towards 9 ka. Since about 4.5 ka these lakes have remained relatively low, with occasional short-lived transgressions. Very schematically, we could consider the interval of high lake levels from 30 to 18 ka as representing a humid glacial phase; the interval of low lake levels from 18 to 12 ka as an arid glacial

phase; the interval of early Holocene high lake levels as a humid interglacial phase; and the interval of late Holocene relatively low lake levels as a dry interglacial phase. Even this fourfold subdivision is a caricature of reality, and perforce ignores local hydrological and geomorphic controls over precipitation, runoff, evaporation, and groundwater inflow and seepage (Fontes *et al.* 1985, Abell and Williams 1989).

Whatever their ultimate causes (Kutzbach and Street-Perrott 1985, Gasse *et al.* 1990, Street-Perrott and Perrott 1990), the consequences of the alternating wetter and drier Quaternary climatic phases are very evident throughout the Sahara. For instance, at the isolated ring-complex of Adrar Bous in the geographical heart of the Sahara (Fig. 26.2), the geomorphic expressions of these past climatic fluctuations include active and stable dunes, lake strandlines and partially deflated lacustrine diatomites, alluvial fans, alluvial terraces, and partly buried palaeochannels and former backswamps (Fig. 26.3). The stratigraphic evidence is equally informative and extends well back into the middle Pleistocene (Williams *et al.* 1987). Phases of rapid erosion with associated deposition of coarse sands and gravels alternated with longer intervals of minimal erosion, fine-grained sedimentation in low energy environments, and soil development in and around the mountain (Williams 1971, 1976). The presence at Adrar Bous of late Pleistocene and Holocene freshwater snails and gastropods allows us to use palaeoecological and isotopic evidence (Williams *et al.* 1987) to test the inferences drawn from sedimentology and geomorphology, and additional evidence is yielded by prehistoric stone tool assemblages, hearths, graves, and middens, the last with burnt remains of locally consumed fauna (Clark *et al.* 1973, Smith 1980).

Similar Quaternary interdisciplinary or multidisciplinary studies are now the norm in different parts of the Sahara, so that despite its vastness and periodic difficulties of access, the Sahara has provided the best dated and most comprehensive evidence of late Quaternary environmental fluctuations so far available from any of our deserts. Among many excellent recent local or regional investigations, mention should be made of the very good interdisciplinary work now emerging from the Maghreb (Fontes *et al.* 1985, Causse *et al.* 1988, 1989, Gibert *et al.* 1990), the equally exciting work emanating from northern Sudan and southern Egypt (Ritchie and Haynes 1987, Brookes 1989, Kowalski *et al.* 1989, Szabo *et al.* 1989, Pachur *et al.* 1990), and the careful palynological and stratigraphic work now in progress along the southern and western margins of the Sahara (Fabre and Petit-Maire 1988, Lézine 1988a, b, 1989, Lézine and Casanova 1989, Lézine *et al.* 1990, Téhet *et al.* 1990).

GEOMORPHIC HISTORY OF THE AUSTRALIAN DESERT

The account which follows is distilled from more detailed discussions by Bowler (1976), Chen (1989), Shackleton and Kennett (1975), Veevers (1984), Williams (1984b, c, 1991), and Williams *et al.* (1991a).

PRECAMBRIAN TECTONIC LEGACY

Until about 2500 Ma, much of what is now western and northern Australia consisted of a granitic basement of Archaean rocks. Localized faulting and rifting created a vast regional sediment trap in northern Australia towards 2500 Ma. Over the next few hundred million years, intercalated marine and non-marine gravels, sands, and muds, together with volcanic rocks, accumulated within this depocentre, attaining a thickness of over 14 000 m. Major regional metamorphism ensued towards 1870 to 1800 Ma, during which the Lower Proterozoic sedimentary and volcanic formations, together with some of the adjacent basement rocks, were folded, faulted, and metamorphosed to form the Lower Proterozoic metasediments which crop out today as rocky strike-ridges in northern Australia. This period of regional metamorphism was followed by uplift, erosion, and by several minor episodes of granite intrusion and volcanic activity. For several tens of millions of years thereafter, prolonged erosion, interrupted by episodic faulting and uplift, ultimately created a Precambrian landscape of gently undulating relief with sporadic hills and shallow valleys. Thereafter, the region has been tectonically stable apart from slow epeirogenic uplift during the late Phanerozoic.

Several hundred metres of horizontal sands, interbedded lavas, and minor basal gravels were laid down across the early Precambrian land surface towards 1690 to 1650 Ma. These Middle and Upper Proterozoic sandstones are the older Precambrian cover rocks in northern Australia and today form rugged sandstone plateaux such as the Arnhem Land plateau with its joint-controlled gorges and steep erosional cliffs. These Precambrian cover rocks or plateau sandstones have protected the underlying Lower Proterozoic metasediments from subsequent erosion. Slow scarp retreat has gradually exhumed the original Precambrian topography, so that the

Figure 26.3 Geomorphic map of Adrar Bous ring-complex in the Tenere Desert of Niger, showing the major landforms and location of the stratigraphic sections discussed in the text (after Williams *et al.* 1987, fig. 3).

present relief of bevelled strike ridges and undulating rock-cut surfaces is, in parts, a resurrected and, except for the modern vegetation cover, a virtually unmodified Lower Proterozoic landscape.

PALAEOZOIC AND MESOZOIC SEDIMENTATION

Palaeozoic sandstones and limestones crop out in the less elevated parts of northern Australia but are conspicuously absent from the stable cratonic areas of western Australia as well as from the summits of the northern Precambrian plateaux.

During the early Cretaceous, towards 135 to 100 Ma, Australia consisted of three large islands separated by shallow seas. The two western islands were the Precambrian shield region of western Australia and the Precambrian and Palaeozoic uplands of northern and central Australia, indicating that these upland areas have had a long history of subaerial erosion.

Some of the present northern Precambrian plateaux, such as the Arnhem Land plateau, have a thin cover of Cretaceous sediments. These Cretaceous mudstones and sandstones also mantle the Lower Proterozoic and Archaean rocks north and west of Arnhem Land, where they are up to 200 m thick. Scarp retreat of the plateau has probably been accelerated by the uplift which followed the 110 Ma Aptian marine transgression, and may be a Cenozoic rather than a Cretaceous phenomenon, since the Cretaceous sediments are uniformly and deeply weathered wherever they occur. In central Australia, the horizontal Mesozoic formations often have a caprock of silcrete. Further north, in what are now the seasonally wet tropics, the caprock consists of ferruginous ironstone (laterite or ferricrete) or even of bauxite. Such deep weathering implies prolonged and efficient leaching under conditions of slow or ineffective mechanical erosion, and normally requires low gradients and high effective precipitation.

CENOZOIC DEEP WEATHERING, UPLIFT, AND EROSION

By late Cretaceous time, the sea had retreated from most of Australia, and in the centre and north there were several prolonged intervals of deep weathering of the newly emerged land surface. This prolonged weathering under conditions of tectonic stability was interrupted by minor intervals of mostly gentle uplift with local faulting and folding, notably in the middle to late Miocene.

At least three post-early Cretaceous erosion surfaces have been identified by different workers in central and northern Australia on the basis of elevation, laterite-capped remnants, and regional slope. Assuming that block-faulting can be ruled out, and assuming that the weathering mantle did indeed develop on a gently sloping surface, both of which at present are unproven assumptions, then the presence of such stepped surfaces is entirely consistent with episodic Cenozoic uplift and associated vertical and lateral erosion. The geomorphic evidence accords well with such an interpretation. Rejuvenation of the drainage in northern Australia has led to vertical incision and the development of rugged relief consisting of steep valleys, rocky strike ridges, boulder-mantled granite hills, and steep-sided sandstone plateaux.

LATE CENOZOIC DESICCATION

Until about 130 Ma, Australia, Antarctica, and Greater India were all part of East Gondwana. Very early in the Cretaceous a rift developed between Greater India and Australia–Antarctica, and the present Indian Ocean began to form. Sea-floor spreading was very rapid between 80 and 53 Ma, attaining rates up to 175 mm y^{-1}. The initial separation of Australia from Antarctica at 90 Ma was at first very slow and remained so until about 30 Ma. During the last 30 m.y., Australia has drifted north at a mean rate of roughly 50 to 70 mm y^{-1}. Concomitant rifting along the southern continental margin and the eastern edge of continental Australia led to separation of the Campbell Plateau, New Zealand, and the Lord Howe rise from Australia, and formation of the Tasman Sea, and, ultimately, of the Southern Ocean.

As Australia drifted north, the Eastern Highlands were the centre of sustained volcanism, although the locus of volcanic activity shifted south *pari passu* as Australia moved north. The Eastern Highlands were uplands well before the Tertiary, and sporadic uplift continued during the late Cretaceous and Cenozoic, even if the detailed pattern of uplift is still unclear. The west-flowing drainage of eastern Australia is thus very old, and great river basins such as the ancestral Murray–Darling were already in existence during the late Cretaceous.

In western Australia, early Cretaceous rifting, volcanism, uplift and later subsidence accompanied the separation of Greater India from Australia. Late Palaeocene to Eocene rifting also accompanied the separation of Australia from Antarctica. As a result of these tectonic upheavals, the once integrated network of drainage in western Australia became progressively disrupted from 130 to 40 Ma (early

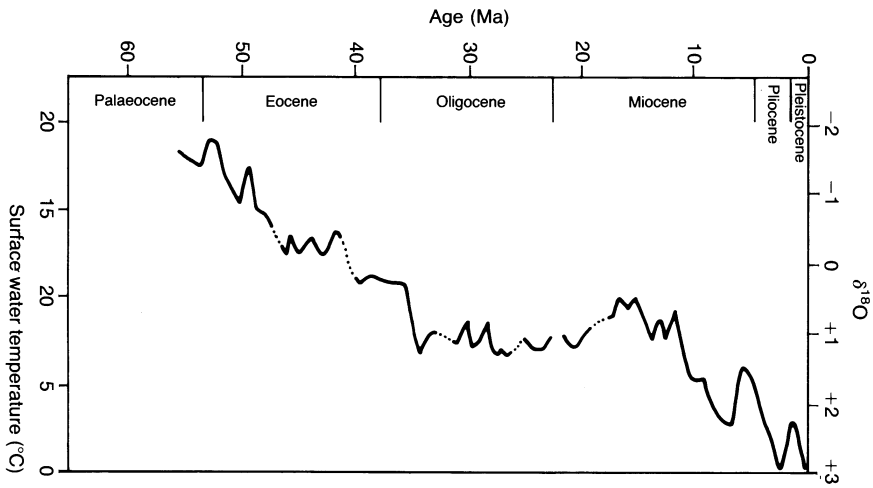

Figure 26.4 Cenozoic sea surface temperatures in the Southern Ocean deduced from changes in oxygen isotopic composition of planktonic Foraminifera at DSDP sites 277, 279, and 281 (after Shackleton and Kennett 1975, fig. 2).

Cretaceous to late Eocene), and the rivers became less and less active during the Oligocene and early Miocene. By mid-Miocene times (15 to 10 Ma), a conspicuous network of linear salt lakes occupied the western half of the Australian continent, a witness to early Cenozoic tectonic disruption and later Cenozoic climatic desiccation.

As Australia moved north away from Antarctica, it came increasingly under the influence of tropical climatic systems and dry, subsiding, anticyclonic air masses. The long-term reduction in precipitation and runoff is reflected in the late Cenozoic trend towards the endoreic and areic drainage systems which are today characteristic of roughly two-thirds of the continent. Cooling of the Southern Ocean accentuated the trend towards aridity evident in the changing flora and fauna of inland Australia. Figure 26.4 shows a fluctuating decline in Southern Ocean sea surface temperatures from roughly 19°C in the early Eocene to only 7°C in the Oligocene, associated with the progressive accumulation of ice in Antarctica discussed earlier in this chapter. The global cooling and ensuing intertropical desiccation which accompanied the late Pliocene expansion of continental ice sheets in North America added the final gloss to the late Cenozoic drying out of Australia's great inland rivers and lakes, which reached its full climax in the second half of the Quaternary.

QUATERNARY CLIMATIC FLUCTUATIONS

Recent palaeomagnetic, geomorphological, and geochemical investigations in the arid Amadeus Basin of central Australia have demonstrated that the onset of aridity did not become apparent until about the Jaramillo subchron (0.91 Ma) below the Brunhes–Matuyama palaeomagnetic boundary (Chen 1989). Before that time, from at least 5 Ma until about 0.9 Ma, the pattern of sedimentation in the Amadeus Basin was dominantly one of fluviolacustrine clay accumulation with intermittent drier intervals. Thereafter, quartz dune sands, groundwater evaporites, and wind-blown gypsum sands indicate an alternation between aridity and less arid intervals characterized by high regional groundwater levels and weak pedogenesis on stabilized dune surfaces (Chen 1989).

It is tempting to equate the change in regional climate evident in the change in depositional regime in central Australia to a change in global atmospheric circulation linked to the astronomically modulated cycles of changing global ice volumes and ocean temperatures. As a working hypothesis, we propose that aridity in both the Sahara and Australian deserts was more severe during the last 0.7 to 0.9 m.y. than previously, and was associated with a change from the low-amplitude, high-frequency 41 000-year obliquity cycle, which dominated the late Pliocene and first half of the Pleistocene, to the high-amplitude but low-frequency 100 000-year orbital eccentricity cycle, which has dominated the last three-quarter million years or more of the middle and late Pleistocene.

A criticism commonly levelled at those involved in palaeoclimatic reconstruction is that they take too little account of present-day climatic and geomorphic

processes and ignore the topographic and other constraints imposed by geography. Figures 26.5, 26.6 and 26.7 are an attempt to meet such criticism. Starting with a morphoclimatic portrayal of Australia today (Fig. 26.5), Figure 26.6 is a preliminary reconstruction of Greater Australia and New Guinea at 18 ka, when sea level was some 135 to 150 m lower than today, and much of Australia was significantly colder and more arid. The return to warmer and wetter post-glacial conditions is illustrated in Figure 26.7 and is broadly representative of interglacial times.

The combined influence of the climatic fluctuations of the past 30 000 years upon a reasonably typical portion of the south-eastern margin of the Australian arid zone is shown schematically in Figure 26.8. The stratigraphic sections indicate several episodes of hillslope instability, aeolian dust accumulation, soil development, migration of source-bordering dunes, and seasonal replenishment of alluvial sands. Few of these processes are very active today, but the sections themselves were created by the current epicycle of gully incision which is probably a result of changing land use as well as historical changes in rainfall seasonality and intensity (Williams *et al.* 1991b).

IMPACT OF CENOZOIC TECTONIC EVENTS AND CLIMATIC CHANGES ON DESERT LANDSCAPES

Throughout this chapter, we have been at pains to emphasize that many of the geomorphic attributes of our present-day deserts have a very ancient geological pedigree. We have stressed the role of Precambrian and early Phanerozoic tectonic inheritance in controlling the disposition of Mesozoic and Cenozoic uplands and lowlands in the Sahara. In Australia, we have seen that certain elements of the modern landscape are exhumed surfaces developed well before the final onset of Tertiary and Quaternary climatic fluctuations, and that some of these surfaces have been remarkably little altered since they were formed during the Precambrian. It is now appropriate to review some of the key tectonic and climatic events of the Mesozoic and Cenozoic which, directly or indirectly, had an important influence on the evolution of our modern deserts. For clarity and simplicity, these events are summarized in Table 26.1.

Both hemispheres played a decisive role in the events which culminated in the late-Cenozoic desiccation of what are now the great tropical and temperate deserts of the world. Since Cenozoic intertropical desiccation was intimately associated with the cooling of Antarctica, we begin with a discussion of tectonic and climatic events in the Southern Hemisphere.

Initial separation of Australia from Antarctica started at 90 Ma and was fully effective by 45 to 50 Ma. Later opening of the Drake Passage between South America and Antarctica towards 30 to 25 Ma resulted in the establishment of a circum-Antarctic ocean current. Antarctica was now thermally isolated from warmer ocean waters to the north, and rapid cooling ensued. In the Southern Ocean, the changing isotopic composition of both planktonic and benthic Foraminifera is evidence of a dramatic cooling of deep ocean water as well as surface water. Cumulative ice build-up in Antarctica saw the creation of mountain glaciers followed by the growth of a major ice cap, first in East Antarctica and later in West Antarctica. Australia, meanwhile, was moving north into dry subtropical latitudes. Within Australia, forest gave way to woodland, and woodland gave way to savanna. The net effects for Australia were climatic desiccation, progressive disruption of the drainage network, expansion of the desert, and successive plant and animal extinctions. We turn now to the Northern Hemisphere.

Collision between Greater India and Asia extends back to about 45 Ma, and by 20 to 15 Ma the resulting underthrusting of Greater India beneath Asia had resulted in early uplift of the Himalayas. This uplift continued at least intermittently during the Miocene, Pliocene and Quaternary and continues to this day. Development of the Indian monsoon during the late Miocene (or earlier) was one climatic outcome of this uplift. Another was the genesis of the easterly jet stream emanating from the Tibetan Plateau.

In East Africa, uplift and rifting created the Neogene depocentres with their unrivalled record of Pliocene and Pleistocene hominid evolution. The emergence of *Australopithecus afarensis*, a bipedal but small-brained early Pliocene hominid, may well be linked to the 6 to 5-Ma Messinian salinity crisis which led to the genetic isolation of Africa from Eurasia. During this terminal Miocene event, the Mediterranean Sea dried out completely, refilled and dried out again on about a dozen occasions, resulting in the accumulation of evaporites and anhydrite deposits up to a kilometre thick, representing roughly 6% of the total oceanic salt supply. The precursors to this 'salinity crisis' were the Miocene and earlier shrinking of the Tethys Sea (with an associated change to a more seasonal rainfall regime with lower annual precipitation) and the more immediate late Miocene glacio-eustatic drop in sea level caused by

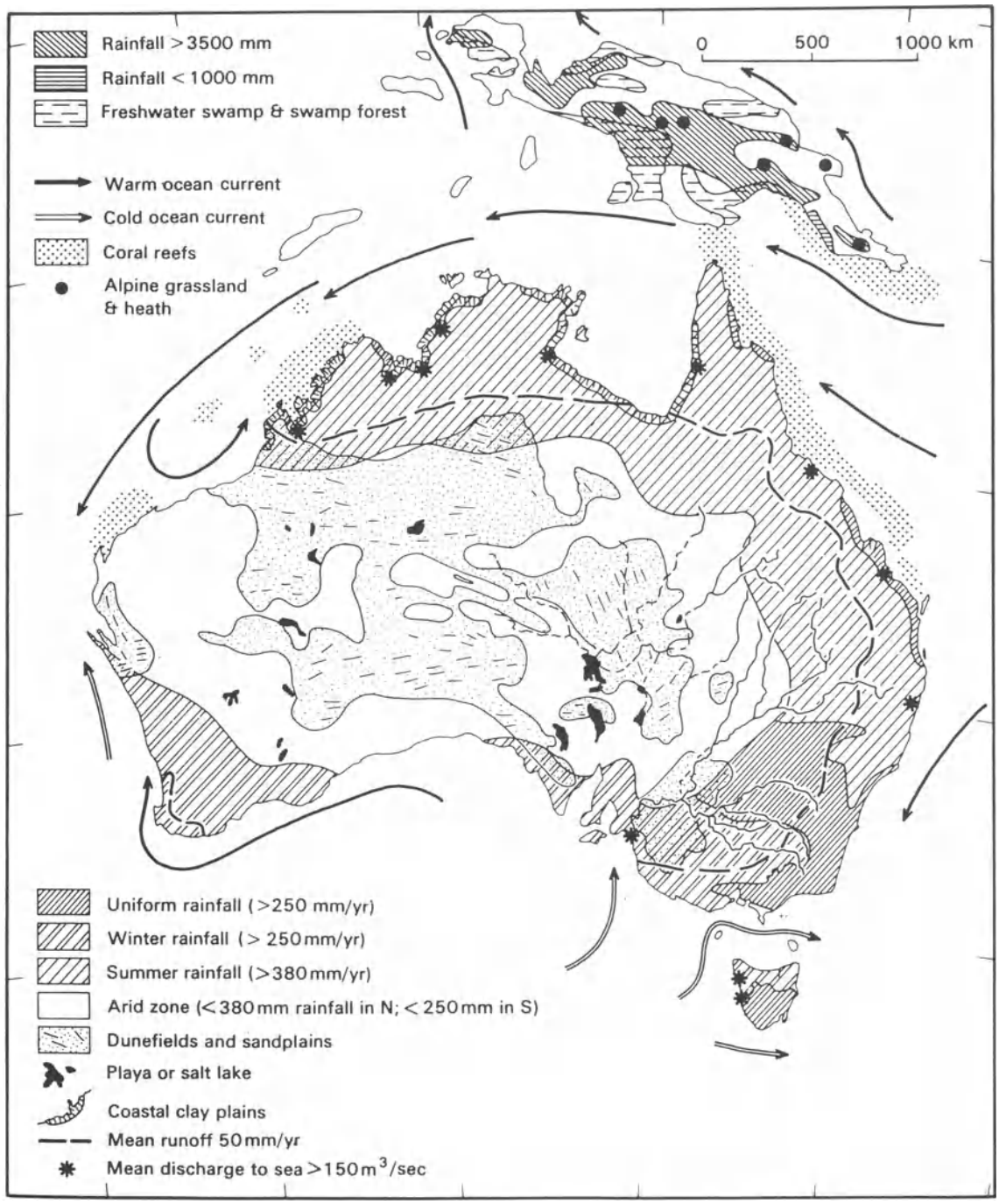

Figure 26.5 Morphoclimatic map of Australia–New Guinea at 0 ka (after Williams 1984c, fig. 37B).

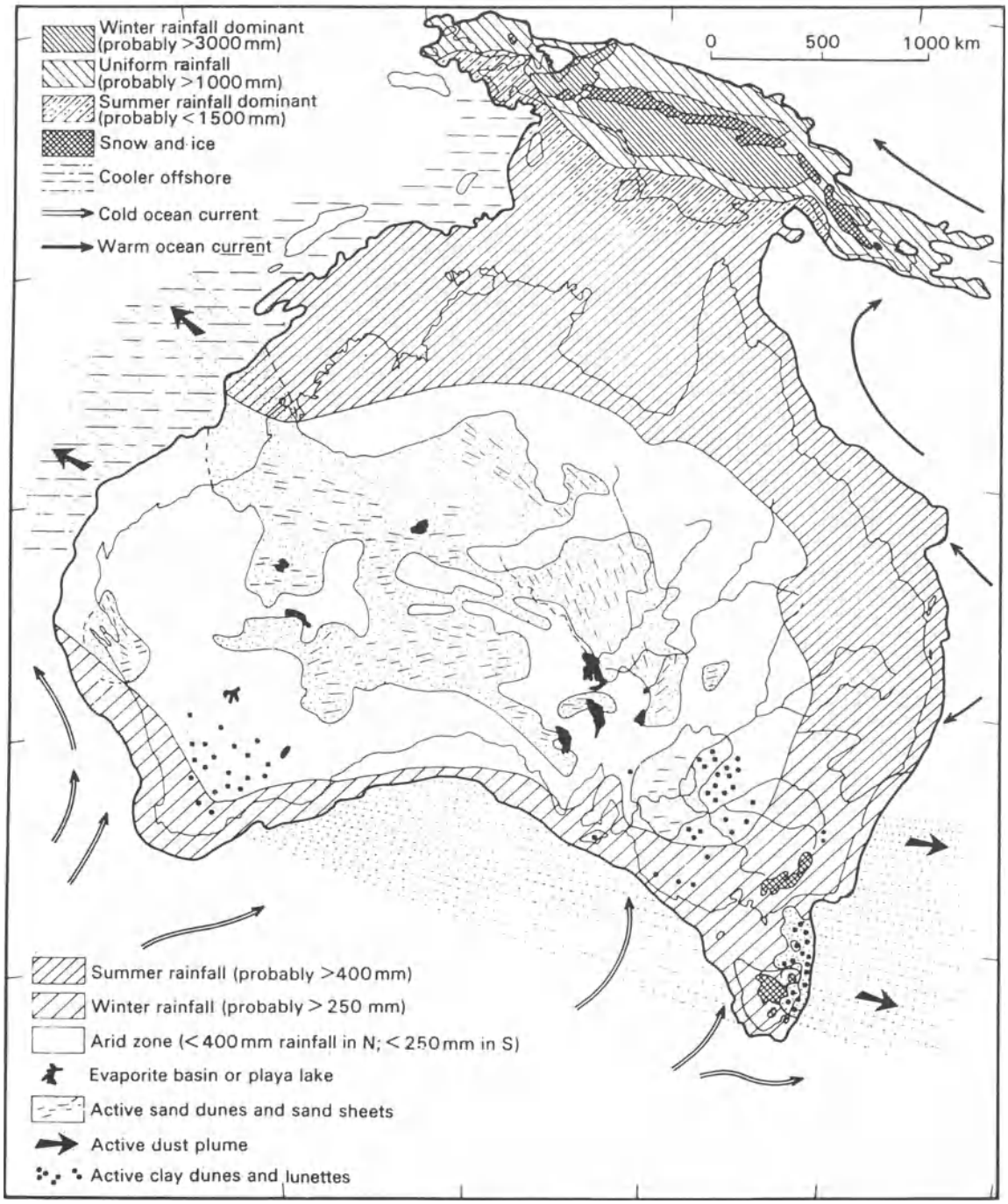

Figure 26.6 Morphoclimatic map of Australia–New Guinea at 18 ka (after Williams 1984c, fig. 37B).

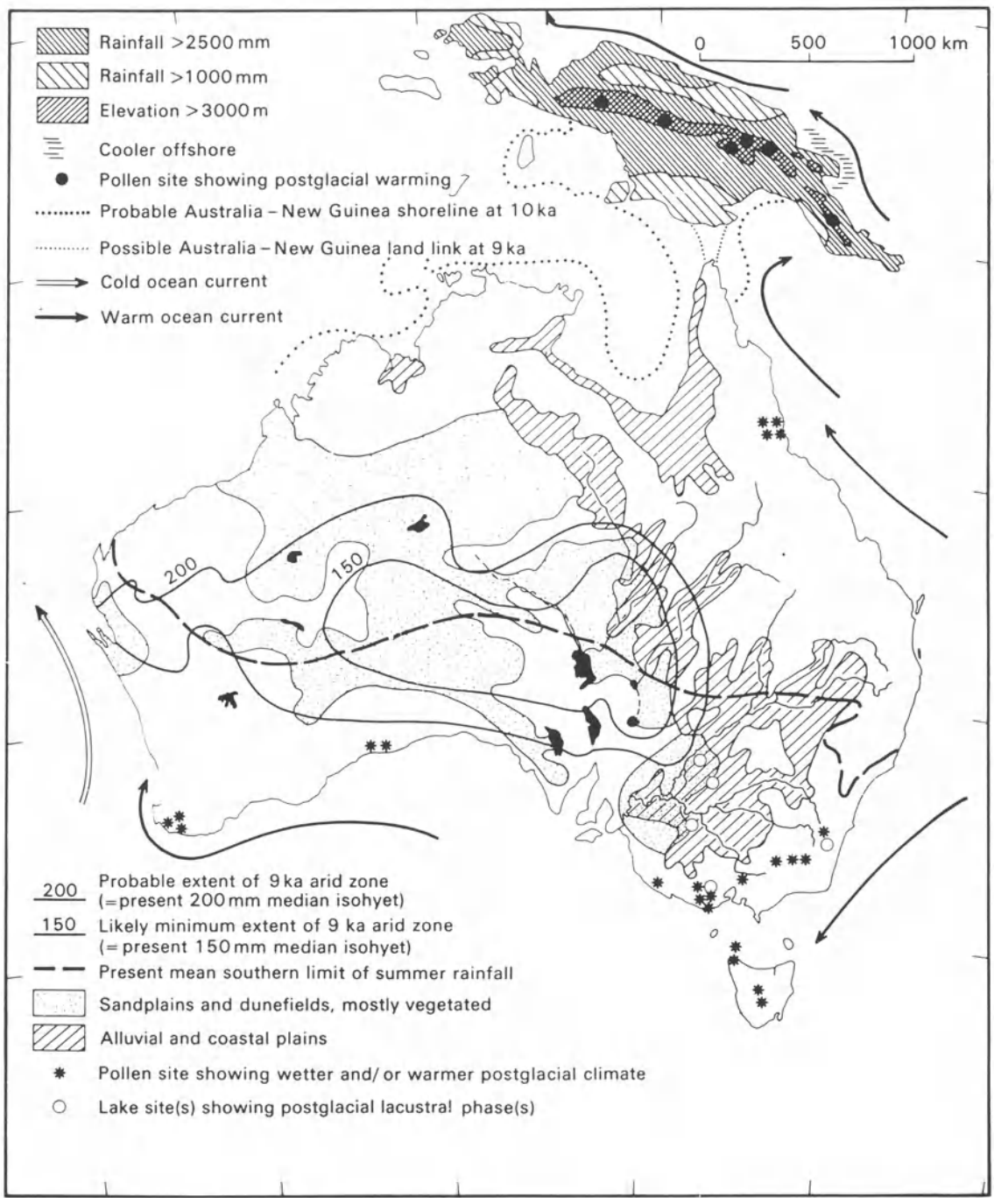

Figure 26.7 Morphoclimatic map of Australia–New Guinea at 9 ka (after Williams 1984c, fig. 37C).

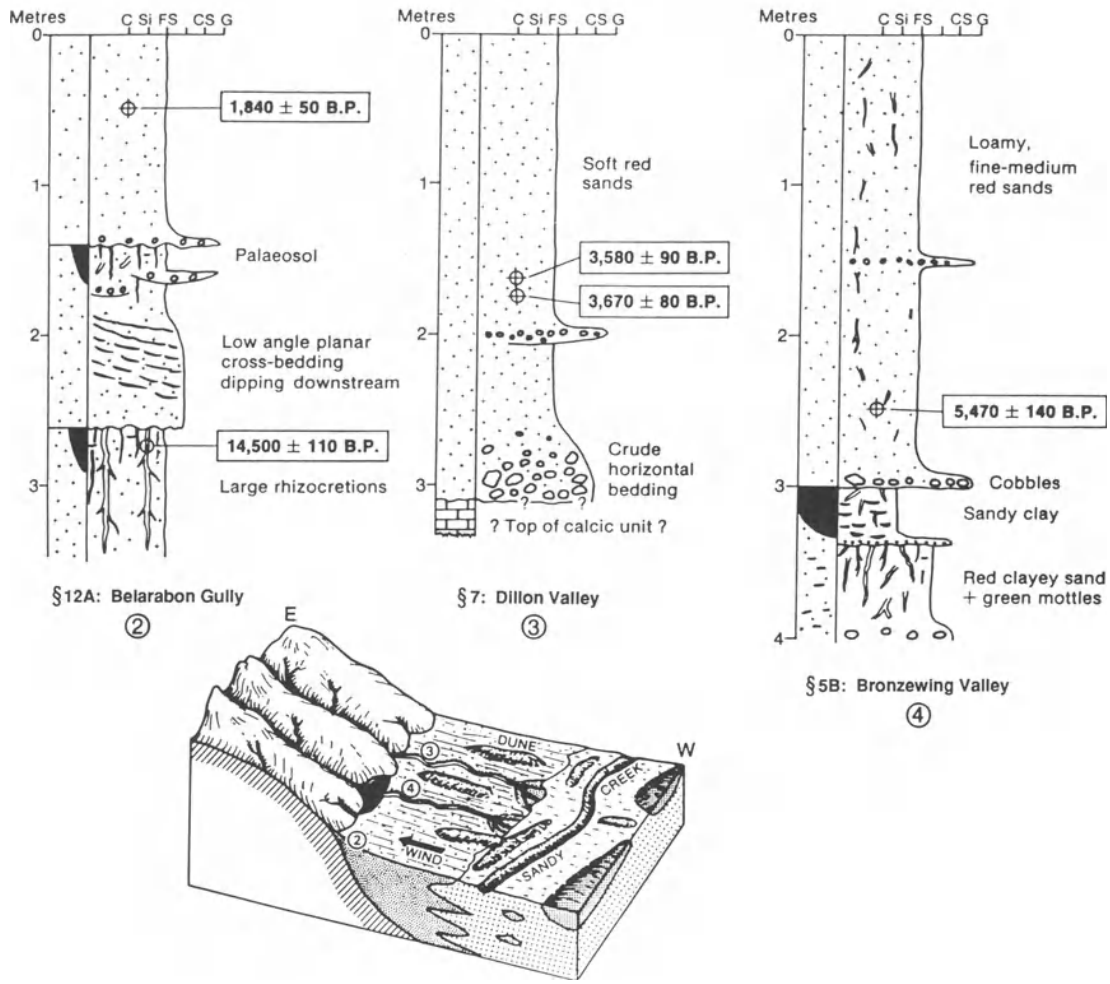

Figure 26.8 Late Quaternary piedmont deposits, Belarabon Range, central western New South Wales. Sandy Creek is today ephemeral, and the late Holocene source-bordering dunes are now vegetated and inactive. The older fanglomerates are late Pleistocene in age, as are the truncated palaeosols with their calcareous rhizocretions (after Williams *et al.* 1991b, fig. 5).

final accumulation of the West Antarctic ice cap. It was the 40-m fall in global sea level in the very late Miocene which exposed the Gibraltar sill separating the Atlantic from the Mediterranean, so that the Mediterranean became a closed basin in which evaporation greatly exceeded inputs from coastal rivers and local rainfall. The result was extreme aridity along the North African littoral, together with fluvial downcutting by the late Miocene Nile to carve a gorge over 1000 km long and up to 2 km deep at its northern end.

Late Pliocene cooling and desiccation towards 2.5 Ma caused the tropical lakes of the Sahara and East Africa to shrink, and in upland areas such as Ethiopia was associated with expansion of grassland at the expense of montane forest. It may be no coincidence that the first stone tools made to a replicated pattern make their first appearance at about this time, together with an increase in meat-eating by our hominid ancestors.

Northern polar cooling towards 15 Ma followed break-up of Laurasia. Antarctic cooling and ice build-up at about this time triggered a major change in ocean bottom water circulation. Pliocene closure of the Panama isthmus was indirectly responsible for enhanced snowfall in high northern latitudes, reflected in Arctic ice accumulation by 3.5 Ma and a rapid expansion of North American ice caps at

Table 26.1 Key tectonic and climatic events in the Mesozoic and Cenozoic relevant to the origin and development of our present-day deserts. Based on information from Adamson and Williams (1987), Macquarie Illustrated World Atlas (1984), National Academy of Sciences (1975), Owen (1983), Press and Siever (1986), Quilty (1984), and Van Andel (1985)

Era	*Date (Ma)*	*Period*	*Epoch*	*Tectonic event*	*Oceanic, climatic, and evolutionary events*
Palaeozoic				Final assembly of Pangaea	Land plants Early forests and trees Early reptiles
Mesozoic	245	Triassic		Opening of Atlantic Ocean	
	208	Jurassic		Pangaea breaking into Laurasia and Gondwana Africa, South America and India are separating from Antarctica Opening of South Atlantic Ocean Indian is moving northward Australia is still firmly part of Gondwanaland	Seaway through west Tethys embayment (200 Ma) Circum-global equatorial current Further warming of Earth Reduced lateral temperature gradient Early birds and mammals
	144	Cretaceous		Formation of Alps North Atlantic and Indian Oceans have widened Rift beginning to separate Africa and South America Separation of Africa from Antarctica (125 Ma)	Flowering plants evolve
Cenozoic	66	Tertiary	Paleocene	Opening of Norwegian Sea and Baffin Bay South America is separated from Africa Continents beginning to resemble their present shape	Ocean flows freely around the Equator Uniform climate and warm ocean, even near poles Temperate broadleaf forests in southern continents No evidence of even minor glaciation
	57		Eocene	Separation of Australia and Antarctica Australia moving northward into subtropics Crowding together of ridges and islands in western Pacific Ocean	Major climatic deterioration (50 to 46 Ma) Start of Cenozoic climatic decline First mountain glaciers in Antarctica (38 Ma) Seaway between Antarctica–Australia fully open (38 Ma)
	37		Early Oligocene	Closure of Tethys in Middle and Near East (35 to 30 Ma) Spain approaching North Africa, formation of Mediterranean Sea Collision of India with Asia	Major climatic deterioation (37 to 35 Ma) Drastic cooling of surface water in far south Equatorial flow weakened, cooler waters turning north and south Deep ocean basins about 10°C cooler, extinction of many bottom dwelling organisms Even cooler water returned to Equator along west coasts of continents, reducing evaporation and hence rainfall there
			Late Oligocene	Opening of Drake Passage (30 to 25 Ma)	Circum-Antarctic current established (30 to 25 Ma) First evidence for Antarctic glaciers at sea level
	24		Early Miocene	Separation of Greenland and Norway produced major seaway in early Miocene Formation of Himalayan Mountains (20 Ma) Uplands and rifts developing in Africa (20 Ma)	Accelerated production of very cold water and modern abyssal circulation

Table 26.1

Era	*Date (Ma)*	*Period*	*Epoch*	*Tectonic event*	*Oceanic, climatic, and evolutionary events*
		Tertiary	Middle Miocene	Mid-Miocene sinking of Iceland–Faroe Ridge	North Atlantic water able to travel south
				Africa meets Europe, mountain building (17 Ma)	Increased precipitation augmented snowfall on southern continent
				Circum-Mediterranean uplift (15 Ma)	Arctic ice cap develops (20 to 15 Ma)
					Change from forest to woodlands in Australia (15 Ma)
					Major climatic deterioration (12 to 10 Ma)
					Growth of Northern Hemisphere mountain glaciers (10 Ma)
			Late Miocene		Sharp global cooling and aridity (6 Ma)
					Glacial advances in Southern Hemisphere at high latitudes (6 to 5 Ma)
					Global fall in sea level due to large ice volume (6 to 5 Ma)
					Isolation of Mediterranean, evaporated to dryness, lowered global oceanic salinity by 6%
					Increasing Equator to poles temperature contrast
					Colder ocean, reduction in continental rainfall
					Replacement of forest with savanna in East Africa and South Asia
					Forest dwelling primates coming out into open (ancestors of *Homo sapiens*?)
	5.3		Early Pliocene	Isthmus of Panama closes, linking North and South America (5 Ma)	Gulf Stream intensified in North Atlantic, providing more moisture for growth of ice in north
				Change in rotation of Pacific plate (5 to 3 Ma)	Global warming and high sea levels (5 to 3 Ma)
				Fusion of Indian and Arabian plates (5 to 3 Ma)	Probable retreat of Antarctic ice sheet (5 to 3 Ma)
					Moist relative to late Miocene (5 to 3 Ma)
					Appearance of hominids – *Australopithecus* (4 Ma)
			Late Pliocene	Rapid elevation of Himalayas–Tibetan Plateau (3 to 2 Ma)	Ice caps form in Northern Hemisphere (3 Ma)
					Global cooling, growth of Antarctic ice sheet (3 to 2 Ma)
					Aridity increased (3 to 2 Ma)
					Establishment of Indian and Asian monsoons (3 to 2 Ma or earlier)
					Onset of strongly seasonal Mediterranean climate (3 to 2 Ma)
					Onset of loess deposition in China (3 to 2 Ma)
					Stone tools appear – *Homo habilis* (3 to 2 Ma)
	2	Quaternary	Pleistocene		World-wide glaciations

2.5 Ma. Initiation of the Laurentide ice sheet ushered in the late Pliocene and Quaternary glacial–interglacial cycles, with consequent glacio-eustatic sea level oscillations and a global pattern of spatially and temporally alternating morphogenetic systems. Glacial maxima were times of desert expansion and desert retreat. During at least the last 0.7 m.y., each cycle was roughly 100 ka long and modulated by the 100-ka orbital eccentricity cycle.

The net effects of the late Cenozoic changes in tectonics, climate, and ocean circulation were therefore a global increase in latitudinal temperature gradients and in the seasonal incidence of rainfall, final evolution of the incipient deserts into regions of scanty and unreliable rainfall, and the emergence in Africa of upright-walking, stone toolmaking ancestral humans who later discovered how to make and use fire, and ultimately occupied every continent except Antarctica.

The story of the Cenozoic tectonic and climatic events which culminated in the slow emergence of the world's great deserts is thus also, in a very real sense, the story of the global environmental changes which were associated with the origins of the first humans in Africa some 2.5 m.y. ago. From that time on, humans began to modify their habitats, sometimes contributing unwittingly to desertification or local expansion of the desert environment. Notwithstanding our destructive proclivities, the great deserts would be where they are even if humans had never appeared on the face of this Earth. We must needs learn to live with our Cenozoic inheritance.

ACKNOWLEDGEMENTS

The fieldwork on which this review is based was supported financially by the Australian Research Council, the National Science Foundation, and the Royal Geographical Society, to all of whom we are deeply grateful. Helen Quilligan gave much appreciated help in compiling Table 26.1. We owe warm thanks to Gary Swinton and Jan Liddicut of Monash University for their care with the figures and manuscript, respectively.

REFERENCES

Abell, P.I. and M.A.J. Williams 1989. Oxygen and carbon isotope ratios in gastropod shells as indicators of palaeoenvironments in the Afar region of Ethiopia. *Palaeogeography, Palaeoclimatology, Palaeoecology* **74**, 265–78.

Adamson, D.A. and F. Williams 1980. Structural geology, tectonics and the control of drainage in the Nile Basin. In *The Sahara and the Nile*, M.A.J. Williams and H. Faure (eds), 225–52. Rotterdam: Balkema.

Adamson, D.A. and M.A.J. Williams 1987. Geological setting of Pliocene rifting and deposition in the Afar Depression of Ethiopia. *Journal of Human Evolution* **16**, 597–610.

Bagnold, R.A. 1933. A further journey in the Libyan Desert. *Geographical Journal* **82**, 103–29, 403–4.

Berger, A.L. 1981. The astronomical theory of palaeoclimates. In *Climatic variations and variability: facts and theories*, A. Berger (ed.), 501–2. Dordrecht: D. Reidel.

Beuf, S., B. Bijou-Duval, O. De Charpal, P. Rognon *et al.* 1971. Les Grès du Paléozoique inférieur au Sahara. *Publication de l'Institut français du Pétrole*. Paris: Technip.

Black, R. and M. Girod 1970. Late Palaeozoic to Recent igneous activity in West Africa and its relationship to basement structure. In *African magmatism and tectonics*, T.N. Clifford and I.G. Gass (eds), 185–210. Edinburgh: Oliver and Boyd.

Bloemendal, J. and P. de Menocal 1989. Evidence for a change in the periodicity of tropical climate cycles at 2.4 Myr from whole-core magnetic susceptibility measurements. *Nature* **342**, 897–900.

Bonnefille, R. 1976. Implications of pollen from the Koobi Fora Formation, East Rudolf, Kenya. *Nature* **264**, 403–7.

Bonnefille, R. 1980. Vegetation history of savanna in East Africa during the Plio-Pleistocene. *IV International Palynological Conference* **3**, 78–89.

Bonnefille, R. 1983. Evidence for a cooler and drier climate in the Ethiopian uplands towards 2.4 myr ago. *Nature* **303**, 487–91.

Bordet, P. 1952. Les appareils volcaniques récents de l'Ahaggar. *Monographic Régionale. Algérie* 1: No. 11, 19^{e} Congrès de Géologie Internationale, Alger.

Bowen, R. and U. Jux 1987. *Afro Arabian geology. A kinematic view*. London: Chapman & Hall.

Bowler, J.M. 1973. Clay dunes: their occurrence, formation and environmental significance. *Earth-Science Reviews* **9**, 315–38.

Bowler, J.M. 1976. Aridity in Australia: age, origins and expression in aeolian landforms and sediments. *Earth-Science Reviews* **12**, 279–310.

Bowles, F.A. 1975. Palaeoclimatic significance of quartz/illite variations in cores from the eastern equatorial North Atlantic. *Quaternary Research* **5**, 225–35.

Breed, C.S., J.F. McCauley and P.A. Davis 1987. Sand sheets of the eastern Sahara and ripple blankets on Mars. In *Desert sediments: ancient and modern*, L. Frostick and I. Reid (eds), 337–59. Geological Society Special Publication No. 35.

Breuil, H. 1928. Les gravures du Djebel Ouenat. *Revue Scientifique, Paris* **66**(4), 125–7.

Brookes, I.A. 1989. Early Holocene basinal sediments in the Dakhleh Oasis region, south central Egypt. *Quaternary Research* **32**, 139–52.

Caporiacco, L. and P. Graziosi 1934. *Le pitture rupestri di Ain Doua (El Auenat)*. Firenze: Centro di Studi Coloniali.

Causse, C., G. Conrad, J.-C. Fontes, F. Gasse, *et al.* 1988. Le dernier humide pléistocène du Sahara nord-occidental daterait de 80–100 000 ans. *Compte Rendu de l'Académie des Sciences de Paris* **306**, II, 1459–64.

Causse, C., R. Coque, J.-C. Fontes, F. Gasse, *et al.* 1989. Two high levels of continental waters in the southern

Tunisian chotts at about 90 and 150 ka. *Geology* **17**, 922–5.
Chappell, J. 1973. Astronomical theory of climatic change: status and problem. *Quaternary Research* **3**, 221–36.
Chappell, J. 1974. Relationships between sealevels, $^{18}0$ variations and orbital perturbations, during the past 250,000 years. *Nature* **252**, 199–202.
Chen, X.Y. 1989. Lake Amadeus, central Australia: modern processes and evolution. Unpublished Ph.D. thesis, Australian National University, Canberra.
Clark, J.D. and S.A. Brandt (eds) 1984. *From hunters to farmers. The causes and consequences of food production in Africa*. Berkeley: University of California Press.
Clark, J.D., M.A.J. Williams and A.B. Smith 1973. The geomorphology and archaeology of Adrar Bous, Central Sahara: a preliminary report. *Quaternaria* **17**, 245–97.
Clark, J.D., B. Asfaw, G. Assefa, J.W.K. Harris, *et al.* 1984. Palaeoanthropological discoveries in the Middle Awash Valley, Ethiopia. *Nature* **307**, 423–8.
Clifford, T.N. and I.G. Gass 1970. *African magmatism and tectonics*. Oliver & Boyd, Edinburgh.
Cooke, H.B.S. 1958. Observations relating to Quaternary environments in east and southern Africa. *South African Geological Society Bulletin* 20, annexure.
Cooke, R.U. and A. Warren 1973. *Geomorphology in deserts*. London: Batsford.
Conrad, G. 1969. *L'évolution continentale post-hercynienne du Sahara algérien*. (Saoura, Erg Chech-Tanezrouft, Ahnet-Mouydir). Paris: CNRS.
Coque, R. 1962. *La Tunisie présaharienne, étude géomorphologique*. Paris: A. Colin.
Cowie, J.W. and M.G. Bassett 1989. 1989 global stratigraphic chart, with geochronometric and magnetostratigraphic calibration. *Supplement to Episodes* **12**(2), June 1989.
Crabb, P. 1980. Alluvium and agriculture in the semi-arid world. In *A land between two Niles*, M.A.J. Williams and D.A. Adamson (eds), 1–11. Rotterdam: Balkema.
Dresch, J. 1959. Notes sur la géomorphologie de l'Air. *Bulletin de l'Association de Géographes français* **280-81**, 2–20.
Deuser, W.G., E.H. Ross and L.S.Waterman 1976. Glacial and pluvial periods: their relationship revealed by Pleistocene sediments of the Red Sea and Gulf of Aden. *Science* **191**, 1168–70.
Eberz, G.W., F.M. Williams and M.A.J. Williams 1988. Plio-Pleistocene volcanism and sedimentary facies changes at Gadeb prehistoric site, Ethiopia. *Geologische Rundschau* **77**, 513–27.
Ehrlich, P.R. and A.H. Ehrlich 1970. *Population, resources, environment*, 2nd edn. San Francisco: Freeman.
El-Gaby, S. and R.O. Greiling (eds) 1988. *The Pan-African belt of northeast Africa and adjacent areas*. Braunschweig: Vieweg & Sohn.
Fabre, J. 1974. Le Sahara: un musée géologique. *La Recherche* **42**(5), 140–52.
Fabre, J. and N. Petit-Maire 1988. Holocene climatic evolution at 22–23° from two palaeolakes in the Taoudenni Area (Northern Mali). *Palaeogeography, Palaeoclimatology, Palaeoecology* **65**, 133–48.
Faure, H. 1962. Reconnaissance géologique des formation-post-paléozoiques du Niger oriental. *Mémoire du Bureau de Recherches Géologiques et Minières* (Dakar) (1966) No. 47.
Faure, H. 1975. Recent crustal movements along the Red Sea and Gulf of Aden coasts in Afar (Ethiopia and TFAI). *Tectonophysics* **29**, 479–86.
Flint, R.F. 1959a. Pleistocene climates in eastern and southern Africa. *Bulletin of the Geological Society of America* **70**, 343–74.
Flint, R.F. 1959b. On the basis of Pleistocene correlation in East Africa. *Geological Magazine* **96**, 265–84.
Flohn, H. 1980. The role of the elevated heat source of the Tibetan Highlands for the large-scale atmospheric circulation (with some remarks on paleoclimatic changes). In: *Proceedings of Symposium on Qinghai-Xizang (Tibet) Plateau (abstracts), Beijing*, China, May 25 – June 1, 1980. Beijing: Academia Sinica.
Fontes, J.C., F. Gasse, Y. Callot and J.-C. Plaziat, *et al.* 1985. Freshwater to marine-like environments from Holocene lakes in northern Sahara. *Nature* **317**, 608–10.
Francis, P.W., R.S. Thorpe and F. Ahmed 1973. Setting and significance of Tertiary–Recent volcanism in the Darfur Province of Western Sudan. *Nature Physical Science* **243**, 30–2.
Frostick, L.E. and I. Reid (eds) 1987. *Desert sediments: ancient and modern*. Geological Society Special Publication No. 35.
Galloway, R.W. 1965. A note on world precipitation during the last glaciation. *Eiszeitalter and Gegenwart* **16**, 76–7.
Gasse, F. 1975. L'évolution des lacs de l'Afar Central (Ethiopie et TFAI) du Plio-Pléistocène à l'Actuel. D.Sc. thesis, University of Paris VI.
Gasse, F., R. Téhet, A. Durand, E. Gibert, *et al.* 1990. The arid–humid transition in the Sahara and the Sahel during the last deglaciation. *Nature* **346**, 141–6.
Gibert, E., M. Arnold, G. Conrad, P. De Deckker, *et al.* 1990. Retour des conditions humides au Tardiglaciaire au Sahara septentrional (sebkha Mellala, Algérie). *Bulletin de la Société Géologique de France* **3**, 497–504.
Glantz, M.H. (ed.) 1987. *Drought and hunger in Africa: denying famine a future*. Cambridge: Cambridge University Press.
Greigert, J. and R. Pougnet 1967. Essai de description des formations géologiques de la République du Niger. *Mémoires du Bureau de Recherches Géologiques et Minières* (Dakar) No. 48, 1–236.
Grove, A.T. 1958. The ancient erg of Hausaland and similar formations on the south side of the Sahara. *Geographical Journal* **124**, 528–33.
Grove, A.T. 1980. Geomorphic evolution of the Sahara and the Nile. In *The Sahara and the Nile*, M.A.J. Williams and H. Faure (eds), 7–16. Rotterdam: Balkema.
Grove, A.T. and A. Warren 1968. Quaternary landforms and climate on the south side of the Sahara. *Geographical Journal* **134**, 194–208.
Habicht, J.K.A. 1979. Paleoclimate, paleomagnetism, and continental drift. *AAPG Studies in Geology No. 9*. Tulsa, Oklahoma: American Association of Petroleum Geologists.
Hays, J.D., J. Imbrie and N.J. Shackleton 1976. Variations in the earth's orbit: pacemaker of the ice ages. *Science* **194**, 1121–32.
Heller, F. and T.-S. Liu 1982. Magnetostratigraphical dating of loess deposits in China. *Nature* **300**, 431–3.
Hume, F.W. 1925. *Geology of Egypt*, Volume 1. Cairo: Government Press.
Imbrie, J. and K.P. Imbrie 1979. *Ice ages: solving the mystery*. London: Macmillan.
Jack, R.L. 1915. The geology and prospects of the region to

the south of the Musgrave Ranges and the geology of the western portion of the Great Artesian Basin. *Bulletin of the Department of Mines, South Australia* **5**, 72.

Kennett, J.P. and D.A. Hodell 1986. Major events in Neogene oxygen isotopic records. *South African Journal of Science* **82**, 497–8.

Kilian, C. 1931. Des principaux complexes continentaux du Sahara. *Compte rendu de la Société géologique de France, 1928–31*, 109–11.

Kowalski, K., W. Van Neer, Z. Brocheński, M. Mlynarski, *et al.* 1989. A last interglacial fauna from the eastern Sahara. *Quaternary Research* **32**, 335–41.

Kutzbach, J.E. and F.A. Street-Perrott 1985. Milankovitch forcing of fluctuations in the level of tropical lakes from 18 to 0 kyr BP. *Nature* **317**, 130–4.

Lézine, A.-M. 1988a. New pollen data from the Sahel, Senegal. *Review of Palaeobotany and Palynology* **55**, 131–54.

Lézine, A.-M. 1988b. Les variations de la couverture forestière mésophile d'Afrique occidentale au cours de l'Holocène. *Compte Rendue de l'Académie des Sciences de Paris* **307**, 439–45.

Lézine, A.-M. and J. Casanova 1989. Pollen and hydrological evidence for the interpretation of past climates in tropical West Africa during the Holocene. *Quaternary Science Reviews* **8**, 45–55.

Lézine, A.-M. 1989. Le Sahel: 20 000 ans d'histoire de la végétation. *Bulletin de la Société Géologique de France* **1**, 35–42.

Lézine, A.-M., J. Casanova and C. Hillaire-Marcel 1990. Across an early Holocene humid phase in western Sahara: pollen and isotope stratigraphy. *Geology* **18**, 264–7.

Loubere, P. and K. Moss 1986. Late Pliocene climatic change and the onset of Northern Hemisphere glaciation as recorded in the northeast Atlantic Ocean. *Bulletin of the Geological Society of America* **97**, 818–28.

Mabbutt, J.A. 1977. *Desert landforms*. Canberra: Australian National University Press.

Mabbutt, J.A. 1978a. Lessons from pediments. In *Landform evolution in Australasia*, J.L. Davies and M.A.J. Williams (eds), 331–47. Canberra: Australian National University Press.

Mabbutt, J.A. 1978b. The impact of desertification as revealed by mapping. *Environmental Conservation* **5**, 45–56.

Mabbutt, J.A. 1985. Desertification of the world's rangelands. *Desertification Control Bulletin*, UNEP, Nairobi No. 12, 1–11.

Macquarie Illustrated World Atlas 1984. Sydney: Macquarie Library.

Maley, J. 1980a. Etudes palynologiques dans le bassin du Tchad et paléoclimatologie de l'Afrique Nord-tropicale de 30 000 ans à l'époque actuelle. D.Sc. thesis, University of Montpellier.

Maley, J. 1980b. Les changements climatiques de la fin du Tertiaire en Afrique: leur conséquence sur l'apparition du Sahara et de sa végétation. In *The Sahara and the Nile*, M.A.J. Williams and H. Faure (eds), 63–86. Rotterdam: Balkema.

May, R.M. 1978. Human reproduction reconsidered. *Nature* **272**, 491–5.

McDougall, I., W.H. Morton and M.A.J. Williams 1975. Age and rates of denudation of Trap Series basalts at Blue Nile Gorge, Ethiopia. *Nature* **254**, 207–9.

McHugh, W.P., C.S. Breed, G.G. Schaber, J.F. McCauley, *et al.* 1988. Acheulian sites along the 'radar rivers', southern Egyptian Sahara. *Journal of Field Archaeology* **15**, 361–79.

McHugh, W.P., G.G. Schaber, C.S. Breed and J.F. McCauley 1989. Neolithic adaptation and the Holocene functioning of Tertiary palaeodrainages in southern Egypt and northern Sudan. *Antiquity* **63**, 320–36.

McKee, E.D. (ed.) 1978. A study of global sand seas. *United States Geological Survey, Professional Paper* 1052.

Milankovitch, M. 1920. *Théorie mathématique des phénomènes thermiques produits par la radiation solaire*. Paris: Gaultier-Villars.

Milankovitch, M. 1930. Mathematische Klimalehre und astonomische Theorie der Klimaschwankungen. In *Handbuch der Klimatologie*, Volume I(A), W. Köppen and R. Geiger (eds), 1–176. Berlin: Gebruder Borntraeger.

National Academy of Sciences 1975. *Understanding climatic change: a program for action*. Washington, DC: National Academy of Sciences.

Owen, H.G. 1983. *Atlas of continental displacement, 200 million years to the present*. Cambridge: Cambridge University Press.

Pachur, H.-J., Kröpelin, P. Hoelzmann, M. Goschin, *et al.* 1990. Late Quaternary fluvio-lacustrine environments in western Nubia. *Berliner geowissenschaftliche Abhandlungen* **120.1**, 203–60.

Parkin, D.W. 1974. Trade-winds during the glacial cycles. *Proceedings of the Royal Society of London A* **337**, 73–100.

Parkin, D.W. and N. Shackleton 1973. Trade-winds and temperature correlations down a deep-sea core off the Saharan coast. *Nature* **245**, 455–7.

Parmenter, C. and D.W. Folger 1974. Eolian biogenic detritus in deep sea sediments: a possible index of equatorial Ice Age aridity. *Science* **185**, 695–8.

Peel, R.F. 1939. An expedition to the Gilf Kebir and 'Uweinat. 4. The Gilf Kebir. *Geographical Journal* **93**, 295–307.

Peel, R.F. 1941. Denudational landforms in the central Libyan Desert. *Journal of Geomorphology* **5**, 3–23.

Peel, R.F. 1966. The landscape in aridity. *Transactions of the Institute of British Geographers* **38**, 1–23.

Pesce, A. 1968. *Gemini space photographs of Libya and Tibesti. A geological and geographical analysis*. Tripoli: Petroleum Exploration Society of Libya.

Petit, J.R., M. Briat and A. Royer 1981. Ice age aerosol content from East Antarctic ice core samples and past wind strength. *Nature* **293**, 391–4.

Prentice, M.L. and G.H. Denton 1988. The deep-sea oxygen isotope record, the global ice sheet system and hominid evolution. In *Evolutionary history of the 'robust' australopithecines*, F.E. Grine (ed.), 383–403. New York: Aldine de Gruyter.

Press, F. and R. Siever 1986. *Earth*. San Francisco: W.H. Freeman.

Quade, J., T.E. Cerling and J.R. Bowman 1989. Development of the Asian monsoon revealed by marked ecological shift during the latest Miocene in northern Pakistan. *Nature* **342**, 163–6.

Quilty, P.G. 1984. Phanerozoic climates and environments of Australia. In *Phanerozoic Earth history of Australia*, J.J. Veevers (ed.), 48–55. Oxford: Clarendon Press.

Raulais, M. 1951. Du Crétacé probable sur les hauts reliefs sahariens. *Compte rendu sommaire des séances de la Société géologique de France, 1951*, 22–3.

Ritchie, J.C. and C.V. Haynes 1987. Holocene vegetation zonation in the eastern Sahara. *Nature* **330**, 645–7.

Rognon, P. 1967. *Le massif de l'Atakor et ses bordures (Sahara central): étude géomorphologique*. Paris: CNRS and CRZA.

Rognon, P. 1989. *Biographie d'un désert*. Paris: Plon.

Rognon, P. and M.A.J. Williams 1977. Late Quaternary climatic changes in Australia and North Africa: a preliminary interpretation. *Palaeogeography, Palaeoclimatology, Palaeoecology* **21**, 285–327.

Ruddiman, W.F. and M.E. Raymo 1988. Northern Hemisphere climate régimes during the past 3 Ma: possible tectonic connections. *Philosophical Transactions of the Royal Society B* **318**, 411–30.

Sandford, K.S. 1933. Geology and geomorphology of the Southern Libyan-Desert. Section 7 in 'A further journey through the Libyan Desert'. *Geographical Journal* **82**, 213–9.

Sarnthein, M. 1978. Sand deserts during glacial maximum and climatic optimum. *Nature* **272**, 43–5.

Sarnthein, M., G. Tetzlaff, B. Koopmann, K. Wolter and U. Pflaumann, 1981. Glacial and interglacial wind regimes over the eastern subtropical Atlantic and north-west Africa. *Nature* **293**, 193–6.

Schnitker, D. 1980. Global paleoceanography and its deep water linkage to the Antarctic glaciation. *Earth-Science Reviews* **16**, 1–20.

Servant, M. 1973. *Séquences continentales et variations climatiques: Evolution du bassin du Tchad au Cénozoique supéricur*. D.Sc. thesis, University of Paris.

Shackleton, N.J. 1977. The oxygen isotope stratigraphic record of the late Pleistocene. *Philosophical Transactions of the Royal Society* **280**, 169–79.

Shackleton, N.J. 1987. Oxygen isotopes, ice volume and sea level. *Quaternary Science Reviews* **6**, 183–90.

Shackleton, N.J. and J.P. Kennett 1975. Paleotemperature history of the Cenozoic and the initiation of Antarctic glaciation: oxygen and carbon isotope analyses in DSDP sites 277, 279 and 281. In *Initial Reports of the deep sea drilling project No. 29*, J.P. Kennett, R.E. Houtz, P.B. Andrews, A.R. Edwards, *et al.* (eds), 743–55. Washington DC: U.S. Government Printing Office.

Shackleton, N.J. and N.D. Opdyke 1977. Oxygen isotope and palaeomagnetic evidence for early Northern Hemisphere glaciation. *Nature* **270**, 216–9.

Shackleton, N.J., J. Backman, H. Zimmerman, D.V. Kent, *et al.* 1984. Oxygen isotope calibration of the onset of ice-rafting and history of glaciation in the North Atlantic region. *Nature* **307**, 620–3.

Smith, A.B. 1980. The Neolithic tradition in the Sahara. In *The Sahara and the Nile*, M.A.J. Williams and H. Faure (eds), 451–65. Rotterdam: Balkema.

Street, F.A. 1980. The relative importance of climate and local hydrogeological factors in influencing lake-level fluctuations. *Palaeoecology of Africa* **12**, 137–58.

Street-Perrott, F.A. and R.A. Perrott 1990. Abrupt climatic fluctuations in the tropics: the influence of Atlantic Ocean circulation. *Nature* **343**, 607–12.

Suc, J.-P. 1984. Origin and evolution of the Mediterranean vegetation and climate in Europe. *Nature* **307**, 429–32.

Szabo, B.J., W.P. McHugh, G.G. Schaber, C.V. Haynes Jr, *et al.* 1989. Uranium-series dated authigenic carbonates and Acheulian sites in Southern Egypt. *Science* **243**, 1053–6.

Talbot, M.R. 1980. Environmental responses to climatic change in the West African Sahel over the past 20,000 years. In *The Sahara and the Nile*, M.A.J. Williams and H. Faure (eds), 37–62. Rotterdam: Balkema.

Téhet, R., F. Gasse, A. Durand and P. Schroeter 1990. Fluctuations climatiques du Tardiglaciaire à l'Actuel au Sahel (Bougdouma, Niger Méridional). *Compte Rendu de l'Académie des Sciences de Paris* **311**, 253–8.

Thomas, D.S.G. (ed.) 1989. *Arid zone geomorphology*. London: Belhaven.

Thorp, M.B. 1969. Some aspects of the geomorphology of the Aïr Mountains, southern Sahara. *Transactions of the Institute of British Geographers* **47**, 25–46.

Tiercelin, J.J. 1987. The Pliocene Hadar Formation, Afar depression of Ethiopia. In: L.E. Frostick and I. Reid (eds), *Desert sediments: ancient and modern*, 221–40. Oxford: Blackwell Scientific, Geological Society Special Publication No. 35.

Twidale, C.R. 1960. Some problems of slope development. *Journal of the Geological Society of Australia* **6**, 131–47.

Twidale, C.R. 1978. Granite platforms and the pediment problem. In *Landform evolution in Australasia*, J.L. Davies and M.A.J. Williams (eds), 288–304. Canberra: Australian National University Press.

UNESCO 1967. 1:10 M Preliminary Geological Map of Africa.

UNESCO 1968. 1:15 M Tectonic Map of Africa.

Vail, J.R. 1972a. Jebel Marra, a dormant volcano in Darfur Province, western Sudan. *Bulletin Volcanologique* **36**, 251–65.

Vail, J.R. 1972b. Geological reconnaissance in the Zalingei and Jebel Marra areas of western Darfur Province, Sudan. *Bulletin of the Geological Survey, Sudan* **19**, 1–50.

Van Andel, T.H. 1985. New views on an old planet. *Continental drift and the history of Earth*. Cambridge: Cambridge University Press.

Veevers, J.J. (ed.) 1984. *Phanerozoic Earth history of Australia*. Oxford: Clarendon Press.

Vincent, P. 1963. Les volcans tertiaires et quaternaires du Tibesti occidental et central (Sahara du Tchad). *Mémoires, Bureau de Recherches Géologiques et Minières* **23**, 1–307.

Vogt, J. and R. Black 1963. Remarques sur la géomorphologie de l'Aïr. *Bulletin, Bureau de Recherches Géologiques et Minières* (Dakar) **1**, 1–29.

Wasson, R.J. 1976. Holocene aeolian landforms in the Belarabon area, S.W. of Cobar, NSW. *Journal and Proceedings, Royal Society of New South Wales* **109**, 91–101.

Williams, D.F., W.S. Moore and R.H. Fillon 1981. Role of glacial Arctic Ocean ice sheets in Pleistocene oxygen isotope and sea level records. *Earth and Planetary Science Letters* **56**, 157–66.

Williams, M.A.J. 1971. Geomorphology and Quaternary geology of Adrar Bous. *Geographical Journal* **137**, 449–55.

Williams, M.A.J. 1975. Late Pleistocene tropical aridity synchronous in both hemispheres? *Nature* **253**, 617–8.

Williams, M.A.J. 1976. Upper Quaternary stratigraphy of Adrar Bous (Republic of Niger, south-central Sahara). In *Proceedings of the Panafrican Congress of Prehistory and Quaternary Studies, Addis Ababa, 1971, VIIth Session*, B. Abebe, J. Chavaillon and J.E.G. Sutton (eds), 435–41.

Williams, M.A.J. 1980. Quaternary environments in Northern Africa. In *A land between two Niles*, M.A.J. Williams and D.A. Adamson (eds), 13–22. Rotterdam: Balkema.

Williams, M.A.J. 1984a. Geology. In *Key environments. Sahara Desert*, J.L. Cloudsley-Thompson (ed.), 31–9. Oxford: Pergamon.

Williams, M.A.J. 1984b. Cenozoic evolution of arid Australia. In *Arid Australia*, H.G. Cogger and E.E. Cameron (eds), 59–78. Sydney: Australian Museum.

Williams, M.A.J. 1984c. Quaternary environments. In *Phanerozoic Earth history of Australia*, J.J. Veevers (ed.), 42–7. Oxford: Clarendon Press.

Williams, M.A.J. 1985. Pleistocene aridity in tropical Africa, Australia and Asia. In *Environmental change and tropical geomorphology*, I. Douglas and T. Spencer (eds), 219–33. London: Allen & Unwin.

Williams, M.A.J. 1986. The creeping desert: what can be done? *Current Affairs Bulletin* **63**, 24–31.

Williams, M.A.J. 1991. Evolution of the landscape. In *Monsoonal Australia. Landscape, ecology and man in the northern lowlands*, M.G. Ridpath, C.D. Haynes and M.A.J. Williams (eds), 207–21. Rotterdam: Balkema.

Williams, M.A.J. and H. Faure (eds) 1980. *The Sahara and the Nile*. Rotterdam: Balkema.

Williams, M.A.J. and D.N. Hall 1965. Recent expeditions to Libya from the Royal Military Academy, Sandhurst. *Geographical Journal* **131**, 482–501.

Williams, M.A.J. and F.M. Williams 1980. Evolution of the Nile Basin. In *The Sahara and the Nile*, M.A.J. Williams and H. Faure (eds), 207–24. Rotterdam: Balkema.

Williams, M.A.J., D.A. Adamson, G.H. Curtis, & F. Gasse, *et al.* 1979. Plio-Pleistocene environments at Gadeb prehistoric site, Ethiopia. *Nature* **282**, 29–33.

Williams, M.A.J., D.A. Adamson, F.M. Williams, W.H. Morton, *et al.* 1980. Jebel Marra volcano: a link between the Nile Valley, the Sahara and Central Africa. In *The Sahara and the Nile*, M.A.J. Williams and H. Faure (eds), 305–37. Rotterdam: Balkema.

Williams, M.A.J., F.M. Williams and P. Bishop 1981. Late Quaternary history of La Besaka, Ethiopia. *Palaeoecology of Africa* **13**, 93–104.

Williams, M.A.J., G. Assefa and D.A. Adamson 1986. Depositional context of Plio-Pleistocene hominid-bearing formations in the Middle Awash Valley, southern Afar Rift, Ethiopia. In *Sedimentation in the African Rifts*, L. Frostick, R. Renaut, I. Reid and J.J. Tiercelin (eds), 233–43. Oxford: Blackwell Scientific, Geological Society Special Publication No. 25.

Williams, M.A.J., P.I. Abell and B.W. Sparks 1987. Quaternary landforms, sediments, depositional environments and gastropod isotope ratios at Adrar Bous, Tenere Desert of Niger, south-central Sahara. In *Desert sediments: ancient and modern*, L. Frostick and I. Reid (eds), 105–25. Geological Society Special Publication No. 35.

Williams, M.A.J., P. De Deckker and A.P. Kershaw (eds) 1991a. *The Cainozoic in Australia: a re-appraisal of the evidence*. Geological Society of Australia, Special Publication No. 18.

Williams, M.A.J., D.A. Adamson, P. De Deckker and M.R. Talbot 1991b. Episodic fluviatile, lacustrine and aeolian sedimentation in a late Quaternary desert margin system, central western New South Wales. In *The Cainozoic in Australia: a re-appraisal of the evidence*, M.A.J. Williams, P. De Deckker and A.P. Kershaw (eds), 258–87. Geological Society of Australia, Special Publication No. 18.

Winkler, H.A. 1939. Rock-pictures at 'Uweinat. Section 5 in 'An expedition to the Gilf Kebir and 'Uweinat, 1938'. *Geographical Journal* **93**, 307–10.

Yemane, K., R. Bonnefille and H. Faure 1985. Palaeoclimatic and tectonic implications of Neogene microflora from the north-western Ethiopian highlands. *Nature* **318**, 653–6.

INDEX